



ภาคผนวก

โครงการการพัฒนาศักยภาพการวิจัยเชิงสถาบันของภาควิชาพืชศาสตร์
และทรัพยากรการเกษตร คณะเกษตรศาสตร์ มหาวิทยาลัยขอนแก่น
เลขที่สัญญา IRG5780003

ศาสตราจารย์สนั่น จอกลอย และคณะ
ภาควิชาพืชศาสตร์และทรัพยากรการเกษตรศาสตร์
คณะเกษตรศาสตร์ มหาวิทยาลัยขอนแก่น

สนับสนุนโดยสำนักงานกองทุนสนับสนุนการวิจัย
และมหาวิทยาลัยขอนแก่น

ResearchGate

See discussions, stats, and author profiles for this publication at: https://www.researchgate.net/publication/271952728

Effect of Pistia stratiotes, cattle manure and wood vinegar (pyroligneous acid) application on growth and yield of organic rainfed rice

Article *in* Paddy and Water Environment · July 2014

DOI: 10.1007/s10333-014-0453-z

CITATIONS
0

READS
94

3 authors, including:



Bubpha Simma
Khon Kaen University
1 PUBLICATION **0** CITATIONS

SEE PROFILE

All content following this page was uploaded by Bubpha Simma on 24 February 2016.

The user has requested enhancement of the downloaded file.

Paddy Water Environ
DOI 10.1007/s10333-014-0453-z

ARTICLE

Effect of *Pistia stratiotes*, cattle manure and wood vinegar (pyroligneous acid) application on growth and yield of organic rainfed rice

Anan Polthanee · Nisit Kumla · Bubpha Simma

Received: 18 September 2013 / Revised: 10 June 2014 / Accepted: 8 July 2014
© The International Society of Paddy and Water Environment Engineering and Springer Japan 2014

Abstract The effect of soil incorporation of water lettuce (*Pistia stratiotes*) and cattle manure and of wood vinegar (pyroligneous acid) foliar application on growth and yield of rainfed rice was studied with a four replications split plot in a farmer's field in Thailand. *P. stratiotes* incorporation significantly increased the grain yield over nonincorporation with *P. stratiotes*. Cattle manure incorporation alone or combined with wood vinegar application significantly increased grain yield over wood vinegar and no-fertilizer application. Incorporation of *P. stratiotes* combined with cattle manure and wood vinegar application could not provide sufficient N to the rice crop, but it adequate for P and K. Plots with cattle manure incorporation combined with wood vinegar application exhibited the maximum K, P and N content in soil after harvest.

Keywords Water lettuce · Cattle manure · Wood vinegar · Organic rice

Introduction

Rice is the most important crop for Thailand, cultivated in more than 17 million ha annually and more than 75 % cultivated under rainfed conditions (Office of Agricultural Economic 2012). Organic rice is currently seen as a promising opportunity. Due to the demand in European countries, its production in Thailand had rapidly increased since 2003 (Economic Research Center 2003). As organic rice must be cultivated without inorganic fertilizer and pesticides, animal manure and crop residues are the most common fertilizers used for its production.

Manure is used as a source of N, P, K, Ca, Mg and S (Johnston 1997; Greenland 1997; Materechera and Salagae 2002; Edmeades 2003). Several studies have shown that crop residues can increase rice yield and allow a reduction of 25–50 % in chemical fertilizer N use (Aulakh et al. 2001; Salem 2006). Algae and aquatic weeds that develop in rice fields constitute a source of organic matter and nutrients that can be used as manure for rice. Average standing crops of the aquatic photosynthetic biomass range from around 500 kg dry weight ha^{-1} in the fields to 1–5 t dry weight ha^{-1} in irrigation canals and water tanks (Roger and Watanabe 1984). Major plants that grow naturally are water hyacinths (*Eichornia spp.*) (Gaur 1984), water lettuce (*Pistia stratiotes*) and duck weed (*Lemaceae* family) (Roger and Watanabe 1984). Application of spontaneous plant (*Pueraria phaseloides* and *Chomolaena* spp.) residures increased rice yield by 29 and 33 % over control (Kone et al. 2010). Water lettuce (*Pistia stratiotes*), abundant in the reservoirs of Northeast Thailand, has a potential as green manure in nearby rice-cultivated areas; however, there is no information about its use for rice production in Thailand. Wood vinegar (pyroligneous acid), a by-product of charcoal burning, has been widely used by farmers in Thailand as foliar fertilizer to improve crop yields (Jun et al. 2006; Katoda and Niimi 2004; Yoshimura et al. 1995). This study investigated the effect of *P. stratiotes*, cattle manure and wood vinegar on growth and yield of organic rice under rainfed conditions.

Materials and methods

This experiment was conducted in a farmer's field in Muang village, Khon Kaen province in 2012. The soil is a loamy sand: pH 4.49, organic matter content 0.69 %, total N 0.037 %,

A. Polthanee (✉) · N. Kumla · B. Simma
Department of Plant Science and Agricultural Resources, Faculty of Agriculture, Khon Kaen University, Khon Kaen, Thailand
e-mail: panan@kku.ac.th

Published online: 23 July 2014

available P 6.37 ppm and exchangeable K 83.74 ppm. The climate of the area is tropical monsoon type with an annual average temperature of 24–30 °C and annual rainfall of 1,000 mm with 895 mm during the rice-growing period.

The experiment was laid out in a split plot design with four replications. *P. stratiotes* incorporation and nonincorporation were the main-plot factors. Cattle manure incorporation and wood vinegar foliar application, alone or combined, were the subplot factors.

Pistia stratiotes was collected from the lake located in Khon Kaen province. Four samples of plants were analyzed for N (2.75 %), P (0.61 %) and K (2.70 %). *P. stratiotes* was chopped to 5 cm length and applied at 2.2 ton ha^{-1} (dry weight). It was uniformly incorporated into the soil at approximately 15 cm depth, 7 days before transplanting. The corresponding amount of nutrients incorporated were 59.2 kg Nha^{-1}, 13 kg Pha^{-1} and 58.0 kg Kha^{-1}.

Cattle manure (0.87 % N, 0.23 % P, 2.16 % K dw.) was incorporated 7 days before transplanting at 3,125 kg ha^{-1} dw, corresponding to 27.3 kg Nha^{-1}, 7.3 kg Pha^{-1} and 67.2 kg Kha^{-1}. Eucalyptus wood vinegar, diluted 300 times, was used for foliar application at 15 days intervals from 30 days after transplanting until 10 days before maturity. Rice variety of KDML 105 was used. Three 30-day-old seedlings were transplanted per hill at a 25 × 25 cm spacing, 7 days after water lettuce and cattle manure application. A manure weeding was performed at tillering. No insecticide or fungicide was used.

Plant height and total above ground dry weight were measured at panicle initiation (PI) and at harvest on five hills from each plot. Nitrogen, phosphorus and potassium contents of leaves were determined at panicle initiation and harvest. The number of panicle per hill was measured at harvest. Ten panicles from each plot were randomly selected to determine the total number of grains per panicle and calculate the percentage of filled grain per panicle. Grain yield was measured from the 2 × 3 m harvesting area of each plot and calculated as kg ha^{-1} at 14 % moisture. The filled grains were randomly selected from the grain yield samples to determine the weight of 1,000 grains. At harvest, soils were sampled at 0–25 cm depth to determine OM (%), total N (%), available P (ppm) and exchangeable K (ppm).

The data were analyzed using analysis of variance procedures, and least significant difference (LSD) was used to compare treatments when the F test was significant.

Results

Growth of rice

P. stratiotes incorporation significantly increased plant height at PI but not at harvest. It had no significant effect on above ground dry weight (Table 1). Cattle manure alone or combined with wood vinegar significantly increased plant height over the control (no-fertilizer) at PI, but no effect was observed at harvest. It significantly increased the above ground dry weight, both at PI and harvest. Wood vinegar application alone had no significant effect on plant height and above ground dry weight.

Table 1 Plant height and above ground dry weight of KDML 105 rice at panicle initiation (PI) and at harvest as affected by plant residue management and application of organic fertilizer

Treatments	Plant height (cm)		Above ground dry weight ($gplant^{-1}$)	
	PI	Harvest	PI	Harvest
Plant residue management (A)				
Water lettuce	86.8a	112.2	11.6	15.2
No-plant residue	77.4b	108.6	9.4	12.9
Type of organic fertilizer (B)				
Cattle manure (C)	88.6a	112.8	11.1ab	14.3ab
Wood vinegar (W)	79.2bc	107.5	9.1c	12.6b
C combined with W	84.5ab	110.8	11.9a	18.7a
No-fertilizer	76.1c	110.6	9.8bc	13.5b
F test				
Plant residue management (A)	**	NS	NS	NS
Type of organic fertilizer (B)	**	NS	**	*
A × B	NS	NS	NS	NS

Means followed by the same letter at the same column are not significantly different by LSD at $P < 0.05$

NS not significant

* Significant at $P < 0.05$, ** significant at $P < 0.01$

Yield components

A higher panicle number per hill, grain number per panicle, filled grain percentage and 1,000 grain weight were observed after *P. stratiotes* incorporation, but the difference was not statistically significant (Table 2). Cattle manure combined with wood vinegar significantly increased the number of panicle per hill over control, but had no significant effect on the grain number per panicle, the filled grain percentage and 1,000 grain weight (Table 2). The interaction between *P. stratiotes* incorporation and the type of organic fertilizer on 1,000 grain weight was highly significant (Table 3). The highest 1,000 grain weight was observed with cattle manure combined with *P. stratiotes* incorporation and with wood vinegar in the absence of *P. stratiotes* incorporation (Table 3).

Table 2 Grain yield and yield components of KDML 105 rice as affected by plant residue management and application of organic fertilizer

Treatments	Panicle (no./hill)	Grain (no./panicle)	Filled grain (%)	1,000 grain weight (g)	Grain yield (kg ha^{-1})
Plant residue management (A)					
Water lettuce	6.89	80.10	75.3	26.86	2,305.1a
No-plant residue	6.30	78.33	70.5	26.78	2,042.5b
Type of organic fertilizer (B)					
Cattle manure (C)	6.90ab	83.25	68.4	27.12	2,319.1a
Wood vinegar (W)	6.30ab	79.22	70.8	26.33	2,048.1b
C combined with W	6.95a	81.25	75.2	27.20	2,404.3a
No-fertilizer	6.22b	73.15	77.5	26.63	2,023.6b
F test					
Plant residue management (A)	NS	NS	NS	NS	*
Type of organic fertilizer (B)	**	NS	NS	NS	**
A × B	NS	NS	NS	**	NS

Means followed by the same letter at the same column are not significantly different by LSD at $P < 0.05$

NS not significant

* Significant at $P < 0.05$, ** significant at $P < 0.01$

Table 3 Interaction between plant residue management and type of organic fertilizer on 1,000 grains weight at harvest

Treatments	1,000 grains weight (g)	
	Water lettuce application	No-plant residue
Cattle manure (C)	27.8a	26.4
Wood vinegar (W)	25.3b	27.4
C combined with W	27.2a	27.2
No-fertilizer	26.8a	26.5

Means followed by the same letter at the same column are not significantly different by LSD

Grain yield

P. stratiotes incorporation had significantly increased the grain yield over nonincorporation treatment (Table 2). Cattle manure alone or combined with wood vinegar significantly increased grain yield over the control. The maximum grain yield was obtained with cattle manure combined with wood vinegar but was not significantly different from that obtained with cattle manure alone (Table 2).

Nutrient concentration in leaves

P. stratiotes incorporation had no significant effect on N, P and K concentrations in leaves at panicle initiation (PI) and harvest (Tables 4 and 5). Cattle manure alone significantly increased P concentration over control at PI and harvest (Tables 4 and 5). The highest P concentration at PI and harvest was observed with cattle manure alone and was not significantly different from that of cattle manure combined with wood vinegar. With *P. stratiotes* incorporation, cattle manure combined with wood vinegar provided the highest N concentration in leaves at PI. Under no *P. stratiotes* incorporation, cattle manure alone gave the maximum N concentration at PI (Table 6).

Table 4 Nitrogen, phosphorus and potassium concentration in leaves of KMDL 105 rice at panicle initiation as affected by plant residue management and application of organic fertilizer

Treatments	Nitrogen (%)	Phosphorus (%)	Potassium (%)
Plant residue management (A)			
Water lettuce	1.37	0.22	2.95
No-plant residue	1.34	0.2	2.83
Type of organic fertilizer (B)			
Cattle manure (C)	1.35	0.23a	2.92
Wood vinegar (W)	1.37	0.19c	2.93
C combined with W	1.35	0.22ab	2.78
No-fertilizer	1.36	0.20bc	2.93
F test			
Plant residue management (A)	NS	NS	NS
Type of organic fertilizer (B)	NS	**	NS
A × B	**	NS	NS

Means followed by the same letter at the same column are not significantly different by LSD at $P < 0.05$

NS not significant

** Significant at $P < 0.01$

Table 5 Nitrogen, phosphorus and potassium content in leaves of KDML 105 rice at harvest as affected by plant residue management and application of organic fertilizer

Treatments	Nitrogen (%)	Phosphorus (%)	Potassium (%)
Plant residue management (A)			
Water lettuce	0.89	0.08	1.11
No-plant residue	0.87	0.07	1.03
Type of organic fertilizer (B)			
Cattle manure (C)	0.89	0.09a	1.05
Wood vinegar (W)	0.86	0.07b	1.11
C combined with W	0.93	0.08ab	1.12
No-fertilizer	0.85	0.07b	0.99
F test			
Plant residue management (A)	NS	NS	NS
Type of organic fertilizer (B)	NS	*	NS
A × B	NS	NS	NS

Means followed by the same letter at the same column are not significantly different by LSD at $P < 0.05$

NS not significant

* Significant at $P < 0.05$

Table 6 Interaction between plant residue management and type of organic fertilizer on nitrogen concentration in leaves at panicle initiation growth stage

Treatments	N concentration in leaves of rice at PI (%)	
	Water lettuce application	No-plant residue
Cattle manure (C)	1.302b	1.388a
Wood vinegar (W)	1.383ab	1.361a
C combined with W	1.403a	1.269b
No-fertilizer	1.30ab	1.341ab

Means followed by the same letter at the same column are not significantly different by LSD

Soil chemical property at harvest

P. stratiotes incorporation had no significant effect on organic matter, total N, available P and exchangeable K in soil (Table 7). Cattle manure alone or combined with wood vinegar significantly increased organic matter, total N, available P and exchangeable K over control (Table 7).

Discussion

P. stratiotes incorporation into the soil as green manure significantly increased the grain yield of KDML 105 rice

Table 7 Soil chemical properties at 0–25 cm depth at harvest as affected by plant residue management and application of organic fertilizer

Treatments	OM (%)	Total N (%)	Available P (ppm)	Exchangeable K (ppm)
Plant residue management (A)				
Water lettuce	0.62	0.03	4.43	66.99
No-plant residue	0.61	0.03	3.40	63.09
Type of organic fertilizer (B)				
Cattle manure (C)	0.67a	0.03a	4.75a	76.06a
Wood vinegar (W)	0.58b	0.02b	3.88bc	55.06b
C combined with W	0.67a	0.03a	4.95a	79.24a
No-fertilizer	0.56b	0.02b	3.44c	49.79b
F test				
Plant residue management (A)	NS	NS	NS	NS
Type of organic fertilizer (B)	**	**	**	**
A × B	*	*	NS	NS

Means followed by the same letter at the same column are not significantly different by LSD at $P < 0.05$

NS not significant

* Significant at $P < 0.05$, ** significant at $P < 0.01$

variety over no-fertilizer treatment. *P. stratiotes* incorporation increased rice grain yield over no-fertilizer by 263 kg ha^{-1} (or 12 %). Application of cattle manure combined with wood vinegar significantly increased rice grain yield (2,404 kg ha^{-1}) over wood vinegar applied alone (2,048 kg ha^{-1}) and without fertilizer application (2,024 kg ha^{-1}) plots. The application of cattle manure combined with wood vinegar produced maximum grain yield (2,404 kg ha^{-1}), but it was not significantly different from that of the cattle manure applied alone (2,319 kg ha^{-1}). In this experiment, application of cattle manure combined with wood vinegar increased rice yield over cattle manure alone by 4 %, due to an increase of the panicle number and filled grain percentage. This agrees with the study by Hiowaka (1994). Manure is used mainly as a source of N, P and S for crop production (Materechera and Salagal 2002; Johnston 1997; Greenland 1997). Polthanee et al. (2012) reported that application of cattle manure at 3,125, 6,250 and 9,375 kg ha^{-1} increased rice yield by 9, 15 and 24 %, respectively. Application of 10 ton ha^{-1} cattle manure to low fertile soil increased grain yields by 108–106 % in long term (Kanika 1998). Application of cattle manure combined with wood vinegar increased rice yield over cattle manure alone by 4 % due to

Table 8 Interaction between plant residue management and type of organic fertilizer on soil organic matter and total nitrogen in soil at harvest

Treatments	Organic matter (%)		Total N (%)	
	Water lettuce application	No-plant residues	Water lettuce application	No-plant residues
Cattle manure (C)	0.695a	0.653b	0.033a	0.031b
Wood vinegar (W)	0.613ab	0.554c	0.029ab	0.026c
C combined with W	0.612ab	0.729a	0.029ab	0.034a
No-fertilizer	0.558b	0.561c	0.026b	0.026c

Means followed by the same letter at the same column are not significantly different by LSD at $P < 0.05$

an increase of panicle number and filled grain percentage. This agrees with the study by Hiowaka (1994) (Table 8).

In our experiment, wood vinegar application did not significantly increased rice yield (1.2 %) over the control, but increased the number of panicle and grain number per panicle. This agrees with the work done by Ruamtaku et al. (2007). Acetic acid, being a main component in wood vinegar, might act as a carbon source that associated with photosynthesis. Mixing acetic acid in medium solution for the culture of seaweeds (*Chondrus crispus*) enhances growth and consequently increased the productivity by 28 % (Amat and Braud 1993).

N concentration in leaves at PI of about 2.6–3.2 % of dry weight (dw) was considered sufficient (Mikkelsen and Hunziker 1971). In our experiment, N in leaves at PI was 1.34–1.37 % of dw for all treatments, indicating a deficiency in N. Such a deficiency is known to reduce grain number per panicle and filled grain percentage (Doberman and Fairhurst 2000).

P concentration in rice leaves at the PI stage was estimated to be sufficient at about 0.17 % dw (Fageria et al. 1988). In our experiment, it was 0.19–0.23 % of dw for all treatments. This indicates that soil could provide an adequate amount for rice growth at PI. The sufficient K concentration in leaves at the PI stage was estimated to be about 1.0–2.2 % dw (Jones et al. 1991). In our study, K in leaves at the PI stage was 2.78–2.95 % dw for all treatments, indicating that soil K was sufficient for rice growth at PI. Nitrogen was obviously the major limiting factor for rice crop production in the site.

The nutrient content in soil at harvest was significantly higher in the cattle manure treated plots, with and without wood vinegar application, as compared with the control. This agrees with the long-term trials by Edmeades (2003) showing that the use of manure relative to fertilizers can result in soils becoming excessively enriched with P, K, Ca and Mg in the top soil.

Conclusion

P. stratiotes incorporation into the soil as green manure significantly increased the grain yield of KDML 105 rice variety over nonincorporation treatment. *P. stratiotes* incorporation combined with cattle manure at a rate of 3,125 kg ha^{-1} could not provide sufficient N to the rice crop, but was adequate for P and K. Application of cattle manure combined with wood vinegar resulted in the maximum grain yield (2,404 kg ha^{-1}) due to an improved number of panicle per hill.

References

Amat M, Brand JP (1993) The use of acetic acid as a source of carbon by cultivated *Chondrus crispus* (Gigartinales, Rhodophyta) Stackhouse. Hydrobiologia 260(261):451–456

Aulakh MS, Khera TS, Doran JW, Broson KF (2001) Managing drop residue with green manure, urea, and tillage in a rice wheat rotation. Soil Sci Soc Am J 65:820–827

Dobermann A, Fairhurst TH (2000) Rice Nutrient Disorders and Nutrient Management. Oxford Graphic Printers Pte Ltd, Singapore, p 199

Economic Research Center (2003) Study on Developing Hom Mali Organic Rice for export to Europe and United State of America (in Thai). Kasetsart University, Faculty of Economics 286p

Edmeades DC (2003) The long-term effects of manures and fertilizers on soil productivity and quality: a review. Nutr Cycl Agroecosyst 66:165–180

Fageria NK, Wright RT, Buligar VC (1988) Rice cultivar evaluation for phosphorus use efficiency. Plant Soil 111:105–109

Gaur AC (1984) Response of rice to organic matter: The Indian experience. Organic matter and rice. International Rice Research Institute, Manila, pp 503–514

Greenland DJ (1997) Soil condition and plant growth. Soil Use Manage. 13:169–177

Hiowaka T (1994) The use of wood vinegar and charcoal in Agriculture. ICCA, Japan

Johnston AE (1997) The value of long-term field experiments in agriculture, ecological and environmental research. Adv. Agron. 59:291–333

Jones JB, Wolf B, Mills HA (1991) Analysis Handbook: A practical sampling, preparation, analysis and interpretation guide. Micro-Macro Inc., USA

Jun ZM, Wen G, Qing LW (2006) Preliminary study of application effect of bamboo vinegar on vegetable growth. Forest Study of China 5(3):43–47

Kanika N (1998) Improvement of paddy soil. Technology for Hom Mali rice production (in Thai). Department of Agriculture, Ministry of Agriculture and Cooperatives, pp 33–45

Katoda M, Niimi Y (2004) Effect of charcoal with pyroligneous acid and barnyard manure on bedding plants. Scientia Horticulture. 101:327–332

Kone F, Kouadio JY, Yapo ES, Visser M (2010) Effects of spontaneous plant residues and rice straw incorporated in soil

on growth and yield parameters of a lowland rice in Subhumid Tropical Area. J. App. Sci. Res. 6(11):1581–1588

Materechera SA, Salagae AM (2002) Use of partially decomposed cattle and chicken manure amended with wood ash in two South African arable soils with contrasting texture: effect on nutrient uptake early growth, and dry matter yield of maize. Commun Soil Sci Plant Anal 33:179–201

Mikkelsen DS, Hunziker RG (1971) A plant analysis survey of California rice. Agri. Chem. 14:18–22

Office of Agricultural Economic (2012) Agricultural Statistics of Thailand. Office of Ministry of Agriculture and Cooperative, Bangkok

Polthanee A, Promkhambut A, Treloges V (2012) Effect of pre-rice mungbean and cattle manure application on growth and yield of organic rice. International Journal of Environmental and Rural Development 3(1):1–9

Roger PA and Watanabe I (1984) Algae and aquatic weeds as source of organic matter and plant nutrients for wetland rice In: Organic matter and rice, International Rice Research Institute, Los banos, Philippines, pp 147–168

Ruamtaku C (2007) Effect of wood vinegar on yield and seed quality of KMDL 105 rice. Master of Science Thesis in Agronomy, Graduate School, Khon Kaen University

Salem AKM (2006) Effect of nitrogen levels, plant spacing and time of farmyard manure application on the productivity of rice. J Appl Sci Res 2(II):980–987

Yoshimura H, Washio H, Yoshuda S, Seino T, Otaka M, Matsubara K, Matsubara M (1995) Promoting effect of wood vinegar compounds on fruit-body formation of *Pleurotus oetratus*. Mycoscience. 36:173–177

View publication stats



Bioscience, Biotechnology, and Biochemistry

ISSN: 0916-8451 (Print) 1347-6947 (Online) Journal homepage: http://www.tandfonline.com/loi/tbbb20

Identification of peanut seed prolamins with an antifungal role by 2D-GE and drought treatment

Waraluk Senakoon, Suporn Nuchadomrong, Robin Y.-Y. Chiou, Gulsiri Senawong, Sanun Jogloy, Patcharin Songsri & Aran Patanothai

To cite this article: Waraluk Senakoon, Suporn Nuchadomrong, Robin Y.-Y. Chiou, Gulsiri Senawong, Sanun Jogloy, Patcharin Songsri & Aran Patanothai (2015) Identification of peanut seed prolamins with an antifungal role by 2D-GE and drought treatment, Bioscience, Biotechnology, and Biochemistry, 79:11, 1771-1778, DOI: 10.1080/09168451.2015.1056508

To link to this article: http://dx.doi.org/10.1080/09168451.2015.1056508

Published online: 18 Jun 2015.

Submit your article to this journal

Article views: 263

View related articles

View Crossmark data

Full Terms & Conditions of access and use can be found at
http://www.tandfonline.com/action/journalInformation?journalCode=tbbb20

Download by: [202.28.119.99] **Date:** 06 September 2017, At: 01:25

Bioscience, Biotechnology, and Biochemistry, 2015
Vol. 79, No. 11, 1771–1778

Identification of peanut seed prolamins with an antifungal role by 2D-GE and drought treatment

Waraluk Senakoon[1], Suporn Nuchadomrong[1,*], Robin Y.-Y. Chiou[2], Gulsiri Senawong[1], Sanun Jogloy[3], Patcharin Songsri[3] and Aran Patanothai[3]

[1]*Faculty of Science, Department of Biochemistry, Khon Kaen University, Khon Kaen, Thailand;* [2]*Department of Food Science, College of Life Sciences, National Chiayi University, Chiayi, Taiwan, ROC;* [3]*Faculty of Agriculture, Department of Plant Science and Agricultural Resources, Khon Kaen University, Khon Kaen, Thailand*

Received January 26, 2015; accepted May 1, 2015
http://dx.doi.org/10.1080/09168451.2015.1056508

Downloaded by [] at 01:25 06 September 2017

This work revealed peanut seed prolamins likely displaying a defensive role besides the known nitrogen storage. Drought stress and proteomic approaches were used in varieties of peanuts to explore the prolamin member in association with a test against *Aspergillus flavus* spore germination. The stress effect was showed by aerial biomass, leaf content of malondialdehyde, and seed contamination by *A. flavus*. Sodium dodecyl sulfate–polyacrylamide gel electrophoresis profiles were not informative for the antifungal polypeptides. From two-dimensional gel electrophoresis, the suspected polypeptides were those with pI 5.45–5.75 and sizes of 22.0–30.5 kDa specifically in Spanish-type peanuts. Regarding to the drought effect in most of these peanuts, the spot peak volume analysis deduced three novel prolamin-related antifungal polypeptides at pI 5.75–5.8 with 30.5, 27.5–28.5, and 22.0–22.5 kDa, which was confirmed after isoelectric purification at pH 5.60. The data could not yet conclude their correlation with resistance to drought and to seed infection by *A. flavus*.

Key words: 2D-GE maps; antifungus; *Aspergillus flavus*; peanut seed prolamins

The market-type peanuts (*Arachis hypogaea* L.) including the runner, Virginia, Spanish, and Valencia are cultivated worldwide in tropical and warm temperate zones. Due to the poor water management in the globule peanut planting areas,[1)] the peanut plant frequently exposes to water deficit (or drought) during crop season. As a result from drought during pod development, peanut pods are at high risk of infection by soil microorganisms, and the most importance is *Aspergillus flavus* infection which is causative for the contamination of aflatoxin.[2)] The drop in seed kernel water activity during drought causes the reduction in phytoalexin synthesis, which was proposed to be the critical involvements.[3,4)] Otherwise, drought causes plant weakness from oxidative impair of cell-to-organ functions which somehow promotes *A. flavus* invasion.[5)]

Several workers have published electrophoretic evidence of seed proteins in peanut genotypes. The simple sodium dodecyl sulfate–polyacrylamide gel electrophoresis (SDS–PAGE) was successful in a few cases.[6,7)] However, extensive successes were obtained using two-dimensional gel electrophoresis (2D-GE) in several aspects.[8–10)] 2D-GE also demonstrated distinct changes in proteomic of total seed storage proteins in response to water deficit solely or in couple with *A. flavus* inoculation, comparing between drought susceptible and resistant genotypes.[11,12)] Those findings were found mostly in association with peanut seed globulins and albumins, in the sense of allergens and antifungal proteins.[9,10,12,13)] Peanut seed proteins contain three known classes of storage proteins including globulins (94–95%), albumins (2–3%), and prolamins (1–2%).[14)] Information of prolamins has been restricted to that of cereal seeds with an importance as primary nitrogen reserves.[15)] Native prolamins are hydrophobic and extractable in aqueous alcohol solutions like 50–55% propanol or 60–70% ethanol.[16)] Our previous work described an extraction method for peanut seed prolamins which retarded *A. flavus* spore germination comparing to the globulin or albumin fraction.[17)] No other works on prolamins have been published in peanut genotypes, but the Ara h 9 (a non-specific lipid transfer protein) in the peanut seed allergen prolamin superfamily displays an antifungal property.[13)]

This study aimed to use the proteomic study, peanut genotypes with different susceptibility to drought and drought treatment as tools to investigate seed prolamin members in association with the anti-*A. flavus* activity. The experiments were conducted with five Spanish-type and one Virginia-type genotypes. A drought condition for peanut plantings was set up in parallel with the non-drought condition since the anti-*A. flavus* prolamin members might be drought-inductive especially in the resistant genotype. To accomplish our purposes, one

*Corresponding author. Email: suporn@kku.ac.th

© 2015 Japan Society for Bioscience, Biotechnology, and Agrochemistry

part of the work prior to the proteomic study was dealt with demonstrations of the drought establishment on peanut plants.

Materials and methods

Planting design. Four drought resistant Spanish-type peanuts from the International Crops Research Institute for Semi-Arid Tropics (ICRISAT; India) included ICGV 98300, 98303, 98305, and 98308.[18] Two genotypes of drought-sensitive traits cropped in Thailand were the Virginia-type KK 60-3 and the Spanish-type Tainan-9.[18] Soil water holding at control field capacity or drought condition at 1/3 available water was instrumentally evaluated at 15.00 and 7.33% v/w, respectively. The water volume for monitoring control or drought condition was calculated.[19] The peanut plant stages were defined by following the classical description.[20]

Peanut plants were grown in plastic pots (38 cm width and 28 cm height) with plugholes during the dry season in November 2011 to March 2012 at the Field Crop Research Station, Khon Kaen University. At the date of 50% blooming (37 DAS; days after sowing), 100-mL spore suspension from fresh *A. flavus* cultures on potato dextrose agar (PDA) medium was applied entirely the soil surface at 1.75×10^7 spores/cm^2 to normalize the infection. The drought stress was started at the beginning pod stage (57 DAS) by stopping water supply a few days in advance from the calculated daily water loss. The apparent soil water status was weekly confirmed by the conventional gravimetric method. The drought continued to the harvest time at the seed maturity stage (110–120 DAS dependent on genotypes).

Plant responses to water status. Samples were taken from the peanut plants at the beginning seed stage (76 DAS). The first fully expanding leaves from the main stem apex ($n = 3$) were detached at noon. One leaf was processed for determining relative water content from leaf fresh weight, turgid weight, and dry weight.[21] The other leaf was immediately dipped in cold absolute ethanol to block wounding stress and shortly kept at −30 °C. On analysis, the leaf was washed in water to remove ethanol, blotted dry, and weighed for the leaf wet weight. The malondialdehyde content in leaves (0.3 g) was quantified by the thiobarbituric acid reaction.[22] The aerial parts of peanut plants ($n = 3$) were dried at 80 °C to a constant weight as the biomass value.

Test for A. flavus seed contamination. Fresh sound mature peanut seeds ($n = 10$) were surface sterilized by rinse once for 30 s with 70% ethanol and subsequent 5-min shake in 1% sodium hypochlorite. After excessive washings with distilled water, seeds were placed on PDA medium at 30 °C for a week.

Preparation of prolamin samples. The kernel from the fresh sound mature seeds was got rid of seed coats to prevent the effect of phenolic compounds,[23] crushed in liquid N_2 and defatted overnight at −20 °C with hexane (25 mL/g). The fat-free kernel meal was air-dried and stored at −70 °C.

The preparation of prolamins followed the two-step extraction,[17] which was performed by stirring the fat-free sample (10 g) in 5 volumes of a specified solvent for 1 h at room temperature. The first step was twice extraction with 2 M NaCl in 50 mM Tris–HCl (pH 6.8). Then, the meal was rinsed with acetone, air-dried, and subjected to second extraction with 70% ethanol. The ethanolic extract was carried out protein precipitation for 1 h on ice with 4 volumes of cold acetone. The precipitates were collected by centrifugation, flushed with N_2 gas, and suspended in 20 mL of distilled water (pH 6.25) in order to obtain homogeneously dispersed powder by lyophilization. The packed dry sample was readily dissolved in water which was cited unusual for prolamins. The freeze-dried powder as crude prolamins was water soluble at the routine preparation of 3 μg protein/μL as determined by the modified Lowry protein assay kit (Pierce, USA).

In an experiment with ICGV 98305 as specified in "*Results*", the crude prolamin powder solution was carefully adjusted with 1 M HCl to pH 5.60 and left for 18 h at 4 °C to partially purify particular members of prolamins by means of the isoelectric precipitation. After centrifugation, the purified precipitate was dissolved and the supernatant was collected. Both fractions were concentrated to a protein concentration of 10 μg/μL by centrifugal ultrafiltration using Vivaspin tube (10 kDa MWCO; GE Healthcare, UK) and processed for test on *A. flavus* and 2D-GE analysis.

Inhibitory assay on fungal spore germination. The aqueous solutions of prolamin powder or those from the isoelectric purification were adjusted for a protein concentration of 3 μg/μL and made sterile by membrane filtration. Spore suspensions were prepared from fresh *A. flavus* culture. In triplicates using a 96-well microplate, 80-μL suspensions (5×10^5 spores) were treated with 10 μL of the sterile prolamin sample (30 μg protein). After 16 h at 30 °C, glutaraldehyde was added at 5% for fixation and germinated spores were determined as a percentage of totally 300 spores/replicate by counting under a light microscopy.

SDS–PAGE analysis. Samples (10 μg protein) were separated in a 13% gel with a Mini-Protean III unit (Bio-Rad, USA) using the standard SDS–PAGE protocol.[24] Protein bands were visible by coomassie brilliant blue R-250.

2D-GE analysis. Isoelectric focusing was performed firstly with the Ettan IPGphore apparatus (GE Healthcare, Sweden). To eliminate the retarding effect by impurities, 1 mL of crude prolamin solution was washed three times in distilled water with fourfold each using the Vivaspin tube. The obtaining cloudy solution was finally adjusted to a total protein concentration of 10 μg/μL. The dry 13-cm immobilized pH

Downloaded by [] at 01:25 06 September 2017

Downloaded by [] at 01:25 06 September 2017

gradient strip (pH 3–10 NL; GE Healthcare, Sweden) was incubated for 12 h at 20 °C with 100 µg of the protein sample solubilized in 250 µL of a solution containing 0.5% IPG buffer (GE Healthcare, Sweden), 4% CHAPS (3-[(3-cholamidopropyl)dimethylammonio]-1-propane sulfonate), 8 M urea, 1 M thiourea, 2 µM DTT (dithiothreitol), and trace of bromophenol blue. Electrophoresis was optimized at 0.5 kV for 1 h, 1 kV for 1 h, 3 kV for 2.5 h, and 8 kV for 5 h, continuously, with a constant current of 50 µA/strip. After that, the strip was treated for 20 min at room temperature in 50 mM Tris–HCl buffer (pH 8.8) containing 8 M urea, 1% DTT, 30% glycerol, 2% SDS, and trace of bromophenol blue, which was followed by 20-min incubation in the same buffer with 0.7% iodoacetamide instead of DTT. Then, the strip was rinsed once with distilled water and subjected to 15% gel SDS–PAGE using a Hoefer™ SE 600 Ruby apparatus (Amersham Biosciences, USA). The gel was processed for protein staining by colloidal coomassie brilliant blue G-250. Protein spots were recorded and analyzed by a LabScan ImageScanner-ImageMaster™ 2D Platinum 5.0 software system (GE Healthcare, Sweden).

Results

Plant responses to water status

All six peanut genotypes had the same trends of leaf relative water content (Table 1). The lower content without leaf wilting was a general indicator for the drought effect on peanut plants. The vegetative parameters for drought response could be observed from growth in terms of biomass or the leaf content of malondialdehyde (MDA; a molecular index for the oxidative stress effect). The drought impact on Tainan-9 (Spanish-type peanut) and KK 60-3 (Virginia-type peanut) as the drought-sensitive models was demonstrated by both indices. Different results were found in the different resistant genotypes (all Spanish type). Except ICGV 98308, the other ICGV genotypes showed good growth adaptation under drought. Meanwhile, ICGV 98305 and ICGV 98308 exhibited better resistance to the drought-induced oxidative stress than the other four genotypes. Drought resistant characteristics in vegetative modes were therefore genotypic dependent.

With 1-week incubation on PDA medium, seeds of the drought-stressed plants differently exhibited outbreaks of fungal mycelium with *A. flavus* characteristic yellow–green spores. The lower outbreaks were found in ICGV 98300, 98303, and 98305. It demonstrated high resistance to *A. flavus* in these genotypes. The more fungal appearance was that of the ICGV 98308 and KK 60-3 while the highest was that of Tainan-9. There was no fungal growth in seeds ($n = 10$) of all genotypes from the control watering.

There was no conclusive evidence to rank the drought resistance of the peanut genotypes in the study. It was seen from indices of biomass, leaf MDA content, and seed resistance to *A. flavus* that ICGV 98300 resembled ICGV 98303 in response to drought, whereas it was different from other genotypes in at least one index. As it could not be expected for the correlation of peanut genotypes and the seed prolamin constituents, all including the two resembled genotypes were used for further investigations.

Characterization of crude prolamin fraction

The seed prolamins obtained by alcohol extraction and subsequent acetone precipitation were examined by SDS–PAGE. The profile contained polypeptides of small sizes to almost 66 kDa. Four major bands were unique at 22.4 kDa to below 14.4 kDa (Fig. 1). Different from the Spanish-type Tainan-9, the profiles within the Spanish-type ICGV peanuts appeared more closely to those of the Virginia-type KK 60-3. The prolamin profiles from SDS–PAGE could not be distinguishable among the peanut genotypes. From band intensity, there were changes in the content of prolamin polypeptides at 17, 20.1, 22.4, 27.5, 31.6, and 66 kDa in some

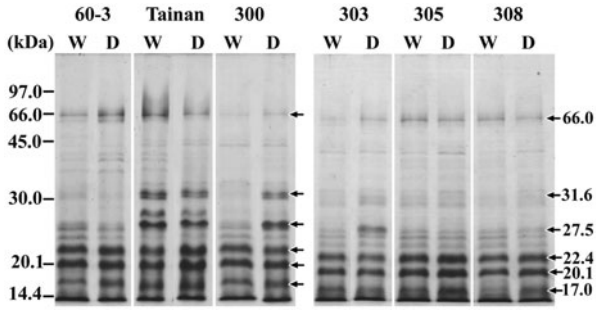


Fig. 1. SDS–PAGE profiles of crude prolamins from seeds of peanuts grown under the control watering (W) and drought (D) conditions.

Notes: The peanut genotypes from left to right are KK 60-3, Tainan-9, ICGV 98300, ICGV 98303, ICGV 98305, and ICGV 98308.

Table 1. Peanut responses to the soil water content at control watering and drought. Mean ± S.D. values with the same superscripts are not significantly different by one-way ANOVA analysis at $p \leq 0.05$.

	Leaf relative water content (%)		Biomass (g/plant)		MDA content (nmol/g leaf wet weight)	
Genotype	Watering	Drought	Watering	Drought	Watering	Drought
Tainan-9	95.9 ± 2.23^{ab}	86.8 ± 1.09^{f}	59.6 ± 0.54^{bc}	53.8 ± 1.53^{d}	14.7 ± 1.22^{f}	25.3 ± 0.47^{b}
98300	97.5 ± 1.95^{a}	92.5 ± 2.17^{cd}	57.2 ± 2.67^{bcd}	55.4 ± 2.49^{cd}	18.7 ± 0.41^{df}	29.0 ± 0.95^{a}
98303	93.9 ± 1.61^{bc}	90.2 ± 0.11^{de}	59.1 ± 3.49^{bc}	60.0 ± 2.53^{bc}	17.0 ± 0.51^{def}	26.3 ± 5.08^{ab}
98305	96.4 ± 1.02^{ab}	88.5 ± 1.18^{ef}	56.7 ± 4.45^{bcd}	57.6 ± 2.06^{bcd}	14.7 ± 0.44^{f}	18.3 ± 0.99^{de}
98308	96.3 ± 1.80^{ab}	88.7 ± 0.58^{ef}	61.1 ± 3.09^{ab}	55.9 ± 4.17^{cd}	19.0 ± 0.65^{df}	20.7 ± 2.45^{cd}
KK 60-3	92.9 ± 1.07^{c}	89.3 ± 2.47^{ef}	65.6 ± 2.30^{a}	58.8 ± 3.50^{bcd}	15.7 ± 1.23^{ef}	24.3 ± 0.99^{bc}

Table 2. Germination of *Aspergillus flavus* spores affected by peanut prolamins. Crude prolamin fractions were prepared from seeds of different peanut genotypes grown under the control watering and drought conditions. Mean ± S.D. values with the same superscripts are not significantly different by one-way ANOVA analysis at $p \leq 0.05$.

	Spore germination (%)	
Prolamin sources	Watering	Drought
Tainan-9	63 ± 2.12^{c}	59 ± 1.22^{d}
98300	53 ± 1.20^{e}	52 ± 0.38^{ef}
98303	57 ± 1.33^{d}	57 ± 1.65^{d}
98305	57 ± 1.43^{d}	50 ± 0.90^{fg}
98308	48 ± 0.73^{g}	46 ± 0.84^{h}
KK 60-3	95 ± 2.51^{a}	96 ± 1.52^{a}

drought-stressed peanuts. However, these changes did not correlate with peanut characteristics to drought stress.

While the *A. flavus* spore germination in water was 84 ± 1.73%, the KK 60-3 prolamin fractions enhanced spore germination (Table 2). Therefore, the KK 60-3 prolamins were used as negative references in the proteomic study for its components in relation to the lack of antifungal activity. The prolamin fractions of all Spanish-type peanuts including Tainan-9 and ICGV genotypes possessed inhibitory activity on *A. flavus* spore germination which was slightly higher in the samples from drought experiments of Tainan-9, ICGV 98305, and ICGV 98308. The inhibition was lower for the Tainan-9 prolamin samples while it was highest in those of ICGV 98308.

Proteomic analysis by 2D-GE

From Fig. 2, the demonstrative profile by that of Tainan-9 revealed that the crude prolamins contained spots of basic (pI 9.8) to acidic polypeptides (pI 4.5). By software evaluation for the resolving distances along the *X*-axis (pH) vs. the *Y*-axis (MW), six dense spots at around pH 5.45–5.75 were detected namely the polypeptide spot 1 (pI 5.75, 30.5 kDa), spot 2 (pI 5.75, 28.5 kDa), spot 3 (pI 5.75, 22 kDa), spot 4 (pI 5.5, 30.5 kDa), spot 5 (pI 5.5, 28.5 kDa), and spot 6 (pI 5.45, 22 kDa). The results in Fig. 3 showed that these six spots were also found commonly in other Spanish-type peanut models (ICGV 98300, ICGV 98303, ICGV 98305, and ICGV 98308). Except for the 22 kDa polypeptides, those around 28.5–30.5 kDa were not clearly detectable by the lower resolution on SDS–PAGE. These spots did not appear in the profiles of the Virginia-type KK 60-3 crude prolamins, but nine spots were found closely at pH 5.05, 5.35, and 5.90. Due to the restricted presence in the Spanish-type peanut models, the spot 1–6 prolamins were prospective for their correlative activity against *A. flavus* spore germination.

The spots 1–6 in the profile from Fig. 3 were undertaken quantitative 3D view analysis for the peak volumes to represent their comparative contents (Fig. 4). The peak volumes and inductive characteristic of spots 1–6 were genotypic dependent. The six spots showed high peak volumes in ICGV 98308, but all were relatively low in Tainan-9 and ICGV 98303. The ICGV

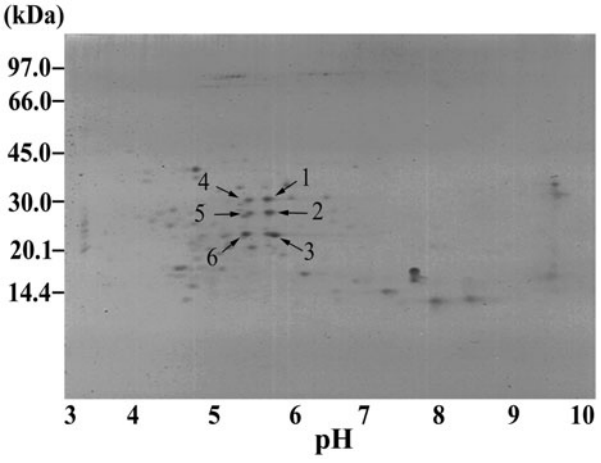


Fig. 2. Demonstrative 2D-GE profile of crude seed prolamins from the Spanish-type Tainan-9 peanut genotype.

Notes: The sample was from seeds of the control watering peanut plants. The arrows point to the six characteristic spots.

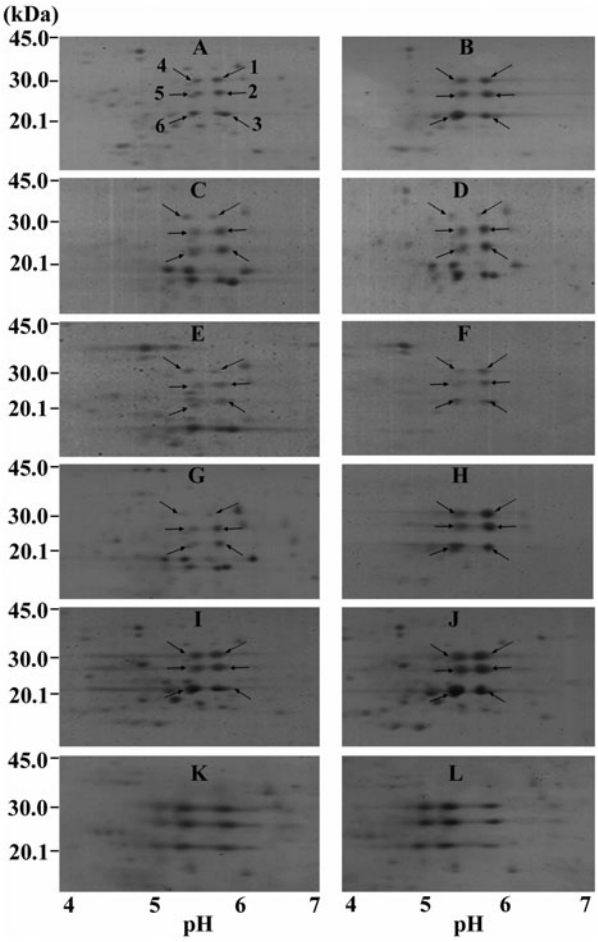


Fig. 3. Intensive 2D-GE profiles of crude seed prolamins zooming-in the common area around characteristic spots in individual genotype.

Notes: The second dimension gels were cropped to focus at the area containing polypeptide spots within the pI range of 4–7 and masses of 14.4–45.0 kDa. The samples were of Tainan-9 (A, B); ICGV 98300 (C, D); ICGV 98303 (E, F); ICGV 98305 (G, H); ICGV 98308 (I, J) and KK 60-3 (K, L). Figures in the left panel are of control watering samples, and those of drought-stressed samples are in the right panel. The spots 1–6 were numbered following the demonstrations in Fig. 2.

Downloaded by [] at 01:25 06 September 2017

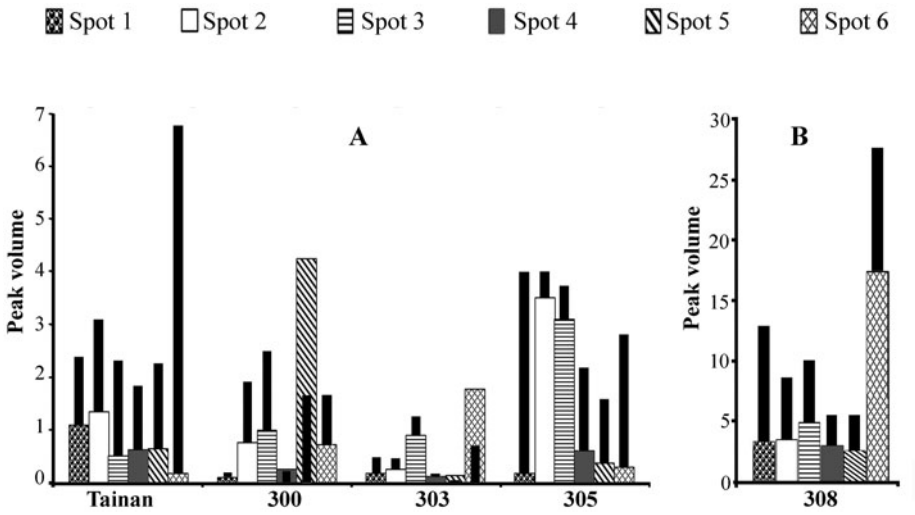


Fig. 4. Relative content of the spots 1–6 crude prolamin polypeptides from Tainan-9, ICGV 98300, ICGV 98303, ICGV 98305, and ICGV 98308.

Notes: The data were obtained from the 3D view analysis for peak volumes of the spots 1–6 in Fig. 3. For each spot, the dark chart stands for the drought-stressed sample which is superimposed on the chart for the control watering sample.

Downloaded by [] at 01:25 06 September 2017

98300 had high volume of spot 5 while ICGV 98305 contained high volumes of spots 2 and 3. The increases in the peak volume were found in most samples from drought treatment except for the unchanged spot 4 in ICGV 98300 and ICGV 98303, as well as the declined level of spot 5 in ICGV 98300 and of spot 6 in ICGV 98303. These data would be discussed with the antifungal activity of the relevant prolamin samples of the Spanish-type peanuts in Table 2.

Isoelectric precipitation of the prospective antifungal prolamins

As considered from the results in Fig. 3, the solution of crude prolamin powder of ICGV 98305 from the drought experiment was chosen for precipitation at pH 5.60 to selectively purify prolamins containing the six prospective polypeptides (pI 5.45–5.75). The yield of the protein precipitate was approximately 6–7% of the original amount in prolamin solution. The 2D-GE profiles were demonstrated for the precipitate or the supernatant portion after precipitation. The precipitate contained immensely nine spots, and six spots among them could be identified as the prospective prolamins with slight shifts in pI and molecular weight (Fig. 5(A)) including the spot 1 (pI 5.8, 30.5 kDa), spot 2 (pI 5.8, 27.5 kDa), spot 3 (pI 5.8, 22.5 kDa), spot 4 (pI 5.5, 30.5 kDa), spot 5 (pI 5.5, 27.5 kDa), and spot 6 (pI 5.5, 23 kDa). The predominant presence of six spots related prolamins of the ICGV 98305 precipitate sample was concurrent with fivefold increase in inhibitory activity against *A. flavus* spore germination (10.34 ± 0.47% germination; 30 μg proteins) comparing to that before precipitation (50 ± 0.90%, Table 2). More abundant spots were detected in the 2D-GE profile of the supernatant portion (Fig. 5(B)) including the three enriched spots considerably equivalent to the spot 4 (pI 5.6, 30 kDa), spot 5 (pI 5.6, 27 kDa), and spot 6 (pI 5.6, 22.5 kDa). Together with the change in the prolamin constituents with the loss in the spot 1–3, the supernatant strikingly enhanced *A. flavus* spore germination to 94.32 ± 0.62%. At this point, the spot 1–3 related peanut seed prolamins were regarded as significant members displaying antifungal activity.

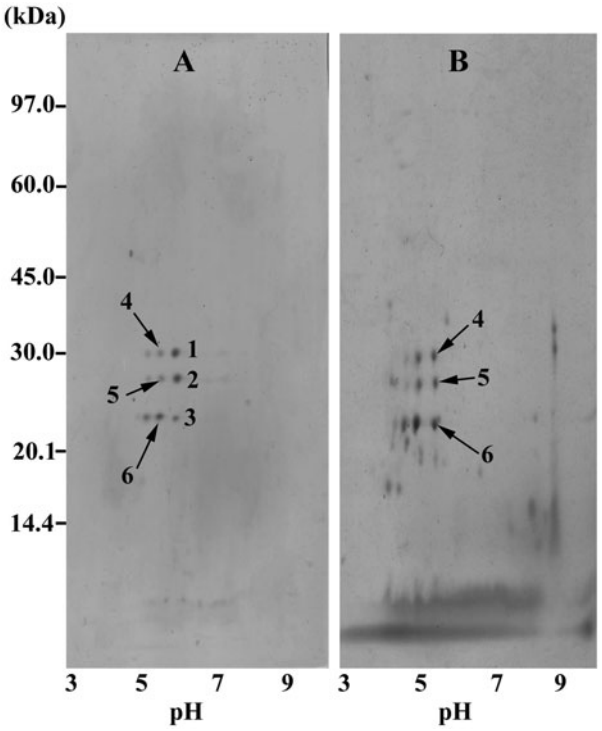


Fig. 5. 2D-GE profiles of ICGV 98305 prolamin samples after isoelectric precipitation at pH 5.60, (A) precipitate and (B) supernatant portions.

Discussion

The peanut seeds are usually attacked by soil microbes, importantly by *A. flavus*. The seed has functional and structural defensive mechanisms including a number of the seed storage water-soluble proteins which are the three 2S albumins (Ara h 2, Ara h 6,

Downloaded by [] at 01:25 06 September 2017

Ara h 7) and a non-specific lipid transfer protein (Ara h 9).[13,16,25,26] Our preliminary work demonstrated the possibility that *A. flavus* spore germination could be significantly inhibited by the crude 70% ethanol-extractable peanut seed prolamins.[17] The investigation on the aqueous alcohol-soluble peanut antifungal prolamin members will provide another biological function of proteins in this group in addition to the known nitrogen storage for seedling growth.

The parameters in the study were water treatments and peanut genotypes to obtain comparative information within and between genotypes. The period of severe drought treatment covered the critical period of water-deficit stress in peanuts.[27] High leaf malondialdehyde (MDA) content is an index of drought-induced oxidative damage due to suppression of photosynthesis from stomatal closure to prevent water loss, while metabolic regulation of its production close to the basal level is promising for the drought resistance.[5] Although it was not our main point, it was found that the drought resistance in vegetative modes (aerial biomass and/or leaf MDA content; Table 1) did not always promise the seed resistance to *A. flavus* as previously reported.[28]

The present data showed inhibitory activity on *A. flavus* spore germination of crude prolamin fractions from different peanut genotypes (Table 2), which could be attributed to their antifungal components. The presence of significant antifungal proteins was suspected in the crude prolamins from the Spanish-type peanut genotypes. The distinct characteristic of Virginia KK 60-3 crude prolamins preliminarily predicted dissimilar components. The antifungal assessment of prolamins *in vitro* did not relate to the occurrence of fungal growth in seed tests, as in the cases of ICGV 98308. Other defensive mechanisms might be dealt with constitutive or drought-inductive seed components.[25,29,30]

In this work, SDS–PAGE was not successful in discriminating prolamin profiles between peanut genotypes, as well as between water statuses (Fig. 1). The prolamin profiles were similar to the previous report.[17] They could be further cited to be free of the bands of globulins and albumins.[31] Therefore, the antifungal activity of the prolamin fractions should not be from 2S albumins. The profiles could not be compared to those of another legume,[32] because of species difference or the extraction method. This study provided the first 2D-GE maps for peanut prolamins which were resolved in the pH range of 4.5–9.8 (Fig. 2). Although the native prolamins are hydrophobic and extractable by high alcohol concentration, polypeptides with acidic pIs to basic pIs were also published for the prolamins of Inca peanut and rice.[32,33] The results revealed six major constitutive polypeptides with sizes of 30.5, 28.5, and 22 kDa at pI 5.45–5.75 restrictedly in seed prolamins of the Spanish-type peanuts (Fig. 3(A–J)). Their presence was concurrent with the relatively high inhibitory activity on *A. flavus* spore germination (Table 2), which was the first clue for their possible significance in that role. Nevertheless, the KK 60-3 prolamin extract might contain the six target prolamin members in low proportion so that the antifungal measurement and 2D-GE resolution were hindered by other prolamins.

There have been neither established 2D-GE maps nor sequence database of peanut seed prolamins. Several resources were searched for indirect information of any peanut seed proteins having related sizes and pIs. The six polypeptides have not been found in 2D-GE maps of total protein extracts from seeds of the established Spanish, Virginia and Valencia peanuts,[8–10] or maps of peanut seed crude globulins.[34] Despite water solubility of the seed albumins, a large amount of the peanut albumins could be extracted by NaCl buffer.[35] In a soybean 2D-GE model, little contamination of globulins and albumins was evident together with other hydrophilic proteins after one-step extraction by relatively high alcohol strength using 40% isopropanol.[36] The authors explained that it was resulted from protein aggregation as aqueous alcohol-soluble molecules. Therefore, we deduced from SDS–PAGE and 2D-GE that excessive extraction by buffered NaCl solution achieved in sufficient elimination of globulins and albumins as well as the antifungal proteins thereof. Thus, it resulted in significant enrichment of prolamins for alcohol extraction in the subsequent step. The spots of the antifungal Ara h 9 (9 kDa and pI around 9–10)[37] did not appear in our 2D-GE maps. The antifungal activity of the peanut prolamins was consequently not from the established 2S albumins and Ara h 9. Peanut seed proteins obtained from subsequent extraction with NaCl buffer and low ethanol concentration (20%) gave 2D-GE maps[38] dissimilar to our results.

Prolamins are abundant storage proteins in cereal seeds which vast knowledge has been gathered from. All prolamins are recognized water insoluble in their native conformation in protein bodies within endoplasmic reticulum originated vacuoles, and they are extractable in water/alcohol mixtures.[39] Despite predominant content of hydrophobic amino acid residues, prolamins from different cereal seeds have different hydrophilic characteristic.[39,40] It was evident that a number of prolamins in wheat, barley, and rye could be directly extracted in water or 0.5 M NaCl at room temperature.[41] These prolamins probably exhibit their water solubility once vacuolar free. Peanut seed prolamin powder extracts in this work were ready to dissolve in water. It is likely that 80% acetone could precipitate prolamins having more hydrophilic nature out of the total prolamins soluble in 70% ethanol after extraction. However, their hydrophobic nature was apparent later since the crude proteins turned dramatically water insoluble under the repeatedly successive ultrafiltration in the sample preparation for 2D-GE. The rehydration buffer with a combination effect of urea and thiourea was consequently used as it has been recommended for 2D-GE analysis of hydrophobic proteins.[33]

In terms of Ara h, they are groups of peanut seed allergenic proteins of which biochemical properties (MW and pI) as well as biological roles have been reviewed.[13,42] The three main allergens are Ara h 1 (7S globulin or conarachin), Ara h 3 (11S globulin or arachin), and Ara h 2 (a 2S albumin with trypsin inhibitor activity against pathogen) comprising about 90% of total allergens.[13] These allergens together with another 2S albumin (Ara h 6; a trypsin inhibitor) have been already suggested as protein markers in

identification, by SDS–PAGE or 2D-GE, of peanut genotypes at the viewpoint of genotypic markers and nutritional awareness.[8–10] Some peanut allergens are pathogenesis-related (PR) proteins including Ara h 8 (ribonuclease-like PR-10) and two defensins (Ara h 12 and Ara h 13). Ara h 9 is the group of non-specific lipid transfer proteins (nsLTPs) and is the last allergen that has activity against pathogens. The 2S albumins and nsLTPs are also alternatively characterized in the same prolamin superfamily due to conserved cysteine residues and intrachain disulfide bridges similar to the seed storage alcohol-soluble prolamin.[13,42] Most Ara h is soluble in water or saline solution except defensins which could be differently obtained by methanol/chloroform extraction of peanut seed meal.[13] Regarding to solubility property, these allergens are hardly present in the aqueous ethanolic prolamin fraction from the peanut seeds. The inhibitory action on *A. flavus* spore germination in Table 2 consequently was neither caused by the relevant Ara h nor the novel water-soluble chitinase-like antifungal hypotin.[30]

The synthesis of a number of peanut seed functional proteins including defensive proteins could be up-regulated according to water stress, *A. flavus* infection, or aflatoxin contamination.[11,12,43–45] Basically, these proteins are less abundant and natively hydrophilic so that they should not be confound in the prolamin fractions after the two-step extraction used in the study.

Based on the analysis of spot peak volumes, the content of spots 1–6 could draw a primary attention for their possible relevance to the inhibitory activity of the prolamin fraction against *A. flavus* spore germination (Fig. 4 and Table 2). The interesting demonstrations were those from the control experiments of Tainan-9 (all low contents/low inhibition) and ICGV 98308 (all high contents/high inhibition). Meanwhile, the intermediate inhibition was observed in ICGV 98300, 98303, and 98305 which the mixed low or high presence of some prospective spots was remarked. However, the results from drought experiments and partial purification by isoelectric precipitation could be finally conclusive for the significance of the prolamin member spots 1–3, not spots 4–6, as antifungal prolamins inhibiting *A. flavus* spore germination. The present data did not inform the native conformation of the spot 1 (pI 5.75, 30.5 kDa), spot 2 (pI 5.75, 28.5 kDa), and spot 3 (pI 5.75, 22.0 kDa) whether they are monomeric or homo-/hetero-multimeric. It seemed that isoelectric precipitation at pH 5.60 with low protein yield obtained highly purified spot 1–3 prolamin polypeptides as considered by the comparative 2D-GE map (Fig. 5) and the increased antifungal activity of the precipitate. Conclusively, the spot 1–3 related peanut seed prolamin storage proteins were closely associated with the antifungal property against spore germination in the *A. flavus* model. Their presence was specifically illustrated in the Spanish-type peanuts and was confirmed up on induction in the drought condition. The relative content of the final three spots herein did not always show positive correlation with the drought resistant genotypes. It was high in ICGV 98308 comparing to those in other ICGV genotypes and in the drought-sensitive Tainan-9 (Fig. 4). Likewise, their content was not in agreement with resistance to *A. flavus* infection in seeds of the drought-stressed peanut plants. For example, the fungal infection was high in ICGV 98308 while it was very low in ICGV 98303. The use of drought-sensitive/resistant genotypes together with water-deficit treatment has been the conventional tool to investigate total protein extract for protein markers of the resistance traits to drought and seed aflatoxin contamination in peanuts.[12,44] That no correspondence was found between the prolamin content and the resistance traits might be resulted from the fractionated extraction procedure. The present data revealed the existence of prolamins with positive test in inhibiting *A. flavus* spore germination. If antibody is raised against these prolamins, it will be useful in further comparative detection for their presence in the total protein extract of peanut seeds in relation with the resistance traits for breeding purpose.

Author contribution

W. Senakoon carried out the whole experiments and made manuscript draft; S. Nuchadomrong was responsible for the main experimental assignments, data analysis and manuscript preparation; R.Y.-Y. Chiou advised in 2D-GE part; G. Senawong took part in antifungal tests; S. Jogloy, P. Songsri, and A. Patanothai guided works in peanut cultivation and water treatment.

Acknowledgment

Miss Senakoon is grateful to a scholarship from the Graduate School Khon Kaen University for her short term work at the National Chiayi University, Taiwan.

Disclosure statement

No potential conflict of interest was reported by the authors.

Funding

This work was supported by the Higher Education Research Promotion and National Research University Project of Thailand, Office of the Higher Education Commission, through the Food and Functional Food Research Cluster of Khon Kaen University, Thailand [grant number NRU541007, FC1.1.7 PhD]; and the Thailand Research Fund, the Commission for High Education and Khon Kaen University through the Distinguish Research Professor Grant of Professor Dr. Aran Patanothai.

References

[1] Pandey MK, Monyo E, Ozias-Akins P, et al. Advances in *Arachis* genomics for peanut improvement. Biotechnol. Adv. 2012;30:639–651.
[2] Canavar Ö, Kaynak MA. Prevention of pre-harvest aflatoxin production and the effect of different harvest times on peanut (*Arachis hypogaea* L.) fatty acids. Food Addit. Contam. Part A 2013;30:1807–1818.
[3] Dorner JW. Management and prevention of mycotoxins in peanuts. Food Addit. Contam. 2008;25:203–208.
[4] Surendranatha Reddy EC, Sudhakar C, Eswara Reddy NP. Aflatoxin contamination in groundnut induced by *Aspergillus flavus* type fungi: a critical review. IJABPT 2011;2:180–192.

Downloaded by [] at 01:25 06 September 2017

[5] Sharma P, Jha AB, Dubey RS, et al. Reactive oxygen species, oxidative damage, and antioxidative defense mechanism in plants under stressful conditions. J. Bot. 2012;2012:1–26.
[6] Bianchi-Hall CM, Keys RD, Stalker HT. Use of seed protein profiles to characterize peanut cultivars. Peanut Sci. 1994;21: 152–159.
[7] Javaid A, Ghafoor A, Anwar R. Seed storage protein electrophoresis in groundnut for evaluating genetic diversity. Pak. J. Bot. 2004;36:25–29.
[8] Liang XQ, Luo M, Holbrook CC, et al. Storage protein profiles in Spanish and runner market type peanuts and potential markers. BMC Plant Biol. 2006;6:24–32.
[9] Kottapalli KR, Payton P, Rakwal R, et al. Proteomics analysis of mature seed of four peanut cultivars using two-dimensional gel electrophoresis reveals distinct differential expression of storage, antinutritional, and allergenic proteins. Plant Sci. 2008;175:321–329.
[10] Schmidt H, Gelhaus C, Latendorf T, et al. 2-D DIGE analysis of the proteome of extracts from peanut variants reveals striking differences in major allergen contents. Proteomics 2009;9: 3507–3521.
[11] Basha SM, Katam R, Naik KSS. Differential response of peanut genotypes to water stress. Peanut Sci. 2007;34:96–104.
[12] Wang T, Zhang E, Chen X, et al. Identification of seed proteins associated with resistance to pre-harvested aflatoxin contamination in peanut (*Arachis hypogaea* L). BMC Plant Biol. 2010;10:267–277.
[13] Bublin M, Breiteneder H. Cross-reactivity of peanut allergens. Curr. Allergy Asthma Rep. 2014;14:426–437.
[14] Sebei K, Gnouma A, Herchi W, et al. Lipids, proteins, phenolic composition, antioxidant and antibacterial activities of seeds of peanuts (*Arachis hypogaea* L.) cultivated in Tunisia. Biol. Res. 2013;46:257–263.
[15] Shewry PR, Tatham AS. The prolamin storage proteins of cereal seeds: Structure and evolution. Biochem. J. 1990;267:1–12.
[16] Shewry PR, Halford NG. Cereal seed storage proteins: Structures, properties and role in grain utilization. J. Exp. Bot. 2002;53:947–958.
[17] Senakoon W, Nuchadomrong S, Senawong G, et al. An alternate fractionation of peanut seed proteins in association with inhibitory assay on *Aspergillus flavus*. APCBEE Procedia 2012;4: 42–47.
[18] Girdthai T, Jogloy S, Vorasoot N, et al. Associations between physiological traits for drought tolerance and aflatoxin contamination in peanut genotypes under terminal drought. Plant Breed. 2010;129:693–699.
[19] Songsri P, Jogloy S, Holbrook CC, et al. Association of root, specific leaf area and SPAD chlorophyll meter reading to water use efficiency of peanut under different available soil water. Agric. Water Manage. 2009;96:790–798.
[20] Boote KJ. Growth stages of peanut (*Arachis hypogaea* L.). Peanut Sci. 1982;9:35–40.
[21] Sharp RE, Hsiao TC, Silk WK. Growth of the maize primary root at low water potentials: II. Role of growth and deposition of hexose and potassium in osmotic adjustment. Plant Physiol. 1990;93:1337–1346.
[22] Sheokand S, Bhankar V, Sawhney V. Ameliorative effect of exogenous nitric oxide on oxidative metabolism in NaCl treated chickpea plants. Braz. J. Plant Physiol. 2010;22:81–90.
[23] White BL, Gökce E, Nepomuceno AI, et al. Comparative proteomic analysis and IgE binding properties of peanut seed and testa (Skin). J. Agric. Food. Chem. 2013;61:3957–3968.
[24] Laemmli UK. Cleavage of structural proteins during the assembly of the head of bacteriophage T4. Nature 1970;227:680–685.
[25] Liang XQ, Luo M, Guo BZ. Resistance mechanisms to *Aspergillus flavus* infection and aflatoxin contamination in peanut (*Arachis hypogaea*). Plant Pathol. J. 2006;5:115–124.
[26] Breiteneder H, Radauer C. A classification of plant food allergens. J. Allergy Clin. Immunol. 2004;113:821–830.
[27] Suleiman AA, Soler CMT, Hoogenboom G. Determining FAO-56 crop coefficients for peanut under different water stress levels. Irrigation Sci. 2013;31:169–178.
[28] Hamidou F, Rathore A, Waliyar F, et al. Although drought intensity increases aflatoxin contamination, drought tolerance does not lead to less aflatoxin contamination. Field Crops Res. 2014;156:103–110.
[29] Ye XY, Ng TB. Hypogin, a novel antifungal peptide from peanuts with sequence similarity to peanut allergen. J. Pept. Res. 2001;57:330–336.
[30] Wang S, Shao B, Rao P, et al. Hypotin, a novel antipathogenic and antiproliferative protein from peanuts with a sequence similar to those of chitinase precursors. J. Agric. Food Chem. 2007;55:9792–9799.
[31] El-Beltagi HES. Effect of roasting treatments on protein fraction profiles, some enzyme activities of Egyptian peanuts. Int. J. Food Sci. Nutr. 2011;62:453–456.
[32] Sathe SK, Kshirsagar HH, Sharma GM. Solubilization, fractionation, and electrophoretic characterization of inca peanut (*Plukenetia volubilis* L.) proteins. Plant Food Hum. Nutr. 2012;67:247–255.
[33] Shigemitsu T, Saito Y, Morita S, et al. Separation and identification of rice prolamins by two-dimensional gel electrophoresis and amino acid sequencing. Biosci. Biotechnol. Biochem. 2012;76:594–597.
[34] Chassaigne H, Trégoat V, Nørgaard JV, et al. Resolution and identification of major peanut allergens using a combination of fluorescence two-dimensional differential gel electrophoresis, Western blotting and Q-TOF mass spectrometry. J. Proteomics 2009;72:511–526.
[35] Porterfield HS, Murray KS, Schlichting DG, et al. Effector activity of peanut allergies: a critical role for Ara h 2, Ara h 6, and their variants. Clin. Exp. Allergy 2010;39:1099–1108.
[36] Natarajan SS, Krishnan HB, Lakshman S, et al. An efficient extraction method to enhance analysis of low abundant proteins from soybean seed. Anal. Biochem. 2009;394:259–268.
[37] Krause S, Reese G, Randow S, et al. Lipid transfer protein (Ara h 9) as a new peanut allergen relevant for a Mediterranean allergic population. J. Allergy Clin. Immunol. 2009;124: 771–778.e5.
[38] Chassaigne H, Brohée M, Nørgaard JV, et al. Investigation on sequential extraction of peanut allergens for subsequent analysis by ELISA and 2D gel electrophoresis. Food Chem. 2007;105: 1671–1681.
[39] Taylor J, Anyango JO, Taylor JRN. Developments in the science of zein, kafirin, and gluten protein bioplastic materials. Cereal Chem. 2013;90:344–357.
[40] Belitz HD, Kieffer R, Seilmeier W, et al. Structure and function of gluten proteins. Cereal Chem. 1986;63:336–341.
[41] Kanerva P, Sontag-Strohm T, Brinck O, et al. Improved extraction of prolamins for gluten detection in processed foods. Agric. Food Sci. 2011;20:206–216.
[42] Offermann LR, Perdue ML, He JZ, et al. Structural biology of peanut allergens. J. Contemp. Immunol. 2015;2:1–26.
[43] Mazhar H, Basha SM. Effects of desiccation on peanut (*Arachis hypogaea* L.) seed protein composition. Environ. Exp. Bot. 2002;47:67–75.
[44] Katam R, Vasanthaiah HKN, Basha SM. Proteomic approach to screen peanut genotypes with enhanced nutritional qualities. FBIT 2007;94:171–176.
[45] Wang Z, Yan S, Liu C, et al. Proteomic analysis reveals an aflatoxin-triggered immune response in cotyledons of *Arachis hypogaea* infected with *Aspergillus flavus*. J. Proteome Res. 2012;11:2739–2753.

Downloaded by [] at 01:25 06 September 2017

Agricultural Water Management 152 (2015) 142–150

Contents lists available at ScienceDirect

Agricultural Water Management

journal homepage: www.elsevier.com/locate/agwat

Variation of inulin content, inulin yield and water use efficiency for inulin yield in Jerusalem artichoke genotypes under different water regimes

Darunee Puangbut[a], Sanun Jogloy[a,*], Nimitr Vorasoot[a], Supalax Srijaranai[b], Corley Carl Holbrook[c], Aran Patanothai[a]

[a] Department of Plant Science and Agricultural Resources, Faculty of Agriculture, Khon Kaen University, Khon Kaen 40002, Thailand
[b] Department of Chemistry, Faculty of Science, Khon Kaen University, Muang, Khon Kaen 40002, Thailand
[c] USDA-ARS, Crop Genetics and Breeding Research Unit, Coastal Plain Experimental Station, Tifton, GA 31793, USA

ARTICLE INFO

Article history:
Received 15 April 2014
Accepted 7 January 2015
Available online 2 February 2015

Keywords:
Helianthus tuberosus
Genotypic
Drought stress
Fructan

ABSTRACT

The information on genotypic variation for inulin content, inulin yield and water use efficiency of inulin yield (WUEi) in response to drought is limited. This study was to investigate the genetic variability in inulin content, inulin yield and WUEi of Jerusalem artichoke (*Helianthus tuberosus* L.) under different water regimes. A field experiment was conducted for two years during September to January 2010/2011 and 2011/2012. A strip plot design with four replications was used in both years. Horizontal factors were three irrigation levels (W1 = 100% evapotranspiration (ET), W2 = 75% ET and W3 = 45% ET) and vertical factors were 12 Jerusalem artichoke genotypes. Data were recorded for inulin content, inulin yield and WUEi at harvest. Significant differences among Jerusalem artichoke genotypes were observed for inulin content, inulin yield and WUEi under W1, W2 and W3 in both years. There were five genotypes (HEL 253, HEL 53, HEL 256, HEL 65 and CN 52867) that exhibited consistently high inulin content and inulin yield across water regimes in both years. Inulin content was increased under W2 conditions but not inulin yield, while WUEi was increased under both W2 and W3 conditions. CN 52867 and HEL 65 were the genotypes with the highest inulin content and inulin yield under limited water conditions in both years. Furthermore, these genotypes showed high WUEi and drought tolerance indices under drought conditions in both years. Improvement of inulin content combined with high WUEi could have contributed to higher inulin yield under limited water conditions. The information on genotypic variation in inulin content and WUEi under drought conditions may have application in genetic improvement of drought resistance in Jerusalem artichoke.

© 2015 Elsevier B.V. All rights reserved.

1. Introduction

Jerusalem artichoke (*Helianthus tuberosus* L.) originated in North America, and has been introduced to many countries for immediate uses and further development particularly in relation to lower production cost and drought tolerance (Denoroy, 1996). Jerusalem artichoke is used for many purposes such as human food, animal feedstock and ethanol production. Currently, it is important as a source of inulin.

Inulin is a polydispers fructan, which has a degree of polymerization between 4-150 (Baldini et al., 2011). The fructans can be used as dietary fiber in the food industry, and fructose resulting from fructan hydrolysis can be used as a low calorie sweetener and has several uses in the non-food medical and pharmaceutical industries (Frese, 1993). Due to these properties, inulin is considered a functional food ingredient.

However, inulin or fructan is dependent upon on many factors such as photosynthesis and temperature (Schubert and Feuerle, 1997; Kocsis et al., 2008). Moreover, low temperature is an important factor affecting growth, tuber yield and inulin yield of Jerusalem artichoke (Kocsis et al., 2008; Puangbut et al., 2012; Ruttanaprasert et al., 2013). Although inulin content responses to low temperature have been extensively studied in this species, the impact of water stress has received little attention.

Drought is a major abiotic stress affecting yield and quality of Jerusalem artichoke as it reduces inulin accumulation in tubers (Gao et al., 2011; Conde et al., 1991; Schittenhelm, 1999; Monti et al., 2005a). Previous study showed that the severity of

* Corresponding author. Tel.: +66 43 364637; fax: +66 43 364637.
E-mail address: Sanun@kku.ac.th (S. Jogloy).

http://dx.doi.org/10.1016/j.agwat.2015.01.005
0378-3774/© 2015 Elsevier B.V. All rights reserved.

drought strongly influenced tuber yield and inulin content (Monti et al., 2005b). Severe water stress decreased inulin accumulation (Monti et al., 2005a), while moderate stress increased inulin content (Monti et al., 2005b; Vandoorne et al., 2012). Although inulin content benefits of mild stress conditions have been demonstrated, the studies involved a limited number of genotypes and inulin yield responses are not fully understood.

In addition, Losavio et al. (1997) reported that water use efficiency for tuber yield (WUEy) was increased with drought conditions. Recently, Yang et al. (2010) reported that WUEy was increased under limited water conditions and this could be due to the increasing in tuber yield. However, there is limited information on genotypic variation for water use efficiency for inulin yield (WUEi) under drought conditions.

Jerusalem artichoke has been reported as a hardy plant that can be grown at low cost with low input techniques and less desirable soils (Kays and Nottingham, 2008). Jerusalem artichoke has been reported non-tolerant to water stress conditions because drought may strongly influence its dry matter production (Monti et al., 2005a; Schittenhelm, 1999; Conde et al., 1991), but the impact of water stress on inulin yield and WUEi remains poorly documented.

Information on genetic variability for economically important traits is important for plant breeding. Screening for water use efficiency for inulin yield in a large number of germplasm accessions has not been reported in the literature. Studies on the effects of drought on inulin content and inulin yield conducted so far have been limited to a small number of accessions (Gao et al., 2011; Zhang et al., 2010; Monti et al., 2005a), and information on genotypic variation in inulin content and inulin yield under drought conditions is lacking. Knowledge on the responses of Jerusalem artichoke genotypes to drought is important for selection of Jerusalem artichoke genotypes with good performance under drought conditions. The objectives of this study were to investigate the genetic variability in inulin content, inulin yield and WUEi of Jerusalem artichoke subjected to different water regimes.

2. Materials and methods

2.1. Plant material and experimental design

Twelve Jerusalem artichoke genotypes were studied during two growing seasons. They included seven genotypes (JA 1, JA 3, JA 16, JA 38, JA 60, JA 89 and CN 52867) from the Plant Gene Resources of Canada (PGRC), four genotypes (HEL 256, HEL 65, HEL 53 and HEL 253) from the Leibniz Institute of Plant Genetics and Crop Plant Research (IPK) of Germany and [JA 102 × JA 89] – 8 a hybrid clone of Khon Kaen University, Thailand.

A field experiment was conducted during two years at the Field Crop Research Station of Khon Kaen University located in Khon Kaen province, Thailand (16°28′N, 102°48′E, 200 masl) during September 2010 to January 2011 and September 2011 to January 2012. The soil type was a Yasothon series (Yt: fine-loamy; siliceous, isohypothermic, Oxic Paleustults). A strip plot design with four replications was used in both years. Horizontal factors were three irrigation levels (W1 = 100% evapotranspiration (ET), W2 = 75% ET and W3 = 45% ET)) and vertical factors were 12 Jerusalem artichoke genotypes. Plot size was 2 × 4 m with a spacing of 50 cm between rows and 30 cm between hills in a row.

2.2. Crop management

Pre-sprouted seed tubers were used as planting materials. To prepare the sprouted seed tubers, the tubers were cut into small pieces each of which had 2–3 buds/piece. The tuber pieces were incubated in plastic bags containing moist coconut peat at the bottom and the top of the bags for 7 days. The plastic bags were kept opened for good aeration. The tuber pieces with active buds and roots were further transferred to plug plastic trays containing a mixture 1:1 soil:burnt rice husk medium about 7 days for germination. The two leaf-sprouted seedlings were then suitable for transplanting in the plot. One seedling was transplanted per hill. Fertilizer formula 15–15–15 of N–P_2O_5–K_2O was applied at 30 days after transplanting at a rate of 156 kg ha^{-1}. A Terraclor (quintozene 24% W/V EC) was applied monthly for 3 months after transplanting at the rate 25 mL/20 L of water for the control of stem rot (*Sclerotium rolfsii*).

2.3. Water regimes

A drip-irrigation system (Super Typhoon®, Netafim Irrigation equipment & Drip systems, Israel) was installed with a distance of 20 cm between emitters and a spacing of 50 cm between drip lines on the soil surface mid way between Jerusalem artichoke rows and fitted with a pressure valve and water meter to supply a uniform measured amount of water. Before transplanting, water was supplied uniformly to the experiment field to field capacity (FC) to a depth of 10 cm using the drip irrigation system for crop establishment until 14 days after transplanting (DAT).

Different water gradients were supplied by the line source sprinkler to the crop at 14 DAT until harvest. The line-source sprinkler system provided three water gradients, which hereafter are referred to as W1 (100% ET), W2 (75% ET) and W3 (45% ET), respectively. The water gradients were dependent on the distances from the line source, which was installed at the center of the field. The water supplied to W1 was expected to be equivalent to the crop water requirement (ET crop). Water supplied to W2 was estimated as 75% of that supplied to W1, and water supplied to W3 was 45% of that supplied to W1.

The amount of water applied was based on crop water requirements using the Doorenbos and Pruitt (1992) methodology along with water loss from surface evaporation as described by Singh and Russell (1981).

Total crop water use for W1 was calculated as the sum of transpiration and soil evaporation. Crop water requirement was calculated using the methods described by Doorenbos and Pruitt (1992):

$$ET_{crop} = ET_o \times K_c$$

where ET_{crop} = crop water requirement (mm/day), ET_o = evapotranspiration of a reference plant under specified conditions calculated by pan evaporation method, K_c = the crop water requirement coefficient for sunflower, which varies with genotype and growth stage. Soil evaporation (E_s) was calculated as (Singh and Russell, 1981):

$$E_s = \beta \times \left(\frac{E_o}{t}\right)$$

where E_s = soil evaporation (mm), β = light transmission coefficient measured depending on crop cover, E_o = evaporation from class A pan (mm/day), t = days from the last irrigation or rain.

As crop coefficient for Jerusalem artichoke is not available in the literature, the crop coefficient for sunflower (Monti et al., 2005a) was used because sunflower and Jerusalem artichoke are closely related species and their morphological characters are similar.

2.4. Soil moisture status

Soil moisture content was measured by gravimetric methods at the depths of 30, 60 and 90 cm at planting and harvesting. Soil moisture content at planting was used for calculating the correct amount of water to be applied to the crop, and soil moisture at harvest was

used for calculating the water use of the crop. The soil water status was also monitored at 7-day intervals using a neutron moisture meter (Type I.H. II SER. No. N0152, Ambe Diccot Instruments Co. Ltd., England), and neutron probe readings were conducted at the depths of 30 and 60 cm at 7–day intervals throughout the course of the experiment.

2.5. Relative water content

Relative water content (RWC) was measured at 40, 60 and 70 DAT. The second fully-expanded leaf from the top of the main stem was sampled for each plot between 10:00 h to 12:00 h. After recording the fresh weight, turgid weight was measured after placing the leaf sample in water for 8 h. Leaf dry weight was measured after oven-drying at 80 C for 48 h. RWC was computed by the following formula:

$$\mathrm{RWC}\,(\%) = \frac{(\mathrm{FW} - \mathrm{DW})}{(\mathrm{TW} - \mathrm{DW})} \times 100$$

where FW = fresh weight, TW = turgid weight and DW = dry weight.

2.6. Tuber dry weight

At harvest, the plants at two ends of the rows were discarded, all plants in an area of 2.1 m^2 were harvested discarding the border rows, cut at the soil surface and separated into shoots and tubers. Tubers were washed in tap water to remove the potting medium. Tuber fresh weight was determined in the field and then the weights were converted to fresh weights per area. A random tuber fresh weight from 10% of plants in each plot was taken, oven-dried at 80 °C for 72 h or until constant weight, and weighed.

2.7. Inulin content and inulin yield

Inulin content was analyzed using the methods described by Saengkanuk et al. (2011). Briefly, the tubers were longitudinally sliced into thin pieces at the middle part of the tubers. Fifty grams of sliced tuber were soaked in absolute ethanol at 4 °C for 24 h and the samples were stored at −20 °C until analyzed. The samples were oven dried at 60 °C for 10 h. To extract inulin, 2 g of dried sample was mixed with distilled water at 80 °C for 20 min. The solution was cooled to room temperature and filtered through a 0.45 μm membrane filter.

The extracts (500 μl) were pipette into 25 ml volumetric flask containing 3% HCl and diluted to 25 ml with water. The mixtures were then heated at 80 °C in a water-bath for 45 min. After cooling, the solutions were stored in plastic bottles before being analyzed by spectrophotometer. The detailed method for measurement for inulin content has been reported by Saengkanuk et al. (2011). Inulin analysis was shown as a percentage of inulin content on a dry weight basis and inulin yield was computed by the following formula (Puangbut et al., 2011):

$$\text{inulin yield}\left(\text{kg ha}^{-1}\right) = \text{inulin content}\,(\%) \times \text{tuber yield}\left(\text{kg ha}^{-1}\right)$$

Simple correlation was used to determine the relationship between tuber dry weight with inulin content measured under W1, W2 and W3 conditions.

2.8. Water use efficiency of inulin yield (WUEi)

Evapotranspiration (ET) under varying water regimes was calculated using the soil water balance equation for the growing season as follows:

$$\mathrm{ET} = I + (Mi - Mf) - D - R$$

where I = the irrigation applications, Mi = starting soil moisture before transplanting, Mf = soil moisture at final harvest (soil moisture was measured by gravimetric method), D = soil water drainage which is assumed as close to zero, and R = surface runoff. Percolation and surface runoff were assumed to be not significant and the values were ignored.

WUEi for each treatment was calculated as inulin yield divided by evapotranspiration (ET):

$$\mathrm{WUEi} = \frac{\text{inulin yield}\,(\mathrm{g})}{\mathrm{ET}\,(kg)}$$

2.9. Drought tolerance index (DTI)

A drought tolerance index was computed for inulin content, inulin yield and WUEi under stress conditions (W2 or W3) compared to that under non-stress conditions (W1) as suggested by Nautiyal et al. (2002), using the relationship as follows:

$$\mathrm{DTI} = \frac{\text{stress treatment}}{\text{non-stress treatment}}$$

2.10. Statistical analysis

Individual analysis of variance was performed for each character in each year followed a strip plot design. Error variances for the two years were tested by Bartlett's test (Hoshmand, 2006). Due to significance of year × genotype as well as water regime × genotype interaction (Table 1) for two of the three dependent variables, data for each year and water regime were analyzed separately according to a randomized complete block design (RCBD) and Duncan's multiple range test (DMRT) was used to compare means.

Multiple-linear regression was used to determine the relative contribution of inulin content and tuber yield to inulin yield under

Table 1
Mean squares from combined analysis of variance for inulin content, inulin yield and water use efficiency for inulin yield (WUEi) observed in 2010/2011 and 2011/2012.

Source of variation	DF	Inulin content	Inulin yield	WUEi
Year (Y)	1	3626.68**	11.84**	3.03**
Reps. within (Y)	6	102.53	2.13	0.25
Water regimes (W)	2	1280.38**	29.16**	2.57**
Error (a)	14	33.32	0.24	0.01
Genotypes (G)	11	203.91**	3.88**	2.09**
Y × G	11	16.8ns	0.86**	0.27**
Error (b)	66	15.71	0.23	0.04
W × G	22	11.77ns	0.37**	0.02**
Y × W × G	22	9.62ns	0.15*	0.02**
Error (c)	132	7.15	0.09	0.01

ns, *,** Non significant and significant at $P < 0.05$ and $P < 0.01$, respectively.

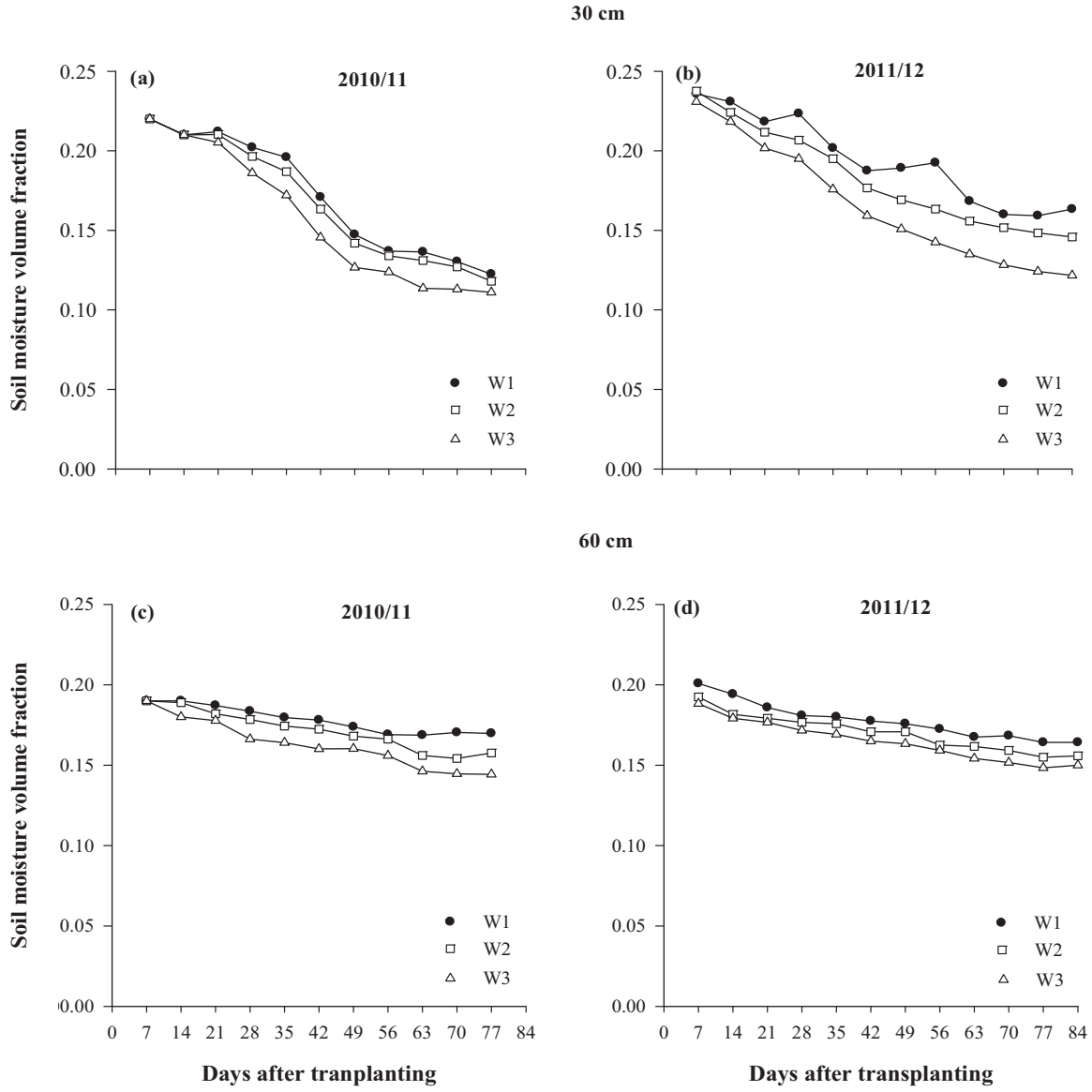


Fig. 1. Soil moisture volume fraction in three water regimes (W1 = 100% ET), W2 = 75% ET, and W3 = 45% ET at 30 (a and b) and 60 cm (c and d) of soil depth in 2010/2011 and 2011/2012.

W1, W2 and W3 conditions. The analysis was based on the following statistical model (Hoshmand, 2006):

$$Y_i = \alpha + \beta_1 X_{1i} + \beta_2 X_{2i} + \delta_i$$

where Y_i is inulin yield of genotype i, α is the Y intercept, X_{1i} and X_{2i} are inulin content and tuber yield of genotype i, respectively, β_1, and β_2 are regression coefficients for the independent variables X_1 and X_2 and δ_i is the associated deviation from regression.

The analysis was conducted by fitting the full model first and then determining the relative importance of the individual independent variables. A sequential fit was then performed by fitting the more important variable first. The relative contributions of the individual independent variables to the inulin yield under drought stress were determined from the percentages of regression sum of squares due to the respective independent variables to total sum of squares in the sequential fitted analysis.

3. Results and discussion

3.1. Soil moisture content and water status

Soil moisture was monitored using a neutron moisture meter at 7-day intervals until harvest (Fig. 1). The results showed reasonable management of soil moisture under different treatments. Clear distinctions between soil moisture levels were noted at 30 and 60 cm of soil depth.

Relative water contents (RWC) averaged over all genotypes for the three soil moisture levels were significantly different at 40, 60 and 80 days after transplanting (DAT). The highest RWC was observed under full irrigation (W1) followed by W2 and then W3, respectively (Fig. 2). Visual wilting was observed in W2 and more severe wilting was observed in W3 in both years.

3.2. Genotypic variability and genotype × environment interactions

Significant differences between water regimes (W) were observed for inulin content, inulin yield and WUEi ($P \leq 0.01$) and

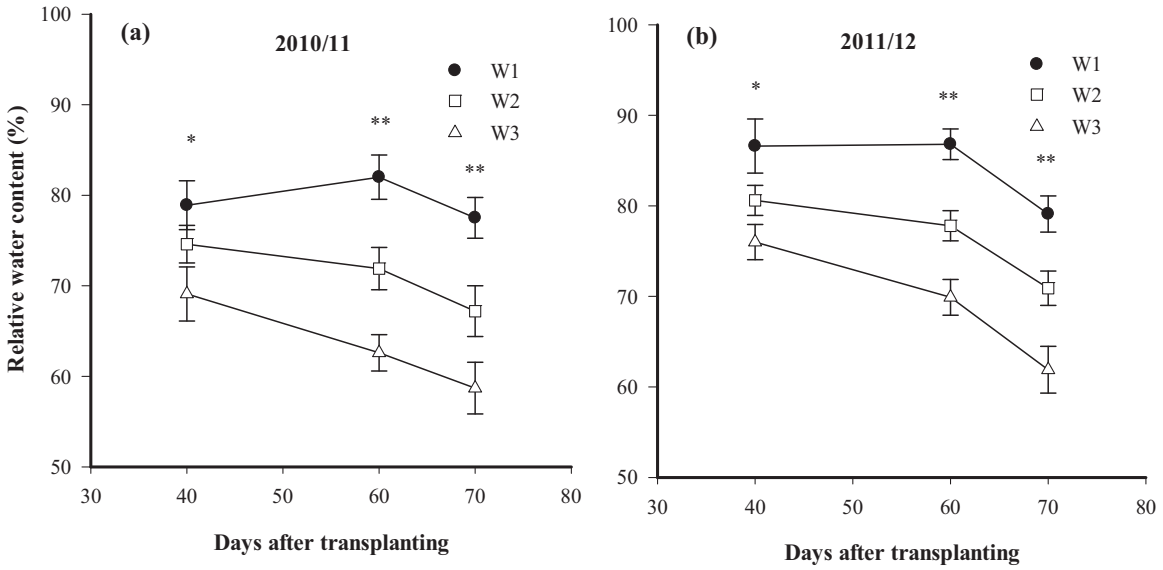


Fig. 2. Averages of relative water content in 12 Jerusalem artichoke genotypes under three water regimes (W1 = 100% ET, W2 = 75% ET, and W3 = 45% ET at 40, 60 and 70 days after transplanting in 2010/2011 (a) and 2011/2012 (b) and vertical bars indicate ± SEM. *, ** Significant at $P < 0.05$ and $P < 0.01$, respectively.

significant differences among Jerusalem artichoke genotypes (G) were observed for all traits (Table 1). Difference in years (Y) was also significant for inulin content, inulin yield and WUEi. The interactions between water regime and Jerusalem artichoke genotype (W × G) were significant for inulin yield and WUEi ($P \leq 0.01$). Genotypes × year (G × Y) interactions were significant for inulin yield and WUEi. Genotype × year × water interactions (G × Y × W) were also significant for inulin yield and WUEi. Two and three way interactions were not significant for inulin content, indicating that the genotypic rankings for inulin content were stable across years and soil moisture levels.

Results from our experiments showed non-significant interaction effects of genotype × environment for inulin content indicating that the genotypic ranking for this trait was more stable than for inulin yield and WUEi, suggesting potential for using this trait for selecting genotypes in Jerusalem artichoke improvement programs.

3.3. Genotypic variation of inulin content under different water regimes

Inulin content differed significantly among genotypes under W1, W2 and W3 conditions in both years (Table 2). W3 reduced inulin content by an average of 5.5% compared with W1 treatment, whereas W2 increased inulin content by 9.3% over the W1 treatment in 2010/2011. Similarly, drought at W2 increased inulin content by an average of 4.5% over the W1 conditions while W3 decreased inulin content by 6.1% in 2011/2012.

In 2010/2011, CN 52867, HEL 65 and HEL 256 were identified as having high inulin content under both drought conditions and DTI for inulin content ranged from 0.93 to 1.23 under W2 and W3 conditions while JA 1, JA 16, JA 60 and JA 38 had low inulin content across water regimes and DTI for inulin content ranged from 0.95 to 1.11 under both W2 and W3 conditions (Table 2). Under well-watered conditions, HEL 253, HEL 65 and CN 52867 had high inulin content.

In 2011/2012, the genotype with high or low inulin content could be identified. HEL 253, HEL 53, HEL 256, HEL 65 and CN 52867 had consistently high inulin content across water regimes and DTI for inulin content ranged from 0.92 to 1.07 under W2 and W3 conditions, whereas JA 1 had low inulin content across water regimes and DTI for inulin content was 0.95 and 1.06 under W2 and W3 conditions, respectively (Table 2).

There were five genotypes (HEL 253, HEL 53, HEL 256, HEL 65 and CN 52867) that exhibited consistently high inulin content across water regimes in both years. HEL 65, HEL 256 and CN 52867 showed consistently high DTI for inulin content under W2 conditions in both years. The highest increase in inulin content under W2 conditions in 2010/2011 was observed in CN 52867 followed by HEL 256 and HEL 65.

In this study, we found that W2 increased inulin content, and the results supported previous findings that mild water stress increased inulin accumulation in tubers, whereas severe drought reduced inulin content (Monti et al., 2005a; Conde et al., 1991). The results indicated that Jerusalem artichoke genotypes showed different ability to tolerate the moderate and severe drought conditions. In addition, Vandoorne et al. (2012) reported that water stress increased inulin content in root chicory. Enhanced inulin content under water stress could be due to the increase of soluble sugar concentration (Vandoorne et al., 2012).

The soluble sugars may directly influence inulin concentration in tuber of Jerusalem artichoke. Sucrose, fructose and glucose have been reported as the main parameters influencing the regulation of the activities of inulin-metabolizing enzymes (Vandoorne et al., 2012; De Roover et al., 2000). Since inulin content was increased under mild water stress this indicates that sucrose transport from source leaves to sink roots was not inhibited under water stress (Vandoorne et al., 2012). Valluru and Van den Ende (2008) reported that increases in inulin accumulation could protect cells from dehydration during water stress. Also, plants have the capacity to synthesize secondary metabolites such as sugar, inulin and fructans, all known as osmolytes that allow this plant to perform osmotic adjustment (Delatorre-Herrera et al., 2010). The results revealed that increasing the osmotic adjustment such as inulin constituting factors of drought resistance in Jerusalem artichoke. Therefore, it could be hypothesized that Jerusalem artichoke genotypes with high inulin content might exhibit improved resistance to water deficit.

Jerusalem artichoke genotypes showed significant differences for inulin content under drought conditions, indicating that this trait could be useful for improving genotypic performance in breeding program for drought resistance. CN 52867 had high inulin content under drought conditions, and, in previous study, this

Table 2
Inulin content of 12 Jerusalem artichoke genotypes under different water regimes in the dry season 2010/2011 and 2011/2012.

Genotypes	Inulin content (%)									
	2010/2011					2011/2012				
	W1	W2	W3	DTI (W2)	DTI (W3)	W1	W2	W3	DTI (W2)	DTI (W3)
[JA102 × JA89] – 8	62.0abc	65.3bcd	58.0bc	1.05c	0.94	67.5bc	69.7d	63.0e	1.03ab	0.93
JA 89	61.2bc	64.3cd	58.0bc	1.05c	0.95	66.5c	69.5d	62.5g	1.05a	0.94
HEL 253	67.0a	68.3bc	57.3bc	1.02d	0.86	71.0ab	75.7ab	68.0b	1.07a	0.96
HEL 53	61.5bc	66.3bcd	57.6bc	1.08c	0.94	71.3ab	74.7ab	68.2b	1.05a	0.96
HEL 256	61.7abc	72.0b	57.6bc	1.17ab	0.93	72.0ab	75.5ab	67.7b	1.05a	0.94
HEL 65	62.7abc	72.0b	60.0ab	1.15ab	0.96	71.7ab	75.2ab	66.2b	1.05a	0.92
CN 52867	65.5ab	78.3a	64.6a	1.23a	0.99	74.5a	78.0a	70.2a	1.05a	0.93
JA 3	61.7abc	68.0bc	61.0ab	1.10c	0.99	69.7b	73.7. b	66.0b	1.06a	0.95
JA 60	58.5 cd	63.0 cd	56.3c	1.08c	0.96	69.2b	71.2c	65.5c	1.03ab	0.95
JA 16	57.5 cd	62.6 cd	55.0c	1.09c	0.96	68.2bc	69.0d	65.2c	1.01abc	0.96
JA 1	55.0d	60.3d	52.0d	1.10c	0.95	64.3c	68.2d	61.2f	1.06a	0.95
JA 38	58.5 cd	65.0bcd	55.3c	1.11b	0.95	66.1c	69.0d	64.0d	1.04ab	0.97
Mean	***61.1***	***66.8***	***57.7***	***1.09***	***0.94***	***69.4***	***72.5***	***65.2***	***1.04***	***0.94***

Means in the same column with the same letters are not significantly different by DMRT ($P < 0.05$). W1 = 100% ET, W2 = 75% ET, and W3 = 45% ET. DTI for a genotype was calculated by the ratio of stress (W2 or W3)/non-stress (W1) conditions.

genotype also had high inulin content and tuber yield under fully irrigated conditions (Puttha et al., 2012; Pimsaen et al., 2010). The high inulin content in CN 52867 under drought conditions could be due to high potential under well-irrigated conditions. Full irrigation seemed to promote aerial growth rather than tuber growth and inulin accumulation, whereas moderate water stress favored the accumulation of inulin.

3.4. Genotypic variation of inulin yield under different water

Jerusalem artichoke genotypes were significantly different for inulin yield under well-watered and limited water conditions in both years (Table 3). Inulin yield was decreased under limited water conditions in both years, especially under W3 where it was decreased by 59.8% compared to W1 in 2010/2011 and 49.4% in 2011/2012.

In 2010/2011, HEL 53, HEL 253, HEL 65, HEL 256, [JA 102 × JA 89] – 8 and JA 89 had high inulin yield across water regimes but CN 52867 exhibited high inulin yield under drought conditions only (Table 3). The genotype with low inulin yield across water regimes were JA 60, JA 16 and JA 1. High DTI for inulin yield was observed for CN 52867 under both W2 and W3 conditions whereas HEL 256, JA 1 and JA 38 had low DTI for inulin yield under W2 and W3 conditions.

In 2011/2012, the genotypes with high inulin yield were HEL 256 and CN 52867 under well-watered conditions, and HEL 65 and CN 52867 across water regimes (Table 3). JA 1 and JA 60 showed consistently low inulin yield across water regimes. The genotypes with high DTI for inulin yield were HEL 65, JA 3, JA 1 and JA 38 under W2 conditions. JA 3 and JA 38 also had high DTI for inulin yield under W3 conditions.

HEL 256, HEL 65, CN 52867 exhibited high inulin yield across water regimes in both years, indicating that genotypes were stable across environments. High DTI for inulin yield was observed in CN 52867 in the first year while HEL 65 had high DTI in the second year.

Although inulin content was slightly increased by W2, inulin yield was decreased due to reduced tuber yield. These results were similar to those reported previously (Monti et al., 2005a; Baldini et al., 2006; Vandoorne et al., 2012). Water stress decreased plant growth, leaf area and photosynthetic capacity which in turn led to a significant decrease in tuber yield and resulted in reduce inulin yield (Vandoorne et al., 2012). The present study revealed tuber yield was the major factor contributing to inulin yield under both fully-irrigated and drought conditions. In contrast, tuber yield was not a major component contributing to inulin content under drought conditions, indicating that two traits were not genetically associated and suggested that these traits could be combined through conventional breeding.

Increase in inulin content could sustain inulin yield under W2 conditions to some extent, although the increase in inulin content did not completely offset the effect of drought on inulin yield. Variation in inulin yield among Jerusalem artichoke accessions was found under drought conditions, and it was possible to identify Jerusalem artichoke genotypes with better inulin yield and high DTI under drought conditions. This germplasm can be used as sources for drought resistance in breeding of Jerusalem artichoke. However, inulin yield had high genotype × environment interaction and this will reduce breeding progress for improved drought resistance in Jerusalem artichoke.

3.5. Genotypic variation of WUEi under different water

Significant differences among Jerusalem artichoke genotypes were observed for WUEi under non-stress and stress conditions in both years (Table 4). WUEi increased with drought conditions at W2 by 12.3% and W3 by 43.2% compared with W1 conditions in 2010/2011, and similarly WUEi was increased under W2 (18.3%) and W3 (38.9%) in 2011/2012.

In 2010/2011, HEL 65, [JA 102 × JA 89] – 8, HEL 53 and JA 89 had high WUEi across water regimes, but CN 52867 had high WUEi under W2 and W3 conditions (Table 4). JA 1 and JA 60 had low WUEi across water regimes. The high DTI for WUEi was observed in JA 60, JA 3 and CN 52867 under both W2 and W3 conditions.

In 2011/2012, HEL 65 showed consistently high WUEi across water regimes, while CN 52867 had high WUEi under W2 conditions only (Table 4). The genotype with high DTI for WUEi under both W2 and W3 conditions were CN 52867 and JA 3.

The genotype with high WUEi across water regimes in both years was HEL 65, while CN 52867 exhibited high WUEi under drought conditions in both years. In addition, CN 52867 showed consistently high WUEi and DTI for WUEi under W2 conditions in both years.

Water use efficiency for inulin yield was increased by W2 and W3. A recent study also reported that water stress increased WUEi in chicory (Vandoorne et al., 2012). Enhanced WUEi could be associated with large root systems allowing plants to absorb additional water from deep soil layers and promoting tuber yield, which in turn contributes to inulin yield. Also, Vandoorne et al. (2012) demonstrated that drought conditions increased inulin content and

Table 3
Inulin yield of 12 Jerusalem artichoke genotypes under different water regimes in the dry season 2010/2011 and 2011/2012.

Genotypes	Inulin yield (kg ha^{-1})									
	2010/2011					2011/2012				
	W1	W2	W3	DTI (W2)	DTI (W3)	W1	W2	W3	DTI (W2)	DTI (W3)
[JA102 × JA89] – 8	2319ab	1654a	845ab	0.71c	0.36c	2407c	1978bc	1203b	0.82b	0.50b
JA 89	2272ab	1788a	944a	0.79bc	0.42b	2746b	1705bc	1236b	0.62d	0.45c
HEL 253	2486a	1826a	1057a	0.73c	0.43b	2044d	1464de	1160b	0.72c	0.57b
HEL 53	2758a	1942a	967a	0.70c	0.35c	2330c	2027bc	1344ab	0.87ab	0.58b
HEL 256	2478a	1553ab	822b	0.63d	0.33c	3425a	1860bc	1100c	0.54e	0.32d
HEL 65	2608a	1673a	1010a	0.64d	0.39c	2771b	2503a	1438a	0.90a	0.52b
CN 52867	1874bc	1698a	1052a	0.91a	0.56a	2926ab	2127ab	1234b	0.73c	0.42c
JA 3	1127de	794c	435c	0.70c	0.39c	1996e	1788bc	1284b	0.90a	0.64a
JA 60	925de	821c	451c	0.89a	0.49b	1698ef	1278f	1008c	0.75c	0.59b
JA 16	1223d	901c	528bc	0.74c	0.43b	2139cd	1618e	1066c	0.76c	0.50b
JA 1	647e	376c	302c	0.58de	0.47b	1418f	1344f	750d	0.95a	0.53b
JA 38	1471cd	933bc	519bc	0.63d	0.35c	2126cd	1814bc	1345b	0.85ab	0.63a
Mean	***1849***	***1329***	***744***	***0.72***	***0.40***	***2336***	***1792***	***1181***	***0.77***	***0.51***

Means in the same column with the same letters are not significantly different by DMRT ($P < 0.05$). W1 = 100% ET, W2 = 75% ET, and W3 = 45% ET. DTI for a genotype was calculated by the ratio of stress (W2 or W3)/non-stress (W1) conditions.

also enhanced WUEi, indicating that inulin content might be associated with WUEi under drought conditions. Previous study reported that inulin was contributed to maintain high WUEi under drought conditions in Aloe Vera plants (Delatorre-Herrera et al., 2010). This may partially explain the contribution of inulin content to WUEi under W2 conditions.

Jerusalem artichoke showed significant differences in inulin content, inulin yield and WUEi. CN 52867 and HEL 65 had the highest inulin content and also had high inulin yield and WUEi under drought conditions across years. The ability of Jerusalem artichoke genotypes with high photosynthesis to enhance accumulation of fructose explains their relatively high inulin content (Monti et al., 2005a; Vandoorne et al., 2012), which in turn increased inulin yield and water use efficiency for inulin yield. The information on inulin content and WUEi under W2 conditions may have application in genetic improvement for drought resistance in Jerusalem artichoke.

Identification of the physiological traits associated with drought resistance of plants under drought conditions is an important goal of breeding programs. Water stress leads to increased WUEy in many plants species (Losavio et al., 1997; Puangbut et al., 2009; Songsri et al., 2009; Vandoorne et al., 2012), and could be used as selection criteria for improving drought resistance in Jerusalem artichoke. This study revealed that WUEi is a drought resistant trait which helps plants to conserve soil moisture and contributes to inulin yield under unpredictable or limiting available soil water conditions.

3.6. Relationship between inulin content and tuber dry weight under different water regimes

Results for tuber dry weight were presented by Ruttanaprasert et al. (2014). They reported that tuber dry weight was decreased by drought conditions. This study, tuber dry weight was used to determine the relationship with inulin content and to determine the relative contributions to inulin yield under drought conditions.

The correlation coefficients between tuber dry weight and inulin content were not significant under W2 and W3 conditions in both years (Figs. 3 and 4). Under drought conditions, HEL 65 had the highest tuber yield while CN 52867 had the highest inulin content in both years. The present study revealed that increased inulin content under W2 was not associated with tuber yield.

3.7. Factors contributing to inulin yield under different water regimes

Multiple regression analysis showed the contributions of inulin content and tuber yield to inulin yield under W1, W2 and

Table 4
Water use efficiency for inulin yield (WUEi) of 12 Jerusalem artichoke genotypes under different water regimes in 2010/2011 and 2011/2012.

Genotypes	Water use efficiency for inulin yield (g kg^{-1})									
	2010/2011					2011/2012				
	W1	W2	W3	DTI (W2)	DTI (W3)	W1	W2	W3	DTI (W2)	DTI (W3)
[JA102 × JA89] – 8	1.15a	1.20ab	1.55a	1.04d	1.35cd	1.07c	1.24b	1.36bc	1.16c	1.27d
JA 89	1.09ab	1.18ab	1.41ab	1.08cd	1.29d	1.13ab	1.26b	1.38bc	1.12c	1.22d
HEL 253	0.99b	1.12b	1.33b	1.13cd	1.34cd	1.02c	1.25b	1.43bc	1.23b	1.40c
HEL 53	1.10ab	1.19ab	1.48ab	1.08cd	1.35cd	1.10ab	1.26b	1.47bc	1.15c	1.34cd
HEL 256	1.10ab	1.13b	1.34b	1.03d	1.22d	1.06c	1.28b	1.34c	1.21b	1.26d
HEL 65	1.19a	1.20ab	1.60a	1.01d	1.34cd	1.23a	1.40ab	1.62b	1.14c	1.32cd
CN 52867	0.96b	1.28a	1.59a	1.33c	1.66bc	1.00c	1.50a	1.71a	1.50a	1.71a
JA 3	0.43cd	0.84c	0.98bc	1.95a	2.28a	0.76e	1.06c	1.25cd	1.39ab	1.64b
JA 60	0.32d	0.52e	0.70d	1.63b	2.19a	0.78e	0.85cd	1.12d	1.09c	1.44c
JA 16	0.53c	0.61d	0.75d	1.15cd	1.42c	0.86d	0.98cd	1.09d	1.14c	1.27d
JA 1	0.36d	0.40f	0.57e	1.11cd	1.58bc	0.62f	0.72d	0.86e	1.16c	1.39c
JA 38	0.57c	0.67de	0.90c	1.18cd	1.58bc	1.08c	1.18bc	1.32c	1.09c	1.22d
Mean	***0.78***	***0.91***	***1.11***	***1.23***	***1.55***	***0.98***	***1.17***	***1.33***	***1.20***	***1.37***

Means in the same column with the same letters are not significantly different by DMRT ($P < 0.05$). W1 = 100% ET, W2 = 75% ET, and W3 = 45% ET. DTI for a genotype was calculated by the ratio of stress (W2 or W3)/non-stress (W1) conditions.

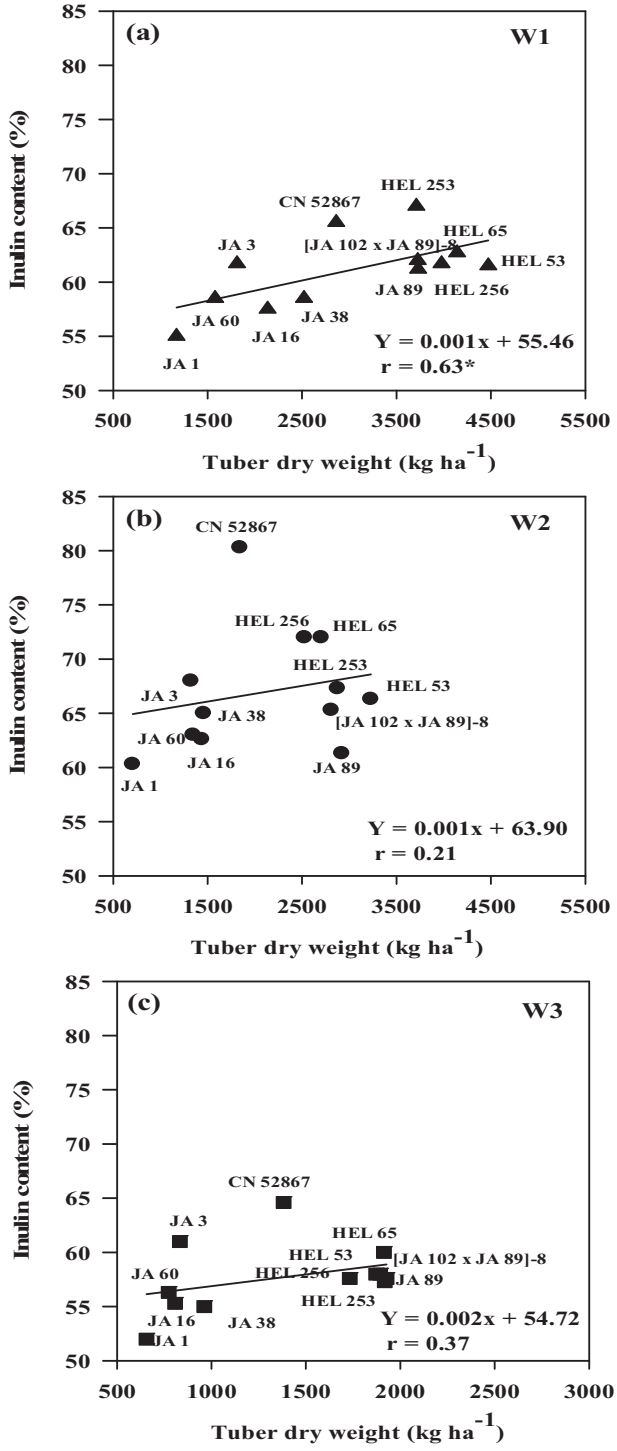


Fig. 3. Relationship between tuber dry weight and inulin content of 12 Jerusalem artichoke genotypes under W1 (100% ET) (a), W2 (75% ET) (b) and W3 (45% ET) (c) in 2010/2011.

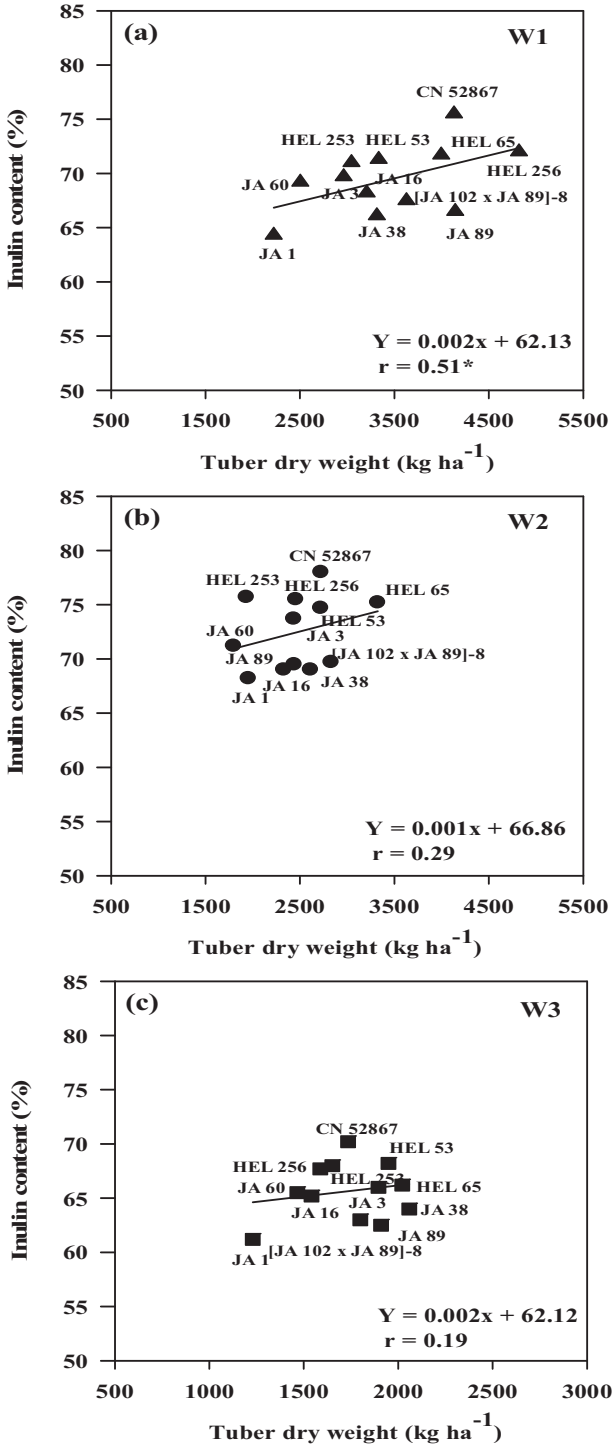


Fig. 4. Relationship between tuber dry weight and inulin content of 12 Jerusalem artichoke genotypes under W1 (100% ET) (a), W2 (75% ET) (b) and W3 (45% ET) (c) in 2011/2012.

W3 conditions in both years (Table 5). In 2010/2011, tuber yield was the major contributing factor to inulin yield under W1 (99.01%), W2 (89.67%) and W3 (83.07%). Similarly, the contribution of tuber yield to inulin yield was still the most important under W1 (98.51), W2 (95.14%) and W3 (93.66%) in 2011/2012.

The present study clearly showed that tuber yield are important trait determinants for inulin yield under both well-watered and water stress conditions. Therefore, it would be useful for selecting genotype for improved tuber yield and useful for crop simulation model to predicating the yield in multi-location trails. Our study expected that physiological traits could be useful for improvement of the crop simulation model to enable it to simulate Jerusalem artichoke productivity in different conditions. Baldini et al. (2011) suggested that the crop simulation model could be useful as a tool for the planning and risk evaluation of production Jerusalem as a crop for inulin production.

Table 5
Contributions of inulin content and tuber yield to inulin yield of 12 Jerusalem artichoke genotypes under different water regimes in 2010/2011 and 2011/2012.

Traits	Explained by regression (%)					
	2010/11			2011/12		
	W1	W2	W3	W1	W2	W3
Regression	99.86**	96.42**	90.55**	99.58**	99.85**	98.25**
Inulin content	0.85*	6.75*	7.48*	1.07*	4.71*	4.59*
Tuber yield	99.01**	89.67**	83.07**	98.51**	95.14**	93.66**

*, ** Significant at $P < 0.05$ and significant at $P < 0.01$, respectively.
W1 = 100% ET, W2 = 75% ET, and W3 = 45% ET

4. Conclusion

Inulin content in these 12 genotypes showed fairly consistent rankings under well watered and drought conditions over two years. The present study revealed that significant genotypic variation in inulin content, inulin yield and WUEi in response to drought conditions, indicating potential for using these traits for selecting genotypes in Jerusalem artichoke improvement programs. Inulin content increased with W2 whereas inulin yield was reduced under drought conditions. WUEi was higher in plants which experienced drought stress. Genotypes with high inulin content and high WUEi under W2 conditions were identified. CN 52867 and HEL 65 showed high inulin content and WUEi under W2 in both years. These traits could be useful for improving the genetic performance of Jerusalem artichoke for drought resistance.

Acknowledgements

This work was supported by the Higher Education Research Promotion and National Research University Project of Thailand, Office of the Higher Education Commission, through the Food and Functional Food Research Cluster of Khon Kaen University. We also thank the Leibniz Institute of Plant Genetics and Crop Plant Research, Germany, the Plant Gene Resource of Canada for the contribution of Jerusalem artichoke germplasm. Grateful acknowledgments are made to the Peanut and Jerusalem artichoke Improvement for Functional Food Research Group and Plant Breeding Research Center for Sustainable Agriculture, Khon Kaen University. Grateful acknowledgement is also made to the Thailand Research Fund, the commission for Higher Education and Khon Kaen University for providing financial supports to this research through the Distinguished Research Professor Grant of Professor Dr. Aran Patanothai.

References

Baldini, M., Danuso, F., Monti, A., Amaducci, M.T., Stevanato, P., Mastro, G.D., 2006. Chicory and Jerusalem artichoke productivity in different areas of Italy, in relation to water availability and time harvest. Ital. J. Agron. 2, 291–307.

Baldini, M., Danuso, F., Rocca, A., Bulfoni, E., Monti, A., Mastro, G.D., 2011. Jerusalem artichoke (*Helianthus tuberosus* L.) productivity in different Italian growing areas: a modelling approach. Ital. J. Agron. 6, 126–132.

Conde, J.R., Tenorio, J.L., Rodriguez-Maribona, B., Ayerbe, L., 1991. Tuber yield of Jerusalem artichoke (*Helianthus tuberosus* L.) in relation to water stress. Biomass Bioenerg. 3, 131–142.

Delatorre-Herrera, J., Delfino, I., Salinas, C., Silva, H., Cardemil, L., 2010. Irrigation restriction effects on water use efficiency and osmotic adjustment in Aloe Vera plants (*Aloe barbadensis* Miller). Agric. Water Manage. 97, 1564–1570.

Denoroy, P., 1996. The crop physiology of *Helianthus tuberosus* L.: a model orienter view. Biomass Bioenerg. 11, 11–32.

De Roover, J., Vandenbranden, K., Van Laere, A., Van den Ende, W., 2000. Drought induces fructan synthesis and 1-SST (sucrose:sucrose fructosyltransferase) in roots and leaves of chicory seedlings (*Cichorium intybus* L.). Planta 210, 808–814.

Doorenbos, J., Pruitt, W.O., 1992. Guideline for predicting crop water requirements. In: FAO Irrigation and Drainage Paper. Food and Agriculture Organization of the United Nations, Rome.

Hoshmand, A.R., 2006. Design of Experiments for Agriculture and the Natural Sciences. Chapman & Hall, Florida.

Frese, L., 1993. Production and utilization of inulin. In: Suzuki, M., Chatterton, N.J. (Eds.), Cultivation and Breeding of Fructans. CRC Press, London, pp. 303–318.

Kays, S.J., Nottingham, S.F., 2008. Biology and Chemistry of Jerusalem Artichoke (*Helianthus tuberosus* L.). CRC Press, Florida.

Kocsis, L., Kaul, H.-P., Praznik, W., Liebhard, P., 2008. Influence of harvest date on tuber growth, tuber dry matter content, inulin and sugar yield of different Jerusalem artichoke (*Helianthus tuberosus* L.) cultivars in the semi-arid production area of Austria. Ger. J. Agron. 12, 8–21.

Gao, K., Zhu, T., Han, G., 2011. Water and nitrogen interactively increased the biomass production of Jerusalem artichoke (*Helianthus tuberosus* L.) in semi-arid area. Afr. J. Biotechnol. 10, 6466–6472.

Losavio, N., Lamascese, N., Vonella, A.V., 1997. Water requirement and nitrogen fertilization in Jerusalem artichoke (*Helianthus tuberosus* L.) grown under Mediterranean conditions. Acta Hortic. 449, 206–209.

Monti, A., Amaducci, M.T., Venturi, G., 2005a. Growth response, leaf gas exchange and fructans accumulation of Jerusalem artichoke (*Helianthus tuberosus* L.) as affected by different water regimes. Eur. J. Agron. 23, 136–145.

Monti, A., Amaducci, M.T., Pritoni, G., Venturi, G., 2005b. Growth, fructan yield, and quality of chicory (*Cichorium intybus* L.) as related photosynthetic capacity, harvest time, and water regime. J. Exp. Bot. 56, 1389–1395.

Nautiyal, P.C., Nageswara Rao, R.C., Joshi, Y.C., 2002. Moisture-deficit-induced changes in leaf water content, leaf carbon exchange rate and biomass production in groundnut cultivars differing in specific leaf area. Field Crops Res. 74, 67–79.

Pimsaen, W., Jogloy, S., Suriharn, B., Kesmala, T., Pensuk, V., Patanothai, A., 2010. Genotype by environment (G × E) interactions for yield components of Jerusalem artichoke (*Helianthus tuberosus* L.). Asian J. Plant Sci. 9, 11–19.

Puangbut, D., Jogloy, S., Vorasoot, N., Akkasaeng, C., Kesmala, T., Rachaputi Rao, C.N., Wright, G.C., Patanothai, A., 2009. Association of root dry weight and transpiration efficiency of peanut genotypes under early season drought. Agric. Water Manage. 96, 1460–1466.

Puangbut, D., Jogloy, S., Srijaranai, S., Vorasoot, N., Kesmala, T., Patanothai, A., 2011. Rapid assessment of inulin content in *Helianthus tuberosus* L. tubers. SABRAO J. Breed. Genet. 43, 188–200.

Puangbut, D., Jogloy, S., Vorasoot, N., Srijaranai, S., Kesmala, T., Patanothai, A., 2012. Influence of planting date and temperature on inulin content in Jerusalem artichoke (*Helianthus tuberosus* L.). Aust. J. Crop Sci. 6, 1159–1165.

Puttha, R., Jogloy, S., Wangsomnuk, P.P., Srijaranai, S., Kesmala, T., Patanothai, A., 2012. Genotypic variability and genotype by environment interactions for inulin content of Jerusalem artichoke germplasm. Euphytica 183, 119–131.

Ruttanaprasert, R., Banterng, P., Jogloy, S., Vorasoot, N., Kesmala, T., Kanwar, R.S., Holbrook, C.C., Patanothai, A., 2014. Genotypic variability for tuber yield, biomass and drought tolerance in Jerusalem artichoke germplasm. Turk. J. Agric. For. 38, 570–580.

Ruttanaprasert, R., Jogloy, S., Vorasoot, N., Kesmala, T., Kanwar, R.S., Holbrook, C.C., Patanothai, A., 2013. Photoperiod and growing degree days effect on dry matter partitioning in Jerusalem artichoke. Int. J. Plant Prod. 7 (3), 393–416.

Saengkanuk, A., Nuchadomrong, S., Jogloy, S., Patanothai, A., Srijaranai, S., 2011. A simplified spectrophotometric method for the determination of inulin in Jerusalem artichoke (*Helianthus tuberosus* L.) tubers. Eur. Food Res. Technol. 233, 609–616.

Schittenhelm, S., 1999. Agronomic performance of root chicory, Jerusalem artichoke and sugarbeet in stress and non-stress environment. Crop Sci. 39, 1815–1823.

Schubert, S., Feuerle, R., 1997. Fructan storage in tuber of Jerusalem artichoke: characterization of sink strength. New Phytol. 136, 115–122.

Singh, S., Russell, M.B.,1981. Water use by maize/pigeonpeas intercrop on a deep vertisol. In: Proceedings of the International Workshop on Pigeonpeas. ICRISAT Center, pp. 271–282.

Songsri, P., Jogloy, S., Holbrook, C.C., Kesmala, T., Vorasoot, N., Akkasaeng, C., Patanothai, A., 2009. Association of root, specific leaf area and SPAD chlorophyll meter reading to water use efficiency of peanut under different available soil water. Agric. Water Manage. 96, 790–798.

Valluru, R., Van den Ende, W., 2008. Plant fructans in stress environment: emergence concepts and future prospects. J. Exp. Bot. 59, 2905–2916.

Vandoorne, B., Matheiu, A.S., Van den Ende, W., Vergauwen, R., Périlleux, C., Javaux, M., Lutts, S., 2012. Water stress drastically reduces root growth and inulin yield in *Cichorium intybus* (var. *sativam*) independently of photosynthesis. J. Exp. Bot. 63, 4359–4373.

Yang, B., Zhang, H.J., You-Xian, L., Xue, Y.L., 2010. Effect of different irrigation on development and water use efficiency of Jerusalem artichoke. Irrig. Drain. 29, 168–175.

Zhang, M., Chen, Q., Shen, S., 2010. Physiological responses of two Jerusalem artichoke cultivars to drought stress induced by polyethylene glycol. Acta Physiol. Plant. 33, 313–318.

Plant Foods Hum Nutr (2015) 70:221–226
DOI 10.1007/s11130-015-0480-y

ORIGINAL PAPER

Preparation of Inulin Powder from Jerusalem Artichoke (*Helianthus tuberosus* L.) Tuber

Bang-orn Srinameb · Suporn Nuchadomrong · Sanun Jogloy · Aran Patanothai · Supalax Srijaranai

Published online: 25 March 2015
© Springer Science+Business Media New York 2015

Abstract The complete procedure for the production of inulin powder from Jerusalem artichoke tubers (JAT) was investigated. The procedure consists of isolation of inulin from JAT, elimination of color from the inulin extract and solidification. Washed tubers were first sliced, dried in a 60 °C oven for 10 h and then milled and sieved into a powder. Inulin was isolated from the JAT powder by hot water extraction using an accelerated solvent extractor (ASE). The effects of temperature and time for the extraction were investigated. The highest extraction efficiency was obtained at the extraction temperature of 80 °C for 20 min. The color of the extract was eliminated using ion exchange process with diethylaminoethyl cellulose as the sorbent. The inulin powder was subsequently obtained by freeze drying. Inulin content and inulin profiles were monitored to evaluate the efficiencies of the complete procedure. The inulin content was indirectly determined by spectrophotometry from free and total fructose measurements using potassium iodide. The inulin profile was monitored using high performance anion exchange chromatography equipped with integrated pulse amperometric detection (HPAEC−PAD). The proposed method provided the inulin production yield of 92.5 %. The present procedure is fast, simple and effective for production of inulin powder from JAT. In addition, infrared spectra and some physico−chemical properties of the obtained inulin powder were determined and compared with the standard inulin.

Keyword Inulin · Jerusalem artichoke · Accelerated solvent extractor · HPAEC−IPAD

Electronic supplementary material The online version of this article (doi:10.1007/s11130-015-0480-y) contains supplementary material, which is available to authorized users.

B.-o. Srinameb · S. Srijaranai (✉)
Materials Chemistry Research Center, Department of Chemistry and Center of Excellence for Innovation in Chemistry, Faculty of Science, Khon Kaen University, Khon Kaen 40002, Thailand
e-mail: supalax@kku.ac.th

S. Nuchadomrong
Department of Biochemistry, Faculty of Science, Khon Kaen University, Khon Kaen 40002, Thailand

S. Jogloy · A. Patanothai
Department of Plant Science and Agricultural Resources, Faculty of Agriculture, Khon Kaen University, Khon Kaen 40002, Thailand

Introduction

Inulin is one group of fructans or fructooligosaccharides which are linear polymers of D−fructose joined by β (2→1) linkages and terminated with a single D−glucose which is linked to D−fructose by an α (1→2) linkage [1–3]. The chain length of D−fructose, known as degree of polymerization (DP), varies from 2−60 [4–6]. The DP of inulin depends on various parameters including specific varieties of plants, harvest time, storage time after harvesting and the production procedure for isolating inulin [6–8]. Inulin has a number of interesting properties that can be applied in various fields. Inulin is a functional food "ingredient" since it can be used as a prebiotic agent [9], can stimulate health−promoting gut microflora [10, 11] and may reduce the risk of cancer [9, 12]. Pharmaceutical and cosmetics applications of inulin have been described [13, 14]. For energy production, inulin is an appropriate source for production of ethanol through fermentation [15, 16].

Inulin is found mainly in the tubers and roots of many plants, such as Chicory artichoke (*Cynara scolymnus* L.), viper's grass (*Scorzonera hispanica* L.), Jerusalem artichoke (*Helianthus tuberosus* L.), globe artichoke (*Cynara cardunculus var. scolymus*) [17], Yacon (*Smallanthus sonchifolius*) [18] and dahlia tubers (*Dahlia Pinata Cav.)* [9, 19]. Inulin is mostly commercialized as a powder, known as

Beneo HP [5] and Raftilin® ST or Fibruline [9, 10]. So far, the major crop used for industrial production of inulin is chicory [2, 20]. However, the Jerusalem artichoke tuber has a large amount of inulin, ca. 14–19 % [2, 5, 21], so it should be a valuable source for inulin production. However, the production of inulin from Jerusalem artichoke tuber has not progressed significantly because it has an undesirable flavor, significant color and limited harvest time [22].

Inulin is isolated from plants using extraction based methods. An important physico−chemical property of pure inulin is that it is almost insoluble in cold water, but highly soluble in hot water [20]. Therefore, one of the most common methods for isolation of inulin from plants is hot water extraction. Conventionally, inulin is extracted from Chicory roots by hot water at 70−80 °C in continuous counter current extractors with an extracting time of 1.5−2 h [23]. The technology of inulin extraction from Chicory root is similar to the saccharose extraction from sugar beets [23]. The extraction of inulin from Jerusalem artichoke is similar to the other plants. The conventional procedure is hot water extraction at various temperatures and times such as extraction at 80 °C with mild shaking for 3 h [24], at 80 °C for 1.5 h [25] and 80 °C for 1 h [26]. Recently, ultrasound−assisted extraction has been introduced as a powerful tool for extraction of inulin from various plant tissues. It applies high−frequency and high−intensity sound waves to interact with materials [2, 19]. Ultrasound disrupts plant cell walls thereby facilitating the release of extractable compounds and enhancing mass transport of solvent from the continuous phase into plant cells [13]. The ultrasound assisted extraction of inulin from JAT was reported using extraction temperature at 76.65 °C for 20 min [2]. Nevertheless, it is considered unsuitable for inulin extraction on the large scale. An alternative method for isolation of inulin is the precipitation of inulin by alcohol. This method is efficient and widely used in laboratory. However, it was uneconomical and unsuitable on an industrial scale [2]. More recently, various strategies have been employed to obtain high extraction efficiency for inulin isolation such as pulsed electric fields (PEF) [27] and three−stage homogenate extraction (TSHE) [26]. Another strategy using high pressure for extraction, known as pressurized liquid extraction (PLE) or accelerated solvent extraction (ASE) has been successfully applied for the isolation of interest compounds from various plants such as peperine from pepper and bioactive molecules from *Hypericum perforatum* L. [28–30]. ASE allows efficient performance, rapid extraction at high temperature and high pressure, minimizing solvent consumption and sample manipulation. To our knowledge, there are no reports of using ASE for the extraction of inulin from plants.

The present study is aimed at investigating the production procedure of inulin powder from Jerusalem artichoke tuber. Besides, high efficiency, rapid and cost effective, the minimizing of inulin degradation during the production is considered. Inulin was extracted from Jerusalem artichoke powder by ASE using water as the extraction solvent. The extract was then subjected to a chromatographic process for elimination of color. Inulin powder was obtained after freeze drying. Inulin content and inulin profile were monitored for all processes. Instrumental analyses of inulin powder by IR and SEM are also reported.

Materials and Methods

Chemicals and Reagents

All chemicals and reagents were of analytical reagent grade. These included sodium hydroxide, potassium iodide, sodium periodate and sodium acetate (Carlo Erba, Rodano, Italy); methanol (Lab-Scan, Bangkok, Thailand); silica gel (0.06 mm for chromatography, Carlo Erba, Val de Reuil, France); diethylaminoethyl cellulose (Sigma, Singapore); barium acetate (Carlo Erba, Val de Reuil, France); citric acid; concentrated hydrochloric acid, and concentrated sulfuric acid (Carlo Erba, Val de Reuil, France), anhydrous D-(−)-fructose and D-(+)-glucose (Univar, New South Wales, Australia). Standards fructooligosaccharide (1-kestose (n=3) and nystose (n=4)) were obtained from Fluka. Standard inulin from chicory was purchased from Sigma. All aqueous solutions were prepared using deionized water from RiOs™ Type I Simplicity 185 (Millipore, USA) with the resistivity of 18.2 MΩ.cm.

Intrumentations

The spectrophotometric experiments were carried out on an Agilent 8453 UV−Vis spectrophotometer (Germany). Chromatographic separations were performed on a Dionex DX −500 Ion Chromatographic system (Sunnyvale, USA), consisting of a GP40 gradient pump and an ED 40 electrochemical detector equipped with a thin−layer type amperometric cell. The cell contained a 1.0−mm diameter gold working electrode and a platinum counter electrode in integrated pulse amperometric detection mode (PAD). The separations were performed on a CarboPac PA 1 column set comprised of a guard column (50×4 mm i.d.) and analytical column (250×4 mm i.d.). The injection volume was 25 μL. Data acquisition and data analysis were under the control of the PeakNet 6.0 Dionex software. The accelerated solvent extractor model ASE−200 (Dionex, USA) with a 22 mL extraction cell and a 30 mL collection cell, was used for the extraction of inulin from Jerusalem artichoke tuber powder. An Isotemp oven (Fisher Scientific, UK) was used for the drying of Jerusalem artichoke tubers. The freeze dryer model ScanSpeed MaxiVac (Scientific, Germany) was employed for preparation of inulin powder. PerkinElmer, Spectrum One (USA), Fourier

transform infrared spectroscopy (FT−IR) was used for IR spectra. Microphotographs were obtained using Scanning electron microscopy (Hitachi, S−3000N, Akishima, Tokyo, Japan).

Sample Preparation

Jerusalem artichoke tubers were washed with tap water to eliminate soil and then were longitudinally sliced to obtain approximately 2−mm thick pieces. The tubers were dried at 60 °C for 10 h in an oven, milled and sieved through an 850−μm sieve. The powdered tubers were kept for short periods of time at an ambient atmosphere in desiccators, until extraction.

Procedure

Extraction of Inulin from Jerusalem Artichoke Powder by ASE

Accurate weight (2 g) of JA powder along with silica gel (3.6 g) was placed into an extraction cell. The powders were then automatically extracted with water (as the extraction solvent) for 20 min at 80 °C and 1500 psi, controlled by the ASE time program. All experiments were conducted in triplicate.

Elimination of Color of the Inulin Extract

The extract was passed through a glass column (15 cm×1 cm ID) packed with 15 g of diethylaminoethyl cellulose (DEAE −cellulose) at a flow rate 2 mL min^{-1}, water was used as the eluent.

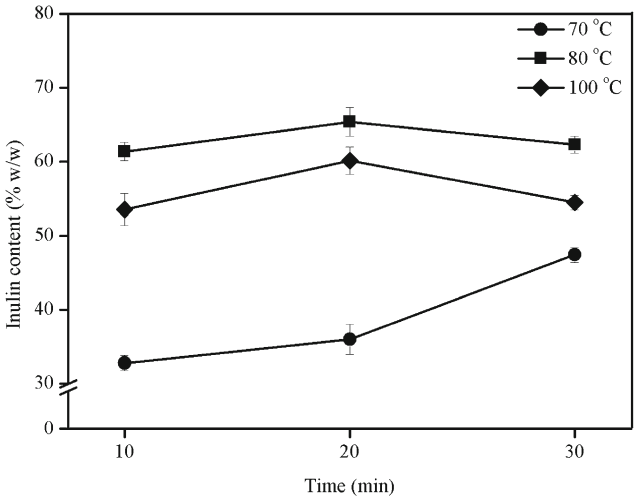


Fig. 1 The effects of extraction time and temperature on the extraction efficiency of inulin from JAT powder

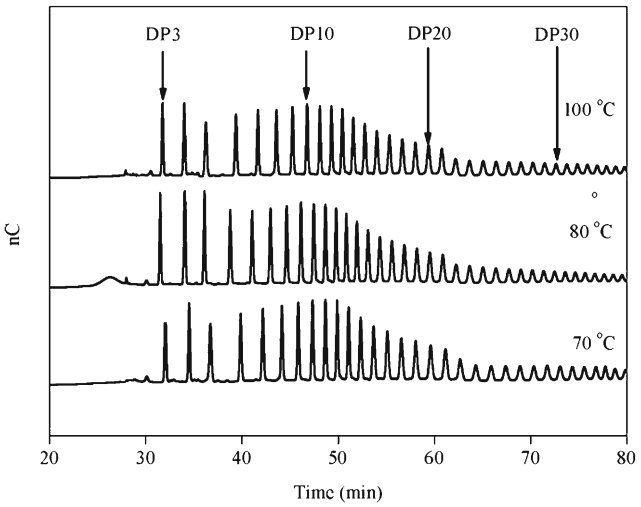


Fig. 2 Inulin profiles showing the distribution of DPs at various extraction temperatures (70–100 °C) for the extraction time of 20 min

Determination of Inulin Content by Spectrophotometry

Determination of Free Fructose Content (F_f)

The extract (150 μL) was pipetted into 10 mL volumetric flask containing 20 mmol L^{-1} citrate buffer 6 (5 mL) and diluted to 10 mL with water. After 5 min, 100 mmol L^{-1} potassium iodide (150 μL) was added, and mixture was left for an additional 5 min. The absorbance was subsequently measured at 350 nm using a UV−Vis spectrophotometer. The concentration of free fructose was deduced from a calibration curve of standard fructose solutions.

Determination of Total Fructose Content (F_{tot})

The extract (0.50 mL) was acidified with 0.2 mol L^{-1} HCl, in a final volume of 25 mL, and subjected to acid hydrolysis at 97 ± 2 °C for 45 min. The solution was then adjusted to pH 7 with NaOH before dilution with water to 25 mL. A 150 μL portion of the neutral hydrolysate was analyzed spectrophotometrically by the same procedure as described previously for free fructose (F_f).

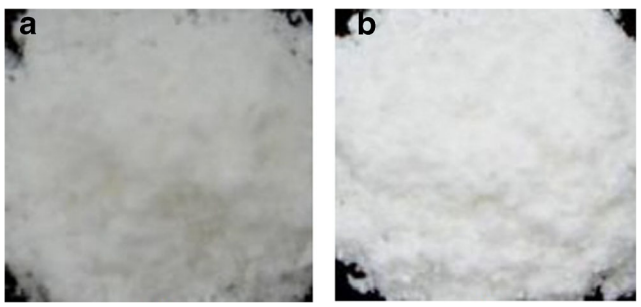


Fig. 3 Photographs of inulin powders from **a** the produced inulin from JAT powder and **b** standard Chicory

Table 1 Effect of extraction temperatures on the inulin composition (peak area) from the extraction of JAT for 20 min

Composition (relative %)	Extraction temperature (°C)		
	70	80	100
DP<3	3.71[a]	3.94[a]	4.00[a]
DP3-10	34.94[b]	37.77[a]	35.95[b]
DP11-20	36.87[a]	37.81[a]	35.37[a]
DP21-30	11.35[a]	10.59[a]	12.11[a]
DP31-40	7.05[a]	5.57[a]	7.45[a]
DP41-50	6.08[a]	4.32[b]	5.12[ab]

Letters "a" and "b" display the significant test using Duncan's multiple range test, the values in a row with different letters "a" and "b" mean that there are significantly different at $*P<0.05$

The inulin content was evaluated using the following equation [5]:

$$I = k(F_{tot} - F_f)$$

where I is the content of inulin, F_{tot} is total fructose content, F_f is free fructose, k is 0.995, it is a correction factor for the glucose part of inulin and water loss during hydrolysis [5, 31].

Determination of Inulin Profile

The profile of inulin was analyzed by High Performance Anion Exchange Chromatography equipped with an Integrated Pulsed Amperometric Detector. The inulin extracts were diluted to appropriate concentrations with water and filtered through a 0.45 μm membrane filter before injection. The separation conditions were 150 mmol L^{-1} NaOH as eluent A, 150 mmol L^{-1} NaOH spiked with 500 mmol L^{-1} sodium acetate as eluent B, a flow rate of 1.0 mL min^{-1}. The elution gradient was 0−15 min with 100 % eluent A, 15−45 min with linear gradient from 0 to 60 % eluent B, 45−90 min with linear gradient from 60 to 90 % eluent B, 90−110 min with linear gradient from 90 to 100 % eluent B, and 110−120 min with linear gradient from 100 to 0 eluent B. The electrical potential and time period (waveform) for the detector were programmed as follows: E1, +0.1 V (*vs.* Ag/AgCl) for 400 ms; E2, −2 V for 20 ms; E3, +0.6 V for 10 ms; E4, −0.1 V for 60 ms [6]. Standards inulin including 1-kestose (DP=3) and nystose (DP=4) were used for the identification of peaks.

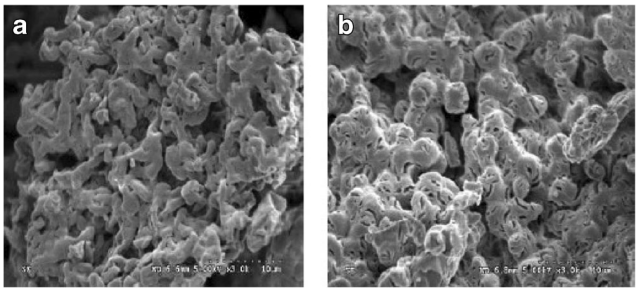


Fig. 5 Microphotographs of inulin powder from **a** the produced inulin from JAT powder and **b** standard Chicory

Results and Discussion

Extraction of Inulin by ASE

In this study, inulin was extracted using water and was performed at high temperature under high pressure by using an accelerated solvent extractor. The extractions were investigated at temperatures 70−100 °C and extraction times in the range of 10−30 min, while the pressure was kept constant at 1500 psi.

The extraction efficiency is expressed as percent of extracted inulin in the extract per dried weight of powdered tuber. As seen in Fig. 1, extraction at 70 °C gave the lowest inulin content for all the studied extraction times. The highest extraction efficiency was obtained at the extraction temperature of 80 °C for 20 min. The decrease in extracted inulin content at longer extractions times was possibly due to the acid−heat sensitivity of the fructose molecule [5].

The inulin profiles under various extraction conditions were also investigated as a typical profile, shown in Fig. 2. The chromatograms show the distribution of DPs, each peak represents each DP. Considering as intervals of DP values as follow: 3−10, 11−20, 21−30, and 31−40. It can be seen that DPs 3–20 provided highest contents. Table 1 summarizes the effect of extraction temperatures for the extraction time of 20 min on the mean (n=2) of relative peak areas of each interval. It is clearly seen that the major DPs at all the studied temperatures are DP 3−10 and DP 11−20, totaling ca. 60

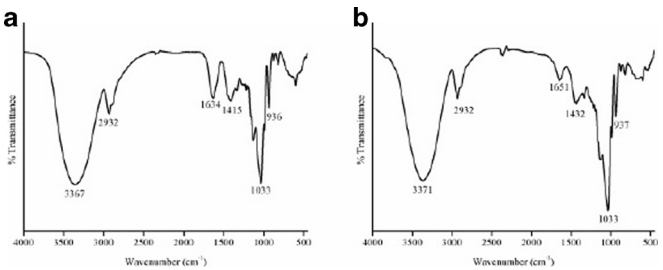


Fig. 4 Infrared spectra of inulin powder from **a** the produced inulin from JAT powder and **b** standard Chicory

−70 %. The separate amounts of DP3−10 and DP11−20 were in the same range of 30−39 % relative area for the extraction at the 80 °C with the average peak area of 37.77 and 37.81 % for DP3−10 and DP11−20, respectively. It can be concluded that the major DPs (DPs 3–20) obtained at 80 °C are higher than those from 70 to 100 °C. Therefore, the inulin profiles reveal the results which are in good agreement with the results in term of the extraction efficiency mentioned previously, *i.e.*, the optimum extraction condition was 80 °C for 20 min.

The primary advantage of using ASE to extract inulin from JAT powder is the rapid extraction time used (20 min), much shorter than the extraction time by the conventional method (1 −1.5 h) [6, 24]. The use of water as the extraction solvent is economical and it is environmentally more desirable since it does not use organic solvents. In addition, the extracts obtained from ASE were clear, without the need for filtration or centrifugation.

Elimination of Color from Inulin Extract

The obtained inulin extract has a dark brown color. Various methods have been used for the elimination of inulin extract color. For example, chemicals such as lead acetate [32], lime and carbon dioxide [33], dialysis process [9], activated carbon [20] and ion exchange resin [9, 34] were reported. In this study, chemical treatment and ion exchange were studied for elimination of the color in the extract. Visual observation as well as the absorption spectra was used to evaluate the effectiveness of the decolorization process. It was found that ion exchange process using anion exchange resin, DEAE −cellulose, is the most effective strategy color in inulin extract. The visual observation (data not shown) is in good agreement with the absorption spectrum (supplementary data) which shows significant reduction in absorbance at all visible wavelengths. In addition, inulin contents and profiles obtained after color elimination by DEAE-cellulose were not significantly different from those before the elimination process.

Preparation of Inulin Powder

In this study, freeze drying was used for solidification of inulin from the inulin extract. Freeze drying was chosen because it is performed at low temperature, thus the degradation of inulin can be minimized. The obtained inulin powder is white (Fig. 3a) and displays a texture similar to the Chicory inulin standard (Fig. 3b).

Some physico-chemical properties of the produced inulin powder were also studied and the results are compared to the standard inulin from Chicory. The infrared spectra are shown in Fig. 4, revealing the similarity of the peaks with the previous works [20, 35]. SEM images of the obtained inulin powder and chicory (Fig. 5a and b), show similar microphotographs of amorphous spherical shapes with some agglomerates.

Conclusion

This is the first report that demonstrates the systematical study for the preparation of inulin powder from Jerusalem artichoke tubers. Inulin was firstly isolated from tuber powder of Jerusalem artichoke using accelerated solvent extraction. The color of the inulin extract was eliminated using DEAE resin. Freeze drying was subsequently used for solidification of the inulin extract. The inulin content and inulin profiles were used to evaluate the efficiency of the procedure. The proposed method is efficient, rapid and is accomplished at a low cost. Under the optimum conditions, the inulin production yield calculated based on the obtained inulin powder and the powdered tuber used was 92.5 %.

Acknowledgments This work was financially supported by the Higher Education Research Promotion and National Research University Project of Thailand, Office of the Higher Education Commission, through the Food and Functional Food Research Cluster of Khon Kaen University (FC 1.1.1. MS) and the center for Innovation in Chemistry (PERCH-CIC). The authors thank Prof. Richard L. Deming (California State University of Fullerton, USA) for assistance with the English.

Conflict of Interest All authors report no conflict of interest.

References

1. Modler HW (1994) Bifidogenic factors-sources, metabolism and applications. Int Dairy J 4:383–407
2. Lingyun W, Jianhua W, Xiaodong Z, Da T, Yalin Y, Chenggang C, Tianhua F, Fan Z (2007) Studies on the extracting technical conditions of inulin from Jerusalem artichoke tubers. J Food Eng 79:1087–1093
3. Panchev I, Naiden D, Kovacheva D, Slavov A (2011) Physicochemical characteristics of inulins obtained from Jerusalem artichoke (*Helianthus tuberosus L.*). Eur Food Res Technol 233: 889–896
4. Prosky L, Hoebregs H (1999) Method of determine food inulin and oligofructose. J Nutr 129:1418s–1423s
5. Saengkanuk A, Nuchadomrong S, Jogloy S, Patanothai A, Srijaranai S (2011) A simplified spectrometric method for the determination of inulin in Jerusalem artichoke (*Helianthus tuberosus* L.) tubers. Eur Food Res Technol 233:609–616
6. Saengthongpinit W, Sajjaanantakul T (2005) Influence of harvest time and storage temperature on characteristics of inulin from Jerusalem artichoke (*Helianthus tuberosus* L.) tubers. Postharvest Biol Technol 37:93–100
7. Leroy G, Grongnet JF, Mabeau S, Corre DL, Baty Julien C (2010) Changes in inulin and soluble sugar concentration in artichokes (*Cynara scolymus* L.) during storage. J Sci Food Agric 90:1203–1209
8. Vulsteke G, Calus A (1990) Influence of variety, date of harvest and storage time on factors connected with the crystallisation on canned

scorzonera (*Scorzonera hispanica*). Plant Foods Hum Nutr 40:149–166
9. López−Molina D, Navarro−Martínez MD, Melgarejo FR, Hiner ANP, Chazarra S, Rodríguez−López JN (2005) Molecular properties and prebiotic effect of inulin obtained from artichoke (*Cynara scolymus* L.). Phytochemistry 66:1476–1484
10. Takeuchi J, Nagashima T (2011) Preparation of dried chips from Jerusalem artichoke (*Helianthus tuberosus*) tubers and analysis of their function properties. Food Chem 126:922–926
11. Roberford MB (2005) Introducing inulin-type fructans. Br J Nutr 93: S13–S25
12. Kiss A, Forgo P (2011) Investigations on inulin-type oligosaccharides with regard to HPLC analysis and prospective food applicability. Monatsh Chem 142:547–553
13. Vinatoru M (2001) An overview of the ultrasonically assisted extraction of bioactive principles from herbs. Ultrason Sonochem 8:303–313
14. Mussatto SI, Mancilha IM (2007) Non-digestible oligosaccharide: a review. Carbohydr Polym 68:587–597
15. Matías J, González J, Royana L, Barrena RA (2011) Analysis of sugar by liquid chromatography-mass spectrometry in Jerusalem artichoke tubers for bioethanol production optimization. Biomass Bioenerg 3:2006–2012
16. Zhao CH, Chi Z, Zhang F, Guo FJ, Li M, Song WB, Chi Z−M (2011) Direct conversion of inulin and extract of tubers of Jerusalem artichoke into single cell oil by co-cultures of *Rhodorula mucilaginosa* TJY15a and immobilized inulinase-producing yeast cells. Bioresour Technol 102:6128–6133
17. Pandino G, Lombardo S, Mauromicale G (2011) Chemical and morphological characteristics of new clones and commercial varieties of globe artichoke (*Cynara cardunculus* var. *scolymus*). Plant Foods Hum Nutr 66:291–297
18. Delgado GT, Tamashiro WM, Maróstica Junior MR, Pastore GM (2013) Yacon (*Smallanthus sonchifolius*): a functional food. Plant Foods Hum Nutr 68:222–228
19. Milani E, Koocheki A, Golimovahhed QA (2011) Extraction of inulin from Burdock root (*Arctium lappa*) using high intensity ultrasound. Int J Food Sci Technol 46:1699–1704
20. Abou−Arab AA, Talaat HA, Abu−Salem FM (2011) Physico−chemical properties of inulin produced from Jerusalem artichoke tubers on bench and pilot plant scale. Aust J Basic Appl Sci 5: 1297–1309
21. Van Loo J, Coussement P, De Leenmheer L, Hoebregs H, Smits G (1995) On the presence of inulin and oligofructose as natural ingredients in the western diet. Crit Rev Food Sci Nutr 35:525–552
22. Modler HW, Jones JD, Mazza G (1993) Observation on long-term storage and processing of Jerusalem artichoke tuber (*Helianthus tuberosus*). Food Chem 48:279–284
23. Van der Poel PW, Schiweek H, Schwartz T (1998) Sugar technology, beet and cane sugar manufacture, 1st edn. Bartens, Berlin
24. Baldini M, Danuso F, Turi M, Vannozzi GP (2004) Evaluation of new clones of Jerusalem artichoke (*Helianthus tuberosus* L.) for inulin and sugar yield from stalks and tubers. Ind Crop Prod 19:25–40
25. Gaafar AM, Serag El-Din MF, Boudy EA, El-Gazar HH (2010) Extraction conditions of inulin from Jerusalem artichoke tubers and its effects on blood glucose and lipid profile in diabetic rats. J Am Sci 6:36–43
26. Li H, Zhu H, Qioa J, Du J, Zhang H (2012) Optimization of the main liming process for inulin crude extract from Jerusalem artichoke tubers. Front Chem Sci Eng 6:348–355
27. Zhu Z, Bals O, Grimi N, Vorobiev E (2012) Pilot scale inulin extraction from chicory roots assisted by pulsed electric fields. Int J Food Sci Technol 47:1361–1368
28. Anand R, Verma N, Gupta DK, Puri SC, Hadda G, Sharma VK, Qazi GN (2005) Comparison of extraction techniques for extraction of bioactive molecules from *Hypericum perforatum* L. plant. J Chromatogr Sci 43(10):530–531
29. Upadhya V, Pai SR, Sharma AK, Hegde HV, Kholkute SD, Joshi RK (2014) Compound specific extraction of camptothecin from *Nothapodyte nimoniana* and piperine from *Piper nigrum* using accelerated solvent extractor. J Anal Methods Chem. doi:10.1155/2014/932036
30. Mey ED, Maere HD, Dewulf L, Paelinck H, Sajewicz M, Fraeye I, Kowalska T (2014) Application of accelerated solvent extraction (ASE) and thin layer chromatography (TLC) to determination of piperine in commercial samples of pepper (*Piper nigrum* L.). J Liq Chromatogr Relat Technol 37:2980–2988
31. Steegmans M, Iliaens S, Hoebregs H (2004) Enzymatic, spectrophotometric determination of glucose, fructose, sucrose, and inulin/oligofructose in foods. J AOAC Int 87:1200–1207
32. Wack M, Blaschek W (2006) Determination of the structure and degree of polymerization of fructans from *Echinacea purpurea* roots. Carbohydr Res 341:1147–1153
33. Zhi−fu Z, Hong−ji Z, Jin−jin Y, Chao L, Gui−yan G, Yi−wei Z (2009) Impurity removal from inulin extract of Jerusalem artichoke tubers by carbonation. Food Sci 30:67–71
34. Krzywonos M, Lapawa A (2012) Decolorisation of sugar beet molasses vinasse by ion exchange. Clean: Soil, Air, Water 40:1408–1414
35. Grube M, Bekers M, Kaminska E (2002) Infrared spectra of some fructans. Spectroscopy 16:289–296

Journal of Food Biochemistry

Journal of Food Biochemistry ISSN 1745-4514

HISTONE DEACETYLASE INHIBITORY ACTIVITY OF PEANUT TESTA EXTRACTS AGAINST HUMAN CANCER CELL LINES

SOMPRASONG KHAOPHA[1], SANUN JOGLOY[2], ARAN PATANOTHAI[2] and THANASET SENAWONG[1,3,4,5]

[1]Department of Biochemistry, Faculty of Science,
[2]Department of Plant Science and Agricultural Resources, Faculty of Agriculture,
[3]Natural Products Research Unit and
[4]Food and Products Chemical Analysis Research Group, Faculty of Science, Khon Kaen University, Khon Kaen 40002, Thailand

[5]Corresponding author.
TEL: 66-43-342-911;
FAX: 66-43-342-911;
EMAIL: sthanaset@kku.ac.th

Received for Publication August 4, 2014
Accepted for Publication February 9, 2015

doi:10.1111/jfbc.12128

ABSTRACT

Inhibition of histone deacetylase (HDAC) is a promising strategy for cancer treatment. In this study, HDAC inhibitory activity of 15 Valencia-type peanut testa extracts was assessed in mammalian cell model. Nine of 15 testa extracts exhibited HDAC inhibitory activity. Two peanut testa extracts (genotypes ICG15042 and KK4) possessing the greatest HDAC inhibitory activity could inhibit the growth of all five human cancer cell lines tested. At 72-h treatment, both ICG15042 and KK4 testa extracts showed the most effective growth inhibition on Jurkat T-leukemia cells with IC_{50} values of 28.81 and 30.00 μg/mL, respectively. Both extracts were more toxic against the cancerous cell lines, but safer toward a noncancer cell line. Growth inhibitory effects of both extracts appeared to be mediated by induction of apoptosis in a dose-dependent manner. Moreover, some phenolic acids including protocatechuic, syringic, *p*-coumaric, ferulic and sinapinic acids, which may underpin their anticancer activity, were also identified and analyzed quantitatively.

PRACTICAL APPLICATIONS

HDAC inhibitory potentials of phenolic-rich testa extracts of 15 Valencia-type peanut genotypes in mammalian cell model were evaluated. The results suggest that peanut skins (testae) of nine peanut genotypes possessed HDAC inhibitory activity and two of them (ICG15042 and KK4), with the highest HDAC inhibitory activity, could inhibit cancer cell growth via apoptosis induction. Accordingly, peanut skins could be useful for application in areas such as alternative medicine for cancer treatment and functional food for dietary prevention of cancer.

INTRODUCTION

Acetylation is one of the most important posttranslational modifications of the N-terminal tails of histones, which, in combination with phosphorylation, methylation and ubiquitination, contributes to a "histone code" determining the activity of target genes (Ververis *et al.* 2013; Chueh *et al.* 2014). Acetylation of core nucleosomal histones is regulated by a balance between the activities of histone acetyltransferases (HATs) and histone deacetylases (HDACs). The balance between HDACs and HATs is often impaired in cancer, which leads to aberrant expressions of tumor suppressor genes and/or proto-oncogenes (Kim and Bae 2011). Increased expression of classical HDACs has been found in several human cancers (Hrabeta *et al.* 2013) whereas decreased activity of the HDACs has been associated with suppression of growth and development of cancer cells (Zupkovitz *et al.* 2006; Montgomery *et al.* 2007). Moreover, both HATs and HDACs can also regulate gene expression indirectly by mediating posttranslational acetylation and deacetylation of several nonhistone protein substrates (Ocker 2010).

Based on the homology to their yeast analogs, HDACs are classified into four categories: (1) class I (HDACs 1, 2, 3 and 8); (2) class IIa (HDACs 4, 5, 7 and 9) and class IIb (HDACs 6 and 10); (3) class III (sirtuins or SIRT 1–7, NAD^+-dependent homologs of the yeast Sir2 proteins); and (4) class IV (HDAC 11, exhibiting features of both classes I and II) (Marks and Xu 2009). Eleven family members of classes I, II and IV, referred to as "classical" HDACs, require Zn^{2+} as

a cofactor for deacetylase activity, whereas class III members require NAD^+ as a cofactor (Witt *et al.* 2009). Accordingly, HDACs can be grouped into two distinct families as Zn^{2+} dependent and NAD^+ dependent based on the mechanisms of removing the acetyl groups.

Many types of HDAC inhibitors have been developed and classified as a new category of chemotherapeutic drugs currently in several clinical trials with promising results (Rasheed *et al.* 2007; Riester *et al.* 2007; Martinez-Iglesias *et al.* 2008; Marks and Xu 2009). The general structural characteristics of HDAC inhibitors that act on classical zinc-dependent HDAC isozymes are: (1) a zinc-binding moiety; (2) an opposite capping group; and (3) a straight chain alkyl, vinyl or aryl linker connecting the zinc-binding moiety and the capping group (Marks and Xu 2009). HDAC inhibitors acting on classical HDACs have been classified into four subtypes based on their chemical structures: (1) aliphatic acids or short chain fatty acids; (2) hydroxamic acids; (3) benzamides; and (4) cyclic peptides (Hrabeta *et al.* 2014). Treatments with HDAC inhibitors usually resulted in growth arrest, apoptosis and inhibition of angiogenesis in cancer cells (Marks and Xu 2009; Sánchez-Tena *et al.* 2013), with the cancer cell apoptosis effect being due to a shift in the balance of pro- and anti-apoptotic genes (Carew *et al.* 2008). Because of their low toxicity, HDAC inhibitors constitute a promising treatment for cancer, especially in combination with other chemotherapeutic agents (Carew *et al.* 2008; Bots and Johnstone 2009; Ma *et al.* 2009). Several studies have demonstrated that HDAC inhibitors enhance the anticancer activity of current anticancer drugs; therefore, the investigation on clinical application of HDAC inhibitors has increased dramatically (Gryder *et al.* 2012). However, serious side effects, such as fatigue, nausea, anorexia, diarrhea, anemia and myalgia, have been observed upon treatment with some HDAC inhibitors, especially pan-HDAC inhibitors (Rikiishi 2011) pointing to the need for safer and more effective HDAC inhibitors.

The phenolic compounds of some plants have been shown to possess HDAC inhibitory activity (Ahn *et al.* 2008; Bora-Tatar *et al.* 2009; Senawong *et al.* 2013). Peanut (*Arachis hypogaea* L.), one of the most popular foods consumed worldwide, is a potential source of natural phenolic compounds, especially in peanut skin (seed coat or testa) (Talcott *et al.* 2005; Khaopha *et al.* 2012). The major phenolic acids found in peanut testa are *p*-coumaric acid and *p*-hydroxybenzoic acid (Yu *et al.* 2005; Khaopha *et al.* 2012). The purified compound *p*-coumaric acid has been shown to exhibit anticancer activity (Janicke *et al.* 2011; Jaganathan *et al.* 2013; Kong *et al.* 2013), hence one can envision a phenolic-rich testa extract may possess anticancer activity due to, at least in part, its active component *p*-coumaric acid. To date, HDAC inhibitory and anticancer activities of peanut testa extracts have not been explored. In this study, we investigated the HDAC inhibitory activity of 15 Valencia-type peanut testae. In addition, two selected testa extracts with the greatest HDAC inhibitory activity and highest amount of phenolic content (KK4 and ICG15042) were investigated for their antiproliferative and apoptosis induction activities against five human cancer cell lines (HeLa, HT29, HCT116, Jurkat and MCF-7 cells) and one noncancer cell line (Vero cells). Moreover, their high-performance liquid chromatography (HPLC) profiles and phenolic acid compositions that may underpin their anticancer activity were also investigated.

MATERIALS AND METHODS

Materials

HCT116, MCF-7, HT29 and HeLa cells were kindly provided by Dr. O. Tetsu (University of California, San Francisco) and Dr. P. Picha (National Cancer Institute, Thailand). Jurkat and Vero cells were obtained from Dr. M. Leid (Oregon State University, Oregon) and Dr. S. Barusrux (Khon Kaen University, Thailand). The 15 Valencia-type peanut kernels (deposited in plastic bags and stored at 4C until used) of the 2010 crop (October 2010 to February 2011) were obtained from the Field Crop Research Station of Khon Kaen University, Thailand. Testae were removed from kernels as previously described (Khaopha *et al.* 2012). Most phenolic acid standards were purchased from Sigma-Aldrich Corporation (St. Louis, MO). Two phenolic acid standards, *m*-hydroxybenzaldehyde and *p*-hydroxybenzoic acid, were purchased from Fluka (Buchs, Switzerland) and Acros Organics (Geel, Belgium), respectively.

Cell Culture

All cell lines (human cervical adenocarcinoma [HeLa cells], human colon adenocarcinoma [HT29 cells], human colorectal carcinoma [HCT116 cells], human T-cell leukemia [Jurkat cells], human breast adenocarcinoma [MCF-7 cells]) and noncancer cell lines (Vero cells) were cultured in RPMI-1640 supplemented with 10% fetal bovine serum, 100 U/mL penicillin and 100 μg/mL streptomycin (Gibco BRL, Grand Island, NY). Cells in the culture media were incubated in a humidified incubator with an atmosphere of 95% air and 5% CO_2 at 37C.

Crude Methanolic Extraction

In a previously published paper, the highest yield of total phenolic compounds in peanut testae removed by direct peeling was obtained by methanolic extraction (Yu *et al.* 2005). Therefore, in this study, 100% methanol was used as a solvent for extraction of phenolic compounds from 15

peanut testae to obtain 15 "phenolic-rich" testa extracts. In brief, 1.0 g of ground testae (ground with a pestle and mortar) was macerated with 40 mL of methanol, stirred for 2 h at room temperature, and then centrifuged at 900 × g for 10 min. The aqueous suspension was filtered through filter paper (Whatman grade No. 4). The filtrate was evaporated to 2 mL using a rotary evaporator, and to dryness ultimately under a gentle stream of nitrogen. The testa extracts were considered phenolic-rich extracts and stored at −20C until used for HDAC inhibition, antiproliferation and apoptosis induction analyses.

Assessment of HDAC Inhibition in Mammalian Cells

Because of their high level of HDAC expression, HeLa cells were chosen as a mammalian cell model for evaluation of HDAC inhibition in mammalian cells. Cells were grown in a 4.5-cm dish and treated with 200 μg/mL of phenolic-rich extracts for 6 h. Cells treated with a potent HDAC inhibitor trichostatin A (TSA; 5 nM) and dimethyl sulfoxide (DMSO; 0.37%) were used as positive and negative controls, respectively. Extraction of histone proteins was performed as previously described (Senawong *et al.* 2013). Hyperacetylation of histone H4 in HeLa cells was determined by acid-urea-Triton (AUT) polyacrylamide gel electrophoresis (PAGE).

AUT X-100 PAGE

AUT gel electrophoresis was used to evaluate hyperacetylation of histone H4 due to HDAC inhibition in mammalian cell model as described previously (Senawong *et al.* 2013). Gels were stained using PageSilver Silver Staining Kit (Fermentas, Burlington, Ontario, Canada).

MTT Assay

Antiproliferative activity of two selected phenolic-rich extracts was determined by MTT assay as described by Senawong *et al.* (2013) with some modifications. Cancer cell lines (HeLa, HT29, HCT116, Jurkat and MCF-7 cells) and a noncancer cell line (Vero cells) were treated with two peanut testa extracts at varied concentrations of 15–90 μg/mL, and incubated for 24, 48 and 72 h. The KK4 and ICG15042 peanut testae were selected because of their high HDAC inhibitory activity (Fig. 1b) and total phenolic content among 15 Valencia-type peanut testae (Khaopha *et al.* 2012). The culture medium was replaced with fresh medium and the cells were treated with 10 μL of MTT for 2 h at 37C. The formazan dye was dissolved in DMSO, and the absorbance at 550 nm was measured with a microplate reader (Bio-Rad Laboratories, Hercules, CA). The absorbance at 655 nm was used as a reference wavelength. The number of viable cells was proportional to the production of formazan.

Analysis of Apoptosis by Flow Cytometry

Vybrant Apoptosis Assay Kit #2 (Molecular Probes, Invitrogen Corporation, Carlsbad, CA) was used for apoptosis analysis according to the manufacturer's instructions. Cells (1×10^6 cells) were seeded into a 4.5-cm dish and treated with different concentrations of KK4 and ICG15042 peanut testa extracts for 24 h. After treatment, cells were collected, washed with phosphate-buffered saline and centrifuged. Cells resuspended in ice-cold annexin-binding buffer were added with the Alexa Fluor 488 Annexin V and propidium iodide (PI) solutions and mixed gently. After 15-min incubation at room temperature in the dark, stained cells were analyzed by flow cytometry using a BD

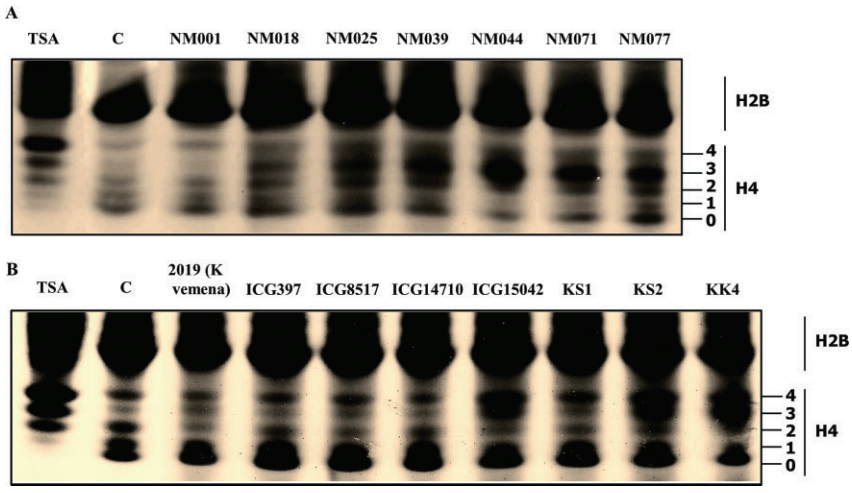


FIG. 1. HDAC INHIBITORY ACTIVITY OF 15 VALENCIA-TYPE PEANUT TESTA EXTRACTS, NEW MEXICO (A) AND OTHER VARIETIES (B), IN MAMMALIAN CELLS (HELA CELLS). CONTROL (C) REPRESENTS THE LEVEL OF HISTONE ACETYLATION IN VEHICLE CONTROL TREATMENT. THE TSA TREATMENT WAS USED AS A POSITIVE CONTROL. THE DEGREE OF HISTONE ACETYLATION OF HISTONE H4 IS INDICATED AS FOLLOWS: 0, NONACETYLATED; 1, MONOACETYLATED; 2, DIACETYLATED; 3, TRIACETYLATED; 4, TETRAACETYLATED. THE DATA SHOWN ARE REPRESENTATIVE OF TWO INDEPENDENT EXPERIMENTS PERFORMED IN DUPLICATE

FACSCantoII Flow Cytometer (Becton Dickinson, San Jose, CA).

Phenolic Acid Extraction

Up to 1.0 g of ground peanut testae was macerated in 40 mL of 100% methanol and stirred continuously for 2 h at room temperature. The mixture was filtered through Whatman grade No. 1 filter paper and the filtrate was then evaporated to 60 mL by a rotary evaporator. Further extraction of free and esterified phenolic acids from the 60 mL filtrate was performed as described by Khaopha *et al.* (2012).

HPLC

Reversed phase HPLC was used for identification of individual phenolic acids in extracts based on matching spectrum and retention times of phenolic acid standards as previously described by Khaopha *et al.* (2012). The individual phenolic acids in samples were analyzed quantitatively by using a standard curve and the internal standard (*m*-hydroxybenzaldehyde; 1 μg).

Statistical Analysis

Data were reported as means ± standard deviation calculated from three replicate experiments. Statistical analyses were carried out by using SPSS 11.5 for Windows (SPSS Corporation, Chicago, IL). Significant differences between groups were determined at $P < 0.05$ using one-way analysis of variance (ANOVA) with Duncan's post hoc test.

RESULTS AND DISCUSSION

HDAC Inhibitory Activity of Peanut Testa Extracts in Mammalian Cells

Inhibition of HDACs causes accumulation of acetylated forms of histone proteins (Marks and Xu 2009). Electrophoresis showed the band pattern for histone H4 acetylation in HeLa cells treated with methanolic crude extract, TSA or DMSO. As shown in Fig. 1, the addition of most phenolic-rich extracts to cell cultures resulted in accumulation of hyperacetylated histone H4 molecules, which could be detected clearly on AUT gel. However, treatment with 200 μg/mL each of the six methanolic crude testa extracts (NM001, 2019 [K vemena], ICG397, ICG8517, ICG14710, KS1) did not cause hyperacetylation of histone H4 in HeLa cells (Fig. 1a,b). Treatment of HeLa cells with phenolic-rich testa extracts of nearly all New Mexico varieties tested (NM018, NM025, NM039, NM044, NM071 and NM077) significantly increased triacetylated H4 molecules with three acetylated lysine residues (band 3) (Fig. 1a). After the cells were treated with phenolic-rich testa extracts of ICG15042, KS2 and KK4, the histone H4 with all four acetylated lysine residues (band 4) was significantly increased (Fig. 1b), indicating that the phenolic-rich testa extracts of these genotypes exhibited a greater HDAC inhibitory activity than those of the New Mexico varieties. The discrepancy on hyperacetylation pattern may be explained by different sensitivities of specific HDAC enzymes to the inhibitor(s) (Khan *et al.* 2008) and/or differences in mechanism of HDAC inhibition (Marks and Xu 2009). Further studies are needed to elucidate the specificity of the phenolic-rich testa extracts and their purified phenolic components for specific HDAC. However, the HDAC inhibitory activity of the methanolic crude extracts was less effective than that of a positive control TSA (5 nM), a very potent HDAC inhibitor (Bora-Tatar *et al.* 2009). These results indicated that phenolic-rich extracts of peanut testae could inhibit HDAC activity in mammalian cells, suggesting that some phenolic compounds in the extracts may function as HDAC inhibitors capable of inhibiting HDACs in the nucleus. Among the genotypes with high HDAC inhibitory activity (ICG15042, KS2 and KK4), ICG15042 and KK4 genotypes were also found to have the highest amount of total phenolic content among all 15 genotypes tested (Khaopha *et al.* 2012). Therefore, ICG15042 and KK4 were chosen for further study on their anticancer activity.

Although the link between hyperacetylation of histone proteins and cellular apoptosis is not fully understood, treatments with HDAC inhibitors usually cause a shift in the balance of pro- and anti-apoptotic genes toward apoptosis (Carew *et al.* 2008). Most HDAC inhibitors studied in clinical trials are synthetic compounds, which are mostly pan-HDAC inhibitors and still cause adverse side effects (Rikiishi 2011). According to our results, most of the phenolic-rich extracts of Valencia-type peanut testae appear to be promising natural sources of HDAC inhibitors, which are generally recognized as safe and edible. However, identification of individual phenolic compounds acting as HDAC inhibitors in peanut testae is needed.

Effect of Two Phenolic-Rich Extracts on Proliferation of Human Cancer Cell Lines

Two phenolic-rich extracts of peanut testae (KK4 and ICG15042) with the greatest HDAC inhibitory activity and phenolic content were investigated for their antiproliferative activity. Both ICG15042 and KK4 testa extracts significantly inhibited the proliferation of HeLa, HT29, HCT116 and Jurkat cells in a concentration- and time-dependent manner (Table 1). In contrast, a breast cancer cell line (MCF-7 cells) and a noncancer cell line (Vero cells) were less sensitive to both extracts (Table 1). The testa extracts of both ICG15042 and KK4 at concentrations less than 90 μg/mL were not cytotoxic toward a nontumorous cell line (Table 1). Based

TABLE 1. HALF MAXIMAL INHIBITORY CONCENTRATIONS (IC_{50}) OF ICG15042 AND KK4 TESTA EXTRACTS AFTER 24-, 48- AND 72-H EXPOSURES TO CANCER CELL LINES

Peanut testa extracts	IC_{50} values (mean ± SD; $n = 3$; μg/mL)																	
	Vero cells*		HeLa cells			HT29 cells			HCT116 cells			MCF-7 cells			Jurkat cells			
	24 h	48 h	72 h	24 h	48 h	72 h	24 h	48 h	72 h	24 h	48 h	72 h	24 h	48 h	72 h	24 h	48 h	72 h
ICG15042	>90	>90	>90	82.5 ± 1.34	57.22 ± 0.16	55.63 ± 1.24	69.13 ± 3.77	55.63 ± 1.24	44.26 ± 1.12	>90	62.42 ± 5.08	56.76 ± 0.70	>90	>90	>90	57.41 ± 2.90	44.62 ± 5.36	30.00 ± 2.11
KK4	>90	>90	>90	>90	69.57 ± 0.31	51.43 ± 1.48	60.01 ± 0.03	46.21 ± 0.45	44.48 ± 2.04	>90	69.57 ± 0.31	50.68 ± 0.25	>90	>90	>90	54.49 ± 4.33	42.36 ± 3.14	28.81 ± 1.91

* Noncancer cell line.

on the IC_{50} values at 24-, 48- and 72-h exposures, the human T-cell leukemia cell line (Jurkat cells) was considered the most sensitive cancer cell line to both ICG15042 and KK4 testa extracts (Table 1).

The HDAC inhibitory activity of phenolic-rich extracts of both ICG15042 and KK4 peanut testae makes the extracts more attractive for combination chemotherapy because HDACs are drug targets different from those of highly effective chemotherapeutic drugs such as cisplatin and doxorubicin. Combination therapy is now considered a standard approach to chemotherapy (Matés *et al*. 2009). In this regard, combining HDAC inhibitors vorinostat and sodium butyrate with aurora kinase inhibitors and doxorubicin, respectively, enhances cancer cell destruction (Cheriyath *et al*. 2011; Kretzner *et al*. 2011).

Effect of Two Phenolic-Rich Extracts on Apoptosis Induction of Human Cancer Cell Lines

To further confirm that induction of apoptosis underlies cancer cell growth inhibition of the two phenolic-rich extracts, their capacity to induce apoptosis in cancer cell lines was examined. As shown in Figs. 2 and 3, the results confirmed that both ICG15042 and KK4 testa extracts induced apoptosis of all cancer cell lines tested in a dose-dependent manner. Both testa extracts were the most effective on apoptosis induction of HeLa and HCT116 cells (Figs. 2 and 3). In contrast, treatment of a noncancer cell line with both ICG15042 and KK4 testa extracts at the highest concentration tested (150 μg/mL) resulted in early apoptotic cell death by only 1.8 ± 0.57% and 1.3 ± 0.14%, respectively. These amounts of apoptotic cells were not significantly different from that of the solvent control treatment (Figs. 2f and 3f), indicating that the noncancer cell line may be resistant to induction of apoptosis by both testa extracts. These results suggest that both ICG15042 and KK4 testa extracts may suppress the growth of human cancer cells through induction of apoptosis.

In this study, the "eat-me" signal of apoptotic cells (Ravichandran 2010), an externalized phosphatidylserine, was detected by a combined Annexin V/PI dual staining assay to confirm the cancer cell death via apoptosis. Although it is evident that both ICG15042 and KK4 testa extracts possessing HDAC inhibitory activity are capable of inducing apoptosis in all cancer cell lines tested, the link between HDAC inhibition by these extracts and cancer cell apoptosis is not clearly understood. HDAC inhibition leads to many changes at the molecular level (Carew *et al*. 2008; Marks and Xu 2009); therefore, further investigation is required to elucidate the consequences of both hyperacetylation and apoptosis induction by treatment with phenolic-rich testa extracts.

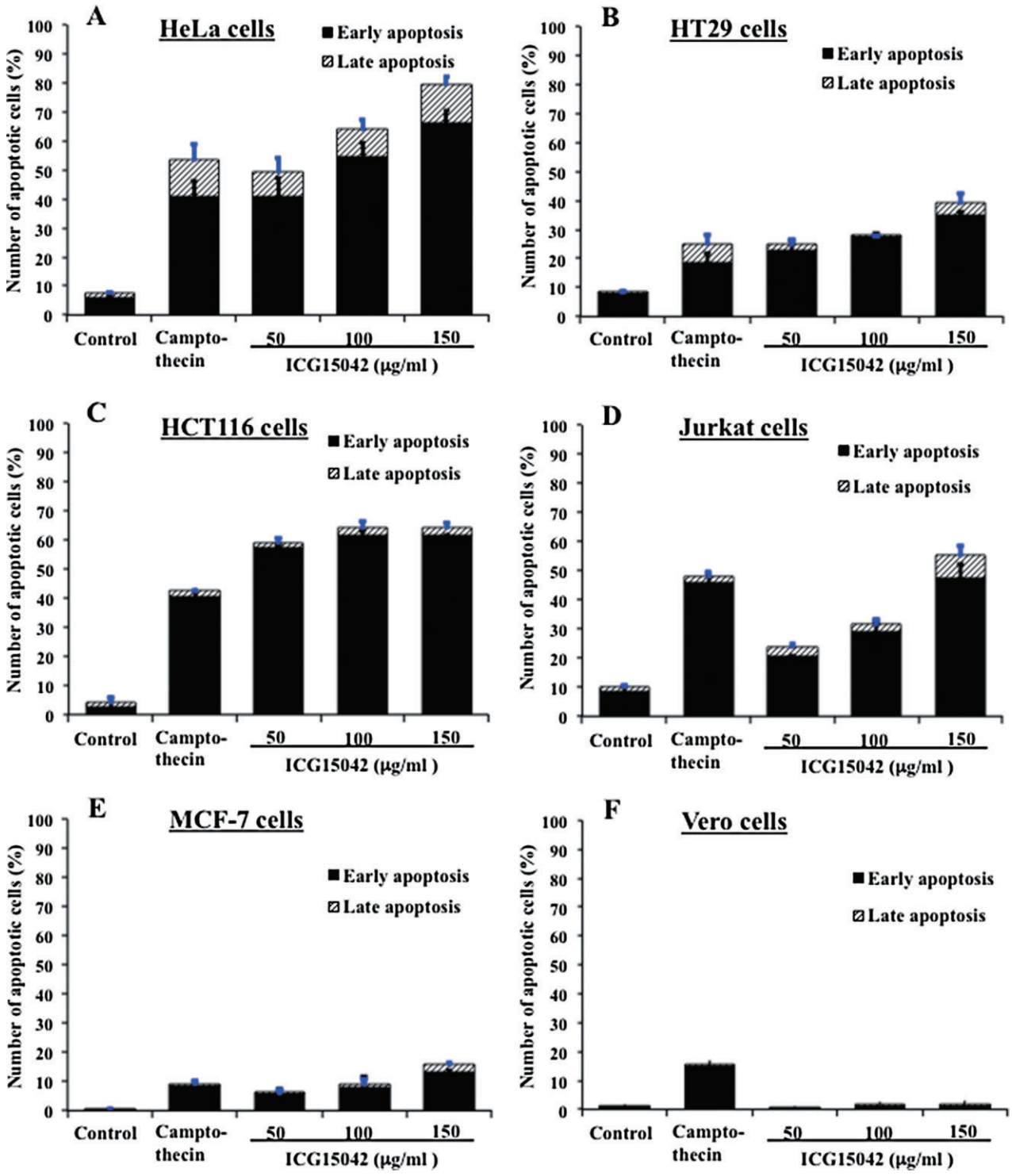


FIG. 2. APOPTOSIS INDUCTION ACTIVITY OF ICG15042 TESTA EXTRACT ON HUMAN CANCER CELL LINES, (A) HUMAN CERVICAL ADENOCARCINOMA CELL LINE (HELA CELLS), (B) HUMAN COLON ADENOCARCINOMA CELL LINE (HT29 CELLS), (C) HUMAN COLORECTAL CARCINOMA CELL LINE (HCT116 CELLS), (D) HUMAN T-CELL LEUKEMIA CELL LINE (JURKAT CELLS), (E) HUMAN BREAST ADENOCARCINOMA CELL LINE (MCF-7 CELLS) AND (F) NONCANCER CELL LINE (VERO CELLS). BAR GRAPH SHOWS THE SUMMARIZED DATA FROM TWO INDEPENDENT EXPERIMENTS PERFORMED IN DUPLICATE

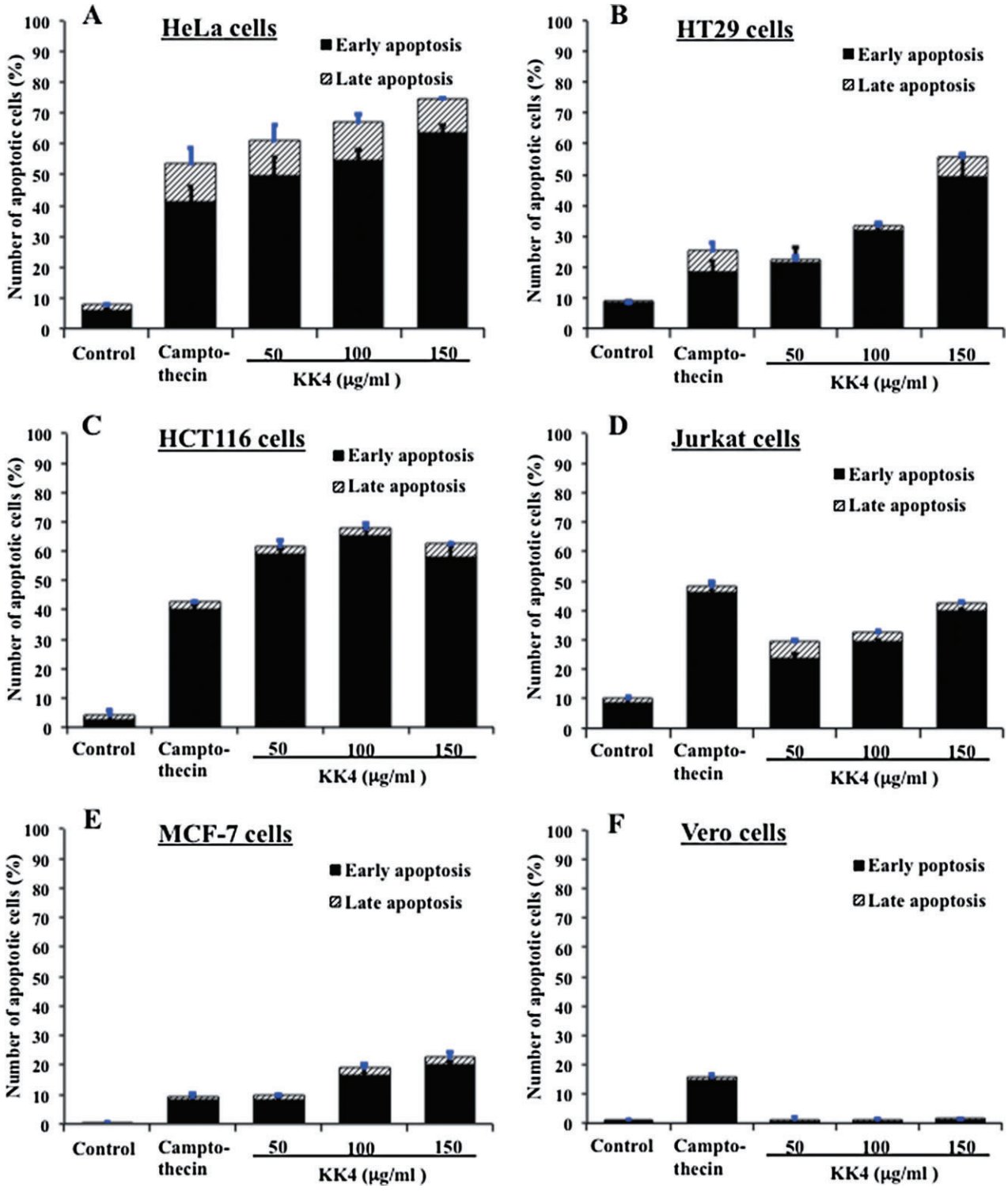
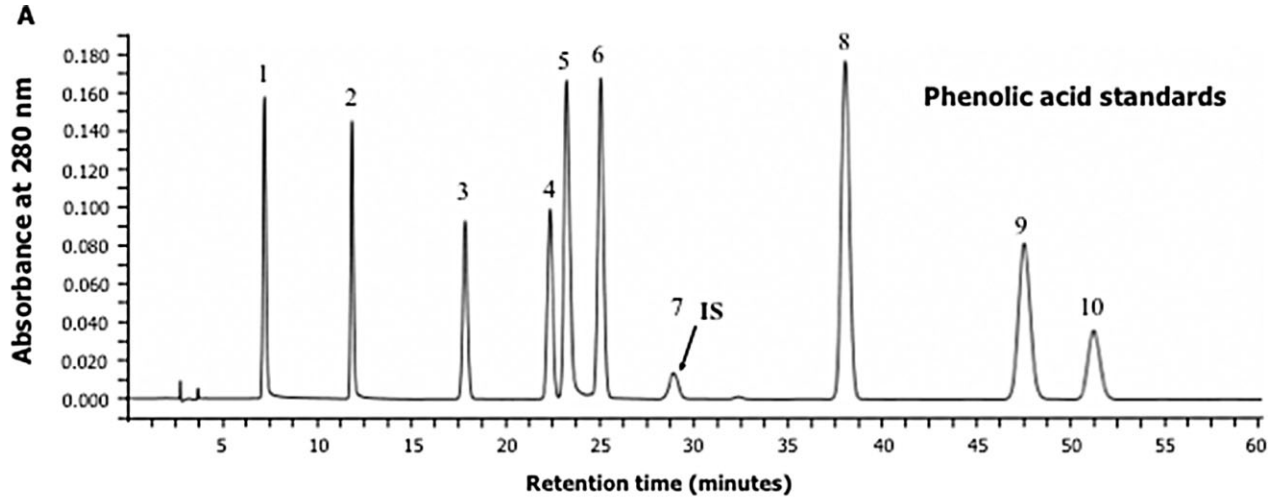
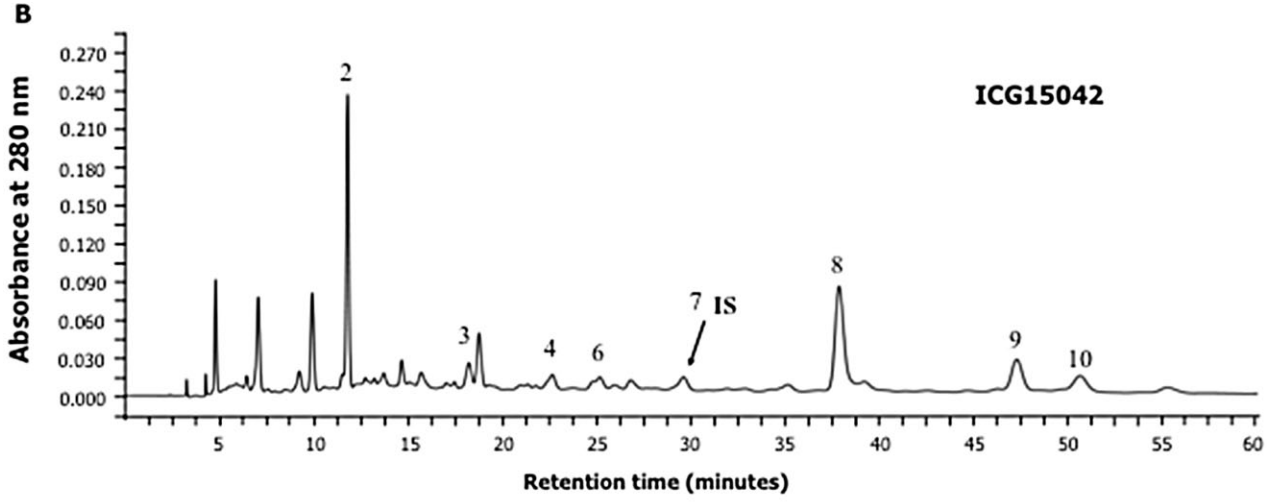


FIG. 3. APOPTOSIS INDUCTION ACTIVITY OF KK4 TESTA EXTRACT ON HUMAN CANCER CELL LINES, (A) HELA CELLS, (B) HT29 CELLS, (C) HCT116 CELLS, (D) JURKAT CELLS, (E) MCF-7 CELLS AND (F) NONCANCER CELL LINE (VERO CELLS). BAR GRAPH SHOWS THE SUMMARIZED DATA FROM TWO INDEPENDENT EXPERIMENTS PERFORMED IN DUPLICATE


A
Absorbance at 280 nm
Phenolic acid standards
1
2
3
4
5
6
7 IS
8
9
10
Retention time (minutes)


B
Absorbance at 280 nm
ICG15042
2
3
4
6
7 IS
8
9
10
Retention time (minutes)

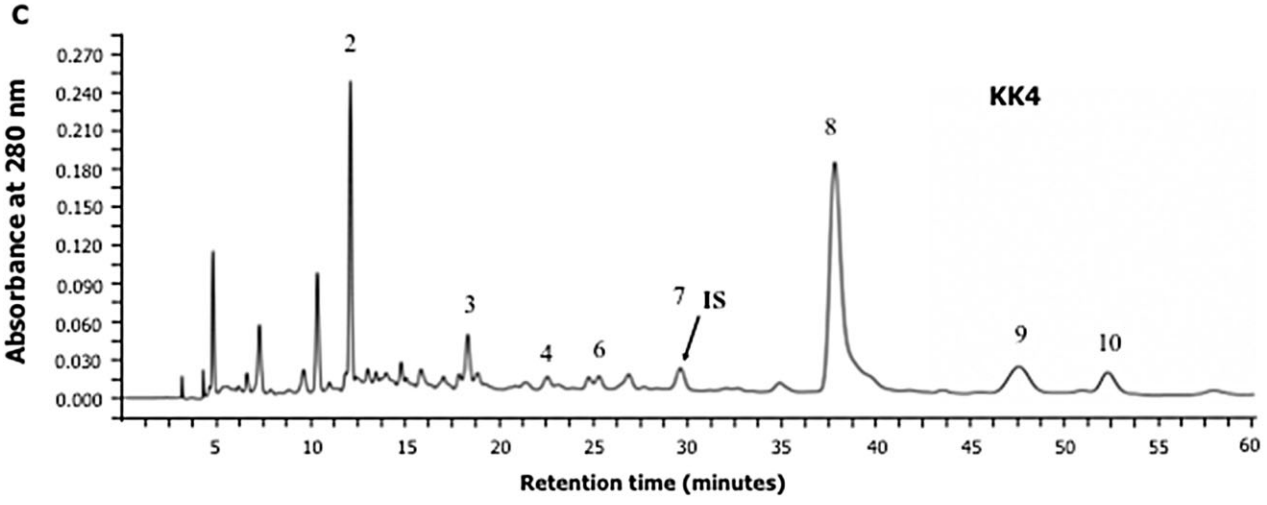

C
Absorbance at 280 nm
KK4
2
3
4
6
7 IS
8
9
10
Retention time (minutes)

FIG. 4. HPLC CHROMATOGRAMS OF PHENOLIC ACID STANDARDS AND ICG15042 AND KK4 TESTA EXTRACTS. HPLC PROFILES OF STANDARD PHENOLIC ACIDS (1 MG EACH) (A), ICG15042 (0.58 MG) (B) AND KK4 (0.68 MG) (C) TESTA EXTRACTS ADDED WITH THE INTERNAL STANDARD (IS), *M*-HYDROXYBENZALDEHYDE (1 MG), ARE DISPLAYED COMPARATIVELY. STANDARD PHENOLIC ACIDS USED ARE GALLIC ACID (1), PROTOCATECHUIC ACID (2), *P*-HYDROXYBENZOIC ACID (3), VANILLIC ACID (4), CAFFEIC ACID (5), SYRINGIC ACID (6), *M*-HYDROXYBENZALDEHYDE (7), *P*-COUMARIC ACID (8), FERULIC ACID (9) AND SINAPINIC ACID (10). THE DATA SHOWN ARE REPRESENTATIVE OF TWO INDEPENDENT EXPERIMENTS PERFORMED IN DUPLICATE

Phenolic Acid Composition of ICG15042 and KK4 Testa Extracts

Phenolic acid profiles of both ICG15042 and KK4 phenolic acid extracts presented in Fig. 4 were consistent with previous results (Khaopha *et al.* 2012). Figure 4 shows typical chromatograms of phenolic acid standards (Fig. 4a) and the two phenolic extracts (Fig. 4b,c). Seven phenolic acids including protocatechuic, *p*-hydroxybenzoic, vanillic, syringic, *p*-coumaric, ferulic and sinapinic acids were identified in both ICG15042 and KK4 testa extracts with protocatechuic and *p*-coumaric acids being the most predominant (Table 2). The confirmation of sample peak was obtained by Liquid chromatography-Mass spectrometry (LC-MS) analysis (data not shown). According to HPLC results, the amount of protocatechuic and vanillic acids in ICG15042 testa extract appeared to be slightly greater than that of KK4 testa extract, whereas the amount of *p*-coumaric and sinapinic acids in KK4 testa extract was greater than that of ICG15042 testa extract (Table 2).

There exists a previous study showing that phenolic acids inhibit HDAC and suppress malignant transformation stimulating apoptosis in HT-29 colon cancer cells (Waldecker *et al.* 2008). Accordingly, protocatechuic acid exhibited antiproliferative activity against HL-60 leukemia cells through induction of apoptosis (Anter *et al.* 2011). Syringic acid possessed proteasome inhibitory activity and inhibited the growth of human malignant melanoma cells (Orabi *et al.* 2013). Ferulic acid showed antiproliferative activities and apoptosis induction toward a bladder cancer cell line (Peng *et al.* 2013). *p*-Coumaric acid has been shown to inhibit the growth of HCT15 and HT29 cells by inducing apoptosis through reactive oxygen species (ROS)-mitochondrial pathway (Jaganathan *et al.* 2013), inhibit the growth of Caco-2 cells by inducing a G2/M phase cell cycle arrest (Janicke *et al.* 2011), and inhibit tumor growth *in vivo* through inhibition of angiogenesis (Kong *et al.* 2013). Recently, sinapinic acid has been shown to possess HDAC inhibitory activity and inhibit the growth of HeLa, HT29 and HCT116 cells (Senawong *et al.* 2013). The cytotoxic activity of both *p*-hydroxybenzoic and vanillic acids has not been reported yet. Nonetheless, the derivatives of *p*-hydroxybenzoic acid exhibited both HDAC inhibitory and anticancer activities (Seidel *et al.* 2013).

CONCLUSION

The results of this study showed that 9 of 15 phenolic-rich testa extracts of Valencia-type peanut genotypes possessed HDAC inhibitory activity in mammalian cell model. The inhibitory effect on five human cancer cell lines (HeLa, HT29, HCT116, Jurkat and MCF-7 cells) of both ICG15042 and KK4 testa extracts is in accordance with their ability to induce cancerous cell apoptosis. Both ICG15042 and KK4 testa extracts contained similar types and amounts of phenolic acids and their antiproliferative activity seemed to correlate with the phenolic acid profiles. Further investigation with details about HDAC inhibitory activity, anticancer activity of individual phenolic compounds found in peanut testae and their combination with other highly effective anticancer drugs is of interest. The findings may validate the use of peanut testae as alternative medicines for cancer treatment or dietary prevention of cancer.

ACKNOWLEDGMENTS

This work was supported by the Higher Education Research Promotion and National Research University Project of

TABLE 2. PHENOLIC ACID COMPOSITION OF PHENOLIC-RICH EXTRACTS OF TWO PEANUT TESTAE ANALYZED BY REVERSED PHASE HPLC

	Phenolic acids* (μg/g dry weight)						
Peanut testae	Protocatechuic acid	*p*-Hydroxybenzoic acid	Vanillic acid	Syringic acid	*p*–Coumaric acid	Ferulic acid	Sinapinic acid
ICG15042	42.30 ± 1.51[a]	15.76 ± 2.10[a]	9.63 ± 1.49[a]	5.68 ± 0.55[a]	16.37 ± 0.03[a]	9.02 ± 0.30[a]	7.57 ± 0.03[a]
KK4	34.09 ± 1.90[b]	11.60 ± 2.65[a]	6.91 ± 0.15[b]	6.12 ± 0.23[a]	29.37 ± 9.25[b]	10.44 ± 1.84[a]	12.09 ± 1.38[b]

* Values are means ± standard deviation of three replicates. Different superscript letters within the same column indicate significant differences ($P < 0.05$).

Thailand, Office of the Higher Education Commission, through the Food and Functional Food Research Cluster of Khon Kaen University. We thank Dr. N. Puppala and Dr. Hori Upadhyaya for providing peanut genotypes. We thank Dr. Prasan Swatsitang for technical advice on peanut extract preparation. This study was partially supported by the Thailand Research Fund (TRF) through the Distinguished Research Professor Grant for Prof. Aran Patanothai.

CONFLICT OF INTEREST

The authors declare that there are no conflicts of interest.

REFERENCES

AHN, M.Y., JUNG, J.H., NA, Y.J. and KIM, H.S. 2008. A natural histone deacetylase inhibitor, Psammaplin A, induces cell cycle arrest and apoptosis in human endometrial cancer cells. Gynecol. Oncol. *108*, 27–33.

ANTER, J., ROMERO-JIMÉNEZ, M., FERNÁNDEZ-BEDMAR, Z., VILLATORO-PULIDO, M., ANALLA, M., ALONSO-MORAGA, A. and MUÑOZ-SERRANO, A. 2011. Antigenotoxicity, cytotoxicity, and apoptosis induction by apigenin, bisabolol, and protocatechuic acid. J. Med. Food *14*, 276–283.

BORA-TATAR, G., DAYANGAC-ERDEN, D., DEMIR, A.S., DALKARA, S., YELEKCI, K. and ERDEM-YURTER, H. 2009. Molecular modifications on carboxylic acid derivatives as potent histone deacetylase inhibitors: Activity and docking studies. Bioorg. Med. Chem. *17*, 5219–5228.

BOTS, M. and JOHNSTONE, R.W. 2009. Rational combinations using HDAC inhibitors. Clin. Cancer Res. *15*, 3970–3977.

CAREW, J.S., GILES, F.J. and NAWROCKI, S.T. 2008. Histone deacetylase inhibitors: Mechanisms of cell death and promise in combination cancer therapy. Cancer Lett. *269*, 7–17.

CHERIYATH, V., KUHNS, M.A., KALAYCIO, M.E. and BORDEN, E.C. 2011. Potentiation of apoptosis by histone deacetylase inhibitors and doxorubicin combination: Cytoplasmic cathepsin B as a mediator of apoptosis in multiple myeloma. Br. J. Cancer *104*, 957–967.

CHUEH, A.C., TÖGEL, L., MARIADASON, J. and TSE, J.W. 2014. Mechanisms of HDAC inhibitor-regulated gene expression in cancer cells. Antioxid. Redox Signal 2014, *5863*, 1–19.

GRYDER, B.E., SODJI, Q.H. and OYELERE, A.K. 2012. Targeted cancer therapy: Giving histone deacetylase inhibitors all they need to succeed. Future Med. Chem. *4*, 505–524.

HRABETA, J., STIBOROVA, M., ADAM, V., KIZEK, R. and ECKSCHLAGER, T. 2014. Histone deacetylase inhibitors in cancer therapy. A review. Biomed. Pap. Med. Fac. Univ. Palacky Olomouc Czech. Repub. *158*, 161–169.

JAGANATHAN, S.K., SUPRIYANTO, E. and MANDAL, M. 2013. Events associated with apoptotic effect of *p*-Coumaric acid in HCT-15 colon cancer cells. World J. Gastroenterol. *19*, 7726–7734.

JANICKE, B., HEGARDT, C., KROGH, M., ONNING, G., AKESSON, B., CIRENAJWIS, H.M. and OREDSSON, S.M. 2011. The antiproliferative effect of dietary fiber phenolic compounds ferulic acid and *p*-coumaric acid on the cell cycle of Caco-2 cells. Nutr. Cancer *63*, 611–622.

KHAN, N., JEFFERS, M., KUMAR, S., HACKETT, C., BOLDOG, F., KHRAMTSOV, N., QIAN, X.Z., MILLS, E., BERGHS, S.C., CAREY, N. *et al*. 2008. Determination of the class and isoform selectivity of small-molecule histone deacetylase inhibitors. Biochem. J. *409*, 581–589.

KHAOPHA, S., SENAWONG, T., JOGLOY, S. and PATANOTHAI, A. 2012. Comparison of total phenolic content and composition of individual phenolic acids in testae and testa-removed kernels of 15 Valencia-type peanut (*Arachis hypogaea* L.) genotypes. Afr. J. Biotechnol. *11*, 15923–15930.

KIM, H.J. and BAE, S.C. 2011. Histone deacetylase inhibitors: Molecular mechanisms of action and clinical trials as anti-cancer drugs. Am. J. Transl. Res. *3*, 166–179.

KONG, C.S., JEONG, C.H., CHOI, J.S., KIM, K.J. and JEONG, J.W. 2013. Antiangiogenic effects of *p*-coumaric acid in human endothelial cells. Phytother. Res. *27*, 317–323.

KRETZNER, L., SCUTO, A., DINO, P.M., KOWOLIK, C.M., WU, J., VENTURA, P., JOVE, R., FORMAN, S.J., YEN, Y. and KIRSCHBAUM, M.H. 2011. Combining histone deacetylase inhibitor vorinostat with aurora kinase inhibitors enhances lymphoma cell killing with repression of c-Myc, hTERT, and micro-RNA levels. Cancer Res. *71*, 3912–3920.

MA, X., EZZELDIN, H.H. and DIASIO, R.B. 2009. Histone deacetylase inhibitors: Current status and overview of recent clinical trials. Drugs *69*, 1911–1934.

MARKS, P.A. and XU, W.S. 2009. Histone deacetylase inhibitors: Potential in cancer therapy. J. Cell. Biochem. *107*, 600–608.

MARTINEZ-IGLESIAS, O., RUIZ-LLORENTE, L., SANCHEZ-MARTINEZ, R., GARCIA, L., ZAMBRANO, A. and ARANDA, A. 2008. Histone deacetylase inhibitors: Mechanism of action and therapeutic use in cancer. Clin. Transl. Oncol. *10*, 395–398.

MATÉS, J.M., SEGURA, J.A., ALONSO, F.J. and MÁRQUEZ, J. 2009. Natural antioxidants: Therapeutic prospects for cancer and neurological diseases. Mini Rev. Med. Chem. *9*, 1202–1214.

MONTGOMERY, R.L., DAVIS, C.A., POTTHOFF, M.J., HABERLAND, M., FIELITZ, J., QI, X., HILL, J.A., RICHARDSON, J.A. and OLSON, E.N. 2007. Histone deacetylases 1 and 2 redundantly regulate cardiac morphogenesis, growth, and contractility. Genes Dev. *21*, 1790–1802.

OCKER, M. 2010. Deacetylase inhibitors-focus on non-histone targets and effects. World J. Biol. Chem. *1*, 55–61.

ORABI, K.Y., ABAZA, M.S., EL SAYED, K.A., ELNAGAR, A.Y., AL-ATTIYAH, R. and GULERI, R.P. 2013. Selective growth inhibition of human malignant melanoma cells by syringic

acid-derived proteasome inhibitors. Cancer Cell Int. 2013, *82*, 1–15.

PENG, C.C., CHYAU, C.C., WANG, H.E., CHANG, C.H., CHEN, K.C., CHOU, K.Y. and PENG, R.Y. 2013. Cytotoxicity of ferulic acid on T24 cell line differentiated by different microenvironments. Biomed Res. Int. 2013, *579859*, 1–7.

RASHEED, W.K., JOHNSTONE, R.W. and PRINCE, H.M. 2007. Histone deacetylase inhibitors in cancer therapy. Expert Opin. Investig. Drugs *16*, 659–678.

RAVICHANDRAN, K.S. 2010. Find-me and eat-me signals in apoptotic cell clearance: Progress and conundrums. J. Exp. Med. *207*, 1807–1817.

RIESTER, D., HILDMANN, C. and SCHWIENHORST, A. 2007. Histone deacetylase inhibitors – Turning epigenic mechanisms of gene regulation into tools of therapeutic intervention in malignant and other diseases. Appl. Microbiol. Biotechnol. *75*, 499–514.

RIKIISHI, H. 2011. Autophagic and apoptotic effects of HDAC inhibitors on cancer cells. J. Biomed. Biotechnol. 2011, *830260*, 1–9.

SÁNCHEZ-TENA, S., VIZÁN, P., DUDEJA, P.K., CENTELLES, J.J. and CASCANTE, M. 2013. Green tea phenolics inhibit butyrate-induced differentiation of colon cancer cells by interacting with monocarboxylate transporter 1. Biochim. Biophys. Acta *1832*, 2264–2270.

SEIDEL, C., SCHNEKENBURGER, M., DICATO, M. and DIEDERICH, M. 2013. Antiproliferative and proapoptotic activities of 4-hydroxybenzoic acid-based inhibitors of histone deacetylases. Cancer Lett. *343*, 134–146.

SENAWONG, T., MISUNA, S., KHAOPHA, S., NUCHADOMRONG, S., SAWATSITANG, P., PHAOSIRI, C., SURAPAITOON, A. and SRIPA, B. 2013. Histone deacetylase (HDAC) inhibitory and antiproliferative activities of phenolic-rich extracts derived from the rhizome of *Hydnophytum formicarum* Jack.: Sinapinic acid acts as HDAC inhibitor. BMC Complement. Altern. Med. *2013*, 232.

TALCOTT, S., PASSERETTI, S., DUNCAN, C. and GORBET, W. 2005. Polyphenolic content and sensory properties of normal and high oleic acid peanuts. Food Chem. *90*, 379–388.

VERVERIS, K., HIONG, A., KARAGIANNIS, T.C. and LICCIARDI, P.V. 2013. Histone deacetylase inhibitors (HDACIs): Multitargeted anticancer agents. Biologics *7*, 47–60.

WALDECKER, M., KAUTENBURGER, T., DAUMANN, H., BUSCH, C. and SCHRENK, D. 2008. Inhibition of histone-deacetylase activity by short-chain fatty acids and some polyphenol metabolites formed in the colon. J. Nutr. Biochem. *19*, 587–593.

WITT, O., DEUBZER, H.E., MILDE, T. and OEHME, I. 2009. HDAC family: What are the cancer relevant targets? Cancer Lett. *277*, 8–21.

YU, J., AHMEDNA, M. and GOKTEPE, I. 2005. Effects of processing methods and extraction solvents on concentration and antioxidant activity of peanut skin phenolics. Food Chem. *90*, 199–206.

ZUPKOVITZ, G., TISCHLER, J., POSCH, M., SADZAK, I., RAMSAUER, K., EGGER, G., GRAUSENBURGER, R., SCHWEIFER, N., CHIOCCA, S., DECKER, T. *et al*. 2006. Negative and positive regulation of gene expression by mouse histone deacetylase 1. Mol. Cell. Biol. *26*, 7913–7928.

Biomass and Bioenergy 81 (2015) 369–377

Contents lists available at ScienceDirect

Biomass and Bioenergy

journal homepage: http://www.elsevier.com/locate/biombioe

Research paper

Root responses of Jerusalem artichoke genotypes to different water regimes

R. Ruttanaprasert [a], S. Jogloy [a, b, *], N. Vorasoot [a], T. Kesmala [a], R.S. Kanwar [c], C.C. Holbrook [d], A. Patanothai [a]

[a] Department of Plant Science and Agricultural Resources, Faculty of Agriculture, Khon Kaen University, Muang, Khon Kaen, Thailand
[b] Peanut and Jerusalem Artichoke Improvement for Functional Food Research Group, Khon Kaen University, Muang, Khon Kaen, Thailand
[c] Department of Agricultural & Biosystems Engineering, Iowa State University, Ames, IA, USA
[d] USDA-ARS, Coastal Plain Experiment Station, P.O. Box 748, Tifton, 31793, GA, USA

ARTICLE INFO

Article history:
Received 10 November 2014
Received in revised form
19 July 2015
Accepted 20 July 2015
Available online 31 July 2015

Keywords:
Drought
Available soil water
Helianthus tuberosus L.
Crop adaptation
Drought tolerance
Bioenergy

ABSTRACT

The objective of this study was to determine effects of drought on selected root growth parameters and develop relationships between root parameters and tuber yield for selected Jerusalem artichoke (JA) genotypes. Three water regimes (Field capacity, 50% available soil water (AW) and 25% AW) and five JA varieties (JA 60, JA 125, JA 5, JA 89 and HEL 65) were planted with factorial treatments in a randomized complete block design with four replications. Data on root dry weight (RDW) and root: shoot ratios (RSR) were measured manually. Root diameter (RD), root length (RL), root surface area (RSA) and root volume (RV) were collected at harvest. Drought tolerance indices (DTI) were calculated for all root parameters. Drought reduced all root parameters and DTI but increased RSR in JA 60, JA 125, JA 5, and HEL 65. JA 125 had high values for all root traits and DTI of these traits under drought stress. JA 60 had high DTI of RDW, RD and RSR under mild and severe water stress. JA 5 had high DTI of RDW, RD, RL, RSR and RV under drought conditions. JA 89 and HEL 65 performed well for RDW, RD, RL and low DTI of all root characteristics. DTI for root parameters were positively correlated with tuber dry weight under mild and severe water stress. The JA 5, JA 60 and JA 125 varieties showed high DTI for some root traits, indicating that better root parameters contributed to higher tuber yield under drought stress.

© 2015 Elsevier Ltd. All rights reserved.

1. Introduction

Jerusalem artichoke (*Helianthus tuberosus* L.) is a tuber crop containing inulin that can be used as raw material in many industries. Inulin can be used as soluble dietary fiber or sugar replacement for diabetes disease in the medicine industry, as a stabilizer in the pharmaceutical industry [1] and as raw material for biofuels [2,3]. Jerusalem artichoke is a new crop that has the potential to be grown in temperate and tropical regions of the world.

Global warming may cause more severe and frequent droughts due to either decreased precipitation and/or increased evaporation [4]. Drought reduces productivity of agricultural crops including Jerusalem artichoke [5–10]. Yield loss of 20% under mild water stress has been reported [5,6] and yield loss higher than 90% has been reported under severe drought stress [11]. Although drought problems can be alleviated by irrigation, management of irrigation systems is sometimes difficult in those geographical areas of the world where water resource are not either readily available or too expensive to maintain. The development and utilization of drought tolerant varieties would be ideal in these drought prone areas of the world.

The selection of Jerusalem artichoke for drought tolerance has primary been based on biomass production and tuber dry weight under drought stress conditions. In tropical regions of the world, JA 5 was reported as a drought tolerant variety with high tuber yield under drought stress conditions [11]. The progress in breeding for drought tolerance varieties has been slow because yield and related traits vary greatly, depending on ecological environmental conditions. A better understanding of some physiological mechanisms of drought resistance varieties should accelerate the progress in breeding for high tuber productivity under drought stress.

Drought tolerance may be enhanced by exploiting drought

* Corresponding author. Department of Plant Science and Agricultural Resources, Faculty of Agriculture, Khon Kaen University, Muang, Khon Kaen 40002, Thailand. Tel./fax: +66 43 364 637.
E-mail address: sjogloy@gmail.com (S. Jogloy).

http://dx.doi.org/10.1016/j.biombioe.2015.07.027
0961-9534/© 2015 Elsevier Ltd. All rights reserved.

avoidance mechanisms such as the ability of roots to extract water from the soil. Root dry weight, root length, root: shoot ratio [12], deep root and root length density [13–16] have been identified as drought-adaptive traits and they could be used as selection criteria for drought resistance traits. However, root characteristics of Jerusalem artichoke in responses to drought have not been clearly investigated. Therefore, the objective of this study was to determine the effects of drought on selected root growth parameters of Jerusalem artichoke and develop relationships between root growth parameters (characters) and tuber yield for selected drought resistance varieties of Jerusalem artichoke genotypes. The new scientific information from this research on the ability of root traits of selected Jerusalem artichoke genotypes contributing to high tuber yield under water stress are likely to reveal the avoidance mechanism and could result in the development of improved breeding strategies for drought tolerance in Jerusalem artichoke.

2. Materials and methods

2.1. Experimental design and treatments

Pot experiments were conducted at the Field Crop Research Station of Khon Kaen University located in Khon Kaen province, Thailand (16°28′ N, 102°48′ E, 200 m above mean sea level). The experimental treatments were arranged in a 3 × 5 factorial experiment in randomized complete block design with four replications for each treatment and experiments were conducted for two years during May to September 2012 and May to September 2013. Factor A consisted of three water regimes including field capacity (FC), 50% available soil water (50% AW) and 25% available soil water (25% AW) and factor B included five Jerusalem artichoke varieties with different drought tolerance levels based on tuber yield under drought stress. The experimental unit consisted of 5 pots requiring a total of 300 pots for each experiment. The varieties JA 60 and JA 125 had low tuber yield, JA 5 had intermediate tuber yield and JA 89 and HEL 65 had high tuber dry weight under drought stress conditions [11].

2.2. Preparation of plants and pot materials

Tubers with uniform size were cut into small pieces with 2–3 buds per piece. The tuber pieces were then pre-sprouted in charred rice husk with mixed trichoderma in the ratio of 3:1 by volume under ambient conditions for 4–7 days to control *Sclerotium rolfsii*. The sprouted tuber pieces were then transferred to germinating plug trays with mixed medium containing soil, charred rice husk and trichoderma (3:2:2) for 7 days to complete sprouting. Healthy and uniform seedlings were then transplanted to plastic pot containers (1 plant pot^{-1}).

The plastic containers with 35 cm in diameters and 25 cm in height were then filled with 20 kg of dry soil which was separated into two layers to create uniform bulk density. The first soil fraction of 10 kg of dry soil was filled in the bottom of the container at 10 cm below the soil surface, and the second soil fraction of remaining 10 kg was filled to 5 cm below the top of the pot. The water tubes were installed at the middle of these soil fractions. One seedling was transplanted into each container. Wood vinegar obtained from slow pyrolysis of wood was sprayed on Jerusalem artichoke plants two times per week at the dilution of 5 cm^3 wood vinegar in a liter of water to control insects in the pots. Weeds were controlled manually after transplanting and fertilizer grade 15-15-15 was applied to each pot at the rate of 2 g per pot or 265 kg ha^{-1} at 15 days after transplanting (DAT).

2.3. Water management

Water was applied to each pot as per each water treatment and based on crop water requirements (ETcrop) [17] plus to meet the daily surface evaporation (S.E.) needs of pots [18]. Crop water requirements for each pot were calculated as per the requirements of experimental treatments and using the methods described by Ref. [17]:

$$\mathrm{ETcrop} = \mathrm{kc} \times \mathrm{ETo},$$

where ETcrop is the crop water requirement (mm day^{-1}), ETo is evapotranspiration of reference crop and kc is the coefficient of the crop at different growth stages. The crop coefficient (kc) of the Jerusalem artichoke was not found in literature, therefore, kc of sunflower was used [8,10].

Surface evaporation (S.E.) was calculated as [18]:

$$\mathrm{S.E.} = \beta(E_o/t),$$

where S.E. is the soil evaporation (mm), β is the light transmission coefficient measured depending on crop cover, E_o is the evaporation from class A pan (mm day^{-1}), t is the days from the last irrigation.

To maintain a uniform water supply in the whole pot, the irrigation was divided into two fractions. Water was supplied to the soil fractions through the plastic tubes previously installed to the containers. At pre-transplanting, water was supplied to all pots and moisture level was maintained at FC (20.5% of soil moisture content) until 10 DAT for uniform establishment of the plants. Water treatments (20.5% of soil moisture content in FC, 13.9% of soil moisture content in 50% AW and 10.6% of soil moisture content in 25% AW) were imposed to the crop after 14 DAT and maintained uniformly with no more than 1% fluctuation until harvest.

The irrigation supplied to each pot was equal to the sum of water used by the crop and to meet the daily soil surface evaporation needs. The soil water status was also monitored by gravimetric method for soil moisture collection at 7-days interval. The added water irrigation was applied to each pot once a week for maintaining the level of soil moisture treatment.

2.4. Data collection

2.4.1. Meteorology conditions

Weather data for two years were recorded daily from transplanting until crop harvest by a weather station located 100 m away from the experimental field. Maximum temperatures, minimum temperature, daily pan evaporation and daily relative humidity were recorded at this experiment station (Fig. 1).

2.4.2. Soil data

The data on soil texture and chemical properties were collected using ten randomly selected points in the field from where the whole soil was collected and mixed to create two sets of soil samples. The first set was analyzed for field capacity and permanent wilting percentage of soil for irrigation management. The second set was analyzed for the soil texture and the soil chemical properties including total N and available P, pH, organic matter, exchangeable K and Ca and cation exchange capacity.

Soil moisture contents were recorded by gravimetric method at 30, 60 and 90 DAT at the depth of 0–20 cm (Fig. 2).

2.4.3. Plant data

Relative water content (RWC) in each experimental unit was measured at 30, 60 and 90 DAT to estimate plant water status. The

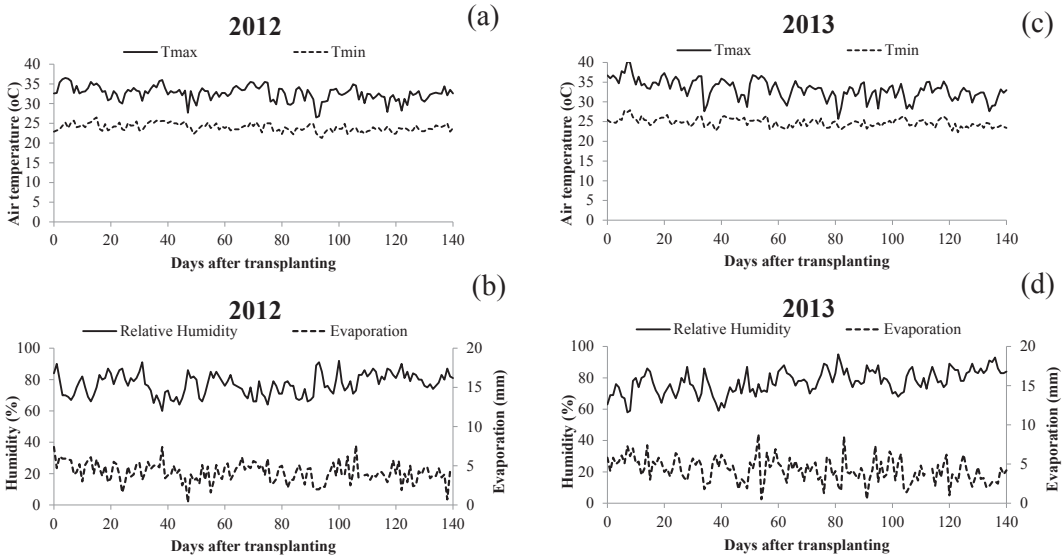


Fig. 1. Maximum temperatures (Tmax), minimum air temperatures (Tmin) (°C), evaporation (mm) and relative humidity (%) in 2012 (a), (b) and 2013 (c), (d).

second leaves from the top of the main stem the five plants in each experimental unit were bored by a disc borer with 1 cm^2 in leaf area. Saturated weight was determined by putting the leaf samples in water for 8 h, blot drying the outer surface, and then measuring leaf weight. The leaf samples were then oven-dried at 80 °C for at least 72 h or until the leaf weights were constant. RWC was calculated as follows [19]:

$$\mathrm{RWC} = \frac{\text{Fresh weight} - \text{Dry weight}}{\text{Saturated weight} - \text{Dry weight}} \times 100$$

The mature plants, which were determined by stem browning of 50%, were cut at the soil surface at harvest. The below ground parts of plants were then separated and washed with tap water to remove soil particles and then separated into tubers and roots. Ten percentage of mass fraction were then taken from the total root mass for further root characteristics including root diameter (mm), root surface (cm^2 $plant^{-1}$), root length (cm $plant^{-1}$) and root volume (cm^3 $plant^{-1}$). Data on root characterization were analyzed using the WINRHIZO Pro2004a software. Roots (plus ten percentage mass fraction of roots) and tubers were then oven-dried at 80 °C for at least 72 h or until the weights were found to be constant. Tuber dry weight (g $plant^{-1}$) and root dry weight (plus ten percentage mass fraction of roots) (g) were recorded.

DTI was calculated for root characteristics (root surface, root length and root volume) using the relationship as follows:

$$\mathrm{DTI} = \frac{\text{Root characteristics under drought stress conditions}}{\text{Root characteristics under non} - \text{drought stress conditions}}$$

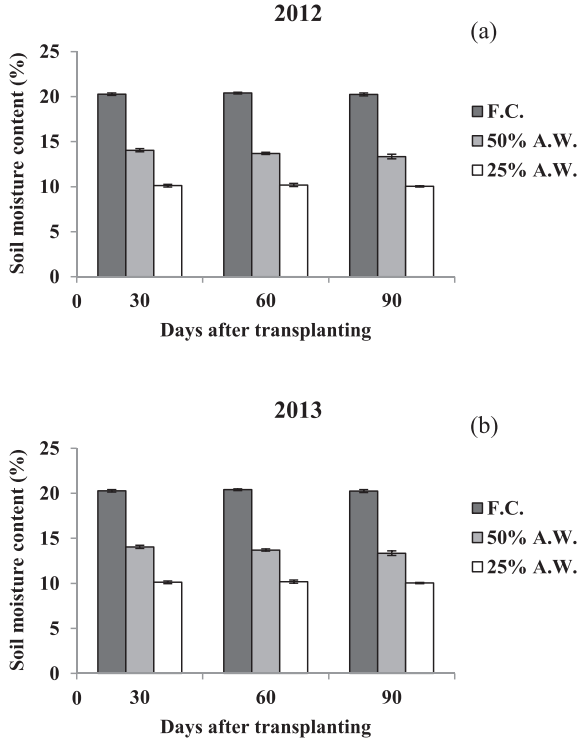


Fig. 2. Soil moisture content (%) under three water regimes (FC = field capacity, 50% AW = 50% of soil available water and 25% AW = 25% of soil available water) at 30 days after transplanting (DAT), 60 DAT and 90 DAT of five Jerusalem artichoke genotypes during 2012 (a) and 2013 (b).

2.5. Statistical analysis

Individual analysis of variance was conducted for each root growth parameter or characteristics for each year according to randomize complete block design (RCBD) [20] and all calculations were done using STATISTIX8 software. Variances for all root growth parameters/characters were tested for homogeneity. Least significant difference (LSD) was used to compare means when the differences of main effects were significant ($p \leq 0.05$). Correlation coefficients between DTI of root traits and tuber dry weight were calculated to determine their relationship between the parameters.

3. Results

3.1. Weather conditions

Maximum temperature (Tmax) and minimum temperature

(Tmin) in 2012 ranged between 26.5 and 36.5 °C and between 21.3 and 26.5 °C, respectively (Fig. 1a), Tmax and Tmin in 2013 ranged between 25.7–40.4 °C and 22.3–27.9 °C, respectively (Fig. 1c).Daily pan evaporation ranged from 0.3 to 7.6 mm per day in 2012 and from 0.5 to 8.8 mm per day in 2013 (Fig. 1b and d). The relative humidity values were 60%–92.0% and 58%–95% in the first and second years, respectively (Fig. 1b and d).

3.2. Soil type, soil moisture contents, and plant water status

The soil used for this experiment was loamy sand in both years and characterized as having proportions of sand ranged from 80 to 81%, silt ranged from 15 to 18% and clay ranged from 2 to 4% (Table 1). The soils had 0.59%–0.64% of organic matter, 0.02%–0.03% of total nitrogen contents, 11.21–15.14 mg kg^{-1} of phosphorus and 69–70 mg kg^{-1} of potassium.

Soil moisture contents for FC, 50% AW and 25% AW at 30, 60 and 90 DAT in 2012 and 2013 are presented in Fig. 2. The differences among water regimes were significant during the experiment periods for both years. The FC (19.5–21.1%) was the highest followed by 50% AW (12.3–14.6%) and 25% AW (9.6–10.8%), respectively. These results indicated that soil moisture content was adequately controlled and well managed during the entire duration of the experiment.

Water regimes were also significantly different for relative water content (RWC) at 30, 60 and 90 DAT in both years (Fig. 3). The differences among water regimes in RWC were rather narrow compared to soil water contents, ranging between 88.5 and 91.7% under well-watered condition, 81.1–87.7% under mild water stress and 70.3–84.8% under severe water stress conditions in 2012. These results were also similar in 2013 and RWC values ranged between 80.2 and 88.7% under well-watered condition, 78.5–82.1% under mild water stress and 75.8–77.6%under severe water stress conditions.

3.3. Combined analysis of variance for water use and root traits (root growth parameters)

Combined analysis of variance indicated that differences between years (Y), among water regimes (W) and among varieties (V) were significant for water use (Table 2). There were also significant interactions between year and water regime (Y × W), between year and variety (Y × V), between water and variety (W × V) and secondary levels interactions (Y × W × V) for water use. The interactions between the year and water regime, between year and variety and the secondary interaction contributed a small percent of sum of squares, therefore data on water use for two years were combined and presented together. A larger percent of sum of squares was contributed by water regime x variety, therefore, data on water use for each year and each water regime were analyzed and presented separately.

Combined analysis of variance showed that differences among water regimes (W) and among varieties (V) were significant for all root traits (characters) (Table 2). However, the difference between years (Y) was significant for most root characters except for root dry weight, root surface area and total root volume.

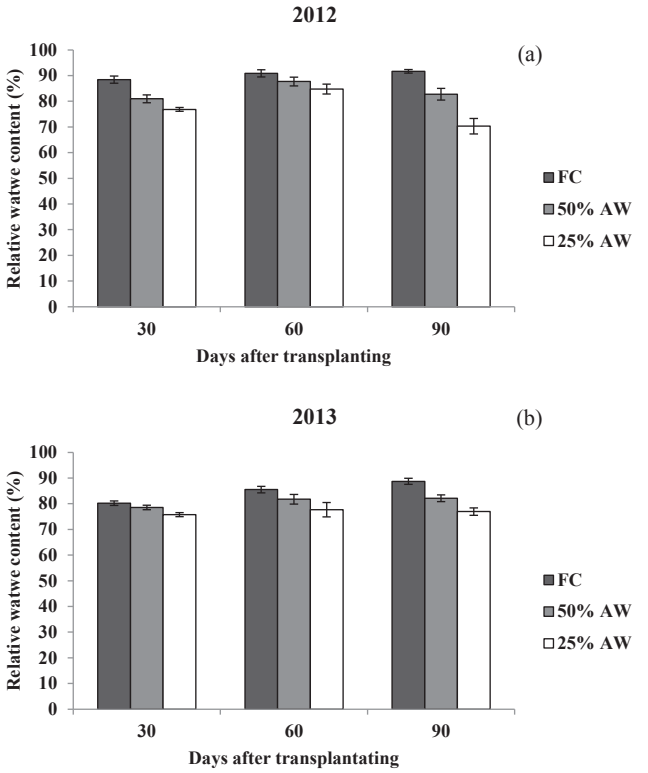


Fig. 3. Leaf relative water content (RWC) under three water regimes (FC = field capacity, 50% AW = 50% of soil available water and 25% AW = 25% of soil available water) at 30 days after transplanting (DAT), 60 DAT and 90 DAT of five Jerusalem artichoke genotypes during 2012 (3a) and 2013 (3b).

The interactions between year and variety (Y × V) were significant for root: shoot ratio, root length, root surface area and root volume. The interactions between water and variety (W × V) were significant for most root characters except for root diameter. The secondary level interactions (Y × W × V) were also found to be significantly different for root shoot ratio, root length and root volume. Due to the significance difference between the year x variety as well as water regime x variety and the secondary interaction for root shoot ratio, root length, root surface area and root volume, data on root traits for each year and for each water regime were analyzed and presented separately.

3.4. Water use

The water use was highest under field capacity conditions, lower under mild water stress and lowest under severe drought stress (Table 3.). The range in values of water use under well water was 60.06–65.07 L pot^{-1}. Under mild water stress, the amount of water use ranged from 30.00 to 32.10 L pot^{-1}. Under severe water stress, the amount of water use ranged from 17.00 to 19.00 L pot^{-1}. In three water conditions, differences among Jerusalem artichoke genotypes were significant for water use. JA 125 showed the highest

Table 1
Soil texture and chemical properties for pot experiments in 2012 and 2013.

Years	Soil texture			Soil type	Soil chemical properties							
	Sand	Silt	Clay		pH	EC (dSm^{-1})	CEC ($cmolkg^{-1}$)	OM (%)	Total N (%)	Available P (mg kg^{-1})	K (mg kg^{-1})	Ca (mg kg^{-1})
2012	80%	18%	2%	Loamy sand	6.4	0.02	17.84	0.59	0.03	11.2	69	1005
2013	81%	15%	4%	Loamy sand	6.1	0.02	7.76	0.64	0.02	15.1	70	823

Table 2
Mean squares for water use (L pot^{-1}), root dry weight (g plant^{-1}), root: shoot ratio, root length (cm plant^{-1}), root surface (cm^2 plant^{-1}), root volume (cm^3 plant^{-1}) and root diameter (mm) of five Jerusalem artichoke genotypes grown under three water regimes (FC = field capacity, 50% AW = 50% of soil available water and 25% AW = 25% of soil available water) in 2012 and 2013.

Source of variance	df	Water use (L pot^{-1})	Root dry weight (g plant^{-1})	Root: shoot ratio	Root length (km plant^{-1})	Root surface (cm^2 plant^{-1})	Root volume (cm^3 plant^{-1})	Root diameter (mm)
Year (Y)	1	0.13 (0.00)**	1.51 (0.11) ns	0.108 (5.92)*	0.0906 (0.60)*	30,49,641 (0.15) ns	6 (0.00) ns	0.0171 (16.17)**
Rep within year	6	0.00 (0.00)	0.61 (0.27)	0.008 (2.63)	0.0079 (0.32)	12,18,461 (0.37)	74 (0.29)	0.0009 (4.92)
Water (W)	2	22,080.80 (99.51)**	461.03 (68.58)**	0.231 (25.28)**	5.1220 (68.49)**	63,28,00,000 (63.68)**	49,764 (65.33)**	0.0043 (8.08)**
Y × W	4	0.03 (0.00)**	0.31 (0.05) ns	0.001 (0.15) ns	0.3889 (0.03) ns	158,083 (0.02) ns	19 (0.02) ns	0.0013 (2.41) ns
Variety (V)	2	40.65 (0.37)**	44.99 (13.38)**	0.018 (3.92)*	0.0023 (10.40)**	740,10,000 (14.89)**	5531 (14.52)**	0.0055 (20.83)**
Y × V	4	0.01 (0.00)**	0.96 (0.29) ns	0.014 (3.17)*	0.0736 (1.97)**	45,87,265 (0.92)*	313 (0.82)**	0.0002 (0.68) ns
W × V	8	6.58 (0.12)**	19.79 (11.78)**	0.060 (26.38)**	0.1839 (9.84)**	329,00,000 (13.24)**	2779 (14.59)**	0.0006 (4.47) ns
Y × W × V	8	0.00 (0.00)**	0.73 (0.44) ns	0.015 (6.66)*	0.0326 (1.74)**	25,53,567 (1.03) ns	158 (0.83)*	0.0004 (3.28) ns
Error	84	0.00 (0.00)	0.82 (5.11)	0.006 (25.89)	0.0116 (6.54)	13,53,413 (5.71)	65 (3.57)	0.0005 (39.15)
Total	119							

Numbers in the parentheses are percent (%) of sum squares to total sum of squares.
ns, *,** Non significant, significant and highly significant at P ≤ 0.05 and ≤ 0.01 probability levels, respectively.

Table 3
Water use (L pot^{-1}), Root dry weight (g plant^{-1}), drought tolerance index (DTI) of root dry weight, root diameter (mm) and DTI of root diameter of five Jerusalem artichoke genotypes grown under different water regimes at harvest in 2012 and 2013.

Genotypes	Water use (L pot^{-1})			Root dry weight (g plant^{-1})					Root diameter (mm)				
	FC	50% AW	25% AW	FC	50% AW	25% AW	DTI (50% AW)	DTI (25% AW)	FC	50% AW	25% AW	DTI (50% AW)	DTI (25% AW)
JA 60	63.06b	32.10b	17.00d	6.70d	3.29b	1.74	0.50b	0.27b	0.3448b	0.3246b	0.3145	0.95	0.91
JA 125	65.05a	33.00a	19.00a	8.32c	5.21a	2.15	0.63a	0.26b	0.3454b	0.3570a	0.34	1.04	0.99
JA 5	60.06c	30.00c	17.00d	4.95e	2.68b	1.69	0.55ab	0.35a	0.3221c	0.3248b	0.3184	1.01	0.99
JA 89	65.07a	32.05b	18.00c	12.86a	4.80a	1.95	0.38c	0.16c	0.3650a	0.3558a	0.327	0.98	0.9
HEL 65	65.06a	32.06b	18.01b	10.05b	4.82a	1.98	0.48bc	0.20bc	0.3651a	0.3615a	0.3452	0.99	0.94
Means	63.66	31.84	17.8	8.58	4.16	1.9	0.51	0.25	0.3485	0.3447	0.329	0.99	0.95

Means in the same column with the same letter(s) are not significantly different by LSD at P ≤ 0.05.
DTI for genotype was calculated by the ratio of stressed (50% soil available water (AW) or 25% AW)/non-stressed (field capacity; FC) conditions.

water use across the three water levels.

3.5. Root characters and drought tolerance index (DTI)

The results of this study showed that drought stress reduced root dry weight and root diameter (Table 3). Means of root dry weight were found to be equal to 8.58, 4.16 and 1.90 g plant^{-1} under well-watered, mild water stress and severe drought stress, respectively. Further, the drought tolerance index (DTI) for root dry weight was reduced by drought stress. Under mild water stress, DTI for root dry weight was 0.51 and it was lower under severe drought stress (0.25).

Means of root diameter were 0.35, 0.34 and 0.33 mm under well-watered, mild water stress and severe water stress, respectively. DTI for root diameter was also reduced by drought stress. DTI values were 0.99 and 0.95 under mild water stress and under severe water stress, respectively.

Severe drought stress (25% AW) increased root: shoot ratio (Table 4). Overall means for root: shoot ratios in 2012 were 0.36, 0.33 and 0.47 under well watered, mild water stress and severe water stress, respectively. In 2013, means for root: shoot ratios were 0.30, 0.26 and 0.42 under well watered, mild water stress and severe water stress, respectively. Mean DTI for root: shoot ratios (1.39 in 2012 and 1.52 in 2013) under severe water stress were higher than under mild water stress (1.00 in 2012 and 0.92 in 2013).

Drought reduced root lengths of all Jerusalem artichoke varieties. Mean roots lengths in 2012 were 0.91, 0.43 and 0.21 km plant^{-1} under well watered, mild water stress and severe water stress, respectively and mean root lengths in 2013 were 0.96, 0.50 and 0.25 km plant^{-1} under well watered, mild water stress and severe water stress, respectively. Mean DTI for root length under mild drought stress were 0.51 in 2012 and 0.53 in 2013 and under severe drought stress were 0.25 in 2012 and 0.28 in 2013.

Roots surface areas were reduced by drought stress in both years. Mean roots surface areas in 2012 were 9988, 4830 and 2037 cm^2 plant^{-1} under well watered, mild drought stress and severe drought stress, respectively. In 2013, mean roots surfaces were 10,162, 5234 and 2415 cm^2 plant^{-1} under well watered, mild drought stress and severe drought stress, respectively. Mean DTI for root surface were 0.54 (in 2012) and 0.52 (in 2013) under mild water stress and 0.24 (in 2012) and 0.25 (in 2013) under severe drought stress.

Drought stress reduced root volumes in both years. Mean root volumes in 2012 were 89, 44 and 18 cm^3 plant^{-1} under well watered, mild drought stress and severe drought stress, respectively. Mean root volumes in 2012 were 88, 44 and 19 cm^3 plant^{-1} under well watered, mild drought stress and severe drought stress, respectively. Mean DTI for root volumes were 0.56 (in 2012) and 0.51 (in 2013) under mild water stress and 0.26 (in 2012) and 0.24 (in 2013) under severe drought stress.

3.6. Variability of root characteristics

Under well watered condition, differences among Jerusalem artichoke genotypes were significant for root dry weight and root diameter (Table 3). Jerusalem artichoke genotypes could be classified into the group with high root dry weight and the group with low root dry weight. JA 89 and HEL 65 exhibited the highest root

Table 4
Root: shoot ratio, drought tolerance index (DTI) of root: shoot ratio, root length (cm plant^{-1}), DTI of root length, root surface (cm^2 plant^{-1}), DTI of root surface, root volume (cm^3 plant^{-1}) and DTI of root volume of five Jerusalem artichoke genotypes grown under different water regimes (FC; field capacity, 50% AW; 50% soil available water and 25% AW; 25% soil available water) at harvest in 2012 and 2013.

Varieties	2012			DTI (50% AW)	DTI (25% AW)	2013			DTI (50% AW)	DTI (25% AW)
	FC	50% AW	25% AW			FC	50% AW	25% AW		
Root: shoot ratio										
JA 60	0.33b	0.33	0.56a	1.01	1.69	0.29bc	0.32	0.51ab	1.10	1.75
JA 125	0.24b	0.39	0.43bc	1.62	1.77	0.22c	0.28	0.58a	1.30	2.66
JA 5	0.30b	0.29	0.53ab	0.97	1.75	0.29bc	0.23	0.36bc	0.78	1.24
JA 89	0.48a	0.26	0.34c	0.55	0.70	0.40a	0.26	0.23c	0.65	0.57
HEL 65	0.46a	0.39	0.48ab	0.84	1.04	0.31b	0.23	0.43ab	0.74	1.40
Means	0.36	0.33	0.47	1.00	1.39	0.30	0.26	0.42	0.92	1.52
Root length (km plant^{-1})										
JA 60	0.71cd	0.37	0.21	0.52	0.30	1.09ab	0.50ab	0.23b	0.46	0.22
JA 125	0.78c	0.46	0.22	0.59	0.28	0.91b	0.67a	0.38a	0.74	0.42
JA 5	0.55d	0.35	0.17	0.64	0.31	0.55c	0.26c	0.20b	0.47	0.37
JA 89	1.39a	0.45	0.21	0.33	0.15	1.28a	0.61ab	0.22b	0.48	0.17
HEL 65	1.13b	0.52	0.22	0.46	0.20	0.96b	0.47b	0.24b	0.49	0.25
Means	0.91	0.43	0.21	0.51	0.25	0.96	0.50	0.25	0.53	0.28
Root surface (cm^2 plant^{-1})										
JA 60	8227c	3846b	2082ab	0.47	0.25	10,025b	5016b	2368b	0.50	0.24
JA 125	8445c	5464a	2623a	0.65	0.31	9142b	7000a	3810a	0.77	0.42
JA 5	3971d	3153b	1539b	0.79	0.39	5855c	2488c	1552b	0.42	0.27
JA 89	15,804a	5682a	1918ab	0.36	0.12	14,476a	6552ab	2122b	0.45	0.15
HEL 65	13,492b	6007a	2022ab	0.45	0.15	11,314b	5115b	2224b	0.45	0.20
Means	9988	4830	2037	0.54	0.24	10,162	5234	2415	0.52	0.25
Root volume (cm^3 plant^{-1})										
JA 60	75c	36a	17	0.48	0.23	83b	37cd	20b	0.45	0.24
JA 125	81c	50a	24	0.62	0.30	84b	53ab	33a	0.63	0.39
JA 5	32d	28b	16	0.87	0.50	48c	26d	17b	0.53	0.35
JA 89	142a	53a	16	0.37	0.12	126a	59a	12b	0.47	0.10
HEL 65	116b	55a	18	0.47	0.15	96b	45bc	15b	0.46	0.15
Means	89	44	18	0.56	0.26	88	44	19	0.51	0.24

Means in the same column with the same letter(s) are not significantly different by LSD at $P \leq 0.05$.
DTI for genotype was calculated by the ratio of stressed (50% available water (AW) or 25% AW)/non-stressed (field capacity; FC) conditions.

dry weight and root diameter. In contrast, JA 5, JA 60 and JA 125 showed the lowest root dry weight and root diameter.

Under mild water stress, JA 125 performed well as it had high root dry weight and DTI for root dry weight, whereas JA 5 and JA 60 had low root dry weight and high DTI of root dry weight. In contrast, JA 89 and HEL 65 were categorized into the group with high root dry weight and low DTI for root dry weight.

JA 125, JA 89 and HEL 65 had high root diameter and high DTI for root diameter, whereas JA 60 and JA 5 had low root diameter and high DTI of root diameter. However, the differences among five Jerusalem artichoke genotypes for root dry weight and root diameter under severe water stress were not significant.

Jerusalem artichoke genotypes responded differently for root: shoot ratio, root length, root surface and root volume under well watered conditions in both years (Table 4). JA 89 and HEL 65 had high root: shoot ratio, root length, root surface area and root volume under well watered conditions in both years. JA 125 and JA 5 had low root: shoot ratio, root length, root surface and root volume under well watered conditions in both years. JA 60 had high, root length, root surface and root volume under well watered conditions in 2013 only.

Severe water stress increased root: shoot ratio in JA 60, JA 125 JA 5 and HEL 65 in both years, whereas JA 89 did not respond to drought for root: shoot ratio. JA 60 performed well for root: shoot ratio under mild and severe water stress conditions in both years. JA 125 also performed well under mild and severe water stresses as it had highest DTI of root: shoot ratio in both years, whereas JA 89 performed poorly as it had low DTI for root: shoot ratio in both years.

JA 125 performed well for root length under mild and severe water stress in both years as it had high root length and DTI of root length in both years. JA 125 and JA 5 had high DTI of root length under mild and severe water stress in both years but JA 89 and HEL 65 had rather low DTI of root length under mild and severe water stress in both years. JA 125 had high root surface and DTI for root surface under mild and severe water stresses in both years, whereas JA 89 and HEL 65 had high root surface but they had low DTI of root surface under mild and severe water stress in both years. JA 125 and JA 5 showed consistently high DTI for root volume under mild and severe water stress. JA 125 had also high root volume under mild and severe water stress in both years.

JA 125 had high root dry weight, root diameter, root: shoot ratio, root length, root surface, root volume across years, and values of DTI for these traits under mild and severe water stress were also high. JA 60 was identified as the genotype with high DTI of root dry weight, root diameter and root: shoot ratio under mild and severe water stress. JA 5 was identified as the genotype with high DTI of root dry weight, root diameter, root length, root surface and root volume under mild and severe water stress. JA 89 and HEL 65 performed well for root dry weigh, root diameter, root length and low DTI of all root characteristics. JA 125, JA 60 and JA 5 consistently performed well under drought stress by maintaining the ability to absorb water by having high DTI of some root traits.

3.7. Relationship between tuber dry weight and root characteristics

Tuber dry weight was positively correlated with DTI for root dry weight under severe water stress ($r = 0.95$, $P \leq 0.05$) and mild water stress ($r = 0.80$, $P > 0.05$) (Fig. 4).

The correlation coefficient between tuber dry weight and DTI for root: shoot ratio was significant under mild water stress ($r = 0.63$, $P \leq 0.05$) but not significant under severe water stress ($r = 0.41$,

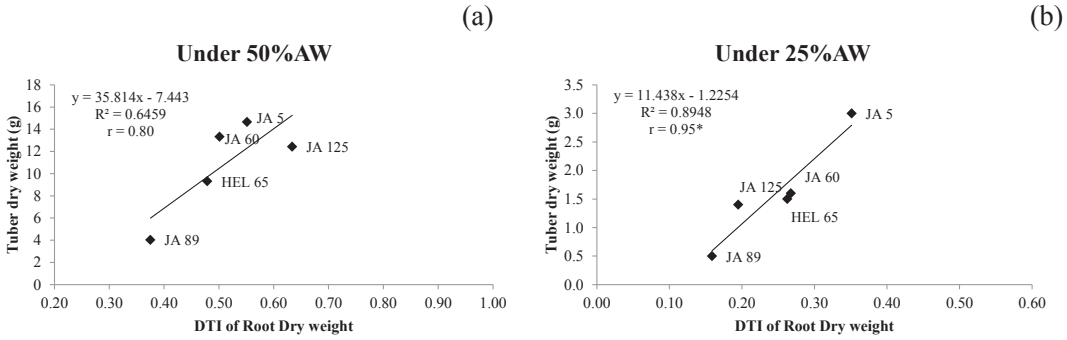


Fig. 4. -Relationship between tuber dry weight (g) and drought tolerance index (DTI) of root dry weight under 50% AW (50% soil available water) (a) and under 25% AW (b) of five Jerusalem artichoke genotypes in 2012 and 2013.

$P > 0.05$) (Fig. 5a and b).Positive correlations coefficients were observed between tuber dry weight with DTI for root length, DTI for root surface and DTI for root volume. Correlation coefficient (0.72, $P \leq 0.01$) between tuber dry weight and DTI for root length was significant under severe water stress, but the correlation was not significant under mild water stress (0.51, $P > 0.05$) (Fig. 5c and d).The correlation coefficients between tuber dry weight and DTI for root surface was positive and significant under severe water stress (0.72, $P \leq 0.01$) (Fig. 5e and f).The correlation coefficients between tuber dry weight and DTI for root volume were not significant under mild water stress ($r = 0.59$, $P > 0.05$) and under severe water stress ($r = 0.61$, $P > 0.05$) (Fig. 5g and h).

4. Discussion

How Jerusalem artichoke could maintain high tuber yield under drought stress has not been clearly understood. A better understanding on the mechanisms underlying high tuber yield under drought stress could lead to the success in breeding of Jerusalem artichoke for drought resistance. The information on the physiological traits related to drought avoidance mechanism that can maintain high water uptake and high tuber yield under drought has not been clearly investigated for Jerusalem artichoke. A better understanding on the root response of Jerusalem artichoke under drought stress should be useful for improving high tuber dry weight under water limited conditions. Drought resistance in crop may be enhanced by improving the extraction of water from the soil. Our study demonstrated that Jerusalem artichoke genotypes responded to drought to maintain high tuber dry weight under mild and severe soil moisture conditions. The results of this study also demonstrated the significant correlations between root traits and tuber weight under mild and severe drought conditions, indicating that roots are important in maintaining tuber yield in Jerusalem artichoke under drought conditions.

The interactions between year and variety for root: shoot ratio, root length, root surface area and root volume, though significant, were very small compared to main effects (water regime and variety). Low interactions indicated that the varieties performed rather consistently across years. The interactions between year and water regime were not significant for all of the root traits. This indicated that the effect of water regime was rather consistent across years. Low interaction level favors selection of better genotypes under both, non-stress or drought stress conditions. Greater variations in root dry weight, root: shoot ratio, root length, root surface, root volume and root diameter were found among varieties. These results clearly indicated that it is possible to select Jerusalem artichoke genotypes for better performance for these traits under differing levels of soil moisture.

The interaction between water regime and variety was significant for root dry weight, root: shoot ratio, root length, root surface and root volume. This revealed that those root traits were expressed under partially mild and severe water stress. Therefore, the selection for high root: shoot ratio of Jerusalem artichoke under severe water stress could be recommended. Likewise, differences for root length, root surface and root volume traits were expressed under mild water stress.

Drought increased root: shoot ratio but it reduced root dry weight, root diameter, root length, root surface area and root volume. Severe water stress resulted in greater reductions of those traits compared to mild water stress. These observations are in agreement with some previous studies. In sunflower, drought stress reduced root volume, total root length [21,22] and root diameter [21]. Del- Rosario and Fajardo [23] found that root dry weight of peanut was reduced by drought but root: shoot ratio was increased. Nevertheless, the response for root dry weight to drought conditions occurred in some genotype which had low leaf water potential. In some drought tolerance varieties of tomato, drought (withholding water) increased root dry weight, root: shoot ratio and root length [12]. Songsri et al. [16] found that root length density in deeper subsoil level was increased in response to drought.

In this study, Jerusalem artichoke varieties responded differently for root traits under both mild water stress and severe water stress. Increase in root traits was related to tuber dry weight, indicating that roots contributed to high tuber yield under drought. The relationships between DTI of root trait and tuber yield in Jerusalem artichoke have not been reported previously. In peanut, Songsri et al. [16] found that the ability to maintain the percentage of root length density (DTI) was related to pod yield, DTI for pod yield and DTI for harvest index. The ability of peanut to maintain a viable root system during water stress may contribute to the crop's drought resistance [24].

Jerusalem artichoke genotypes were classified into the group with high DTI values for root dry weight, root diameter, root: shoot ratio, root length, root surface area and root volume and the group with low DTI values for these traits. These Jerusalem artichoke genotypes were previously identified as drought tolerant varieties based on tuber yield, but their responses to drought based on root traits was not investigated. JA 125, JA 5 and JA 60 showed the highest DTI values for root parameters, and JA 89 and HEL 65 showed the lowest DTI values for root parameters.

JA 89 had the highest root dry weight but it had the lowest DTI values for root traits under mild water stress and severe water stress. In this genotype, the contribution of dry matter was partitioned to vegetative growth rather than harvestable organ. The sink competition between the harvestable part and the root sink should

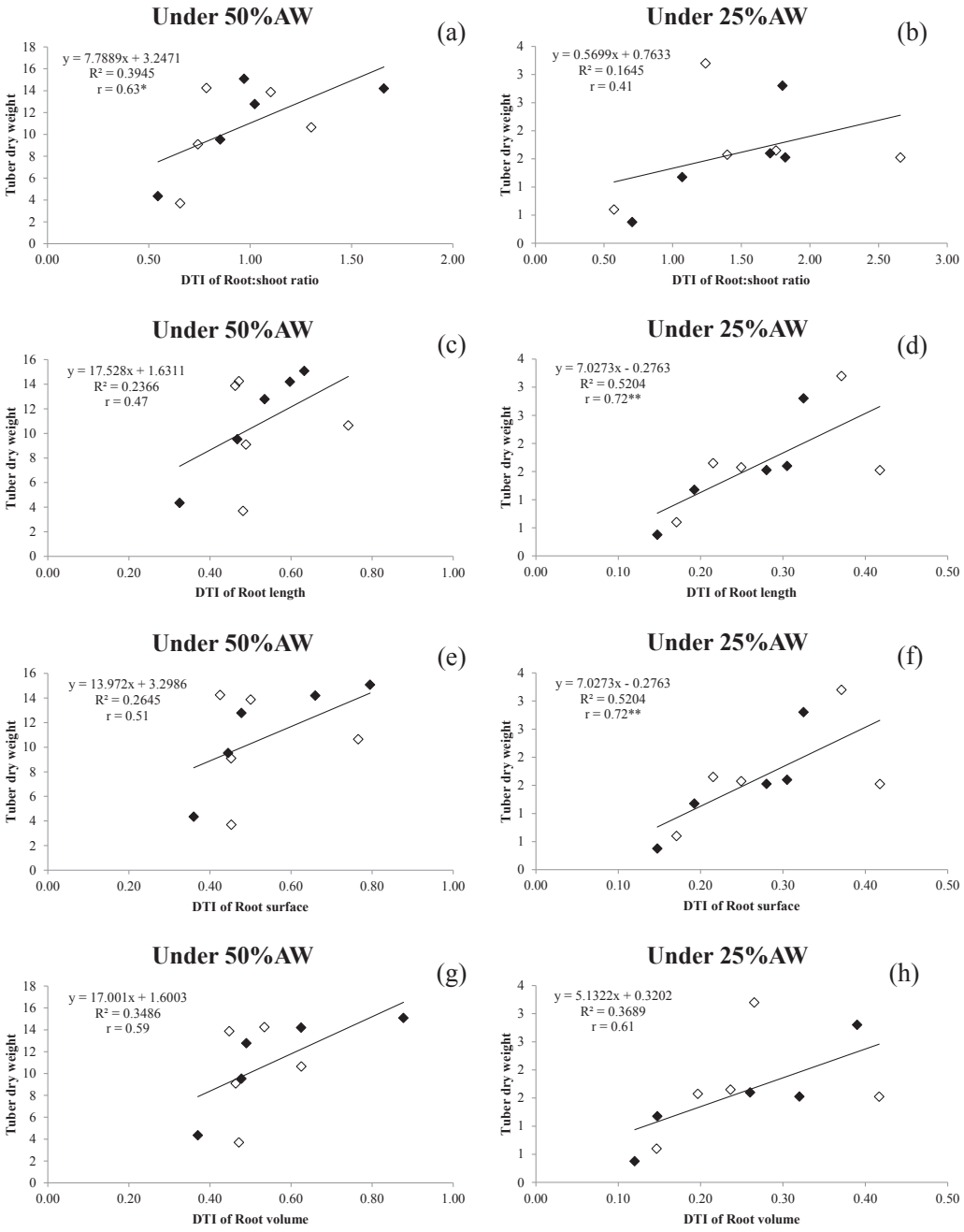


Fig. 5. Relationship between tuber dry weight (g) and drought tolerance index (DTI) of root: shoot ratio under 50% AW (50% soil available water) (a) and under 25% AW (b), between tuber dry weight (g) and DTI for root length under 50% AW (c) and under 25% AW (d), between tuber dry weight (g) and DTI for root surface under 50% AW (e) and under 25% AW (f), between tuber dry weight (g) and DTI of root volume under 50% AW (g) and under 25% AW (h) of five Jerusalem artichoke genotypes in 2012 and 2013.

be considered when devising breeding strategies to improve drought resistance [25]. JA 125, JA 5 and JA 60 were classified as a group with high tuber dry weight under mild water stress, and JA 5 was identified as the drought tolerant genotypes under severe drought stress because it had the highest tuber dry weight under severe water stress. Some varieties had low means for root parameters but they had high DTI values for these parameters. The results indicated that Jerusalem artichoke varieties changed root growth patterns in response to drought to mine more water from drying soils, and, therefore, these varieties could maintain high tuber yield under drought.

5. Conclusion

Drought stress reduced root dry weight, root diameter, root length, root surface area, root volume, and DTI for these root characteristics in all Jerusalem artichoke varieties. Drought stress increased root: shoot ratio of JA 60 and JA 125 varieties. Tuber dry weight was positively correlated with DTI for root dry weight, root diameter, root: shoot ratio, root length, root surface and root volume under mild water stress and severe water stress. Variations in responses to drought for root traits were observed among Jerusalem artichoke genotypes. Based on DTI for root traits, JA 5, JA 60 and

JA 125 were identified as the varieties with drought avoidance mechanism because these varieties could stabilize tuber yield and have the capability to absorb water under drought conditions. This mechanism might help Jerusalem artichoke to obtain higher tuber yields under drought conditions. Breeding for maintaining yield under water-limited conditions by the adaptation of root parameters may facilitate the development of improved Jerusalem artichoke varieties in specific water limited-environments.

Acknowledgments

The Royal Golden Jubilee Ph.D. Program (jointly funded by Khon Kaen University and the Thailand Research Fund) (grant no. PHD/0026/2551), the Thailand Research Fund, provided financial supports to this research through the Senior Research Scholar Project of Professor Dr. Sanun Jogloy and the project was partially supported by the Plant Breeding Research Center for Sustainable Agriculture, Khon Kaen University. The Higher Education Promotion and National Research University Project of Thailand of the Office of Higher Education Commission were also acknowledged for funding support through the Food and Functional Food Research Cluster of Khon Kaen University. Finally, we would like to thank the Thailand Research Fund (TRF) Khon Kaen University (KKU) and Faculty of Agriculture KKU for providing financial support for training on manuscript preparation.

References

[1] T. Barclay, M. Ginic-Markovic, P. Coope, N. Petrovsky, Inulin—a versatile polysaccharide with multiple pharmaceutical and food chemical uses, J. Excip. Food Chem. 1 (3) (2010) 27–50.
[2] T. Zhang, Z. Chi, C.H. Zhao, Z.M. Chi, F. Gong, Bioethanol production from hydrolysates of inulin and the tuber meal of Jerusalem artichoke by *Saccharomyces sp.* W0, Bioresour. Technol. 101 (21) (2010) 8166–8170.
[3] F. Yang, Q. Liu, X. Bai, Y. Du, Conversion of biomass into 5–hydroxymethylfurfural using solid acid catalyst, Bioresour. Technol. 102 (3) (2011) 3424–3429.
[4] A. Dai, Increasing drought under global warming in observations and models, Nat. Clim. Ch. 3 (2013) 52–58.
[5] J.R. Conde, J.L. Tenorio, B. Rodriguez-Maribona, L. Ayerbe, Tuber yield of Jerusalem artichoke (*Helianthus tuberosus* L.) in relation to water stress, Biomass Bioenerg. 1 (3) (1991) 137–142.
[6] N. Losavio, N. lamascese, A.V. Vonella, Water requirements and nitrogen fertilization in Jerusalem artichoke (*Helianthus tuberosus* L.) grown under Mediterranean conditions, Acta Hortic. 449 (1997) 205–209.
[7] S. Schittenhelm, Agronomic performance of root chicory, Jerusalem artichoke and sugar beet in stress and non-stress environment, Crop Sci. 39 (1999) 1815–1823.
[8] A. Monti, M.T. Amaducci, G. Venturi, Growth response, leaf gas exchange and fructans accumulation of Jerusalem artichoke (*Helianthus tuberosus* L.) as affected by different water regimes, Eur. J. Agron. 23 (2005) 136–145.
[9] Z.X. Liu, J.H.J. Spiertz, S. Jing, X. Shuai, H.X. Guang, Growth and yield performance of Jerusalem artichoke clones in a semiarid region of China, Agron. J. 104 (6) (2012) 1538–1546.
[10] R. Ruttanaprasert, B. Poramate, S. Jogloy, N. Vorasoot, T. Kesmala, R.S. Kanwar, et al., Genotypic variability for tuber yield, biomass and drought tolerance in Jerusalem artichoke germplasm, Turk J Agric For 38 (2014) 570–580.
[11] R. Ruttanaprasert, S. Jogloy, N. Vorasoot, T. Kesmala, R.S. Kanwar, C.C. Holbrook, et al., Effects of water stress on total biomass, tuber yield and harvest index in Jerusalem artichoke, Agr. Water Manage. (2015) (Submitted).
[12] K. Nahar, R. Gretzmacher, Response of shoot and root development of seven tomato cultivars in hydrophonic system under water stress academic, Acad. J. Plant Sci. 4 (2) (2011) 57–63.
[13] M.M. Ludlow, R.C. Muchow, A critical evaluation of traits for improving crop yields in water–limited environments, Adv. Agron. 43 (1990) 107–153.
[14] T. Matsui, B.B. Singh, Root characteristics in cowpea related to drought tolerance at the seedling stage, Exp. Agric. 39 (2003) 29–38.
[15] L. Taiz, E. Zeiger, Stress physiology, in: L. Taiz, E. Zeiger (Eds.), Plant Physiology, fourth ed., Sinauer Associates Inc, Sunderland, Massachusetts, 2006, pp. 671–681.
[16] P. Songsri, S. Jogloy, N. Vorasoot, C. Akkasaeng, A. Patanothai, C.C. Holbrook, Root distribution of drought-resistant peanut genotypes in response to drought, J. Agron. Crop Sci. 194 (2008) 92–103.
[17] J. Doorenbos, W.O. Pruitt, Guideline for Predicting Crop Water Requirements, FAO Irrigation and Drainage Paper No. 24, FAO, Rome, 1992, pp. p.1–p65.
[18] S. Singh, M.B. Russell, Water use by maize/pigeonpeas intercrop on a deep vertisol, in: Y.L. Nene, V. Kumble (Eds.), International Workshop on Pigeonpeas Volume 1. Proceeding of The International Workshop on Pigeonpeas Volume 1; 1980 Dec 15–19, ICRISAT Center Patancheru, India, AP, 1980, pp. 271–282.
[19] P.J. Kramer, Drought, stress and the origin of adaptation, in: N.C. Turner, P.J. Kramer (Eds.), Adaptation of Plant to Water and High Temperature Stress, John Wiley & Sons, New York, 1980, pp. 7–20.
[20] K.A. Gomez, A.A. Gomez, Statistical Procedures for Agricultural Research, second ed., John Wiley & Sons, New York, 1984.
[21] M. Perbea, E. Petcu, The effect of soil water content on sunflower seedlings, Rom. Agric. Res. (2000) 43–47.
[22] M.I. Hossain, A. Khatun, M.S.A. Talukder, M.M.R. Dewan, M.S. Uddin, Effect of drought on physiology and yield contributing characters of sunflower, Bangladesh J. Agric. Res. 35 (2010) 113–124.
[23] D.A. Del-Rosario, F.F. Fajardo, Morphophysiological responses of ten peanut (*Arachis hypogaea* L.) varieties to drought stress, Philipp. Agric 71 (1988) 447–459.
[24] T.Y. Reddy, V.R. Reddy, V. Anbumozhi, Physiological responses of groundnut (*Arachis hypogaea* L.) to drought stress and its amelioration: a critical review, Plant Growth Regul. 41 (2003) 75–88.
[25] R. Ruttanaprasert, S. Jogloy, N. Vorasoot, T. Kesmala, R.S. Kanwar, et al., Photoperiod and growing degree days effect on dry matter partitioning in Jerusalem artichoke, Int. J. Plant Prod. 7 (3) (2013) 393–416.



International Journal of Plant Production 9 (4), October 2015
ISSN: 1735-6814 (Print), 1735-8043 (Online)
www.ijpp.info

GUASNR

Responses of inulin content and inulin yield of Jerusalem artichoke to seasonal environments

D. Puangbut[a], S. Jogloy[a,b,*], N. Vorasoot[a], C.C. Holbrook[c], A. Patanothai[a]

[a]*Department of Plant Science and Agricultural Resources, Faculty of Agriculture, Khon Kaen University, Khon Kaen, Thailand.*
[b]*Peanut and Jerusalem Artichoke Improvement for Functional Food Research Group, Khon Kaen University, Khon Kaen, Thailand.*
[c]*United States Department of Agriculture-Agricultural Research Service, Coastal Plain Experiment Station, Tifton, Georgia, USA.*
*Corresponding author. E-mail: sjogloy@gmail.com

Received 30 May 2015; Accepted after revision 21 July 2015; Published online 28 September 2015

Abstract

Seasonal variation (e.g. temperature and photoperiod) between growing seasons might affect inulin content and inulin yield of Jerusalem artichoke. However, there is limited information on genotypic response to seasons for inulin content and inulin yield. The objective of this study was to investigate the variability in genotypic response to seasons for inulin content and inulin yield of Jerusalem artichoke. Field experiments were conducted during the early-rainy season from June to September 2011 and the post-rainy season from September to December in 2011 and these 2 seasons were repeated in 2012 at the Field Crop Research Station of Khon Kaen University. A randomized complete block design (RCBD) with 5 replications was used. Four Jerusalem artichoke genotypes were studied during both seasons in each year. Data were recorded for brix value, inulin content, tuber yield, inulin yield, biomass and harvest index at harvest. The results revealed that seasonal variations had significant effects on inulin content, inulin yield, tuber yield, biomass and harvest index but not on brix value. The results indicated that growing Jerusalem artichoke in the early-rainy season with high temperature and long photoperiod resulted in greater inulin content and biomass. In contrast, growing Jerusalem artichoke in the post-rainy season with low temperature and short photoperiod resulted in greater tuber yield and inulin yield. The present study revealed that temperature and photoperiod were important for producing tuber yield and inulin yield. This information can be used to select the appropriate growing seasons for sustainable production of inulin content, inulin yield and tuber yield of Jerusalem artichoke in Thailand.

Keywords: Sunchoke; Growing season; Temperature; Photoperiod; Tuber yield; Fructan.

Introduction

Inulin, non-digestible oligosaccharides belong to a class of carbohydrates known as fructans. Inulin is a prebiotic that can be used to selectively stimulate growth of bifidobacteria and lactobacilli but limit growth of non-beneficial bacteria such as *Escherichia* in the intestine and thus improve host health (Coudray et al., 2005; Gibson et al., 2004). Additionally, inulin can increase intestinal absorption of minerals in humans and animals and help to prevent the development of deficiency diseases (Coudray et al., 2005). Inulin is considered as functional food that is beneficial to human health through reduction in the risk of some diseases like intestinal infections, constipation, non-insulin dependent diabetes, obesity and colon cancer (Roberfroid,

2002; Roberfroid, 2007). Several studies have shown that inulin reduces the risk of colon cancer and improve the management of inflammatory bowel diseases (Roberfroid, 2002; Pool-Zobel, 2005; Rafter et al., 2007). Clausen et al. (2012) indicated that inulin is suitable for a diabetic diet because it did not increase blood glucose levels. Moreover, inulin has low caloric value, thus, it is consumed as a dietary supplement for obese people (Kaur and Gupta, 2002). Therefore, inulin has been increasingly used in various foods due to its beneficial nutritional attributes.

Inulin a storage carbohydrate is found in many plants including leek, onion, garlic, wheat, banana, yacon, chicory and Jerusalem artichoke (Kaur and Gupta, 2002). However, only a limited number of species are suitable for non-food and industrial food applications. The main sources of inulin that are used in the food industry are chicory and Jerusalem artichoke. Jerusalem artichoke is a major source for inulin production in the tropics, where chicory cannot be grown commercially.

Jerusalem artichoke (*Helianthus tuberosus* L.) is native to North America (Kays and Nottingham, 2008) and is cultivated widely in many countries for different purposes such as for the food industry and also for the production of ethanol (Kleessen et al., 2007; Kerckhoffs and Renquist, 2013). Jerusalem artichoke can be grown successfully across a wide range of climatic environments including tropical climates in Thailand (Ruttanaprasert et al., 2013; Ruttanaprasert et al., 2014; Puangbut et al., 2012). Jerusalem artichoke can successfully be grown in two seasons (early-rainy and late-rainy) in Thailand due to its wide range of adaptability (Puttha et al., 2012). In the early-rainy season, Jerusalem artichoke is grown during May to September under high temperatures and long days while during the late-rainy season the crop is grown under medium temperatures and short days of September to December. Seasonal variations such as photoperiod, temperature and maturity, might affect inulin content and inulin yield of Jerusalem artichoke.

Previous studies indicated inulin content can be affected by photosynthesis, temperature and maturity (Ernst et al., 1995; Saengthongpinit and Sajjaanantakul, 2005; Kocsis et al., 2008; Puangbut et al., 2012). Legnani and Miller (2001) stated that inulin accumulation was increased by long photoperiod and high temperature conditions in *Dahli*a. Recent studies indicated that genotypes, days to maturity and rainfall affected tuber yield and inulin content (Puttha et al., 2012; Kocsis et al., 2008). Ruttanaprasert et al. (2013) also reported that photoperiod and growing degree days affected dry matter and partitioning of Jerusalem artichoke. However, there is limited information of genotypic response to different seasons for inlulin content and inulin yield in Jerusalem artichoke. Variation in genotype, season and genotype × season interaction can affect tuber yield, biomass, inulin content and inulin yield of Jerusalem artichoke.

Information of genotypic response for inulin content and inulin yield to different environments is important for breeding programs. High variation in genotype and genotype × year interactions (G × Y) were observed for inulin content and tuber yield and extensive evaluation in many years is necessary (Pimsaen et al., 2010; Puttha et al., 2012). However, the information on genotypic response to different seasons for inulin traits is rather limited and the extent to which the genotypic interact with the seasons has not been adequately researched. This information can then be used to develop appropriate management strategies for suitable production of inulin yield between growing seasons. The objective of this study was investigating the variability in genotypic response to seasons for inulin content and inulin yield of Jerusalem artichoke.

Materials and Methods

Plant materials and experimental design

Four Jerusalem artichoke genotypes representing three maturity classes (early, intermediate and late) were studied in both seasons for two years. CN 52867 is early maturity, JA 89 and KT 50-4 are intermediate maturity and HEL 65 is late maturity. CN 52867 and JA 89 were kindly donated from the Plant Gene Resources of Canada (PGRC), HEL 65 was kindly donated from the Leibniz Institute of Plant Genetics and Crop Plant Research (IPK) of Germany and KT 50-4 is a hybrid clone from Khon Kaen University, Thailand.

Field experiments were conducted during the early-rainy season from June to September 2011 and the post-rainy seasons from September to December in 2011 and the two seasons were repeated in 2012 at the Field Crop Research Station of Khon Kaen University. A randomized complete block design (RCBD) with five replications was used. Plot size was 6×6 m with a spacing of 50 cm between rows and 50 cm between hills in a row.

Crop management

Pre-sprouted seed tubers were used as planting materials. To prepare the sprouted seed tubers, the tubers were cut into small pieces each of which had two or three buds. The tuber pieces were incubated in plastic bags containing moist coconut peat at the bottom and the top of the bags for 7 days. The plastic bags were kept opened for good aeration. The tuber pieces with active buds and roots were further transferred to plug plastic trays containing a mixture 1:1 soil: burnt rice husk medium for about 7 days for germination. The fourth leaf-sprouted (V4) seedlings were then suitable for transplanting in the plot. One seedling was transplanted per hill. Fertilizer grade 15-15-15 was applied at 30 days after transplanting (DAT) at a rate of 156 kg per ha^{-1}. A Terraclor (quintozene 24% W/V EC) was applied monthly for 3 months after transplanting at the rate 25 mL to 20 L of water for control of stem rot (*Sclerotium rolfsii*). Supplementary irrigation was applied to the crop with an overhead sprinkler system at two day intervals.

Tuber yield, biomass and harvest index

At harvest, five plants in each plot were sampled randomly and used for determination of tuber yield, biomass, harvest index (HI) and inulin content. The stems were cut at the crowns, tubers were dug and roots were discarded. Tubers were washed in tap water to remove the potting medium. Fresh shoot weight and tuber fresh weight were determined in the field and then the weights were converted to fresh weights per area. A one kg random sample of shoot and tuber fresh weight was taken and oven-dried at 80 °C for 72 hours or until constant weight and weighed. Biomass was calculated from shoot dry weight and tuber dry weight. HI was calculated as tuber dry weight divided by the total biomass.

Total soluble solids

Three tubers of each plot were randomly selected and used for determination of total soluble solids. The tubers were cut longitudinally into small pieces. Juice containing total soluble solids was extracted from small fresh samples of tubers using a hydraulic press. A juice sample of a few milliliters was used to determine total soluble solids using a digital refractometer "model FG 103" (ATAGO, Tokyo, Japan).

Inulin content and inulin yield

Inulin content was analyzed using the methods described by Saengkanuk et al. (2011). Briefly, the tubers were longitudinally sliced into thin pieces at the middle part of the tubers. Fifty grams of sliced tuber was soaked in absolute ethanol at 4 °C for 24 h and the samples were stored at -20 °C until analyzed. The samples were oven dried at 60 °C for 10 hours. To extract inulin, 2 g of dried sample was mixed with distilled water at 80 °C for 20 minutes. The solution was cooled to room temperature and filtered through a 0.45 µm membrane filter.

The extracts (500 µl) were pipette into 25 ml volumetric flasks containing 3% HCl and diluted to 25 ml with water. The mixtures were then heated at 80 °C in a water-bath for 45 minutes. After cooling, the solutions were stored in plastic bottles before being analyzed by spectrophotometer. The detailed method for measurement for inulin content has been reported by Saengkanuk et al. (2011). Inulin analysis was shown as a percentage of inulin content on a dry weight basis and inulin yield was computed by the following formula (Puangbut et al., 2011).

Inulin yield ($kgha^{-1}$)= inulin content (%) × tuber yield ($kgha^{-1}$)

Statistical analysis

Analysis of variance was performed for individual seasons and error variances were tested for homogeneity by Bartlett's test (Hoshmand, 2006). Because of, genotype × seasons interactions were significant for all characters (Table 1), data were reported for individual seasons. Duncan's multiple range tests (DMRT) was used to compare means within genotypes and Least significant difference (LSD) was used to compare means between seasons for each genotype. Calculations procedures were done using MSTAT-C package (Bricker, 1989).

Table 1. Mean square from combine analysis of variance for brix value, inulin content, inulin yield, tuber yield (TY), biomass (BIO) and harvest index (HI) of four Jerusalem artichoke genotypes in two years and two seasons.

SOV	df	Brix value	Inulin content	Inulin yield	TY	BIO	HI
Year (Y)	1	14.0^{ns}	39.8^{ns}	19251^{ns}	143059^{ns}	4347315^{ns}	0.003^{ns}
Season (S)	1	6.4^{ns}	2010.0^{**}	839210^{*}	$1.2E+07^{**}$	$2.1E+08^{**}$	1.601^{**}
Y × S	1	3.8^{ns}	25.9^{ns}	$2.2E+07^{**}$	$4.0E+07^{**}$	$1.7E+08^{**}$	0.001^{ns}
Reps. within Y and S	16	4.5	80.6	326231	1025222	9971915	0.002
Genotypes (G)	3	72.5^{**}	111.7^{**}	1112169^{*}	1774666^{*}	$2.2E+07^{*}$	0.036^{**}
G × Y	3	2.3^{ns}	15.8^{ns}	242053^{ns}	512100ns	5427433^{ns}	0.005^{ns}
G × S	3	25.4^{**}	96.2^{**}	3029435^{**}	3999924^{**}	$2.6E+07^{*}$	0.001^{ns}
Y × S × G	3	3.3^{ns}	16.4^{ns}	412364^{ns}	387817^{ns}	9253937^{ns}	0.004^{ns}
Pooled error	48	284.4	8.2	556286	880234	9990803	0.006

ns, * and ** non-significant, significant at P<0.05 and significant at P<0.01.

Results and Discussion

Weather conditions

Daily temperatures and photoperiod during growth in the early-rainy season and the post-rainy season in each year are shown in Figure 2. The seasonal means of maximum and minimum air temperatures ranged between 22.9 and 31.3 ºC in the early-rainy season and 20.2 and 30.6 ºC in the post-rainy season in 2011 (Figure 2a). Maximum and minimum air temperatures ranged between 23.0 and 32.4 ºC in the early-rainy season and 21.7 and 32.0 ºC in the post-rainy season in 2012 (Figure 2b). The averaged photoperiod in the early-rainy season was 13.0 h and 11.6 h in the post-rainy season in both years (Figure 2).

The mean temperature during the growing season in the early-rainy season was higher than in the post-rainy season in both years. Photoperiod in the post-rainy season was shorter than in the early-rainy season in both years. Differences in temperature and photoperiod between the seasons might have affected inulin content, inulin yield and tuber yield. Our results demonstrated that vegetative growth and tuber growth are significantly different between seasons (Figure 1). Ruttanaprasert et al. (2013) also reported that Jerusalem artichoke grown during high temperature (32.3 ºC) and long photoperiod (13.0 h) took longer to mature than when grown during low temperature (17.5 ºC) and short photoperiod (11.2 h). In addition, short photoperiod conditions gave higher rate of partitioning of dry matter to tuber (HI) and enhance tuber dry weight (Ruttanaprasert et al., 2013). The present study revealed that low temperature and short photoperiod were favorable for tuber growth and resulted in a rapid increase in dry matter in tuber.



Figure 1. Vegetative growth and tuber growth of HEL 65 Jerusalem artichoke grown in the early-rainy season (a, b) and in the post- rainy season (c,d).

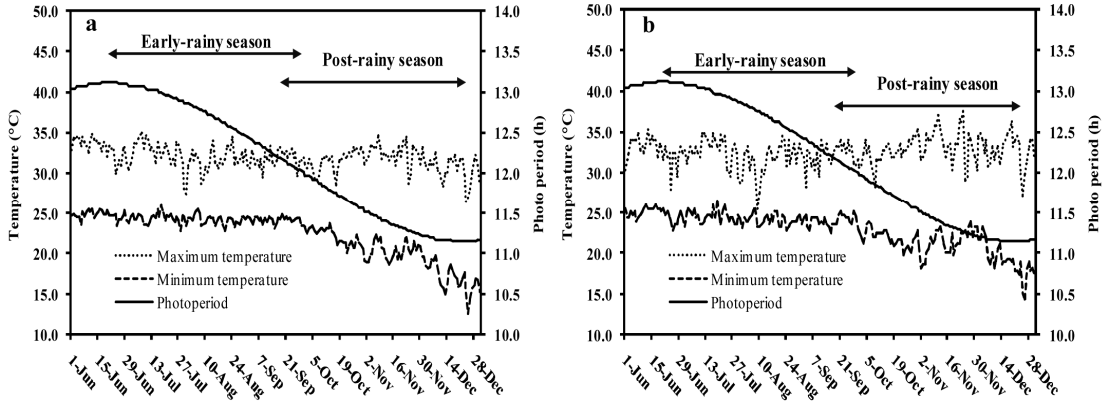


Figure 2. Daily maximum temperature, minimum temperature and photoperiod during the early-rainy and post-rainy seasons in 2011 (a) and in 2012 (b).

Combined analysis of variance

Variations between years (Y) were not significant for brix value, inulin content, inulin yield, tuber yield, biomass and harvest index (HI) (Table 1). Seasons were significant difference for all traits except brix value. This result indicated the effect of season was larger than year. The results also revealed that brix value was more stable than other traits across seasons. Jerusalem artichoke genotypes were significantly different for all traits and there were significant genotype × season interactions (G × S) for these traits. The contribution of season was higher than that genotype for inulin content and HI while genotype contributed a larger portion to the variations in Brix value, inulin yield, tuber yield and biomass. The second level interactions (Y × S × G) were not significant for all traits.

Seasonal variations in brix value and inulin content

The crop grown in the early-rainy season had higher inulin content than did the crop grown in the post-rainy season (Table 2), while brix value showed no significant differences between seasons. The results revealed that brix value was more stable than inulin content across seasons. This was in agreement with Puangbut et al. (2011) who reported that brix values were stable across years with different environments and this trait should be applicable in Jerusalem artichoke breeding programs. In contrast, Puttha et al. (2012) reported that inulin content was stable across seasons. The different observations on the stability of inulin content may be due to the use of different genetic material. Significant differences among Jerusalem artichoke genotypes were found for brix value and inulin content with CN 52867 having the highest brix value and inulin content in both seasons (Table 2).

The results indicated that inulin contents were increased in the early-rainy seasons. This could be due to high photosynthesis that resulted in high assimilate (sucrose) (Schubert and Feuerle, 1997; Legnani and Miller, 2001). Sucrose, fructose and glucose have been reported as the main parameters influencing the regulation of the activities of inulin-metabolizing enzymes (Vandoorne et al., 2012; De Roover et al., 2000). Inulin synthesis is initiated by sucrose: sucrose1-fructosyltransferase, which catalyses the transfer of a fructose moiety between two sucrose molecules to produce glucose and the trisaccharide 1-kestose (Vandoorne et al., 2012). Plant appearance in the early-rainy

seasons in comparison to the post-rainy season (Figure 1) illustrated enhanced leaf area which would be expected to lead to high photosynthesis that could have contributed to the increased inulin content. Enhanced photosynthetic capacity would also enhance accumulation of fructose resulting in relatively high inulin content (Monti et al., 2005; Vandoorne et al., 2012). Jerusalem artichoke tubers produced during the early-rainy season in Thailand should be expected to have higher inulin content than those produced during the post-rainy season.

Table 2. Brix value and inulin content of four Jerusalem artichoke genotypes grown during the early-rainy seasons (ERS) and the post-rainy seasons (PRS) for two years.

Genotype	Brix value		LSD	Inulin content (%)		LSD
	ERS	PRS		ERS	PRS	
JA 89	21.1^{b}	21.9^{ab}	ns	83.0^{b}	74.9^{ab}	**
HEL 65	19.8^{b}	21.6^{ab}	ns	81.4^{b}	75.2^{ab}	**
CN 52867	25.7^{a}	23.5^{a}	ns	90.0^{a}	78.1^{a}	**
KT 50-4	21.8^{b}	19.1^{b}	ns	88.0^{a}	70.3^{b}	**
Mean	22.1	20.9		85.6	74.6	

Means in the same column with the same letters are not significantly different by DMRT (P≤0.05).
ns and ** non-significant and significant at P≤0.01, respectively by LSD.

Seasonal variations on tuber yield, inulin yield, biomass and harvest index

The effect of season was significant for tuber yield, inulin yield, biomass and harvest index (HI) (Table 1). On average, tuber yield and inulin yield in the post-rainy season was higher than the early-rainy season (Table 3). There were significant differences among Jerusalem artichoke genotypes for tuber yield and inulin yield in both seasons. The highest for tuber yield was KT-50 in both the early-rainy and the post-rainy seasons. KT 50-4 was also highest inulin yield in the early-rainy seasons while CN 52867 had the highest inulin yield in the post-rainy seasons.

Over all genotypes, biomass in the early-rainy season was higher than the post-rainy seasons while HI in the post-rainy season was higher than the early-rainy season (Table 4). Significant differences among Jerusalem artichoke genotypes were found for biomass and HI in both seasons. The highest biomass was observed in HEL 65 and CN 52867 in the early-rainy and the post-rainy seasons, respectively, whereas KT 50-4 had the highest HI in both seasons.

Table 3. Tuber yield and inulin yield of four Jerusalem artichoke genotypes grown during the early-rainy seasons (ERS) and the post-rainy seasons (PRS) for two years.

Genotype	Tuber yield (kg ha^{-1})		LSD	Inulin yield (kg ha^{-1})		LSD
	ERS	PRS		ERS	PRS	
JA 89	3,478^{b}	4,510^{ab}	**	2,834^{b}	3,378^{b}	*
HEL 65	3,655^{b}	4,140^{b}	ns	3,076^{b}	3,113^{b}	ns
CN 52867	3,324^{b}	4,775^{a}	**	2,990^{b}	3,729^{a}	*
KT 50-4	4,572^{a}	4,780^{a}	ns	4,028^{a}	3,360^{b}	ns
Mean	3,757	4,630		3,232	3,454	

Means in the same column with the same letters are not significantly different by DMRT (P≤0.05).
ns, * and ** non-significant, significant at P≤0.05 and significant at P≤0.01, respectively by LSD.

Table 4. Biomass of four Jerusalem artichoke genotypes grown during the early-rainy seasons (ERS) and the post-rainy seasons (PRS) for two years.

Genotypes	Biomass (kg ha^{-1})		LSD	Harvest index		LSD
	ERS	PRS		ERS	PRS	
JA 89	9,271^{ab}	7,128^{ab}	**	0.39^{ab}	0.65^{b}	**
HEL 65	12,656^{a}	6,532^{ab}	**	0.35^{b}	0.65^{b}	**
CN 52867	7,816^{b}	7,433^{a}	ns	0.43^{ab}	0.65^{b}	**
KT 50-4	10,151^{ab}	6,397^{b}	**	0.45^{a}	0.74^{a}	**
Mean	9,973	6,872		0.40	0.67	

Means in the same column with the same letters are not significantly different by DMRT ($P \leq 0.05$).
ns and ** non-significant and significant at $P \leq 0.01$, respectively by LSD.
Harvest index (HI) was calculated as tuber dry weight divided by the total biomass of the plant.

The present study supported previous findings that Jerusalem artichoke grown in the early-rainy season with high temperatures and long photoperiod produced higher biomass but lower tuber yields than when grown in the post-rainy season (Ruttanaprasert et al., 2013; Puangbut et al., 2012). This is similar to potato where Kozia et al. (1995) reported that total dry matter increased with long photoperiod. Jerusalem artichoke grown in the post-rainy season with low temperature and short photoperiod had higher tuber yield which contributed to high inulin yield. Our results demonstrated that the post-rainy season was favorable for inulin yield while the early-rainy season promoted accumulation of inulin content in tubers.

The present study revealed that seasonal variation was more effect on inulin content, tuber yield and inulin yield but not for brix value. The results indicated that the post-rainy season were favorable conditions for tuber yield and inulin yield while the early-rainy season was induced inulin content. This information will enable growers to make decisions and choose suitable growing seasons for Jerusalem artichoke production for high inulin content or high inulin yield in Thailand.

Acknowledgements

This work was supported by the Higher Education Research Promotion and National Research University Project of Thailand, Office of the Higher Education Commission, through the Food and Functional Food Research Cluster of Khon Kaen University. We also thank the Leibniz Institute of Plant Genetics and Crop Plant Research, Germany, the Plant Gene Resource of Canada for the contribution of Jerusalem artichoke germplasm. Grateful acknowledgments are made to the Peanut and Jerusalem artichoke Improvement for Functional Food Research Group and Plant Breeding Research Center for Sustainable Agriculture, Khon Kaen University and to the Thailand Research Fund for providing financial supports to this research through the Senior Research Scholar Project of Professor Dr. Sanun Jogloy. Acknowledgement is extended to the Thailand Research Fund (IRG 578003), Khon Kaen University and Faculty of Agriculture, KKU for providing financial support for manuscript preparation activities.

References

Bricker, A.A., 1989. MSTAT-C User's Guide. Michigan State University, Michigan.

Clausen, M.R., Bach, V., Edelenbos, M., Bertram, H.C., 2012. Metabolomics reveals drastic compositional changes during overwintering of Jerusalem artichoke (*Helianthus tuberosus* L.) tubers. J. Agric. Food Chem. 60, 9495-9501.

Coudray, C., Rambeau, M., Feillet-Coudray, C., Tressol, J.C., Demigne, C., Gueux, E., Mazur, A., Rayssiguier, Y., 2005. Dietary inulin intake and age can significantly affect intestinal absorption of calcium and magnesium in rats: a stable isotope approach. J. Nutr. 136, 117-122.

De Roover, J., Vandenbranden, K., Van Laere, A., Van den Ende, W., 2000. Drought induces fructan synthesis and 1-SST (sucrose:sucrose fructosyltransferase) in roots and leaves of chicory seedlings (*Cichorium intybus* L.). Planta 210, 808-814.

Ernst, M., Chatterton, N.J., Harrison, P.A., 1995. Carbohydrate changes in chicory (*Cichorium intybus* L. var. *foliosum*) during growth and storage. Sci. Hortic. 63, 251-261.

Gibson, G.R., Probert, H.M., Loo, J.V., Rastall, R.A., Roberfroid, M.B., 2004. Dietary modulation of the human colonic microbiota: updating the concept of prebiotics. Nutr. Res. Rev. 17, 259-275.

Hoshmand, A.R., 2006. Design of Experiments for Agriculture and the Natural Sciences. Chapman & Hall, Florida.

Kaur, N., Gupta, A.K., 2002. Applications of inulin and oligofructose in health and nutrition. J. Biosci. 27, 703-714.

Kays, S.J., Nottingham, S.F., 2008. Biology and chemistry of Jerusalem artichoke (*Helianthus tuberosus* L.) CRC press, Florida.

Kerckhoffs, H., Renquist, R., 2013. Biofuel from plant biomass. Agron. Sustain. Dev. 33, 1-19.

Kleessen, B., Schwarz, S., Boehm, A., Fuhrmann, H., Richter, A., Henle, T., Krueger, M., 2007. Jerusalem artichoke and chicory inulin in bakery products affect faecal microbiota of healthy volunteers. Brit. J. Nutr. 98, 540-549.

Kocsis, L., Kaul, H.P., Praznik, W., Liebhard, P., 2008. Influence of harvest date on tuber growth, tuber dry matter content, inulin and sugar yield of different Jerusalem artichoke (*Helianthus tuberosus* L.) cultivars in the semi-arid production area of Austria. Ger. J. Agron. 12, 8-21.

Kozia, T., Watanabe, K., Jeong, B.R., 1995. Stem elongation and growth of *Solanum tuberosum* L. in vitro in response to photosynthetic photon flux, photoperiod and difference in photoperiod and dark period temperatures. Sci. Hortic. 64, 1-9.

Legnani, G., Miller, W.B., 2001. Short photoperiods induce fructan accumulation and tuberous root development in *Dahli*a seedling. New phytol. 149, 445-454.

Monti, A., Amaducci, M.T., Venturi, G., 2005. Growth response, leaf gas exchange and fructans accumulation of Jerusalem artichoke (*Helianthus tuberosus* L.) as affected by different water regimes. Eur. J. Agron. 23, 136-145.

Pimsaen, W., Jogloy, S., Suriharn, B., Kesmala, T., Pensuk, V., Patanothai, A., 2010. Genotype by environment (G × E) interactions for yield components of Jerusalem artichoke (*Helianthus tuberosus* L.). Asian J. Plant Sci. 9, 11-19.

Pool-Zobel, B.L., 2005. Inulin-type fructans and reduction in colon cancer risk: review of experimental and human data. Br. J. Nutr. 93, 73-90.

Puangbut, D., Jogloy, S., Srijaranai, S., Vorasoot, N., Kesmala, T., Patanothai, A., 2011. Rapid assessment of inulin content in *Helianthus tuberosus* L. tubers. SABRAO J. Breed. Genet. 43, 188-200.

Puangbut, D., Jogloy, S., Vorasoot, N., Srijaranai, S., Kesmala, T., Holbrook, C.C., Patanothai, A., 2012. Influence of planting date and temperature on inulin content in Jerusalem artichoke (*Helianthus tuberosus* L.). Aust. J. Crop Sci. 6, 1159-1165.

Puttha, R., Jogloy, S., Wangsomnuk, P.P., Srijaranai, S., Kesmala, T., Patanothai, A., 2012. Genotypic variability and genotype by environment interactions for inulin content of Jerusalem artichoke germplasm. Euphytica. 183, 119-131.

Rafter, J., Bennen, M., Caderni, G., Clune, Y., Hughes, R., Karlsson, P.C., Klinder, A., O'Riordan, M., O'Sullivan, G.C., 2007. Dietary synbiotics reduce cancer risk factors in polypectomized and colon cancer patients. Am. J. Clin. Nutr. 85, 488-496.

Roberfroid, M.B., 2002. Functional foods: concepts and application to inulin and oligofructose. Brit. J. Nutr. 87, 139-143.

Roberfroid, M.B., 2007. Inulin-type fructans: functional food ingredients. J. Nutr. 137, 2493-2502.

Ruttanaprasert, R., Banterng, P., Jogloy, S., Vorasoot, N., Kesmala T, Kanwar, R.S., Holbrook, C.C., Patanothai, A., 2014. Genotypic variability for tuber yield, biomass and drought tolerance in Jerusalem artichoke germplasm. Turk. J. Agric. For. 38, 570-580.

Ruttanaprasert, R., Jogloy, S., Vorasoot, N., Kesmala, T., Kanwar, R.S., Holbrook, C.C., Patanothai, A., 2013. Photoperiod and growing degree days effect on dry matter partitioning in Jerusalem artichoke. Int. J. Plant Prod. 7, 393-416.

Saengkanuk, A., Nuchadomrong, S., Jogloy, S., Patanothai, A., Srijaranai, S., 2011. A simplified spectrophotometric method for the determination of inulin in Jerusalem artichoke (*Helianthus tuberosus* L.) tubers. Eur. Food Res. Technol. 233, 609-616.

Saengthongpinit, W., Sajjaanantakul, T., 2005. Influence of harvest time and storage temperature on characteristics of inulin from Jerusalem artichoke (*Helianthus tuberosus* L.) tubers. Postharvest Biol. Tec. 37, 93-100.

Schubert, S., Feuerle, R., 1997. Fructan storage in tuber of Jerusalem artichoke: characterization of sink strength. New phytol. 136, 115-122.

Vandoorne, B., Matheiu, A.S., Van den Ende, W., Vergauwen, R., Périlleux, C., Javaux, M., Lutts, S., 2012. Water stress drastically reduces root growth and inulin yield in *Cichorium intybus* (var. *sativam*) independently of photosynthesis. J. Exp. Bot. 63, 4359-4373.

Copyright of International Journal of Plant Production is the property of Gorgan University of Agricultural Sciences & Natural Resources and its content may not be copied or emailed to multiple sites or posted to a listserv without the copyright holder's express written permission. However, users may print, download, or email articles for individual use.

Scientia Horticulturae 195 (2015) 108–115

Contents lists available at ScienceDirect

Scientia Horticulturae

journal homepage: www.elsevier.com/locate/scihorti

Responses of growth, physiological traits and tuber yield in *Helianthus tuberosus* to seasonal variations under tropical area

D. Puangbut[a], S. Jogloy[a,b,*], N. Vorasoot[a], A. Patanothai[a]

[a] Department of Plant Science and Agricultural Resources, Faculty of Agriculture, Khon Kaen University, Khon Kaen 40002, Thailand
[b] Peanut and Jerusalem Artichoke Improvement for Functional Food Research Group, Khon Kaen University, Khon Kaen, Thailand

ARTICLE INFO

Article history:
Received 10 March 2015
Received in revised form 26 August 2015
Accepted 6 September 2015

Keywords:
Jerusalem artichoke
Temperature
Development pattern
Tuber growth rate

ABSTRACT

Seasonal variations affect growth and yield of a crop, primarily by changing its phenological developmental processes. The objective of the present study was to evaluate seasonal variation effects on growth and development of Jerusalem artichoke. The experiment was conducted during the early-rainy seasons in June–September 2011 and the post-rainy seasons in September–December in 2011, and two seasons were repeated in 2012 at the Field Crop Research Station of Khon Kaen University. A randomize complete block design (RCBD) with 5 replications was used. Four Jerusalem genotypes including JA 89, HEL 65, CN 52867 and KT 50-4 were used. Results indicated similar phenological development between the early and post rainy-seasons. However, high temperature combined with long photoperiod during the early-rainy seasons delayed tuber initiation and extended maturity. Low temperature and short photoperiod was a favorable condition for tuber development but reduced vegetative and reproductive development. On average, tuber dry weights and tuber growth rate were higher in the post-rainy season compared to the early-rainy season. On the other hand, biomass and crop growth rates were higher in the early-rainy seasons compared to the post-rainy seasons. The knowledge obtained in this study is important for Jerusalem artichoke production and selection of Jerusalem artichoke genotypes in the tropical climate.
© 2015 Elsevier B.V. All rights reserved.

1. Introduction

Jerusalem artichoke is generally grown in temperate regions (Denoroy et al., 1996) but it can perform well in the Semi-Arid Tropics (Pimsaen et al., 2010; Puangbut et al., 2012; Ruttanaprasert et al., 2013). Ruttanaprasert et al. (2013) concluded that Jerusalem artichoke can be grown successfully across a wide range of climatic environments including tropical climates. The Jerusalem artichoke tolerance to both low and high temperatures has contributed to its wide geographic, morphological and habitat adaption, extending from temperate areas in the North America to Semi-Arid Tropics areas in Southeast Asia.

However, growth, development and yield of this crop is influenced by environmental factors, including solar radiation, temperature, length of the growing season and rainfall (Monti et al., 2005; Kays and Nottingham, 2007). Temperature is often cited as main driver of Jerusalam artichoke growth and development (Kocsis et al., 2007, 2008). Several reports indicated that low temperature reduced growth and tuber yield of Jerusalem artichoke in both temperate and semi-arid tropical regions (Kocsis et al., 2007, 2008; Puangbut et al., 2012).

Furthermore, photoperiod also influences growth and development of Jerusalem artichoke (Soja and Dersch, 1993; Kays and Kultur, 2005; Kocsis et al., 2007). Ruttanaprasert et al. (2013) reported that tuber yield was enhanced when Jerusalem artichoke plants were grown during short photoperiods. The proportion of assimilate that produced tuber was also found to be photoperiod sensitive (Ruttanaprasert et al., 2013).

Experimental and farm research trials in Thailand have also shown adaptability, as Jerusalem artichoke production has been successful in both early-rainy and post-rainy seasons (Puttha et al., 2012). In the early-rainy seasons, Jerusalem artichoke is subjected to high temperature and humidity (May–June). During June and July, when the plant has both vegetative and reproductive growth, temperatures range from 28 to 35 °C. In contrast, the post-rainy season beginning in September and October is moderate in temperature (25–31 °C) with the reproductive phase of this crop subjected

* Corresponding author. Fax: +66 43364637.
E-mail address: sjogloy@gmail.com (S. Jogloy).

http://dx.doi.org/10.1016/j.scienta.2015.09.008
0304-4238/© 2015 Elsevier B.V. All rights reserved.

to temperatures in November and December ranging from 12 to 20 °C.

Certainly the environmental conditions affect growth and development. Reproductive and tuberization stages during the early-rainy crop take relatively longer due to their long days as compared with the post-rainy season crop where reproductive and tuberization stages take place under short days (Ruttanaprasert et al., 2013). However, only a limited number of studies have evaluated growth and developmental patterns and other physiological traits of Jerusalem artichoke genotypes across different environments, to show how the differences in physiological traits may explain yield performance. Growth analysis of Jerusalem artichoke breeding lines conducted during different growing seasons can provide additional information concerning the growth habit of released genotypes for different environmental conditions, leading to a better understanding of the physiological determinants of tuber yield of these genotypes. This information can then be used to determine additional selection criteria for Jerusalem artichoke breeding programs, and to develop appropriate management strategies for Jerusalem artichoke production for different growing seasons. The objective of the present study was to evaluate effects of seasonal and genetic variation on growth and development of Jerusalem artichoke.

2. Materials and methods

2.1. Plant materials and experimental design

Four Jerusalem artichoke genotypes were studied in both seasons for two years. These genotypes were selected because they are commonly cultivated in Thailand. KT 50-4, a hybrid clone of Khon Kaen University, Thailand and it takes 110 days to maturity. Two genotypes (CN 52867 and JA 89) were kindly donated by the Plant Gene Resource of Canada (PGRC). CN52867 is an early maturity (100 days) and JA 89 with 110-day maturity. HEL 65 is late maturity (115 days) from the Leibniz Institute of Plant Genetics and Crop Plant Research of Germany (IPK).

Field experiments were conducted during the early-rainy season in June–September 2011 and the post-rainy seasons in September–December in 2011, and the two seasons were repeated in 2012 at the Field Crop Research Station of Khon Kaen University. A randomized complete block design (RCBD) with five replications was used. Plot size was 6 × 6 m with a spacing of 50 cm between rows and 50 cm between hills in a row, giving population density of 40,000 plants per hectare.

2.2. Crop management

Pre-sprouted seed tubers were used as planting materials. To prepare the sprouted seed tubers, the tubers were cut into small pieces each of which had two or three buds. The tuber pieces were incubated in plastic bags containing moist coconut peat at the bottom and the top of the bags about 7 days under ambient conditions (Puttha et al., 2012). The plastic bags were kept opened for good aeration. The tuber pieces with active buds and roots were further transferred to plug plastic trays containing a mixture 1:1 soil: burnt rice husk medium about 7 days for germination. When the fourth leaf-sprouted (V4) the seedlings were then transplanting into the plots at the rate of one seedling per hill. Fertilizer formula 15-15-15 was applied at 30 days after transplanting (DAT) at a rate of 156 kg/ha. Terraclor (quintozene 24% W/V EC) was applied monthly for 3 months after transplanting at the rate 25 ml in 20 l of water for the control of stem rot (*Sclerotium rolfsii*). The disease also causes yield loss in Jerusalem artichoke (McCarter and Kays, 1984). Therefore, plants were observed for disease severity (data not shown). Supplementary irrigation was applied to the crop with an overhead sprinkler system.

Table 1
Physical and chemical properties of the soil from the experimental field site.

Soil properties/depth	0–30 cm
Physical properties	
Sand (%)	88.3
Silt (%)	7.3
Clay (%)	4.4
Chemical properties	
pH (1:2.5H_2O)	5.52
CEC (c mol kg^{-1})	5.56
Oganic matter (%)	0.53
Total N (%)	0.029
Available P (mg kg^{-1})	48.8
Exchangeable K (mg kg^{-1})	45.7
Exchangeable Ca (mg kg^{-1})	444

2.3. Data collection

Plant growth and development traits were recorded for both early rainy and post rainy seasons. The developmental data recorded were: time from emergence to second true leaf expansion (V2), to four nodes present on the main stem beginning with the unifoliated node (V4), plants with first flower initiation (R1), plants with first open flower (R3), plants with the disk flower corollas become yellow and brown (R6), plants with stolon develop (T1), plants with first the trip of stolon being swell (T2), plant with first tuber initiation and appreciable enlarging (T3), plant with first tuber cell expand (T4), plant with tuber skin become to yellow and brown (T5) and plant with tuber skin become dark brown and stem turn yellow or brown and loses leave (T6) (Puangbut et al., 2015). V and R stages were observed on three-plants sampled at 2-day intervals while T stage was observed on three plants sampled at 5-day intervals in each replication. The occurrence of each stage was defined as when 50% of the observed plants reached that stage. Crop growth characteristics were obtained at six developmental stages (T1–T6) and were collected according to Puangbut et al. (2015). Total, leaf, stem and tuber dry weight was measured at 20, 40, 60, 80 and 100 DAT from three plants in area 0.75 m^2 and this dry weight were converted to dry weight per square meter.

At harvest, plants each end of the rows were discarded, and all plants in an area of 3.5 m^2 were harvested discarding the border rows. Plants were cut at the soil surface and separated into shoots and tubers. Tubers were washed in tap water to remove the potting medium. Fresh shoot weight and tuber fresh weight were determined in the field and then the weights were converted to fresh weights per area. One kg samples of fresh shoots and tubers for each plot were taken, oven-dried at 80 °C for 72 h or until the weight was constant. Tuber dry weight and biomass including shoot dry weight and tuber dry weight were recorded.

Leaf area was measured at 25, 50, 75 DAT and harvest, using a leaf area meter (LI-3100 area meter, LI-COR, Inc., USA). The total leaf area of the subsample was used to convert leaf biomass into total leaf area and LAI for each plot. Biomass data were used to determine crop growth rate (CGR) and tuber growth rate (TGR) of the individual genotypes in each season. CGR was calculated as an average rate for the entire season. Similarly, TGR was calculated as an average rate for the entire tuber development period (T2–T6).

Daily maximum and minimum temperatures (°C), rainfall (mm), and solar radiation (MJ m^{-2} day^{-1}) were obtained from the KKU Field Crops Research Station where the experiment was conducted.

Temperature and photoperiod was computed from day of sprout development (VE) to harvest time (T6). These data was calculated for eight periods of phenology development: sprout development to vegetative (VE–V4), vegetative to floral bud formation (V4–R1),

floral bud formation to seed set (R1–R6), vegetative to stolon (V4–T1), stolon to tuber development (T1–T3), tuber development to tuber maturity (T3–T6), stolon to tuber maturity (T1–T6) and vegetative to tuber maturity (V4–T6).

2.4. Statistical analysis

Comparisons were made for phenological development and growth characteristics of genotypes during the different seasons. Analysis of variance was performed for each character in each seasons followed a Randomize complete block design. Error variances for the two years were tested for homogeneity by Bartlett's test (Hoshmand, 2006). Although error variances of two year were homogenous (data not shown), there were significant genotype × season interaction for all characters (data not shown), data were reported for individual seasons. Duncan's multiple range tests (DMRT) was used to compare means within genotypes and *F*-test was used to compare means between seasons for each genotype. Calculation procedures were done using STATISTIX 8 software program (Statistix 8, 2003).

3. Results and discussion

3.1. Soil properties and weather conditions

The soil series on the experimental site is Yasothon (Yt; fine-loamy, siliceous, isohypothermic, Oxic Paleustults), a sandy soil with pH 5.52, 0.53% organic matter and 0.03% total N (Table 1). The proportions of sand, silt and clay in the soil were 88.3%, 7.3% and 4.4%, respectively. Available P was 48.8 mg kg^{-1} and extractable K and Ca were 45.7 and 444 mg kg^{-1}, respectively. Cation exchange capacity (CEC) was 5.56 c mol kg^{-1}. The soil in this study (tropics) was sandy with low organic matter, low nitrogen, medium phosphorus and medium potassium. However, Jerusalem artichoke can grow in dry regions with poor soil (Kays and Nottingham, 2007).

Seasonal mean maximum temperature in the early-rainy season was 32.0 °C and it was 30.4 °C in the post-rainy seasons in 2011 (Fig. 1). Seasonal mean minimum temperature in the early-rainy season was 23.0 °C and it was 20.2 °C in the post-rainy season in 2011. Seasonal mean maximum temperature in the early-rainy season was 32.4 °C and it was 31.0 °C in the post-rainy season in 2012 (Fig. 2). Seasonal mean minimum temperature in the early-rainy season was 23.0 °C and it was 21.7 °C in the post-rainy season in 2012.

The mean solar radiation in the early-rainy season was 12.3 MJ/m^{-2} per day and it was 12.5 MJ/m^2 per day in the post-rainy season in 2011 (Fig. 1). In 2012, the mean solar radiation in the early-rainy season was 16.2 MJ/m^{-2} per day and it was 17.2 MJ/m^2 per day in the post-rainy season (Fig. 2).

Rainfall in the early-rainy season totaled 815 mm and it totaled 276 mm in the post-rainy season in 2011 (Fig. 1). Rainfall in the early-rainy season totaled 480 mm and it totaled 108 mm in the post-rainy season in 2012 (Fig. 2).

Results indicated that solar radiation, daily temperatures during the period from reproductive to tuberization stages of the post-rainy season were considerably lower than in the early-rainy seasons, especially during tuber initiation (T2) to the tuber maturity stages (T6) (Table 2). Rainfall was well distributed throughout the crop cycle in the early-rainy seasons in both years, and no water stress was observed during the growing seasons for post-rainy seasons in either year.

3.2. Crop development

In making comparisons, the stages of phenological development were grouped into eight periods: sprout development to vegetative (VE–V4), vegetative to floral bud formation (V4–R1), floral bud formation to seed set (R1–R6), vegetative to stolon (V4–T1), stolon to tuber development (T1–T3), tuber development to tuber maturity (T3–T6), stolon to tuber maturity (T1–T6) and vegetative to tuber maturity (V4–T6) representing the periods of vegetative development, reproductive development and tuber development. Table 2 shows the means of each Jerusalem artichoke genotypes for the whole crop growth and the eight phenological development periods along with the photoperiod for each period.

Table 2
Means for duration of individual phenological development periods for early-rainy seasons (ERS) and post-rainy seasons (PRS) of four Jerusalem artichoke genotypes and the corresponding values of photoperiod.

	Duration (days)			Photoperiod (h)	
Stage[a]	ERS	PRS	*T*-test	ERS	PRS
JA 89					
VE–V4	14	14	ns	13.1	12.3
V4–R1	35	36	*	13.0	12.1
R1–R6	45	37	**	12.6	11.6
V4–T1	25	30	*	13.0	12.1
T1–T3	43	27	**	12.7	11.8
T3–T6	42	39	ns	12.1	11.6
T1–T6	85	66	**	12.4	11.3
V4–T6	110	96	**	12.5	11.2
HEL 65					
VE–V4	14	14	ns	13.1	12.3
V4–R1	44	41	**	13.0	11.2
R1–R6	48	43	**	12.4	11.4
V4–T1	20	27	**	13.1	12.0
T1–T3	42	25	**	12.8	11.7
T3–T6	53	42	**	12.1	11.3
T1–T6	95	67	**	12.4	11.4
V4–T6	115	94	**	12.5	11.6
CN 52867					
VE–V4	14	14	ns	13.1	12.3
V4–R1	35	33	*	13.0	12.0
R1–R6	39	32	**	12.6	11.4
V4–T1	19	25	**	13.1	12.0
T1–T3	40	25	**	12.8	11.7
T3–T6	39	39	ns	12.3	11.3
T1–T6	79	64	**	12.5	11.4
V4–T6	98	88	**	12.6	11.6
KT 50-4					
VE–V4	14	14	ns	13.1	12.3
V4–R1	42	40	**	13.0	11.9
R1–R6	43	35	**	12.4	11.4
V4–T1	25	30	**	13.0	12.0
T1–T3	39	25	**	12.7	11.6
T3–T6	46	46	ns	12.1	11.3
T1–T6	85	71	**	12.4	11.4
V4–T6	110	100	**	12.5	11.6

Ns, * and ** non-significant, significant at $p < 0.05$ and significant at $p < 0.01$.
[a] VE, sprout development; V4, The fourth true leaf (transplanting); R1, Flower initiation; R6, seed maturity; T1, stolon; T3, tuber formation; T6, tuber maturity.

The duration from transplanting to physiology maturity differed between early-rainy seasons and post-rainy seasons for all Jerusalem artichoke genotypes. The duration across all genotypes in the early-rainy seasons averaged 108 days, while the post-rainy seasons duration averaged 96 days, HEL 65 was the latest maturing in early-rainy seasons (115 day), while KT 50-4 was the latest maturing in the post-rainy seasons (100 day). In contrast, the duration of CN 52867 was shorter in both early-rainy seasons and post-rainy seasons (98 and 88 days, respectively). The durations of VE-V4 did not differ between early-rainy seasons and post-rainy seasons but T1–T3 and T1–T6 was substantially longer for the early-rainy seasons. It was apparent that the long duration of crop growth of Jerusalem artichoke in the early-rainy seasons was mainly due to a longer period from stolon to tuber maturity (T1–T6), which

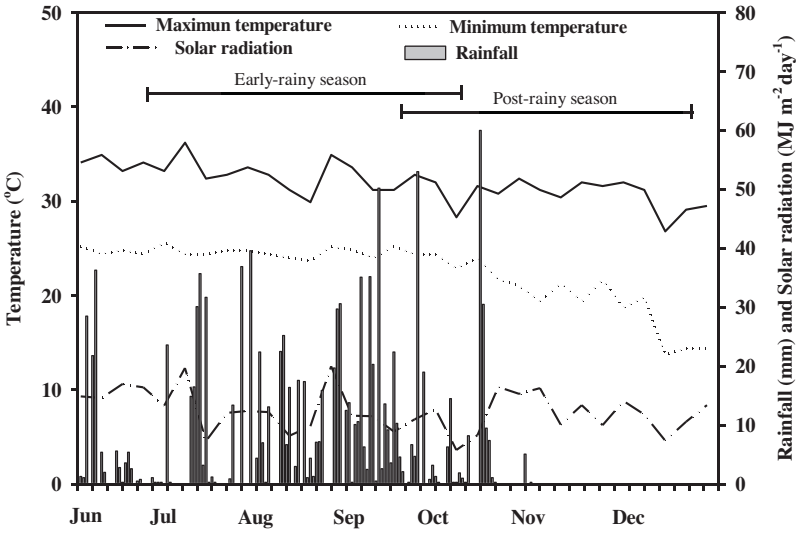


Fig. 1. Daily maximum temperature, minimum temperature, solar radiation and rainfall during the early-rainy and post-rainy seasons in 2011.

coincided with a period of relatively long photoperiod and high temperature (28 °C).

The duration of growth was longer in the early-rainy seasons due to a longer period from stolon to tuber maturity for all genotypes. In early-rainy seasons, the duration from stolon to tuber maturity averaged 83 days while in the post-rainy season it was 65 days. The differences of tuber growth rate in different growing seasons are due to variation of photoperiod and temperature that affect growth and maturity of Jerusalem artichoke (Soja and Dersch, 1993; Kays and Nottingham, 2007; Ruttanaprasert et al., 2013). The present study demonstrated that the rate of phenological development from stolon to tuber maturity is mainly controlled by photoperiod and temperature and suggested that these factors was the main affect growth and yield of Jerusalem artichoke. Several papers also revealed that temperature and photoperiod is the main forcing factor affecting plant development and yield (Soja and Dersch, 1993; Schwartz, 2003; Kays and Nottingham, 2007; Heide, 2008; Ruttaprasert et al., 2013).

3.3. Dry matter accumulation and leaf area expansion

Dry matter accumulation and leaf area expansion at different growth stages for two seasons for four genotypes are shown in Figs. 3–5. In both seasons, total, tuber, leaf and stem dry weight increased continuously throughout the growing season. The delay in phenological development during the reproductive and tuberization stages in the early-rainy seasons when temperatures were high was reflected in a delay in tuber formation in all genotypes (Fig. 3). Total biomass for all genotypes, was higher in the early-rainy seasons than in the post-rainy seasons. Tuber dry weights in the post-rainy seasons were significantly higher than in the early-rainy seasons for CN 52867 only. Furthermore, this study revealed that tuber size in the post-rainy seasons (23 g per tuber) was large than in the early-rainy seasons (16 g per tuber) (data not shown).

Previous research indicated that low temperature and short photoperiod were favorable conditions for tuber development in both temperate and tropical regions but not for vegetative and reproductive development (Soja and Dersch, 1993; Somda et al.,

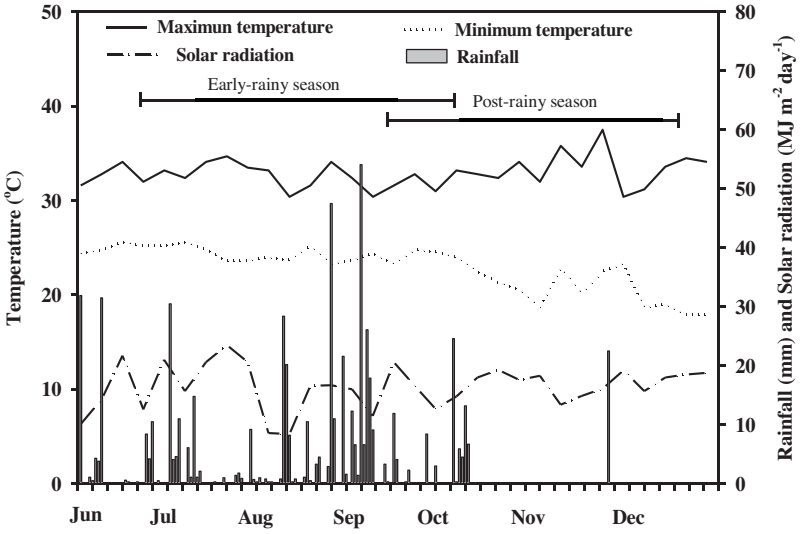


Fig. 2. Daily maximum temperature, minimum temperature, solar radiation and rainfall during the early-rainy and post-rainy seasons in 2012.

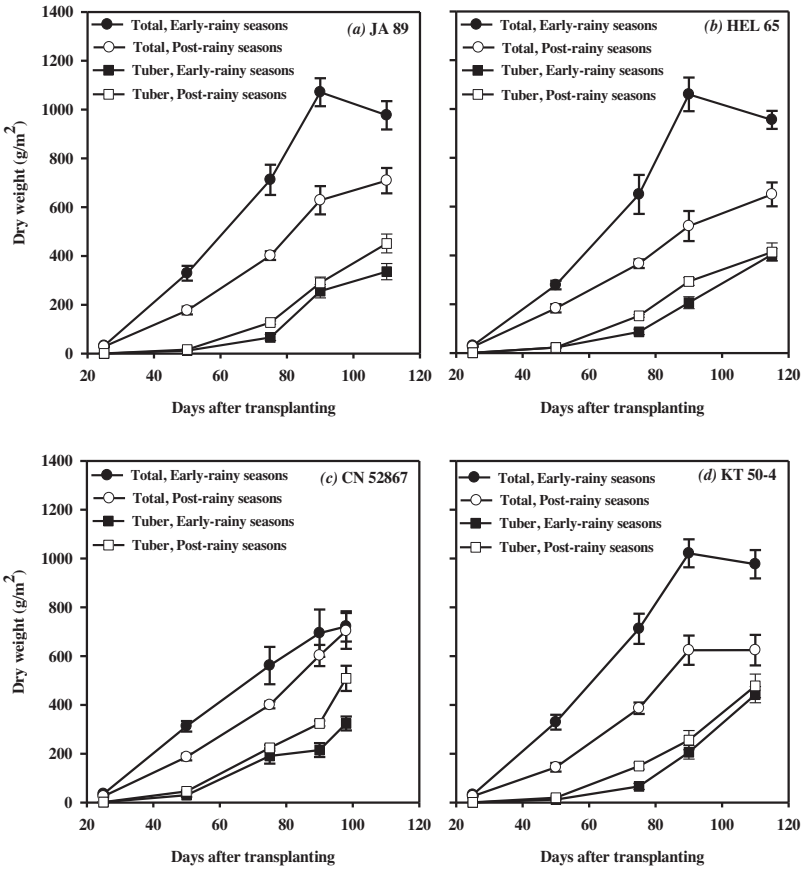


Fig. 3. Total and tuber dry weights of four Jerusalem artichoke genotypes in the early-rainy seasons and post-rainy seasons. Vertical bars are standard errors of the means (n = 5).

1999; Kays and Nottingham, 2007). The present study revealed that Jerusalem artichoke plants grown during short photoperiod (11 h) produced larger tubers and resulted in an increase tuber yield. Similar to Ruttanaprasert et al. (2013), they also noted that short photoperiod reduced the number of tuber but increase tuber size and resulted in enhance tuber dry weight. Enhanced tuber yield may be due to the plant allocating most of the dry matter to tuber organs, thus increasing tuber dry matter (Soja and Dersch, 1993; Somda et al., 1999; Ruttanaprasert et al., 2013). The results suggested that low temperature and short photoperiod conditions during tuber formation can increase tuber yield of Jerusalem artichoke in tropical regions.

The crop grown in the early-rainy seasons had higher leaf dry weights and stem dry weights than did the crop grown in the post-rainy seasons (Fig. 4). All Jerusalem artichoke genotypes showed similar pattern for leaf dry weight and stem dry weight in both seasons.

In the early-rainy seasons, the growth pattern of four Jerusalem artichoke genotypes was similar to that of the post-rainy seasons. The most rapid increase of vegetative growth (leaf and stem) occurred between 25 and 90 DAT and peaked at 80 DAT and then declined thereafter (Fig. 4). However, total dry weight accumulation was significantly different between seasons. In the early-rainy season, total dry weight increased continuously until 90 DAT and then declined thereafter for all Jerusalem artichoke genotypes while in the post-rainy season was increased continuously from tuber formation to tuber maturity (Fig. 3). The reduction of total dry weight could be due to Southern stem rot. Although the stem rot was well-controlled in both experiments, there was noticed the disease severity in the early-rainy season in both years. This diseases incited by *S. rolfsii* is more prevalent under the high temperature and high humidity conditions of the rainy seasons (Sennoi et al., 2012, 2013). High disease severity may cause reduced stem, leaf and tuber dry weight in the early-rainy season (Sennoi et al., 2013).

Generally, the accumulation of dry matter in the leaves and stems increased continuously from vegetative stage to tuber formation and then declined when tuber cell expended (Somda et al., 1999). These could be due to the nutrient accumulations were allocated from stem senescence to storage organ (tuber). Thus, aboveground plant parts, in particular stems (shoots and branches), constituted the primary temporary sink for carbohydrates remobilized later into the developing stolons and tubers (Somda et al., 1999).

The results indicated that the dry matter in vegetative structures (leaf and stem) decreased with the onset of rapid tuber development. During the stage of shoot senescence, the dry matter in shoot (temporary sink) is allocated to storage organs (tuber and root) thus causing a rapid increase in tuber dry matter (Somda et al., 1999).

The results revealed that temperature and photoperiod during tuber formation period was quite different between seasons. The present study indicated that all Jerusalem artichoke genotypes showed a rapid tuber growth under post-rainy season (Table 2). It was apparent that tuber growth was associated with short photoperiod and low temperature. Likewise, Ruttanaprasert et al. (2013) revealed that temperature and photoperiod was correlated with harvest index and tuber yield.

Several reports demonstrated that higher temperature and long photoperiod can result in a return to vegetative growth (Denoroy, 1996; Kays and Kultur, 2005). These conditions delayed tuber ini-

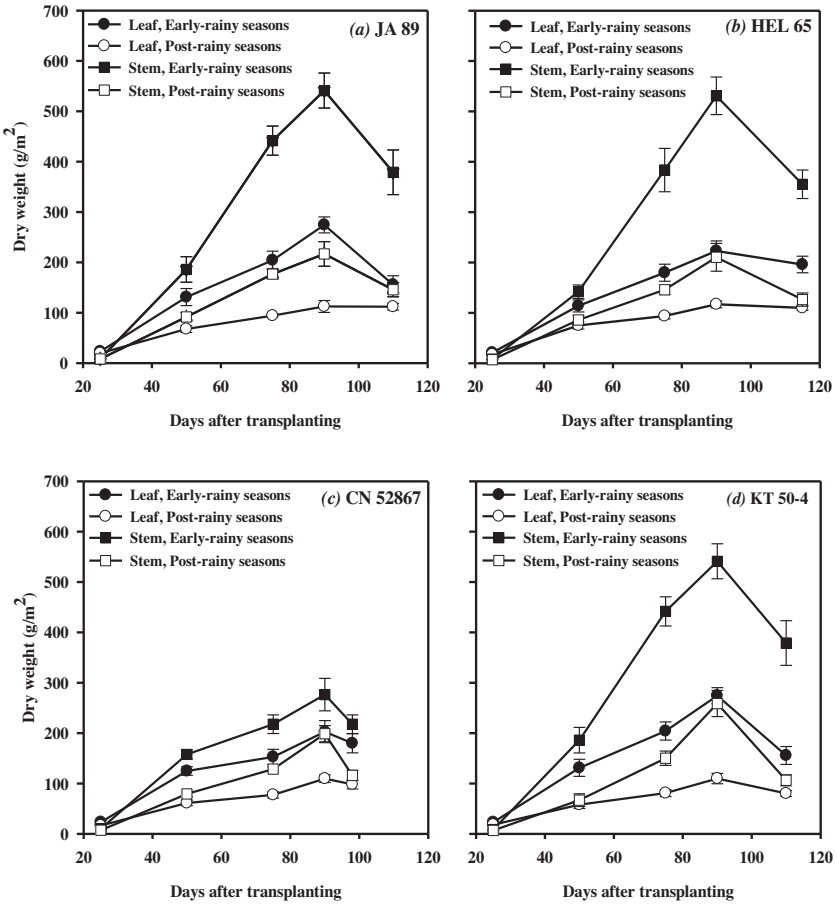


Fig. 4. Leaf and stem dry weights of four Jerusalem artichoke genotypes in the early-rainy seasons and post-rainy seasons in year 2011 and 2012. Vertical bars are standard errors of the means ($n = 5$).

tiation, induced vegetative growth and reduced allocation of dry matter to tuber. On the contrary, low temperature and short photoperiod induced tuber initiation. Similar to Okubo et al. (1992) reported that tuberous root formation was induced by short photoperiod in winged bean. Thus, tuber initiation needs sufficiently low temperature and short photoperiod (Djurhuus, 1985; Soja and Dersch, 1993; Kays and Nottingham, 2007). These finding were similar to other tuber crops such as potato. In potato, high temperatures delay tuber initiation and reduces assimilate portioning to the tuber (Van Dam et al., 1996). Physiological changes to climatic variations triggering a translocation rate increase, and accelerating the remobilization of reserves from stalks to tubers have been noted by Baldini et al. (2011).

LAI in most of genotypes increased to maximum value at 75 DAT and then progressively declined except in HEL 65 for both seasons (Fig. 5). HEL 65 still increased LAI even at the last sampling date in the early-rainy season. Growth rates for LAI were high in all genotypes during the VE–R6 stage (averaged 82 DAT) in the early-rainy seasons. In contrast, growth rates for LAI were low in all genotypes in the post-rainy seasons during the VE–T6 stage.

LAI can also influence photosynthetic capacity and tuber yield (Kays and Nottingham, 2007; Gao et al., 2011). The present study revealed low LAI in the post-rainy season compared to the early-rainy seasons and this could be due to small plant and large canopy gaps. Therefore, increasing the plant population density in the post-rainy season may increase tuber yield. Rebora et al. (2011) found that raising plant density from two to eight plants per square meter increased yield per unit area but reduced tuber size. Our study suggested that increasing plant density from four to six plants per square meter in the post-rainy season could increase both tuber yields per unit area and tuber size. However, the optimal plant density is still undetermined in the tropical area.

3.4. Variation among genotypes in tuber yield and physiological traits

Tuber yield, biomass, crop growth rate (CGR), tuber growth rate (TGR) and duration of tuber enlargement for individual genotypes in the rainy-seasons and post-rainy seasons are shown in Tables 3 and 4. Mean tuber dry weight and TGR were higher but the duration of tuber enlargement was shorter in the post-rainy seasons. In contrast, biomass and CGR were lower while the duration of tuber enlargement was longer in the early-rainy seasons.

The variation in tuber yield, biomass, CGR and TGR among genotypes was significantly different for both seasons. In the rainy-

Table 3
Tuber dry weight and biomass for the early-rainy seasons (ERS) and the post-rainy seasons (PRS) of four Jerusalem artichoke genotypes.

	Tuber dry weight ($g\,m^{-2}$)			Biomass ($g\,m^{-2}$)		
Genotypes/clone	ERS	PRS	F-test	ERS	PRS	*F*-test
JA 89	336 b	451 b	**	856 ab	703 b	*
HEL 65	403 ab	414 c	ns	956 a	650 c	**
CN 52867	324 bc	509 a	**	721 b	709 a	ns
KT 50-4	442 a	478 b	*	977 a	625 c	**
Mean	377	463	**	878	672	**

Means in the same column with the same letters are not significantly different by DMRT ($p < 0.05$) ns, * and ** non-significant, significant at $p < 0.05$ and significant at $p < 0.01$.

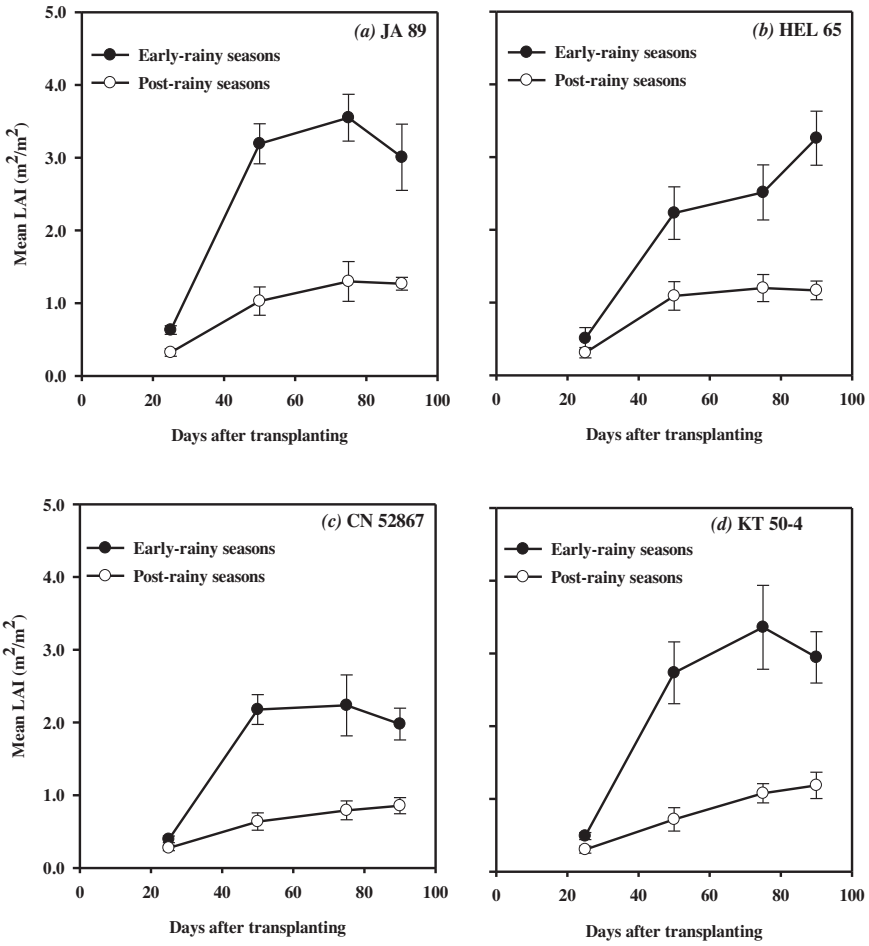


Fig. 5. Leaf area index (LAI) of four Jerusalem artichoke genotypes in the early-rainy seasons and post-rainy seasons. Vertical bars are standard errors of the means ($n = 5$).

season, KT 50-4 and HEL 65 had high tuber dry weight and biomass while the highest in CGR and TGR was observed in HEL 65 and KT 50-4, respectively. CN 52867 was the highest for tuber dry weight, CGR and TGR in the post-rainy seasons (Tables 3 and 4).

All Jerusalem artichoke genotypes showed higher yield in the post-rainy seasons than that in the early-rainy seasons. In contrast, all genotypes showed higher biomass accumulation in the early-rainy season when compared to the post-rainy season. This finding supports previous studies that plant grown during the post-rainy seasons increase more partitioning of dry matter (HI) towards the tuber (Ruttanaprasert et al., 2013). Therefore a study of dry matter production and distribution in the various plant organs during development is important to determine a cultivar's growth rate and production.

Table 4
Crop growth rate (CGR), tuber growth rate (TGR) for the early-rainy seasons (ERS) and the post-rainy seasons (PRS) of four Jerusalem artichoke genotypes.

	CGR ($g\,m^{-2}\,day^{-1}$)			TGR ($g\,m^{-2}\,day^{-1}$)			Tuber enlarging duration (days)		
Genotypes	ERS	PRS	*F*-test	ERS	PRS	F-test	ERS	PRS	*F*-test
JA 89	10.4 b	9.1 b	*	4.4 b	7.7 b	**	73 b	55 a	**
HEL 65	13.7 a	9.1 b	**	4.7 b	7.0 b	**	84 a	56 a	**
CN 52867	10.2 b	10.7 a	ns	4.7 b	9.6 a	**	67 c	52 ab	*
KT 50-4	11.6 b	7.9 c	**	5.7 a	7.3 b	**	75 b	58 a	**
Mean	11.5	9.2		4.9	7.9		75	55	

Means in the same column with the same letters are not significantly different by DMRT ($p < 0.05$) ns, * and ** non-significant, significant at $p < 0.05$ and significant at $p < 0.01$.

The yield differences among genotypes could be accounted for by measured physiological traits. The results suggested that TGR was the major component contributing to tuber yield and it was increased with lower temperature conditions. Similar to potato crop, Ascione et al. (2013) suggested that TGR was an important trait in determining tuber yield.

Therefore, TGR would be useful when selecting genotypes for improved tuber yield. Our study suggested that physiological traits could be useful for improvement of the crop simulation models to enable it to simulate Jerusalem artichoke productivity in different conditions. Similar to Baldini et al. (2011) suggested that the crop simulation model could be useful as a tool for the planning and risk evaluation of production Jerusalem artichoke as a crop for inulin production.

4. Conclusions

The present study demonstrated that seasonal variation was the main effect on growth, physiological traits and tuber yield. The results revealed that the post-rainy seasons were more favorable for tuber growth but not for vegetative and reproductive development. Over all genotypes, tuber yield and TGR in the post-rainy seasons were higher than those traits in the early-rainy season. This information is very important for Jerusalem artichoke production in different growing season and could be useful for selection of Jerusalem artichoke genotypes in the tropics.

Acknowledgements

This work was supported by the Higher Education Research Promotion and National Research University Project of Thailand, Office of the Higher Education Commission, through the Food and Functional Food Research Cluster of Khon Kaen University, Thailand. We also thank the Leibniz Institute of Plant Genetics and Crop Plant Research, Germany, the Plant Gene Resource of Canada, Canada for the contribution of Jerusalem artichoke germplasm. Grateful acknowledgments are made to the Thailand Research Fund for providing financial support through the Senior Research Scholar Project of Prof. Dr. Sanun Jogloy (Project no. RTA 5880003) and to Plant Breeding Research Center for Sustainable Agriculture, Khon Kaen University. Grateful acknowledgement is also made to the Thailand Research Fund (Project no. IRG 5780003), Khon Kaen University (KKU) and Faculty of Agriculture, KKU for providing financial support for manuscript preparation activities.

References

Ascione, S., Ruggiero, C., Vitale, C., 2013. Contribution of growth components on relative plant, crop and tuber growth rate of nine potato cultivars in southern Italy. Int. J. Sci. 2, 1–11.

Baldini, M., Francesco, D., Alvaro, R., Elena, B., Monti, A., Giuseppe, D.M., 2011. Jerusalem artichoke (*Helianthus tuberosus* L.) productivity in different Italian growing areas: a modelling approach. Ital. J. Agron. 6, 126–132.

Denoroy, P., 1996. The crop physiology of *Helianthus tuberosus* L.: a model orienter view. Biomass Bioenerg. 11, 11–32.

Djurhuus, R., 1985. The effect of photoperiod and temperature on growth and development of Begonia × tuberhybrida 'Karelsk Jomfru'. Sci. Hortic. 27, 123–131.

Gao, K., Zhu, T., Han, G., 2011. Water and nitrogen interactively increased the biomass production of Jerusalem artichoke (*Helianthus tuberosus* L) in semi-arid area. Afr. J. Biotechnol. 10, 6466–6472.

Heide, O.M., 2008. Interaction of photoperiod and temperature in the control of growth and dormancy of Prunus species. Sci. Hortic. 115, 309–314.

Hoshmand, A.R., 2006. Design of Experiments for Agriculture and the Natural Sci-ences. Chapman & Hall, Florida.

Kays, S.J., Kultur, F., 2005. Genetic variation in Jerusalem artichoke (*Helianthus tuberosus* L.) flowering date and duration. Hortscience 40, 1675–1678.

Kays, S.J., Nottingham, S.F., 2007. Biology and chemistry of Jerusalem artichoke (*Helianthus tuberosus* L.). CRC Press, Florida.

Kocsis, L., Kaul, H.-P., Praznik, W., Liebhard, P., 2007. Influence of harvest date on shoot and tuber yield ofdifferent Jerusalem artichoke (*Helianthus tuberosus* L.) cultivars in the semiarid production area of Austria. Ger. J. Agron. 11, 67–76.

Kocsis, L., Kaul, H.-P., Praznik, W., Liebhard, P., 2008. Influence of harvest date on tuber growth tuber dry matter content, inulin and sugar yield of different Jerusalem artichoke (*Helianthus tuberosus* L.) cultivars in the semi-arid production area of Austria. Ger. J. Agron. 12, 8–21.

McCarter, S.M., Kays, S.J., 1984. Disease limiting production of Jerusalem artichokes in Georgia. Plant Dis. 68, 299–302.

Monti, A., Amaducci, M.T., Venturi, G., 2005. Growth response, leaf gas exchange and fructans accumulation of Jerusalem artichoke (*Helianthus tuberosus* L.) as affected by different water regimes. Eur. J. Agron. 23, 136–145.

Okubo, H., Masunaga, T., Yamashita, H., Uemoto, S., 1992. Effects of photoperiod and temperature on tuberous root formation in winged bean (*Psophocarpus tetragonolobus*). Sci. Hortic. 49, 1–8.

Pimsaen, W., Jogloy, S., Suriharn, B., Kesmala, T., Pensuk, V., Patanothai, A., 2010. Genotype by environment (G × E) interactions for yield components of Jerusalem artichoke (*Helianthus tuberosus* L.). Asian J. Plant Sci. 9, 11–19.

Puangbut, D., Jogyloy, S., Vorassot, N., Patanothai, A., 2015. Growth and phenology of Jerusalem artichoke (*Helianthus tuberosus* L.). Pak. J. Bot. (in press).

Puangbut, D., Jogloy, S., Vorasoot, N., Srijaranai, S., Kesmala, T., Patanothai, A., 2012. Influence of planting date and temperature on inulin content in Jerusalem artichoke (*Helianthus tuberosus* L.). Aust. J. Crop Sci. 6, 1159–1165.

Puttha, R., Jogloy, S., Wangsomnuk, P.P., Srijaranai, S., Kesmala, T., Patanothai, A., 2012. Genotypic variability and genotype by environment interactions for inulin content of Jerusalem artichoke germplasm. Euphytica 183, 119–131.

Rebora, C., Barguren, L., Lelio, H., Gómez, L., 2011. Effect of plant population density on yield of Jerusalem artichoke urban waste water irrigated. Rev. Fac. Cienc. Agrar. 43, 83–90.

Ruttanaprasert, R., Jogloy, S., Vorasoot, N., Kesmala, T., Kanwar, R.S., Holbrook, C.C., Patanothai, A., 2013. Photoperiod and growing degree days effect on dry matter partitioning in Jerusalem artichoke. Int. J. Plant Prod. 7, 393–416.

Schwartz, M.D., 2003. Phenology: An Integrative Environmental Science. Kluwer Academic Publishers, Netherlands.

Sennoi, R., Jogloy, S., Saksirirat, W., Kesmala, T., Patanothai, A., 2013. Effects of host growth stage, re-isolation and culture medium on screening for resistance to stem rot disease caused by *Sclerotium rolfsii* Sacc. in Jerusalem artichoke. Pak. J. Bot. 45, 1825–1829.

Sennoi, R., Jogloy, S., Saksirirat, W., Kesmala, T., Singkham, N., Patanothai, A., 2012. Levels of *Sclerotium rolfsii* inoculum influence identification of resistant genotypes in Jerusalem artichoke. Afr. J. Microbiol. Res. 6, 6755–6760.

Soja, G., Dersch, G., 1993. Plant development and hormonal status in the Jerusalem artichoke (*Helianthus tuberosus* L.). Ind. Crops. Prod. 1, 219–228.

Somda, Z.C., Mclaurin, W.J., Kays, S.J., 1999. Jerusalem artichoke growth, development, and field storage. II. Carbon and nutrient element allocation and redistribution. J. Plant Nutr. 22, 1315–1334.

Statistix 8, 2003. Statistix8: analytical software user's manual. Tallahassee, Florida.

Van Dam, J., Kooman, L.P., Struik, P.C., 1996. Effects of temperature and photoperiod on early growth and final number of tuber in potato (*Solanum tuberosum* L). Potato Res. 39, 51–62.

Pak. J. Bot., 47(6): 2207-2214, 2015.

GROWTH AND PHENOLOGY OF JERUSALEM ARTICHOKE (*HELIANTHUS TUBEROSUS* L.)

DARUNEE PAUNGBUT[1], SANUN JOGLOY[1,2*], NIMITR VORASOOT[1] AND ARAN PATANOTHAI[1]

[1]*Department of Plant Science and Agricultural Resources, Faculty of Agriculture, Khon Kaen University, Khon Kaen, 40002, Thailand*
[2] *Peanut and Jerusalem artichoke Improvement for Functional Food Research Group, Khon Kaen University, Khon Kaen, 4002, Thailand*
[*]*Corresponding author e-mail: sjogloy@gmail.com*

Abstract

A standardized, accurate, and easy system is needed to describe Jerusalem artichoke (*Helianthus tuberosus* L.) plant development. Therefore, this study was designed to define stages of development descriptions for Jerusalem artichoke. Field experiments were conducted during early rainy season and the post rainy season of 2011 and 2012. Data were collected and uniform growth stage descriptions, based on visually observable events, were developed for the vegetative (V), reproductive (R) and tuberization (T) stages. The V stage was determined by counting the number of developed nodes on the main axis of the Jerusalem artichoke, beginning with emergence of the sprout seedling and ending with the initial visual appearance of the inflorescence. The proposed R stages include R1 (Floral bud formation), R2 (beginning bloom), R3 (flowering), R4 (beginning of anthesis), R5 (seed set) and R6 (seed maturity). The T stage include T1 (stolonization), T2 (tuber initiation), T3 (tuber formation), T4 (tuber bulking), T5 (skin set) and T6 (tuber maturity). The V, R and T stages can be measured separately and concurrently and apply to populations or single plants. The present study revealed that reproductive and tuberization development occurred more rapidly in the post-rainy season than in the early-rainy season. The proposed standard descriptions of Jerusalem artichoke development will help research and extension personnel better communicate results and recommendations related to this crop.

Key words: Sunchoke, Vegetative stage, Reproductive stage, Tuberization stage.

Introduction

Jerusalem artichoke (*Helianthus tuberosus* L.) is crop native to North America which stores the carbohydrate inulin (instead of starch) in its tubers. It was originally grown in temperate climates and has been introduced to most parts of the world including in the semi-arid tropics in Thailand. It is cultivated widely in many countries for different purposes such as food industry, medical applications and also for the production of ethanol (Muir *et al*., 2007; Kiru & Nasenko, 2010). Jerusalem artichoke tubers contain 20% carbohydrates, 70 % to 90% of which is inulin (Abou-Arab *et al*., 2011; Puttha *et al*., 2012). Inulin is considered as functional food that is beneficial to human health and can reduce the risk of many diseases (Roberfroid, 2002).

Uniform growth stage descriptions have been developed most crops, and these descriptions have aided communication among producers, researchers, and educators. They are especially useful to producers in the scheduling of cultural practices, irrigation, fertilizer and harvest (Carneiro, 2007). In addition, the precise knowledge of plant growth stages is important for researchers to use as model on the effects of pest and disease infestations, to devise and implement action thresholds for pest management and to develop a plant breeding program (Leather, 2010).

Jerusalem artichoke (*Helianthus tuberosus)* has no relationship to Jerusalem or artichoke (*Cynara cardunculus var. scolymus*) it belongs to the genus *Helianthus* which is often cultivated for its tuber. Jerusalem artichoke is a close relative of the sunflower (above ground) and potato (underground). Growth stages have been defined for both sunflower (*Helianthus annuus* L.) (Schneiter & Miller, 1981) and potato (*Solanum tuberosum*) (Jefferies & Lawson, 1991). However, staging of Jerusalem artichoke development has been proposed by at least one researcher.

There are a few published reports on the growth stages of Jerusalem artichoke. Most previous research on growth stage has been limited to temperate regions, hence there was a little information of growth and phenology in the tropical climate. Denoroy (1996) reviewed and concluded there were five developmental stages of Jerusalem artichoke. However, they have not described the morphology and phenology stage of Jerusalem artichoke. Kays & Nottingham (2007) have described vegetative and reproduction stages, but not tuberization stage. Both Jerusalem artichoke staging reports provided definition of needed crop development stages, yet additional definition is needed of subterranean development (stolonisation and tuberization). We also found that some of the criteria used in tuberization stages were not reliable, nor were they clearly defined. Thus, the description of tuberization stage is needed to increase communication among agricultural sciences and phenological observation networks. Therefore, the objective of this study was to design stages of development descriptions for Jerusalem artichoke.

Materials and Methods

Plant materials and experimental design: Field experiments were conducted during early rainy season (June to September) in 2011 and 2012, and during the post rainy season (September to December) in 2011 and 2012 at the Field Crop Research Station of Khon Kaen University. A randomized complete block design (RCBD) with five replications was used in this study. Two

Jerusalem artichoke genotypes (HEL 65 (late maturity) and CN 52867 (early maturity) were used. Plot size was 6 × 6 m with a spacing of 50 cm between rows and 50 cm between hills with in a row.

Pre-sprouted seed tubers were used as planting materials. To prepare the sprouted seed tubers, the tubers were cut into small pieces each having 2-3 buds/piece. The tuber pieces were then pre-sprouted in charred rice husk with mixed trichoderma at in the ratio of 3:1 under ambient conditions for 7 days. The tuber pieces with active buds and roots were then transferred to plastic plug trays containing a 3:1:1 mixture of soil and burnt rice husk and trichoderma for 7 days. Those tuber pieces with two leaf-sprouted seedlings were then transplanted, at a density of one seedling per hill into the plots. Fertilizer (15-15-15 of N- P_2O_5-K_2O) was applied at 30 days after transplanting (DAT) at a rate of 156 kg per ha^{-1}. A Terraclor (quintozene 24 % W/V EC) was applied monthly for 3 months after transplanting at the rate of 25 mL/ 20 L of water for control of stem rot. This diseases incited by *Sclerotium rolfsii* is more prevalent under the high temperature and high humidity conditions (Sennoi *et al*., 2013). The plots were sprinkler irrigated every 2 days.

Data collection: Data were collected for vegetative (V) and reproductive (R) stages on three-plants sampled at 2-day intervals. The tuberization (T) stage data was made from observations of on three plants sampled at 5-day intervals in each replication.

Vegetative stages: Determination of the vegetative (V) stages was based on the number of developed nodes on the main axis, beginning with emergence of the sprout seedling and ending with the initial visual appearance of the inflorescence. Nodes, rather than leaves, are used for stage determination because they are permanent, whereas early leaves may be lost. When a Jerusalem artichoke leaf drops, the node can easily be identified by either the stipules, the petiole scar or by presence of a branch in the former axils of the leaf. The individual stages after emergence are determined by true leaf number.

Reproductive stages: Determination of the reproductive stages was based on visually observable events related to flower initiation, beginning of flower bloom, flowering and seed set. The number of days between reproductive stages is variable and dependent upon genotypic and environmental factors.

Tuberization stages: Determination of the tuberization stages was based on visually observable events related to stolon, tuber initiation, tuber expanded, tuber skin set and maturity. The number of days between tuberization stages is variable and dependent upon genotypic and environmental factors.

Daily maximum and minimum temperatures and solar radiation during the two seasons were recorded daily from transplanting until harvest by a meteorological station located near the experimental site.

Growing degree days (GDD) for each growth stage for each genotype was calculated as the summation of daily mean temperatures above the 0°C base-temperature from day of transplanting to harvest. GDD for reproductive stage was calculated from the day of transplanting to floral bud formation (R1), beginning bloom (R2), flowering (R3), beginning of anthesis (R4), seed set (R5) and seed maturity (R6). GDD for tuberization stage was calculated from the day of transplanting to stolonization (T1), tuber initiation (T2), tuber formation (T3), tuber bulking (T4), skin set (T5) and tuber maturity (T6).

Statistical analysis: Comparisons were made for growing degree days of each growth stage for each genotype between seasons. Mean differences between seasons were tested by t-test in each genotype. Calculation procedures were done using STATISTIX8 software program (Statistix8, 2003).

Results and Discussion

Soil properties and weather conditions: The soil in tropics is sandy with low organic matter (0.53%), low nitrogen (0.029%), medium phosphorus (49 mg kg^{-1}) and medium potassium (46 mg kg^{-1}) (Table 1). In contrary, the soil in temperate regions is usually with medium organic matter (1.76%), high phosphorus (126 mg kg^{-1}), and rich potassium (121 mg kg^{-1}) (Danilcenko *et al*., 2013). However, Jerusalem artichoke can grow in dry regions with poor soil (Kays & Nottingham, 2007). The differences of soil properties between growing environments would cause significant differences in plant growth and yield.

Table 1. Physical and chemical properties of the soil from the experimental field

Soil properties / depth	0-30 cm
Physical properties	
Sand (%)	88.3
Silt (%)	7.3
Clay (%)	4.4
Texture class	Sand
Chemical properties	
pH (1:2.5 H_2O)	5.52
Organic Matter (%)	0.53
Total N (%)	0.029
Available P (mg kg^{-1})	48.8
Exchangeable K (mg kg^{-1})	45.7

Seasonal mean maximum temperature in the early-rainy seasons were 32.0ºC and 30.4ºC in the post-rainy seasons in 2011 and minimum temperature in the rainy-seasons were 23.0°C and 20.2°C in the post-rainy season in 2011 (Fig. 1). Maximum temperature in the early-rainy seasons were 32.4ºC and 31.0ºC in the post-rainy seasons in 2012 and minimum temperature in the early-rainy seasons were 23.0°C and 21.7°C in the post-rainy seasons in 2012 (Fig. 2).

The growing conditions were different between tropical and temperate regions where the crop was originated. The difference between regions could be due to difference in temperatures. As Jerusalem artichoke was grown in tropics, the growing temperatures were much higher than temperate regions (Puttha *et al*., 2012). In temperate regions, the average temperatures during the growing season are between of 6ºC to 26ºC and the crop required at least 4 to 5 months for tuber maturity (Kays & Nottingham, 2007). Therefore, temperature is directly related to the rate of tuber growth. Maturity in tropical area (approximately 4 months) is generally shorter than in the temperate regions (Ruttanaprasert *et al*., 2013).

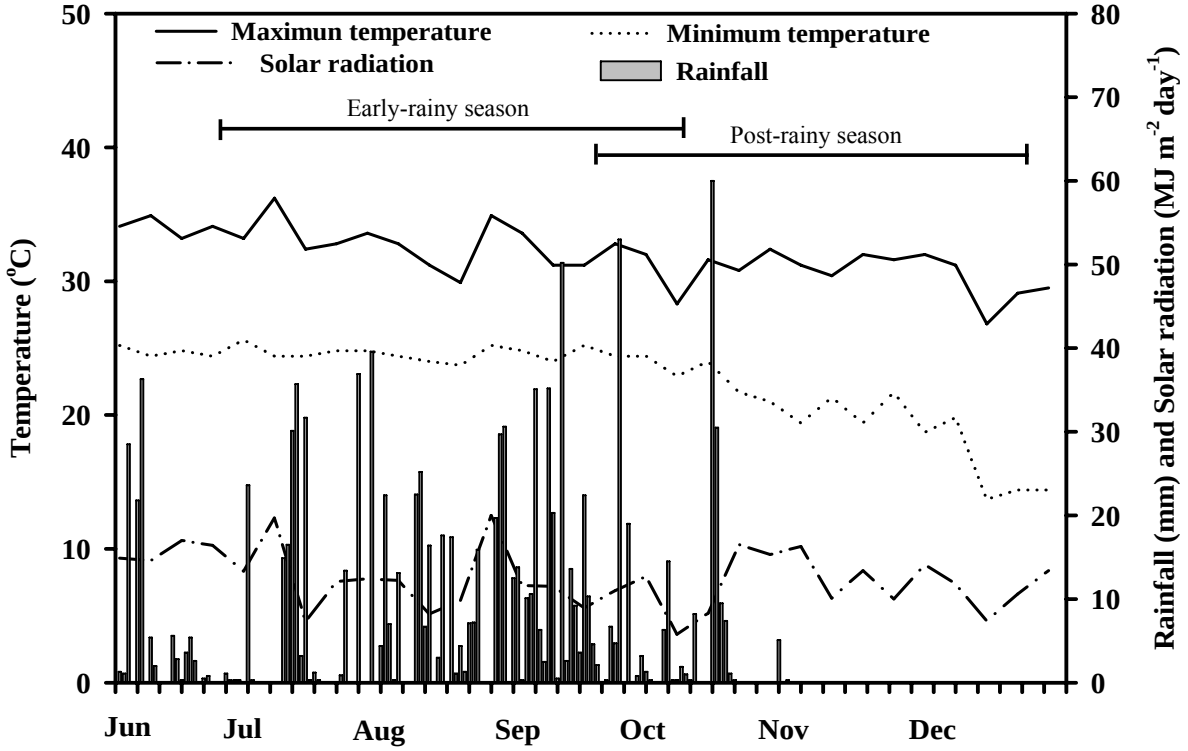


Fig. 1. Daily maximum temperature, minimum temperature, solar radiation and rainfall during the early-rainy and post-rainy seasons in 2011.

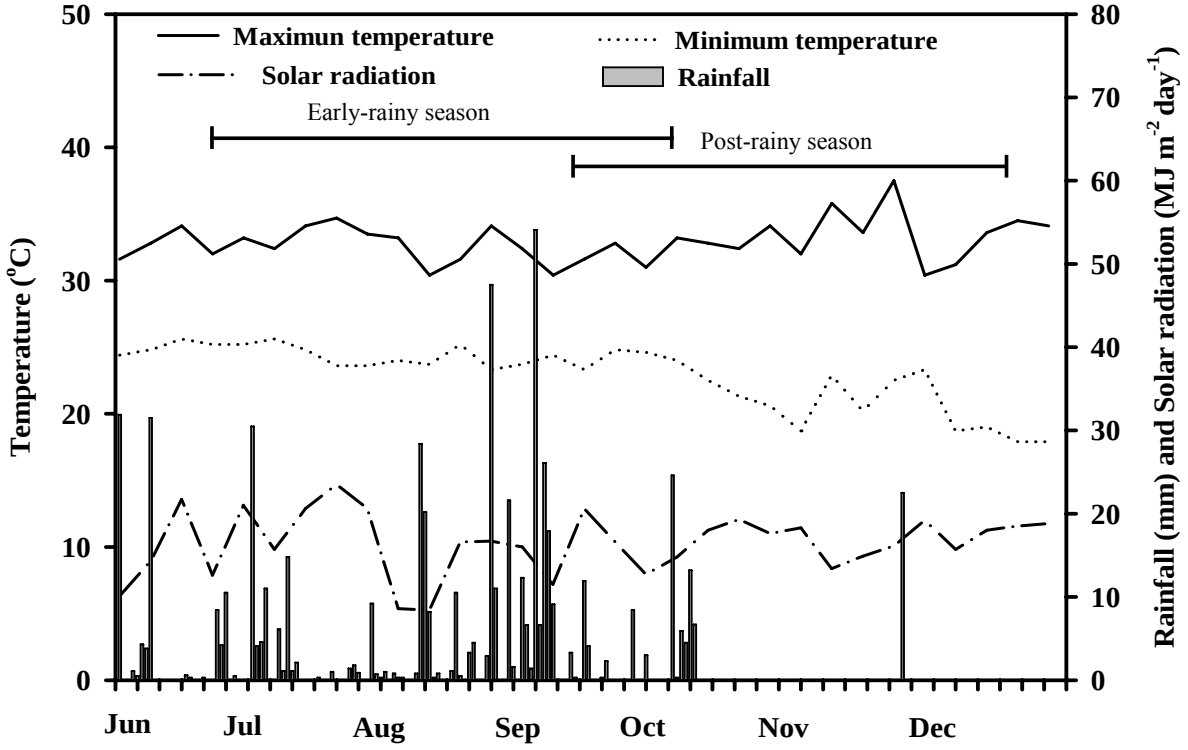


Fig. 2. Daily maximum temperature, minimum temperature, solar radiation and rainfall during the early-rainy and post-rainy seasons in 2012.

Seasonal biome dynamics are controlled by recurrent variations of environmental conditions, especially temperature changes driven by weather. Although temperature is the main factor affecting plant development, other environmental factors also play a role.

The means of solar radiation in the early-rainy seasons were 12.3 MJ m^{-2} d^{-1} and 12.5 MJ m^{-2} d^{-1} in the post-rainy seasons in 2011 (Fig. 1). In 2012, the means of solar radiation in the early-rainy seasons were 16.2 MJ m^{-2} d^{-1} and 17.2 MJ m^{-2} d^{-1} in the post-rainy seasons (Fig. 2). Rainfalls in the early-rainy seasons were 815 mm and 276 mm in the post-rainy seasons in 2011 (Fig. 1) and in rainfall in the early-rainy seasons were 480 mm and 108 mm in the post-rainy seasons in 2012 (Fig. 2).

The solar radiation in temperate regions for growing season was 17 MJ m^{-2} d^{-1}, indicating that there is not a significant different between tropical conditions and temperate regions. Solar radiation was not expected to significantly affect the growth and development of Jerusalem artichoke grown in tropics. However, solar radiation is the one factor which effect on photosynthesis and yield of Jerusalem artichoke grown in shade conditions (Kays and Nottingham, 2007). Rainfall well distributed throughout the crop cycle in the early-rainy seasons in both years. However, no water stress was observed during the growing seasons for post-rainy seasons in both years.

Vegetative development: The sprout development "VE" is when the sprouts develop from buds on the tuber (Table 2, Fig. 3). As did Kays & Nottingham (2007) and others, we noted the length of time to this stage which was dependent on temperature, available soil water, tuber dormancy and cultivar. In temperate regions, Jerusalem artichoke requires at least 6.7ºC of soil temperature for sprout development (Kays & Nottingham, 2007), while in this experiment high temperature (approximately 28 ºC) for sprout development was required. However, cold temperatures are needed to break dormancy (5°C or less) (Denoroy, 1996).

The vegetative stage V1 is when the first leaf develops from an aboveground node along the emergence sprout (Fig. 3). Vegetative stage V2 is defined as one developed node with two true leaves that are flat. Subsequent V stages up to V_N are based on N developed nodes on the main axis of the plant, counting the uppermost last node having true leaves that are flat. Leaf attachment in Jerusalem artichoke appears to begin in an opposite arrangement and gradually develops a spiral phyllotaxy of alternate phyllotaxy leaves. Our results were similar to those of Kays & Nottingham (2007), where the first leaves are arranged opposite on the stem, but by the 19th node the plant has switched to alternate. Both ours and those of Kays & Nottingham (2007) also noted that the location of the shift from opposite to alternate appears to vary with cultivar. In our study CN 52867 changed its leaf orientation from opposite to alternate around the node 23 while HEL 65, changed orientation at node 25.

Reproductive development: Growing degree days (GDD) from transplanting (V4) to specific R stages are given in Table 3 for CN 52867 and HEL 65 in both seasons. Growth stages are given in Table 2, while Fig. 4 shows the identifying traits associated with the reproductive stages R1-R6. Although these photographs are of CN 52867, the visual traits for these stages in HEL 65 are very similar except for HEL 65's larger flower size.

Reproductive stage R1, Floral bud formation, is when the plants have one floral bud at any node on the plant (Fig. 4). The GDD was calculated from transplanting (V4) to R1 for both genotypes. GDD to reach R1 was 997°C and 1248°C for CN 52867 and HEL 65 in the early-rainy season (Table 3). In the post-rainy seasons, CN 52867 and HEL 65 required 909 and 1121°C GDD to reach R1.

Table 2. Growth stage descriptions for Jerusalem artichoke (*Helianthus tuberosus* L.).

Stage no.	Abbreviated stage title	Description
	Vegetative Stages	
VE	Sprout development	Sprouts develop from bud on tuber (Fig 3, VE).
V1	Vegetative stage	The first leaf develops from an above ground node along emergence sprout (Fig 3, V1).
V2-Vn	The second true leaf to N leave	Two to N leaves have developed on nodes on main stem, a node is counted when its true leaf are flat (Fig 3, V2-Vn).
	Reproductive Stages	
R1	Floral bud formation	One floral bud at any node on plant (Fig 4, R1).
R2	Beginning bloom	One flower begins to unroll or ligules yellow-green (ray flower corollas) beginning to elongate (Fig 4, R2).
R3	Flowering	First open flower with petals that are completely horizontal (Fig 4, R3).
R4	Beginning of anthesis	50% of the plants have one open flower flowering and the anthers and first stigma have emerged on the outer whorl (Fig 4, R4).
R5	Seed set	50% of the ray flowers are wilting, disk flower petals are intact and the seed is starting to set (Fig 4, R5).
R6	Seed maturity	The first flowers have shed their ligules and the disk flower corollas are wilting (Fig 4, R6)
	Tuberization Stages	
T1	Stolon	Stolons develop at below ground node. The plants have one stolon (2-5 cm in length) (Fig 5, T1)
T2	Tuber initiation	The trip of stolon being to swell to at least twice the width of T1 stage (Fig 5, T2).
T3	Tuber formation	Tuber diameter enlarged to greater than 1 cm or twice the T2 stage (Fig 5, T3).
T4	Tuber bulking	Tuber diameter is at least 2.5 cm or four times of T2 stage (Fig 5, T4).
T5	Skin set	Tuber skin becomes yellow and brown (Fig 5, T5).
T6	Tuber maturity	Stems turn yellow or brown and lose leaves, tuber skin becomes dark (Fig 5, T6).

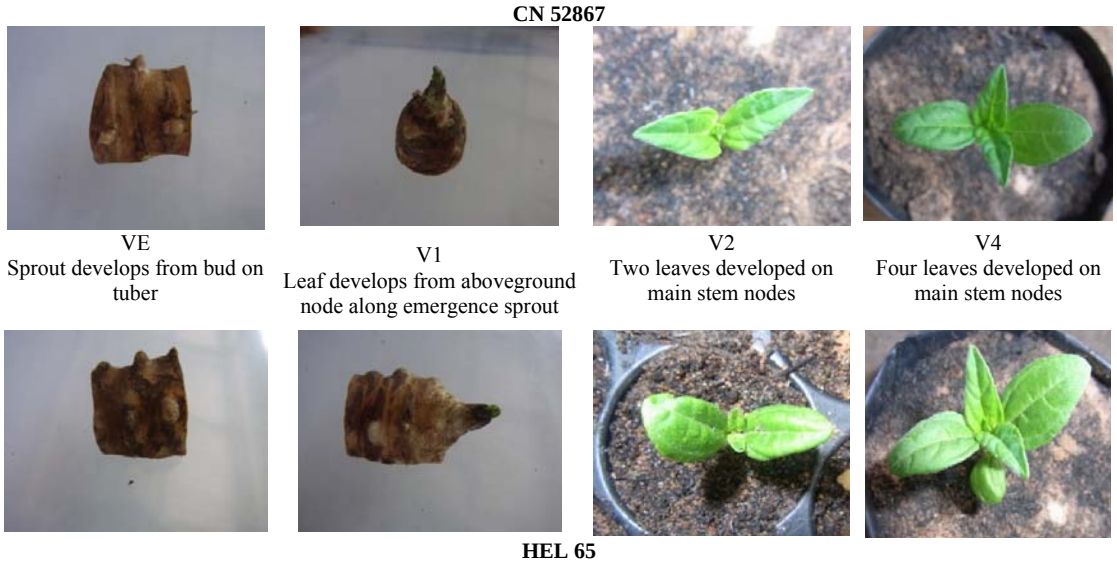


Fig. 3. Vegetative stages for CN 52867 and HEL 65 of Jerusalem artichoke (*Helianthus tuberosus* L.).

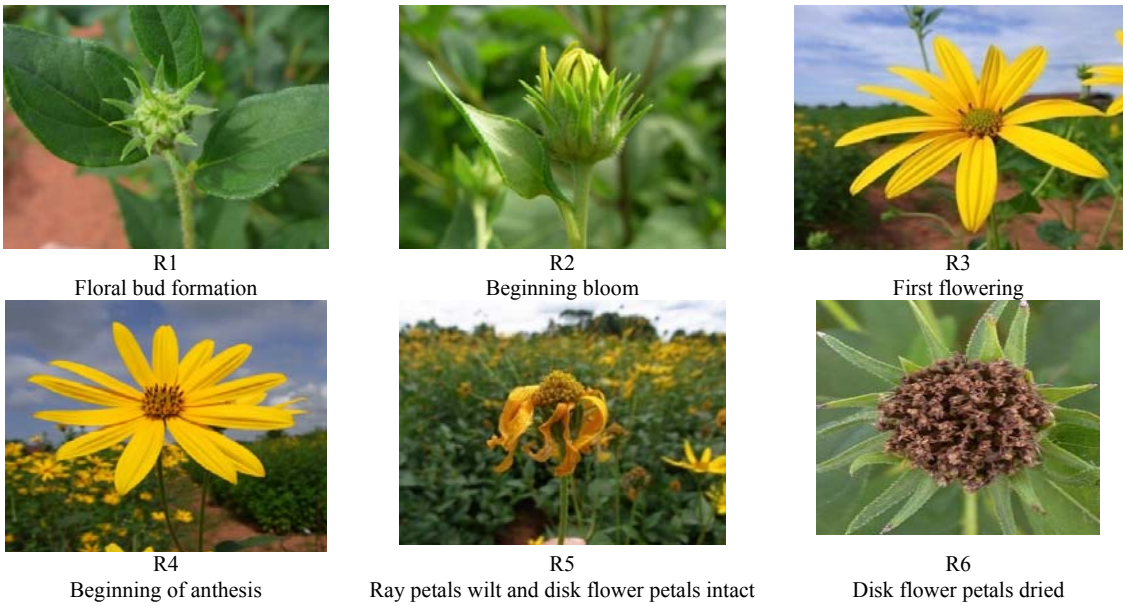


Fig. 4. Reproductive stages of Jerusalem artichoke (*Helianthus tuberosus* L.).

The results indicated that the GDD to reach floral bud formation (R1) in the early-rainy season was higher than in the post-rainy-seasons. Thus, floral bud formation in the post-rainy seasons (short day) occurred earlier than in the early-rainy season (long day) because long day favored development of aerial growth rather than reproductive and tuber growth, similar to other reports by Ruttanaprasert *et al*. (2013); Kays & Kultur (2005). Similar to Fenner (1998) reported that seasonal changes in photoperiod may be a major determinant of flowering time in individual species.

Kays & Nottingham (2007) noted that Jerusalem artichoke is a photoperiod-sensitive short-day plant that requires long light periods followed by shorter light periods to trigger the shift to reproductive stage of development. In tropical and temperate regions GDD during the growing season is a main factor affecting growth and yield of Jerusalem artichoke (Kocsis *et al*., 2007; Puangbut *et al*., 2012; Rattanaprasert *et al*., 2014).

In addition, temperature is also important factor affecting floral buds and inflorescence formation (Fenner, 1998; Hassan *et al*., 2005; Dasumiati *et al*., 2015). Several reports indicated that low temperature delayed floral bud formation in many plant (Konvalinková, 2003; Kaleem *et al*., 2010). Therefore, floral bud formation needs sufficiently high temperatures. A cooler temperature can result in a return to vegetative growth. Thus, short day reduced the number of days to flowering.

Table 3. Growing degree days (GDD) for each growth stages of CN 52867 and HEL 65 Jerusalem artichoke genotypes in the early-rainy season (ERS) and post-rainy season (PRS) in year 2011 and 2012.

Growth stage	Growing degree days (°C)					
	CN 52867		T-test	HEL 65		T-test
	ERS	PRS		ERS	PRS	
Reproductive stages						
R1	997	909	*	1248	1121	*
R2	1222	1094	**	1416	1309	*
R3	1276	1229	ns	1527	1413	*
R4	1416	1360	ns	1725	1548	**
R5	1583	1495	ns	1856	1731	*
R6	2088	2023	ns	2596	2254	**
Tuberization stages						
T1	546	692	**	633	747	*
T2	945	987	*	997	1041	*
T3	1670	1335	**	1753	1413	**
T4	1978	1628	**	2061	1549	**
T5	2257	1996	**	2398	1996	**
T6	2760	2350	**	3217	2493	**

T-test is the differences between seasons in each growth stage

R2, Beginning bloom, is when plants have one flower beginning to unroll or ligules yellow-green (ray flower corollas) beginning to elongate (Fig. 4). Seasons were significant difference for GDD to reach R2 in both genotypes (Table 3). GDD to reach R2 in the early-rainy season were 1222 and 1416°C for CN 52867 and HEL65, respectively while GDD to reach R2 was 1094 and 1309°C for CN 52867 and HEL65 in the post-rainy seasons (Table 3).

R3, Flowering, is when plants have their first open flower with petals completely horizontal, and the first disk flowers on the outer whorl have their anthers emerging from corollas (Fig. 4). Seasons were significant difference for GDD to reach R3 in HEL 65 only. In the early-rainy seasons, CN 52867 and HEL 65 required 1276 and 1527°C GDD to reach R3, respectively while GDD to reach R3 was 1229 and 1413°C for CN 52867 and HEL 65 in the post-rainy seasons (Table 3).

Previously reports indicate that the onset and duration of flowering vary widely among genotypes and planting date, location production and conditions (Kays & Nottingham, 2007; Kays & Kultur, 2005). In this (tropics) condition, the onset of flowering started at 45 days after transplanting and then earlier than plants grown in temperate zone (Kays & Kultur, 2005). Recent studies indicated that photoperiod and temperature is an important factor influence on plant phenology including the timing of flowering (Rejŝková *et al*., 2010; Song *et al*., 2013). However, understanding the mechanisms by which plants integrate both photoperiod and temperature cues to control flowering is not well understood.

R4, Beginning of anthesis, is when 50% of the plants have one completely open flower and the anthers and first stigma have emerged on the outer whorl (Fig. 4). In the early-rainy seasons, CN 52867 and HEL 65 required 1416 and 1725°C GDD to reach R4, respectively while GDD to reach R4 was 1360 and 1548°C for CN 52867 and HEL 65 in the post-rainy seasons (Table 3). The results revealed that HEL 65 showed significant differences between seasons for GDD to reach R4.

R5, Seed set, is when 50% of the ray flowers are wilting, disk flower petals are intact and the seed is starting to set (Fig. 4). Generally there are a few seed per flower. In the early-rainy seasons, CN 52867 and HEL 65 required 1583 and 1856°C GDD to reach R5 while GDD to reach R4 was 1495 and 1731°C for CN 52867 and HEL 65 in the post-rainy seasons (Table 3). The results indicated that GDD to reach R5 were different between seasons in HEL 65 only.

R6, Seed maturity, is when the first flowers have shed their ligules and the disk flower corollas are wilting (Fig. 4). Mature seeds are flattened, wedge shaped and smooth (Kays & Nottingham, 2007). Their external color or pericarp is mottled black or brown with black spots. Seed size ranges from 5-7 mm in length and 1-2 mm in width and vary among genotypes. In the early-rainy seasons, GDD to reach R6 of CN 52867 and HEL 65 were 2088 and 2596°C, respectively while GDD to reach R6 was 2023 and 2254°C for CN 52867 and HEL 35 in the post-rainy seasons (Table 3). However, only HEL 65 showed significant difference between seasons for GDD to reach R6.

Seed production varies with clone (Konvalinková, 2003) and usually wild clones produce more seed per flower (5) than cultivated clones (1 or 2) (Kays & Nottingham, 2007). Several factors contribute to this low seed production including self-incompatibility, late flowering and cool temperatures during seed development. These challenges have slowed progress in Jerusalem artichoke breeding programs.

Tuberization development: Tuberization stage T1, Stolonization, is when the plants have one stolon (2-5 cm in length) (Fig. 5). To assist readers in visualizing tuberization stages defined in Table 2. Seasons were significantly different for GDD to reach T1 in both genotypes (Table 3). In the early-rainy seasons, CN 52867 and HEL 65 required 546 and 633 °C GDD to reach T1, respectively (Table 3). In the post-rainy season, GDD to reach T1 was 692 and 747 °C for CN 52867 and HEL 65. The results indicated that the GDD accumulation for tuber initiation in the post-rainy seasons (October) occurred later than in the early-rainy seasons (July) because of the longer day length, which will delay the stolonization stage and induce aerial growth (Denoroy, 1996; Kays & Kultur, 2005).

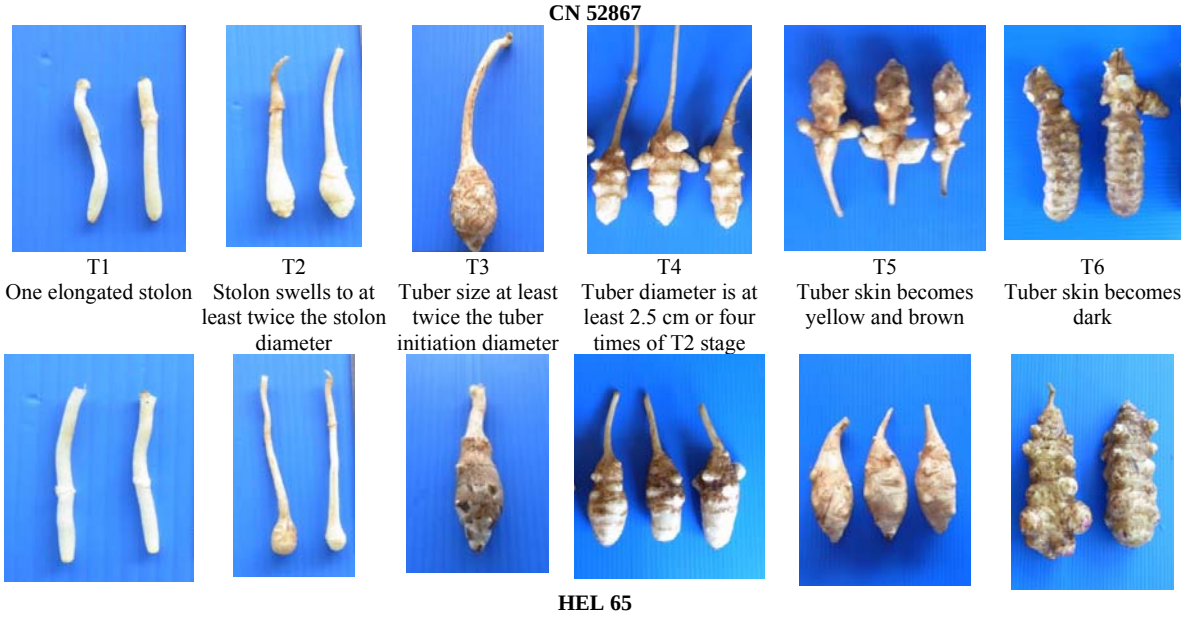


Fig. 5. Tuberization stages for CN 52867 and HEL 65 Jerusalem artichoke genotypes.

T2, Tuber initiation, is when 50% of the plants have stolon tips being to swell to at least twice the width of those in the T1 stage, indicating the initiation of tubers (Fig. 5). Two genotypes showed significant differences between seasons for GDD to reach T2 (Table 3). In the early-rainy season, GDD to reach T2 was 945 and 997°C for CN 52867 and HEL 65. In the post-rainy seasons, CN 52867 and HEL 65 required 987 and 1041°C GDD to reach T2 (Table 3).

T3, Tuber formation, is when 50% of the plants have a tuber diameter greater than 1 cm or twice the T2 stage (Fig. 5). Seasons were significantly different for GDD to reach T3 in both genotypes (Table 3). In the early-rainy seasons, GDD to reach T3 for CN 52867 and HEL 65 were 1670 and 1753°C, respectively while CN 52867 and HEL 65 required 1335 and 1413°C GDD to reach T3 in the post-rainy seasons (Table 3).

T4, Tuber bulking, is when 50% of the plants have tuber diameter is at least 2.5 cm or four times of T2 stage (Fig. 5). Seasons were significantly different for GDD to reach T4 in both genotypes (Table 3). In the early-rainy seasons, GDD to reach T4 for CN 52867 and HEL 65 were 1978 and 2016°C, respectively while GDD to reach T4 was 1628 and 1549°C for CN 52867 and HEL 65 in the post-rainy seasons (Table 3).

T5, Skin set, is when 50% of the plants have a yellow and brown tuber skin (Fig. 5). Seasons were significantly different for GDD to reach T5 in both genotypes (Table 3). In the early-rainy seasons, GDD to reach T5 of CN 52867 and HEL 65 were 2257 and 2398°C, respectively while CN 52867 and HEL 65 required 1996 and 1996°C GDD to reach T5 in the post-rainy seasons (Table 3).

T6, Tuber maturity, is when 50% of the plants have a stem which has turned yellow or brown, is losing leaves and has a dark tuber skin (Fig. 5). Seasons were significantly different for GDD to reach T6 in both genotypes (Table 3). In the early-rainy seasons, GDD to reach T6 of CN 52867 and HEL 65 were 2760 and 3217°C, respectively while CN 52867 and HEL 65 required 2350 and 2493 °C GDD to reach T6 in the post-rainy seasons (Table 3).

The results indicated that GDD to tuber maturity had higher in the early-rainy season than in the post-rainy seasons. However, tuber maturity occurred more rapidly in post-rainy season than in the early-rainy seasons. Recent report, GDD was associated with temperature and photoperiod (Rattanaprasert *et al*., 2014). The result revealed that low GDD or low temperature favored development of tuber growth. Similar to Puangbut *et al*. (2012) and Rattanaprasert *et al*. (2014) reported that tuber yield increased with low GDD (temperature sum) and short photoperiod. In our studies, as Denoroy's (1996) and others, tuber was influenced by daylength, temperature and genotype. Tuberization occurred more rapidly in the post-rainy seasons than in the early-rainy seasons. Short day length has been documented to favor tuber formation over flowers (Denoroy, 1996), although this mechanism is not well understood. While temperature is known to affect tuber yield, it is also known to influence inulin content (Hassan *et al*., 2005; Puangbut *et al*., 2011; Ruttanaprasert *et al*., 2013, 2014). The present study indicated that Jerusalem artichoke grown under tropical climate had early maturity (100-120 days) than did the crop grown in temperate regions (125-150 days) and this could be due to speed up of growth rate in regions near the equator (Kays & Nottingham, 2007).

Our results revealed that GDD could be used to determine growth stage of Jerusalem artichoke in different environment conditions. The current study supports earlier findings that GDD was used to estimate plant development suggesting that it gave better estimates for determining various physiological stages in response to environmental conditions (Noreen *et al*., 2013). The accumulation of GDD determines the maturity of crop as well as performance and quality of produce.

Conclusions

The present study demonstrated that seasonal variation was influenced on phenological development and growth stages. The crop maturity in the post-rainy season required low GDD than that in the early-rainy season which resulted in more rapid of tuber maturity in the post-rainy season. The scope of this study provided the opportunity to describe the developmental stages for Jerusalem artichoke with emphasis on details important for researchers. Certain stages, such as tuberization stage, were described in detail because of their importance to producers, researchers and educators. We have outlined a number of visually identifiable events in the vegetative, reproductive and tuberization stages of Jerusalem artichoke. These stages will be useful in describing research results and provide a more precise basis for scheduling cultural practices rather than use of general descriptors.

Acknowledgements

We appreciate the support of the Higher Education Research Promotion and National Research University Project of Thailand, Office of the Higher Education Commission, through the Food and Functional Food Research Cluster of Khon Kaen University. We also thank the Leibniz Institute of Plant Genetics and Crop Plant Research, Germany, the Plant Gene Resource of Canada for the contribution of Jerusalem artichoke germplasm. Grateful acknowledgments are made to the Peanut and Jerusalem artichoke Improvement for Functional Food Research Group and Plant Breeding Research Center for Sustainable Agriculture, Khon Kaen University, and to the Thailand Research Fund for providing financial supports to this research through the Senior Research Scholar Project of Professor Dr. Sanun Jogloy (Project no. RTA 5880003). Acknowledgement is extended to the Thailand Research Fund (IRG 5780003), Khon Kaen University and Faculty of Agriculture, KKU for providing financial support for manuscript preparation activities. Finally, we are grateful extended to Dr. Kvien Craig, Department of Crop and Soil Sciences, The University of Georgia, USA for his kind suggestion.

References

Abou-Arab, A.A., H.A. Talaat and F.M. Abu-Salem. 2011. Physico-chemical properties of inulin produced from Jerusalem artichoke tubers on bench and pilot plant scale. *Aust. J. Basic Appl. Sci*., 5: 1297-1309.

Carneiro, J.W.P. 2007. Stevia rebaudiana (Bert.) Bertoni: Stages of plant development. *Can. J. Plant Sci*., 87: 861-865.

Danilcenko, H., E. Jariene, M. Gajewski, B. Sawicka, J. Kulaitiene and J. Cerniauskiene. 2013. Changes in amino acids content in tubers of Jerusalem artichoke (*Helianthus tuberosus* L.) cultivars during storage. *Acta Sci. Pol*., 12: 97-105.

Dasumiati, Miftahudin, Triadiati and A. Hartana. 2015. Flower characteristics and phenology of andromonoecious Jatropha curcas. *Pak. J. Bot*., 47(4): 1501-1510.

Denoroy, P. 1996. The crop physiology of *Helianthus tuberosus* L: a model orientated view. *Biomass Bioenerg*., 11: 11-32.

Fenner, M. 1998. The phenology of growth and reproduction in plants. Perspect. Perspect. *Plant Ecol. Evol. Syst*., 1: 78-91.

Hassan, F.U., G. Qadir and M. A Cheema. 2005. Growth and development of sunflower in response to seasonal variations. *Pak. J. Bot*., 37(4): 859-864.

Jefferies, R.A. and H.M. Lawson. 1991. A key for the stages of development of potato (*Solanum tuberosum*). *Ann. Appl. Biol*., 119: 387-389.

Kaleem, S., U.F. Hassan, M. Farooq, M, Rasheed and A. Munir. 2010. Physio-morphic traits as influenced by seasonal variation in sunflower: a review. *Int. J. Agr. Biol*., 12: 468-473.

Kays, S.J. and F. Kultur. 2005. Genetic variation in Jerusalem artichoke (*Helianthus tuberosus* L.) flowering date and duration. *Hortscience*, 40: 1675-1678.

Kays, S.J. and S.F. Nottingham. 2007. Biology and Chemistry of Jerusalem Artichoke (*Helianthus tuberosus* L.). CRC Press, Florida.

Kiru, S. and I. Nasenko. 2010. Use of genetic resources from Jerusalem artichoke collection of N. Vavilov Institute in breeding for bioenergy and health. *Agron. Res*., 8: 625-632.

Kocsis, L., H-P. Kaul, W. Praznik and P. Liebhard. 2007. Influence of harvest date on shoot and tuber yield ofdifferent Jerusalem artichoke (*Helianthus tuberosus* L.) cultivars in the semiarid production area of Austria. *Ger. J. Agron*., 11: 67-76.

Konvalinková, P. 2003. Generative and vegetative reproduction of *Helianthus tuberosus*, an invasive plant in Central Europe: Plant invasions: Ecological threats and management solutions. In: (Eds.): Child, L, J.H. Brock, G. Brundu, K. Prach, K. Pysěk, P.M Wade and M. Williamson. Backhuys, Leiden, Netherlands, pp. 289-298.

Leather, S.R. 2010. Precise knowledge of plant growth stages enhances applied and pure research. *Ann. Appl. Biol*., 157: 159-161.

Muir, J.G., S.J. Shepherd, O. Roselia, R. Rose, J.S. Barrett and P.R. Gibson. 2007. Fructan and free fructose content of common Australian vegetables and fruit. *J. Agr. Food Chem*., 55: 6619-6627.

Noreen, S., H.U.R Athar and M. Ashraf. 2013. Interactive effects of watering regimes and exogenously applied osmoprotectants on earliness indices and leaf area index in cotton (*Gossypium hirsutum* L.) crop. *Pak. J. Bot*., 45(6): 1873-1881.

Puangbut, D., S. Jogloy, S. Srijaranai, N. Vorasoot, T. Kesmala and A. Patanothai. 2011. Rapid assessment of inulin content in (*Helianthus tuberosus* L.) tubers. *SABRAO J. Breed. Genet*., 43: 188-200.

Puangbut, D., S. Jogloy, N. Vorasoot, S. Srijaranai, T. Kesmala and A. Patanothai. 2012. Influence of planting date and temperature on inulin content in Jerusalem artichoke (*Helianthus tuberosus* L.). *Aust. J. Crop Sci*., 6: 1159-1165.

Puttha, R., S. Jogloy, P.P. Wangsomnu, S. Srijaranai, T. Kesmala, and A. Patanothai. 2012. Genotypic variability and genotype by environment interactions for inulin content of Jerusalem artichoke germplasm. *Euphytica*, 183: 119-131.

Rejšková, A., J. Bromb, J. Pokorny´ and J. Korečko. 2010. Temperature distribution in light-coloured flowers and inflorescences of early spring temperate species measured by Infrared camera. *Flora*, 205: 282-289.

Roberfroid, M.B. 2002. Functional foods: concepts and application to inulin and oligofructose. *Br. J. Nutr*., 87: 139-143.

Ruttanaprasert, R., P. Banterng, S. Jogloy, N. Vorasoot, T. Kesmala, R.S. Kanwar, C.C. Holbrookand and A. Patanothai. 2014. Genotypic variability for tuber yield, biomass, and drought tolerance in Jerusalem artichoke germplasm. *Turk. J. Agric. For*., 38: 570-580.

Ruttanaprasert, R., S. Jogloy, N. Vorasoot, T. Kesmala, R.S. Kanwar, C.C. Holbrook and A. Patanothai. 2013. Photoperiod and growing degree days effect on dry matter partitioning in Jerusalem artichoke. *Int. J. Plant Prod*., 7: 393-416.

Schneiter, A. A. and J.F. Miller. 1981. Description of sunflower growth stages. *Crop Sci*., 21: 901-903.

Sennoi, R., S. Jogloy, W. Saksirirat, T. Kesmala and A. Patanothai. 2013. Effects of host growth stage, re-isolation and culture medium on screening for resistance to stem rot disease caused by *Sclerotium rolfsii* Sacc. in Jerusalem artichoke. *Pak. J. Bot*., 45(5): 1825-1829.

Song, Y.H., S. Ito and T. Imaizumi. 2013. Flowering time regulation: photoperiod and temperature-sensing in leaves. *Trends Plant Sci*., 18: 575-583.

Statistix 8, 2003. Statistix8: analytical software user's manual. Tallahassee, Florida.

(Received for publication 7 January 2015)

Journal of Food Composition and Analysis 44 (2015) 1–9

Contents lists available at ScienceDirect

Journal of Food Composition and Analysis

journal homepage: www.elsevier.com/locate/jfca

Original Research Article

Bioactive, antioxidant and enzyme activity changes in frozen, cooked, mini, super-sweet corn (*Zea mays* L. saccharata 'Naulthong')

Kamonporn Sitthitrai [a], Danupol Ketthaisong [b,c], Kamol Lertrat [b,c], Ratchada Tangwongchai [a,*]

[a] Department of Food Technology, Faculty of Technology, Khon Kaen University, Khon Kaen 40002, Thailand
[b] Department of Plant Science and Agricultural Resources, Faculty of Agriculture, Khon Kaen University, Khon Kaen 40002, Thailand
[c] Plant Breeding Research Center for Sustainable Agriculture, Khon Kaen University, Khon Kaen 40002, Thailand

ARTICLE INFO

Article history:
Received 12 December 2014
Received in revised form 30 May 2015
Accepted 1 June 2015
Available online 6 June 2015

Keywords:
Food analysis
Food composition
Mini, supersweet corn
Zea mays L. *saccharata* 'Naulthong'
Steaming
ABTS-scavenging
Lipoxygenase
Peroxidase
Frozen storage

ABSTRACT

We investigated changes in the antioxidant and enzyme activities of cooked, mini, super-sweet corn (*Zea mays* L. *saccharata* 'Naulthong'). After steaming, samples of whole-ear and cut mini corncobs were vacuum- or atmospheric-packaged then frozen for 6 months. Lutein, zeaxanthin, ferulic acid, total phenolics, 2,2′-azinobis-3-[ethylbenzothiazoline-6-sulfonic acid] (ABTS), 2,2-diphenyl-1-picrylhydrazyl (DPPH) and ferric-reducing antioxidant power (FRAP) generally decreased in relation to storage time, which differed significantly depending on the serving pattern and type of packaging. Cut pieces with atmospheric packaging had the highest peroxidase (POD) and lipoxygenase (LOX) activity. For all storage periods, whole ears had higher levels of bioactive compounds and antioxidant activity than cut-pieces. Vacuum-packaging provided greater quality maintenance than atmospheric-packaging of frozen, cooked, mini, super-sweet ears. Preparation style and packaging during frozen storage affect nutritional quality and guide consumer choices.

© 2015 Elsevier Inc. All rights reserved.

1. Introduction

Interest in the bioactive compounds in fruits and vegetables has grown dramatically among consumers and scientists; as epidemiological studies suggest that regular consumption of natural antioxidants is associated with a lower risk of cardiovascular disease and cancer (Temple, 2000) as well as being protective against diabetes (Tsuda et al., 2003). Vegetables—particularly supersweet corn—are good sources of antioxidant phytochemicals like phenolic compounds, anthocyanin and carotenoids (Adefegha and Oboh, 2011; Chipurura et al., 2010; Harakotr et al., 2014). Lutein and zeaxanthin are carotenoids and also present in supersweet corn (Dewanto et al., 2002; Junpatiw et al., 2013; Kurilich and Juvik, 1999; Scott and Eldridge, 2005).

Sweet corn is a vegetable best consumed when fresh. It is boiled or steamed then served whole or cut. Cooking induces many changes in the physico-chemical and functional properties of the kernels (Scott and Eldridge, 2005); including the concentration and bioavailability of bioactive compounds (Turkmen et al., 2005).

Corn is processed to retain eating quality and increase storability. Freezing is one of the most important techniques for preserving and prolonging the shelf-life of fresh agricultural products. Frozen fruit and vegetable marketing have flourished with ongoing potential; especially frozen sweet corn, due to its convenience and better quality than canned sweet corn. Blanching before freezing can inhibit enzyme activity (including peroxidase, lipoxygenase and catalase), which prevent deterioration during storage and after thawing (Rickman et al., 2007; Scott and Eldridge, 2005).

Numerous factors affect the chemical composition of sweet corn and play roles in determining its nutriceutical bio- and enzyme activity (Lee and Kader, 2000) and processing can alter the bioactive compounds (Dewanto et al., 2002; Scott and Eldridge, 2005). Murcia et al. (2003) and Mazzeo et al. (2011) reported that food processing conditions, storage duration, storage temperature and packing conditions (i.e., vacuum and modified atmosphere) can influence enzyme and microbial activity.

* Corresponding author. Tel.: +66 43 36 2132; fax: +66 43 36 2131.
E-mail address: ratchada@kku.ac.th (R. Tangwongchai).

http://dx.doi.org/10.1016/j.jfca.2015.06.001
0889-1575/© 2015 Elsevier Inc. All rights reserved.

Several studies determined enzyme activity and the morphological characteristics of fresh commercial sweet corn cultivars (Boyes et al., 1997; Dewanto et al., 2002; Lee and Hammes, 1979). Few studies, however, have evaluated the bioactive compounds and antioxidants of cooked, mini supersweet corn after frozen storage. The objective of the current study was to evaluate the effect of different serving-styles and packaging conditions on bioactives, antioxidant and the enzyme activity of frozen, cooked, mini supersweet corn. The results will help to establish parameters for consumers and food scientists vis-à-vis preparation-styles and packaging conditions for frozen storage, yielding longer shelf-life and improved nutritional quality of the new hybrid, sweet corn varieties.

2. Materials and methods

2.1. Plant materials and sample preparation

The new mini supersweet corn hybrid (*Zea mays* L. *saccharata cv*. 'Naulthong') was harvested during the 2011/2012 dry season from a demonstration farm, at the Plant Breeding Research Center for Sustainable Agriculture, Faculty of Agriculture, Khon Kaen University, Thailand. The samples were harvested at the milky stage; 18 days after pollination (DAP). The fresh ears harvested for chemical analyses were further selected by size (~12–13 cm length) to ensure uniform maturity. Husks and silks were removed before cleaning in water. Then the tip-end of the ear (~1–2 cm) was cut-off to achieve uniformity of the kernels. Samples were separated into two groups (viz., whole ears and cut-pieces of 10–12 cm and 5–6 cm in length, respectively) before cooking. Steaming conditions were optimized by preliminary experiments conducted for each treatment. Whole ears and cut-pieces were steamed (~99 ± 1 °C) in a stainless-steamer over boiling water for 16 and 12 min, respectively. The cooked mini supersweet corn was immediately frozen using an air-blast freezer at −35 °C. Frozen samples were labeled, packed in polyethylene bags and sealed, both under vacuum and atmospheric packaging conditions. All samples were stored at −18 °C for 6 months, and several bioactive components analyzed during storage.

2.2. Chemicals

All chemical used in extraction were Analytical grade and the chemicals used in HPLC separation were HPLC grade. Ferulic acid (99%), 6-Hydroxy-2,5,7,8-tetramethylchromane-2-carboxylic acid (Trolox, 97%), gallic acid (≥98%), butylated hydroxytoluene (BHT ≥99%), 2,2′-azino-bis [3-ethylbenzthiazoline-6-sulphonic acid] (ABTS, ≥99%), 1,1-diphenyl-2-picrylhydrazyl (DPPH), phosphate buffer saline pH 7.4 were obtained from Sigma–Aldrich (Steinheim, Germany). 2,4,6-Tris (2-pyridyl)-*S*-triazine (TPTZ, 99%) was obtained from Fluka (Buchs, Switzerland). Folin-Ciocalteu's RS reagent was purchased from Carlo Erba (Milan, Italy). Absolute ethanol, methanol, acetonitrile, dichloromethane, ethyl acetate (HPLC grade), acetic acid (99.7%) were obtained from RCI Labscan (Bangalore, India). Sodium hydroxide (NaOH, 99%) and potassium hydroxide (99%) were purchased from VWR International (Leuven, Begium). Lutein and zeaxanthin (95.8%) were purchased from Chromadex Inc (Irvine, CA, USA).

2.3. Extraction of lutein and zeaxanthin from corn kernels

The extraction was done as per Galicia et al. (2009), with slight modifications. Fresh weight (fw) 500 mg of ground corn kernels were dispersed in 6 mL of absolute ethanol containing 0.1% BHT (w/v), then mixed using a vortex mixer and incubated at 85 °C for 5 min. To the cloudy sample, 120 μL of 80% potassium hydroxide solution was added to hydrolyze the carotenol ester. The mixture was then gently mixed and stored at 85 °C for 10 min. Since the high temperature could cause isomerization of the carotenoids, the effect of heating should not exceed 85 °C. During the process, cold deionized water (3 mL) was added and mixed with a vortex mixer then immediately placed in an ice bath. Petroleum ether-diethyl ether (3 mL at 2:1, v/v) was added, thoroughly mixed and centrifuged at 1400 × *g* for 10 min using a Sorvall legend 1.6R Mach centrifuge (Thermo Scientific, Waltham, MA, USA). The supernatant was collected and the extraction repeated two more times. Supernatants were pooled then evaporated at 40 °C under vacuum. The extracts were stored at −20 °C until analyzed.

2.4. Quantification of lutein and zeaxanthin

Quantification of lutein and zeaxanthin in the corn kernels was determined as per Kurilich and Juvik (1999), with slight modifications. Each sample was dispersed in 500 μL of mobile phase (acetonitrile:dichloromethane:methanol, 70:20:10, v/v/v), then mixed until dissolved. Analytical chromatographic separation was determined using high-performance liquid chromatography (HPLC). The HPLC system (Waters; Milford, MA, USA) was connected to a Phenomenex C18 security guard cartridge column (Torrance, CA, USA), which included a SIL-10AD VP auto-injector; SCL-10A VP system controller; UV-VIS detector) at a wavelength of 450 nm; YMC carotenoid C30, 4.6 mm × 250 mm column. The mobile phase was filtered and pumped into the HPLC at a flow rate of 1 mL/min. A 50-μL aliquot was injected into the HPLC system and the lutein and zeaxanthin separation took place at 11.69 and 15.02 min, respectively. The entire HPLC run time was 30 min. A calibration curve for each chromatogram was constructed using lutein and zeaxanthin as the standards (Fig. 1). Data analyses were performed using 717 Pluse Waters Millennium 32 software version 3.05 (Waters, Milford, MA, USA). Each sample was analyzed in duplicate.

2.5. Extraction for ferulic acid

Extraction of ferulic acid was done as per Adom and Liu (2002) with slight modifications. Briefly, corn kernels (2 g) were extracted with 40 mL of 1 M NaOH and sonicated for 3 h. Each sample was filtered through Whatman #40 filter paper. The filtrate was normalized by adding 20 mL of 2 M HCl, and 30 mL of ethyl acetate added then mixed until the sample dissolved. After centrifugation at 5000 × *g* for 5 min, the upper aqueous layer was removed; and extraction repeated 3 times. The supernatants were pooled then evaporated at 40 °C under vacuum.

2.6. Determination of ferulic acid

Ferulic acid content was determined following Butsat et al. (2009), with slight modifications. The sample extract was re-dissolved in 3 mL of deionised water–methanol (1:1, v/v) before analysis by HPLC. Reversed-phase HPLC analysis of ferulic acid was performed using a 1525 Water-HPLC system with a binary pump and a 484 UV-VIS detector (Water, Milford, MA, USA). Chromatographic separations were performed using a C-18 column (3.9 mm × 150 mm, i.d. 5 μm). The mobile phase comprised 1% acetic acid in deionized water (phase A) and acetonitrile (phase B) at a flow rate of 1 mL/min. Gradient elution was performed as follows: 0–15 min, 3% phase B; 16–39 min, 35–100% phase B; and 40–50 min, and 3% phase B. Operating conditions were as follows: column temperature 25 °C, injection volume 10 μL, and UV-visible detection at 280 nm. The calibration curve was constructed by plotting the peak areas of the analyte against the concentration of ferulic acid. Data analyses were performed

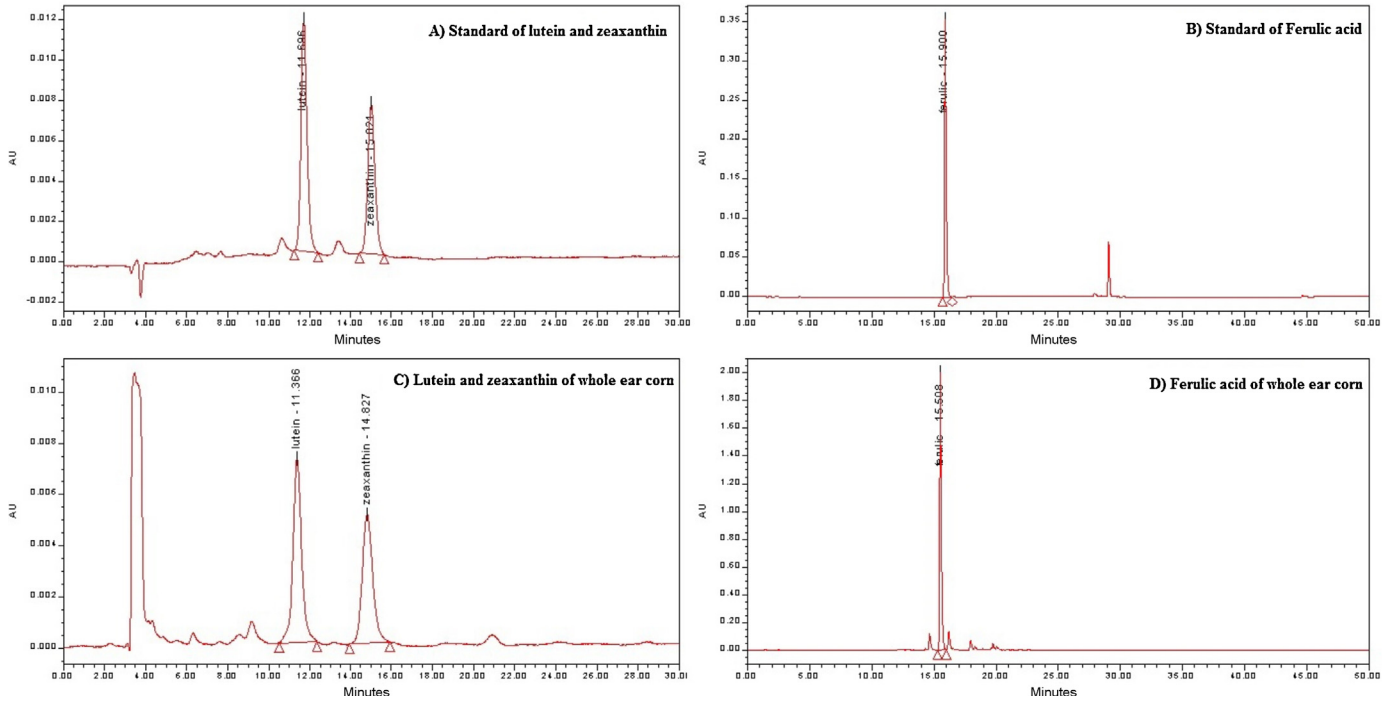


Fig. 1. HPLC Chromatograms: (A) standards of lutein and zeaxanthin, (B) standard of ferulic acid, (C) lutein and zeaxanthin and (D) ferulic acid in cooked whole-ear corn at 0 month storage.

using 717 Pluse Waters Millennium 32 software version 3.05 (Water, Milford, MA, USA). Each sample was analyzed in duplicate.

2.7. Extractions of kernels for total phenolics and antioxidant activity

Total phenolic compounds in mini supersweet corn kernels were extracted as per Dewanto et al. (2002), with slight modifications. About 2 g of corn kernels were added to a flask containing 20 mL of 80% aqueous methanol. The sample was shaken on a platform shaker at 200 rpm for 30 min. After centrifugation at 10,000 × *g* at 4 °C for 20 min, the supernatant was collected for determination of total phenolics and antioxidant activity.

2.8. Determination of total phenolics

Total phenolic content was determined using the Folin–Ciocalteu (F–C) method described by Kahkonen et al. (1999). The dilutions of extracts were oxidized with F–C reagent for 30 min, and the reaction neutralized with sodium carbonate. The sample was completely reacted in the dark. The absorbance of the color was measured at 725 nm, and the total phenolic content expressed as mg of gallic acid equivalent per g of fresh weight (mg GAE/g FW).

2.9. Antioxidant activity determinations

2.9.1. ABTS assay

We followed the ABTS procedure as per Re et al. (1999) with some modifications. The stock solutions included 7 mM $ABTS^{\bullet+}$ solution and 2.45 mM potassium persulfate solution. The stock solution was prepared by mixing 7 mM ABTS and 2.45 mM potassium persulfate at a ratio of 2:1 (v/v) and allowing them to react for 12 h in the dark at room temperature. The solution was diluted with phosphate buffered saline (pH 7.4) to obtain an absorbance of 0.7 ± 0.02 units at 734 nm using a spectrophotometer. The $ABTS^{\bullet+}$ solution was freshly prepared for each assay. Corn extracts (150 μL each) were allowed to react with 3 mL of $ABTS^{\bullet+}$ solution for 2 h in the dark. The absorbance was obtained at 734 nm using a spectrophotometer. The standard curve was linear between 50 and 500 μM of Trolox solution. Results are expressed in μmolTrolox equivalents (TE)/g fresh weight.

2.9.2. DPPH radical-scavenging activity

The DPPH antioxidant-activity assay was performed as per Brand-Williams et al. (1995) with modifications. The stock solution was prepared by dissolving 24 mg DPPH with 100 mL methanol. Corn extracts (77 μL) were added to react with 3 mL of the DPPH solution for 15 min in the dark. The absorbance was taken at 515 nm. The standard curve was linear between 50 and 500 μM of Trolox solution. Results are expressed in μmolTrolox/g fresh weight.

2.9.3. FRAP assay

The FRAP (ferric reducing antioxidant power) assay was done as per Benzie and Strain (1999) with slight modifications. The stock solutions included 300 mM acetate buffer (pH 3.6); 10 mM TPTZ solution in 40 mM HCl; and 20 mM $FeCl_3.6H_2O$ solution. Fresh working solution was prepared by mixing 25 mL of acetate buffer; 2.5 mL of TPTZ solution; and 2.5 mL of $FeCl_3.6H_2O$ solution. Corn extract (200 μL) was allowed to react with 3.8 mL of the FRAP solution for 30 min in the dark. The colored products were taken at 593 nm. The standard curve was linear between 50 and 400 μM of Trolox solution. Results are expressed in μmolTrolox/g fresh weight.

2.10. Sample preparation for enzyme activity

Ground corn (2 g) was added to 20 mL of 0.1 M Tris–HCl buffer (pH 8) then mixed with a vortex mixer for 5 min. After centrifugation at 10,000 × *g* for 30 min at 4 °C, the supernatant as crude enzyme extract was collected for analysis.

2.11. Enzyme activity analysis

2.11.1. Peroxidase activity

Peroxidase (POD) activity was measured by a spectrophotometric assay as per Boyes et al. (1997) with modifications. The reaction mixture was prepared freshly in a total volume of 100 mL 0.2 M sodium phosphate buffer (pH 6.5) containing 560 μL guaiacol (100%) and 195 μL H_2O_2 (30%). The reaction was carried out in a quartz cuvette. Crude enzyme extract (0.15 mL) was pipetted into the cuvette containing 3.6 mL of substrate solution. The increase in absorbance was measured at 470 nm. The results are presented in Unit/g fresh weight.

2.11.2. Lipoxygenase activity

LOX (lipoxygenase) activity was determined as per Tangwongchai et al. (2000) with some modifications. The reaction mixture contained 7.1 mL of 1% linoleic acid in absolute ethanol, 0.2 mL of Tween 20, and 10 mL of 1% absolute ethanol. The reaction mixture was evaporated at 40 °C under vacuum for 30 min. The residue was reconstituted with 150 mL of 0.05 M Na_2HPO_4 (pH 6.5). Enzyme extract (0.15 mL) was added to a cuvette containing 3.6 mL of substrate solution. The increase in absorbance was measured at 234 nm for 15 min. The results are expressed in Unit/g fresh weight.

2.12. Statistical analyses

Analysis of variance (ANOVA) was performed to identify impacts of the packaging condition and storage time following a factorial experiment in randomized complete block design (RCBD) with the same serving style, and 3 replicates. Data were expressed as mean values ± SD. The program SPSS 17.0 (SPSS Inc., Chicago, IL, USA) was used for statistical data analysis at 5% significance level ($p < 0.05$). Duncan's new multiple range test (DMRT) was used to compare mean differences.

3. Results and discussion

3.1. Changes in lutein and zeaxanthin of cooked mini supersweet corn during frozen storage

The lutein and zeaxanthin of cooked mini supersweet corn kernels, measured by a HPLC, are presented in Fig. 2. The lutein and zeaxanthin—separated from the cooked kernels—are shown in Fig. 1C and D. According to the lutein and zeaxanthin patterns, the profile behaviors of different serving styles were greatly affected by packaging conditions and the frozen storage time (0–6 months). The lutein level of the vacuum packaged cooked kernels was higher than that of atmospheric packaging for all treatments ($p \leq 0.05$).

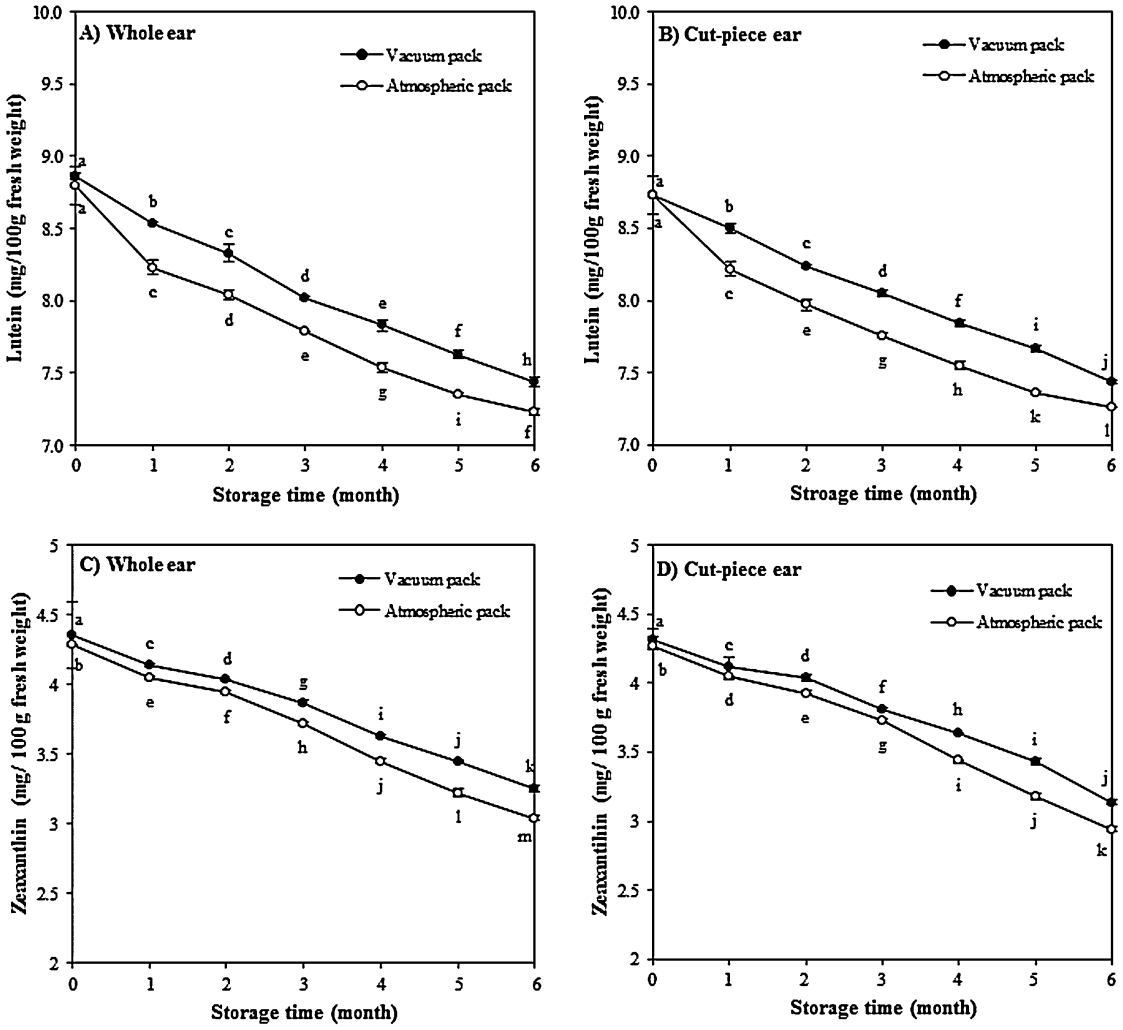


Fig. 2. Changes in lutein and zeaxanthin contents of cooked mini, super-sweet corn ear: vacuum and atmospheric packaging conditions during frozen storage: (A, C) whole ear and (B, D) cut-pieces corn. The lutein and zeaxanthin contents are represented as the means of 6 determinations. The different letters indicates significant differences between treatments under the same serving style ($p \leq 0.05$).

The lutein content of vacuum-packaged, whole-ear corn decreased from 8.86 ± 0.02 to 7.44 ± 0.03 mg/100 g fresh weight during 0–6 month storage, while those under atmospheric packaging decreased from 8.80 ± 0.13 to 7.23 ± 0.02 mg/100 g fresh weight (Fig. 2A). The lutein content of vacuum-packed, cut-pieces decreased from 8.73 ± 0.13 (at month 0) to 8.50 ± 0.03 mg/100 g fresh weight (after 1 month) then decreased rapidly to 8.24 ± 0.01, 7.84 ± 0.02 to 7.44 ± 0.01 mg/100 g fresh weight during storage for 2, 4 and 6 months, respectively ($p \leq 0.05$). Lutein in atmospheric packaging similarly decreased during storage (Fig. 2B).

Like lutein, the zeaxanthin in vacuum-packed whole-ear corn exhibited a higher content than that in atmospheric packaging (Fig. 2C). The zeaxanthin values of vacuum-packed whole-ear corn decreased from 4.35 ± 0.24 to 3.25 ± 0.02 mg/100 g fresh weight while those of atmospheric packaging decreased from 4.28 ± 0.01 to 3.04 ± 0.02 mg/100 g fresh weight during storage ($p \leq 0.05$). A similar trend was observed for cut-pieces in vacuum and atmospheric packaging (Fig. 2D). The results suggest that lutein and zeaxanthin trend to decrease during frozen storage, as reported previously for sweet corn (Junpatiw et al., 2013), oranges (Dias et al., 2014) and broccoli (Martınez-Hernández et al., 2013).

In the current study, after one month of frozen storage, the lutein and zeaxanthin of the cooked whole-ear corn with atmospheric packaging decreased to 6.48% and 5.38%, respectively while those of the cut-pieces fell to 5.84% and 5.15%. Our results agree with Junpatiw et al. (2013) who reported a reduction of the two bioactives of small-ear, bi-color corn for the same storage period were 5.5–17.6 and 2.6–18.0%, respectively. This may have been due to oxidative degradation causing extensive losses of the carotenoids, which depends on (a) the availability of oxygen, (b) stimulation by light, (c) enzymes, (d) metals and (e) co-oxidation with lipid hydroperoxides (Rodriguez-Amaya, 2001)."

3.2. Changes in ferulic acid and total phenolic compounds in cooked, mini supersweet corn during frozen storage

Ferulic acid is a species of soluble phenolic compounds found in corn. The correlation coefficient (r^2) of ferulic acid and total phenolics in corn was 0.78–0.80 (Table 2; $p \leq 0.01$). The ferulic acid in cooked mini supersweet corn at different frozen storage times are shown in Fig. 3. Serving styles and packaging accounted for significant differences in levels ($p \leq 0.05$). The variations of ferulic acid in whole-ears decreased from 83.26 ± 0.16 to 30.26 ± 0.04 mg/100 g fresh weight (vacuum packaging) and 83.30 ± 0.27 to 28.27 ± 0.03 mg/100 g fresh weight (in atmospheric packaging); while in cut-pieces it decreased from 83.52 ± 0.05 to 30.73 ± 0.03 mg/100 g fresh weight and 83.22 ± 0.14 to 27.71 ± 0.04 mg/100 g fresh weight in vacuum vs. atmospheric packaging, respectively. Ferulic acid in all samples decreased relative to storage time from 0 to 6 months. The kernels of vacuum-packed whole-ear corn had higher ferulic content than that under atmospheric packaging for all storage periods (Fig. 3A).

The same trends (a decrease in relation to storage time at −18 °C) were observed for cut-piece corn under vacuum and atmospheric packaging (Fig. 3B). The results indicate that ferulic acid and bioactive compounds in corn kernels will decrease during frozen storage; probably because of degradation (oxidation) of the free ferulic acid released from esterified and insoluble bound forms (Dewanto et al., 2002). There were significant changes in total phenolic content during frozen storage at −18 °C among the samples from different serving styles, packing conditions and storage times. The effects of serving styles and packing conditions on phenolic stability of frozen, cooked, mini-supersweet corn are shown in Fig. 4. Both in whole-ear and cut-piece corn, the phenolic content of vacuum- and atmospheric-packaged samples increased in the early stage of storage time (1st month) then decreased ($p \leq 0.05$; Fig. 4A, B). The total phenolics of vacuum-packed, cooked, whole ears had higher levels than those packed under atmospheric conditions.

In whole-ear corn storage, phenolic content of vacuum-packaged corn-kernels increased from 13.59 ± 0.12 to 16.08 ± 0.01 mg GAE/100 g fresh weight after the 1st month storage (+18.3%), then further significantly decreased from 9.35 ± 0.06 to 6.34 ± 0.25 mg GAE/100 g fresh weight by the 4th (−31.2%) and 6th (−53.4%) month of storage, respectively (Fig. 4A). The phenolic content in corn-kernels kept under atmospheric condition increased from 13.49 ± 0.05 to 15.16 ± 0.99 mg GAE/100 g fresh weight during the 0–1 months of storage (+12.3%), then decreased to 5.36 ± 0.12 mg GAE/100 g fresh weight by the 6th month of storage (−60.3%). For cut-pieces of vacuum-packed, mini supersweet corn, total phenolic content increased from 13.48 ± 0.07 to 16.05 ± 0.03 mg GAE/100 g fresh weight during the 0–1 months of storage (+19.1%), then decreased until the end of the storage (−46.9%; Fig. 4B). A similar profile was observed in those kept frozen under atmospheric conditions; perhaps because of losses of phenolic compounds during cold storage.

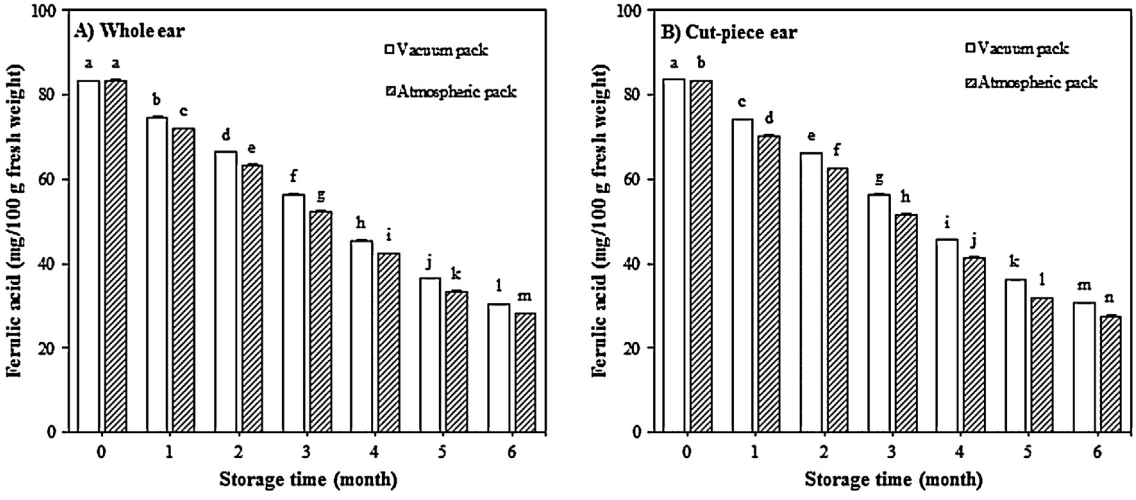


Fig. 3. Changes in ferulic acid of cooked mini, super-sweet corn ear packed under vacuum and atmospheric conditions during frozen storage: (A) whole ear and (B) cut-piece corn. The ferulic acid contents are represented as the means of 6 determinations. The different letters indicates significant differences between treatments under the same serving style ($p \leq 0.05$).

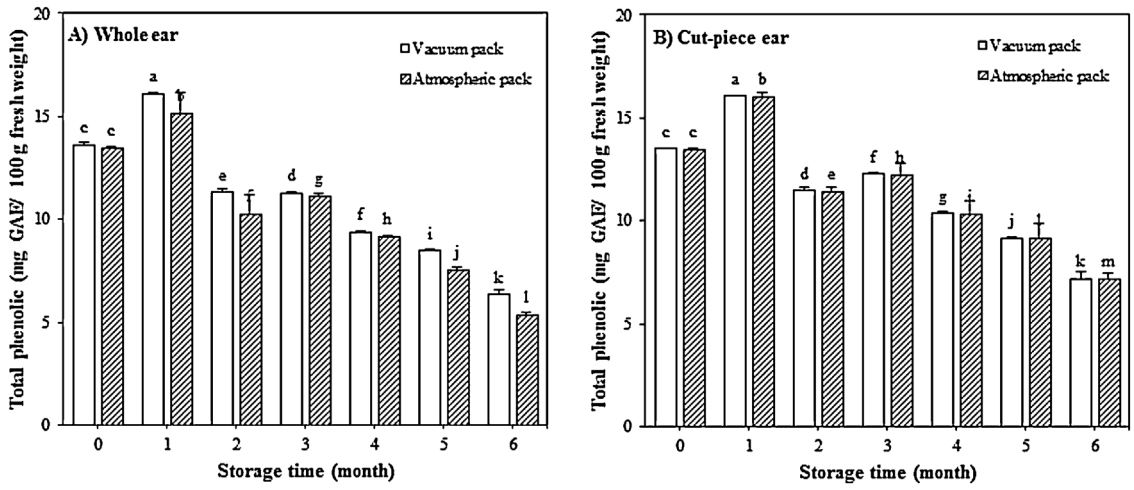


Fig. 4. Total phenolic content of cooked mini, super-sweet corn ear packed under vacuum and atmospheric conditions during frozen storage: (A) whole ear and (B) cut-piece corn. The total phenolic contents are represented as the means of 6 determinations. Different letters indicates significant differences between treatments under the same serving style ($p \leq 0.05$).

The result demonstrated that mini supersweet corn is a good source of total phenolics in comparison to plant-based products; thus, it represents a healthy food choice. Normally, phenolic content may decrease or increase in fruits and vegetables, depending on the storage conditions (Kalt, 2005). Packing style/method causes a significant decrease in total phenolic content ($p \leq 0.05$), suggesting that packaging conditions were sufficient to magnify impacts on quality components. In addition, other reports found that frozen storage induced the reduction in total phenolic content in plants such as spinach, sweet corn, pea (BajČan et al., 2013); pomegranate juice (Mirsaeedghazi et al., 2014); as well as spinach (Bunea et al., 2008). Our results agree with those of BajČan et al. (2013) who found that total phenolics in sweet corn increased to 20.0% in the first month then decreased (i.e., to 9.02%, −1.22%, and −5.01% in the 6th, 9th and 10th month storage, respectively). The increase in total phenolic contents in the first month storage was probably due to water loss from the kernel during frozen storage (Song et al., 2013). The mechanism(s) for these findings remains unclear. The changes in ferulic acid (i.e., a soluble phenolic) content were in line with those of lutein, zeaxanthin and phenolics, which trended to decrease progressively during frozen storage.

The amounts of lutein, zeaxanthin, ferulic acid and total phenolics decreased over the frozen storage time. Ioannou et al. (2012) described that the decrease could be enhanced by the progressive enzymatic or chemical oxidation of phenolics. This was confirmed by the reversibility of oxidizing enzyme activity (i.e., peroxidase and Lipoxygenase) (Table 3).

3.3. Antioxidant activity

Antioxidant activities of cooked corn during frozen storage at −18 °C as determined by the ABTS, DPPH and FRAP assays showed significant variation among the samples from different serving styles, packing conditions and storage times ($p \leq 0.05$, Table 1). During storage, antioxidant activities of both whole and cut-piece corn decreased in relation to storage periods (at 6 months) as well as vacuum packaging. The antioxidant activity under vacuum packaging was higher than that of atmospheric conditions ($p \leq 0.05$). These results suggest that cooked whole ears in vacuum packaging preserved all antioxidants compared to cut-pieces under atmospheric packaging for any storage period. Other studies have reported that atmospheric conditions were generally observed to be destructive to antioxidant activities during storage (Karpińska-Tymoszczyk, 2014; Murcia et al., 2003).

The ABTS assay showed the highest activity after the 1st month of storage (161.81 ± 0.18 and 161.41 ± 0.10 μmol TE/g fresh weight for whole-ear under vacuum and atmospheric conditions, respectively), while the activity in cut-pieces was 161.37 ± 0.19 and 161.52 ± 0.16 μmol TE/g fresh weight for whole-ear under vacuum and atmospheric conditions, respectively. Antioxidant activity by ABTS assay increased during the 1st storage period, then decreased after 2–6 months of storage ($p \leq 0.05$). Vacuum-packaged, whole-ear corn had higher average ABTS-antioxidant activity than that of atmospheric conditions. The ABTS assay indicated that activity increased from 158.65 ± 0.39 (0 months) to 161.81 ± 0.18 μmol-molTrolox/g fresh weight (1 month), then decreased to 97.52 ± 0.17 (4th month) and 71.26 ± 0.12 μmolTrolox/g fresh weight (6th month). Under atmospheric conditions, activity increased from 158.29 ± 0.39 (0 month) to 161.41 ± 0.10 μmolTrolox/g fresh weight (1 month) and decreased from 95.30 ± 0.20 (4th month) to 68.18 ± 0.16 μmolTrolox/g fresh weight (6th month), respectively. A similar profile was observed for cut-piece corn under both vacuum and atmospheric conditions.

In terms of the DPPH radical scavenging capacity, the greatest antioxidant potential was observed in vacuum-packed, whole-ear corn after 1-month storage (Table 1) (75.55 ± 0.11 μmolTrolox/g fresh weight), which decreased through 6-months frozen storage (50.72 ± 0.07 μmolTrolox/g fresh weight). The average DPPH antioxidant activity for vacuum-packed whole-ear corn was significantly higher than that of atmospheric packed samples ($p \leq 0.05$). The same trend was observed for cut-piece corn for both vacuum and atmospheric conditions.

The respective FRAP activity of samples was significantly different according to serving style and packing conditions throughout the storage period. All bio-activity in mini supersweet corn was drastically decreased during frozen storage (from 0 to 6 months) (Table 1). The respective average FRAP activity of whole-ear corn in vacuum vs. atmospheric packaging deceased between 56.24 ± 0.46 and 39.22 ± 0.44 vs. 56.20 ± 0.06 to 36.21 ± 0.05 μmolTrolox/g fresh weight. In cut-pieces, the respective decease was 56.23 ± 0.03 to 38.19 ± 0.06 vs. 56.20 ± 0.05 to 34.63 ± 0.47 μmolTrolox/g fresh weight. The effects of different serving styles, packaging conditions and duration of frozen storage might explain the large variability. These results suggest that frozen storage negatively influenced the ferric reducing antioxidant power

Table 1
Antioxidant activity changes in whole and cut-pieces of cooked mini, super-sweet corn under different packaging conditions during frozen storage[#]

Month	ABTS (μmolTrolox/g fresh weight)				DPPH (μmolTrolox/g fresh weight)				FRAP (μmolTrolox/g fresh weight)			
	Whole ear		Cut-piece ear		Whole ear		Cut-piece ear		Whole ear		Cut-piece ear	
	Vacuum	Atmospheric	Vacuum	Atmospheric	Vacuum	Atmospheric	Vacuum	Atmospheric	Vacuum	Atmospheric	Vacuum	Atmospheric
0	158.65 ± 0.39 c	158.29 ± 0.39 d	158.79 ± 0.42 b	157.77 ± 0.33 c	72.71 ± 0.21 c	72.55 ± 0.11 d	72.22 ± 0.13 c	72.58 ± 0.10 e	56.24 ± 0.46 b	56.20 ± 0.06 b	56.23 ± 0.03 b	56.20 ± 0.05 b
1	161.81 ± 0.18 a	161.41 ± 0.10 b	161.37 ± 0.19 a	161.52 ± 0.16 a	75.55 ± 0.11 a	75.32 ± 0.13 b	74.66 ± 0.09 a	73.43 ± 0.10 b	58.13 ± 0.08 a	56.13 ± 0.07 b	57.18 ± 0.11 a	55.23 ± 0.06 c
2	114.94 ± 0.20 e	110.77 ± 0.13 f	110.72 ± 0.19 d	110.85 ± 0.23 d	72.61 ± 0.14 cd	70.12 ± 0.05 f	70.44 ± 0.14 d	70.08 ± 0.05 g	54.78 ± 0.56 c	51.22 ± 0.05 d	54.46 ± 0.04 d	50.03 ± 0.09 e
3	106.77 ± 0.31 g	103.95 ± 0.28 h	106.31 ± 0.15 e	102.88 ± 0.23 f	70.56 ± 0.14 e	64.82 ± 0.10 h	68.45 ± 0.14 f	63.62 ± 0.10 i	50.10 ± 0.10 e	44.30 ± 0.07 g	49.63 ± 0.11 f	43.82 ± 0.05 h
4	97.52 ± 0.17 i	95.30 ± 0.20 j	96.48 ± 0.14 g	93.68 ± 0.13 h	65.28 ± 0.08 g	55.15 ± 0.10 j	62.67 ± 0.12 h	54.38 ± 0.12 k	45.32 ± 0.48 f	40.36 ± 0.06 h	44.21 ± 0.05 g	39.97 ± 0.09 i
5	83.55 ± 0.12 k	80.35 ± 0.11 l	82.21 ± 0.14 i	79.28 ± 0.15 j	57.60 ± 0.14 i	50.39 ± 0.11 l	54.69 ± 0.14 j	48.10 ± 0.15 m	40.22 ± 0.56 h	38.08 ± 0.07 j	38.32 ± 0.05 j	34.62 ± 0.46 k
6	71.26 ± 0.12 m	68.18 ± 0.16 n	70.55 ± 0.07 k	66.35 ± 0.10 l	50.72 ± 0.07 k	45.09 ± 0.15 m	48.44 ± 0.15 l	42.47 ± 0.12 n	39.22 ± 0.44 i	36.21 ± 0.05 k	38.19 ± 0.06 j	34.63 ± 0.47 l

Means in columns under the same serving style with different letters are significantly different ($p < 0.05$) determined by Duncan's multiple range test (DMRT).
[#] Values are means ± SD ($n = 6$). ABTS: 2,2′-azinobis-(3-ethylbenzothiazoline-6-sulfonic acid); DPPH: 2,2-diphenyl-1-picrylhydrazyl and FRAP, ferric reducing antioxidant power.

of cooked kernels. The antioxidant activities in vegetables depressed after thermal processing are likely heat sensitive while the water-soluble bioactive compounds undergo oxidation during frozen storage (Gokmen et al., 2005; Thaipong et al., 2006). The antioxidant activities of cooked-frozen kernels depend upon various factors, such as plant structures, packaging conditions and storage periods (Dewanto et al., 2002; Martínez et al., 2013). Table 2 shows correlation coefficients (r^2) between bioactives and antioxidant activities of the cooked corn under vacuum packing condition throughout the frozen storage period. There were strong positive correlations between bioactives in corn and antioxidant activities by ABTS, FRAP and DPPH assays with r^2 of 0.90–0.93, 0.83–0.92 and 0.72–0.91, respectively ($p \leq 0.01$). Antioxidant activities in corn resulted from both hydrophilic and hydrophobic antioxidant systems. The r^2 of cooked corn under atmospheric packing condition was on likewise in line. Other researchers reported the same trend (Chuah et al., 2008; Ismail et al., 2004; Stahl & Sies, 2003; Wachtel-Galor et al., 2008 cited in Song et al., 2013).

3.4. Enzyme activity

The enzyme activities of steamed mini supersweet corn were significantly different at various serving styles, packing conditions and storage periods ($p \leq 0.05$). POD-activity in corn kernels initially increased during frozen storage (−18 °C) and increased after 6 months storage (Table 3). The average POD-activity of cut-pieces was comparable to that of whole-ear corns with the same packaging. For whole-ear serving style, the POD-activity in corn-kernels of atmospheric packaging after 1-month storage was higher (5.08 ± 0.01 Unit/g fresh weight) than that of vacuum packaging (4.49 ± 0.02 Unit/g fresh weight). After 6 months storage, the POD-activity was increased to 64.84 ± 0.60 and 59.94 ± 0.44 unit/g fresh weight for atmospheric and vacuum packaging, respectively.

For cut-pieces, POD-activity in corn-kernels in vacuum packaging was 2.77 ± 0.02, 6.72 ± 0.02, 21.61 ± 0.15 and 60.66 ± 0.12 Unit/g fresh weight at 0, 2, 4 and 6 month storage, respectively. A similar trend was observed for cut-pieces with atmospheric packaging during frozen storage. The results revealed a reversible increase in POD-activity during frozen storage. These results agree with Lee and Hammes (1979) and Boyes et al. (1997) who reported that steaming at 99 °C for 15 min completely inactivated POD-activity, but that enzyme activity was reversible during frozen storage at −18 °C for 9 months. This was due to enzyme conformational changes during storage (Gonçalves et al., 2009; Lisiewska and Kmiecik, 2000).

Like POD, the LOX-activity in corn-kernels (both whole and cut-pieces) generally increased with storage time at −18 °C (Table 3). LOX activity of vacuum-packed whole-ears was lower than that under atmospheric condition after 6 months of storage. The average LOX-activity for all samples ranged from 1.91 ± 0.00 Unit/g fresh weight at the beginning, and gradually increased to 8.42 ± 0.02 to 9.92 ± 0.05 Unit/g fresh weight after 6 months of storage. Both whole-ear and cut-pieces with atmospheric packaging exhibited the highest LOX-activity at 6 months of storage (9.92 ± 0.05 and 9.93 ± 0.11 Unit/g fresh weight, respectively) followed by cut-piece and whole-ear corn in vacuum packaging (8.56 ± 0.02 and 8.42 ± 0.02 unit/g fresh weight, respectively). These results indicate that the inactivation of LOX in steam-cooked mini-supersweet corn kernels was reversible since its activity continually increased during frozen storage. These results agree with the LOX-activity of cooked green beans during frozen storage (Bahçeci et al., 2005). LOX has been associated with quality degradation because it causes off flavors and odors, as well as loss of carotenoids and chlorophylls (Tangwongchai et al., 2000).

Table 2
Correlation coefficients (r^2) between bioactive compounds in vacuum-packed, frozen whole and cut ears of cooked, mini, super-sweet corn.

Variables	Lutein	Zeaxanthin	Ferulic acid	Total phenolic	ABTS	DPPH	FRAP
Lutein							
(whole ear)	1.000						
(cut-piece ear)	1.000						
Zeaxanthin							
(whole ear)	0.987	1.000					
(cut-piece ear)	0.975	1.000					
Ferulic acid							
(whole ear)	0.993	0.994	1.000				
(cut-piece ear)	0.990	0.982	1.000				
Total phenolics							
(whole ear)	0.761	0.762	0.779	1.000			
(cut-piece ear)	0.747	0.787	0.796	1.000			
ABTS							
(whole ear)	0.921	0.907	0.926	0.930	1.000		
(cut-piece ear)	0.896	0.896	0.913	0.922	1.000		
DPPH							
(whole ear)	0.724	0.790	0.756	0.821	0.782	1.000	
(cut-piece ear)	0.815	0.881	0.824	0.913	0.847	1.000	
FRAP							
(whole ear)	0.831	0.886	0.862	0.830	0.863	0.964	1.000
(cut-piece ear)	0.860	0.920	0.873	0.835	0.829	0.972	1.000

Values were significantly different at $p < 0.01$.
ABTS: 2,2′-azinobis-(3-ethylbenzothiazoline-6-sulfonic acid); DPPH: 2,2-diphenyl-1-picrylhydrazyl and FRAP, ferric reducing antioxidant power.

Table 3
Enzyme activity changes in frozen, whole and cut, cooked, mini, super-sweet corn with different packaging.

Month	POD (Unit/g fresh weight)				LOX (Unit/g fresh weight)			
	Whole ear		Cut-piece ear		Whole ear		Cut-piece ear	
	Vacuum	Atmospheric	Vacuum	Atmospheric	Vacuum	Atmospheric	Vacuum	Atmospheric
0	2.77 ± 0.02 l	2.77 ± 0.02 l	2.77 ± 0.02 l	2.77 ± 0.02 l	1.91 ± 0.00 l	1.91 ± 0.00 l	1.91 ± 0.00 l	1.91 ± 0.00 l
1	4.49 ± 0.02 k	5.08 ± 0.01 j	4.47 ± 0.02 k	5.12 ± 0.02 j	2.24 ± 0.13 k	2.39 ± 0.01 j	2.24 ± 0.01 l	2.53 ± 0.01 jk
2	6.75 ± 0.05 i	7.06 ± 0.05 i	6.72 ± 0.02 i	7.12 ± 0.04 i	2.42 ± 0.00 j	2.57 ± 0.01 i	2.46 ± 0.08 k	2.60 ± 0.06 i
3	11.67 ± 0.03 h	13.09 ± 0.08 g	11.79 ± 0.27 h	13.24 ± 0.04 g	2.75 ± 0.07 h	2.93 ± 0.12 g	2.80 ± 0.03 h	2.94 ± 0.02 g
4	21.66 ± 0.10 f	23.23 ± 0.12 e	21.61 ± 0.15 f	23.34 ± 0.05 e	4.21 ± 0.03 f	4.50 ± 0.02 e	4.32 ± 0.03 f	4.59 ± 0.05 e
5	38.46 ± 0.33 d	42.08 ± 0.43 c	39.35 ± 0.94 d	42.80 ± 0.04 c	6.19 ± 0.04 d	6.62 ± 0.02 c	6.21 ± 0.09 d	6.61 ± 0.02 c
6	59.94 ± 0.44 b	64.84 ± 0.60 a	60.66 ± 0.12 b	66.40 ± 0.10 a	8.42 ± 0.02 b	9.92 ± 0.05 a	8.56 ± 0.02 b	9.93 ± 0.11 a

Values are means ± SD ($n = 6$). POD: peroxidase; LOX: lipoxiginase.
Means in columns under the same serving style with different letters are significant ($p < 0.05$) determined by Duncan's multiple range test (DMRT).

4. Conclusions

Bioactives, lutein and zeaxanthin in cooked, frozen mini supersweet corn showed significant differences in relation to various serving styles, packing conditions and storage times. Ferulic acid, total phenolic content and antioxidant activity of whole-ear corn were higher under vacuum packing than those of cut-pieces with atmospheric packing; however, bioactives in vacuum-packaged, whole-ear corn decreased more slowly than cut-piece corn with atmospheric packaging during 6 months of frozen storage. POD- and LOX-activities for all treatments increased for all periods of frozen storage.

Acknowledgements

This work was supported by the Higher Education Research Promotion and National Research University Project of Thailand, Office of the Higher Education Commission, through the Food and Functional Food Research Cluster of Khon Kaen University. The authors thank (a) the Plant Breeding Research Center for Sustainable Agriculture, Faculty of Agriculture, Khon Kaen University, for plant material and (b) Mr. Bryan Roderick Hamman for assistance with the English-language presentation. This work was under the Incubation Researcher Project, Khon Kaen University.

References

Adefegha, S.A., Oboh, G., 2011. Cooking enhances the antioxidant properties of some tropical green leafy vegetables. Afr. J. Biotechnol. 10, 632–639.
Adom, K.K., Liu, R.H., 2002. Antioxidant activity of grains. J. Agric. Food Chem. 6182–6187.
Bahçeci, S.K., Serpen, A., Gökmen, V., Acar, J., 2005. Study of lipoxygenase and peroxidase as indicator enzymes in green beans: change of enzyme activity, ascorbic acid and chlorophylls during frozen storage. J. Food Eng. 66, 187–192.
BajČan, D., Tomáš, J., Uhlířová, G., Árvay, J., Trebichalský, P., Stanovič, R., Šimanský, V., 2013. Antioxidant potential of spinach, peas, and sweetcorn in relation to freezing period. Czech J. Food Sci. 6, 613–618.
Benzie, I.F.F., Strain, J.J., 1999. Ferric reducing antioxidant power assay: direct measure of total antioxidant activity of biological fluids and modified version for simultaneous measurement of total antioxidant power and ascorbic acid concentration. Methods Enzymol. 299, 15–27.
Boyes, S., Chevis, P., Perera, C., 1997. Peroxidase isoforms of corn kernels and corn on the cob: preparation and characteristics. LWT-Food Sci. Technol. 30, 192–201.
Brand-Williams, W., Cuvelier, M.E., Berset, C., 1995. Use of a free radical method to evaluate antioxidant activity. Lebensmittel-Wissenschaft and Technologie 26, 25–30.
Bunea, A., Andjelkkovic, M., Socaciu, C., Bobis, O., Neacsu, M., Verhé, R., Camp, J.V., 2008. Total and individual carotenoids and phenolic acids content in fresh, refrigerated and processed spinach (*Spinacia oleracea* L.). Food Chem. 108, 649–656.
Butsat, S., Weerapreeyakul, N., Siriamornpun, S., 2009. Changes in phenolic acids and antioxidant activity in Thai rice husk at five growth stages during grain development. J. Agric. Food Chem. 57, 4566–4571.
Chipurura, B., Muchuwei, M., Manditseraa, F., 2010. Effect of thermal treatment on the phenolic content and antioxidant activity of some vegetables. Asian J. Clin. Nutr. 2, 93–100.

Dewanto, V., Wu, X., Liu, R.H., 2002. Processed sweet corn has higher antioxidant activity. J. Agric. Food Chem. 50, 4959–4964.
Dias, M.G., Camões, M.F.G.F.C., Oliveira, L., 2014. Carotenoid stability in fruits, vegetables and working standards – effect of storage temperature and time. Food Chem. 156, 37–41.
Galicia, L., Nurit, E., Rosales, A., Palacios-Rojas, N., 2009. Laboratory Protocols: Maize nutrition quality and plant tissue analysis laboratory. CIMMYT, Mexico.
Gokmen, V., Bahceci, K.S., Serpen, A., Acar, J., 2005. Study of lipoxygenase and peroxidase as blanching indicator enzymes in peas: change of enzyme activity, ascorbic acid and chlorophylls during frozen storage. LWT-Food Sci. Technol. 38, 903–908.
Gonçalves, M.E., Cruz, S.M.R., Abreu, M., Brandã, R.R.T., Silva, M.L.C., 2009. Biochemical and colour changes of watercress (*Nasturtium officinale* R. Br.) during freezing and frozen storage. J. Food Eng. 93, 32–39.
Harakotr, B., Suriharn, B., Tangwongchai, R., Scott, M.P., Lertrat, K., 2014. Anthocyanin, phenolics and antioxidant activity changes in purple waxy corn as affected by traditional cooking. Food Chem. 164, 510–517.
Ioannou, I., Hyardin, A., Charbonnel, C., Ghoul, M., 2012. Comparative study of antioxidant activity between basic and convenience foods. J. Food Res. 1, 143–156.
Junpatiw, A., Lertrat, K., Lomthaisong, K., Tangwongchai, R., 2013. Effects of steaming, boiling and frozen storage on carotenoid contents of various sweet corn cultivars. Int. Food Res. J. 20, 2219–2225.
Kahkonen, M.P., Hopia, A.I., Vuorela, H.J., Rauha, J.P., Pihlaja, K., Kujala, T.S., 1999. Antioxidant activity of plant extracted containing phenolic compounds. J. Agric. Food Chem. 47, 3954–3962.
Kalt, W., 2005. Effects of production and processing factors on major fruit and vegetable antioxidants. J. Food Sci. 70, 11–19.
Karpińska-Tymoszczyk, M., 2014. The effect of antioxidants, packaging type and frozen storage time on the quality of cooked turkey meatballs. Food Chem. 148, 276–283.
Kurilich, C.A., Juvik, A.J., 1999. Quantification of carotenoid and tocopherol antioxidants in *Zea mays*. J. Agric. Food Chem. 47, 1948–1955.
Lee, Y.C., Hammes, J.K., 1979. Heat inactivation of peroxidase in corn-on-the-cob. J. Food Sci. 44, 785–787.
Lee, S.K., Kader, A.A., 2000. Pre-harvest and post-harvest factors influencing vitamin C content of horticultural crops. Postharvest Biol. Technol. 20, 207–220.
Lisiewska, Z., Kmiecik, W., 2000. Effect of storage period and temperature on the chemical composition and organoleptic quality of frozen tomato cubes. Food Chem. 70, 167–173.
Martínez, S., Pérez, N., Carballo, J., Franco, I., 2013. Effect of blanching methods and frozen storage on some quality parameters of turnip greens ("grelos"). LWT-Food Sci. Technol. 51, 383–392.
Martınez-Hernández, B.G., Artés-Hernández, F., Gómezb, A.P., Artés, F., 2013. Induced changes in bioactive compounds of kailan-hybrid broccoli after innovative processing and storage. J. Funct Foods 5, 133–143.
Mazzeo, T., N'Dri, D., Chiavaro, E., Visconti, A., Fogliano, V., Pellegrini, N., 2011. Effect of two cooking procedures on phytochemical compounds, total antioxidant capacity and colour of selected frozen vegetables. Food Chem. 128, 627–633.
Mirsaeedghazi, H., Emam-Djomeh, Z., Ahmadkhaniha, R., 2014. Effect of frozen storage on the anthocyanins and phenolic components of pomegranate juice. J. Food Sci. Technol. 52, 382–386.
Murcia, A.M., Martínez-Tomé, M., Nicolás, C.M., Vera, M.A., 2003. Extending the shelf-life and proximate composition stability of ready to eat foods in vacuum or modified atmosphere packaging. Food Microbiol. 20, 671–679.
Re, R., Pellegrini, N., Proteggente, A., Pannala, A., Yang, M., Evans, C.R., 1999. Antioxidant activity applying an improved ABTS radical cationde colorization assay. Free Rad. Biol. Med. 9, 1231–1237.
Rickman, J.C., Bruhn, C.M., Barrett, D.M., 2007. Nutritional comparison of fresh, frozen and canned fruits and vegetables II. Vitamin A and carotenoids, vitamin E, minerals and fiber. J. Sci. Food Agric. 87, 1185–1196.
Rodriguez-Amaya, D.B., 2001. General procedure and sources of errors in carotenoid analysis. In: A guide to carotenoid analysis in foods. International Life Sciences Institute. ILSI Press, Washington, D.C., 23 p.
Scott, C.E., Eldridge, A.L., 2005. Comparison of carotenoid content in fresh, frozen and canned corn. J. Food Compos. Anal. 18, 551–559.
Song, J., Liu, C., Li, D., Meng, L., 2013. Effect of cooking methods on total phenolic and carotenoid amounts and DPPH radical scavenging activity of fresh and frozen sweet corn (*Zea mays*) kernels. Czech J. Food Sci. 6, 607–612.
Tangwongchai, R., Ledward, D.A., Ames, J.M., 2000. Effect of high-pressure treatment on lipoxygenase activity. J. Agric. Food Chem. 48, 2896–2902.
Temple, N.J., 2000. Antioxidants and disease: more questions than answers. Nutr. Res. 20, 449–459.
Thaipong, K., Boonprakob, U., Crosby, K., Cisneros-Zevallos, L., Byrne, D.H., 2006. Comparison of ABTS, DPPH, FRAP and ORAC assays for estimating antioxidant activity from guava fruit extracts. J. Food Compos. Anal. 19, 669–675.
Tsuda, T., Horio, F., Uchida, K., Aoki, H., Osawa, T., 2003. Dietary cyanidin 3-O-b-D glucoside-rich purple corn color prevents obesity and ameliorates hyperglycemia in mice. J. Nutr. 133, 2125–2130.
Turkmen, N., Sari, F., Velioglu, Y.S., 2005. The effect of cooking methods on the total phenolics and antioxidant activity of selected green vegetables. Food Chem. 93, 713–718.

J Food Sci Technol (October 2015) 52(10):6529–6537
DOI 10.1007/s13197-015-1750-2

ORIGINAL ARTICLE

Physicochemical and morphological properties of starch from fresh waxy corn kernels

Danupol Ketthaisong · Bhalang Suriharn · Ratchada Tangwongchai · Jay-lin Jane · Kamol Lertrat

Revised: 14 January 2015 / Accepted: 30 January 2015 / Published online: 26 February 2015
© Association of Food Scientists & Technologists (India) 2015

Abstract
The characteristics on physicochemical and morphological properties of starches were investigated in fresh waxy corn kernels. Starches were isolated from eight waxy corn genotypes at the immature kernel stage growing in Thailand. The starch content showed variation with genotypes and ranged from 77.76 to 90.97 %. Granule size distribution showed a two population of starch granules with peak values ranged from 0.8 to 1.1 μm (small) and 9.0 to 12.2 μm (large). Genotypes were also significantly different for average chain length (CL), unit chain length distribution and pasting properties. The small granule (<5 μm) was negatively correlated with CL and degree of polymerization (DP) 25–36 of amylopectin (−0.82 and −0.67, respectively, $P < 0.01$). And a strong relationship between trough and final viscosity was consistent with the contribution of pasting properties.

Highlights
- Immature starches showed variation on starch content, granule sizes and chain length distribution of amylopectin.
- A two population of starch granules with peak values ranged from 0.8 to 1.1 μm (small) and 9.0 to 12.2 μm (large).
- Small granule population was negative correlation with CL and DP 25–36 of amylopectin.

D. Ketthaisong · B. Suriharn · K. Lertrat (✉)
Department of Plant Science and Agricultural Resources, Faculty of Agriculture, Khon Kaen University, Khon Kaen 40002, Thailand
e-mail: Kamol9@gmail.com

K. Lertrat
e-mail: danupol63@gmail.com

R. Tangwongchai
Department of Food Technology, Faculty of Technology, Khon Kaen University, Khon Kaen 40002, Thailand

J.-l. Jane
Department of Food Science and Human Nutrition, Iowa State University, Ames, IA 50011, USA

Keywords Microstructure · Granule size · Viscosity · Amylopectin distribution

Introduction

Waxy or glutinous corn (*Zea mays* L. var. *ceratina*) is traditional vegetable, consumed similar to sweet corn as cooked green ears. This corn has been developed and cultivated in many Asian countries, including, some parts of China, Japan, Vietnam, Lao, Myanmar, Korea, Taiwan and Thailand (Lertrat and Thongnarin 2008). Waxy corn has similar properties to sticky rice because its endosperm starch consists of mainly amylopectin. Small-scale farmers in Thailand and Southeast Asia have grown waxy corn as a cash crop next to rice for fresh consumption for more than a century. A good eating quality is the main goal for waxy corn breeding program (Lertrat and Thongnarin 2008).

Breeding for fresh kernel has become economically beneficial because the development of niche markets for specialty ear. In addition, it has been increasing numbers of vertically integrated vegetable corn systems can capture the added value in an improved quality food for health benefit. The market share of waxy corn in the seed industry has increased. Seed companies in southeast Asia have shown interests in improving quality of waxy corn and develop new varieties. An objective breeding is to produce starch with novel properties for making new products. New varieties of waxy corn have been developed with improved consistency, taste and shelf life, which affected by the physicochemical properties of starch. Numerous researches exhibited the basic component of starch can affect the textural properties of several food crops such rice (Kang et al. 2006), potato (Sing et al. 2005) and sorghum (Cagampang and Kirleis 1984).

Starch is the main energy storage of plants. The chemical compositions of starch in corn kernels are amylose and

amylopectin, and some intermediate materials that retain characteristics of both fractions. Amylose is linear or slightly branched molecules whereas amylopectin is highly branched molecules (Jane et al. 1999). These two polymers have different physical properties. Therefore, lots efforts have be interested to improve novel starch for unique properties by changing the proportions of the two molecules. Functional properties of starch are affected by the amylose content and branched chain length distribution of amylopectin (Hanashiro et al. 1996; Jane et al. 1999). The physicochemical properties of waxy corn starches from mature seeds have been reported (Fiedorowicz and Rebilas 2002; Jane et al. 1999; Jiranuntakul et al. 2011; Singh et al. 2003), but the properties of kernel starches at immature stage are less understood. Including, the variation of varieties are affected to physicochemical properties of waxy corn starch. The immature ears are consumed during kernel development about 16 to 22 days after pollination (DAP), which depend on genetics and environment. Genetic information in the physicochemical properties is important for breeders to select breeding lines that starch characteristics to relate the quality and also for market to select the quality foods with desired properties for consumer. The objectives of this study were to characterization on the physicochemical properties of waxy corn starch at the immaturity stage and study the correlation among physicochemical traits. This information will be useful for developing practical strategies to improve waxy corn for good-eating quality in the future and also this will be useful in selecting the appropriate variety for end use suitability.

Materials and methods

Plant materials Eight genotypes of waxy corn were used in this study including, KKU-BK, KKU-JP, KKU-UB, KKU-JD, KKU-G2 and KKU-N7 and the two check commercial F_1-hybrid varieties ("BigW" and "Violet"). The inbred lines were extracted from a local population with high adaptability, early maturity as well as high and low performance in traits related to eating quality of cooked green ears (Ketthaisong et al. 2014). The breeding lines were selected by Plant Breeding Research Center for Sustainable Agriculture, Khon Kaen University, Thailand. The seeds were grown at Khon Kaen University, Khon Kaen Province, Thailand during November 2011 to January 2012. Standard agronomic practices were used to provide adequate nutrition and kept the plots disease-free. For each variety, fifteen sib-pollinated ears were harvested 16 to19 days after pollination (DAP) and stored at −20 °C in plastic bags until analysis.

Isolation of starches Waxy corn starches were isolated using a method of Jiranuntakul et al. (2011) with slight modifications. Corn kernels, 400 g for each sample, were steeped in water containing 0.16 % sodium hydrogen sulfite at 45 °C for 12 h to inactivate the enzymes. The grains were ground in a blender and then screened through a 250, 106 and 63 μm sieves, respectively. The cloudy supernatant was removed, and the sediment was re-slurried in 0.2 % sodium hydroxide solution. The supernatant was discarded, and the starch cake was re-suspended in water for five times. The starch slurry was then passed through a 63 μm sieve. The cake was given repeated washings with water until the pH of starch slurry reached seven. The starch cake was then dried in an oven at 40 °C for 24 h.

Amylose and starch contents The amylose content was determined using the iodine adsorption method of Hoover and Ratnayake (2001), and starch content was obtained using the Total Starch Kit (Megazyme, Co, Wicklow, Ireland).

Starch granule morphology Starch powders were fixed onto a circular specimen stub with double-side tape, coated with vacuum-coated with a mixture of 60 % gold and 40 % palladium particles then observed using a scanning electron microscope (SEM, JEOL, JSM-5300LV, Japan) with an accelerating voltage of 10 kV.

Particle size analysis Starch granules were suspended in water, and then the particle size distribution was measured with a laser particle size analyzer Model Master sizer S long bed Ver.2.11.

Unit chain distribution of amylopectin Unit chain distribution of amylopectin was determined following the procedure described by Jiranuntakul et al. (2012) with slight modifications. Starch 28 mg (dry basis, db) was dispersed in 2.8 mL of distilled water and heated in boiling water until the sample was completely dissolved. Distilled water (3.85 mL) and 0.35 mL of 10 mM acetate buffer (pH 3.5) were added, then mixed with a vortex mixer and incubated at 45 °C for 10 min. A solution of isoamylase (0.03 unit/mg of substrate) from *Pseudomonas* sp. (1000 U/ml, EC 3.2.1.68, Lot 90701b,

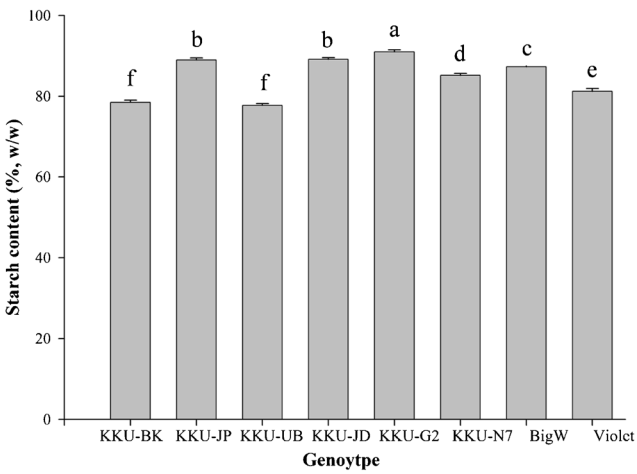


Fig. 1 Starch contents (%, w/w) of eight waxy corn genotypes harvested at immature stage; 16 DAP (KKU-BK) and 19 DAP (KKU-JP, KKU-UB, KKU-JD, KKU-G2, KKU-N7, "BigW" and "Violet")

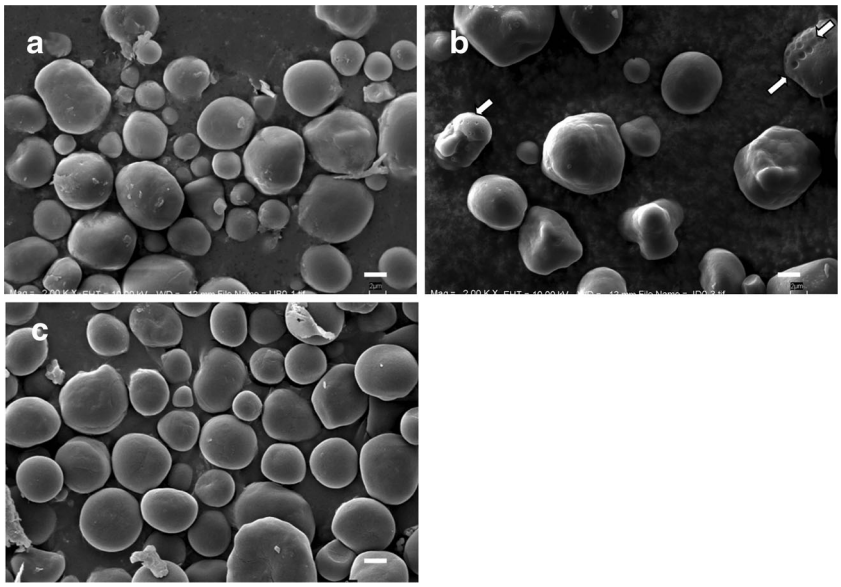


Fig. 2 SEM of starch granules separated from waxy corn varieties at immature stages; **a** KKU-UB (*2000x*), **b** KKU-JD (*2000x*), and **c** "Violet" (*2000x*). *Arrowheads*: starch granule with pinholes on the surface and *scale bar* 2 μm

Megazyme) was added to sample. Samples were debranched for 12 h at 45 °C in a water bath. After debranching, the enzyme activity was stopped by heating in boiling water for 5 min. The debranched amylopectin solutions were dried using a freeze dryer at −80 °C and kept in a sealed plastic container until analyzed. The unit chain distribution of debranched amylopectin was determined using the High Performance Size Exclusion Chromatograph (HPSEC). The HPSEC system included of a pump (Water 1525; Millipore Waters, USA), an injector, two 6.2×250 mm columns connected in series (Zorbax PSM 60S; Agilent Technologies, Santa Clara, CA), packed with 5 mm porous silica microspheres, and a Refractive Index Detector (RI, RID-2414; Waters). A calibration curve for each chromatogram was constructed using maltoheptaose, pullulan 6000 and pullulan 12, 000 standards. The data were analyzed by using Breeze two software (Waters, USA), and each sample was analyzed in duplicate. The *y*-axis of the chromatogram was converted from the RI value to a molar response using the calibration curve.

Pasting properties The pasting properties of waxy corn starches were measured with a Rapid Visco-Analyzer (RVA-4 Series, Newport Scientific Pvt Ltd, Warriewood, NSW, Australia). The starch slurry at concentration 6 % (w/w, db) were determined, at a fixed a paddle rotation speed of 160 rpm. Each sample was heated from 50 to 95 °C at 12 °C/min, maintained at 95 °C for 2.5 min, and then cooled to 50 °C at the same rate, and finally held at 50 °C for 2 min.

Statistical analysis The data of starch characteristics and properties were subjected to analysis of variance according to a Randomized Complete Block Design (RCBD) with three replications, and expressed as mean values for standard deviations. The Least Significant Difference (LSD) was used to compare mean difference at $P<0.05$. The relationships among traits were calculated by the Pearson's correlation analysis using accession means (Gomez and Gomez 1984).

Results and discussion

Amylose and starch content The amylose content of starch separated from different waxy corn genotypes at immature stage were not significantly different (data not shown). Amylose content was very low because every line exhibited inbreeding depression for a waxy gene. Inbreeding is the consequence of the mating between two related individuals. As an effect of selfing, recessive genes, earlier masked in the heterozygous forms, become homozygous (Hallauer et al. 2010). An amylose content of 0.30 % in mature waxy corn starches were reported by Fredriksson et al. (1998), 2.06 % (Jiranuntakul et al. 2011) and 1.00 % (Rocha et al. 2012). The starch content of different genotypes showed significant differences. The variation in starch content ranged from 77.76 to 90.97 %, the KKU-G2 line showed the highest value, whereas the lowest value was observed in KKU-BK line (Fig. 1). In addition, the starch content has been shown to vary among immature botanical sources, with 37 % from kidney bean (Yoshida et al. 2003), 13.70 % from canna (Puncha-arnon et al. 2007) and 74.50 % from yam (Huang et al. 2006). The accumulation of starch depends on developmental stage, organ of plants, types of corn and environment which can affected to physicochemical properties of starch (Li et al. 2007).

Starch granule morphology The scanning electron micrographs (SEM) of starch granules isolated from immature

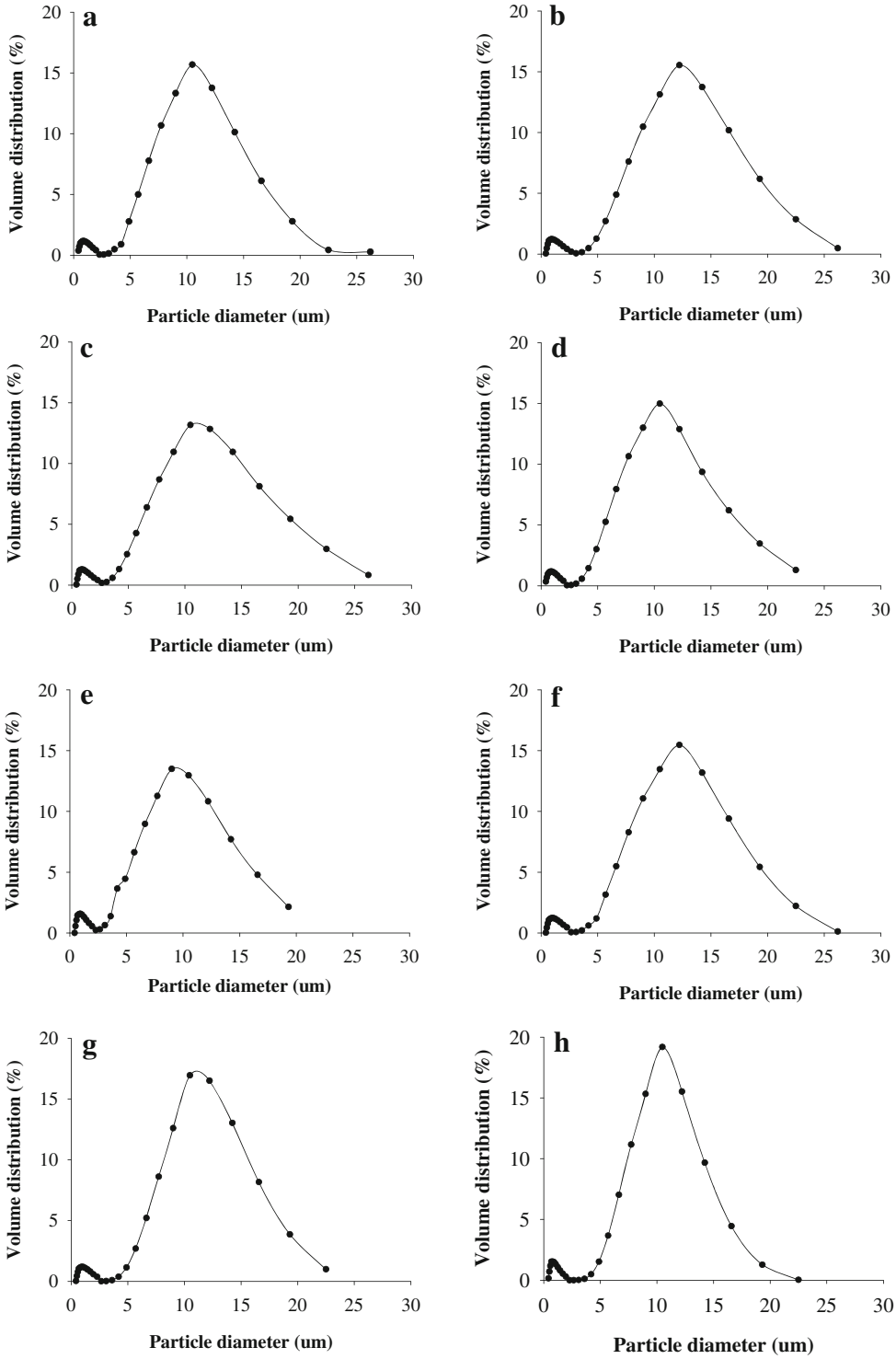


Fig. 3 Granules size distribution (%) of starches from immature waxy corn genotypes. **a**) KKU-BK, **b** KKU-JP, **c**) KKU-UB, **d** KKU-JD, **e**) KKU-G2, **f** KKU-N7, **g**) "BigW" and **h** "Violet"

kernel are shown in Fig. 2. The granule sizes ranged from 2 to 20 μm in diameter. Granules were found to be oval in shape and have smooth surfaces. The SEM images showed irregularly granule shape similar to the granules of immature sweet corn (Jane and Kasemsuwan 1994), but the surface has been smooth then. Starch from KKU-JD line showed few starch granules with pinholes on the surface at immature kernels (Fig. 2B), which the affects from endogenous enzyme to hydrolyzed starch (Li et al. 2007). The internal structure of corn starch granule is determined during the biosynthesis and development of starch granules by the expression of starch synthase activities during the maturation of kernels (Jane 2007). Whereas, the accumulations of amylose in normal corn kernels were increased during kernel development and correlated with a

Table 1 Volume distributions of immature waxy corn starch granules (%)

Genotype	Particle diameter of immature starch granule (μm)		
	Large-granule (>15 μm)	Medium-granule (5–15 μm)	Small-granule (<5 μm)
KKU-BK	9.5±0.6 b	76.9±0.7 b	13.6±0.1 c
KKU-JP	19.2±0.1 f	68.5±0.4 f	12.3±0.4 d
KKU-UB	17.4±0.0 g	67.3±0.0 g	15.3±0.0 b
KKU-JD	11.1±0.2 c	74.1±0.0 c	14.7±0.0 c
KKU-G2	7.2±0.6 d	71.2±0.0 d	21.6±0.6 a
KKU-N7	17.2±0.1 e	70.3±0.2 e	12.4±0.1 e
"BigW"	12.6±0.1 b	76.7±0.1 b	11.4±0.7 f
"Violet"	5.8±0.0 a	81.5±0.0 a	12.7±0.0 e

Means with different letters (a, b, …) in the same column are significantly different ($P<0.05$). Mean ± standard deviation

number of pinholes and activity of granule bound starch synthase I (GBSSI) (Li et al. 2007). The starch granules isolate from normal corn showed few or no pores on immature stage, but those from kernels harvested at fully matured showed a large number of pores (Li et al. 2007). The pinholes could be distributed to endogenous enzyme hydrolysis during kernel development and also are openings to channels for providing an approach to channels that provide an approach to the interior of granules via channel and the surface pores (Miao et al. 2011).

Granule size distribution Starches from genotypes showed significant differences in distribution and also in the volume of the granules (Fig. 3). The granule sizes exhibited a bimodal distribution with peak values in the ranges of 0.8 to 1.1 μm (small) and 9.0 to 12.2 μm (large) for all starches. The limits between the two populations were described as the minimum of the curves that occurred at ~2.7 μm. The granule sizes were classified into large (>15 μm), medium (5–15 μm), and small (<5 μm) granules (Ketthaisong et al. 2013). Average diameter of large, medium, and small granules ranged between 16.6 to 26.2, 5.7 to 14.2 and 0.4 to 4.9 μm, respectively. Among all starches, medium-granules had a highest contribution to the total volumes (68.5 to 81.5 %), followed by small (11.4 to 21.6 %) and large (5.8 to 19.2 %) granules. "Violet" showed the largest proportion of medium-granules and lowest proportion of large-granules, while KKU-UB starch showed the smallest proportion of medium-granules with 67.3 % (Table 1). The variation in size distribution of starch granules may be due to the difference in genotypes, and it is an important factor that affects the starch quality (Li et al. 2008; Singh et al. 2010).

Unit chain distribution of debranched immature waxy corn starches The chain-length distributions as well as the data listed in Table 2. The classification of amylopectin branched chain in the A, B1, B2, and B3 groups conform to chains with a DP of 6–12, 13–24, 25–36 and ≥37, respectively (Hanashiro et al. 1996). In the cluster model of amylopectin, A and B1 chains are located within a single cluster where they form double helices, and form one crystalline lamella, whereas B2 and B3+ chains extend through two or more clusters. Therefore, B2 and longer chains are present in both the crystalline and amorphous lamellae (Hizukuri 1986). Branch chain lengths of amylopectin from the immature starches were significantly different between genotypes for the amount of starch in each group. Average chain length (CL) of starches ranged between 15.2 and 19.4 for KKU-N7 and "BigW", respectively. The increase of CL can affect the physicochemical properties of starches (Jane et al. 1999). In addition, the numerous reported of mature kernels showed CL with 23.5 (Jane et al. 1999), 20.5 (Wang and Wang 2003), and 16.6 (Jiranuntakul et al. 2012), which differences in stages of plants and also the method of determined.

Table 2 Average chain length and unit chain distribution of debranched amylopectins from immature waxy corn starches[a]

Genotype	CL	Distribution (%)			
		DP 6–12	DP 13–24	DP 25–36	DP ≥37
KKU-BK	17.3±0.2 b	73.3±0.2 ab	15.1±0.0 cd	9.6±0.2 d	2.1±0.1 abc
KKU-JP	18.1±1.6 ab	73.4±1.2 ab	15.2±0.7 c	10.0±0.6 cd	1.3±0.0 c
KKU-UB	18.3±1.6 ab	73.9±1.0 ab	13.8±0.0 d	10.1±0.4 cd	2.1±0.6 abc
KKU-JD	18.3±1.5 ab	73.2±1.7 ab	15.5±0.5 c	11.2±0.2 bc	1.8±1.0 abc
KKU-N7	15.2±0.1 c	75.3±0.3 a	14.6±0.7 cd	8.3±1.0 e	1.8±0.1 abc
KKU-G2	18.4±0.5 ab	72.3±0.4 b	15.1±0.1 cd	10.0±0.1 cd	2.6±0.3 a
"BigW"	19.4±1.1 a	67.9±2.3 c	18.0±1.2 b	11.7±0.7 b	2.4±0.4 ab
"Violet"	19.0±1.0 ab	65.5±0.6 d	19.9±0.6 a	13.0±0.5 a	1.6±0.5 cd

Means with different letters in the same column are significantly different ($P<0.05$). Mean ± standard deviation

CL Average chain length, *DP* Degree of polymerization

[a] Molar basis

Table 3 Pasting properties of eight waxy corn starches separated from immature kernels

Genotype	PV (RVU)	TV (RVU)	BV (RVU)	FV (RVU)	SV (RVU)	PT (°C)
KKU–BK	145.5±0.5 c	77.0±3.5 e	68.4±3.4 a	87.4±3.4 c	10.8±2.9 b	77.4±0.4 d
KKU–JP	163.9±1.6 a	110.8±0.9 a	53.1±2.4 cd	123.3±1.4 a	12.4±2.3 b	80.1±0.0 b
KKU–UB	161.7±1.6 b	110.8±1.0 a	50.9±2.7 d	124.1±0.5 a	13.3±1.2 b	79.3±0.0 c
KKU–JD	136.9±1.6 e	69.2±1.2 f	67.8±1.2 a	76.5±0.4 d	7.4±0.8 c	80.7±0.5 ab
KKU–G2	139.3±0.6 d	82.7±0.3 d	56.5±0.3 bc	87.8±0.8 c	5.0±0.6 c	81.0±0.0 a
KKU–N7	128.9±0.3 f	106.3±0.5 b	22.6±0.6 e	123.3±0.5 a	17.0±0.9 a	80.1±0.0 b
BigW	161.0±0.8 b	103.1±1.8 c	57.9±2.5 b	116.5±0.6 b	13.4±2.4 b	77.9±0.4 d
Violet	140.2±0.8 d	71.3±0.5 f	68.9±1.3 a	78.4±0.4 d	7.1±0.1 c	80.1±0.8 b

Means with different letters in the same column are significantly different ($P \leq 0.05$). Mean ± standard deviation

PV peak viscosity, *TV* trough viscosity, *BV* breakdown viscosity, *FV* final viscosity, *SV* setback viscosity and *PT* pasting temperature. *RVU* rapid visco unit

Eight genotypes exhibited a larger proportion of A chains than of B1, B2 and B3+. KKU-N7 line had the greatest proportions of short branch chain (DP 6–12), 75.3 % and the "Violet" showed smallest proportion, 65.5 %. In mature kernel starches the proportions of amylopectin branch-chains were reported to be DP of 13–24 and DP 25–36 which is lower than those of waxy corn starches (Jiranuntakul et al. 2012). The result suggested that KKU-UB line had 73.9 and 13.8 % of DP 6–12 and 13–24, respectively and KKU-JD line showed a smaller proportion of DP 6–12, but a larger proportion of DP 13–24 with 73.2 and 15.5 %, respectively, whereas, the F_1-hybrid varieties showed a smaller proportion with DP 6–12 (65.5 to 67.9 %) than breeding lines (72.3 to 75.3 %). For comparison, waxy corn starch exhibited a small proportions of chains with DP 13–36 but larger proportions of chains with DP 6–12 and >36 (Mendez-Montealvoa et al. 2011). However, some waxy corn starches showed a proportion of debranched amylopectin with DP 13–24 greater than DP 5–12 for 43.3 and 35.2 %, respectively (Wang and Wang 2003). In addition, normal corn starches exhibited a large proportion of branch chains with DP 13–24, 6–12 and 25–36, respectively (Ai et al. 2011; Wang and Wang 2003).

Pasting properties of starches The pasting properties of immature waxy corn starches showed significant difference between all genotypes. The peak viscosity exhibited a range of 128.9 to 163.9 RVU for KKU-N7 and KKU-JP lines, respectively (Table 3). Sandhu and Singh (2007) reported peak viscosity in the range between 67.0 and 104.5 RVU and break down viscosity range with 27.0 to 115.7 RVU for selected corn lines. Miles et al. (1985) reported that increase in final viscosity might be due to the aggregation of the amylose molecules. Pasting properties are dependent on the rigidity of starch granules. Setback viscosities for starch ranged from 5.0 RVU for KKU-G2 line to 17.0 RVU for KKU-N7 line. In addition, the breeding lines and F_1–hybrid varieties exhibited high peak viscosity because it had high proportion of short branch-chains of amylopectin, which can affected to starch properties (Jane et al. 1999). Therefore, the waxy starch samples displayed a similar high peak viscosity, easy breakdown, and low setback viscosity (Jiranuntakul et al. 2011), whereas the rapid increase in viscosity at the early stage of pasting for the gelatinized waxy corn starch powders effected from the rapid hydration and swelling of the amorphous starch powders (Xing and Lim 2012). Pasting properties of starch have been reported to be affected by amylose and branch chain-length distribution of amylopectin. Also, the chain length of amylopectin and molecular size of amylose create synergistic effects on the viscosity of starch pastes (Jane and Chen 1992). This data may be used as criteria for evaluation of physicochemical properties of waxy corn starch between selection lines in breeding program.

Correlation of traits Estimation of simple correlation between various physicochemical characters may provide good information necessary for waxy corn breeders, when, selection is based on two or more traits simultaneously. However, breeding program, precise evaluation of eating quality in early generation is critical. Simple correlation coefficient can help the plant breeders to predict traits. Correlation coefficient is important in plant breeding, because it measures the degree of association, genetic and environment interaction, between two or more characters. If genetic association exists, selection for one trait will cause changes in other traits, basically a correlated response (Hallauer et al. 2010).

Possible correlation coefficients between 14 parameters in eight waxy corn starches at immature stage are summarized in Table 4. The granule size of <5 μm (small) was negatively correlated with CL and DP 25–36 (−0.82 and −0.67, respectively, $P<0.01$), and positively correlated with DP 6–12 (0.63, $P<0.01$), whereas the granule size 5–15 μm (medium) showed positively correlated with DP 13–24 and DP 25–36 (0.91 and 0.78, respectively, $P<0.01$), but exhibited

Table 4 Simple correlation coefficients (*r*) between physicochemical properties of immature starches separated from different waxy corn genotypes

	Starch content	Small[a]	Medium	Large	CL	DP 6–12	DP 13–24	DP 25–36	DP ≥37	PV	TV	BV	FV	SV
Small	0.15													
Medium	0.01	−0.37												
Large	−0.12	−0.33	−0.74 **											
CL	−0.28	−0.82 **	0.40	0.18										
DP 6–12	−0.11	0.63 **	−0.85 **	0.41 *	−0.75 **									
DP 13–24	−0.12	−0.49 *	0.91 **	−0.57 **	0.61 **	−0.95 **								
DP 25–36	−0.22	−0.67 **	0.78 **	−0.32	0.75 **	−0.87 **	0.86 **							
DP ≥37	−0.43	−0.22	−0.19	0.36	0.19	0.06	−0.09	0.02						
PV	−0.13	−0.05	−0.05	0.09	−0.10	0.09	−0.14	0.05	0.44 *					
TV	−0.00	0.18	0.10	−0.22	−0.12	0.01	0.10	0.05	0.07	0.52 **				
BV	−0.11	−0.25	−0.15	0.33	0.05	0.07	−0.23	−0.01	0.29	0.26	−0.69 **			
FV	−0.06	0.17	0.12	−0.24	−0.10	−0.02	0.13	0.06	0.07	0.48 *	0.99 **	−0.71 **		
SV	−0.28	0.10	0.17	−0.24	0.02	−0.13	0.22	0.09	0.03	0.22	0.73 **	−0.64 **	0.82 **	
PT	0.40	−0.11	0.15	−0.07	0.14	−0.13	0.17	0.08	−0.30	−0.52 **	−0.31	−0.08	−0.37	−0.52 **

*, ** Significant at $P \leq 0.05$ and 0.01 probability levels, respectively

CL average chain length, *DP* degree of polymerization, *PV* peak viscosity, *TV* trough viscosity, *BV* viscosity, *FV* final viscosity and *SV* setback viscosity

[a] Small (<5 μm), medium (5–10 μm) and large (>5 μm) granules

negatively correlated with granule size >15 μm (large) and DP 6–12 (−0.74 and −0.85, respectively, $P<0.01$). A strong negative relationship between DP 6–12 to DP 13–24 and DP 25–36 (−0.96 and −0.96, $P<0.01$, respectively) was consistent with the contribution of swelling towards pasting properties. Trough viscosity was positively correlated with final viscosity and setback viscosity (0.99 and 0.73, $P< 0.01$, respectively) and negatively correlated with breakdown viscosity (−0.69, $P<0.01$), whereas final viscosity showed highly positive correlation with setback viscosity (0.83, $P< 0.01$). Similar positive correlation between final viscosity and peak viscosity, and negative correlation between setback viscosity and pasting temperature has been reported by Sandhu and Singh (2007). The structure of amylopectin has been reported to play an important role in the pasting properties of starches. An increase in molecular weight of amylopectin has been effete to decrease the amount of long-branch chain length as well as branching degree of amylopectin, which affected to an increase with peak viscosity and breakdown and decrease in setback and final viscosity (Takeda et al. 1989).

Conclusions

Immature waxy corn starches from different genotypes showed variation on starch contents, granule morphology, granule sizes and chain length distribution of amylopectin. The amount of starch in the small granule population was negative correlation with CL and long branched of amylopectin. Which, the physicochemical properties trait is criteria of choice for evaluation of waxy corn lines in breeding program.

Acknowledgments We thank The Royal Golden Jubilee Ph.D. Program (RGJ), Choncharean Farm, Chia Tai Ltd., The National Science and Technology Development Agency (NSTDA), Pathumthani, Thailand, The Plant Breeding Research Center for Sustainable Agriculture, Faculty of Agriculture, Khon Kaen University, Thailand and Dr. Paul Scott, USDA-ARD, Corn Insects and Crop Genetics Research Unit.

References

Ai Y, Medic J, Jiang H, Wang D, Jane J (2011) Starch characterization and ethanol production of sorghum. J Agric Food Chem 59:7385–7329

Cagampang BG, Kirleis AW (1984) Relationship of sorghum grain hardness to selected physical and chemical measurements of grain quality. Cereal Chem 61:100–105

Fiedorowicz K, Rebilas K (2002) Physicochemical properties of waxy corn starch and corn amylopectin illuminated with linearly polarised visible light. Carbohydr Polym 50:315–319

Fredriksson H, Silverio J, Andersson R, Eliasson AC, Aman P (1998) The influence of amylose and amylopectin characteristics on gelatinization and retrogradation properties of starches. Carbohydr Polym 35:119–134

Gomez KA, Gomez AA (1984) Statistical procedures for agricultural research. John Wiley and Sons, Singapore

Hallauer RA, Carena MJ, Miranda JB (2010) Handbook of plant breeding. Quantitative genetics in maize breeding. Springer, New York

Hanashiro I, Abe J, Hizukuri S (1996) A periodic distribution of the chain length of amylopectin as revealed by high–performance anion–exchange chromatography. Carbohydr Res 283:151–159

Hizukuri S (1986) Polymodal distribution of the chain lengths of amylopectins and its significance. Carbohydr Res 147:342–347

Hoover R, Ratnayake WS (2001) Determination of total amylose content of starch. In: Wrolstad RE, Acree TE, An H, Decker EA, Penner MA, Reid DS, Schwartz SJ, Shoemaker CF, Sporns P (eds) Current protocols in food analytical chemistry. Wiley, USA, pp 2–3, unit E

Huang C, Lin M, Wang CR (2006) Changes in morphological, thermal and pasting properties of yam (*Dioscorea alata*) starch during growth. Carbohydr Polym 64:524–531

Jane J (2007) Structure of starch granules. J Appl Glyco 54:31–36

Jane J, Chen JF (1992) Effects of amylose moleculr size and amylopectin branch chain length on paste properties of starch. Cereal Chem 69: 60–65

Jane J, Kasemsuwan T (1994) Anthology of starch granule morphology by scanning electron microscopy. Starch-Stärke 46:121–129

Jane J, Chen YY, Lee LF, McPherson AE, Wong KS, Radosavljevic M, Kasemsuwan T (1999) Effects of amylopectin branch chain length and amylose content on the gelatinization and pasting properties of starch. Cereal Chem 76:629–637

Jiranuntakul W, Puttanlek C, Rungsardthong V, Puncha-arnon S, Uttapap D (2011) Microstructural and physicochemical properties of heat-moisture treated waxy and normal starches. J Food Eng 104:246–258

Jiranuntakul W, Puttanlek C, Rungsardthong V, Puncha-arnon S, Uttapap D (2012) Amylopectin structure of heat-moisture treated starches. Starch-Stärke 64:470–480

Kang HJ, Hwang IK, Kim KS, Choi HC (2006) Comparison of the physicochemical properties and ultrastructure of japonica and indica rice grains. J Agric Food Chem 54:4833–4838

Ketthaisong D, Suriharn B, Tangwongchai R, Lertart K (2013) Changes in physicochemical properties of waxy corn starches at different stages of harvesting. Carbohydr Polym 98:241–248

Ketthaisong D, Suriharn B, Tangwongchai R, Lertart K (2014) Combining ability analysis in complete diallel cross of waxy corn (*Zea mays* var. *ceratina*) for starch pasting viscosity characteristics. Sci Hortic 175:229–235

Lertrat K, Thongnarin N (2008) Novel approach to eating quality improvement in local waxy corn: Improvement of sweet taste in local waxy corn variety with mixed kernels from super sweet corn. Acta Hortic 769:145–150

Li L, Blanco M, Jane J (2007) Physicochemical properties of endosperm and pericarp starches during maize development. Carbohydr Polym 67:630–639

Li W, Yan S, Yin Y, Li Y, Liang T, Gu F, Dai Z, Wang Z (2008) Comparison of starch granule size distribution between hard and soft wheat cultivars in eastern China. Agric Sci China 7:907–914

Mendez-Montealvoa G, Wanga Y, Campbell M (2011) Thermal and rheological properties of granular waxy maize mutant starches after β-amylase modification. Carbohydr Polym 83:1106–1111

Miao M, Zhang T, Mu W, Jiang B (2011) Structural characterizations of waxy maize starch residue following *in vitro* pancreatin and amyloglucosidase synergistic hydrolysis. Food Hydrocoll 25:214–220

Miles MJ, Morris VJ, Orford PD, Ring GS (1985) The roles of amylose and amylopectin in the gelation and retrogradation of starch. Carbohydr Res 135:271–281

Puncha-arnon S, Puttanlek C, Rungsardthong V, Pathipanawat W, Uttapap D (2007) Changes in physicochemical properties and

morphology of canna starches during rhizomal development. Carbohydr Polym 70:206–217

Rocha ST, Felizardo SG, Jane J, Franco CML (2012) Effect of annealing on the semicrystalline structure of normal and waxy corn starches. Food Hydrocoll 29:93–99

Sandhu SK, Singh N (2007) Some properties of corn starches II: physicochemical, gelatinization, retrogradation, pasting and gel textural properties. Food Chem 101:1499–1507

Sing KN, Ezekiel L, Guraya R, Sing H (2005) Microstructure, cooking and textural characteristics of potato (*Solanum tuberrosum* L.) tubers in relation to physicochemical and functional properties of their flours. J Sci Food Agric 85:1275–1284

Singh N, Singh J, Kaur L, Sodhi NS, Gill BS (2003) Morphological, thermal and rheological properties of starches from different botanical sources. Food Chem 81:219–231

Singh S, Singh N, Isono N, Noda T (2010) Relationship of granule size distribution and amylopectin structure with pasting, thermal, and retrogradation properties in wheat starch. J Agric Food Chem 58: 1180–1188

Takeda Y, Takeda C, Suzuki A, Hizukuri S (1989) Structure and properties of sago starches with low and high viscosities on amylograph. J Food Sci 54:177–182

Wang Y, Wang L (2003) Physicochemical properties of common and waxy corn starches oxidized by different levels of sodium hypochlorite. Carbohydr Polym 52:207–217

Xing Z, Lim S (2012) Pasting viscosity and *in vitro* digestibility of retrograded waxy and normal corn starch powders. Carbohydr Polym 87:235–239

Yoshida H, Nozaki K, Hanashiro I, Yagi F, Ito H, Honma M (2003) Structure and physicochemical properties of starches from kidney bean seeds at immature, premature and mature stages of development. Carbohydr Res 338:463–469

Euphytica (2015) 203:237–248
DOI 10.1007/s10681-014-1240-z

Genotypic variability in anthocyanins, total phenolics, and antioxidant activity among diverse waxy corn germplasm

Bhornchai Harakotr · Bhalang Suriharn · Marvin Paul Scott · Kamol Lertrat

Received: 9 January 2014 / Accepted: 18 August 2014 / Published online: 24 August 2014
© Springer Science+Business Media Dordrecht 2014

Abstract Identification of germplasm sources of waxy corn (*Zea mays* L. var. *ceratina*) with high variability for anthocyanins, phenolic compounds, and antioxidant activity is an important phase for waxy corn breeding for improvement of useful phytochemicals. The objectives of this study were to evaluate 49 genotypes of waxy corn for color parameters, monomeric anthocyanin content (MAC) and total phenolic content (TPC), and antioxidant activities. The experiment was conducted under field conditions in a randomized complete block design with three replications for two seasons in the rainy and the dry season 2010. Corn genotypes and seasons were significantly different ($P \leq 0.01$) for most traits under study except for TPC. Variations due to genotype were large for all characters, accounting for 74.43–95.70 % of total variations. The interactions between genotype and season were significant for all characters. Forty-nine corn genotypes were divided into four groups based on antioxidants and their activities. Significant and positive correlations were found among the anthocyanins, phenolics, and antioxidant activities, and correlation coefficients between anthocyanins with 2,2-diphenyl-1-picrylhydrazyl (DPPH) radical scavenging ability and Trolox equivalent antioxidant capacity (TEAC) assays were high (r = 0.94 and 0.88, respectively). All of the Hunterlab color parameters, including chroma and hue angle were highly correlated with anthocyanins, phenolics and their activities and therefore could be used as indirect selection criteria for improving levels of antioxidants and antioxidant activity in waxy corn.

Keywords Diversity · Crop breeding · Cluster analysis · Indirect selection · Phytochemicals · *Zea mays* L.

B. Harakotr · B. Suriharn · K. Lertrat (✉)
Department of Plant Science and Agricultural Resources, Faculty of Agriculture, Khon Kaen University, Khon Kaen 40002, Thailand
e-mail: kamol9@gmail.com

B. Harakotr · B. Suriharn · K. Lertrat
Plant Breeding Research Center for Sustainable Agriculture, Khon Kaen University, Khon Kaen 40002, Thailand

M. P. Scott
USDA-ARS Corn Insects and Crop Genetics Research Unit, Iowa State University, Ames, Iowa 50011, USA

Introduction

Consumption of fruits, vegetables, and un-polished grains is strongly associated with the reduced risk of developing chronic diseases such as cancer and cardiovascular disease (Isabelle et al. 2010; Liu 2004). Flavonols, flavonones, phenolic compounds, vitamins E and C, carotenoids, and anthocyanins in natural foods might confer these health protective benefits by alleviating oxidative stress such as

preventing free radicals proteins, DNA, and lipids (Duthie et al. 2000; Huang et al. 2005). Anthocyanins are among the most abundant polyphenols in many foods (de Pascual-Teresa and Sanchez-Ballesta 2008). They constitute the largest group of water-soluble pigments in the plant kingdom, being responsible for the vivid blue, purple, and red colors displayed by many flowers, fruits and leaves. These pigments are usually present in red fruits, vegetables, roots, legumes and cereals (Clifford 2000; He and Giusti 2010). Among cereals, corn not only has a sufficient amount of carotenoids, tocopherols, protein, oil, and starch but also has a comparable content of anthocyanin compared with other cereals such as colored rice and wheat (Abdel-Aal et al. 2006; Chander et al. 2008). Purple corn is a special type of corn that is rich in anthocyanin, and can be used as viable a source of antioxidants for functional foods (de Pascual-Teresa et al. 2002). This corn type gained popularity as a functional colorant and functional food ingredient because of its high antioxidant compounds (Montilla et al. 2011).

Waxy corn (*Zea mays* L. var. *ceratina*) is harvested at immature stage and consumed as fresh vegetable in many countries of Asia such as China, Korea, Thailand, Vietnam, Laos and Myanmar, and the demand for waxy corn is increasing (Hu and Xu 2011; Chung et al. 2010). Phytochemical compositions and concentrations vary significantly according to the kernel colors. Especially, waxy corn has various kernel colors, including white, yellow, red, purple, and black. Moreover, the pigmented corn contains anthocyanins, carotenoids, phenolic compounds, and antioxidant activity than non-pigmented corn (Lopez-Martinez et al. 2009; Montilla et al. 2011; Žilić et al. 2012). Pigments and other substances are genetically regulated and can be improved through selection and combined with high-yielding characters (Graham et al. 1999; Rodriguez et al. 2013). Therefore, the opportunity to develop waxy corn varieties with high phytochemicals is great.

Breeding corn may increase antioxidants intake with higher antioxidant properties. The success of breeding depends on identifying genetic variation for the traits, and knowledge of the impacts of environmental parameters on its expression (Conner et al. 2002; Dooner et al. 1991). However, studies on variation among genotypes and the effects of environments are scant. Substantial and significant variations in phytochemical content and antioxidant activity were observed between a set of corn genotypes and even among classes of colors, and the potential health benefits provided by corn depended firstly on corn genotypes (Kuhnen et al. 2011). Kernel color can be easily identified visually and, therefore, can be increased through phenotypic selection (Rodriguez et al. 2013; Shen et al. 2009). Although visual assessment is and an easy method, it lacks consistency due to human is poor in color memory and compromises genotype comparisons (Hasting et al. 2012; Hutchings 1999). The application of colorimetric systems, based on uniform color spaces (CIELUV and CIELAB) and non-uniform color spaces (CIE-XYZ), is of great value for the quantification and characterization of the color properties of diverse pigments and foods (Hernanz et al. 2008; Wrolstad et al. 2005; Yang et al. 2008). Thus, the objectives of this study were to assess variability for color parameters, monomeric anthocyanin content, total phenolic content, and antioxidant activities and to investigate the correlations between these traits and color parameters. The results of this study could provide corn breeders and eventually commercial corn grower with new opportunities to promote the production of corn with enhanced levels of the antioxidant compounds.

Materials and methods

Waxy corn germplasm and crop management

Forty-nine genotypes of waxy corn (Table 1) collected from China, England, Japan, Laos, Myanmar, South Korea, Taiwan, Thailand, USA, and Vietnam were evaluated in this study. The Vegetable Corn Improvement Project, Plant Breeding Research Center for Sustainable Agriculture, Khon Kaen University in Thailand collected these genotypes, which included commercial and landrace cultivars. The entries were assigned in a randomized complete block design with three replications for two seasons in the rainy season (June–August 2010) and the dry season (November 2010–January 2011) at the Research Farm, Khon Kaen University. The plot size was a single-row plot with 5 m long with spacing 0.8 m between row and 0.25 m between plants within rows. Soil preparation, planting and other agronomic practices were carried out uniformly according to the recommendations for

Table 1 Waxy corn genotypes, origin and pigmentation

Entry no.	Genotypes	Origin	Pigmentation
1	KKU-WX211001	Thailand	Light purple
2	KKU-WX211002	Thailand	Light purple
3	KKU-WX211003	Thailand	Light purple
4	KKU-WX211004	Thailand	Purple–yellow
5	KKU-WX212003	Laos	Light purple
6	KKU-WX212004	Laos	Light purple
7	KKU-WX212005	South Korea	Light purple
8	KKU-WX212006	China	Dark pink
9	KKU-WX212007	Laos	Purple–white
10	KKU-WX212008	South Korea	purple–white
11	KKU-WX221001	Thailand	Light purple
12	KKU-WX221058	Thailand	Yellow–white–purple
13	KKU-WX211022	Thailand	Yellow–purple
14	KKU-WX211024	Thailand	Light purple
15	KKU-WX212006	Japan	Dark pink
16	KKU-WX221059	Thailand	Light purple
17	KKU-WX221060	Thailand	Light purple
18	KK composite	Thailand	Yellow–purple–white
19	KKU-WX111031	Thailand	Purplish black
20	KKU-WX111033	Thailand	Purple–white–yellow
21	KKU-WX111034	Thailand	Purple–yellow
22	KKU-WX111035	Thailand	Purple–white
23	KKU-WX112091	Thailand	Light purple
24	KKU-WX112092	Thailand	Purple–white–yellow
25	KKU-WX112096	Thailand	Purple–white
26	KKU-WX112097	Thailand	Purple–white–yellow
27	KKU-WX112098	Thailand	Light purple
28	KKU-WX112099	Thailand	White–yellow–purple
29	KKU-WX121063	Laos	Purple–white–yellow
30	KKU-WX121065	Laos	Purple–white
31	KKU-WX121069	China	Light purple
32	KKU-WX112095	Thailand	Light purple
33	KKU-WX121068	Taiwan	Light purple
34	KKU-WX122026	Taiwan	Light purple
35	KKU-WX122027	Vietnam	White–pink
36	KKU-WX122028	Vietnam	Light purple
37	KKU-WX122031	China	Purple–white
38	KKU-WX122032	Myanmar	Light purple
39	KKU-WX122033	China	Light purple–white
40	KKU-WX122035	Thailand	Purplish black
41	KKU-WX122036	Thailand	Purplish black
42	Local Isan2	Thailand	Purple–white
43	Sweet violet	Thailand	Light purple–white
44	Japan stripe	Japan	Stripe red
45	Europe stripe	England	Stripe red

Table 1 continued

Entry no.	Genotypes	Origin	Pigmentation
46	Thai mountaineer	Thailand	Purple–white
47	KKU KNG	Thailand	Purplish black
48	White	Thailand	Creamy white
49	Yellow	Thailand	Creamy yellow

commercial production of corn. The populations were sib-pollinated with the plants in the same populations to avoid contamination of stray pollens. Five ears for each population were randomly harvested at physiological maturity (35 days after pollination; DAP) and oven-dried at 40 °C (moisture content $\leq$ 13 %). The kernels were manually separated from the cobs and then color values were measured prior to milling. The samples were milled into fine powder (CM190, Cemotec^{TM}), sieved through 60-mesh screen mesh, thoroughly mixed and stored at −20 °C until analysis. Maximum and minimum temperatures during the two seasons were record daily by a meteorological station near the experimental site.

Color measurements

Color attributes was measured by HunterLab miniscan XE PLUS colorimeter (Mod. PL50, Hunter Associates Laboratory Inc., VA, USA), and the colorimeter was calibrated prior to data collection with a HunterLab calibration standard white reflector plate. The color value was determined from random samples of 100 kernels from five corn ears of purple-colored genotypes which the terminal tip ends of 3 cm were discarded. The color was expressed in C* and h°. The chroma (C*) represents color intensity which is the distance of a color from the origin (a* + b* = 0) in a* and b* plane. Hue angle (h°) expresses in degree ranged from 0° to 360°, where 0° (red) locates on the +a axis and then rotates anticlockwise to 90° (yellow) for the +b* axis, 180° (green) for −a* and 270° (blue) for −b* (McGuire 1992).

Sample extraction

The anthocyanins in ground waxy corn kernels were extracted according to the method described by Rodriguez-Saona and Wrolstad (2001), Jing et al. (2007) with slight modifications. Approximately 2 g of each sample were added to a flask containing 25 mL of 70 % aqueous acetone acidified by the addition of HCl to 0.01 % and mixed well. The flasks were shaken on a platform shaker (LabScientific Inc., Livingston, NJ, USA) at 200 rpm and room temperature for 2 h. Each sample was filtered through Whatman # 1 filter paper under vacuum using a Büchner funnel, and the slurry was washed with 10 mL of acidified 70 % acetone. The filtrate was transferred to a separatory funnel, and 15 mL of chloroform were added. The mixture was gently mixed by turning the funnel upside down a few times. The samples were stored overnight at 4 °C or until a clear partition between the two phases was obtained. The solution was transferred to a centrifuge tube and centrifuged at 11,538 × g and 4 °C for 10 min. The upper aqueous layer containing the acetone/water mixture was collected, and the chloroform/acetone layer was carefully discarded. The residual acetone and chloroform were removed from the anthocyanin extract using a rotary evaporator at 40 °C under vacuum. The volume of the extracts was increased to 25 mL in a volumetric flask by the addition of 0.01 % HCl-acidified methanol.

Monomeric anthocyanin content (MAC)

The total monomeric anthocyanin content was measured using the pH differential method, as described by Giusti and Wrolstad (2001). A UV–vis spectrophotometer (GENESYS 10S, ThermoScientific, Waltham, MA, USA) was used to measure the absorbance at 510 and 700 nm. Anthocyanin levels were expressed as μg of cyanidin-3-glucoside equivalents per g of dry weight (μg CGE/g DW), using the reported molar extinction coefficient of 26,900 M^{-1} cm^{-1} and a molecular weight of 449.2 g/mol.

Total phenolic content (TPC)

The phenolic content was determined using the Folin-Ciocalteu (F–C) assay as described by Hu and Xu (2011). Briefly, the appropriate dilutions of the

extracts were oxidized with F–C reagent for 90 min, and the reaction was neutralized with sodium carbonate. The absorbance of the resulting blue color was measured at 765 nm, and the phenolic content was expressed as mg of gallic acid equivalents per g of dry weight (mg GAE/g DW).

Measurements of antioxidant activity

The activity for scavenging 2,2-diphenyl-1-picrylhydrazyl (DPPH) radical was assessed by measuring the bleaching of a black-colored methanol solution containing DPPH radicals, as described by Yao et al. (2010). Trolox was used as the reference compound. The results are expressed in μmol of Trolox equivalents per g of dry weight (μmol TE/g DW).

The Trolox equivalent antioxidant capacity (TEAC) assay, which measures the reduction of radical cations of ABTS by antioxidants, was conducted as described by Lopez-Martinez et al. (2009). Trolox was used as the reference compound. The results are expressed in μmol of Trolox equivalents per g of dry weight (μmol TE/g DW).

Statistical analysis

Analysis of variance was performed separately for each season, and error variances were tested for homogeneity (Gomez and Gomez 1984). Where error variances were homogeneous, the data of two seasons for monomeric anthocyanin, phenolic content, antioxidant activity and color parameter were combined. Duncan's multiple range test (DMRT) was used to compare mean difference between groups at 0.05 probability level. The Pearson correlation coefficients were calculated to determine the relationships among variables. Hierarchical agglomerative clustering was then performed for antioxidants and their activity, using the Ward criterion. All calculations were performed using JMP Pro software (version 10.0, SAS institute Inc., Chicago, IL, USA).

Results

Variations in color parameters, antioxidants and antioxidant activity

Differences in seasons were significant ($P \leq 0.01$) for chroma (C*), and hue angle (h°) (Table 2). However,

Table 2 Mean squares for color parameters, monomeric anthocyanin content, total phenolic content and antioxidant activity in kernels of 49 waxy corn genotypes evaluated in the rainy and dry seasons 2010

SOV	df	Color parameters		Antioxidants		Antioxidant capacity	
		Chroma (C*)	Hue angle (h°)	MAC	TPC	DPPH	TEAC
Season (S)	1	211.5* (3.64)[a]	6830.9** (9.71)	167,905** (1.05)	0.003NS (0)	150.3** (0.83)	5211.4** (1.33)
Genotype (G)	48	223.9** (88.67)	2276.2** (74.43)	314,420** (94.85)	13.9** (92.30)	360.8** (95.70)	7596.8** (93.62)
S × G	48	17.5** (6.94)	355.2** (11.62)	13,174** (3.97)	1.04** (6.90)	11.7** (3.11)	383.4** (4.73)
Error	192	0.5 (0.73)	30.5 (3.99)	105.0 (0.13)	0.03 (0.71)	0.3 (0.36)	6.2 (0.3)
C.V. (%)		4.25	5.29	4.41	7.25	5.28	6.58

SOV source of variance, *df* degree of freedom, *MAC* monomeric anthocyanin content, *TPC* total phenolic content, *DPPH* 2,2-diphenyl-1-picrylhydrazyl radical scavenging ability, *TEAC* Trolox equivalent antioxidant capacity, *NS* non-significant

*,** Significant at $P \leq 0.05$ and 0.01, respectively

[a] Number within the parentheses is percentage of sum squares to total sum of squares

Table 3 Means for colors, antioxidant content, and antioxidant activity in kernels of 49 waxy corn genotypes evaluated in the rainy and dry seasons 2010

Parameters	Seasons		Minimum	Maximum	Average
	Rainy	Dry			
Colors					
Chroma (C*)	15.07 ± 5.88	16.84 ± 6.76	2.9	29.4	15.95 ± 6.37
Hue angle (h°)	292.73 ± 21.67	314.03 ± 40.42	274.5	355.0	306.88 ± 22.18
Antioxidant content					
MAC (μg CGE/g DW)	225.23 ± 1.34	273.03 ± 1.35	2.5	1,063.0	249.13 ± 3.57
TPC (mg GAE/g DW)	6.74 ± 0.01	6.70 ± 0.01	4.3	11.8	6.73 ± 0.01
Antioxidant activity					
DPPH (μmol TE/g DW)	10.25 ± 0.02	11.68 ± 0.02	0.1	39.4	10.96 ± 0.02
TEAC (μmol TE/g DW)	34.62 ± 0.22	41.22 ± 0.22	0.1	184.6	37.91 ± 0.22

Data are expressed as the mean ± SD of triplicate samples

MAC monomeric anthocyanin content, *TPC* total phenolic content, *DPPH* 2,2-diphenyl-1-picrylhydrazyl radical scavenging ability, *TEAC* Trolox equivalent antioxidant capacity

variations in seasons had small contributions to total variations for these traits (3.64 and 9.71 %, respectively). The results indicated that the traits were consistent across seasons. Corn genotypes were significantly different for all traits, and there were large contributions of corn genotype to total variations for C* and h° (88.67 and 74.43 %, respectively). The interactions between genotype by season were significant ($P \leq 0.01$) for all traits. However, most interactions had small contributions (6.94 % for C* and 11.62 % for h°) to total variations for these traits. Although the differences between seasons were low for these parameters, the maximum and minimum values for these parameters were rather wide, ranging from 2.9 to 29.4 for C*, and 274.5° to 355.0° for h° (Table 3). The averaged means of two-season data were 15.95 and 306.88° for C* and h°, respectively.

Genotype was the most important source of variations in monomeric anthocyanin content (MAC), accounting for 94.85 % of total variation, whereas season accounted for only 1.05 % although the difference between seasons was significant (Table 2). Genotype by season interaction was significant ($P \leq 0.01$) and contributed to 3.97 % of total variation. The monomeric anthocyanin contents of corn grown in the rainy season and the dry season ranged from 2.5 to 1,063.0 μg CGE/g DW (Table 3). The averaged means of two-season data was 249.13 μg CGE/g DW. Genotype was still the main source of variation in total phenolic content (TPC), accounting for 92.3 % of total variation, whereas difference in seasons was not significant (Table 2). Genotype by season interaction was significant ($P \leq 0.01$) and contributed to 6.9 % of total variation. TPC values ranged from 4.3 to 11.8 mg GAE/g DW (Table 3). The averaged means of two-season data was 6.73 mg GAE/g DW.

Genotype contributed to the largest portions of total variations in 2,2-diphenyl-1-picrylhydrazyl (DPPH) radical scavenging ability (95.70 %) and Trolox equivalent antioxidant capacity (TEAC) (93.62 %), whereas season contributed to the smallest portions for DPPH (0.83 %) and TEAC (1.33 %) (Table 2). The differences among genotypes were significant ($P \leq 0.01$) for these traits, and the interactions between genotype and season were also significant ($P \leq 0.01$). However, the contributions of the interactions between genotype and season were small, accounting for only 3.11 % for DPPH and 4.73 % for TEAC. DPPH values ranging from 0.1 to 39.4 μM TE/g DW were observed among waxy corn genotypes, and the averaged means of two-season data was 10.96 μM TE/g DW (Table 3). Similarly, TEAC values ranging from 0.1 to 184.6 μM TE/g DW were found, and the averaged means of two-season data was 37.91 μM TE/g DW.

Cluster analysis

A dendrogram, which was constructed based on MAC, TPC, DPPH, and TEAC, could classify the corn

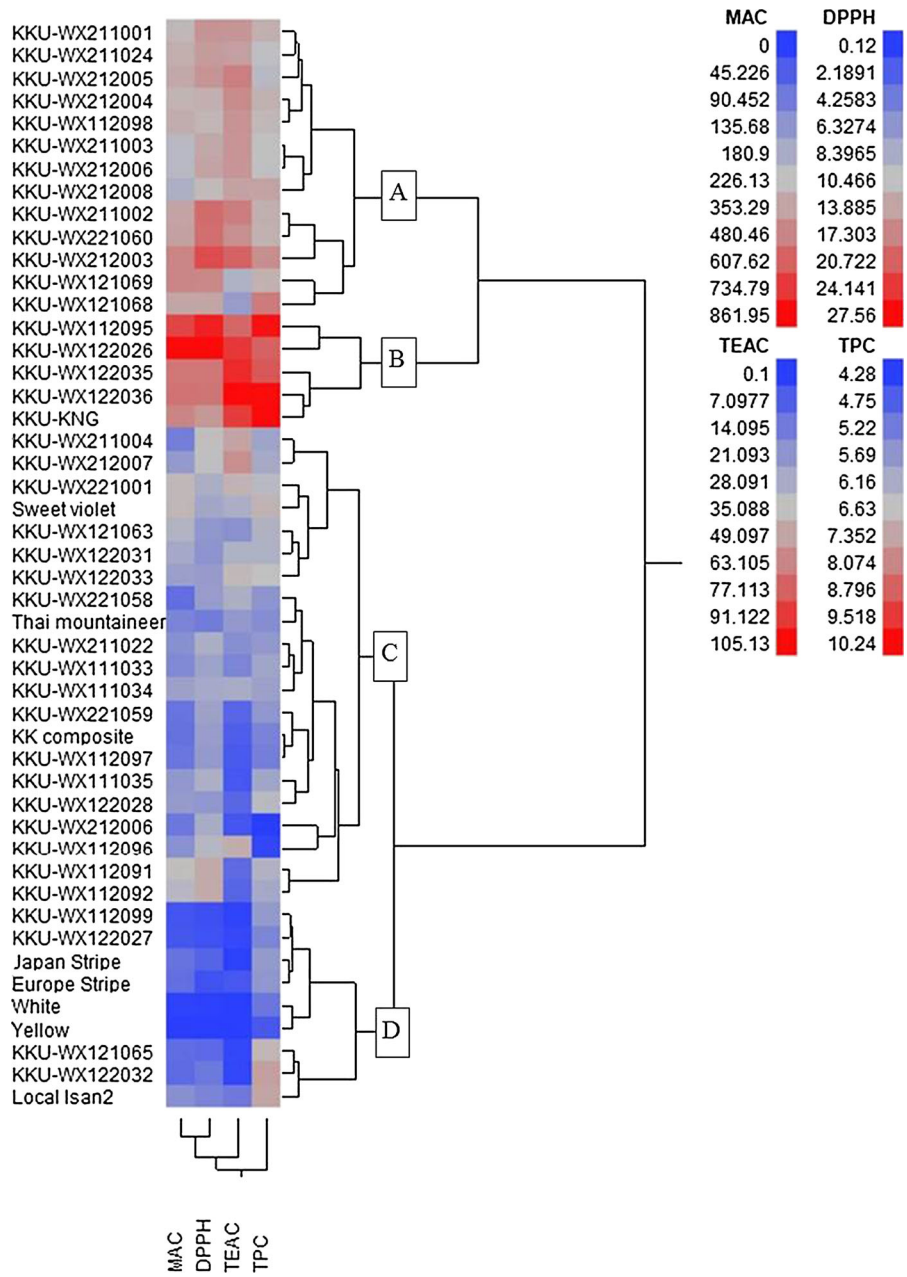


Fig. 1 Dendogram of genetic relationships among 48 waxy corn genotypes. Four main clusters (*A* to *D*) were formed. Two ways clustering method was Ward's cluster analysis based on antioxidants and antioxidant activities traits (scale: Distance scale) [a]

[a] Cluster together *columns* as well as *rows*; the *columns* must be measured on the same scale

genotypes into four distinct groups (Fig. 1). KKU-WX111031was considered as the out-group and it was not included in the dendrogram because it had the extremely high values of antioxidants and their activities. Therefore, forty-eight genotypes were included in the analysis.

There were 13 corn genotypes in group A consisting of KKU-WX211001, KKU-WX211024, KKU-WX211005, KKU-WX211004, KKU-WX112098, KKU-WX211003, KKU-WX212006, KKU-WX212008, KKU-WX211002, KKU-WX221060, KKU-WX212003, KKU-WX121069, and KKU-WX121068. Most corn genotypes this group had high values of MAC, TPC, DPPH, and TEAC except for KKU-WX121068, which showed the low value of TEAC.

Group B comprised 5 corn genotypes with the highest values of antioxidants and their activities (Table 4). This

Table 4 List of top high and low performing genotypes for monomeric anthocyanin content, total phenolic content and antioxidant activities in kernel of waxy corn genotypes averaged over two seasons

Genotypes/Groups	MAC	TPC	Antioxidant activities (μmol TE/g DW)	
	(μg CGE/g DW)	(mg GAE/g DW)	DPPH	TEAC
High group				
KKU-WX111031	1,063.0 ± 108.4a[a]	11.8 ± 0.4a	36.8 ± 2.8a	178.4 ± 8.1a
KKU-WX112095	699.3 ± 47.2c	10.1 ± 0.3b	26.1 ± 2.2c	78.0 ± 10.3f
KKU-WX122026	870.0 ± 59.4b	8.8 ± 0.3 cd	27.6 ± 1.5b	91.4 ± 8.3e
KKU-WX122035	544.9 ± 135.7f	9.0 ± 0.2c	19.0 ± 2.7f	95.8 ± 13.5d
KKU-WX122036	636.4 ± 202.7e	10.2 ± 0.8b	21.6 ± 4.4e	105.1 ± 15.9b
KKU KNG	664.9 ± 256.5d	10.2 ± 0.3b	21.4 ± 5.5e	99.1 ± 20.5c
Low group				
KKU-WX112099	29.6 ± 5.1ć	5.8 ± 0.6o-t	1.4 ± 0.4é	1.2 ± 0.5w
KKU-WX122027	35.9 ± 15.2b́ć	5.4 ± 0.6stu	1.4 ± 0.5é	7.1 ± 6.2stu
Japan stripe	75.1 ± 7.8zá	5.8 ± 0.6o-t	2.6 ± 0.4x	0.6 ± 0.6w
Euro stripe	74.8 ± 27.7zá	5.7 ± 0.6q-t	1.4 ± 0.5y	2.5 ± 1.6vw
KKU-WX121065	70.6 ± 14.6á	7.0 ± 0.7g-l	3.0 ± 1.0ć	1.5 ± 0.8w
KKU-WX122032	70.5 ± 20.8á	7.5 ± 1.5fg	3.7 ± 0.6b́	1.2 ± 0.8w
Local Isan	126.4 ± 12.9uv	7.4 ± 0.1fgh	4.8 ± 1.2zá	14.1 ± 4.8r
White	2.5 ± 1.2d́	5.2 ± 0.9uv	0.3 ± 0.2f́	0.5 ± 0.3w
Yellow	ND	4.7 ± 1.1vw	0.1 ± 0.1f́	0.1 ± 0.5w

Data are expressed as the mean ± SD of six determinations

MAC monomeric anthocyanin content, *TPC* total phenolic content, *DPPH* 2,2-diphenyl-1-picrylhydrazyl radical scavenging ability, *TEAC* Trolox equivalent antioxidant capacity, *ND* not detected

[a] Means in the same columns with different letters are significant ($P \leq 0.05$) determined by DMRT

group consisted of KKU-WX112095, KKU-WX122026, KKU-WX122035, KKU-WX122036, and KKU KNG. Most genotypes were collected in Thailand except for KKU-WX122026 from Taiwan.

Group C was the largest group consisting of KKU-WX211004, KKU-WX212007, KKU-WX221001, Sweet violet, KKU-WX121063, KKU-WX122031, KKU-WX122033, KKU-WX221058, Thai mountaineer, KKU-211022, KKU-WX111033, KKU-WX111034, KKU-WX221059, KK composite, KKU-112097, KKU-111035, KKU-WX122028, KKU-WX212006, KKU-WX122096, KKU-WX122091, and KKU-WX122092. This group showed medium values of antioxidants and antioxidant activities. However, the genotypes KKU-WX211004 and KKU-WX212007 showed high TEAC values, and KKU-WX122091 and KKU-WX122092 demonstrated high DPPH values.

Group D comprised 9 corn genotypes including KKU-WX122099, KKU-WX122027, Japan stripe,

Table 5 Pearson correlation coefficients between color parameters, monomeric anthocyanin content, total phenolic content, and antioxidant activities of purple colored waxy corn genotypes

	Color parameters		MAC	TPC	DPPH
	C*	h°			
C*					
h°	0.76**				
MAC	0.68**	0.84**			
TPC	0.75**	0.80**	0.84**		
DPPH	0.57**	0.77**	0.94**	0.78**	
TEAC	0.60**	0.78**	0.88**	0.79**	0.89**

Values are from six determinations

*C** chroma, *h°* hue angle, *MAC* monomeric anthocyanin content, *TPC* total phenolic content, *DPPH* 2,2-diphenyl-1-picrylhydrazyl radical scavenging ability, *TEAC* Trolox equivalent antioxidant capacity

** The correlation is significant at $P \leq 0.01$

Euro stripe, KKU-WX121065, KKU-WX122032, Local Isan, White, and Yellow (Table 4). This group had the lowest values of antioxidants except for KKU-WX122032 and Local Isan, which showed high TPC.

Relationship among monomeric anthocyanin, phenolic content, antioxidant activity, and color traits

The chromatic parameter (C*) was significantly correlated with hue angle (h°) (0.76; $P \leq 0.01$) (Table 5). C* was positively correlated with monomeric anthocyanin content (MAC), total phenolic content (TPC), 2,2-diphenyl-1-picrylhydrazyl (DPPH) radical scavenging ability and Trolox equivalent antioxidant capacity (TEAC), and the correlation coefficients ranged from 0.57 to 0.75; $P \leq 0.01$. Similarly, color parameter h° was also significantly correlated with antioxidants and their properties, and the correlation coefficients ranged from 0.77 to 0.84; $P \leq 0.01$. The correlation coefficients among MAC, TPC, DPPH and TEAC were positive and significant, ranging from 0.78 to 0.94; $P \leq 0.01$.

Discussion

Variations in color parameters, antioxidants and antioxidant activity

Phytochemicals in food are beneficial to health due to their high antioxidant properties, which is related to prevention of cardiovascular disease, diabetes or obesity and mutagenesis or cancer (He and Giusti 2010; Tsuda et al. 2003). In corn, colored corn has different pigments and other compounds with antioxidant activity that can be highly beneficial for human health (Rodriguez et al. 2013). The hypothesis underlying this investigation is that color parameters are related to antioxidant compounds and their activity, and, therefore, color parameters, monomeric anthocyanin content (MAC), total phenolic content (TPC), 2,2-diphenyl-1-picrylhydrazyl (DPPH) radical scavenging ability and Trolox equivalent antioxidant capacity (TEAC) were investigated in 49 corn genotypes with different levels of colors from white to purplish black. This investigation also explored the possibility to use color parameters as an alternative tool to select corn genotypes with high antioxidant activity.

In this study, corn genotypes were significantly different for color traits, MAC, TPC, DPPH, and TEAC, and the contributions of genotype to total variations in these characters were highest, ranging from 74.43 to 95.70 %. Direct comparison of studies in waxy corn is not available. However, genotype was more important source of variations in anthocyanin and other phytochemicals in corn (Chander et al. 2008; Mahan et al. 2013) than environment and genotype by environment interaction. The results indicated that selection for individual characters would be possible as sample variations are available for these characters.

Season had very small effects on total variations in color parameters, MAC, TPC, DPPH, and TEAC accounting for 0 % for TPC to 9.71 % for hue angle. The results indicated that these characters were rather stable. In previous investigation in cereals, environmental factor had small effects on antioxidant characters and this should allow for easy selection (Santra et al. 2005). Therefore, in corn breeding programs, selection of corn genotypes with high antioxidant activity in a few seasons should result in improved anthocyanin concentration combined with other desirable antioxidant compounds. However, environmental factors such as UV radiation, cold temperature, drought and water stress could induce high accumulation of anthocyanin in corn (Jing et al. 2007) and other plants (Chalker-Scott 1999; Liang et al. 2009). The contrasting results among different studies would be possible due to the differences in materials used and experimental conditions.

The interaction effects were generally small compared to main effects except for TPC (6.9 %), color parameter C* (6.94 %) and h° (11.62 %). When low interaction effects were considered, MAC, DPPH, and TEAC were rather stable and might be useful as selection criteria for improvement of corn genotypes with high antioxidant capacity. The low interactions of genotype × environment are preferable, indicating that the relative performance in one season is reliable in predicting relative performance in another season (Knievel et al. 2009; Hasting et al. 2012; Mahan et al. 2013). With low G × E interaction and little error variance, the relative performance across seasons or environment should be similar.

Relationships among color parameters, antioxidants and antioxidant activity

Pearson correlations coefficients among Hunterlab color parameters, chroma (saturation or vividness of color) and hue angle (tint of color, an angular measure) with anthocyanins, phenolic content, and antioxidant activity were explored in this study. The color parameters C* and h° correlated strongly with the levels of anthocyanins, phenolic and their activities ($r = 0.60–0.84$), except correlation between C* and DPPH ($r = 0.57$). A positive correlation between antioxidants and antioxidant activity would be expected because any increase in antioxidants would increase color intensity and hue angle. These results were in agreement with those reported by Yang et al. (2008) who evaluated the correlations among the yield of anthocyanins with C* and h° in extractible anthocyanin of purple corncob. Interestingly, the colored waxy corn genotypes (high C* and h° values) may better develop in phytochemicals and/or antioxidant activity. C* and h° may be a suitable for use as indirect selection criteria in screening of corn genotypes with high antioxidants.

In this study, the relationships among monomeric anthocyanin content (MAC), total phenolic content (TPC) and antioxidant activity (2,2-diphenyl-1-picrylhydrazyl radical scavenging ability and Trolox equivalent antioxidant capacity) were strong and positive. In previous study, MAC was significantly positive correlated with TPC because anthocyanin is the phenolic subgroup with same biosynthetic pathway and localization (pericarp and/or aleurone layer of kernel) (Hu and Xu 2011; Žilić et al. 2012). As anthocyanin is related to antioxidant in colored corn, breeding for high anthocyanin would result in high antioxidant.

Although MAC and TPC had significant positive correlation with both DPPH and TEAC, antioxidant activities were more closely correlated with anthocyanin than with phenolic compounds. The results suggested that anthocyanins had higher contribution to antioxidant properties than did phenolic compounds due to relatively high concentrations of anthocyanins compared with the overall phenolic compounds. In contrast to this study, phenolic components had higher contribution to antioxidant activity than did anthocyanin pigments (Pitija et al. 2013). The contrasting results of different studies would be possibly due to materials used, evaluation methods for antioxidation, and complicated extracts containing two or more antioxidants (del Pozo-Insfran et al. 2006). A better understanding on the relationship among phytochemicals and antioxidant activities in corn is important for improvement of corn varieties with high nutritional value.

Cluster analysis

Dendrogram could classified corn genotypes into four distinct clusters and one genotype (KKU-WX111031) was an out-group because of its high values of TAC, TPC, DPPH, and TEAC. Cluster B had the highest values of antioxidants and their activity. The differences between high group (group B) and low group (group D) were significant for TAC, TPC, DPPH, and TEAC, and the genotype with low and high antioxidants and antioxidant activity were readily identified (Table 4). The use of phytochemicals and antioxidant activity in clustering corn genotypes was successful in this study. The use of phytochemicals and antioxidant activity for germplasm in identifying superior genotypes with high antioxidant activity is useful. The corn genotypes in cluster B (KKU-WX112095, KKU-WX122026, KKU-WX122035, KKU-WX122036, and KKU KNG) and the out-group (KKU-WX111031) can be used as parents for improvement of nutraceutical properties in corn.

Implications for waxy corn breeding

The prime goal of corn breeders is always yield enhancement, but views of improving the livings through increased levels of antioxidants and their activity in grains is highly warranted. Thus, high anthocyanins, phenolic compounds and antioxidant activity as percent mean along with wide variation estimates observed for these important traits indicated the considerable scope for improving the phytochemical status of corn. A few breeders have studied the prospects for development of corn hybrids with high functional and antioxidant materials. As a primary step to achieve this goal, it is necessary to investigate the genotypic diversity in the phytochemicals among diverse corn germplasm, to find a way to enrich these compositions by breeding.

In this study, contributions of genotype to total variations in these traits were highest. Elite genotypes were identified as a genetic stock for enhanced levels of antioxidants and their capacity. The pigment was

found in the aleurone layer and pericarp of the kernel. Although the naked-eye color of the kernel and location of the pigment in corn genotypes were the same, the content of antioxidants varied (Moreno et al. 2005). Modern color instrumentation has made a measurement of chroma and hue angle indices and easy (Wrolstad et al. 2005). It is interesting to note here that strong correlations between color parameters C* and h° with antioxidants and antioxidant activity, suggests that color traits could be used as indirect indexes to select corn breeding germplasm with high antioxidant components. Moreover, pre-screening using a colorimeter could significantly reduce the number of samples, expensive extraction and long time for analysis.

Conclusion

The wide range of antioxidants and their activity levels found in this study indicates that adequate genetic variability is present potentially to develop corn varieties with enhanced health benefits. Large contributions of genotypes and low interactions between genotype and environment to total variations in these characters indicated that evaluation for these traits could be carried out in few locations or seasons in order to identify superior genotypes. The relationships of these traits with kernel color traits, including of chroma (C*) and hue angle (h°) could serve as indexes to indirectly select waxy corn genotypes with high anthocyanin, phenolics, and their activities. KKU-WX111031, KKU-WX112095, KKU-WX122026, KKU-WX122035, KKU-WX122036, and KKU-KNG were identified as genotypes with high anthocyanin, high phenolic content and high antioxidant activities. The information is useful for corn breeders to develop superior lines and hybrids with high level of antioxidant compounds.

Acknowledgments The authors would like to thank for financial support from: the Royal Golden Jubilee Ph.D. Program (RGJ); National Science and Technology Development Agency, Thailand; the Plant Breeding Research Center for Sustainable Agriculture, Faculty of Agriculture, Khon Kaen University, Thailand. We also wish to thanks Assist. Prof. Dr. Sakunkan Simla (Faculty of Technology, Mahasarakham University, Thailand) for collecting data regarding kernel color parameters. Mr. Thawan Kesmala is acknowledged for his generosity in providing constructive comments.

References

Abdel-Aal ES, Young M, Rabalski JC (2006) Anthocyanin composition in black, blue, pink, purple, and red cereal grains. J Agric Food Chem 54:4696–4704

Chalker-Scott L (1999) Environmental significance of anthocyanins in plant stress responses. Photochem Photobiol 70:1–9

Chander S, Meng Y, Zhang Y, Yan J, Li J (2008) Comparison of nutritional traits variability in selected eighty-seven inbreds from Chinese maize (*Zea mays* L.) germplasm. J Agric Food Chem 56:6506–6511

Chung H, Lee HB, Yamakawa T (2010) Major agricultural characteristics and antioxidants analysis of the new developed colored waxy corn hybrids. J Fac Agr Kyushu Uni 55:55–59

Clifford MN (2000) Anthocyanin-nature, occurrence and dietary burden. J Sci Food Agr 80:1063–1072

Conner AM, Luby JJ, Tong CBS, Finn CE, Hancock JF (2002) Genotypic and environmental variation in antioxidant activity, total phenolic content, and anthocyanin content among blueberry cultivars. J Amer Soc Sci 127:89–97

de Pascual-Teresa S, Sanchez-Ballesta MT (2008) Anthocyanins: from plant to health. Phytochem Rev 7:281–299

de Pascual-Teresa S, Santos-Buelga C, Rivas-Gonzalo JC (2002) LC–MS analysis of anthocyanins from purple corn cob. J Sci Food Agric 82:1003–1006

del Pozo-Insfran D, Brenes CH, Serna S, Talcott ST (2006) Polyphenolic and antioxidant content of white and blue corn (*Zea mays* L.) products. Food Res Int 36:696–703

Dooner HK, Robbins TP, Jorgensen RA (1991) Genetic and developmental control of anthocyanin biosynthesis. Annu Rev Genet 25:173–199

Duthie GG, Duthie SJ, Kyle JA (2000) Plant polyphenols in cancer and heart disease: implications as nutritional antioxidants. Nutr Res Rev 13:79–106

Giusti MM, Wrolstad RE (2001) Characterization and measurement of anthocyanins by UV-visible spectroscopy. In: Wrolstad RE, Acree TE, Decker EA, Penner MA, Reid DS, Schwartz SJ, Shoemaker CF, Sporns P (eds) Current Protocols in Food Analytical Chemistry. John Wiley and Sons, New York, pp F1.2.1–F1.2.13

Gomez KA, Gomez AA (1984) Statistical procedure for agricultural research. John Wiley and Sons, New York

Graham R, Senadhira D, Beebe S, Iglesis C, Monasterio I (1999) Breeding for micronutrient density in edible portions of staple food crops: conventional approaches. Field Crop Res 60:57–80

Hasting T, Osorio LF, Whitaker VM (2012) Estimation of genetic parameters and gains for color traits of strawberry. Euphytica 186:303–311

He J, Giusti MM (2010) Anthocyanins: natural colorants with health-promoting properties. Annu Rev Food Sci Technol 1:63–187

Hernanz D, Recamales AF, Melendez-Martinez AJ, Gonzalez-Miret ML, Heredia F (2008) Multivariate statistical analysis of the color-anthocyanin relationships in different soilless-grown strawberry genotypes. J Agric Food Chem 56:2735–2741

Hu QP, Xu JG (2011) Profiles of carotenoids, anthocyanins, phenolics, and antioxidant activity of selected color waxy corn grains during maturation. J Agric Food Chem 59:2026–2033

Huang D, Ou B, Prioir RL (2005) The chemistry behind antioxidant capacity assays. J Agric Food Chem 53:1841–1856

Hutchings JB (1999) Food color and appearance. Aspen Publishers, Gaithersburg

Isabelle M, Lee BL, Lim MT, Koh WP, Huang D, Ong CN (2010) Antioxidant activity and profiles of common fruits in Singapore. Food Chem 123:77–84

Jing P, Noriega V, Schwartz SV, Giusti MM (2007) Effects of growing conditions on purple corncob (*Zea mays* L.) anthocyanins. J Agric Food Chem 55:8625–8629

Knievel DC, Abdel-Aal ESM, Rabalski I, Nakamura T, Hucl T (2009) Grain color development and the inheritance of high anthocyanin blue aleurone and purple pericarp in spring wheat (*Triticum aestivum* L.). J Cereal Sci 50:113–120

Kuhnen S, Lemos PMM, Campestrini LH, Ogliari JB, Dias PF, Maraschin M (2011) Carotenoid and anthocyanin contents of grains of Brazilian maize landraces. J Sci Food Agric 9:1548–1553

Liang Z, Yang C, Yang J, Wu B, Wang L, Cheng LiS (2009) Inheritance of anthocyanins in berries of *Vitis vinifera* grapes. Euphytica 167:113–125

Liu RH (2004) Potential synergy of phytochemicals in cancer prevention: mechanism of action. J Nutr 134:3479S–3485S

Lopez-Martinez LX, Oliart-Ros RM, Valerio-Alfaro G, Lee CH, Parkin KL, Garcia HS (2009) Antioxidant activity, phenolic compounds and anthocyanins content of eighteen strains of Mexican maize. LWT - Food Sci Technol 42:1187–1192

Mahan AL, Murray SC, Rooney LW, Crosby KM (2013) Combining ability for total phenols and secondary traits in a diverse set of colored (red, blue, and purple) maize. Crop Sci 53:1–8

McGuire RG (1992) Reporting of objective color measurements. HortScience 27:1254–1255

Montilla EC, Hillebrand S, Antezana A, Winterhalter P (2011) Soluble and bound phenolic compounds in different Bolivian purple corn (*Zea mays* L.) cultivars. J Agric Food Chem 59:7068–7074

Moreno YS, Sanchez GS, Hernandez DR, Lobato NR (2005) Characterization of anthocyanins extracts from maize kernels. J Chromatogr Sci 43:483–487

Pitija K, Nakornriab M, Sriseadka T, Vanavichit A, Wongpornchai S (2013) Anthocyanin content and antioxidant capacity in bran extracts of some Thai black rice varieties. Int J Food Sci Technol 48:300–308

Rodriguez VM, Soengas P, Landa A, Ordas A, Revilla P (2013) Effects of selection for color intensity on antioxidant capacity in maize (*Zea mays* L.). Euphytica 193:339–345

Rodriguez-Saona LE, Wrolstad RE (2001) Extraction, isolation, and purification of anthocyanins. In: Wrolstad RE, Acree TE, Decker EA, Penner MA, Reid DS, Schwartz SJ, Shoemaker CF, Sporns P (eds) Current protocols in food analytical chemistry. John Wiley and Sons, New York, pp F1.2.1–F1.2.13

Santra M, Santra DK, Rao VS, Taware SP, Tamhankar SA (2005) Inheritance of β-carotene in durum wheat (*Triticum turgidum* L. ssp. durum). Euphytica 144:215–221

Shen Y, Jin L, Xiao P, Lu Y, Bao J (2009) Total phenolics, flavonoids, antioxidant capacity in rice grain and their relations to grain color, size and weight. J Cereal Sci 49:106–111

Tsuda T, Horio F, Uchida K, Aoki H, Osawa T (2003) Dietary cyanidin 3-0-β-D glucoside-rich purple corn color prevents obesity and ameliorates hyperglycemia in mice. J Nutr 133:2125–2130

Wrolstad RE, Durst RW, Lee J (2005) Tracking color and pigment changes in anthocyanin products. Trend Food Sci Tech 16:423–428

Yang Z, Fan G, Gu Z, Han Y, Chen Z (2008) Optimization extraction of anthocyanins from purple corn (*Zea mays* L.) cob using tristimulus colorimetry. Eur Food Res Technol 227:409–415

Yao Y, Sang W, Zhou M, Ren G (2010) Antioxidant and α-glucosidase inhibitory activity of colored grains in China. J Agric Food Chem 58:770–774

Žilić S, Serpen A, Akıllıoğlu G, Gökmen V, Vančetović J (2012) Phenolic compounds, carotenoids, anthocyanins and antioxidant capacity of colored maize (*Zea mays* L.) kernels. J Agric Food Chem 5:1224–1231

ResearchGate

See discussions, stats, and author profiles for this publication at: https://www.researchgate.net/publication/266027625

Influence of variety and harvest maturity on phytochemical content in corn silk

Article *in* Food Chemistry · February 2015

DOI: 10.1016/j.foodchem.2014.07.136 · Source: PubMed

CITATIONS
8

READS
415

4 authors, including:



Eakrin Sarepoua
Khon Kaen University
1 PUBLICATION **8** CITATIONS
SEE PROFILE



Ratchada Tangwongchai
Khon Kaen University
17 PUBLICATIONS **185** CITATIONS
SEE PROFILE



Bhalang Suriharn
Khon Kaen University
45 PUBLICATIONS **269** CITATIONS
SEE PROFILE

Some of the authors of this publication are also working on these related projects:



Effect of Development Stage on Phytochemical Content of Leaf and Fruit in Carissa carandas View project

All content following this page was uploaded by Ratchada Tangwongchai on 30 September 2014.

The user has requested enhancement of the downloaded file.

Food Chemistry 169 (2015) 424–429

Contents lists available at ScienceDirect

Food Chemistry

journal homepage: www.elsevier.com/locate/foodchem

Influence of variety and harvest maturity on phytochemical content in corn silk

Eakrin Sarepoua [a], Ratchada Tangwongchai [b], Bhalang Suriharn [a,c], Kamol Lertrat [a,c,*]

[a] Department of Plant Science and Agricultural Resources, Faculty of Agriculture, Khon Kaen University, Khon Kaen 40002, Thailand
[b] Department of Food Technology, Faculty of Technology, Khon Kaen University, Khon Kaen 40002, Thailand
[c] Plant Breeding Research Center for Sustainable Agriculture, Faculty of Agriculture, KhonKaen University, Khon Kaen 40002, Thailand

ARTICLE INFO

Article history:
Received 9 April 2014
Received in revised form 7 July 2014
Accepted 30 July 2014
Available online 17 August 2014

Keywords:
Phenolic compounds
Flavonoid
Anthocyanin
Vegetable corn
Functional food

ABSTRACT

Corn silk has been used as a traditional herb in Asia. The objective of this study was to evaluate variability in phytochemicals in corn varieties at three maturity stages of corn silk. Ten vegetable corn varieties were evaluated in a completely randomized design with three replications. Data were recorded for total phenolic (TPC), total flavonoids (TFC), total anthocyanin (TAC) and antioxidant activity (AA) by DPPH free-radical-scavenging assays. Differences among corn varieties were observed for all parameters at all maturity stages, and the interactions between maturity stage and corn variety were significant. TPC and TAC were highest at the milky stage, whereas TFC and AA were highest at the silking stage. TPC, TFC and AA were highest in super sweet corn and white corn at the silking stage. PWC5 variety of purple waxy corn at the milky stage had the highest values for all parameters, and it is useful for further development of functional food products.

© 2014 Elsevier Ltd. All rights reserved.

1. Introduction

Silk of corn (*Zea mays* L.) has been used as a herb for traditional medicine by native Americans, Chinese and people in many parts of the world. Phytochemicals in corn silk have antioxidant properties and are beneficial for health. Therefore, it can be used as dietary fibre and as a food additive for the prevention of several diseases (Hasanudin, Hashim, & Mustafa, 2012). Corn silk is rich in polyphenol compounds with strong free radical scavenging activity, and it is a good source of natural antioxidants (Nurhanan, Rosli, & Mohsin, 2012). Corn silk contains many bioactive compounds such as proteins, vitamins, carbohydrates, calcium, potassium, magnesium and sodium salts, volatile oils and steroids, alkaloids, flavonoids and other phenolic compounds with beneficial effects on human health (Ebrahimzadeh, Pourmorad, & Hafezi, 2008). Its potential antioxidant and healthcare applications as a diuretic agent, in hyperglycemia reduction, as an antidepressant and for anti-fatigue use have been claimed in several reports. Other uses of corn silk include teas and supplements to treat urinary related problems. The potential use is very much related to its properties and mechanism of action of its plant's bioactive constituents such as flavonoids and terpenoids (Hasanudin et al., 2012).

Corn silk is usually considered as waste and discarded during processing of baby corn and super sweet corn products. Corn silk provides natural colour and can be used as a food additive and flavouring (Maksimovic, Malencic, & Kovacevic, 2005). For example, corn silk powder is used as a food additive to improve the nutrient content and physical characteristics of beef patties (Rosli, Nurhanan, Solihah, & Mohsin, 2011). Corn silk can be utilised commercially as an ingredient to produce a wide variety of value-added products such corn silk tea, snacks, cosmetics and medicines.

Corn is consumed at different maturity stages. It can be used as baby corn as a vegetable, immature corn, mature corn, and corn silk. At these different maturity stages there may be a difference in phytochemicals and antioxidant activity (Žnidarčič, 2012). A recent study showed that the total flavonoid content of the butanol fraction of corn silk extract is in good correlation with the total phenolic content (Liu et al., 2011), and corn silk from upper parts of ears (dark brown) had higher amounts of total phenolics, total anthraquinones and total flavonoids than the lower parts of ears (Alam, 2011). Corn silk from baby corn had the highest yield and corn silk from purple waxy corn had the highest content of total phenolic, total flavonoid and total anthocyanin (Sarepoua, Tangwongchai, Suriharn, & Lertrat, 2013).

* Corresponding author at: Department of Plant Science and Agricultural Resources, Faculty of Agriculture, Khon Kaen University, Khon Kaen 40002, Thailand. Tel.: +66 43202696.
E-mail addresses: i.eak_@hotmail.com (E. Sarepoua), ratchada@kku.ac.th (R. Tangwongchai), sphala@kku.ac.th (B. Suriharn), kamol9@gmail.com (K. Lertrat).

http://dx.doi.org/10.1016/j.foodchem.2014.07.136
0308-8146/© 2014 Elsevier Ltd. All rights reserved.

The information on phytochemicals and antioxidant activity of corn silk at different maturity stages is still lacking. The objectives of this study were to evaluate the effects of maturity on total phenolic compounds, flavonoid and anthocyanin contents of corn and to identify corn varieties with high phytochemicals. This information will be useful in the commercial production of functional foods using corn silk and exploitation of agricultural waste to produce value-added products.

2. Materials and methods

2.1. Plant materials and sample preparations

Ten corn hybrids including five purple waxy corns, three white waxy corns and two super sweet corns were selected because of the differences in silk colours (Table 1). Silk colours and kernel colours were similar and varied from yellow-green, yellow-brown and purple. Three types of corn were classified based on harvest times at different maturity stages. Group 1 is baby corn which was harvested at the silking stage (7–10 days after anthesis) or R1. Group 2 is vegetable corn which was harvested at immature stages (18 days after anthesis) or R4, and group 3, the corn for seed production, was harvested at the physiological maturity stage (30 days after anthesis) or R6. The corn varieties were grown in a Completely Randomized Design (CRD) with three replications at the Vegetable Farm, Khon Kaen University, Khon Kaen, Thailand (18° 51′ N, 98° 45′ E, 200 masl) in the rainy season during May to July 2012.

At anthesis, the ears were sib-pollinated to ensure good pollination of the ears, the ears were harvested at three maturity stages as described above. The samples of corn silk were washed with distilled water and oven-dried at 60 °C for 24 h until the samples reached a final moisture content of 10% (Hu, Zhang, Li, Ding, & Li, 2010). Dry samples were ground into powder using a grinder, sealed in vacuum plastic bags and stored at below −20 °C until analysis. The ground samples were analysed for bioactives and antioxidant activity in triplicates.

2.2. Extraction of phytochemicals from corn silk

Corn silk samples were extracted using a modified method (Nurhanan et al., 2012). Briefly, 3 g of corn silk powder was mixed with 30 ml of 80% methanol in a flask and extracted at 70 °C in a water bath shaker (WB14/SV1422, GmbH Co. KG Memmert, Shanghai, China). After 1.5 h, the extract was filtrated through filter paper Whatman No. 1 to remove the debris. The filtrate was evaporated using a rotary flash evaporator (Eyela SB-651, Kokusan Enshinki Co., Tokyo, Japan) to remove the solvent. The residue was reconstituted with 5 ml methanol and stored at 0–4 °C until analysis.

The extract was analysed on a UV–Vis spectrophotometer (10S, Thermo Scientific Genesys, Australia) to determine total phenolic content (TPC), total flavonoid content (TFC), total anthocyanin content (TAC), and antioxidant activity was analysed by DPPH free-radical-scavenging activity assay.

2.3. Determination of total phenolic content

Total phenolic content was determined using the Folin–Ciocalteu colorimetric method and gallic acid was used as a standard (Liu & Yao, 2007). Folin–Ciocalteu reagent was diluted with distilled water at a ratio of 1:10. 0.5 ml of corn silk extract was mixed with 3 ml of the diluted Folin–Ciocalteu reagent and 2.5 ml of 0.2% (w/v) Na_2CO_3 solution. The mixture was allowed to stand for 30 min at room temperature (ca. 25 °C) and the absorbance of the resulting solution was read at 750 nm using a spectrophotometer. The blank consisted of all regents and solvents except for the sample. The total phenolic content was determined using a standard calibration curve and expressed as gallic acid equivalents per dry mass of corn silk sample (μg GAE/g dried sample).

Table 1
List of 10 varieties of Thai corn used in this study.

Entry No.	Varieties	Types of corn[a]	Silk colour[b]	Kernel colour[c]	Origin
1	PWC1	Purple waxy corn	Purple	Purple	Khon Kaen University
2	PWC2		Purple	Purple	Khon Kaen University
3	PWC3		Purple	Purple	Khon Kaen University
4	PWC4		Purple	Purple	Khon Kaen University
5	PWC5		Purple	Purple	Pacific Seeds (Thai) Ltd.
6	WWC1	White waxy corn	Green	White	Khon Kaen University
7	WWC2		Green	White	Khon Kaen University
8	WWC3		Green	White	Khon Kaen University
9	SSC1	Super sweet corn	Green	Yellow	Pacific Seeds (Thai) Ltd.
10	SSC2		Green	Yellow	Syngenta Seeds Ltd.

[a] Vegetable corn.
[b] Colour of silk at milky stage.
[c] Colour of kernel at milky stage.

2.4. Determination of total flavonoid contents

Total flavonoid content was determined using a modified colorimetric aluminium chloride method and rutin hydrate was used as a standard (Liu et al., 2011). Briefly, 0.5 ml diluted corn silk extract in 2.5 ml methanol was mixed with 3 ml of 0.01 M aluminium chloride in methanol. Then the mixture was allowed to stand for 10 min at room temperature (ca. 25 °C). The absorbance of the resulting solution was read at 400 nm using a spectrophotometer. The total flavonoid content was determined using a rutin calibration curve at concentrations from 0-0.100 mg/ml in methanol and expressed as rutin hydrate equivalents per dry mass of corn silk sample (μg RE/g dried sample).

2.5. Determination of total anthocyanin content

Total anthocyanin content was determined according to the pH-differential method (Ku, Kin, & Kang, 2009). Corn silk extract from each sample was mixed with pH 1.5 buffers in 1% HCl to 6 ml in methanol extract. After extracting at room temperature (ca. 25 °C) for 20 min, absorbance was measured for each solution at 530 nm and 700 nm against blanks of pH 1.0 and 4.5 buffers. Total anthocyanin content was determined by the following equation:

$$\text{Total anthocyanin } (\text{mg/L}) = (A \times \text{MW} \times 1000 \times \text{DF})/(\varepsilon \times 1)$$

where A was adjusted absorbance calculated from (A530–A700) at buffer 1.0 − (A520–A700) at buffer 4.5, 1000 was a converting factor from molar to ppm, and DF was a dilution factor.

For a quantification of total anthocyanin content, external calibration was carried out for cyanidin-3-glucoside with molecular weight (MW) of 449.2, and molar absorptivity of 1% HCl in methanol (ε) was 34,300. The results were expressed as microgram of cyanidin-3-glucoside equivalents per dry mass of corn silk sample (μg C3G/g dried sample).

2.6. Antioxidant activity assay

Antioxidant activity was measured using the DPPH free radical scavenging activity assay (Liu et al., 2011). Initially, 0.2 ml of corn silk extract was added to 1 ml of 0.2 mM freshly prepared DPPH methanol solution. The reaction was mixed and allowed to stand for 30 min under dark conditions. The control contained all reagents except the extract fraction was used as blank. Absorbance was read against a blank at 517 nm using a spectrophotometer. The percentage inhibition of absorbance was calculated and plotted as a function of the concentration of standard and corn silk extract to determine the ascorbic acid equivalent antioxidant concentration. The percentage of DPPH radical scavenging activity (%) of sample was calculated as follows:

$$\text{DPPH radical scavenging activity (\%inhibition)} = (1 - A\ \text{sample}/A\ \text{control}) \times 100$$

where A sample is the absorbance of the extract or standard and A control is the absorbance of the control. All tests were run in duplicates and analyses of the samples were run in triplicates.

2.7. Statistical analysis

Analysis of variance was performed for each parameter according to a completely randomized block design, and least significant difference (LSD) was used to compare means at $p < 0.05$. Data were expressed as mean ± standard deviation (SD) of three replication analysis. All analyses were done in SPSS v19 (SPSS Inc., USA).

3. Results

3.1. Total phenolic content and total flavonoid content

Total phenolic content ranging from 26.5 to 206.8 μg GAE/g of dry samples was observed among corn varieties evaluated across three maturity stages from silking to physiological maturity (Table 2). Based on total phenolic content, corn varieties could be roughly divided into a high or low group. The high group consisted of all varieties in purple waxy corn with total phenolic content higher than 100 μg GAE/g, and the low group comprised all corn varieties in white waxy corn and super sweet corn with total phenolic content lower than 100 μg GAE/g.

Maturity stages were also different for total phenolic content. On average across the three types of corn, milky stage (R4) had the highest total phenolic content (121.3 μg GAE/g) followed by silking stage (R1) (110.7 μg GAE/g) and physiological maturity stage (R6) (97.8 μg GAE/g), respectively (Table 6).

On average across three maturity stage, PWC5 had the highest total phenolic content (189.1 μg GAE/g) followed by PWC3 (153.2 GAE/g) and PWC1 (150.8 μg GAE/g), respectively (Table 2). PWC5 was also the highest at milking stage (206.8 ± 5.5 μg GAE/g). The corn varieties with the lowest total phenolic content were WWC3 (59.6 μg GAE/g) and WWC1 (61.2 μg GAE/g) of white waxy corn. WWC1 was also the lowest at physiological maturity stage (26.5 ± 2.1 μg GAE/g).

Total flavonoid contents ranging from 33.2 to 136.0 μg RE/g dried samples were observed among corn varieties across three maturity stages (Table 3). On average across corn varieties, silking stage had the highest total flavonoid content of 88.5 μg RE/g followed by milky stage (85.3 μg RE/g) and physiological maturity stage (69.1 μg RE/g) (Table 6).

On average across the three maturity stages, PWC5 was the highest for total flavonoid content (119.6 μg RE/g) followed by PWC4 (111.1 μg RE/g) and PWC1 (96.1 μg RE/g), respectively, whereas WWC3, WWC2 and WWC1 had the lowest flavonoid contents (52.3, 40.1 and 41.9 μg GAE/g, respectively) (Table 3). It is clear that purple corns had the highest total flavonoid content. Super sweet corns were intermediate and white waxy corns were the lowest.

PWC5 and PWC4 of purple waxy corn had the highest total flavonoid content at the milky stage (R4) (136.0 ± 2.2 and 129.2 ± 3.2 μg RE/g, respectively), whereas WWC1 and WWC2 of white waxy corn had the lowest total flavonoid content at the silking stage of 41.9 and 40.1 μg RE/g, respectively.

3.2. Total anthocyanin content

Differences among corn varieties at three maturity stages were significant for total anthocyanin contents ranging from 0.3 to 63.4 μg C3G/g of dried samples (Table 4). On average across corn varieties, silking stage had the highest total anthocyanin content (27.9 μg C3G/g) followed by physiological maturity stage (23.8 μg C3G/g) and milking stage (4.4 μg C3G/g), respectively (Table 6).

Based on total anthocyanin content, corn varieties could be clearly classified into a high and low group. The high group consisted PWC5, PWC1, PWC3, PWC2 and PWC4 in purple waxy corn with total anthocyanin contents ranging from 23.9 to 46.0 μg C3G/g, and low group included other varieties in white waxy corn and super sweet corn (Table 4). PWC5 in purple waxy corn had the highest total anthocyanin content at milking stage (63.4 ± 1.7 μg C3G/g) and physioligical maturity stage (62.7 ± 1.7 μg C3G/g),

Table 2
Total phenolic content in silk of 10 corn varieties evaluated at different reproductive stages.

Type of corn	Varieties	Total phenolic content (μg GAE/g dried sample)			
		Silking stage (R1)	Milky stage (R4)	Maturity stage (R6)	Mean
Purple waxy corn	PWC1	123.8 ± 3.8 *h*	179.6 ± 3.2 *cd*	149.1 ± 2.6 *f*	150.8 *b*
	PWC2	112.8 ± 2.1 *i*	169.2 ± 2.4 *e*	114.7 ± 3.1 *i*	132.2 *c*
	PWC3	127.0 ± 2.7 *h*	185.3 ± 1.9 *bc*	147.4 ± 2.8 *f*	153.2 *b*
	PWC4	115.6 ± 2.2 *i*	147.7 ± 3.3 *f*	134.5 ± 2.4 *g*	132.6 *c*
	PWC5	173.4 ± 2.6 *de*	206.8 ± 5.5 *a*	187.1 ± 3.2 *b*	189.1 *a*
White waxy corn	WWC1	99.8 ± 1.3 *j*	57.3 ± 2.3 *q*	26.5 ± 2.1 *t*	61.2 *fg*
	WWC2	89.6 ± 2.5 *kl*	56.8 ± 2.4 *q*	47.6 ± 1.8 *r*	64.7 *f*
	WWC3	85.9 ± 1.8 *l*	56.7 ± 2.1 *q*	36.1 ± 1.9 *s*	59.6 *g*
Super sweet corn	SSC1	85.5 ± 2.4 *lm*	75.2 ± 3.2 *no*	65.5 ± 2.0 *p*	75.4 *e*
	SSC2	93.4 ± 3.2 *jk*	78.3 ± 3.1 *mn*	69.4 ± 2.2 *op*	80.3 *d*

Values are mean ± standard deviation of three replicate analysis.
Means with the same letter(s) in the same column are not significantly different ($p < 0.05$) by LSD.
R1 is 7–10 days after silking, R4 is milky stage at 18 days after silking and R6 is maturity stage at 30 days after silking.

Table 3
Total flavonoid content in silk of 10 corn varieties evaluated at different reproductive stages.

Type of corn	Varieties	Total flavonoids content (μg RE/g dried sample)			
		Silking stage (R1)	Milky stage (R4)	Maturity stage (R6)	Mean
Purple waxy corn	PWC1	83.6 ± 1.9 *k*	104.6 ± 2.1 *e*	100.0 ± 1.7 *f*	96.1 *c*
	PWC2	74.1 ± 3.1 *l*	99.8 ± 3.2 *f*	61.8 ± 4.4 *o*	78.6 *g*
	PWC3	74.4 ± 2.1 *l*	94.5 ± 1.4 *g*	86.8 ± 1.0 *j*	85.2 *f*
	PWC4	99.0 ± 2.3 *f*	129.2 ± 3.2 *b*	105.3 ± 4.3 *e*	111.1 *b*
	PWC5	121.5 ± 2.4 *c*	136.0 ± 2.2 *a*	101.4 ± 1.9 *f*	119.6 *a*
White waxy corn	WWC1	57.6 ± 3.3 *p*	35.0 ± 2.3 *r*	33.2 ± 3.5 *r*	41.9 *i*
	WWC2	50.9 ± 3.2 *q*	35.7 ± 3.1 *r*	33.6 ± 4.1 *r*	40.1 *j*
	WWC3	87.4 ± 3.3 *ij*	35.7 ± 3.2 *r*	33.8 ± 3.4 *r*	52.3 *h*
Super sweet corn	SSC1	117.6 ± 3.4 *d*	90.3 ± 3.1 *hi*	65.5 ± 2.4 *n*	91.1 *e*
	SSC2	119.1 ± 3.2 *cd*	92.2 ± 3.8 *gh*	69.2 ± 3.9 *m*	93.5 *d*

Values are mean ± standard deviation of three replicate analysis.
Means with the same letter(s) in the same column are not significantly different ($p < 0.05$) by LSD.
R1 is 7–10 days after silking, R4 is milky stage at 18 days after silking and R6 is maturity stage at 30 days after silking.

Table 4
Total anthocyanin content in silk of 10 corn varieties evaluated at different reproductive stages.

Type of corn	Varieties	Total anthocyanin content (μg C3G/g dried sample)			
		Silking stage (R1)	Milky stage (R4)	Maturity stage (R6)	Mean
Purple waxy corn	PWC1	5.8 ± 2.2 *ij*	53.2 ± 1.5 *cd*	52.2 ± 1.1 *d*	37.1 *b*
	PWC2	5.3 ± 2.4 *ij*	59.9 ± 1.9 *b*	39.8 ± 1.6 *f*	35.0 *c*
	PWC3	6.0 ± 2.5 *i*	53.7 ± 1.3 *c*	48.4 ± 1.2 *e*	36.0 *bc*
	PWC4	4.3 ± 2.3 *jk*	39.5 ± 1.1 *f*	27.9 ± 1.5 *g*	23.9 *d*
	PWC5	11.7 ± 3.4 *h*	63.4 ± 1.7 *a*	62.7 ± 1.7 *a*	46.0 *a*
White waxy corn	WWC1	1.7 ± 2.1 *lmnop*	1.2 ± 1.2 *nop*	0.5 ± 0.3 *op*	1.1 *f*
	WWC2	3.1 ± 2.2 *kl*	2.9 ± 1.8 *klm*	2.5 ± 1.3 *lmn*	2.8 *e*
	WWC3	1.6 ± 2.2 *mnop*	1.5 ± 1.4 *mnop*	0.3 ± 0.2 *p*	1.1 *f*
Super sweet corn	SSC1	2.1 ± 2.3 *lmn*	2.0 ± 1.7 *lmno*	1.8 ± 0.4 *lmnop*	2.0 *ef*
	SSC2	2.3 ± 2.2 *lmn*	1.9 ± 1.3 *lmno*	1.5 ± 0.3 *mnop*	1.9 *ef*

Values are mean ± standard deviation of three replicate analysis.
Means with the same letter(s) in the same column are not significantly different ($p < 0.05$) by LSD.
R1 is 7–10 days after silking, R4 is milky stage at 18 days after silking and R6 is maturity stage at 30 days after silking.

whereas PWC2 and PWC1 had the highest total anthocyanin contents of 59.9 ± 1.9 and 53.2 ± 1.5 μg C3G/g, respectively, at the milky stage.

3.3. Radical DPPH scavenging activity

Differences among corn varieties at three maturity stages were significant for radical DPPH scavenging activity (Table 5). The DPPH values of radical scavenging activity of corn varieties evaluated across the three maturity stages ranged from 11.0% to 86.0%. Silking stage had the highest DPPH values of 61.5% followed by milky stage (56.6%) and physiological maturity stage (43.6%), respectively (Table 6). On average across three maturity stages, purple waxy corn constituted the highest DPPH values ranging from 78.3% to 64.2%, and PWC5 and PWC3 were highest (78.3% and 71.0%, respectively) (Table 5). Super sweet corns were intermediate ranging from 61.3% to 63.7%, and white waxy corn was lowest ranging from 21.3% to 33.4%. PWC5 of purple waxy corn was highest for DPPH values at milky stage (86.0 ± 4.5%) and silking stage (78.1%), whereas WWC1 WWC3 and WWC2 of white waxy corn had the lowest DPPH values of 11.0 ± 3.3, 15.0 ± 3.3 and 19.8 ± 3.5%, respectively, at physiological maturity stage.

4. Discussion

4.1. Phytochemicals at three maturity stages

Corn is usually harvested and consumed at three maturity stages such as baby corn, vegetable immature corn and mature corn. Baby corn is harvested at the silking stage. Vegetable corns such as super sweet corn and waxy corn are harvested at the immature stage which is normally at 21 days after silking or slightly later but not at physiological maturity stage, and corn is also harvest at physiological maturity stage for seed production (Žnidarcic, Ban, Peršuric, Oplanic, & Koncar, 2008). At all maturity stages, ears and kernels are used for food, and silk is normally discarded as waste. However, silk can be used as a food ingredient as it is rich in photochemicals with antioxidant activity. Therefore, this study was carried out to determine total phenolic, flavonoid and anthocyanin content and antioxidant activity in the silk of purple waxy corn, white waxy corn and super sweet corn at the silking stage, immature stage and physiological maturity stage.

In this study, purple waxy corn is most suitable for use as a source of phenolic compounds, flavonoids and anthocyanins as the contents of these phytochemicals were generally higher than white waxy corn and super sweet corn at all maturity stages. In the previous study, phenolic compounds (Ebrahimzadeh et al., 2008; Liu et al., 2011) and flavonoids (Ebrahimzadeh et al., 2008; Hu, Zhang, Li, Ding, & Li, 2010; Liu et al., 2011) were the major components of phytochemicals in corn silk, and the contents of these phytochemicals varied depending on extraction methods, plant tissues and the origin of the plants (Ebrahimzadeh et al., 2008). Purple waxy corn has high anthocyanin accumulation (Jian & Monica, 2010; Yang & Zhai, 2010) as there are derivatives unique among flavonoids and phenolic compounds as their structures undergo reversible transformation at different pHs in aqueous solution (Jian & Monica, 2010). Anthocyanins also accumulate in other parts of corn such as in silk, leaves and seeds (Fossen, Slimestad, & Andersen, 2001).

Table 5
Scavenging activity in silk of 10 corn varieties evaluated at different reproductive stages.

Type of corn	Varieties	Scavenging activity (%inhibition DPPH)			
		Silking stage (R1)	Milky stage (R4)	Maturity stage (R6)	Mean
Purple waxy corn	PWC1	70.7 ± 4.1 *d*	74.7 ± 5.4 *c*	52.0 ± 5.2 *i*	65.8 *c*
	PWC2	70.3 ± 5.5 *d*	74.6 ± 6.5 *c*	47.7 ± 4.2 *j*	64.2 *d*
	PWC3	74.7 ± 4.4 *c*	77.1 ± 6.3 *b*	61.3 ± 4.3 *f*	71.0 *b*
	PWC4	57.3 ± 4.2 *g*	61.4 ± 5.3 *f*	45.9 ± 4.5 *k*	54.9 *f*
	PWC5	78.1 ± 5.3 *b*	86.0 ± 4.5 *a*	70.8 ± 4.6 *d*	78.3 *a*
White waxy corn	WWC1	33.2 ± 3.6 *l*	19.7 ± 3.4 *n*	11.0 ± 3.3 *p*	21.3 *i*
	WWC2	32.5 ± 3.1 *l*	23.6 ± 3.6 *m*	19.8 ± 3.5 *n*	25.3 *h*
	WWC3	61.5 ± 7.1 *f*	23.6 ± 3.9 *m*	15.0 ± 3.3 *o*	33.4 *g*
Super sweet corn	SSC1	65.3 ± 4.2 *e*	60.3 ± 5.5 *f*	58.2 ± 4.6 *g*	61.3 *e*
	SSC2	71.1 ± 4.6 *d*	65.2 ± 5.2 *e*	54.9 ± 4.2 *h*	63.7 *d*
Asorbic acid (40 μg/mL)				75.5 ± 2.1 *bc*	

Values are mean ± standard deviation of three replicate analysis.
Means with the same letter(s) in the same column are not significantly different ($p < 0.05$) by LSD.
R1 is 7–10 days after silking, R4 is milky stage at 18 days after silking and R6 is maturity stage at 30 days after silking.

Table 6
Means for total phenolic content (TPC), total flavonoids content (TFC), total anthocyanin content (TAC) and scavenging activity (SA) in silk of 10 corn varieties evaluated at different reproductive stages.

Reproductive stage	TPC (μg GAE/g dried sample)	TFC (μg RE/g dried sample)	TAC (μg C3G/g dried sample)	SA (%inhibition DPPH)
Silking stage	110.7 *b*	88.5 *a*	4.4 *c*	61.5 *a*
Milky stage	121.3 *a*	85.3 *b*	27.9 *a*	56.6 *b*
Maturity stage	97.8 *c*	69.1 *c*	23.8 *b*	43.6 *c*

Means with the same letter(s) in the same column are not significantly different ($p < 0.05$) by LSD.

In this study, harvest of purple waxy corn at the milky stage was most suitable for higher phytochemicals. This harvest time is normal for commercial production of purple waxy corn. The best harvest time for super sweet corn that gave the highest phytochemicals was at silking stage. However, super sweet corn is also harvested commercially at milky stage which produced somewhat lower phytochemicals than at the silking stage. Harvest at physiological maturity stage is not suitable as it produced low phytochemicals for all types of corn.

In previous investigations, total anthocyanin content in corn silk of purple waxy corn varieties was highest at the milky stage and maturity stage (Yang & Zhai, 2010). In general, low concentrations of anthocyanins were found in white waxy corn and super sweet corn varieties (Kasim, Sulusoglu, & Ufuk, 2011). Purple waxy corn had the highest total phenolic content, total flavonoid content and total anthocyanin content (Sarepoua et al., 2013).

The results in this study supported previous reports and indicated that corn silk is suitable for use as a raw material for the production of functional food products. However, harvest at different maturity stages resulted in differences in silk quality. If phytochemicals are considered, harvest at silking stage gave the best quality of silk. Harvest at immature stage had intermediate quality, and harvest at physiological maturity stage had rather low quality. Although corn silk has been used as a traditional herb, the scientific information on the health promoting properties of corn silk has not been clearly elucidated. This study provided useful information on the differences of corn silk of different corn types harvested at different maturities for phenolic compounds, flavonoids and anthocyanins which were closely related to antioxidant activity (Ardestani & Yazdanparast, 2007). Corn silk contains phytochemicals that have health benefits, and it is useful for use as raw material for extraction of natural phytochemicals for use in food industry. The use of corn silk should reduce agricultural waste.

4.2. Antioxidant activity at three maturity stages

Plants are an important source of natural antioxidants especially for phenolics, flavonoids, tannins and anthocyanidins that are safe and bioactive (Mohsen & Ammar, 2009). Natural antioxidants extracted from fruits, teas, vegetables and medicinal plants have been investigated extensively because they are effective in eliminating free radicals and less toxic than synthetic antioxidants (Zhu, Lian, Guo, Peng, & Zhou, 2011). Corn silk is an important bioactive source of natural antioxidants (Hasanudin et al., 2012), and total phenolic content in corn silk was correlated with free-radical scavenging activity (Ardestani & Yazdanparast, 2007). If DPPH radical scavenging activity is considered, corn silk with the best quality can be harvested at the silking stage, which is in accordance with the harvest time of baby corn. Therefore, silk of baby corn is the best source of antioxidant activity. Harvest at the milking stage also yielded the best quality silk especially for purple waxy corn which was the best type of corn for high DPPH radical scavenging activity. Harvest at physiological maturity stage yielded the lowest quality of corn silk.

In earlier studies, DPPH radical scavenging activity was correlated with total phenolic content and total flavonoid content, and, although the relationship between DPPH radical scavenging activity and anthocyanin content was not significant, it was still high and positive ($r = 0.40$) (Sarepoua et al., 2013). Phenolic compounds, flavonoids and anthocyanins in corn silk can reduced DPPH radicals and provide high antioxidant activity (Nurhanan et al., 2012). Therefore, corn silk harvested at different maturity stages can be used as a raw material for production of value-added functional food products.

High pigmentation generally occurs at the early maturity phase of corn silk, and it is related directly to high antioxidant activity. Different parts of corn silk also differ in antioxidant activity. The upper part of corn silk had higher pigmentation than the lower part of corn silk, and it also had a higher total antioxidant capacity (Alam, 2011). The highest antioxidant activity was found in corn silk from purple waxy corn varieties PWC5 at the milky stage and silking stage.

5. Conclusion

This study evaluated total phenolic, flavonoid and anthocyanin content and antioxidant activity in corn silk of different types at different maturity stages. The questions underlying the research project were what harvest times are most suitable and which corn types and varieties are most suitable for production of corn silk

with high concentrations of the phytochemicals and antioxidant activity. Milky stage was the best time for harvest, and corn silk that was harvest at this maturity stage had the highest total phenolic content, total flavonoid content, total anthocyanin content and antioxidant activity. Corn silk harvest at the silking stage had lower quality than corn silk harvested at the milky stage, but harvest at physiological maturity produced corn silk with the lowest quality. In general, purple waxy corn had silk with the highest total phenolic content, total flavonoid content, total anthocyanin content and antioxidant activity. Super sweet corn also provided silk of good quality although the quality was lower than that produced from purple waxy corn. However, silk of white waxy corn has the lowest quality. PWC5 of purple waxy corn was the best genotypes for silk quality especially at milking growth stage.

Acknowledgements

This work was supported by the Higher Education Research Promotion and National Research University Project of Thailand, Office of the Higher Education Commission, through the Food and Functional Food Research Cluster of Khon Kaen University and Plant Breeding Research Center for Sustainable Agriculture, Faculty of Agriculture, Khon Kaen University, Thailand.

References

Alam, E. A. (2011). Evaluation of antioxidant and antibacterial activities of Egyptian Maydis stigma (*Zea mays* hairs) rich in some bioactive constituents. *The Journal of American Science, 7*(4), 726–729.

Ardestani, A., & Yazdanparast, R. (2007). Antioxidant and free radical scavenging potential of *Achillea santolina* extracts. *Food Chemistry, 104*(1), 21–29.

Ebrahimzadeh, M. A., Pourmorad, F., & Hafezi, S. (2008). Antioxidant activities of Iranian corn silk. *Turkish Journal of Biology, 32*, 43–49.

Fossen, T., Slimestad, R., & Andersen, O. M. (2001). Anthocyanins from maize *Zea mais* and reed canarygrass *Phalaris arundinacea*. *Journal of Agricultural and Food Chemistry, 49*, 2318–2321.

Hasanudin, K., Hashim, P., & Mustafa, S. (2012). Corn silk (Stigma Maydis) in healthcare: a phytochemical and pharmacological review. *Molecules, 17*, 9697–9715.

Hu, Q. L., Zhang, L. J., Li, Y. N., Ding, Y. J., & Li, F. L. (2010). Purification and antifatigue activity of flavonoids from corn silk. *International Journal of Physical Sciences, 5*(4), 321–326.

Jian, H., & Monica, G. M. (2010). Anthocyanins: natural colorants with health-promoting properties. *Annual Review of Food Science and Technology, 1*, 63–87.

Kasim, R., Sulusoglu, M., & Ufuk, K. M. (2011). Relationship between total anthocyanin level and colour of natural cherry laurel (*Prunuslaurocerasus* L.) fruits. *African Journal of Plant Science, 5*(5), 323–328.

Ku, K. M., Kin, S. K., & Kang, Y. H. (2009). Antioxidant activity and functional components of corn silk (*Zea mays* L.). *Korean Journal of Plant Research, 22*(4), 323–329.

Liu, J., Wang, C., Wang, Z., Zhang, C., Lu, S., & Liu, J. (2011). The antioxidant and free-radical scavenging activities of extract and fractions from corn silk (*Zea mays* L.) and related flavone glycosides. *Food Chemistry, 126*, 261–269.

Liu, Q., & Yao, H. Y. (2007). Antioxidant activities of barley seeds extracts. *Food Chemistry, 102*(3), 732–737.

Maksimovic, Z., Malencic, D., & Kovacevic, N. (2005). Polyphenol contents and antioxidant activity of Maydis stigma extracts. *Bioresource Technology, 96*, 873–877.

Mohsen, S. M., & Ammar, A. S. M. (2009). Total phenolic contents and antioxidant activity of corn tassel extracts. *Food Chemistry, 112*(3), 595–598.

Nurhanan, A. R., Rosli, W. I. W., & Mohsin, S. S. J. (2012). Total polyphenol content and Free radical scavenging activity of Cornsilk (*Zea mays* hairs). *Sains Malaysiana, 41*(10), 1217–1221.

Rosli, W. I. W., Nurhanan, A. R., Solihah, M. A., & Mohsin, S. S. J. (2011). Cornsilk improves nutrient content and physical characteristics of beef patties. *Sains Malaysiana, 40*(2), 155–161.

Sarepoua, E., Tangwongchai, R., Suriharn, B., & Lertrat, K. (2013). Relationships between phytochemicals and antioxidant activity in corn silk. *International Food Research Journal, 20*(5), 2073–2079.

Yang, Z., & Zhai, W. (2010). Identification and antioxidant activity of anthocyanins extracted from the seed and cob of purple corn (*Zea mays* L.). *Innovative Food Science and Emerging Technologies, 11*, 169–176.

Zhu, K. X., Lian, C. X., Guo, X. N., Peng, W., & Zhou, H. M. (2011). Antioxidant activities and total phenolic contents of various extracts from defatted wheat germ. *Food Chemistry, 126*, 1122–1126.

Žnidarčič, D. (2012). Performance and characterization of five sweet corn cultivars as influenced by soil properties. *Journal of Food, Agriculture and Environment, 10*(1), 495–500.

Žnidarčič, D., Ban, D., Peršurič, A. S. I., Oplanič, M., & Končar, A. B. (2008). Yield and quality of sweet corn (*Zea mays* L. var. saccharata Korn.) cultivars grown on different soil types. *Cereal Research Communications, 36*(Suppl.), 1–4. http://dx.doi.org/10.1556/CRC .36.2008.Suppl.13.

View publication stats

Hindawi Publishing Corporation
Evidence-Based Complementary and Alternative Medicine
Volume 2015, Article ID 301029, 11 pages
http://dx.doi.org/10.1155/2015/301029

Research Article

The Combined Extract of *Zingiber officinale* and *Zea mays* (Purple Color) Improves Neuropathy, Oxidative Stress, and Axon Density in Streptozotocin Induced Diabetic Rats

Jintanaporn Wattanathorn,[1,2] Paphaphat Thiraphatthanavong,[2] Supaporn Muchimapura,[1,2] Wipawee Thukhammee,[1,2] Kamol Lertrat,[3] and Bhalang Suriharn[3]

[1]*Department of Physiology, Faculty of Medicine, Khon Kaen University, Khon Kaen 40002, Thailand*
[2]*Integrative Complementary Alternative Medicine Research and Development Center, Khon Kaen University, Khon Kaen 40002, Thailand*
[3]*Faculty of Agriculture, Khon Kaen University, Khon Kaen 40002, Thailand*

Correspondence should be addressed to Jintanaporn Wattanathorn; jintanapornw@yahoo.com

Received 25 December 2014; Accepted 10 March 2015

Academic Editor: Yoshiji Ohta

Copyright © 2015 Jintanaporn Wattanathorn et al. This is an open access article distributed under the Creative Commons Attribution License, which permits unrestricted use, distribution, and reproduction in any medium, provided the original work is properly cited.

Based on the protective effect of the combined extract of purple waxy corn and ginger (PWCG) on oxidative stress related disorders in diabetic condition, we aimed to determine the effect of PWCG on the functional, biochemical, and structural change of the lesion nerve in streptozotocin- (STZ-) diabetic rats. PWCG at doses of 100, 200, and 300 mg·kg^{-1} BW were orally given to STZ-diabetic rats which were subjected to chronic constriction (CCI) at right sciatic nerve for 21 days. The blood sugar was assessed before and at the end of study whereas the sciatic function index (SFI), paw withdrawal threshold intensity (PWTI), and paw withdrawal latency (PWL) were assessed every 3 days until the end of study. At the end of study, the determination of nerve conduction velocity (NCV), axon density, oxidative stress status, and aldose reductase (AR) activity of the lesion nerve were performed. It was found that PWCG improved SFI, PWTI, PWL, and NCV together with the improved oxidative stress status and the axon density in the lesion nerve. No changes of AR activity or blood sugar level were observed. Therefore, PWCG might improve the functional and structural changes in STZ-diabetic rats plus CCI via the improved oxidative stress status.

1. Introduction

Diabetic neuropathy (DN), a common and costly complication of diabetic mellitus [1], affects more than 50% of diabetic patients [2]. It has been reported that chronic hyperglycemia can destroy sensory, motor, and autonomic fibers especially at distal extremities [3]. The manifestation of DN is varied depending on the affected nerve ranging from sensory deficit, weakness, and autonomic dysfunction. DN is regarded as a leading cause of nontraumatic amputation [4] due to the loss of protective limb mechanical sensations. In addition, approximate 11% of DN cases are associated with chronic painful condition which markedly decreases the quality of life of diabetic patients [5]. Since diabetic condition is dramatically increased worldwide, the importance of DN is also increasing. However, the current therapeutic efficiency is still limited.

Recently, it has been demonstrated that hyperglycemia can induce nerve damage by many mechanisms such as the enhanced oxidative stress, the increase of advanced glycation end product formation [6–8], the accumulation of sorbitol due to the increased aldose reductase activity [9], and nerve hypoxia/ischemia [6–8]. However, accumulative lines of evidence have suggested that both the excess oxidative stress and the elevation of aldose reductase may possibly be the important cause for the development of DN. This raises

the hypothesis that substances which can suppress oxidative stress and aldose reductase should improve DN.

Herbal medicine is used for treating numerous ailments on the long term. It has been believed that it is much safer than synthetic drugs. Therefore, herbal medicine is very popular and gains much attention nowadays. To decrease the high medical cost and expenditure, the dietary therapy by using herb-based food has gained much attention. Recently, it has been reported that *Zingiber officinale* and *Zea mays* (purple color) could improve diabetes and diabetic conditions [10–12]. In addition, recent study of our group has clearly shown that the combined extract of *Z. officinale* and *Z. mays* (purple waxy corn var. purple color) significantly improves diabetic cataract and diabetic retinopathy by suppressing oxidative stress and aldose reductase [13]. Therefore, the beneficial effect of the combined extract of purple waxy corn and ginger (PWCG) might be able to improve DN in streptozotocin-(STZ-) diabetic rats. Due to the lack of supported evidence, this study was undertaken to determine the effect of PWCG on DN in STZ-diabetic rats. In addition, the effects of PWCG on oxidative stress markers, aldose reductase activity, and axonal change were also investigated.

2. Materials and Methods

2.1. Plant Material and Extract Preparation. The plant materials used in this study were dried seeds of purple waxy corn or *Zea mays* L. (purple color; KKU open pollinated cultivar) and rhizomes of ginger or *Zingiber officinale* Roscoe. They were harvested during September 2012 and authenticated by Associate Kamol Lertrat and Dr. Bhalang Suriharn, Faculty of Agriculture, Khon Kaen University, Khon Kaen, Thailand. The voucher specimens (voucher specimens 2012001 and 2012002) were kept at the Integrative Complementary Alternative Medicine Research and Development Center, Khon Kaen University. The dried seeds of purple waxy corn and rhizomes of ginger were extracted with 50% hydroalcoholic solvent by maceration method at a ratio of 2 : 5 and 1 : 5 (weight : volume), respectively. The samples were macerated at room temperature for 3 days. Both of the yielded extracts were concentrated by lyophilization and kept at 4°C for further study. The percentage yields of purple waxy corn and ginger extracts were 5.72 and 25.26, respectively. The combination extract was prepared by mixing the extracts of purple waxy corn and ginger at a ratio of 1 : 4 (this ratio provided the highest anticataract potential). The content of total phenolic compounds in the combination extract was 44.82 ± 2.37 mg/L GAE/mg extract. The extract contained quercetin, gingerol, anthocyanin, and gallic acid at concentrations of 14.421 mg quercetin equivalent (QE)/100 mg PWCG extract, 10.701 mg gingerol/100 mg PWCG extract, 0.089 mg cyanidin-3-glucoside/100 mg PWCG, and 0.022 mg gallic acid/100 mg PWCG, respectively. The fingerprint chromatogram was shown in Figure 1.

2.2. Experimental Design. Male Wistar rats, weighing 250–280 g, were used in this study ($n = 8$ per group). The animals were maintained and treated in accordance with

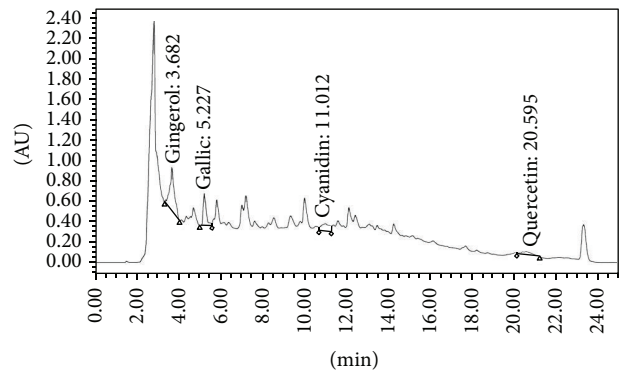


Figure 1: Fingerprint chromatogram of the combination extract of purple waxy corn (*Z. mays* var. purple color) and ginger (*Z. officinale* rhizome) or PWCG.

the guideline and approval of the Ethical Committee on Animals Experiments of Khon Kaen University (AEKKU 98/2555). All rats were divided into various groups as the following:

group I: control group (all rats in this group were normal rats which are subjected to sham operation and received citrate buffer, a vehicle of streptozotocin (STZ)),

group II: DM + CCI + vehicle of the extract or distilled water,

group III: DM + CCI + GABApentin at dose of 50 mg·kg^{-1} BW,

group IV: DM + CCI + ascorbic acid at dose of 100 mg·kg^{-1} BW,

groups V–VII: DM + CCI + PWCG at doses of 100, 200, and 300 mg·kg^{-1} BW, respectively.

In all rats in groups II–VII, diabetes mellitus was induced by a single injection of STZ which was dissolved in citrate buffer (pH 4.5) at dose of 55 mg·kg^{-1} BW. All diabetic rats which showed the blood sugar level more than 250 mg·dL^{-1} were selected for further study by inducing peripheral neuropathy with neuropathic pain by using the chronic constriction injury (CCI) of sciatic nerve [14, 15]. All rats were treated with the assigned interventions once daily after chronic constriction injury throughout the 21-day study period. The behavioral tests including hot plate test, von Frey filament, and foot print analysis were evaluated every 3 days until the end of study. At the end of study, nerve conduction velocity was investigated and the lesion nerves were evaluated upon the following parameters: histomorphology, aldose reductase, and oxidative stress markers including malondialdehyde (MDA) level and the activities of superoxide dismutase (SOD), catalase (CAT), and glutathione peroxidase (GPx) enzymes.

2.3. Induction of Diabetic Neuropathy: Chronic Constriction Injury. Diabetic neuropathy was induced as previously described [14, 15]. After the anesthesia with ethyl ether, the

right hind limb was immobilized in extended and slightly elevated position. The biceps femoris muscle was exposed and the femur bone was used as a landmark for direction of incision. The silk thread number 4.0 was slipped under the sciatic nerve trifurcation and ligated. After the nerve ligation, the muscle and skin layers were sutured. Each animal was allowed to recover for 24 hours before the investigation was carried out further. In this experiment, the contralateral thighs of all treated groups were not subjected to the operation.

2.4. Determination of Walking Track Analysis. Since walking track analysis is one of the commonly used tools to assess the function of innervated target organs after nerve injury, it was used as the evaluation tool in this study. In brief, the hind paws of the animals were dipped in the ink and they were allowed to walk along the wooden walking alley (8.2 × 42 cm) with one closed end and the white paper was placed at the floor. From the footprints, the following parameters were obtained: print length (PL): distance from the heel to the third toe, toe spread (TS): distance from the first to the fifth toe, and intermediate toe spread (ITS): distance from the second to the fourth toe. The mean distances of all measurements mentioned earlier were used to calculate the following factors (dynamic and static):

$$\begin{aligned}\text{Toe spread factor (TSF)} &= \frac{(\text{OTS} - \text{NTS})}{\text{NTS}}\\ \text{Intermediate toe spread factor (ITSF)} &= \frac{(\text{OITS} - \text{NITS})}{\text{NITS}}\\ \text{Print length factor (PLF)} &= \frac{(\text{OPL} - \text{NPL})}{\text{NPL}}.\end{aligned} \tag{1}$$

Then, these values were used to calculate the sciatic function index (SFI) by the following formula [16]:

$$\begin{aligned}\text{SFI} = {} & (-38.3 \times \text{PLF}) + (109.5 \times \text{TSF})\\ & + (13.3\text{I TSF}) - 8.8.\end{aligned} \tag{2}$$

According to this calculation, the normal values of SFI were in the range between +11 and −11 and a value of −100 indicated the total impairment [17].

2.5. Determination of Sensory Function by Using von Frey Filament Test. A series of 10 von Frey filaments (0.1 Gr, 0.2 Gr, 0.4 Gr, 0.8 Gr, 1.0 Gr, 1.2 Gr, 1.5 Gr, 2.5 Gr, 3.6 Gr, and 4.0 Gr) were used to evoke paw withdrawal response. Testing starts with the lowest filament of the series and each hind paw was stimulated 5 times. The intensity of withdrawal responses of each filament in a 3-second stimulation duration was recorded [18].

2.6. Determination of Sensory Function by Using Hot Plate Test. The rats were gently dropped into a plastic box with a metal floor that was preheated to a certain temperature (hot plate) [19]. The time duration between the initiation of the hot plate exposure and the time which the paw was raised from the floor was recorded and considered as paw withdrawal latency. Each animal was measured foot withdrawal reflex 5 times per session, with time interval of 5 min between tests. The average paw withdrawal latency was calculated and used as index. Minimal and maximal cut-offs were assigned at 0.5 to 20 seconds, respectively.

2.7. Determination of Sciatic Nerve Conduction by Nerve Conduction Velocity (NCV). In this experiment, the sciatic nerve conduction velocity was performed by modifying the measurement of conduction velocity in human. In brief, the sciatic nerve of the animal was stimulated and the response of gastrocnemius which was supplied by this nerve was recorded as nerve activity [20]. In brief, the rat was anesthetized with thiopental sodium via intraperitoneal injection. The right sciatic nerve of each rat was exposed and gently dissected away from the surrounding muscle tissue and the electrodes were placed at two different points. The stimulating electrode was placed at proximal site of the lesion whereas the recording electrode was place at distal site of the lesion. The sciatic nerve was stimulated using electrical stimuli at an interval of 0.5 ms and amplitudes between 50 and 2000 mV. The response latency was recorded. Then the location of recoding electrode was moved from the original site. The change of muscle response latency was then recorded. The nerve conduction velocity was calculated by dividing the distance obtained from the displacement of recording electrode with the change of muscle response latency which occurred as the result of the displacement of recording electrode.

2.8. Fasting Blood Glucose Level. Blood samples were taken from rat tails after overnight fasting. The fasting blood glucose level was monitored at the end of experiment by using ACCU-CHEK active.

2.9. Homogenate Preparation. At the end of experiment, homogenate of right sciatic nerve was prepared in 1 mL of 0.1 M phosphate buffer, pH 7.4. The obtained nerve homogenate was adjusted to 10% w/v and centrifuged with microcentrifuge (SIG 1-15PK) at 10,000 g, 4°C for 1 hour. The supernatant was harvested and processed for the estimation of biochemical parameters.

2.10. Biochemical Parameters Assessments

2.10.1. Determination of Malondialdehyde (MDA) Level. Level of malondialdehye (MDA), a lipid peroxidation marker, was monitored by using thiobarbituric acid reacting substances (TBARS) assay. In brief, 100 μL of sample was mixed with the solution containing 100 μL of 8.1% (w/v) sodium dodecyl sulphate (Sigma-Aldrich), 750 μL of 20% (v/v) acetic acid (Sigma-Aldrich) (pH 3.5), and 750 μL of 0.8% thiobarbituric acid (TBA) (Sigma-Aldrich). The solution was heated in a water bath at 95°C for one hour and cooled immediately under running tap water. Then, 500 μL of chilled water and 2500 μL of butanol and pyridine (Sigma-Aldrich) [15 : 1 v/v] were added into each tube and mixed

thoroughly with vortex (Vortex-Genie 2). Then, the solution was centrifuged at 800 ×g for 20 minutes. The upper layer was separated and absorbance was measured at 532 nm with spectrophotometer (GENESYS 20). 1,3,3-tetraethoxypropane (TEP) (Sigma-Aldrich) was used as in [21]. The level of MDA was expressed as U/mg·protein.

2.10.2. Determination of Superoxide Dismutase (SOD) Activity. The determination of SOD activity was carried out via nitroblue tetrazolium (NBT) reduction assay. In this assay, the xanthine-xanthine oxidase system was used as a superoxide generator. In brief, the reaction mixture contained 20 μL of sample and 200 μL of reaction mixture consisting of 57 mM phosphate buffer solution (KH_2PO_4) (Sigma-Aldrich), 0.1 mM EDTA (Sigma-Aldrich), 10 mM cytochrome C solution (Sigma-Aldrich), and 50 μM of xanthine solution (Sigma-Aldrich) and 20 μL of xanthine oxidase solution (Sigma-Aldrich) (0.90 mU/mL) was prepared at 25°C. The optical density was determined at 415 nm with a UV-spectrophotometer (Pharmacia LKB-Biochrom4060). A system devoid of enzyme was served as the control and three parallel experiments were conducted [22]. SOD activity was expressed as U/mg·protein.

2.10.3. Determination of Catalase (CAT) Activity. Nerve catalase activity was assessed based on the ability of the enzyme to break down H_2O_2. In brief, 10 μL of sample was mixed with the reaction mixture which contained 50 μL of 30 mM hydrogen peroxide (Sigma-Aldrich) (in 50 mM phosphate buffer, pH 7.0), 25 μL of H_2SO_4 (Sigma-Aldrich), and 150 μL of $KMnO_4$ (Sigma-Aldrich). After mixing thoroughly, the optical density was measured at 490 nm using GENESYS 20 spectrophotometer. A system devoid of the substrate (hydrogen peroxide) was served as the control. The difference in absorbance per unit time was expressed as the activity. An amount of enzyme required to decompose 1.0 M of hydrogen peroxide per minute at pH 7.0 and 25° is regarded as one unit [23]. The value of CAT activity was expressed as U/mg·protein.

2.10.4. Determination of Glutathione Peroxidase (GPx) Activity. This assay was performed based on the glutathione recycling method by using 5,5′-dithiobis (2-nitrobenzoic acid) (DTNB) (Sigma-Aldrich) and glutathione reductase (Sigma-Aldrich). According to this method, the reaction between DTNB and GSH gave rise to the generation of 2-nitro-5-thiobenzoic acid and GSSG. Since 2-nitro-5-thiobenzoic acid was a yellow colored product, GSH concentration could be determined by measuring absorbance at 412 nm. In brief, a mixture containing 20 μL of sample and the reaction mixture consisting of 10 μL of dithiothreitol (DTT) (Sigma-Aldrich) in 6.67 mM potassium phosphate buffer (pH 7), 100 μL of sodium azide (Sigma-Aldrich) in 6.67 mM potassium phosphate buffer (pH 7), 10 μL of glutathione solution, and 100 μL of hydrogen peroxide was mixed thoroughly and incubated at room temperature for 5–10 minutes. Then, 10 μL of DTNB (5,5-dithiobis-2-nitrobenzoic acid) was added and the optical density at 412 nm was recorded at 25°C over a period of 5 min by using UV-spectrophotometer (Pharmacia LKB-Biochrom4060). Activities were expressed as nmoles/min/mg lens protein [24]. GPx activity was expressed as U/mg·protein.

2.10.5. Determination of Aldose Reductase (AR) Activity. Aldose reductase activity was evaluated using colorimetric method. An assay mixture containing 0.7 mL of phosphate buffer (0.067 mol), 0.1 mL of NADPH (Sigma-Aldrich) (25×10^{-5} mol), 0.1 mL of DL-glyceraldehyde (Sigma-Aldrich) (substrate, 5×10^{-4} mol), and 0.1 mL of nerve supernatant was prepared. Absorbance was recorded against a reference cuvette containing all other components except the substrate, DL-glyceraldehyde. The final pH of the reaction mixture was adjusted to pH 6.2. The determination was performed after adding the substrate or DL-glyceraldehyde by measuring the decrease in NADPH absorbance at 390 nm over a 4-minute period via a UV-spectrophotometer (Pharmacia LKB-Biochrom4060) [25]. The enzyme activity was expressed as nmol/min/mg.

2.11. Histopathology Study. After anesthesia with sodium pentobarbital (60 mg/kg BW), the animals were perfused with 0.9% normal saline. Sciatic nerve was collected and immersed sequentially for 24 h in 10% formalin. The frozen sample was immersed in a stainless steel container filled with optimal cutting temperature (OCT) compound; the container was selected to fit the size of the sample. The specimens were frozen rapidly and 5 μm thick sections were made using cryostat.

2.12. Determination of Axonal Density. The nerve sample was stained with toluidine blue and the axon density in the lesion sciatic nerve was determined. In brief, the sections were stained with 0.1% toluidine blue for 10–30 s, rinsed with running water for about 5 min, and mounted with glycerin under a cover glass. Histological analysis was performed by light microscope and the density of axons was accessed by using Image Pro-plus 5.1 program.

2.13. Statistical Analysis. All parameters were compared using one-way analysis of variance (ANOVA). The post hoc test was used to identify specific mean differences. They were represented as mean ± standard error mean (mean ± SEM). Statistical analysis was carried out using SPSS version 15. Differences were considered significant at P value < .05.

3. Results

3.1. Effect of PWCG on Fasting Blood Glucose Concentration. The average fasting blood glucose levels of all the experimental groups were shown in Figure 2. It was found that the blood sugar levels of all diabetic rats were more than 250 mg·dL^{-1} throughout the study period. PWCG failed to produce a significant reduction of the fasting blood glucose level in all treated groups.

Table 1: Effect of PWCG on the sciatic function index evaluated by walking track analysis (n = 8/group).

Time	Sciatic function index (SFI)						
	Control	DM + CCI + vehicle	DM + CCI + GABApentin (50 mg·kg^{-1} BW)	DM + CCI + ascorbic acid (100 mg·kg^{-1} BW)	DM + CCI + PWCG (100 mg·kg^{-1} BW)	DM + CCI + PWCG (200 mg·kg^{-1} BW)	DM + CCI + PWCG (300 mg·kg^{-1} BW)
Baseline	−9.29 ± 3.51	−10.49 ± 3.80	−7.40 ± 4.56	−8.25 ± 1.82	−8.65 ± 2.95	−10.56 ± 3.89	−7.59 ± 6.86
Day 1	−7.98 ± 1.35	−91.72 ± 1.58$^{###}$	−84.36 ± 7.12	−87.93 ± 2.04	−85.03 ± 2.45	−90.76 ± 1.69	−88.86 ± 2.21
Day 3	−7.86 ± 2.00	−91.94 ± 1.36$^{###}$	−90.59 ± 1.75	−86.28 ± 1.93	−89.02 ± 2.09	−90.45 ± 1.46	−80.81 ± 3.79*
Day 6	−7.74 ± 1.73	−91.82 ± 1.48$^{###}$	−89.86 ± 2.28	−86.28 ± 1.93	−83.69 ± 1.82**	−83.56 ± 1.54**	−84.93 ± 2.31*
Day 9	−9.98 ± 1.89	−91.53 ± 1.77$^{###}$	−91.72 ± 1.58	−86.73 ± 1.79*	−86.54 ± 2.22*	−84.41 ± 0.62**	−83.54 ± 1.71***
Day 12	−9.78 ± 2.40	−92.19 ± 1.11$^{###}$	−90.24 ± 2.05	−84.32 ± 1.79**	−84.01 ± 2.17**	−87.14 ± 1.50*	−86.38 ± 1.94*
Day 15	−6.75 ± 2.54	−91.53 ± 1.77$^{###}$	−91.89 ± 1.41	−85.50 ± 1.57	−89.65 ± 5.21	−90.56 ± 4.40	−85.52 ± 1.76
Day 18	−7.19 ± 1.37	−91.69 ± 1.61$^{###}$	−90.88 ± 2.42	−82.42 ± 9.04	−93.91 ± 5.52	−84.20 ± 1.52	−88.24 ± 2.00
Day 21	−7.48 ± 1.75	−91.53 ± 1.77$^{###}$	−89.15 ± 2.74	−81.45 ± 10.32	−89.85 ± 3.63	−83.03 ± 2.37	−87.57 ± 1.88

$^{###}P$-value <.001; compared to control rats.
$^{*,**,***}P$-value <.05, .01 and .001 respectively; compared to DM rats with CCI which received vehicle.

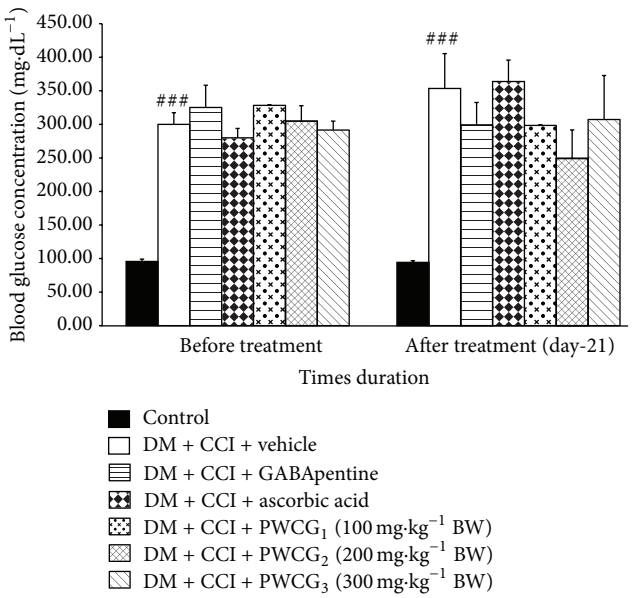


Figure 2: The effect of PWCG on fasting blood glucose concentration (n = 8/group). $^{###}P$ value < .001; compared to control rats.

3.2. Effect of PWCG on Function Recovery in Peripheral Neuropathy in Diabetic Rats. Table 1 showed that, before CCI (baseline data), no significant changes among groups were observed. In addition, all groups still showed normal SFI. Diabetic rats plus CCI which received vehicle showed the significant reduction of SFI (P value < .001 all, compared to control group) and showed the impaired SFI throughout the study period. Diabetic rats which are subjected to CCI and received GABApentin failed to produce the significant change of SFI throughout the study period. Ascorbic acid significantly improved SFI of diabetic rats which are subjected to CCI at 9 and 12 days of treatment (P value < .05 and .01, resp.; compared with diabetic rats plus CCI which received vehicle). PWCG at dose of 100 and 200 mg·kg^{-1} BW significantly improved SFI of diabetic rats which are subjected to CCI at 6 (P value < .01 all, compared with diabetic rats plus CCI which received vehicle), 9 (P value < .05 and .01, resp., compared with diabetic rats plus CCI which received vehicle), and 12 days of treatment (P value < .01 and .05, resp., compared with diabetic rats plus CCI which received vehicle). It was found that diabetic rats plus CCI which were orally given PWCG at dose of 300 mg·kg^{-1} BW produced significant improvement in SFI since day 3 to day 12 of treatment (P value < .05, .05, .001, and .05, resp., compared with diabetic rats plus CCI which received vehicle). No significant improvement of SFI was observed in any treatment groups at the other treatment duration.

The effect of PWCG on sensory function of sciatic nerve was also evaluated by both von Frey filament test and hot plate test and data were shown in Tables 2 and 3. In Table 2, it was found that no significant differences among groups were observed at baseline data. Diabetic rats which received CCI and were orally given vehicle showed the significant reduction in paw withdrawal threshold which was evaluated via von Frey filament test every 3 days throughout a 21-day experimental period (P value < .01, .05, .01, .01, .05, .05, and .05, resp., compared to control group). GABApentin significantly mitigated the decreased paw withdrawal threshold induced by CCI in diabetic rats since day 3 to day 15 of treatment (P value < .01, .05, .05, .01, and .05, resp., compared to diabetic rats plus CCI which received vehicle). Diabetic rats plus CCI which received ascorbic acid showed the significant increase in paw withdrawal threshold in response to mechanical stimuli in diabetic rats plus CCI only at 12 days of treatment (P value < .5, compared to diabetic rats plus CCI which received vehicle). Interestingly, PWCG at dose of 100 mg·kg^{-1} BW significantly mitigated the decrease of paw withdrawal threshold in response to mechanical stimuli induced by CCI in diabetic rats at 9 and 12 days of treatment (P value < .05 all, compared to diabetic rats plus CCI which received vehicle) whereas PWCG at doses of 200 and

Table 2: Effect of PWCG on paw foot withdrawal threshold intensity evaluated by von Frey filament test. (N = 8/group) $^{\#,\#\#}P$-value <.05 and .01 respectively; compared to control rats. $^{*,**}P$-value <.05 and .01 respectively; compared to DM rats with CCI which received vehicle.

Time	Paw withdrawal threshold intensity (g)						
	Control	DM + CCI + vehicle	DM + CCI + GABApentin (50 mg·kg^{-1} BW)	DM + CCI + ascorbic acid (100 mg·kg^{-1} BW)	DM + CCI + PWCG (100 mg·kg^{-1} BW)	DM + CCI + PWCG (200 mg·kg^{-1} BW)	DM + CCI + PWCG (300 mg·kg^{-1} BW)
Baseline	3.92 ± 0.08	3.92 ± 0.08	3.92 ± 0.08	3.92 ± 0.08	3.95 ± 0.05	3.95 ± 0.05	3.90 ± 0.02
Day 3	3.92 ± 0.08	3.02 ± 0.32$^{\#\#}$	3.84 ± 0.10**	3.70 ± 0.30	3.61 ± 0.17	3.58 ± 0.24	3.66 ± 0.08*
Day 6	3.84 ± 0.10	2.70 ± 0.56$^{\#}$	3.84 ± 0.10*	3.70 ± 0.30	3.54 ± 0.30	3.31 ± 0.3	3.40 ± 0.13
Day 9	4.00 ± 0.00	2.80 ± 0.56$^{\#\#}$	3.84 ± 0.10*	3.50 ± 0.50	3.66 ± 0.18*	3.71 ± 0.18*	3.71 ± 0.11*
Day 12	3.92 ± 0.08	2.90 ± 0.48$^{\#\#}$	3.84 ± 0.10**	3.70 ± 0.30*	3.61 ± 0.17*	3.71 ± 0.18*	3.71 ± 0.09*
Day 15	3.92 ± 0.08	3.10 ± 0.37$^{\#}$	3.92 ± 0.08*	3.70 ± 0.30	3.66 ± 0.22	3.76 ± 0.23*	3.71 ± 0.10*
Day 18	4.00 ± 0.00	3.12 ± 0.49$^{\#}$	3.92 ± 0.08	3.70 ± 0.30	3.48 ± 0.22	3.53 ± 0.23	3.53 ± 0.10
Day 21	4.00 ± 0.00	3.24 ± 0.31$^{\#}$	3.84 ± 0.10	3.70 ± 0.30	3.54 ± 0.30	3.61 ± 0.17	3.71 ± 0.18

Table 3: Effect of PWCG on paw foot withdrawal threshold intensity evaluated by hot plate test test. (N = 8/group). $^{\#\#\#}P$-value< .001; compared to control rats. $^{*,**,***}P$-value <.05, .01 and .001 respectively; compared to DM rats with CCI which received vehicle.

Time	Paw withdrawal latency (sec)						
	Control	DM + CCI + vehicle	DM + CCI + GABApentin (50 mg·kg^{-1} BW)	DM + CCI + ascorbic acid (100 mg·kg^{-1} BW)	DM + CCI + PWCG (100 mg·kg^{-1} BW)	DM + CCI + PWCG (200 mg·kg^{-1} BW)	DM + CCI + PWCG (300 mg·kg^{-1} BW)
Baseline	4.47 ± 0.33	4.53 ± 0.53	4.60 ± 0.38	4.40 ± 0.32	4.54 ± 0.41	4.25 ± 0.26	4.21 ± 0.36
Day 3	4.20 ± 0.25	1.40 ± 0.16$^{\#\#\#}$	2.87 ± 0.17**	2.40 ± 0.07*	2.00 ± 0.15	2.17 ± 0.14	2.50 ± 0.51*
Day 6	4.86 ± 0.29	1.60 ± 0.13$^{\#\#\#}$	2.70 ± 0.32***	2.47 ± 0.23**	1.87 ± 0.18	2.21 ± 0.14*	2.17 ± 0.09*
Day 9	4.20 ± 0.23	1.70 ± 0.13$^{\#\#\#}$	2.93 ± 0.07**	2.73 ± 0.30**	2.33 ± 0.34	2.42 ± 0.14*	2.46 ± 0.20*
Day 12	4.07 ± 0.40	1.33 ± 0.18$^{\#\#\#}$	2.66 ± 0.21***	2.40 ± 0.29**	1.90 ± 0.16	2.00 ± 0.22*	2.04 ± 0.10*
Day 15	3.53 ± 0.45	1.53 ± 0.20$^{\#\#\#}$	2.33 ± 0.15*	2.27 ± 0.13*	1.46 ± 0.13	1.67 ± 0.14	1.92 ± 0.10
Day 18	4.33 ± 0.40	1.40 ± 0.13$^{\#\#\#}$	1.93 ± 0.12	1.90 ± 0.14	1.33 ± 0.13	1.58 ± 0.12	1.67 ± 0.13
Day 21	4.40 ± 0.45	1.60 ± 0.13$^{\#\#\#}$	2.27 ± 0.19	2.09 ± 0.21	1.38 ± 0.17	1.46 ± 0.15	1.50 ± 0.15

300 mg·kg^{-1} BW produced the significant mitigation effect on the reduction of paw withdrawal threshold in response to mechanical stimuli induced by CCI in diabetic rats between day 9 and day 15 of treatment (P value < .05 all, compared to diabetic rats plus CCI which received vehicle).

Table 3 showed that the diabetic rats which are subjected to CCI and received vehicle also decreased paw withdrawal latency in response to temperature stimuli evaluated by hot plate test (P value < .001 all, compared to control group). Both diabetic rats plus CCI which received GABApentin and diabetic rats plus CCI which received ascorbic acid significantly mitigated the decreased paw withdrawal latency in response to temperature stimuli since day 3 to day 15 of treatments (P value < .01 and .05; .001 and .01; .01 all; .001 and .01; .05 all, resp., compared to diabetic rats plus CCI which received vehicle). Low dose of PWCG failed to modulate paw withdrawal latency throughout the study period. However, diabetic rats plus CCI which received medium dose of PWCG significantly mitigated the increased paw withdrawal latency from day 6 to day 12 of treatment (P value < .05 all, compared to diabetic rats plus CCI which received vehicle) while those which received high dose of PWCG showed the significant improvement of paw withdrawal latency between day 3 and day 12 of treatment (P value < .05 all, compared to diabetic rats plus CCI which received vehicle).

3.3. Effect of PWCG on Nerve Conduction Velocity. The effect of PWCG on nerve conduction velocity was also evaluated. It was found that diabetic rats which are subjected to CCI significantly decreased sciatic nerve conduction velocity as shown in Figure 3. Diabetic rats which are exposed to CCI and received GABApentin failed to show the significant increase in NCV of sciatic nerve. Interestingly, diabetic rats plus CCI which received either ascorbic acid treatment or PWCG at the range used in this study significantly improved sciatic nerve conduction velocity (P value < .05, .05, .01, and .01, resp., compared with diabetic rats plus CCI which received vehicle).

3.4. Effect of PWCG on Oxidative Stress Markers and Aldose Reductase Activity. Based on the previous findings that oxidative stress plays a crucial role in diabetic neuropathy, we also investigated the effect of PWCG on oxidative stress

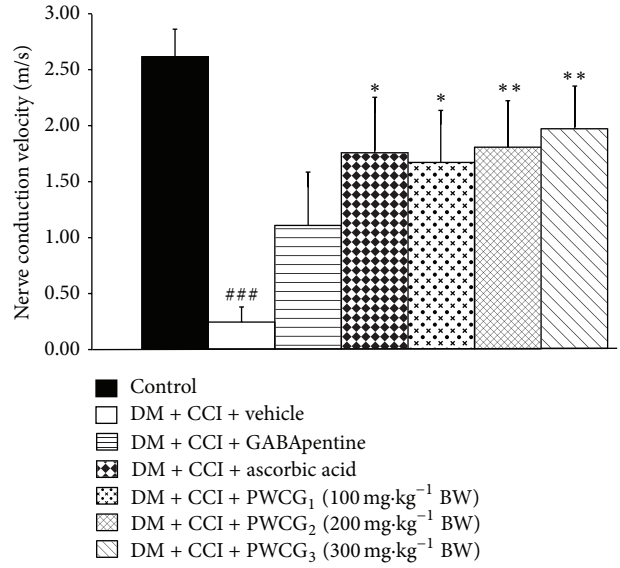


Figure 3: Effect of PWCG on sciatic nerve conduction velocity (n = 8/group). ### P value < .001, compared to control group. *,** P value < .05 and .01, respectively, compared to diabetic rats which were subjected to CCI and received vehicle.

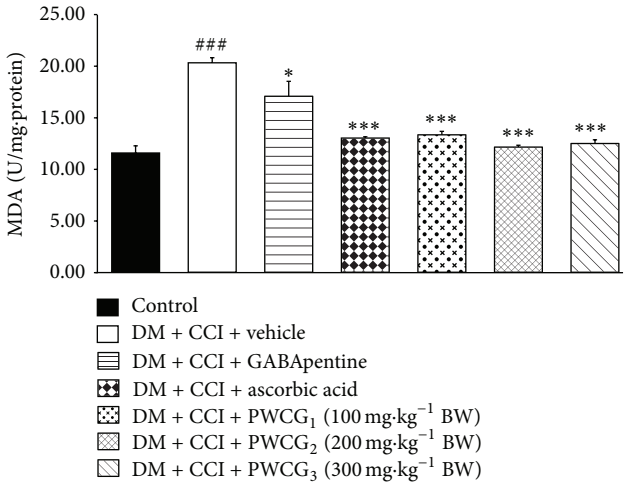


Figure 4: Effect of PWCG on malondialdehyde (MDA) level in the lesion sciatic nerve (n = 8/group). ### P value < .001, compared to control group. *,*** P value < .05 and .001, respectively, compared to diabetic rats which were subjected to CCI and received vehicle.

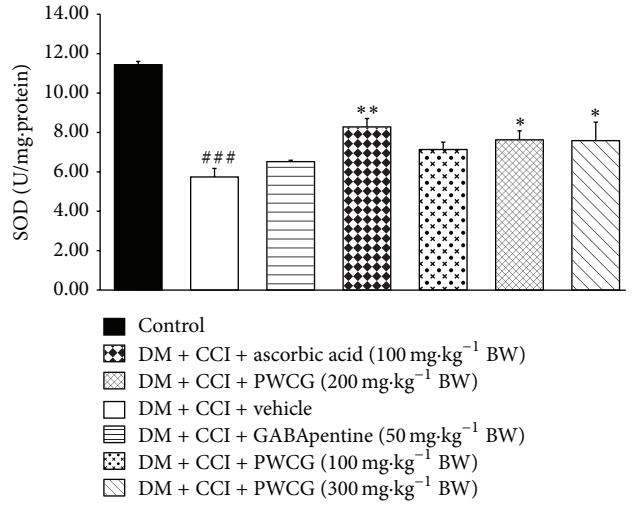


Figure 5: Effect of PWCG on superoxide dismutase (SOD) activity in the lesion sciatic nerve (n = 8/group). ### P value < .001, compared to control group. *,** P value < .05 and .01, respectively, compared to diabetic rats which were subjected to CCI and received vehicle.

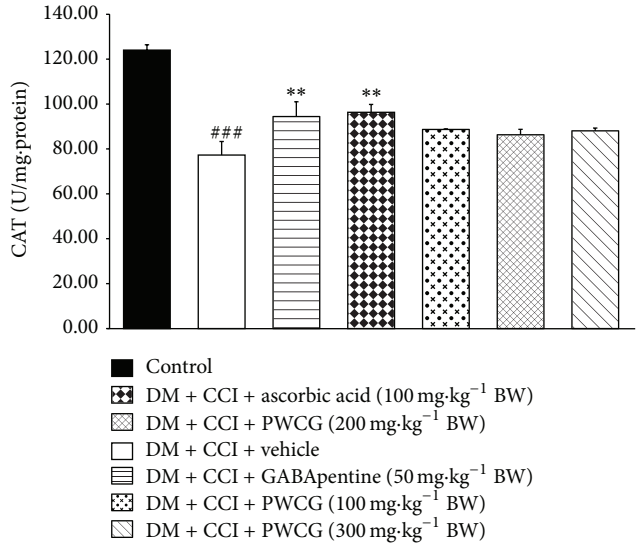


Figure 6: Effect of PWCG on catalase (CAT) activity in the lesion sciatic nerve (n = 8/group). ### P value < .001, compared to control group. ** P value < .01, compared to diabetic rats which were subjected to CCI and received vehicle.

markers including the level of MDA and the activities of SOD, CAT, and GPx in the lesion nerve and results were shown in Figures 4–7. It was found that diabetic rats plus CCI which received vehicle produced the significant reduction of MDA level in the lesion sciatic nerve (P value < .001, compared to control group). However, the activities of SOD, CAT, and GPx in diabetic rats plus CCI which received vehicle were markedly reduced (P value < .001 all, compared to control group). Diabetic rats plus CCI which received GABApentin significantly decreased MDA level but increased CAT activity in the lesion sciatic nerve (P value < .05 and .01, resp., compared to diabetic rats plus CCI which received vehicle). Ascorbic acid treatment could decrease MDA level but decreased SOD, CAT, and GPx activities in the lesion sciatic nerve of diabetic rats plus CCI (P value < .001, .01, .01, and .001, resp., compared to diabetic rats plus CCI which received vehicle). PWCG treatment at dose of 100 mg·kg^{-1} BW significantly decreased MDA level but increased GPx activity in the lesion sciatic nerve. Diabetic rats plus CCI which received PWCG at doses of 200 and 300 mg·kg^{-1} BW produced significant changes of the reduction of MDA level and the increase of SOD activity

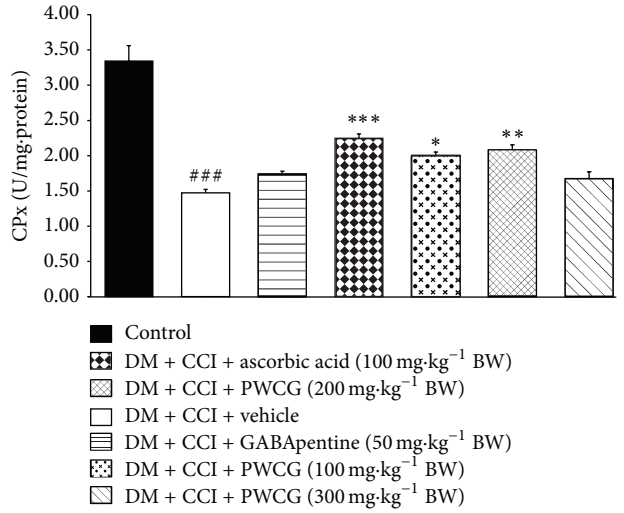


Figure 7: Effect of PWCG on glutathione peroxidase (GPx) activity in the lesion sciatic nerve (n = 8/group). $^{###}P$ value < .001, compared to control group. $^{*,**,***}P$ value < .05, .01, and .001, respectively, compared to diabetic rats which were subjected to CCI and received vehicle.

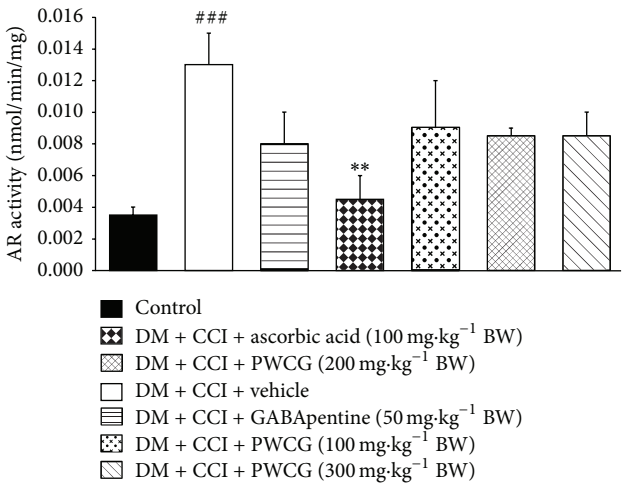


Figure 8: Effect of PWCG on aldose reductase (AR) activity in the lesion sciatic nerve. (n = 8/group) $^{###}P$ value < .001, compared to control group. $^{**}P$ value < .01, compared to diabetic rats which were subjected to CCI and received vehicle.

in the lesion sciatic nerve (P value < .001 all and .05 all, resp., compared to diabetic rats plus CCI which received vehicle). In addition, diabetic rats plus CCI which received the medium dose of PWCG also decreased GPx activity in the lesion sciatic nerve (P value < .01, compared to diabetic rats plus CCI which received vehicle).

The effect of PWCG on aldose reductase, a rate limiting enzyme in polyol pathway, was also investigated and data were shown in Figure 8. Diabetic rats plus CCI which received vehicle markedly increased aldose reductase activity in the lesion sciatic nerve (P value < .001, compared to control group). The only significant reduction of aldose reductase

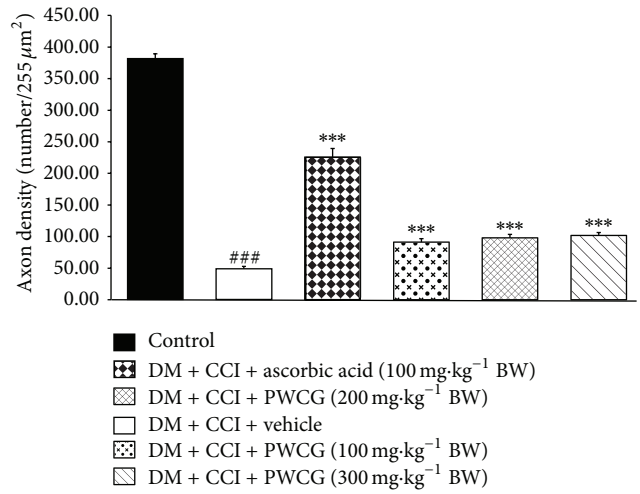


Figure 9: Effect of PWCG on the density of myelinated fibers evaluated by using toluidine blue stain (n = 8/group). $^{###}P$ value < .001, compared to control group. $^{***}P$ value < .001, compared to diabetic rats which were subjected to CCI and received vehicle.

activity in the lesion sciatic nerve was observed only in ascorbic acid treatment group (P value < .01, compared to diabetic rats plus CCI which received vehicle). No other groups showed the significant change of this parameter.

3.5. Effect of PWCG on Density of Axon. The effect of PWCG on density of myelinated axon in sciatic nerve evaluated by toluidine blue stain was investigated and results were shown in Figure 9. Diabetic rats plus CCI which were treated with vehicle significantly decreased density of myelinated axon (P value < .0001, compared to control group). Interestingly, ascorbic acid and all doses of PWCG used in this study mitigated the reduction of density of myelinated axon (P value < .001 all, compared to diabetic rats plus CCI which received vehicle).

4. Discussion

The current data has demonstrated that PWCG successfully improves the myelinated nerve fiber loss and nerve dysfunction in neuropathy with neuropathic pain in diabetic condition. PWCG also improves oxidative stress status in the lesion nerve while no suppression of aldose reductase activity is observed. In addition, no change of blood sugar was observed in PWCG treated rats.

Streptozotocin (STZ) can induce pancreatic beta cell toxicity and is often used to induce diabetes in experimental animals [26, 27]. STZ, a nitrosourea analogue, enters the pancreatic beta cell by using glucose transporter type 2 (GLUT 2) and produces the toxicity mainly via alkylation method. STZ alkylates DNA and protein in the cells leading to cell death. In addition to the alkylation, STZ can also produce oxidative stresses such as superoxide and hydroxyl radicals and nitric oxide (NO) which in turn induce beta cell destruction. Due to the decreased survival beta cell in

pancreas, insulin secretion was also decreased leading to the decreased glucose uptake into peripheral tissues and finally resulting in hyperglycemia [28]. The results obtained from this study are also in agreement with the previous studies. Although the reduction of blood glucose can also improve neuropathy, no reduction of blood glucose was observed in PWCG treated groups. Therefore, the improved neuropathy in this study might not relate to this mechanism.

It has been reported that the pathophysiology of diabetic neuropathy involves the interplay of hyperglycemia, ischemia, and oxidative stress. The increased ischemic condition and oxidative stress status can exacerbate morphological changes of peripheral nerve in diabetic rat [29] and reduce the time duration to induce the damage of peripheral nerve and the clinical manifestation development. Therefore, the ischemic condition of nerve by using CCI in STZ-diabetic rats was performed [14]. Based on the previous finding, it has been reported that oxidative stress and the accumulation of sorbitol via the enhanced polyol pathway are responsible for the development of peripheral diabetic neuropathy [30, 31]. In this study, CCI can develop the impairment of motor function especially walking pattern together with the hyperalgesia conditions which are in agreement with the clinical manifestation observed in patients with diabetic neuropathy [32, 33].

Oxidative stress and the accumulation of sorbitol via the enhanced polyol pathway are reported to be responsible for the development of peripheral diabetic neuropathy [30, 31]. Both oxidative stress and sorbitol can damage the myelin sheath leading to the myelin degradation and the decreased NCV. In addition, both factors can decrease the myelinated nerve fiber density. It has been well known that myelinated fibers play the important role in the transmission of proprioception information which in turn plays the crucial role in postural stability. The abnormal gait which reflects the postural instability observed in this study may be due to the loss of myelinated fiber resulting in the decreased myelinated nerve density which in turn disturbs gait stability as shown by the impairment of SFI. Although hyperglycemia has been previously reported to be the important cause of nerve dysfunction, our data show that PWCG improve nerve dysfunction in diabetic condition without the change of hyperglycemic. Our finding is in agreement with previous study which showed that the nerve dysfunction is associated with the decreased myelinated nerve fiber density [31, 34].

Accumulative lines of evidence also demonstrate that oxidative stress plays an important role in neuropathic pain [35–39]. In addition, neuropathic pain can be attenuated by substances possessing antioxidant activity [34, 37]. Since the data obtained from our study showed that PWCG significantly increased SOD and GPx activities which in turn decreased the oxidative stress reflecting by the decreased MDA level, therefore we suggested that the antihyperalgesic effect of PWCG might occur partly via the decreased oxidative stress which in turn decreased the damage of peripheral nerve fiber resulting in the decreased pain fiber stimulation from potassium ion and prostaglandin which had been released from nerve injury. In addition to oxidative stress, neuropathic pain is also under the influence of many factors including polyol pathway [39]. The increased polyol pathway activity can induce nerve damage directly via the accumulation of sorbitol, a toxic substance, or indirectly via the increased oxidative stress. However, our data failed to show the suppression of aldose reductase in the lesion nerve. Therefore, the improved hyperalgesia in diabetic rats plus CCI which received PWCG might not be associated with the suppression of aldose reductase.

The inhibition of γ-aminobutyric acid or GABA pathway also plays a crucial role in modulating the response of peripheral nerve injury [40]. It has been reported that the activity of GABA pathway is decreased in neuropathic pain condition [41]. Therefore, the improved GABA activity might play a role in the improved neuropathic pain. However, it has been reported that quercetin, the main flavonoids in PWCG, was the GABA antagonist so it was less likely to produce antineuropathic pain via the increased GABA activity [42]. Unfortunately, the determination of GABA activity had not been performed in this study. Therefore, this was the limitation of our study and required further study to confirm the exclusion of the modulation of GABA pathway by PWCG.

In this study, no dose dependent manner of PWCG was observed. The possible explanation might be due to the masking effect of the other ingredients and the interaction effect among the ingredients on the effect of active ingredient (s). In addition, PWCG might not exert the effect directly on the observed parameters but it might exert the modulation effect via other mediators such as the signal molecules.

Taking all data together, PWCG might increase SOD and GPx activities which in turn decreased oxidative stress status in the lesion nerve giving rise to the improved nerve damage leading to the increased myelinated nerve fiber density and the improved SFI. In addition, the decreased nerve damage due to the decreased oxidative stress also decreased the stimulation of pain fiber leading to the improved paw withdrawal threshold intensity in response to mechanical stimuli and the improved paw withdrawal latency in response to thermal stimuli. However, another mechanism such as the involvement of GABA pathway may also play a role in the improvement of hyperalgesia and this requires further investigation. In addition, the improved oxidative stress might improve the damage of myelin sheath giving rise to the increased NCV of sciatic motor function. Although PWCG mitigated the neuropathy in diabetic condition, no reduction of blood glucose or the suppression of aldose reductase activity in the lesion nerve was observed. Therefore, both hypoglycemic effect and the suppression of polyol pathway may not be involved in antineuropathy effect of PWCG.

5. Conclusion

PWCG is the potential candidate to serve as functional food to improve peripheral neuropathy in diabetic patient. However, further researches about the pharmacokinetics and interactions with diabetic drugs are very much necessary before serving as the adjuvant therapy.

Abbreviations

DN: Diabetic neuropathy
PWCG: The combination extract of purple waxy corn and ginger
Z. officinale: *Zingiber officinale*
Z. mays: *Zea mays*
STZ: Streptozotocin
CCI: Chronic constriction injury
SFI: Sciatic function index
PWTI: Paw withdrawal threshold intensity
PWL: Paw withdrawal latency
NCV: Nerve conduction velocity
AR: Aldose reductase
mg: Milligram
kg: Kilogram
BW: Body weight
PL: Print length
TS: Toe spread
ITS: Intermediate toe spread
TSF: Toe spread factor
mV: Millivolt
MDA: Malondialdehyde
SOD: Superoxide dismutase
CAT: Catalase
GPx: Glutathione peroxidase
QE: Quercetin equivalent
TBARS: Thiobarbituric acid reacting substances
NBT: Nitroblue tetrazolium
U: Unit
mL: Milliliter
mM: Millimole
dL: Deciliter
GABA: γ-Aminobutyric acid.

Conflict of Interests

The authors declare that there is no conflict of interests regarding the publication of this paper.

Acknowledgments

This study was supported by the Higher Education Research Promotion and National Research University Project of Thailand, Office of the Higher Education Commission, through the Food and Functional Food Research Cluster of Khon Kaen University, Targeted Research, Faculty of Medicine and the Integrative Complementary Alternative Medicine Research and Development Center, Khon Kaen University, Thailand. The great thanks were also extended to Research and Development Center of Herbal Health Product, for providing the opportunity to collaborate in the subcluster.

References

[1] A. Gordois, P. Scuffham, A. Shearer, A. Oglesby, and J. A. Tobian, "The health care costs of diabetic peripheral neuropathy in the U.S.," *Diabetes Care*, vol. 26, no. 6, pp. 1790–1795, 2003.

[2] R. E. Maser, A. R. Steenkiste, J. S. Dorman et al., "Epidemiological correlates of diabetic neuropathy. Report from Pittsburgh epidemiology of diabetes complications study," *Diabetes*, vol. 38, no. 11, pp. 1456–1461, 1989.

[3] M. J. Brown and A. K. Asbury, "Diabetic neuropathy," *Annals of Neurology*, vol. 15, no. 1, pp. 2–12, 1984.

[4] S. Thomson and L. Jacques, "Demographic characteristics of patients with severe neuropathic pain secondary to failed back surgery syndrome," *Pain Practice*, vol. 9, no. 3, pp. 206–215, 2009.

[5] C. E. Argoff, B. E. Cole, D. A. Fishbain, and G. A. Irving, "Diabetic peripheral neuropathic pain: clinical and quality-of-life issues," *Mayo Clinic Proceedings*, vol. 81, no. 4, pp. S3–S11, 2006.

[6] I. G. Obrosova, C. van Huysen, L. Fathallah, X. C. Cao, M. J. Stevens, and D. A. Greene, "An aldose reductase inhibitor reverses early diabetes-induced changes in peripheral nerve function, metabolism, and antioxidative defense," *The FASEB Journal (Bethesda, MD)*, vol. 16, no. 1, pp. 123–125, 2002.

[7] P. S. van Dam, "Oxidative stress and diabetic neuropathy: Pathophysiological mechanisms and treatment perspectives," *Diabetes/Metabolism Research and Reviews*, vol. 18, no. 3, pp. 176–184, 2002.

[8] A. M. Vincent, J. W. Russell, P. Low, and E. L. Feldman, "Oxidative stress in the pathogenesis of diabetic neuropathy," *Endocrine Reviews*, vol. 25, no. 4, pp. 612–628, 2004.

[9] S. S. M. Chung, E. C. M. Ho, K. S. L. Lam, and S. K. Chung, "Contribution of polyol pathway to diabetes-induced oxidative stress," *Journal of the American Society of Nephrology*, vol. 14, supplement 3, pp. S233–S236, 2003.

[10] Y. Li, V. H. Tran, C. C. Duke, and B. D. Roufogalis, "Preventive and protective properties of *Zingiber officinale* (Ginger) in diabetes mellitus, diabetic complications, and associated lipid and other metabolic disorders: a brief review," *Evidence-Based Complementary and Alternative Medicine*, vol. 2012, Article ID 516870, 10 pages, 2012.

[11] M. Y. Kang, S. S. Lim, J. Y. Lee, K. M. Yeo, and Y. H. Kang, "Anthocyanin-rich purple corn extract inhibit diabetes-associated glomerular angiogenesis," *PLoS ONE*, vol. 8, no. 11, Article ID e79823, 2013.

[12] P. Thiraphatthanavong, J. Wattanathorn, S. Muchimapura et al., "Preventive effect of *Zea mays* L. (purple waxy corn) on experimental diabetic cataract," *BioMed Research International*, vol. 2014, Article ID 507435, 8 pages, 2014.

[13] P. Thiraphatthanavong, J. Wattanathorn, S. Muchimapura, W. Thukham-mee, K. Lertrat, and B. Suriharn, "The combined extract of purple waxy corn and ginger prevents cataractogenesis and retinopathy in streptozotocin-diabetic rats," *Oxidative Medicine and Cellular Longevity*, vol. 2014, Article ID 789406, 11 pages, 2014.

[14] J. Khongrum, J. Wattanathorn, S. Muchimapura et al., "*Moringa oleifera* leaves extract attenuates neuropathic pain induced by chronic constriction injury," *American Journal of Applied Sciences*, vol. 9, no. 8, pp. 1182–1187, 2012.

[15] G. J. Bennett and Y.-K. Xie, "A peripheral mononeuropathy in rat that produces disorders of pain sensation like those seen in man," *Pain*, vol. 33, no. 1, pp. 87–107, 1988.

[16] J. R. Bain, S. E. Mackinnon, and D. A. Hunter, "Functional evaluation of complete sciatic, peroneal, and posterior tibial nerve lesions in the rat," *Plastic and Reconstructive Surgery*, vol. 83, no. 1, pp. 129–136, 1989.

[17] L. de Medinaceli, W. J. Freed, and R. J. Wyatt, "An index of the functional condition of rat sciatic nerve based on measurements made from walking tracks," *Experimental Neurology*, vol. 77, no. 3, pp. 634–643, 1982.

[18] H. Hsu, N. Tang, Y. Lin, T. Li, H. Liu, and C. Hsieh, "Effect of electroacupuncture on rats with chronic constriction injury-induced neuropathic pain," *The Scientific World Journal*, vol. 2014, Article ID 129875, 9 pages, 2014.

[19] Y. Liu, L. Wang, X. Li, C. Lv, D. Feng, and Z. Luo, "Tanshinone IIA improves impaired nerve functions in experimental diabetic rats," *Biochemical and Biophysical Research Communications*, vol. 399, no. 1, pp. 49–54, 2010.

[20] P. S. van Dam, B. Bravenboer, B. S. van Asbeck, J. J. M. Marx, and W. H. Gispen, "High rat food vitamin E content improves nerve function in streptozotocin-diabetic rats," *European Journal of Pharmacology*, vol. 376, no. 3, pp. 217–222, 1999.

[21] H. Ohkawa, N. Ohishi, and K. Yagi, "Assay for lipid peroxides in animal tissues by thiobarbituric acid reaction," *Analytical Biochemistry*, vol. 95, no. 2, pp. 351–358, 1979.

[22] Y. Sun, L. W. Oberley, and Y. Li, "A simple method for clinical assay of superoxide dismutase," *Clinical Chemistry*, vol. 34, no. 3, pp. 497–500, 1988.

[23] L. Góth, "A simple method for determination of serum catalase activity and revision of reference range," *Clinica Chimica Acta*, vol. 196, no. 2-3, pp. 143–151, 1991.

[24] J. T. Rotruck, A. L. Pope, H. E. Ganther, A. B. Swanson, D. G. Hafeman, and W. G. Hoekstra, "Selenium: biochemical role as a component of glatathione peroxidase," *Science*, vol. 179, no. 4073, pp. 588–590, 1973.

[25] M. B. Patel and S. M. Mishra, "Aldose reductase inhibitory activity and anticataract potential of some traditionally acclaimed antidiabetic medicinal plants," *Oriental Pharmacy and Experimental Medicine*, vol. 9, no. 3, pp. 245–251, 2009.

[26] M. S. Islam and D. T. Loots, "Experimental rodent models of type 2 diabetes: a review," *Methods and Findings in Experimental and Clinical Pharmacology*, vol. 31, no. 4, pp. 249–261, 2009.

[27] L. Wei, Y. Lu, S. He et al., "Induction of diabetes with signs of autoimmunity in primates by the injection of multiple-low-dose streptozotocin," *Biochemical and Biophysical Research Communications*, vol. 412, no. 2, pp. 373–378, 2011.

[28] S. Lenzen, "The mechanisms of alloxan- and streptozotocin-induced diabetes," *Diabetologia*, vol. 51, no. 2, pp. 216–226, 2008.

[29] Y. Wang, J. D. Schmelzer, A. Schmeichel, H. Iida, and P. A. Low, "Ischemia-reperfusion injury of peripheral nerve in experimental diabetic neuropathy," *Journal of the Neurological Sciences*, vol. 227, no. 1, pp. 101–107, 2004.

[30] M. Dobretsov, D. Romanovsky, and J. R. Stimers, "Early diabetic neuropathy: triggers and mechanisms," *World Journal of Gastroenterology*, vol. 13, no. 2, pp. 175–191, 2007.

[31] G. Sundkvist, L.-B. Dahlin, H. Nilsson et al., "Sorbitol and myo-inositol levels and morphology of sural nerve in relation to peripheral nerve function and clinical neuropathy in men with diabetic, impaired, and normal glucose tolerance," *Diabetic Medicine*, vol. 17, no. 4, pp. 259–268, 2000.

[32] R. Courtemanche, N. Teasdale, P. Boucher, M. Fleury, Y. Lajoie, and C. Bard, "Gait problems in diabetic neuropathic patients," *Archives of Physical Medicine and Rehabilitation*, vol. 77, no. 9, pp. 849–855, 1996.

[33] C. Gooch and D. Podwall, "The diabetic neuropathies," *Neurologist*, vol. 10, no. 6, pp. 311–322, 2004.

[34] K. F. Eriksson, H. Nilsson, F. Lindgarde et al., "Diabetes mellitus but not impaired glucose tolerance is associated with dysfunction in peripheral nerves," *Diabetic Medicine*, vol. 11, no. 3, pp. 279–285, 1994.

[35] H. K. Kim, S. K. Park, J. L. Zhou et al., "Reactive oxygen species (ROS) play an important role in a rat model of neuropathic pain," *Pain*, vol. 111, no. 1-2, pp. 116–124, 2004.

[36] Z.-Q. Wang, F. Porreca, S. Cuzzocrea et al., "A newly identified role for superoxide in inflammatory pain," *Journal of Pharmacology and Experimental Therapeutics*, vol. 309, no. 3, pp. 869–878, 2004.

[37] M. Tal, "A novel antioxidant alleviates heat hyperalgesia in rats with an experimental painful peripheral neuropathy," *NeuroReport*, vol. 7, no. 8, pp. 1382–1384, 1996.

[38] A. K. Naik, S. K. Tandan, S. P. Dudhgaonkar et al., "Role of oxidative stress in pathophysiology of peripheral neuropathy and modulation by *N*-acetyl-l-cysteine in rats," *European Journal of Pain*, vol. 10, no. 7, pp. 573–579, 2006.

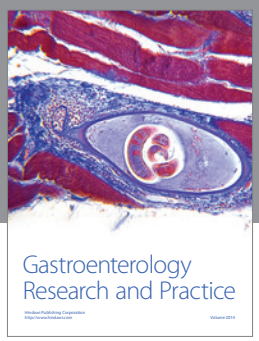
[39] A. Hosseini and M. Abdollahi, "Diabetic neuropathy and oxidative stress: therapeutic perspectives," *Oxidative Medicine and Cellular Longevity*, vol. 2013, Article ID 168039, 15 pages, 2013.

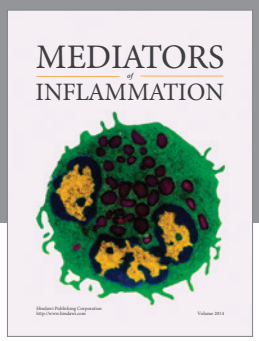
[40] L. Sivilotti and C. J. Woolf, "The contribution of GABAA and glycine receptors to central sensitization: disinhibition and touch–evoked allodynia in the spinal cord," *Journal of Neurophysiology*, vol. 72, no. 1, pp. 169–179, 1994.

[41] C.-O. Stiller, J.-G. Cui, W. T. O'Connor, E. Brodin, B. A. Meyerson, and B. Linderoth, "Release of γ-aminobutyric acid in the dorsal horn and suppression of tactile allodynia by spinal cord stimulation in mononeuropathic rats," *Neurosurgery*, vol. 39, no. 2, pp. 367–375, 1996.

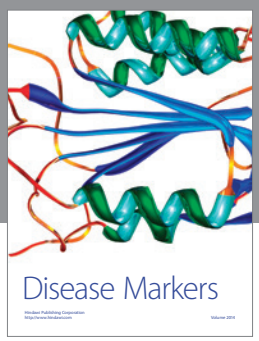
[42] J. D. Goutman and D. J. Calvo, "Studies on the mechanisms of action of picrotoxin, quercetin and pregnanolone at the GABA ρ1 receptor," *British Journal of Pharmacology*, vol. 141, no. 4, pp. 717–727, 2004.



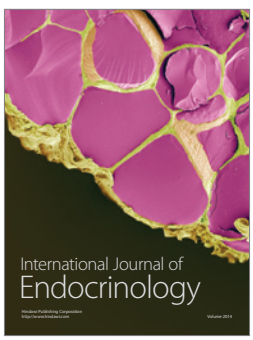






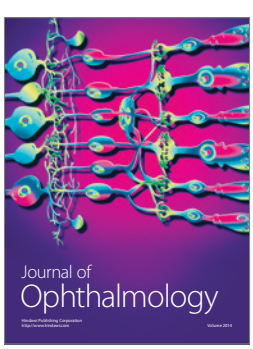


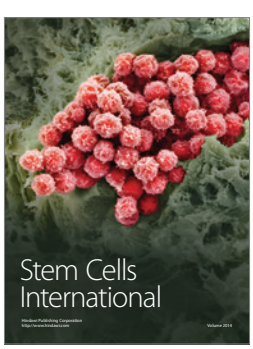


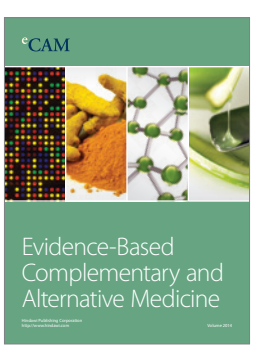






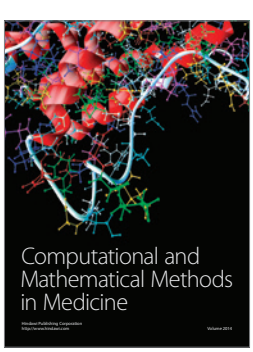


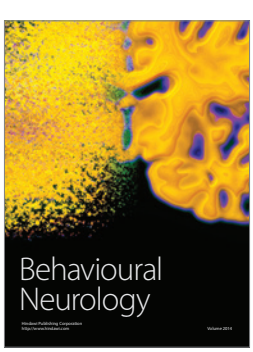




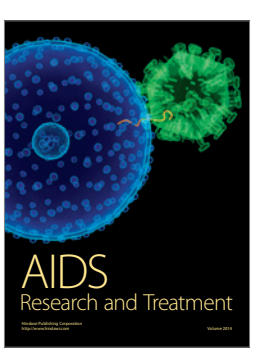


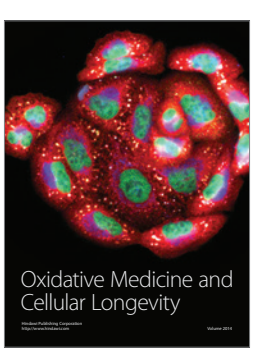












Hindawi

Submit your manuscripts at
http://www.hindawi.com

Scientia Agricola
http://dx.doi.org/10.1590/0103-9016-2013-0380

CSM-CERES-Rice model to determine management strategies for lowland rice production

Saythong Vilayvong[1], Poramate Banterng[1,2]*, Aran Patanothai[1], Krirk Pannangpetch[1]

[1]Khon Kaen University/Faculty of Agriculture – Dept. of Plant Science and Agricultural Resources – Khon Kaen – 40002 – Thailand.
[2]Khon Kaen University/Faculty of Agriculture – Plant Breeding Research Center for Sustainable Agriculture.
*Corresponding author <pbanterng@hotmail.com>

Edited by: Gerrit Hoogenboom

Received November 21, 2013
Accepted December 19, 2014

ABSTRACT: The cropping system model, namely, the crop environment resource synthesis-rice (CSM-CERES-Rice) model, is a decision supporting tool for the design of crop management. This study aimed to determine management practices for increasing rice (*Oryza sativa* L.) production in Laos by using the CSM-CERES-Rice model. The model was evaluated with data sets from the TDK8 and TDK11 cultivars in farmers' fields in the Vientiane plain in 2012. Anthesis and harvesting dates, growth and yield for various management scenario combinations (eight transplanting dates × two levels of plant densities × three rates of nitrogen (N) fertilizer application) for both cultivars were simulated by the model from 1980 to 2012. The model evaluation results showed strong agreement between simulated and observed data for days to harvest with a difference within four days. The model provided acceptable accuracy for grain yields with normalized root mean square error values ranging between 1 and 16 %. The results from the model application indicated that TDK8 and TDK11 produced similar yields. Transplanting TDK8 with two plant densities produced similar yields. The highest yield for both cultivars was achieved on the transplanting date of 15 Jan. N-fertilizer application at 60 and 120 kg N ha^{-1} was able to increase yield for TDK8 by 50 and 87 %, respectively, and for TDK11 by 54 and 70 %, respectively. Rice transplanted on 15 Jan with 5 seedlings $hill^{-1}$ and N-fertilizer at 120 kg N ha^{-1} had the highest average yield for both cultivars with 6,460 and 6,351 kg ha^{-1} for TDK8 and TDK11, respectively. The CSM-CERES-Rice model is an alternative tool in determining crop management practices for rice production.
Keywords: crop simulation, N-fertilizer application, planting practice, transplanting date

Introduction

Rice (*Oryza sativa* L.) is the most important food for half of the world's population especially in Asia (Schiller et al., 2006). In Laos, rice is mostly cultivated in the plain areas which account for more than 80 % of the agricultural areas of the country. Records from the Office of Agricultural Statistics of Laos indicate that the average rice yield is lower than the expected yield level of 2.5 t ha^{-1}. There are several factors that impact rice production, including management practices such as cultivar use, transplanting date, plant density, fertilizer application, irrigation amongst others. Identification of suitable crop management practices could provide information for designing a plan to increase the rice yield of this production area. However, this process is time consuming and expensive as many years of experimental trials are required. In addition, cropping systems are extremely complex and many factors have to be considered to achieve long-term sustainability (Geng et al., 1990) in major rice growing areas.

The CSM-CERES-Rice model has been developed to support decision making in agronomic research, crop production and land-use planning. It has been included in the decision support system for agrotechnology transfer (DSSAT). The CSM-CERES-Rice model is physiologically based and simulates daily canopy photosynthesis, respiration, growth, biomass partitioning and crop development as a function of input information, including daily weather conditions, soil properties, management practices and cultivar characteristics (Jones et al., 2003).

This model was introduced as a decision-supporting tool and its performance has been assessed for rice-wheat cropping systems to increase land and resource use efficiency (Timsina and Connor, 2001; Sarkar and Kar, 2006; Timsina and Humphreys, 2006). The model has been evaluated in a number of agro-environments and crop management strategies (Cheyglinted et al., 2001; Singh et al., 2007; Vilayvong et al., 2012; Yao et al., 2005). It has also been used to determine better rice management systems under irrigated conditions (Ahmad et al., 2012) and simulate rice yield under certain agronomic management practices and changing climatic scenarios (Lamsal and Amgain, 2010). Therefore, the CSM-CERES-Rice model offers the opportunity of a tool to determine crop management for improving rice productivity.

Currently, the lack of this model assessment has limited the application in investigating the interaction of transplanting dates, plant densities and N-fertilizer application for lowland rice under both irrigated and rainfed conditions in tropical regions such as Laos. This study aimed to determine management practices that will increase rice production in Laos by using the CSM-CERES-Rice model.

Materials and Methods

Model evaluation

The input data required to evaluate the CSM-

CERES-Rice model in the DSSAT v4.5 include rice management practices, crop details, soil properties, daily weather conditions and genetic coefficients. Data on rice management, including cultivars used, transplanting date, planting method, plant spacing, fertilization, weed control, irrigation, pest control, harvest time and others production practices were obtained from farmer interviews (nine households) in 2012 in the Xaythani district (18°4′ N, 102°36′ E and 170 m above mean sea level), Vientiane, Laos. These data cover the range of rice management practices in Vientiane. Therefore, it would constitute information representative of rice production in this area. Crop details include harvest maturity date and dry weight of grain yield for TDK8 and TDK11 cultivars from nine farmers' fields.

The sample plots (three plots for each cultivar) were selected for the collection of data from an area of 4 m^2 for each plot. The soil surface and soil profile characteristics for two soil groups in the Vientiane plain were obtained from the Soil Survey and Land Classification Center, National Agriculture and Forestry Research Institute, Ministry of Agriculture and Forestry, Laos (Table 1). The genetic coefficients of TDK8 and TDK11 (Table 2) were obtained from our previous study (Vilayvong et al., 2012), that also indicated that the genetic coefficients of TDK8 and TDK11 cultivars are sufficiently accurate for further application of CSM-CERES-Rice to support decision making.

The management, soil, climatic and crop data for nine farmers' fields and the genetic coefficients of TDK8 and TDK11were used as input data in the DSSAT v4.5. Model evaluation was performed by comparing the simulated values with their corresponding observed values from nine farmers' fields. The root mean square error ($RMSE_n$) value (Wallach and Goffinet, 1987) was used to test the agreement between simulated and observed data. Low RMSE value indicates strong agreement between the data sets. The $RMSE_n$ value gives a measure (%) of the relative difference of simulated versus observed data. The simulation is considered excellent if the $RMSE_n$ value is less than 10 %, good if the $RMSE_n$ is greater than 10 % and less than 20 % and fair if the $RMSE_n$ is greater than 20 % and less than 30 % (Loague and Green, 1991).

Table 1 – The information for the top soil layer (depth 0-15 and 15-30 cm) for two soil groups in the Vientiane plain, Laos.

Soil characteristic	Soil group			
	Acrisols		Alisols	
	0-15 cm	15-30 cm	0-15 cm	15-30 cm
Soil texture	Loam	Loam	Sandy loam	Sandy loam
Sand (%)	52	46	54	55
Clay (%)	18	24	15	16
Silt (%)	30	30	31	29
pH in H_2O	5.1	5.1	5.0	5.1
Total N (%)	0.2	0.2	0.1	0.1
Organic matter (%)	3.2	3.2	2.2	2.4
Bulk density (g cm^{-3})	1.5	1.5	1.5	1.5

Table 2 – The genetic coefficients of the TDK8 and TDK11 cultivars for the CSM-CERES-Rice model.

Genetic coefficient	Cultivar	
	TDK8	TDK11
Phenology coefficient		
P1: Growing degree day (GDD) for the basic vegetative phase (°C day)	415	409
P2R: Photoperiod sensitivity coefficient (°C day)	195	199
P5: GDD from the beginning of grain filling to physiological maturity (°C day)	520	400
P20: Critical day length (h)	10.6	11.2
Growth coefficient		
G1: Potential spikelet number coefficient	40	42
G2: Single grain weight (g)	0.025	0.025
G3: Tillering coefficient	0.8	0.9
G4: Temperature tolerance	0.8	0.8

Source: Vilayvong et al. (2012)

Simulation for different management scenarios

The input data required for model simulation include genetic coefficients, soil properties, daily weather conditions and rice management. The genetic coefficients of TDK8 and TDK11 (Table 2) were obtained from Vilayvong et al. (2012). The historical daily weather data for Vientiane from 2001 to 2012 (12 years) include maximum and minimum temperatures, solar radiation and rainfall (Figure 1). These historical weather data were then used as the input data for the WeatherMan program in DSSAT v4.5 to generate the weather parameters for long-term simulation.

Model simulation for different management scenarios was conducted to determine crop management practices for rice production in the Vientiane plain. The scenarios for crop management were first defined by following both local extension recommendations and current farmers' management practices. Growing rice in-season under both rainfed and irrigated conditions were specified for seven transplanting dates in the rainy season, e.g. 15 June, 30 June, 15 July, 30 July, 15 Aug, 30 Aug and 15 Sept. Another growing rice off-season under irrigated conditions was also set as 15 Jan transplanting date (Figure 1).

Irrigation and water management for all planting dates were set as automatic application when required by the crop. The common plant densities of 1 seedling $hill^{-1}$ and 5 seedlings $hill^{-1}$ with 20 cm × 20 cm of plant spacing were employed. N-fertilizer was applied at the rates of 60 kg N ha^{-1} (the rate recommended by Linquist and Sengxua (2001) for lowland rice in Laos) and 120 kg N ha^{-1} (two times the recommended rate) with three splits (recommended by Iqbal et al., 2008) of 35 % at 20-25 days after transplanting (DAT), 45 % at 40-45 DAT and 20 % at 60 DAT. The most popular glutinous rice cultivars TDK8 and TDK11 in Vientiane plain were used for simulation scenarios.

The crop management scenario combinations (eight transplanting dates × two plant densities × three

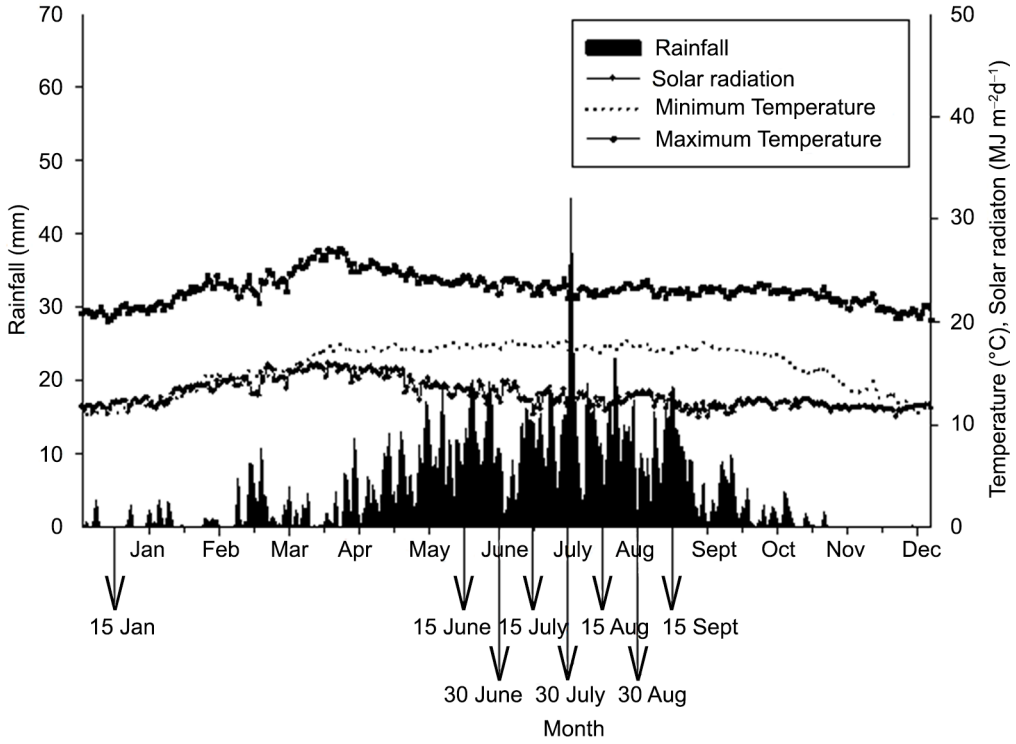


Figure 1 – Average daily maximum temperature, minimum temperature, solar radiation and rainfall over 12 years (2001-2012) for the Vientiane plain, Laos.

rates of N-fertilizer application) were run by the CSM-CERES-Rice model for TDK8 and TDK11 cultivars. The simulation was conducted for 33 years from 1980 to 2012. The seasonal analysis program of DSSAT v4.5 was used to evaluate and compare between different combinations of crop management practices.

The simulated data were analyzed statistically using the analysis of variance technique. Treatment means were compared by the least significant difference (LSD) method. All statistical analyses were performed using Statistix8 software by following Gomez and Gomez (1984). The total production cost and gross income (average simulated yield for 2012 × price of rice) for TDK8 and TDK11 productions under three different rates of N-fertilizer application were also evaluated and they were then used to calculate the net income. The relative values (%) for total production cost, grain yield and net income were calculated by using the value of each N-fertilizer application rate multiplied by 100 and then divided by the corresponding value for no N-fertilizer application.

Results

Model evaluation

Differences between the simulated data and observed data for days to harvest ranged from +2 to -4 days (Table 3). The greatest difference (-4 days) was found for TDK8 grown on 13 June 2013 with N-fertilizer at a rate of 80 kg N ha^{-1} followed by -3 days for TDK11 grown on 10 July 2011 with N-fertilizer at a rate of 73 kg N ha^{-1}. Most differences between the simulated data and observed data for grain yield were low, ranging from 31 to 154 kg ha^{-1} for RMSE values and 1 to 6 % for $RMSE_n$ values (Table 4). However, the highest RMSE value of 556 kg ha^{-1} and $RMSE_n$ value of 16 % were found for TDK8 transplanted on 7 July 2012 with N-fertilizer at a rate of 42 kg N ha^{-1}.

Simulation for management scenarios

The simulated results for 33 years (from 1980 to 2012) indicated that there were differences ($p < 0.05$) between TDK8 and TDK11 for days to anthesis, days to harvest, biomass and harvest index, whereas there was no difference ($p > 0.05$) between TDK8 and TDK11 in terms of grain yield (Table 5). The results for simulated data showed that TDK8 flowered at 83 DAT and had 122 days to harvest, whereas TDK11 bloomed at 76 DAT and could be harvested at 108 days. TDK8 was also higher than TDK11 in biomass production (13,712 and 12,354 kg ha^{-1} for TDK8 and TDK11, respectively), but it was lower than TDK11 as regards harvest index (0.31 and 0.34 for TDK8 and TDK11, respectively). However, these cultivars had no differences in grain yield (4,165 and 4,209 kg ha^{-1} for TDK8 and TDK11, respectively).

Table 3 – Simulated (S) and observed (O) values for days to harvest of TDK8 and TDK11 cultivars grown under different transplanting dates and N-fertilizer application rates in 2012 in Vientiane plain, Laos.

Cultivar	Transplanting date	No. of seedling hill^{-1}	N-fertilizer	Days to harvest (DAT[a])		
				S	O	S – O
			kg N ha^{-1}			
TDK8	13 June 2012	1	80	112	116	-4
	23 June 2012	5	129	115	114	+1
	1 July 2012	5	112	118	117	+1
	3 July 2012	5	80	115	115	0
	5 July 2012	5	73	113	115	-2
	7 July 2012	5	42	114	113	-1
TDK11	8 July 2012	5	117	103	103	0
	10 July 2012	5	73	98	101	-3
	15 July 2012	5	112	102	102	0

[a]DAT is days after transplanting.

Table 4 – Simulated (S) and observed (O) values, root mean square error (RMSE) and normalized RMSE ($RMSE_n$) for grain yield of TDK8 and TDK11 cultivars grown under different transplanting dates and N-fertilizer application rates in 2012 in Vientiane plain, Laos.

Cultivar	Transplanting date	No. of seedling hill^{-1}	N-fertilizer	Grain yield			
				S	O	RMSE	$RMSE_n$
			kg N ha^{-1}	kg ha^{-1}			%
TDK8	13 June 2012	1	80	4,023	3,825	114	3
	23 June 2012	5	129	5,190	5,100	52	1
	1 July 2012	5	112	4,633	4,888	147	3
	3 July 2012	5	80	3,922	3,975	31	1
	5 July 2012	5	73	3,352	3,613	150	4
	7 July 2012	5	42	2,437	3,400	556	16
TDK11	8 July 2012	5	117	4,337	4,250	50	1
	10 July 2012	5	73	3,029	2,763	154	6
	15 July 2012	5	112	4,121	4,038	48	1

Table 5 – Simulated days to anthesis, days to harvest, biomass and grain yield of TDK8 and TDK11 for two plant densities, three rates of N-fertilizer application and eight transplanting dates for 33 years (from 1980 to 2012) in the Vientiane plain, Laos.

Management	Days to anthesis[a] (DAT[b])		Days to harvest[a] (DAT[b])		Biomass[a] (kg ha^{-1})		Grain yield[a] (kg ha^{-1})		Harvest index[a]	
	TDK8	TDK11	TDK8	TDK11	TDK8	TDK11	TDK8	TDK11	TDK8	TDK11
Plant density										
1 Seedling hill^{-1}	83 A	76 A	124 A	110 A	13,518 B	11,996 B	4,154 A	4,232 A	0.3128 A	0.3553 A
5 Seedlings hill^{-1}	82 B	75 B	121 B	106 B	13,905 A	12,712 A	4,177 A	4,186 B	0.3074 B	0.3326 B
$LSD_{0.05}$	0.18	0.17	0.24	0.22	60.09	55.60	29.81	24.00	0.002	0.001
N rate (kg N ha^{-1})										
0	82 B	75 B	120 C	106 C	9,097 C	8,669 C	2,850 C	2,954 C	0.3207 A	0.3460 A
60	83 A	76 A	122 B	108 B	14,472 B	13,270 B	4,405 B	4,556 B	0.3077 B	0.3456 A
120	83 A	76 A	124 A	109 A	17,566 A	15,123 A	5,241 A	5,117 A	0.3018 C	0.3404 B
$LSD_{0.05}$	0.22	0.21	0.30	0.27	73.60	68.09	36.51	29.39	0.002	0.002
Transplanting date										
15 Jan	82 D	74 D	114 F	101 F	14,811 C	13,953 B	4,889 A	4,766 A	0.3320 B	0.3414 D
15 June	85 A	78 A	120 E	108 C	11,096 H	10,383 H	3,760 G	3,840 F	0.3446 A	0.3726 A
30 June	84 B	78 A	121 D	108 C	11,552 G	10,610 G	3,769 G	3,823 F	0.3315 B	0.3637 B
15 July	83 C	77 B	120 E	107 D	12,331 F	11,203 F	3,893 F	3,861 F	0.3192 C	0.3472 C
30 July	82 D	75 C	120 E	106 E	13,036 E	11,597 E	4,080 D	3,940 E	0.3152 D	0.3406 D
15 Aug	82 D	75 C	123 C	107 D	14,131 D	12,304 D	4,341 C	4,247 D	0.3081 E	0.3449 C
30 Aug	82 D	75 C	128 B	111 B	15,669 B	13,589 C	4,601 B	4,571 C	0.2943 F	0.3366 E
15 Sept	82 D	74 D	130 A	114 A	17,066 A	15,192 A	3,990 E	4,624 B	0.2359 G	0.3047 F
$LSD_{0.05}$	0.37	0.34	0.49	0.45	120.18	111.20	59.62	47.99	0.003	0.003
Average[a]	83 a	76 b	122 a	108 b	13,712 a	12,354 b	4,165 a	4,209 a	0.3101 b	0.3440 a
$LSD_{0.05}$ for average	0.15		0.29		187.12		55.58		0.002	

[a]Values in the column (capital letters) and row (small letters) followed by the same letter are not different ($p < 0.05$). [b]DAT is days after transplanting.

Differences in plant population densities affected ($p < 0.05$) days to anthesis, days to harvest, biomass and harvest index for both cultivars, but it did not affect ($p > 0.05$) grain yield of TDK8 (Table 5). Biomass of TDK8 and TDK11 grown at 5 seedlings hill^{-1} was higher than that grown at 1 seedling hill^{-1}, but both TDK8 and TDK11 grown at 1 seedling hill^{-1} had a higher harvest index than those grown at 5 seedlings hill^{-1}.

N-fertilizer rates also affected ($p < 0.05$) days to anthesis, days to harvest, biomass, grain yield and harvest index for both rice cultivars (Table 5). For both cultivars with higher N-fertilizer application, days to anthesis and days to harvest were slightly delayed, whereas biomass and grain yield were increased. However, N-fertilizer reduced the harvest index in both cultivars.

Transplanting date affected ($p < 0.05$) days to anthesis, days to harvest, biomass, grain yield and harvest index (Table 5). The longest days to anthesis was recorded for the crop transplanted on 15 June in TDK8 (85 DAT) and 15 June and 30 June in TDK11 (78 DAT). Whereas the longest days to harvest was recorded for the crop transplanted on 15 Sept for both cultivars with 130 and 114 DAT for TDK8 and TDK11, respectively. The shortest periods of life cycle were recorded for both cultivars transplanted on 15 Jan.

The crop transplanted on 15 Sept produced the highest above ground biomass with 17,066 kg ha^{-1} for TDK8 and 15,192 kg ha^{-1} for TDK11. The crop grown on other transplanting dates during the period 15 June to 15 Aug had low biomass. The crop transplanted on 15 Jan produced the highest grain yield with 4,889 and 4,766 kg ha^{-1} for TDK8 and TDK11, respectively. TDK8 and TDK11 transplanted on 15 June had the highest harvest index. Both cultivars had the lowest harvest index when they were planted on 15 Sept.

According to simulated results for all management combinations, a delay in transplanting dates and an increase in the rate of N-fertilizer application could increase grain yields for all cultivars and plant densities, except for a combination of the crop transplanted on 15 Jan with 1 seedling hill^{-1} and 120 kg N ha^{-1} (Figure 2). A plant density of 5 seedlings hill^{-1} along with 120 kg N ha^{-1} and a transplanting date of 15 Jan had the highest average grain yield for both TDK8 (6,460 $\pm$ 403 kg ha^{-1}) and TDK11 (6,351 $\pm$ 410 kg ha^{-1}) when compared to the other management combinations. In addition, the range of the simulated rice grain yield around the median for this management combination was also small, especially in TDK8.

Contribution of N-fertilizer application to production cost, grain yield and income

Economic assessment for rice production under three rates of N-fertilizer application was also made by using the simulated results from 2012. The results indicated that N-fertilizer rates of 60 and 120 kg N ha^{-1} increased total production costs of 6 and 12 %, respectively, for both TDK8 and TDK11 (Table 6). N-fertilizer rates of 60 and 120 kg N ha^{-1} contributed to yield increases of 50 and 87 % for TDK8 and 54 and 70 % for TDK11, indicating that TDK8 responded to fertilizer application better than did TDK11. The net incomes for growing TDK8 with 0, 60 and 120 kg N ha^{-1} were 147.5, 563.0 and 855.2 US$ ha^{-1}, respectively, while the net incomes for growing TDK11 were 201.9, 678.5 and 794.5 US$ ha^{-1}, respectively. The relative net income for TDK8 went up by 382 and 580 % when the rate of N application was increased from 0 to 60 and 120 kg N ha^{-1}, respectively, it went up by 336 and 393 % for TDK11, respectively.

Discussion

Model evaluation

Differences in simulated data and observed data for days to harvest were in the range between +1 to -4 days and the major differences were TDK8 with N-fertilizer at a rate of 80 kg N ha^{-1} (-4 days) and TDK11 with N-fertilizer at a rate of 73 kg N ha^{-1} (-3 days). The differences were partially due to inaccuracy in determining crop maturity which caused harvest delays by farmers.

The differences between observed and simulated yields were not particularly great. Most differences between simulated yield and observed yield were lower than 10 % except for one crop cut which had a 16 % difference. The simulated results are considered acceptable if the difference between simulated yield and actual yield is lower than 10 % (Loague and Green, 1991). The disparities between the observed and simulated values were attributable to the fact that the crop in the actual farmers' fields had been affected by weeds, diseases and pests and other factors which were not taken into account by the model. In addition, error from fertility data could also result in differences between observation and simulation (Oteng-Darko et al., 2012; Yao et al., 2007).

The CSM-CERES-Rice model provided good simulated yields of glutinous lowland rice (Vilayvong et al., 2012). Overall, variations between observed and simulated yields are adequately accounted for and the CSM-CERES-Rice model could be used to determine the appropriate management practices for improving rice production in the Vientiane plain, Laos.

Simulation for different management scenarios

There was no difference in the yields of TDK8 and TDK11 although they were different in days to anthesis, days to harvest, biomass and harvest index. Difference in days to harvest is very useful for rice production. TDK11 may be better under terminal drought because it completes the life cycle earlier. Thus, it can alleviate the effect of terminal drought. In cases where soil preparation was delayed, TDK11 is also better than TDK8.

The increase in plant population density from 1 seedling hill^{-1} to 5 seedlings hill^{-1} slightly increased biomass and reduced harvest index, whereas grain yield seemed to be reduced for TDK11 cultivars. In previous investigations, 1 seedling hill^{-1} gave a higher net as-

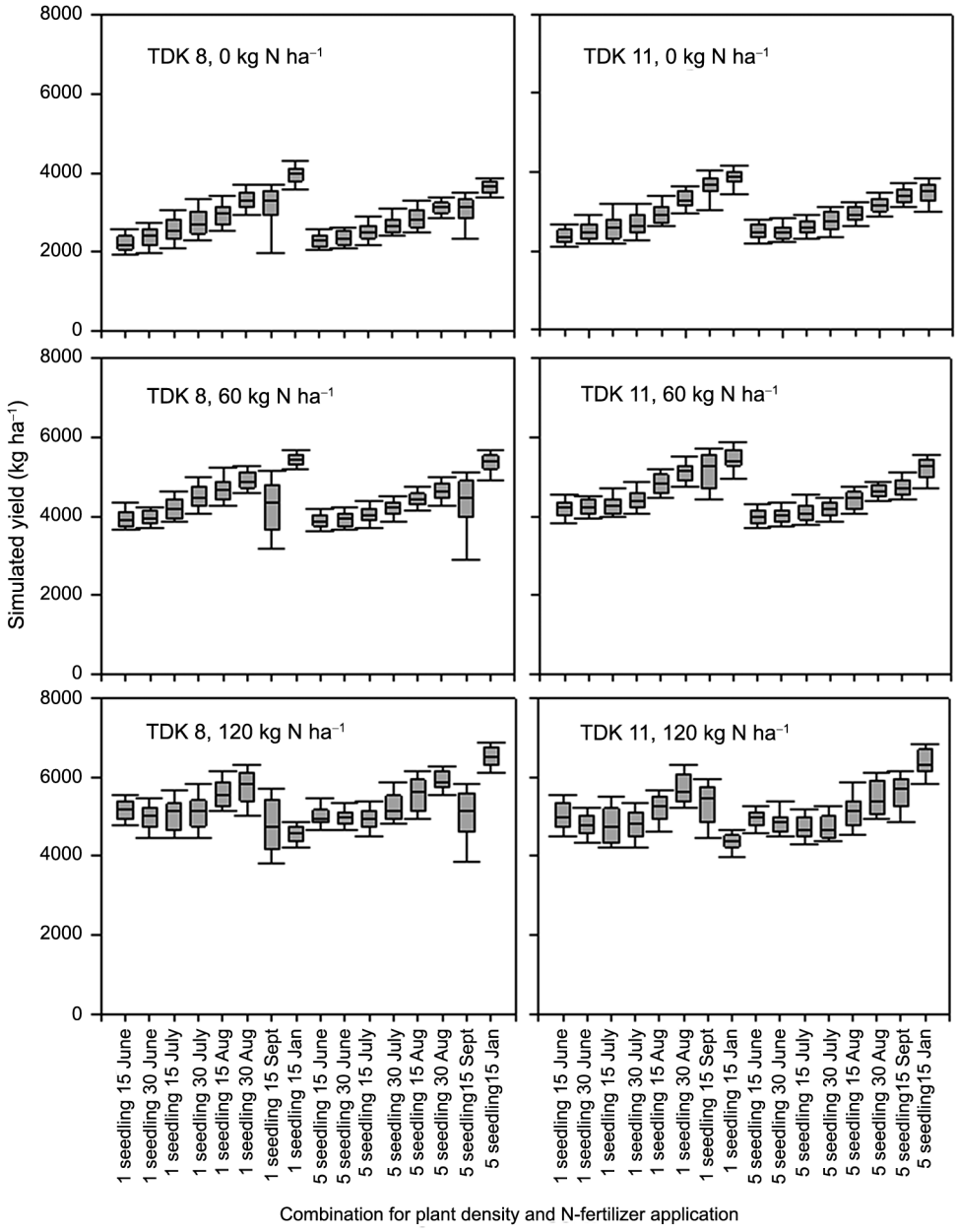


Figure 2 – Simulated grain yield for two rice cultivars, three rates of N-fertilizer application, two rates of plant density and eight planting dates. The model was run for 33 years (from 1980 to 2012) for two soil types in the Vientiane plain, Laos. Box limits represent the 25th and 75th percentiles, box central line represents the median and outliers represent the minimum and maximum values.

similation rate which is the physiological potential for converting the total dry matter into grain yield (Baloch et al., 2006). Similarly, plant density of 1 seedling hill^{-1} of rice gave higher grain when compared to plant density of 2 seedlings hill^{-1} (Srinivasulu et al., 1999). In this study, a high assimilation rate did not contribute much to grain yield because the crop grown at 5 seedlings hill^{-1} had higher biomass than the crop grown at 1 seedling hill^{-1}. Grain yield in this study seems to be related to the harvest index instead of biomass. However, attaining high grain yield may be difficult in different contexts because grain yield is dependent on several factors such as soil moisture, soil fertility, agronomic practices, pests and diseases.

Increases in N-fertilizer rates could increase both biomass and grain yield but they seemed to reduce harvest index. Greater increases in grain yield were found for N-fertilizer at a rate of 60 kg N ha^{-1} and grain yield

Table 6 – Contribution of N-fertilizer application on total production cost, simulated grain yield for 2012 and income for TDK8 and TDK11 cultivars in Vientiane plain, Laos.

Items	Cultivar and N-fertilizer rate (kg N ha^{-1})					
	TDK8			TDK11		
	0	60	120	0	60	120
Total production cost (US$ ha^{-1})	772.9	818.4	863.8	772.9	818.4	863.8
Relative total production cost (%)	100	106	112	100	106	112
Average simulated grain yield (kg ha^{-1})	2,789	4,186	5,209	2,954	4,536	5,025
Relative grain yield (%)	100	150	187	100	154	170
Gross income (US$ ha^{-1})[a]	920.4	1,381.4	1,719.0	974.8	1,496.9	1,658.3
Net income (US$ ha^{-1})	147.5	563.0	855.2	201.9	678.5	794.5
Relative net income (%)	100	382	580	100	336	393

[a]Price of grain rice: 0.33 US$ kg^{-1} in Vientiane, May 2013.

was increased albeit at a reducing rate when the crop was applied with N-fertilizer at a rate of 120 kg N ha^{-1}. Application of N-fertilizer supports crop growth and final yield (Baloch et al., 2006). If the crop is not labile to natural disasters such as flooding, drought, insect pests and diseases, higher N-fertilizer rate is highly recommended for attaining maximum yield and maximum profit.

Production of glutinous rice in this area depends heavily on N-fertilizer input. In this study, application of N-fertilizer at the rates of 60 and 120 kg N ha^{-1} increased total production costs for both cultivars by 6 and 12 %, respectively. At these N-fertilizer rates, changes in grain yield and net income were much higher than changes in production costs. In general, adding N-fertilizer application under good management conditions farmers could obtain a satisfactory income from their rice growing.

The farmers in Laos usually transplant rice in-season (from June to Aug) depending on rainfall and rain distribution and they can also grow off-season rice in Jan with irrigation. In this study, we simulated in-season rice starting from 15 June to 15 Sept (seven transplanting dates) and off-season rice on 15 Jan to understand the effects of the transplanting date on growth and yield. For in-season rice, delayed transplanting from June to Sept caused slightly early anthesis in both TDK8 and TDK11. However, both cultivars seemed to have increased days to harvest with late transplanting dates. These results are similar to the observed values measured by Vilayvong et al. (2012) who maintained that TDK8 and TDK11 are non-photosensitive cultivars. Therefore, the variation in transplanting times would also have a key effect on life duration of these rice cultivars (Fukai, 1999).

Both TDK8 and TDK11 increased biomass with late transplanting dates of in-season rice but they reduced harvest index. Growing rice off-season with a transplanting date of 15 Jan gave high biomass, grain yield and harvest index when compared to in-season rice. This was caused by high solar radiation during the growing season. The average values of solar radiation for the entire growing season were 19.9, 16.7, 15.9, 15.4, 15.1, 14.9, 14.8 and 14.8 MJ m^{-2} day^{-1} for the transplanting dates of 15 Jan, 15 Sept, 30 Aug, 15 Aug, 30 July, 15 July, 30 June and 15 June, respectively.

A high solar radiation value for the entire growing season contributes to the high level of crop yield (Banterng et al., 2010). Solar radiation provides the energy for the processes that drive photosynthesis, affecting carbohydrate partitioning and biomass growth of the individual plant components (Hoogenboom, 2000). Considering the transplanting date, therefore, farmers are recommended to grow rice under both rainfed and irrigated conditions on 15 Jan, 30 July, 15 Aug, 30 Aug and 15 Sept to attain acceptable grain yield.

The highest simulated grain yield for the combination of rice transplanted on 15 Jan with 5 seedlings hill^{-1} and 120 kg N ha^{-1} would be related to the effects of high solar radiation during crop life duration, high N-fertilizer input as well as suitable plant density. However, low values of simulated grain yields for the transplanting date of 15 Jan with 1 seedling hill^{-1} and 120 kg N ha^{-1} were also recorded and this because of over N-fertilizer application. The simulated output from the model indicated that stress or nutrient toxicity was the result of a high input of N-fertilizer during the panicle initiation stage to the beginning of the grain filling stage for the crop transplanted on 15 Jan along with 1 seedling hill^{-1} and 120 kg N ha^{-1} and it reduced the total number of panicles and ultimately grain yield. Under no N-fertilizer application, however, transplanting with 5 seedlings hill^{-1} may face nutrient deficiency stress during the panicle initiation phase.

We demonstrated how the CSM-CERES-rice model could potentially assist in the determination of crop management schemes for rice production in tropical regions such as Laos. The model could provide valuable information in the design of agricultural management practices that will increase rice production in the Vientiane plain. To be able to identify crop management practices for a specific region, however, we suggest that the results both from a few years of actual experiments and from long-term simulation should be used to help design the best recommendations.

Conclusion

CSM-CERES-Rice model is an alternative tool for determining management practices for lowland rice in

the Vientiane plain, Laos. The model evaluation results showed strong agreement between observed and simulated data. TDK8 and TDK11 cultivars were similar for grain yield. The transplanting methods of 1 seedling hill^{-1} and 5 seedlings hill^{-1} produced similar grain yield for TDK8. Application of N-fertilizer at the rates of 60 and 120 kg N ha^{-1} could increase grain yield and net income. The transplanting date of 15 Jan gave the highest grain yield for both TDK8 and TDK11 when compared with the other transplanting dates. The management combination of irrigated rice transplanted on 15 Jan with 5 seedlings hill^{-1} and N-fertilizer at 120 kg N ha^{-1} is recommended for improving lowland rice production in Laos.

Acknowledgements

This study was supported by the Thailand research fund through the CLMV-T DSS graduate degree program research initiative: 1st phase grant number RDG52O0003-LV05 of Assoc. Prof. Dr. Attachai Jintrawet, Chiang Mai University, Thailand. Assistance in conducting the work was received from the plant breeding research center for sustainable agriculture, Khon Kaen University, Khon Kaen, Thailand. Acknowledgement is also extended to Khon Kaen University and the Faculty of Agriculture for providing financial support for manuscript preparation activities.

References

Ahmad, S.; Ahmad, A.; Tojo Soler, C.M.; Ali, H.; Zia-Ul-Haq, M.; Anothai, J.; Hussain, A.; Hoogenboom, G.; Hasanuzzaman, M. 2012. Application of the CSM-CERES-Rice model for evaluation of plant density and nitrogen management of fine transplanted rice for an irrigated semiarid environment. Precision Agriculture 13: 200-218.

Baloch, M.S.; Awan, I.U.; Hassan, G. 2006. Growth and yield of rice as affected by transplanting dates and seedlings per hill under high temperature of Dera Ismail Khan, Pakistan. Journal of Zhejiang University SCIENCE B 7: 572-579.

Banterng, P.; Hoogenboom, G.; Patanothai, A.; Singh, P.; Wani S.P.; Pathak, P.; Tongpoonpol, S.; Atichart, S.; Srihaban, P.; Buranaviriyakul, S.; Jintrawet, A.; Nguyen, T.C. 2010. Application of the cropping system model (CSM)-CROPGRO-Soybean for determining optimum management strategies for soybean in tropical environments. Journal of Agronomy and Crop Science 196: 231-242.

Cheyglinted, S.; Ranamukhaarachchi, S.L.; Singh, G. 2001. Assessment of the CERES-Rice model for rice production in the central plain of Thailand. Journal of Agricultural Science 137: 289-298.

Fukai, S. 1999. Phenology in rainfed lowland rice. Field Crops Research 64: 51-60.

Geng, S.; Hess C.E.; Auburn, J. 1990. Sustainable agricultural systems: concepts and definitions. Journal of Agronomy and Crop Science 165: 73-85.

Gomez, K.A.; Gomez, A.A. 1984. Statistical Procedures for Agricultural Research. 2ed. John Wiley, New York, NY, USA.

Hoogenboom, G. 2000. Contribution of agrometeorology to the simulation of crop production and its applications. Agricultural and Forest Meteorology 103: 137-157.

Iqbal, S.; Ahmad, A.; Hussain, A.; Ali, M.A.; Khaliq, T.; Wajid, S.A. 2008. Influence of transplanting date and nitrogen management on productivity of paddy cultivars under variable environment. International Journal of Agriculture and Biology 10: 288-292.

Jones, J.W.; Hoogenboom, G.; Porter, C.H.; Boote, K.J.; Batchelor, W.D.; Hunt, L.A.; Wilkens, P.W.; Singh, U.; Gijsman, A.J.; Ritchie, J.T. 2003. The DSSAT cropping system model. European Journal of Agronomy 18: 235-265.

Lamsal, A.; Amgain, L.P. 2010. Simulation of growth and yield of rice under varied agronomic management and changing climatic scenario by using DSSAT ver. 4.0 crop model in Chitwan, Nepal. Journal of Hill Agriculture 1: 114-123.

Linquist, B.; Sengxua, P. 2001. Nutrient Management in Rainfed Lowland Rice in the Lao PDR. International Rice Research Institute, Los Banos, Philippines.

Loague, K.; Green, R.E. 1991. Statistical and graphical methods for evaluating solute transport models: overview and application. Journal of Contaminant Hydrology 7: 51-73.

Oteng-Darko, P.; Kyei-Baffour, N.; Ofori, E. 2012. Simulating rice yields under climate change scenarios using the CERES-Rice model. *African Crop Science Journal* 20: 401-408.

Sarkar, R.; Kar, S. 2006. Evaluation of management strategies for sustainable rice-wheat cropping system, using DSSAT seasonal analysis. Journal of Agricultural Sciences 144: 421-434.

Schiller, J.M.; Ladsavong, H.; Doungsila, K. 2006. A history of rice in Laos. p. 9-28. In: Schiller, J.M.; Chanphengxay, M.B.; Linqiust, B.; Appa Rao, S., eds. Rice in Laos. International Rice Research Institute, Los Banos, Philippines.

Singh, H.; Singh, K.N.; Hasan, B. 2007. Evaluation of CERES-rice model (V. 4.0) under temperate conditions of Kashmir valley, India. *Cereal Research Communications* 35: 1723-1732.

Srinivasulu, K.; Veeraraghavaiah, R.; Madhavi, K. 1999. Growth performance of rice hybrids under different methods and densities of planting. Crop Research 18: 1-7.

Timsina, J.; Connor, D.J. 2001. Productivity and management of rice-wheat cropping systems: issues and challenges. Field Crops Research 69: 93-132.

Timsina, J.; Humphreys, E. 2006. Performance of CERES-rice and CERES-wheat models in rice-wheat systems: a review. Agricultural System 90: 5-31.

Vilayvong, S.; Banterng, P.; Patanothai, A.; Pannangpetch, K. 2012. Evaluation of CSM-CERES-Rice in simulating the response of lowland rice cultivars to nitrogen application. Australian Journal of Crop Science 6: 1534-1541.

Wallach, D.; Goffinet, B. 1987. Mean squared error of prediction in models for studying ecological and agronomics systems. Biometrics 43: 561-573.

Yao, F.; Xu, Y.; Feng, Q.; Lin, E.; Yan, X. 2005. Simulation and validation of CERES-rice model in main rice ecological zones in China. Acta Agronomica Sinica 31: 545-550.

Yao, F.; Xu, Y.; Lin, E.; Yokozawa, M.; Zhang, J. 2007. Assessing the impacts of climate change on rice yields in the main rice areas of China. Climatic Change 80: 395-409.

Turkish Journal of FIELD CROPS

Turk J
Field Crops
2015, 20(2), 142-149

EVALUATION OF BLACK GLUTINOUS RICE GENOTYPES FOR STABILITY OF GAMMA ORYZANOL AND YIELD IN TROPICAL ENVIRONMENTS

Poramate BANTERNG[1,2] and Anchalee JORALEE[1]*

[1] Khon Kaen University, Faculty of Agriculture, Department of Plant Science and Agricultural Resources, Khon Kaen, THAILAND
[2] Khon Kaen University, Faculty of Agriculture, Plant Breeding Research Center for Sustainable Agriculture, Khon Kaen, THAILAND
[*]Corresponding author: bporam@kku.ac.th

Received: 29.09.2014

ABSTRACT

Gamma oryzanol is an important phytochemical of black glutinous rice as it has positive effects on human health. The objective of this study was to evaluate stability of gamma oryzanol content and grain yield for black glutinous rice genotypes grown under different environments. Twenty-five black glutinous rice genotypes and 2 white glutinous rice genotypes were evaluated during 2011 and 2012 in 8 farmers' fields of Thailand. The experimental trials were laid out in a randomized complete blocks design (RCBD) with 3 replications. Soil data before growing, weather data during growing season, yield components, grain yield and gamma oryzanol content were recorded. The results indicated that location (L), genotype (G) and G×L interaction were highly significant for number of panicles per hill, number of filled grains per panicle, 1000-grain weight, grain yield, gamma oryzanol per grain weight and gamma oryzanol yield. The GGE biplot analysis indicated that KKU-GL-BL-06-023 (V17), Khaokam Gs.no. 88084 (V5) and KKU-GL-BL-11-001 (V25) had both high mean performance and stability for grain yield. The superior genotypes for gamma oryzanol per grain weight were KKU-GL-BL-11-001 (V25) and KKU-GL-BL-06-043 (V23). The desirable genotypes for gamma oryzanol yield were KKU-GL-BL-11-001 (V25), Niewdam Gs.no. 21427 (V3) and KKU-GL-BL-06-043 (V23).

Key words: Breeding, Combined analysis, Germplasm, GGE biplot, Sticky rice

INTRODUCTION

Glutinous rice with purple or red color in pericarp (black glutinous rice) has been recognized in many countries of Asia. It has been used for making diverse products including functional food, drink, medicine and cosmetics. According to the popularity of healthy consumption trend in this present, black glutinous rice is considered as one of the crops with high potential for making such products. In addition, black glutinous rice is a crop thought to have herbal properties and it has been used traditionally in various kinds of medical treatments. The purple pigment (anthocyanin: cyaniding-3-glucoside) in the husk (hull) and pericarp and gamma oryzanol from rice bran oil are advantageous antioxidants (Xu et al., 2001; Juliano et al., 2005; Vorarat et al., 2010; Pitija et al., 2013). Black rice contained two to three times the amount of anthocyanin and gamma oryzanol higher than did white rice (Ryu et al., 1998; Boonsit et al., 2010). For gamma oryzanol, it is a mixture of phytosteryl ferulate esters in the rice bran oil (Bergman and Xu, 2003; Boonsit et al., 2010) with properties that are beneficial to health including improving the plasma lipid profile, reducing total plasma cholesterol, increasing high-density lipoprotein (HDL) cholesterol levels and inhibiting platelet aggregation (Cicero and Gaddi, 2001).

In Thailand, black glutinous rice has been increasingly attractive as a high value-added crop and it has become a key driving force in economic development. It is grown under rainfed condition in both upland and lowland environments. The farmers mostly grow local genotypes of black glutinous rice with low yield (Saenjum et al., 2012; Somsana et al., 2013). In order to improve the productivity, growing the suitable genotypes is an alternative option for sustainable farming systems. Therefore, growing the recommended rice genotypes with good adaptation to various environments and high yield is very important for the farmers. However, inconsistency of crop performance and yield in different environments has always been a problem and it also causes a big task for plant breeders (Romagosa and Fox, 1993; Yan and Hunt 2003; Sayar et al., 2013). The relative performances of rice genotypes for quantitative traits such as yield and

gamma oryzanol content varied from one environment to another (Bergman and Xu, 2003). If there is multitude of environment, it would also be difficult to develop suitable black glutinous rice genotypes for each environment. Thus, it seems more practical to determine and release a genotype with adaptation to more than a single environment. However, the research on this aspect for black glutinous rice in the tropical environments has been done very less so far. The objective of this study was to evaluate stability of gamma oryzanol content and grain yield for black glutinous rice genotypes grown under different environments.

MATERIALS AND METHODS

Twenty seven rice genotypes were used in this study (Table 1). Twenty-five black glutinous rice genotypes were obtained from Plant Breeding Research Center for Sustainable Agriculture, Faculty of Agriculture, Khon Kaen University, Thailand and 2 white glutinous rice genotypes were kindly donated from Rice Department of Thailand. The performances of all genotypes were evaluated in both upland and lowland conditions at a total of 8 farmers' fields during the main growing season of 2011 and 2012 in Khon Kaen province, Thailand (Table 2). The tested rice genotypes were laid out in a randomized complete blocks design (RCBD) with 3 replications. The entries were planted in the plots with 15 m^2 in size. For upland condition, five seeds were planted per hill with a plant spacing of 30 x 25 cm (Table 2) and seedlings were thinned to 3 plants per hill at 20 days after planting. All plots were fertilized at 45 days after planting with N, P_2O_5 and K_2O at the rate of 23.4 kg ha^{-1}. Urea fertilizer was also applied to all plots at the rate of 31.3 kg ha^{-1} during early booting stage. For lowland condition, rice seedlings at approximate 30 days old after planting were transplanted with a plant spacing of 25 x 25 cm and with 1 seedling per hill (Table 2). N, P_2O_5 and K_2O were applied for all experimental plots at 15 days after transplanting at the rate of 30, 30 and 15 kg ha^{-1}, respectively. Urea fertilizer was applied at the rate of 31.3 kg ha^{-1} during early booting stage. For both upland and lowland conditions, supplemental irrigation was supplied during the dry periods in the rainy season. Weeds, pests and diseases were controlled as necessary.

Table 1. Glutinous rice genotypes used for the study.

No.	Genotype name	No.	Genotype name
1	Niewdam Gs.no. 00621 (V1)	15	KKU-GL-BL-05-010 (V15)
2	Niewdam Gs.no. 09475 (V2)	16	KKU-GL-BL-05-011 (V16)
3	Niewdam Gs.no. 21427 (V3)	17	KKU-GL-BL-06-023 (V17)
4	Niewdam Gs.no. 21629 (V4)	18	KKU-GL-BL-06-034 (V18)
5	Khaokam Gs.no. 88084 (V5)	19	KKU-GL-BL-06-035 (V19)
6	Khaokam Gs.no. 87090 (V6)	20	KKU-GL-BL-06-038 (V20)
7	KKU-GL-BL-05-001 (V7)	21	KKU-GL-BL-06-039 (V21)
8	KKU-GL-BL-05-002 (V8)	22	KKU-GL-BL-06-041 (V22)
9	KKU-GL-BL-05-003 (V9)	23	KKU-GL-BL-06-043 (V23)
10	KKU-GL-BL-05-004 (V10)	24	KKU-GL-BL-06-050 (V24)
11	KKU-GL-BL-05-005 (V11)	25	KKU-GL-BL-11-001 (V25)
12	KKU-GL-BL-05-006 (V12)	26	RD6 (V26)
13	KKU-GL-BL-05-008 (V13)	27	HY 71 (V27)
14	KKU-GL-BL-05-009 (V14)		

Table 2. Location, land type and crop management for each experiment in Khon Kaen province, Thailand.

Location	Land type	Planting/Transplanting date	Spacing (cm x cm)
1. Ban Kham Pom (L1)	Upland	21 June 2011	30x25
2. Ban Wang Wa (L2)	Upland	18 June 2011	30x25
3. Ban Koh Nang Ngam (L3)	Lowland	6 August 2011	25x25
4. Ban Muang (L4)	Lowland	8 August 2011	25x25
5. Ban Kham Pom (L5)	Upland	23 June 2012	30x25
6. Ban Wang Wa (L6)	Upland	19 June 2012	30x25
7. Ban Nong Por (L7)	Lowland	14 August 2012	25x25
8. Ban Muang (L8)	Lowland	9 August 2012	25x25

For data collection, soil samples were collected from the experimental sites before the experiment was conducted at 3 spots and at the depths of 0-15 cm. The soil samples were then analysed for physical and chemical properties. Maximum and minimum air temperatures and rainfall during growing period were recorded from the nearest meteorological stations (Table 3). At final harvest, the 10 sub-samples of each experimental plot were randomly chosen to determine number of panicles per hill, number of filled grains per panicle and 1,000-grain weight. The center rows in each experimental plot were harvested to observe grain yield. In addition, gamma oryzanol values from rice bran of 27 tested genotypes were also recorded by using high performance liquid

chomatography (HPLC) method (Xu and Godber, 1999). Analysis of variance for individual locations and combined analysis of variances of 8 locations were performed by following the procedure described by Gomez and Gomez (1984). Duncan's multiple range test (DMRT) was also used to compare mean differences. All calculations were done using MSTAT-C package (Freed et al., 1989). Stability analysis was done by the GGE biplot method using the GGE biplot software (Yan, 2001). The GGE biplot was constructed from the first two components (PC1 and PC2) that were derived from subjecting environment-centered crop data to singular value decomposition (SVD).

Table 3. Soil property before land preparation and weather condition during the growing season for each experiment.

Location	Soil property						Weather condition		
	Textural class	Total N (%)	Available P (ppm)	Exchangeable K (ppm)	C.E.C. (c mol kg^{-1})	pH	Maximum temperature (^{o}C)	Minimum temperature (^{o}C)	Rainfall (mm)
1. Ban Kham Pom (L1)	Sand	0.02	15.5	31.6	1.7	5.5	31.60	23.12	864.4
2. Ban Wang Wa (L2)	Sand	0.01	8.2	19.3	3.9	5.3	31.65	23.21	865.9
3. Ban Koh Nang Ngam (L3)	Sandy Loam	0.10	9.2	100.8	14.1	5.2	31.53	23.17	1064.1
4. Ban Muang (L4)	Sand	0.03	5.4	47.5	3.9	5.4	31.53	23.21	1064.1
5. Ban Kham Pom (L5)	Sand	0.01	10.9	34.9	2.9	5.1	32.79	23.41	528.2
6. Ban Wang Wa (L6)	Sand	0.02	8.8	53.3	0.3	5.1	32.78	23.44	528.2
7. Ban Nong Por (L7)	Sandy Loam	0.02	3.6	52.4	2.8	6.2	32.53	23.66	544.4
8. Ban Muang (L8)	Sand	0.02	6.4	35.9	1.6	4.8	32.54	23.67	544.4

RESULTS AND DICUSSION

Combined analysis of variance

Location (L), genotype (G) and G×L interaction were highly significant (p<0.01) for number of panicles per hill, number of filled grains per panicle, 1000-grain weight, grain yield, gamma oryzanol per grain weight and gamma oryzanol yield (Table 4). The variations due to locations shared the largest portions of total variations for number of panicles per hill (45.7%), number of filled grains per panicle (52.2%) and 1000-grain weight (70.7%). The G×L interactions contributed to the large portions of total variations for grain yield (36.0%), gamma oryzanol per grain weight (32.7%) and gamma oryzanol yield (35.6%). The contributions of genotypic variations were rather small for number of panicles per hill, number of filled grains per panicle, 1000-grain weight, grain yield and gamma oryzanol yield when compared to the variation of locations. This indicated that growing environments had greater effect on these crop performances than did genotypes. In order to select the genotypes with optimized levels of these crop characteristics, therefore, it is necessary to grow the breeding materials in multiple years and environments.

Table 4. Mean squares for number of panicles per hill, number of filled grains per panicle, 1000-grain weight (g), grain yield (kg ha^{-1}), gamma oryzanol per grain weight (mg g^{-1} grain) and gamma oryzanol yield (g ha^{-1}) for 27 tested genotypes in 8 locations.

Source of variation	Degree of freedom	Mean square					
		Number of panicles per hill	Number of filled grains per panicle	1000-grain weight (g)	Grain yield (kg ha^{-1})	Gamma oryzanol per grain weight (mg g^{-1} grain)	Gamma oryzanol yield (g ha^{-1})
Location (L)	7	150.1 (45.7)**	30230.4 (52.2)**	839.6 (70.7)**	8632369.0 (27.6)**	0.08909 (28.3)**	961561.0 (29.4)**
Replication/L	16	6.4 (4.5)	547.8 (2.2)	3.7 (0.7)	312980.0 (2.3)	0.00223 (1.6)	61636.0 (4.3)
Genotype (G)	26	11.8 (13.4)**	2778.7 (17.8)**	30.5 (9.5)**	1036843.0 (12.3)**	0.0254 (29.9)**	86254.0 (9.8)**
G×L	182	3.0 (23.8)**	291.3 (13.1)**	5.7 (12.5)**	432147.0 (36.0)**	0.00396 (32.7)**	44827.0 (35.6)**
Pooled error	416	0.7 (12.7)	143.9 (14.8)	1.3 (6.5)	114207.0 (21.7)	0.0004 (7.5)	11504.0 (20.9)
Total	647						
%C.V. (GxE)		33.39	23.68	7.57	31.8	17.98	54.38
%C.V. (GxRxE)		11.16	12.14	4.43	19.21	7.64	23.5

Numbers within the parentheses are percent (%) of sum squares to total sum of squares.
** = significant difference (p<0.01)

For gamma oryzanol per grain weight, the results showed that genotypic variation was slightly higher than the variation due to locations, whereas the G×L interaction was observed. Therefore, the experiments in various environments are also still important for selecting rice genotypes with high level of this trait. A report from Bergman and Xu (2003) indicated that genotype and environment played a significant role in controlling gamma oryzanol per grain weight. They also suggested evaluation of the tested genotypes in multiple environments before selecting the best genotype with enhanced gamma oryzanol level.

Range of the tested environments

There were significant differences (p<0.01) for all crop traits among 8 environments. This could be explained by the differences in the weather and soil conditions as well as management practices. Means for all tested environments ranged from 5.90–9.27 for number of panicles per hill, 77.00–130.60 for number of filled grains per panicle, 21.79–29.26 g for 1000-grain weight, 1274.50–2155.27 kg ha^{-1}for grain yield, 0.224–0.323 mg g^{-1} grain for gamma oryzanol per grain weight and 323.83–662.64 g ha^{-1} for gamma oryzanol yield (Table 5).

Ban Koh Nang Ngam produced the highest values for number of filled grains per panicle, 1000-grain weight, grain yield, gamma oryzanol per grain weight and gamma oryzanol yield because Ban Koh Nang Ngam is a lowland environment with higher soil fertility as well as high total amount of rain fall during the crop duration (Table 2 and 3). In order to select the suitable location for yield and gamma oryzanol production, therefore, this location would be identified as more favorable environment for crop growth when compared with the others tested locations.

Table 5. Mean performance for number of panicles per hill, number of filled grains per panicle, 1000-grain weight (g), yield (kg ha^{-1}), gamma oryzanol per grain weight (mg g^{-1} grain) and gamma oryzanol yield (kg ha^{-1}) of 8 locations.

Location	Number of panicles per hill	Number of filled grains per panicle	1000-grain weight (g)	Grain yield (kg ha^{-1})	Gamma oryzanol per grain weight (mg g^{-1} grain)	Gamma oryzanol yield (g ha^{-1})
1. Ban Kham Pom (L1)	8.49 b	113.11 b	27.29 c	2155.27 a	0.224 g	476.50 b
2. Ban Wang Wa (L2)	8.08 c	98.01 c	28.61 b	1909.62 b	0.269 c	502.93 b
3. Ban Koh Nang Ngam (L3)	6.18 d	130.60 a	29.26 a	2097.35 a	0.323 a	662.64 a
4. Ban Muang (L4)	5.95 d	112.18 b	28.68 b	1689.14 c	0.298 b	483.19 b
5. Ban Kham Pom (L5)	8.34 bc	81.97 d	21.79 f	1331.90 d	0.236 f	323.83 d
6. Ban Wang Wa (L6)	9.27 a	77.45 d	23.78 d	1696.30 c	0.243 ef	400.77 c
7. Ban Nong Por (L7)	8.57 b	100.24 c	23.04 e	1919.80 b	0.250 de	472.83 b
8. Ban Muang (L8)	5.90 d	77.00 d	21.92 f	1274.50 d	0.257 d	328.56 d

Values in the column followed by the same letter (s) are not significantly different at the $p<0.01$ level by DMRT.

Performance and stability of rice genotypes

The results indicated significant differences ($p<0.01$) among tested genotypes for all crop traits. KKU-GL-BL-05-005 (V11) and KKU-GL-BL-05-008 (V13) had the highest means for number of panicles per hill with 8.66 and 8.64 panicles per hill, respectively. Whereas the highest means for number of filled grains per panicle were found for Niewdam Gs.no. 21427 (V3) (120.10) and Niewdam Gs.no. 00621 (V1) (116.73) (Table 6). For 1000-grain weight, KKU-GL-BL-05-004 (V10) and KKU-GL-BL-05-001 (V7) gave the highest values with 27.36 and 27.34 g, respectively.

RD6 (V26) gave the highest value of grain yield (2304 kg ha^{-1}) but the values for gamma oryzanol per grain weight (0.168 mg g^{-1} grain) and gamma oryzanol yield (409.4 g ha^{-1}) were rather low when compared with the other genotypes (Table 7). Niewdam Gs.no. 21427 (V3) and KKU-GL-BL-11-001 (V25) had the highest means for gamma oryzanol per grain weight with 0.327 and 0.318 mg g^{-1} grain, respectively, whereas the highest mean for gamma oryzanol yield was found for Niewdam Gs.no. 21629 (V4) (564.4 g ha^{-1}). Therefore, these genotypes with high mean performance would be recommended as the parental sources for further development of new rice genotypes with high productivity for both grain yield and gamma oryzanol content in plant breeding programs.

Based on gamma oryzanol per grain weight, the results also indicated that all 25 black glutinous rice genotypes had higher amount of gamma oryzanol per grain weight than did 2 white rice check genotypes, suggesting that these particular black rice genotypes would also have a higher amount of health and medicinal substances. Furthermore, anthocyanin involving free radical scavenging and antioxidant is also the main phytochemical in black rice (Pitija et al., 2013). Thus, black rice would be more advantageous for medicinal property and it is also a rice genetic resource for improving rice as a functional food crop.

Table 6. Mean performance for number of panicles per hill, number of filled grains per panicle and 1000-grain weight (g) of 27 tested genotypes in 8 locations.

Genotype name	Number of panicles per hill	Number of filled grains per panicle	1000-grain weight (g)
Niewdam Gs.no. 00621 (V1)	5.75 i	116.73 a	26.21 c-f
Niewdam Gs.no. 09475 (V2)	7.09 efg	106.55 bc	24.65 h-k
Niewdam Gs.no. 21427 (V3)	6.38 h	120.10 a	25.24 g-j
Niewdam Gs.no. 21629 (V4)	8.17 a-d	100.96 c-g	23.90 k
Khaokam Gs.no. 88084 (V5)	8.32 abc	94.36 d-g	24.13 k
Khaokam Gs.no. 87090 (V6)	7.53 def	104.53 bcd	24.58 h-k
KKU-GL-BL-05-001 (V7)	7.74 cde	92.05 gh	27.34 a
KKU-GL-BL-05-002 (V8)	7.44 efg	94.63 d-g	23.96 k
KKU-GL-BL-05-003 (V9)	8.37 abc	83.79 hi	26.85 a-d
KKU-GL-BL-05-004 (V10)	8.49 ab	77.54 i	27.36 a
KKU-GL-BL-05-005 (V11)	8.66 a	76.41 i	27.10 abc
KKU-GL-BL-05-006 (V12)	6.75 gh	107.2 bc	24.66 h-k
KKU-GL-BL-05-008 (V13)	8.64 a	93.59 e-h	26.13 d-g
KKU-GL-BL-05-009 (V14)	7.78 b-e	92.63 fgh	25.86 efg
KKU-GL-BL-05-010 (V15)	7.75 cde	83.63 hi	24.19 k
KKU-GL-BL-05-011 (V16)	7.45 d-g	113.83 ab	26.43 a-f
KKU-GL-BL-06-023 (V17)	8.36 abc	93.44 e-h	27.26 ab
KKU-GL-BL-06-034 (V18)	7.27 efg	107.06 bc	25.20 g-j
KKU-GL-BL-06-035 (V19)	6.90 fgh	103.91 b-e	26.38 b-f
KKU-GL-BL-06-038 (V20)	7.20 efg	98.13 c-g	25.55 fgh
KKU-GL-BL-06-039 (V21)	7.71 cde	98.09 c-g	25.49 f-i
KKU-GL-BL-06-041 (V22)	7.24 efg	103.44 cde	26.23 c-f
KKU-GL-BL-06-043 (V23)	7.37 efg	100.54 c-g	24.75 h-k
KKU-GL-BL-06-050 (V24)	7.53 def	102.61 c-f	26.66 a-e
KKU-GL-BL-11-001 (V25)	7.18 efg	103.6 cde	24.54 ijk
RD6 (V26)	8.34 abc	106.45 bc	24.64 h-k
HY 71 (V27)	7.79 b-e	92.46 fgh	24.49 jk

Values in the column followed by the same letter (s) are not significantly different at the $p<0.01$ level by DMRT.

Table 7. Mean performance and ranking for yield (kg ha^{-1}), gamma oryzanol per grain weight (mg g^{-1} grain) and gamma oryzanol yield (kg ha^{-1}) of 27 tested genotypes in 8 locations.

Genotype name	Grain yield		Gamma oryzanol per grain weight		Gamma oryzanol yield	
	Mean (kg ha^{-1})	Rank	Mean (mg g^{-1} grain)	Rank	Mean (g ha^{-1})	Rank
RD6 (V26)	2304 a	1	0.168 n	27	409.4 f-i	21
KKU-GL-BL-06-023 (V17)	2203 ab	2	0.223 m	25	487.0 a-f	9
Khaokam Gs.no. 88084 (V5)	2023 bc	3	0.247 kl	21	506.4 a-e	6
KKU-GL-BL-05-001 (V7)	2012 bc	4	0.245 kl	22	491.7 a-f	8
Niewdam Gs.no. 21629 (V4)	1998 bc	5	0.285 cde	6	564.4 a	1
KKU-GL-BL-06-050 (V24)	1872 cd	6	0.262 h-k	15	480.1 a-f	10
KKU-GL-BL-05-011 (V16)	1810 cde	7	0.242 l	23	427.9 d-i	17
KKU-GL-BL-11-001 (V25)	1801 cde	8	0.318 a	2	556.7 ab	3
HY 71 (V27)	1792 cde	9	0.214 m	26	400.8 f-i	24
KKU-GL-BL-05-008 (V13)	1789 cde	10	0.252 i-l	18	453.1 c-h	14
KKU-GL-BL-06-043 (V23)	1788 cde	11	0.302 b	3	531.3 abc	4
Niewdam Gs.no. 09475 (V2)	1782 cde	12	0.289 bc	4	520.5 a-d	5
KKU-GL-BL-06-041 (V22)	1763 cde	13	0.28 c-g	9	492.1 a-f	7
Niewdam Gs.no. 21427 (V3)	1752 c-f	14	0.327 a	1	561.7 ab	2
Khaokam Gs.no. 87090 (V6)	1682 d-g	15	0.269 e-h	11	447.8 c-h	15
KKU-GL-BL-06-034 (V18)	1673 d-g	16	0.262 h-k	14	407.6 f-i	22
KKU-GL-BL-05-005 (V11)	1661 d-g	17	0.272 d-h	10	442.2 c-i	16
Niewdam Gs.no. 00621 (V1)	1658 d-g	18	0.282 c-f	8	477.1 a-f	11
KKU-GL-BL-06-038 (V20)	1644 d-g	19	0.288 bcd	5	470.0 b-g	12
KKU-GL-BL-05-003 (V9)	1634 d-g	20	0.259 h-k	17	411.0 f-i	20
KKU-GL-BL-05-004 (V10)	1633 d-g	21	0.261 h-k	16	417.1 e-i	18
KKU-GL-BL-05-006 (V12)	1627 d-g	22	0.227 m	24	378.9 ghi	25
KKU-GL-BL-05-009 (V14)	1619 d-g	23	0.285 cde	7	461.7 c-g	13
KKU-GL-BL-06-035 (V19)	1600 d-g	24	0.248 kl	20	401.4 f-i	23
KKU-GL-BL-06-039 (V21)	1534 efg	25	0.267 f-i	12	415.2 e-i	19
KKU-GL-BL-05-002 (V8)	1460 fg	26	0.249 jkl	19	360.1 hi	26
KKU-GL-BL-05-010 (V15)	1387 g	27	0.265 g-j	13	349.8 i	27

Values in the column followed by the same letter (s) are not significantly different at the $p<0.01$ level by DMRT.

The significance of G×L interactions for all crop traits indicated the differential response of varying genotypes under change in the environments and the difficulty in identifying the superior genotypes. High G×L interaction complicates plant breeding programs to explore the superior genotypes in various environments (Comstock and Moll, 1963). Numerous methods have been commonly proposed to reveal patterns of interaction

between genotypes and environments and to assess stability of the genotypes across various environments. In present, however, the GGE biplot method is an effective tool to consider both G and G×L interaction effects. It allows visual examination of the relationships among the test environments, genotypes and the G×L interactions (Yan, 2001). Therefore, it was used to evaluate mean performance and stability of each tested genotype in this study.

The results of mean performance and stability evaluation of 27 rice genotypes by GGE biplot method are shown in Figure 1 for number of panicles per hill, number of filled grains per panicle and 1,000-grain weight and Figure 2 for yield, gamma oryzanol per grain weight and gamma oryzanol yield. An ideal genotype should have high mean performance and be absolutely stable. In each figure, a small circle in the center of a biplot indicates average environment coordination (AEC) which is the average of environmental PC1 and PC2 scores. The center of the concentric circles represents the position of a reference for genotype evaluation. A genotype is more favorable if it is closer to the concentric circles. The genotype on the right side of the line with double arrows has yield performance greater than mean yield, whereas the genotype on the left side of this line has yield less than mean yield. The ideal position is defined by a projection on the mean-environment axis that equals the longest vector of the genotypes having above-average mean yield and by a zero projection on to the perpendicular line (Yan and Hunt 2003).

Based on the results from GGE biplot, there were different desirable genotypes in different crop traits. KKU-GL-BL-05-008 (V13), KKU-GL-BL-06-023 (V17), RD6 (V26) and Khaokam Gs.no. 88084 (V5) were close to the concentric center, and they can be considered as genotypes with both high mean performance and stability for number of panicles per hill (Figure 1), whereas the genotypes with high mean performance and stability for number of filled grains per panicle were KKU-GL-BL-05-006 (V12), Niewdam Gs.no. 09475 (V2) and RD6 (V26). For 1,000-grain weight, KKU-GL-BL-05-004 (V10), KKU-GL-BL-06-050 (V24), KKU-GL-BL-05-011 (V16) and KKU-GL-BL-06-035 (V19) showed good performance in both mean and stability when compared to the other genotypes.

According to GGE biplot for grain yield in Figure 2, more close to concentric circle indicated that KKU-GL-BL-06-023 (V17), Khaokam Gs.no. 88084 (V5) and KKU-GL-BL-11-001 (V25) had both high mean performance and stability. RD6 (V26) had high mean performance genotype as it was located on far right hand side of the line with double arrows. However, a long projection on to the perpendicular line indicated that this genotype had rather low yield stability. The best genotypes in term of both high mean performance and stability for gamma oryzanol per grain weight were KKU-GL-BL-11-001 (V25) and KKU-GL-BL-06-043 (V23), whereas the best genotypes for gamma oryzanol yield were KKU-GL-BL-11-001 (V25), Niewdam Gs.no. 21427 (V3) and KKU-GL-BL-06-043 (V23).

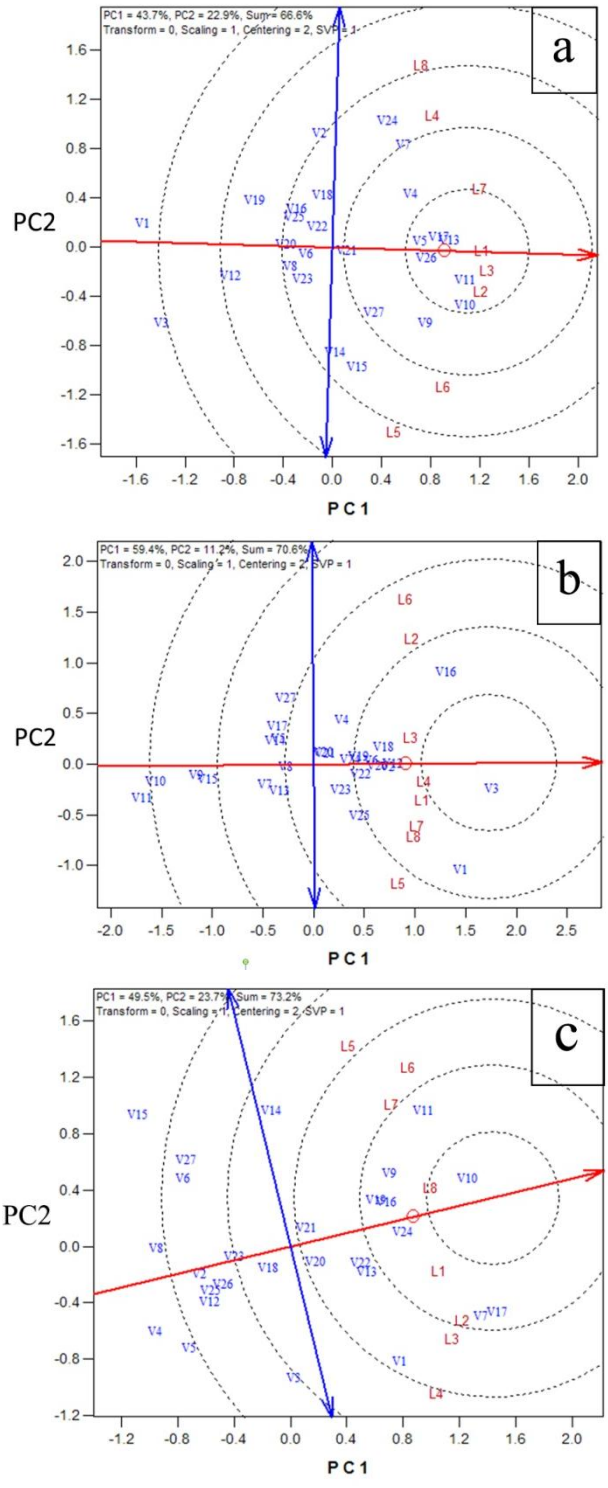


Figure 1. Number of panicles per hill (a), number of filled grains per panicle (b) and 1,000-grain weight (c) comparisons of 27 tested genotypes (see Table 1 and 2 for genotype and location descriptions, respectively) in 8 locations, using GGE-biplot (PC 1 and PC 2 are first and second principal components, respectively).

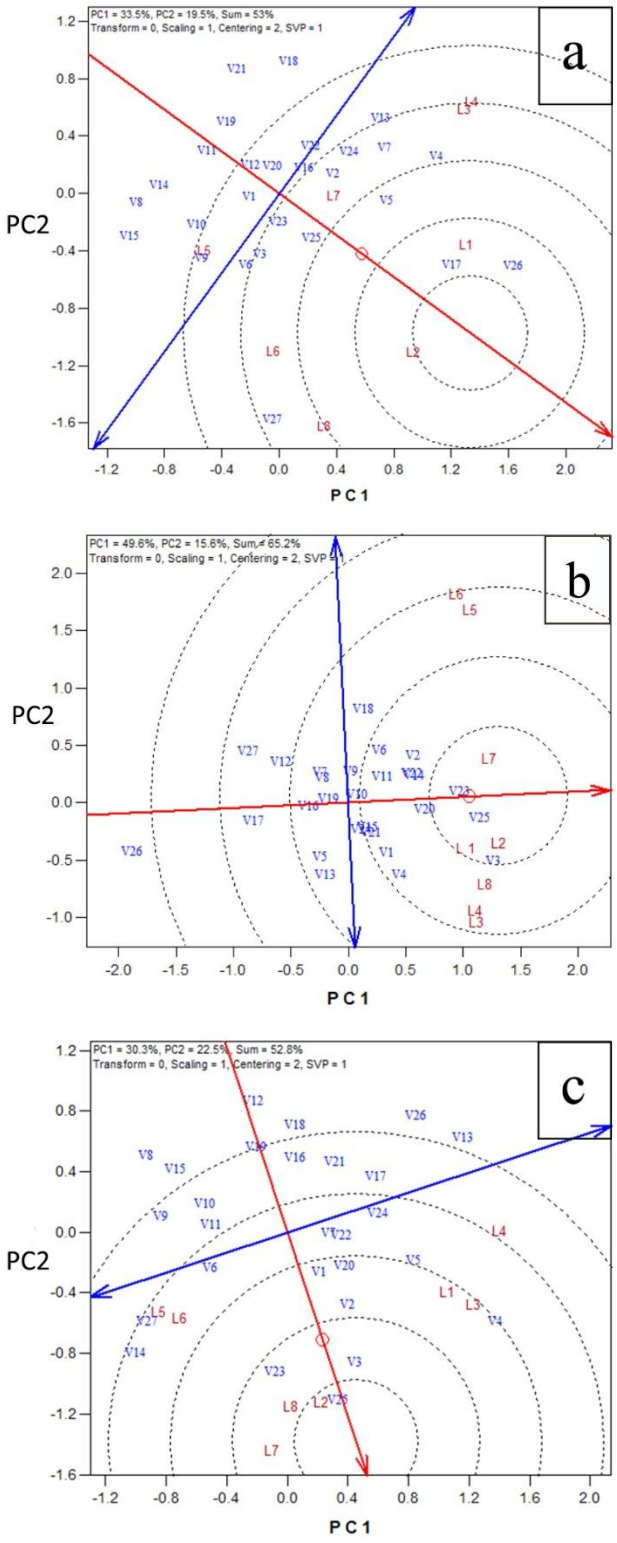


Figure 2. Yield (a), gamma oryzanol per grain weight (b) and gamma oryzanol yield (c) comparisons of 27 tested genotypes (see Table 1 and 2 for genotype and location descriptions, respectively) in 8 locations, using GGE-biplot (PC 1 and PC 2 are first and second principal components, respectively).

Although all recorded crop traits are very important for genotype evaluation across various environments, in this study, however, we paid more emphasis in grain yield, gamma oryzanol per grain weight and gamma oryzanol yield. When these three crop traits were considered, KKU-GL-BL-11-001 (V25) was identified as one of desirable genotypes in term of both high mean performance and stability. The analysis results indicated that this genotype had higher general adaptability when compared to the other tested genotypes. Therefore, it would be recommended as a parental genotype for further improvement in breeding programs and for growing in a commercial scale under both lowland and upland in tropical environments.

In addition, based on the purpose of gamma oryzanol extraction for pharmaceutical and cosmetic industries, the rice genotypes with high gamma oryzanol content per grain weight are more preferable than the genotypes with high gamma oryzanol yield per area. Not only KKU-GL-BL-11-001 (V25), therefore, Niewdam Gs.no. 21427 (V3) and KKU-GL-BL-06-043 (V23) would also be selected for this particular aspect. However, the results showed that these three genotypes are not the highest yielding genotypes. This indicates that breeding to improve both yield and gamma oryzanol content in rice is also the challenge for plant breeders.

CONCLUSION

The combined analysis of variance revealed that there were the significant effect of L, G and G×L interaction for number of panicles per hill, number of filled grains per panicle, 1000-grain weight, grain yield, gamma oryzanol per grain weight and gamma oryzanol yield. The G×L interactions shared the largest portion of total variations for grain yield (36.0%), gamma oryzanol per grain weight (32.7%) and gamma oryzanol yield (35.6%). The results from GGE biplot analysis indicated that KKU-GL-BL-06-023 (V17), Khaokam Gs.no. 88084 (V5) and KKU-GL-BL-11-001 (V25) were the superior genotypes for both high mean performance and stability in grain yield. The best genotypes for gamma oryzanol per grain weight were KKU-GL-BL-11-001 (V25) and KKU-GL-BL-06-043 (V23), whereas the desirable genotypes for gamma oryzanol yield were KKU-GL-BL-11-001 (V25), Niewdam Gs.no. 21427 (V3) and KKU-GL-BL-06-043 (V23). This would be valuable information for black glutinous rice production with high level of gamma oryzanol content and grain yield. It is also helpful information for plant breeders to improve gamma oryzanol content in rice.

ACKNOWLEDGEMENTS

This study was supported by Khon Kaen University, Thailand. Assistance in conducting the work was also received from the Plant Breeding Research Center for Sustainable Agriculture, Khon Kaen University. Acknowledgement is extended to the Thailand Research Fund (Project code : IRG5780003) and Faculty of Agriculture, Khon Kaen University for providing financial support for manuscript preparation activities.

LITERATURE CITED

Bergman, C.J. and Z. Xu. 2003. Genotype and environment effects on tocopherol, tocotrienol, and γ-oryzanol contents of southern U.S. rice. Cereal Chem. 80(4): 446–449.

Boonsit, P., P. Pongpiachan, S. Julsrigival and D. Karladee. 2010. Gamma oryzanol content in glutinous purple rice landrace varieties. C.M.U. J. Nat. Sci. 9(1): 151–157.

Cicero, A.F.G. and A. Gaddi. 2001. Rice bran oil and γ-oryzanol in the treatment of hyperlipoproteinemias and other conditions. Phytother. Res. 15: 277–289.

Comstock, R.E. and R.H. Moll. 1963. Genotype x Environment Interactions. Symposium on Statistical Genetics and Plant Breeding. In: Statistical Genetics and Plant Breeding, ed. Hanson, W.D. and Robinson H.F., 164–196, National Academy Science National Research Council No. 982, Washington, D.C.

Freed, R., S.P. Eisensmith, S. Goetz, D. Reicosky, V.W. Smail and P. Wolberg. 1989. User's Guide to MSTAT-C. East Lansing, MI: Michigan State University, USA.

Gomez, K.A. and A.A. Gomez. 1984. Statistical Procedures for Agricultural Research. 2nd ed. John Wiley and Sons, New York. 680 p.

Juliano, C., M. Cossu, M.C. Alamanni and L. Piu. 2005. Antioxidant activity of gamma-oryzanol: Mechanism of action and its effect on oxidative stability of pharmaceutical oils. Int. J. Pharm. 299: 146–154.

Pitija, K., M. Nakornriab, T. Sriseadka, A. Vanavichit and S. Wongpornchai. 2013. Anthocyanin content and antioxidant capacity in bran extracts of some Thai black rice varieties. Int. J. Food Sci Tech. 48: 300–308.

Romagasa, I. and P.N. Fox. 1993. Genotype x environment interaction and adaptation. In: Plant breeding, Principles and prospects, ed. Hayward, M.D., Bosemark, N.O. and Romagosa I., 373–387, Chapman & Hall, London.

Ryu, S.N., S.Z. Park and C.T. Ho. 1998. High performance liquid chromatographic determination of anthocyanin pigments in some varieties of black rice. J. Food Drug Anal. 6: 729–736.

Saenjum, C., C. Chaiyasut, S. Chansakaow, M. Suttajit and B. Sirithunyalug. 2012. Antioxidant and anti-inflammatory activities of gamma-oryzanol rich extracts from Thai purple rice bran. J. Med. Plants Res. 6(6): 1070–1077.

Sayar M.S., A.E. Anlarsal and M. Basbag. 2013. Genotype–environment interactions and stability analysis for dry-matter yield and seed yield in Hungarian vetch (*Vicia pannonica* Crantz.). Turk. J. Field Crops 18(2): 238-246.

Somsana, P., P. Wattana, B. Suriharn and J. Sanitchon. 2013. Stability and genotype by environment interactions for grain anthocyanin content of Thai black glutinous upland rice (*Oryza sativa*). SABRAO J. Breed. Genet. 45 (3): 523–532.

Vorarat, S., C. Managit, L. Iamthanakul, W. Soparat and N. Kamkaen. 2010. Examination of antioxidant activity and development of rice bran oil and gamma-oryzanol microemulsion. J. Health Res. 24(2): 67–72.

Xu, Z. and J.S. Godber. 1999. Purification and identification of components of γ-oryzanol in rice bran oil. J. Agric. Food Chem. 47: 2724–2728.

Xu, Z., N. Hua and J.S. Godber. 2001. Antioxidant activity of tocopherol, tocotrienols, and gamma-oryzanol components from rice bran against cholesterol oxidation accelerated by 2,2'-azobis(2-methylpropionamidine) dihydrochloride. J. Agric. Food Chem. 49: 2077–2081.

Yan, W. 2001. GGE biplot: A windows application for graphical analysis of multi-environment trail data and other types of two-way data. Agron. J. 93: 1111–1118.

Yan, W. and L.A. Hunt. 2003. Biplot analysis of multi-environment trial data. In: Quantitative Genetics, Genomics, and Plant Breeding, ed. Kang, M.S., 289–303, CAB International, Wallingford, Oxon, UK.

Turkish Journal of FIELD CROPS

Turkish Journal of Field Crops
2015, 20(1), 15-23

EFFECT OF LOCATION, GENOTYPE AND THEIR INTERACTIONS FOR ANTHOCYANINS AND ANTIOXIDANT ACTIVITIES OF PURPLE WAXY CORN COBS

Suchittra KHAMPAS[1], Kamol LERTRAT[1, 3], Khomsorn LOMTHAISONG[2], Sakunkan SIMLA[4], Bhalang SURIHARN [1, 3]*

[1]Khon Kaen University, Faculty of Agriculture, Department of Plant Science and Agricultural Resources, Khon Kaen, THAILAND
[2]Khon Kaen University, Faculty of Science, Department of Biochemistry, Khon Kaen, THAILAND
[3]Khon Kaen University, Plant Breeding Research Center for Sustainable Agriculture, Khon Kaen, THAILAND
[4]Mahasarakham University, Faculty of Technology, Department of Agricultural Technology, Mahasarakham, THAILAND
**Corresponding author: bsuriharn@gmail.com*

Received: 22.05.2014

ABSTRACT

Selection of purple waxy corn genotypes for high and stable anthocyanin content in corn cobs is important for breeding programs and anthocyanin production. The objectives of this study were to evaluate the effects of location, genotype and their interaction on anthocyanin content and antioxidant activities and to identify purple waxy corn genotypes with high and stable anthocyanin content. Five purple waxy corn and a white waxy corn genotypes were evaluated in a randomized complete block design with three replications at four locations with different elevations in Thailand. Location (L), genotype (G) and GxL interaction were significant for all characters. Waxy corn grown in Nakhon Ratchasima had the highest total anthocyanin content (TAC), cyanidin 3-glucoside (C3G), pelargonidin 3-glucoside (Pg3G), and peonidin 3-glucoside (Pn3G), DPPH radical scavenging activity of phenolics (DPPH) and Trolox equivalent antioxidant potential (TEAC). Genotype KNDM4 had the highest TAC, Pg3G, Pn3G and DPPH. Its regression coefficient (b_i) was close to one but it had the highest Sd^2, indicating specific adaptation to favorable environments. KNDM4 genotype performed better than other genotypes at unfavorable environments for all studied traits. This information is useful for breeding programs and anthocyanin production from purple waxy corn.

Keywords: Anthocyanin production, Different elevations, Favorable environments, Regression coefficient, Specific adaptation

INTRODUCTION

Waxy corn (*Zea mays* L. var. *ceratina*) is an important vegetable crop in East and Southeast Asia including China, Vietnam, Cambodia, Taiwan, Korea and Thailand. The world production of vegetable waxy corn is low compared to field corn and sweet corn. It is popular among people in these countries because of its glutinous starch in endosperm due to high amylopectin. Unlike field corn, waxy corn has received little interest for genetic improvement through breeding. The increase in demand for waxy corn and market potential arouses more attention from breeders to improve waxy corn. There are numerous special cultivars that contain colored pigments and give rise to numerous varieties of black and purple corn. Purple corn produced the anthocyanin pigment throughout the plant, especially high in the husk and cob regions, although anthocyanin levels varied significantly among different plant parts (Li et al., 2008).

Anthocyanins have health benefits in reducing the incidence of cardiovascular disease, cancer, hyperlipidemias and other chronic diseases (de Pascual-Teresa and Sanchez-Ballesta, 2008; Wang and Stoner, 2008). Purple waxy corn genotypes had the highest total anthocyanin and antioxidant activity in seed at both immature and harvesting stages in comparison with white waxy corn, super sweet corn and field corn (Khampas et al., 2013). Recently, a study showed that purple waxy corn is a source of anthocyanins with a protective property against diabetic cataract (Thiraphatthanavong et al., 2014). Kernels and cobs of purple corn possess an excellent antioxidant activity, and the application of these natural food colorants by the food industry would be increased

considerably (Yang and Zhai, 2010). Corn cob contributed the most in phenolic compounds and antioxidant capacity, and can be considered as excellent novel sources of natural antioxidants for the functional food and dietary supplement markets (Cevallos-Casals and Cisneros-Zevallos, 2003). This makes it more attractive for nutraceutical and functional food market.

High and stable yield across a range of environments is the primary goal of plant breeding programs. Recently, breeding for high anthocyanins is a priority of waxy corn breeding program at Khon Kaen University as this character defines it possible use as colorants and functional food. Most previous studies on stability and genotype by environment interaction in agronomic traits of cereal crops have focused on yield and the studies on quality traits such anthocyanin content and antioxidant activity are still lacking (Altay, 2012; Mitrović et al., 2012; Mohammadi et al., 2012). In wheat, cultivars Kate A1 and Mufitbey were found to be the most stable genotypes for all the environments whereas cultivar Gerek-79 was found to be the best performer for under poor soil and weather conditions (Altay, 2012), and significant genotype×environment interactions were observed among wheat genotypes (Altay, 2012; Mohammadi et al., 2012). In maize, environment accounted for the largest portion (77.83%) of total variation in grain yield, whereas genotype and genotype by environment accounted for 30% of total variation (Mitrović et al., 2012).

Several factors such as genetic, agronomic, pH, temperature, light intensity, type of light, and metallic ions, processing and storage affect anthocyanin stability (Bordignon-Luiz et al., 2007; de Rosso and Mercadante 2007; Mollov et al., 2007; Veigas et al., 2007; de Pascual-Teresa and Sanchez-Ballesta, 2008). Anthocyanin was mainly affected by pH and temperature (Cevallos-Casals and Cisneros-Zevallos, 2004). However, Zhao et al. (2008) found that anthocyanin in five Chinese purple corn hybrids was rather stable across a wide range of temperatures and times. Soil potassium concentration and population density did not significantly affect anthocyanin concentration in cobs, but growing location affected anthocyanin levels and the percentage of anthocyanins to total phenolics (Jing et al., 2007).

However, effects of various factors such as genotypes, environments and their interaction on purple waxy corn anthocyanin have not been adequately studied. The objectives of this study were to evaluate the effects of location, genotype and their interaction on anthocyanin content and antioxidant activities and to identify purple waxy corn genotypes with high and stable anthocyanin content. The information obtained from this study is important for breeding of waxy corn for high anthocyanin content and antioxidant activity and selection of locations for production of waxy corn for use as raw material for functional food products.

MATERIAL AND METHODS

Plant Materials

Five purple waxy corn genotypes (KGW1, KGW2, KGW3, KNDM4 and Fancy 111) and one white waxy corn genotype (Fancy 121) were used as plant material in the study (Table 1). Most of them are F_1 hybrids except for KNDM4, which is an open-pollinated variety (Hussanun et al., 2014).

Table 1. The waxy corn varieties used in this study.

Genotypes	Seed color	Cob color	Types
1. KGW1	Purple	Purple	Hybrid
2. KGW2	Purple	Purple	Hybrid
3. KGW3	Purple	Purple	Hybrid
4. KNDM4	Purple	Purple	Opened-pollinated
5. FANCY 111[1/]	Purple	Purple	Hybrid
6. FANCY 121[1/]	White	White	Hybrid

[1/] Commercial variety

Field Experiment

Six genotypes of waxy corn were evaluated in a randomized complete block design with three replications at four locations (Saraburi, Khon Kaen, Nakhon Ratchasima and Chiang Rai) with differences in elevations from 120 to 380 meters above sea level in the dry season 2012/13. These locations represented waxy corn growing areas in Thailand from the central plain to the North of Thailand. The details of locations were presented in Table 2.

Table 2. The testing locations used in this study.

Locations	Geographical coordinates	Elevations (masl)	Planting date
Saraburi	N 14° 43′ E 100° 47′	120	Dec 2012
Khon Kaen	N 16° 28′ E 102° 49′	200	Nov 2012
Nakhon Ratchasima	N 14° 30′ E 101° 30′	356	Dec 2012
Chiang Rai	N 20° 24′ E 99° 53′	380	Feb 2013

The genotypes were grown in four-row plots with 5 m long and spacing of 0.80 m between rows and 0.25 m between plants within rows. Recommended cultural practices were used for all locations. The crop at all location was well-irrigated for optimum growth and yield. Sprinkler irrigation was available at the locations in Khon Kaen, Nakhon Ratchasima and Chiang Rai, whereas furrow irrigation was performed in Saraburi.

15-15-15 Fertilizer of N-P-K as basal dose at the rate of 171 kg ha^{-1} was incorporated into the soil during soil preparation. Two splits of the fertilizer at the rate of 93.75 kg ha^{-1} plus urea (46-0-0) at the rate of 93.75 kg ha^{-1} for

first split and the fertilizer at the rate of 125 kg ha^{-1} plus urea at the rate of 62.5 kg ha^{-1} for second split were applied to the crop at 14 days after planting (DAP) and 30 DAP, respectively. At flowering stage, 13-13-21fertilizer was applied at the rate of 156.25 kg ha^{-1}. Therefore, total dose of fertilizers consisted of 150.65 kg ha^{-1} nitrogen, 78.78 kg ha^{-1} phosphorus and 91.27 kg ha^{-1} potassium, respectively. Weather and soil data for all locations were presented in Table 3 and Table 4, respectively.

Table 3. Weather data at four locations.

Days after planting	Average Temperature (^oC)	Solar radiation ($MJ\ m^{-2}day^{-1}$)	Total rainfall (mm)	Relative humanity (%)
Saraburi				
0-30	28.5	15.3	49	68.7
31-60	27.1	17.8	0	62.7
61-90	29.7	18.9	3	66.8
mean	28.4	17.3		66.1
Khon Kaen				
0-30	26.9	17.1	23	60.0
31-60	23.7	17.6	0	52
61-90	26.7	17.1	6	52
mean	25.8	17.3		78.6
Nakhon Ratchasima				
0-30	25.1	16.9	5	68.4
31-60	25.0	18.2	46	62.4
61-90	26.7	19.7	42	71.1
mean	25.6	18.3		67.3
Chiang Rai				
0-30	25.2	16.9	53	74.3
31-60	27.1	19.8	8	71.4
61-90	28.8	20.8	84	62.3
mean	27.0	19.2		69.4

Table 4. Soil physical and chemical properties.

Locations	Soil types	pH (1:1 H_20)	EC (1:5 H_20) (dS/m)	Organic Matter (%)	Total nitrogen (%)	Available Phosphorus (mg/kg)	Available potassium (mg/kg)	Available calcium (mg/kg)
Saraburi	Sandy loam	7.4	0.09	1.22	0.06	234	155	2,432
Khon Kaen	Sandy	4.9	0.01	0.73	0.03	307	139	54
Nakhon Ratchasima	Loamy sand	7.1	0.13	2.49	0.13	52	162	3,137
Chiang Rai	Loamy sand	5.6	0.08	3.40	0.09	45	149	593

Corn cobs were collected at harvest maturity stage (R6) or 90 days after planting and stored at room temperature for analysis of anthocyanin and antioxidant activity. Data were recorded for total anthocyanin content (TAC), cyanidin 3-glucoside (C3G), pelargonidin 3-glucoside (Pg3G), and peonidin 3-glucoside (Pn3G), DPPH radical scavenging activity of phenolics (DPPH) and the Trolox equivalent anti-oxidant potential (TEAC) as described by Yang et al. (2008).

Sample extraction

The portions of 0.5 g cob powder samples were weighted and pounded to fine powder using mortar and pestle. The extraction method used for TAC and antioxidant activity analysis was modified from the method reported previously (Yang et al., 2008). The samples were extracted in 25 ml of methanol containing 1% 1 M citric acid in falcon tubes. The mixtures were vortexed and stored at 4 ºC for 24 hours. The homogenates were centrifuged at 5000 rpm at 4 ºC for 15 minutes. After centrifugation, the mixtures were acquired by filtration through Whatman No.1 filter papers, adjusted to 25 ml and stored in dark room at -20 ºC until analysis for TAC and antioxidant activity.

Analysis of total anthocyanin content (TAC)

TAC was quantified by pH differential method (Giusti and Wrolstad, 2001). The absorbance of diluted extracts was measured to detect anthocyanins level at 510 nm and 700 nm with UV-Visible Spectrophotometer (model Specord 250 plus, Analytik jena, Germany) against a blank cell filled with distilled water. The absorbance was calculated as Abs = (Abs_{510} - A_{700}) pH 1.0-(Abs_{510}-A_{700}) pH 4.5. Then monomeric anthocyanin pigment in samples was calculated as;

Monomeric anthocyanin pigment = (Abs x MW x DF X 1000)/(ε x 1),

Where MW is the molecular weight of cyanidin 3-glucoside (MW of 449.2 g/mol), DF is dilution factor of the sample and ε is the molar extinction coefficient (Equal to 26900 M^{-1} cm^{-1}).

Anthocyanin levels were presented in mg of cyanidin 3-glucoside equivalents (CGE) per 100 g of dry weight (DW).

HPLC analysis of anthocyanin components

Total anthocyanin content was determined by the method described by Kim et al. (2007) with minor modification, and individual anthocyanin components were quantified with high-performance liquid chromatography (HPLC), Shimadzu LC-20AC pushes (Shimadzu Co., Kyoto, Japan), SPD-M20A with a photodiode array detector (Waters, USA). A XselectCHS C-18 line (4.6 mm x 250 mm, i.d. 5 µm). The extracts of cob samples were filtered through a 0.22 µm filter at 30 °C. The anthocyanins were eluted at 1 mL/min using gradient system consisting of two solvents: (A) acidified methanol (methanol 0.1% HCl, 85:15, v/v) and (B) 10% formic acid. The gradient elutions of solvent B were performed as follows: for 0.0-0.5 min (80%), 0.5-9.5 min (15%), 9.5-10.0 min (5%), 10.0-15.0 min (80%), and 15.0-20.0 min (80%). The divided solutions were consequently detected and identified at 520 nm for chromatographic retention times. Three purified anthocyanins consist of cyanidin 3-glucoside, pelargonidin 3-glucoside, and peonidin 3-glucoside and one anthocyanidin (cyanidin chloride) (Sigma, USA) were used for quantification.

The purified anthocyanins extractions were utilized to aid the identification of individual anthocyanins. The standard solutions were prepared in acidified methanol (pH 1) by weighing exactly 200-300 µg in 200 µL; 20 µL of standard solutions and then diluted to 500 µL to prepare working standard. The standard anthocyanins revealed a linear relationship with a HPLC optimum peak area with a concentration range of 0.0-1.0 µg. The coefficient of dedication (r^2) varied from 0.9933 to 0.9998 for a mixture of purified anthocyanins, which were divided by HPLC using 5, 10, and 15 µL of operating standard solution.

Analysis of antioxidant activity

DPPH radical scavenging activity of methanolic extracts was determined according to Xu et al. (2010). Briefly, 0.5 mL of sample extract was added and mixed with 4.5 mL of 60 µM DPPH demolished in methanol. The mixture was shaken thoroughly and allowed to stand for half an hour in the dark room. The absorbance was detected at 517 nm against the solvent blank. Trolox solution (100-1000 µM) was used as a reference conventional. The outcomes were provided in micromoles Trolox equivalents (TE) per g of DW.

Analysis of Trolox equivalent antioxidant capacity (TEAC) measured by the reduction in radical cation of ABTS by anti-oxidants was carried out as previously described by Jemai et al. (2009). Briefly, ABTS+ radical cation was conducted with a result of 7 mmol/L ABTS and 2.45 mmol/L potassium per sulfate. The combination was allowed to stay in dark room at ambient temperature 16-24 hours prior to use and should be used within 2 days. The ABTS solution was diluted with methanol for absorbance of 0.700 ± 0.050 at 734 nm. All samples were diluted appropriately to provide 20-80% inhibition of the blank absorbance. 50 µL of the diluted extract was taken by a pipette and combined with 1.9 mL of diluted ABTS solution. The analysis of the combination was performed in three replications. The combination was allowed to stand for 6 min at ambient temperature and the absorbance was instantly measured at 734 nm. Trolox solution (100-1000 µM) was used as a reference point. The outcomes were indicated as micromoles Trolox equivalents (TE) per g of DW.

Statistical Analysis

Data for each location were analyzed separately and error variances were tested for variance homogeneity. As variances were homogeneous and the differences of error variances were not larger than 3 folds, then combined analysis of variance was performed across the locations. Linear regression was carried out to study stability of corn genotypes by plotting cultivar's means against environmental means for each genotype as described by Eberhart and Russell (1966). Means were compared statistically using least significant difference (LSD) at $P \leq 0.05$.

RESULTS AND DISCUSSION

Variations in anthocyanin and antioxidant activity

Location (L), genotype (G) and GxL interaction were significant ($P \leq 0.01$) for total anthocyanin content (TAC), cyanidin 3-glucoside (C3G), pelargonidin 3-glucoside (Pg3G), and peonidin 3-glucoside (Pn3G), DPPH radical scavenging activity of phenolics (DPPH) and the Trolox equivalent anti-oxidant potential (TEAC) (Table 5). Location contributed to large portions of total variations in TAC (44%), C3G (56%), Pg3G (60%), Pn3G (62%), DPPH (52%) and TEAC (57%).

Genotype contributed to relatively large portion of total variation in TAC (42%), but genotype contributed to rather small portions of total variations in C3G (18%), Pg3G (20%), Pn3G (2%), DPPH (24%) and TEAC (11%). G x L interactions contributed to medium to small portions of total variations in TAC (13%), C3G (25%), Pg3G (20%), Pn3G (15%), DPPH (22%) and TEAC (32%).

Anthocyanins are phytochemicals that commonly occur in many cereal and fruit crops, and the trait is quantitatively inherited (Vizzotto et al., 2007). In corn, anthocyanins are present in all tissues and found at high concentrations in kernel skin and cobs (Moreno et al., 2005). In fruit crops such as grape, grapes may be either white or colored, ranging from the lightest pink to the darkest purple tones according to the amount of

anthocyanin accumulated in the berry skin, which is a crucial trait for both wine quality and human nutrition (Fournier-Level et al., 2009). In peach, anthocyanin content, phenolic content, and antioxidant activity were higher in red-flesh than in light-colored flesh peaches (Vizzotto et al., 2007). Genetic variation in anthocyanins has been reported in maize (Chander et al., 2008), grape (Fournier-Level et al., 2009) and wheat (Knievel et al., 2009). The results indicated that selection for high TAC would be possible among purple waxy corn genotypes. Variation among locations also indicated the importance of selection for the best location for anthocyanin production in corn.

Table 5. Mean squares for total anthocyanin content (TAC), cyanidin 3-glucoside (C3G), pelargonidin 3-glucoside (Pg3G), and peonidin 3-glucoside (Pn3G), DPPH radical scavenging activity of phenolics (DPPH) and the Trolox equivalent anti-oxidant potential (TEAC) of six waxy corn lines/cultivars.

SOV	df	TAC mg/100 gDW	C3G mg/100 gDW	Pg3G mg/100 gDW	Pn3G mg/100 gDW	DPPH µmol/gDW	TEAC µmol/gDW
Location (L)	3	1,004,062** (44)	60,464** (56)	6,320** (60)	1,564** (62)	179.4** (52)	86.1** (57)
Replication (R)/L (a)	8	432	50	6	2	1.4	0.1
Genotype (G)	4	15,975** (42)	14,582** (18)	1,542** (20)	411** (2)	61.4** (24)	12.3** (11)
G x L	12	75,107** (13)	6,596** (25)	512** (20)	96** (15)	18.5** (22)	12.0** (32)
Error (b)	32	2,726	67	5	3	0.4	0.1
C.V. (%) (a)		4.1	15.6	14.0	12.5	8.0	7.5
C.V. (%) (b)		10.3	18.1	12.0	15.2	4.1	5.4

** Highly significant difference at $p \leq 0.01$
Values in parenthesis are percentages of sum squares.

Effects of location and genotype on anthocyanins and antioxidant activity

Location was the main source of variation in TAC, C3G, Pg3G, Pn3G, DPPH and TEAC of five purple waxy corns and one white waxy corn. Nakhon Ratchasima had the highest TAC of 730 mg/100 gDW followed by 418 mg/100 gDW in Saraburi, whereas Khon Kaen and Chiang Rai had rather low TAC, accounting for 275 and 271 mg/100 gDW, respectively (Table 6). Similar patterns were also observed for C3G, Pg3G, Pn3G and DPPH. For these parameters, Nakhon Ratchasima was still highest followed by Saraburi, whereas Khon Kaen and Chiang Rai were similar and lower than Nakhon Ratchasima and Saraburi. Nakhon Ratchasima was also highest for TAEC followed by Khon Kaen, Saraburi and Chiang Rai, respectively.

In general, the highest TAC and anthocyanin components in corn cobs were found in Nakhon Ratchasima compared to the nearest locations in Khon Kaen and Saraburi. Nakhon Ratchasima is located at higher alleviation and had lower temperature during growing season and lower phosphorus. Low temperature and low phosphorus might be the cause of the high TAC and its components.

Low temperature induced anthocyanin synthesis in maize seedlings (Christie et al., 1994). Anthocyanin concentration increased rapidly during low temperature in apple and peach shoots (Leng et al., 2000). Anthocyanins and phenolics contents were enhanced with higher light intensity and lower temperature in potato tubers (Reyes et al., 2004). Visible and UVB radiation, cold temperatures and water stress has been shown to induce anthocyanin synthesis in plant tissue (Chalker-Scott, 1999).

However, low temperatures in the absence of either visible light or UVB prevent anthocyanin biosynthesis (Janda et al., 1996; Oren-Shamir and Levi-Nissim, 1997). Wang and Zheng (2001) also found that high temperature (30/22 day/night ^{o}C) condition enhanced phenolic acid, flavonols, and anthocyanins in strawberry.

Phosphorus deficiency induces anthocyanins accumulation in maize (Cobbina and Miller, 1987). Antocyanin content was increased and growth was decreased on nitrogen and phosphorus deficiency in Cruciferous (Hodges and Nozzolillo 1996). However, Chiang Rai also had low phosphorus but it had the lowest anthocyanins possibly due to high temperature and high solar radiation during reproductive periods. It should be note that stresses of low temperature and low phosphorus were the factors enhancing anthocyanin accumulation.

Nakhon Ratchasima (low temperature and low phosphorus) also had the highest antioxidant activities (DPPH and TEAC) but Chiang Rai (high temperature and low phosphorus) had the lowest highest antioxidant activities. These results were in agreement with previous study of Lachman et al. (2008) who reported that low temperature during vegetative period showed high antioxidant activity in potatoes.

Table 6. Means for total anthocyanin content (TAC), cyanidin 3-glucoside (C3G), pelargonidin 3-glucoside (Pg3G), and peonidin 3-glucoside (Pn3G), DPPH radical scavenging activity of phenolics (DPPH) and the Trolox equivalent anti-oxidant potential (TEAC) of six waxy corn lines/cultivars evaluated in four locations 2012/13.

	Saraburi	Khon Kaen	Nakhon Ratchasima	Chiang Rai
TAC (mg/100gDW)				
KGW1	247^{j}	$67l^{m}$	609^{e}	129^{kl}
KGW2	449^{g}	341^{h}	982^{c}	373^{h}
KGW3	328^{hi}	263^{ij}	547^{ef}	330^{hi}
KNDM4	$1,132^{ab}$	826^{d}	$1,166^{a}$	490^{fg}
FANCY111	346^{h}	148^{k}	$1,076^{b}$	302^{hij}
FANCY121	4^{m}	6^{m}	3^{m}	2^{m}
Means	418^{B}	275^{C}	730^{A}	271^{C}
C3G (mg/100g DW)				
KGW1	5^{fg}	4^{fg}	37^{d}	1^{g}
KGW2	27^{de}	9^{fg}	246^{a}	2^{g}
KGW3	16^{ef}	7^{fg}	93^{b}	3^{g}
KNDM4	96^{b}	23^{e}	246^{a}	5^{fg}
FANCY111	9^{f}	2^{g}	72^{c}	1^{g}
FANCY121	1^{g}	1^{g}	1^{g}	1^{g}
Means	26^{B}	8^{C}	116^{A}	2^{D}
Pg3G (mg/100g DW)				
KGW1	3^{hi}	3^{hi}	9^{f}	2^{hi}
KGW2	11^{f}	5^{gh}	54^{c}	3^{hi}
KGW3	10^{f}	5^{ghi}	29^{d}	3^{hi}
KNDM4	30^{d}	15^{e}	86^{a}	7^{fg}
FANCY111	16^{e}	5^{gh}	63^{b}	3^{hi}
FANCY121	2^{hi}	2^{i}	2^{hi}	2^{hi}
Means	12^{B}	6^{C}	41^{A}	3^{D}
Pn3G (mg/100g DW)				
KGW1	3^{ghi}	3^{ghi}	5^{fg}	2^{i}
KGW2	15^{c}	7^{ef}	35^{a}	3^{ghi}
KGW3	9^{de}	5^{fg}	26^{b}	3^{ghi}
KNDM4	26^{b}	11^{d}	35^{a}	5^{fgh}
FANCY111	9^{de}	3^{ghi}	28^{b}	2^{hi}
FANCY121	2^{i}	1i	2^{i}	2^{i}
Means	11^{B}	5^{C}	22^{A}	3^{D}
DPPH (µmol/gDW)				
KGW1	11^{i}	10^{i}	18^{cde}	8^{jk}
KGW2	17^{ef}	14^{h}	18^{cd}	10^{i}
KGW3	17^{de}	13^{h}	19^{cd}	9^{j}
KNDM4	22^{a}	18^{cd}	15^{g}	16^{fg}
FANCY111	19^{c}	13^{h}	21^{b}	11^{i}
FANCY121	5^{l}	5^{l}	4^{l}	7^{k}
Means	15^{A}	12^{B}	16^{A}	10^{C}
TEAC (µmol/gDW)				
KGW1	0.8^{mn}	2.8^{h}	5.3_{e}	1.3^{kl}
KGW2	6.4^{d}	3.8^{g}	8.1^{b}	1.3^{lk}
KGW3	7.3^{c}	3.7^{g}	6.9^{c}	2.2^{ij}
KNDM4	1.1^{lm}	5.7^{e}	8.2^{b}	4.2^{f}
FANCY111	1.4^{k}	2.5^{hi}	10.2^{a}	2.1^{j}
FANCY121	0.3^{op}	0.0^{p}	0.0^{p}	0.5^{no}
Means	2.9^{B}	3.1^{B}	6.4^{A}	1.9^{C}

Means of varieties in the same column and means of locations in the same row with the same letter(s) are not significantly different at $P \leq 0.05$ by LSD

As the interactions between location and genotype were significant for all parameters, identification of the best genotypes for each parameter was difficult. The varieties that showed good performance in one location did not perform well in other locations. However, KNDM4 showed consistently the highest values for TAC, C3G, Pg3G and Pn3G across locations. High values for these parameters in KNDM4 would be due to the fact that it is an open-pollinated variety and other hybrids had one parent with white kernels. For DPPH, KNDM4 was highest in Saraburi, Khon Kaen and Chiang Rai, whereas FANCY111 was highest in Nakhon Ratchasima. For

TEAC, KNDM4 was the winner in two locations in Khon Kaen and Chiang Rai. FANCY111 was still highest in Nakhon Ratchasima, whereas KGW3 was highest in Saraburi. FANCY111, which is the waxy corn, showed consistently the lowest values for all parameters across locations.

Stability analysis for anthocyanins and antioxidant activity

The genotypes with stable yield should have high mean yield across locations, regression coefficient close to one (b_i=1) and deviation from regression (Sd^2) close to zero (Eberhart and Russell, 1966). KNDM4 had the highest TAC (903 mg/100 gDW) and regression coefficient close to one (0.9), but it showed high deviation from regression (254) (Table 7). KNDM4 was the highest variety for TAC across locations. It did not performed well under unfavorable environment in Chiang Rai but it was still better than others (Table 6). However, anthocyanins of KNDM4 was rather fluctuated across environments as it has high Sd^2. KNDM4 was suitable for favorable environments. KGW2 had the second rank for TAC (536 mg/100g DW), regression coefficient close to one (1.1) and low deviation from regression (67). This genotype was most stable for TAC across environments.

Table 7. Stability parameters for total anthocyanin content (TAC), cyanidin 3-glucoside (C3G), pelargonidin 3-glucoside (Pg3G), and peonidin 3-glucoside (Pn3G) of six waxy corn lines/cultivars.

Genotypes	TAC (mg/100 gDW)			C3G (mg /100 gDW)			Pg3G (mg /100 gDW)			Pn3G (mg /100 gDW)		
	Mean	b[1/]	Sd^2	Mean	b	Sd^2	Mean	b	Sd^2	Mean	b	Sd^2
Purple waxy corn												
KGW1	263[e]	0.9	34	12[e]	0.3**	2	4[e]	0.2**	1	3.5d	0.1**	0.4
KGW2	536[b]	1.1	67	71[b]	1.8	14	18[c]	1.2	2	15.1b	1.4**	0.3
KGW3	367[d]	0.5	45	30[c]	0.7	4	11[d]	0.6**	1	10.9c	1.0	1.7
KNDM4	903[a]	0.9	254	93[a]	1.7	24	35[a]	1.7**	3	19.2a	1.3	5.4
FANCY111	468[c]	1.6	120	21[d]	0.5	4	22[b]	1.4**	1	10.4c	1.1	1.9
White waxy corn												
FANCY121	4			1			2			1.9		

** Significant different from 1 at *P≤0.01*

Means in the same column with the same letter(s) were not significantly different at *P≤0.05* probability level by LSD.

[1/]Regression coefficients were analyzed without white waxy corn.

KNDM4 had the highest C3G (93 mg /100 gDW) followed by KGW2 (71 mg /100 gDW) and their regression coefficients were not different from one (1.7 and 1.8, respectively). However, their deviations from regression were high, indicating that they performed well under favorable conditions but performed poorly under unfavorable conditions (Chiang Rai). KGW1 had the lowest C3G (12 mg/100 gDW) and regression coefficient (0.3**) was significantly lower than one, indicating that this genotype had low C3G and stability for C3G across environments.

Regression coefficients for Pg3G for most genotypes were significantly different from one except KGW2, indicating that these genotypes were not stable for this trait. KNDM4 had the highest Pg3G of 35 mg/100 g DW followed by FANCY111 (22 mg/100g DW) but regression coefficients (1.7** and 1.4**, respectively) were significantly higher than one, indicating that these genotypes performed well under favorable conditions but they had low Pg3G under unfavorable conditions.

KNDM4 had the highest Pn3G (19.2 mg/100 gDW), regression coefficient close to one (1.3) and high deviation from regression. However, it performed best for all locations but it had low Pn3G under unfavorable conditions (Chiang Rai) (Table 5). KGW2 showed high Pn3G (15.1 mg/100 gDW) but it had regression coefficient higher than one (1.4**) and low deviation from regression, indicating that it performed well for Pn3G under favorable conditions but performed poorly under unfavorable conditions.

KNDM4 had the highest DPPH (18.0 μmol/gDW), regression coefficient smaller than one (0.3**) and high deviation from regression (13.6) (Table 8). This genotype showed good adaptation to favorable conditions but it had poor adaptation to unfavorable conditions. KGW3 and KGW2 had high TEAC and regression coefficient close to one with high deviation from regression. Therefore, they may be suitable for some specific conditions.

Table 8. Stability parameters for DPPH radical scavenging activity of phenolics (DPPH) and the Trolox equivalent anti-oxidant potential (TEAC) of six waxy corn lines/cultivars.

Genotypes	DPPH (µmol / gDW)			TEAC (µmol / gDW)		
	Mean	**b**	**Sd^2**	**Mean**	**b**	**Sd^2**
Purple waxy corn						
KGW1	11.8[d]	1.0	3.0	2.6[d]	0.8	0.9
KGW2	14.6[c]	1.1	0.3	4.9[ab]	1.0	2.0
KGW3	14.3[c]	1.3**	0.3	5.0[a]	0.6	2.4
KNDM4	18.0[a]	0.3**	13.6	4.8[b]	0.9	2.5
FANCY111	15.9[b]	1.3	1.3	4.1[c]	1.6**	1.5
White waxy corn						
FANCY121	5.2			0.2		

** Significant different from 1 at *P≤0.01*

Means in the same column with the same letter(s) were not significantly different at *P≤0.05* probability level by LSD.

Khampas et al. (2013) and Harakotr et al. (2014) reported that kernels of purple waxy corn had high TAC and antioxidant activity (DPPH, FRAP and TEAC). In this study, cobs of purple waxy corn also had high TAC and antioxidant activity, and cobs can be used for production of natural colorant with health benefits.

CONCLUSION

Location (L), genotype (G) and GxL interaction were highly significant for all characters. Location contributed to large portion of total variation in anthocyanin content and antioxidant activity in corn cobs, whereas genotype and genotype by location interaction contributed smaller portions of total variations in these traits. Nakhon Ratchasima, which was characterized by low temperature and low phosphorus, was the highest location for TAC and C3G. KNDM4 gave the highest TAC and C3G, and its regression coefficients (b) were close to one. However, KNDM4 also had the highest Sd^2, indicating that it had specific adaptation to favorable environments. KNDM4 performed well under unfavorable environments for all traits. This information is useful for breeding programs in multi-location trails and production of anthocyanins from purple waxy corn.

ACKNOWLEDGEMENTS

The project was funded by the Thailand Research Fund, the commission for High Education and Khon Kaen University through the Distinguished Research Professor Grant of Professor Dr. Aran Patanothai and the Plant Breeding Research Center for Sustainable Agriculture, Faculty of Agriculture, Khon Kaen University, Thailand. Acknowledgement is extended to Khon Kaen University and the Faculty of Agriculture for providing financial support for manuscript preparation activities.

LITERATURE CITED

Altay, F. 2012. Yield stability of some Turkish winter wheat (*Triticum aestivum* L.) genotypes in the western transitional zone of Turkey. Turk. J. Field Crops 17:129-134.

Bordignon-Luiz, M.T., C. Gauche, E.F. Gris and L.D. Falcao. 2007. Colour stability of anthocyanins from Isabel grapes (*Vitis labrusca* L.) in model systems. LWT-Food Sci. Technol. 40:594-599.

Cevallos-Casals, B.A. and L. Cisneros-Zevallos. 2003. Stoichiometric and kinetic studies of phenolic antioxidants from Andean purple corn and red-fleshed sweet potato. J. Agric. Food Chem. 51:3313-3319.

Cevallos-Casals, B.A. and L. Cisneros-Zevallos. 2004. Stability of anthocyanin-based aqueous extracts of Andean purple corn and redfleshed sweet potato compared to synthetic and natural colorants. Food Chem. 86:69-77.

Chalker-Scott, L. 1999. Environmental significance of anthocyanins in plant stress responses. J. Photochem. Photobiol. 70:1-9.

Chander, S., Y. Meng, Y. Zhang, J. Yan and J. Li. 2008. Comparison of nutritional traits variability in selected eighty-seven inbreds from Chinese maize (*Zea mays* L.) germplasm. J. Agric. Food Chem. 56:6506-6511.

Christie, P.J., M.R. Alfenito and V. Walbot. 1994. Impact of low-temperature stress on general phenylpropanoid and anthocyanin pathways: enhancement of transcript abundance and anthocyanin pigmentation in maize seedlings. Planta. 194:541-549.

Cobbina J. and M.H. Miller. 1987. Purpling in maize hybrids as influenced by temperature and soil phosphorus. Agron. J. 79:576-582.

de Pascual-Teresa S. and M.T. Sanchez-Ballesta. 2008. Anthocyanins: from plant to health. Phytochem. Rev. 7(12):281-299.

de Rosso, V.V. and A.Z. Mercadante. 2007. Evaluation of colour and stability of anthocyanins from tropical fruits in an isotonic soft drink system. Innovative Food Sci. Emerging Technol. 8:347-352.

Eberhart, S.A. and W.A. Russel. 1966. Stability parameters for controlling variation. Crop Sci. 6:36-40.

Fournier-Level, A., L. Le Cunff, C. Gomez, A. Doligez, A. Ageorges, C. Roux, Y. Bertrand, J.M. Souquet, V. Cheynier and P. This. 2009. Quantitative genetic bases of anthocyanin variation in grape (*Vitis vinifera* L. ssp. *sativa*) Berry: A Quantitative trait locus to quantitative trait nucleotide integrated study. Genetics 183:1127-1139.

Giusti, M.M. and R.E. Wrolstad. 2001. Characterization and measurement of anthocyanins by UV-visible spectroscopy. In: Current Protocol in Food Analytical Chemistry, ed. Wrolstad, R.E., 5:1-13, John Willy & Sons Inc., New York.

Harakotr, B., B. Suriharn, R. Tangwongchai, M.P. Scott and K. Lertrat. 2014. Anthocyanins and antioxidant activity in coloured waxy corn at different maturation stages. J. Funct. Foods 9:109-118.

Hodges D.M. and C. Nozzolillo. 1996. Anthocyanin and anthocyanoplast content of cruciferous seedlings subjected to mineral nutrient deficiencies. J. Plant Physiol. 147:749-754.

Hussanun, S., B. Suriharn, K. Lertrat. 2014. Yield and early maturity response to four cycles of modified mass selection in purple waxy corn. Turk. J. Field Crops 19:84-89.

Janda, T., G. Szalai and E. Paldi. 1996. Chlorophyll fluorescence and anthocyanin content in chilled maize plants after return to a non-chilling temperature under various irradiances. Biol. Plant. 38:625-627.

Jemai, H., M. Bouaziz and S. Sayadi. 2009. Phenolic composition, sugar contents and antioxidant activity of Tunisian sweet olive cultivar with regard to fruit ripening. J. Agric. Food Chem. 57:2961-2968.

Jing, P., V. Noriega, S.J. Schwartz and M.M. Giusti. 2007. Effects of growing conditions on purple corncob (*Zea mays* L.) anthocyanins. J. Agric. Food Chem. 55:8625-8629.

Khampas, S., K. Lertrat, K. Lomthaisong, and B. Suriharn. 2013. Variability in phytochemicals and antioxidant activity in corn at immaturity and physiological maturity stages. Inter. Food Res. J. 20:3149-3157.

Kim, M.J., J.N. Hyun, J.A. Kim, J.C. Park, M.Y. Kim, J.G. Kim, S.J. Lee, S.C. Chun and I.M. Chung. 2007. Relationship between phenolic compounds, anthocyanins content and antioxidant activity in colored barley germplasm. J. Agric. Food Chem. 55:4802-4809.

Knievel, D.C., E.S.M. Abdel-Aal, I. Rabalski, T. Nakamura and T. Hucl. 2009. Grain color development and the inheritance of high anthocyanin blue aleurone and purple pericarp in spring wheat (*Triticum aestivum* L.). J. Cereal Sci. 50:113-120.

Lachman, J., K. Hamouz, M. Orsák, V. Pivec and P. Dvořák. 2008. The influence of flesh colour and growing locality on polyphenolic content and antioxidant activity in potatoes. Sci. Hortic. 117:109-114.

Leng, P., H. Itamura, H. Yamamura and X.M. Deng. 2000. Anthocyanin accumulation in apple and peach shoots during cold acclimation. Sci. Hortic. 83:43-50.

Li, C.Y., H.W. Kim, S.R. Won, H.K. Min, K.J. Park, J.Y. Park, M.S. Ahn and H.I. Rhee. 2008. Corn husk as a potential source of anthocyanins. J. Agric. Food Chem. 56:11413-11416.

Mitrović, B., D. Stanisavljevi, S. Treski, M. Stojaković, M. Ivanović, G. Bekavac and M. Rajković. 2012. Evaluation of Experimental Maize Hybrids Tested in Multi-Location Trials Using AMMI and GGE Biplot Analyses. Turk. J. Field Crops 17:35-40.

Mohammadi, M., R. Karimizadeh, N. Sabaghnia and M.K. Shefazadeh. 2012. Genotype x environment interaction and yield stability analysis of new improved bread wheat genotypes. Turk. J. Field Crops 17:67-73.

Mollov, P., K. Mihalev, V. Shikov, N. Yoncheva and V. Karagyozov. 2007. Colour stability improvement of strawberry beverage by fortification with polyphenolic copigments naturally occurring in rose petals. Innovative Food Sci. Emerging Technol. 8:318-321.

Moreno, Y.S., G.S. Sánchez, D.R. Hernández, N.R. Lobato. 2005. Characterization of anthocyanin extracts from maize kernels. J. Chromatogr. Sci., 43:483-487.

Oren-Shamir, M. and A. Levi-Nissim 1997. UV-light effect on the leaf pigmentation of *Cotinus coggygria* 'Royal Purple'. Sci. Hort. 71:59-66.

Reyes, L.E., J.C. Miller, and L. Cisneros-Zevallos. 2004. Environmental conditions influence the content and yield of anthocyanins and total phenolics in purple- and red-flesh potatoes during tuber development. Amer. J. of Potato Res. 81:187-193.

Thiraphatthanavong, P., J. Wattanathorn, S. Muchimapura, W. Thukham-mee, P. Wannanon, T. Tong-un, B. Suriharn, and K. Lertrat. 2014. Preventive Effect of *Zea mays* L. (Purple Waxy Corn) on Experimental Diabetic Cataract. Biomed. Res. Int., 1-8.

Veigas, J.M., M.S. Narayan, P.M. Laxman and B. Neelwarne. 2007. Chemical nature, stability and bioefficacies of anthocyanins from fruit peel of *syzygium cumini* Skeels. Food Chem. 105:619-627.

Vizzotto, M., L. Cisneros-Zevallos and D.H. Byrne. 2007. Large variation found in the phytochemical and antioxidant activity of peach and plum germplasm. J. Amer. Soc. Hort. Sci. 132(3):334-340.

Wang, L. and G.D. Stoner. 2008. Anthocyanins and their role in cancer prevention. Cancer Lett. 269:281-290.

Wang, S.Y. and W. Zheng. 2001. Effects of plant growth temperature on antioxidant capacity in strawberry. J. Agric. Food Chem. 49:4977-4982.

Xu, J.G., Q.P. Hu, X.D. Wang, J.Y. Luo, Y. Liu and C.R. Tian. 2010. Changes in the main nutrients, phytochemicals, and antioxidant activity in yellow corn grain during maturation. J. Agric. Food Chem. 58:5751-5756.

Yang, Z., G. Fan, Z. Gu, Y. Han and Z. Chen. 2008. Optimization extraction of anthocyanins from purple corn (*Zea mays* L.) cob using tristimulus colorimetry. Eur. J. Lipid Sci. Tech. 227:409-415.

Yang, Z. and W. Zhai. 2010. Identification and antioxidant activity of anthocyanins extracted from the seed and cob of purple corn (*Zea mays* L.). Innovative Food Sci. Emerging Technol. 11:169-176.

Zhao, X., M. Corrales, C. Zhang, X. Hu, Y. Ma and B. Tauscher. 2008. Composition and thermal stability of anthocyanins from chinese purple corn (*Zea mays* L.). J Agric Food Chem. 56:10761-10766.

Eur J Plant Pathol (2015) 143:725–736
DOI 10.1007/s10658-015-0723-7

Phenotypic and genotypic responses of chili (*Capsicum annuum* L.) progressive lines with different resistant genes against anthracnose pathogen (*Colletotrichum* spp.)

Patcharaporn Suwor · Petcharat Thummabenjapone · Jirawat Sanitchon · Sanjeet Kumar · Suchila Techawongstien

Accepted: 22 July 2015 / Published online: 5 August 2015
© Koninklijke Nederlandse Planteziektenkundige Vereniging 2015

Abstract Anthracnose disease caused by *Colletotrichum* spp. is a serious disease of chili (*Capsicum annuum*), particularly in tropical countries. Host plant resistance breeding is one of the most effective disease management strategies. It requires identification of parents with genes resistant to *Colletotrichum* species predominant in a given region. For phenotypic evaluation, 35 chili lines consisting of progressive lines of *C. annuum* derived from *C. baccatum* PBC80 (34 lines) and from *C. chinense* PBC932 (one line) were inoculated with two aggressive isolates of *Colletotrichum acutatum* (Ca) and *C. capsici* (Cc) by injection into the pericarp of green and red-ripe fruit. Lesion diameters were scored at seven days after inoculation. Two simple sequence repeat (SSR) and one sequence characterized amplified region (SCAR) markers were used for validation in four progressive lines and three each of susceptible and resistant checks for genotypic response. The progressive lines were classified into 10 groups based on their responses to two pathogens and at the two fruit stages. Four progressive lines (101, 205, 210 and 215) were selected and used for developing crosses to combine resistance genes from two sources resistant to Ca and Cc at both fruit stages. Progressive lines derived from PBC80 showed DNA fragment 231 bp amplified by primer HpmsE032 associated with Cc at green fruit stages. Hence the HpmsE032 marker could be considered useful in the selection of resistant genotypes derived from PBC80.

Keywords DNA marker · Fruit rot · Hot pepper · Pathogenicity · Resistance

P. Suwor · P. Thummabenjapone · J. Sanitchon · S. Techawongstien (✉)
Department of Plant Science and Agricultural Resources, Faculty of Agriculture, Khon Kaen University, Khon Kaen 40002, Thailand
e-mail: suctec.kku@gmail.com

S. Kumar
AVRDC – The World Vegetable Center, P.O. Box 42, Shanhua, Tainan 74199, Taiwan

Introduction

Among the five domesticated species of the genus *Capsicum*, *C. annuum* L. is the most commonly cultivated for its pungent (chili) and non-pungent (sweet pepper) fruits valued as spices and vegetables. The cultivated area under chili around the world in 2013 was 3.91 million hectares, with 1.78 t/ha average productivity of dry chili pods (FAO 2013). The major chili producers in Asia are China, India, Indonesia and Thailand. In Thailand, chili is cultivated under irrigated and rain-fed production systems. Productivity is severely affected by anthracnose caused by the *Colletotrichum* species complex (Kim et al. 2008a; Than et al. 2008a). The pathogen can damage chili leaves and stems, but pre- and postharvest decay of mature fruit is the major cause of economic loss, which can be up to 80 % (Poonpolgul and Kumphai 2007). A number of *Colletotrichum* species have been found to be associated with chili anthracnose, of which *C. acutatum* J.H. Simmonds., and *C. capsici* (H.Syd.) E. Butl. and Bisby are most prevalent, aggressive and problematic in Thailand (Than et al.

2008a). The use of anthracnose-resistant cultivars is an integral component of cost effective and safer disease management tactics.

Breeding anthracnose-resistant cultivars remains challenging because of the presence of the *Colletotrichum* species complex, pathotypes within species, and poor understanding of their taxonomy (Than et al. 2008b). Commercially important *C. annuum* chilies are considered to be anthracnose-susceptible species. Broad spectrum resistance sources have been identified in *C. baccatum* L. (PBC80, PBC81, PI594137, PI497985-1 and PI260550) and *C. chinense* Jacq. (PBC932) (Montri et al. 2009; Park et al. 2009). PBC80 (VI046804) and PBC81 (VI046805) were resistant to most of the isolates, while PBC932 showed resistance to some isolates of *C. acutatum, C. capsici* and *C. gloeosporioide* (Benz.) Penz. and Sacc. (Kim et al. 2008b; Than et al. 2008a; Park et al. 2009). At AVRDC – The World Vegetable Center (AVRDC), Taiwan, resistance from *C. chinense* PBC932 was successfully transferred to *C. annuum* progressive lines through conventional backcrossing. In South Korea, resistance from *C. baccatum* PBC81 was introgressed into *C. annuum* by overcoming the interspecific hybridization barrier using embryo rescue (Yoon et al. 2006). At Maejo University, Thailand, putative anthracnose resistant *C. annuum* progressive lines were developed using *C. baccatum* PBC80 through embryo rescue (introgressed into susceptible lines PBC398 and PBC758). Depending on resistance sources, pathotypes and fruit maturity stages, inheritance of anthracnose resistance is reported to be polygenic (Voorrips et al. 2004; Lee et al. 2010), monogenic recessive (Pakdeevaraporn et al. 2005; Kim et al. 2008a, b, c) and duplicate genes (Lin et al. 2007).

In the recent past, sequence characterized amplified regions (SCAR) (Wang 2011) , simple sequence repeats (SSR) (Lee et al. 2010), sequence-tagged sites (STS), and cleavage amplified polymorphic sequences (CAPS) (Lee et al. 2011) markers associated with chili anthracnose resistance have been developed. Among these, SSR markers were developed for a resistance trait in PBC81 against *C. acutatum* (Korean isolate) and *C. capsici* (Thai isolate), while a SCAR marker was developed for a resistance trait in PBC932 against *C. acutatum* (Taiwanese isolate). To improve Thai chili varieties with good horticultural traits and resistance to anthracnose, it is necessary to incorporate resistance from diverse sources against locally prevalent pathogen isolates. We describe the results of phenotypic responses of an array of chili progressive lines derived from two sources of anthracnose resistance along with validation of molecular markers associated with anthracnose resistance in chili.

Materials and methods

Plant materials

Plant materials consisted of four groups of chili genotypes (Table 1). The first group included AVPP0207 (code 101) was a *C. annuum* progressive line possessing anthracnose resistance from *C. chinense* PBC932 in BC_3F_7 generation (Fig. 1). The second group included two subsets of 34 progressive lines (code 201–219 and code 220–234) possessing anthracnose resistance from *C. baccatum* PBC80 in BC_2F_4 generation (Fig. 1). Hence all these 35 lines were derived from interspecific cross and we used four lines in the crossing program to develop advanced populations, hence called "progressive lines" (Fig. 1; Table 1). Three *C. annuum* susceptible checks (code 301–303) constituted third group and the fourth group had three resistant checks (code 401–403) belonging to *C. chinense* and *C. baccatum* (Table 1). Forty-one plants of each progressive line were grown in a greenhouse during May – October 2011 at the Faculty of Agriculture, Khon Kaen University, Thailand. Sixty fruits (30 at the green stage and 30 at the red-ripe stage) of all 41 plants of each genotype were harvested and surface-sterilized in Clorox solution (0.25 % of NaOCl). Fruits were washed twice with sterile water, placed on a sterile paper towel and air-dried. Sterile fruits were separated into three replications in a completely randomized design and placed in a plastic moisture box (18× 28×11 cm).

For genotypic or marker analyses, four progressive lines (101, 205, 210 and 215) and three of each susceptible (301, 302 and 303) and resistant (401, 402 and 403) checks were selected (Table 1). The progressive lines were selected based on the expression of resistant reactions against either each or both isolates or at each or both fruit stages to combine resistance traits by developing three-way cross and generation advancement and selection (Fig. 1).

Table 1 Chili genotypes used for phenotypic and genotypic analysis with anthracnose resistance-associated markers during the rainy seasons of 2011

No.	Code	Name/Pedigree (species)	Status	No.	Code	Name/Pedigree (species)	Status
1	101[a]	AVPP0207/(0038-9155-5-1)	BC_3F_7	21	220[b]	PBC758x80 C_5 (1)5/7, 6/17-12	BC_2F_4
2	201[b]	PBC398x80 C_5 (1)8/14, 1/17-14	BC_2F_4	22	221[b]	PBC758x80 C_5 (1)5/7, 6/17-13	BC_2F_4
3	202[b]	PBC398x80 C_5 (1)8/14, 1/17-21	BC_2F_4	23	222[b]	PBC758x80 C_5 (1)5/7, 6/17-14	BC_2F_4
4	203[b]	PBC398x80 C_5 (1)8/14, 2/17-15	BC_2F_4	24	223[b]	PBC758x80 C_5 (1)5/7, 6/17-15	BC_2F_4
5	204[b]	PBC398x80 C_5 (1)8/14, 2/17-17	BC_2F_4	25	224[b]	PBC758x80 C_5 (1)5/7, 6/17-16	BC_2F_4
6	205[b]	PBC398x80 C_5 (1)8/14, 2/17-21	BC_2F_4	26	225[b]	PBC758x80 C_5 (1)5/7, 6/17-17	BC_2F_4
7	206[b]	PBC398x80 C_5 (1)8/14, 2/17-22	BC_2F_4	27	226[b]	PBC758x80 C_5 (1)5/7, 6/17-22	BC_2F_4
8	207[b]	PBC398x80 C_5 (1)8/14, 2/17-23	BC_2F_4	28	227[b]	PBC758x80 C_5 (1)5/7, 6/17-25	BC_2F_4
9	208[b]	PBC398x80 C_5 (1)8/14, 2/17-24	BC_2F_4	29	228[b]	PBC758x80 C_5 (1)5/7, 6/17-26	BC_2F_4
10	209[b]	PBC398x80 C_5 (1)8/14, 2/17-25	BC_2F_4	30	229[b]	PBC758x80 C_5 (1)5/7, 6/17-27	BC_2F_4
11	210[b]	PBC398x80 C_5 (1)8/14, 2/17-31	BC_2F_4	31	230[b]	PBC758x80 C_5 (1)5/7, 13/14-12	BC_2F_4
12	211[b]	PBC398x80 C_5 (1)8/14, 2/17-34	BC_2F_4	32	231[b]	PBC758x80 C_5 (1)5/7, 13/14-13	BC_2F_4
13	212[b]	PBC398x80 C_5 (1)8/14, 6/17-12	BC_2F_4	33	232[b]	PBC758x80 C_5 (1)5/7, 13/14-21	BC_2F_4
14	213[b]	PBC398x80 C_5 (1)8/14, 6/17-11	BC_2F_4	34	233[b]	PBC758x80 C_5 (1)5/7, 13/14-24	BC_2F_4
15	214[b]	PBC398x80 C_5 (1)8/14, 17/17-12	BC_2F_4	35	234[b]	PBC758x80 C_5 (1)5/7, 13/14-32	BC_2F_4
16	215[b]	PBC398x80 C_5 (1)8/14, 17/17-13	BC_2F_4	36	301[c]	Perennial	Pure line
17	216[b]	PBC398x80 C_5 (1)8/14, 17/17-14	BC_2F_4	37	302[c]	Yodson Kaem 80	Pure line
18	217[b]	PBC398x80 C_5 (1)8/14, 17/17-15	BC_2F_4	38	303[c]	Manbangchang	Pure line
19	218[b]	PBC398x80 C_5 (1)8/14, 17/17-31	BC_2F_4	39	401[d]	PBC932-6-2	Pure line
20	219[b]	PBC398x80 C_5 (1)8/14, 17/17-32	BC_2F_4	40	402[d]	Orange Selex (PBC80)	Pure line
				41	403[d]	Jin's Delight (PBC81)	Pure line

[a] 101; *C. annuum* progressive line derived from PBC932

[b] 201–234; *C. annuum* progressive lines derived from PBC80

[c] 301–303; *C. annuum* susceptible checks

[d] 401–403; *C. chinense* (401) and *C. baccatum* (402–403) resistant checks

Anthracnose inoculums, inoculation and evaluation

Two isolates of anthracnose pathogen, namely *C. acutatum* 'MUJ5' and *C. capsici* 'Cap26' were used as inocula. They were collected from naturally infected *C. annuum* chili plants very commonly cultivated in the Northeast regions of Thailand. These isolates are prevalent in each region and were identified as the most virulent isolates. Standard protocols of the single spore method for preparation of inoculums and the micro dropping method for inoculation were applied (Park and Kim 1992), and post-inoculation observations (Montri et al. 2009) were followed. Both isolates were grown on potato dextrose agar (PDA) at 25 ° C under fluorescent lights for 5–7 days. The concentration of inoculum was adjusted to 5×10^5 conidia/ml. For both fruit stages (green and red-ripe), five fruits per isolate with three replications were inoculated. A wound one millimeter in depth was made on each fruit at two sites (top and end; bottom of fruit) and 2.0 μl of the conidia suspension was injected into the wounds. Inoculated fruits were incubated in plastic moisture boxes at high relative humidity (95–98 %) and 28 ° C in optimum ambient light regimes (12 h light/12 h dark) (Yu et al. 2013) for seven days. The disease symptoms were scored seven days after inoculation. The lesion diameter and fruit size were measured with vernier calipers to determine the disease percentage of the fruit. Percentage of disease severity (PDS) was then calculated by dividing lesion size to total fruit area and PDS values were transformed to indication of levels of aggressiveness with six severity scores (0 to 9 scale) (Table 2; Montri

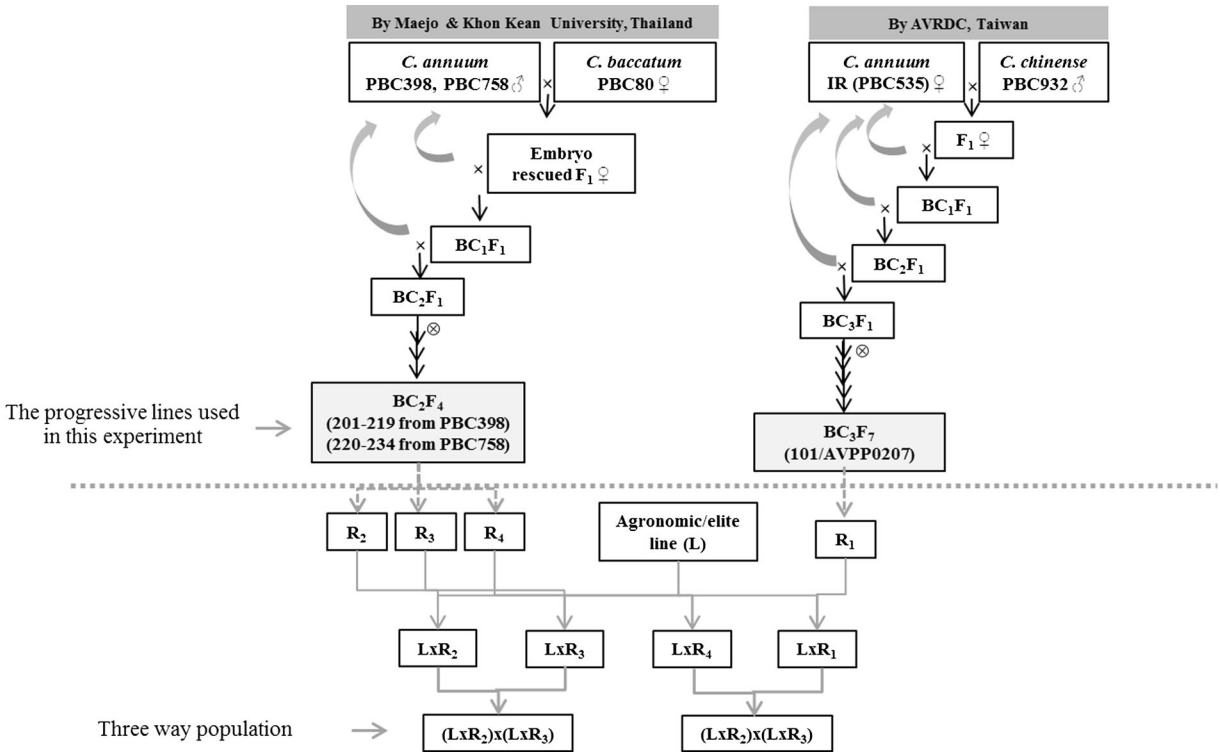


Fig. 1 Developmental description of progressive lines and advanced populations developed during this study. R_1=101, R_2=205, R_3=210 and R_4=215 (progressive lines resistant to *C. capsici* and *C. acutatum* at different stages); L=301 (a line with good horticultural traits with high pungency)

et al. 2009). Data were analyzed using Statistic 8 (V.2) developed by the United States Department of Agriculture (USDA) Natural Resources Conservation Service (NRCS). The means were calculated in percentage (%) and separated by (LSD) (P=0.05) (Gomez and Gomez 1984).

Table 2 Anthracnose disease severity scores, resistance levels and symptom description of chili fruits

Score	Resistance level	Symptom description
0	HR, highly resistant	No infection
1	R, resistant	1–2 % of the fruit with necrotic lesion or a larger water soaked lesion surrounding the infection site
3	MR, moderately resistant	2 to 5 % of the fruit with necrotic lesion, possibly acervuli may be present
5	MS, moderately susceptible	5 to 10 % of the fruit with a necrotic lesion, possibly acervuli
7	S, susceptible	10 to 25 % of the fruit covered with a necrotic lesion with acervuli
9	HS, highly susceptible	25 % of the fruit showing necrosis

Source; Adapted from Montri et al. (2009)

Marker analyses

Two SSR and one SCAR markers previously reported (Table 3) to be associated with an anthracnose-resistance locus were used. All three markers amplified different DNA fragments in different resistant and susceptible varieties (Table 3). The SSR HpmsE032 and HpmsE143 primers amplified DNA fragment of 231 and 107 bp in resistant genotype PBC81, and 240 and 110 bp in susceptible genotype SP26, respectively (Lee et al. 2011). In addition, the Indel primer with the SCAR technique amplified DNA fragments of 100 bp in resistant variety AVPP0207 and 90 bp in susceptible variety AVPP9905 (Wang 2011). Genomic DNA was prepared from 2 to 3 young fresh leaves from 25 to 30 day-old seedlings according to the CTAB method (Doyle and Doyle 1987) and was separated into two replications. Polymerase chain reaction (PCR) was performed in a 25 μl reaction mixture containing 1 μl genomic DNA,

Table 3 Two simple sequence repeat (SSR) and one sequence characterized amplified region (SCAR) markers associated with anthracnose resistance used for validation study

Marker	Position	Product size[a] and sources	Primer sequence	Reference
SSR -HpmsE032	LG12	231 bp (R) (PBC81), 240 bp (S) (SP26)	F:ATGCGCAAAGGGAGAAAATTCA R:CGAACTAACCGTTCATGGTGGA	Lee et al. 2011
SSR- HpmsE143	LG09	107 bp (R) (PBC81), 110 bp (S) (SP26)	F:CCATTCAGCTAGGGTTCAGTCCA R:CGACCAAATCGAATCTTCGTGA	
SCAR-Indel	P5	100 bp (R) (AVPP0207) 90 bp (S) (AVPP9905)	F:GGTATCTTATTTCATAGGGACCAGGCA R:TTTGCGGTAGTGACAACAACTTTACAGCCA	Wang 2011

[a] R=resistant variety (parent), S=susceptible variety (parent)

10 μM of each primer, 50 μM dNTP, 2.5 μM Mg^{2+}, 1 unit of Taq DNA polymerase with the final volume adjusted with dH_2O. The PCR program was as follows: an initial denaturation at 94 ° C for 3 min; 30 cycles of amplification each consisting of 94 ° C for 40 s, 55 ° C for 60 s, and 72 ° C for 1 min; and a final extension period at 72 ° C for 10 min (Yi et al. 2006). The PCR products were separated on 6 % polyacrylamide gels, stained with ethidium bromide solution and visualized in ultraviolet light. The amplified fragments were scored by size.

Results

Highly differential disease reactions

All the 41 chili genotypes were categorized in 10 groups based on disease reactions after being challenged by inoculation with *C. acutatum* and *C. capsici* isolates at both green and red-ripe fruit stages (Table 4). The first group consisted of two resistant *C. baccatum* checks, PBC80 (402) and PBC81 (403). As expected, PBC80 (402) did not develop measurable lesions at either fruit stages when challenged with both the isolates, while PBC81 *C. baccatum* (403) showed highly resistant reactions. PBC932 (401), a resistant *C. chinense* check, developed more than 5 % PDS (moderately susceptible) against *C. acutatum* at the green-mature stage and more than 10 % PDS (susceptible) against both isolates at both stages (group 10, Table 4). The qualitative classification shows that 20 genotypes (18 progressive lines and two resistant checks) had at least one resistant reaction against any of the two isolates and fruit stages (Table 4). The second group showing resistance to *C. acutatum* at the green fruit stage and *C. capsici* at both fruit stages consisted of progressive lines 101 and 205 (Table 4). One progressive line (derived from PBC80) in group three (210), four (215), six (222), and seven (207) showed different reactions (Table 4). Four progressive lines (203, 206, 212 and 213) showed resistance to *C. acutatum* at both fruit stages, and they were identified as the fifth group. Six progressive lines (204, 208, 216, 227, 232 and 233) and two progressive lines (209 and 211) were placed in the eighth and ninth reaction groups against *C. capsici* isolate at green and ripe fruit stages, respectively. The remaining 21 genotypes including one resistant and three susceptible checks were placed in the tenth reaction group because of their susceptibility to both *Colletotrichum* species at both green and red-ripe fruit stages (Table 4).

Aggressiveness of *C. acutatum* and *C. capsici* isolates

At the quantitative level (based on lesion size), different reactions to two isolates of *Colletotrichum* species were displayed in all 41 genotypes (Table 4). The highest level of disease severity was 100 % from *C. acutatum*, while *C. capsici* displayed 47.26 % disease severity. Disease severity in 34 progressive lines ranged from 0 to 100 % (against *C. acutatum* MUJ5) and 0 to 35.81 % (against *C. capsici* cap26) at both green and red-ripe fruit stages. Both the *C. baccatum* resistant checks (402 and 403) expressed resistant (R) to highly resistant (HR) reactions against *C. acutatum* and *C. capsici* at both fruit stages with disease severity ranging from 0 to 2.33 %. However, PBC932 *C. chinense* resistant check (401) showed moderately susceptible (MS) to susceptible (S) reactions with disease severity ranging from 5.13 to 21.81 %. As expected, all three susceptible checks had highly susceptible (HS) reactions against both isolates and both fruit stages with disease severity ranging from

Table 4 Anthracnose disease reactions of chili genotypes inoculated at green and red-ripe fruit stages with two aggressive *Colletotrichum* isolates

No.	Code number [a]	*C. acutatum*_MUJ5				*C. capsici*_Cap26				Group[c]
		Ca - green mature		Ca - ripe mature		Cc - green mature		Cc - ripe mature		
		Disease severity	Disease reaction[b]	Disease severity	Disease reaction[b]	Disease severity	Disease reaction[b]	Disease severity	Disease reaction[b]	
1	101	4.130o	MR	7.63q	MS	0.00 k	HR	0.00j	HR	2
2	201	20.41kl	S	10.22pq	S	ND	–	ND	–	10
3	202	100.00a	HS	ND	–	16.72efg	S	ND	–	10
4	203	74.99d	HS	ND	–	0.90 k	HR	0.57ij	HR	5
5	204	25.30li	HS	11.25opq	S	0.00 k	HR	ND	–	8
6	205	0.00o	HR	20.82ijkl	S	0.00 k	HR	0.00j	HR	2
7	206	100.00a	HS	100.00a	HS	0.00 k	HR	0.00j	HR	5
8	207	13.70n	S	0.00r	HR	ND	–	ND	–	7
9	208	12.01n	S	14.04nop	S	0.00 k	HR	16.23de	S	8
10	209	15.41 m	S	15.18mno	S	13.86fgh	S	2.67hij	MR	9
11	210	28.89hi	HS	0.00r	HR	3.96jk	MR	0.00j	HR	3
12	211	28.99hi	HS	14.30nop	S	11.46ghi	S	0.00j	HR	9
13	212	100.00a	HS	ND	–	0.00 k	HR	0.00j	HR	5
14	213	14.19 m	S	24.35hjk	S	0.00 k	HR	2.80hij	MR	5
15	214	86.30c	HS	79.90c	HS	17.29efg	S	ND	–	10
16	215	0.00o	HR	60.47d	HS	3.06jk	MR	7.55fgh	MS	4
17	216	18.49 lm	S	13.00nop	S	1.36 k	R	11.71ef	S	8
18	217	18.37 lm	S	17.19lmn	S	ND	–	ND	–	10
19	218	100.00a	HS	100.00a	HS	8.15hij	MS	ND	–	10
20	219	41.32e	HS	47.48e	HS	6.44ijk	MS	ND	–	10
21	220	42.71e	HS	30.11 fg	HS	28.23ab	HS	32.21bc	HS	10
22	221	38.90ef	HS	28.44 fgh	HS	20.18def	S	ND	–	10
23	222	3.91o	MR	24.86hij	S	33.78a	HS	36.96a	HS	6
24	223	24.68ijk	S	19.92klm	S	22.94cdf	S	30.48c	HS	10
25	224	34.44 fg	HS	25.35hi	HS	24.58bcd	S	35.81ab	HS	10
26	225	20.19kl	HS	48.44e	HS	20.37def	S	31.16bc	HS	10
27	226	32.20gh	HS	26.03gh	HS	8.74hij	MS	19.22d	S	10
28	227	20.97jkl	S	30.49 fg	HS	0.37 k	HR	8.23 fg	MS	8
29	228	26.90i	HS	31.26f	HS	13.37gh	S	ND	–	10
30	229	31.96gh	HS	20.50jkl	S	26.96bc	HS	ND	–	10
31	230	ND	–	87.03b	HS	29.56ab	HS	ND	–	10
32	231	92.36b	HS	31.62f	HS	ND	–	ND	–	10
33	232	95.06b	HS	95.27a	HS	0.00 k	HR	5.10ghi	MS	8
34	233	21.66jkl	S	12.21opq	S	0.49 k	HR	10.50f	S	8
35	234	14.96mn	S	20.75ijkl	S	12.03ghi	S	7.38fgh	MS	10
36	301	60.74d	HS	60.93d	HS	47.26a	HS	32.36bc	HS	10
37	302	39.97e	HS	39.88ef	HS	46.20a	HS	38.47ab	HS	10
38	303	42.73e	HS	39.99ef	HS	29.86ab	HS	29.07c	HS	10
39	401	12.27mn	S	20.90jkl	S	5.13ij	MS	21.81d	S	10

Table 4 (continued)

No.	Code number [a]	*C. acutatum*_MUJ5				*C. capsici*_Cap26				Group[c]
		Ca - green mature		Ca - ripe mature		Cc - green mature		Cc - ripe mature		
		Disease severity	Disease reaction[b]	Disease severity	Disease reaction[b]	Disease severity	Disease reaction[b]	Disease severity	Disease reaction[b]	
40	402	0.00o	HR	0.00r	HR	0.00 k	HR	0.00j	HR	1
41	403	1.24o	R	0.00r	HR	0.00 k	HR	2.33j	R	1
CV%		7.38		8.85		21.38		28.07		

[a] Abbreviations of serial code number for 41 chili lines are described in Table 4.

[b] Disease reaction; HR-(highly resistant), R-(resistant) MR-(moderately resistant), MS-(moderately susceptible), S-(susceptible), HS-(highly susceptible), ND and - not detected, in a column, a mean followed by common letters are significantly different at 5 % level by LSD

[c] Ten reaction groups for resistance to anthracnose, i.e., 1=resistant to *C. acutatum* at green fruit stage (Ca-G) and red-ripe fruit stage (Ca-R) and *C. capsici* at green (Cc-G) and red-ripe fruit stage (Cc-R); 2=resistant to Ca-G, Cc-G and Cc-R; 3=resistant to Ca-R, Cc-G and Cc-R; 4=resistant to Ca-G and Cc-G; 5=resistant to Cc-G and Cc-R; 6=resistant to Ca-G; 7=resistant to Ca-R; 8=resistant to Cc-G; 9=resistant to Cc-R and 10=susceptible to both species at both fruit stages

29.07 to 60.93 %. The 16 and 6 progressive lines were identified as resistant to *C. capsici* and *C. acutatum*, respectively. Moreover, the 13 progressive lines at green fruit stage and nine progressive lines at red-ripe fruit stage were resistant to *C. capsici* while the resistant reactions in response to *C. acutatum* were four lines at green fruit stage and two lines at ripe fruit stage (Table 4).

Marker reproducibility and validation

Ten selected representative genotypes were subjected to marker analyses using three previously reported markers associated with anthracnose resistance (Table 5, Fig. 2). The SSR-HpmsE032 primer amplified DNA fragments of 231 bp in *C. baccatum* (both resistant checks, e.g., 402 and 403). SSR-HpmsE032 generated two DNA fragments (231 and 240 bp). In the progressive lines 101 (derived from PBC932) and 205 (derived from PBC80) a 240 bp fragment similar to those in three susceptible checks (301–303) was amplified, and also in the *C. chinense* PBC932 resistant check (401). All three progressive lines derived from PBC80 (205, 210 and 215) had 231 bp fragments similar to those in resistant checks 402 and 403. The SSR-HpmsE032 marker was not validated for a resistance gene derived from *C. chinense* PBC932; however, this will be useful as a resistance marker in lines derived from *C. baccatum* PBC80. An extra DNA fragment (approximately 240 bp) was amplified in progressive line 205, which distinguished it from lines 210 and 215. With the SSR-HmpsE143 primer, 110 bp fragments were amplified in all progressive lines examined, similar to three susceptible check varieties and one resistant check *C. chinense* PBC932 (401), whereas a 107 bp fragment was amplified from resistant checks *C. baccatum* PBC80 and PBC81 (402 and 403). The SCAR-Indel primer amplified two different DNA fragments of 90 and 100 bp. Two susceptible checks (302 and 303) had 90 bp fragments amplified, while a 100 bp fragment was amplified in progressive line 101, susceptible check 301, and three resistant checks (401–403). Both of these DNA fragments (90 and 100 bp) were amplified in all three progressive lines derived from PBC 80 (205, 210 and 215) (Table 5, Fig. 2).

Discussion

Identification of resistant parental sources with diverse genetic backgrounds is required for breeding chili varieties with anthracnose resistance. The resistance sources for this study came from two different *Capsicum* species, *C. baccatum* (PBC80) and *C. chinense* (PBC932) with different resistance genes (Vorripps et al. 2004; Mahasuk et al. 2009a, b; Lee et al. 2010; Sun et al. 2015). The inheritance of resistance in both of these sources has been extensively studied and genetic control has been found highly variable depending on a number

Table 5 Reproducibility of markers and their validation with phenotypic data of anthracnose resistance of four progressive lines and three each of susceptible and resistant checks

No.	Code number	Genotypic data			Green fruit stage[1/]				Ripe fruit stage[1/]			
		Hpms E032	Hpms E143	Indel	Disease reaction	Marker validated			Disease reaction	Marker validated		
						Hpms E032	Hpms E143	Indel		Hpms E032	Hpms E143	Indel
C. acutatum												
1	101	240	110	100	MR	–	–	++	MS	++	++	–
2	205	231/240	110	90/100	HR	−+	–	−+	S	−/+	++	−+
3	210	231	110	90/100	HS	–	++	−+	HR	++	–	−+
4	215	231	110	90/100	HR	++	–	−+	HS	–	++	−+
5	301	240	110	100	HS	++	++	++	HS	++	++	–
6	302	240	110	90	HS	++	++	++	HS	++	++	++
7	303	240	110	90	HS	++	++	++	HS	++	++	++
8	401	240	110	100	S	++	++	++	S	++	++	–
9	402	231	107	100	HR	++	++	++	HR	++	++	++
10	403	231	107	100	R	++	++	++	HR	++	++	++
C. capsici												
1	101	240	110	100	HR	–	–	++	HR	–	–	++
2	205	231/240	110	90/100	HR	−+	–	−+	HR	−+	–	−+
3	210	231	110	90/100	MR	++	–	−+	HR	++	–	−+
4	215	231	110	90/100	MR	++	–	−+	MS	–	–	−+
5	301	240	110	100	HS	++	++	–	HS	++	++	–
6	302	240	110	90	HS	++	++	++	HS	++	++	++
7	303	240	110	90	HS	++	++	++	HS	++	++	++
8	401	240	110	100	MS	++	++	–	S	++	++	–
9	402	231	107	100	HR	++	++	++	HR	++	++	++
10	403	231	107	100	HR	++	++	++	R	++	++	++

[1/] Abbreviation of marker (validated +/, not validated – and validated or not validated −/+)

of factors like the use of pathogen species/pathotype, inoculation method, fruit maturity stage and susceptible parent genotype. For instances, resistance reaction in PBC932 against *C. acutatum* at green fruit stages was controlled by two dominant genes and at ripe fruit resistance was under control of two recessive genes (Lin et al. 2007). In PBC932, however, resistance against *C. capsici* was found to be monogenic recessive at both green and ripe fruit stages (Mahasuk et al. 2009a). Resistance in PBC80 was controlled by single recessive and dominant gene at green and ripe fruit stage, respectively (Mahasuk et al. 2009b). We used only one *C. annuum* F_7 progressive line (101) with resistance derived from *C. chinense* PBC932, but used many (34 lines) BC_2F_4 generation progressive resistance lines derived from *C. baccatum* PBC80 because they were segregating and would offer more selection potential for locating targeted genotypes (Tanksley and Nelson 1996).

The reaction of 35 progressive lines and three resistant and susceptible checks were categorized into 10 groups, based on their different disease responses to *Colletotrichum* species and isolates and/or both fruit maturity stages. Second, third and fourth groups were selected because they expressed resistant reactions in more than one combination of isolates and fruit stages (Table 4). Hence, four *C. annuum* progressive lines derived from PBC932 (line 101) and PBC80 (lines 205, 210 and 215) were selected to validate three potential markers to use in crossing and selection

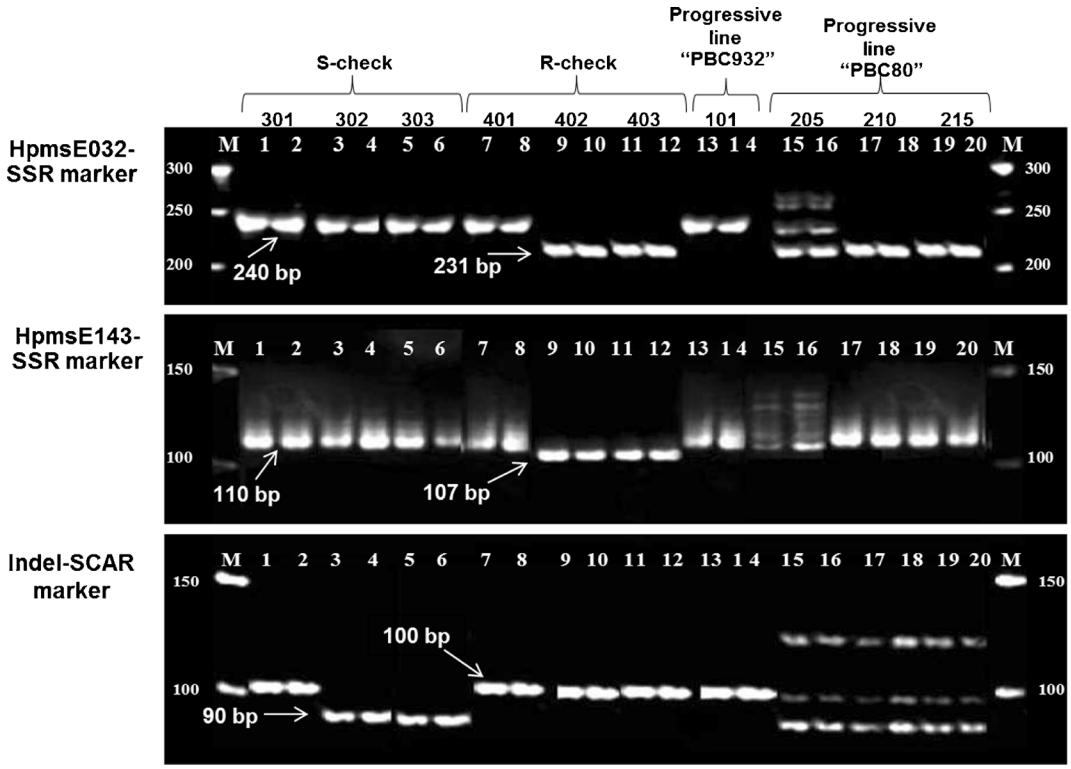


Fig. 2 DNA fingerprints 2 SSR primers (*HpmsE032*, *HpmsE143*), 1 SCAR primer (*Indel*). M: 50 bp Molecular base ladder; well, 1–6 (susceptible checks; S-check); 7–12 (resistant check; R-check), well 13–14 (progressive lines derived from PBC932) and well 15–20 (progressive lines derived from PBC80)

programs for combining resistance against both isolates at both stages.

The comparison between the two *Colletotrichum* species revealed that the percentage of disease severity (PDS) for *C. acutatum* was the maximum level (100 % PDS), while those for *C. capsici* was less than 50 % PDS. The larger number of progressive lines showing resistance against *C. capsici* compared to

Table 6 Phenotypic and genotypic responses of 10 chili genotypes used for marker analysis

No.	Code number	Phenotypic data				Genotypic data		
		C. acutatum		*C. capsici*		SSR-HpmsE032	SSR-HpmsE143	SCAR-Indel
		Green	Ripe	Green	Ripe			
1	101	MR	MS	HR	HR	240	110	100
2	205	HR	S	HR	HR	231/240	110	90/100
3	210	HS	HR	MR	HR	231	110	90/100
4	215	HR	HS	MR	MS	231	110	90/100
5	301	HS	HS	HS	HS	240	110	100
6	302	HS	HS	HS	HS	240	110	90
7	303	HS	HS	HS	HS	240	110	90
8	401	S	S	MS	S	240	110	100
9	402	HR	HR	HR	HR	231	100	100
10	403	R	HR	HR	R	231	100	100

C. acutatum suggests that the *C. acutatum* isolate was more aggressive than the *C. capsici* isolate (Lewis-Ivey et al. 2004; Taylor et al. 2007; Harp et al. 2008; Kim et al. 2008a; Than et al. 2008a). On the other hand, it might be considered that environmental condition such as incubation temperature (28 °C) and high humidity (95–98 % RH) might have favored more aggressiveness to *C. acutatum* than *C. capsici*.

The four selected progressive lines derived from PBC932 and PBC80, and the three resistant and three susceptible checks showed different genotypic responses in terms of amplification for two SSR markers (HpmsE032 and HpmsE143) and one SCAR-Indel marker. The SSR-HpmsE032 and SCAR-Indel markers showed more polymorphism among progressive lines compared to SSR-HpmsE143. The results revealed that the 231 bp fragment amplified by SSR-HpmsE032 in the three progressive lines derived from PBC80 (lines 205, 210 and 215) and two resistant checks (402 and 403) was associated with disease resistance in response to *C. capsici* at the green fruit stage (Tables 5 and 6). Yi et al. (2006) found that the HpmsE032-SSR marker was on a linkage group on chromosome 12 (LG12), and associated with resistant source PBC81 at both mature fruit stages (Lee et al. 2010). In addition, the resistance genes from PBC80 and PBC81 were reported as the similar broad-spectrum resistance source for many *Colletotrichum* species (Yoon et al. 2004; Montri et al. 2009). The 100 bp fragment amplified by the SCAR-Indel primer in all four lines (101, 205, 210 and 215) was similar to the previous report of Wang (2011). However, this marker was also present in one of the susceptible checks (301), hence this marker cannot be used for marker-assisted selection in these populations. The discrepancy in our results compared to Wang (2011) may be because of the use of different pathotypes and application of molecular markers is case specific especially for highly complex pathosystem of *Capsicum* spp. and *Colletotrichum* spp. The pathogenic variability of *Colletotrichum* isolates in relation to virulence is well known and documented in chili cultivars (Montri et al. 2009; Park et al. 2009; Temiyakul et al. 2010; Mahusuk et al. 2013). Chili anthracnose resistance affected by different stages of fruits (Silva et al. 2014) and virulence of *C. acutatum* influenced by light quality (Yu et al. 2013) have also been demonstrated.

Although the phenotypic response (disease reaction) against *C. capsici* at green fruit stage of line 101 was similar to the other three progressive lines (205, 210 and 215); the 231 bp fragment amplified by SSR-HpmsE032 was absent in 101. This further confirms that 101 contain a different resistance locus than the other three lines. It is known that resistance in 101 is under the control of recessive genes (*co1-co3*) from PBC932, while in the other lines, depending on the parental combination, resistance has been under the control of recessive (*co4*) or dominant (*Co5*) gene from PBC80 (Mahasuk et al. 2009a, b). The resistance gene of line 101 was located on chromosome P5. Resistance genes from the other three lines (which belong to *C. baccatum*) were located on LG12 (Lee et al. 2010; Sun et al. 2015). It is interesting to note that line 101 showed a resistant reaction, yet its donor parent (resistant check PBC932; 401) was found to be susceptible. This suggests that the resistant reaction in line 101 (AVPP0207) might be conditioned by the minor genes of the susceptible parent, as reported previously (Kim et al. 2007). The susceptible reaction of line 401 (pure line of PBC932) may be due to the different pathotypes used for our studies and those done previously (Montri et al. 2009).

It can be concluded that three progressive lines (205, 210, 215) derived from PBC80 and one line (101, AVPP0207) derived from PBC932 showed a desirable level of resistance against prevalent *Colletotrichum* isolates from North and Northeast Thailand. Hence, these four lines were used in a crossing program to combine resistance genes from two sources at two fruit stages (Fig. 1). The SSR-HpmsE032 marker was validated in our genotypes and will be useful for marker-assisted selection during generation advancement of three-way crosses developed using resistant progressive lines.

Acknowledgments The authors are grateful to The Royal Golden Jubilee (RGJ) Ph.D. Program, Thailand Research Fund (TRF); The National Science and Technology Agency (NSTDA); National Research University Project of Thailand, Office of the Higher Education Commission, through the Food and Functional Food Research Cluster of Khon Kaen University; Plant Breeding Research Center for Sustainable Agriculture, Khon Kaen University for funding the research, Thailand Research Fund(TRF) (Project code : IRG5780003), Khon Kaen University (KKU) and the Faculty of Agriculture KKU for providing financial support for manuscript preparation activities and RGJ fellowship to the first author. The authors are also grateful to AVRDC – The

World Vegetable Center, Taiwan and Asst. Prof. Chalermsri Nontaswatsri, Maejo University, Thailand for providing seeds of genotypes.

References

Doyle, J. J., & Doyle, J. L. (1987). A rapid DNA isolation procedure for small quantities of fresh leaf tissue. *Phytochemical Bulletin, 19*, 11–15.

FAO. (2013). *Food and Agriculture Statistics*. (2013). (cited 9 May 2015). Available from: http://www.faostat.fao.org.

Gomez, K. A., & Gomez, A. A. (1984). *Statistical procedures for agricultural research*. New York: John Wiley and Sons.

Harp, T. L., Pernezny, K., Lewis Ivey, M. L., Miller, S. A., Kuhn, P. J., & Datnoff, L. (2008). The etiology of recent pepper anthracnose outbreaks in Florida. *Crop Protection*, 1380–1384.

Kim, S. H., Yoon, J. B., Do, J. W., & Park, H. G. (2007). Resistance to anthracnose caused by *Colletotrichum acutatum* in chili pepper (*Capsicum annuum* L.). *Journal of Crop Science and Biotechnology, 10*(4), 277–280.

Kim, J. T., Park, S. Y., Choi, W., Lee, Y. H., & Kim, H. T. (2008a). Characterization of *Colletotrichum* isolates causing anthracnose of pepper in Korea. *Plant Pathology, 24*(1), 17–23.

Kim, S. H., Yoon, J. B., Do, J. W., & Park, H. G. (2008b). Inheritance of anthracnose resistance in a new genetic resource *Capsicum baccatum* PI594137. *Journal of Crop Science and Biotechnology, 11*, 13–16.

Kim, S. H., Yoon, J. B., Do, J. W., & Park, H. G. (2008c). A major recessive gene associated with anthracnose resistance to *Colletotrichum capsici* in chilli pepper (*Capsicum annuum* L.). *Breeding Science, 58*, 137–141.

Lee, J., Hong, J. H., Do, J. W., & Yoon, J. B. (2010). Identification of QTLs for resistance to anthracnose to two *Colletotrichum* species in pepper. *Journal of Crop Science and Biotechnology, 13*(4), 227–233.

Lee, J., Jee, H. H., Jae, W. D., & Jae, B. Y. (2011). Development of STS markers linked to the major QTLs for resistance to the pepper anthracnose caused by *Colletotrichum acutatum* and *C. capsici. Horticulture Environment and Biotechnology, 52*(6), 596–601.

Lewis Ivey, M. L., Nava-Diaz, C., & Miller, S. A. (2004). Identification and management of *Colletotrichum acutatum* on immature bell peppers. *Plant Disease, 88*, 1198–1204.

Lin, S. W., Gniffke, P. A., & Wang, T. C. (2007). Inheritance of resistance to pepper anthracnose by *Colletotrichum acutatum. Acta Horticulture (ISHS), 760*, 329–334.

Mahasuk, P., Khumpeng, N., Wasee, S., Taylor, P. W. J., & Mongkolporn, O. (2009a). Inheritance of resistance to anthracnose (*cColletotrichum capsici*) at seedling and fruiting stages in chilli pepper (*Capsicum* spp.). *Plant Breeding, 128*, 701–706.

Mahasuk, P., Taylor, P. W. J., & Mongkolporn, O. (2009b). Identification of two new genes conferring resistance to *Colletotrichum acutatum* in *Capsicum baccatum*. *Phytopathology, 99*(9), 1100–1104.

Mahasuk, P., Chinthaisong, J., & Mongkolporn, O. (2013). Differential resistances to anthracnose in *Capsicum baccatum* as responding to two *Colletotrichum* pathotypes and inoculation methods. *Breeding Science, 63*, 333–338.

Montri, P. P., Taylor, P. W. J., & Mongkolporn, O. (2009). Pathotypes of *Colletotrichum capsici* the causal agent of chili anthracnose in Thailand. *Plant Disease, 93*, 17–20.

Pakdeevaraporn, P., Wasee, S., Taylor, P. W. J., & Mongkolporn, O. (2005). Inheritance of resistance to anthracnose caused *Colletotrichum capsici* in *Capsicum. Plant Breeding, 124*, 206–208.

Park, K. S., & Kim, C. H. (1992). Identification, distribution, and etiological characteristics of anthracnose fungi of red pepper in Korea. *Korean Journal Plant Pathology, 8*, 61–69.

Park, K. S., Kim, S. H., Park, H. G., & Yoon, J. B. (2009). *Capsicum* germplasm resistance to pepper anthracnose differentially interacts with *Colletotrichum* isolates. *Horticulture Environment and Biotechnology, 50*(1), 17–23.

Poonpolgul, S., & Kumphai, S. (2007). Chili pepper anthracnose in Thailand. First International Symposium. on Chili Anthracnose, Seoul National University, Korea, 23.

Silva, S. A., Rodrigues, R., Goncalves, L. S. A., Sudre, C. P., Bento, C. S., Carmo, M. G. F., & Medeiros, A. M. (2014). Resistance in Capsicum spp. to anthracnose affected by different stages of fruit development during pre- and post harvest. *Tropical Plant Pathology, 39*(4), 335–341.

Sun, C., Mao, S. L., Zhang, Z. H., Palloix, A., Wang, L. H., & Zhang, B. X. (2015). Resistances to anthracnose (*Colletotrichum acutatum*) of *Capsicum* mature green and ripe fruit are controlled by a major dominant cluster of QTLs on chromosome P5. *Scientia Horticulturae, 181*, 81–88.

Tanksley, S. D., & Nelson, J. C. (1996). Advanced backcross QTL analysis: a method for the simultaneous discovery and transfer of valuable QTLs from unadapted germplasm into elite breeding lines. *Theoretical and Applied Genetics, 92*, 191–203.

Taylor, P. W. J., & Ford, R. (2007). Diagnostics, genic diversity and pathogenic variation of Ascochyta blight of cool season food and feed legumes. *European Journal of Plant Pathology, 119*, 127–133.

Temiyakul, P., Taylor, P. W. J., & Mongkolporn, O. (2010). Development of a double-inoculation method to assess resistance to anthracnose in trispecies *Capsicum* hybrid. *Journal of Phytopathology, 158*, 561–565.

Than, P. P., Jeewon, R., Hyde, K. D., Pongsupasamit, S., Mongkolporn, O., & Taylor, P. W. J. (2008a). Characterization and pathogenicity of *Collecotrichum* species associated with anthracnose disease on chili (*Capsicum* ssp.) in Thailand. *Plant Pathology, 57*(3), 562–572.

Than, P. P., Prihastuti, H., Phoulivong, S., Taylor, P. W. J., & Hyde, K. D. (2008b). Chili anthracnose disease caused by *Colletotrichum* species. *Journal Zhejiang University Science Biomedicine and Biotechnology, 9*(10), 764–778.

Voorrips, R. E., Finkers, R., Sanjaya, L., & Groenwold, R. (2004). QTL mapping of anthracnose (*Colletotrichum* spp.) resistance in a cross between *Capsicum annuum* and *C. chinense. Theoretical and Applied Genetics, 109*, 1275–1282.

Wang, Y. W. (2011). Development of Sequence characterized amplified region (SCAR) markers associated with pepper anthracnose (*Colletotrichum acutatum*) resistance. Master Thesis, Department of Agronomy, National Chiayi University, Taiwan.

Yi, G., Lee, J. M., Lee, S., Choi, D., & Kim, B. D. (2006). Exploitation of pepper EST-SSRs and an SSR-based linkage map. *Theoretical and Applied Genetics, 114*, 113–130.

Yoon, J. B., Yang, D. C., Lee, W. P., Ahn, S. Y., & Park, H. G. (2004). Genetic resources resistant to anthracnose in the genus *Capsicum*. *Journal of the Korean Society for Horticultural Science, 45*, 318–323.

Yoon, J. B., Yang, D. C., Do, J. W., & Park, H. G. (2006). Overcoming two post-fertilization genetic barriers in interspecific hybridization between *Capsicum annuum* and *C. baccatum* for introgression of anthracnose resistance. *Breeding Science, 56*, 31–38.

Yu, S. M., Ramkumar, G., & Lee, Y. H. (2013). Light quality influences the virulence and physiological responses of *Colletotrichum acutatum* causing anthracnose in pepper plants. *Journal of Applied Microbiology, 115*(2), 509–516.

Est. 1984

ORIENTAL JOURNAL OF CHEMISTRY
An International Open Free Access, Peer Reviewed Research Journal

www.orientjchem.org

ISSN: 0970-020 X
CODEN: OJCHEG
2015, Vol. 31, No. (3):
Pg. 1331-1343

The Synergistic Effect of Anionic Surfactant on Adsorption Enhancement of the Carotenoids Extract using Mesoporous Hydroxyapatite Nanoparticles

SUPALAK KONGSRI[1], SUCHILA TECHAWONGSTIEN[2] and SAKSIT CHANTHAI[1]*

[1]Department of Chemistry and Center of Excellence for Innovation in Chemistry, Faculty of Science, Khon Kaen University, Khon Kaen 40002, Thailand.
[2]Department of Plant Science and Agricultural Resources, Faculty of Agriculture, Khon Kaen University, Khon Kaen 40002, Thailand.
*Corresponding author E-mail: sakcha2@kku.ac.th

http://dx.doi.org/10.13005/ojc/310310

(Received: April 04, 2015; Accepted: June 04, 2015)

ABSTRACT

Fish hydroxyapatite (FHAp) was prepared from fish scale waste by alkaline heat treatment. The obtained nanoparticles (21 nm) of FHAp with high crystallinity (89.5%) were used as biocompatible adsorbent for an adsorption of plant carotenoids extract. For optimum conditions of batch adsorption study, experimental parameters including pH of solution, adsorbent dosage, an initial concentration of carotenoids, amount of sodium dodecyl sulfate (SDS), contact time and temperature were investigated in details. From the results, the carotenoids adsorption of the FHAp was drastically enhanced in the presence of SDS through their hydrophobic interactions between the carotenoids and the cationic element FHAp via the anionic head of SDS by electrostatic and ion-exchange interactions and surface complexation. The adsorption behaviors fitted well by pseudo-second order kinetic model and Freundlich adsorption isotherm. Thermodynamic data demonstrated that the adsorption behaviors of the carotenoids on the hydroxyapatite nanoparticles were spontaneously endothermic and physisorption process.

Key words: Hydroxyapatite; Fish scale waste; Carotenoid; Freundrich adsorption isotherm.

INTRODUCTION

Fish waste is the residual by-product mostly generated from the fish processing industry. Almost all the waste is often deposited in an environment causing pollution and health problem. The use of this waste as alternative biomaterials has been increasingly encouraged the attention of researcher all around the world during last two decades. The utilizations of fish waste not only increase the production of value-added products but also reduce the amount of waste. Fish processing residues including scale, bone, skin, viscera and head are possible sources of proteins, unsaturated essential fatty acids, minerals and antioxidants[1,2]. The waste investigated in this study was the fish scale that

contained a numerous valuable inorganic components, mainly hydroxyapatite (HAp) and was considered for hydroxyapatite source in recent years because of its widely available waste[2-4].

Hydroxyapatite, formulated as $Ca_{10}(PO_4)_6(OH)_2$ is chemically similar to the main component of hard tissues in bones. It has high commercial value in manufacturing functional food, drug delivery, biomaterials, cosmetics and biomedical products. HAp can be produced either from natural source or synthesis process. This latter process is relatively complicated and expensive due to the use of high purity of reagents. The HAp derived from fish scale has the advantages that they inherit some chemical properties and can be processed by simple, inexpensive and environmental friendly. In this work, HAp was prepared from fish scale waste using alkaline heat treatment, which was modified from an alkaline hydrolysis method. The method was carried out using a mild agent (dilute hydrochloric acid and sodium hydroxide solutions) and soft conditions (temperature of 70-100°C). The preparation of HAp from fish scales is, thus, biologically safe, easy and cheap. A great interest towards the use of nanocrystalline HAp as an ideal adsorbent for a wide range of compounds (e.g. Cd, Pb, As, Mn, Al and Ni) because of its high adsorption capacity, low water solubility, availability, low cost and high stability under oxidizing and reducing conditions[5-8]. Some adsorption mechanisms are involved including ion-exchange, surface complexation, dissolution of HAp and precipitation of metal phosphates, substitution of Ca in HAp by metals during recrystallization (coprecipitation) which have been proposed in order to describe the uptake of heavy metals from aqueous solutions[9,10]. Nanocrystalline HAp has the ability to exchange their calcium, phosphate and hydroxyl ions with other ions without the loss of the crystalline structure. There are a few works reporting about antioxidants adsorbed on the HAp substrate. Thus, the antioxidant adsorbed by nanocrystalline of FHAp was investigated in order to improve the concern about the FHAp properties that can be utilized as medical materials.

Tomatoes are rich in carotenoids, especially lycopene. It is well known as a powerful antioxidant in the group of carotenoid compounds which play an important role to prevent human from the risk of cardiovascular disease and cancers by destruction of free radical intermediates[11]. It has been reported for some beneficial actions in bone diseases. Previous work showed that the daily consumption of lycopene may moderate the risk of osteoporosis[12]. Consequently, the incorporation of lycopene into apatites may actually be possible to use for pain relief of osteoporosis. From literature, no work of the lycopene incorporated into hydroxyapatite has ever been reported elsewhere.

In this study, the fish scale waste was utilized as a raw material to prepare nanocrystalline hydroxyapatite by alkaline heat treatment method. The possibility of using FHAp as an adsorbent for caroteniod adsorption in the presence of sodium dodecyl sulfate (SDS) was investigated for the first time. Other physiochemical parameters that influence the adsorption process in a batch adsorption including pH, adsorbent dosage, initial concentration and contact time were investigated. The experimental data were analyzed using adsorption isotherm, adsorption kinetic and thermodynamic parameters aiming for their adsorption process.

MATERIALS AND METHODS

Preparation and characterization of FHAp nanoparticles

All chemicals were analytical reagent grade and the aqueous solutions were prepared using deionized water with a resistivity of 18.2 MΩ cm used throughout the experiment was from RiO_s^{TM} Type I Simplicity 185 (Millipore water, USA). Nanocrystalline of FHAp adsorbents used in this study was prepared by alkaline heat treatment. This method was described in our previous work[13]. Briefly, fish scale waste was initially deproteinized through an external washing with 0.1 M HCl and washed several times with distilled water. The remaining proteins of fish scale were treated with 5% (w/v) NaOH, heated and stirred at 70°C for 5 h. The obtained fine white precipitate was washed with distilled water and dried at 60°C. For the next step of alkaline heat treatment, 50% (w/v) NaOH was added into the treated scale powder, heated up to 100°C and stirred for 1 h. The obtained FHAp nanopowder was washed thoroughly with deionized water until

the washing solution became neutral and then dried at 60°C.

The crystallinity and particle size of the FHAp sorbent was identified by X-ray diffraction (XRD), using Shimadzu model XRD-6000 with Cu K_α radiation (λ = 1.5406 Å). The XRD patterns were collected from 2θ = 20°-60° with scan step 0.02°. The specific surface area of nanocrystalline FHAp was determined by nitrogen adsorption at 77 K (Quantachrome Autosorb-1 Instrument). Surface area was calculated from adsorption data using Brunauer–Emmett–Teller (BET) equation. The determination of average pore size and pore volume was carried out at relative pressure (P/P_o) equal to 1. The Fourier transform infrared spectroscopy (FT–IR) was done by Perkin Elmer Spectrum One with resolution of 4 cm^{-1} in the frequency range of 4000-400 cm^{-1}.

Carotenoid extraction

Tomato powder (3 g) was extracted with 30 mL mixed solvent of hexane, ethanol and acetone (2:1:1, v/v/v) into Teflon extraction vessel. Each vessel was placed in microwave assisted extraction apparatus (Anton Parr 3000, Austria). The extraction was performed at a constant power of 300 W. After microwave heating, the mixtures in the extraction vessels were allowed to cool down at room temperature. The supernatants were filtered and hexane layer was evaporated off under reduced pressure at 50°C by a rotary evaporator (Büchi R-200 Rotavapor, Switzerland). Then, the residue was thawed into the flask before used and diluted to an appropriate concentration with ethanol. The quantitative analysis of the carotenoid content in the tomato extract was performed using a calibration curve of working standard solution of lycopene[14].

Adsorption experiments

The batch adsorption experiments were performed at ambient temperature (30 ±2 °C). An adsorbent (0.1 g) was added into a 125-mL conical flask containing 25 mL of the carotenoid extract (10 mg L^{-1}) with a fixed amount of SDS solution and the pH of the solution was adjusted and shaken by an orbital shaker (Yamato Scientific, Japan) at approximately 250 rpm until equilibrium was reached. In order to study the optimum conditions for the batch adsorption, various experimental parameters were studied including the effect of pH (3-10), SDS concentration, adsorbent dosage, initial concentration, ionic strength, contact time and temperature. After a period of shaking, the aqueous sample was centrifuged, and the residual concentration of the carotenoids in the supernatant was measured at 470 nm by UV-Visible spectrophotometer (Model 6400, Jenway, Germany).

All experiments were conducted in triplicate under the same conditions. The adsorption capacity (q_e, mg g^{-1}) of the carotenoid extract at the equilibrium state was determined as follows:

$$q_e = (C_0 - C_e)V/m \quad ...(1)$$

where C_o is the initial concentration (mg L^{-1}) of the carotenoid extract in the mixture solution, C_e is the carotenoid concentration (mg L^{-1}) at the equilibrium state, V is the volume (L) of the mixture solution, and m is the mass (g) of the adsorbent used.

RESULTS AND DISCUSSION

Characterization of FHAp nanoparticles

The XRD pattern of FHAp nanocrystalline obtained from alkaline heat treatment method and the commercial hydroxyapatite were very similar (data not shown). The XRD (002), (211), (300), (202), (222) and (213) diffraction lines were used to evaluate the crystallite size by Scherer's formula, giving its estimated crystal size of 21 nm. Since the sharpness of vibration bands relates to crystallinity, their crystallinity can also be calculated. For XRD, the crystallinity degree (X_c) of FHAp was evaluated by the relation:

$$B_{002}\sqrt[3]{X_c} = K \quad ...(2)$$

where K is a constant found equal to 0.24 for a very large number of different HAp powders and B_{002} is FWHM (°) of reflection (002)[15]. The crystallinity of 89.5 % was obtained indicating good crystals and confirmed that all nanopowders were composed of a crystalline hydroxyapatite phase. For IR, the crystallinity index (CI_{IR}) is calculated following equation:

$$CI_{IR} = \left(A_{603} + A_{567}\right) / A_{590} \quad ...(3)$$

where A_x is the absorbance at the wave number *x*, assuming a straight baseline between 750 and 450 cm^{-1}.[16] The CI_{IR} of 4 indicates also that FHAp is a crystal form.

The structural characterization was also analyzed by FT-IR (data not shown). The FTIR spectrum exhibited at 628, 590 and 567 cm^{-1} corresponding to the triple degenerate bending vibrations of phosphate groups in HAp and the sharpness of these peak indicates that the FHAp is crystalline. The broad band peaks at 3467 cm^{-1} and 1637 cm^{-1} are attributed to the –OH stretching and bending of the H_2O molecules while the bands (876, 1458, and 1417 cm^{-1}) are assigned to asymmetric stretching of the carbonate group (B-type carbonate)[17,18].

Figure 1 shows the N_2 adsorption–desorption isotherms of FHAp. The results represent the type IV adsorption isotherm with hysteresis loop which is associated with capillary condensation taking place in mesopores and the limiting uptake over a range of high P/P_o. The initial part of the type IV adsorption isotherm is ascribed to monolayer-multilayer adsorption because it follows the same path as the corresponding part of a type II adsorption isotherm obtained with the given adsorption on the same surface area of adsorbent in a non-porous form. From the shape of the hysteresis loop pattern, FHAp can be classified with specific pore structures. This type of hysteresis loop shows no overlapping between adsorption and desorption of gaseous molecules. This indicates that a difference in mechanism between condensation and evaporation process takes place in pores with narrow necks and wide bodies like ink bottom pores. The result was confirmed by Barrett-Joyner-Halenda (BJH) adsorption as illustrated in the Fig. 1. The result from BJH adsorption plot shows that the pores are distributed as narrow pores indicating that mesopores (2-50 nm) are in the FHAp structure. Analysis of surface characteristics with BET and BJH models showed that the specific surface area of FHAp was 110.6 m^2/g and the sizes of the pores were lower than 13.2 nm.

Adsorption of carotenoid from tomato extract
Effect of pH

The pH of an aqueous solution is an important parameter affecting the adsorption process because of ionization of both adsorbent and adsorbate in the solution. The effect of pH on the adsorption can be described on the basis of the pH of point zero charge (pH_{pzc}), which is the point at

Table 1: Langmuir and Freundlich isotherm data for the adsorption of the carotenoids extract onto the SDS-FHAp compared with FHAp itself

Adsorbent	Langmuir isotherm				Freundlich isotherm		
	q_m (mg g^{-1})	K_L (L mg^{-1})	R_L	R^2	K_F [(mg g^{-1})(L mg^{-1})$^{1/n}$]	1/*n*	R^2
SDS-FHAp	64.103	0.0052	0.9165	0.9894	0.2675	0.9183	0.9952
FHAp	7.8988	0.0146	0.7965	0.9706	0.1027	0.9699	0.9924

Table 2: Adsorption kinetic data for the adsorption of the carotenoids extract onto the SDS-FHAp compared with FHAp itself

Adsorbent	$q_{e,exp}$	Pseudo-first order			Pseudo-second orderIntra-particle diffusion					
	(mg g^{-1})	q_1 (mg g^{-1})	k_1 (h^{-1})	R^2	q_2 (mg g^{-1})	k_2 [g (mg h)$^{-1}$]	R^2	k_p [mg (g $h^{1/2}$)$^{-1}$]	*C* (mg g^{-1})	R^2
SDS-FHAp	3.1741	1.0994	0.8820	0.9714	3.1736	0.3404	0.9998	0.5312	2.2045	0.9654
FHAp	1.4544	0.9440	0.2718	0.9677	1.6221	0.3912	0.9885	0.5291	0.0017	0.9880

which the net charge of the adsorbent is zero. The pH_{pzc} of the FHAp was determined by the batch equilibrium method[19]. It was evident in our work[13] that the FHAp exhibits excellent buffering properties and performs as a buffer over a wide pH range of 4-9 at 30°C. The surface properties of HAp in aqueous solutions were demonstrated as the following reactions[5]:

$$\equiv PO^- + H^+ \Leftrightarrow \equiv POH^\circ \quad ...(4)$$

$$\equiv CaOH_2^+ \Leftrightarrow \equiv CaOH^\circ + H^+ \quad ...(5)$$

At $pH < pH_{pzc}$, the HAp surface is protonated by hydrogen ions (H^+) in the solution resulting in the surface of HAp becomes positively charged $\equiv CaOH_2^+$ and neutral $\equiv POH^\circ$ on HAp surface. In contrast, when the HAp surface is deprotonated by hydroxide ion (OH^-) at $pH > pH_{pzc}$, it produces the negatively charged $\equiv PO^-$ and neutral $\equiv CaOH^\circ$. The pH_{pzc} value of FHAp was previously reported to be 7.86. The effect of pH was investigated by determining the adsorption of carotenoids onto FHAp nanocrystals either in the presence or in the absence of SDS at pH ranging from 3 to 10 and the results are given in Fig. 2a. The results show that the adsorption capacity increased with increasing pH until pH 6 and it decreased at pH higher than this point. When the solution pH was below the pH_{pzc}, anionic surfactant SDS was attracted to the positively charged surface of FHAp. The accumulation of anionic surfactant SDS on the surface leads to the interactions between carotenoid and SDS through hydrophobic interactions onto FHAp. Thus, the adsorption capacity of FHAp increased in the present of SDS. For pH values above 7.86, the FHAp is mainly negative charge. Since the electrostatic repulsion between anionic surfactant SDS and the active sites at the surface of FHAp, the adsorption capacities decreased with increasing of pH. The maximum adsorption capacities were 1.1004 and 0.8725 mg g^{-1} for SDS-FHAp and FHAp, respectively, at pH 6 implying the optimum pH for carotenoid adsorption. Therefore, the solution pH 6 was carried out throughout for further studies.

Effect of SDS concentration

The influence of SDS concentration was also considered in the adsorption of carotenoids on FHAp substrate as shown in Fig. 2b. The results are presented by plotting the adsorption capacity versus the concentration of SDS in the reaction mixture. It is clear that the adsorption of carotenoid on FHAp increased with increasing SDS concentration (below the critical micelle concentration, *cmc*) because of the release of phosphate ion from the FHAp surface. Above the *cmc*, the adsorption of carotenoid on the FHAp remained almost constant with the increase of SDS concentration because the SDS in the aqueous solution had become micelle form leading more stable than the aggregate formation on the FHAp surface[20]. Therefore, this study was done at the SDS concentration lower than the *cmc* point.

Effect of adsorbent dosage

Figure 2c shows the effect of adsorption dosage. The adsorption percentage (%) and adsorption capacity (q_e) of carotenoid were plotted as a function of adsorbent dosage. It was observed that the adsorption percentages of adsorbent increase with increasing the adsorbent dosages. With the increase in SDS-FHAp dosage from 0.025 to 0.20 g, the adsorption percentages increased rapidly from 34.53 % to 72.79 % and approach a plateau at dosage higher than 0.15 g. This trend increased with increasing adsorbent dosage due to the increment of the available surface area and adsorption site; therefore, more adsorbate can be attached to their surfaces. On the other hand, the plot of adsorption capacity revealed that the decrease of adsorption capacity with increasing the

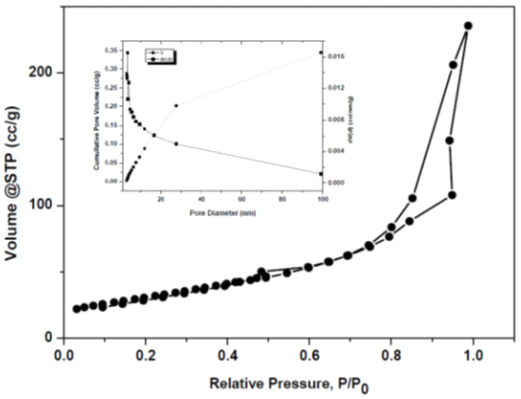
Table 3: Thermodynamic data for the adsorption of the carotenoids extract onto the SDS-FHAp compared with FHAp itself

Adsorbent	ΔS°	ΔH°	ΔG° (kJ mol^{-1})			
	(J mol^{-1}K^{-1})	(kJ mol^{-1})	30 °C	40 °C	50 °C	60 °C
SDS-FHAp	11.9971	2.8600	-0.7747	-0.8946	-1.0145	-1.1344
FHAp	60.7587	19.3134	0.8907	0.2840	-0.3245	-0.9322

adsorbent dosage is due to the unsaturated adsorption sites during the adsorption process[21]. This can be explained that the amount of adsorbent for adsorption increased but the amount of adsorbate remained the same. The optimum adsorbent dosages were considered at 0.15 g and 0.05 g for SDS-FHAp and FHAp, respectively, for further studies.

Effect of an initial concentration of carotenoids

The effect of an initial carotenoid concentration was investigated in the range of 1-17.5 mg L^{-1} at pH 6. Fig. 2d shows a plot of adsorption capacity versus the initial concentration of carotenoid on both SDS-FHAp and FHAp. It was observed that the equilibrium adsorption capacity of the carotenoid increased proportionally with an increasing carotenoid concentration. This was



Inset: the pore diameter determined by BJH adsorption method

Fig. 1: The nitrogen adsorption-desorption isotherms of FHAp

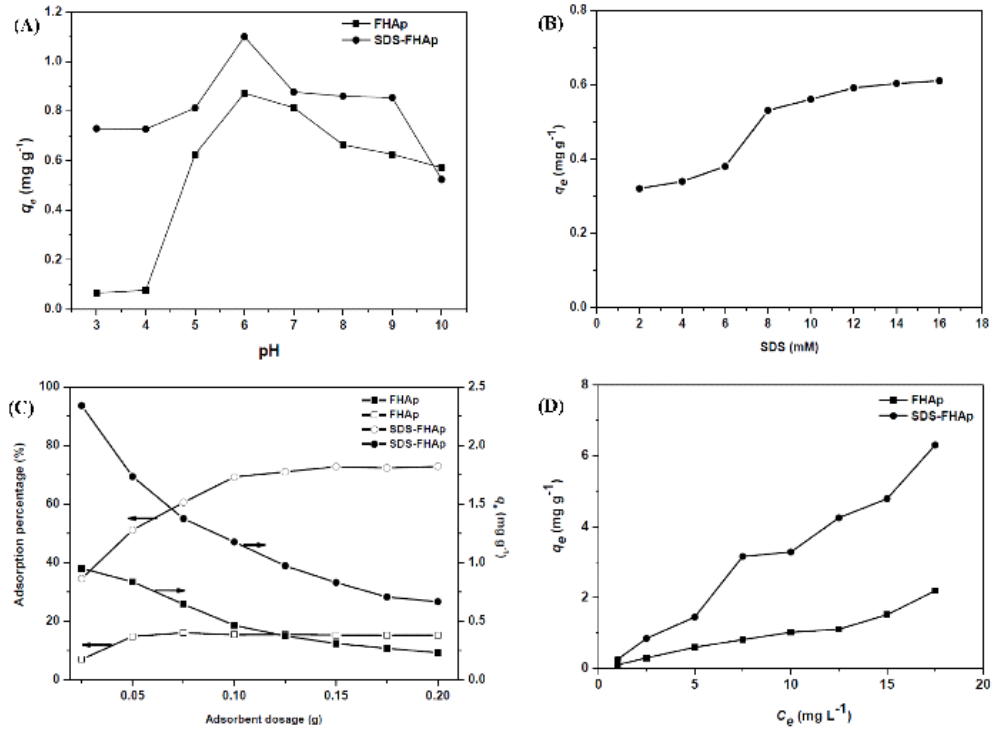


Fig. 2: Effects of (a) pH, (b) SDS concentration, (c) adsorbent dosage, and (d) initial concentration on the carotenoid adsorption. Adsorption conditions: (a) adsorbent dosage at 0.1 g, initial concentration at 10 mg L^{-1}, and 24 h contact time at 30±2°C; (b) solution pH 4, adsorbent dosage at 0.1 g, initial concentration at 10 mg L^{-1}, and 24 h contact time at 30±2°C; (c) solution pH 6, initial concentration at 10 mg L^{-1}, and 24 h contact time at 30±2°C; (d) solution pH 6, adsorbent dosage at 0.15 g for SDS-FHAp and 0.05 g for FHAp, and 24 h contact time at 30±2°C. Symbols: full symbols refer to adsorption capacities (mg g^{-1}); hollow symbols refer to adsorption percentage (%); FHAp in the presence of SDS (circle); FHAp in the absence of SDS (square)

attributed to a higher initial concentration provided a driving force to overcome all mass transfer resistances of the carotenoid between the aqueous and solid phase[22]. The adsorption capacity of SDS-FHAp shows the q_e trend which is higher than FHAp, indicating that the present of SDS can enhance adsorption capacity drastically. In this study, Langmuir and Freundlich adsorption isotherms were also used to describe the experimental results. The Langmuir isotherm model[23,24] assumes that an adsorption occurs on a homogenous adsorbent surface. The adsorption takes place only at specific sites of the adsorbent surface that is equally available and energetically equivalent, each site is carrying equal numbers of molecules and no interaction between the adsorbate molecules. The linear form of Langmuir isotherm model is valid for monolayer adsorption onto a surface, which can be written as follows[25]:

$$1/q_e = 1/(q_m K_L C_e) + 1/q_m \quad ...(6)$$

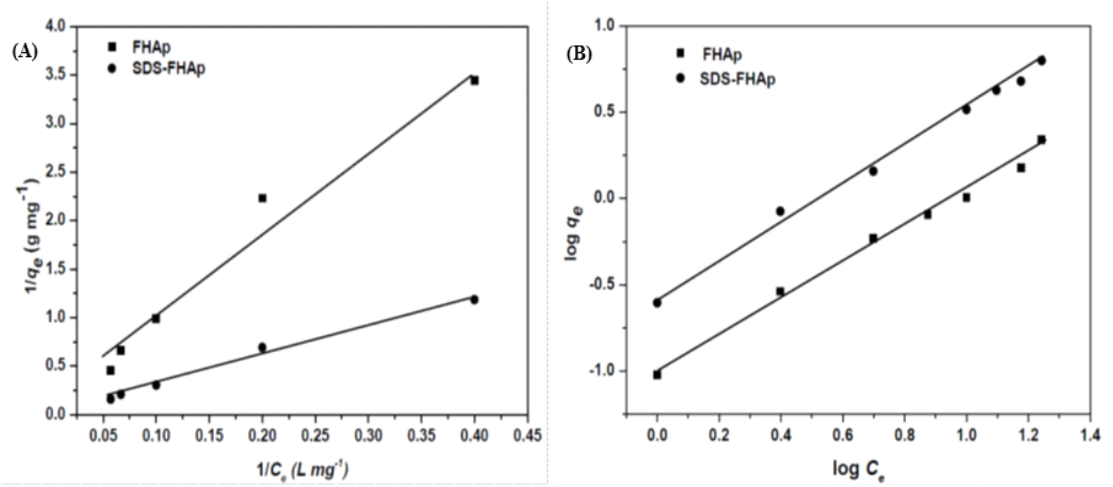


Fig. 3: Langmuir (a) and Frundlich (b) adsorption isotherms for the carotenoids adsorption onto FHAp in the presence and absence of SDS Symbols: SDS-FHAp (circle) and FHAp (square)

where q_m is the maximum amount of the carotenoid adsorbed per unit weight of adsorbent (mg g^{-1}) to form a complete monolayer covered on the surface at equilibrium carotenoid concentration, C_e is the concentration of carotenoid in aqueous solution at equilibrium (mg L^{-1}), q_e is the carotenoid adsorption capacity for adsorbent at equilibrium (mg g^{-1}), K_L is the Langmuir constant (L mg^{-1}). The values of q_m and K_L can be calculated from the intercepts and slopes the of the straight line by plotting $1/q_e$ versus $1/C_e$ (Fig. 3a). The model for Langmuir adsorption isotherm can be evaluated by dimensionless constant separation factor or equilibrium parameter, R_L, given as the following equation[26]:

$$R_L = 1/(1 + K_L C_0) \quad ...(7)$$

where C_0 is the initial concentration of carotenoid in aqueous solution (mg L^{-1}). The R_L value indicates at which the adsorption process is unfavorable ($R_L > 1$) or favorable ($0 < R_L < 1$). The R_L values for the adsorption of SDS-FHAp and FHAp are illustrated in Table 1.

The Freundlich isotherm model assumes that the adsorption process occurs on a heterogeneous surface with difference in energy of adsorption sites and the adsorption capacity is related to the concentration of an adsorbate at equilibrium. The mathematical description of the model for Freundlich adsorption isotherm can be represented by the linear form as follows[27]:

$$\log q_e = \log K_F + 1/n \log C_e \quad ...(8)$$

where K_F is the Freundlich constant related to the adsorption capacity (mg g^{-1})/(L mg^{-1})^n and n is

the intensity of adsorption. Values of 1/*n* are in the range 0.1 < 1/*n* < 1, the adsorption process is favorable. Both values of K_F and 1/*n* were calculated from the intercepts and slopes of the plots of log q_e versus log C_e (Fig. 3b). The constant values obtained from both Langmuir and Freundlich adsorption isotherms and their correlation coefficients, R^2, were calculated and are also summarized in Table 1. It can be concluded that Freundlich isotherm model fitted the experimental data better than Langmuir isotherm model because of high value of the correlation coefficient ($R^2 > 0.99$). A value of 1/n of 0.9183 indicates favorable adsorption and high affinity for carotenoids onto FHAp in the presence of SDS.

Effect of contact time

The effect of contact time on the adsorption of carotenoid onto SDS-FHAp and FHAp were investigated using 0.1 g dosage with 10 mg L^{-1} of the initial carotenoid concentration at pH 6 as shown in Fig. 4a. It was evident that the rate of adsorption increased rapidly at the initial period of contact time and then got down gradually with time until the adsorption reached at the equilibrium point as a plateau value in approximately 3 h and 6 h for SDS-FHAp and FHAp, respectively. No further adsorption was occurred with a prolonged contact time.

Kinetics of the adsorption is desirable information about the mechanism of adsorption, which is important for the adsorption process. The nature of the adsorption process depends on either physical or chemical characteristics of the adsorbent and the adsorbate. In order to elucidate the adsorption process of the carotenoid on both SDS-FHAp and FHAp, three kinetic models including a pseudo-first order, a pseudo-second order and an intraparticle diffusion models were used to analyze the experimental data. The pseudo-first order equation of Lagergren can be expressed as Eq. (9)[28,29].

$$\log(q_1 - q_t) = \log q_1 - k_1 t/2.303 \qquad ...(9)$$

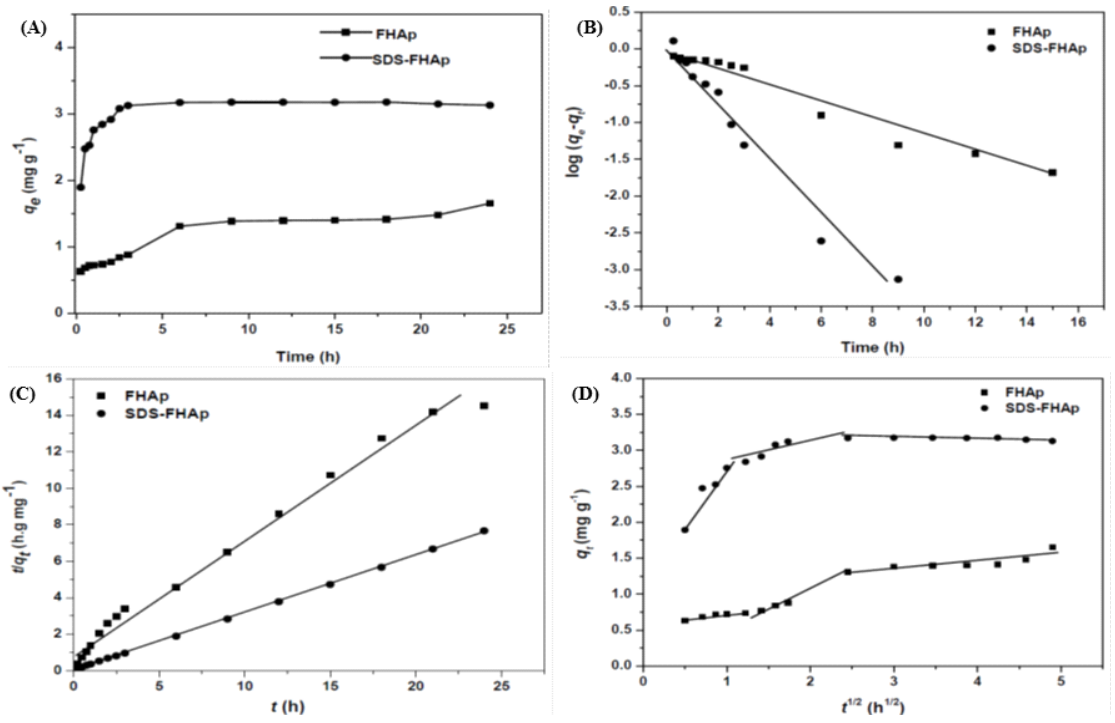


Fig. 4: Studies on contact time (a), pseudo-first order kinetic (b), pseudo-second order kinetic (c) and intraparticle diffusion kinetic (d) models for the carotenoids adsorption onto FHAp in the presence and absence of SDS at temperature of 30±2°C. For Symbols see Fig. 3

where q_t is the amount of carotenoid adsorbed at time t (mg g^{-1}), q_1 is the maximum adsorption capacity for pseudo-first-order kinetic model (mg g^{-1}). k_1 is the equilibrium rate constant of pseudo-first-order kinetic model (min^{-1}). The values of k_1 and q_1 are calculated from slope and intercepts of the plots of log (q_e-q_t) versus t (as shown in Fig. 4b). The linear form of the pseudo-second order kinetic model is expressed by following equation[30,31].

$$t/q_t = 1/\left(k_2 q_2^2\right) + t/q_2 \quad ...(10)$$

where q_2 is the maximum adsorption capacity (mg g^{-1}) for the pseudo-second-order adsorption, q_t is the amount of carotenoids adsorbed at equilibrium (mg g^{-1}) at time t (min) and k_2 is the rate constant of the pseudo-second-order adsorption (g (mg min)$^{-1}$). The values of q_2 and k_2 were calculated from slopes and intercepts of the plots (as shown in Fig. 4c) of t/q_t versus t.

The rate-limiting step which is an important factor is used to predict the adsorption process. For a solid-liquid adsorption process, the adsorption of an adsorbent and adsorbate usually takes place

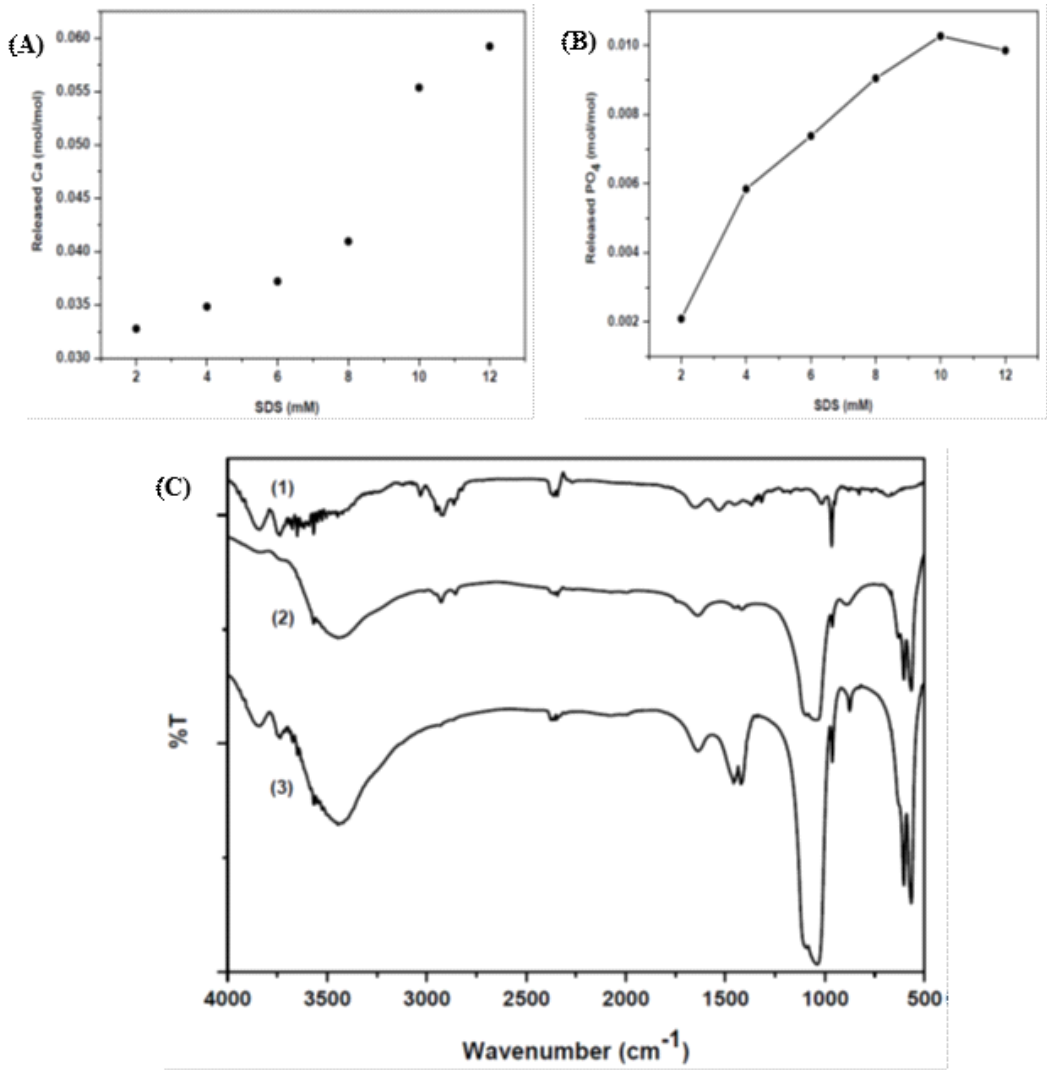


Fig. 5: The analysis of (a) calcium and (b) phosphate released into the aqueous solution after adsorption of SDS onto FHAp and (c) FT-IR spectra of (1) carotenoid standard, (2) carotenoid adsorbed onto FHAp in the presence of SDS and (3) FHAp

through four steps: bulk solution transport, film diffusion, pore diffusion, and adsorption on the surface or pores. Generally, the rate-limiting step is determined by the slowest step, which may be either film diffusion or diffusion into particle pores (intra-particle diffusion) or both. To investigate whether or not the intra-particle diffusion is the rate-controlling step, the intra-particle diffusion model was expressed as[31,32]:

$$q_t = k_p t^{1/2} + C \quad ...(11)$$

where q_t is the amount of carotenoid adsorbed at equilibrium (mg g^{-1}) at time t, C is the intercept and k_p is the intraparticle diffusion rate constant (mg (g $min^{1/2})^{-1}$). The values of k_p and C were calculated from slopes and intercepts of the plots of q_t versus $t^{1/2}$ (Fig. 4d).

Figure 4d shows the intraparticle diffusion plots for adsorption of carotenoid on SDS-FHAp and FHAp. The adsorption processes have three steps involving an initial linear portion, a second linear portion and plateau portion[32,33]. The first portion, rapid sharper portion is attributed to the diffusion of adsorbate through the solution to the external surface of adsorbent or the boundary layer diffusion of solute molecules. The second portion describes the gradual adsorption stage where intra-particle diffusion is the rate limiting. The third portion is the final equilibrium stage where intraparticle diffusion

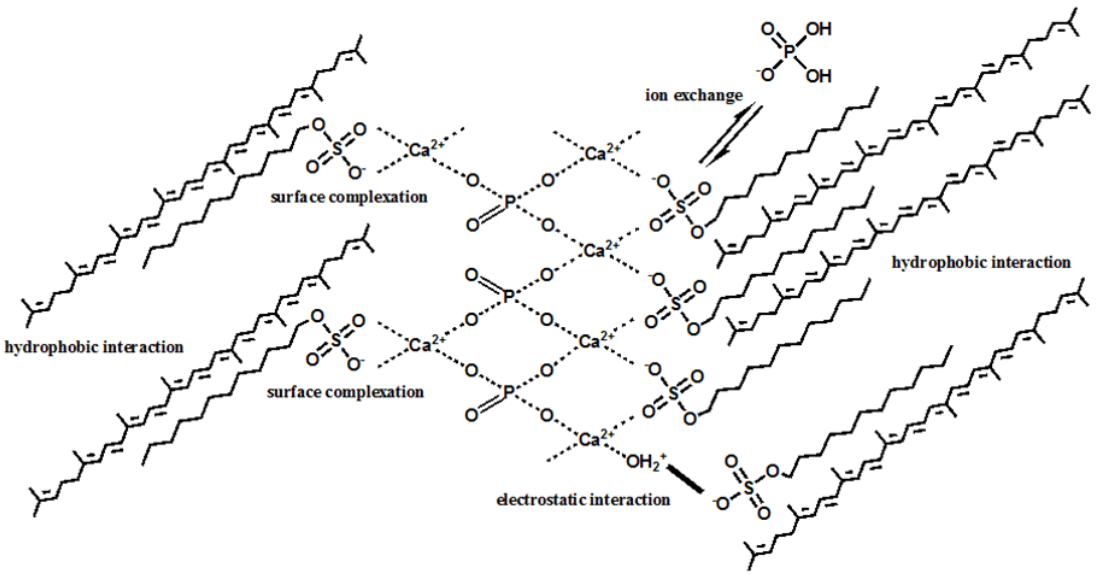


Fig. 6: The proposed adsorption interactions of the carotenoids extract onto the surface of FHAp in the presence of SDS

starts to slow down due to extremely low adsorbate concentrations left in the solutions. An intraparticle diffusion model was used to determine the rate-limiting step of the adsorption process. If the intraparticle diffusion occurs, then q_t versus $t^{1/2}$ will be linear and if the linear plot passes through the origin, it evidents that the rate-limiting step is only due to the intraparticle diffusion. This figure shows the linear plots did not pass through the origin, indicating that the intraparticle diffusion was not only the rate-limiting step in this process. The C value was greater than zero for SDS-FHAp implying that more than one process affected in this adsorption process. For FHAp, the value of C is zero which indicates that the rate of adsorption is controlled by intraparticle diffusion over all adsorption process.

The kinetic parameters for carotenoid adsorption onto SDS-FHAp and FHAp were calculated from Eq. (9) - (11) and are shown in Table 2. It was found that the pseudo-second order model fitted the experimental data better than the pseudo-first order model. It was noted that the values of correlation coefficient were very high (R^2 >0.999) and the calculated, $q_{e,cal}$ values were closer to the experimental $q_{e,exp}$ values.

Effect of temperature

In order to understand the effect of temperature on the adsorption process, both free energy change and entropy change factors should be considered to determine what processes will occur spontaneously. Thermodynamic parameters such as Gibbs free energy changes (ΔG°), enthalpy changes (ΔH°) and entropy changes (ΔS°) were calculated using the following equation[28,34]:

$$\ln K_d = \left(\Delta S^\circ / R\right) - \left(\Delta H^\circ / RT\right) \quad ...(12)$$

$$\Delta G^\circ = -RT \ln K_d \quad ...(13)$$

$$\Delta G^\circ = \Delta \mathrm{H}^0 - T\Delta S^0 \quad ...(14)$$

where ΔG° is Gibbs free energy change (kJ mol^{-1}), ΔH° is enthalpy change (kJ mol^{-1}) and ΔS° is entropy change (kJ mol^{-1} K^{-1}). T is temperature (K), R is gas constant (8.314 J mol^{-1} K^{-1}) and K_d is distribution coefficient of adsorbent (mL g^{-1}) and equal to C_s/C_e. Where, C_s and C_e are the amount of adsorbate adsorbed (mg g^{-1}) and the adsorbate concentration (mg L^{-1}) at the equilibrium state. The values of ΔH° and ΔS° could be obtained from slope and intercept of the plot of *ln* K_d versus $1/T$ at different temperatures. The data of thermodynamic parameters for the adsorption of carotenoid onto SDS-FHAp and FHAp are shown in Table 3. The negative values of ΔG° at various temperatures indicated that the adsorption process of the carotenoid on these sorbents was spontaneous nature. The degree of spontaneity on adsorption process is also increased with increasing temperature. Meanwhile, the positive values of ΔH° showed that this adsorption process was endothermic nature, which can also be predicted from the increase of the carotenoid adsorbed on the adsorbent with increasing in temperature. In addition, the positive values of ΔS° can be explained that this process is an increment in the randomness at the solid/liquid interface during the adsorption of the carotenoid onto both SDS-FHAp and FHAp[35].

Proposed adsorption interactions

At the surface of FHAp nanocrystal, there are three ion groups (phosphate ion, calcium ion and hydroxide ion) that can possibly interact with carotenoids in the presence of sodium dodecyl sulfate (SDS) through various mechanisms such as ion exchange, hydrophobic interaction and electrostatic forces. Therefore, the effect of adsorption and/or release of these ions were examined in order to support the mechanisms for the carotenoids sorption by FHAp. According to previous work[20] described that sulfate group of SDS can be replaced with phosphate ion on the FHAp surface by an ion exchange mechanism because both phosphate and sulfate are oxoacidic and tetrahedral and the interatomic distance of S-O of sulfate group (1.49 Å) is slightly different from P-O of phosphate ion (1.55 Å), so it can easily substitute PO_4^{3-} in the FHAp nanocrystal. Therefore, the one possible mechanism model is the formation of a monolayer at solid-liquid interface via an ion exchange between the sulfate group of SDS and the phosphate ion which occurred at the FHAp surface. After that, the carotenoids were adsorbed on the surface of the FHAp through hydrophobic interactions between polyunsaturated hydrocarbon of the carotenoids and the hydrocarbon tail of SDS at FHAP surface which is previously replaced. The relations between Ca^{2+} and PO_4^{3-} released into solution after the adsorption experiment were measured to confirm the release of Ca^{2+} and PO_4^{3-} from FHAp at different SDS concentration in solution (Fig . 5a and 5b). The result shows that an ion exchange mechanism is involved in the adsorption process. When the concentration of SDS is lower than *cmc*, it gave a good linear relationship between phosphate ion released into solution and an increasing of SDS concentration. On the other hand, the concentration of phosphate ion decreased with increasing SDS concentration above the *cmc*. In fact, SDS in aqueous solution is micelle form leading more stable than the aggregate formation on the FHAp surface resulting in the decrease in phosphate ion in solution. However, the ion exchange was not a dominant mechanism because no proportional ratio at 1:1 between the phosphate ion released and the SDS concentration was observed. Another possible mechanism may be an electrostatic interaction between the negatively charged dodecylsulfate of SDS and calcium ion on the surface site of FHAp[20], which leads the carotenoid adsorption on the FHAp through hydrophobic interactions between the hydrocarbon tail of SDS and the hydrophobic part of the carotenoids. Therefore, the experiment should be performed at the concentration of SDS lower

than the *cmc* to reduce the calcium released. FT-IR spectra of the carotenoid adsorptions in the presence or absence of SDS are shown in Fig. 5c. The new bands were obtained from the stretching vibration of =C-H at 3035 cm^{-1}, the stretching vibrations of non-symmetric and symmetric methyl bands at 2970 and 2852 cm^{-1}. It can confirm that the surface complex has occurred on the FHAp surface. Moreover, the electrostatic interactions between the protonated groups of the hydroxyl group (OH_2^+) of FHAp and the anionic SDS, followed by hydrophobic interactions between the tail of SDS and the hydrophobic part of the carotenoid can be occurred. Figure 6 illustrates the possible mechanisms of the carotenoid adsorption onto FHAp substrate in the presence of SDS.

CONCLUSION

Nanocrystalline FHAp was prepared by alkaline heat treatment method. The adsorption of carotenoid from tomato extract was carried out using nanocrystalline FHAp (with high specific surface area and crystallinity) in the presence of SDS. The carotenoid adsorption was enhanced by the hydrophobic group of SDS that adsorbed on the surface of FHAp via sulfate group. The adsorption was obeyed with Freundlich isotherm and well fitted by pseudo-second order kinetic model. The adsorption process was spontaneous, endothermic and physisorption process in nature. We expect this work to be utilized for many scientific fields such as pharmaceutical, medical, chemical applications and waste management.

ACKNOWLEDGEMENTS

The authors thank the Higher Education Research Promotion and National Research University Project of Thailand, Office of the Higher Education Commission, through the Food and Functional Food Research Cluster of Khon Kaen University (Grant No: NRU541019) for financial support. We are also grateful to the Center of Excellence for Innovation in Chemistry (PERCH-CIC), Commission on Higher Education, and Ministry of Education National for financial support.

REFERENCES

1. Ferraro, V.; Cruz, I. B.; Jorge, R. F.; Malcata, F. X.; Pintado, M. E.; Castro Paula, M. L. *Food Res. Int.* **2010**, *43*, 2221-2233.
2. Huang, Y. C.; Hsiao, P. C.; Chai, H. J. *Ceram. Int.* **2011**, *37*, 1825-1831.
3. Tongchan, P.; Prutipanlai, S.; Niyomwas, S.; Thongraung, C. *As. J. Food Agric.-Ind.* **2009**, *2*(04), 669-676.
4. Mondal, S.; Mondal, B.; Dey, A.; Mukhopadhyay, S. S. *J. Miner. Mater. Charact. Eng.* **2012**, *11*, 55-67.
5. Xu, Y.; Schwartz, F. W.; Traina, S. J. *Environ. Sci. Technol.* **1994**, *28*, 1472-1480.
6. Chen, X.; Wright, J. W.; Conca, J. L.; Peurrung, L. M. *Environ. Sci. Technol.* **1997**, *31*(3), 624-631.
7. Chaturvedi, P. K.; Seth, C. S.; Misra, V. *Chemosphere* **2006**, *64*, 1109-1114.
8. Mobasherpour, I.; Salahi, E.; Pazouki, M. *Desalination* **2011**, *266*, 142-148.
9. Sheha, R. R. *J. Colloid Interface Sci.* **2007**, *310*, 18-26.
10. Corami, A.; Mignardi, S.; Ferrini, V. *J. Hazard. Mater* **2007**, *146*, 164-170.
11. Rahman, K. *Clin. Intervention Aging* **2007**, *2*(2), 219-236.
12. Rao, L. G.; Mackinnon, E. S.; Josse, R. G.; Murray, T. M.; Strauss, A.; Rao, A. V. *Osteoporosis Int.* **2007**, *18*, 109-115.
13. Kongsri, S.; Janpradit, K.; Buapa, K.; Techawongstien, S.; Chanthai, S. *Chem. Eng. J.* **2013**, 215-216, 522-532.
14. Olives Barba, A. I.; Cámara Hurtado, M.; Sánchez Mata, M. C.; Fernández Ruiz, V.; López Sáenz de Tejada, M. *Food Chem.* **2006**, *95*, 328-336.
15. Landi, E.; Tampieri, A.; Celotti, G.; Sprio, S. *J. Eur. Ceram. Soc.* **2000**, *20*, 2377-2387.
16. Pucéat, E.; Reynard, B.; Lécuyer, C. *Chem. Geol.* **2004**, *205,* 83-97.
17. Markovic, M.; Fowler, B. O.; Tung, M. S. *J. Res. Nat. Inst. Stand. Technol.* **2004**, *109*, 553-568
18. Zaragoza, D. L.; Guzman, E. T. R.; Gutierrez, L. R. R. *J. Miner. Mater. Charact. Eng.* **2009**, *8*, 591-609.
19. Corami, A.; Mignardi, S.; Ferrini, V. *J. Colloid*

Interface Sci. **2008**, *317*, 402-408.
20. Shimabayashi, S.; Nishine, S.; Uno, T.; Hino, T. *ACS Symp. Ser.* **2002**, 105-116.
21. Han, R. P.; Zou, W. H.; Zhang, Z. P.; Shi, J.; Yang, J. J. *J. Hazard. Mater.* **2006**, *137*, 384-395.
22. Mobasherpour, I.; Salahi, E.; Pazouki, M. *Arabian J. Chem.* **2012**, *5,* 439-446.
23. Wong, Y. C.; Szeto, Y. S.; Cheung, W. H.; McKay, G. *Process Biochem.* **2004**, *39*, 693-702.
24. Konaganti, V. K.; Kota, R.; Patil, S.; Madra, G. *Chem. Eng. J.* 2010, *158*, 393-401.
25. Lin, K.; Pan, J.; Chen, Y.; Cheng, R.; Xu, X. *J. Hazard. Mater.* **2009**, *161*, 231-240.
26. Hameed, B.; Salman, J.; Ahmad, A. *J. Hazard. Mater.* **2009**, *163*, 121-126.
27. Sundaram, C. S.; Viswanathan, N.; Meenakshi, S. *J. Hazard. Mater.* **2008**, *155*, 206-215.
28. Islam, M.; Patel, R. K. *J. Hazard. Mater.* **2007***, 143*, 303-310.
29. Islam, M.; Mishra, P. C.; Patel, R. K. *J. Environ. Manage.* **2010**, *91*, 1883-1891.
30. Ho, Y. S.; McKay, G. *Chem. Eng. J.* **1998**, *70*, 115-124.
31. Gupta, N.; Kushwaha, A. K.; Chattopadhyaya, M. C. *J. Taiwan Inst. Chem. Eng.* **2012**, *43*, 604-613.
32. Ahmad, A. L.; Chan, C. Y.; Shukor, S. R.; Mashitah, M. D. *Chem. Eng. J.* 2009, *148*, 378-384.
33. Moussavi, G,; Khosravi, R. *J. Hazard. Mater.* **2010**, *183*, 724-730.
34. Wang, Y.; Chen, N.; Wei, W.; Cui, J.; Wei, Z. *Desalination* **2011**, *276*, 161-168.
35. Zhang, D.; Luo, H.; Zheng, L.; Wang, K.; Li, H.; Wang, Y,; Feng, H. *J. Hazard. Mater.* **2012**, 241-242, 418- 426.

Chiang Mai J. Sci. 2015; 42(2) : 304-316
http://epg.science.cmu.ac.th/ejournal/
Contributed Paper

Antibacterial Agents from *Trichoderma harzianum* Strain T9 Against Pathogenic Bacteria

Weeraya Phupiewkham [a,b], Pisan Sirithorn [c,d], Weerasak Saksirirat [c,d] and Sompong Thammasirirak*[a,b]

[a] Protein and Proteomics Research Center for Commercial and Industrial Purposes (ProCCI), Khon Kaen University, Khon Kaen, 40002, Thailand.

[b] Department of Biochemistry, Faculty of Science, Khon Kaen University, Khon Kaen, 40002, Thailand.

[c] Center of Excellence on Agricultural Biotechnology: (AG-BIO/PERDO-CHE), Bangkok, 10900, Thailand and Agricultural Biotechnology Research Center for Sustainable Economy, Khon Kaen University, Khon Kaen, 40002, Thailand.

[d] Department of Plant Science and Agriculture Resources, Faculty of Agriculture, Khon Kaen University, Khon Kaen , 40002, Thailand.

*Author for correspondence; e-mail: somkly@kku.ac.th

Received: 19 June 2013
Accepted: 21 August 2013

ABSTRACT

Trichoderma harzianum is an important fungus that well known for their ability to produce a wide range of secondary metabolite, antibiotic substance and cell-wall degrading enzyme (CWDE) against phytopathogenic fungi. However, information on the antimicrobial agent in *T. harzianum* isolate T9 has not been reported. Hence, this research is the first report about antibiotic activity of *Trichoderma* metabolites against human pathogenic bacteria and enterobacteria. Data for antimicrobial activity were measured at 3 (TS3), 6 (TS6), 9 (TS9), 12 (TS12) and 15 (TS15) days after culture. All culture supernatants from each culture day showed broad-spectrum activity in inhibiting growth of human pathogens and enterobacteria. Especially, inhibiting the growth of *Salmonella typhi* ATCC5784, this is a human-specific pathogen. Moreover, it was stable to thermal and pronase digestion. Therefore, these culture supernatants were further characterized by thin layer chromatography (TLC), high-performance liquid chromatography (HPLC) and proteomics analysis. The TLC fractions activity shows that their activity was loss when compared with the crude compound. Due to the higher antimicrobial activity of TS3 and TS12, their fractions were chosen for further purification by C_{18} Reversed-phase HPLC. The results showed that antibacterial activity against *Staphylococcus aureus* ATCC25923 of these samples was found only one peak of TS3 (F1) and two peaks of TS12 (F1 and F2). Additionally, proteomics analysis shows that the secreted proteins in log and early late log phase appeared to be a proteases enzyme. From our results, it is likely that *T. harzianum* isolate T9 against human pathogenic bacteria and enterobacteria with multiple mechanisms including release of antimicrobial agent and CWDE.

Keywords: *Trichoderma harzianum*, biological control, pathogenic fungi, purification, proteomics

1. INTRODUCTION

Trichoderma are free-living fungi which are highly interactive in root, soil and foliar environments. They are commonly used in the biocontrol of soil-borne plant pathogens of several economically important plant-pathogenic fungi [1]. *Trichoderma harzianum* most frequently used in biocontrol on cereals, fruits and plantation crops [2]. The classical mechanisms of control have included antibiosis, mycoparasitism and competition for nutrients [3]. *Trichoderma* strains inhibit or kill plant-pathogenic fungi through production of antifungal antibiotics and/or hydrolytic enzymes.

Antibiotic production of *Trichoderma* spp. was first described by Weindling [4]. There are many reports of compounds derived from *Trichoderma* species having antibacterial activity: volatile (e.g. ethylene, hydrogen cyanide, alcohols, monoterpenes, aldehydes and ketones up to C4 chain-length) and non-volatile (e.g. peptaibols and diketopiperazine-like gliotoxin and gliovirin) compounds [5]. Szekeres et al [6] have reviewed antagonistic metabolites produced by *Trichoderma* spp. The metabolites are linear, amphipathic polypeptides, namely, peptaibols and peptaibiotics. They also discussed the physico-chemical and biological properties of these antibiotic compounds which included the disruption of lipid membranes, anti-microbial activities and induction of plant resistance.

There are many strains of *Trichoderma* spp. that discovered the beneficial qualities for use as controlling plant disease such as brown spot disease in rice using *T. harzianum* and *T. viride*. And also in potato and tomato plants which found *T. harzianum* T39 could reduce the disease caused by *Phytophthora erythroseptica*. For *T. harzianum* strain T9, Saksirirat et al. [7] reported that it had an antimicrobial agent which shown to be effective against *Fusarium* sp. of tomato and can induce resistance against foliar diseases in tomato as well as showing broad-spectrum activity, thermal stability and resistance to pronase digestion [8]. Moreover, *T. harzianum* strain T9 kills plant-pathogenic fungi by cell-wall degrading enzymes (CWDEs), for instance, several kinds of CWDEs composed of chitinase, cellulase, β-1, 3-glucanase and xylanase [9]. From this information, only functions on their ability to against phytopathogenic fungi on plants have been reported. To the best of our knowledge, the functions of *Trichoderma* spp. on their ability to against human pathogenic bacteria and enterobacteria have not been reported. Therefore, in this research, the antibiotic activities of *T. harzianum* strain T9 against human pathogenic bacteria and enterobacteria which would be important in the medical pharmaceutical industry were examined and the antimicrobial agents were further characterized by thin layer chromatography (TLC), high-performance liquid chromatography (HPLC) and proteomics.

2. MATERIALS AND METHODS

2.1 Strains and Culture Conditions

T. harzianum strain T9 was obtained from Department of Plant Science and Agricultural Research, Faculty of Agriculture, Khon Kaen University, Thailand. It was cultivated and maintained on potato dextrose agar (PDA, HEMEDIA, HiMedia Laboratories Pvt.Ltd, India) at 30°C for 7 days. The inoculum (10^8 unit/ml) in potato dextrose broth (PDB: HEMEDIA, HiMedia Laboratories Pvt.Ltd, India) was incubated at 25°C in an incubator shaker at 125 rpm for 15 days. The culture supernatants were collected at day 3, 6, 9, 12 and 15.

The collected supernatants were filtrated

by Whatman® No. 1 and concentrated by evaporation. The culture filtrates were tested for biochemical properties and studied for proteomic analysis. In addition, the culture filtrates were purified by TLC.

2.2 Target Microorganisms

The target microorganisms consisted of 7 Gram positive bacteria, *Bacillus subtilis* TISTR008, *Bacillus subtilis* ATCC6633, *Bacillus amyloloquefaciens* TISTR1045, *Bacillus cereus* ATCC11778, *Bacillus lichenisformis* TISTR1010, *Staphylococcus aureus* ATCC25923, *Staphylococcus aureus* ATCC1466 and 3 Gram negative bacteria, *Escherichia coli* O157:H7, *Vibrio cholerae* isolate (clinical) and *Salmonella typhi* ATCC5784.

2.3 Antibacterial Activity Assay

The antibacterial activity was tested by using a disc diffusion assay with minor modification of Juan et al method. [10]. For the target microorganisms, each strain was grown on nutrient broth (NB: HEMEDIA, HiMedia Laboratories Pvt.Ltd, India) media at 37°C for 6-8 h. The culture was diluted to a final OD_{600} of approximately 0.01 and swabbed it onto a nutrient agar (NA: HEMEDIA, HiMedia Laboratories Pvt.Ltd, India) plate. After that, 6 mm paper discs were applied on the plate, then 30 µl of samples were pipetted onto the disc and incubated at 37°C for 5-6 h. The inhibition zone was measured after 6-8 h of incubation. A potato dextrose broth (PDB) was used as a negative control. Broad-spectrum antibiotic streptomycin (10 µg) disc was used as positive control as described by Juan et al. [10].

2.4 Biochemical Property Assay

The culture filtrates at 3, 6, 9, 12 and 15 days of *T. harzianum* strain T9 were heated at different temperature in the ranges of 60°C - 121°C for 15 min for thermal stability assay. For enzyme stability, culture supernatants were digested with pronase (5.82 U) and 500 mM $CaCl_2$ was added as co-factor. The inhibiting growth of microorganisms was tested by disc diffusion assay.

2.5 Isolation of Antibacterial Agents by Thin-layer Chromatography (TLC)

The culture filtrates at 3, 6, 9, 12 and 15 days were purified by TLC [11]. The active methanol: chloroform (90:10) fraction was concentrated and developed on analytical and preparative silica-gel TLC plate (silica Gel 60 F254, Merck). The spots were visualized by ninhydrin and I_2 vapor. All fractions from TLC were screened for their antibacterial activity by disc diffusion assay. The target microorganism for testing was *S. aureus* ATCC25923. The active fractions were extracted by methanol and evaporated to dryness, then dissolved in a minimum volume of sterile distilled water and applied to RP-HPLC.

2.6 Purification of Antibacterial Agents by Reverse Phase High-performance Liquid Chromatography (RP-HPLC)

The active fractions from TLC were separated by RP-HPLC (ODS-AM 120-S5 4.60 × 250 mm C_{18} column). The mobile phase was 0.1% formic acid and methanol at a flow rate of 0.2 ml/min. The column effluent was monitored for absorbance at 220 nm and 280 nm. Each fraction was collected and dried, then dissolved in a minimum volume of sterile-distilled water and assayed for antibacterial activity by a disc diffusion method. The inhibition zone in the paper disc was measured after 6-8 h of incubation. The mobile phase; 0.1% formic acid and methanol were also dried and dissolved in a minimum volume of sterile-distilled water. Then the re dissolved of 0.1% formic acid, methanol and sterile

distilled water were used as a negative control. Tetracycline (30 μg) discs were used as positive controls.

2.7 Proteomics of Antibacterial Agents by 2-Dimensional Polyacrylamide Gel Electrophoresis (2D-PAGE)

The culture filtrate at 3, 6, 9, 12 and 15 days of *T. harzianum* strain T9 was cleaned to remove the contaminating substances by 2D-Clean up kit protocol (Amersharm Bioscience, Sweden). Protein samples were re-suspended in rehydration buffer (7M urea, 2M thiourea, or 2% of CHAPS (0.5 g), 2mM dithiothreitol (DTT), focused immobilized pH gradient (IPG) buffer and 0.2% bromophenol blue). An adequate amount of protein was loaded on the strip holder (100 μg of protein sample for 7 cm). The samples were separated in the first dimension on IPG strips pH 4-7 size 7 cm. IPG strips were rehydrated for 12 h at 20°C, followed by step 1 at 250 Vhr (500V, 30 min), step 2 at 800 Vhr (1,000V, 30 min), step 3 at 8500 Vhr (5,000V, 100 min) until the run was completed. The IPG strips were equilibrated for 15 min by DTT-containing equilibration solution (50 mM Tris-HCl pH 8.8, 6 M urea, 30% glycerol, 2% SDS and 0.002% bromophenol blue). After that, a second equilibration was made in iodocetamide (IAA)-containing equilibration solution (without DTT) for 15 min. IPG strips were transferred onto 15% SDS-PAGE without a stacking gel and the gel was inserted in the electrophoresis apparatus and electrophoresis started. SDS-gels were run at 10 mA per gel for 15 min. Subsequently this gel was increased to 20 mA per gel until the run was stopped. Proteins were visualized by placing gels directly into the colloidal coomassie brilliant blue G250 staining solution.

2.8 Identication of Protein by Liquid Chromatography Coupled to Mass Spectrometry (LC/MS-MS) Configuration

The proteins were purified and identified by methods of Prajanban et al. [12] Briefly, protein spots were excised from the 2D-gels and digested with trypsin. The peptide solutions were dried overnight in an incubator at 40°C. The dried peptides were stored at -20°C until LC/MS-MS analysis was performed. The digested peptides were further subjected to LC/MS-MS; a nanoACQUITY system (Waters Corp., Milford, MA, USA) that was composed of a Symmetry C18 Trap column and a BEH130 C18 analytical reverse phase column (Waters Corp., Milford, MA, USA) to attain the highest chromatographic resolution before MS detection. Each tryptic peptide was detected using a SYNAPTTMHDMS mass spectrometer (Waters Corp., Manchester, UK) in positive nanoelectrospray ion mode. The peptides were analyzed using a local Mascot server (Matrix Science) and the following search parameters: a specified trypsin enzymatic cleavage with one possible missed cleavage, +/-0.6 Da mass tolerances for MS and MS/MS, a peptide tolerance of 1.2 Da, 1+, 2+, 3+ ions, methionine oxidation variable modification, carbamidomethyl (C) fixed modification, monoisotopic mass were used. The p*I* and molecular mass value, MASCOT score, number of peptide matches, peptide sequence and sequence coverage were used to estimate the data base search results.

3. RESULTS AND DISCUSSION

The *T. harzianum* strain T9 culture supernatants of TS3, TS6, TS9, TS12 and TS15 were effective against human pathogens and enterobacteria including

B. subtilis TISTR008, *B. subtilis* TISTR6633, *B. amyloloquefaciens* TISTR1045, *B. cereus* ATCC11778, *B. lichenisformis* TISTR1010, *S. aureus* ATCC25923, *S. aureus* ATCC1466, *E. coli* O157:H7, *V. cholerae* isolate (clinical) and *S. typhi* ATCC5784 excepted that TS3 was not effective against *V. cholerae* (clinical isolate) (Table 1). Especially, the substance from *T. harzianum* strain T9 showed the highest activity in inhibiting the growth of *S. typhi* ATCC5784, which is a human-specific pathogen causing systemic febrile illness typhoid fever. When compared the antimicrobial activity among them, TS12 and TS15; the early late log phase showed the highest activity. This evidence might be due to the metabolites at different growth phases. At the early late log phase, most of secretion agents were found to be a secondary metabolite and several antibiotics which cause to exhibit several pathogens [13]. Secondary metabolites such as Gliotoxin, a secondary metabolite is produced by *T. viride* against several phytopathogenic fungi [14] and butenolide and harzianopyridone produced by *T. harzianum* strains T22 and T39, respectively was strong even at low concentrations against *Gaeumannomyces graminis* var. *tritici*. [15]. Whereas, days 3-7 which are a log phase, several reports suggested that the most secretory agents were important for their growth. Therefore, from the best activity against human pathogen of substance, it has a great potential to be used as new sources of development for antibiotic instead of currently used antibiotic as drug resistant.

Table 1. Antibacterial activity of culture supernatant from *T. harzianum* strain T9 on the target microorganisms.

Microorganisms	Inhibition				
	Culture supernatant				
	TS3	TS6	TS9	TS12	TS15
B. subtilis TISTR008	+	+	+	+ +	+ +
B. subtilis ATCC6633	+	+	+	+ +	+ +
B. cereus ATCC11778	+ +	+ +	+ + +	+ + +	+ + +
B. amyloliquefaciens TISTR1014	+	+	+ +	+ +	+ +
B. lichenisformis TISTR1010	+	+	+ +	+ +	+ +
S. aureus ATCC1466	+ +	+ +	+ +	+ +	+ +
S. aureus ATCC25923	+ +	+ +	+ +	+ +	+ +
E. coli O157:H7	+	+	+	+ +	+ +
V. cholerae (clinical)	-	+	+ +	+ +	+ +
Salmonella typhi ATCC5784	+ + +	+ + +	+ + +	+ + +	+ + +

Activities were classified according to the diameter of the inhibition zones around the disc [10]: - : non activity (6 mm), + : inhibition zone 7-12 mm, + + : inhibition zone 13-19 mm, + + + : inhibition zone 20-27 mm, TS3 to TS15: Culture filtrate during culture process at 3, 6, 9, 12 and 15 days, respectively.

Although both of TS12 and TS15 exhibited the highest antimicrobial activity, the culture supernatants from all days were used for testing the thermal and enzyme stability. The thermal stability results indicated that antibacterial agent from all culture date (TS3-TS15) showed stable and remained biologically active over a temperature range from 60 to 100°C (Figure 1a). Moreover, to prove the antimicrobial agents are the

protein, the pronase digestion assay which is more rapid and straightforward was used to indicate an active protein. Pronase activity extends to both denatured and native proteins leading to complete and nearly complete digestion into individual amino acids. Therefore, if the antimicrobial agents are the protein, the activity of them should be loss. And our results found there were still antimicrobial activity against representative strains (i.e. *B. cereus* ATCC11778 and *S. aureus* ATCC25923) (Figure 1b). These results similar with Song *et al*. [16] that found the antimicrobial substance named Trichokonins isolated from *Trichoderma koningii* SMF2 was stable and remained biological active over a wide pH (3-10) and temperature range (50-121°C). In addition, Trichokonins were shown insensitive to proteolytic enzymes and (most of) their antimicrobial activity was retained following exposure to different proteolytic enzymes. These results suggested that the active compounds might be not a protein in nature.

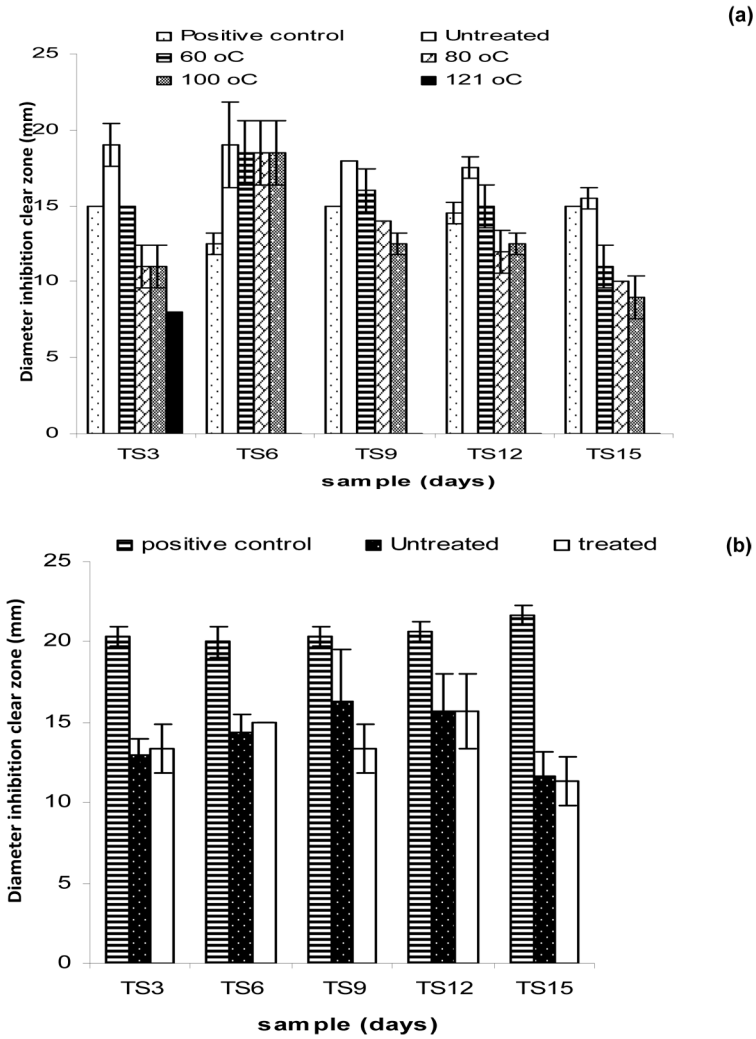


Figure 1. Thermal-stability (a) and pronase-stability (b) of culture filtrates, inhibition zone as examined by disc diffusion assay. TS3 to TS15: Culture filtrates of day 3, 6, 9, 12 and 15, respectively. Streptomycin was used as a positive control.

The TLC was a simple technique for separating known or unknown compound and visualizing of the components of a reaction mixture and very easily to detect protein, peptide, aromatic compound, etc. [17]. This method can identify several compounds depending on TLC staining, iodine has a high affinity for both unsaturated and aromatic compounds [18]. After the TLC analysis, 5 fractions from TS3, 5 fractions from TS6, 4 fractions from TS9, 5 fractions from TS12 and 3 fractions from TS15 were obtained. These substances were detected by iodine vapor but not clearly visible by ninhydrin (Figure 2). Furthermore, all of the fractions at TS3-TS15 were extracted and tested for antibacterial activity. Only fraction F1 from TS3 and TS12 showed antibacterial activity against *S. aureus* ATCC 25923 as could be seen in Table 2. The purified agents were loss their activity when comparing with crude supernatants. The antibacterial agents might be contained a large polymer complex in their structure which was insoluble in mobile phase and the function of antibacterial substances might be inhibited pathogens by cohesion with a complex structure of the compound. These results coincided with the report of biocontrol agent from *T. viride* that was detected by iodine vapor and the substance has aromatic ring in their structure [19].

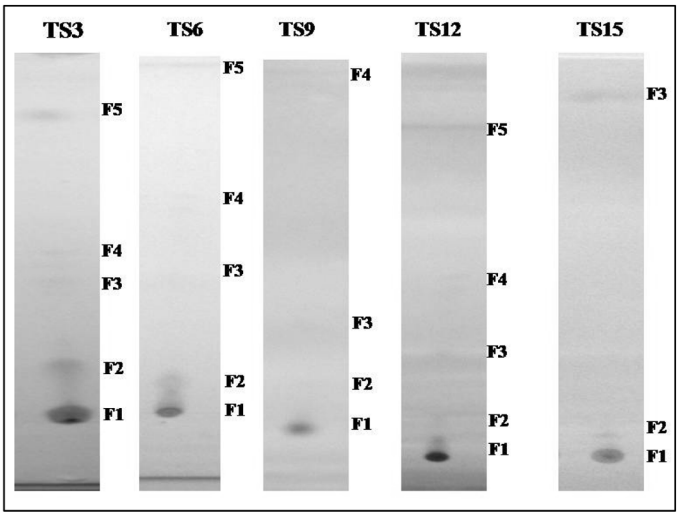


Figure 2. TLC pattern of culture supernatant from *T. harzianum* isolate T9 detected by iodine vapor. TS3 (0.65 μg/μl, 4μl); TS6 (0.55 μg/μl, 4μl); TS9 (0.85 μg/μl, 4μl); TS12 (0.85 μg/μl, 4μl); TS15 (0.55 μg/μl, 4μl).

Table 2. Antibacterial activity of TLC fractions against *S. aureus* ATCC25923.

Fraction No.	Positive control	Negative control	Fraction tested
TS3 F1	✓	-	✓
F2	✓	-	-
F3	✓	-	-
F4	✓	-	-
F5	✓	-	-
TS6 F1	✓	-	-
F2	✓	-	-
F3	✓	-	-
F4	✓	-	-
F5	✓	-	-
TS9 F1	✓	-	-
F2	✓	-	-
F3	✓	-	-
F4	✓	-	-
TS12 F1	✓	-	✓
F2	✓	-	-
F3	✓	-	-
F4	✓	-	-
F5	✓	-	-
TS15 F1	✓	-	-
F2	✓	-	-
F3	✓	-	-

✓ Inhibition zone appears

\- Inhibition zone does not appear

The active fraction F1 of TS3 and TS12 were further purified by C_{18} RP-HPLC. They were observed that the HPLC separation showed at least 16 peaks and 7 peaks for TS3 and TS12, respectively (Figure 3). The HPLC fractions that exhibited antimicrobial activity against *S. aureus* ATCC25923 occurred at only one peak of TS3 (F1) (Figure 4a) and two peaks of TS12 (F1 and F2) (Figure 4b). The elution time of TS3F1, TS12F1 and TS12F2 was approximately 15-17 min. The closely of elution time might be implied that TS3F1, TS12F1 and TS12F2 were the same compound.

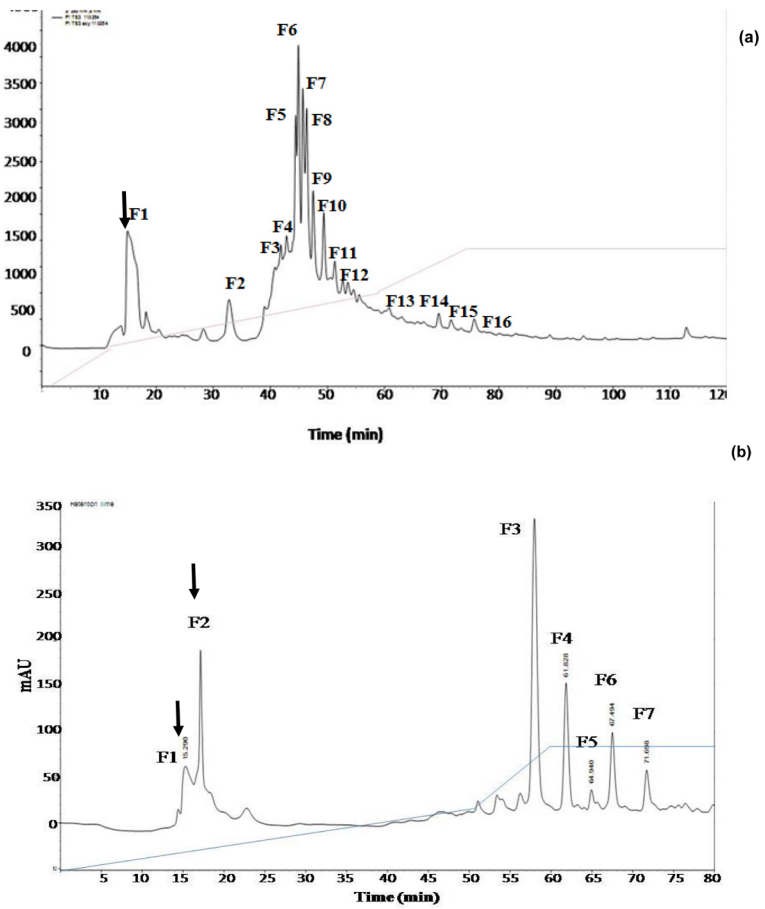


Figure 3. HPLC chromatogram of culture supernatant from *T. harzianum* isolate T9 on RP-HPLC (C18 column) detected with 280 nm. The mobile phase was 0.1% formic acid as solvent A and methanol as solvent B. (a): Chromatogram of TS3 and the arrow indicated the active fraction (F1), (b): Chromatogram of TS12 and the arrow indicated the active fraction (F1 and F2).

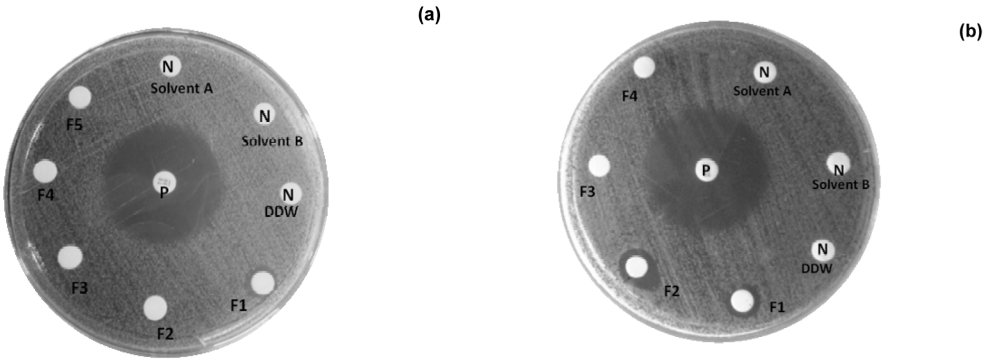


Figure 4. Antibacterial activity of HPLC fractions toward *S. aureus* ATCC 25923. P: Tetracycline (30 μg) used as a positive control; N: Solvent A, solvent B and distilled water (DDW) used as a negative control; F4 to F5: fraction purified by HPLC; (a): the antibacterial activity of HPLC fractions from TS3; (b): the antibacterial activity of HPLC fraction from TS12.

In general, *Trichoderma* spp. has evolved numerous mechanisms to control phytopathogenic bacteria or fungi which not only produced secondary metabolite but also especially secretion of CWDE, peptaibols or protein to kill plant pathogen [20]. In order to analyze the protein associated with biological control, the proteomics study is the first choice to choose for analyzing them. The antibacterial substances at log phase (between first day to 7 days) and early late log phase (between 8 to15 days) were separated by 2D-PAGE and found that 65 spots were observed on both phase. They showed molecular mass between 14 to 97 kDa and all of the major spots were located in a p*I* between 4 to 5. The difference of protein expression patterns between log and early late log phase were found as showed in Figure 5. At log phase (3-7 days), most of the proteins showed molecular mass between 30-97 kDa and all of them had major spots located at p*I* between 4 to 5. The protein patterns showed clear spots, without streaking (Figure 5a). Whereas the protein patterns at early late log phase (8-15 days) showed molecular mass between 14-67 kDa and major spots located at p*I* between 4 to 5 (Figure 5b).

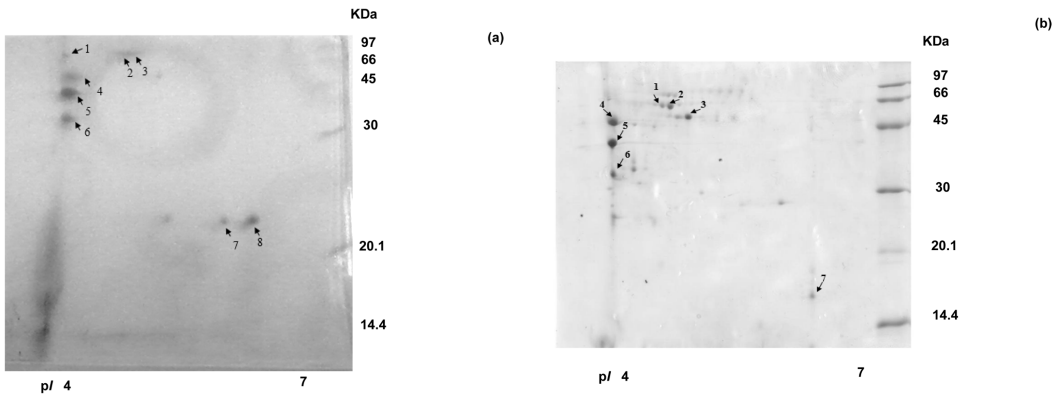


Figure 5. 2D-PAGE analysis of protein expression from culture supernatant of *T. harzianum* isolate T9 during culture process at 6 days, representing log phase (a) and at 12 days, representing early late log phase (b). The first dimension, 100 μg of protein was loaded on an IPG strip with a linear gradient of pH 4-7. The second dimension, 15% polyacrylamide gel was used.

Each protein spots were excised from each gel and identified by LC/MS-MS. Only fifteen spots were successfully identified by mass spectrometry after standard trypsin hydrolysis. Eight spot proteins were analyzed at log phase (Figure 5A). Three of eight proteins submitted to Mascot search were identied with known functions, namely; putative aspartate protease, putative aspartic protease and extracellular small protein 1 (Esp1) (Table 3). Seven spots of protein in early late log phase (Figure 5B) were analyzed. 3 of 7 proteins submitted to Mascot search were identied with known functions, namely; Chain A glycoside hydrolase Family 15, glucoamylase, Alpha-N-arabinofuranosidase and conserved hypothetical protein (Table 4). After identified, all of the proteins spots at log phase and early late log phase were showed in proteases especially the CWDEs. This data coincide with previous report they found mostly CWDEs such as proteases, hydrolase, glucoamylase and chitinase are major lytic enzymes that are secreted and attack the cell wall of phytopathogenic fungi to cause cell lysis and subsequent death [21].

Table 3. Protein identification by LC/MS-MS of antibacterial substance from *T. harzianum* strain T9 in log phase (6 days).

Spot No.	Matched protein	Theoretical MW/p*I*	Experimental MW/p*I*	Sequences coverage(%)	Matched peptide	Species	Accession number	Score
4	Putative Aspartate Protease	42.41/4.65	55/4.2	2	2	*Hypocrea lixii* (*T. harzianum*)	gi| 11558498	79
5	Putative Aspartic Protease	39.65/5.61	41/4.2	6	2	*Hypocrea lixii* (*T. harzianum*)	gi| 82173725	194
8	Extracellular Small Protein 1 (Esp15)	14.64/5.76	22.55/6.2	7	1	*Hypocrea virens* (*T. virens*)	gi| 73672053	51

Table 4. Protein identification by LC/MS-MS of antibacterial substance from *T. harzianum* strain T9 in early late log phase (12 days).

Spot No.	Matched protein	Theoretical MW/p*I*	Experimental MW/p*I*	Sequences coverage(%)	Matched peptide	Species	Accession number	Score
1	Chain A,64.44/4.85 Glycoside Hydrolase Family 15		66/5	2	2	*Hypocrea jecorina* (*Trichoderma* sp.)	gi| 261825113	90
2	Glucoamylase	66.89/9.04	66/5.2	2	2	*Hypocrea sp.* (*Trichoderma* sp.)	gi| 61657886	69
3	Alpha-N arabinofuranosidase	51.71/6.05	55.2/5	3	2	Trichoderma reesei	ABF1_TRIRE	55
4	Conserved hypothetical protein	43.34/9.34	50.9/4	36	2	Talaromyces stipitatus	gi| 242761842	80

4. CONCLUSION

Our study has demonstrated that *T. harzianum* strain T9 shows a variety of antibacterial activities against human pathogens and enterobacteria that would be the great importance in medicine or alimentary industry. In the future, the structure of this substance would be characterized.

ACKNOWLEDMENTS

This Research is partially supported by the Center of Excellence on Agricultural Biotechnology, Science and Technology Postgraduate Education and Research Development Office. Office of Higher Education Commission, Ministry of Education (AG-BIO/PERDO-CHE) and Agricultural Biotechnology Research Center for Sustainable Economy, Khon Kaen University, and by Protein and Proteomics Research Center for Commercial and Industrial Purposes (ProCCI), Khon Kaen University. We wish to acknowledge the support of the Khon Kaen University Publication Clinic, Research and Technology Transfer Affairs, Khon Kaen University, for their assistance.

REFERENCES

[1] Howell C.R., The Role of Antibiosis in Biocontrol; in Harman G.E. and Kubicek C.P., eds., *Trichoderma and Gliocladium*,

Vol 2. *Enzymes, Biological Control, and Commercial Applications*, Taylor & Francis, London, 1998; 173-184.

[2] Benitez T., Rincon A.M., Limon M.C. and Codon A.C., Biocontrol mechanisms of *Trichoderma* strains, *Int. Microbiol*., 2004; **7**: 249-260.

[3] Chet I., *Trichoderma*: Application, Mode of Action and Potential as Biocontrol Agent of Soilborne Plant Pathogenic Fungi; in Chet I., ed., *Innovative Approaches to Plant Disease Control*, John Wiley & Sons, New York, 1987; 137-160.

[4] Weindling R., Studies on a lethal principle effective in the parasitic action of *Trichoderma lignorum* on *Rhizoctonia solani* and other soil fungi, *Phytopathology*, 1934; **24**: 1153-1179.

[5] Sivasithamparam K. and Ghisalberti E.L., Secondary metabolism in *Trichoderma* and *Gliocladium*; in Harman G.E. and Kubicek C.P., eds., *Trichoderma and Gliocladium*, Taylor & Francis, London, 1998; 139-149.

[6] Szekeres A., Leitgeb B., Kredics L., Antal Z., Hatvani L., Manczinger L. and Vagvolgyi C., Peptaibols and related peptaibiotics of *Trichoderma*. A review, *Acta Microbiol. Immunol. Hungary*, 2005; **52**: 137-68. DOI 10.1556AMicr.52.2005.2.2.

[7] Saksirirak W., Chareerak P. and Bunyatrachata W., Induced systemic resistance of biocontrol fungus, *Trichoderma* spp. against bacterial and gray leaf spot in tomatoes, *As. J. Food Ag-Ind., Special Issue*, 2009; 99-104.

[8] Phupiewkham W., Sirithorn P., Saksirirat W. and Thammasirirak S., Characterization of cell-wall degrading enzymes produced by *T. harzianum* isolate T9, *Lao J. Appl. Sci*., 2001; **2(1)**: 140-143.

[9] Phupiewkham W., Sirithorn P., Saksirirat W. and Thammasirirak S., Study of biological activity of *Trichoderma harzianum* isolate T9, *KKU Res. J. (Graduate Studies)*, 2010; **10(1)**: 9-13.

[10] Juan A.V., Luis S.Z., Angela B.I., Francisca V.N., Santiago G., Hermosa M.R. and Enrique M., Screening of antimicrobial activities in *Trichoderma* isolates representing three *Trichoderma* sections, *Mycol. Res*., 2005; **109(12)**: 1397-1406. DOI 10.1017/S0953756205003898.

[11] Thomson K.S. and Moland E.S., The new β-lactamases of Gram-negative bacteria at the dawn of the new millennium, *Microbes Infect*., 2000; **2**: 1225-1235.

[12] Prajanban B., Shawsuan L., Daduang S., Kommanee J., Roytrakul S., Dhiravisit A. and Thammasirirak S., Identification of five reptile egg whites protein using MALDI-TOF mass spectrometry and LC/MS-MS analysis, *J. Proteomics*, 2012; **75**: 1940-1959. DOI 10.1016 j.jprot. 2012.01.004.

[13] Benitez T., Rincon A.M., Limon M.C. and Codon A.C., Biocontrol mechanisms of *Trichoderma* strains, *Int. Microbiol*., 2004; **7**: 249-260. DOI 10.1590/S0074-02762003000200010.

[14] Geetha I., Paily K.P., Padmanaban V. and Balaraman K., Oviposition response of the mosquito, *Culex quinquefasciatus* to the secondary metabolite(s) of the fungus, *Trichoderma viride*, *Mem. Inst. Oswaldo Cruz*, *Rio de Janeiro*, 2003; **98(2)**: 223-226. DOI 10.1111/j.1472-765X.2006.01939.x.

[15] Vinale F., Marra R., Scala F., Ghisalberti E.L., Lorito M. and Sivasithamparam K., Major secondary metabolites produced by two commercial *Trichoderma* strains active

against different phytopathogens, *Lett. Appl. Microbiol*., 2006; **43**: 143-148. DOI 10.1111/j.1574-6968.2006.00316.x.

[16] Song X.Y., Shen Q.Tao., Xie S.T., Chen X.L., Sun C.Y. and Zhang Y. Z., Broad-spectrum antimicrobial activity and high stability of Trichokonins from *Trichoderma koningii* SMF2 against plant pathogens, *FEMS Microbiol. Lett*., 2006; **260**: 119-125.

[17] Jork, H.H., Funk W., Fischer W. and Wimmer H., *Thin-layer Chromatography Reagents and Detection Methods, vol. 1a. Physical and Chemical Detection Methods: Fundamentals, Reagents,* VHC, Weinheim, Germany, 1990. DOI 10.1007/BF0263 5828.

[18] Sims A.P.R. and Larose J.A.C., The use of iodine vapor as a general detecting agent in the thin layer chromatography of lipids, *J. Am. Oil Chem. Soc*., 1962; **39**: 232. DOI 10.1111/j.1365-2915.1994. tb00103.x.

[19] Beehler W.J., Millar G.J. and Mulla S.M., Protein hydrolysates and associated contaminants as oviposition attractants for the mosquito *Culex quinquefasciatus*, *Med. Vet. Entomol*., 1994; **8**: 381-385. DOI 10.1094/PHYTO-96-0190.

[20] Harman G.E., Overview of mechanisms and uses of *Trichoderma* spp, *Phytopathology*, 2006; **96**:190-194. DOI 10.1016/S0065-2164(04)56010-0.

[21] Harman G.E., Lorito M. and Lynch J.M., Uses of *Trichoderma* spp. to alleviate or remediate soil and water pollution, *Adv. Appl. Microbiol*., 2004; **56**: 313-330.

Scientia Horticulturae 184 (2015) 85–92

Contents lists available at ScienceDirect

Scientia Horticulturae

journal homepage: www.elsevier.com/locate/scihorti

Development of seed agglomeration technology using lettuce and tomato as model vegetable crop seeds

Potjana Sikhao[a,b], Alan G. Taylor[a,*], Edward T. Marino[a], Catharine M. Catranis[a], Boonmee Siri[b]

[a] Department of Horticulture, New York State Agricultural Experiment Station, Cornell University, Geneva, NY 14456, USA
[b] Agronomy Division, Faculty of Agriculture, Department of Plant Science and Agricultural Resources, Khon Kaen University, Khon Kaen 40002, Thailand

ARTICLE INFO

Article history:
Received 27 August 2014
Received in revised form 9 December 2014
Accepted 19 December 2014
Available online 14 January 2015

Keywords:
Tomato seed
Lettuce seed
Seed agglomeration
Seed pelleting
Seed coating
Multiple seeds

ABSTRACT

Seed agglomeration is a coating technology with the purpose to sow multiple seeds of the same seed lot, or multiple seeds of different seed lots, varieties or species. The objective of this study was to develop agglomeration technology by producing single agglomerates or pellets using lettuce and tomato as model vegetable crop seeds. Physical properties of dry and wet pellets were measured and seedling emergence assessed. Pellets were formed by a molding technique with a mixture of filler, binder, and seeds. Diatomaceous earth (DE) was used as the filler, and two binders were tested: polyvinyl alcohol (PVA) and a commercial organic binder. Each binder solution was mixed with DE, and seeds were added during the agglomeration process. Oval and cylindrical pellets were molded with known compression forces. Cylindrical pellet strength increased, as PVA binder concentration increased from 8% to 16% and pellet strength was greater for pellets produced with 3 kg than with 1 kg compression. The percent seedling emergence and speed of emergence were not affected by a compression force of 1 kg and 3 kg for PVA-pelleted lettuce and tomato, respectively compared to the non-pelleted control. Cylindrical pellets formed using the commercial organic binder at 1 and 3 kg force without lecithin showed significantly less seedling emergence and speed of emergence for lettuce seed; no significant differences were observed for tomato seed. Seedling emergence and speed of emergence for lettuce seed from oval pellets formed with the commercial organic binder and lecithin at 1 kg and 3 kg compression grouped with the non-pelleted control. Cylindrical pellets made without lecithin and with the commercial organic binder using 3 kg compression force containing three tomato seeds produced plants with greater combined leaf area, fresh and dry weight than plants grown from single non-pelleted seeds, 26 days after being sown in the greenhouse.
© 2015 Elsevier B.V. All rights reserved.

1. Introduction

Seed treatment and coating technologies are used worldwide for the application of materials to seeds including seeds sown in planter boxes, as well as conventional liquid treatments, film coating and pelleting (Taylor, 2003). The goal of these seed coating technologies is to apply materials uniformly over the surface of seed in the same lot while maintaining singulation during the coating process. An alternate coating technology is required to sow multiple seeds of the same seed lot, or multiple seeds of different seed lots, varieties or species. Agglomeration is a technology that combines particles of different sizes and shapes into a single unit; seeds are examples of particles that can be formed into agglomerates with the purpose of sowing multiple seeds into a single dispersal unit. The seed agglomeration technology has broad applications for many crop seeds including vegetable, flower, grass, cover crop, and biofuel species.

A review of agglomeration and coating technologies to produce propagules with multiple seeds is largely found in patents. Three patents were issued for making seed capsules (Adams, 1971; Brink, 1971; Clifford, 1971), using a two step process that positioned a seed in the depression of a lower, partially compressed pellet volume then covered the seed with a top layer of the pelleting material and compressed the entire mass into one pellet. Mechanized seed pelleting incorporated advances of seed coating technologies to produce seed pellets 'comprising a core of at least two seeds, an organic substrate such as loess, organic fertilizer, fungicides, and a wetting agent enclosed by a water permeable coating' (Gerber, 1988). Later versions of the multi-seed pellet addressed problems with pelletizing very small seeds such as flower seeds and methods have been patented that use an inert core (e.g., glass bead, perlite,

* Corresponding author. Tel.: +1 315 787 2243; fax: +1 315 787 2216.
E-mail addresses: potja_noi@hotmail.com (P. Sikhao), agt1@cornell.edu (A.G. Taylor).

http://dx.doi.org/10.1016/j.scienta.2014.12.028
0304-4238/© 2015 Elsevier B.V. All rights reserved.

bentonite granules), surrounded by an intermediate layer (e.g., clay, vermiculite, polyvinyl acetate) around which 'at least two seeds of the same or different species were distributed in an adhesive layer formulated from a combination of binders and fillers (e.g., polyvinyl alcohol, clay, gypsum)' (Legro, 1997). Recently, Conrad (2012) submitted a patent application for a method of producing 'a cast pellet comprising a mixture of one or more plant seeds'. As multi-seed pelletizing processes were being developed, a process was proposed to encapsulate multiple seed units utilizing pharmaceutical capsules composed of hard gelatin to contain one or more seeds (Trias and Takahashi, 2014). However, a molding technique that incorporates multiple seeds within a pellet comprised entirely of organic materials (US Government Printing Office, 2014) has not been reported.

Rotary pan technology has been adapted to make agglomerates using a solution of polyvinyl alcohol as the binder and diatomaceous earth as the filler material on bluebunch wheatgrass (*Pseudoroegneria spicata* (Pursh) Á. Love) seeds (Madsen et al., 2012). Based on the same planting density, the agglomerated treatment had greater seedling emergence than the non-coated control under simulated soil crusting (clay soils) and non-crusting (sandy soil) conditions in greenhouse studies. Focused research conducted on agglomeration seed coating technology (Kavak and Taylor, unpublished) examined the effect of pelletizing on seed germination. Pellets were formed by compressing lettuce seeds in a mixture of 85% red clay thoroughly mixed with 15% liquid binder (Spectrum 100, Germains Seed Technology, Gilroy, CA, USA) at 3 kg compression force; a 5 kg compression force was used for onion seeds. Pelleting decreased the seedling emergence rate but did not affect total emergence, based on the total seeds sown in both crops seeds. Additionally, when using compressive force to produce seed containing pellets, ease of removal of the compressed pellet from the molding form is a critical component of efficient manufacture. Soy lecithin, a plant based extract with amphipathic molecules aligning the nonpolar fatty acid portion facing the surface provides a "non-sticking" property (Xu et al., 2011). To our knowledge, the effect of incorporating soy lecithin in multi-seed pellets on seed pellet three-dimensional strength, seed germination and seedling growth has not been reported. Overall, the effect of mechanical aspects used to form multi-seed compressed pellets, as well as the possible inhibitory or stimulatory effects of formulation components on seedling germination and growth, must be considered as critical design features during the development of multi-seed pellets.

The goal of this study was to produce agglomerates using a molding technique to form single pellets containing multiple seeds of lettuce or tomato, the model vegetable crops used in this study. The objectives of this study were: (1) the production of a pellet of uniform size and shape which is three-dimensionally strong for use in mechanical planter; (2) the development of a formulation and pelletizing process that permits more than one seed per pellet; and (3) proposal of a multi-seed process that has no negative effect on germination and seedling growth under greenhouse conditions. The optimum compression force for producing multi-seed lettuce and tomato seed pellets without negative growth effects was determined from data on three-dimensional strength, dissolution period, germination, and seedling growth.

2. Materials and methods

2.1. Seed agglomeration materials

Single seed lots of two vegetable crops were used in all laboratory and greenhouse experiments. Lettuce (*Lactuca sativa* L.), 'Jupiter' was provided by Nunhems USA, Inc., Parma, ID, USA, and tomato (*Solanum lycopersicum* L.), 'Talladega' was provided by Syngenta Seeds, Inc., Boise, ID, USA. Diatomaceous earth (DE) obtained from Perma-Guard, Inc., Albuquerque, NM, USA was used as the filler material for all pellet formulations. SELVOL™ polyvinyl alcohol (Selvol-205®), a water-soluble copolymer was provided from Sekisui Specialty Chemicals America, LLC, Dallas, TX, USA. A commercial organic binder, SOL034 was provided by Incotec, Salinas, CA, USA. Natural Soya Lecithin (Rite Aid Pharmacy, Camp Hill, PA, USA) was used in selected experiments as a non-sticking agent, to prevent sticking of the seed containing filler material to the molding tips.

2.2. Agglomeration methods and physical properties of pellets

Two properties are essential to the production and utility of agglomerated seeds: (1) a suitable concentration of binder sufficient to provide adequate mechanical strength for dry pellets used in mechanized planting, and (2) water permeability allowing pellet dissolution and seed germination. To examine pellet three-dimensional strength, pellets were prepared with one of two binders over a range of compression forces without the addition of seeds. Polyvinyl alcohol (PVA) crystals were dissolved in water at a range of concentrations from 8% to 16% (w:v) in 2% increments, to prepare the non-organic binder. The commercial organic binder, SOL034 was prepared by diluting the concentrate with water to 12.5%, 25%, 50% (v:v) and by using undiluted, 100% SOL034. Each binder solution was thoroughly mixed with diatomaceous earth, DE filler at ratio 5:4 (w:w) to form a moist, friable powder.

Two 6.3 mm × 100 mm × 100 mm plates composed of ultra high molecular weight (UHMW) polyethylene were used for molding the pellets. The first plate was solid with a smooth hard surface and served as the base during molding process (Fig. 1A, right). The second plate was drilled with 16 holes of 5 mm diameter and equidistantly spaced (Fig. 1A, left); the holes served to contain the friable binder–filler powder during pellet formation under pressure. To form pellets, the second plate was placed on top of the first plate and the holes were filled with binder–filler. The binder–filler mixture in the holes was compressed at specific force measured in kg with an Extech "Fruit Hardness Tester" (model FHT200, Extech Instruments Corp., Waltham, MA, USA; www.extech.com) (Fig. 1B). The 5 mm tip of the Extech fruit hardness tester had a flat end that produces a cylindrical pellet. After compression, the pellets were removed by pressing the pellet from the mold using the flat top of a drill bit shank. After removal from the mold, all compressed pellets were dried in forced air oven at 30 °C for 4 h.

Physical properties, including three-dimensional strength and dissolution period of the pellets were determined. Ten pellets were placed on the undrilled, solid base plate and the three-dimensional mechanical strength of individual pellets was assessed by applying force on the top (height of cylinder) or side (diameter of cylinder) of the pellet with the Extech fruit hardness tester. The dimensional force required to crush each pellet was recorded. An additional ten pellets from each production batch were individually dissolved in 30 ml of water contained in weigh boats; the total dissolution period for the pellets to dissolve was recorded with a laboratory timer.

2.3. Effect of compression forces on seedling emergence

Lettuce and tomato seed pellets were prepared with 8% PVA binder and DE filler (binder:filler, 5:4, w:w) at different compression forces; 250 seeds of either crop were mixed with the binder–filler mixture in a single batch. The lettuce mixture was filled into the holes of the mold plate and compressed at 0 kg, 0.5 kg, 1 kg, 2 kg or 3 kg. The same procedure was conducted for tomato seeds using compression forces of 0 kg, 1 kg, 3 kg, 5 kg or 7 kg. The

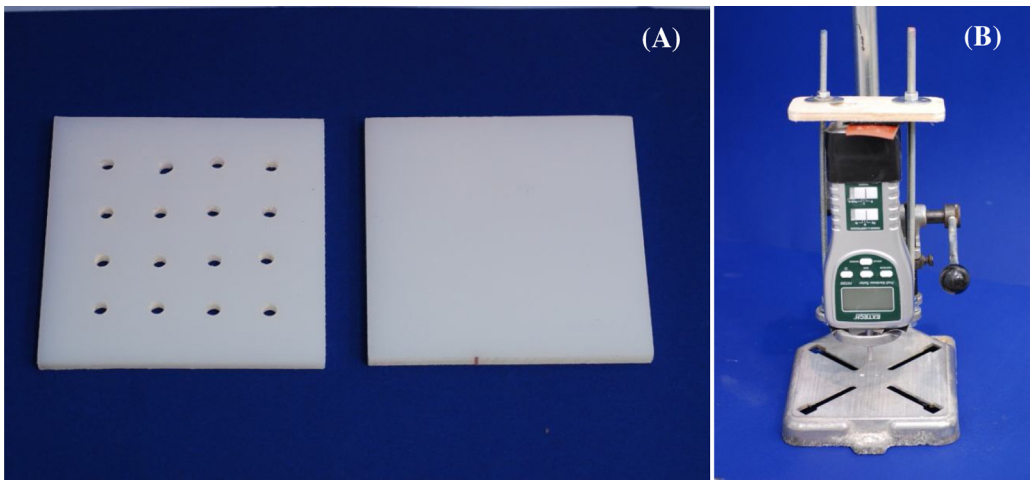


Fig. 1. (A) Plates used in the seed molding process. (B) The Extech Fruit Hardness Tester Model 200 (Extech Model FHT200) was used to provide a known compression force.

0 kg treatments were prepared without the compression force of the Extech fruit hardness tester by filling the mold holes and then gently removing the soft pellet with the flat end of the drill bit shank. All pellets were dried (30 °C for 4 h).

To test the effect of compression on seed germination and seedling growth, pellets were dissolved in water, and the seeds were removed from the pellet-water solution and dried 12 h at room temperature (22 °C). Four replicates of 25 seeds per replicate from each treatment including a non-pelleted control were sown in the greenhouse for seedling emergence trials. Potting mix ("Cornell mix") containing: 0.323 cubic meters compressed bale peat moss; 0.340 cubic meters vermiculite; 9.071 kg dolomitic limestone; and 2.721 kg 11–5–11 (N–P–K) fertilizer was used for sowing all seed and seed pellets; this mix is used as the standard potting mix for all greenhouses of Cornell University. Seed pellets and non-pelleted seed controls were sown at a depth of 1 cm in Cornell mix in 50 cm × 36 cm × 8 cm flats. The temperature was maintained at alternating 20/25 °C and flats were watered to maintain a moist surface in each flat. Lettuce and tomato seedling emergence were recorded daily for 7 and 14 days, respectively. Only normal seedlings, based on criteria of the International Seed Testing Association (ISTA, 2008) were counted. Percentage of seedling emergence was calculated on the last day using the following formula:

$$\text{Percentage of seedling emergence} = \left(\frac{\text{Number of normal seedlings}}{\text{Total number of seed sown}}\right) \times 100$$

The speed of emergence was calculated from the daily counts using the following formula:

$$\text{Speed of emergence} = \sum \left(\frac{\text{No. of seedlings}}{\text{Days of first count}} \cdots + \cdots \frac{\text{No. of seedlings}}{\text{Days of final count}}\right)$$

2.4. Molding and pellet shape

The objective of this study was to develop and compare pellets that were cylindrical in shape with pellets with rounded ends, an "oval" shape. The cylindrical shaped pellets were prepared with a flat-ended tip as described in Section 2.2. Cylindrical pellets were produced with 100% SOL034 with and without lecithin; oval pellets were produced with 100% SOL034 and required the addition of lecithin to maintain conformational integrity. The oval shaped pellets were produced from two custom made metal tips that were machined at the pellet-forming end to produce a concave surface; one concave tip was used as the bottom of the chamber, replacing the solid UHMW polyethylene plastic base plate and the other concave tip was used to compress the pellet. The oval pellets required the addition of soya lecithin to retain their shape; the lecithin was thoroughly mixed into filler-binder mixture at 5:4:0.5 (53%:42%:5%, w:w:w, DE:binder:lecithin, respectively). Lettuce and tomato seed pellets were prepared with a compression force of 1 kg and 3 kg, respectively. To ensure that the same number of seeds were contained in each pellet, three seeds were placed into each mold during pellet preparation. After the seed containing pellets were dried (30 °C for 4 h), physical tests were performed on mechanical strength and the dissolution period. Top and side crushing three-dimensional strength was tested for cylindrical pellets; only side crushing strength was determined for the oval pellets, due to the difficulty in maintaining a consistent impact position for top crushing. Data were recorded as described in Section 2.2; seedling emergence studies were conducted with seed containing pellets using non-pelleted seed as controls, as described in Section 2.3.

2.5. Effect of agglomeration on plant growth

Cylindrical pellets containing three tomato seeds were prepared using 100% SOL034 as the binder and DE as the filler (binder:filler, 5:4, w:w) and with a compression force of 3 kg as described in Section 2.3. Three seeds were placed into the mold during pellet preparation. Four replications of 15 pots each of pelleted and non-pelleted seed were sown in the Cornell mix for the plant growth trials. One non-pelleted seed or one pellet containing three seeds per pellet was sown in the Cornell mix in separate pots; seeds were germinated and seedlings were grown under greenhouse conditions. The temperature was maintained at alternating 20/25 °C and pots were watered to maintain a moist surface in each pot. Tomato plant growth attributes, including leaf area, seedling fresh weight and dry weight were determined at harvest, 26 days after sowing. Leaves for each plant were cut at the end of their petiole and the total leaf area for each leaf was measured with a leaf area meter (model CI-202, CID Bio-Science, Inc., Camas, WA, USA). Each tomato plant was cut at the planting medium level; fresh weight recorded for each plant (all leaf and stem tissue). Harvested plants were dried in an oven set at 80 °C for 48 h and the tissue was reweighed to obtain the dry weight data.

2.6. Statistical analyses

The experiment was a completely randomized design (CRD). The seedling emergence data were arcsine-transformed and analyzed

Table 1
Physical properties of cylindrical pellets prepared with different concentrations of SOL034 binder and DE filler (binder:filler, 5:4, w:w) at 1 or 3 kg of pellet forming compression.

SOL conc. (%)	1 kg compression force			3 kg compression force		
	Top crush (kg)	Side crush (kg)	Dissolution period (s)	Top crush (kg)	Side crush (kg)	Dissolution period (s)
12.5	0.16b	0.08c	13a	0.54c	0.21b	15a
25	0.24b	0.12bc	9b	0.75bc	0.22b	11b
50	0.40a	0.24ab	7b	0.94b	0.30b	10b
100	0.45a	0.27a	8b	1.48a	0.62a	12b
F-test	**	*	**	**	**	**
CV (%)	5.23	8.13	2.62	3.55	4.47	1.89

Treatments significantly different at $^{*}P \leq 0.05$ and $^{**}P \leq 0.01$. Means within columns with different letters are significantly different ($P \leq 0.05$). Coefficient of variation, CV (%), is the variation in the mean across treatments ($n = 10$ for each SOL034 concentration, compression class, and force aspect).

by one-way ANOVA. The difference between treatments was tested by Duncan's new multiple range test (DMRT).

3. Results

3.1. Physical properties of pellets

Three-dimensional strength was tested and the dissolution periods were recorded over the range of PVA binder concentrations and at 1 or 3 kg compression forces (Fig. 2A and B). In general, the force needed to crush the cylindrical pellet increased as PVA concentration increased from 8% to 16% (Fig. 2A) and pellet strength was greater for pellets made with 3 kg compression than for pellets made with 1 kg compression, at each PVA concentration. Cylindrical pellets withstood greater crushing force applied to the top than to the side for each PVA concentration and each compression force used (Fig. 2A). Pellets withstood over 10 kg top compression and over 2 kg side compression crushing force, for 3 kg-compressed pellets. In comparison, the crushing force for 1 kg-compressed cylindrical pellets was reduced by half. Similar trends for pellet strength were observed for pellets produced with the SOL034 binder (Table 1). Pellet strength increased as the SOL034 binder concentration increased and with increased compression force used for pellet molding, maximally withstanding top-crushing forces of 0.45 kg (1 kg compressed pellets) and 1.48 kg (3 kg compressed pellets); maximum side crushing forces of for 1 kg compressed pellets, 0.27 kg was approximately half that of 3 kg compressed pellets, 0.62 kg.

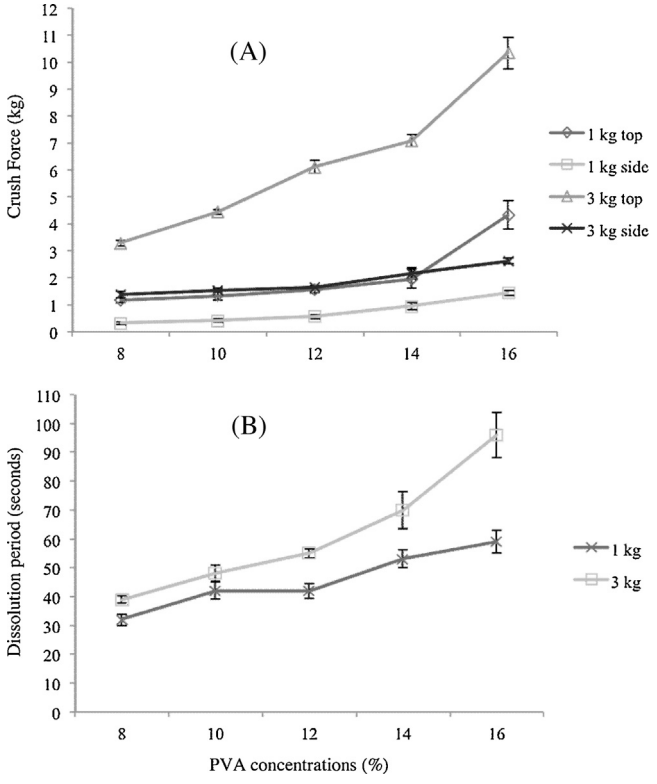


Fig. 2. Physical properties of cylindrical pellets prepared with different concentrations of polyvinyl alcohol (PVA) binder and DE filler (binder:filler, 5:4, w:w) at 1 kg or 3 kg of compression. (A) Force needed to crush pellets: pellets made with 1 kg compression were crushed with top force (diamond) and side force (square) and pellets made with 3 kg compression were crushed with top force (triangle) and side force (×) ($n = 10$ for each PVA concentration, compression class, and force aspect). (B) Dissolution period for pellets made with 1 kg force (×) and 3 kg force (square) ($n = 10$ for each concentration and compression class). Error bars for (A) and (B) represent standard error.

The elapsed time required for dissolving the pellets in water, the dissolution period increased as PVA concentration increased from an average of 35 s (8%) to an average of 60 s (16%) for pellets formed using 1 kg compression (Fig. 2B). PVA concentration was associated with greater differences in dissolution period for pellets formed with 3 kg compression, ranging from an average of 45 s (8%) to 95 s (16%) (Fig. 2B). Consistently, PVA containing pellets formed with 3 kg compression took longer to dissolve than PVA containing pellets formed using 1 kg compression (Fig. 2B). Additionally, dissolution period for PVA-containing pellets were consistently greater than for SOL034-containing pellets, regardless of compression force used for pellet formation. For pellets formed using either the 1 kg or the 3 kg compression force, the dissolution period was greatest and statistically significantly different with 12.5% SOL034 binder ($P \leq 0.01$), compared to all higher concentrations of SOL034 binder (Table 1). Overall, increased pellet forming compression force was associated with greater differences in dissolution period for PVA-containing pellets than SOL034-containing pellets.

3.2. Seedling emergence and speed of emergence

Lettuce seeds and tomato seeds were agglomerated with different compression forces, as described in Section 2.3. Seeds were removed from the pellets, as described, to determine the effect of compression forces and eliminated any confounding effect of the pellet or pellet components on seedling emergence in the greenhouse. For pelleted lettuce and tomato seed, the percent seedling emergence ($P \leq 0.05$) and the speed of emergence ($P \leq 0.05$ for lettuce and $P \leq 0.01$ for tomato) were significantly affected by the compression forces used to produce the pellets (Tables 2 and 3). While seedling emergence and speed of emergence for lettuce seed pellets produced with the 0 kg, 0.5 kg and 1 kg compression force were not significantly different from the non-pelleted control, compression forces of 2 kg and 3 kg negatively impacted both lettuce seedling emergence parameters compared to the control (Table 2). For tomato, the 0 kg, 1 kg and 3 kg compression force treatments grouped statistically with the non-pelleted control for both percent and speed of emergence (Table 3). However, speed of tomato seedling emergence for seed from pellets produced with the 5 kg

Table 2
Lettuce seedling emergence and speed of emergence from cylindrical pellets made with 8% PVA and DE filler (binder:filler, 5:4, w:w) with selected compressions forces. Seeds were removed from the pellets and then sown in the greenhouse. Four replications of 25 seeds per replicate from each treatment including a non-pelleted control were sown in the greenhouse for seedling emergence trials.

Pellet compression force	Seedling emergence (%)	Speed of emergence (seedlings/day)
Non-pelleted	100a	25.0a
0 kg	97ab	24.2a
0.5 kg	95abc	23.7ab
1 kg	95abc	23.4abc
2 kg	91bc	22.3bc
3 kg	88c	21.9c
F-test	*	*
CV (%)	4.79	4.87

Treatments significantly different at $^{*}P \leq 0.05$. Means within columns with different letters are significantly different ($P \leq 0.05$). Seedling emergence data were transformed using arcsine transformation. Coefficient of variation, CV (%), is the variation in the mean across treatments ($n = 100$ for each pellet compression force treatment class).

compression force was significantly reduced, compared to treatments grouping with the control; seed from pellets produced with 7 kg compression were showed significantly lower percent seedling emergence and speed of emergence, when compared to other treatments as well as the control (Table 3).

3.3. Molding methods

Cylindrical pellets produced without lecithin and 3 kg compression required significantly more side-crushing force ($P \leq 0.01$) than either the oval pellets or the cylindrical pellets produced with lecithin (Table 4). The same trend was observed with 1 kg compression, though not significant ($P \leq 0.01$). The addition of lecithin significantly increased the dissolution period required for the pellets ($P \leq 0.01$). In general, the pellets produced at 3 kg compression required more force to crush the pellet and a greater dissolution period, compared to pellets made with 1 kg compression.

Lettuce seedling emergence ($P \leq 0.05$) and speed of emergence ($P \leq 0.01$) for oval and cylindrical pellet shapes with lecithin were not significantly different from the non-pelleted control (Table 5). However, cylindrical lettuce seed pellets formed without lecithin produced at 1 kg compression had significantly lower percent seedling emergence than cylindrical pellets made at either 1 kg or 3 kg compression with lecithin and oval pellets made with 3 kg compression ($P \leq 0.05$). Moreover, cylindrical lettuce seed pellets with lecithin as an additive had greater speed of seedling emergence ($P \leq 0.01$) than cylindrical pellets without lecithin made at the same compression (Table 5). No statistically significant differences were observed between treatments for tomato seedling emergence and speed of emergence ($P \leq 0.05$) (Table 5).

Table 3
Tomato seedling emergence and speed of emergence from cylindrical pellets made with 8% PVA and DE filler (binder:filler, 5:4, w:w) with selected compressions forces. Seeds were removed from the pellets and then sown in the greenhouse. Four replications of 25 seeds per replicate from each treatment including a non-pelleted control were sown in the greenhouse for seedling emergence trials.

Pellet compression force	Seedling emergence (%)	Speed of emergence (seedlings/day)
Non-pelleted	98a	19.4a
0 kg	98a	19.3a
1 kg	98a	19.3a
3 kg	98a	19.4a
5 kg	94ab	18.2b
7 kg	88b	16.4c
F-test	*	**
CV (%)	4.51	3.54

Treatments significantly different at $^{*}P \leq 0.05$ and $^{**}P \leq 0.01$. Means within columns with different letters are significantly different ($P \leq 0.05$). Seedling emergence data were transformed using arcsine transformation. Coefficient of variation, CV (%), is the variation in the mean across treatments ($n = 100$ for each pellet compression force treatment class).

3.4. Plant growth

On a per plant basis, tomato leaf area was significantly greater ($P \leq 0.05$) for the single seed than the pelleted seed (Table 6). However, the total leaf area for plants grown from the pelleted seed was almost double that of the plant grown from the single seed. No statistically significant differences were observed for either fresh weight or dry weight on a per plant basis ($P \leq 0.05$). Both fresh weight and dry weight were significantly greater for plants grown from the pellet compared with those from the single seed ($P \leq 0.01$).

4. Discussion

A pellet molding-based agglomeration technology was developed using a synthetic binder, PVA or an organic binder, SOL034 and tomato or lettuce as model crop seeds. The results suggest that the molding procedure described produce sufficient three-dimensional strength of the combined filler and binder within the pellet when compressed and dried for the pellet to withstand mechanical handling and sowing. To date, this method has used lettuce and tomato as model crops. However, prior patent research and the results presented herein indicate that this method could be applied to produce multiple-species flower seed pellets as well as pellets containing multiple grass species. Proof of concept results have recently been reported for agglomerated seed of perennial bunchgrass species; increased biomass for plants grown from agglomerated seed indicate potential for use in rangeland restoration (Madsen et al., 2012). In multiple-species pellet combinations, the advantage would be from the inclusion of species with a range of environmental tolerance. For example, grass species representing a range of drought tolerance could be included in one pellet. Production of a multiple species, environmentally competent seed pellet provides an alternative to single species sowing under environmentally variable conditions. In addition to the capability of at least some of the pellet's species suite to survive variable environmental conditions, there is an inherent "prescriptive" property to vary species composition based on site requirements such as seasonal drought, soil salinity and basic pH.

In the results presented, the pellet three-dimensional strength produced in PVA and SOL034 pellets was dependent on the binder concentration and the compression forces used to make the pellet. The force required to crush the pellets, generally, increased with increased compressive force used to form the pellet and increased binder concentration. For example, the greatest crush force was required at the highest PVA concentration, 16% and greatest compressive force, 3 kg indicating that adhesive strength increased as PVA concentration increased from 8% to 16% (Fig. 2A). Bardin and Huang (2003) reported results for the adhesive properties of ten binders that were used to adhere coating materials of chitin or flax straw powder onto sugar beet seeds; a 10% PVA solution was found optimal to adhere more material to the seed than all other binders tested. In comparison with PVA, while a similar relationship between required crush force and binder concentration is apparent, pellets made with SOL034 required less force to crush the pellet (Table 1); the proprietary components of this commercial binder are approved for organic use (Incotec, Personal Communication). Consistent for both PVA and SOL034 pellets, more force was required to crush cylindrical pellets from the top compared to the side, because the force is better distributed over the top than the side surface of a cylinder (Fig. 2A, Table 1).

Table 4
Physical properties of cylindrical and oval shaped pellets formed at 1 or 3 kg compression. Lecithin ("Lec") is an additive incorporated into the 100% SOL034 binder and DE filler (5:4:0.5, w:w:w, DE:binder:lecithin).

Pellet shape and additive	1 kg compression force		3 kg compression force	
	Side crush (kg)	Dissolution period[a] (s)	Side crush (kg)	Dissolution period[a] (s)
Cylinder	0.52	4c	1.36a	13c
Cylinder + Lec	0.49	2000a	0.93b	5490a
Oval + Lec	0.32	360b	0.54c	860b
F-test	ns	**	**	**
CV (%)	4.42	9.18	2.83	7.14

Treatments not significantly different (ns) and significantly different at $^{**}P \leq 0.01$. Means within columns with different letters are significantly different ($P \leq 0.05$). Coefficient of variation, CV (%), is the variation in the mean across treatments ($n = 10$ for each pellet shape class, compression class, and force aspect).

[a] Dissolution periods for pellets made with lecithin have been rounded to nearest 10 s.

Table 5
Lettuce and tomato seedling emergence and speed of emergence from cylindrical and oval shaped pellets formed at 1 or 3 kg compression. Lecithin ("Lec") is an additive incorporated into the 100% SOL034 binder and DE filler (5:4:0.5, w:w:w, DE:binder:lecithin). Four replications of 25 seeds per replicate from each treatment including a non-pelleted control were sown in the greenhouse for seedling emergence trials.

Pellet shape and treatment	Lettuce seed		Tomato seed	
	Seedling emergence (%)	Speed of emergence (seedlings/day)	Seedling emergence (%)	Speed of emergence (seedlings/day)
Non-pelleted	99a	24.8a	97	14.3
Cylinder @ 1 kg	91c	21.8bc	95	12.9
Cylinder @ 3 kg	92bc	21.2c	95	13.2
Cylinder + Lec @ 1 kg	97ab	24.1a	97	13.8
Cylinder + Lec @ 3 kg	98ab	23.7a	98	13.5
Oval + Lec @ 1 kg	96abc	23.5a	97	13.2
Oval + Lec @ 3 kg	97ab	23.2ab	97	13.9
F-test	*	**	ns	ns
CV (%)	3.65	4.40	3.10	4.64

Treatments not significantly different (ns) and significantly different at $^{*}P \leq 0.05$ and $^{**}P \leq 0.01$. Means within columns with different letters are significantly different ($P \leq 0.05$). Seedling emergence data were transformed using arcsine transformation. Coefficient of variation, CV (%), is the variation in the mean across treatments ($n = 100$ for each pellet shape and pellet compression force treatment class).

One of the more critical requirements for plant growth is water uptake by the pellet; the rapidly dissolving pellet thereby avoids being a physical barrier for gas exchange or radicle growth. In this study, the time required to dissolve pellets in water was also dependent on PVA concentration and compression forces (Fig. 2B); pellets made with the highest concentration of PVA (16%) and greatest compression force (3 kg) required less than 2 min to dissolve. PVA is soluble in highly polar and hydrophilic solvents such as water (Kadajji and Betagevi, 2011); PVA pellets were easily dissolved after a brief soak in water. While cylindrical SOL034 pellets required greater crushing force with increased binder concentration (Table 1), dissolution period decreased with increased binder concentration (Table 1) This interaction suggests increased hydrophilicity with increased SOL034 concentration; the maximal dissolution period, 15 s presents no barrier to seed performance. Similar to PVA, SOL034 dissolution period was greater for the 3 kg compressive force than 1 kg compressive force at each concentration tested (Table 1). The results for both binders, as used in pellet formulations without lecithin, indicate increased three-dimensional strength with increasing binder concentration and compressive force with a 2 min or less dissolution period.

While similar trends were observed for three-dimensional strength for PVA and SOL034 binders, the SOL034 binder demonstrated an inversely proportional relationship for both the top and side crushing force with the dissolution period at both compressive forces used for cylindrical pellets formed without lecithin (Table 1). It can be suggested that this relationship is tied to increased availability of water-soluble molecules associated with increased SOL034 concentration. At the same SOL034 concentration, dissolution period increases with increased compressive force but the relationship between crushing force and dissolution period persists, indicating that increased compressive force may reduce access to water soluble molecules. This increased dissolution period for 3 kg compressed pellets may be due to reduced porosity associated with the increased compression. Additionally, the inversely proportional relationship between side crushing force and dissolution period persisted with pellets made with added lecithin. The significant increase for dissolution period for cylindrical pellets made with added lecithin may be due to the presence phospholipids in the added lecithin; soya lecithin is approximately 65–75% phospholipids combined with triglycerides (Scholfield, 1981). Phospholipids are not water-soluble. The

Table 6
Tomato plant growth of non-pelleted and pelleted tomato seed made using a cylindrical form with 100% SOL034 and DE and 3 kg compression force. Four replications of 15 pots each containing one pellet with three seeds or one non-pelleted seed were sown in the greenhouse for this seedling emergence trial.

Treatment	Leaf area per plant (cm^2)	Leaf area per pot (cm^2)	Fresh wt per plant (g)	Fresh wt per pot (g)	Dry wt per plant (g)	Dry wt per pot (g)
Non-pelleted seed (1 seed/pot)	44.4a	44.4b	0.690	0.690b	0.145	0.145b
Pellets (3 seeds/pellet)	28.4b	85.1a	0.590	1.711a	0.141	0.423a
F-test	*	**	ns	**	ns	**
CV (%)	2.24	2.39	2.67	2.96	2.10	2.27

Treatments not significantly different (ns) and significantly different at $^{*}P \leq 0.05$ and $^{**}P \leq 0.01$. Means within columns with different letters are significantly different ($P \leq 0.05$). Coefficient of variation, CV (%), is the variation in the mean across treatments ($n = 60$ for pelleted seed and $n = 60$ for non-pelleted seed).

presence of phospholipids would tend to reduce access to water soluble molecules, increasing the dissolution period, as demonstrated with the cylindrical pellets made with 5% lecithin (Table 4). Further, the dissolution period is more than doubled with increased compression, perhaps due to decreased porosity. Dissolution period for oval pellets produced with 5% lecithin was significantly less than that for the cylindrical pellet made with added lecithin; 18% of the 1 kg compressed cylindrical pellet and 16% of the 3 kg compressed cylindrical pellet. The decreased dissolution period associated with the oval shape and the least crushing force indicates that reduced three-dimensional strength may be associated with increased porosity and consequent increased access to water-soluble molecules.

The agglomeration process, including the compression forces required to form the pellet, should not harm the seeds by impairing either the percent or rate of seedling emergence. Compression forces of 0.5 kg or 1 kg did not significantly affect lettuce seedling emergence or speed of emergence ($P \leq 0.05$). However, increasing the force to 2 kg or 3 kg significantly decreased both the percent and speed of seedling emergence compared to the non-pelleted control ($P \leq 0.05$, Table 2). A dark-seeded variety of lettuce was used in this research and varietal differences may exist in the seed's susceptibility to compression. Peñaloza et al. (2005) found that black-seeded lettuce varieties had higher seed quality than white-seeded lettuce varieties in seed quality tests. Near isogenic lines of bean (*Phaseolus vulgaris* L.) with dark and white colored seed coats were tested for the compressive force required for seed breakage (Bay et al., 1996). The dark-seeded line withstood greater force for whole seed breakage than the white-seeded line. Further, the compressive strength increased as the seed water activity (moisture content) increased. Similarly, under the same test conditions, percent seedling emergence and speed of emergence for tomato seed were not significantly reduced by 1 kg, 3 kg, or 5 kg compressive force ($P \leq 0.05$, Table 3) but did show significant reductions at 7 kg compression. It is not known why tomato seed is negatively affected at a higher compression than lettuce seed but seed shape may play a role. Collectively, crop species differences may exist to withstand seed compression. Consequently, preliminary testing should be performed to determine the maximum compression for each crop seed.

Conventional seed pelleting can also reduce stand establishment potential and research has focused on ameliorating these negative effects by the pellet composition (Halmer, 1988; Hill, 1999). One objective of this project was the development of the molding technique to produce a more spherical agglomerated pellet using a set of two molding tips each with a concave end. However, moist pellet formulation was found to adhere inside of the concave tips, resulting in broken pellets. To alleviate this problem, lecithin was added as a non-sticking agent; lecithin is commonly used as a non-stick additive in food cooking spray. The addition of lecithin to formulations used in producing the cylindrical pellets with 3 kg compression made softer pellets as indicated by reduced side-crushing strength (Table 4). However, the more dramatic effect was observed with the increased time required to dissolve the pellets. Soya lecithin is composed of 65–75% phospholipids together with triglycerides and other compounds (Scholfield, 1981) making the substance soluble in both water and lipids. Moreover, in comparing the cylinder shaped pellets produced at 1 kg or 3 kg, the lecithin was associated with both the increased percent and increased speed of seedling emergence and was comparable to levels observed in the non-pelleted control ($P \leq 0.05$, Table 5). This may indicate a possible beneficial effect from lecithin for seedling emergence.

Agglomeration is a coating technology to produce a dispersal unit to sow multiple seeds of the same seed lot, or multiple seeds of different seed lots, varieties or species. This technology could be used on a wide range of crop seeds including vegetable, flower, grass, and mixed species. The molding technique described here is analogous to technologies used in the pharmaceutical industry for making tablets. Traditional seed coating equipment and methods have previously been adapted to make agglomerates using rotary pan technology (Madsen et al., 2012). Both multi-seed pelleting technologies illustrate benefits such as enhanced seedling emergence and increased above ground biomass for seedlings grown from multi-seed pellets. The advantage of the molding technique described herein is uniformity of pellet size; there is limited control of agglomerate size produced with conventional seed coating (rotary pan) equipment. This paper describes the components and compression forces required to produce pellets with good seedling emergence potential using lettuce and tomato as model crops. The apparatus to produce the molded pellets is a prototype that requires further engineering efforts for large-scale production.

5. Conclusions

A method is described to agglomerate multiple-seeds from multiple species in a single pellet with a unique molding technique forming either cylindrical or oval pellets. Diatomaceous earth (DE) is applicable for use as the filler for all pellet formulations at both 1 kg and 3 kg compression forces and for both the cylindrical and oval conformations. Polyvinyl alcohol (PVA), used as a binder, produces pellets with the overall greatest three-dimensional strength and would likely provide pellets with the greatest durability for mechanical seed planting.

Compared to the PVA binder, SOL034, a proprietary binder with OMRI organically approved components produces cylindrical pellets with almost 10-fold less top and side-dimensional strength than PVA-containing pellets. This reduction in three-dimensional strength indicates limited options for use of the SOL034 containing formulation for mechanical seeding. More specifically, SOL034-containing oval pellets formed with 3 kg compression required significantly less side-crushing force ($P \leq 0.01$) than cylindrical pellets, suggesting that the cylindrical pellets are the more durable candidate for mechanical seeding and that, overall, the 3 kg compressed cylindrical PVA-containing pellets are the most durable.

All SOL034 containing pellets made without added lecithin dissolve in less time than pellets produced with PVA, showing lower potential for SOL034 containing formulations to act as a barrier to seed imbibition after planting. Differences for required dissolution period between 1 kg compressed pellets and 3 kg-compressed pellets is less for SOL034 containing pellets than PVA containing pellets. However, the greatest dissolution period for pellets made without added lecithin, 95 s required for 3 kg compressed 16% PVA pellets, represents little if any barrier to seed germination. The greatest dissolution period for pellets made with added lecithin, 91 min required for cylindrical pellets at 3 kg compression is well within physiological range to allow normal germination and seedling emergence.

The optimal compression force for producing multi-seed, cylindrical, PVA-containing lettuce and tomato seed pellets with good three-dimensional strength and no negative growth effect is 1 kg and 3 kg, respectively. These different optima indicate species-associated growth related differences for the compressive forces used. The percent seedling emergence and speed of seedling emergence from multi-seed, oval, SOL034 containing lettuce and tomato seed pellets sown under greenhouse conditions show no significant differences ($P \leq 0.05$, Table 5) from the non-pelleted, single seed control, indicating no inhibitory growth related effects for compression or added lecithin.

Acknowledgements

This research was supported by the Royal Golden Jubilee Ph.D. Program (Grant no. PHD/0174/2550) of the Thailand Research Fund and the senior research scholarship project of Assoc. Prof. Dr. Boonmee Siri. This research was supported in Prof. Dr. Alan G. Taylor's lab at Cornell University under Multi-State project, W-2168. Finally, we give a special thanks to Dr. Chananat Kaewmanee for editing the manuscript.

References

Adams, W.J., Jr., February 9, 1971. Seed capsule and method of making same. US Patent 3,561,159.

Bardin, S.D., Huang, H.-C., 2003. Efficacy of stickers for seed treatment with organic matter or microbial agents for the control of damping-off of sugar beet. Plant Pathol. Bull. 12, 19–26.

Bay, A.P.M., Bourne, M.C., Taylor, A.G., 1996. Effect of moisture content on compressive strength of whole bean (*Phaseolus vulgaris* L.) and separated cotyledons. Int. J. Food Sci. Technol. 31, 327–331.

Brink, E.H., January 19, 1971. Seed capsule and method of making same. US Patent 3,555,730.

Clifford, P.J., November 2, 1971. Seed capsule. US Patent 3,616,573.

Conrad, R., April 5, 2012. Cast pellets for planting seeds. US Patent Application 201102395535 A1.

Gerber, D., July 26, 1988. Seed pellets and process for their manufacture. US Patent 4,759,151.

Halmer, P., 1988. Technical and commercial aspects of seed pelleting and film-coating. In: Martin, T.J. (Ed.), Applications to Seeds and Soil. British Crop Protection Council, Alton, England, pp. 191–204.

Hill, H.J., 1999. Recent developments in seed technology. J. New Seeds 1, 105–112.

International Seed Testing Association, 2008. International Rules for Seed Testing, Seed Science and Technology 27, Supplement.

Kadajji, V.G., Betagevi, G.V., 2011. Water soluble polymers for pharmaceutical applications. Polymers 3, 1972–2009.

Legro, R.J., April 29, 1997. Pills or pellets containing seeds and inert carrier material and method for their preparation. US Patent 5,623,781.

Madsen, M.D., Davies, K.W., Williams, C.J., Svejcar, T.J., 2012. Agglomerating seeds to enhance native seedling emergence and growth. J. Appl. Ecol. 49, 431–438.

Peñaloza, P., Ramirez-Rosales, G., McDonald, M.B., Bennett, M.A., 2005. Lettuce (*Lactuca sativa* L.) seed quality evaluation using seed physical attributes, saturated salt accelerate aging and the seed vigour imaging system. Electron. J. Biotechnol. 8 (3), 299–307.

Scholfield, C.R., 1981. Composition of soybean lecithin. J. Am. Oil Chem. Soc. 58 (10), 889–892.

Taylor, A.G., 2003. Seed treatments. In: Thomas, B., Murphy, D.J., Murray, B.G. (Eds.), Encyclopedia of Applied Plant Sciences. Elsevier Academic Press, Oxford, England, pp. 1291–1298.

Trias, J., Takahashi, L.K., March 27, 2014. Promotion of plant growth using collagen based gelatin. US Patent Application 20140087942.

United States Government Printing Office (US GPO), August 12, 2014. United States Electronic Code of Federal Regulations. Title 7, Subtitle B, Chapter 1, Subchapter M, Part 205. National Organic Program. Available from: http://www.ecfr.gov/cgi-bin/retrieveECFR?gp=1&SID=464284b01c17808a7934d2e902c79005&ty=HTML&h=L&r=PART&n=pt7.3.205

Xu, Q., Nakajima, M., Liu, Z., Shiina, T., 2011. Soybean-based surfactants and their applications. In: Ng, T.-B. (Ed.), Soybean – Applications and Technology. , pp. 341–358, Available from: http://www.intechopen.com/books/soybean-applications-and-technology/soybean-based-surfactants-and-their-applications

LAND DEGRADATION & DEVELOPMENT
Land Degrad. Develop. **26**: 300–310 (2015)
Published online 15 March 2013 in Wiley Online Library (wileyonlinelibrary.com) **DOI**: 10.1002/ldr.2208

SOIL PROPERTIES AND MAIZE GROWTH IN SALINE AND NONSALINE SOILS USING CASSAVA-INDUSTRIAL WASTE COMPOST AND VERMICOMPOST WITH OR WITHOUT EARTHWORMS

A. N. OO[1,2], C. B. IWAI[2]* AND P. SAENJAN[2]

[1]*Department of Agricultural Chemistry, Yezin Agricultural University, Nay Pyi Taw, Myanmar*
[2]*Department of Plant Science and Agricultural Resources, Land Resources and Environment Section, Faculty of Agriculture, Khon Kaen University, Khon Kaen 40002, Thailand*

Received: 18 April 2012; Revised: 28 November 2012; Accepted: 15 January 2013

ABSTRACT

The aim of this study was to investigate the effectiveness of compost and vermicompost as soil conditioners in alleviating salt-affected soils and increasing maize productivity. A greenhouse trial, consisting of seven soil amendment treatments in a completely randomized design with three replications, was carried out at Khon Kaen University, Thailand, during the rainy season of 2011. Plant height and total dry matter of maize increased in treatments with compost and vermicompost application when compared with the control (no fertilizer) in two types of soils (saline and nonsaline) during the growing season. Soil pH and electrical conductivity in saturation paste extracts were decreased by compost and vermicompost amendments with or without earthworms when compared with unamended treatments in the saline soil. Compost and vermicompost amendments improved cation exchange capacity, soil organic carbon, total nitrogen and extractable phosphorus in both soils. These amendments also increased exchangeable K^+, Ca^{2+} and Mg^{2+} while decreasing exchangeable Na^+ in the saline soil, which suggested that Ca^{2+} was exchanged for Na^+, exchangeable Na^+, then leached out, and soil salinity reduced as a result. Soil microbial activities including microbial C and N and basal soil respiration were improved by the application of compost and vermicompost amendments with or without earthworms when compared with the control in both soils. This experiment showed that the compost and vermicompost were effective in alleviating salinity and improving crop growth. Copyright © 2013 John Wiley & Sons, Ltd.

KEYWORDS: salinity; microbial biomass; soil respiration; hybrid maize

INTRODUCTION

Soil degradation resulting from salinity is a major obstacle to the optimal utilization of land resources. Salt-affected soils are widely distributed throughout the world, with around 20 per cent of the world's cultivated land affected (Sumner, 2000). In Northeast Thailand, approximately 17 per cent of the land is salt-affected because of salt-bearing rocks (Land Development Department, 1991), predominantly in the Nakhon Ratchasima, Khon Kaen, Roi-Et and Mahasarakham provinces (Department of Mineral Resources, 1982). The salinization of soils in Northeast Thailand has several unique characteristics and has been accelerated by human activities such as improper land management practices, deforestation, irrigation, salt making and construction of roads and reservoirs (Mitsuchi *et al*., 1986). All of these human activities except salt making are believed to promote salinization by causing the level of saline groundwater to rise towards the surface. Eventually, low-lying paddy fields become subject to rapid salinization. The present extent of salt-affected soils in the northeast already substantially restricts crop production in many areas. Concerns regarding the potential future expansion of areas of salt-affected soils and their effects on land and water resources have been reported to be one of the most important issues for farmers who live in affected areas (Kohyama and Subhasaram, 1993; Topark-Ngarm, 2010).

Soil salinity has become a serious threat to crop productivity. Many previous studies (Keren, 2000; Levy, 2000; Liang *et al*., 2003; Sardinha *et al*., 2003) have reported on the adverse effects of excessive amounts of salts on the physical and chemical properties of soils and on plant growth and yield. Salt-affected soils exhibit unique structural problems resulting from soil physical processes such as slaking, swelling and dispersion of clay, which in turn cause degradation of soil structure (Boivin *et al*., 2004; Tejada and Gonzalez, 2005). These structural changes can affect water and air movement, plant-available water holding capacity, root penetration, seedling emergence, runoff and erosion, as well as tillage and sowing operations (Oster and Jayawardane, 1998). Salinity also affects soil chemical properties through the presence of highly soluble salt concentrations (Sumner, 2000). This alters the osmotic and matric potential of the soil solution, thereby adversely affecting soil microbial communities and their activity (Zahran, 1997; Sardinha *et al*., 2003; Rietz and Haynes, 2003). This in turn can have a negative influence on plant growth and yield (Marschner, 1995). In addition, changes in the proportions of exchangeable ions in the soil solution have osmotic and ion-specific effects that can produce imbalances in plant nutrients, including deficiencies of several nutrients

Correspondence to: C. B. Iwai, Department of Plant Science and Agricultural Resources, Land Resources and Environment Section, Faculty of Agriculture, Khon Kaen University, Khon Kaen 40002, Thailand.
E-mail: chulee_b@kku.ac.th*

Copyright © 2013 John Wiley & Sons, Ltd.

or conversely high levels of Na^+ (Grattan and Grieve, 1999; Mengel and Kirkby, 2001). To solve such problems, expansion of amelioration actions and improved management practices are needed to reclaim salt-affected soils (Qadir *et al*., 2001; Suarez, 2001; Barrett-Lennard, 2002).

The amelioration of salt-affected soils can be accomplished through many effective methods, such as water leaching, chemical remediation and phytoremediation (Sharma and Minhas, 2005; Qadir *et al*., 2007). The amelioration of salt-affected soils using chemical agents, including gypsum, calcite, calcium chloride and organic matter (farmyard manure, green manure, organic amendments and municipal solid waste), is a successful approach that has been implemented worldwide (Mitchell *et al*., 2000; Hanay *et al*., 2004; Sharma and Minhas, 2005; Tejada *et al*., 2006). According to Melero *et al*. (2007), the application of organic matter conditioners has become a common practice in salt-affected areas in the last several decades and constitutes an important method of soil regeneration and fertility enhancement.

Organic matter is very important for maintaining structural stability in soils as well as improving the physical, chemical and biological properties of soils. Salt-affected soils generally exhibit poor structural stability due to low organic matter. The addition of organic materials (green, farmyard and poultry manures, compost, food processing wastes, etc.) has been suggested for improving structural stability by many researchers (More, 1994; Nelson and Oades, 1998). Barzegar *et al*. (1997) found that addition of plant residues improved the water-stable aggregate because of increased organic matter content and decreased soil salinity. The application of organic matter for soil remediation is considered essential for sustainable land use and crop productivity.

Disposal of agro-industrial wastes is a major problem for industries in many countries, including Thailand (Iwai, 2009; Iwai *et al*., 2011). Dumping of agro-industrial wastes in the vicinity of industrial areas causes environmental hazards. Increasing pressure to reduce and recycle waste has prompted industries to look at the removal of organic wastes. Recycling of agro-industrial wastes is both a disposal mechanism and an approach to resource management. New and improved technologies are being developed for treating industrial wastes such as agro-industrial waste and cassava processing wastes. One such technology is vermicompost using earthworms. Vermiculture has been developed as a means of converting industrial wastes into value-added products that can be utilized for improving soil structure and fertility. Agro-industrial wastes could effectively be tapped for resource recovery through vermicomposting technology to produce a product for use in land rehabilitation. Adding compost or vermicompost to soils can help to replenish soil organic carbon, which can help to improve soil health and promote further primary productivity (Lal, 2004; Iwai *et al*., 2010; 2011).

Earthworms are known to have beneficial effects on the physical, chemical and biological properties of soils and thereby contribute to increased plant growth and crop yields in both natural and managed agro-ecosystems (Edwards and Bohlen, 1996; Edwards, 1998). Their beneficial effects have been attributed to improvements in soil properties and structure, greater availability of mineral nutrients to plants (Gilot, 1997) and enhanced microbial populations and activity, thereby producing biologically active metabolites such as plant growth regulators (Doube *et al*., 1997).

The objective of this study was to investigate the effectiveness of compost and vermicompost with and without earthworms as soil conditioners for alleviating salt-affected soils and to determine the effect of these amendments on the growth of maize under greenhouse conditions.

MATERIALS AND METHODS

Preparation of Soil, Compost and Vermicompost

An experiment was carried out to investigate the short-term effects of compost and vermicompost produced from cassava waste on soil properties of a saline soil and a nonsaline soil and on the growth of maize under greenhouse conditions at Khon Kaen University, Thailand, during the rainy season of 2011. The saline soil (Khorat soil series) was a composite of samples taken at a depth of 0–15 cm from various places in salt-affected areas in Borabue district (16°01′N, 103°05′E), Mahasarakham Province, Thailand. Nonsaline soil (Nam Phong soil series) was taken from an uncultivated field at Khon Kaen University. The soils were air-dried and passed through a 2-mm-mesh sieve to remove stones and other debris. The initial physical and chemical properties of the two soils before the start of the experiment are shown in Table I.

Compost and vermicompost were prepared in a laboratory of the Land Resources and Environment Department, Faculty of Agriculture, Khon Kaen University. They were produced from cassava waste materials incubated for 2 months in black plastic pots. The earthworm species used to produce the vermicompost was *Eudrilus eugeniae*. The chemical properties of the compost and vermicompost used are shown in Table II.

Table I. Physical and chemical properties of the saline and nonsaline soils at the beginning of the experiment

Property	Saline soil	Nonsaline soil
Soil texture	Loamy-sand	Loamy-sand
Sand (per cent)	87·50	80·50
Silt (per cent)	7·00	12·50
Clay (per cent)	5·50	7·00
pH (1:2·5)	7·30	6·89
Electrical conductivity of saturated paste extract ($dS\,m^{-1}$)	4·26	0·66
Cation exchange capacity ($cmol_c\,kg^{-1}$)	4·40	8·25
Organic carbon ($g\,kg^{-1}$)	4·66	5·76
Total N ($g\,kg^{-1}$)	0·24	0·49
Extractable P ($mg\,kg^{-1}$)	11·47	31·36
Exchangeable K^+ ($cmol_c\,kg^{-1}$)	0·22	0·22
Exchangeable Na^+ ($cmol_c\,kg^{-1}$)	1·32	0·07
Exchangeable Ca^{2+} ($cmol_c\,kg^{-1}$)	2·87	2·69
Exchangeable Mg^{2+} ($cmol_c\,kg^{-1}$)	0·21	0·44

Copyright © 2013 John Wiley & Sons, Ltd.

Table II. Chemical properties of compost and vermicompost made from cassava waste materials

Property	Compost	Vermicompost
pH (1:5)	5·25	7·17
Electrical conductivity (dS m^{-1}) (1:10)	5·45	1·05
Organic carbon (g kg^{-1})	172·56	62·16
Total N (g kg^{-1})	5·46	4·13
Total P (g kg^{-1})	0·89	1·24
Total K (g kg^{-1})	1·00	1·70
Total Na (g kg^{-1})	0·19	0·36
Total Ca (g kg^{-1})	16·80	11·49
Total Mg (g kg^{-1})	0·68	1·12
C : N	31·64	15·04

Experimental Design

The experiment was laid out in a completely randomized design with three replications (Gomez and Gomez, 1984). Two types of soils were used, saline soil and nonsaline soil. Seven treatments were compared: T_1 = control (no fertilizer applied), T_2 = earthworms only (20 individuals per pot), T_3 = compost only (10 Mg ha^{-1}), T_4 = compost + earthworms, T_5 = vermicompost only (5 Mg ha^{-1}), T_6 = vermicompost + earthworms and T_7 = chemical fertilizers (100 kg N ha^{-1} as urea, 50 kg P_2O_5 ha^{-1} as triple superphosphate and 25 kg K_2O ha^{-1} muriate of potash, which are the recommended rates for the region of study).

Seven kilogrammes of 2-mm-sieved air-dried soil was placed in each black plastic pot of 30-cm height and 25-cm diameter for each treatment (42 pots in total for both types of soil). Compost and vermicompost were applied before planting. Urea application was split into two equal amounts. The first half of the urea (50 kg N ha^{-1}) was applied together with all the triple superphosphate (50 kg P_2O_5 ha^{-1}) and muriate of potash (25 kg K_2O ha^{-1}) before planting. The other half of the urea was applied at 40 days after sowing. Equal amounts of water were added to all pots at the time of planting maize. Soil moisture was kept at field capacity during the entire growing period. Maize (F1 hybrid) seed was obtained from the Khon Kaen University Research Station.

Plant Data Collection

Plant height was measured every 2 weeks starting from 2 weeks after sowing until termination to determine the growth rate of maize plants. At 12 weeks after sowing, the experiment was terminated. Maize plants, including roots, were removed from the soil and then were dried at 80 °C for 48 h by a hot air oven to measure dry weights.

Soil Analyses

Triplicate soil samples were collected at a depth of 0–10 cm by taking a soil core from each pot at the end of the experiment. The soil samples were analysed for soil physical and chemical properties at the laboratory of the Land Resources and Environment section, Faculty of Agriculture, Khon Kaen University. Soil texture was determined by a hydrometer (Bouyoucos, 1951). Soil pH was determined in a 1:2·5 soil-to-water solution by a pH meter. Electrical conductivity (EC_e) in saturated paste extracts was measured following the method described by the USDA (1954). Cation exchange capacity (CEC) was determined by the 1-N ammonium acetate method (Schollerger and Simmon, 1945), and total soil organic carbon was determined by the method of Walkley and Black (1934). Total nitrogen was measured by the Kjeldahl method (Bremner, 1960). Extractable phosphorus was determined by the Bray II method (Bray and Kurtz, 1945). Exchangeable potassium, sodium, calcium and magnesium were extracted with 1-N ammonium acetate (pH 7·0) (Schollerger and Simmon, 1945). The concentrations of K^+ and Na^+ from these extracts were analysed by flame photometry, whereas those of Ca^{2+} and Mg^{2+} were analysed by atomic absorption spectrometry following a standard procedure.

After the removal of maize plants at the end of the experiment, microbial biomass C (MBC) and N (MBN) were immediately determined in field-moist subsamples after sampling by the chloroform fumigation extraction method (Amato and Ladd, 1988). For MBC, 20 g of fumigated and unfumigated soils was extracted with 100 ml of 0·5-M K_2SO_4. MBC in the extracts was determined after oxidation with $K_2Cr_2O_7$. For MBN, 20 g of soil was extracted with 100 ml of 1-M KCl. Extracts were taken from nonfumigated samples immediately after sampling. MBN was determined by the ninhydrin-reactive N method (Amato and Ladd, 1988). MBC and MBN were calculated as the difference between fumigated and unfumigated values, using k_{EC} and k_{EN} factors of 0·33 (Sparling and West, 1988) and 3·1 (Amato and Ladd, 1988) to convert extracted organic C and N to microbial C and N, respectively.

Basal soil respiration (BSR) was determined by the titrimetric method (Anderson, 1982). This method is based on the determination of CO_2 evolution from incubated soil. Field-moist soil was placed in an airtight jar containing a vial with 15 ml of 1·0-M NaOH and incubated at 28 °C. After 1 day of incubation, the NaOH vial was removed from the jar, an excess 0·5-M $BaCl_2$ and phenolphthalein were added to precipitate carbonate out from the NaOH solution as insoluble barium carbonate and, finally, the excess NaOH was titrated out with 0·5 M HCl. Soil respiration as CO_2-C was computed from the titration value according to the equation of Anderson (1982),

$$CO_2\text{-}C\ (\text{mg}) = (B - V)\,NE \tag{1}$$

where B is the volume (ml) of acid (HCl) used to titrate the alkali (NaOH) of a blank solution (not incubated with soil), V is the volume (ml) of acid used to titrate the alkali solution incubated with the soil sample, N is the normality of the acid (HCl) and E is the equivalent weight of CO_2-C.

The metabolic quotient (qCO_2) (Anderson and Domsch, 1986) of each sampling period was calculated as

$$qCO_2 = CO_2\text{-}C/\text{MBC} \tag{2}$$

where CO_2-C (mg kg^{-1} soil) is soil respiration and MBC (mg kg^{-1} soil) is microbial biomass of carbon.

Copyright © 2013 John Wiley & Sons, Ltd.

Statistical Analysis

The data collected were statistically analysed using analysis of variance techniques. Treatment means were compared by the least significant difference method at the 5 per cent level. All data analyses were performed by using Statistix 8.0 (Analytical Software, 2003).

RESULTS

Maize Growth and Dry Matter Yield

The heights of maize plants measured from 2 to 12 weeks after sowing are shown in Figure 1. Maize plant heights were not significantly different among treatments at early growth stages in either soil. In contrast, the application of compost and vermicompost amendments with or without earthworms increased plant height significantly compared with the treatment of no fertilizer application at 6, 8, 10 and 12 weeks after sowing in both soils.

Total dry matter at termination of the experiment is shown in Figure 2. The application of compost and vermicompost resulted in higher total dry matter yield when compared with the control, followed by inorganic fertilizer application in both soils. In contrast, earthworms alone and no fertilizer application both had very low dry matter yields in the saline soil. The saline soil showed significantly ($P \leq 0{\cdot}01$) lower dry matter yield compared with the nonsaline soil. No interaction between soil type and treatments was found for dry matter yield.

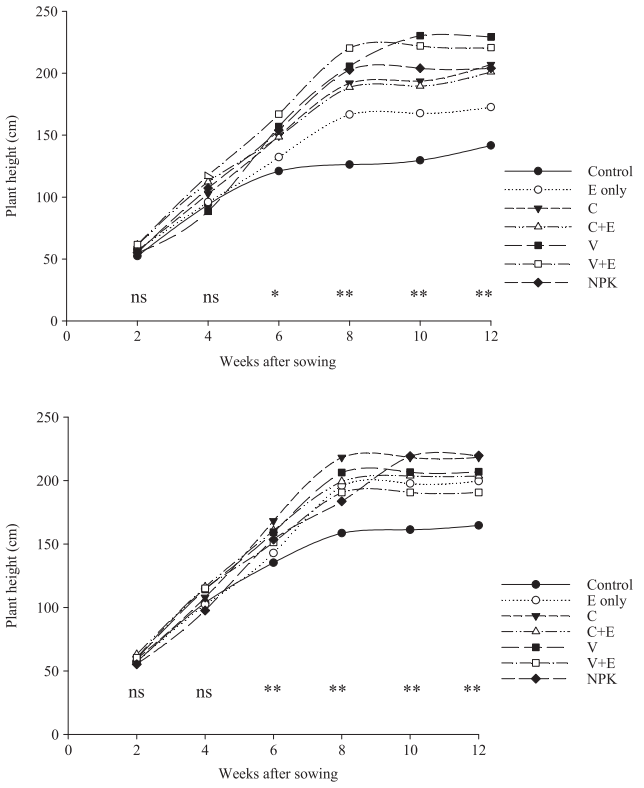


Figure 1. Effect of compost (C), vermicompost (V), earthworms (E) and chemical fertilizer (NPK) on maize plant heights at different growth stages in (a) saline soil and (b) nonsaline soil. **Significantly different at $P \leq 0{\cdot}01$; *significantly different at $P \leq 0{\cdot}05$; ns, not significant.

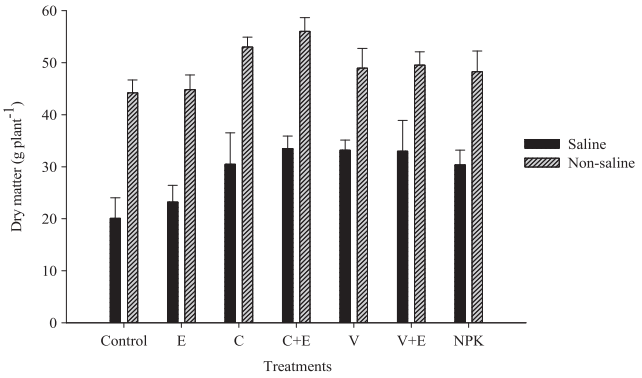


Figure 2. Effects of compost (C), vermicompost (V), earthworms (E) and chemical fertilizer (NPK) on the total dry matter of maize 12 weeks after planting. (Bars indicate standard error.)

Soil Properties

Table III shows the effects of compost and vermicompost amendments on soil salinity characteristics. In the saline soil, the pH of the soils remained greater than 7·0 in the treatments without organic amendments, whereas it was lower in the treatments with inorganic fertilizers (average of 6·4). In contrast, the pH of nonsaline soils was less than 7·0 in all treatments. In both soils, the application of vermicompost with or without earthworms resulted in pH values near neutrality (7·0). There was an interaction for pH between soils and treatments, with organic treatments having a pH reduction effect in saline soils but not in nonsaline soils.

Soil EC_e values differed significantly among treatments in both soils. The application of compost and vermicompost resulted in lower EC_e than other treatments in saline soil, with the lowest values found in the vermicompost application with earthworms ($1{\cdot}86\,dS\,m^{-1}$). In contrast, the application of compost to nonsaline soil increased EC_e, whereas vermicompost application decreased it. There was an interaction for EC_e between soils and treatments, indicating that EC_e was affected in each soil by compost and vermicompost applications.

The CEC was significantly different among treatments and soils (Table IV). In both soils, the application of compost and vermicompost gave higher CEC compared with treatments without organic amendments. The absence of an interaction for CEC between soils and treatments indicates that the effects of compost and vermicompost on CEC were similar for both tested soils. Similarly, there were significant differences in soil organic C among the treatments in both soils (Table IV). The treatment of compost with earthworms had the highest soil organic C content ($8{\cdot}24\,g\,kg^{-1}$ for saline soil and $8{\cdot}68\,g\,kg^{-1}$ for nonsaline soil), whereas the treatment with no fertilization had the lowest value ($3{\cdot}18\,g\,kg^{-1}$ in saline soil and $6{\cdot}09\,g\,kg^{-1}$ in nonsaline soil). The application of compost and vermicompost resulted in more organic carbon accumulation in the soil when compared with inorganic sources or no fertilization in both soils. There was an interaction for soil organic C between soil and treatments, indicating that soil organic C was affected in each soil by compost and vermicompost applications.

Copyright © 2013 John Wiley & Sons, Ltd.

Table III. Effect of compost and vermicompost on soil pH and EC_e in saline and nonsaline soils

	pH			EC_e (dS m^{-1})		
Treatments	Saline	Nonsaline	Mean	Saline	Nonsaline	Mean
Control	7·18ab (0·11)	6·74ab (0·04)	6·96	3·60a (0·19)	0·53b (0·04)	2·07
Earthworm (E)	7·46a (0·16)	6·78a (0·06)	7·11	3·68a (0·11)	0·58b (0·04)	2·13
Compost (C)	6·50c (0·18)	6·59bc (0·12)	6·55	3·03ab (0·40)	2·30a (0·06)	2·66
Compost + E (C + E)	6·82bc (0·21)	6·52c (0·06)	6·67	2·99ab (0·25)	2·56a (0·25)	2·78
Vermicompost (V)	6·66c (0·26)	6·74ab (0·04)	6·70	2·29bc (0·32)	0·53b (0·10)	1·41
Vermicompost + E (V + E)	6·83bc (0·09)	6·85a (0·05)	6·85	1·86c (0·19)	0·69b (0·07)	1·27
NPK fertilizers	6·41c (0·12)	6·88a (0·01)	6·65	3·29a (0·11)	0·59b (0·05)	1·94
Mean	6·84	6·73		2·96	1·11	
A (soil factor)	ns			**		
B (management)	**			**		
A × B	**			**		
CV (per cent)	3·27			16·32		

Values in the same column followed by the same letter are not significantly different at the 5 per cent level by the least significant difference test. Standard error is presented in parentheses.
EC_e, electrical conductivity; ns, not significant.
**Significantly different at $P \leq 0{\cdot}01$.

Total N content was significantly different among treatments, but there were no differences between the two soils (Table V). The treatment of vermicompost with earthworms had the highest total N content (0·32 g kg^{-1} for saline soil and 0·33 g kg^{-1} for nonsaline soil), whereas the treatment with no fertilization had the lowest values (0·19 g kg^{-1} in saline soil and 0.22 g kg^{-1} in nonsaline soil). There were significant differences in extractable P between soils and among treatments (Table V). Vermicompost without earthworms had the highest soil extractable P among the different treatments (56·74 mg kg^{-1} in saline soil and 63·07 mg kg^{-1} in nonsaline soil), followed by vermicompost with earthworms (53·80 mg kg^{-1} in saline soil and 58.84 mg kg^{-1} in nonsaline soil). No interaction for total N and extractable P was found between soil and management treatments. This indicates that the effects of compost and vermicompost were similar for both tested soils.

Tables VI and VII show that there were significant differences in exchangeable cations between treatments in saline and nonsaline soils. Treatments with organic amendments had more accumulation of exchangeable K^+ in both soils. Application of vermicompost with earthworms had the highest exchangeable K^+ (0·72 cmol$_c$ kg^{-1} in saline soil and 0·96 cmol$_c$ kg^{-1} in nonsaline soil), followed by vermicompost without earthworms (0·61 cmol$_c$ kg^{-1} in saline soil and 0·92 cmol$_c$ kg^{-1} in nonsaline soil). Exchangeable Na^+ was significantly different between treatments in saline soil, but it was not different in nonsaline soil. Treatments without organic amendments had high exchangeable Na^+ similar to the original saline soil (Table I), with the highest values found in the control (1·04 cmol$_c$ kg^{-1}). There were significant differences in the exchangeable Ca^{2+} among treatments in both soils. The use of compost and vermicompost with or without earthworms resulted in more

Table IV. Effect of compost and vermicompost on CEC and soil organic carbon in saline and nonsaline soils

	CEC (cmol$_c$ kg^{-1})			Soil organic C (g kg^{-1})		
Treatments	Saline	Nonsaline	Mean	Saline	Nonsaline	Mean
Control	4·18c (0·53)	6·10e (0·29)	5·14	3·18c (0·24)	6·09d (0·41)	4·63
Earthworm (E)	4·38c (0·09)	7·40d (0·30)	5·89	3·27c (0·23)	6·99bcd (0·31)	5·13
Compost (C)	5·03abc (0·44)	8·08cd (0·07)	6·56	8·12a (0·51)	7·76ab (0·25)	7·94
Compost + E (C + E)	5·70ab (0·50)	8·73bc (0·33)	7·22	8·24a (0·36)	8·68a (0·14)	8·46
Vermicompost (V)	5·75a (0·41)	9·17ab (0·16)	7·46	6·64b (0·28)	7·36bc (0·44)	7·00
Vermicompost + E (V + E)	5·80a (0·42)	9·73a (0·49)	7·77	6·81b (0·13)	7·48bc (0·51)	7·15
NPK fertilizers	4·47bc (0·36)	7·48d (0·20)	5·98	3·75c (0·29)	6·69cd (0·11)	5·22
Mean	5·05	8·10		5·72	7·29	
A (soil factor)	**			**		
B (management)	**			**		
A × B	Ns			**		
CV (per cent)	9·46			8·69		

Values in the same column followed by the same letter are not significantly different at the 5 per cent level by the least significant difference test. Standard error is presented in parentheses.
CEC, cation exchange capacity; ns, not significant.
**Significantly different at $P \leq 0{\cdot}01$.

Copyright © 2013 John Wiley & Sons, Ltd.

Table V. Effect of compost and vermicompost on total nitrogen and extractable phosphorus in saline and nonsaline soils

	Total N ($g\,kg^{-1}$)			Extractable P ($mg\,kg^{-1}$)		
Treatments	Saline	Nonsaline	Mean	Saline	Nonsaline	Mean
Control	0·19c (0·03)	0·22d (0·02)	0·20	13·99d (0·67)	23·14c (0·97)	18·57
Earthworm (E)	0·21c (0·02)	0·23cd (0·01)	0·22	16·52d (1·64)	23·32c (2·61)	19·92
Compost (C)	0·23c (0·01)	0·28ab (0·02)	0·26	25·53c (2·02)	33·28b (2·40)	29·41
Compost + E (C + E)	0·24bc (0·02)	0·27bc (0·01)	0·26	25·68c (1·28)	38·37b (0·61)	32·02
Vermicompost (V)	0·31ab (0·01)	0·29ab (0·01)	0·30	56·74a (1·41)	63·07a (2·48)	59·91
Vermicompost + E (V + E)	0·32a (0·03)	0·33a (0·02)	0·33	53·80a (2·13)	58·84a (2·07)	56·32
NPK fertilizers	0·21c (0·02)	0·23cd (0·01)	0·22	31·30b (2·26)	38·31b (1·76)	34·81
Mean	0·25	0·27		31·94	39·76	
A (soil factor)	ns			**		
B (management)	**			**		
A × B	ns			ns		
CV (per cent)	13·41			8·94		

Values in the same column followed by the same letter are not significantly different at the 5 per cent level by the least significant difference test. Standard error is presented in parentheses.
ns, not significant.
**Significantly different at $P \leq 0{\cdot}01$.

accumulation of exchangeable Ca^{2+} in both soils. The response to organic amendments differed between the two soils for the exchangeable Ca^{2+}. Application of compost without earthworms had the highest exchangeable Ca^{2+} in saline soil ($7{\cdot}77\,cmol_c\,kg^{-1}$), but compost with earthworm treatment had the highest value in nonsaline soil ($9{\cdot}82\,cmol_c\,kg^{-1}$). Exchangeable Mg^{2+} was significantly different among treatments in both soils. Application of vermicompost with earthworms had the highest values ($0{\cdot}46\,cmol_c\,kg^{-1}$ in saline soil and $0.52\,cmol_c\,kg^{-1}$ in nonsaline soil) among the different treatments. The preceding differences in responses depending on soil reflected significant interactions for exchangeable K^+, Na^+ and Ca^{2+} between soils and management treatments. However, no interaction was found for exchangeable Mg^{2+}.

Soil Biological Properties

Tables VIII and IX show effects on soil biological properties in saline and nonsaline soils. There were significant differences in MBC among the treatments in both soils. Treatments with organic amendments had higher MBC in both soils. In saline soil, MBC was the highest in the treatment with application of vermicompost with earthworms ($209{\cdot}5\,mg\,kg^{-1}$), but in nonsaline soil, the treatment with application of compost with earthworms was the highest ($340{\cdot}3\,mg\,kg^{-1}$). In both soils, the treatment with no fertilization was the lowest ($88{\cdot}0\,mg\,kg^{-1}$ in saline soil and $139{\cdot}8\,mg\,kg^{-1}$ in nonsaline soil). Saline soil showed a significantly lower MBC value compared with the nonsaline soil. No interaction was found for MBC between soils and treatments, indicating that the effects of compost and vermicompost on MBC were similar overall for both tested soils.

Similarly, there were significant differences in MBN among treatments in both soils. The treatment with application of vermicompost with earthworms gave the highest MBN in both soils ($56{\cdot}9\,mg\,kg^{-1}$ in saline soil and $74{\cdot}8\,mg\,kg^{-1}$ in nonsaline soil), whereas the treatment with no fertilization was lowest in

Table VI. Effects of compost and vermicompost on exchangeable cations K^+ and Na^+ in saline and nonsaline soils

	Exchangeable K^+ ($cmol_c\,kg^{-1}$)			Exchangeable Na^+ ($cmol_c\,kg^{-1}$)		
Treatments	Saline	Nonsaline	Mean	Saline	Nonsaline	Mean
Control	0·05c (0·01)	0·08d (0·01)	0·07	1·04a (0·12)	0·05b (0·00)	0·55
Earthworm (E)	0·05c (0·01)	0·08d (0·00)	0·07	0·94ab (0·08)	0·05b (0·00)	0·50
Compost (C)	0·36b (0·04)	0·41b (0·04)	0·39	0·72bc (0·09)	0·06ab (0·00)	0·39
Compost + E (C + E)	0·38b (0·04)	0·50b (0·04)	0·44	0·75bc (0·04)	0·07a (0·01)	0·41
Vermicompost (V)	0·61a (0·11)	0·92a (0·07)	0·76	0·43d (0·07)	0·05b (0·00)	0·24
Vermicompost + E (V + E)	0·72a (0·05)	0·96a (0·04)	0·84	0·57cd (0·09)	0·06ab (0·01)	0·32
NPK fertilizers	0·17c (0·02)	0·24c (0·02)	0·21	0·92ab (0·03)	0·06ab (0·01)	0·50
Mean	0·34	0·46		0·77	0·06	
A (soil factor)	**			**		
B (management)	**			**		
A × B	*			**		
CV (per cent)	19·04			24·04		

Values in the same column followed by the same letter are not significantly different at the 5 per cent level by the least significant difference test. Standard error represents in parenthesis.
**Significantly different at $P \leq 0{\cdot}01$;
*Significantly different at $P \leq 0{\cdot}05$.

Copyright © 2013 John Wiley & Sons, Ltd.

Table VII. Effects of compost and vermicompost on exchangeable cations Ca^{+} and Mg^{+} in saline and nonsaline soils

	Exchangeable Ca^{2+} ($cmol_c\,kg^{-1}$)			Exchangeable Mg^{2+} ($cmol_c\,kg^{-1}$)		
Treatments	Saline	Nonsaline	Mean	Saline	Nonsaline	Mean
Control	2·82c (0·28)	2·58c (0·16)	2·70	0·27b (0·02)	0·36b (0·03)	0·11
Earthworm (E)	2·33c (0·14)	2·60c (0·16)	2·46	0·35ab (0·04)	0·38b (0·03)	0·36
Compost (C)	7·77a (0·69)	8·99ab (0·37)	8·38	0·28b (0·06)	0·31b (0·01)	0·29
Compost + E (C + E)	7·44a (0·42)	9·82a (0·40)	8·63	0·27b (0·03)	0·31b (0·03)	0·29
Vermicompost (V)	6·21b (0·25)	8·24b (0·38)	7·22	0·38ab (0·05)	0·41ab (0·06)	0·40
Vermicompost + E (V + E)	7·40a (0·38)	8·42b (0·41)	7·91	0·46a (0·06)	0·52a (0·05)	0·49
NPK fertilizers	2·26c (0·13)	2·78c (0·09)	2·52	0·28b (0·02)	0·37b (0·01)	0·33
Mean	5·17	6·21		0·33	0·38	
A (soil factor)	**			*		
B (management)	**			**		
A × B	**			ns		
CV (per cent)	10·46			19·14		

Values in the same column followed by the same letter are not significantly different at the 5 per cent level by the least significant difference test. Standard error is presented in parentheses.
ns, not significant.
**Significantly different at $P \leq 0{\cdot}01$;
*Significantly different at $P \leq 0{\cdot}05$.

both soils (17·8 mg kg^{-1} in saline soil and 34·4 mg kg^{-1} in nonsaline soil). No interaction was found for MBN between soils and treatments, indicating that the effects of compost and vermicompost on MBN were similar overall for both soils.

Table IX shows that BSR differed significantly among treatments in both soils. Treatments with compost and vermicompost amendments had increased BSR in both soils. BSR was the highest in the treatment with application of compost with earthworms in both soils (16·13 μg CO_2-C g^{-1} day^{-1} in saline soil and 20·90 μg CO_2-C g^{-1} day^{-1} in nonsaline soil). In contrast, it was the lowest in the treatment with no fertilizer input in both soils (10·08 μg CO_2-C g^{-1} day^{-1} in saline soil and 13·02 μg CO_2-C g^{-1} day^{-1} in nonsaline soil). Saline soil had a significantly lower BSR value compared with the nonsaline soil. Metabolic quotients (qCO_2) were significantly different among treatments in both soils. It was the lowest in the treatment with application of vermicompost with earthworms in both soils (3·05 μg CO_2-C mg^{-1} MBC h^{-1} in saline soil and 2·48 μg CO_2-C mg^{-1} MBC h^{-1} in saline soil). The qCO_2 was generally higher in unamended soils. No interactions were found for BSR and qCO_2 between soils and treatments, indicating that the effects of compost and vermicompost were similar for both tested soils.

DISCUSSION

Maize Growth and Dry Matter Yield

The increased plant height and dry matter yield (Figures 1 and 2) observed in the treatments with compost and vermicompost amendments might be due to better physiological growth of plants, as the addition of organic matter is known to increase the water holding capacity of soil, CEC of soil, improved availability of macronutrients as well as micronutrients and improved soil physical properties under saline and nonsaline conditions.

Table VIII. Effect of compost and vermicompost on soil MBC and MBN in saline and nonsaline soils

	MBC (mg kg^{-1})			MBN (mg kg^{-1})		
Treatments	Saline	Nonsaline	Mean	Saline	Nonsaline	Mean
Control	88·0b (7·35)	139·8d (14·07)	113·9	17·8c (1·57)	34·4d (0·91)	26·1
Earthworm (E)	98·8b (7·65)	155·6cd (10·31)	127·2	23·1c (3·44)	36·1cd (1·79)	29·6
Compost (C)	177·5a (10·09)	278·6b (10·47)	228·0	41·0ab (4·93)	59·3b (3·78)	50·1
Compost + E (C + E)	200·4a (22·36)	340·3a (23·68)	270·4	45·0ab (9·77)	69·9ab (3·91)	57·4
Vermicompost (V)	185·5a (14·35)	278·9b (15·26)	232·2	53·7a (8·28)	72·3a (6·64)	63·0
Vermicompost + E (V + E)	209·5a (15·47)	291·6b (12·40)	250·5	56·9a (3·93)	74·8a (4·07)	65·9
NPK fertilizers	99·5b (1·49)	188·9c (15·49)	144·2	28·0bc (4·38)	47·0c (2·29)	37·5
Mean	151·3	239·1		37·9	56·3	
A (soil factor)	**			**		
B (management)	**			**		
A × B	ns			ns		
CV (per cent)	12·22			18·05		

Values in the same column followed by the same letter are not significantly different at the 5 per cent level by the least significant difference test. Standard error is presented in parentheses.
MBC, microbial biomass carbon; MBN, microbial biomass nitrogen; ns, not significant.
**Significantly different at $P \leq 0{\cdot}01$;

Copyright © 2013 John Wiley & Sons, Ltd.

Soil Properties

It is commonly known that application of organic materials such as compost and other sources improves soil physical, chemical and biological properties. Soil pH may either increase or decrease depending on the initial pH of the amendment material. This increase or decrease in pH will depend on site-specific factors including the pH of the original soil. The significant differences in soil pH value observed among different treatments could be explained by the fact that the initial pH of the organic amendment materials that was composted was quite acid, with a pH of 5·25 (Table II).

A general decrease in EC_e was seen in the treatments with compost and vermicompost compared with other treatments. This could be due to the effect of organic amendments in increasing soil porosity and aeration (Tejada *et al*., 2008). Leaching of saline water has been found to increase when organic matter is mixed in the soil (Kahlown and Azam, 2003). Moreover, the compost and vermicompost used in this study contain calcium and magnesium, which act as bases because they exist as oxides, hydroxides and carbonates when applied to soil. As a consequence of increased Ca^{2+} concentration in the soil solution, Na^+–Ca^{2+} exchange increases at the soil's cation exchange sites, permitting greater leaching of exchanged Na^+ in percolating water and subsequent reduction in soil salinity (Qadir and Oster, 2004). The effects of the compost and vermicompost application in salt-affected soils, resulting in diminished salinity and consequent improved soil characteristics, observed in this study are most likely due to increased leaching of salts by the aforementioned mechanism. Reduction of pH and EC of the soil from the addition of vermicompost was also observed by Wahid *et al*. (1998).

Soil organic matter not only is a pool of plant nutrients but also affects soil physical, chemical and biological properties, which in turn enables it to play a key role in establishing and maintaining the level of soil fertility (Fageria, 2009). In this study, compost and vermicompost amendments had positive effects on soil organic carbon compared with unamended treatments in both soils. This might be due to increased organic carbon content in the soil from the application of compost and vermicompost. In particular, in this study, soil amended with compost had higher organic carbon content than soil amended with vermicompost. Chaoui *et al*. (2003) reported that compost contained a much higher level of soluble organic C than the earthworm cast material in vermicompost. This is indicative of the lesser degree of decomposition that compost has undergone and suggests that it is still rich in labile carbon compounds, which can serve as an energy source for microbes. The noticeable increase in CEC in the treatments with compost and vermicompost might be primarily attributed to the increase of organic carbon (Tisdale *et al*., 1993; Oo *et al*., 2010).

Soils treated with vermicompost had significantly higher contents of total nitrogen and extractable phosphorous compared with the other treatments in both soils. Frederickson *et al*. (2007) reported that N and P levels of vermicompost were higher than those of compost. It appears that earthworms increased the amount of N available to the plants. In this study, only low amounts of N remained in both soils at the end of the experiment, suggesting that most of the N was removed from the soil by the plant roots. Exchangeable cations including K^+, Ca^{2+} and Mg^{2+} were significantly higher in treatments where compost and vermicompost were applied to the soil. This may be due to the initial high content of these elements in the amendment material.

Soil Microbial Activities

The addition of readily metabolizable C in organic waste products is likely to have been the most influential factor contributing to the biomass C increases measured, as has been observed previously by Tejada *et al*. (2006). Blagodatsky *et al*. (2000) and Tejada and Gonzalez (2004) reported that soil microbial biomass responds rapidly to additions of readily

Table IX. Effect of compost and vermicompost on basal soil respiration and metabolic quotient (qCO_2) in saline and nonsaline soils

	Basal soil respiration (μg CO_2-C g^{-1} day^{-1})			Metabolic quotient (qCO_2) (μg CO_2-C mg^{-1} MBC h^{-1})		
Treatments	Saline	Nonsaline	Mean	Saline	Nonsaline	Mean
Control	10·08c (1·12)	13·02d (1·12)	11·55	4·76ab (0·17)	3·99a (0·60)	4·38
Earthworm (E)	11·18c (0·92)	13·57cd (0·73)	12·38	4·83ab (0·71)	3·64ab (0·12)	4·24
Compost (C)	15·22ab (0·66)	19·25ab (0·32)	17·23	3·60bc (0·27)	2·88bcd (0·06)	3·24
Compost + E (C + E)	16·13a (0·73)	20·90a (1·10)	18·52	3·40c (0·22)	2·58cd (0·20)	2·99
Vermicompost (V)	15·03ab (0·97)	16·87bc (1·32)	15·95	3·40c (0·24)	2·52d (0·15)	2·96
Vermicompost + E (V + E)	15·40a (1·68)	17·23b (0·97)	16·32	3·05c (0·16)	2·48d (0·19)	2·76
NPK fertilizers	11·73bc (1·60)	15·77bcd (1·04)	13·75	4·91a (0·68)	3·51abc (0·46)	4·21
Mean	13·54	16·66		3·99	3·09	
A (soil factor)	**			**		
B (management)	**			**		
A × B	ns			ns		
CV (per cent)	13·48			17·98		

Values in the same column followed by the same letter are not significantly different at the 5 per cent level by the least significant difference test. Standard error is presented in parentheses.
ns, not significant.
**Significantly different at $P \leq 0{\cdot}01$

Copyright © 2013 John Wiley & Sons, Ltd.

available C. In this study, the application of compost and vermicompost provided additional substrates for microbiota, which would explain the increased soil microbial biomass and respiration observed (Tables VIII and IX). Additional substrate can also alleviate osmotic and salinity stress on microorganisms while improving soil physical and chemical conditions (Chander *et al*., 1994). The presence of organic matter can provide a buffer in the soil solution for soil microorganisms and their activities, particularly where salinity increases (McCormick and Wolf, 1980) or, as in this study, where salinity levels are already high. In the saline soil of this study, the lowest MBC values were found in unamended soils where CO_2 evolution was low and EC_e remained high.

Soil basal respiration, as measured by carbon dioxide production, is a direct indicator of microbial activities and indirectly reflects the availability of organic material (Parkin *et al*., 1996; Gomez *et al*., 2001). In this study, addition of organic amendments stimulated soil basal respiration, paralleling results obtained by Marinari *et al*. (2000). They interpreted their results as likely due either to a synergic effect of soil and amendment microorganisms or to the stimulation of microbial growth by organic substrates in the amendments. Most of the carbon supplied by these amendments consists of partially decomposed material, easily degradable for use as energy and nutrient sources for soil microorganisms. This is then reflected in increased soil microbial respiration (Stevenson, 1986).

The metabolic quotient (qCO_2) was used here to assess the effects of stress on the microbial community. The qCO_2 was generally higher in soils that were not amended with organic material in both soils (Table IX). This is probably due to the initial low organic matter content of both soils due to their sandy texture. The saline soil showed significantly higher qCO_2 compared with the nonsaline soil, probably because of the unfavourable effects of salinity, which result in low substrate utilization efficiency in saline soils (Yuan *et al*., 2007). Following the addition of compost and vermicompost, the qCO_2 was generally lower (Table VII) compared with the qCO_2 in unamended soil, suggesting that greater amounts of C were utilized in microbial synthesis rather than respiration. It is likely that the addition of compost and vermicompost alleviates stress on microbial population by providing additional substrate, as described previously. Therefore, we can conclude that qCO_2 decreased as the microbial biomass increased because of the additional substrate provided by the organic material in both saline and nonsaline soils.

Effects of Earthworm Addition

Earthworms are known to have beneficial effects on physicochemical and biological soil properties by their feeding, burrowing and casting activities. In this study, the addition of compost and vermicompost with earthworms resulted in increased organic carbon, total nitrogen and extractable phosphorus and potassium compared with the treatment with earthworms alone, probably because these organic substrates provide easily available food for earthworms (Curry, 2004). In addition, several studies have indicated that earthworms may stabilize soil organic matter through the incorporation and protection of organic matter in their casts (Martin, 1991; Guggenberger *et al*., 1996; Bossuyt *et al*., 2004, 2005; Pulleman *et al*., 2005) and increase the available form of mineral nutrients for plants (Gilot, 1997). In this study, soil microbial C and N and basal respiration increased in treatments with compost and vermicompost added with earthworms, compared with treatments with those materials without earthworms (Tables VIII and IX). Earthworms secrete polysaccharides, proteins and other nitrogenous compounds from their body, thereby providing an additional energy source for microorganisms (Sinha and Sinha, 2008). Thus, the activities of earthworms not only help replenish natural soil fertility but also can contribute to improved soil pH and reduced soil salinity.

CONCLUSIONS

The preceding results showed the beneficial effects of compost and vermicompost application, both with and without earthworms, in increasing maize growth. The results of soil analysis from the two soils showed that application of compost and vermicompost significantly increased soil organic carbon, CEC and soil N, P and K contents. Organic amendments can thus serve as a source of essential nutrients for plants as well as contribute to improved soil properties. In addition, these amendments increased exchangeable K^+, Ca^{2+} and Mg^{2+} while decreasing exchangeable Na^+ in the saline soil, thereby reducing soil salinity. Soil microbial activities as indicated by microbial C and N contents and BSR were also improved by the application of compost and vermicompost amendments with or without earthworms in both soils. These results suggest that the use of compost and vermicompost is likely to be helpful for both alleviating salinity and improving crop productivity in salt-affected areas. The addition of earthworms as soil conditioners can also contribute to improved physical, chemical and biological properties of the soil and thereby increase its nutritive value for plants.

ACKNOWLEDGEMENTS

This study was supported by the Research Projects 'Agro-industrial Waste Management and Utilization' funded by the Office of the Higher Education Commission, Thailand; 'Problem Soils in Northeast Thailand' and 'Using Soil Biota for Biological Monitoring and Ecological Zoning in the Salt affected Area in Northeast Thailand' research funded in year 2012 by the Khon Kaen University, Thailand and Khon Kaen University, Higher Education Research Promotion and National Research University Project of Thailand, Office of the Higher Education Commission. This work was also partly supported by the Graduate School Research Fund and Development Center for Integrated Water Resource Management in Northeast Thailand and GWRC, Khon KaenUniversity, Thailand. The authors would like to thank

Copyright © 2013 John Wiley & Sons, Ltd.

Dr John S. Caldwell, Japan International Research Center of Agriculture Science (JIRCAS), for English editing and suggestions for the manuscript.

REFERENCES

Amato M, Ladd JN. 1988. Assay for microbial biomass based on ninhydrin reactive nitrogen in extracts of fumigated soil. *Soil Biology and Biochemistry* **20**: 107–114, DOI: 10.1016/0038-0717(88)90134-4.

Analytical Software. 2003. Statistix 8: User's Manual. Analytical Software: Tallahassee.

Anderson JPE. 1982. Soil respiration. In Agronomy Monograph Number 9, Part II. Chemical and Biological Properties, 2nd edition, Page AL, Miller RH, Keeney DR (eds). American Society of Agronomy and Soil Science Society of America: Madison; 831–871.

Anderson TH, Domsch KH. 1986. Carbon link between microbial biomass and soil organic matter. In Perspectives in Microbial Ecology, Proceedings of the 4th International Symposium on Microbial Ecology, Ljubljana; 467–471.

Barrett-Lennard EG. 2002. Restoration of saline land through revegetation. *Agricultural Water Management* **53**: 213–226, DOI: 10.1016/S0378-3774(01)00166-4.

Barzegar AR, Nelson PN, Oades JM, Rengasamy P. 1997. Organic matter, sodicity and clay type: influence on soil aggregation. *Soil Science Society of America Journal* **61**: 1131–1137.

Blagodatsky S, Heinemeyer O, Richter J. 2000. Estimating the active and total soil microbial biomass by kinetic respiration analysis. *Biology and Fertility of Soils* **32**: 73–81, DOI: 10.1007/s003740000219.

Boivin P, Saejiew A, Grunberger O, Arunin S. 2004. Formation of soils with contrasting textures by translocation of clays rather than ferrolysis in flooded rice fields in Northeast Thailand. *European Journal of Soil Science* **55**: 713–724, DOI: 10.1111/j.1365-2389.2004.00644.x.

Bossuyt H, Six J, Hendrix PF. 2004. Rapid incorporation of fresh residue-derived carbon into newly formed stable microaggregates within earthworm casts. *European Journal of Soil Science* **55**: 393–399. DOI: 10.1111/j.1351-0754.2004.00603.x.

Bossuyt H, Six J, Hendrix PF. 2005. Protection of soil carbon by microaggregates within earthworm casts. *Soil Biology and Biochemistry* **37**: 251–258, DOI: 10.1016/j.soilbio.2004.07.035.

Bouyoucos GH. 1951. A recalibration of the hydrometer for making mechanical analysis of soils. *Agronomy Journal* **43**: 434–438.

Bray RH, Kurtz LT. 1945. Determination of total organic and available form of phosphorus in soil. *Soil Science* **59**: 39–46.

Bremner JM. 1960. Determination of nitrogen in soil by the Kjeldahl method. *Journal of Agricultural Science* **55**: 11–33, DOI: 10.1017/S0021859600021572.

Chander K, Goyal S, Kapoor KK. 1994. Effect of sodic water irrigation and farm yard manure application on soil microbial biomass and microbial activity. *Applied Soil Ecology* **1**: 139–144, DOI: 10.1016/0929-1393(94)90033-7.

Chaoui HI, Zibilske LM, Ohno T. 2003. Effects of earthworms casts and compost on soil microbial activity and plant nutrient availability. *Soil Biology and Biochemistry* **35**: 295–302, DOI: 10.1016/S0038-0717(02)00279-1.

Curry JP. 2004. Factors affecting the abundance of earthworms in soils. In Earthworm Ecology, 2nd edition, Edwards CA (ed). CRC Press: Boca Raton; 91–113.

Department of Mineral Resources. 1982. Geologic Map of Thailand. Department of Mineral Resources: Bangkok.

Doube BM, Williams PML, Willmott PJ. 1997. The influence of two species of earthworm (*Aporrectodea trapezoides* and *Aporrectodea rosea*) on the growth of wheat, barley and faba beans in three soil types in the greenhouse. *Soil Biology and Biochemistry* **29**: 503–509, DOI: 10.1016/S0038-0717(96)00037-5.

Edwards CA, Bohlen PJ. 1996. Biology and Ecology of Earthworms. Chapman & Hall: London; 426.

Edwards CA. 1998. The use of earthworms in the breakdown and management of organic wastes. In Earthworm Ecology, Edwards CA (ed). CRC Press: Boca Raton, FL; 327–354.

Fageria NK. 2009. The Use of Nutrients in Crop Plants. CRC Press: Boca Raton, FL.

Frederickson J, Howell G, Hobson AM. 2007. Effect of pre-composting and vermicomposting on compost characteristics. *European Journal of Soil Biology* **43**: S320–S326, DOI: 10.1016/j.ejsobi.2007.08.032.

Gilot C. 1997. Effects of a tropical geophageous earthworm, *M. anomala* (Megascolecidae), on soil characteristics and production of a yam crop in Ivory Coast. *Soil Biology and Biochemistry* **29**: 353–359, DOI: 10.1016/S0038-0717(96)00046-6.

Gomez E, Ferreras L, Toresani S, Ausilio A, Bisaro V. 2001. Changes in some soil properties in a vertic Argiudoll under short term conservation tillage. *Soil Tillage Research* **61**: 179–186, DOI: 10.1016/S0167-1987(01)00193-3.

Gomez, KA, Gomez AA. 1984. Statistical Procedures for Agricultural Research, 2nd edition. John Wiley & Sons: New York.

Grattan SR, Grieve CM. 1999. Salinity–mineral nutrient relations in horticultural crops. *Scientia Horticulturae* **78**: 127–157, DOI: 10.1016/S0304-4238(98)00192-7.

Guggenberger G, Thomas RJ, Zech W. 1996. Soil organic matter within earthworm casts of an anecic–endogeic tropical pasture community, Colombia. *Applied Soil Ecology* **3**: 263–274, DOI: 10.1016/0929-1393(95)00081-X.

Hanay A, Büyüksönmez F, Kiziloglu FM, Canbolat MY. 2004. Reclamation of saline-sodic soils with gypsum and MSW compost. *Compost Science and Utilization* **12**: 175–179.

Iwai CB, Arporn M, Seripong S. 2010. Earthworm distribution under different land use systems in Northeast of Thailand—benefit for land resource. *International Journal of Environmental and Rural Development* **1**(1): 37–42.

Iwai CB, Ta-oun M, Seripong S, Champar-ngam N. 2011. Vermiculture Technology. Faculty of Agriculture, Khon Kaen University: Khon Kaen, Thailand (Book in Thai).

Iwai CB. 2009. Agroprocessing waste management in Thailand. Country paper, Multicountry Observational Study Mission on Waste Management in the Agroprocessing Industry, Seoul, South Korea, 16–19 June.

Kahlown MA, Azam M. 2003. Effect of saline drainage effluent on soil health and crop yield. *Agricultural Water Management* **62**: 127–138, DOI: 10.1016/S0378-3774(03)00096-9.

Keren R. 2000. Salinity. In Handbook of Soil Science, Sumner ME (ed). CRC Press: Boca Raton; G3–G25.

Kohyama K, Subhasaram T (eds). 1993. Salt-affected Soils in Northeast Thailand, Their Salinization and Amelioration. ADRC Technical Paper No. 12. ADRC Khon Kaen: Khon Kaen.

Lal R. 2004. Soil carbon sequestration to mitigate climate change. *Geoderma* **123**: 1–22, DOI: 10.1016/j.bbr.2011.03.031.

Land Development Department. 1991. Distribution of Salt-affected Soil in the Northeast Region 1:100,000 Map. Department of Land Development: Bangkok.

Levy GJ. 2000. Sodicity. In Handbook of Soil Science, Sumner ME (ed). CRC Press: Boca Raton; G27–G63.

Liang YC, Yang YF, Yang CG, Shen QQ, Zhou JM, Yang LZ. 2003. Soil enzymatic activity and growth of rice and barley as influenced by organic matter in an anthropogenic soil. *Geoderma* **115**: 149–160, DOI: 10.1016/S0016-7061(03)00084-3.

Marinari S, Masciandaro G, Ceccanti B, Grego S. 2000. Influence of organic and mineral fertilisers on soil biological and physical properties. *Bioresource Technology* **72**: 9–17, DOI: 10.1016/S0960-8524(99)00094-2.

Marschner H. 1995. Mineral Nutrition of Higher Plants, 2nd edition. Academic Press: London.

Martin A. 1991. Short- and long-term effects of the endogeic earthworm *Millsonia anomala* (Omodeo) (Megascolecidae, Oligochaeta) of tropical savannas. *Biology and Fertility of Soils* **11**: 234–238, DOI: 10.1007/BF00335774.

McCormick RW, Wolf DC. 1980. Effect of sodium chloride on CO_2 evolution, ammonification, and nitrification in a sassafras sandy loam. *Soil Biology and Biochemistry* **12**: 153–157, DOI: 10.1016/0038-0717(80)90052-8.

Melero S, Madejon E, Ruiz JC, Herencia JF. 2007. Chemical and biochemical properties of a clay soil under dryland agriculture system as affected by organic fertilization. *European Journal of Agronomy* **26**: 327–334, DOI: 10.1016/j.eja.2006.11.004.

Mengel K, Kirkby EA. 2001. Principles of Plant Nutrition. Kluwer Academic: Dordrecht.

Mitchell JP, Shennan C, Singer MJ, Peters DW, Miller RO, Prichard T, Grattan SR, Rhoades JD, May DM, Munk DS. 2000. Impacts of gypsum and winter cover crops on soil physical properties and crop productivity when irrigated with saline water. *Agricultural Water Management* **45**: 55–71, DOI: 10.1016/S0378-3774(99)00070-0.

Mitsuchi M, Wichaidit P, Jeungnijnirund S, 1986. Outline of Soils of the Northeast Plateau. Their Characteristics and Constraints. ADRC: Khon Kaen, Technical Paper No. 1, 24–35.

Copyright © 2013 John Wiley & Sons, Ltd.

More SD. 1994. Effect of farm wastes and organic manures on soil properties, nutrient availability and yield of rice–wheat grown on sodic vertisols. *Journal of the Indian Society of Soil Science* **42**: 253–256.

Nelson PN, Oades JM. 1998. Sodicity and soil structure. In Sodic Soils: Distribution, Properties, Management, and Environmental Consequences, Sumner ME, Naidu R (eds). Oxford UP: New York; 67–91.

Oo AN, Banterng P, Polthanee A, Trelo-Ges V. 2010. The effect of different fertilizers management strategies on growth and yield of upland black glutinous rice and soil property. *Asian Journal of Plant Sciences* **9**: 414–422, DOI: 10.3923/ajps.2010.414.422.

Oster JD, Jayawardane NS. 1998. Agricultural management of sodic soils. In Sodic Soil: Distribution, Management and Environmental Consequences, Sumner ME, Naidu R (eds). Oxford UP: New York; 126–147.

Parkin TB, Doran JW, Franco-Vizcarno E. 1996. Field and laboratory tests of soil respiration. In Methods for Assessing Soil Quality, Doran JW, Jones AJ. (eds). SSSA Special Publication No. 49; 231–245.

Pulleman MM, Six J, Uyl A, Marinissen JCY, Jongmans AG. 2005. Earthworms and management affect organic matter incorporation and microaggregate formation in agricultural soils. *Applied Soil Ecology* **29**: 1–15, DOI: 10.1016/j.apsoil.2004.10.003.

Qadir M, Oster JD, Schubert S, Noble AD, Sahrawat KL. 2007. Phytoremediation of sodic and saline-sodic soils. *Advances in Agronomy* **96**: 197–247.

Qadir M, Oster JD. 2004. Crop and irrigation management strategies for saline-sodic soils and waters aimed at environmentally sustainable agriculture. *Science of the Total Environment* **323**: 1–19. DOI: 10.1016/j.scitotenv.2003.10.012.

Qadir M, Schubert S, Ghafoor A, Murtaza G. 2001. Amelioration strategies for sodic soils: a review. *Land Degradation and Development* **12**: 357–386, DOI: 10.1002/ldr.458.

Rietz DN, Haynes RJ. 2003. Effects of irrigation induced salinity and sodicity on soil microbial activity. *Soil Biology and Biochemistry* **35**: 845–854, DOI: 10.1016/S0038-0717(03)00125-1.

Sardinha M, Muller T, Schmeisky H, Joergensen RG. 2003. Microbial performance in soils along a salinity gradient under acidic conditions. *Applied Soil Ecology* **23**: 237–244, DOI: 10.1016/S0929-1393(03)00027-1.

Schollerger CJ, Simmon RH. 1945. Determination of exchange capacity and exchangeable bases in soil-ammonium acetate method. *Soil Science* **59**: 13–24.

Sharma BR, Minhas PS. 2005. Strategies for managing saline/alkali waters for sustainable agricultural production in South Asia. *Agricultural Water Management* **78**: 136–151, DOI: 10.1016/j.agwat.2005.04.019.

Sinha RK, Sinha R. 2008. Environmental Biotechnology: Role of Plants, Microbes and Earthworms in Environmental Management & Sustainable Development. Aavishkar Publishers, Distributors: India.

Sparling GP, West AW. 1988. A direct extraction method to estimate soil microbial C: calibration in situ using microbial respiration and ^{14}C labeled cells. *Soil Biology and Biochemistry* **20**: 337–343, DOI: 10.1016/0038-0717(88)90014-4.

Stevenson FJ. 1986. Cycles of Soil: Carbon, Nitrogen, Phosphorus, Sulfur, Micronutrients. John Wiley & Sons: New York.

Suarez DL. 2001. Sodic soil reclamation: modelling and field study. *Australian Journal of Soil Research* **39**: 1225–1246, DOI: 10.1071/SR00094.

Sumner ME. 2000. Handbook of Soil Science. CRC Press: Boca Raton.

Tejada M, Garcia C, Gonzalez JL, Hernandez MT. 2006. Use of organic amendment as a strategy for saline soil remediation: influence on the physical, chemical and biological properties of soil. *Soil Biology and Biochemistry* **38**: 1413–1421, DOI: 10.1016/j.soilbio.2005.10.017.

Tejada M, Gonzalez JL, Garcia-Martinez AM, Parrado J. 2008. Effects of different green manures on soil biological properties and maize yield. *Bioresource Technology* **99**: 1758–1767, DOI: 10.1016/j.biortech.2007.03.052.

Tejada M, Gonzalez JL. 2004. Effects of application of a byproduct of the two-step olive oil mill process on maize yield. *Agronomy Journal* **96**: 692–699. DOI: 10.2134/agronj2004.0692.

Tejada M, Gonzalez JL. 2005. Beet vinasse applied to wheat under dryland conditions affects soil properties and yield. *European Journal of Agronomy* **23**: 336–347, DOI: 10.1016/j.eja.2005.02.005.

Tisdale SL, Nelson WL, Beaton JD, Havlin JL. 1993. Soil Fertility and Fertilizers, 5th edition. Macmillan Publishing Co: New York.

United States Department of Agriculture (USDA). 1954. Diagnosis and improvement of saline and alkali soils. In Agriculture. Handbook No. 60, Richards LA. (ed). Oxford and IBH Publishing Company: New Delhi; 1–160.

Wahid A, Akhtar S, Ali I, Rasul E. 1998. Amelioration of saline-sodic soils with organic matter and their use of wheat growth. *Communications in Soil Science and Plant Analysis* **29**, 2307–2318, DOI: 10.1080/00103629809370112.

Walkley A, Black JA. 1934. An examination of the dichromate method for determining soil organic matter and a proposed modification of the chromic acid titration method. *Soil Science* **37**: 29–38.

Yuan B, Li Z, Liu H, Gao M, Zhang Y. 2007. Microbial biomass and activity in salt affected soil under arid condition. *Applied Soil Ecology* **35**: 319–328, DOI: 10.1016/j.apsoil.2006.07.004.

Zahran Z. 1997. Diversity, adaptation and activity of the bacterial flora in saline environments. *Biology and Fertility of Soils* **25**: 211–223. DOI: 10.1007/s003740050306.

Copyright © 2013 John Wiley & Sons, Ltd.

JEB
Journal of Environmental Biology

Journal Website : www.jeb.co.in
E-mail : editor@jeb.co.in
ISSN: 0254-8704 (Print)
ISSN: 2394-0379 (Online)
CODEN: JEBIDP

Potential use of acetylcholinesterase, glutathione-*S*-transferase and metallothionein for assessment of contaminated sediment in tropical chironomid, *Chironomus javanus*

A. Somparn[1], C.B. Iwai[1,2*] and B. Noller[3]

[1]Department of Plant Sciences and Agricultural Resources, Land Resources and Environment Division, Faculty of Agriculture, Khon Kaen University, Khon Kaen, Thailand,40002.

[2]Integrated Water Resource Management Research and Development Center in Northeast Thailand, Khon Kaen, Thailand,40002.

[3]The University of Queensland, Centre for Mined Land Rehabilitation (CMLR), Brisbane, 4072 Australia.

*Corresponding Author's E-mail : chulee_b@kku.ac.th

Publication Info

Paper received:
11 May 2014

Revised received:
14 February 2015

Accepted:
20 March 2015

Abstract

Heavy metals and organophosphorus insecticide is known to act as disruptors for the enzyme system, leading to physiologic disorders. The present study was conducted to investigate the potential use of these enzymes as biomarkers in assessment of contaminated sediments on tropical chironomid species. Acetylcholinesterase (AChE), glutathione-S-transferase (GST) and metallothionein (MT) activity was measured in the fourth-instar chironomid larvae, *Chironomus javanus*, Kieffer, after either 48-hr or 96-hr exposure to organophosphorus insecticide, chlorpyrifos (0.01- 0.25 mg kg^{-1}) or heavy metal cadmium (0.1-25 mg kg^{-1}). Exposure to chlorpyrifos (0.01 mg kg^{-1}) at 48 and 96 hr significantly of AChE activity (64.2 % - 85.9%) and induced GST activity (33.9 - 63.8 %) when compared with control ($P<0.05$). Moreover, exposure to cadmium (0.1mg kg^{-1}) at 48 and 96 hr also showed significant increas GST activity (11.7 - 40 %) and MT level (9.0 % - 70.5 %) when compared with control ($P<0.05$). The results indicated the impact of enzyme activity on chlorpyrifos and cadmium contamination. Activity of AChE, GST and MT could serve as potential biomarkers for assessment and biomonitoring the effects of insecticide and heavy metal contamination in tropical aquatic ecosystems.

Key words

Acetylcholinesterase, Cadmium, Chlorpyrifos, Glutathione *S*-transferase, Metallothionein.

Introduction

Measurement of toxicant concentration is the most common and simplest way to assess environment quality and occurrence of biological effects from exposure to pollution (Van der Oost *et al*., 2003). However, use of biochemical markers such as enzyme activity, which is closely related to molecular biology, immunological or physiological activity of an organism, has been proposed as sensitive 'early warning' tool for assessing biological effects (Callaghan *et al*., 2000; Van der Oost *et al*., 2003). Acetylcholinesterase (AChE), a carboxylesterase enzyme, has a key role in maintaining normal nerve function in the invertebrate organisms (Callaghan, 2001) and is inhibited by neurotoxic compounds such as phosphate and carbamate esters (commonly used as insecticides) that bind to the enzyme and lead to accumulation of acetylcholine in the synapse resulting in disruption of normal functioning of nervous system (Olsen *et al*., 2001). AChE inhibition has been used as a specific biomarker for organophosphate and carbamate pesticides (Domingues, 2008). Glutathione-*S*-transferases (GST) represents a family of enzymes that catalyzes the conjugation of various compounds having electrophilic centers (nitro compounds, organophosphates and organochlorines) with tripeptide glutathione. Glutathione conjugation products are rendered less toxic and become more soluble in water, facilitating their excretion (Olsen et al.,2001; Hyne and Maher, 2003). Increase in GST

© Triveni Enterprises, Lucknow (India)

activity has been used as a biomarker of organic contamination (Domingues, 2008). Metallothioneins (MTs) are small (6–7 kDa) cytosolic proteins involved in metal homeostasis and detoxification processes that contain about 60 amino acids (none of which is aromatic) and high content of cysteine residues (Coyle *et al*., 2002; Costa *et al*., 2008). The thiol groups (-SH) of cysteine residues enable MTs to bind particular heavy metal for their storage, transport or detoxification (Amiard *et al*., 2006). In organisms, it has been reported that MT level increase every 48 hr after being exposured to heavy metals ions. Thus, this response can be used for the monitoring the effects of heavy metal contamination in the environment (Rome´o *et al*., 2000; Strouhal *et al*., 2003; Kraemer *et al*., 2005; Prusa *et al*.,2006).

Application of biomarker data is relatively new in ecotoxicological study but has limitations in tropical countries such as Thailand due to availability of ecotoxicological data on aquatic organisms. Similar to the situation with many developing countries, there has been a revision of overseas ecotoxicological data, especially from temperate locations, regarding the significance of contaminants affecting organism in the environment (Dominues *et al*., 2007). Direct comparison of temperate-zone climate with tropical ecotoxicological data may not be suitable, because organisms from tropical locations may be more or less sensitive to contaminants than surrogate species. The characteristics of sediment and water in river systems may differ from other temperate locations that might influence toxicity and sensitivity of organisms to contaminants (Somparn *et al*., 2010). The assessment of toxic effects of pesticides and heavy metals in tropical climate ecosystems should be performed with local species, since their sensitivity to toxicants may differ considerably from those of laboratory standardized organisms from temperate-zone studies.

Chironomid species have been adopted as test species for ecotoxicological assessment in both water and sediment because they are an important component of freshwater ecosystems, which represents one of the most widely distributed groups of benthic organisms adapted to almost every type of aquatic ecosystem (Vos, 2000). These species are important prey for juvenile and adult fish and aquatic birds and can easily be cultured under laboratory conditions with relatively short life cycle (Taenzler, 2007). Two species of chironomid, typically used in ecotoxicity testing, are *C. tentans* and *C. riparius* (Watts and Pascoe, 2000). Since these species are not commonly found in Thailand freshwater ecosystem, local chironomid species was used in study to represent an accurate adverse effect of pollution on the tropical invertebrate species in Thailand. Therefore, the aim of the present study was to investigate the effects of chlorpyrifos and cadmium on enzyme activity (AChE, GST and MT) in tropical chironomid, *Chironomus javanus*.

Materials and Methods

Test organisms: Chironomid larvae *(Chironomus javanus*) were collected in the Ecotoxicology and Environmental Sciences Laboratory, Khon Kaen University, Thailand were since 2009.The culture was modified from OECD (2004). In brief, test species where maintained at 25±1.0°C and kept under static conditions at 6:18 hr (light- dark) photo-period. The culture water had a dissolved oxygen (DO) concentration at 5 -7 mgl^{-1} and pH of 7-8. Test species was fed with 0.5 mg of ground commercial fish food (TetraMin®, Melle,Germany). Continuous gentle aeration was provided, using an air pump to maintain optimum oxygen level, and the culture was maintained till further use.

Study design: AChE, GST and MT assays were performed to determine the activity of enzymes in chironomid larvae after exposure to chlorpyrifos and cadmium for 48 and 96hr at 25±1.0°C. Artificial sediment was spiked with chlorpyrifos to give test concentration of 0.01, 0.05, 0.1 and 0.25 mg kg^{-1} and cadmium 0.1, 1, 10 and 25 mg kg^{-1}as described by OECD (2004) test procedure. Four replication of five 4^{th} instar larvae per treatment and control were used.

Measurement of AChE and GST activity: All the steps were carried out at 4°C. Whole frozen chironomid was homogenized in ice-cooled buffer (0.02 M phosphate buffer pH 8.0, containing 1% Triton X-100) using a tissue homogenizer. Homogenate was centrifuged at 14,000 ×*g* at 4°C for 15 min. And supernatant of each sample was stored at –20°C for not more than a week, until enzymatic activities were complete. Total protein content in homogenate was measured following the method of Bradford (1976), at 595 nm, using bovine serum albumin as standard protein.

AChE activity assay was based on the method described by Ellaman *et al*. (1961), with some modification. In brief, the sample was mixed with 8 mM 5,5-di-thio-nitrobenzene acid (DTNB) in phosphate buffer containing 0.75 mgl^{-1} $NaHCO_3$ and 50 µl of 16 mM acetylthiocholine iodide. After incubation at 30°C for 5 min, AChE activity was determined by kinetic measurement at 412 nm. Results were expressed as nmol mg^{-1} protein min^{-1}.

GST activity assay was based on the method of Habig et al. (1974), with some modification adapted to microplate. In brief, the sample was mixed with assay buffer containing 1-chloro-2,4-dinitrobenzene as substrate and glutathione in sodium phosphate buffer at pH 7.5. All GST activity assays were realized in conditions of linearity with respect to incubation time. The rate was measured as ΔOD/min at 340 nm. Extinction coefficient of 9.6 was used with a light path of 0.600 cm for activity calculations. The results were expressed as nmol mg^{-1} protein min^{-1}.

MT levels was estimated by the method of Viarengo *et al*. (1997). Chironomid larvae was homogenized in three volumes

of 0.5 M sucrose, 20 mM Tris-HCl buffer, pH 8.6, with added 0.006 mM leupeptine,0.5 mM phenylmethyl sulphonylfluoride (PMSF) and 0.01% B-mercaptoethanol. The homogenate was then centrifuged at 30,000g for 30 min at 4^{o}C to obtain a supernatant. The supernatant was then treated with 1.05 ml of cold absolute ethanol and 80 µl of chloroform of 1 ml of supernatant. The samples were and then at 6000 g for 10 min. This supernatant sample was then centrifuged at 3000 g for 5 min at 4 °C; the supernatant absorbance was evaluated at 412 nm following the method of Ellaman *et al*. (1961), and MT level was estimated by utilizing reduced glutathione (GSH) as standard. The data expressed as ng mg^{-1} protein

Statistical analysis: The data obtained from different experiments were analyzed using ANOVA by Statistical 8 software (Version 8,USA) to detect significant difference in variance (P<0.05) between treatment group of concentrations and control.

Results and Discussion

The result of the effect of chlorpyrifos on AChE and GST activity is tabulated of in Table1. Chlorpyrifos inhibited AChE activity in a concentration duration manner. After exposure to highest concentration (0.25 mg kg^{-1}) chlorpyrifos for 48 hr, the AChE activity in chironomid was inhibited up to 76.5 % and when exposed for 96 hr inhibition reached 91.1 % (Table 1). This inhibition effect might be due to binding of chlorpyrifos-inhibited AChE activity to active site serine, resulting in irreversible inhibition of enzymes and thereby increasing both the level and duration of action of the neurotransmitter acetylcholine. Accumulation of acetylcholine will results in prolonged muscle contraction and prolonged electrical activity at nerve endings causing uncontrolled movement (Olsen *et al*., 200; Handy and Galloway, 2003). Previous studies have reported chlorpyrifos the ability of inhibit AChE in *C. tentans* and *C. riparius* in a dose and time-dependent manner (Dominingues *et al*., 2008; Callaghan *et al*., 2002). These studies also indicate that chironomid was sensitive to low concentrations of chlorpyrifos (0.01 mg/ kg^{-1}) and inhibited AChE activity to over 50 % after 24 hrs exposure, and that AChE activity can be used as a biomarker for assessing chlorpyrifos contamination that has low persistence in the environment (PMRA, 2000).

At highest concentration GST activity increased by 272 % and 192% at 48 and 96 hr, respectively (Table 1). It is well established that chlorpyrifos is effective in the inducting GST activity in chironomid by catalyzing the conjugation reaction of molecules with electrophilic sites with reduced glutathione and with a group of compounds like organophosphates and organochlorines (Olsen *et al*, 2001; Kheir, 2001; Crane, 2002). GST can alter the structure of pesticide to less toxic form and enhance elimination of toxicity from the organism. (Olsen *et al*.,2001; Hyne and Maher,. 2003). It is also known that GST is important in detoxification of organophosphates and organochlorines, and is induced by these pesticides in many aquatic organisms (Crane *et al*., 2002). Printes *et al*. (2007) reported that *C. xanthus* increased GST activity after exposure to chlorpyrifos for 96 hr. Moreover, there were significant differences in GST activity over time with higher activity at 48 hr, compared to 96 hr (Table1) because the chironomid absorbs chlorpyrifos in its body which causes the chironomid to create GST and remove chlorpyrifos from the body, resulting in less toxicity of chlorpyrifos.

Table 2 shows MT level and GST activity in chironomid after exposure to cadmium at 48 and 96 hr. The level of MT in

Table 1.: Effects of chlorpyrifos concentration on AChE and GST activity of *C. javanus* at 48 and 96 hr.

Chlorpyrifos (mg kg-1)	AChE activity (nmol mg l^{-1} protein)		GST activity (nmol mg l^{-1} protein)	
	48hr	96hr	48hr	48hr
0	33.7±1.0a (0)	39.7±1.6b (0)	50.6±4.7 (100)	51.1±2.7 (100)
0.01	12.1±0.9*a (64.29)	5.6±0.9*b (85.9)	67.8±2.5*d (134)	83.7±3.6*c (164)
0.05	9.89±1.2*a (70.9)	5.6±1.2*b (85.9)	99.1±2.1*c (196)	69.6±2.4*d (136)
0.10	9.5±1.8*a (71.9)	5.1±1.0*b (87.1)	127±1.1*b (250)	90.9±1.5*c (178)
0.25	7.9±1.4*a (76.6)	3.5±1.3*b (91.1)	138±2.93*a (272)	98.1±2.2*b (192)

Note: Values are mean of four replications ±SD; * indicate significant difference from control (LSD, P < 0.05); different letters in superscript indicate significant difference among different values as each exposure time; Value in parentheses indicate values of % AchE inhibition and % GST induction relative to the control.

Table 2: Effect of cadmium on MT level and GST activity of *C. javanus* at 48 and 96 hr.

Cadmium (mg kg^{-1})	MT level (ng g^{-1}tissue)		GST activity (nmol mg l^{-1} protein)	
	48hr	96hr	48hr	48hr
0	110±1.2^{a} (100)	69.5±1.9^{b} (100)	19.6±1.7 (100)	20.1±1.2 (100)
0.1	120±1.6^{*d} (109)	118±1.1^{*e} (171)	21.9±1.9^{b} (112)	28.2±1.2^{*c} (141)
1	136±1.1^{*c} (123)	140±1.9^{*d} (201)	28.9±4.7^{*b} (147)	32.95±2.20^{*c} (164)
10	172±0.7^{*b} (155)	159±1.8^{*c} (229)	26.3±3.3^{*b} (134)	33.5±1.1^{*c} (205)
25	233±0.7^{*a} (211)	167±1.1^{*b} (240)	76.2±2.0^{*a} (388)	41.2±1.1^{*b} (205)

Note: Values are mean of four replications ±SD; * indicate significant difference from control (LSD, P < 0.05); different letters in superscript indicate significant difference among different values as each exposure time; Value in parentheses indicate values of % MT and % GST induction relative to the control.

control tissues was 110.39 and 69.47 ng g^{-1} after 48 hr and 96 hr, respectively. There was significant increase in MT level in the chironomid at of 0.1 mg kg^{-1} concentration at 48 and 96 hr as compared to control (Table 2). In the present study, cadmium administration to the chironomid resulted in rapid increase of MT level up to maximum cadmium dose of 25 mg kg^{-1}. MT is a protein that can eliminate heavy-metal toxicants from organisms (Nordberg and Nordberg, 2000; Amiard *et al*., 2006) and its.

Induction represents an important defense mechanism against the toxic effects of cadmium to the chironomid. Similarly, Fabrik *et al*. (2008) observed that less toxicity of cadmium on the *C. riparius* was correlated to decrease MT in concentration, indicating the role of MT on heavy metal detoxification. The effect of cadmium was evident when chironomid was exposed to lowest concentration (0.1 mg kg^{-1}) as there was significant effect of cadmium on chironomid. The results presented for exposure times 48 and 96 hr, showed that the MT level in chironomid at of 96 hr decreased when compared to 48 hr (Table 2), which indicated that MTs needed some time to be induced. The LOEC value for cadmium exposed to *C. javanus* was 0.1 mg kg^{-1} indicating sensitivity of biomarker to cadmium exposure.

Regarding GST, the mean value for GST activity in chironomid for control obtained from the experiment with cadmium at 48 and 96 hr is presented in Table 2. After 48 hrs of exposure to 25 mg kg^{-1} cd, there was a significant increase in GST activity in chironomid (Table 2). After 96 hr, a significant change was observed in GST activity in chironomid for all the tested concentrations of cadmium (Table 2). Previous data have reported different effects of cadmium on GST activity in aquatic organism. An increase in GST activity in chironomid, *Propsilocerus akamusi* exposed to 50 mmol l of cadmium was observed at 96 hr (Zheng *et al*., 2011), and induction of GST activity has also been observed in crayfish *Procambarus clarkii* that exposed to 100 $\mu g l^{-1}$ cadmium for 96 hrs. This study indicated that GST activity also responded to cadmium. For comparison of GST activity in chironomid between exposure times of 48 and 96 hr, the results showed that no effect of cadmium on GST activity in chironomid for an exposure time of 48 hr (Table 2). Jamee *et al*. (2007) described that GST activity was possible, since it depended on the type of chemical, time and dose exposure and showed that the values of both MT level and GST activity in *C. javanus* could serve as one of the several biomarkers of cadmium contamination. However, changing MT level in chironomid at 48 hr (cadmium 0.1 mg kg^{-1}) showed higher potential as a biomarker of cadmium exposure than GST activity (Table 2).

Taken together, AChE and GST activity, as well as MT levels, show an impact on chironomid and thus represent an early toxicity response to chlorpyrifos and cadmium contamination. Therefore, assessment of AChE and GST, activity as well as MT levels in chironomid could be promising biomarkers of chlorpyrifos and cadmium contamination in sediment. The assay will be an environmental risk-assessment tool for pesticide and heavy-metal contamination in the tropical ecosystem.

Acknowledgments

This work was supported by the Higher Education Research Promotion and National Research University Project of Thailand, Office of the Higher Education Commission, Graduate School, Integrated Water Resource Management Research and Development Center in Northeast Thailand, Research center for environmental and hazardous substance management and Center of Excellence on Hazardous Substance Management, Khon Kaen University, Thailand.

References

Amiard, J.C., C. Amiard-Triquet, S. Barka , J. Pellerin and P.S. Rainbow: Metallothioneins in aquatic invertebrates: Their role in metal detoxification and their use as biomarkers *Aquat Toxicol*., **76**, 160-202 (2006).

Beauvais, S.L., S.B. Jones, J.T. Parris, S.K. Brewer and E.E. Little: Cholinergic and behavioral neurotoxicity of carbaryl and cadmium to larval rainbow trout (*Oncorynchusmykiss*). *Eco. Environ. Saf.,* **49**, 84-90 (2001).

Bradford, M.A.: Rapid and sensitive method for the quantification of microgram quantities of protein utilizing the principle of protein-dye binding. *Anal Biochem.,* **72**, 248-254 (1997).

Callaghan, A.,C. Fisher, A. Grosso, J. Holloway and M. Crane: Effect of temperature and pirimiphos methyl on biochemical biomarkers in *Chironomus riparius*, Meigen. *Eco. Environ. Saf*., **52**, 128-133 (2002).

Costa, P.M., T. Repolho, S. Caeiro, M.E. Diniz, I. Moura and M.H. Costa: Modeling metallothionein induction in the liver of *Sparus aurata* exposed to metal-contaminated sediments. *Ecotox Environ Safe*., **71**, 117-124 (2008).

Coyle, P.J., C. Philcox, L.C. Carey and A. M. Rofe: Metallothionein: The multipurpose protein., *Cell. Mol. Life Sci*., **59**, 627-647 (2002).

Crane, M., W. Sildanchandra, R. Kheir and C. Callaghan: Relationship between biomarker activity and developmental endpoints in *Chironomus riparius* Meigen exposed to an organophosphate insecticide. *Ecotox. Environ. Saf*., **53**, 361-369 (2002).

Domingues, I., L.Guilhermino, A.M.V.M. Soares and A.J.A. Nogueira: Assessing dimethoate contamination in temperate and tropical climates: potential use of biomarkers in bioassays with two chironomid species. *Chemosphere*., **69**, 145-154 (2007).

Domingues, I., S.Kriengkrai, Y. Amararatne, M.V.M. Soares and A.J.A Nogueira: In situ assay with the midge *Kiefferulus calligaster* for contamination evaluation in aquatic agro-systems in central Thailand. *Chemosphere*.,**71,** 1877-1887 (2008).

Ellman, G., K.Courtney, J.V. Andres and R. Featherstone: A new and rapid colorimetric determination of acetylcholi-nesterase activity. *Biochem. Pharmaco*.,**7**, 88-95 (1961).

Fabrik, I., Ruferova, Z., Hilscherova, K., Adam, V., Trnkova, L. and Kizek, R.: Determination of metallothionein in larvae of freshwater a midges (*Chironomus riparius*) using Burdick Reaction. *Sensors*., **8**, 4081-4094 (2008).

Handy, R.D., T.S. Galloway and M.H. Depledge: A proposal for the use of biomarkers for the assessment of chronic pollution and in regulatory toxicology. *Ecotox.,* **12**, 331-343 (2003).

Hyne, R.V. and W.A. Maher: Invertebrate biomarkers: Links to toxic is that predict population decline. *Ecotoxicol Environ Saf.,* **54**, 366-

374 (2003).

Jemec, A., D. Damjana,T. Tišler and S.Kristina: Biochemical biomarkers in environmental studies-lessons learnt from enzymes catalase, glutathione *S*-transferase and cholinesterase in two crustacean species. *Environ Sci Pollut Res.,* **17**, 71-81 (2009).

Kraemer, L.D., P.G.Campbell and L.Hare: Dynamics of cd and zn accumulation in organs and sub-cellular fractions in field transplantated juvenile yellow perch (*Percaflavescens*). *Environ. Pollut.,* **138**, 324-337 (2005).

Kheir, R., H. Ibrahim, J. Lewis, A. Callaghan and M. Crane: Comparison of acetylcholinesterase and glutathione-*S*-transferase activity in *Chironomus riparius* Meigen exposed to chemical-spiked sediments. *Bull Environ Contam Toxicol*., **66**,603-610 (2001).

Kovarova, J, R. Kizek , A. Vojtech, D. Harustiakova, O. Celechovska, and Z. Svobodova:Effect of Cadmium Chloride on Metallothionein levels in carp. *Sensors.,* **9**, 4789-4803 (2009).

Nordberg, M and G.F. Nordberg: Toxicological aspects of metallothionein. *Cell Mol Biol.,* **46**, 451-463 (2000).

OECD: Test guideline 218 sediment-water chironomid toxicity test using spiked sediment (2004) .

Olsen, T., L. Ellerbeck, T. Fisher, A. Callaghan and M.Crane: Variability in acetylcholinesterase and glutathione *S*-transferaseactivities in *Chironomus riparius* Meigen deployed in situ at uncontaminated field sites. *Environ Toxicol Chem.,* **20**, 1725-1732 (2001).

PMRA (Pest Management Regulatory Agency): Environmental assessment of chlorpyrifos. environmental assessment. Division, Pest Management Regulatory Agency, Ottawa, Ontario (2000).

Prusa, R., M.Svoboda, O.Blastik, V.Adam, O.Zitka, M.Beklova, T.Eckschlager and R.Kizek: Increase in content of metallothionein as marker of resistance to cisplatinin a human germ cell tumor cell line. *Clin. Chem.,* ***52***, 174-175 (2006).

Pery, A. R., R. V.Ducrot, R. Mons, C. Miege, J. Gahou, D. Gorini and J. Garric: Survival test with *Chrironomus riparius* exposured to spiked sediment can profit DEBtox model. *Water Res*., **37**, 2691-2699 (2003).

Printes, L. B. E. L. G. Espindola and M. N. Fernandes: Biochemical biomarkers in individu all larvae of *Chironomus xanthus* (Rempel, 1939) (Diptera, Chironomidae). *J. Braz. Soc. Ecotoxicol.,* **2**, 53-60 (2007).

Rome´o, M., M. Bennani,M.Gnassia-Barelli, M. Lafaurie and J.P. Girard: Cadmium and copper display different responses to oxidative stress in the kidney of the sea bass *Dicentrarchuslabrax*. *AquaToxico*., **48**, 185 -194 (2000).

Roesijadi, G.: Mercury-binding proteins from the marine mussel, *Mytilus edulis*. *Environ Health Perspect*., **65**, 45-48 (1986).

Somparn, A., C.B Iwai, and B. Noller: Development of the indigenous chironomid species ecotoxicology test : Tool for water quality management in Thailand. *IJERD*., **1**, 32-36 (2010).

Strouhal, M., R.Kizek, J.Vecek, L.Trnkova and M. Nemec: Electrochemical study of heavymetals and metallothionein in yeast *Yarrowialipolytica*. *Bioelectrochem.,* **60**, 29-36 (2003).

Taenzler,V., B. Eric ,D. Michael, P.Verena and W. Lennart: Chironomids: suitable test organisms for risk assessment investigations on the potential endocrine disrupting properties of pesticides. *Ecotox*., **16**, 221-223 (2007).

Van der Oost, R., J.Beyer and N.P.E. Vermeulen: Fish bioaccumulation and biomarkers in environmental risk assessment: a review. *Environ Toxicol Pharmacol*., **13**, 57-149 (2003).

Vos, J.H., M.A.G.Ooijevaar, J.E.Postma and W.Admiraal: Interaction between food availability and food quality during growth of early instar chironomid larvae. *J North Am Benthol Soc*., **19**, 158-168 (2000).

Watts, M.M.P. and D.Pascoe: A comparative study of *Chironomus riparius* Meigen and *Chironomus tentans,* Fabricius (Diptera: Chironomidae) in aquatic toxicity tests. *Arch Environ. Contam. Toxicol*., **33**, 299-306 (2000).

Wheelock, C.E., K.J. Eder, I.Werner, H. Huang, P.D. Jones, B.F. Brammell, A.A. Elskus and B.D. Hammock: Individual variability in esterase activity and CYP1Alevels in Chinook salmon (*Oncorhynchuststshawytscha*) exposed to esfenvalerate and chlorpyrifos. *Aqua Toxico.,* **74 ,** 172-192 (2005).

Zheng X, W.Long, Y. Guo and M. Enbo: Effects of cadmium exposure on lipid peroxidation and the antioxidant system in fourth-instar larvae of *Propsilocerus akamusi* (diptera: Chironomidae) under laboratory conditions. *J .Econ Entomo.,* **104**, 827-832 (2011).

Online Copy

Hort. Environ. Biotechnol. 56(1):27-35. 2015.
DOI 10.1007/s13580-015-0064-7

ISSN (print) : 2211-3452
ISSN (online) : 2211-3460

Research Report

Water Use Efficiency, Nutrient Leaching, and Growth in Potted Marigolds Affected by Coconut Coir Dust Amended in Substrate Media

Panupon Hongpakdee[1*] and Soraya Ruamrungsri[2]

[1]*Department of Plant Science and Agricultural Resources, Faculty of Agriculture, Khon Kaen University, Khon Kaen, 40002 Thailand*
[2]*Department of Plant Science and Natural Resources, Faculty of Agriculture, Chiang Mai University, Chiang Mai, 52000 Thailand*

*Corresponding author: panupon@kku.ac.th

Received June 2, 2014 / Revised January 19, 2015 / Accepted January 19, 2015
Ⓒ Korean Society for Horticultural Science and Springer 2015

Abstract. Coconut coir dust amended in substrate had effects on water use and some growth in potted marigolds (*Tagetes erecta* 'Antigua Yellow'). This study was performed to clarify the effect of coir dust amended in substrate media on water use efficiency and nutrient leaching in potted marigold. 'Antigua Yellow' seeds were sown in peat moss to develop 2 pairs of true leaf, then seedlings were randomly transplanted into 15 cm plastic pots containing soilless mix media (40% rice husk charcoal, 20% rice husk, 20% sand and 20% compost leaves; by volume) and followed by coconut coir dust amended treatments with 0, 25, 50 and 75% (v/v). The results exhibited that all amended coconut treatments could improve the physical properties of mix media by decreasing the estimated bulk density, but increased the total porosity (%) and water filled pore (%). Fifty percent coir dust treatment seems to reduce accumulated ET, crops evapotranspiration (ETc) and transpiration per leaf area unit per day. Hence, 50% coir dust portion gave the highest water use efficiency (WUE) and the lowest crop co-efficient (Kc) parameter. Nevertheless, 75% coir dust portion also reduced some nutrient leachate in the runoff solution; nitrate (NO_3^-) leachate at early growth stage and phosphate leachate (PO_4^{3-}) at flowering and senescence. Positive correlation was observed between total leachate volume and total phosphate concentration leachate (R = 0.98). Almost all plant growth parameters had diverse responses during the comparison of each different coconut coir dust portion, but flowering yield (total FW and total number) were prone to be promoted by 75% coir dust treatment.

***Additional key words*:** coco-peat, containerized marigold, mixed media, nutrient leachate, water regimes

Introduction

Marigold (*Tagetes erecta*) is one of the most important flowering crops in the world. It was ranked in the top five of bedding plants in USA (USDA, 2013), widely used as an Asian ornamental potted plant and grown on a large scale for landscaping decoration, making garlands and cut flowers (Sangwan et al., 2010). In Thailand, potted marigold is still very popular with a high demand for many years, mainly because of its vivid yellowish flower colors, long lasting shelf life and its auspicious local Thai name 'Dao Rueng' which means 'condensed gold' (Marigold Asia, 2013). This has led to an appearance of various new marigold seeds companies and retail nurseries.

The potted plant industry was partially responsible for significant water losses during its agricultural activities which contributed to an increase in economic cost and nutrient leaching, this, in turn, led to chemical contamination in the surface and ground water (Pannkuk et al., 2011). Effective water management practices in plant nurseries must include water supply via an estimated plant water requirement, suitable irrigation methods and growing substrate media properties improvement. Evapotranspiration (ET) was a common method of measuring the water balance of plants. Irrigation amounts should be sufficient to replace water the plant and substrates have evapotranspirated, which can be estimated by measuring the change in weight (Argo and Biernabaum, 1994). Modifications of growing substrate medium in terms of physical, chemical and biological characteristic which enhances plant growth, water use efficiency and nutrient availability has been reported in various flowers and ornamental plants (Klock-Moore and Broschat, 2001; Wilson and Stoffella,

2003).

Soilless media is widely used in greenhouse crop production because it is relatively lightweight, free from diseases, readily available, and more uniform and more suitable for containerization than mineral soils (Nelson, 1991). Peat, vermiculite, perlite, bark, and rock wool are used extensively (Lin et al., 1996). These components, however, are more expensive. Coconut coir dust was a local by-product material from manufacturing processes, usually used as a growing medium for numerous ornamental plant productions (Meerow, 1997), since it had a large water holding capacity, high containment of some nutrient (K, Na, and Mg) (Abad et al., 2005), renewable resource and low price (Abad et al., 2002). It was an alternative to a traditional, commercially available peat-moss which is mentioned in a sustainable agricultural context regarding non-renewable resources (Erwan et al., 2013). Coconut coir dust amended in substrate media has been reported to improve flower quality and prolong shelf life in potted marigolds and celosia (Awang and Ismail, 1997). While the use of mixed coir dust and fermented rice husk with added superphosphate fertilizer is still the best as is peat moss (Sittinam, 2007). There is little information concerning the effect on water use requirements and nutrient leachate in potted marigold. There is considerable pressure on the flower and ornamental plant industry to produce crops more efficiently, to reduce water regimes and nutrient leaching in an effort to be environmental friendly.

The purpose of this study was to clarify the effect of coconut coir dust amended in substrate media on water use efficiency and nutrient leaching in potted marigold, growing under tropical conditions.

Materials and Methods

Experimental Site

The experiment was conducted at the Flower and Ornamental Nursery, Faculty of Agriculture, Khon Kaen University, Khon Kean, Thailand (latitude16°28'N, longitude 102°48'E, 200 m above mean sea level), during June and July, 2012.

Plant Materials and Experimental Condition

Tagetes erecta 'Antigua Yellow' seeds were sown in peat moss and grown for 20 days before being transplanted in to 15 cm plastic pots (1.32 L), then filled with a mixture of substrate media (40% rice husk, 20% rice husk charcoal, 20% sand and 20% fermented leaf compost by volume) and amended with different coconut coir dust portions as treatment 0, 25, 50 and 75% (v/v), respectively. All coconut coir dusts were soaked in tap water overnight 3 times for dilution of the sodium ion and chloride ion prior to mix in substrate as a treatment.

The pinching technique was completed when plants reached a 4 leaf pair (27 days after sowing: DAS). Throughout the experiment, plants received top dressing fertilizer with 15N-15P_2O_5-15K_2O at 2.5 g/plant each week and sprayed with 21N-21P_2O_5-21K_2O foliar fertilizer (Tween Ferty, Saeree Agricultural Chemistry & Industrial, Bangkok, Thailand) twice a week. All amended coir dust treatments were replicated four times (5 pots per replication) and arranged in a completely randomized design on a bench top under plastic greenhouse of tropical conditions (approximately 29°C, 76% RH and 17.68 $MJ \cdot m^{-2} \cdot d^{-1}$ solar radiation). Each pot was irrigated daily with 380 mL of tap water by hand watering throughout the growth periods.

Data Collection

The physical and chemical properties i.e. bulk density, total porosity, air-filled pore, water fill pore, EC and pH of substrate media mixture were evaluated pre- and post-planting as previously described by Spomer (1979) with some modification.

Twenty randomly selected plants per treatment were harvested in 5 growth stages 1) pinching (27 DAS), 2) axillary bud growing (30 DAS), 3) vegetative growth (37 DAS), 4) flowering (48 DAS) and 5) ceased flower (56 DAS) for investigating their growth and development in terms of shoot-root dry weight (DW), plant height, leaf area, flower number, flower fresh weight (FW) and flower size.

The potted plant weighing method by Argo and Biernabaum (1994) procedure was used to determine the evapotranspiration rate (ET) by balances, estimated crop evapotranspiration (ETc) was determined by the soil-water balance method, crop co-efficients (Kc) were estimated dividing ETc by the FAO modified Penman ETo according to Doorenbos and Pruitt (1992) based on meteorological data automatically recorded. Measurement of water use efficiency (WUE) by gravimetric approach involves the calculation of the dry matter accumulated over the specific periods of time (difference in the initial and final dry matter of each growth stage) and the total water consumed during the experiment (Jaleel et al., 2008), while the transpiration per leaf area unit per day was derived by dividing water consumed in each growth stage by leaf area which was measured using a LI-3100C leaf area meter (LI-COR Bioscience, Lincoln, NE, USA).

The leaching fraction was quantified as the water volume leached from the pot divided by the total water applied (Bañón et al., 2009). Total leachate volumes were recorded and 150 mL sample aliquots were collected in vials and immediately frozen until used to analyze for NO_3^-, PO_4^{3-} and K with reflectometer (RQ flex 10, Merck KGaA, Darmstadt, Germany). The leachate sample was filtered through a filter paper (110 mm, Whatman) before analysis of nutrients in

Table 1. Physical properties of substrate media amended with different rates of coconut coir dust.

Treatment	Substrate physical properties			
	Bulk density ($g \cdot cm^{-3}$)	Total porosity (%)	Air filled pore (%)	Water filled pore (%)
		Pre-planting		
0% Coir dust	0.07 a[z]	44.7 d	1.23 b	43.12 d
25% Coir dust	0.06 b	47.6 c	1.60 a	45.95 c
50% Coir dust	0.05 c	51.4 b	1.28 b	49.89 b
75% Coir dust	0.03 d	59.4 a	1.82 a	57.27 a
LSD at $p < 0.05$	*	*	*	*
% CV	7.80	1.72	13.6	1.83
		Post-planting		
0 % Coir dust	0.07 a	44.8 d	1.22 c	43.11 c
25 % Coir dust	0.05 b	51.3 c	2.21 b	46.79 b
50 % Coir dust	0.04 c	52.9 b	1.64 c	51.12 a
75 % Coir dust	0.03 d	55.5 a	2.78 a	53.75 a
LSD at $p < 0.05$	*	*	*	*
% CV	7.83	1.93	16.43	4.51

[z]Means with the same letter within column are not significant different by LSD ($p < 0.05$).

leachate. Nitrate was analyzed using reflectoquant nitrate test strips (No.116999, Merck KGaA, Darmstadt, Germany) by the reaction between acidic buffer nitrite ions with an aromatic amine to form a diazonium salt, which in turn reacts with N-(1-naphthyl)-ethylenediamine to form a red-violet azo dye (Merck, 2012a). Phosphate was analyzed using phosphate reflectoquant phosphate test strips (No. 116978, Merck KGaA, Darmstadt, Germany) by the reaction of ortho-phosphate ions (PO_4^{3-}) in sulfuric solution with molybdate ions to form molybdophosphoric acid before reduced to phosphomolybdenum blue (PMB) (Merck, 2012b). Potassium was analyzed using reflectoquant potassium test strips (No. 116992, Merck, Darmstadt, Germany) by reaction of potassium ions with dipicrylamine to form an orange-colored complex which was determined reflectometrically (Merck, 2012c).

Statistical Analysis

Data was subjected to analysis of variance (ANOVA) using Statistic 8 analytical software (SXW Tallahassee, FL, USA). Least significant difference at $p < 0.05$ was used to determine significant differences in physical and chemical properties of substrate media in pre- and post-planting, growth, water consumption (with 4 replicates per treatment), leaching fraction and nutrient leachate (4 replicates, 5 plants per replicate). A linear regression and correlation coefficient analysis was performed at $p < 0.05$.

Results

Substrate Physical and Chemical Properties

All coconut coir dust amended treatments resulted in substantially improved media physical properties as reflected in the decrease of the estimated bulk density, but increased in the percentage of total porosity and water fill pore in both pre-and post-planting. The increasing coir dust portion was seen to increase the percentage of air fill pore (Table 1). Among the tree coir dust portions, 75% coir dust was found to be the most effective for substrate media physical improvement (Table 1). This amended treatment alters the substrate chemical properties by significantly increasing the pH value compared with coir dust base free treatment (Table 2).

Plant Growth and Development

The total dry weight of potted marigold was mainly partitioned to shoot more than 50% in each stage, except the axillary bud growth stage (Fig. 1). At axillary bud growth stage, both 0 and 75% coir dust portions gave the highest flower DW accumulation (68 and 62%, respectively) compared with remaining portions (Figs. 1A and 1D). Root DW partition seemed to gradually decrease from early stages to the end of growth in each treatment (Fig. 1). When plants reached the vegetative growth stage, a sharp decrease of DW occurred in root and continued to the lowest (less than 2%) at senescence stage.

The growth of plants in terms of total root dry weight,

Table 2. Effects of coconut coir dust amended substrate media on growth, flower quality, leaching fraction, electrical conductivity (EC) and pH of leachate solution in potted marigold.

Growth parameter	Coconut coir dust (%)			
	0	25	50	75
Plant growth at flowering				
Shoot dry weight (g)	27.81 a[z]	27.05 a	21.70 b	27.25 a
Root dry weight (g)[ns]	2.50	2.25	2.36	2.28
Root-shoot ratio	0.09 b	0.09 b	0.12 a	0.08 b
Plant height (cm)[ns]	29.50	30.30	29.80	29.70
Total leaf area (cm^2)[ns]	725.05	766.33	767.98	732.68
Flower quality				
Total flower number	5.95 b	4.45 c	5.00 bc	7.20 a
Total flower fresh weight (g)	40.44 b	36.17 bc	35.42 c	48.86 a
Flower diameter (cm)[ns]	3.89	4.08	4.21	4.07
Leaching fraction (%)	31.51 b	28.77 c	38.16 a	31.95 b
EC ($dS \cdot m^{-1}$)	1.95 ab	2.00 ab	2.15 ab	1.85 b
pH	6.06 b	6.90 a	6.96 a	7.06 a

[z]Means with the same letter within row are not significant different by LSD ($p < 0.05$).
[ns]Not significant.

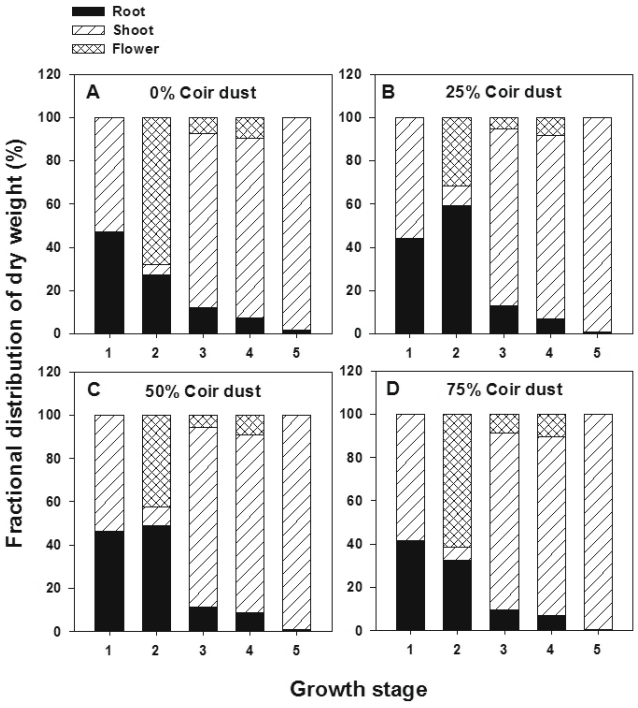


Fig. 1. Fractional distribution of dry weight (%) to component plant part (roots, shoots and flowers) of potted marigold (*Tagetes erecta* 'Antigua Yellow') when grown in 4 different levels of coconut coir dust amended substrate media 0 (A), 25 (B), 50 (C) and 75% (D) at 5 growth stages: 1, pinching (27 DAS); 2, axillary bud growing (30 DAS); 3, vegetative growth (37 DAS); 4, flowering (48 DAS); and 5, ceased flower (56 DAS).

plant height and total leaf area were not affected by the coir dust amended treatment (Table 2). However, the 50% coir dust treatment also reduced shoot dry weight, but induced the highest root-shoot ratio (Table 2). The 75% amended coir dust treatment seems to increase flower yields in terms of its total number and total FW (Table 2).

Water Regimes Parameters

The greatest leaching fraction percentage was found in plants which were grown under the 50% coir dust treatment (38.16%). All coir dust treatments induced spectacular increases in the leachate pH, compared with coir dust base free treatment (Table 2).

The daily ET and accumulated ET in all treatments during the experimental time are presented in Fig. 2. During the first two growing periods (pinching and axillary bud growth), the daily ET was ranked between 33 and 141 mL/pot (Fig. 2A) and continued to increase when plants reached the vegetative growth (37 DAP), followed by 28 to 268 mL/pot at flowering period (48 DAP). The highest peak of daily ET was found in ceased flower stage at 432 mL/pot under the 75% coir dust treatment and sharply decreased when they reached the last 2-3 day of floral senescent (Fig. 2A).

The 50% coir dust in substrate treatment gave the lowest accumulated ET (L/pot) and transpiration rate per leaf area unit per day of potted marigold in flowering and ceased flower stage (Figs. 2B and 3B). The decreasing of calculated average ETc ($mm \cdot d^{-1}$) in the last few growth stages was observed in the 50% coir dust, compare with the non-coir dust treatment (Fig. 3A). This result showed a similar pattern as described above, and achieved spectacular increases in water use efficiency: WUE (mg $DW \cdot mL^{-1}$) of plant when

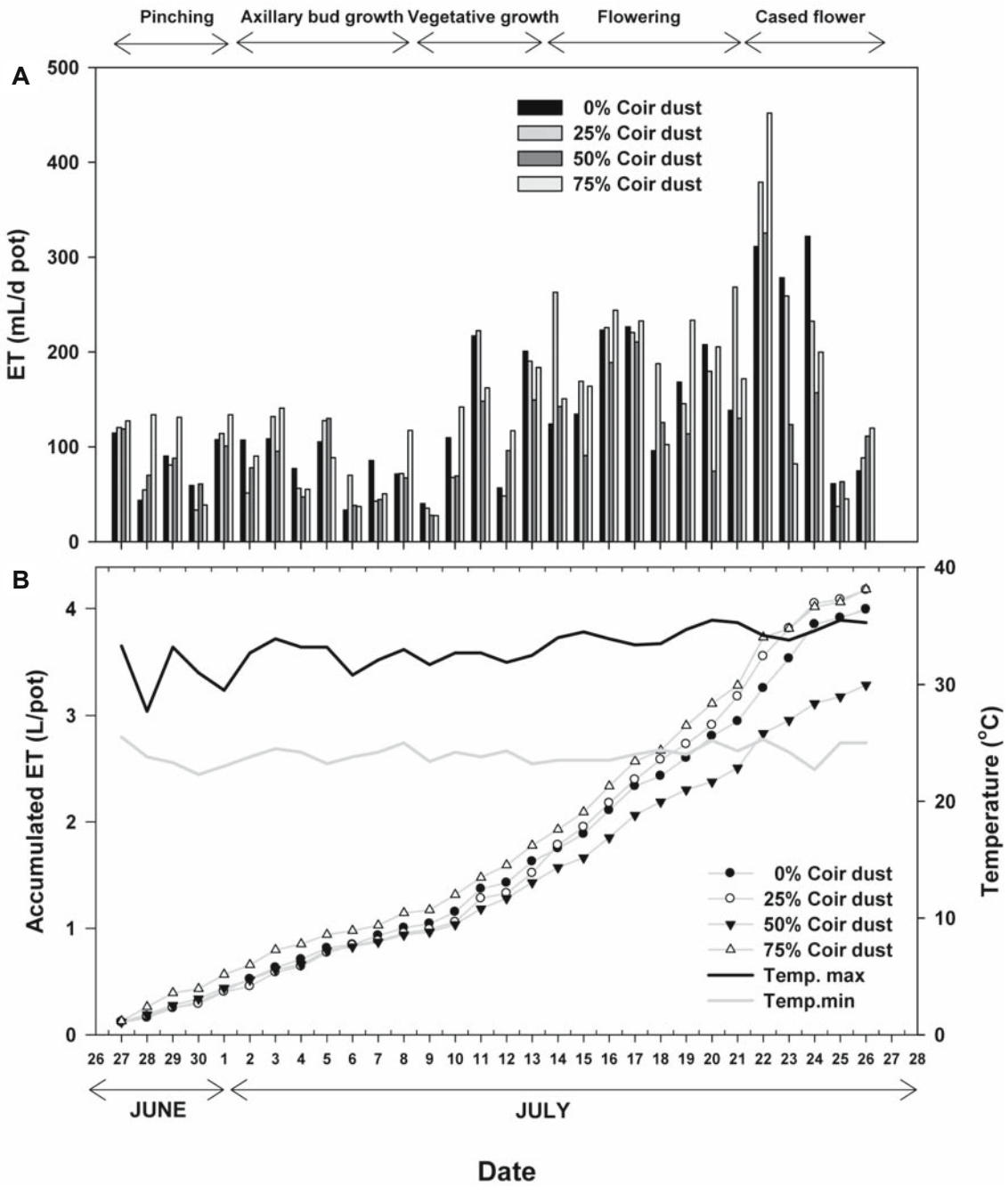


Fig. 2. Evapotranspiration (mL/pot) (A), accumulated ET (L/pot) and temperature (°C) (B) of potted marigold (*Tagetes erecta* 'Antigua Yellow') when grown in 4 different levels of coconut coir dust amended substrate media 0, 25, 50 and 75% at 5 growth stages: 1, pinching (27 DAS); 2, axillary bud growing (30 DAS); 3, vegetative growth (37 DAS); 4, flowering (48 DAS); and 5, ceased flower (56 DAS).

grown in the 50% coir dust treatment at vegetative growth stage (Fig. 3C).

The crop-co efficient (Kc) of potted marigold was ranked between 0.38 to 3.85, with the 50% coir dust treatment, showing the best result for reduced Kc in each growth stage (Fig. 4).

Nutrient Leachate in Leaching Solution

The 75% coir dust amended treatment gave the lowest leaching nitrate (NO_3^-) from drainage solution in first two phases (pinching, and vegetative growth) 4.33 and 6.50 mg·L^{-1}, respectively (Fig. 5A). Thereafter, when plants started flowering and senescence, the non-coir dust free substrate treatment had the least leaching NO_3^- 44.75 and less than 3.0

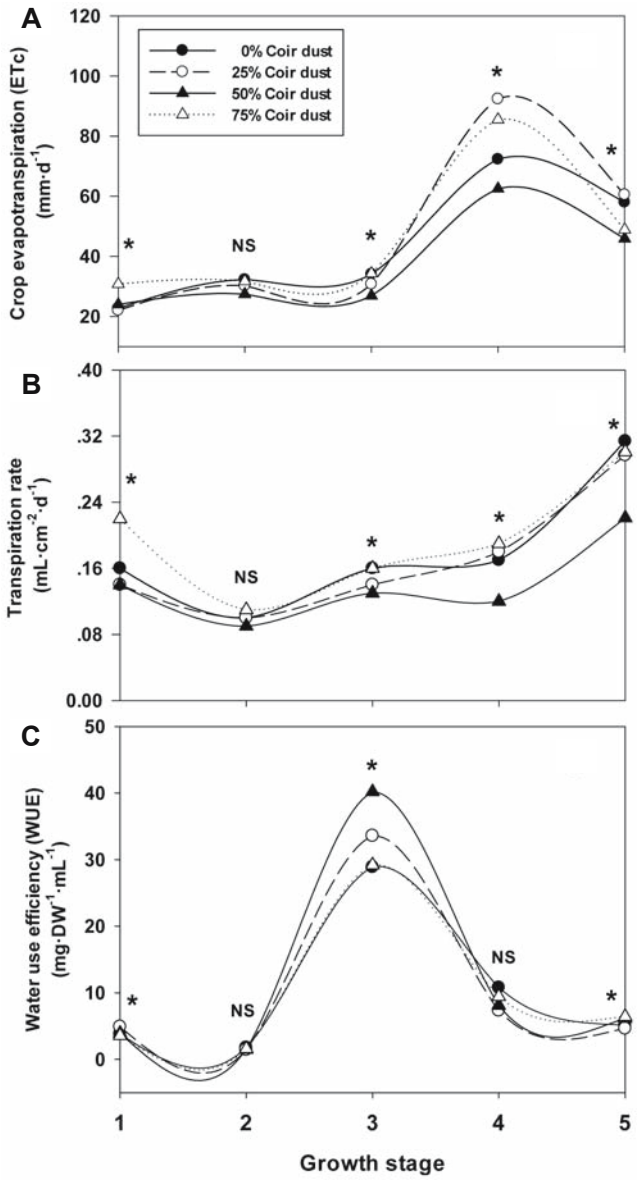


Fig. 3. Crop evapotranspiration (A), transpiration rate (B) and water use efficiency (C) of potted marigold (*Tagetes erecta* 'Antigua Yellow') when grown in 4 different levels of coconut coir dust amended substrate media 0, 25, 50 and 75% at 5 growth stages: 1, pinching (27 DAS); 2, axillary bud growing (30 DAS); 3, vegetative growth (37 DAS); 4, flowering (48 DAS); and 5, ceased flower (56 DAS).

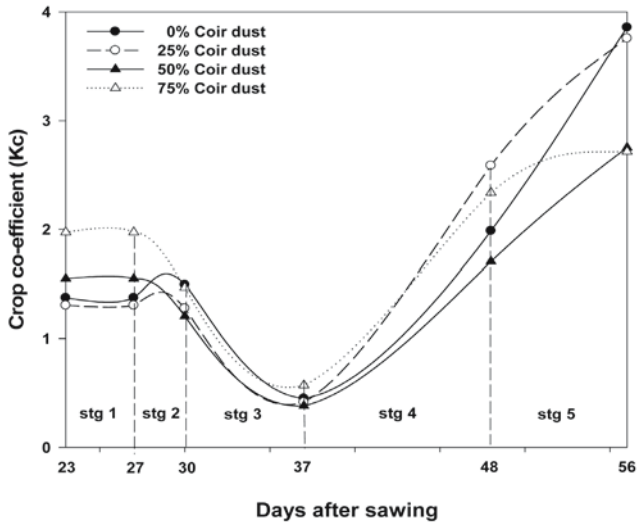


Fig. 4. Crop co-efficient (Kc) of potted marigold (*Tagetes erecta* 'Antigua Yellow') when grown in 4 different levels of coconut coir dust amended substrate media 0, 25, 50 and 75% at 5 growth stages: 1, pinching (27 DAS); 2, axillary bud growing (30 DAS); 3, vegetative growth (37 DAS); 4, flowering (48 DAS); and 5, ceased flower (56 DAS).

$mg \cdot L^{-1}$ (Fig. 5A).

Amended coir dust into substrate over 25% could reduce leaching phosphate (PO_4^{3-}) at the flowering and senescent stages, compared with the non-coir dust free substrate. The lowest PO_4^{3-} concentration was found in both leachate solution of the 50 and 75% coir dust treatments when plants reached floral senescent (Fig. 5B).

All coir dust amending did not affect any leaching potassium (K) of potted marigolds in each growth stage, except 25 and 75% coir dust portion had the least K leachate concentration after pinching (Fig. 5C).

Correlation between Total Leachated Volume and Nutrient Leachate Concentration

During an experimental period of potted marigolds (stages 1 to 5), positive correlations were found between total leachate volume and total leaching phosphate (PO_4^{3-}) concentration (R = 0.98), total potassium (K) concentration (R = 0.68) and leaching phosphate concentration at pinching (R = 0.59). However, the negative correlation was only found between total leachate volume and leaching phosphate concentration at flower senescent (R = -0.79) (Table 3).

Discussion

Due to rising costs and uncertain future availability of peat moss, there is a need in the potted ornamental and floriculture industry for alternative components in commercial potting substrates (Bachman and Metzger, 2008). One material gaining interest in agricultural is coconut coir dust, usually used as a growing medium for numerous ornamental plant production (Meerow, 1997; Valdez-Aguilar et al., 2009). Many previous studies have been slightly focused on its suitable physical and chemical properties, but little information is available on the effects of coir dust to water use and nutrient leaching in potted plants.

In this experiment, coconut coir dust amended in substrate media partially affected all water regimes parameters of the potted *T. erecta* 'Antigua Yellow', improving the physical

Table 3. Correlation between total leachate volumes and nutrient leachate concentration in runoff solution of potted marigolds when grown under different coconut coir dust amended in substrate media. The linear regression and correlation coefficients *R* are presented at $p > 0.05$. Data was calculated from means at each stage.

Parameter[z] (X axis vs. Y axis)	n	Regression equation	*R*	*p* - value	Significance $p < 0.05$
X axis					
Total leachate vol.					
Y axis					
Total NO_3^- conc.	20	y = -0.46x + 403	-0.39	0.2142	ns
Total PO_4^{3-} conc.	20	y = 2.52x – 94.78	0.98	0.0000	*
Total K conc.	20	y = 0.35x + 1436	0.68	0.0147	*
PO_4^{3-} conc. stage[y] 1	20	y = 0.76x + 45.97	0.59	0.0488	*
PO_4^{3-} conc. stage 2	20	y =-0.02x + 26.59	-0.06	0.1601	ns
PO_4^{3-} conc. stage 3	20	y = 0.12x + 80.58	0.47	0.4322	ns
PO_4^{3-} conc. stage 4	20	y = 0.74x + 8.42	0.24	0.1640	ns
PO_4^{3-} conc. stage 5	20	y = -0.462x + 108.2	-0.79	0.0176	*

[z]Vol., volume; vs., versus; conc., concentration; NO_3^-, nitrate; PO_4^{3-}, phosphate; K, potassium; ns, not significant.
[y]Stages 1, pinching (27 DAS); stage 2, axillary bud growing (30 DAS); stage 3, vegetative growth (37 DAS); stage 4, flowering (48 DAS); and stage 5, ceased flower (56 DAS).

properties of mixed media, reducing the total leaching fraction (%) and some nutrient leachate in the run off solution. The plant growth parameters had diverse responses amongst the comparisons of each different coconut coir dust portions, and flowering yield is likely to be promoted.

It has been proposed that the uses of coconut coir dust as the container medium shows a comparative higher ability to hold water (Abad et al., 2005) and the reverse for aeration properties of sphagnum peat (Abad et al., 2005; Evans et al., 1996). In this experiment, the increasing of coir dust portions (0-75%, v/v) was seen to substantially improve some media physical properties by increasing the total porosity (%) and the water fill pore (%), and this led to losses of its estimated bulk density, because the coir dust was evaluated as a light-weight (bulk density) material and had high total porosity by volume (Abad et al., 2005).

There was a similar water volume applied to each plant during the growth stage (1.9 L), but the leaching fraction (%) was slightly dependent on the coir dust portion in substrate (Table 2), because the run off solution volume was different (data not shown). The 50% coir dust portion gave the greatest leaching fraction (38.16%) and sufficient to regulate leachate EC (2.15 $dS \cdot m^{-1}$). Our result was consistent with Bañón et al. (2009), who also recorded the lower leaching fraction with an insufficient EC from retained water in coconut base media, while the opposite occurred in peat base. However, previous studies reported that marigold 'First Lady', bedding plant marigolds 'French Vanilla' 'Flagstaff', and 'Yellow Climax' exhibited abnormal growth and toxicity symptoms when irrigated with water EC (ECw) was higher than 8 $dS \cdot m^{-1}$ (Huang and Cox, 1988; Valdez-Aguilar et al., 2009). Generally, coconut coir dust had been reported to contain high saline ion, especially chloride and sodium (Abad et al., 2002), which might cause problems when using as substrate for growing certain salt sensitive ornamental plant. In this experiment, the EC value was varied in the range between 1.85 to 2.15 $dS \cdot m^{-1}$ in all treatments (Table 2) which was below marigold growth and toxicity saline water level (Valdez-Aguilar et al., 2009). Although we could not evaluate saline ions of tap water before watering, less 70 ppm of chloride ion concentration has been previously reported by Namwichai and Nam-moonnoi (1996) and those amount of chloride ion is generally safe for watering all plants without damaging (Bauder et al., 2011).

The leaf area was related to canopy transpiration and associated with the plant water consumption, but the total leaf area of potted marigolds was not altered by the treatment (Table 2).

The daily ET of potted marigolds was slightly increased when plants were developed in the first two growing stages (pinching and axillary bud growth) and increased again when they reached the flowering stage. This indicates the fast growing in the reproductive phase, when plants generally require high amounts of water to be applied. Thereafter, the highest daily ET occurred in the ceased flower stage (Fig. 2A). In addition, several reports indicated the reduction of ET/d during the flowering and senescence phase, which might be caused by less active physiological function in plants (Lorenzo et al., 1998). All of daily ET (mL/pot) results were related with some dependence on the changes of daily temperature, since the sharp decrease in temperature at 2-3 beginning dates did not reasonably induce the lowest ET (Fig. 2A).

For the duration of the experiment, the 50% coir dust

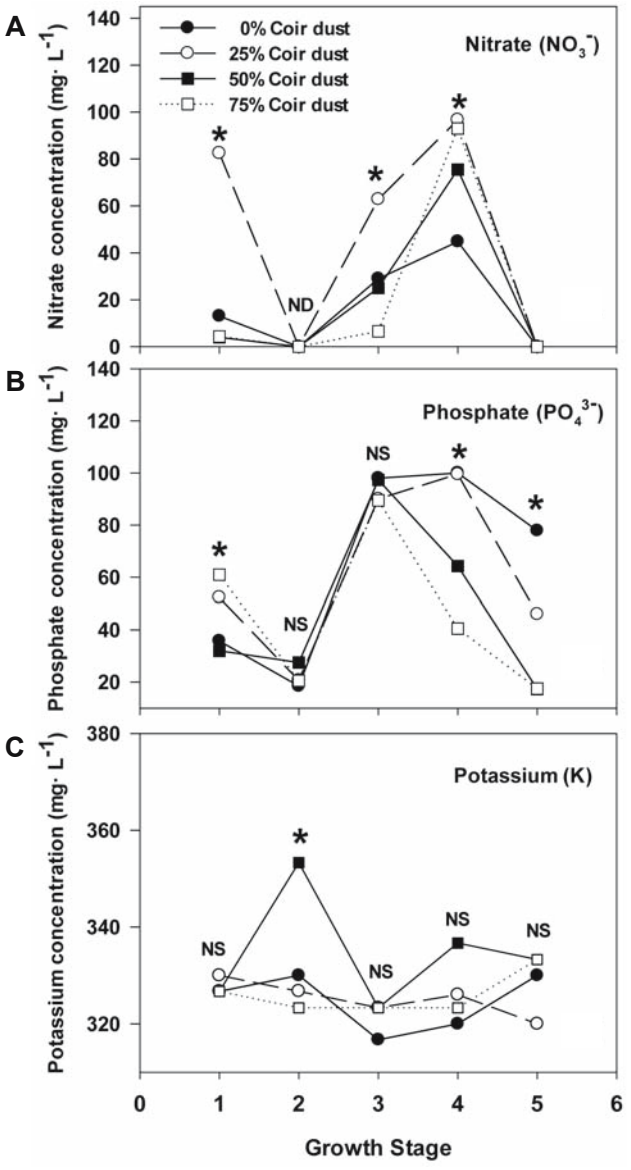


Fig. 5. Nitrate (A), phosphate (B) and potassium (C) in leaching solution of amended substrate media with coconut coir dust (0, 25, 50 and 75%) in potted marigolds (*Tagetes erecta* 'Antigua Yellow') at 5 growth stages: 1, pinching (27 DAS); 2, axillary bud growing (30 DAS); 3, vegetative growth (37 DAS); 4, flowering (48 DAS); and 5, ceased flower (56 DAS). NS = no significant, * = significant at $p < 0.05$, ND = no detection (concentration less than 3 mg·L^{-1}).

amended treatment comparably showed the lowest accumulated ET (L/pot) among the treatments (Fig. 2B). Similar results were represented in crop evapotranspiration; ETc at flowering and senescence stage (Fig. 3A). Regarding the non-significant total leaf area of potted marigold and the lowest ET in 50% coir dust, it might partially cause a reduction to the transpiration rate per leaf area unit per day and gave the lowest one in the 50% coir dust treatment at both growing periods. However, the maximum of water use efficiency, WUE (mg DW·mL^{-1}), occurred only in the 50% coir dust amended at vegetative growth stage. This finding might be explained by the highest sharply increase of difference in the initial and final aboveground dry weight from stage 2 to stage 3 (data not shown) and the lowest water consumption at stage 3 occurs only in the 50% coir dust treatment. A concern, when prior marigolds usually become flowering, is that the greatest aboveground dry weight with large canopy exhibit on less water applied (Khumdee, 2003). Crop co-efficient; Kc, was the ratio between crop evapotranspiration (ETc) and reference evapotranspiration (ETo). Both parameters were measured by a water balance using drainage lysimeters in similar climatic conditions (Fernandez et al., 2000). In *T. erecta* cv. 'Yellow Galore', Kc was lowest at the pinching stage (1.6) and gradually increased to the highest peak of Kc value account 6.2 at the post blooming stage, and this pattern is similar with the increasing of canopy size during growth stage (Khumdee, 2003). In this experiment, Kc values in the early stages (pinching and axillary bud growth stage) were higher than in the vegetative growth stage. This occurrence might be due to the higher media surface evaporation than non-covering pot canopy plant transpiration. Kc value was the lowest (0.38) at vegetative growth and continued to the highest (3.86) at senescence. While the 50% coir dust ratio was seen to be the best result for reducing Kc from vegetative growth, reproductive growth continued until the end of senescence (Fig. 4).

All coir dust amended in substrate media showed fluctuating results in reducing nutrient leaching from drainage solution in each growth stage. Nevertheless, the 75% coir dust treatment gave the lowest leaching nitrate (NO_3^-) only at vegetative growth stage. Similar coir dust portion shows the best result for reducing leaching phosphate (PO_4^{3+}) at flowering and senescence stages. However, the coir dust portion did not alter any leaching potassium (K). The current result might be explained with a study by Tyler et al. (1996), who reported the leachate N and P responded with the reduction in irrigation volume, K loss only decreased by reducing fertilizer rate. The present finding of declined P loss via the amending of coir dust portions also confirms the closely relation with effluent by the significantly positive correlations between total leachate volume and total leaching phosphate concentration (R = 0.98) (Table 3). This result might indicate that, reducing water loss by improving the media physical properties seem to induce less leaching phosphate solution.

These experimental conditions, suggest that effective strategies to reduce nutrient losses, increase water use efficiency, and promote flowering yield might partially be amended in substrate media with both 50 and 75% coconut coir dust for the production of potted marigolds. In order to avoid the problem of excess salt and high EC affecting plant growth, re-washing coconut coir dust material with pure water in many times should be done before use them as substrate

media amendment.

Acknowledgements: This research was supported by New Researcher Scholar Program 2012 through Khon Kaen University. Acknowledgement is extended to the Faculty of Agriculture for providing financial support for manuscript preparation activities.

Literature Cited

Abad, M., F. Fornes, C. Carrión, and V. Noguera. 2005. Physical properties of various coconut coir dusts compared to peat. HortScience 40:2138-2144.

Abad, M., P. Noguera, R. Puchades, A. Maquieira, and V. Noguera. 2002. Physico-chemical and chemical properties of some coconut coir dusts for use as a peat substitute for containerised ornamental plants. Bioresource Technol. 82:241-245.

Argo, W. and J. Biernabaum. 1994. Irrigation requirements root-medium pH and nutrient concentrations of Easter lilies grown in five peat-based media with and without an evaporation barrier. J. Amer. Soc. Hort. Sci. 119:1151-1156.

Awang, Y. and M. Ismail. 1997. The growth and flowering of some annual ornamentals on the coconut dust. Acta Hort. 450:31-38.

Bachman, G.R. and J.D. Metzger. 2008. Growth of bedding plants in commercial potting substrate amended with vermicompost. Bioresource Technol. 99:3155-3161.

Bañón, S., J. Miralles, A. Navarro, and M.J. Sánchez-Blanco. 2009. Influence of paclobutrazol and substrate on daily evapotranspiration of potted geranium. Sci. Hort. 122:572-578.

Bauder, T.A., R.M. Waskom, P.L. Sutherland, and J.G. Davis. 2011. Irrigation water quality criteria. Colorado State Extension University. http://www.ext.colostate.edu/pubs/crops/00506.html.

Doorenbos, J. and W.O. Pruitt. 1992. Calculation of crop water requirement. In: Crop water requirement. FAO, The United Nation, Rome, Italy.

Erwan, M.R.I., H.M. Saud, R. Othman, S.H. Habib, H. Kausar, and L. Naher. 2013. Effect of oil palm frond compost amended coconut coir dust soilless growing media on growth and yield of cauliflower. Int. J. Agric. Biol. 15:731-736.

Evans, M.R., S. Konduru, and R.H. Stamps. 1996. Source variation in physical and chemical properties of coconut coir dust. HortScience 31:965-967.

Fernandez, M.D., M. Gallardo, S. Bonachela, F. Orgez, and E. Fereres. 2000. Crop coefficients of pepper crop grown in plastic greenhouses in Almeria, Spain. Acta Hort. 537:461-469.

Huang, Z.T. and D.A. Cox. 1988. Salinity effects on annual bedding plants in a peat-perlite medium and solution culture. J. Plant Nutri.11:145-159.

Jaleel, C.A., R. Gopi, B. Sankar, M. Gomathinayagam, and R. Panneerselvam. 2008. Differential responses in water use efficiency in two varieties of *Catharanthus roseus* under drought stress. C.R. Biologies 331:42-47.

Khumdee, W. 2003. Water use of potted marigold at different growth stages. B.S. Department of Horticulture, Kasetsart University, Bangkok, Thailand.

Klock-Moore, K.A. and T.K. Broschat. 2001. Effect of four growing substrates on growth of ornamental plants in two irrigation systems. HortTechnology 11:456-460.

Lin, Y.P., E.J. Holcomb, and J.P. Lynch. 1996. Marigold growth and phosphorus leaching in a soilless medium amended with phosphorus-charged alumina. HortScience 31:94-98.

Lorenzo, P., E. Medrano, and M.C. Sánchez-Guerrero. 1998. Greenhouse crop transpiration: An implement to soilless irrigation management. Acta Hort. 458:113-122.

Marigold Asia. 2013. The history of marigold. http://www.marigoldasia.com.

Merck. 2012a. Instruction for use MQuant nitrate test. http://www.merckmillipore.com/TH/en/product/Nitrate-Test,MDA_CHEM-110020#anchor_PI.

Merck. 2012b. Instruction for use MQuant phosphate test. http://www.merckmillipore.com/TH/en/product/Phosphate-Test,MDA_CHEM-110428#anchor_PI.

Merck. 2012c. Instruction for use MQuant potassium test. http://www.merckmillipore.com/TH/en/product/Potassium-Test,MDA_CHEM-117985#anchor_PI.

Meerow, A.W. 1997. Coir dust, a viable alternative to peat moss. Greenhouse Product News January:17-21.

Namwichai, N. and S. Nam-moonnoi. 1996. The determinations of chemical properties of local tap water in Ampher Mueng Khon Kaen and Khon Kaen University. B.S. Department of Chemistry, Khon Kaen University, Khon Kaen, Thailand.

Nelson, P.V. 1991. Greenhouse operation and management. 4th ed. Prentice-Hall, Englewood Cliffs, NJ, USA.

Pannkuk, T.R., J.A. Aitkenhead-Peterson, K. Steinke, J.C. Thomas, D.R. Chalmers, and R.H. White. 2011. Carbon, nitrogen, and orthophosphate leaching from soil under single- and mixed-species landscapes. HortScience 46:1533-1539.

Sangwan, P., V.K. Garg, and C.P. Kaushik. 2010. Growth and yield response of marigold to potting media containing vermicompost produced from different wastes. Environmentalist 30:123-130.

Sittinam, T. 2007. Effect of substrate and fertilizers on germination and growth of some flowering pot plant. M.S. (Agriculture) Thesis, Department of Horticulture, Kasetsart University, Thailand.

Spomer, L.A. 1979. Three simple demonstrations of the physical effects of soil amendment. HortScience 14:75-77.

Tyler, H.H., S.L. Warren, and T.E. Bilderback. 1996. Reduced leaching fractions improve irrigation use efficiency and nutrient efficacy. Environ. Hort. 14:199-204.

United States Department of Agriculture (USDA). 2013. New release: Selected North Carolina floriculture crop values up. http://www.ncagr.gov/stats/release/Floriculture.pdf.

Valdez-Aguilar, L.A., C.M. Grieve, and J. Poss. 2009. Salinity and alkaline pH in irrigation water affect marigold plants: I. Growth and shoot dry weight partitioning. HortScience 44:1719-1725.

Wilson, S.B. and P.J. Stoffella. 2003. Compose amended media and irrigation system influence containerized perennial salvia. J. Amer. Soc. Hort. Sci. 128:260-268.

frontiers in
PLANT SCIENCE

ORIGINAL RESEARCH ARTICLE
published: 06 January 2015
doi: 10.3389/fpls.2014.00753

A simple framework to analyze water constraints on seasonal transpiration in rubber tree (*Hevea brasiliensis*) plantations

Jessada Sopharat[1]*, Frederic Gay[2,3], Philippe Thaler[2,3], Sayan Sdoodee[1], Supat Isarangkool Na Ayutthaya[4], Charlchai Tanavud[5], Claude Hammecker[6] and Frederic C. Do[6]

[1] *Department of Plant Science, Faculty of Natural Resources, Prince of Songkla University, Songkhla, Thailand*
[2] *UMR Eco&Sols, French Agricultural Research Centre for International Development (CIRAD), Montpellier, France*
[3] *Hevea Research Platform in Partnership, DORAS Centre, Kasetsart University, Bangkok, Thailand*
[4] *Department of Plant Science and Agricultural Resources, Faculty of Agriculture, Khon Kaen University, Khon Kaen, Thailand*
[5] *Department of Earth Science, Faculty of Natural Resources, Prince of Songkla University, Songkhla, Thailand*
[6] *UMR Eco&Sols, Institut de Recherche pour le Développement, Montpellier, France*

Edited by:
Laurent Deluc, Oregon State University, USA

Reviewed by:
Jyostna Devi Mura, North Carolina State University, USA
Claudio Lovisolo, University of Turin, Italy

****Correspondence:***
Jessada Sopharat, Department of Plant Science, Faculty of Natural Resources, Prince of Songkla University, Hat Yai, Songkhla 90112, Thailand
e-mail: jessadaso@gmail.com

Climate change and fast extension in climatically suboptimal areas threaten the sustainability of rubber tree cultivation. A simple framework based on reduction factors of potential transpiration was tested to evaluate the water constraints on seasonal transpiration in tropical sub-humid climates, according pedoclimatic conditions. We selected a representative, mature stand in a drought-prone area. Tree transpiration, evaporative demand and soil water availability were measured every day over 15 months. The results showed that basic relationships with evaporative demand, leaf area index and soil water availability were globally supported. However, the implementation of a regulation of transpiration at high evaporative demand whatever soil water availability was necessary to avoid large overestimates of transpiration. The details of regulation were confirmed by the analysis of canopy conductance response to vapor pressure deficit. The final objective of providing hierarchy between the main regulation factors of seasonal and annual transpiration was achieved. In the tested environmental conditions, the impact of atmospheric drought appeared larger importance than soil drought contrary to expectations. Our results support the interest in simple models to provide a first diagnosis of water constraints on transpiration with limited data, and to help decision making toward more sustainable rubber plantations.

Keywords: potential transpiration model, drought, high evaporative demand, canopy phenology, relative extractable soil water

INTRODUCTION

The rubber tree (*Hevea brasiliensis*) is a major tree crop in Southeast Asia. Globally, it covers 9.82 million hectares mainly exploited by smallholders (UNCTAD, 2013). The tree is a native from the rainforests of the equatorial region of the Amazon basin (Priyadarshan et al., 2005). Traditionally, it has been cultivated in the equatorial belt and humid zones with a tropical and monsoonal climate (Raj et al., 2005). Currently, Thailand is the world's top producer of natural rubber. The plantations are mainly located where conditions are optimal in southern Thailand. However, in the last 30 years, the rubber plantations have largely expanded into climatically sub-optimal areas in north and northeast Thailand. The dynamic of land use is similar to that in other rubber-producing countries, with expansions also recorded in northeast India, the highlands and coastal areas of Vietnam, southern China, and the southern plateau of Brazil (Priyadarshan et al., 2005). In such areas, rubber can be constrained by drought, low temperature and high altitude or conversely by periodic heavy rainfall. Moreover, with climate change, higher frequencies of extreme events (flooding, drought) in the rainy season and an increase in temperature and evaporative demand in the dry season are expected in both traditional and new areas (Masaki et al., 2011). In addition, despite the large extension of land covered by rubber plantation, little is known of its environmental impacts and particularly about carbon and water balances (Guardiola-Claramonte et al., 2010; Kumagai et al., 2013). To address the sustainability of rubber plantations and to choose appropriate plant material and management practices, it is necessary to forecast rubber tree behavior on a large scale and over long periods of time. Hence the availability of simple models with limited data to analyze water constraints on tree transpiration and consequences on growth, production and soil water balance is a key issue (Guardiola-Claramonte et al., 2010; Boithias et al., 2012; Carr, 2012).

Our final objective is to evaluate, on an annual basis, the relative contributions of soil water shortage and atmospheric drought to the regulation of maximal transpiration in rubber tree stands under various pedoclimatic conditions. The use of a robust and

simple model based on reduction factors of potential transpiration simulation appeared as a reasonable first approach to schematically separate the main controls. Granier et al. (1999) proposed such a model of daily water balance called BILJOU to evaluate water constraints in forest stands. It has been successfully used in temperate and tropical humid forests (Granier et al., 1999; Wagner et al., 2011). Transpiration models based on canopy conductance regulation have been also assessed and used (Jarvis, 1976; Stewart, 1988; Granier et al., 2000, 2007). However, they require an hourly step, more parameters and input data. As a first approach we chose to use the framework of BILJOU99 (Granier et al., 1999). The model assumes, under non-limiting soil water, a linear response of maximal transpiration (T_{max}) vs. potential evapotranspiration (*PET*) for a leaf area index (*LAI*) inferior to 6, the slope being the ratio "*rm*" depending on the *LAI*. The model assumes that under a soil water shortage, *rm* decreases linearly below a threshold of relative extractable water (*REW*) of 0.4. Like many models, it does not consider direct constraint due to atmospheric drought (Boote et al., 2013). However, Isarangkool Na Ayutthaya et al. (2011) have shown that transpiration in mature rubber trees was strongly regulated above a threshold of evaporative demand, whatever the soil water availability. Such a regulation was related to an isohydric behavior expressed by stability of minimum leaf water potential and maximum whole-tree hydraulic conductance. The idea was to add a reduction factor above a critical climatic demand.

To test our modeling approach based on BILJOU99 framework, we selected a representative mature stand where trees faced the full range of soil and atmospheric drought conditions over a complete annual cycle. Tree transpiration, the evaporative demand and the soil water availability were measured every day over 15 months. The first objective was to test simplified controls of transpiration through evaporative demand, leaf area index and relative extractable water. We hypothesized that the basic relationships hold, except when the evaporative demand becomes too high. The second objective was to test an evolution of the model including sensitivity to atmospheric drought. We assumed that it would provide a reasonable indication of the trend in seasonal transpiration. The third objective was to assess by modeling the hierarchy between soil water and atmospheric constraints on transpiration on an annual basis. We assumed a predominant control by soil drought according to common thinking.

MATERIALS AND METHOD

STUDY SITE

The plantation was located at Baan Sila (N15° 16′ 23″ E103° 04′ 51.3″), Khu-Muang, Buri Ram province in northeast Thailand. The experiments were conducted in a monoclonal plot (clone RRIM 600), planted at 2.5 × 7.0 m spacing (571 trees ha^{-1}). The trees were 11 years old and had been tapped for 4 years for latex harvesting. The soil is deep with a loamy sand texture. The mean contents of clay, loam and organic matter varied from 9.9, 24.2, to 0.78% in the surface layer (0–0.2 m) to 20.2, 23.6, and 0.34% at a depth of 1.5 m, respectively. In this non-traditional rubber tree plantation area, the environmental conditions are water limiting for *H. brasiliensis*. The dry season lasts 6 months, from November to April, and average annual rainfall is 1176 mm. Canopy yellowing and defoliation occurred between December and March. In a sample of 237 trees, canopy fullness was assessed every 2 weeks for each tree according to seven categories of the percentage of green leaves (100, 90, 75, 50, 25, 10, and 0%). When the defoliation was almost complete, the maximum leaf area index (LAI_{max}) was estimated from leaves collected in nine 1 m² litter traps. A schematic change in the *LAI* over the year was deduced from observations of canopy fullness and litter fall measurements.

CLIMATIC MEASUREMENTS

The local microclimate was monitored automatically in an open field at a distance of 50 m from any trees. An automatic weather station (Minimet automatic weather station, Skye Instruments Ltd, Llandrindod Wells, UK) recorded half-hourly values of air temperature, relative humidity, incoming short wave radiation, wind speed and rainfall. The reference evapotranspiration was calculated according to the FAO 56 formula in Allen et al. (1998).

SOIL WATER CONTENT MEASUREMENTS

Volumetric soil water content (θ) was measured with a neutron probe (3322, Troxler, Research Triangle Park, NC, USA) calibrated for the experimental soil with separate calibrations for the upper (0–0.2 m) and lower (below 0.2 m) layers. Twelve 2 m-long tubes were set up in pairs; in each pair, one tube was located in the planting line between two trees, and the other in the middle of the inter-row. Measurements were made every 0.2 m, from a depth of 0.1 to 1.5 m every 2 weeks. Based on observed fluctuations in soil water, the soil profile was separated into two layers: topsoil (0–0.6 m) and subsoil (0.6–1.6 m). The average field capacity and permanent wilting points were measured as 0.21 and 0.07 m^3 m^{-3} for the topsoil, and 0.25 and 0.10 m^3 m^{-3} for the subsoil, respectively (Isarangkool Na Ayutthaya et al., 2010). Additionally, θ was measured continuously with a capacitance probe (EnvironSCAN System, Sentek Sensor Technologies, Adelaide, SA, Australia). The vertical probe included nine sensors located every 0.2 m at the same level as the neutron probe measurements. For each sensor, θ was estimated from cross-calibration with the neutron probe measurements over the whole seasonal range. Relative extractable water was calculated for each layer according to Granier et al. (1999):

$$REW_i = (W - W_m)/(W_f - W_m) \quad (1)$$

where REW_i is the relative extractable water in each soil layer *i*, W_m is the minimum soil water content, W_f is the soil water content at field capacity and W is the actual soil water content. To calculate the total *REW* for the sensitive root zone, REW_i was weighted by the percentage of fine root length within each layer. As the soil profiles showed low soil water availability and little change in the subsoil (**Figure 1B**), for modeling purpose the total *REW* was calculated for the top soil (0–0.6 m). In this site, the top soil contained 83% of the fine root length accumulated down to 1.6 m (Gonkhamdee et al., 2009). The fraction of fine root length used for weighting the *REW* in the top soil was 0.63, 0.32, and 0.05 for the layers 0–0.2, 0.2–0.4, and 0.4–0.6 m, respectively.

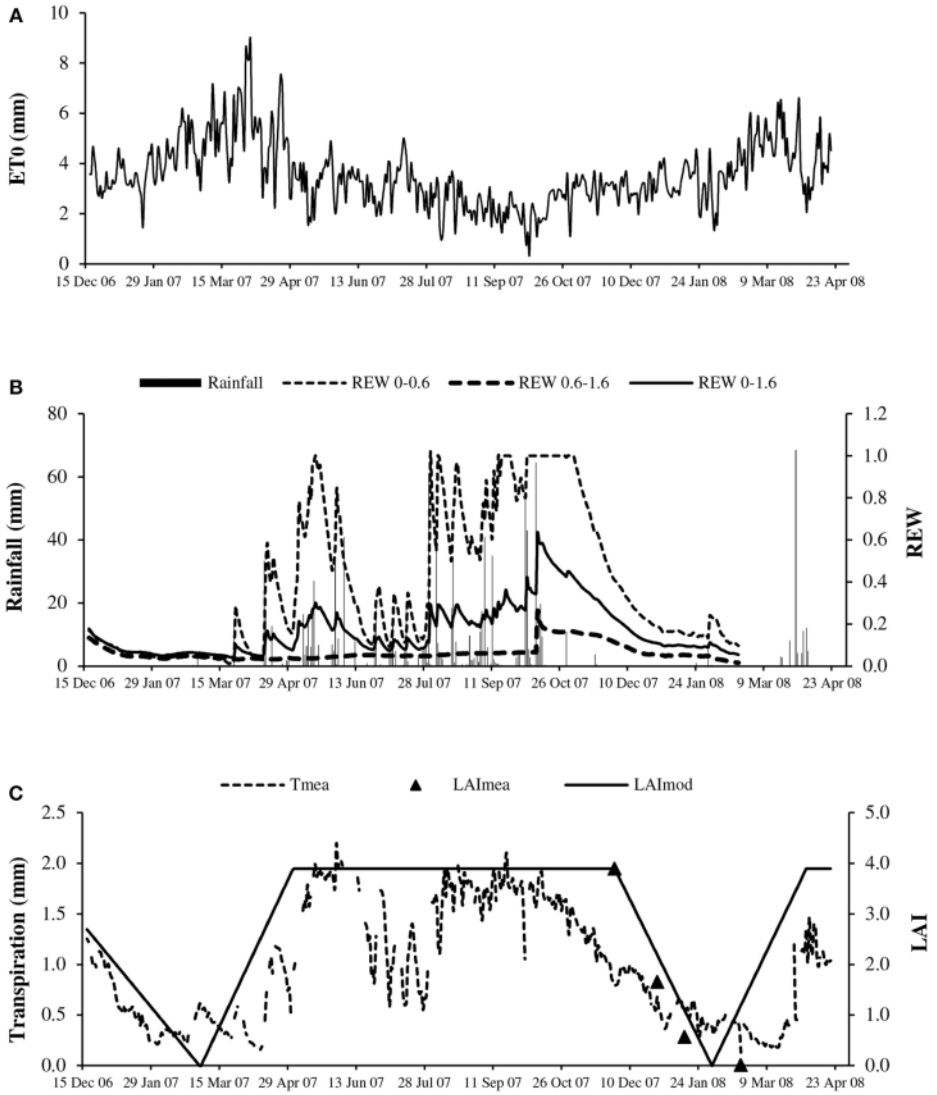


FIGURE 1 | Seasonal course of: (A) reference evapotranspiration (*ET0*); (B) rainfall (solid bar) and relative extractable water of bulk soil (*REW*) for layers 0–0.6 m (*REW* 0–0.6), 0.6–1.6 m (*REW* 0.6–1.6) and 0–1.6 m (*REW* 0–1.6); and (C) measured transpiration (T_{mea}, dotted line) and leaf area index estimated from litterfall (LAI_{mea}, triangles) and schematic shape (LAI_{mod}, solid line).

TRANSPIRATION MEASUREMENT

The xylem sap flow density was measured using the transient thermal dissipation method (TTD, Isarangkool Na Ayutthaya et al., 2010). The TTD method is based on using the same Granier probe design and heating power but uses a cyclic schedule of heating and cooling to assess a transient thermal index over a 10-min rise in temperature. The hourly sap flux density (J_s; kg m^{-2} h^{-1}) was calculated according to the non-species-specific calibration assessed by Isarangkool Na Ayutthaya et al. (2010):

$$J_s = 12.95 \times K_a \times 10^2 \quad (2)$$

where K_a is the transient thermal index. A temperature signal (ΔT_a) was defined as

$$\Delta T_a = \Delta T_{on} - \Delta T_{off} \quad (3)$$

where ΔT_{on} is the temperature difference reached at the end of the 10-min heating period and ΔT_{off} is the temperature difference before heating. To measure J_s every half hour with a heating period of 10 min, a cycle of 10 min heating and 20 min cooling was applied and the temperature signals were recorded every 10 min. ΔT_{off} wasinterpolated at the time of ΔT_{on} from ΔT_{off} surrounding measurements. The transient thermal index was calculated as:

$$K_a = (\Delta T_{0a} - \Delta T_{ua})/\Delta T_{ua} \quad (4)$$

where ΔT_{0a} is the maximum temperature difference obtained under zero flow conditions and ΔT_{ua} is the measured signal at a given J_s. the zero flux signal was determined every night assuming that sap flow was negligible at the end of the night. This

assumption was strongly supported by slight change of daily ΔT_{0a} over the study period and minimum nocturnal *VPD* always lower than 0.3 kPa (Donovan et al., 2001). The probes were inserted into the trunks at a height of 1.8 m above the soil. At this height, average sapwood area was estimated to be 1.97×10^{-2} m^2. After removal of the bark, the 2-cm-long probes were inserted to a depth of 2.5 cm into the sapwood, in such a way that the whole probe was fully inside the conductive sapwood. Three probes were inserted into each trunk to account for circumferential variability. The trunk area containing the probes was protected from direct solar radiation and rainfall by a deflector. Probes were connected to a data logger (CR10X, Campbell Scientific, Leicester, UK). Hourly sap flow density (J_s), measured in the outermost ring of the sapwood, was accumulated over 24 h to calculate daily J_s (J_{out_day} expressed in kg m^{-2} d^{-1}). To account for radial variation in the sap flux density in the deep sapwood, a reduction coefficient of 0.874 was applied to the J_s measured in the outermost ring of conducting xylem (Isarangkool Na Ayutthaya et al., 2010). Finally, neglecting tree water storage, transpiration (T; mm d^{-1}) was estimated according to the equation:

$$T = 0.874 \times 10^{-2} \times J_{out_day} \times (\text{sapwood area/tree spacing area}) \quad (5)$$

CANOPY CONDUCTANCE CALCULATION

The canopy conductance (G_c; mm s^{-1}) was calculated by inverting an approximate of the Penman-Monteith equation. The approximation assumes that tree stand transpiration is well coupled to the atmosphere, i.e., decoupling coefficient (Ω) close to 0 (Jarvis and McNaughton, 1986; Phillips and Oren, 1998):

$$G_c = \frac{\gamma \cdot \lambda \cdot T}{C_p \cdot \rho \cdot VPD} \quad (6)$$

where γ is the psychrometric constant (Pa K^{-1}), γ is the latent heat of water vaporization (J kg^{-1}), T is transpiration, C_p is the specific heat of dry air at constant pressure (J kg^{-1} K^{-1}), ρ is the atmospheric density (kg m^{-3}) and *VPD* is the air vapor pressure deficit (kPa). G_c was calculated at midday (G_{c_md}) from the maximum vapor pressure deficit (VPD_{max}) and the daily maximum transpiration estimated from the sap flow (T_{max}; mm s^{-1}).

MODELING

Basic relationships

The main relationships of BILJOU99 framework have been described in the introduction and more details are provided in Granier et al. (1999). The model inputs are daily data of leaf area index, rainfall and Penman potential evapotranspiration (*PET*). Instead of *PET* we used the FAO reference evapotranspiration *ET0* (Allen et al., 1998) which is currently available in world weather networks. The model can simulate the soil water balance by daily tipping buckets if runoff is negligible, which was not the case here. The present study was focused on transpiration controls and for the sake of accuracy we used only measured soil water availability.

Details of calculation

Potential, climatic or maximal transpiration was first calculated from the following equation:

$$T_{max} = rm * ET0 \quad (7)$$

where *rm* depends on LAI_{max};

Second, T_{max} could be decreased according to the *LAI* pattern by the following reduction coefficient:

$$rLAI = (LAI / LAI_{max}) \quad (8)$$

The effect of soil water shortage was simulated by the calculation of a reduction coefficient (*rREWc*) as:

$$rREWc = rLAI \quad if\ REW > REWc \quad (9)$$
$$rREWc = (rLAI/REWc) * REW \quad if\ REW \leq REWc$$

where *REWc* is the critical value of relative soil water content.

Hence the transpiration was calculated according to the following formula:

$$T_{mod} = rREWc * T_{max} \quad (10)$$

The expected saturation of transpiration at high evaporative demand was introduced in the BILJOU99 framework by applying a reduction coefficient above a critical value of *ET0*:

$$T_{mod_ET0c} = min(rREWc; rET0c) * T_{max} \quad (11)$$

For simplicity of writing we could have included the negative effect of high *ET0* in equation [7]. But we have preferred to separate the effects because of functional reasons. Equation [7] represents a general climatic driving effect (positive) on transpiration whatever plant species. While *rET0c* in equation [11] expresses a negative effect which varies according species and which is attributed to plant hydraulic limitations (Oren and Pataki, 2001; Bush et al., 2008; Isarangkool Na Ayutthaya et al., 2011; Ocheltree et al., 2014).

Diagnosis of hierarchy between water constraints

The approach was to use the calibrated framework to simulate independently or in combination the factors that control the regulation of transpiration on an annual basis and to separate the rainy season and dry season. The regulations of transpiration was expressed as the ratio between the cumulated potential transpiration, driven by evaporative demand and stand characteristics under full canopy conditions (LAI_{max}), and the cumulated actual transpiration possibly reduced by defoliation, soil water availability or sensitivity to air dryness. Such a calculation assumes that reduction factors act independently which is certainly not true in the details. The annual cycle of transpiration was considered from January 1 to December 31, and the rainy season from May 1 to October 31. The few gaps in the daily transpiration were interpolated from *ET0* using an average ratio *T/ET0* measured on surrounding data (at least 4 days).

DATA ANALYSIS

Statistics were performed using the XLSTAT software (Addinsoft, Paris, France). The agreement between measured and simulated data was quantified by using the coefficient of determination (R^2), root mean square error (*RMSE*) and relative root mean square error (*RRMSE*). Absolute and relative root mean square errors were calculated according to the following formulas:

$$RMSE = \sqrt{\frac{\sum_{i=1}^{n}(x_{mea,i} - x_{\mathrm{mod,i}})^2}{n}},$$

$$RRMSE = \sqrt{\frac{\sum_{i=1}^{n}\left(x_{mea,i} - x_{\mathrm{mod,i}}/x_{mea,i}\right)^2}{n}} \quad (12)$$

where $x_{mea,i}$ is the measured value, $x_{\mathrm{mod,i}}$ is the simulated value at place *i* and *n* is the number of values.

RESULTS

SEASONAL VARIATIONS OF ENVIRONMENTAL WATER CONSTRAINTS, *LAI*, AND TRANSPIRATION

The evaporative demand as expressed by *ET0* largely fluctuated between 1 and 9 mm d^{-1} with a cumulative value of 1247 mm $year^{-1}$ (**Figure 1A**), 23% above the cumulative rainfall (965 mm) in 2007. *ET0* values were particularly high during the 6 months of the dry season, from 3 mm d^{-1} in November up to 9 mm d^{-1} in March, corresponding to a *VPD* value above 1.0 kPa. The evaporative demand remained relatively high in the first part of the rainy season (from May to July) and decreased markedly in August, September and October, with *ET0* and *VPD* values below 2.0 mm d^{-1} and 0.7 kPa, respectively.

The water availability of the bulk soil or *REW* logically followed the rain occurrence (**Figure 1B**), with values close to 1.0 at the start of the rainy season in the topsoil (0–0.6 m). The availability decreased sharply to 0.2 in July, in the middle of the rainy season. The *REW* again reached high values (above 0.5) from August to October. *REW* values above 1 at the end of October suggested temporary water logging in the topsoil which was confirmed by observations. The *REW* quickly decreased in the dry season, reaching 0.2 in January. In the deep soil (0.6–1.6 m), the *REW* value indicated low water availability with little change over the year (maximum 0.26).

As represented by the schematic change in the *LAI* (**Figure 1C**), leaf shedding occurred in January and February, immediately followed by leaf flushing, with the latter occurring when the evaporative demand was the highest. The maximum *LAI* deduced from litterfall measurements averaged 3.9 at the end of 2007 ($n = 9$, $SD = 0.7$). The period with full canopy included approximately the period of highest soil water availability and lowest evaporative demand.

The maximum transpirations estimated by sap flow measurements (T_{mea}) were steady (approximately 2.0 mm d^{-1}) throughout the period with full canopy (**Figure 1C**). The intermittent decreases evident in June and July related to the evolution of the *REW* in the topsoil (**Figure 1B**). The lowest transpiration corresponded to the time of leaf shed. However, it never reached zero values despite almost complete defoliation. However, the sap flow measurement using the TTD method has low accuracy at very low flow rates (Isarangkool Na Ayutthaya et al., 2010). The minimum recorded transpiration was 0.1 mm d^{-1} on April 11, 2007 and the maximum value was 2.2 mm d^{-1} on May 31, 2007.

TRANSPIRATION vs. *ET0*, *REW*, AND *LAI*

ET0

Under conditions of full canopy and non-limiting soil water (*REW*> 0.5), transpiration plotted vs. *ET0* showed a linear response at low evaporative demand but it exhibited a pseudo-plateau above approximately 2.3 mm d^{-1} (**Figure 2A**). The average slope of the linear section crossing the origin was estimated as 0.9 (± 0.052). Such a slope corresponds to *rm*, the $T_{\max}/ET0$ ratio, in the model framework (Equation [7]). Several values of $T_{\max}/ET0$ were above 1.0 at low *ET0*. First, *ET0* is a reference value which does not necessarily represent the maximum *ET* for this particular stand. Second, transpiration could have been overestimated by sap flow measurement, particularly for rainy days and low flow rates. In **Figure 2B**, $T_{\max}/ET0$ was plotted vs. *ET0* discarding y values above 1. The relationship fitted well a Lohammar's function ($y = -0.585\ln(x) + 1.2492$; $R^2 = 0.87$). The R^2 has little meaning here because the variables were directly related by *ET0* in the calculation. However, Lohammar's function provided better results of $T_{\mathrm{mod_ET0c}}$ than a linear adjustment. The plot of midday canopy conductance (G_{c_md}) vs. $VPD_{\max}$ confirmed the underlying mechanism of stomatal regulation at increasing *VPD* (**Figure 3**). According to the fitted Lohammar's function (Lohammar et al., 1980), the reference G_c at 1 KPa and the sensitivity term equal 4.74 mm s^{-1} and 7.6, respectively.

LAI

Transpiration estimated by sap flow measurements (T_{mea}) followed in the expected manner the *LAI* seasonal pattern (**Figure 1C**) which supports a strong control of transpiration by the *LAI*. However, the soil water availability decreased at the same time in the dry season.

REW

The plot of *T/ET0* vs. *REW* showed scatters of points consistent with the assumption of a threshold around $REW = 0.4$ (**Figure 4**). Above a threshold between 0.4 and 0.5, *T/ET0* exhibited a pseudo-plateau averaging 1.0, with large variability. Below the critical *REW*, a linear decrease toward 0:0 crossed the scatter of points. However, the assessment of the value critical *REW* was approximate due to the lack of soil data between 0.4 and 0.5 *REW*.

SIMULATION OF TRANSPIRATION

Conditions of simulation

For the calculations described in the Modeling paragraph of Material and Methods:

- *rm* was tested between 0.9 and 1.0 according to **Figures 2A**, **4**, and finally 1.0 was kept.
- $LAI_{\max}$ was taken equal to 3.9 as measured.
- *REW* was calculated for the top soil (0–0.6 m) with weighting by percentage of fine root length distribution as described in paragraph 2.3.
- The active soil depth and weighting by root distribution were kept constant over the annual cycle.

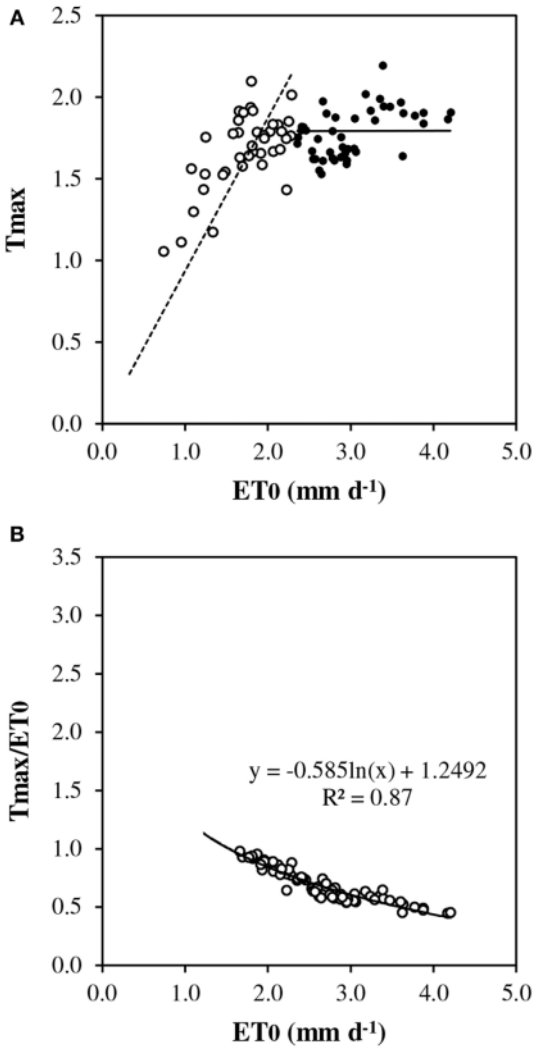


FIGURE 2 | Daily transpiration vs. reference evapotranspiration (*ET0*): (A) measured maximum transpiration (T_{max}) in the absence of soil water stress (*REW* 0–0.6 ≥ 0.5), closed circles indicate *ET0* > 2.3 mm d^{-1}, open circles indicate *ET0* < 2.3 mm d^{-1}, dotted line represents the linear regression below 2.3 *ET0* and crossing origin; (B) relative transpiration (T_{max}/*ET0*).

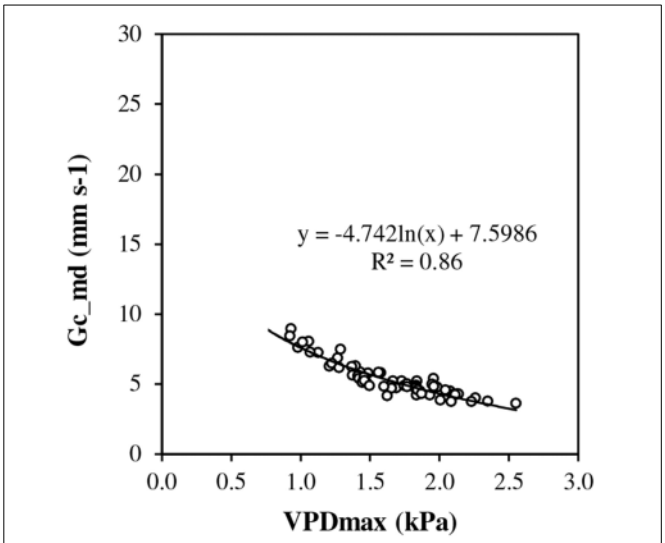


FIGURE 3 | Midday canopy conductance (G_{c_md}) vs. maximum vapor pressure deficit (VPD_{max}) at full canopy period and in the absence of soil water stress (*REW* 0–0.6 ≥ 0.5).

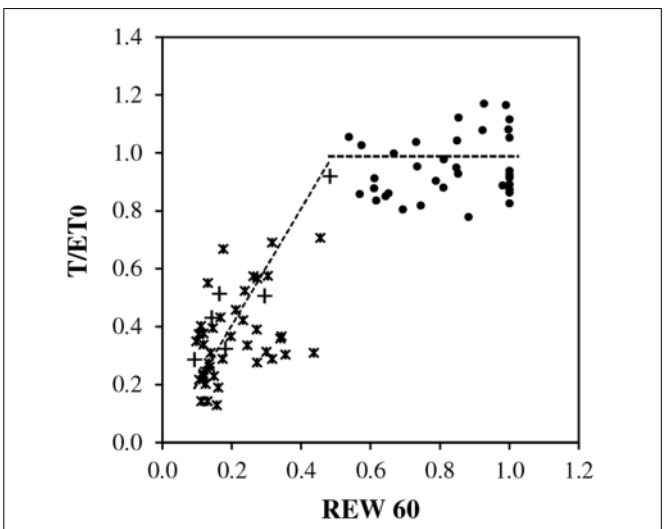


FIGURE 4 | Relative transpiration (*T/ET0*) vs. relative extractable soil water (*REW*) in top soil (0–0.6 m) during full canopy period (LAI_{max}), closed circles indicate *REW* ≥ 0.5 and *ET*0 < 2.3 mm d^{-1}, asterisks indicate *REW* < 0.5 and *ET*0 ≥ 2.3 mm d^{-1} and plus signs indicate *REW* < 0.5 and *ET*0 < 2.3 mm d^{-1}. Trends are shown as dotted lines, averaged as 1.0 for *REW* ≥ 00.5 and as a reduction coefficient for *REW* < 0.5.

- *REWc* was taken equal to 0.4 according to BILJOU99 framework and **Figure 4**.
- *rET0c* was calculated according the function deduced from **Figure 2B**:
  If $ET0 \leq ET0c$, $rET0c = 1$
  If $ET0 > ET0c$, $rET0c = a * \ln(ET0) + b$
  with $ET0c = 2.3$ mm d^{-1}, $a = -0.585$ and $b = 1.2492$.

Simulated transpiration

The transpirations simulated with the original framework of BILJOU99 (T_{mod}), largely overestimated during the full canopy period, particularly in April, May, June, August and November, during periods of high evaporative demand (**Figure 5**). The values simulated with regulation at high *ET0* (T_{mod_ET0c}) logically better expressed the seasonal change of transpiration; however substantial inaccuracy remained in the dry season with overestimates in November and underestimates in other periods (**Figure 5**). **Table 1** summarizes the previous observations: large errors with T_{mod} and the substantial improvement with regulation at high evaporative demand in the rainy season (*RRMSE* < 35%). In the dry season, the errors were substantial (*RRMSE* >

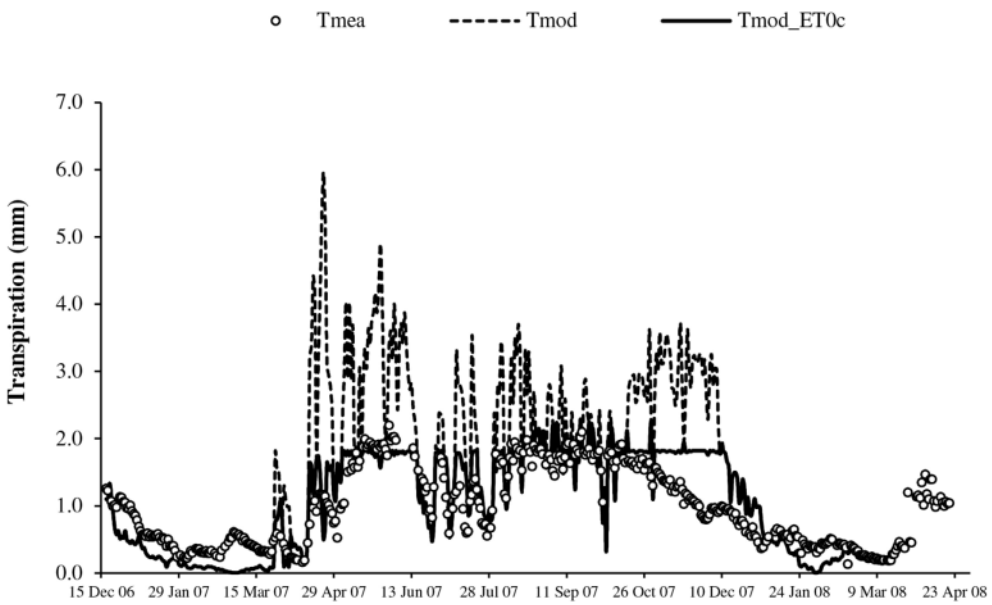


FIGURE 5 | Seasonal change of transpiration from measurement (T_{mea}), simulation with original BILJOU99 framework (T_{mod}) and with evolution including threshold of *ET0* (T_{mod_ET0c}).

Table 1 | Evaluation metrics of simulations of transpiration according to two frameworks: original BILJOU (T_{mod}), simulation with reduction coefficient of *ET0* (T_{mod_ET0c}).

Model	Observation No.	R^2	Whole year *RMSE(RRMSE)*(mm.d^{-1})	Wet season *RMSE(RRMSE)*(mm.d^{-1})	Dry season *RMSE(RRMSE)*(mm.d^{-1})
T_{mod}	379	0.56	1.06 (1.01)	1.00 (0.67)	1.10 (1.19)
T_{mod_ET0c}	379	0.77	0.39 (0.56)	0.30 (0.31)	0.45 (0.68)

RMSE; root mean square error and RRMSE; relative root mean square. Wet season from May 1 to October 31, 2007 and Dry season from December 18, 2006 to April 4, 2007 and November 1, 2007 to February 22, 2008.

60%); however they are emphasized by the relative expression vs. the low absolute values.

HIERARCHY BETWEEN REDUCTION FACTORS OF ANNUAL TRANSPIRATION

On an annual basis, the cumulative measured transpiration (430 mm) was 66% lower than the potential annual transpiration (1247 mm). The regulation was substantial in the rainy season (−39%) and twofold higher in the dry season (−81%). The simulated data provided close estimates of transpiration reduction (−64.5%) when all constraints were considered (*LAI* × *REWc* × *ET0c* in **Figure 6**). When considering only one reduction factor, the *LAI* variation induced the lowest reduction, logically located in the dry season, at the time of defoliation. The impacts of *REWc* and *ET0c* were similar with substantial reduction around −45%, slightly higher for *ET0c* (−50.1%). The *ET0c* constraint was significantly higher than the *REWc* constraint in the rainy season (**Figure 6B**). It was noteworthy that the overall effect of the *ET0c* constraint alone already represented 76% of the total reduction with the combination of the three factors of constraint. The combination with two factors of constraints supported the proposal that *ET0c* had a larger impact than *REWc*. The small difference in the simulation between *REWc* and *REWc* x *LAI* suggested that the *REWc* constraint included already the *LAI* effect. The *REWc* × *ET0c* interaction induced a reduction equivalent to the reduction with three factors, which confirmed the previous suggestion.

DISCUSSION

BASIC RELATIONSHIPS OF BILJOU99 FRAMEWORK

Our results confirmed that the basic relationships of the original framework (Granier et al., 1999) hold except that the regulation of transpiration at high evaporative demand was not well simulated.

ET0$_c$

Experimental data showed a strong regulation of transpiration under non-limiting soil water at high evaporative demand, when the *ET0* was approximately above 2.3 mm d^{-1}. The analysis of the corresponding canopy conductance confirmed a dramatic decrease above *VPD* values equal to 1 kPa. This result supports the previous analysis of Isarangkool Na Ayutthaya et al. (2011) where such a response was related to isohydric behavior with a stable maximal value of the whole tree hydraulic conductance

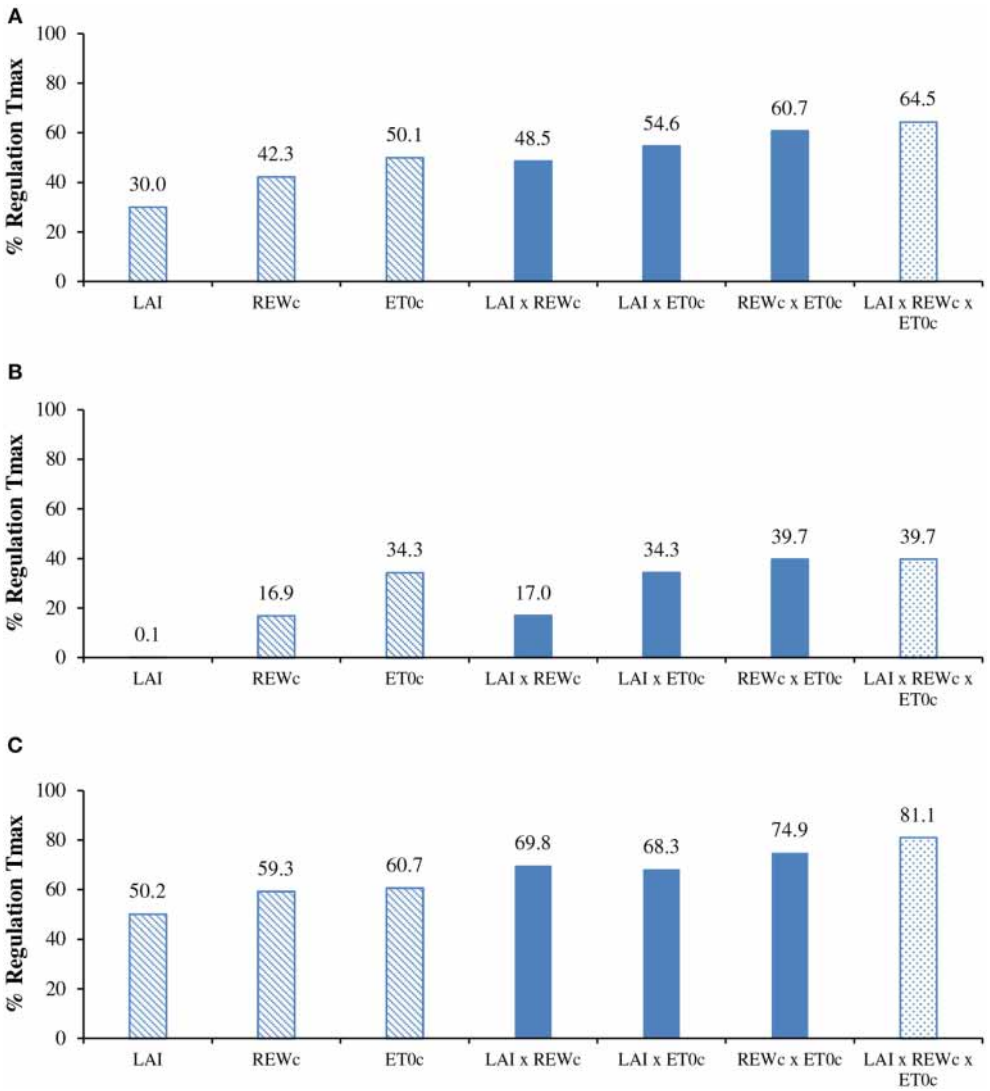


FIGURE 6 | Regulation of seasonal transpiration (simulated with constraints/maxima) for: (A) the annual cycle; (B) the rainy season; and (C) the dry season, according to reduction factors issued from the *LAI* change, critical relative extractable water (*REWc*) and critical potential evapotranspiration (*ET0c*). For details of simulation see paragraphs Modeling and Simulation of transpiration.

and a stable minimum value of the leaf water potential. Such regulation of transpiration vs. high evaporative demand is known for several species (Pataki and Oren, 2003; David et al., 2004; Ocheltree et al., 2014). However, the sensitivity of this response appears dependent on wood anatomy and hydraulic conductivity. *Hevea brasiliensis* is a diffuse-porous species (Richter and Dallwitz, 2000). And our results follow the general trend that stomatal control vs. high evaporative demand is stricter in diffuse-porous species than in ring-porous species. (Oren and Pataki, 2001; McCulloh and Woodruff, 2012).

$T_{max}/ET0$

Below the threshold of critical evaporative demand, the simple and common concept of a stable *rm* ratio between maximal transpiration and reference evapotranspiration under non-limiting conditions held with our data, as *rm* ranged around 1.0 for a maximum *LAI* estimated at 3.89. These values appear relatively high compared to the range of 0.70–0.80 quoted by Granier et al. (1999). However, the latter quotation concerned the ratio vs. *PET* (Potential Evapotranspiration with the Penman equation) which should be higher than *ET0*, the reference evapotranspiration using the Penman-Monteith formula and FAO56 coefficients (Allen et al., 1998). Moreover the accuracy on absolute value of transpiration by sap flow measurement including scaling from tree to stand level is estimated around 20% (Isarangkool Na Ayutthaya et al., 2010).

REWc

Our data supported the general assumption of a linear decrease of $T_{max}/ET0$ below a critical value around 0.4 for the *REW* (Granier et al., 1999; Bréda et al., 2006). This threshold of 0.4 was also quoted for other classical expressions of soil water availability,

i.e., the plant available soil moisture or PAW (Sadras and Milroy, 1996) or the fraction of transpirable soil water or FTSW (Sinclair et al., 2005).

LAI

The seasonal pattern of transpiration followed remarkably the main trend in the *LAI*. However, this observation did not confirm here the well-known control of transpiration by the *LAI* because the *REW* was also decreasing in the dry season. Moreover, simulations in paragraph 3.3 have shown that the decrease in the *REW* was already sufficient to reduce transpiration.

SIMULATION OF TRANSPIRATION WITH MODEL EVOLUTION

Transpiration

Our results confirmed that including regulation by high evaporative demand in the model largely improved the accuracy in simulation of transpiration. However, substantial errors remained and particularly in the dry season. Besides inaccuracy on estimate of absolute transpiration by sap flow measurement, several points could explain this result with such a simple model. The model relationships were mainly tested in the rainy season and under full canopy conditions and they were applied on the annual cycle. The change in the *LAI* was estimated roughly from litter fall measurements and canopy fullness observations. Temporary water logging could have decreased transpiration in November. Also, stomatal regulation could change with leaf age, particularly during senescence and refoliation (Kositsup et al., 2010). Moreover, the profile of fine root length activity changes in the dry season as shown by Gonkhamdee et al. (2009) while in the simulation, the *REW* calculation used the same soil depth and root profile for weighting. However, at the end, the simulation provided a reasonable indication of trends in seasonal regulation of transpiration which was the objective of the tested framework.

Several models of water balance previously used for rubber tree did not consider atmospheric constraints on transpiration: CROPWAT (Allen et al., 1998), WANULCAS (VanNoordwich and Lusiana, 1999; Guardiola-Claramonte et al., 2010; Boithias et al., 2012). The consequences could be (1) an overestimate of transpiration and root water uptake and (2) a further underestimation of stomatal regulation and consequently an overestimation of C assimilation. In a recent review, Boote et al. (2013) included this process as a current limitation of many crop models. Bregaglio et al. (2014) reported the good performance of a simple approach in arid environments based on transpiration use efficiency that explicitly accounts for the negative impact of vapor pressure deficit on photosynthesis.

A limitation of the reduction factor based on *ET0*c is likely the generality of the relationship and value of *ET0*c which has to be tested in different experimental conditions.

DIAGNOSIS OF THE HIERARCHY BETWEEN WATER CONSTRAINTS

The simple framework of simulation has allowed comparing the relative impact of the different constraints on annual and seasonal transpiration. The soil water shortage did not appear as the major water constraint on transpiration in the studied area. High evaporative demand, as expressed by *ET0*, appeared at least of similar importance, if not higher, than soil water shortage. The provided hierarchy is contrary to expectations in this growing area known as climatically under-optimal due to the low amount and variability of rainfall. Clermont-Dauphin et al. (2013) recently provided evidence that soil water shortage was not the main cause of low growth rates in young rubber plantations of North East Thailand and they suggested the importance of high evaporative demand and temporary water logging.

The results from the simulation are directly due to the fact that the sensitivity to air dryness was taken into account in the model. Such a type of response is dependent on the species or variety. We studied the most-planted clone in Thailand (RRIM 600) and the response may change with other varieties of *Hevea brasiliensis*. But the recent of work of Kobayashi et al. (2014) in Cambodia confirmed the sensitivity of canopy stomatal conductance to *VPD* for mature rubber trees of another clone (RRIC 100). However, the details of the response may likely change according to the clone, age and stand characteristics, root development (Devakumar et al., 1999), spatiotemporal acclimation and root proliferation (Liu et al., 2014). We doubt in the generality of the relationship and critical *ET0* used in the framework to simulate sensitivity to air dryness. The results of Sangsing et al. (2004) on young plants of RRIM 600 and RRIT 251 did not show isohydric behavior under water constraints as observed in mature trees. The variability of water relations and sensitivity to air dryness certainly deserves more study.

On the other end, the lower influence of soil water shortage vs. evaporative demand cannot be attributed to a relatively low soil water constraint in the experiment. The growing area of Buri Ram (south of Northeast Thailand) is known as soil water limited with an average annual rainfall of around 1150 mm, which is far below the recommended threshold of 1500 mm. Moreover, the year of study was particularly dry with a rainfall amount of 965 mm. The measurements of soil water availability confirmed the severity of water shortage in both the top soil and deep soil, in the dry season as in the rainy season (**Figure 1B**).

Defoliation is usually limited to 1–2 months, with the defoliation peak between mid-January and mid-February. However, in dry years such as in the year of study, the period of defoliation could last over 3 months, from January to March. In addition to internal controls, canopy phenology can be influenced by both soil and atmospheric droughts (Eamus and Prior, 2001; Do et al., 2005). These relationships were not taken explicitly into account in the model. It is likely that such inclusions could have changed the results of simulation in the details. However, it is doubtful that they could change completely the conclusion and particularly the fact that impact of atmospheric drought on transpiration regulation was at least of similar importance than soil drought.

CONCLUSION

In conclusion, the adapted framework of BILJOU99 had allowed analyzing the relative contribution of soil water shortage and atmospheric drought to the regulation of transpiration on a seasonal scale. This paper provides two main insights. The first stresses the importance of taking into account the direct regulation of transpiration vs. high evaporative demand which often is omitted in simple agro-climatic models. According species, water constraint due to evaporative demand could have been

underestimated in previous studies in the sub-humid tropics. The second relies on the interest in simple agro-climatic models to provide a first diagnosis of water constraints on transpiration, in order to help the evolution of cultural choices and practices toward greater sustainability.

AUTHORS CONTRIBUTION

Jessada Sopharat: data analysis, modeling, paper writing. Supat Isarangkool Na Ayutthaya: experimental design, data collection, data analysis. Frederic Gay: paper writing, editorial advising. Philippe Thaler: paper writing, editorial advising. Sayan Sdoodee: paper writing, editorial advising. Charlchai Tanavud: paper writing, editorial advising. Claude Hammecker: paper writing, editorial advising. Frederic C. Do: experimental design, data collection, supervising the work, modeling, paper writing.

ACKNOWLEDGMENTS

This work was carried out as part of a PhD and was supported by the Higher Education Research Promotion and National Research University Project of Thailand (NRU), Office of the Higher Education Commission and the Graduate School, Prince of Songkla University. In particular, the field experiment was supported by funding from the French Institute for Rubber (IFC) and associate companies (Michelin, Socfinco, SIPH).

REFERENCES

Allen, R. G., Pereira, L. S., Raes, D., and Smith, M. (1998). "Crop evapotranspiration guidelines for computing crop water requirements," in *FAO Irrigation and Drainage Paper 56*. (Rome: Food and Agriculture Organization of the United Nations).

Boithias, L., Do, F. C., Isarangkool Na Ayutthaya, S., Junjittakarn, J., Siltecho, S., et al. (2012). Transpiration, growth and latex production of a *Hevea brasiliensis* stand facing drought in Northeast Thailand: the use of the WaNuLCAS model as an exploratory tool. *Exp. Agric.* 48, 49–63. doi: 10.1017/S001447971100086X

Boote, K. J., Jones, J. W., White, J. W., Asseng, S., and Lizaso, J. I. (2013). Putting mechanisms into crop production models. *Plant. Cell. Environ.* 36, 1658–1672. doi: 10.1111/pce.12119

Bréda, N., Huc, R., Granier, A., and Dreyer, E. (2006). Temperate forest trees and stands under severe drought: a review of ecophysiological responses, adaptation processes and long-term consequences. *Ann. For. Sci.* 63, 625–644. doi: 10.1051/forest:2006042

Bregaglio, S., Frasso, N., Pagani, V., Stella, T., Francone, C., Cappelli, G., et al. (2014). New multi-model approach gives good estimations of wheat yield under semi-arid climate in Morocco. *Agron. Sustain. Dev.* doi: 10.1007/s13593-014-0225-6. (in press).

Bush, S. E., Pataki, D. E., Hultine, K. R., West, A. G., Sperry, J. S., and Ehleringer, J. R. (2008). Wood anatomy constrains stomatal responses to atmospheric vapor pressure deficit in irrigated, urban trees. *Oecologia* 156, 13–20. doi: 10.1007/s00442-008-0966-5

Carr, M. K. V. (2012). The water relations of rubber (*Hevea brasiliensis*): a review. *Exp. Agric.* 48, 176–193. doi: 10.1017/S0014479711000901

Clermont-Dauphin, C., Suvannang, N., Hammecker, C., Cheylan, V., Pongwichian, P., and Do, F. C. (2013). Unexpected absence of control of rubber tree growth by soil water shortage in dry subhumid climate. *Agron. Sustain. Dev.* 33, 531–538. doi: 10.1007/s13593-012-0129-2

David, T. S., Ferreira, M. I., Cohen, S., Pereira, J. S., and David, J. S. (2004). Constraints on transpiration from an evergreen oak tree in southern Portugal. *Agr. Forest. Meteorol.* 122, 193–205. doi: 10.1016/j.agrformet.2003.09.014

Devakumar, A. S., Prakash, P. G., Sathik, M. B. M., and Jacob, J. (1999). Drought alters the canopy architecture and micro-climate of *Hevea brasiliensis* trees. *Trees* 13, 161–167. doi: 10.1007/PL00009747

Do, F., Goudiaby, V. A., Gimenez, O., Diagne, A. L., Diouf, M., Rocheteau, A., et al. (2005). Environmental influence on canopy phenology in the dry tropics. *Forest Ecol. Manag.* 215, 319–328. doi: 10.1016/j.foreco.2005.05.022

Donovan, L., Linton, M., and Richards, J. (2001). Predawn plant water potential does not necessarily equilibrate with soil water potential under well-watered conditions. *Oecologia* 129, 328–335. doi: 10.1007/s004420100738

Eamus, D., and Prior, L. (2001). Ecophysiology of trees of seasonally dry tropics: comparisons among phenologies. *Adv. Ecol. Res.* 32, 113–197. doi: 10.1016/S0065-2504(01)32012-3

Gonkhamdee, S., Maeght, J. L., Do, F., and Pierret, A. (2009). Growth dynamics of fine *Hevea brasiliensis* root along a 4.5 m soil profile. *Khon. Kaen. Agr. J.* 37, 265–276.

Granier, A., Bréda, N., Biron, P., and Villette, S. (1999). A lumped water balance model to evaluate duration and intensity of drought constraints in forest stands. *Ecol. Model.* 116, 269–283. doi: 10.1016/S0304-3800(98)00205-1

Granier, A., Loustau, D., and Bréda, N. (2000). A generic model of forest canopy conductance dependent on climate, soil water availability and leaf area index. *Ann. For. Sci.* 57, 755–765. doi: 10.1051/forest:2000158

Granier, A., Reichstein, M., Bréda, N., Janssens, I. A., Falge, E., Ciais, P., et al. (2007). Evidence for soil water control on carbon and water dynamics in European forests during the extremely dry year: 2003. *Agr. Forest. Meteorol.* 143, 123–145. doi: 10.1016/j.agrformet.2006.12.004

Guardiola-Claramonte, M., Troch, P. A., Ziegler, A. D., Giambelluca, T. W., Durcik, M., Vogler, J. B., et al. (2010). Hydrologic effects of the expansion of rubber (*Hevea brasiliensis*) in a tropical catchment. *Ecohydrol.* 3, 306–314. doi: 10.1002/eco.110

Isarangkool Na Ayutthaya, S., Do, F. C., Pannengpetch, K., Junjittakarn, J., Maeght, J., Rocheteau, A., et al. (2010). Transient thermal dissipation method of xylem sap flow measurement: multi-species calibration and field evaluation. *Tree Physiol.* 30, 139–148. doi: 10.1093/treephys/tpp092

Isarangkool Na Ayutthaya, S., Do, F. C., Pannangpetch, K., Junjittakarn, J., Maeght, J. L., Rocheteau, A., et al. (2011). Water loss regulation in mature *Hevea brasiliensis*: effects of intermittent drought in the rainy season and hydraulic regulation. *Tree Physiol.* 31, 751–762. doi: 10.1093/treephys/tpr058

Jarvis, P. G. (1976). The interpretation of the variations in leaf water potential and stomatal conductance found in canopies in the field. *Philos. Trans. R. Soc. Lond. B* 273, 593–610. doi: 10.1098/rstb.1976.0035

Jarvis, P. G., and McNaughton, K. G. (1986). Stomatal control of transpiration: scaling up from leaf to region. *Adv. Ecol. Res.* 15, 1–49. doi: 10.1016/S0065-2504(08)60119-1

Kobayashi, N., Kumagai, T., Miyazawa, Y., Matsumoto, K., Tateishi, M., Lim, T. K., et al. (2014). Transpiration characteristics of a rubber plantation in central Cambodia. *Tree Physiol.* 34, 285–301. doi: 10.1093/treephys/tpu009

Kositsup, B., Kasemsap, P., Thanisawanyangkura, S., Chairungsee, N., Satakhun, D., Teerawatanasuk, K., et al. (2010). Effect of leaf age and position on light-saturated CO_2 assimilation rate, photosynthetic capacity, and stomatal conductance in rubber trees. *Photosynthetica* 48, 67–78. doi: 10.1007/s11099-010-0010-y

Kumagai, T., Mudd, R. G., Miyazawa, Y., Liu, W., Giambelluca, T. W., Kobayashi, N., et al. (2013). Simulation of canopy CO_2/H_2O fluxes for a rubber (*Hevea brasiliensis*) plantation in central Cambodia: the effect of the regular spacing of planted trees. *Ecol. Model.* 265, 124–135. doi: 10.1016/j.ecolmodel.2013.06.016

Liu, W., Li, J., Lu, H., Wang, P., Luo, Q., Liu, W., et al. (2014). Vertical patterns of soil water acquisition by non−native rubber trees (*Hevea brasiliensis*) in Xishuangbanna, southwest China. *Ecohydrology* 7, 1234–1244. doi: 10.1002/eco.1456

Lohammar, T., Larsson, S., Linder, S., and Falk, S. O. (1980). "FAST – Simulation models of gaseous exchange in Scots pine," in *Structure and Function of Northern Coniferous Forests. An Ecosystem Study,* ed T. Persson (Stockholm: Ecological Bulletins), 505–523.

Masaki, Y., Ishigooka, Y., Kuwagata, T., Goto, S., Sawano, S., and Hasegawa, T. (2011). Expected changes in future agro-climatological conditions in Northeast Thailand and their differences between general circulation models. *Theor. Appl. Climatol.* 106, 383–401. doi: 10.1007/s00704-011-0439-3

McCulloh, K. A., and Woodruff, D. R. (2012). Linking stomatal sensitivity and whole-tree hydraulic architecture. *Tree physiol.* 32, 369–372. doi: 10.1093/treephys/tps036

Ocheltree, T. W., Nippert, J. B., and Prasad, P. V. V. (2014). Stomatal responses to changes in vapor pressure deficit reflect tissue-specific differences in hydraulic conductance. *Plant Cell. Environ.* 37, 132–139 doi: 10.1111/pce.12137

Oren, R., and Pataki, D. E. (2001). Transpiration in response to variation in microclimate and soil moisture in southeastern deciduous forests. *Oecologia* 127, 549–559. doi: 10.1007/s004420000622

Pataki, D. E., and Oren, R. (2003). Species differences in stomatal control of water loss at the canopy scale in a mature bottomland deciduous forest. *Adv. Water. Resour.* 26, 1267–1278. doi: 10.1016/j.advwatres.2003.08.001

Phillips, N., and Oren, R. (1998). A comparison of daily representations of canopy conductance based on two conditional time averaging methods and the dependence of daily conductance on environmental factors. *Ann. For. Sci.* 55, 217–235. doi: 10.1051/forest:19980113

Priyadarshan, P. M., Hoa, T. T. T., Huasun, H., and de Gonçalves, P. S. (2005). Yielding potential of rubber (*Hevea brasiliensis*) in sub-optimal environments. *JCRIP* 14, 221–247. doi: 10.1300/J411v14n01_10

Raj, S., Das, G., Pothen, J., and Dey, S. K. (2005). Relationship between latex yield of *Hevea brasiliensis* and antecedent environmental parameters. *Int. J. Biometeorol.* 49, 189–196. doi: 10.1007/s00484-004-0222-6

Richter, H. G., and Dallwitz, M. J. (2000). *Commercial Timbers: Descriptions, Illustrations, Identification, and Information Retrieval. Version: 25th June 2009*. Available online at: http://delta-intkey.com

Sadras, V. O., and Milroy, S. P. (1996). Soil-water thresholds for the responses of leaf expansion and gas exchange: a review. *Field. Crop. Res.* 47, 253–266. doi: 10.1016/0378-4290(96)00014-7

Sangsing, K., Kasemsap, P., Thanisawanyangkura, S., Sangkhasila, K., Gohet, E., Thaler, P., et al. (2004). Xylem embolism and stomatal regulation in two rubber clones (*Hevea brasiliensis* Muel. Arg.). *Trees* 18, 109–114. doi: 10.1007/s00468-003-0286-7

Sinclair, T. R., Holbrook, N. M., and Zwieniecki, M. A. (2005). Daily transpiration rates of woody species on drying soil. *Tree Physiol.* 25, 1469–1472. doi: 10.1093/treephys/25.11.1469

Stewart, J. B. (1988). Modelling surface conductance of pine forest. *Agric. For. Meteorol.* 43, 19–35. doi: 10.1016/0168-1923(88)90003-2

UNCTAD. (2013). *Area Under NR Cultivation.* Available online at: http://www.unctad.info/en/Infocomm/Agricultural_Products/Caoutchouc/Crop/Area-under-NR-cultivation/ Accessed 19 November 2013

VanNoordwich, M., and Lusiana, B. (1999). WaNuLCAS, a model of water, nutrient and light capture in agroforestry systems. *Agrofor. Syst.* 43, 217–242. doi: 10.1023/A:1026417120254

Wagner, F., Hérault, B., Stahl, C., Bonal, D., and Rossi, V. (2011). Modeling water availability for trees in tropical forests. *Agr. Forest. Meteorol.* 151, 1202–1213. doi: 10.1016/j.agrformet.2011.04.012

Conflict of Interest Statement: The authors declare that the research was conducted in the absence of any commercial or financial relationships that could be construed as a potential conflict of interest.

Received: 29 September 2014; accepted: 08 December 2014; published online: 06 January 2015.

*Citation: Sopharat J, Gay F, Thaler P, Sdoodee S, Isarangkool Na Ayutthaya S, Tanavud C, Hammecker C and Do FC (2015) A simple framework to analyze water constraints on seasonal transpiration in rubber tree (Hevea brasiliensis) plantations. Front. Plant Sci. **5**:753. doi: 10.3389/fpls.2014.00753*

This article was submitted to Crop Science and Horticulture, a section of the journal Frontiers in Plant Science.

Copyright © 2015 Sopharat, Gay, Thaler, Sdoodee, Isarangkool Na Ayutthaya, Tanavud, Hammecker and Do. This is an open-access article distributed under the terms of the Creative Commons Attribution License (CC BY). The use, distribution or reproduction in other forums is permitted, provided the original author(s) or licensor are credited and that the original publication in this journal is cited, in accordance with accepted academic practice. No use, distribution or reproduction is permitted which does not comply with these terms.

Hydrol. Earth Syst. Sci., 19, 1193–1207, 2015
www.hydrol-earth-syst-sci.net/19/1193/2015/
doi:10.5194/hess-19-1193-2015
© Author(s) 2015. CC Attribution 3.0 License.

Hydrology and Earth System Sciences
Open Access

Use of field and laboratory methods for estimating unsaturated hydraulic properties under different land uses

S. Siltecho[1,4,5], C. Hammecker[2], V. Sriboonlue[3,4], C. Clermont-Dauphin[2], V. Trelo-ges[1,4], A. C. D. Antonino[6], and R. Angulo-Jaramillo[7]

[1]Department of Plant Science and Land Resource, Faculty of Agriculture, Khon Kaen University, Khon Kaen, Thailand
[2]Institut de Recherche pour le Développement (IRD), UMR 210, place Viala, Montpellier, France
[3]Department of Agricultural Engineering, Faculty of Engineering, Khon Kaen University, Khon Kaen, Thailand
[4]Ground Water Research Center, Khon Kaen University, Khon Kaen, Thailand
[5]Land Development Regional Office No. 5, Land Development Department, Ministry of Agriculture, Khon Kaen, Thailand
[6]Universidade Federal de Pernambuco, Centro de Tecnologia e Geociências, Departamento de Energia Nuclear, Recife, Brazil
[7]Université de Lyon – UMR5023 Ecologie des Hydrosystèmes Naturels et Anthropisés, Université Lyon 1, ENTPE, CNRS, 3, rue Maurice Audin, 69518 Vaulx-en-Velin, France

Correspondence to: C. Hammecker (claude.hammecker@ird.fr)

Received: 23 April 2014 – Published in Hydrol. Earth Syst. Sci. Discuss.: 10 June 2014
Revised: 26 December 2014 – Accepted: 7 February 2015 – Published: 3 March 2015

Abstract. Adequate water management is required to improve the efficiency and sustainability of agricultural systems when water is scarce or over-abundant, especially in the case of land use changes. In order to quantify, to predict and eventually to control water and solute transport into soil, soil hydraulic properties need to be determined precisely. As their determination is often tedious, expensive and time-consuming, many alternative field and laboratory techniques are now available. The aim of this study was to determine unsaturated soil hydraulic properties under different land uses and to compare the results obtained with different measurement methods (Beerkan, disc infiltrometer, evaporation, pedotransfer function). The study has been realized on a tropical sandy soil in a mini-watershed in northeastern Thailand. The experimental plots were positioned in a rubber tree plantation in different positions along a slope, in ruzi grass pasture and in an original forest site. Non-parametric statistics demonstrated that van Genuchten unsaturated soil parameters (K_s, α and n) were significantly different according to the measurement methods employed, whereas the land use was not a significant discriminating factor when all methods were considered together. However, within each method, parameters n and α were statistically different according to the sites. These parameters were used with Hydrus1D for a 1-year simulation and computed pressure head did not show noticeable differences for the various sets of parameters, highlighting the fact that for modeling, any of these measurement methods could be employed. The choice of the measurement method would therefore be motivated by the simplicity, robustness and its low cost.

1 Introduction

The rubber tree (*Hevea brasiliensis*) has become a crop of high economic interest in the northeast of Thailand since the rise in price of natural rubber on the international market and the policy of the Thai government to extend rubber tree plantation. Despite climatic and edaphic conditions being very different to those of the original growing region (south of Thailand), rubber tree plantation extended by about 170 000 ha between 2004 and 2006 (Rantala, 2006). The introduction of the rubber tree in the northeast of Thailand may also contribute to important land use changes affecting soil and water resources. In this area, the average annual rainfall (1.1–1.2 m) does not completely meet the minimal requirements for rubber trees (1.3 m), and therefore it is necessary to design a wise water management to be able to ensure sustainable rubber tree farming. In order to achieve this practical goal, numerical modeling of water flow in soils is a valu-

able tool for quantifying precisely the water balance and the different mechanisms involved (Soares and Almeida, 2001; Antonino et al., 2004; Anuraga et al., 2006) and therefore for trying to forecast the evolution of the system, as the new land use may be leading to changes in the general water balance. In order to achieve accurate quantification of these changes with modeling, it is therefore necessary to estimate precisely the hydrodynamical properties of the vadose zone.

Several laboratory methods are commonly used to determine the hydraulic properties of soil, like the pressure plate method (Klute and Dirksen, 1986; Bittelli and Flury, 2009) to determine the retention curve, and hydraulic conductivity measurements like hot air, crust, one-step outflow, and sorptivity-based methods (Stolte et al., 1994). Some in situ methods have mainly been developed to measure hydraulic conductivity in the field, like the tension disc infiltrometer (Perroux and White, 1988; Akeny et al., 1991; Angulo-Jaramillo et al., 2000). In any of these cases, the determination of the hydraulic parameters of unsaturated soil is always tedious and time-consuming. Therefore, the quest for alternative methods of determination is a research issue. For example, the development of pedotransfer functions (PTFs), which provide relationships between soil hydraulic parameters and more easily measurable properties such as particle size distribution (PSD), has become successful amongst soil scientists and hydrologists (Bouma, 1989; Pachepsky et al., 2006). They are mainly based on the textural properties of soil, but show some inadequacy in describing structural aspects of soil. Consequently, specific methods taking into account structural properties have been developed to tackle this problem. For example, the Beerkan method (Haverkamp et al., 1996; Braud et al., 2005) is a field and laboratory measurement method that aims to determine retention curves and hydraulic conductivity curves by particle size distribution and single ring infiltration data, in order to describe the contribution of the texture and the structure to hydraulic properties. But, the main interest of this method is to provide an efficient and low cost estimation of soil hydraulic properties. These basic data are processed with the Beerkan Estimation of Soil Transfer parameters (BEST) algorithm according to this theory (Lassabatere et al., 2006) to provide acceptable estimations of hydraulic parameters to a complete characterization of hydraulic characteristic curves. We also compared it to a laboratory evaporation method inspired by the method proposed by Wind (1968), which is based on an evaporation measurement to estimate soil water retention and hydraulic conductivity. Wind's method has become very popular and is constantly improved by the introduction of inverse modeling (Tamari et al., 1993; Simunek et al., 1998a; Richard et al., 2001), and has been adapted for infiltration procedures (Bruckler et al., 2002). Though hydraulic conductivity is well predicted for the dry part of the curve, Wind's method is generally inadequate near saturation for hydraulic gradients that are too low (Tamari et al., 1993; Wendroth et al., 1993; Richard et al., 2001). In this study, we considered only part of the evaporation technique, in order to determine experimentally the retention curve.

Land use changes are known to modify soil properties and especially the unsaturated soil hydraulic characteristics (Zimmermann et al., 2006; Price et al., 2010), as the soil structure might be affected by different tillage methods, different root densities and sizes, and different biological activities of macro-fauna. Therefore, the hydraulic conductivity of the top soil will be affected and the infiltration capacity will be modified. In the context of tropical rain patterns with heavy rainfall followed by long dry periods, with these shallow soils, the infiltration capacity is an important factor in the soil water balance. The efficiency of the rainfall highly depends on the infiltration capacity.

Different land uses such as rubber tree plantation, pasture or natural forest in the same soil series are expected to show very different soil properties. The purpose of this study is to verify this hypothesis and to compare the performance of different measurement techniques for estimating the soil-hydraulic properties of top soil in a typical mini-watershed of northeastern Thailand, in order to model soil water flow accurately.

2 Materials and methods

2.1 Site and soil description

The study area is set up in a small watershed located near Ban Noon Tun, Phra Yuen District, Khon Kaen Province, Thailand (16°19′43.90″ N, 102°45′07.91″ E) at about 19 km southwest of the city of Khon Kaen. This area is subject to a tropical savanna climate, with annual rainfall of 1.3 and 1.96 m in 2007 and 2008, respectively, and an average annual temperature of 29 °C. The site is located in the typically undulating landscape of northeastern Thailand, with an elevation ranging from 165 to 181 m above medium sea level and an average slope of 3.5 % (Fig. 1). The surface area of the mini-watershed is estimated to be 200 m × 104 m, where most of the surface is covered with rubber trees (*Hevea brasiliensis*) and ruzi grass (*Brachiaria ruziziensis*) cultivated for seeds. The area dedicated to rubber tree plantation is approximately 120 m × 104 m, and previously the land was planted with jute (*Corchorus capsularis*), cassava (*Manihot esculenta*) and ruzi grass. Following the governmental policy and the bright economical perspectives for the farmers, the soil use changed to a rubber tree plantation in 2004.

The soil is generally shallow; in the upper part of the toposequence, the soil thickness is about 0.70 m, 0.90 m midslope, and 2.5 m downslope. The soil texture is classified as sand to sandy clay loam, with a bulk density ranging from 1.38 to 1.54×10^3 kg m^{-3}. According to the USDA classification system, the soil fit into three subgroups, i.e., Typic Haplustult, Arenic Paleustalf, and Typic Paleustult. The soil profile is comprised of an unstructured superficial sandy

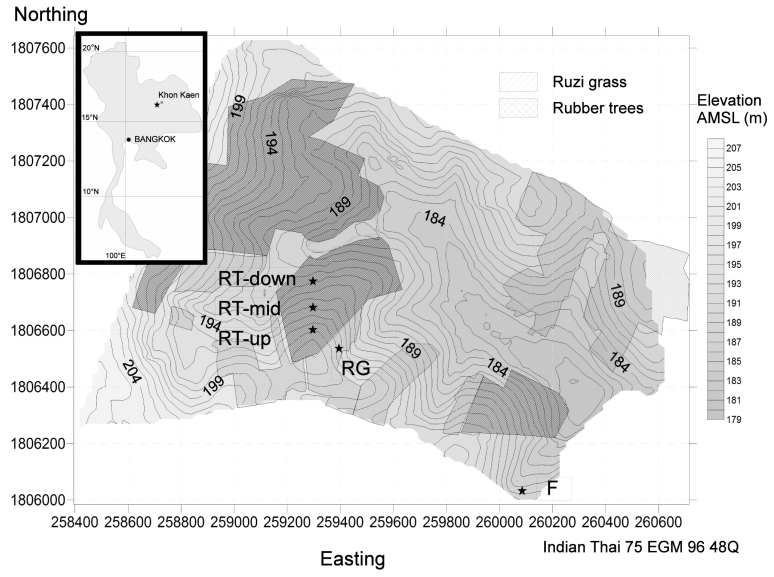


Figure 1. Location of the experimental watershed with the different different land uses and measurement sites; F: forest, RG: ruzi grass, RT-up: rubber tree upslope, RT-mid: rubber tree midslope, RT-down: rubber tree downslope, and location of meteorological station MS.

Table 1. Physical and chemical properties of the topsoil at the different sites.

	Sand	Silt %	Clay	Bulk density kg m^{-3}	Organic matter %	pH
Rubber tree						
Upslope	89.3	7.1	3.5	1.39×10^3	0.49	6.0
Midslope	88.5	7.5	4.1	1.38×10^3	0.71	6.4
Downslope	85.5	12.2	2.3	1.46×10^3	0.70	6.4
Ruzi grass	89.0	7.5	3.5	1.47×10^3	0.63	6.6
Forest	84.6	11.1	4.3	1.54×10^3	0.76	6.4

layer with low clay and organic matter contents, overlying a 0.20 to 0.50 m thick grey clayey layer colored locally with red weathered material from the bedrock (Wiriyakitnateekul et al., 2009). The bedrock, which is also probably the parental material, is a fine red sandstone or siltstone, containing clay minerals and feldspars (orthoclase), thoroughly weathered in its upper part, and densely fractured. The physical and chemical properties of the soil measured in the laboratory (Table 1) show that the texture of the top soil is sandy for rubber trees (upslope and midslope) and ruzi grass and loamy sand for rubber tree (downslope) and forest. Moreover, they show slightly acidic soils with very low organic matter content, though slightly higher in the forest (Table 1).

The first situation considered for measuring soil hydraulic properties was a toposequence of 300 m along a gentle slope (3 %) in the rubber tree plantation (i.e., RT site, Fig. 1) where three positions were selected: upslope, midslope, and downslope. Next to the rubber tree plantations, important extensions of ruzi grass pasture are still present in this small watershed, which are ploughed once a year, during the rainy season, just before sowing. The second measurement site was located in a ruzi grass pasture plot close to the rubber tree plantation (i.e., RG site, Fig. 1). The third measurement site was located in the upper part of the watershed, where an original Dipterocarpus forest has been conserved (i.e., F site, Fig. 1). Experimental soil water flow measurement devices, namely, tensiometers with pressure sensors (SKT 850T, SDEC, Reignac-sur-Indre, France) and soil moisture sensors (Enviroscan probe, Sentek, Stepney SE, Australia), were installed at the different sites (RT upslope, midslope, downslope, RG and F) and monitored every 2 h continuously from 2007 to 2009. Tensiometric data were recorded at 0.10, 0.25, 0.40, 0.60 and 1.10 m and soil moisture was measured at 0.10, 0.30, 0.50, 0.70, 0.90, 1.10 and 1.40 m. Meteorological data (rainfall, temperature, air humidity, wind speed, solar radiation) were recorded continuously at a single site in the small watershed (Fig. 1). At each experimental site (RT upslope, midslope, downslope, RG and F), Beerkan infiltration experiments were performed in the field during the dry season, from November 2007 to February 2008, and soil cylinders were collected for laboratory evaporation method measurements. The soil volumetric water content at 0–0.10 m depth, measured when the Beerkan infiltration experiments were performed, was 0.01 (m^3 m^{-3}) for RT upslope and F and 0.02 for the other sites.

2.2 Estimation of soil unsaturated hydraulic properties

Modeling and quantifying water flow in the vadose zone is mostly described by Richards' equation (Richards, 1931), and in order to solve this equation, one is required to deter-

mine (i) the soil water retention function, relating the pressure head to the soil water content $h(\theta)$,

$$S_e = \left(\frac{\theta - \theta_r}{\theta_s - \theta_r}\right) = \left(1 + (\alpha h)^n\right)^{-m}, \quad (1)$$

$$m = 1 - \frac{k}{n}, \quad (2)$$

and (ii) the hydraulic conductivity based on the Brooks and Corey (1964) model (Eq. 3),

$$\frac{K(\theta)}{K_s} = (S_e(\theta))^{\eta}, \quad (3)$$

or the van Genuchten relationship:

$$K(\theta) = K_s S_e^l \left[1 - \left(1 - S_e^{1/m}\right)^m\right]^2. \quad (4)$$

These equations are defined by several parameters where h is the pressure head (L), S_e is the effective saturation (–), θ ($L^3\,L^{-3}$) is the volumetric water content, θ_r and θ_s are the residual and saturated water content, m (–) and n (–) are shape parameters, and k is an integer usually chosen to be 1 (Mualem, 1976) or 2 (Burdine, 1953). α (L^{-1}) is the scale-fitting parameter, K_s ($L\,T^{-1}$) is the saturated hydraulic conductivity, and l (–) and η (–) are other shape parameters, with l usually considered to be 1/2.

2.2.1 The Beerkan method

The experimental procedure of this method consisted of two distinct processes, i.e., the soil particle size distribution analysis and a single ring infiltration test. According to the theory developed in Braud et al. (2005) and Lassabatere et al. (2006), 3-D axisymmetric infiltration was realized with a zero pressure head at the soil surface. It was achieved with a pulse flux of small volumes of water, and the infiltration tests were performed in situ with a 0.102 m diameter cylinder. The choice of the cylinder diameter for the Beerkan method was motivated by the experience from the literature (Braud et al., 2005) and the availability of the material. As the soil in this area is sandy and has little or no structure, it was assumed that the diameter of the infiltration cylinder would not impact the representativity of measurement.

The infiltration cylinder was driven firmly into the soil for about 0.01 to 0.02 m in order to prevent lateral loss of water from the infiltration cylinder (Fig. 2b). A series of constant volume of water ($120 \times 10^{-6}\,m^3$) was poured into the cylinder and the time was recorded after each volume of water had been completely infiltrated. Each volume represented a maximum of 0.015 m of pounding pressure at the soil surface when the cylinder was freshly refilled. Haverkamp et al. (1998) showed that small variations in pounding pressure did not influence significantly the infiltration rate, and the surface pressure head in the present case could be considered to be nil. The soil surface micro-topographic irregularities

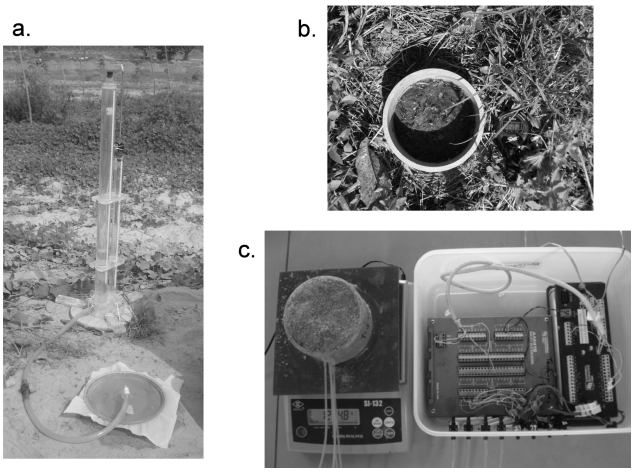


Figure 2. Photographs of some of the experimental measurement methods: **(a)** disc infiltrometer; **(b)** Beerkan method; and **(c)** evaporation method.

in a cylinder of 0.102 m in diameter are therefore negligible as regards the surface pressure. The time reading for each added volume was recorded precisely when the last free water puddle vanished completely from the soil surface. A new volume was added immediately to ensure continuous water supply. This procedure was continued until the steady-state infiltration rate was reached. Undisturbed and disturbed soil samples were collected at the test spot to determine dry bulk density, PSD by the sedimentation method, and initial (θ_0) and final (θ_s) volumetric water content. At each site, when the results were homogeneous, a minimum of three infiltration tests have been conducted. When the variability of infiltration was higher, the number of infiltration tests was increased to seven in some cases. The results were analyzed with the BEST algorithm (Lassabatere et al., 2006) in order to obtain both, the water retention curve (Eq. 1) with the Burdine condition, $k = 2$ (Eq. 2), and the hydraulic conductivity (Eq. 3). The details of this calculation procedure can be found in Lassabatere et al. (2006). However, in order to compare the results with other methods and to be able to use these parameters in numerical models like Hydrus1D (Simunek et al., 2005), the curves obtained with BEST were then adjusted to the van Genuchten with Mualem conditions ($k = 1$ in Eq. 2). The retention curve was plotted according to the Burdine parameters and the equation with the Mualem condition ($m = 1 - 1/n$) was adjusted with a Marquardt procedure to fit the new parameters.

2.2.2 Disc infiltrometer

This common field technique to measure saturated hydraulic conductivity was used at the different sites with the SW080 B device (SDEC, Reignac-sur-Indre, France). The principle of the tension disc infiltrometer is based on maintaining the water in the apparatus under a controlled tension, so that only

pores with lower matric potential can be filled. With this technique, the bio-macropores, cracks and other structures promoting preferential flow can be ignored, to measure hydraulic conductivity strictly in the soil matrix. A tension disc infiltrometer consists of a water reservoir, a Mariotte bubbling tower, and a contact disc of diameter 0.20 m covered with a microporous nylon membrane (with a pore diameter of 20×10^{-6} m). The water reservoir outlet was connected to the center of the disc with a flexible plastic tube (Fig. 2a). The tension applied to water in the device is controlled in the Mariotte tube; the depth of the air inlet under the water surface controls the minimal tension necessary to draw water out of the infiltrometer throughout the disc. Infiltration is realized until it reaches the constant infiltration rate successively with decreasing tension. The soil surface has to be cleared of vegetation and leveled to ensure perfect contact with the infiltration disc. Usually, the soil surface was slightly covered with clean fine sand to get a smooth horizontal surface and to provide a good contact between the base of the disc and the soil below. The relative position of the infiltration disc with the water reservoir is not necessarily constant. Therefore, it is important to measure it in order to calculate the actual water potential head controlled with the immersed tube of the Mariotte device. In order to calculate saturated hydraulic conductivity with the multi-potential method (Perroux and White, 1988; Smettem and Clothier, 1989), the infiltration measurements have been realized for two different tension values and interpreted with Wooding's method (Wooding, 1968; Akeny et al., 1991; Angulo-Jaramillo et al., 2000). The tension values used for the experiments were not always exactly the same, as they were partly controlled by the soil microtopography. But, they were generally between -15 and -10 hPa for the higher tension and between -7 and -3 hPa for the lower tension.

2.2.3 Evaporation method

Two undisturbed soil samples were collected in the field at each location (RT upslope, midslope, downslope, RG, F) by driving a PVC cylinder (height 9 cm and diameter 15 cm) into the previously wetted soil surface. The soil cylinders were air-dried, ensuring that the soil structure was preserved, and slowly saturated with tap water to control the initial water content. Four micro-tensiometers (3×10^{-2} m length $\times$ 1.5×10^{-2} m diameter) filled with de-aired water were connected to pressure transducers (Honeywell 15 PSI model, Honeywell Aerospace Plymouth, Plymouth MN) and inserted into the soil sample at four depths: at 0.011, 0.034, 0.056 and 0.079 m from the top of the soil sample (Fig. 2c). The cylindrical soil sample was dried from the upper surface in a ventilated thermostatic oven at an air temperature of 40 °C, imposing very slow evaporation conditions with a constant evaporation rate of 2.3×10^{-8} m s^{-1}. Pressure and the weight were recorded during evaporation at a regular time interval (30 min) on a data logger (CR10 model, Campbell Scientific, Logan UT). The measurements continued until the air entry limit of the ceramic cup of the tensiometer was reached. The soil was removed from the PVC cylinder and oven-dried at 105 °C during 24 h, and the final water content and dry bulk density were calculated. As the evaporation rate was set to be slow with a quasi steady-state flux, the pressure head gradient in the soil sample was close to zero, with a uniform pressure head profile. Therefore, it was legitimate to derive the retention curve from the average tension measured in the four tensiometers and from the water content variation during the drying of the soil cylinder. The relationship of van Genuchten (1980), Eq. (1) with the Mualem condition ($k = 1$), has been used to fit to the experimental water retention curves.

2.2.4 The inverse method

The original method of Wind is known for introducing some biases into the calculation of the hydraulic conductivity near saturation, especially as the hydraulic gradient is low (Tamari et al., 1993; Wendroth et al., 1993; Richard et al., 2001). Therefore, the same experimental data set as for the evaporation method was used to derive the soil hydraulic parameters by numerical inverse modeling with Hydrus1D (Simunek et al., 2005). The height of the simulated domain was set to 0.09 m, with four observation points corresponding to the positions of the tensiometers in the soil cylinder. The boundary conditions were set to Neumann conditions; namely, the lower boundary condition was set to zero flux and the upper boundary condition was set to the experimental evaporation flux. The inversion procedure is based on the minimization of an objective function describing the difference between observed and computed values. The estimated unsaturated soil characteristics were chosen to be described by the van Genuchten (1980) relationship (Eqs. 1 and 4) with the Mualem condition ($k = 1$, Eq. 2). In order to improve the fitting procedure, the values of θ_r, θ_s, n, and α obtained with the evaporation method and the values of K_s obtained with the disc infiltrometer were used as initial guesses for the inversion procedure. The water content parameters θ_r and θ_s were kept fixed, whereas the parameters n, α, K_s were fitted, and l was set to 0.5.

2.2.5 Pedotransfer function

Many pedotransfer functions relating simple PSD to the soil water characteristics (SWC) and especially the water retention curve have been developed in the last decades (Pachepsky and Rawls, 2003; Mohammadi and Vanclooster, 2011). Therefore, a well-established model was chosen for this study.

The model proposed by Arya et al. (1999) based on the original work of Arya and Paris (1981) is a partly physically based model, deriving from the pore size distribution of a soil from the PSD data, according to the following equation:

$$r_i = R_i \sqrt{\frac{2en_j^{1-\alpha_i}}{3}}, \quad (5)$$

where r_i is the mean pore radius and R_i the mean particle radius for the ith particle size fraction, e is the void ratio of the natural structured soil sample, n_i is the equivalent number of spherical particles in the ith particle size fraction, and α_i is a scale factor. The calculation details for these parameters can be found in Arya et al. (1999). Finally, the pore radii, r_i, are converted into equivalent pressure heads h_i, using the capillary rise equation

$$h_i = \frac{2\eta \cos\Theta}{\rho_w g r_i}, \quad (6)$$

where η is the water surface tension at the air–water interface, Θ is the contact angle, ρ_w is the density of water, and g is the acceleration due to gravity. The volumetric water content, θ_i ($m^3\,m^{-3}$), is obtained from successive summation of water-filled pore volumes according to

$$\theta_i = (\varepsilon S_w) \sum_{j=1}^{j=i} w_j, \quad (7)$$

where ε is the total porosity ($m^3\,m^{-3}$), and S_w is the saturation rate.

2.3 Evaluation of the methods

Experimental soil water flow measurement devices, namely, tensiometers and soil moisture sensors (Enviroscan probe, Sentek, Stepney SE, Australia) were installed in the different soil locations, and were continuously recorded every 2 h for several years. In order to evaluate the goodness of the soil parameter estimation methods, a reference was needed. The final use for these parameters was modeling of soil water flow, and no intrinsic correct values were known, so these parameters were evaluated by modeling with Hydrus1D, a robust and well-documented software (Simunek et al., 2005), and by comparing modeled results with experimental data. The calculation has been performed on a uniform 0.35 m deep domain with two tensiometric boundary conditions measured in the field at 0.10 m as the upper boundary condition and at 0.45 m for the bottom boundary condition. This choice has been motivated by the necessity to perform the simulation with well-constrained boundaries. The development of matric potential during an almost 1-year period was calculated for the intermediate tensiometer located at 0.25 m. These calculations were performed with the combination of the unsaturated soil parameters measured with the different methods (i.e., the Beerkan, disc infiltrometer, PTF, evaporation and inverse methods) and were compared to the experimental tension values measured in the five different locations (i.e., in the forest, ruzi grass, and the three positions in the rubber plantation). The four criteria generally proposed were used to evaluate the performance of modeling (Table 2), namely the root mean squared error (RMSE), the coefficient of determination (CD), the modeling efficiency index (EF) and the coefficient of residual mass (CRM) (Loague and Green, 1991; Kim et al., 1999).

2.4 Statistics

Firstly, the estimated variables, namely saturated hydraulic conductivity (K_s), parameter α and parameter n, were analyzed using standard statistics to calculate their mean and coefficient of variation values. The statistical R package (R Development core team, 2008) was used to test the normality of data frequency distribution with the Anova test.

However, as the number of repetitions were uneven and sometimes very low (from 3 to 10 samples per method tested in each site), Kruskal–Wallis non-parametric tests were also used to check the hypothesis of the same continuous distribution for the different cases. This test determines equality between means or medians of different groups of data, without presuming any specific hypothesis on the distribution.

3 Results

3.1 Beerkan method

With a simple 3-D infiltration experiment combined with PSD analysis, the BEST software (Lassabatere et al., 2006) derived the main shape parameter n and scale parameter K_s and α describing the unsaturated hydraulic properties. The results displayed in Table 3 show relatively low variation between the different sites. Saturated hydraulic conductivity (K_s) ranged from 5.59 to $10.23 \times 10^{-6}\,m\,s^{-1}$ within the different sites and showed a clear gradient along the slope in the rubber tree plantation. The highest values of K_s were found upslope and on the lowest downslope, probably due to the accumulation of finer particles in the lower part, as mentioned by other authors (Heddadj and Gascuel-Odoux, 1999; Jing et al., 2008) describing topographic variation of hydraulic conductivity. Average K_s values were found to be very similar for the soil under ruzi grass and under forest (5.84 and $5.93 \times 10^{-6}\,m\,s^{-1}$, respectively), though the standard deviation was much higher for ruzi grass than for forest (3×10^{-6} and $9 \times 10^{-7}\,m\,s^{-1}$, respectively). Along the slope, the relative standard error on K_s was also quite high, with values ranging from 49 to 62 %. The retention curve parameters, α and n, also showed little variation between the different sites: for most of the cases, the average value of α was 1.4 or $1.5 \times 10^{-4}\,m^{-1}$, except for the forest (F), where α displayed higher values ($2.8 \times 10^{-4}\,m^{-1}$). The shape parameter n followed a similar trend as K_s, namely, decreasing values along the slope (2.33, 2.26 and 2.06, respectively, in the upslope, midslope and downslope positions). Outside the plantation, the average value for n in ruzi grass (R) was within the range previously observed, namely 2.23, but it was significantly

Table 2. Evaluation criteria for performance of modeling.

$\mathrm{RMSE} = \sqrt{\frac{\sum_{i=1}^{N}(T_i - M_i)^2}{N}}$	Indicates that the degree of deviation between the experimental determinations and calculated values tends to zero when the calculated and experimental values tend to be equal.
$\mathrm{CD} = \frac{\sum_{i=1}^{N}(M_i - \overline{M})^2}{\sum_{i=1}^{N}(T_i - \overline{M})^2}$	Describes the ratio between the dispersion of experimental determinations and the dispersion of the calculated values, tending towards unity when the experimental and calculated values are consistent.
$\mathrm{EF} = \frac{\sum_{i=1}^{N}(M_i - \overline{M})^2 - \sum_{i=1}^{N}(T_i - \overline{M})^2}{\sum_{i=1}^{N}(M_i - \overline{M})^2}$	Indicates whether the model provides a better estimate of experimental determinations than the mean value of these determinations. The expected value for EF tends towards 1.
$\mathrm{CRM} = \frac{\sum_{i=1}^{N} M_i - \sum_{i=1}^{N} T_i}{\sum_{i=1}^{N} M_i}$	Indicates whether the model tends to overestimate (CRM < 0) or underestimate (CRM > 0) compared to experimental values. The optimal value for CMR tends towards zero.

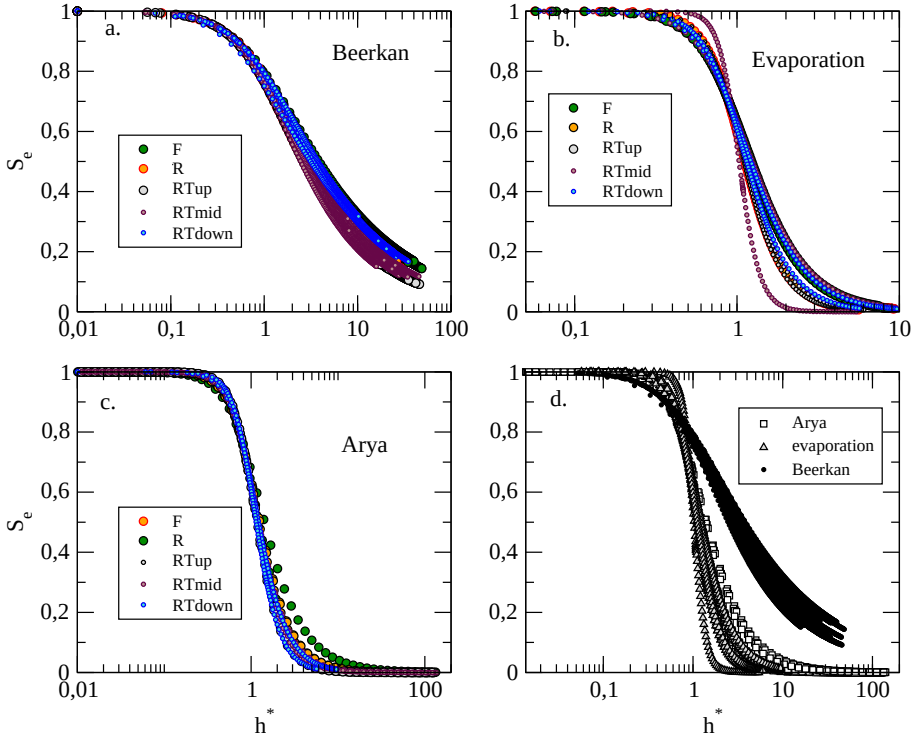


Figure 3. Scaled retention curves for **(a)** the Beerkan method, **(b)** the evaporation method, **(c)** the method based on Arya's PTF, and **(d)** the different methods.

Table 3. Means and standard errors for the main van Genuchten parameters with Mualem conditions ($n = 1/\{1 - m\}$) determined for the different methods at the different sites. The number of samples is indicated in parentheses.

$K_s \times 10^{-6}$ (m s^{-1})				
	Beerkan	Disc infiltrometer	Inverse	
Forest	5.94 ± 0.94 (3)	6.65 ± 4.41 (6)	10.00 ± 2.04 (3)	
Ruzi	5.82 ± 3.55 (4)	6.93 ± 5.45 (7)	18.48 ± 7.12 (3)	
RT downslope	5.59 ± 2.56 (7)	3.48 ± 2.38 (6)	10.18 ± 0.82 (3)	
RT midslope	8.53 ± 4.22 (11)	5.11 ± 4.60 (7)	14.66 ± 8.90 (3)	
RT upslope	10.23 ± 6.38 (10)	6.89 ± 5.31 (6)	22.06 ± 5.27 (2)	
α (m^{-1})				
	Arya	Beerkan	Inverse	Evaporation
Forest	1.5 ± 0.9 (6)	2.8 ± 0.47 (3)	1.8 ± 0.058 (3)	1.8 ± 0.058 (3)
Ruzi	0.6 (1)	1.5 ± 0.56 (10)	1.87 ± 0.21 (3)	1.87 ± 0.21 (3)
RT downslope	0.6 (6)	1.4 ± 0.55 (11)	1.97 ± 0.21 (3)	1.97 ± 0.21 (3)
RT midslope	0.54 ± 0.05 (5)	1.5 ± 0.85 (7)	1.87 ± 0.21 (2)	1.87 ± 0.3 (3)
RT upslope	0.5 (5)	1.5 ± 0.9 (4)	2.55 ± 0.35 (3)	1.97 ± 0.21 (3)
n				
	Arya	Beerkan	Inverse	Evaporation
Forest	2.83 ± 0.17 (6)	2.00 ± 0.03 (3)	2.29 ± 0.09 (3)	3.29 ± 0.50 (3)
Ruzi	1.82 ± 1.22 (3)	2.23 ± 0.11 (4)	2.90 ± 0.44 (3)	3.82 ± 0.69 (3)
RT downslope	2.72 ± 0.07 (6)	2.06 ± 0.02 (7)	2.48 ± 0.29 (3)	3.20 ± 0.54 (3)
RT midslope	3.35 ± 0.14 (5)	2.26 ± 0.06 (11)	2.31 ± 0.08 (3)	2.96 ± 0.14 (3)
RT upslope	3.17 ± 1.01 (6)	2.33 ± 0.03 (10)	2.18 ± 0.02 (2)	3.32 ± 0.67 (3)

lower in the forest situation, with a value of 2. Normalized or scaled retention curves (Fig. 3d) were established with dimensionless values of water content (S_e) and of the matric potential ($h^* = h\,\alpha$), in order to simplify the retention curve $h(\theta)$, and to compare the shape parameters. They showed very similar shapes for all the locations, with a small shift for the F soil samples, indicating differences in shape parameters for the soil in forest resulting from a slightly higher clay content. As hydraulic conductivity is mainly ruled by shape parameters like texture that vary less in local than in scale parameters, scaled hydraulic conductivity curves (not shown here) were all grouped together and were therefore less informative.

3.2 Disc infiltrometer

Results obtained for K_s with the disc infiltrometer showed a behavior similar to that with the Beerkan method, namely, a progressive decrease down the slope in the rubber tree plantation, though the actual values for K_s were systematically lower, namely, 6.9, 5.1 and 3.5×10^{-6} m s^{-1} from upslope to downslope positions, respectively (Table 3). The average values of K_s in the forest and ruzi grass were larger than those for the Beerkan method (6.65 and 6.93×10^{-6} m s^{-1}, respectively). The relative standard errors for this method were significantly larger than for the Beerkan method, with values ranging from 66 to 90 %. The higher dispersion for hydraulic conductivity values derived from the disc infiltrometer could be explained by the fact that measurements are very dependent on the quality of the contact between the disc and the soil surface. Despite all the efforts to meet this requirement, it can be quite difficult to fulfill, and therefore affects the kinetics of infiltration. The precise infiltration surface area was also subjected to uncertainty when sand was applied to improve the contact, as the sand could overlap the actual disc surface. Moreover, in sandy soils, local hydrophobicity can occur (especially in rubber tree plantations, where natural rubber can modify water repellent properties of soil), and therefore affects infiltration dynamics and more specifically the measurements with the disc infiltrometer, as soil suction was the driving force. The presence of macro-pores related to biological activity (earthworms, ants, termites) could also partly explain the differences between the Beerkan method and the disc infiltrometer, as with this latter method, water can only infiltrate into the soil matrix.

3.3 Evaporation method and the associated inverse method

Theoretically, the water retention curve obtained from the evaporation method could be considered a reference, for it corresponds to direct experimental data with no model as-

sumed a priori. In order to compare the results more easily with the other methods, the van Genuchten model with Mualem conditions was used to fit to the experimental retention curves. Parameter α varied only in a very narrow interval between 1.8×10^{-4} and $2.5 \times 10^{-4}\,\mathrm{m}^{-1}$, and was found to be equal for both methods. Nevertheless, the values were found to be slightly larger than for the Beerkan method. Values for shape parameter n are significantly different between the two methods, with higher values for the evaporation method. By comparison, the n values obtained with the Beerkan method are much lower than those derived from the evaporation and inverse methods. The scaled retention curves depicted in Fig. 3c for the evaporation method clearly show slight variations between the different situations. A single soil sample from the RT in the midslope position stood out, with a noticeably larger value for n. Saturated hydraulic conductivity obtained with the inverse method was much more important than when determined with other methods, as it ranged from 10 to $22 \times 10^{-6}\,\mathrm{m\,s}^{-1}$. Regarding K_s along the slope, the same pattern was found, namely, showing an increase along the slope from the bottom to the upper position. Unlike the disc infiltrometer and Beerkan methods, K_s for ruzi grass and for forest soils was found to be very different, with a very high K_s value for ruzi grass: $22 \times 10^{-6}\,\mathrm{m\,s}^{-1}$ instead of $6 \times 10^{-6}\,\mathrm{m\,s}^{-1}$ with the other methods.

3.4 Arya method

Van Genuchten water retention parameters were fitted on the experimental curves and showed little variation for parameter α between the different sites, reflecting a low variability of PSD. On the other hand, the values for α were found to be significantly lower than for the other estimation methods. The shape parameter n showed very high variability, with average values ranging from 1.82 for RG to 3.35 for RT-mid and an important standard deviation running from 3 to 67 %. The scaled retention curves (Fig. 3b) for this method were very similar, though the forest soil samples showed a slightly particular behavior. Nevertheless, when all are represented on the same graph, the slight variations of scaled retention curves corresponding to the location of the soil samples seemed negligible compared to the differences due to the measurement methods (Fig. 3a). The value of the shape parameter n represented by the slope of the retention curve was lowest for the Beerkan method, intermediate for Arya method and highest for the evaporation method. Retention curves obtained with the Arya and Beerkan methods were, respectively, strictly based on PSD, and on PSD partly influenced by infiltration data. As for these methods, the values for n were lower, and the pore size distribution was not as sharp as for the evaporation method. One can therefore suppose that part of the porous volume was not drained with the evaporation method. In fact, by imposing a low evaporation rate to avoid overly important hydraulic gradients inside the soil sample, the energy necessary to draw out water from the smallest or less accessible pores is probably not sufficient.

3.5 Statistical analysis

The number of replicates for each method was not equal, because it depended on (i) the time necessary to perform the measurement, and on (ii) the quality of the measurement. For example, only a few evaporation measurements have been performed, as each measurement took up to 2 weeks to be completed. On the other hand, more Beerkan and disc infiltrometer measurements have been performed, as the infiltration experiments lasted only between 30 and 60 min, and between 2 and 6 h, respectively. The number of results was also controlled by the data processing of the infiltration experiment, as some experiments had finally to be discarded.

The statistical analysis of the van Genuchten unsaturated soil water parameters for the different locations with the different experimental techniques was performed with the Kruskal–Wallis non-parametric method. Both κ^2 and p values (Table 4) showed clearly that measured unsaturated soil water parameters were highly dependent on the measurement techniques. As already pointed out on the scaled retention curves, parameter n seemed to be the most dependent on the type of method, considering the high value of κ^2 and the extremely low p value. The shape parameter α showed the highest κ^2 value, but saturated hydraulic conductivity K_s is also highly dependent on the measurement method. The influence of location was found to be secondary or even negligible, with a p value of 0.11, 0.94 and almost 1 for α, n and K_s, respectively, except for α showing a relatively high value for κ^2 (7.15), but still under the acceptable limit (9.49) for the corresponding degrees of freedom (4). Saturated hydraulic conductivity K_s was therefore not a discriminating parameter for the different situations, whereas parameter n tended to show an evolution with the different sites. When data were considered globally, regrouping all the measurement methods, the variability of the results was higher considering the measurement method rather than the measurement location. When studied separately for each measurement method (Table 4), some parameters seemed to differentiate clearly the different sites. For example, with the Beerkan method, the shape parameter n appeared to be significantly different for the different sites. With the pedotransfer function of Arya, scale parameter α was the most discriminating parameter, with an extremely low p value, though parameter n also showed a low p value (< 0.05). In both cases, it was shown that the particle size distribution and the derived parameters were significantly different at the various sites for these two measurement methods. With the others, no clear distinction between the different sites was observed, as the p values were very high, between 0.15 and 0.86.

Table 4. Medians and parameters of Kruskal–Wallis, chi-squared (κ^2), degree of freedom df, and p value for the van Genuchten parameters for different methods and different sites, in general and in detail for each method, $K_S \times 10^{-6}$ ($m\,s^{-1}$) and α (m^{-1}). B: beerkan, I: inverse, A: Arya, E: evaporation, D: disc. * indicates a statistically significant difference between values.

	General	Arya	Beerkan	Disc inf.	Inverse	Evapor.	κ^2	df	p value
	α	0.6	1.6	–	1.9	1.8	28.171	3	3.34×10^{-6}
	K_S	–	7.15	4.76	12.16	–	19.364	2	6.24×10^{-5}
	n	2.979	2.251	–	2.331	3.117	47.981	3	2.15×10^{-10}
		Forest	RT down	RT mid	RT up	Ruzi			
	α	1.9	1.4	1.6	1.5	1.7	7.15	4	1.28×10^{-1}
	K_S	6.42	4.497	8.39	9.53	6.97	4.40	4	3.54×10^{-1}
	n	2.703	2.597	2.318	2.361	2.387	1.72	4	7.87×10^{-1}
Method	Detail	Forest	RT down	RT mid	RT up	Ruzi	κ^2	df	p value
B	K_S	5.99	4.93	8.81	9.53	4.93	4.251	4	0.3731
	α	2.72	1.39	1.59	1.505	1.44	6.16	4	0.1878
	n	2.01	2.06	2.26	2.33	2.20	24.54	4	6.23×10^{-5}*
I	K_S	92.68	90.00	169.86	190.60	140.28	6.35	4	0.1750
	α	1.80	1.90	1.80	2.55	1.80	6.05	4	0.1955
	n	2.28	2.60	2.28	2.18	3.09	6.77	4	0.1490
A	α	1.5	0.6	0.5	0.5	10.9	21.22	4	0.0003*
	n	2.84	2.72	3.4	3.553	2.84	12.97	4	0.0114
E	α	1.8	1.9	1.8	1.9	1.8	1.29	4	0.8627
	n	3.07	3.42	2.89	3.60	4.01	3.47	4	0.483
D	K_S	44.51	25.85	24.24	58.03	59.71	2.71	4	0.6077

3.6 Modeling validation

Unsaturated soil water parameters are generally determined for use in mathematical models simulating soil water flow. Their evaluation was therefore performed with Hydrus1D, and the computed matric potentials at 0.25 m were compared to the experimental data. The different locations could be divided into two distinctive groups where (i) infiltration was strictly 1-D with vertical water flow, corresponding to the forest and ruzi grass, and (ii) with a possible lateral flow component due to the slope in the rubber tree plantation. The results obtained in the forest and at the ruzi grass sites showed good conformity with the experimental data (Fig. 4) and with RMSE values less than 40 hPa and EF values close to unity, especially for the forest site (0.83–0.95). The numerical simulations obtained with unsaturated soil water parameters issued from the different methods show very few differences. In both cases (F and RG), the best fit was obtained with parameters derived from the combination of the Arya method for retention curves and the disc infiltrometer for hydraulic conductivity. Simulations performed with parameters from the Beerkan method showed a slightly higher RMSE value, whereas the results obtained with the evaporation-method-based parameters seemed to fit worse to experimental data. These trends were confirmed by the other modeling evaluation indexes (DR, EF). CRM showed a systematic small negative value for the forest site, regardless of the measurement method, indicating an underestimation in the computed matric potential values. The scatterplots of computed vs. experimental matric pressure heads (Fig. 5) showed good agreement for all models in the forest and a slight underestimation for the high values in the ruzi grass. For the rubber tree plantation, concordance between computed results and experimental data was much worse (Figs. 4 and 5). The general trend was preserved but often overestimated compared to experimental data, as depicted in Table 4 and quantified by CRM in Table 5. During the rainy season, the fit between computed and experimental matric potential was generally better than during the drier period (Fig. 5). This discrepancy can be explained mainly by the slope in the rubber tree plantation and the inevitable subsurface lateral flow. Indeed, in the soil profile, an impervious clayey layer lying over the bedrock promoted the generation of a perched water table during the rainy season. Though the slope of the terrain was only 3 %, the actual slope of the interface on which the water table built up was more important, as the soil profiles increased from upslope to downslope. It has been shown that 40 % of the annual rainfall actually contributed to lateral flow along the slope (Seltacho et al., 2013). Therefore, the water flow in the field was not 1-D, and could not be com-

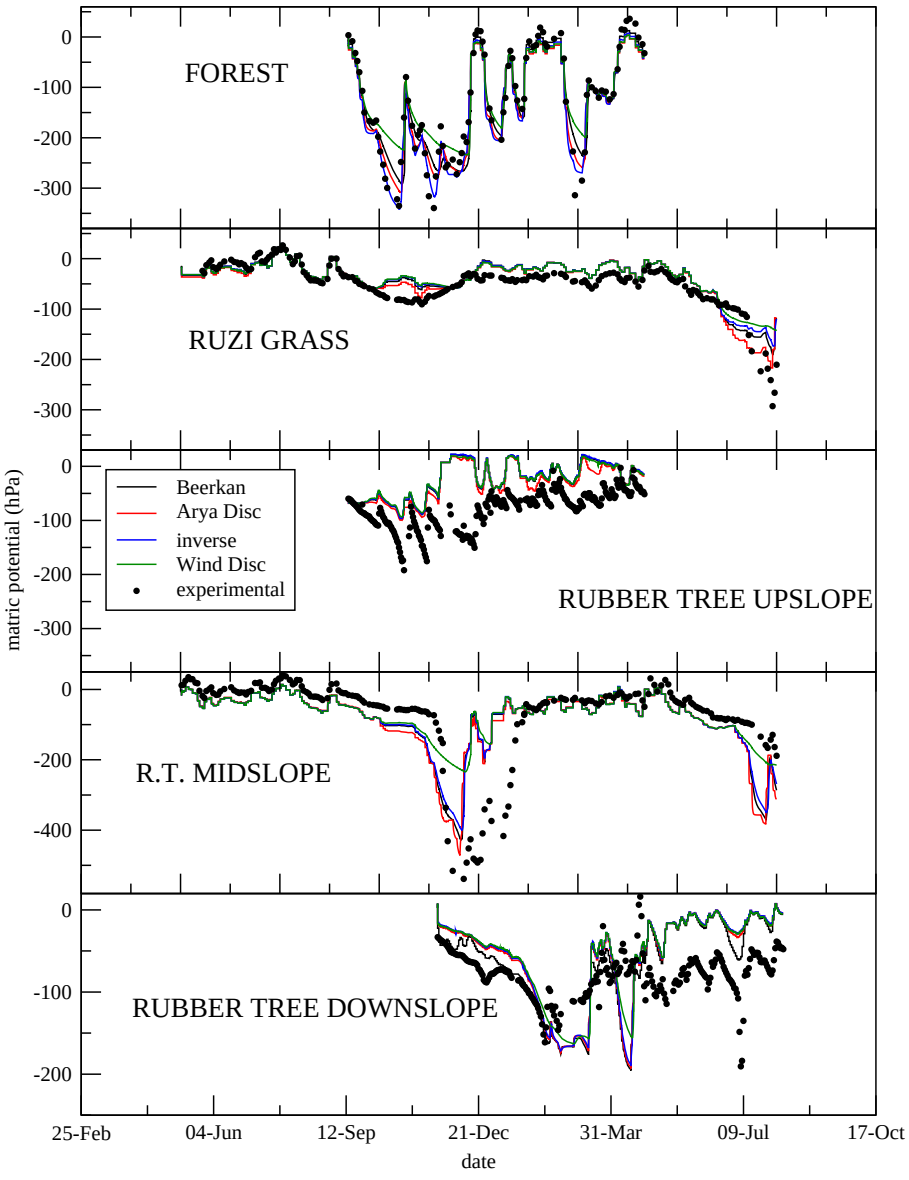


Figure 4. Development of the matric potential at 0.25 m depth in the different locations (black dots) and results of modeling with Hydrus1D (continuous lines).

puted adequately; in upslope and midslope positions, water was lost laterally and accumulated in the downslope position. Nevertheless, when lateral flow was taken into account in a 2-D simulation with Hydrus2D (Seltacho et al., 2013), computed and experimental values fitted well. In any case, when contemplated from a yearly timescale, the differences between the different methods for simulating the water flow in soil seemed negligible in terms of water stock. Regardless of whether the computed results fitted the experimental data, as for forest and ruzi grass, or did not, as with the rubber tree plantation, no method could clearly stand out as being more efficient than any other one in modeling water flow for these different situations. These results are informative about the non-uniqueness of the parameters for modeling water flow in soil. Despite not describing exactly the development of soil water potential, different combinations of soil parameters lead to very similar results when used in Hydrus1D on a yearly timescale. The efforts to determine the soil hydraulic parameters precisely can therefore be seriously questioned. In any case, to improve the modeling performance for a longer time series or to forecast different scenarios, the parameters need to be adjusted by inverse modeling (Seltacho et al., 2013).

Table 5. Four modeling evaluation criteria for matric potential for the different situations with the different parameters used in Hydrus1D.

RMSE (hPa)	Beerkan	Arya disc	Inverse	Evaporation disc
Forest	33.15	27.47	24.09	42.50
Ruzi grass	23.02	22.56	24.45	26.71
RT upslope	64.94	60.06	65.78	64.61
RT midslope	100.59	102.25	99.62	98.25
RT downslope	52.63	49.06	53.21	51.22
DR	Beerkan	Arya disc	Inverse	Evaporation disc
Forest	1.2	1.25	1.05	1.83
Ruzi grass	0.56	1.05	1.42	1.65
RT upslope	0.30	0.35	0.29	0.31
RT midslope	2.43	2.25	2.61	4.87
RT downslope	1.33	0.27	0.24	0.27
ME	Beerkan	Arya disc	Inverse	Evaporation disc
Forest	0.9	0.93	0.95	0.83
Ruzi grass	0.62	0.76	0.72	0.66
RT upslope	−2.47	−1.97	−2.56	−2.44
RT midslope	0.32	0.30	0.33	0.35
RT downslope	0.85	−2.06	−2.60	−2.43
CRM	Beerkan	Arya disc	Inverse	Evaporation disc
Forest	−0.03	−0.06	−0.09	0.08
Ruzi grass	−0.51	0.15	0.24	0.27
RT upslope	0.69	0.62	0.70	0.69
RT midslope	−0.11	−0.15	−0.09	0.02
RT downslope	0.33	0.23	0.35	0.41

4 Discussion

A major result of this study is the apparent high dependence of unsaturated hydraulic properties on the measurement method. Several factors can explain this discrepancy, especially the size of the soil sample on which the measurement has been performed.

The measurements have been performed on soil samples of different sizes for the different methods, depending on the availability of equipment and materials. For example, the diameter of the disc infiltrometer was almost twice the diameter of the infiltration cylinder. However, according to Anderson and Bouma (1997) and Bouma (1980), the representative elementary volume of sandy soil for measuring hydraulic conductivity is usually considered to be around $1 \times 10^{-4}\,m^3$. Consequently, considering the texture (mainly sandy) and especially the lack of structure of the soil in the different locations (except in the forest), the volumes of the soil samples exceed the representative elementary volume. Therefore, despite not having been measured on strictly the same volumes or areas, but still on the order of magnitude (Beerkan $8 \times 10^{-4}\,m^3$, disc infiltrometer $2 \times 10^{-3}\,m^3$, evaporation $1.5 \times 10^{-3}\,m^3$), the results for the different methods should not be affected by the scale.

On the other hand, the differences can be explained by the specific properties of each method with their limitations and inherent assumptions for deriving the parameters.

The Beerkan method is popular for the straightforwardness of the experimental setup and rapid infiltration process; a constant infiltration rate is generally reached in less than an hour. However, the derivation of the unsaturated parameters is based on a rigorous hypothesis about the unsaturated hydraulic properties; namely, they are supposed to follow strictly the retention model of van Genuchten with Burdine's condition and the expression of Brooks and Corey for hydraulic conductivity. Even though this assumption agrees well in most of the cases, situations like bimodal porous networks, for example, are not taken into account.

With the disc infiltrometer, the experiment is more difficult to set up, as it needs a perfectly flat contact between the soil surface and the disc and is prone to many technical failures (leaks, etc.). Moreover, each experiment usually takes a very long time to reach a constant infiltration rate (sometimes several hours for finely textured soils). Wooding's model used to derive saturated hydraulic conductivity from disc infiltration measurements assumes an exponential relationship between hydraulic conductivity and matric potential that is quite different from the van Genuchten function.

The evaporation method is the only one for which the retention curves were actually measured without any a priori model. The slow evaporation rate imposed at the surface generated a very slight tension gradient inside the soil, with a uniform water content distribution. Average water content and pressure head values could therefore be calculated. The drawbacks of this method are the length of time needed for a soil sample to dry completely (up to 2 weeks) and the costly equipment (oven, computer, balance, microtensiometers, pressure gauge, data logger).

The pedotransfer function is an extremely easy method to derive the retention curve based only on particle size distribution. The Arya relationship is physically based, deriving the size of the voids between the grains by assuming a packing model. Nevertheless, as this model, unlike the Beerkan method, is exclusively governed by the PSD and the bulk density of the soil, little information about the the soil structure is available in the computed retention curve.

These technical and theoretical differences between the two infiltration methods can explain the contrast between their results. The shape of the hydraulic conductivity equations, Brooks and Corey for the Beerkan method and an exponential relationship for the disc infiltrometer, are different, especially near saturation. Saturated hydraulic conductivity determined through an exponential function with the Wooding method takes into account pressure head values near saturation, whereas in the BEST procedure, the Brooks and Corey equation is derived over a wider range of pressure head values. Therefore, saturated hydraulic conductivity determined with the disc infiltrometer is higher than when derived with the Beerkan method (Simunek et al., 1998b).

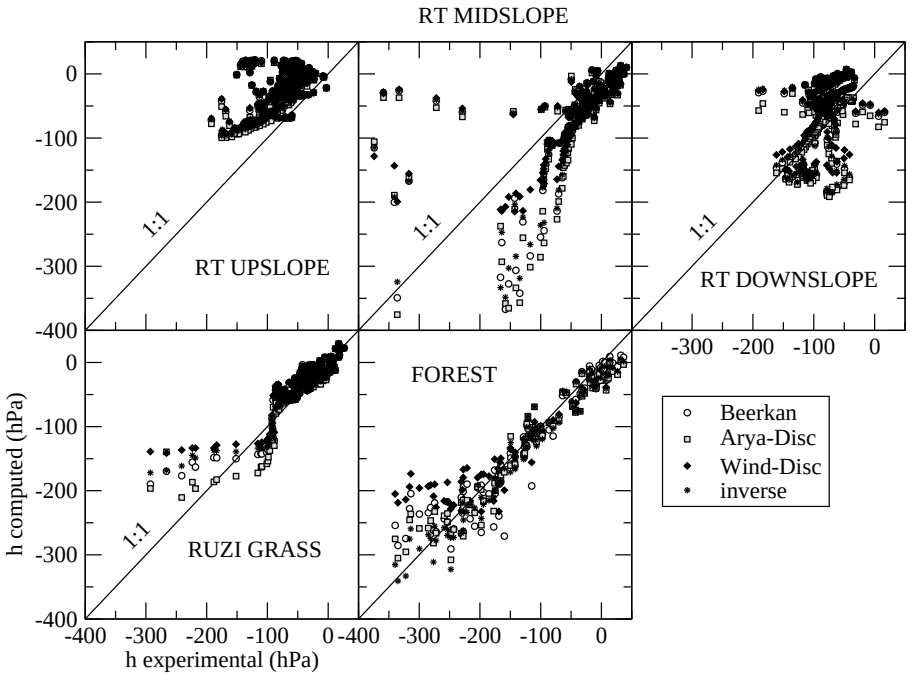


Figure 5. Scatterplots of computed vs. experimental matric potential values in the different locations for different combinations of parameters.

When K_s is derived by inverse modeling from the evaporation experiment, it is systematically higher than with the infiltration methods. The use of the van Genuchten equation (Eq. 4) with Mualem conditions in the fitting procedure seems to be responsible for the overestimation of K_s. More generally, the use of different type of equations, valid in different domains of pressure head or soil water content to derive K_s, invariably leads to a wide range of values. The same conclusions could be drawn for the scale and shape parameters (α and n), as equivalent procedures were used to derive them.

Nevertheless, for each measurement method, a decrease in hydraulic conductivity down the slope in the rubber tree plantation was systematically observed, and could probably be related to the translocation of finer particles downslope (Wiriyakitnateekul et al., 2009). Despite showing slightly higher levels of organic matter, and unlike what would commonly be expected, forest soil had the lowest hydraulic conductivity. The higher content in finer particles (clay and silt) was most probably responsible for lower K_s values at the forest site and to some extent at the ruzi grass site. During the early stages of the rubber tree plantation, the soil surface was not covered and was therefore more vulnerable to erosion. The fine soil particles were translocated downslope and down the soil profile, whereas under forest and ruzzi grass clay translocation was not as active.

The final use of these van Genuchten (VG) parameters was to use them in Hydrus1D to compute the water balance at these different sites. This study showed clearly that the uniqueness of VG parameters did not apply in this case, as many different combinations provided similar or equivalent results when a yearly timescale was considered. The simulation results obtained with the parameters derived from different methods were generally equivalent when the different validation parameters were considered. In any case, to perform efficient and reliable modeling of water flow in soil, these parameters should be carefully adjusted by inverse modeling procedures on experimental data over a time series describing contrasted situations and then validated. The measured VG parameters should be used as appropriate first guess values for the inverse modeling procedure. No single method could be considered without doubt as producing better results than the others. It should therefore be recommended to use the easiest and cheapest methods for the experimental evaluation of the first set of VG parameters and, in this case, the Beerkan method would surely be the best option.

5 Conclusions

In order to determine the unsaturated hydraulic properties of soil for different land use, several experimental methods have been used in a small watershed in northeastern Thailand. They included laboratory methods like the evaporation method, inverse methods and PTF (Arya et al., 1999), and also field evaluations like the Beerkan method and a disc infiltrometer.

Statistical analysis of the results obtained during this study showed clearly that significative differences in VG parame-

ter measurements appeared, depending on the measurement method. Though the impact of land use and position was not completely negligible, the primary factor for measurement variability was found to be in the experimental methods. It was stated that the actual values of VG parameters depend on the method employed to determine them. However, when each measurement method was considered separately, the discrimination by site was significant for the Beerkan method and Arya's PTF method. As both methods are based on particle size distribution, parameters n and α, respectively, could distinguish the different sites. Unsaturated soil properties of this sandy soil seemed to be governed mainly by textural parameters related to the pedogenesis rather than by structural properties associated with land use and management.

Amongst the different methods tested in this study, none could clearly be considered superior to the others in terms of providing better parameters for modeling soil water flow. Therefore, the cheapest and easiest method to derive the VG parameters, like the Beerkan method, should be used to fulfill this task. The important land use changes taking place in northeastern Thailand can therefore be evaluated easily with numerical modeling and the consequences of rubber tree plantation for the water balance on different scales can therefore be predicted (Seltacho et al., 2013).

The Supplement related to this article is available online at doi:10.5194/hess-19-1193-2015-supplement.

Acknowledgements. The work was funded by IRD (Institut de Recherche pour le Développement), UMR210, the Land Development Department (LDD), the Groundwater Research Center of Khon Kaen University and the PHC-Siam Franco-Thai cooperation program. We would also like to express our thanks to the research assistants of IRD for their valuable contribution to the field measurements (Nitjaporn Koonklang, Worraphan Chintachao and Weerawut Yotjamrut), and the staff of the Land Development Department laboratory. Finally, we were very grateful to Apichai Keansuwan and Vachira Jariyapaiboon, respectively, the owner and manager of the rubber tree plantation, for giving us the opportunity to perform this experiment in this field.

In memory of our colleague and friend Roland Poss.

Edited by: B. Kronvang

References

Ankeny, M. D., Ahmed, M., Kaspar, T. C., and Horton, R.: Simple field method for determining unsaturated hydraulic conductivity, Soil Sci. Soc. Am. J., 55, 467–470, 1991.

Anderson, J. L., and Bouma, J.: Relationships between hydraulic conductivity and morphometric data of an argillic horizon, Soil Sci. Soc. Am. Proc., 37, 413–421, 1997.

Angulo Jaramillo, R., Vandervaere, J.-P., Roulier, S., Thony, J.-L., Gaudet, J.-P., and Vauclin, M.: Field measurement of soil surface hydraulic properties by disc and ring infiltrometers: a review and recent developments, Soil Till. Res., 55, 1–29, 2000.

Antonino, A. C. D., Angulo-Jaramillo, R., Hammecker, C., Netto, A. M., Montenegro, S. M. L. G., Lira, C. A. B. O., and Cabral, J. J. S. P. A.: A simplified water transfer model of the reservoir-ebb tide system, including preferential flow, in the semi-arid region in Northeastern Brazil, J. Hydrol., 287, 147–160, 2004.

Anuraga, T., Ruiz, L., Kumar, M. M., Sekhar, M., and Leijnse, A.: Estimating groundwater recharge using land use and soil data: a case study in South India, Agr. Water Manage., 84, 65–76, 2006.

Arya, L. M. and Paris, J. F.: A physicoempirical model to predict the soil moisture characteristics from particle-size distribution and bulk density data, Soil Sci. Soc. Am. J., 45, 1023–1030, 1981.

Arya, L. M., Leij, F. J., Shouse, P. J., and van Genuchten, M. T.: Relationship between the hydraulic conductivity function and the particle-size distribution, Soil Sci. Soc. Am. J., 63, 1063–1070, 1999.

Bittelli, M. and Flury, M.: Errors in water retention curves determined with pressure plates, Soil Sci. Soc. Am. J., 73, 1453–1460, 2009.

Bouma, J.: Field measurement of soil hydraulic properties characterizing water movement through swelling clay soils, J. Hydrol., 4, 149–158, 1980.

Bouma, J.: Using soil survey data for quantitative land evaluation, Adv. Soil S., 9, 177–213, 1989.

Braud, I., De Condappa, D., Soria, J. M., Haverkamp, R., Angulo-Jaramillo, R., Galle, S., and Vauclin, M.: Use of scaled forms of the infiltration equation for the estimation of unsaturated soil hydraulic properties (the Beerkan method), Eur. J. Soil Sci., 56, 361–374, 2005.

Brooks, R. H. and Corey, C. T.: Hydraulic properties of porous media, Hydrol. Paper 3, Colorado State University, Fort Collins, 1964.

Bruckler, L., Bertuzzi, P., Angulo-Jaramillo, R., and Ruy, S.: Testing an infiltration method for estimating soil hydraulic properties in the laboratory, Soil Sci. Soc. Am. J., 66, 384–395, 2002.

Burdine, N. T.: Relative permeability calculation from pore size distribution data, Petr. Trans. Am Inst. Min. Metall. Eng., 198, 71–77, 1953.

Haverkamp, R., Arrue, J. L., Vandervaere, J.-P., Braud, I., Boulet, G., Laurent, J. P., Taha, A., Ross, P. J., and Angulo-Jaramillo, R.: Hydrological and thermal behaviour of the vadose zone in the area of Barrax and Tomelloso (Spain): experimental study, analysis and modeling Project UE no EV5C-CT 92 00 90, Laboratoire d'étude des Transferts en Hydrologie et Environnement, Grenoble, 1996.

Haverkamp, R., Bouraoui, C., Zammit, R., Angulo-Jaramillo, R., and Delleur, J. W.: Soil properties and moisture movement in the unsaturated zone, in: The Handbook of Groundwater Engineering, edited by: Delleur, J. W., CRC, Boca Raton, FL, 2931–2935, 1998.

Heddadj, H. and Gascuel-Odoux, C.: Topographic and seasonal variations of unsaturated hydraulic conductivity as measured by tension disc infiltrometers at the field scale, Eur. J. Soil Sci., 50, 275–283, 1999.

Jing, Y.-S., Zhang, B., Thimm, A., and Zepp, H.: Anisotropy of soil hydraulic properties along arable slopes, Pedosphere, 18, 353–362, 2008.

Kim, D. J., Angulo-Jaramillo, R., Vauclin, M., Feyen, J., and Choi, S. I.: Modeling of soil deformation and water flow in a swelling soil, Geoderma, 92, 217–238, 1999.

Klute, A. and Dirksen, C.: Hydraulic conductivity and diffusivity: laboratory methods, in: Methods of Soil Analysis, Part 1. Physical and Mineralogical Methods, edited by: Klute, A., 2nd Edn., ASA and SSSA, Madison, WI, 687–734, 1986.

Lassabatere, L., Angulo-Jaramillo, R., Soria Ugalde, J. M., Cuenca, R., Braud, I., and Haverkamp, R.: Beerkan, Estimation of soil transfer parameters through infiltration experiments – BEST, Soil Sci. Soc. Am. J., 70, 521–532, 2006.

Loague, K. M. and Green, R. E.: Statistical and graphical methods for solute transport models, J. Contam. Hydrol., 7, 51–73, 1991.

Mohammadi, M. H. and Vanclooster, M.: Predicting the soil moisture characteristic curve from particle size distribution with a simple conceptual model, Vadose Zone J., 10, 594–602, 2011.

Mualem, Y.: A new model for predicting the hydraulic conductivity of unsaturated porous media, Water Resour. Res., 12, 513–522, 1976.

Pachepsky, Y. A., Rawls, W., and Lin, H.: Hydropedology and pedotransfer functions, Geoderma, 131, 308–316, 2006.

Pachepsky, Y. A. and Rawls, W. J.: Soil structure and pedotransfer functions, Eur. J. Soil Sci., 54, 443–452, 2003.

Perroux, K. M. and White, I.: Design for disc permeameters and soil dispersion, Soil Sci. Soc. Am. J., 48, 50–55, 1988.

Price, K., Jackson, C. R., and Parker, A. J.: Variation of surficial soil hydraulic properties across land uses in the southern Blue Ridge Mountains, North Carolina, USA, J. Hydrol., 383, 256–268, 2010.

Rantala, L.: Rubber plantation performance in the Northeast and East of Thailand in relation to environmental conditions, Ms thesis, Dep. of Forest Ecology, University of Helsinky, Finland, 70 pp., 2006.

R Development Core Team: R: A Language and Environment for Statistical Computing, R Foundation for Statistical Computing, Vienna, Austria, available at: http://www.R-project.org (last access: 22 November 2013), 2008.

Richard, G., Sillon, J., and Marloie, O.: Comparison of inverse and direct evaporation methods for estimating soil hydraulic properties under different tillage practices, Soil Sci. Soc. Am. J., 65, 215–224, 2001.

Richards, L. A.: Capillary conduction of liquids through porous media, J. Appl. Phys., 1, 318–333, doi:10.1063/1.1745010, 1931.

Seltacho, S., Sriboonlue, V., Suwanang, N., Wiriyakitnateekul, W., and Hammecker, C.: Quantification and modeling of water flow in sandy soils in Northeast Thailand, in: Advances in Unsaturated Soils, edited by: Caicedo, B., Murillo, C., Colmenares, L. H. J. E., and Berdugo, I. R., CRC Press, London, 573–577, 2013.

Simunek, J., Wendroth, O., and van Genuchten, M. T.: Parameter estimation analysis of the evaporation method for determining soil hydraulic properties, Soil Sci. Soc. Am. J., 62, 894–905, 1998a.

Simunek, J., Wang, D., Shouse, P. J., and Van Genuchten, M. T.: Analysis of field tension disc infiltrometer data by parameter estimation, Int. Agrophys., 12, 167–180, 1998b.

Simunek, J., van Genuchten, M. T., and Sejna, M.: The HYDRUS-1D software package for simulating the movement of water, heat and multiple solutes in a variably saturated media, Version 3.0 HYDRUS, University of California Riverside, Riverside, California, USA, 2005.

Smettem, K. R. J. and Clothier, B. E.: Measuring unsaturated sorptivity and hydraulic conductivity using multiple disc permeameters, J. Soil Sci., 40, 563–568, 1989.

Soares, J. V. and Almeida, A. C.: Modeling the water balance and soil water fluxes in a fast growing Eucalyptus plantation in Brazil, J. Hydrol., 253, 130–147, 2001.

Stolte, J., Freijer, J. I., Bouten, W., Dirksen, C., Halbertsma, J. M., van Dam, J. C., van den Berg, J. A., Veerman, G. J., and Wösten, J. H. M.: Comparison of six methods to determine unsaturated soil hydraulic conductivity, Soil Sci. Soc. Am. J., 58, 1596–1603, 1994.

Tamari, S., Bruckler, L., Halbertsma, J., and Chadoeuf, J. A.: Simple method for determining soil hydraulic properties in the laboratory, Soil Sci. Soc. Am. J., 57, 642–651, 1993.

van Genuchten, M. T.: A closed form equation for predicting the hydraulic conductivity of unsaturated soils, Soil Sci. Soc. Am. J., 44, 892–898, 1980.

Wendroth, O., Ehlers, W., Hopmans, J. W., Kage, H., Halbertsma, J., and Wosten, J. H. M.: Reevaluation of the evaporation method for determining hydraulic functions of unsaturated soils, Soil Sci. Soc. Am. J., 57, 1436–1443, 1993.

Wind, G. P.: Capillary conductivity data estimated by a simple method, in: Water in the Unsaturated Zone, Vol. 1, edited by: Rijtema, P. E. and Wassink, H., Proc. Wageningen Symp., June 1966, Int. Assoc. Scientific Hydrol., Gentbrugge, Belgium, 181–191, 1968.

Wiriyakitnateekul, W. C., Hammecker, C., Anusontpornperm, S., and Boonrod, S.: Clay mineralogy of soils developed on sandstone along a toposequence in Northeast Thailand, XIV International Clay Conference, 14–20 June 2009, Castellaneta Marina, Italy, 520–520, 2009.

Wooding, R. A.: Steady infiltration from a shallow circular pond, Water Resour. Res., 4, 1259–1273, 1968.

Zimmermann, B., Elsenbeer, H., and De Moraes, J. M.: The influence of land-use changes on soil hydraulic properties: implications for runoff generation, Forest Ecol. Manage., 222, 29–38, 2006.

ResearchGate

See discussions, stats, and author profiles for this publication at: https://www.researchgate.net/publication/282496772

Heterosis and Combining Ability of F Hybrid Sweet Sorghum in Thailand

Article *in* Crop Science · January 2015

DOI: 10.2135/cropsci2014.05.0363

CITATION
1

READS
40

5 authors, including:



Darika Bunphan
Faculty of Technology Mahasarakham Univer…
3 PUBLICATIONS **2** CITATIONS
SEE PROFILE



Jirawat Sanitchon
Srinagarind Hospital - Khon Khaen Universit…
37 PUBLICATIONS **188** CITATIONS
SEE PROFILE



Joseph E. Knoll
United States Department of Agriculture
25 PUBLICATIONS **329** CITATIONS
SEE PROFILE

Some of the authors of this publication are also working on these related projects:



Evaluation of the tolerance of Thai indigenous upland rice germplasm to early drought stress using multiple selection criteria View project



Southeastern Biofuel Feedstock Production View project

All content following this page was uploaded by Darika Bunphan on 28 July 2016.

The user has requested enhancement of the downloaded file.

RESEARCH

Heterosis and Combining Ability of F_1 Hybrid Sweet Sorghum in Thailand

Darika Bunphan, Prasit Jaisil, Jirawat Sanitchon, Joseph E. Knoll,* and William F. Anderson

ABSTRACT

Sweet sorghum [*Sorghum bicolor* (L.) Moench] is a sugar-based biofuel crop that is well-suited to tropical environments. Most sweet sorghum cultivars are open-pollinated, but hybrids could offer yield and seed production advantages. Fifteen hybrids were generated among five female and three male parents. The hybrids, parents, and three inbred checks were evaluated for sugar yield and related traits under two environments in Thailand in 2013: Field Crop Research Station at Khon Kaen University, Khon Kaen, and National Corn and Sorghum Research Center, Nakhon Ratchasima. Theoretical sugar yield was positively correlated with juice dissolved solids (Brix), plant height, stalk diameter, biomass yield, stripped stalk yield, and theoretical juice yield. Grain yield was negatively correlated with juice dissolved solids and theoretical sugar yield. Positive heterosis for juice dissolved solids was not observed, though five hybrids had negative mid-parent heterosis for this trait. Positive heterosis for biomass yield, theoretical juice yield, and grain yield was observed in some hybrids. General combining ability was observed for most traits, but specific combining ability (SCA) effects were of greater importance. Overall, the hybrids KKA-11 × BJ248, KKA-11 × KKU40, KKA-139 × BJ248, KKA-14 × KKU40, and KKA-53 × Theis had the greatest SCA for theoretical sugar yield. In producing ethanol from both sugar and grain fractions, two of the hybrids in this study (KKA-11 × BJ248 and KKA-139 × BJ248) could produce approximately 4600 L ha^{-1} ethanol in Thailand.

D. Bunphan, P. Jaisil, and J. Sanitchon, Plant Breeding Research Center for Sustainable Agriculture and Dep. of Plant Science and Agricultural Resources, Faculty of Agriculture, Khon Kaen Univ., Khon Kaen 40002, Thailand; and J.E. Knoll and W.F. Anderson, USDA–ARS, Crop Genetics and Breeding Research Unit, 115 Coastal Way, Tifton GA 31793. Received 15 May 2014. *Corresponding author (Joe.Knoll@ars.usda.gov).

Abbreviations: E, environment; G, genotype; GCA, general combining ability; HPH, high-parent heterosis; KKU, Khon Kaen University; LPH, low-parent heterosis; MPH, mid-parent heterosis; NCSRC, National Corn and Sorghum Research Center; QTL, quantitative trait loci; SCA, specific combining ability.

Sweet sorghum (*Sorghum bicolor* (L.) Moench) is a promising biofuel crop, which accumulates soluble sugars in its stalk, similar to its close relative sugarcane (*Saccharum officinarum* L.). Sweet sorghum accumulates 100 to 250 g L^{-1} sugar in its stem juice near grain maturity (Reddy et al., 2008; Ritter et al., 2008). The juice is suitable as a feedstock for direct fermentation to ethanol or for production of other bio-based chemicals that use sugars as reactant. The leaves, bagasse, and grain portions of the crop can also be used to produce biofuels or can be used as animal feed. The bagasse can be burned for heat or power generation, or used to make valuable coproducts, such as pulp and particle board (Somani and Taylor, 2003). As a biofuel crop, sweet sorghum has many favorable characteristics, such as wide adaptability, rapid growth (Reddy and Reddy, 2003; Reddy et al., 2008), drought tolerance (Reddy and Reddy, 2003; Tesso et al., 2005), waterlogging tolerance, salinity resistance (Reddy and Reddy, 2003; Almodares et al., 2008), and high biomass production (Almodares and Hadi,

Published in Crop Sci. 55:178–187 (2015).
doi: 10.2135/cropsci2014.05.0363
© Crop Science Society of America | 5585 Guilford Rd., Madison, WI 53711 USA

All rights reserved. No part of this periodical may be reproduced or transmitted in any form or by any means, electronic or mechanical, including photocopying, recording, or any information storage and retrieval system, without permission in writing from the publisher. Permission for printing and for reprinting the material contained herein has been obtained by the publisher.

2009; Reddy and Reddy, 2003). It should be well-suited to the tropical growing environment of Thailand.

Although sweet sorghum is highly productive, replacing the current inbred line sweet sorghum cultivars with hybrids could increase stalk and sugar yields. The development of hybrid sorghum relies on a cytoplasmic-genetic male sterility system, which requires male-sterile (A), sterility-maintainer (B), and fertility-restorer (R) lines. An A-line (female) and R-line (male) are crossed to produce a male-fertile F_1 hybrid. A B-line (male) is crossed with its sister A-line to regenerate the male-sterile seed parent. This system has been used for decades in grain and forage sorghum, but only recently has it been applied to sweet sorghum. In sweet sorghum, nonrestorer B-lines can also be used as pollen parents if male-sterile hybrids that do not produce grain are desired (Pfeiffer et al., 2010). This is, however, not practical in regions where sorghum ergot (*Claviceps africana* Frederikson, Mantle and De Milliano) is endemic, as sterile florets are more easily infected by this fungus (Pfeiffer et al., 2010; Bandyopadhyay et al., 1998). This disease has been reported in Thailand (Bandyopadhyay et al., 1998), so fertile grain-producing hybrids will be needed in this region.

Recent studies have shown the value of using hybrid sweet sorghum for biofuel production. Makanda et al. (2009) studied combining ability in 64 hybrids of sweet sorghum under off-season (winter) conditions in the tropical lowlands of Mozambique and South Africa. Two male lines, ZLR1 and ICSVP3046, showed significant and positive general combining ability (GCA) effects for juice dissolved solids (Brix), while 13 crosses showed positive and significant specific combining ability (SCA) effects. In general the hybrids had greater biomass than the inbreds, contributing to greater sugar production in this study. Indhubala et al. (2010) studied 35 F_1 hybrids, derived from five females and seven males. Thirteen characteristics were measured including plant height, stem thickness, days to 50% flowering, grain yield, total biomass yield, fresh stripped cane yield, juice yield, juice extractability, juice Brix and related sugar traits, and ethanol yield. Overall, males showed greater GCA effects than the females for most traits, but as in other studies, SCA effects were of greater significance. Pedersen et al. (2013) created hybrids using six A-lines and six sweet sorghum cultivars as pollen parents, and then evaluated them for sugar, biomass, and grain production in Nebraska. The results showed that five of the A-lines could be used as seed parents (A-Dwarf Kansas Sourless, AKS9, A-N36, A-N39, and A-N4692) to produce hybrids with sugar yields that were usually comparable to those of the inbred male parents. Heterosis for most traits was not widely observed in this study, and only one hybrid showed positive high-parent heterosis (HPH) for sugar yield. However, hybrids tended to have increased grain yields compared with their inbred male parents. In the absence of heterosis, hybrids still have an advantage in that hybrid seed can be easily produced in large quantities on short-statured plants. Reddy et al. (2011) conducted a very large study of 171 hybrids from 19 female and 9 male parents. They grew these under both rainy and post-rainy seasons in India and observed that SCA effects were more important than GCA effects for sugar yield and that genotype by environment interaction was highly significant. They identified different sets of crosses that were best suited to growing in the different seasons.

Because of strong genotype by environment (G × E) effects, such tests need to be conducted in the target environments where the hybrids will be grown, but relatively few studies of heterosis in sweet sorghum hybrids have been reported in Thailand. Pothisoong and Jaisil (2011) studied 20 F_1 hybrids of sweet sorghum during the dry season that were crossed from 10 female and 2 male parents. Heterosis for some traits was observed. The objectives of the current study were to evaluate the general and specific combining abilities for sugar yield and related traits of 8 parents and 15 hybrids of sweet sorghum and to measure heterosis of those hybrids to determine which crosses are most effective to grow as feedstock for bio-ethanol production in Thailand.

MATERIALS AND MATHODS

Plant Materials

Five male-sterile A-lines (KKA-11, KKA-14, KKA-48, KKA-53, and KKA-139) were used as female parents. Each female was crossed to each of three male-fertile lines (KKU40, BJ248, and Theis) in line × tester design to produce 15 F_1 hybrids. All five females and male KKU40 were developed at Khon Kaen University. BJ248 was introduced from China and Theis was introduced from the United States (Broadhead et al., 1978). Three cultivars, Keller (Broadhead, 1982), Urja, and Suwan Sweet Extra, were used as check varieties. Suwan Sweet Extra was developed from three sweet sorghum cultivars (Suwan Sweet 3, KKU40, and Urja) and was selected for high sugar yields. All 15 hybrids, 8 parents, and 3 checks were evaluated in the field experiments. The female parents were represented in the experiments by their male-fertile (B-line) versions.

Experimental Sites

The experiment was conducted in two different environments: Field Crops Research Station, Khon Kaen University (KKU), Khon Kaen Thailand (latitude 16°26′ N and longitude 102°50′ E, altitude 190 m above sea level, average rainfall 1327 mm yr^{-1}, average temperature 27.8°C, humidity 85.4%, and soil texture—sand); and National Corn and Sorghum Research Center (NCSRC), Nakhon Ratchasima, Thailand (latitude 14°30′ N and longitude 101°0′ E, altitude 388 m above sea level, rainfall 1000–2000 mm yr^{-1}, average temperature 30°C, humidity 85%, and soil texture—clay). The monthly rainfall and monthly average temperatures recorded at both environments are presented in Fig. 1. The experiment was conducted in a randomized complete block design with three replications in each environment. Each plot was four rows of 4-m length with 75 × 10 cm spacing.

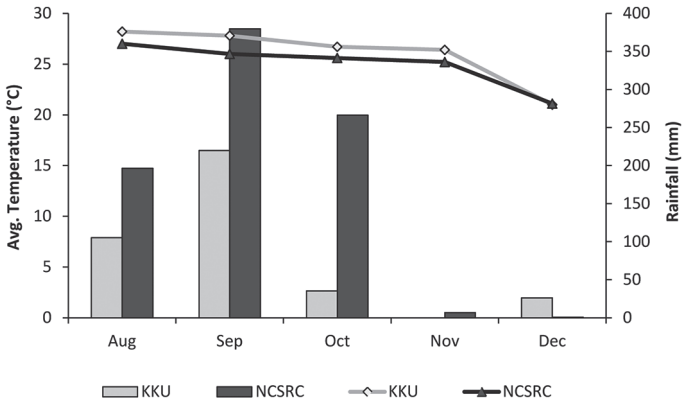


Figure 1. Average temperature (lines; left vertical axis) and monthly rainfall (bars; right vertical axis) from August to December 2013 at Khon Kaen University (KKU) and National Corn and Sorghum Research Center (NCSRC) in Thailand.

Planting occurred on 22 Aug. 2013 at KKU and 9 Sept. 2013 at NCSRC. Recommended agronomic practices were followed throughout the crop season. A basal fertilizer (grade 15–15–15 NPK at rate 156 kg ha^{-1}) was applied at planting and again 1 mo after planting at the same rate. The fields were kept weed free by hand-weeding just before applying fertilizer. Irrigation was applied once per week in each environment, as needed to maintain leaf turgor, unless sufficient rainfall was received. Each plot was harvested by hand approximately 30 d after anthesis (hard dough stage), and only the middle two plot rows were harvested to minimize edge effects. Harvesting occurred during December 2013 at KKU and from December 2013 through early January 2014 at NCSRC.

Data Collection

Days to 50% flowering were recorded when half the plants in a plot shed pollen. Total biomass yield including leaves and panicles was measured using all plants from the middle two plot rows, excluding the edge plants. At harvest, 10 randomly chosen plants per plot were sampled for plant height, panicle length, stalk diameter, juice yield, and juice soluble solids. Plant height was measured from the ground to panicle tip, and panicle length was measured from the first primary branch to the panicle tip. Stalk diameter was measured using a digital vernier caliper at three positions along the stalk: one-quarter, one-half, and three-quarters of the height of the stalk between the ground and flag leaf. The average of these three measurements was recorded. Grain yield was measured from these same 10 plants. Panicles were removed and allowed to dry in the sun for 2 d and were then manually threshed. Grain yield was then converted to Mg ha^{-1} on the basis of plant and row spacing. After removing leaves and panicles, the 10 stalks were weighed and then passed through a small diesel-powered sugarcane extractor three times to quantify actual juice yields. Juice dissolved solids (also known as Brix, and assumed to be mostly sugars) was measured using a hand-held refractometer. The juice and bagasse were weighed after extraction; on average, approximately 7.6% of total stripped stalk mass was lost in the extraction process. The bagasse was then dried in an oven at 80°C until constant weight (approximately 72 h) to measure dry stripped stalk yield. Theoretical juice yield was estimated by subtracting dry stripped stalk yield from fresh stripped stalk yield. Theoretical sugar yield was estimated from theoretical juice yield using the following formula, adapted from Somani and Taylor (2003):

$$\text{Sugar yield (kg ha}^{-1}) = [(\text{Brix} - 3)/100] \times \text{SG} \times \text{juice yield (L ha}^{-1})$$

where Brix is the juice dissolved solids in degrees Brix (1°Bx = 1 g sucrose in 100 g solution) and SG is the specific gravity of the sweet sorghum juice.

Statistical Analysis

Analysis of variance was performed using PROC GLIMMIX in SAS v. 9.3 (SAS Institute). Location, entry, and location × entry were included as fixed effects with replications as a random effect, nested within location. Theoretical sugar yield was log-transformed before ANOVA using the DIST = LOGNORMAL option in the MODEL statement, and all means comparisons for this trait were made on the log scale. Back-transformed values are reported. Mid-parent heterosis (MPH) and high-parent heterosis (HPH) were calculated for all traits according to Hayes et al. (1955). Low-parent heterosis (LPH) was calculated as the percentage deviation from the lowest performing parent in a cross. Tukey's HSD test was used to compare means and to determine significance of heterosis. All differences are declared significant at $\alpha \leq 0.05$. Correlations between juice dissolved solids, days to flowering, plant height, stalk diameter, stripped stalk yield, biomass yield, theoretical juice yield, theoretical sugar yield, grain yield, and panicle length were computed using PROC CORR in SAS (SAS).

Analysis of variance for combining ability was performed using only the data from hybrid entries. Location, female parent effect (GCA_{female}), male parent effect (GCA_{male}), and all possible interactions were included as fixed effects with replications as a random effect, nested within location. Significance of individual GCA and SCA effects was determined using the analysis of means (PDIFF = ANOM) option in the LSMEANS statement.

RESULTS

Field Performance of F_1 Hybrids, Parental Lines, and Check Varieties

The mean performance of 15 F_1 hybrids, their parents, and checks for 11 characteristics, averaged over both environments (KKU and NCSRC), are presented in Table 1. The mean number of days to flowering was not different between the two locations. The check variety Suwan Sweet Extra was the latest flowering (74.8 d), while the hybrid KKA-48 × KKU40 flowered earliest (65 d) on average (Table 1). Several entries showed an interaction with environment: KKB-11, KKA-139 × BJ248, and KKA-53 × BJ248 flowered earlier at KKU, while BJ248 and KKA-14 × BJ248 flowered earlier at NCSRC (data not shown). Overall, Suwan Sweet Extra and KKU40 had the highest juice dissolved solids readings (203 and 177 g kg^{-1}, respectively), while KKA-48 × BJ248 was lowest (102 g kg^{-1}; Table 1). The mean juice dissolved solids reading at harvest was greater at KKU (153 g kg^{-1}) than at NCSRC

Table 1. Mean performance of 15 sorghum F_1 hybrids, their parents, and three check varieties for key biofuel traits, averaged across two locations (Khon Kaen University and National Corn and Sorghum Research Center) in Thailand in 2013.

Entry	Days to flowering	Dissolved solids	Plant height	Stem diameter	Biomass yield	Stripped stalk yield	Theoretical juice yield	Juice extractability	Grain yield	Panicle length	Theoretical sugar yield†
	d	g kg^{-1}	cm	mm	Mg ha^{-1}	Mg ha^{-1}	L ha^{-1}	%	Mg ha^{-1}	cm	Mg ha^{-1}
KKB-11	72.5	147	245	15.0	66.0	35.0	28,954	34.3	5.15	21.5	3.42 bcd
KKB-139	68.0	123	237	15.2	73.1	36.0	30,477	40.5	5.77	22.9	2.76 cdef
KKB-14	66.2	146	236	15.3	63.3	32.9	27,554	36.7	6.02	23.5	3.11 bcdef
KKB-48	67.0	119	223	15.6	58.3	33.0	27,773	36.7	5.38	23.2	2.40 defg
KKB-53	68.3	146	237	14.9	68.3	30.1	24,827	37.1	5.87	22.3	2.82 cdef
BJ248	73.7	158	188	15.4	57.4	32.2	26,669	36.7	4.26	24.2	3.43 bcd
KKU40	70.7	167	262	15.7	74.7	39.3	37,404	45.1	3.67	25.4	5.69 a
Theis	71.0	148	267	16.4	82.3	41.3	34,934	43.4	4.77	26.9	4.10 abc
KKA-11 × BJ248	72.5	107	260	17.3	83.7	46.8	39,470	40.9	7.83	24.0	3.01 cdef
KKA-11 × KKU40	66.2	135	228	16.0	68.1	37.9	31,844	40.5	5.64	26.5	3.25 bcde
KKA-11 × Theis	66.7	106	192	14.7	57.3	24.4	20,645	38.7	5.47	24.7	1.48 h
KKA-139 × BJ248	68.0	145	221	16.7	76.4	35.4	29,803	35.6	6.98	24.6	3.40 bcd
KKA-139 × KKU40	70.2	125	251	14.7	76.5	34.1	28,381	36.5	7.04	23.7	2.54 def
KKA-139 × Theis	66.8	130	226	15.7	66.4	31.9	26,862	41.0	5.47	24.4	2.65 def
KKA-14 × BJ248	68.8	107	227	15.4	67.2	32.0	27,178	33.2	6.31	23.9	2.09 fgh
KKA-14 × KKU40	70.5	133	266	16.0	78.9	38.4	32,228	42.2	5.66	25.6	3.35 bcd
KKA-14 × Theis	65.3	144	236	14.5	52.9	24.4	20,148	38.5	4.59	24.1	2.37 defg
KKA-48 × BJ248	68.2	102	237	16.8	89.3	42.1	35,907	38.0	6.43	24.8	2.33 defg
KKA-48 × KKU40	65.0	108	233	15.9	82.4	40.6	34,712	36.8	7.47	24.0	1.65 gh
KKA-48 × Theis	71.7	133	218	13.6	50.6	24.9	20,612	39.5	3.98	22.2	2.14 efgh
KKA-53 × BJ248	69.5	147	216	14.2	56.8	30.4	25,336	35.1	4.78	26.7	2.97 cdef
KKA-53 × KKU40	69.8	123	235	14.6	70.4	33.9	28,520	36.9	5.49	25.1	2.70 cdef
KKA-53 × Theis	70.5	129	246	15.9	68.8	40.0	33,824	41.2	2.95	25.4	3.40 bcd
Keller	69.3	177	262	15.8	74.7	44.4	33,588	44.0	4.17	22.4	4.66 ab
Suwan Sweet Extra	74.8	203	267	15.7	66.7	38.4	31,085	38.0	2.23	23.5	5.62 a
Urja	71.3	133	236	16.4	75.4	37.9	33,274	45.5	4.88	26.5	3.47 bcd
Min. significant difference	6.6	32	38	2.8	17.8	8.4	7370	6.9	1.38	3.6	–

† Means comparisons for sugar yield were computed using log-transformed data, so a single minimum significant difference value cannot be calculated. Back-transformed values are reported; means with the same letter are not significantly different.

(120 g kg^{-1}), but two entries (KKA-11 × KKU40 and KKA-53 × Theis) had significantly higher juice dissolved solids readings at NCSRC (data not shown). Mean plant height was also greater at KKU than at NCSRC (266 cm vs. 207 cm, respectively). Suwan Sweet Extra and Theis were tallest (267 cm), while BJ248 was shortest (188 cm; Table 1). The interaction between genotype and location was relatively small for this trait. Only two entries did not differ in height between the two locations: KKA-139 × BJ248 and KKA-14 × Theis (data not shown). Stem diameter ranged from 13.6 mm (KKA-48 × Theis) to 17.3 mm (KKA-11 × BJ248), but most entries did not differ from each other (Table 1). Overall, the mean stem diameter was not different between locations, except that three entries (KKA-11 × KKU40, KKA-53 × BJ248, and KKA-53 × Theis) had thicker stems at KKU (data not shown).

Yields of total fresh biomass were greater at KKU (74.5 Mg ha^{-1}) than at NCSRC (64.4 Mg ha^{-1}). Likewise, stripped stalk yields were also greater at KKU than at NCSRC (37.8 Mg ha^{-1} vs. 32.8 Mg ha^{-1}, respectively). However, three entries (KKA-139 × BJ248, KKA-48 × KKU40, and Theis) had greater biomass and stripped stalk yields at NCSRC (data not shown). Overall, hybrid KKA-48 × BJ248 had the greatest biomass yield (89.3 Mg ha^{-1}), and hybrid KKA-11 × BJ248 had the greatest stripped stalk yield (46.8 Mg ha^{-1}). Three hybrids of Theis (KKA-11 × Theis, KKA-14 × Theis, and KKA-48 × Theis) had the lowest stripped stalk yields, all below 25 Mg ha^{-1} (Table 1), but the inbred Theis yielded 41.3 Mg ha^{-1} stripped stalks (Table 1).

Stalk moisture content (total stalk juice) ranged from 808 g kg^{-1} (Suwan Sweet Extra) to 879 g kg^{-1} (Urja), with relatively few differences between entries (data not shown). Using the sugarcane extractor, the actual amount of juice recovered (extractability) ranged between 33.2% (KKA-14 × BJ248) and 45.5% (Urja) of the total juice in the stalk (Table 1). Theoretical juice yield was marginally greater (p = 0.052), on average, at KKU (31,262 L ha^{-1}) than at NCSRC (28,123 L ha^{-1}). KKA-11 × BJ248 had the greatest average theoretical juice yield (39,470 L ha^{-1}; Table 1). Sugar yield was estimated on the basis of theoretical juice yields and juice dissolved solids, both of which tended to be greater at KKU, thus sugar yields at KKU

Table 2. Pearson correlations (*r*) among key biofuel traits in sweet sorghum grown at two locations (Khon Kaen University [KKU] and National Corn and Sorghum Research Center [NCSRC]) in Thailand.

Correlations	Dissolved solids	Days to flowering	Plant height	Stalk diameter	Stripped stalk yield	Biomass yield	Theor. juice yield	Grain yield	Panicle length
					KKU				
Days to flowering	0.21								
Plant height	0.13	0.10							
Stalk diameter	−0.16	−0.04	0.28*						
Stripped stalk yield	−0.11	0.13	0.51***	0.65***					
Biomass yield	−0.17	0.11	0.48***	0.66 ***	0.75***				
Theor. juice yield	−0.14	0.12	0.510***	0.63 ***	0.99***	0.72***			
Grain yield	−0.57 ***	−0.05	0.01	0.28*	0.21	0.39***	0.21		
Panicle length	−0.43 ***	−0.44***	0.05	0.46***	0.21	0.28*	0.25*	0.38***	
Theor. sugar yield	0.68 ***	0.21	0.46***	0.29**	0.60***	0.35**	0.58***	−0.35**	−0.15
					NCSRC				
Days to flowering	0.45***								
Plant height	0.20	0.20							
Stalk diameter	−0.16	0.02	0.42***						
Stripped stalk yield	0.00	0.11	0.44***	0.51***					
Biomass yield	−0.34**	−0.04	0.40***	0.61***	0.82***				
Theor. juice yield	−0.07	0.05	0.41***	0.54***	0.99***	0.83 ***			
Grain yield	−0.68***	−0.30**	0.04	0.42***	0.26*	0.60***	0.30**		
Panicle length	0.18	0.10	0.03	0.09	0.14	0.05	0.15	−0.26*	
Theor. sugar yield	0.86***	0.44***	0.40***	0.16	0.47***	0.09	0.41***	−0.49 ***	0.24*

* Indicates significance at $\alpha \leq 0.05$.

** Indicates significance at $\alpha \leq 0.01$.

*** Indicates significance at $\alpha \leq 0.001$.

averaged 3.77 Mg ha^{-1}, and 2.32 Mg ha^{-1} at NCSRC. Of the hybrids, KKA-139 × BJ248 and KKA-53 × Theis had the greatest average theoretical sugar yield (3.40 Mg ha^{-1}), which was significantly less than inbreds KKU40 (5.69 Mg ha^{-1}) and Suwan Sweet Extra (5.62 Mg ha^{-1}), which had the highest theoretical sugar yields (Table 1).

In contrast to biomass and sugar-related traits, average grain yield was greater at NCSRC (6.04 Mg ha^{-1}) than at KKU (5.44 Mg ha^{-1}), but there were some significant interactions; KKA-11 × KKU40, KKA-53 × BJ248, and KKA-53 × Theis had lower grain yields at NCSRC than at KKU (data not shown). The highest average grain yield was 7.83 Mg ha^{-1} (KKA-11 × BJ248), and the lowest grain yield was 2.23 Mg ha^{-1} (Suwan Sweet Extra; Table 1). Panicle length was not affected by location, and ranged from 21.5 cm (KKB-11) to 26.9 cm (Theis; Table 1).

Biomass yield and stripped stalk yield were found to be highly correlated at both locations (r = 0.754 at KKU and r = 0.821 at NCSRC; Table 2). Theoretical juice yields were highly correlated with actual juice yields (r = 0.907 at KKU and r = 0.917 at NCSRC; data not shown). Theoretical juice yield was highly correlated with stripped stalk yield (r = 0.993 at KKU and r = 0.991 at NCSRC; Table 2). At KKU panicle length and grain yield were positively correlated (r = 0.382), while at NCSRC, they were slightly negatively correlated (r = −0.255; Table 2).

Heterosis of Hybrid Sweet Sorghum

No significant heterosis, positive or negative, was observed for days to flowering, stem diameter, or panicle length. Positive MPH was observed for plant height in two hybrids: KKA-11 × BJ248 (20.0%) and KKA-53 × BJ248 (18.0%; Table 3). Five hybrids demonstrated negative MPH for juice dissolved solids, while positive heterosis for this trait was not observed. Three hybrids showed positive MPH for biomass yield, while one hybrid (KKA-138 × Theis) demonstrated negative MPH for biomass (−34.8%; Table 3). One hybrid, KKA-11 × BJ248, showed positive MPH for biomass yield, stripped stalk yield, and theoretical juice yield (35.6, 39.2, and 41.9%, respectively; Table 3). Three hybrids demonstrated negative MPH for theoretical juice yield, and seven had negative MPH for theoretical sugar yield. Positive heterosis for theoretical sugar yield was not observed. Five hybrids had positive MPH for grain yield, while only one had negative MPH for this trait (KKA-53 × Theis; Table 3).

Four hybrids showed significant LPH for juice dissolved solids (26.8–30.1% below the lowest parent in the cross; Table 3). For biomass yield, one hybrid, KKA-139 × Theis, showed LPH (−30.8%) for biomass yield, while KKA-48 × BJ248 had HPH for biomass (31.2%). Hybrid KKA-11 × BJ248 had HPH for stripped stalk yield and theoretical juice yield, while KKA-139 × Theis and KKA-48 × KKU40 both demonstrated LPH for these two traits (Table 3). Only two hybrids had LPH for theoretical sugar yield, KKA-11 × Theis and KKA-14 × BJ248. Three hybrids showed

Table 3. Percentage mid-parent or high- or low-parent heterosis for seven biofuel traits of sweet sorghum hybrids grown at two locations in Thailand in 2013. The first number is mid-parent heterosis, the number in parentheses is high-parent heterosis (if positive) or low-parent heterosis (if negative).

Hybrid	Plant height	Dissolved solids	Biomass yield	Stripped stalk yield	Theor. juice yield	Theor. sugar yield	Grain yield
KKA-11 × BJ248	20.0	–29.9 (–27.3)	35.6	39.2 (33.7)	41.9 (36.3)	–	66.4 (52.1)
KKA-11 × KKU40	–	–	–	–	–	–41.7	–
KKA-11 × Theis	–	–27.1 (–26.8)	–	–	–	–56.1 (–51.8)	50.8 (45.2)
KKA-139 × KKU40	–	–26.1	–	–	–	–50.5	–
KKA-139 × Theis	–	–	–34.8 (–30.8)	–35.5 (–30.7	–37.0 (–32.4)	–37.7	–
KKA-14 × BJ248	–	–30.6 (–27.8)	–	–	–23.9	–54.7 (–52.4)	–
KKA-48 × BJ248	–	–	32.2 (31.2)	–	–	–	44.8 (29.7)
KKA-48 × KKU40	–		–	–32.5 (–26.0)	–38.2 (–27.5)	–41.4	–
KKA-53 × BJ248	18.0	–	–	–	–	–	39.0
KKA-53 × KKU40	–	–34.8 (–30.1)	24.9	–	–	–45.1	28.1
KKA-53 × Theis	–	–	–	–	–	–	–44.6 (–38.2)

Table 4. F values from analysis of variance for general combining ability (GCA) and specific combining ability (SCA) of hybrid sweet sorghum for key biofuel traits across two locations in Thailand.

Effect	DF†	Days to flowering	Dissolved solids	Plant height	Stalk diameter	Stripped stalk yield	Biomass yield	Theor. juice yield	Grain yield	Panicle length	Theor. sugar yield‡
Location (L)	1/4	3.10^{ns}§	84.4***	88.7***	1.97^{ns}	20.72*	20.32*	12.63 *	18.01*	1.45^{ns}	157.4 ***
GCA_{female} (F)	4/56	1.06^{ns}	8.17***	2.00^{ns}	1.71^{ns}	4.04**	3.41*	4.20 **	30.51***	3.67*	10.2 ***
L × F	4/56	1.61^{ns}	16.2***	1.36^{ns}	2.82*	3.93**	3.18*	4.64 **	22.54***	0.52^{ns}	21.8 ***
GCA_{male} (M)	2/56	1.43^{ns}	1.86^{ns}	7.83***	6.11**	40.36***	30.78 ***	39.46 ***	86.58***	1.92^{ns}	4.72 *
L × M	2/56	1.95^{ns}	6.47**	2.07^{ns}	0.20^{ns}	0.91^{ns}	2.16^{ns}	0.57^{ns}	12.39***	1.88 ^{ns}	8.63 ***
SCA (F × M)	8/56	5.18***	8.86***	7.39***	4.23***	17.40***	8.27***	17.18 ***	8.56***	2.11 *	10.0 ***
L × F × M	8/56	3.53**	9.36***	2.65*	1.57^{ns}	9.69***	10.67***	9.64 ***	15.43***	0.55^{ns}	6.91 ***

* Indicates significance at $\alpha \leq 0.05$.

** Indicates significance at $\alpha \leq 0.01$.

*** Indicates significance at $\alpha \leq 0.001$.

† DF = degrees of freedom (numerator/denominator).

‡ Sugar yield was estimated using the formula of Somani and Taylor (2003) and was then log-transformed (*ln*) before ANOVA.

§ ns = not significant.

significant HPH for grain yield, and only one hybrid, KKA-53 × Theis, had LPH for grain yield (Table 3).

General Combining Abilities of Sweet Sorghum Parent Lines

Analysis of variance (*F* statistics) of combining abilities for 10 characteristics measured in two locations is presented in Table 4. Female GCA effect was significant for all traits except days to flowering, plant height, and stalk diameter, while location × GCA_{female} interaction was significant for all traits except days to flowering, plant height, and panicle length. Male GCA effect was significant for all traits except days to flowering, juice dissolved solids, and panicle length. Location × GCA_{male} interaction was only significant for juice dissolved solids, grain yield, and theoretical sugar yield.

The global *F* test for female GCA was not significant for days to flowering (Table 4), although female parent KKA-53 did show a marginally significant ($p = 0.045$) GCA effect in comparison with the overall hybrid mean (1.30 d; Table 5). General combining ability for juice dissolved solids was significant for all female parents except KKA-14 (Table 5). KKA-139 and KKA-53 showed positive GCA for juice dissolved solids (8.2 and 8.3 g kg^{-1}, respectively) while KKA-11 and KKA-48 had negative GCA for juice dissolved solids (−9.1 and −10.6 g kg^{-1}, respectively; Table 5). Across locations male GCA effects for juice dissolved solids were not significant, and this is because nearly opposite male GCA effects were observed for this trait at the two locations (location × GCA_{male} interaction). At NCSRC, where juice dissolved solids was generally lower, Theis showed positive GCA effect (10.6 g kg^{-1}), while the other two males showed negative GCA effects (−5.2 g kg^{-1} for BJ248 and −5.4 g kg^{-1} for KKU40). At KKU, the GCA effect of Theis was slightly negative (−3.6 g kg^{-1}) and for KKU40 it was slightly positive (5.1 g kg^{-1}; data not shown). Though these effects were not statistically significant at KKU, they contributed to the strong location × GCA_{male} interaction for juice dissolved solids, which obscured the main GCA_{male} effect (data not shown). KKA-14 had a marginal GCA effect for plant height (10.13 cm) in comparison with the overall mean. Among males, KKU40 contributed positive (9.71 cm)

Table 5. General combining ability (GCA) effects (deviations from the mean) for key biofuel traits of five female parents and three male parents of sweet sorghum in hybrid combinations, across two locations in Thailand.

	Days to flowering	Dissolved solids	Plant height	Stalk diameter	Biomass yield	Stripped stalk yield	Theor. juice yield	Theor. sugar yield†	Grain yield	Panicle length
	d	g kg^{-1}	cm	mm	Mg ha^{-1}	Mg ha^{-1}	L ha^{-1}	kg ha^{-1}	Mg ha^{-1}	cm
Females										
KKA-11	−0.20^{ns}	−9.1**	−6.11^{ns}	0.53^{ns}	−0.01^{ns}	1.89*	1622 *	−134^{ns}	0.57***	0.43^{ns}
KKA-139	−0.31^{ns}	8.2**	−0.02^{ns}	0.24^{ns}	3.39^{ns}	−0.65^{ns}	−683^{ns}	270*	0.76***	−0.38^{ns}
KKA-14	−0.42^{ns}	3.2^{ns}	10.13*	−0.16^{ns}	−3.35^{ns}	−2.89**	−2513 **	−21^{ns}	−0.22^{ns}	−0.13^{ns}
KKA-48	−0.37^{ns}	−10.6***	−3.66^{ns}	−0.04^{ns}	4.38*	1.38^{ns}	1379^{ns}	−554***	0.22^{ns}	−1.00**
KKA-53	1.30*	8.3**	−0.34^{ns}	−0.57*	−4.40*	0.27^{ns}	195^{ns}	439***	−1.33***	1.07**
Males										
BJ248	0.76^{ns}	−3.4^{ns}	−0.46^{ns}	0.62**	4.97***	2.86***	2507 ***	146*	0.73***	0.14^{ns}
KKU40	−0.31^{ns}	−0.1^{ns}	9.71***	−0.02^{ns}	5.54***	2.49***	2106 ***	47^{ns}	0.52***	0.35^{ns}
Theis	−0.44^{ns}	3.5^{ns}	−9.26**	−0.59**	−10.50***	−5.35***	−4613 ***	−248**	−1.25***	−0.50^{ns}

* Indicates that the GCA is significantly different from the mean at $\alpha \leq 0.05$.

** Indicates that the GCA is significantly different from the mean at $\alpha \leq 0.01$.

*** Indicates that the GCA is significantly different from the mean at $\alpha \leq 0.001$.

† Sugar yield was estimated using the formula of Somani and Taylor (2003) and was then log-transformed (*ln*) before ANOVA. Back-transformed values are shown here.

ns not significant.

and Theis contributed negative (−9.26 cm) GCA effects for plant height. Among females only KKA-53 showed a GCA effect for stem diameter, and it was slightly negative (−0.57 mm). Among males, only BJ248 showed a positive GCA effect (0.62 mm) for stem diameter (Table 5).

Stripped stalk yield, biomass yield, and juice yield were most strongly affected by male GCA effects, though female effects were also observed. Female KKA-11 showed positive GCA effect for stripped stalk yield and theoretical juice yield, while KKA-48 showed positive GCA for total biomass yield. KKA-14 had negative GCA for stripped stalk yield and theoretical juice yield, while KKA-53 GCA for biomass was negative (Table 5). Among males, BJ248 and KKU40 had highly positive GCA for stripped stalk yield, biomass yield, and theoretical juice yield, while Theis showed negative GCA for these traits. Females KKA-139 and KKA-53 had positive GCA effects for theoretical sugar yield (270 and 439 kg ha^{-1}, respectively), as did male BJ248 (146 kg ha^{-1}). Two females (KKA-11 and KKA-139) and two males (BJ248 and KKU40) showed positive GCA effects for grain yield, while two parents, KKA-53 and Theis, had negative GCA for this trait. Despite this, KKA-53 had positive GCA for panicle length.

Specific Combining Abilities of Sweet Sorghum Hybrids

Specific combining ability effect was significant for all characteristics. However, location × SCA was also significant except for stalk diameter and panicle length (Table 4). Specific combining ability was, however, important in determining days to flowering in hybrids, and a location × SCA interaction was also detected (Table 4). Among hybrids, KKA-48 × KKU40, KKA-14 × Theis and KKA-11 × KKU40 tended to flower earlier (negative SCA), while KKA-11 × BJ248 and KKA-48 × Theis flowered later (positive SCA; Table 6). Positive SCA for juice dissolved solids was observed for hybrids KKA-139 × BJ248, KKA-14 × Theis, and KKA-53 × BJ248, while five hybrids had negative SCA for juice dissolved solids (Table 6). Specific combining ability for juice dissolved solids also showed interactions with location (Table 4). The most extreme rank change contributing to this genotype by environment interaction was observed in the hybrid KKA-48 × KKU40. At KKU this entry had the highest SCA for juice dissolved solids (27.5 g kg^{-1}), while at NCSRC it was by far the lowest (−62.1 g kg^{-1}; data not shown). Only KKA-11 × BJ248, KKA-139 × KKU40, and KKA-14 × KKU40 had positive SCA for plant height (Table 6). Three hybrids had positive SCA for stem diameter, and two had negative SCA.

Hybrids KKA-11 × BJ248, KKA-14 × KKU40, KKA-48 × BJ248, and KKA-48 × KKU40 had positive SCA for biomass yield, stripped stalk yield, and theoretical juice yield. KKA-53 × Theis had positive SCA for stripped stalk yield (5.50 Mg ha^{-1}) and theoretical juice yield (4793 L ha^{-1}), despite the fact that Theis showed negative GCA for both of these traits. Five hybrids demonstrated positive SCA for theoretical sugar yield. KKA-139 × BJ248 had the greatest SCA for theoretical sugar yield (831 kg ha^{-1}), followed closely by KKA-53 × Theis (829 kg ha^{-1}). KKA-11 × Theis had the most highly negative SCA for theoretical sugar yield (−1,091 kg ha^{-1}; Table 6). Six hybrids demonstrated positive SCA for grain yield, and four had negative SCA (Table 6). The greatest positive SCA effect for grain yield was observed in hybrid KKA-11 × BJ248 (2.09 Mg ha^{-1}; Table 6). Specific combining ability for grain yield also showed a strong interaction with location. Hybrid KKA-48 × KKU40 had grain yield SCA effect of 4.38 Mg ha^{-1} at NCSRC, but at KKU its SCA effect was −0.92 Mg ha^{-1} (data not shown). A similar trend was observed

Table 6. Specific combining ability (SCA) effects (deviations from the mean) for key biofuel traits of five female parents and three male parents of sweet sorghum in hybrid combinations, across two locations in Thailand.

Hybrids	Days to flowering	Dissolved solids	Plant height	Stalk diameter	Biomass yield	Stripped stalk yield	Theor. juice yield	Theor. sugar Yield†	Grain yield	Panicle length
	d	g kg^{-1}	cm	mm	Mg ha^{-1}	Mg ha^{-1}	L ha^{-1}	kg ha^{-1}	Mg ha^{-1}	cm
KKA-11 × BJ248	3.86**	−18.0**	27.25***	1.88***	13.95***	12.34***	10439***	434*	2.09***	−0.66^{ns}
KKA-11 × KKU40	−2.48*	10.2^{ns}	−4.60^{ns}	0.48^{ns}	−1.56^{ns}	3.42*	2813*	683**	−0.10^{ns}	1.88**
KKA-11 × Theis	−1.98^{ns}‡	−19.5***	−40.98***	−0.77^{ns}	−12.43***	−10.09***	−8386***	−1091***	−0.27^{ns}	0.06^{ns}
KKA-139 × BJ248	−0.64^{ns}	20.0***	−11.49^{ns}	1.23*	6.72^{ns}	0.95^{ns}	772^{ns}	831***	1.24***	−0.02^{ns}
KKA-139 × KKU40	1.52^{ns}	0.1^{ns}	18.42*	−0.75^{ns}	6.75^{ns}	−0.34^{ns}	−650^{ns}	−31^{ns}	1.30***	−0.91^{ns}
KKA-139 × Theis	−1.81^{ns}	4.7^{ns}	−6.99^{ns}	0.23^{ns}	−3.31^{ns}	−2.56^{ns}	−2170^{ns}	83^{ns}	−0.27^{ns}	−0.21^{ns}
KKA-14 × BJ248	0.19^{ns}	−17.8**	−5.61^{ns}	−0.09^{ns}	−2.48^{ns}	−2.50^{ns}	−1853^{ns}	−482*	0.57*	−0.77^{ns}
KKA-14 × KKU40	1.86^{ns}	07.8^{ns}	32.89***	0.56^{ns}	9.22*	3.89*	3197*	774**	−0.08^{ns}	0.99^{ns}
KKA-14 × Theis	−3.31**	19.4***	3.12^{ns}	−0.95^{ns}	−16.79***	−10.06***	−8883***	−200^{ns}	−1.15***	−0.60^{ns}
KKA-48 × BJ248	−0.48^{ns}	−22.9***	3.84^{ns}	1.34*	19.58***	7.62***	6875***	−239^{ns}	0.69**	0.11^{ns}
KKA-48 × KKU40	−3.64**	−17.3**	−0.10^{ns}	0.46^{ns}	12.64***	6.07***	5681***	−923***	1.73***	−0.67^{ns}
KKA-48 × Theis	3.02*	8.2^{ns}	−14.73*	−1.91***	−19.09***	−9.54***	−8419***	−436 *	−1.76***	−2.45***
KKA-53 × BJ248	0.86^{ns}	21.9***	−16.30*	−1.27*	−12.94***	−4.08*	−3696**	399^{ns}	−0.96***	2.03**
KKA-53 × KKU40	1.19^{ns}	−1.5^{ns}	1.99^{ns}	−0.86^{ns}	0.64^{ns}	−0.60^{ns}	−511^{ns}	130^{ns}	−0.25^{ns}	0.48^{ns}
KKA-53 × Theis	1.86^{ns}	4.5^{ns}	13.29^{ns}	0.43^{ns}	−0.90^{ns}	5.50***	4793***	829***	−2.79***	0.71^{ns}

* Indicates that the SCA is significantly different from the mean at $\alpha \leq 0.05$.

** Indicates that the SCA is significantly different from the mean at $\alpha \leq 0.01$.

*** Indicates that the SCA is significantly different from the mean at $\alpha \leq 0.001$.

† Sugar yield was estimated using the formula of Somani and Taylor (2003) and was then log-transformed (*ln*) before ANOVA. Back-transformed values are shown here.

‡ ns = not significant.

for hybrids KKA-48 × BJ248 (SCA effect = 1.89 Mg ha^{-1} at NCSRC vs. −0.52 Mg ha^{-1} at KKU) and KKA-139 × BJ248 (SCA effect = 2.77 Mg ha^{-1} at NCSRC vs. −0.29 Mg ha^{-1} at KKU; data not shown).

DISCUSSION

As expected in field studies of this type, differences in performance were observed between the two locations for most traits, and genotype by environment interactions were also noted. The major factors contributing to these differences would likely be soil properties and weather conditions, specifically precipitation. Although irrigation was provided at both locations when needed, NCSRC received 463 mm more rainfall than did KKU during the study period (Fig. 1). Surprisingly biomass yields tended to be greater at the drier site KKU. It is possible that water was in excess at NCSRC, leading to reduced biomass yields, though average grain yield was higher at the wetter site. A previous study by Pothisoong and Jaisil was conducted at NCSRC to compare sweet sorghum yields in which some of the same cultivars were planted (KKU40, Keller, and Urja). Although irrigation was used in the previous study, it was conducted during the dry season (December through March), and stripped stalk yields of these three cultivars were higher and their grain yields lower than the current study. Juice dissolved solids was higher for Keller and KKU40 in this study, and dissolved solids for Urja was only slightly lower. Interestingly, days to flowering and plant height were similar between the two studies, except that KKU40 flowered about 10 d later in this study. The soil at KKU is sandy with low organic matter, while the soil at NCSRC is clay. Perhaps these genotypes are more suited to drier conditions or sandier soils.

Overall, flowering time in this study was considerably earlier than reported by Ali et al. (2008) in Nebraska. In that study Theis flowered 111 d after planting and Keller at 99 d; both were considerably taller as well. This is likely because of the significantly longer daylength during the summer growing season in Nebraska (latitude 40°50′ N) compared with the fall growing season in Thailand (latitude 16°26′ N and 14°30′ N). Long days delay flowering in cultivars of sorghum depending on the degree of photoperiod sensitivity; the maximum optimal photoperiod for most sorghum is around 12 h. At planting time the daylength at KKU would have been 12 h, 35 min, and at NCSRC the daylength would have been 12 h, 18 min, and decreasing at both locations. In Nebraska Ali et al. (2008) would have planted when the daylength was 14 h, 17 min, and getting longer (NOAA, 2014).

Positive heterosis for stem juice dissolved solids was not observed in this set of hybrids, and several crosses showed negative heterosis for this trait, similar to previous sweet sorghum hybrid studies. Of 12 hybrids, only one (A_3 N100 × Dale) showed positive heterosis for juice dissolved solids (HPH = 3.6%), and in the other crosses heterosis for this trait was not significant (Pfeiffer et al., 2010). Of 20 hybrids studied by Pothisoong and Jaisil (2011) in Thailand, positive heterosis for juice dissolved solids was detected for only three hybrids, and the highest value was only 7.6%, while many more crosses showed negative heterosis. Similarly,

negative HPH for juice dissolved solids was reported by Umakanth et al. (2012) for 12 of the 16 hybrids in that study, with only 1 hybrid showing positive MPH of 9%. It is unclear why positive heterosis for juice dissolved solids is relatively rare in hybrid sweet sorghum. Yun-long et al. (2006) identified quantitative trait loci (QTL) that explained up to 25% of the phenotypic variance in sugar concentration. They also noted an overdominance effect and suggested that heterosis in hybrids should be expected. Several other investigators (Murray et al., 2008; Murray et al., 2009; Ritter et al., 2008) have also identified QTL for juice Brix or sugar concentration, but they were mostly of small effects. It may be that juice dissolved solids, or sugar concentration, is controlled by multiple genes of relatively small effect in most sweet sorghum lines and that many of the alleles favoring higher solids concentration are recessive in hybrid combination. Perhaps to achieve high sugar yields in hybrids, sweet sorghum breeders will need to develop seed parents and pollen parents with high juice sugar concentration to produce hybrids that also have high juice sugar concentration, and then exploit positive heterosis for other traits such as stalk yield.

The highest theoretical sugar yields in this study were obtained using pure line varieties, KKU40 (5.69 Mg ha^{-1}) and the checks Suwan Sweet Extra (5.62 Mg ha^{-1}) and Keller (4.66 Mg ha^{-1}). The two hybrids with greatest theoretical sugar yield were KKA-139 × BJ248 and KKA-53 × Theis, which produced about 3.40 Mg ha^{-1} of sugar each. Based on an ethanol conversion rate of 0.53 L kg^{-1} (Somani and Taylor, 2003), KKU40 could yield approximately 3000 L ha^{-1} ethanol. The top-yielding hybrids would produce approximately 1800 L ha^{-1} ethanol from sugar. One major reason for the greater sugar yields of the inbreds was the higher dissolved solids concentration of the juice. The nominal increase in juice volumes in the hybrids did not fully compensate for lower sugar concentration, which is evidenced by high correlation between juice dissolved solids and theoretical sugar yield in this study. Murray et al. (2008) also reported this correlation, but a study by Alhajturki et al. (2012) found no correlation between these two traits in well-watered conditions and a negative correlation under drought conditions. In previous studies (Alhajturki et al., 2012; Umakanth et al., 2012) juice yield appears to be the most important factor determining sugar yield, and though it was also important in this study, juice dissolved solids was equally important. Three hybrids in this study showed positive heterosis for biomass yield, but only one of these also had positive heterosis for stripped stalk yield and theoretical juice yield. Previously, Pfeiffer et al. (2010) found that 6 of 12 hybrids had positive HPH for sugar yield, and of these, 3 had significant positive HPH for juice yield. Umakanth et al. (2012) found positive HPH for juice yield in six hybrids, all of which had positive HPH for computed ethanol yield as well. In the current study the water content of the stalks did not vary greatly, but among sorghum there is a wide variation in "juiciness" of stalks. One would expect that dry pithy stalks should weigh less than juicy stalks of similar size. Also, given the high correlation between stripped stalk yields and theoretical juice yields observed in this study, selection on the basis of stripped stalk yields and juice dissolved solids could be a simple strategy for rapid early-generation selection for sugar yield in sweet sorghum, reducing the need to quantify juice directly. Though extractability of the juice did vary somewhat between the entries in this study, there was a very high correlation between theoretical juice yields and the actual amount of juice recovered from the extractor.

The grain portion can also be converted to ethanol, and in the United States, sorghum grain is currently used as an ethanol feedstock. Grain yields averaged 4.74 Mg ha^{-1} for inbreds and checks and 5.74 Mg ha^{-1} for hybrids. Pedersen et al. (2013) also reported heterosis for grain yield in hybrid sweet sorghum in Nebraska, and yields among hybrids were similar to those observed in this study. On the basis of a conversion factor of 402 L Mg^{-1} grain (USDA, 2006), some of the hybrids in this study could potentially produce over 3000 L ha^{-1} ethanol from grain alone. Adding ethanol production from both sugar and grain fractions, two of the hybrids in this study (KKA-11 × BJ248 and KKA-139 × BJ248) could produce approximately 4600 L ha^{-1} ethanol. Obviously this is theoretical, and juice yields are probably overestimated given that they were based on stalk moisture percentage, and grain yields may also be slightly inflated from measuring in small plot sizes. Nonetheless, the advantages of hybrids are quite apparent, if dual-purpose plants can be efficiently harvested and processed. One challenge to development of dual-purpose sweet and grain sorghum is the negative correlation between juice dissolved solids and grain yield that was observed in this study and was also reported by Murray et al. (2008) and Ritter et al. (2008). It may be difficult to maximize both of these traits in the same plant, but genetic analysis by Murray et al. (2008) concluded that it should be possible. An additional consideration is that higher grain yields on very tall plants may increase the incidence of lodging (Pfeiffer et al., 2010). Lodging should be another target for improvement through breeding.

CONCLUSIONS

Heterosis in sweet sorghum was observed for several traits related to ethanol production, but overall, theoretical sugar yields of hybrids were often not greater than that of inbred lines. However, hybrids have an advantage over inbreds in that seed is more easily produced and mechanically harvested using short male-sterile lines. In this study hybrids generally produced more grain than inbreds, which can also be used for producing ethanol. Parental lines were

identified with positive GCA for various sugar-related traits and for grain yield. Two female lines (KKA-139 and KKA-53) and one male (BJ248) showed positive GCA for theoretical sugar yield. These lines should be included in future hybrid breeding studies. For most traits, particularly biomass yield, stripped stalk yield, theoretical juice yield, and theoretical sugar yield, SCA effects were greater in magnitude than GCA effects, and environmental interaction was important. The hybrids KKA-11 × BJ248, KKA-11 × KKU40, KKA-139 × BJ248, KKA-14 × KKU40, and KKA-53 × Theis had positive SCA for theoretical sugar yield and would be recommended for further testing in more locations. Hybrid KKA-11 × BJ248 had positive SCA for plant height, stalk diameter, stripped stalk yield, biomass yield, theoretical juice yield, and grain yield, although SCA for juice dissolved solids was negative for this cross. This study suggests that F_1 hybrids have advantages over pure lines except that juice solids concentrations of F_1 hybrids were lower than pure lines. Therefore juice sugar concentration should be the first target for further improvement in this sorghum improvement program.

Acknowledgments

The researchers would like to thank the Royal Golden Jubilee Ph.D. Program (RGJ) under the Thailand Research Fund, Research and Researcher for industry (RRi), Plant Breeding Research Center for Sustainable Agriculture, Department of Plant Science and Agricultural Resources, Faculty of Agriculture and Khon Kaen University Research Fund. We are also grateful to Dr.Thamrongsilpa Pothisoong at the NCSRC for assistance.

References

Alhajturki, D., M. Aljamali, A. Kanbar, and F. Azmah. 2012. Potential of some sweet sorghum [*Sorghum bicolor* (L.) Moench] genotypes under two regimes for sugar and bio-ethanol production. Sugar Tech. 14(4):376–382. doi:10.1007/s12355-012-0181-x

Ali, M.L., J.F. Rajewski, P.S. Baenziger, K.S. Gill, K.M. Eskridge, and I. Dweikat. 2008. Assessment of genetic diversity and relationship among a collection of US sweet sorghum germplasm by SSR markers. Mol. Breed. 21:497–509. doi:10.1007/s11032-007-9149-z

Almodares, A., and M.R. Hadi. 2009. Production of bioethanol from sweet sorghum: A review. African J. Agric. Res. 4(9):772–780.

Almodares, A., M.R. Hadi, and H. Ahmadpour. 2008. Sorghum stem yield and soluble carbohydrates under phenological stages and salinity levels. Afr. J. Biotechnol. 7:4051–4055.

Bandyopadhyay, R., D.E. Frederickson, N.W. McLaren, G.N. Odvody, and M.J. Ryley. 1998. Ergot: A new disease threat to sorghum in the Americas and Australia. Plant Dis. 82(4):356–366. doi:10.1094/PDIS.1998.82.4.356

Broadhead, D.M. 1982. Registration of Keller sweet sorghum. Crop Sci. 22(6):1263. doi:10.2135/cropsci1982.0011183X002200060055x

Broadhead, D.M., K.C. Freeman, O.H. Coleman, and N. Zummo. 1978. Registration of Theis sweet sorghum. Crop Sci. 18(1):165. doi:10.2135/cropsci1978.0011183X001800010052x

Hayes, H.K., I.R. Immer, and D.C. Smith. 1955. Methods of plant breeding. McGraw-Hill Book Company Inc., New York.

Indhubala, M., K. Ganesamurthy, and D. Punitha. 2010. Combining ability studies for quality traits in sweet sorghum [*Sorghum bicolor* (L.) Moench]. Madras Agric. J. 97(1–3):17–20.

Makanda, I., P. Tongoona, and J. Derera. 2009. Combining ability and heterosis of sorghum germplasm for stem sugar traits under off-season conditions in tropical lowland environments. Field Crops Res. 114:272–279. doi:10.1016/j.fcr.2009.08.009

Murray, S.C., A. Sharma, W.L. Rooney, P.E. Klein, J.E. Mullet, S.E. Mitchell, and S. Kresovich. 2008. Genetic improvement of sorghum as a biofuel feedstock: I. QTL for stem sugar and grain nonstructural carbohydrates. Crop Sci. 48:2165–2179. doi:10.2135/cropsci2008.01.0016

Murray, S.C., W.L. Rooney, M.T. Hamblin, S.E. Mitchell, and S. Kresovich. 2009. Sweet sorghum genetic diversity and association mapping for brix and height. Plant Gen. 2:48–62. doi:10.3835/plantgenome2008.10.0011

NOAA. 2014. NOAA solar calculator. www.esrl.noaa.gov/gmd/grad/solcalc/ (accessed 30 Oct. 2014).

Pedersen, J.F., S.E. Sattler, and W.F. Anderson. 2013. Evaluation of public sweet sorghum A-lines for use in hybrid production. Bioenerg. Res. 6. doi:10.1007/s12155-012-9231-1

Pfeiffer, T.W., M.J. Bitzer, J. Toy, and J.F. Pedersen. 2010. Heterosis in sweet sorghum and selection of a new sweet sorghum hybrid for use in syrup production in Appalachia. Crop Sci. 50:1788–1794. doi:10.2135/cropsci2009.09.0475

Pothisoong, T., and P. Jaisil. 2011. Yield potential, heterosis and ethanol production in F_1 hybrids of sweet sorghum [*Sorghum bicolor* (L.) Moench]. KMITL Sci. Technol. J. 11(1):17–24.

Reddy, B.V.S., S. Ramesh, A.A. Kumar, S.P. Wani, R. Ortiz, H. Ceballos, and T.K. Sreedevi. 2008. Bio-fuel crops research for energy security and rural development in developing countries. Bioenerg. Res. 1:248–258. doi:10.1007/s12155-008-9022-x

Reddy, B.V.S., and P.S. Reddy. 2003. Sweet sorghum: Characteristics and potential. Int. Sorghum Millets Newsl. 44:26–28.

Reddy, P.S., B.V.S. Reddy, and P. Srinivasa. 2011. Genetic analysis of traits contributing to stalk sugar yield in sorghum. Cereal Res. Commun. 39(3):453–464. doi:10.1556/CRC.39.2011.3.15

Ritter, K.B., D.R. Jordan, S.C. Chapman, I.D. Godwin, E.S. Mace, and C.L. McIntyre. 2008. Identification of QTL for sugar-related traits in a sweet × grain sorghum [*Sorghum bicolor* (L.) Moench] recombinant inbred population. Mol. Breed. 22:367–384. doi:10.1007/s11032-008-9182-6

Somani, R.B., and J.R.N. Taylor. 2003. Sorghum: A potential source of raw material for agro-industries. Alternative uses of sorghum and pearl millet in Asia. CFC Technical Paper No. 34. Proceedings of the Expert Meeting, Patancheru, Andhra Pradesh, India, 1–4 July 2003. ICRISAT, Patancheru, Andhra Pradesh, India; and Common Fund for Commodities, Amsterdam, Netherlands. p. 146–168.

Tesso, T.T., L.E. Claflin, and M.R. Tuinstra. 2005. Analysis of stalk rot resistance and genetic diversity among drought tolerant sorghum genotypes. Crop Sci. 45:645–652. doi:10.2135/cropsci2005.0645

Umakanth, A.V., J.V. Patil, C. Rani, S.R. Gadakh, S.S. Kumar, S.S. Rao, and T.V. Kotasthane. 2012. Combining ability and heterosis over environments for stalk and sugar related traits in sweet sorghum [*Sorghum bicolor* (L.) Moench.]. Sugar Tech 14(3):237–246. doi:10.1007/s12355-012-0166-9

USDA. 2006. The economic feasibility of ethanol production from sugar in the United States. www.fsa.usda.gov/Internet/FSA_File/ethanol_fromsugar_july06.pdf (accessed 30 Oct. 2014).

Yun-long, B., Y. Seiji, I. Maiko, and C. Hong-wei. 2006. QTLs for sugar content of stalk in sweet sorghum [*Sorghum bicolor* (L.) Moench]. Agric. Sci. China 5(10):736–744. doi:10.1016/S1671-2927(06)60118-1

View publication stats

Field Crops Research 175 (2015) 26–36

Contents lists available at ScienceDirect

Field Crops Research

journal homepage: www.elsevier.com/locate/fcr

Genotypic variation in grain yield and flowering pattern in terminal and intermittent drought screening methods in rainfed lowland rice

T. Monkham [a], B. Jongdee [a,*], G. Pantuwan [b], J. Sanitchon [a], J.H. Mitchell [c], S. Fukai [c]

[a] Faculty of Agriculture, Khon Kaen University, Khon Kaen 40002, Thailand
[b] Bureau of Rice Research and Development (BRRD), Rice Department, Bangkok, Thailand
[c] The University of Queensland, School of Agriculture and Food Sciences, Brisbane 4072, Australia

ARTICLE INFO

Article history:
Received 8 October 2014
Received in revised form 31 January 2015
Accepted 2 February 2015
Available online 21 February 2015

Keywords:
Water deficit
Rice maturity group
Drought resistance
Delay in flowering
Aerobic rice
Intermittent stress

ABSTRACT

Rainfed lowland rice in the Mekong region is mostly grown in drought-prone areas, and drought resistant varieties could be selected using either terminal drought (severe water stress after flowering) or intermittent drought (frequent mild stress) screening. Delay in flowering is considered as a putative trait for selection of drought resistant genotypes, and its effectiveness as an indirect selection trait and its association with genotype's flowering duration, i.e. the time taken from the first to last flower in a plot, was evaluated under the two drought screening methods. These screening methods together with flood control were used at two locations, Chum Phae and Ubon in north-east Thailand using a total of 70 genotypes with different growing duration. Delay in flowering was estimated for the two drought screening methods and flowering of individual panicles within a plot was recorded to determine flowering duration of each genotype in the flood and terminal drought conditions.

Mean reduction in grain yield was 52–55% under the terminal drought screening while it was 10–19% for the whole population and 23–33% for early flowering genotypes in the intermittent drought. Delay in flowering under intermittent drought condition at both locations was associated with yield reduction; genotypes that exhibited shorter delay in flowering had smaller yield reduction percentage and larger number of panicles. At Chum Phae, where grain yield reduction was associated with flowering time, genotypes with longer flowering duration under terminal drought had smaller yield reduction, and this was found even among genotypes that flowered about the same time under flood condition. However, there was no association between delay in flowering and flowering duration. It is concluded that delay in flowering appears promising as a selection criterion under intermittent drought conditions, provided a higher yield reduction can be achieved for example by using an increased irrigation interval.

© 2015 Elsevier B.V. All rights reserved.

1. Introduction

In the Mekong region, the majority of rice growing areas are classified as rainfed lowland ecosystem (OAE, 2003). Grain yield is low and varied across years and locations due to large environmental variability across the toposequence positions, soil types and seasonal rainfall patterns (Ouk et al., 2007; Kamoshita et al., 2008). The rainfed lowland rice crop is subjected to frequent drought especially late in the growing season, around October in north-east Thailand (late season terminal drought) but other types of drought, early season drought and intermittent drought are also common (Kamoshita et al., 2008; Fukai and Ouk, 2012). Different types of drought develop in rainfed rice fields, and characterization of the prevalent drought regimes for the region concerned is essential for identifying appropriate drought screening methods and also drought resistance traits that could be used for screening.

The success of a specific drought screening method is dependent on the discrimination of traits/genotypes reflecting that of the target environment. In order to make greater progress in selecting for drought resistant rice varieties, the use of managed environments in research stations was advocated by Lafitte et al. (2002). While the application of uniform, repeatable and controlled stress environment can be achieved more readily in the dry season and this may possibly maximize the genetic component of the observed variation, the extrapolation of results to natural target environments in the wet season can be difficult (Kamoshita et al., 2008). Phenotyping facilities for screening rice genotypes for drought resistance are increasingly available. While terminal drought is commonly used for drought screening in the Mekong region (Pantuwan et al., 1997; Fukai and Ouk, 2012), the drought stress level may be too severe to

* Corresponding author.
E-mail address: boonrat@brrd.mail.go.th (B. Jongdee).

http://dx.doi.org/10.1016/j.fcr.2015.02.003
0378-4290/© 2015 Elsevier B.V. All rights reserved.

be representative of the drought that commonly develops during the wet season. Thus, intermittent drought screening methodology was suggested to target the moderately severe drought that is common during the wet season (Xangsayasane et al., 2014b). However, they found the drought stress level in the intermittent screening in the wet season was too low for discriminating genotypes for drought resistance, but by combining both wet and dry season screenings, genotypes identified as drought resistant were found to perform well in farmer's rainfed lowland fields in the wet season in Laos (Xangsayasane et al., 2014a).

While grain yield is commonly used as a selection criterion, determining grain yield accurately for a large number of genotypes can require a large input of resources, and indirect selection may be more efficient for a breeding program if we can identify a trait that can be determined with reduced resources but is highly heritable and is related to the genotypic variation in grain yield. Delay in flowering under drought stress has been found to be one of the traits associated with drought resistance in rice (Bernier et al., 2007) and it can be used for prediction of genotypic performance in drought-prone rainfed lowlands (Pantuwan et al., 2002b). While the delay in flowering under drought conditions appeared to be related to drought susceptibility, in experiments reported by Kumar et al. (2009), the results were confounded by the flowering time of genotypes, as shorter delays were found in early flowering genotypes which escaped from severe drought that developed late in the season. Commonly, delay in flowering is calculated as the difference in flowering time of genotype under stress condition and under flooded control (Pantuwan et al., 2002b; Sellamuthu et al., 2011; Xangsayasane et al., 2014b), and the flowering time is estimated on the whole plot basis. However, the delay in flowering may not be accurately estimated in this manner, as flowering time varies not only among plants but also within a plant depending on the number of tillers and panicles (Yoshida, 1981). The time interval for flowering of an entire panicle is normally four to seven days (Moldenhauer and Slaton, 2004). Within the same panicle it may take 7–10 days for all the spikelets to complete anthesis. Further, drought affects tillering pattern and subsequent panicle number (Sellamuthu et al., 2011; Kanjoo et al., 2012), and these may also affect flowering duration within a plot. Thus, the measurement of the duration of flowering (i.e. time taken from the first to the last flower) within a plot under flood and drought conditions may provide better understanding of the delay in flowering on the plot basis. The objective of the present work was to identify the importance of plant characters associated with drought resistance, particularly delay in flowering under intermittent and terminal drought conditions and its relationship to flowering duration under terminal drought conditions.

2. Materials and methods

2.1. Experimental sites and conditions

Two identical experiments were conducted at Chum Phae (CPA; latitude 16°32′2.6″N, 102°6′0″E) and Ubon Ratchathani (UBN; latitude 15°19′52.35″N, longitude 104°40′55.15″E) Rice Research Centers in Northeast Thailand, during the 2009 wet season. The soils at the experimental sites were sampled from 3 trial areas (flood, intermittent drought and terminal drought trials) but as the soil characteristics did not differ greatly among these areas only the mean is shown in Table 1. The soil texture was characterized as clay-loam and sand, at CPA and UBN, respectively.

To ensure the terminal drought trial was exposed to severe drought without interference of rainfall, the sowing date of all trials was delayed to 20 August at CPA and 15 August 2009 at UBN, and transplanting was done on 17 and 7 September at CPA and UBN, respectively. Transplanting was done using 1 seedling per hill, at hill spacing of 20 cm × 20 cm. The plot size was 1 m × 1 m (25 plants per plot) and harvest area was 0.6 × 0.6 m (3 plants × 3 plants).

Table 1
Soil pH, organic matter (OM), N, P and K availability, CEC, and soil texture at CPA and UBN.

	CPA	UBN
pH (1:1 H_2O)	5.2	4.8
Organic matter (%)	1.1	0.5
Total N (%)	0.1	0.0
Available P (ppm)	20.6	26.6
Extractable K (ppm)	202.4	32.4
CEC (c mol/kg)	10.7	2.0
Sand (%)	27.0	91.9
Silt (%)	40.6	6.6
Clay (%)	32.8	1.5
Texture class	Clay loam	Sand

2.2. Water condition trials

There were three water condition trials; flood, intermittent and terminal drought conditions. Under the flood condition the paddy was flooded with rainwater and irrigation to a height of 1–10 cm above the soil surface throughout the crop growth. Under the intermittent drought condition, surface irrigation was applied in the same manner as the flood condition until 53–54 days after sowing (DAS), and then water was drained out of the paddy. The paddy was irrigated at 63, 75, 87, 96 and 105 DAS at CPA, and at 62, 71, 77, 89, 98 and 107 DAS at UBN before the plants showed any visual symptom of drought stress such as leaf wilting or rolling. On the day of irrigation, the paddy was flooded in the morning for 5–6 h and drained out in the afternoon and this cycle was repeated until mid-grain filling.

Under the terminal drought condition the paddy was supplied with irrigation water in the same manner as in the flood condition until the flood water was drained out at 67 DAS at both locations, 13–14 days later than the intermittent drought condition, after which no further irrigation was applied.

2.3. Genotypes

Two types of genotypes were used in the experiments; one group consisted of 37 photoperiod insensitive genotypes selected in the previous dry season, while the other group consisted of 26 photoperiod sensitive genotypes based on RD6 as a parent and selected in the previous wet season. There were also 7 parents and varieties. The selection had been based on high grain yield and leaf water potential (LWP) under flood, aerobic and drought conditions. The former group included 5 double haploid lines derived from CT9993-5-10-1-M/IR62266-42-6-2, and 26 lines from Surin1 backcross with drought resistant donor (Surin1*3/IR68586-CA-143). The latter group included 7 lines from RD6 backcross with drought resistant donor (RD6*2/IR58821-23-B-1-2-1) and a number of lines extracted from crosses between RD6 and various local varieties (3 lines each from cross with Haew Jan and Hom Bang, 2 lines each from cross with Luang Ema, Kiew, Pong Aew1, and Daw Yoa, and 1 line each from cross with Hom Bai, Loa, Daw Noi, Hom Toong1, Kaao Kaew and Jaao Daeng), and 5 lines from cross between RD6 and selected line UBN95009-SRN-41-2-1-1).

2.4. Measurements

Days to flower (DTF) were estimated by visual observation from the number of days after sowing to the day 50% of plants flowered in each plot under flood, intermittent and terminal drought conditions. The flowering delay under intermittent and terminal drought

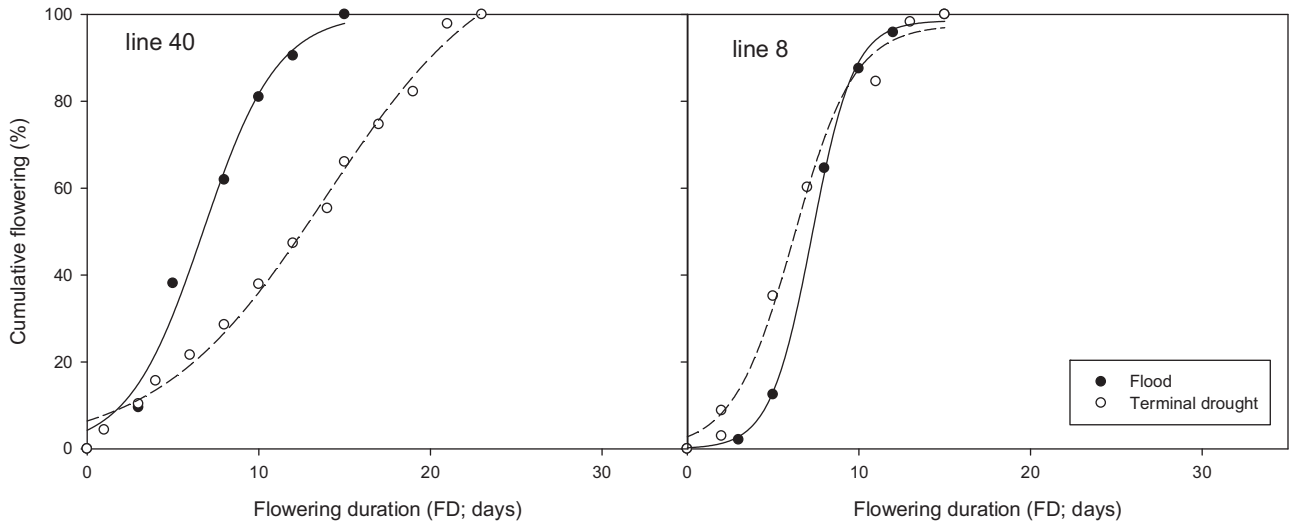


Fig. 1. Cumulative flowering (%) of two genotypes (line 40 and line 8) when grown under flood and terminal drought conditions.

condition was calculated from the difference between DTF under water deficit conditions (intermittent and terminal) and DTF under flood conditions.

Flowering duration (FD), the duration from the first flowering to the last flowering was calculated for each plot from observation of flowering of all panicles on the centre 3 plants every 1–3 days, under flood and terminal conditions. The cumulative flowering percentage at any time was calculated as, (cumulative number of flowering panicles/total number of panicles that flowered) × 100, and was determined by fitting the following equation, $y = (100/1 + e^{a+bx})$, where y is cumulative flowering (%) and a and b are constants. Data sets with only correlation coefficient (r) between observed and fitted flowering (%) showing greater than 0.80 were accepted, and 7 and 10 genotypes were discarded at CPA and UBN, respectively. When $y = 100/2$, i.e. 50% flowering ($x = x_{50}$), $100/2 = \left(100/\left(1 + e^{a+bx_{50}}\right)\right)$. Then the x_{50} was multiplied by 2 for the total duration of flowering (FD), hence $FD = -(a/b)$.

Fig. 1 shows two examples (line 8 and line 40) of flowering pattern obtained under flood and terminal drought conditions at CPA; line 40 showed prolonged flowering duration under drought condition while line 8 had similar flowering pattern under flood and terminal drought conditions.

Tiller number per hill was determined at 60–61 DAS and panicle number per hill was determined at 103–104 DAS, from 4 randomly selected plants in the middle rows of each plot, and grain yield was determined from the 9 plants in the middle rows. Plants were harvested at ground level and air dried for 10–15 days for determination of total dry matter, and harvest index was calculated as grain yield/total dry matter. The number of filled and unfilled grain were counted to determine the percentage of filled grain.

Mid-day leaf water potential (LWP; 11.00–14.00 h) was determined at 82 and 94 DAS under flood, 82 and 91 DAS under intermittent and 82, 88 and 97 DAS under terminal drought condition at CPA, and at 87, 89 and 95 DAS under flood, intermittent and terminal drought conditions, respectively, at UBN. On each measurement occasion, the youngest fully expanded leaf was randomly sampled from each plot. To prevent transpirational water loss, a long-narrow plastic sheath, 2 cm wide and 20 cm long, was placed over the leaf tip and pulled down to cover the whole leaf blade, then the leaf was cut with scissors just above the leaf collar. The leaf sample was immediately taken to measure LWP using the pressure chamber (model 3005 Plant Water Status Console, Soil Moisture Equipment, USA).

Daily rainfall data was collected from the meteorology station within each Rice Research Center. Data on soil moisture in the experiment was collected about once a week after draining commenced from intermittent and terminal drought conditions (only intermittent at UBN). Soil samples to 15 cm depth were collected (3 samples per replication), and fresh weight determined. Soils were dried in an oven at 105 °C for 48 h then weighed and gravimetric soil moisture content determined.

2.5. Statistical analysis

Analysis of all traits was based on a randomized complete block design with 3 replications in all trials. Correlation analysis on a genotype mean basis was used to determine the genotypic consistency between water conditions and also the factors contributing to grain yield variation in each water condition.

3. Results

3.1. Water environment

The total rainfall after transplanting was 352 mm at CPA (Fig. 2a). After standing water was drained out from the intermittent drought condition at 54 DAS, soil moisture content declined to around 15% and it went up to around 18% with irrigation water applied, and soil moisture content cycled between these values (Fig. 2a). In this intermittent drought condition, there were at least 2 cycles of drought and irrigation before early flowering genotypes flowered. Draining water from the terminal drought condition started 14 days later than in the intermittent condition with the soil moisture content lower than that in the intermittent drought by the time early genotypes started to flower at around 80 DAS, and it became well below the moisture content in intermittent condition thereafter. Leaf water potential also decreased sharply from around −1.0 to −2.25 MPa in CPA and −2.01 MPa in UBN in the terminal drought condition, and by the time of the last measurement at 82–97 DAS, LWP in terminal condition was well below that of the intermittent condition (−1.12 and −0.9 MPa at CPA and UBN, respectively).

Rainfall before transplanting was higher at UBN than at CPA, and UBN also experienced a heavy rainfall around 45DAS and some rain occurred subsequent to draining of the intermittent drought (Fig. 2b). The intermittent condition received 6 irrigation events, and soil moisture fluctuated around 13–22%. At 89 DAS, LWP under

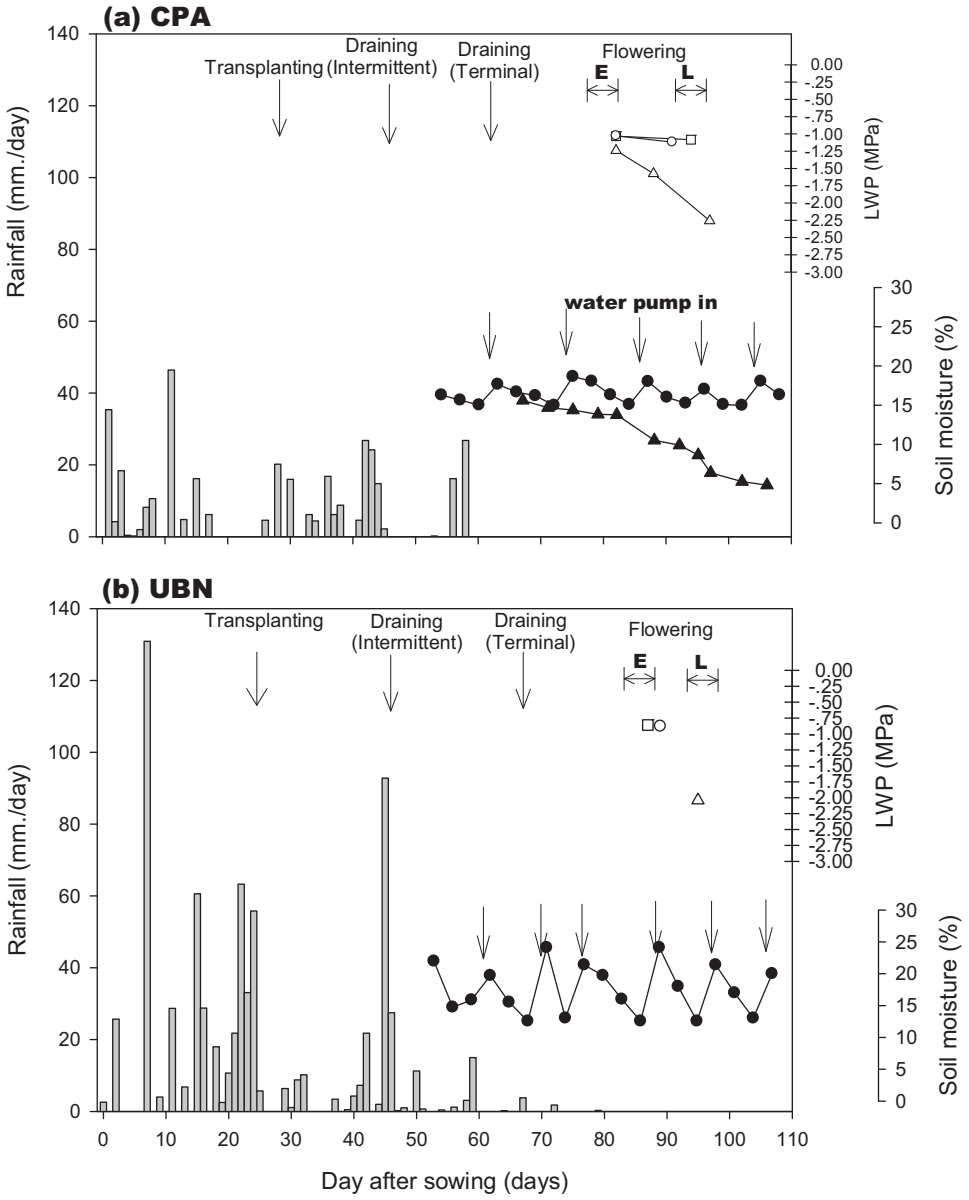


Fig. 2. Daily rainfall, soil moisture (%) and leaf water potential (LWP) at CPA (a), and at UBN (b), under intermittent and terminal drought conditions (black arrow is time of water pumped in under intermittent condition, E and L are flowering time of early and late genotype groups. For LWP, white circle is for flood condition, white square for intermittent condition and white triangle for terminal drought condition.

intermittent condition was about the same as in flood condition. There was no effective rainfall in the terminal condition once the drought condition had been imposed.

3.2. Grain yield, panicle number and flowering pattern

At both locations, mean grain yield reduction due to intermittent drought condition was small (10–19%) but terminal drought condition reduced yield by more than 50% (Table 2). However, genotypes differed in their responses with a significant genotype by water condition interaction effect at both locations. The mean yield reduction was due to both reductions in total dry matter and harvest index. Individual panicle dry weight was reduced by both drought conditions, while water condition effect on the number of panicles was 11–25% reduction under terminal drought condition and less in the intermittent drought. The panicle number at 103–104 DAS was slightly but significantly greater in later flowering genotypes (about 6–7 panicles/plant) than earlier flowering genotypes (about 5–6 panicles/plant) under flood and intermittent conditions. Under terminal drought, there were about 5 panicles/plant with no effect of flowering time.

Mean days to flowering was 87 and 90 DAS in flood conditions and 1 and 3 days longer for both intermittent and terminal drought conditions in CPA and UBN, respectively. Genotypic variation in flowering delay was significant at UBN, but not at CPA. When two locations were combined, there was highly significant genotypic variation and also significant water condition by genotype interaction effect (Table 2).

The duration of flowering was significantly affected by location, genotypes and location by water condition interaction; mean duration of flowering was prolonged by 1.2 days with drought at CPA but was shortened by one day (from 14.4 to 13.4 days) at UBN. While the level of probability of significance of genotype effect for flowering duration was 0.05–0.07 at each location, it was highly significant when the two locations were combined. However there was no significant genotype by location or genotype by water

Table 2
Mean grain yield (GY), grain yield reduction (%), total dry matter (TDM), harvest index (HI), Panicle number per hill, panicle grain weight (PGW), day to flowering (DTF), delay in flowering, duration of flowering and leaf water potential (LWP) of 70 genotypes at two locations in wet season 2009.

	Conditions	GY (g/m^2)	Reduction (%)	TDM (g/m^2)	HI	Panicle (per hill)	PGW (g/panicle)	DTF (days)	Delay (days)	Flowering duration (days)	LWP[a] (MPa)
CPA	Flood	276		619	0.44	5.9	1.84	87	–	13.4	−1.09
	Intermittent	244	10.0	576	0.42	5.8	1.66	88	0.61	–	−1.12
	Terminal	121	55.3	440	0.25	5.1	1.19	88	0.82	14.6	−2.25
p-Value											
Condition (C)		*<0.001*		*<0.001*	*<0.001*	*<0.001*	*<0.001*	*<0.001*	*0.372*	*0.007*	*<0.001*
Genotypes (G)		*<0.001*		*<0.001*	*<0.001*	*<0.001*	*<0.001*	*<0.001*	*0.214*	*0.046*	*0.529*
C × G		*<0.001*		*0.003*	*<0.001*	*0.107*	*0.808*	*<0.001*	*0.522*	*0.553*	*0.412*
UBN	Flood	287		717	0.40	6.6	1.77	90	–	14.4	−0.88
	Intermittent	234	18.5	630	0.36	6.5	1.39	93	2.56	–	−0.90
	Terminal	138	51.9	590	0.23	4.9	1.09	93	3.07	13.4	−2.01
p-Value											
Condition (C)		*<0.001*		*<0.001*	*<0.001*	*<0.001*	*<0.001*	*<0.001*	*0.134*	*0.043*	*<0.001*
Genotypes (G)		*<0.001*		*<0.001*	*0.013*	*<0.001*	*<0.001*	*<0.001*	*0.040*	*0.071*	*0.039*
C × G		*0.026*		*0.011*	*0.297*	*0.839*	*0.196*	*<0.001*	*0.676*	*0.623*	*0.709*
Combined											
p-value											
Location (L)		*0.002*		*<0.001*	*<0.001*	*<0.001*	*0.020*	*0.010*	*<0.001*	*0.030*	*<0.001*
Condition (C)		*<0.001*		*<0.001*	*<0.001*	*<0.001*	*<0.001*	*<0.001*	*0.456*	*0.150*	*<0.001*
L × C		*<0.001*		*<0.001*	*<0.001*	*<0.001*	*<0.001*	*<0.001*	*0.488*	*0.028*	*<0.001*
Genotypes (G)		*<0.001*		*<0.001*	*<0.001*	*<0.001*	*<0.001*	*<0.001*	*<0.001*	*0.001*	*0.136*
L × G		*0.011*		*0.004*	*0.065*	*0.183*	*0.993*	*<0.001*	*0.913*	*0.473*	*0.355*
C × G		*0.005*		*0.102*	*0.009*	*0.017*	*0.312*	*0.015*	*0.036*	*0.525*	*0.309*
L × C × G		*0.009*		*<0.001*	*0.053*	*0.974*	*1.000*	*0.005*	*1.000*	*0.749*	*0.966*

[a] LWP measured at 94, 91 and 97 DAS under flood, intermittent and terminal drought, respectively at CPA and 87 89 and 95 DAS under flood, intermittent and terminal drought, respectively at UBN.

condition interaction effect. Genotypes that flowered later tended to have up to 2 days shorter flowering duration.

The correlation coefficients of genotypes for grain yield and some attributes between water conditions are shown in Table 3. Grain yield under intermittent conditions was correlated to those under flooded and terminal drought condition at both locations, but grain yield under flood and terminal drought was significantly correlated only in CPA. There was significant correlation for tiller number between flood, intermittent and terminal drought at both conditions and also for panicle number at CPA. The duration of flowering was correlated between flood and terminal drought condition at CPA but not at UBN. Leaf water potential which had significant genotypic variation only at UBN was correlated between flood and intermittent and between intermittent and terminal drought condition at this location.

There was no significant association between days to flower and grain yield under all conditions at UBN, but it was significant under both drought conditions at CPA (Fig. 3). At CPA under intermittent drought yield of early flowering genotypes were lower than late flowering genotypes, resulting in a positive effect ($r = 0.568^{**}$, $n = 70$) of flowering time on grain yield. On the other hand, with drought becoming more severe with time under terminal drought condition, the yield of late flowering genotypes was more affected by the terminal drought ($r = -0.584^{**}$).

For each drought condition at each location, grain yield reduction (%) as well as delay in flowering due to drought was calculated and plotted against days to flower under flood condition. Under intermittent condition at both locations (Fig. 4a and b), both grain yield reduction (%) and delay in flowering was greater in earlier flowering genotypes than in later flowering genotypes. These results are in contrast to the terminal drought condition in which grain yield reduction was higher in genotypes that flowered later under flood condition (CPA) or not significantly affected by the flowering time (UBN) (Fig. 4c and d). However, delay in flowering in the terminal drought was generally longer in earlier flowering genotypes at both locations.

The correlation coefficients between traits of 70 genotypes under intermittent condition are shown in Table 4a. At both UBN where there was no significant effect of time of flowering on grain yield and CPA where grain yield reduction (%) was smaller with later flowering genotypes, yield reduction (%) was significantly correlated with delay in flowering; the shorter the delay the smaller the grain yield reduction. At CPA, the earlier flowering genotypes with larger yield reduction were also associated with higher LWP ($r = -0.386^{**}$), resulting in apparently smaller yield reduction in genotypes with higher LWP ($r = 0.292^{*}$).

Under terminal drought, grain yield reduction was not related to delay in flowering at both locations (Table 4b). On the other hand, grain yield reduction was smaller in genotypes with longer flowering duration in CPA where earlier flowering genotypes tended to have smaller yield reduction and longer flowering duration. This yield reduction-flower duration association was not observed with flowering duration determined under flood condition ($r = 0.085^{ns}$ data not shown), indicating that this association was induced by the drought. At UBN, there was no significant effect of attributes on yield reduction (%), but genotypes with longer delay tended to have lower LWP ($r = -0.325^{**}$). At both locations there was no relationship between delay in flowering and flowering duration, indicating that the longer delay was not caused by prolonged flowering duration.

Table 5 shows contrasting genotypes selected under particular drought condition at each location. Table 5a lists six selected genotypes from a total of 70 genotypes under intermittent drought at UBN where there was no effect of flowering time on grain yield reduction and yield reduction (%) was strongly associated with delay in flowering. Three selected genotypes for small yield

Table 3
Phenotypic correlation of grain yield (GY), day to flowering (DTF), tiller and panicle number, duration of flowering and leaf water potential (LWP) of 70 genotypes grown under flood, intermittent and terminal drought at (a) CPA and (b) UBN in wet season 2009.

	GY		DTF		Tiller number		panicle number		flowering duration		LWP[a]	
	F	I	F	I	F	I	F	I	F	I	F	I
(a)CPA												
I	0.432**		0.952**		0.417**		0.627**		–		0.145ns	
T	0.200*	−0.209*	0.963**	0.938**	0.281*	0.422**	0.478**	0.462**	0.236*	–	0.021ns	0.031ns
(b)UBN												
I	0.520**		0.320**		0.534**		0.650**		–		0.253*	
T	0.193ns	0.307*	0.605**	0.342**	0.424**	0.726**	0.252*	0.174ns	0.097ns	–	0.131ns	0.276*

* and ** represent significant levels at $p < 0.05$ and $p < 0.01$, respectively, ns represent non significant.
F = flood, I = intermittent drought and T = terminal drought.
[a] LWP measured at 94, 91 and 97 DAS under flood, intermittent and terminal drought, respectively at CPA and 87 89 and 95 DAS under flood, intermittent and terminal drought, respectively at UBN.

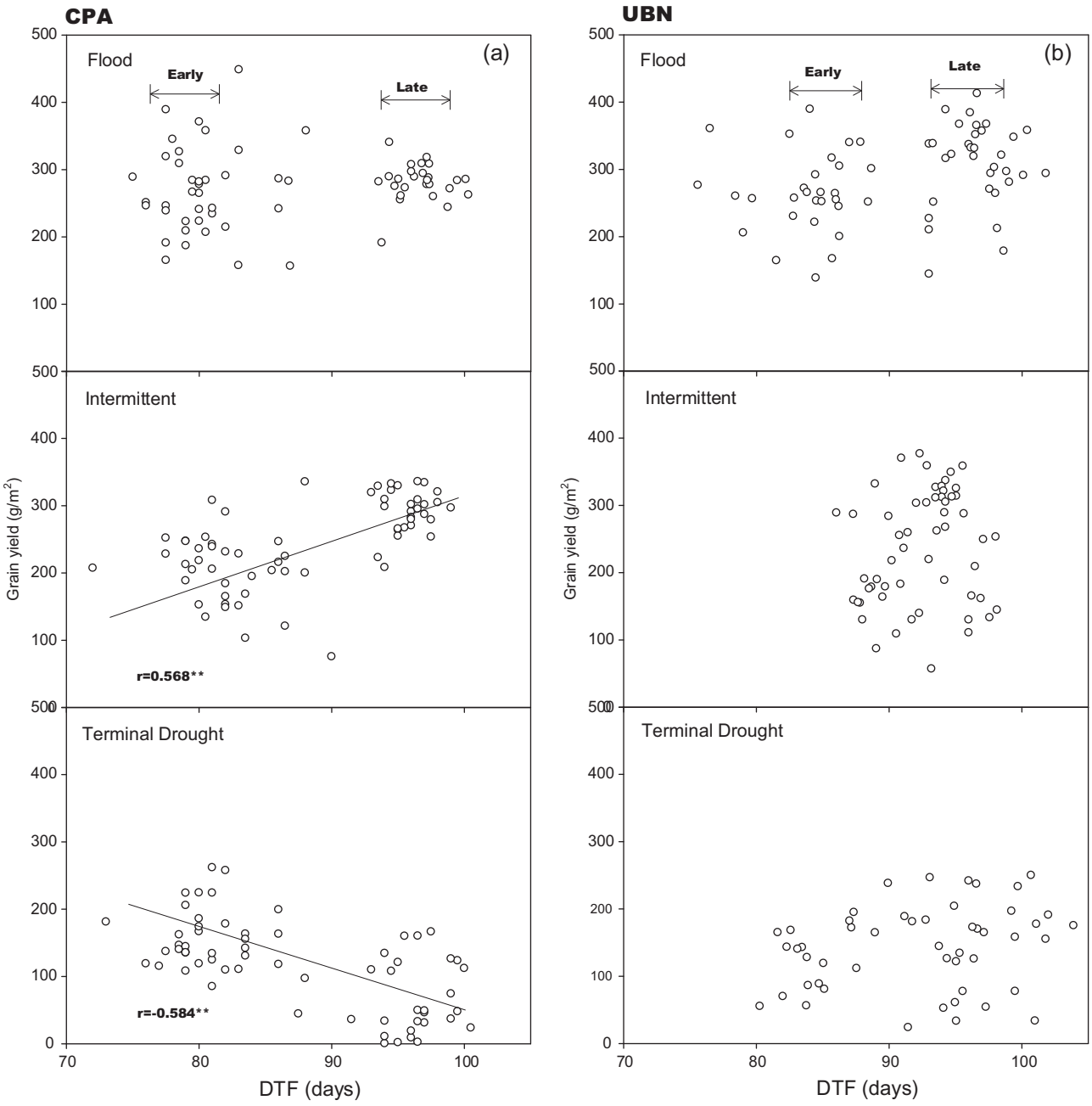


Fig. 3. Relationship between grain yield and day to flowering (DTF) of 70 genotypes grown under flood, intermittent and terminal drought conditions at CPA (a) and UBN (b) in wet season 2009.

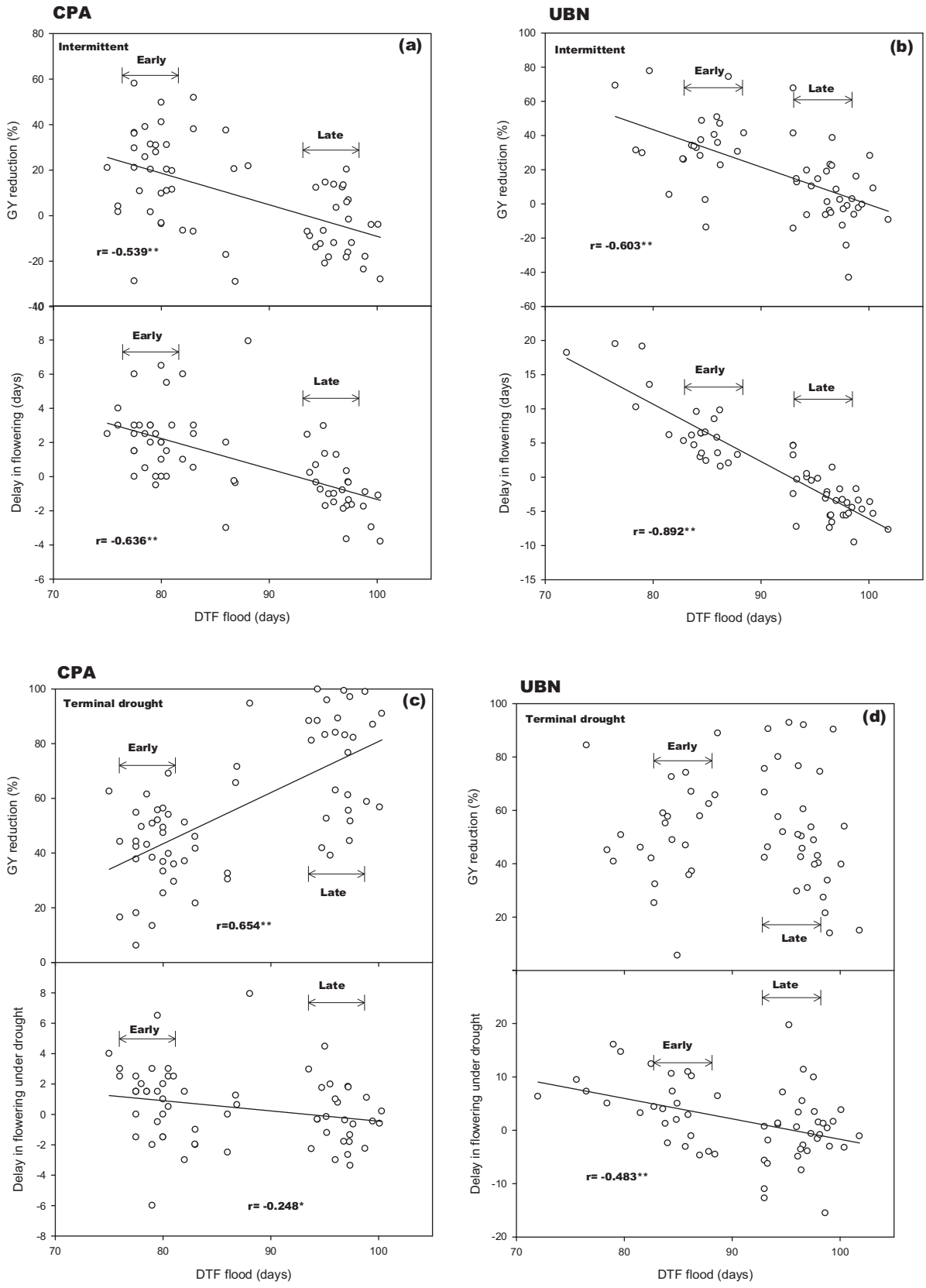


Fig. 4. Relationship between DTF under flood and grain yield reduction (%) and/or delay in flowering under intermittent (a and b) and terminal drought condition (c and d) at CPA (a and c) and UBN (b and d) of 70 genotypes in wet season 2009 (horizontal arrow shows early and late groups that were selected).

Table 4
Correlation coefficient matrix of traits, (a) under intermittent drought and (b) under terminal drought, of 70 genotypes at CPA (left columns) and UBN (right columns) in WS2009. DTF, days to flower; LWP, leaf water potential.

(a) Intermittent drought

	GY reduction (%)	DTF	Panicle number	Delay (days)	LWP (MPa)[a]
GY reduction	1.000				
DTF	−0.556**, −0.056	1.000			
Panicle number	−0.341**, −0.458**	0.421**, 0.451**	1.000		
Delay	0.453**, 0.617**	−0.291*, 0.105	−0.430**, −0.271*	1.000	
LWP	0.292*, −0.043	−0.386**, 0.313**	0.010, 0.326**	0.111, 0.004	1.000

(b) Terminal drought

	GY reduction (%)	DTF	Panicle number	Delay (days)	LWP (MPa)[a]	Flowering duration
GY reduction	1.000					
DTF	0.679**, −0.059	1.000				
Panicle number	0.156, −0.299*	0.220*, −0.187	1.000			
Delay	0.022, −0.113	−0.021, 0.325**	−0.111, −0.153	1.000		
LWP	0.067, −0.002	0.404**, 0.409**	0.262*, 0.134	−0.125, −0.324**	1.000	
Flowering duration	−0.711**, −0.006	−0.512**, −0.077	−0.138, −0.237*	−0.006, −0.158	−0.185, −0.167	1.000

* And ** represent significant levels at $p < 0.05$ and $p < 0.01$, respectively.
[a] LWP measured at 94, 91 and 97 DAS under flood, intermittent and terminal drought, respectively, at CPA and 87 89 and 95 DAS under flood, intermittent and terminal drought, respectively, at UBN.

reduction (less than 23%) had no delay in flowering, in fact flowering was hastened, while those with large yield reduction (larger than 33%) had flowering delay of at least 8 days. Leaf water potential varied between −0.8 and −1.0 MPa with no particular trend. Under terminal drought conditions, yield reduction of all 6 genotypes was similar between 46 and 58%.

Because of the effects of flowering time on grain yield reduction particularly at CPA, genotypes that flowered within 5 days of each other under flood condition were grouped together to form either early or late flowering group at each location as shown in Fig. 4, and are further analysed in the next section.

3.3. Relationship between grain yield and some attributes among genotypes of similar flowering time

Two groups of genotypes, early and late groups, were identified based on days to flower under flood condition; the early group flowered between 77–81 and 83–87 DAS at CPA and UBN, respectively. However within the late group, grain yield variation was not significant, and hence the results of the early group genotypes only are shown here.

In the early group there was significant genotypic variation in grain yield under intermittent drought at CPA and terminal drought

Table 5
Various characteristics of the 6 selected contrasting genotypes at CPA and UBN. DTF—days to flower, delay—delay in flowering (days), LWP—leaf water potential (MPa). FD—flowering duration (days).

(a) UBN. Genotypes contrasting in grain yield reduction (%) under intermittent drought

Entry	Genotypes	Flood	Intermittent drought			Terminal drought			
		DTF	GY reduction%	Delay	LWP	GY reduction%	Delay	FD	LWP
	Small yield reduction								
66	IRUBN030063-9-22	93	15	−7.3	−1.00	46	−6.3	11.4	−1.70
58	IRUBN030054-10-136	96	23	−5.6	−0.90	50	−7.5	13.4	−1.75
47	AO148-1-5	100	9	−5.3	−0.85	54	−3.2	14.2	−1.75
	Large yield reduction								
5	B6144	86	40	8.5	−0.90	47	−3.1	4.8	−1.65
8	IR82870-48	84	33	9.6	−0.90	58	−2.4	6.2	−2.20
34	IRUBN050037-B-10-B	80	78	13.5	−0.80	51	14.7	11.2	−2.35
	Mean of 70 genotypes	*90*	*19*	*1.4*	*−0.90*	*51*	*1.8*	*13.4*	*−2.01*

(b) CPA. Genotypes selected from early flowering group under terminal drought

Entry	Genotypes	Intermittent drought			Terminal drought			
		GY reduction%	Delay	LWP	GY reduction%	Delay	FD	LWP
	Small yield reduction							
12	Y364-UBN-15	2	2.0	−1.28	13	−5.0	17.4	−2.38
15	Y453-UBN-5	−4	2.0	−1.12	25	0.0	20.0	−2.15
40	IRUBN050044-B-11-B	36	2.5	−1.14	6	1.5	25.0	−2.05
	Large yield reduction							
8	IR82870-48	31	5.5	−0.93	69	2.5	13.0	−2.20
31	IRUBN050035-B-8-B	31	3.0	−1.19	51	3.0	12.2	−2.30
35	IRUBN050039-B-8-B	31	2.5	−0.81	56	6.5	16.0	−2.77
	Mean of 26 genotypes	*11*	*0.8*	*−1.13*	*42*	*−2.1*	*16.2*	*−2.32*

Table 6
Mean grain yield (GY), yield reduction percentage, tiller and panicle number per plant, panicle grain weight (PGW), flowering duration, delay in flowering and leaf water potential (LWP) in early group at CPA ($n = 27$) and UBN ($n = 23$), wet season 2009.

		GY (g/m^2)	Reduction (%)	Tiller number	Panicle number	PGW (g/panicle)	Flowering duration (days)	Delay in flowering (days)	LWP[a] (MPa)
CPA									
Flood		267*		6.5^{ns}	5.5*	1.50^{ns}	13.8^{ns}	–	−1.22^{ns}
Intermittent	202**	23	6.3^{ns}	5.3**	1.61*	–	0.39^{ns}	−1.20*	
Terminal Drought	154^{ns}	41	6.3^{ns}	5.0^{ns}	1.15 **	14.0^{ns}	0.59^{ns}	−2.42^{ns}	
p Value									
Condition(C)	*<0.001*		*0.07*	*0.023*	*<0.001*	*0.784*	*0.683*	*<0.001*	
Genotypes(G)	*<0.001*		*0.007*	*<0.001*	*<0.001*	*0.632*	*0.899*	*0.099*	
C × G	*0.039*		*0.561*	*0.38*	*<0.001*	*0.849*	*0.777*	*0.123*	
UBN									
Flood		264*		7.3^{ns}	6.3**	1.87*	14.8*	–	−0.82^{ns}
Intermittent	178^{ns}	33	7.8**	6.0**	1.67^{ns}	–	2.27^{ns}	−0.82^{ns}	
Terminal Drought	144*	43	7.3**	5.3^{ns}	1.25*	13.2^{ns}	2.93^{ns}	−1.85^{ns}	
p Value									
Condition(C)	*<0.001*		*0.209*	*<0.001*	*<0.001*	*0.446*	*0.236*	*<0.001*	
Genotypes(G)	*<0.001*		*<0.001*	*<0.001*	*<0.001*	*0.024*	*0.028*	*0.662*	
C × G	*0.757*		*0.618*	*0.886*	*0.535*	*0.504*	*0.647*	*0.969*	

* and ** represent significant levels at $p < 0.05$ and $p < 0.01$, respectively, ns represent non significant.
[a] LWP measured at 94, 91 and 97 DAS under flood, intermittent and terminal drought, respectively at CPA and 87 89 and 95 DAS under flood, intermittent and terminal drought, respectively at UBN.

Table 7
Correlation coefficient between traits under intermittent drought of early flowering groups at CPA (left columns; $n = 27$) and UBN (right columns; $n = 23$) in wet season 2009.

(a) Intermittent drought

	GY reduction	Delay	LWP[a]
GY reduction	1.000		
Delay	0.385*, 0.105	1.000	
LWP[a]	−0.005, −0.021	−0.268, −0.041	1.000

(b) Terminal drought

	GY reduction	Delay	LWP[a]	Flowering duration
GY reduction	1.000			
Delay	0.347, −0.343	1.000		
LWP[a]	−0.1888, −0.223	−0.007, −0.393*	1.000	
Flowering duration	−0.813**, 0.179	0.029, −0.296	0.230, −0.330	1.000

*, ** Represent significant levels at $p < 0.05$ and $p < 0.01$, respectively.
[a] LWP measured at 94, 91 and 97 DAS under flood, intermittent and terminal drought, respectively at CPA and 87 89 and 95 DAS under flood, intermittent and terminal drought, respectively at UBN.

at UBN (Table 6). The yield reduction was 23–33% in the intermittent drought and 41–43% in the terminal drought. By comparing mean values under different water availability conditions at each location, drought effect on tiller number production was negligible at both locations, but terminal drought conditions reduced the mean panicle number at UBN, and also reduced the individual panicle weight at both locations.

Under intermittent drought condition, early flowering genotypes with larger yield reduction (%) were associated with longer delay in flowering, and this was significant at CPA (Table 7a). Under terminal drought conditions at this location, similar association was obtained although it was not significant at 5% probability level ($r = 0.347$, $p = 0.08$). Grain yield reduction was strongly correlated with flowering duration; genotypes with smaller yield reduction had longer flowering duration. Genotypes with longer delay tended to have lower LWP at UBN. These results were similar to those found earlier with the 70 genotypes, despite the grain yield reduction being greatly affected by flowering time in the larger population set.

Among early flowering genotypes three were selected for small yield reduction (less than 25%) and another three were selected for large yield reduction (more than 50%) under terminal drought at CPA where grain yield was strongly related to flowering time and flowering duration was measured (Table 5b). Under the terminal drought, the former group of genotypes had a flowering duration of 17.4–25.0 days, while the latter had flowering duration of 16 days or less. Delay was less than 1.5 days in the genotypes with small yield reduction while the delay was greater than 2.5 days in the latter group. Some genotypes that performed well under terminal drought also had small yield reduction under intermittent drought, but this was not so with one line (IRUBN050044-B-11-B).

4. Discussion

In order to enhance the drought resistance of germplasm in rainfed lowland rice, the present work has evaluated delay in flowering as a potential selection trait in intermittent stress conditions. It has also examined delay in flowering in relation to flowering duration under terminal conditions. The small reduction (10–19%) in grain yield under intermittent drought conditions and larger reduction in terminal drought conditions (52–55%) in the wet season in rainfed lowland ecosystem obtained in NE Thailand in the present work was similar to that obtained in Laos under similar intermittent and terminal drought conditions (mean yield reduction of 13% and 35%) by Xangsayasane et al. (2014b). They concluded the intermittent drought did not provide sufficient drought damage to discriminate genotypes for drought resistance, and suggested to reduce irrigation frequency for screening under intermittent drought

condition in wet season. However in the present work, the intermittent drought effect was greater in early flowering genotypes; i.e. yield reduction of 23–33% for early genotypes that flowered between 77–81 DAS and 83–87 DAS under flood condition at CPA and UBN, respectively. While soil water content under the intermittent drought condition at both locations fluctuated in a similar manner for a long period (Fig. 2), the delay in flowering and yield reduction were greater in genotypes that flowered early under flood conditions (Fig. 4), suggesting their susceptibility to drought under intermittent drought condition. This could be related to particular groups of early and late genotypes tested in the experiments, or the smaller yield reduction in late maturing genotypes in intermittent drought condition may be associated with their ability to recover from the initial drought stress as Lilley and Fukai (1994) had shown under upland conditions. In addition, the late flowering genotypes were exposed to several intermittent drought periods before flowering, and this may have helped them to adjust to the drought conditions (Lilley and Ludlow, 1996; Jongdee et al., 2002; Nio et al., 2011), resulting in rather small adverse effect of drought on yield. In any case, the reduction in irrigation frequency as suggested by Xangsayasane et al. (2014b) is likely to increase the reliability of drought screening, and hence is recommended.

While the overall effect of intermittent and terminal drought conditions was similar between the two locations, there was indication that the crop was slightly more severely affected by drought in UBN where the soil was sand compared to clay loam soil in CPA, particularly under intermittent drought conditions. This can be seen as longer delay in flowering (3 vs 1 days) and larger yield reduction under intermittent conditions (18.5 vs 10.0% for all the genotypes and 33 vs 23% for the early flowering genotypes). There was also a difference in responses of 70 genotypes to drought conditions at CPA and UBN. At CPA, the effect of flowering time on grain yield was significant under both intermittent and terminal drought conditions. Under terminal drought at this location increased soil water deficit with time resulted in more severe grain yield reduction in later flowering genotypes as was also found by others (Pantuwan et al., 2002a; Jongdee et al., 2006; Kumar et al., 2012). Drought stress was severe after flowering in terminal drought condition and this resulted in smaller individual panicles. The rather negligible effect on panicle number was also found in intermittent drought, and most drought effect on grain yield was through reduced individual panicle weight.

The result of terminal drought condition at UBN was different from that obtained at CPA, because in UBN genotype's flowering time had rather small effect on grain yield and other attributes. Some late flowering genotypes were able to produce 70–80% of yield obtained under flood condition. While the reason for this is not known, our later experiments show that the late genotypes had higher root density and larger root number under 0–10 cm depth (Monkham et al. unpublished). In the terminal drought condition at both locations in the present experiment, the higher LWP was found in later flowering genotypes which was also found by Jongdee et al. (2002) under terminal drought condition.

Delay in flowering is a potential selection criterion that can be used by breeders for selection of drought resistant varieties in rainfed lowland rice (Pantuwan et al., 2002b). The present work has shown that under intermittent drought condition where drought stress was mild and yield reduction was small, delay in flowering can be used to select drought resistant genotypes, because genotypes with smaller yield reduction (%) were associated with shorter delay in flowering, $r = 0.453^{**}$ and 0.617^{**} at CPA and UBN, respectively. The delay in flowering may be related to loss of turgor (Blum 2011), particularly in genotypes with lower LWP (Jongdee et al., 2002; Kumar et al., 2006); this LWP- delay association was also found in terminal drought at UBN where significant genotypic variation in LWP was found. In the present intermittent condition where irrigation was applied every 6–12 days, mild drought that developed was interrupted frequently by irrigation, and it is likely that resistant genotypes with better plant water status under drought condition took a shorter time to recover and flowered sooner, resulting in shorter delay.

On the other hand, under terminal drought there was no correlation between grain yield reduction and delay in flowering at both locations, but later flowering genotypes had longer delay in flowering than earlier flowering genotypes. At CPA where soil moisture data were available from both terminal and intermittent drought conditions, by the time early flowering genotypes were about to head under terminal drought condition, the plants were already sufficiently stressed, and without further water supply, some panicles died and there was no significant relationship between yield reduction and delay in flowering. However smaller reduction in yield under terminal drought was associated with longer flowering genotypes at CPA when either all 70 genotypes with different flowering dates or only early flowering genotypes were examined. It appears that under this situation of increasing drought stress condition, only more advanced panicles within a crop canopy emerged and flowered. Susceptible genotypes stopped flowering earlier while resistant ones apparently kept flowering resulting in longer duration of flowering. This appears to be the case even within the early flowering genotypes as there was highly significant correlation between yield reduction (%) and flowering duration ($r = -0.813^{**}$) under terminal drought condition at this location. These results suggest timing and severity of drought appear important in determining success or otherwise of delay in flowering as a selection criterion, and flowering of susceptible genotypes may be delayed under rather mild drought conditions that develop immediately prior to the time of flowering.

In a recent work in Laos under intermittent and terminal drought conditions, Xangsayasane et al. (2014b) found no correlation between delay in flowering and grain yield when 227 genotypes were subjected to drought screening. However, they found significantly lower yield in genotypes with longer delay when genotypes were grouped into 3 maturity types. Thus, drought development patterns and genotype's maturity may need to be considered for delay in flowering to be used successfully as a drought screening trait. Another possible reason for this difficulty may be related to errors in determining the flowering date of a whole plot because of flowering time variation both within a plant and between the plants (Yoshida, 1981; Shahidullah et al., 2009). The present work has shown that flowering took place for several days in each canopy, and there was significant genotypic variation in flowering duration. The canopy flowering duration was found to be related to genotype's flowering date, but it was not related to delay in flowering in the present experiments. Thus, it is likely that the longer flowering delay was not caused by flowering duration becoming prolonged with drought.

While there is a requirement to utilize an irrigated control to enable calculation of the delay in flowering due to drought, delay in flowering based on a plot can be determined without any specialized equipment, just by visual observation and recording of flowering date. Therefore, this trait can be used to screen a large number of genotypes within a rather short time if drought timing and severity are managed for maximum discrimination of genotypes. The screening efficiency is likely to increase if the intermittent drought period is longer than the period used in the present work and hence genotypes screened under slightly more severe drought conditions, in addition analysis needs to be conducted on groups of genotypes according to their maturity. The latter should be readily achieved particularly for advanced plant materials which have been tested during earlier stages of selection process.

It can be concluded that the drought screening under intermittent stress condition was suitable at both locations and it is likely

that reduction in irrigation frequency and subsequent increase in each intermittent drought duration will further improve discrimination among genotypes for drought resistance. When drought effect is mild and interrupted frequently as in intermittent drought, delay in flowering can be used as indirect selection trait. While genotypes with longer flowering duration had smaller yield reduction under terminal drought at one location, flowering duration was not related to delay in flowering.

Acknowledgements

The authors wish to thank the Generation Challenge Program for financial support of the work reported here and the Royal Golden Jubilee Ph.D. Program (grant no. PHD/0029/2551) for the support of the senior author. We gratefully acknowledge the involvement of staff of Faculty of Agriculture, Khon Kaen University and Chum Phae and Ubon Ratchathani Rice Research Center (CPA and UBN), and the provincial staff for their technical assistance.

References

Bernier, J., Kumar, A., Ramaiah, V., Spaner, D., Atlin, G., 2007. A large-effect QTL for grain yield under reproductive-stage drought stress in upland rice. Crop Sci. 47, 505–516.

Fukai, S., Ouk, M., 2012. Increase productivity of rainfed lowland rice cropping system of the Mekong region. Crop Pasture Sci. 63, 944–973.

Jongdee, B., Fukai, S., Cooper, M., 2002. Leaf water potential and osmotic adjustment as physiological traits to improve drought tolerance in rice. Field Crops Res. 76, 153–163.

Jongdee, B., Pantuwan, G., Fukai, S., Fischer, K.S., 2006. Improving drought tolerance in rainfed lowland rice: an example for Thailand. Agric. Water Manage. 80, 225–240.

Kamoshita, A., Babu, R.C., Boopathi, N.M., Fukai, S., 2008. Phenotypic and genotypic analysis of drought-resistance traits for development of rice cultivars adapted to rainfed environments. Field Crop Res. 109, 1–23.

Kanjoo, V., Punyawaew, K., Siangliw, J.L., Jearakongman, S., Vanavichit, A., Toojinda, T., 2012. Evaluation of agronomic traits in chromosome segment substitution lines of KDML105 containing drought tolerance QTL under drought stress. Rice Sci. 19, 117–124.

Kumar, A., Verulkar, S., Dixit, S., Chauhan, B., Bernier, J., Venuprasad, R., Zhao, D., Shrivastava, M.N., 2009. Yield and yield-attributing traits of rice (*Oryza sativa* L.) under lowland drought and suitability of early vigor as a selection criterion. Field Crop Res. 114, 99–107.

Kumar, A., Verulkar, S.B., Mandal, N.P., Variar, M., Shukla, V.D., Dwivedi, J.L., Singh, B.N., Singh, O.N., Swain, P., Mall, A.K., Robin, S., Chandrababu, R., Jain, A., Haefele, S.M., Piepho, H.P., Raman, A., 2012. High-yielding, drought-tolerant, stable rice genotypes for the shallow rainfed lowland drought-prone ecosystem. Field Crop Res. 133, 37–47.

Kumar, R., Sarawgi, A.K., Ramos, C., Amarante, S.T., Ismail, A.M., Wade, L.J., 2006. Partitioning of dry matter during drought stress in rainfed lowland rice. Field Crops Res. 98, 1–11.

Lafitte, H.R., Courtois, B., Arraudeau, M., 2002. Genetic improvement of rice in aerobic system: progress from yield to genes. Field Crop Res. 75, 171–190.

Lilley, J.M., Fukai, S., 1994. Effect of timing and severity of water deficit on four diverse rice cultivars. III. Phenological development, crop growth and grain yield. Field Crops Res. 37, 225–234.

Lilley, J.M., Ludlow, M.M., 1996. Expression of osmotic adjustment and dehydration tolerance in diverse rice lines. Field Crop Res. 48, 185–197.

Moldenhauer, K., Slaton, N., 2004. 1-Rice growth and development. In: Slaton, N. (Ed.), Rice Production Handbook. University of Arkansas, Division of Agriculture, Little Rock, Arkansas, U.S.A.

Nio, S.A., Cawthray, G.R., Wade, L.J., Colmer, T.D., 2011. Pattern of solutes accumulated during leaf osmotic adjustment as related to duration of water deficit for wheat at the reproductive stage. Plant Physiol. Biochem. 49, 1126–1137.

OAE, 2003. Rice Growing Area in Thailand. OAE, Retrieved October 13, 2013. From ⟨http://www.oae.go.th⟩.

Ouk, M., Basnayake, J., Tsubo, M., Fukai, S., Fisher, K.S., Kang, S., Men, S., Thun, V., Cooper, M., 2007. Genotype-by-environment interactions for grain yield associated with water availability at flowering in rainfed lowland rice. Field Crops Res. 101, 145–154.

Pantuwan, G., Fukai, S., Cooper, M., O'Toole, J.C., Sarkarung, S., 1997. Root traits to increase drought resistance in rainfed lowland rice. In: Fukai, S., Cooper, M., Salisbury, J.E. (Eds.), Proceedings of an International Workshop. Australian Centre for International Agricultural Research, Canberra, ACT, Ubon Ratchathani, Thailand, pp. 170–179.

Pantuwan, G., Fukai, S., Cooper, M., Rajatasereekul, S., O'Toole, J.C., 2002a. Yield response of rice (*Oryza sativa* L.) genotypes to different types of drought under rainfed lowlands Part 1. Grain yield and yield components. Field Crop Res. 73, 153–168.

Pantuwan, G., Fukai, S., Cooper, M., Rajatasereekul, S., O'Toole, J.C., 2002b. Yield response of rice (*Oryza sativa* L.) genotypes to different types of drought under rainfed lowlands, Part 2. Selection of drought resistant genotypes. Field Crop Res. 73, 169–180.

Sellamuthu, R., Liu, G.F., Ranganathan, C.B., Serraj, R., 2011. Genetic analysis and validation of quantitative trait loci associated with reproductive-growth traits and grain yield under drought stress in a doubled haploid line population of rice (*Oryza sativa* L.). Field Crop Res. 124, 46–58.

Shahidullah, S.M., Hanafi, M.M., Ashrafuzzaman, W.M., Salam, M.A., Khair, A., 2009. Flowering response and crop duration of aromatic rices in diverse environments. C.R. Biol. 332, 909–916.

Xangsayasane, P., Fukai, S., Mitchell, J.H., Jongdee, B., Jothityangkoon, D., Pantuwan, G., Inthapanya, P., 2014a. Genotypic performance in multi-location on-farm trials for evaluation of different on-station screening methods for drought-prone rainfed lowland rice in Lao PDR. Field Crops Res. 160, 1–11.

Xangsayasane, P., Jongdee, B., Pantuwan, G., Fukai, S., Mitchell, J.H., Inthapanya, P., Jothiyangkoon, D., 2014b. Genotypic performance under intermittent and terminal drought screening in rainfed lowland rice. Field Crop Res. 156, 281–292.

Yoshida, S., 1981. Fundamentals of Rice Crop Science. IRRI, Los Baños, Philippines, P.O. Box 933, Manila (269 pp.).

Plant Prod. Sci. 18(1): 32—42 (2015)

Effects of Salt Stress after Late Booting Stage on Yield and Antioxidant Capacity in Pigmented Rice Grains and Alleviation of the Salt-Induced Yield Reduction by Exogenous Spermidine

Sumitahnun Chunthaburee[1], Jirawat Sanitchon[2], Wattana Pattanagul[1] and Piyada Theerakulpisut[1]

([1]Department of Biology, Faculty of Science, Khon KaenUniversity, Khon Kaen 40002, Thailand;
[2]Department of Plant Science and Agricultural Resources, Faculty of Agriculture, Khon Kaen University, Khon Kaen 40002, Thailand)

Abstract: Pigmented rice is receiving much attention due to the large amounts of bioactive compounds and various health benefits. However, little information is available on its agronomic and physiological aspects. This research aimed to explore the effects of salinity on yield and grain quality of pigmented rice and the modulation of salinity responses by exogenous application of spermidine (Spd). Four cultivars of rice were grown in pots until the early booting stage. Thereafter, the plants were sprayed with 1 mM Spd for 7 successive days before being irrigated with 25 mM NaCl instead of tap water until maturity. Grain yield, yield components and harvest index in all rice cultivars were negatively affected by this salinity stress. Pretreatment with Spd dramatically improved yield and yield components of salt-treated plants, particularly the salt-sensitive cultivar. The major yield components which were improved and contributed most to the dramatic increase in seed yield were the number of filled grains per panicle and panicle fertility. Moreover, Spd pretreatment resulted in an increase in K^+/Na^+ ratio in rice grains. Salt stress increased nutritional quality of mature grains, i.e., total phenolic content, anthocyanins, proanthocyanins and antioxidant activities (evaluated by FRAP, DPPH and ABTS assays) in all rice cultivars. Furthermore, all aspects of health-promoting nutritional characters were further enhanced by Spd pretreatment. Thus foliar spraying of Spd to rice plants prior to salt application improved grain yield as well as nutritional quality of colored rice grains in relation to total phenolics, flavonoid pigments and antioxidant capacities.

Key words: Antioxidant activity, Pigmented rice, Salt stress, Spermidine.

Soil salinity is one of the most important abiotic stress factors affecting rice productivity in the arid and semi-arid regions of the world (Flowers, 2004). It is considered the most serious threat to agriculture and to the environment in many parts of the world (Parida and Das, 2005). Salinity stress causes a low soil water potential, accumulation of toxic sodium ions, nutritional imbalance and subsequently leads to an over-accumulation of reactive oxygen species (ROS) (Roychoudhury et al., 2008). Salinity results in growth reduction during the vegetative growth stage and yield reduction during the reproductive stage. Attempts to improve yield under stress conditions by genetic improvement have been difficult with limited success due to the complex polygenic nature of abiotic stress regulation. Recently, exogenous protectants such as osmoprotectants, plant hormones, antioxidants and polyamines have been found effective in mitigating the salt-induced damage in plants (Hamdia and Shaddad, 2010; Yusuf et al., 2012)

Polyamines (PAs) are low molecular weight organic cations present in a wide range of organisms from bacteria to plants and animals (Bouchereau et al., 1999). The most common PAs are putrescine (Put), spermidine (Spd) and spermine (Spm) that are implicated in regulations of many physiological processes in plants (Alcázar et al., 2006). Mechanisms of action of PAs in protecting cells from abiotic stress damage have mainly been demonstrated during vegetative growth stages. Endogenous PAs which are induced by abiotic stresses play multifaceted roles in protecting plant cells against environmental stresses (Shabala et al., 2007; Farooq et al., 2009; Hussain et al., 2011). Synthesis of PAs during reproductive development has been demonstrated to be essential for normal seed development (Liang and Lur, 2002; Urano et al., 2005)

Received 13 February 2014. Accepted 26 May 2014. Theerakulpisut (piythe@kku.ac.th, fax +66 43 202530).

Abbreviations: ABTS, 2,2′-azinobis (3-ethylbenzothiazoline 6-sulfonic acid); DPPH, 2,2´-diphenyl-1-picrylhydrazyl; FRAP, ferric reducing antioxidant power; GAE, gallic acid equivalents; NO, nitric oxide; PAs, polyamines; Put, putrescine; ROS, reactive oxygen species; Spd, spermidine; Spm, spermine; TPC, total phenolic content; TE, trolox equivalents; TPTZ, 2, 4, 6-tripyridyl-*s*-triazine.

Table 1. Description of rice cultivars used in this study.

No.	Cultivar	Rice type	Pericarp colour	Salt tolerance at seedling stage	Source
1	Pokkali	non-glutinous rice	red	tolerant	India
2	KKU-LLR-012	non-glutinous rice	red	tolerant	Thailand
3	Niewdam Gs.no.00621	glutinous rice	black	tolerant	Thailand
4	KKU-LLR-039	glutinous rice	black	sensitive	Thailand

and their actions are antagonized by ethylene (Yang et al., 2006). Exogenous PAs have been shown to reduce salinity stress-induced damages in several plants including rice. Exogenous application of PAs either as seed priming, foliar spray or root soaking has proved beneficial for vegetative growth of rice under salt stress (Krishnamurthy and Bhagwat, 1989; Roychoudhury et al., 2011; Saleethong et al., 2011). During vegetative growth PAs have been shown to reduce the accumulation of Na^+, alleviate the loss of K^+, reduce ROS accumulation and enhance the activity of antioxidative enzymes and non-enzymatic antioxidants, alleviate chlorophyll loss and membrane leakage, and increase compatible osmolytes (Chattopadhayay et al., 2002; Roy et al., 2005; Ndayiragije and Lutts, 2006; Quinet et al., 2010; Roychoudhury et al., 2011; Saleethong et al., 2011). Exogenous application of PAs has also been reported to promote reproductive development and offers protection to reproductive structures leading to yield improvement under cold stress in chickpeas (Nayyar, 2005) and salt stress in rice (Ndayiragije and Lutts, 2007; Saleethong et al., 2013). However, the effects of exogenous PAs on the nutritional quality of harvested seeds were not addressed in previous studies. Relatively little information is available on the effects of exogenous PAs application on reproductive development and yield of rice exposed to salt stress (Ndayiragije and Lutts, 2007; Saleethong et al., 2013). Exogenous PA application has been suggested to be a convenient and effective approach for enhancing salinity tolerance of crops and eventually improving crop productivity under high salinity (Chattopadhayay et al., 2002; Verma and Mishra, 2005).

Red rice and black rice have become increasingly popular due to numerous health benefits because they contain large amounts of phenolic compounds, especially anthocyanins in pericarp (Abdel-Aal et al., 2006). However, little information exists on the effects of stresses on the production of beneficial pigments and antioxidant capacities of colored rice. The present study, therefore, aims to investigate the effects of salinity and exogenous Spd on yields as well as the grain quality in relation to antioxidant capacities of four cultivars of pigmented rice with different levels of salt tolerance. The information from the present investigation is expected to provide an insight into the mechanism of action and the potential application of PAs in modulating the reproductive development of rice under salt stress.

Materials and Methods

1. Plant growth conditions

Seeds of three accessions of pigmented rice (*Oryza sativa* L.) were kindly provided by Faculty of Agriculture, Khon Kaen University and those of the cultivar Pokkali by Rice Gene Discovery Unit, Biotec, Thailand. Description of rice cultivars and their salt tolerance levels (Chunthaburee et al., 2012) are summarized in Table 1. The experiment was carried out in a net house (with walls of nylon net) during the months of June to November 2011. Plants were raised in black plastic pots (30 cm in height, 30 cm in diameter) containing 12 kg homogeneous mixture of 3:1 (v/v) soil and farmyard manure. Five seeds were planted in each pot (27 June 2011) and the plants were thinned to three per pot at 14 days after germination. The water level in each pot was maintained at 5 cm above the soil surface using tap water. At the early booting stage, the plants were divided into three groups, one control and two treatments including (1) NaCl and (2) NaCl + Spd. Six pots per treatment were arranged in a completely randomized design. For the NaCl + Spd group, the plants were treated with 1 mM Spd as a foliar spray between 1600 and 1700 for 7 successive days (28 September to 4 October 2011) at a volume of 50 mL per pot. The same amount of distilled water was sprayed in the control and the NaCl treatment groups. After the Spd treatment ended, salinity treatment was imposed as NaCl and NaCl + Spd treatments by adding 25 mM NaCl to the pots (5 October 2011 until harvest), while the control continued to be fed with tap water. The heading date of the plants was between 9 October and 11 October 2011. At maturity, the panicles were harvested and threshed manually. Yield and yield components were measured as number of panicles per plant, panicle length, number of filled grains per panicle, number of unfilled grains per panicle, 1000-grain weight, grain yield per plant and harvest index (%). The mean for each parameter was calculated from 6 repetitions, each was calculated as an average of three plants.

2. Extraction procedure to determine the antioxidant properties

The method of extraction for determination of antioxidant properties of rice grains was adapted from

Sompong et al. (2011). De-hulled rice samples were finely ground and samples (1.5 g) were extracted with 85% aqueous ethanol for 30 min. The mixtures were centrifuged at 2,500 × g for 10 min and the supernatants were collected. The residues were re-extracted twice under the same conditions, resulting in a final volume of 50 mL crude extract and the supernatants were pooled. Extracts were used to determine total phenolic content (TPC) and antioxidant capacity and the measurements were replicated four times.

3. Determination of total phenolic content

TPC was assayed by Folin–Ciocalteu's reagent method (Singleton et al., 1999). Briefly, 120 μL of extract was placed into test tubes and then 600 μL of freshly diluted 10-fold Folin–Ciocalteu's reagent was added. After 2 min, 480 μL of sodium carbonate solution (75 g L^{-1}) was added. The mixtures were vigorously shaken and allowed to stand for 40 min. The absorbance of the resulting blue colour was measured at 760 nm. Gallic acid was used as standard and TPC was expressed as mg gallic acid equivalents (GAE) equivalent per g flour weight.

4. Determination of ferric reducing antioxidant power (FRAP)

The FRAP assay was adapted from Benzie and Strain (1999). Briefly, 200 μL of rice extract is mixed with 1.3 mL of the FRAP reagent. Absorption was measured at 595 nm using a spectrophotometer after 30 min incubation at 37ºC. FRAP reagent consisting of 0.3 M acetate buffer (pH 3.6), 10 mM TPTZ (2, 4, 6-tripyridyl-*s*-triazine) in 40 mM HCl and 20 mM $FeCl_3$ at a ratio of 10:1:1 (v/v/v) was freshly prepared as required. The FRAP value was expressed as milligrams of Trolox equivalents (TE) per g dry weight.

5. Determination of 2,2´-diphenyl-1-picrylhydrazyl (DPPH) radical-scavenging assay

DPPH radical-scavenging ability of rice extracts was estimated according to the method of Brand-Williams et al. (1995). The reaction mixture contained 1.5 mL DPPH working solution (4.73 mg of DPPH in 100 mL ethanol HPLC-grade) and 100 μL rice extract. The mixture was shaken and incubated for 1 hr in the dark at room temperature. The absorbance was read at 515 nm relative to the control using a spectrophotometer. Trolox was used to develop standard curves. The percentage of inhibition was measured according to the equation:

$$\% \text{ inhibition} = 100 \times (A_{control} - A_{sample}) / A_{control}$$

6. Determination of 2,2´-azinobis (3-ethylbenzothiazoline 6-sulfonic acid) (ABTS) radical-scavenging assay

The ABTS radical cation scavenging assay was conducted by a modification of the method of Re et al. (1999). A stable stock solution of ABTS radicals was produced by adding potassium persulfate to a 7 mM aqueous solution of ABTS in the dark at room temperature and allowing to react for 12 – 16 hr before use. Rice extract (120 μL) was allowed to react with 1.5 mL of a diluted ABTS radical solution (absorbance of 0.70 ± 0.02 at 734 nm). The absorbance at 734 nm of the mixture was measured after 30 min reaction time. The percentage of inhibition was measured according to the equation:

$$\% \text{ inhibition} = 100 \times (A_{blank} - A_{sample}) / A_{blank}$$

7. Total anthocyanins

Concentration of anthocyanins was determined according to the method of Abdel-Aal and Hucl (1999). Briefly, rice grains were finely ground with a mortar and pestle. Approximately 0.1 g of sample was soaked for 72 hr in 10 mL of acidified ethanol (ethanol and HCl 1.0 N, 85:15, v/v). The tube was centrifuged at 15,000 × g for 30 min. The suspension was filtered through Whatman No.1 filter paper (Sigma-Aldrich, St. Louis, MO, USA) and absorbance was measured at 535 nm.

8. Total proanthocyanidins

Rice grains were finely ground with a mortar and pestle. Rice flour (1 g) of each sample was extracted with 50 mL methanol for 24 hr followed by centrifugation at 15,000 × g for 15 min. The supernatant was collected for analysis. The total proanthocyanidins were measured using the modified vanillin assay described by Sun et al. (1998). In brief, the rice extract (0.5 mL) was mixed with 3 mL of 4% vanillin in methanol (w/v) solution and 1.5 mL hydrochloric acid. Absorption of the mixture was measured within 15 min at 500 nm. Total proanthocyanidins content was expressed as catechin equivalents (mg g^{-1}) using the equation based on the calibration curve.

9. Determination of the Na^+ and K^+ content

The grain husk was removed and the rice grains were ground with a mortar and pestle for analysis. Approximately 0.5 g powder of each dried sample was subjected to chemical analyses by digesting in 10 mL of nitric acid at 300ºC, 5 mL perchloric acid at 200ºC and 20 mL of 6 M hydrochloric acid at 200ºC, for 30 min, respectively. The Na and K ions were measured using an atomic absorption spectrometer (Model GBC932AAA, England).

10. Statistical analysis of data

Analysis of variance was performed using SPSS 16.0 for Windows (SPSS, Inc., Chicago, IL). Significant difference between means among treatments was determined by Duncan's multiple range test (DMRT). The p values smaller than 0.05 were considered as statistically significant.

Table 2. Effects of salt stress without and with Spd pretreatment on yield and yield components of rice cvs. Pokkali, KKU-LLR-012, Niewdam Gs.no.00621and KKU-LLR-039.

Cultivars	Treatment	Panicle number / plant	Panicle length (cm)	Filled grain number / panicle	Unfilled grain number / panicle	Total number of spikelet / panicle	1000- grain weight (g)	Panicle fertility (%)	Grain yield / plant (g)	Harvest index (%)
Pokkali	Control	7.67^{de}	30.02^{g}	165.75^{bc}	15.42^{bcd}	181.17^{b}	34.12^{h}	91.41^{de}	31.61^{ef}	60.20^{f}
	NaCl	6.83^{cd}	27.97^{de}	149.92^{b}	24.92^{f}	174.83^{b}	33.54^{g}	85.69^{b}	27.66^{de}	51.49^{d}
	NaCl + Spd	7.42^{d}	29.11^{f}	155.42^{bc}	21.67^{ef}	177.08^{b}	33.94^{h}	87.76^{c}	29.27^{def}	55.75^{def}
KKU-LLR-012	Control	9.89^{g}	27.03^{bc}	196.17^{e}	10.00^{a}	206.17^{c}	22.65^{b}	95.15^{g}	32.53^{f}	59.39^{f}
	NaCl	8.67^{ef}	25.88^{a}	184.39^{de}	19.22^{de}	203.61^{c}	21.84^{a}	90.66^{d}	29.13^{def}	53.27^{de}
	NaCl + Spd	9.28^{fg}	26.58^{ab}	191.61^{e}	14.33^{bc}	205.94^{c}	22.31^{b}	93.23^{efg}	30.91^{ef}	57.40^{ef}
Niewdam Gs.no.00621	Control	5.61^{ab}	28.16^{de}	169.33^{cd}	11.33^{ab}	180.67^{b}	32.44^{f}	93.70^{fg}	26.19^{cd}	51.44^{d}
	NaCl	5.11^{a}	27.03^{bc}	152.61^{bc}	21.06^{ef}	173.67^{b}	31.73^{e}	87.78^{c}	20.21^{ab}	40.00^{b}
	NaCl + Spd	5.22^{a}	27.55^{cde}	159.78^{bc}	16.50^{cd}	176.28^{b}	32.29^{f}	90.46^{d}	23.49^{bc}	45.74^{c}
KKU-LLR-039	Control	6.60^{bcd}	29.17^{f}	166.27^{bc}	14.60^{bc}	180.87^{b}	25.89^{d}	91.77^{def}	26.06^{cd}	52.63^{de}
	NaCl	5.73^{abc}	27.49^{cd}	121.87^{a}	34.20^{g}	156.07^{a}	24.82^{c}	78.18^{a}	17.05^{a}	32.48^{a}
	NaCl + Spd	6.20^{abc}	28.37^{ef}	148.93^{b}	24.40^{f}	173.33^{b}	25.60^{d}	85.84^{bc}	22.31^{bc}	43.04^{bc}
Cultivars (C)		155.7*	53.7*	40.0*	951.0*	12401.3*	1414.0*	532.2*	962.5*	2334.5*
Treatment (T)		11.2*	34.5*	7547.1*	2213.0*	1606.7ns	10.0*	854.1*	478.5*	2064.2*
C × T		0.46 ns	0.76 ns	913.2 ns	100.4*	420.6 ns	0.18 ns	69.0*	25.6 ns	146.2*
CV (%)		21.18	3.84	13.32	28.09	12.80	1.67	2.93	19.63	13.28

*, significant at $p < 0.05$ level. ns, not significant. The values are the means of 6 replicates. Means with different letters are significantly different at $p < 0.05$ according to Duncan's multiple range test.

Results

1. Yield and yield components

Salinity-induced changes in yield-related parameters of rice are given in Table 2. In general, rice exposed to salt stress from the late booting stage through to maturity showed a reduction in yield and all yield components. Panicle number per plant and panicle length decreased in all cultivars. Salinity caused a significant reduction in grain yield per plant in KKU-LLR-039 (–35%) and Niewdam Gs.no.00621 (–23%). Grain yield per plant for Pokkali and KKU-LLR-012 showed a small non-significant reduction (–13% and –10% respectively). The greatest reduction in grain yield per plant in KKU-LLR-039 resulted from the highest percentage reduction in most parameters including panicle number (–13%), filled grain number per panicle (–27%), 1000-grain weight (–4%) and panicle fertility (–15%). The increase in unfilled grain number was also greatest in KKU-LLR-039 (+134%) compared with 92, 86 and 61% increase in KKU-LLR-012, Niewdam Gs.no.00621and Pokkali, respectively. Yield reduction was less severe in Niewdam Gs.no.00621and resulted from significant reduction in 1000-grain weight (–2%) and panicle fertility (–6%). The most dramatic effect of salt stress was demonstrated in the harvest index of KKU-LLR-039 and Niewdam Gs.no.00621. The salinity effect on harvest index was less severe in Pokkali and KKU-LLR-012.

Treatment with Spd prior to salt stress showed a tendency to improve all yield-related characters. The number of panicles in all cultivars increased although the means were not significantly different. The length of panicles significantly increased from 27.97 cm in the salt-treated plants to 29.11 cm in the Spd-pretreated group in Pokkali (+4%) and 27.49 cm to 28.37 cm (+3%) in KKU-LLR-039 but was not significantly increased in KKU-LLR-012 or Niewdam Gs.no.00621. Grain yield per plant increased considerably in KKU-LLR-039 (+30%). The amount of increase in grain yield was less and non-significant in the remaining cultivars, i.e., +16%, +2% and +2% in Niewdam Gs.no.00621, KKU-LLR-012 and Pokkali, respectively. Spd treatment showed a tendency to increase the filled grain number in all cultivars, but the increase was significant only in KKU-LLR-039 (+22%). The 1000-grain weight and panicle fertility, on the other hand, were significantly increased in all cultivars by Spd treatment. The pronounced effect of Spd was observed on the improvement of harvest index. The increase in harvest index followed the same ranking as the increase in grain yield i.e. +33%, +14%, +8% and +8% for KKU-LLR-039, Niewdam Gs.no.00621, Pokkali and KKU-LLR-012 respectively.

The variations in yield and yield component were

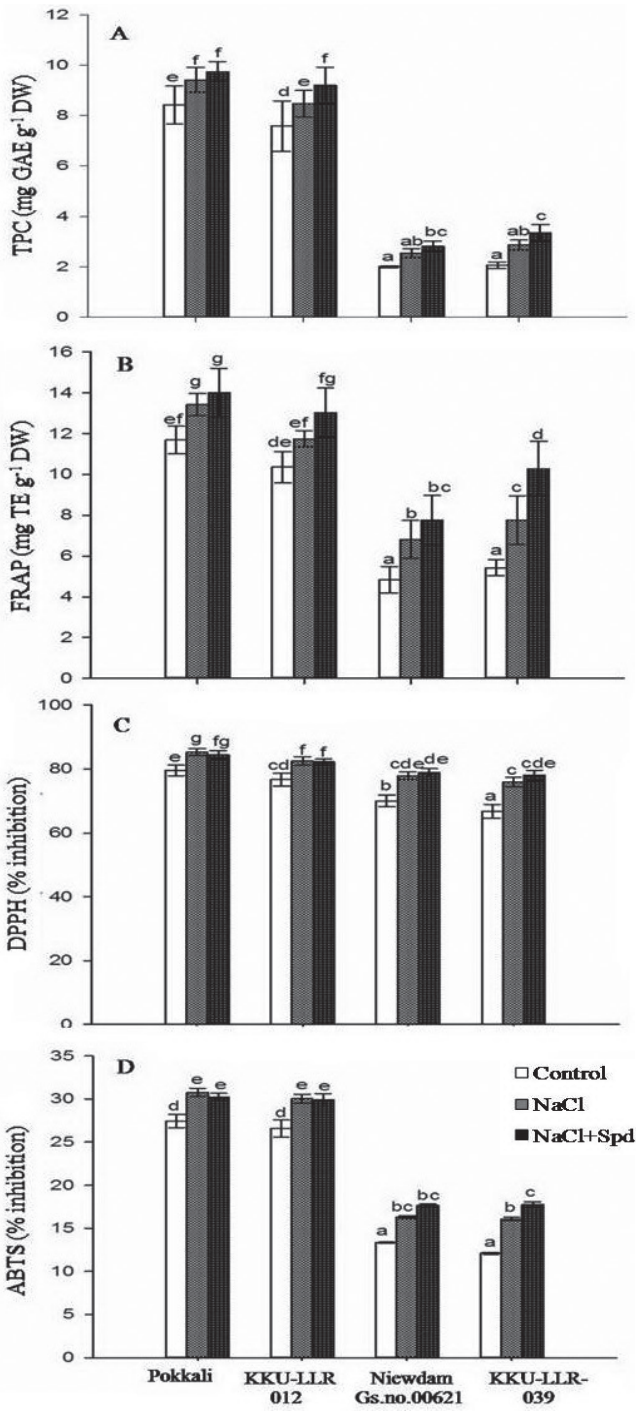


Fig. 1. Effects of salt stress without and with Spd pretreatment on total phenolic content (A) and antioxidant activities based on FRAP (B), DPPH (C) and ABTS (D) assays in mature grains of rice cvs. Pokkali, KKU-LLR-012, Niewdam Gs.no.00621and KKU-LLR-039. Data are shown as means ± SD of four independent measurements. Values with different letters are significantly different at $p < 0.05$ according to Duncan's multiple range test.

observed in Table 2. The main effect of cultivars (C) was highly significant and the interaction of treatments (T) was also significant for all yield parameters except the total number of spikelets per panicle. The interactions between cultivars and treatment (C × T) were significant for unfilled grain number per panicle, panicle fertility and harvest index, but not for the other traits were not significant.

2. TPC and antioxidant capacity

The amount of TPC (Fig. 1A) in the red-pericarp grains was 3- to 4-fold that in the black-pericarp grains. All cultivars tended to accumulate a larger amount of TPC by salinity treatment with further increase after Spd treatment. The increase of TPC by salt treatment was more pronounced in KKU-LLR-039 (39%) and Niewdam Gs. no.00621 (27%) which had black-pericarp than in Pokkali (12%) and KKU-LLR-012 (12%), which had red-pericarp. When salt stress was coupled with 1mM Spd treatment, the level of TPC increased significantly only in KKU-LLR-039 (17%) and KKU-LLR-012 (9%). However, the effect of Spd on enhancement of TPC was not significant in Pokkali (3.5%) or Niewdam Gs.no.00621 (11%).

The antioxidant activities of crude extracts from rice grains were determined by DPPH, ABTS and FRAP assays. Under salt stress, the FRAP values of all cultivars (except KKU-LLR-012) significantly increased as shown in Fig. 1B. The FRAP values in the black glutinous rice were 53% (KKU-LLR-039) and 40% (Niewdam Gs.no.00621) higher in salt-stressed conditions compared with the controls. On the other hand, the extent of salt-enhanced FRAP activity was much lower in the red rice (Pokkali; +15%; KKU-LLR-012; +13%). Similarly, after salinity stress DPPH radical scavenging activity significantly increased in all cultivars being more pronounced in the black than the red grains (Fig. 1C). The percentage increases were 14%, 11%, 8% and 7% in KKU-LLR-039, Niewdam Gs.no.00621, KKU-LLR-012 and Pokkali respectively. Salinity stress also increased the ABTS radical scavenging activity significantly in all cultivars (Fig. 1D), especially in KKU-LLR-039 which showed a 33% increase followed by Niewdam Gs.no.00621 (22%), Pokkali (13%) and KKU-LLR-012 (12%).

Exogenous Spd treatment increased the levels of FRAP in all cultivars but the effect was statistically significant only in KKU-LLR-039. Treatment with Spd before salt stress had no significant effects on DPPH activity in any cultivars. Spd tended to increase DPPH activity in the black rice but reduce it in the red rice. The ABTS activity showed similar patterns of response to Spd pretreatment, i.e., the activity further increased in the black rice but slightly decreased in the red rice. In addition, the extent of the increase in ABTS activities was most pronounced in KKU-LLR-039 (11%) followed by Niewdam Gs.no.00621 (8%).

3. Total anthocyanins and proanthocyanidins

Changes in anthocyanin content are presented in Fig. 2A. The black rice grains naturally contain more than 10

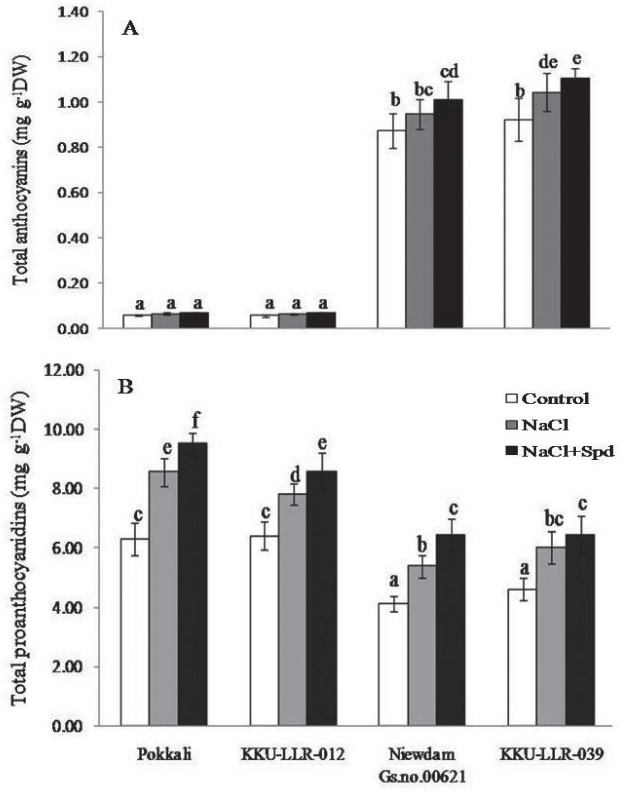


Fig. 2. Effects of salt stress without and with Spd pretreatment on anthocyanins (A) and proanthocyanidins content (B) in mature grains of rice cvs. Pokkali, KKU-LLR-012, Niewdam Gs.no.00621and KKU-LLR-039. Data are shown as means ± SD of four independent measurements. Values with different letters are significantly different at $p < 0.05$ according to Duncan's multiple range test.

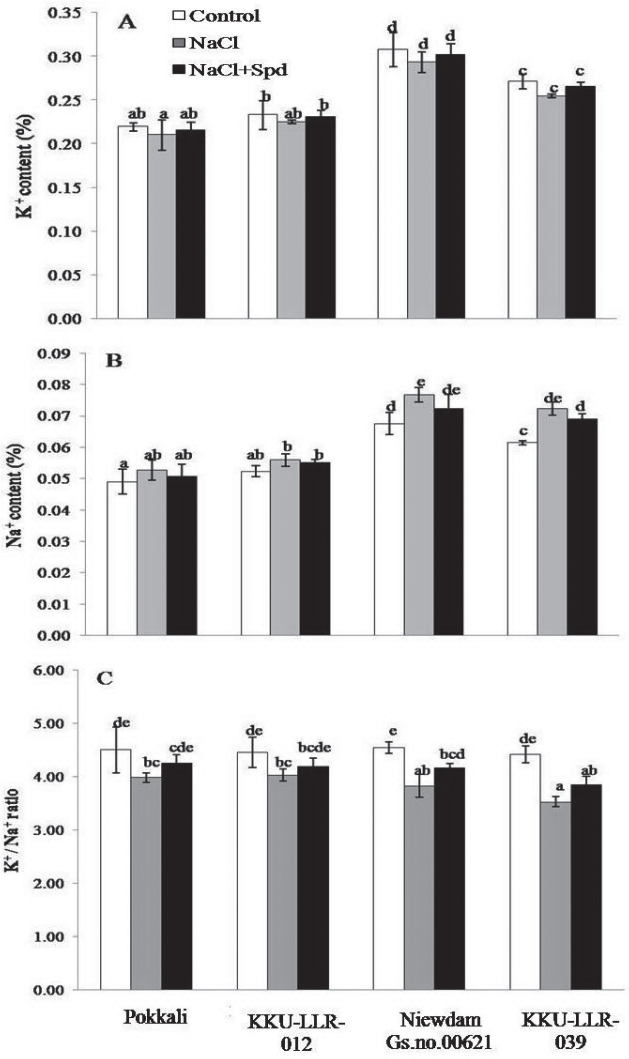


Fig. 3. Effects of salt stress without and with Spd pretreatment on K^+ (A), Na^+ (B) and K^+/Na^+ ratio (C) in mature grains of rice cvs. Pokkali, KKU-LLR-012, Niewdam Gs.no.00621and KKU-LLR-039. Data are shown as means ± SD of four independent measurements. Values with different letters are significantly different at $p < 0.05$ according to Duncan's multiple range test.

fold more anthocyanins than the red rice grains. Salinity stress tended to increase anthocyanin contents in all rice cultivars although not significantly except in KKU-LLR-039 (+13%). Spd treatment further increased anthocyanin content in all rice cultivars although not statistically significant. As shown in Fig. 2B, total proanthocyanidins markedly increased with salt stress in all cultivars. The most responsive cultivar was Pokkali (+36%) followed by Niewdam Gs.no.00621 (+31%), KKU-LLR-039 (+30%) and KKU-LLR-012 (+22%). Spd treatment significantly increased proanthocyanidin contents in the more tolerant cultivars (10 – 19%) but not in the sensitive KKU-LLR-039.

4. Ion concentration

Salinity stress reduced the K^+ concentration in mature grains of all rice cultivars (Fig. 3A) and Spd application led to a non-significant increase. On the contrary, salinity increased the Na^+ concentration (Fig. 3B). Spd pretreatment led to a slight non-significant reduction in all rice cultivars. The K^+/Na^+ ratio in mature grains decreased in all cultivars under salt stress. As shown in Fig. 3C, the K^+/Na^+ ratio was more affected by salt stress in KKU-LLR-039 than in other cultivars. In KKU-LLR-039 the ratio decreased from 4.41 in the control to 3.52 by salt stress (–20%) followed by –16%, –9% and –12% in Niewdam Gs.no.00621, KKU-LLR-012 and Pokkali, respectively. Pretreatment with Spd considerably raised the K^+/Na^+ ratio in all cultivars, especially in KKU-LLR-039 and Niewdam Gs.no.00621 where the ratios increased from 3.52 and 3.83, respectively, in the salt-treated plants to 3.85 and 4.17, respectively, in the Spd-pretreated plants (both +9%).

Discussion

The four rice cultivars showed different levels of sensitivity to salt stress. Lower percentages of reductions in yield and most yield components were noted in Pokkali and KKU-LLR-012 while KKU-LLR-039 showed the highest

percentage reduction in yield and all yield components. The cultivars KKU-LLR-012 and Niewdam Gs.no.00621 which attained similar level of salt tolerance at the seedling stage in a previous study (Chunthaburee et al., 2012) displayed a wide difference in yield reduction; a non-significant 10% reduction in the former and a significant 23% reduction in the latter. Shereen et al. (2005) also found that three rice inbred lines which showed similar levels of tolerance at the seedling stage (10 – 20% reduction in shoot growth) expressed a large difference in yield reduction (2 – 47%). However, Ali et al. (2004) reported that among ten rice cultivars tested salt tolerance scores based on visual symptoms at the seedling stage related well to grain yield under saline conditions. The observed varietal difference in salt-induced yield reduction hence depended on several factors including the intensity and duration of salt exposure as well as the developmental stage at which the plants were salinized (Asch and Wopereis, 2001; Zeng et al., 2001; Shereen et al., 2005).

In the present study, salt stress was initiated at the late booting stage and continued to maturity: therefore later formed yield components (filled grain number, unfilled grain number, 1000-grain weight and panicle fertility) were more severely affected than the earlier formed components (panicle length, tiller/panicle number per plant and total number of spikelets per panicle). However, an exception was noted in KKU-LLR-039 in which salt stress also negatively affected the total number of spikelets because reproductive development of this cultivar lagged behind the other cultivars for 3 – 4 days. This differential sensitivity to salt stress was most pronounced in the most sensitive cultivar KKU-LLR-039. The total number of spikelets was already fixed at panicle initiation (Hoshikawa, 1989) long before the commencement of salt stress and therefore was hardly affected by salinity whereas the panicle fertility and grain weight were more severely affected leading to high percentage increase in unfilled grain number and reduction in 1000-grain weight. Abdullah et al. (2001) reported multiple causes of sterility in seed set of rice under salinity including elevated Na^+/K^+ ratio in floral parts, reduction in pollen viability and stigma receptivity. Reduction in grain yield was also attributed to increased and decreased uptake of sodium and potassium ions respectively into rice panicles leading to reductions in K^+/Na^+ ratio in mature grains (Fig. 3) which was most pronounced in the salt-sensitive KKU-LLR-039. The importance of ion imbalance in determining grain yield was previously illustrated that grain yield reduction was correlated with sodium concentration in developing panicles (Asch et al., 1999), Na^+/K^+ ratio in spikelets (Abdullah et al., 2001), young leaves at the late vegetative stages (Asch et al., 2000) and the shoots (Castillo et al., 2007). Reduction in grain weight could be due to limited soluble carbohydrate translocation from leaves to spikelets and inhibition of starch synthetase activity in developing rice grains (Abdullah et al., 2001). Final grain weight is also determined by grain filling rate which has been associated with ratio between ABA and ethylene in developing grains (Yang et al., 2006) and activity of sucrose synthase (Tang et al., 2009). In contrast to this study, when rice plants were exposed to salinity earlier in the vegetative stages, the reduction in tiller number per plant and total spikelet number per panicle were the major causes of yield loss (Zeng and Shannon, 2000; Zeng et al., 2001; Zeng et al., 2002). Similarly Asch and Wopereis (2001) concluded that the strongest salinity effects on yield were observed around panicle initiation and the most affected yield components were the total spikelet number per panicle.

The reversal of the inhibitory effects of salinity on yield by exogenous Spd was more pronounced in the sensitive cultivar than the more tolerant ones. Although Spd application significantly increased panicle fertility and 1000-grain weight in all four cultivars, significant improvement in grain yield per plant was observed only in KKU-LLR-039 (+31%). The large improvement in grain yield in KKU-LLR-039 resulted from significant increases in all later formed yield components including panicle length (3.23%), panicle fertility (+9.8%), 1000-grain weight (+3.13%) and harvest index (+32.51%). Similar results were obtained by Ndayiragije and Lutts (2007) who reported that the exogenous application of Put and Spd to salt-sensitive rice cv. I Kong Pao significantly improved yield in salt-treated plants. The beneficial effects of PAs were similarly related to an improvement in panicle number per plant and total number of spikelets per panicle. Put also had positive effects on seed set and 1000-grain weight but Spd did not. In that study, the number of panicles was improved because PAs were applied to the plants from early vegetative growth. The promotive effects of PAs on post-anthesis development of rice were demonstrated by Tan et al. (2009) who found that the grain filling rate and brown rice weight were highly correlated with endogenous Spd and Spm concentration in developing grains in six rice cultivars. Wang et al. (2012) also found that endogenous Spd and Spm concentrations in the developing panicles were positively correlated with the grain filling rate but negatively correlated with ethylene evolution rate. In developing maize grains, Cao et al. (2010) demonstrated that Spd concentration has much higher positive correlations with seed weight and quality than Put and Spm. Although the mechanism underlying salt stress alleviation by PAs has not yet been fully elucidated, several suggestions have been made including the reduced accumulation of toxic Na^+ in leaves (Chattopadhayay et al., 2002; Quinet et al., 2010; Saleethong et al., 2011), shoots and roots (Ndayiragije and Lutts, 2007) and increased K^+/Na^+ ratio in grains (Saleethong et al., 2013). Shabala et al. (2007) suggested

that PAs alleviated salinity effects by the reduction of Na^+ uptake and K^+ leakage from pea mesophyll cells by directly blocking the non-selective K^+ and Na^+ permeable cation channels. Evidence also pointed to an interplay between PAs and ROS generation and NO signaling in ABA-mediated stress responses leading to stomatal regulation and Na^+/K^+ homeostasis (Alcázar et al., 2010).

The content of health promoting total phenolics in rice grains has been shown to be highly dependent on the bran color being several times higher in the red and purple than in the light brown (Goffman and Bergman, 2004) and white rice (Shen et al., 2009). Shen et al. (2009) and Sompong et al. (2011) found higher mean TPC in the black rice than in the red rice and very high within-color variations. However, the highest TPC value was found in the red variety (Shen et al., 2009). The red rice cultivars used in this study also contained higher TPC than the black ones. More importantly the antiradical efficiency showed a high positive correlation with TPC (Goffman and Bergman, 2004; Shen et al., 2009), suggesting that phenolics are the main compounds responsible for radical-scavenging activity. As expected, the red rice grains had higher antioxidant capacities as determined by the FRAP assay, ABTS radical cation scavenging activity and DPPH radical-scavenging ability. Although these assays detected the antioxidant capacity based on a similar mechanism, i.e., single electron transfer reactions (Prior et al., 2005), the FRAP assay was more responsive to Spd treatment than the others. Exogenous Spd may have stimulated the metabolic pathways leading to synthesis of certain groups of phenolic compounds responsible for the reducing ability in FRAP assays. This result confirmed earlier findings of greater antiradical ability in the red rice than in the black rice (Choi et al., 2007; Jun et al., 2012). Although the negative effects of salt stress on grain yield of rice have been widely reported, few studies have dealt with grain quality. To our knowledge, the present study demonstrated for the first time, the promotive effects of salinity on nutritional values of rice grains in terms of TPC and antioxidant activity.

The major types of flavonoids in seeds are flavonols, anthocyanins, phlobaphenes, isoflavones and proanthocyanidins (Lepiniec et al., 2006). Anthocyanins are primary pigments in the red and black rice grains (Abdel-Aal et al., 2006). Black rice had ten times higher anthocyanin contents than the red rice. On the contrary, the red rice had higher proanthocyanidin contents. Min et al. (2012) reported higher proanthocyanin content in red rice, and Furukawa et al. (2006) reported higher anthocyanin contents in black or purple rice. The anthocyanin and proanthocyanidin synthesis pathways share dihydroflavonols as precursor molecules. Cross talk between anthocyanin- and proanthocyanidin-specific branches existed where down-regulation of anthocyanidin reductase resulted in the accumulation of anthocyanins and inhibition of proanthocyanidin synthesis (Abrahams et al., 2002) while its overexpression led to down-regulation of anthocyanin and accumulation of proanthocyanidins (Xie et al., 2003). Regulation of flavonoid pathway branch is regulated by complex network of signals triggered by internal metabolic cues and external signals including abiotic stress factors (Abeynayake et al., 2012). Flavonoid pigments particularly anthocyanins and proanthocyanidins have been reported to be highly correlated with antioxidant capacities of colored rice grains (Finocchiaro et al., 2007; Min et al., 2012). Anthocyanin accumulation can be induced by biotic and abiotic stressors, such as UV-B irradiation, drought, cold, toxic metals in soils and pathogens attack (Chalker-Scott, 1999). Salinity stress-induced accumulation of anthocyanins in leaves has been observed in several glycophytes. In rice, Roychoudhury et al. (2008) and Chutipaijit et al. (2011) reported that the level of anthocyanins in leaves of salt-tolerant rice was higher than in salt-sensitive rice under salinity stress. The enhancement of anthocyanins synthesis under salinity has been suggested to be important in the protection against salt-induced oxidative damages by binding the ions and thereby reduced toxicity on cytoplasmic structure (Wahid and Ghazanfar, 2006; Hichem et al., 2009). Furthermore, Roychoudhury et al. (2011) revealed that salinity-induced anthocyanin accumulation in seedlings of three rice cultivars was significantly enhanced by Spd application. Proanthocyanidins in the grains of all four rice cultivars were also significantly increased under salinity stress. It is interesting to note that the salt-enhanced increase in proanthocyanidins was more pronounced than that for anthocyanins. Moreover, the increase was greatest in the salt-tolerant red-grain cultivar (Pokkali). The enhanced level of proanthocyanidins under salt stress conditions has also been reported in seedlings of two maize varieties (Hichem et al., 2009) and salt-tolerant *Acacia saligna* (Elfeel and Backhashwain, 2012). Higher proanthocyanidins accumulation in the more salt-tolerant variety of maize was associated with greater antioxidant capacity (Hichem et al., 2009). The present study demonstrated for the first time in cereal grains that the concentration of anthocyanins was slightly increased and that of proanthocyanidins was significantly increased in response to salinity stress and that the accumulation of both pigments was further promoted significantly by exogenous Spd treatment. Although the mechanisms of action of Spd on modulation of flavonoid biosynthesis pathways leading to enhanced accumulation of anthocyanins and proanthocyanidins under salt stress is currently unknown, metabolic regulation by Spd has emerged as a promising approach relevant to practical application to improve rice grain nutritional qualities.

Conclusions

Salinity stress negatively affected yield and most yield

component parameters in four pigmented rice cultivars in a pot experiment and the extent of yield reduction was highest in the most sensitive cultivar. Foliar application of Spd prior to salt application resulted in an improvement in yield and yield components. Surprisingly, salt-stressed plants of all cultivars tended to produce grains with higher TPC, anthocyanins and proanthocyanidins resulting in enhanced antioxidant capacities. Exogenous Spd further increased all aforementioned health promoting characters. To our knowledge, this is the first report on the promotive effects of Spd on rice grain quality which warrants further in-depth research aimed at agricultural application as well as a better understanding of the physiological and molecular basis of Spd functions.

Acknowledgements

This research was funded by the Food and Functional Food Cluster under the National Research University Program of Khon Kaen University. We also acknowledge financial support from Khon Kaen University's Salt Tolerant Rice Research Group. We would also like to thank Prof. D.C. Slack, Department of Agricultural and Biosystems Engineering, University of Arizona, USA for critical reading the manuscript. Special thanks are also extended to Dr. Poramet Buntaung, Faculty of Agriculture, Khon Kaen University and Dr. Teerayut Toojinda, BIOTEC, Thailand for the generous gift of rice seeds.

References

Abdel-Aal, E.M. and Hucl, P. 1999. A rapid method for quantifying total anthocyanins in blue aleurone and purple pericarp wheats. *Cereal Chem.* 76: 350-354.

Abdel-Aal, E.M., Young, J.C. and Rabalski, I. 2006. Anthocyanin composition in black, blue, pink, purple, and red cereal grains. *J. Agric. Food Chem.* 54: 4696-4704.

Abdullah, Z., Khan, M.A. and Flowers, T.J. 2001. Causes of sterility in seed set of rice under salinity stress. *J. Agron. Crop Sci.* 187: 25-32.

Abeynayake, S.W., Panter, S., Chapman, R., Webster, T., Rochfort, S., Mouradov, A. and Spangenberg, G. 2012. Biosynthesis of proanthocyanidins in white clover flowers: cross talk within the flavonoid pathway. *Plant Physiol.* 158: 666-678.

Abrahams, S., Tanner, G.J, Larkin, P.J. and Ashton, A.R. 2002. Identification and biochemical characterization of mutants in the proanthocyanidin pathway in *Arabidopsis*. *Plant Physiol.* 130: 561-576.

Alcázar, R., Marco, F., Cuevas, J.C., Patron, M., Ferrando, A., Carrasco, P., Tiburcio, A.F. and Altabella, T. 2006. Involvement of polyamines in plant response to abiotic stress. *Biotechnol. Lett.* 28: 1867-1876.

Alcázar, R., Altabella, T., Marco, F., Bortolotti, C., Reymond, M., Koncz, C., Carrasco, P. and Tiburcio, A.F. 2010. Polyamines: molecules with regulatory functions in plant abiotic stress tolerance. *Planta* 231: 1237-1249.

Ali, Y., Aslam, Z., Awan, A.R., Hussain, F. and Cheema, A.A. 2004. Screening rice (*Oryza saliva* L.) lines/cultivars against salinity in relation to morphological and physiological traits and yield components. *Int. J. Agric. Biol.* 6: 572-575.

Asch, F., Dingkuhn, M., Wittstock, C. and Doerffling, K. 1999. Sodium and potassium uptake of rice panicles as affected by salinity and season in relation to yield and yield components. *Plant Soil* 207: 133-145.

Asch, F., Dingkuhn, M., Dörffling, K. and Miezan, K. 2000. Leaf K/Na ratio predicts salinity induced yield loss in irrigated rice. *Euphytica* 113: 109-118.

Asch, F. and Wopereis, M.C.S. 2001. Responses of field-grown irrigated rice cultivars to varying levels of floodwater salinity in a semi-arid environment. *Field Crop Res.* 70: 127-137.

Benzie, I.F.F. and Strain, J.J. 1999. Ferric reducing/antioxidant power assay: Direct measure of total antioxidant activity of biological fluids and modified version for simultaneous measurement of total antioxidant power and ascorbic acid concentration. *Methods Enzymol.* 299: 15-27.

Bouchereau, A., Aziz, A., Larher, F. and Martin-Tanguy, J. 1999. Polyamines and environmental challenges: recent development. *Plant Sci.* 140: 103-125.

Brand-Williams, W., Cuvelier, M.E. and Berset, C. 1995. Use of a free radical method to evaluate antioxidant activity. *Lwt-Food Sci. Technol.* 28: 25-30.

Cao, D.D., Hu, J., Zhu, S.J., Hu, W.M. and Knapp, A. 2010. Relationship between changes in endogenous polyamines and seed quality during development of sh_2 sweet corn (*Zea mays* L.) seed. *Sci. Hortic.* 123: 301-307.

Castillo, E.G., Tuong, T.P., Ismail, A.M. and Inubushi, K. 2007. Response to salinity in rice: Comparative effects of osmotic and ionic stresses. *Plant Prod. Sci.* 10: 159-170.

Chalker-Scott, L. 1999. Environmental significance of anthocyanins in plant stress responses. *Photochem. Photobiol.* 70: 1-9.

Chattopadhyay, M.K., Tiwari, B.S., Chattopadhyay, G., Bose, A., Sengupta, D.N. and Ghosh, B. 2002. Protective role of exogenous polyamines on salinity-stressed rice (*Oryza sativa*) plants. *Physiol. Plant.* 116: 192-199.

Choi, Y., Jeong, H.S. and Lee, J. 2007. Antioxidant activity of methanolic extracts from some grains consumed in Korea. *Food Chem.* 103: 130-138.

Chunthaburee, S., Sanitchon, J., Pattanagul, W. and Threerakulpisut, P. 2012. Salinity tolerance of black glutinous rice seedlings is related to Na^+/K^+ and proline but not the anthocyanin content. *In* Proc. The 12th SABRAO Congress on Plant Breeding towards 2025: Challenges in a Rapidly Changing World. Thailand. 105.

Chutipaijit, S., Cha-um, S. and Sompornpailin, K. 2011. High contents of proline and anthocyanin increase protective response to salinity in *Oryza sativa* L. spp. *Indica*. *Aust. J. Crop Sci.* 5: 1191-1198.

Elfeel, A.A. and Bakhashwain, A.A. 2012. Salinity effects on growth attributes mineral uptake, forage quality and tannin contents of *Acacia saligna* (Labill.) H. Wendl. *Res. J. Environ. Earth Sci.* 4: 990-995.

Farooq, M., Wahid, A. and Lee, D.J. 2009. Exogenously applied polyamines increase drought tolerance of rice by improving leaf water status, photosynthesis and membrane properties. *Acta. Physiol. Plant* 31: 937-945.

Finocchiaro, F., Ferrari, B., Gianinetti, A., Dall'Asta, C., Galaverna, G.,

Scazzina, F. and Pellegrini, N. 2007. Characterization of antioxidant compounds of red and white rice and changes in total antioxidant capacity during processing. *Mol. Nutr. Food Res.* 51: 1006-1019.

Flower, T.J. 2004. Improving crop salt tolerance. *J. Exp. Bot.* 55: 307-319.

Furukawa, T., Maekawa, M., Oki, T., Suda, I., Iida, S., Shimada, H., Takamure, I. and Kadowaki, K. 2006. The *Rc* and *Rd* genes are involved in proanthocyanidin synthesis in rice pericarp. *Plant J.* 49: 91-102.

Goffman, F.D. and Bergman, C.J. 2004. Rice kernel phenolic content and its relationship with antiradical efficiency. *J. Sci. Food. Agric.* 84: 1235-1240.

Hamdia, M.A. and Shaddad, M.A.K. 2010. Salt tolerance of crop plants. *J. Stress Physiol. Biochem.* 6: 64-90.

Hichem, H., Mounir, D. and Naceurc, E.A. 2009. Differential responses of two maize (*Zea mays* L.) varieties to salt stress: Changes on polyphenols composition of foliage and oxidative damages. *Ind. Crop. Prod.* 30: 144-151.

Hoshikawa, K. 1989. The Growing Rice Plants - an Anatomical Monograph. Nosan Gyoson Bunka Kyokai (Nobunkyo), Tokyo, Japan. 148-149.

Hussain, S.S., Ali, M., Ahmad, M. and Siddique, K.H. 2011. Polyamines: Natural and engineered abiotic and biotic stress tolerance in plants. *Biotechnol. Adv.* 29: 300-311.

Jun, H.I., Song, G.S., Yang, E.I., Youn, Y. and Kim, Y.S. 2012. Antioxidant activities and phenolic compounds of pigmented rice bran extracts. *J. Food Sci.* 77: 759-764.

Krishnamurthy, R. and Bhagwat, K.A. 1989. Polyamines as modulators of salt tolerance in rice cultivars. *Plant Physiol.* 91: 500-504.

Lepiniec, L., Debeaujon, I., Routaboul, J.M., Baudry, A., Pourcel, L., Nesi, N. and Caboche, M. 2006. Genetics and biochemistry of seed flavonoids. *Annu. Rev. Plant Biol.* 57: 405-430.

Liang, Y.L. and Lur, H.S. 2002. Conjugated and free polyamine levels in normal and aborting maize kernels. *Crop Sci.* 42: 1217-1224.

Min, B., Gu, L., McClung, A.M., Bergman, C.J. and Chen, M.H. 2012. Free and bound total phenolic concentrations, antioxidant capacities, and profiles of proanthocyanidins and anthocyanins in whole graij rice (*Oryza sativa* L.) of different bran colours. *Food Chem.* 133: 715-722.

Nayyar, H. 2005. Putrescine increases floral retention, pod set and seed yield in cold stressed chickpea. *J. Agron. Crop Sci.* 191: 340-345.

Ndayiragije, A. and Lutts, S. 2006. Do exogenous polyamines have an impact on the response of a salt sensitive rice cultivar to NaCl? *J. Plant Physiol.* 163: 506-516.

Ndayiragije, A. and Lutts, S. 2007. Long term exogenous putrescine application improves grain yield of a salt-sensitive rice cultivar exposed to NaCl. *Plant Soil* 291: 225-238.

Parida, A.K. and Das, A.B. 2005. Salt tolerance and salinity effects on plants: a review. *Ecotox. Environ. Safe.* 60: 324-349.

Prior, R.L., Wu, X. and Schaich, K. 2005. Standardized methods for the determination of antioxidant capacity and phenolics in foods and dietary supplements. *J. Agric. Food Chem.* 53: 4290-4302.

Quinet, M., Ndayiragije, A., Lefevre, I., Lambillotte, B., Dupont-Gillain, C.C. and Lutts, S. 2010. Putrescine differently influences the effect of salt stress on polyamine metabolism and ethylene synthesis in rice cultivars differing in salt resistance. *J. Exp. Bot.* 61: 2719-2733.

Re, R., Pellegrini, N., Proteggente, A., Pannala, A., Yang, M. and Rice-Evans, C. 1999. Antioxidant activity applying an improved ABTS radical cation decolorisation assay. *Free Radic. Biol. Med.* 26: 1231-1237.

Roy, P., Niyogi, K., Sengupta, D.N. and Ghosh, B. 2005. Spermidine treatment to rice seedlings recovers salinity-stress-induced damage of plasma membrane and PM-bound H^+-ATPase in salt tolerant and salt-sensitive rice cultivars. *Plant Sci.* 168: 583-591.

Roychoudhury, A., Basu, S., Sarkar, S.N. and Sengupta, D.N. 2008. Comparative physiological and molecular responses of a common aromatic indica rice cultivar to high salinity with non-aromatic indica rice cultivars. *Plant Cell Rep.* 27: 1395-1410.

Roychoudhury, A., Basu, S. and Sengupta, D.N. 2011. Amelioration of salinity stress by exogenously applied spermidine or spermine in three varieties of indica rice differing in their level of salt tolerance. *J. Plant Physiol.* 168: 317-328.

Saleethong, P., Sanitchon, J., Kong-ngern, K. and Theerakulpisut, P. 2011. Pretreatment with spermidine reverses inhibitory effects of salt stress in two rice (*Oryza sativa* L.) cultivars differing in salinity tolerance. *Asian J. Plant Sci.* 10: 245-254.

Saleethong, P., Sanitchon, J., Kong-ngern, K. and Theerakulpisut, P. 2013. Effects of exogenous spermidine (Spd) on yield, yield-related parameters and mineral composition of rice (*Oryza sativa* L. ssp. *indica*) grains under salt stress. *Aust. J. Crop Sci.* 7: 1293-1301.

Shabala, S., Cuin, T.A. and Pottosin, I. 2007. Polyamines prevent NaCl-induced K^+ efflux from pea mesophyll by blocking non-selective cation channels. *FEBS Lett.* 581: 1993-1999.

Shen, Y., Jin, L., Xiao, P., Lu, Y. and Bao, J. 2009. Total phenolics, flavonoids, antioxidant capacity in rice grain and their relations to grain color, size and weight. *J. Cereal Sci.* 49: 106-111.

Shereen, A., Mumtaz, S., Raza, S., Khan, M.A. and Solangi, S. 2005. Salinity effects on seedling growth and yield components of different inbred rice lines. *Pak. J. Bot.* 37: 131-139.

Singleton, V.L., Orthofer, R. and Lamuela-Raventós, R.M. 1999. Analysis of total phenols and other oxidation substrates and antioxidants by means of Folin–Ciocalteu reagent. *Methods Enzymol.* 299: 152-178.

Sompong, R., Siebenhandl-Ehn, S., Linsberger-Martin, G. and Berghofer, E. 2011. Physicochemical and antioxidative properties of red and black rice varieties from Thailand, China and Sri Lanka. *Food Chem.* 124: 132-140.

Sun, B., Ricardo-Da-Silva, J.M. and Spranger, I. 1998. Critical factors of vanillin assay for catechins and proanthocyanidins. *J. Agric. Food Chem.* 46: 4267-4274.

Tang, T., Xie, H., Wang, Y., Lü, B. and Liang, J. 2009. The effect of sucrose and abscisic acid interaction on sucrose synthase and its relationship to grain filling of rice (*Oryza sativa* L.) *J. Exp. Bot.* 60: 2641-2652.

Tan, G.L., Zhang, H., Fu, J., Wang, Z.Q., Liu, L.J. and Yang, J.C. 2009. Post-anthesis changes in concentration of polyamines in superior and inferior spikelets and their relation with grain filling of super rice. *Acta Agron. Sin.* 35: 2225-2233.

Urano, K., Hobo, T. and Shinozaki, K. 2005. *Arabidopsis ADC* genes involved in polyamine biosynthesis are essential for seed development. *FEBS Lett.* 579: 1557-1564.

Verma, S. and Mishra, S.N. 2005. Putrescine alleviation of growth in salt stressed *Brassica juncea* by inducing antioxidative defense system. *J. Plant Physiol.* 162: 669-677.

Wahid, A. and Ghazanfar, A. 2006. Possible Involvement of some secondary metabolites in salt tolerance of sugarcane. *J. Plant Physiol.* 163: 723-730.

Wang, Z., Xu, Y., Wang, J., Yang, J. and Zhang, J. 2012. Polyamine and ethylene interactions in grain filling of superior and inferior spikelets of rice. *Plant Growth Regul.* 66: 215-228.

Xie, D.Y., Sharma, S.B., Paiva, N.L., Ferriera, D. and Dixon, R.A. 2003. Role of anthocyanin reductase, encoded by *BANYULS* in plant flavonoid biosynthesis. *Science* 299: 396-399.

Yang, T., Zhang, J., Wang, Z., Liu, K. and Wang, P. 2006. Post-anthesis development of inferior and superior spikelets in rice in relation to abscisic acid and ethylene. *J. Exp. Bot.* 57: 149-160.

Yusuf, M., Fariduddin, Q., Varshney, P. and Ahmad, A. 2012. Salicylic acid minimizes nickel and/or salinity-induced toxicity in Indian mustard (*Brassica juncea*) through an improved antioxidant system. *Environ. Sci. Pollut. Res.* 19: 8-18.

Zeng, L. and Shannon, M.C. 2000. Salinity effects on seedling growth and yield components of rice. *Crop Sci.* 40: 996-1003.

Zeng, L., Shannon, M.C. and Lesch, S.M. 2001. Timing of salinity stress affects rice growth and yield components. *Agric. Water Manage.* 48: 191-206.

Zeng, L., Shannon, M.C. and Grieve, C.M. 2002. Evaluation of salt tolerance in rice genotypes by multiple agronomic parameters. *Euphytica* 127: 235-245.

Industrial Crops and Products 63 (2015) 349–356

Contents lists available at ScienceDirect

Industrial Crops and Products

journal homepage: www.elsevier.com/locate/indcrop

Estimation methods and parameter assessment for ethanol yields from total soluble solids of sweet sorghum

Darika Bunphan[a], Prasit Jaisil[a], Jirawat Sanitchon[a], Joseph E. Knoll[b], William F. Anderson[b,*]

[a] Plant Breeding Research Center for Sustainable Agriculture and Department of Plant Science and Agricultural Resources, Faculty of Agriculture, Khon Kaen University, Khon Kaen 40002, Thailand
[b] USDA/ARS Crop Genetics and Breeding Research Unit, 115 Coastal Way, Tifton, GA 31793, USA

ARTICLE INFO

Article history:
Received 9 May 2014
Received in revised form 2 October 2014
Accepted 5 October 2014
Available online 8 November 2014

Keywords:
Sugar content
Sucrose content
Brix value
Bio-ethanol
Fermentable sugar

ABSTRACT

Estimation methods and evaluation of ethanol yield from sweet sorghum (*Sorghum bicolor* (L.) Moench) based on agronomic production traits and juice characteristics is important for developing parents and inbred lines of sweet sorghum that can be used by the bio-ethanol industry. The objectives of this study were to compare published indirect methods for the calculation of ethanol yields from sweet sorghum and test them against direct ethanol production in laboratory, as well as to determine the relationships among total soluble sugar and juice traits with ethanol concentrations over time. Four sorghum varieties (KKU40, Theis, BJ248 and SPV1411) were compared for juice characters and ethanol yield in a randomized complete block design with four replications. Agronomic and juice traits of sweet sorghum were recorded during flowering and at harvest. Juice of sweet sorghum was fermented by yeast (*Saccharomyces cerevisiae*) to obtain ethanol yields in the laboratory, which were then compared with ethanol yields calculated based upon five calculation methods from the literature. Ethanol yield estimates calculated from published methods were generally higher than laboratory values. However, estimates based upon Somani and Taylor (2003) and on Smith et al. (1987) when multiplying theoretical yields by 80% were not significantly different from laboratory results. Though ethanol yield are strongly correlated with sugar yields, juice traits influenced the rate of fermentation of sugars over time. For example, glucose, fructose and nitrogen content in the juice had a positive effect on ethanol concentration after 12 h of fermentation while multiple juice traits were significantly associated with ethanol concentrations after 24, 36 and 48 h of fermentation.

Published by Elsevier B.V.

1. Introduction

Bio-ethanol is a renewable energy source produced mainly from agricultural crops such as sugarcane (Ratnavathi et al., 2010), maize (*Zea mays* L.), and cassava (*Manihot esculenta* Crantz) (Ali et al., 2008). These feedstocks are generally used for human and animal consumption and for other industries, for which the competition for these feedstocks is high (Jia et al., 2013). Therefore, alternative or supplemental feedstocks for bio-ethanol production are necessary during raw material shortage and for expansion of the industry (Shen et al., 2011). Sweet sorghum is an attractive crop as feedstock for bio-ethanol production (Ratnavathi et al., 2010). The juice from the fresh stems of sweet sorghum contains sucrose, glucose and fructose, which can be directly fermented to produce alcohol (Tew et al., 2008; Sipos et al., 2009). Moreover, the crop can be used as feedstock for producing sugar, syrup, fodder, bedding, roofing, fencing and paper in many areas of the world (Doggett, 1988; Laopaiboon et al., 2007; Liu et al., 2008). Genetically, sweet sorghum is similar to grain sorghum except for genes controlling plant height and sweet juice in the stalks (Ratnavathi et al., 2010). In addition, sweet sorghum is similar to sugarcane due to the high sugar content in the stalk which can range from 16 to 23% Brix (Smith et al., 1987; Murray et al., 2009; Ratnavathi et al., 2011). Sweet sorghum accumulates large amounts of sugar in stem parenchyma cells, beginning after internode elongation is complete (Hoffmann-Thoma et al., 1996), and peaking from anthesis to physiological maturity (Pfeiffer et al., 2010).

Ethanol yield of sweet sorghum can be determined directly from fermentation of sweet sorghum juice with bacteria or yeast (*Saccharomyces cerevisiae*) (Liu et al., 2008; Ratnavathi et al., 2011) or

* Corresponding author. Tel.: +1 229 386 3170.
E-mail address: bill.anderson@ars.usda.gov (W.F. Anderson).

http://dx.doi.org/10.1016/j.indcrop.2014.10.007
0926-6690/Published by Elsevier B.V.

ethanol yield can be estimated indirectly from many calculation methods (Ratnavathi et al., 2010; Tew et al., 2008; Somani and Taylor, 2003; Smith and Buxton, 1993; Dalvi et al., 2011). Tew et al. (2008) estimated the ethanol yield of five sweet sorghums (Dale, M81-E, Rio, Theis and Topper) and two non-flowering sorghum × sudangrass forage hybrids by using Brix and the percent sucrose [1.05 (%sucrose) + 1.00 (%Brix − %sucrose)] to estimate hexose and then using a conversion rate of 1.7 kg hexose L^{-1} ethanol. This estimate did not take into account soluble solids in Brix other than sugars. Smith et al. (1987) assumed that fermentation would use every sugar molecule and produce ethanol and carbon dioxide and that 5.83 kg of hexose or 5.54 kg sucrose was needed to convert to one gallon (3.78 L) of ethanol. Smith and Buxton (1993) revised their theoretical ethanol yields by dividing total sugar yield by 5.68, and assuming only 80% efficiency due to other metabolic factors. Hills et al. (1990) reduced all sugars to hexose by multiplying sucrose by the factor 1.05 then uses an ethanol conversion rate of 15.02 lbs (6.81 kg) hexose for each gallon (1.8 kg hexose L^{-1}). This conversion rate of hexose to ethanol is slightly less than that used by Tew et al. (2008). Somani and Taylor (2003) estimated alcohol yield from sweet sorghum juice by using specific gravity (SG) and adjusting sugar estimates by subtracting 3 from each reading in the formula: (Brix − 3) × SG × 0.59 L ethanol kg^{-1} sucrose. This equation takes into account non-sugars in Brix but does not take into account possible differences in the sugar profile. All ethanol estimates of sweet sorghums were useful for comparisons among genotypes or treatments within the studies. However, comparisons of ethanol yields obtained from different estimates with measured ethanol yields from the lab have not been reported for sweet sorghum genotypes. Information is needed to determine the most accurate methods for estimating ethanol yield from juice components of sweet sorghum.

It is also important to determine how variation in juice parameters affects the conversion of sweet sorghum juice to ethanol. The pH of sweet sorghum juice has been shown to range from 4.4 to 5.5 (Davila-Gomez et al., 2011; Chohnan et al., 2011). This range is optimum for yeast growth and ethanol production (Mountney and Gould, 1988) with optimum ethanol production at about pH 5 (Raikar, 2012). Sufficient nitrogen and zinc are needed in the fermentation medium for sufficient growth and reproduction of the yeasts (Bisson, 1999; De Nicola and Walker, 2009). Clarity of the juice is diminished by cellulose fiber which can have a negative effect on ethanol yield (Han et al., 2012). How these parameters vary among sweet sorghum lines and how they corporately affect ethanol yields are important to understand.

The objectives of this study were to compare available estimation methods for ethanol yields of sweet sorghum with those obtained directly in the laboratory, and to determine relationships between characteristics of the juice and ethanol concentration from fermentation. The information obtained from this study will be useful for choosing the best methods to estimate ethanol yields from field production of soluble sugars and juice characteristics responsible for conversion efficiency through fermentation of sweet sorghum.

2. Materials and methods

2.1. Plant materials

Four genotypes of sweet sorghums (KKU40, Theis, BJ248 and SPV1411) were used in this study. KKU40 is a pure line variety developed at Khon Kaen University, Thailand. Theis (Broadhead et al., 1978) and BJ248 are also pure line varieties introduced from United States and China, respectively. SPV1411 was a variety donated from the International Crops Research Institute for the Semi-Arid Tropics (ICRISAT), India. The four genotypes of sweet sorghum were planted during early rainy season on 8 May 2013 at the Field Crops Research Station (fine loamy, siliceous, Oxic Paleustult, Korat soil series), Faculty of Agriculture, Khon Kaen University, Khon Kaen, Thailand (latitude 16.26° N, longitude 102.50° E).

2.2. Experimental design

A randomized complete block design (RCBD) with four replications was used in this study. The plot size was a 4-row plot with 4 m in length and spacing of 75 cm between rows and 10 cm between plants. Manual planting was carried out for all plots at the seed rate higher than normal planting, and the seedlings were later thinned to obtain one plant per hill 15 days after planting. Fertilizer grade 15–15–15 (N–P–K) at the rate of 156 kg ha^{-1} was applied to the plots at planting and then again as top dressing at 30 days after planting.

2.3. Data collection

Data were recorded for days to 50% flowering when 50% of total plants shed pollen. Total soluble solids (Brix) was recorded at the days to 50% flowering, soft dough (10 days after flowering), hard dough (20 days after flowering), and at harvest (30 days after flowering) from 10 randomly chosen intact plants in each plot using a hand refractometer. Three internode positions (top, middle and bottom) along the stems were tapped to extract juice, and total soluble solids were averaged from three positions (Makanda et al., 2009).

At harvest (30 days after flowering for each sweet sorghum cultivar starting in mid-September 2013), a 3 m long section of plants in each plot was harvested manually, and the stems were cut at ground surface. Plant height and stalk diameter were recorded from 10 randomly chosen plants in each plot. Plant height was measured from the ground to panicle tip (IBPGR and ICRISAT, 1993), and stalk diameter (SD) in mm was measured using a digital vernier caliper and averaged from three positions along the stalks. The plants were cut at the top to remove panicles, and all leaves were also removed. All stalks in the harvest area in each plot were measured, and stripped stalk weight was recorded.

The stalks of sweet sorghum were crushed to extract juice using a sugarcane three-roller crusher, and juice weight and juice volume were determined. Extracted juice was then immediately stored from each harvest at −20 °C for subsequent analysis and use. Specific gravity was then calculated as juice weight divided by juice volume. Total juice yield was calculated by subtracting stalk dry weight from fresh stripped stalk weight. The pH, total soluble solid, total sugar, reducing sugar, fructose, glucose and sucrose of the juice were recorded. The pH of each replicate was measured with a pH meter. Total soluble solids of the juice were recorded using a handheld refractometer (Ade Advanced Otpic®) to measure Brix immediately after squeezing from the stalks. Reducing sugars, fructose, glucose and sucrose of the juice was determined using high-performance liquid chromatography (HPLC) (LC-10AD, Shimadzu, Japan).

2.4. Fermentation

Two hundred and fifty milliliters of juice from each replication of the four sweet sorghum varieties were immediately placed in an ice bath. The juice was autoclaved at 110 °C for 28 min then cooled overnight in flasks prior to fermentation. Yeast (*S. cerevisiae*) TISTR 5048 provided by the culture collection of the Thailand Institute of Scientific and Technological Research (TISTR), Bangkok, Thailand, was grown in malt extract medium and placed on a rotating shaker

at 100 rpm, 30 °C for 18 h (Laopaiboon et al., 2007). Juice was inoculated with 1×10^8 cells per flask of yeast and allowed to ferment at 30 °C without adjustment of pH (juice pH was 4.8).

2.5. Ethanol concentration during fermentation

During fermentation, samples were taken from the flasks at 12, 24, 36 and 48 h from initiation to quantify ethanol concentration (Laopaiboon et al., 2007). Briefly, ethanol concentration was analyzed by gas–liquid chromatography GLC (Shimadzu GC-14B, Japan, solid phase: polyethylene glycol (PEG-20 M), carrier gas: nitrogen, 90 ○C isothermal packed column, injection temperature 160 °C, flame ionization detector temperature 230 ○C; C-R7 Ae plus Chromatopac Data Processor) and isopropanol was used as an internal standard.

2.6. Estimation of ethanol from total sugar or juice yields

Five published estimation methods for calculation of ethanol yield from the sugar yields were compared to measured ethanol yield obtained in the laboratory. These equations, which are listed below, will be referred to as (1) Smith 1 – theoretical ethanol yield Smith et al. (1987), (2) Smith 2 – 80% of theoretical Smith et al. (1987), (3) Hills et al. (1990), (4) Tew et al. (2008), and (5) Somani and Taylor (2003):

$$\frac{\text{L ethanol}}{\text{ha}} = \frac{\text{kg sugar}}{\text{ha}} \times \frac{\text{gal ethanol}}{5.68\,\text{kg sugar}} \times \frac{3.78\,\text{L}}{\text{gal}} \quad (1)$$

$$\frac{\text{L ethanol}}{\text{ha}} = \frac{\text{kg sugar}}{\text{ha}} \times \frac{\text{gal ethanol}}{5.68\,\text{kg sugar}} \times \frac{3.78\,\text{L}}{\text{gal}} \times 0.8 \quad (2)$$

$$\frac{\text{L ethanol}}{\text{ha}} = \frac{(1.05(\%\text{suc}) + \%\text{glc} + \%\text{frc})\,\text{kg hex}}{100\,\text{L juice}} \times \frac{\text{L juice}}{\text{ha}} \times \frac{\text{L ethanol}}{1.8\,\text{kg hex}} \quad (3)$$

$$\frac{\text{L ethanol}}{\text{ha}} = \frac{(1.05(\%\text{suc}) + (\text{Brix} - \%\text{suc}))\,\text{kg hex}}{100\,\text{L juice}} \times \frac{\text{L juice}}{\text{ha}} \times \frac{\text{L ethanol}}{1.7\,\text{kg hex}} \quad (4)$$

$$\frac{\text{L ethanol}}{\text{ha}} = \frac{(\text{Brix} - 3)\,\text{kg suc}}{100\,\text{kg juice}} \times \frac{\text{SG kg juice}}{\text{L juice}} \times \frac{\text{L juice}}{\text{ha}} \times \frac{0.53\,\text{L ethanol}}{\text{kg suc}} \quad (5)$$

where suc = sucrose, glc = glucose, frc = fructose, hex = hexose, and SG = specific gravity. Smith 1 and Smith 2 (Smith et al., 1987) equations use measurement of total sugar that was harvested and assume a theoretical conversion of total sugars to ethanol of 5.68 kg gal^{-1} (1.5 kg L^{-1}). This conversion rate of 5.68 is taken as an average between the theoretical conversion rate of 5.83 kg of hexose and 5.54 kg of sucrose for each gallon of ethanol. Thus they are assuming the same sugar composition for all entries. Smith 2 assumes a conversion rate of 80% compared to the 100% conversion in Smith 1. Hills et al. (1990) use actual rates of sucrose (adjusting for conversion to hexoses by 1.05), and the hexoses glucose and fructose to determine conversion. They use the theoretical conversion of 1.8 kg hexose L^{-1} ethanol which is lower than that used by Smith 1 and Smith 2, but assumes 100% conversion. Tew et al. (2008) relies on Brix as an estimate of total sugars and thus subtracts sucrose from Brix to estimate hexose sugars. This estimate does not take into account that up to 25% of the total soluble solids are non-sugars. They use a conversion rate of sugars to ethanol of 1.7 kg hexose L^{-1} ethanol which is between Smith et al. (1987) and Hills et al. (1990). Somani and Taylor (2003) also use Brix but compensate for the non-sugars by subtracting 3 from Brix and also adjusting estimates by using the specific gravity to estimate the sucrose in the juice. Their conversion estimate was 0.59 L ethanol kg^{-1} sucrose (1.7 kg sucrose L^{-1} ethanol). They do not take into account the presence of hexoses and assume 100% sucrose.

2.7. Statistical analysis

Analysis of variance was performed for all parameters according to a randomized complete block design using PROC GLM (SAS, 1999). Least significant difference test (LSD) (Gomez and Gomez, 1984) was used to compare means. Unless otherwise noted, all comparisons are considered significant at $\alpha \leq 0.05$. Simple correlation coefficients among parameters were calculated based on entry means. Stepwise regression (PROC LOGISTIC of SAS) (SAS, 1999) was performed on ethanol concentration at 12, 24, 36 and 48 h with juice traits to determine important parameters for ethanol conversion at different times.

3. Results

3.1. Agronomic traits

Sweet sorghum varieties were significantly different for days to 50% flowering and total soluble solids, but they were not significantly different for plant height, stripped stalk yield or juice specific gravity (Table 1). KKU40 had the earliest maturity, Theis and BJ248 had intermediate maturity, and SPV1411 had late maturity. Theis and KKU40 had significantly higher total soluble solids than SPV1411. SPV1411 had significantly higher fiber content in the juice compared to KKU 40 while Theis and BJ248 were intermediate.

3.2. Juice quality

The differences in juice pH between the different sweet sorghum varieties were not significant (range between 4.81 and 4.87). Total sugar and sucrose were lower for SPV1411 than for the other

Table 1
Means for days to 50% flowering, plant height, % fiber, stripped stalk yield, total soluble solids, and specific gravity of four sorghum varieties at harvest (four replications).

Cultivar	Days to 50% flowering (days)	Plant height (cm)	Fiber (g kg^{-1})	Stripped stalk yield (t ha^{-1})	Total soluble solid (%Brix × 10/SG)	Specific gravity
KKU40	76^{c}	318^{a}	101^{b}	38.75^{a}	169.9^{ab}	1.055^{a}
Theis	80^{b}	291^{a}	114^{ab}	30.73^{a}	174.5^{a}	1.050^{a}
BJ248	80^{b}	312^{a}	111^{ab}	31.94^{a}	156.9^{b}	1.051^{a}
SPV1411	84^{a}	333^{a}	140^{a}	35.40^{a}	179.3^{a}	1.044^{a}
Mean	80	314	116	34.21	170.1	1.050
	***	ns	*	ns	*	ns

ns, non-significant; *,*** significant at 0.05 and 0.001 probability levels, respectively.
Means in the same column followed by the same letter(s) are not significantly different (at $p < 0.05$) by LSD.

Table 2
Means for pH, total sugar, fructose, glucose, and sucrose of four sorghum varieties replicated four times.

Cultivar	pH	Total sugar ($g\,L^{-1}$)	Fructose ($g\,L^{-1}$)	Glucose ($g\,L^{-1}$)	Sucrose ($g\,L^{-1}$)
KKU40	4.83[a]	165.4[ab]	15.43[ab]	18.28[ab]	131.66[a]
Theis	4.80[a]	170.8[a]	14.49[ab]	16.71[b]	139.60[a]
BJ248	4.86[a]	166.9[ab]	14.22[b]	16.46[b]	136.27[a]
SPV1411	4.87[a]	151.8[b]	16.39[a]	20.19[a]	115.26[b]
Mean	4.84 ns	163.7 *	15.13 *	17.91 *	130.70 **

ns, non-significant; *,**significant at 0.05 and 0.01 probability levels, respectively.
Means in the same column followed by the same letter(s) are not significantly different (at $p < 0.05$).

Table 3
Means for nitrogen, phosphorus, potassium, magnesium, iron, and zinc in juice of four sweet sorghum varieties ($mg\,L^{-1}$).

Cultivar	Nitrogen	Phosphorus	Potassium	Magnesium	Iron	Zinc
KKU40	185[b]	160[a]	3553[ab]	348[b]	8.68[c]	1.12[a]
Theis	228[a]	240[a]	3629[ab]	389[b]	12.47[b]	1.09[a]
BJ248	155[b]	197[a]	4321[a]	637[a]	9.79[c]	1.37[a]
SPV1411	304[a]	201[a]	2659[b]	398[b]	18.16[a]	0.92[a]
Mean	218 **	200 ns	3541 *	443 ***	12.27 ***	1.13 ns

ns, non-significant; *,**,*** significant at 0.05, 0.01, and 0.001 probability levels, respectively.
Means in the same column followed by the same letter(s) are not significantly different (at $p < 0.05$) by LSD.

Table 4
Means for % soluble solids (%Brix) at flowering, soft dough stage (10 days after flowering), hard dough stage (20 days after flowering and harvest (30 days after flowering).

Cultivar	Flowering	Soft dough	Hard dough	Harvest
KKU40	14.24[a]	15.60[b]	17.33[b]	18.40[a]
Theis	14.49[a]	16.89[a]	19.36[a]	18.82[a]
BJ248	14.11[a]	15.79[a]	16.48[bc]	17.85[a]
SPV1411	10.70[b]	14.96[b]	16.25[c]	16.37[b]
Mean	13.38 ***	15.81 *	17.35 ***	17.86 *

*,*** significant at 0.05, and 0.001 probability levels, respectively.
Means in the same column followed by the same letter(s) are not significantly different (at $p < 0.05$) by LSD.

varieties but this variety showed the highest glucose and fructose concentrations (Table 2).

3.3. Comparison of estimated versus measured ethanol yield

No significant differences were found among the four sweet sorghum varieties for juice yield, sugar yield and subsequent ethanol yield. However, numerically, KKU40 had the highest harvested sugar yields and the highest ethanol yield ($2240\,L\,ha^{-1}$). The other three varieties ranged from 1425 to $1824\,L\,ha^{-1}$. Ethanol yields measured in the laboratory for all genotypes were compared with estimates reported in the literature. There were significant differences between estimations from published methods and measured ethanol levels (Fig. 1). Estimated ethanol yields for sweet sorghum obtained by the Smith 1 and by the method of Tew et al. (2008) equations were significantly higher (via *t*-tests) than actual ethanol yields. Yields estimated from the equation derived from Smith 2 (Smith et al., 1987) and Somani and Taylor (2003) were very close to actual yields for sweet sorghum. The Smith 2 method which estimates ethanol yield as 80% of theoretical was also used by Rani and Umakanth (2012). The estimation from Hills et al. (1990) resulted in higher yields. All estimates were highly correlated ($r = 0.94–0.95$) with measured laboratory yields suggesting that even though some estimates were not accurate they were precise enough for use as comparisons among genotypes or treatments within a study.

3.4. Mineral content of juice

Significant differences were observed among the four sweet sorghum varieties for concentrations of N, K, Mg, Fe, and Zn (Table 3). Theis and SPV1411 had significantly higher levels of N and P, while BJ248 had higher levels of Mg. SPV1411 had significantly higher Fe and significantly lower Zn than the other varieties (Table 3).

Table 5
Ethanol concentration ($g\,L^{-1}$) at different periods of fermentation from 12 to 48 h of four sweet sorghum varieties replicated four times.

Cultivar	12 h	24 h	36 h	48 h
KKU40	28.1[a]	59.2[a]	70.2[a]	72.9[a]
Theis	22.3[b]	59.8[a]	67.3[a]	72.8[a]
BJ248	20.9[b]	42.3[b]	63.0[a]	68.3[a]
SPV1411	29.4[a]	55.9[a]	64.1[a]	76.4[a]
Mean	25.2 *	54.3 ***	66.2 ns	70.4 ns

ns, non-significant; *,*** significant at 0.05 and 0.001 probability levels, respectively.
Means in the same column followed by the same letter(s) are not significantly different (at $p < 0.05$) by LSD.

3.5. Changes in total soluble solids

Total soluble solids were recorded at 50% flowering date, soft dough (10 days after flowering), hard dough (20 days after flowering), and harvest (30 days after flowering) to determine the most suitable time for harvest of the four sweet sorghum varieties. Other than SPV1411 total soluble solids were similar among cultivars at flowering (Table 4). At the hard dough stage Theis had significantly higher percent soluble solids, while KKU40 and BJ248 continued to increase until harvest. SPV1411 had increased soluble solids up to the hard dough stage but was consistently lower than the other cultivars.

3.6. Changes in ethanol concentration during fermentation

Ethanol concentrations were recorded at 12, 24, 36 and 48 h after initiation of fermentation. Accumulations of ethanol after 36 and 48 h of fermentation were similar among the four sweet sorghum varieties (Table 5) with all genotypes reaching the highest concentrations at 48 h. However, BJ248 fermentation lagged behind the others through the first 24 h.

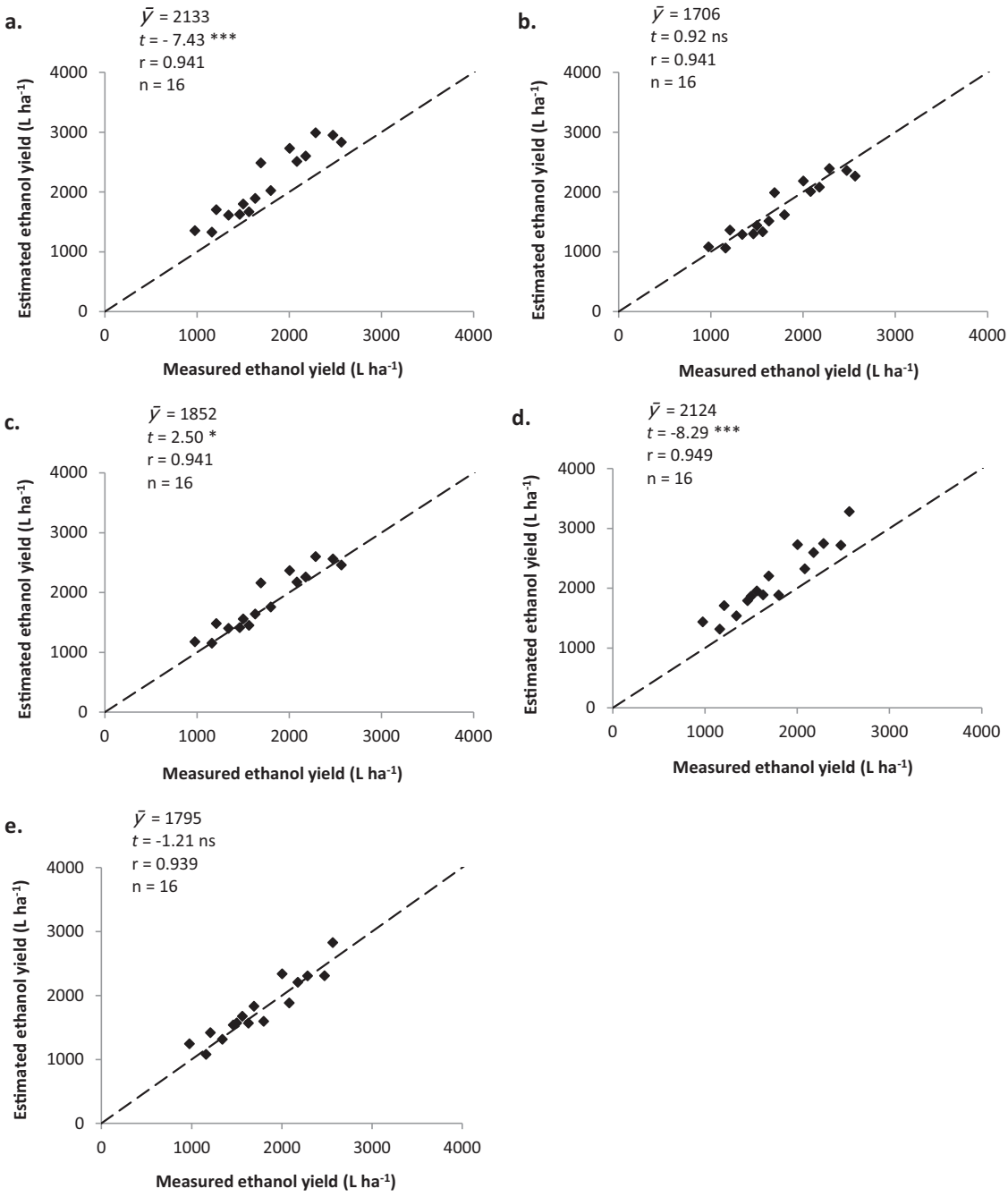


Fig. 1. Plots of laboratory ethanol yields (*x*-axes) versus estimated ethanol yields (*y*-axes) from Smith 1 (a), Smith 2 (b), Hills et al. (c) Tew et al. (d), and Somani and Taylor (e). $\bar{y}$ = mean of estimated ethanol yield; *t* = *t*-test statistic, where ns means non-significant differences between estimated and measured ethanol yield, *,*** means significant differences between estimated and measured ethanol yield at the 0.05 and 0.001 probability levels, respectively; *r* = Pearson correlation coefficient; *n* = sample number. Dashed diagonal line represents *x* = *y*.

3.7. Correlations among traits

Total sugar content of the sweet sorghum juice extracted from samples of each sweet sorghum was highly correlated with sucrose ($r = 0.94^{***}$). The amount of fructose and glucose were highly correlated with each other ($r = 0.95^{***}$) and each was significantly correlated with ethanol levels after 12 h ($r = 0.55^{*}$ and 0.58^{*} for fructose and glucose, respectively). None of the other sugar components were significantly correlated with ethanol production at the different time intervals. Among minerals present in the juice, nitrogen content was highly correlated with iron content ($r = 0.86^{***}$). Nitrogen was the only mineral to affect fermentation and was significantly correlated with ethanol at 12 h ($r = 0.55^{*}$).

The multiple stepwise regression procedure requires a significance level of 0.3 to allow a variable into a model and a significance level of 0.35 to stay in the model. Multiple traits attributed to ethanol yield differences at all fermentation sampling times (Table 6). Glucose and fructose levels appeared to be important during early fermentation. The minerals N, P, K and Fe influenced ethanol levels after 12 h, while N and K remained important throughout the first 36 h. Final ethanol production (48 h) was significantly influenced by sucrose, P and fiber levels (Table 6).

Table 6
Final model for inclusion of juice traits affecting conversion to ethanol over time by stepwise regression analysis.

Order of insertion into stepwise model	Effect	$p > \chi^2$
Ethanol concentration after 12 h		
1	Glucose	0.012
2	Phosphorus	0.021
3	Nitrogen	0.168
4	Iron	0.016
5	Fiber	0.067
6	Potassium	0.191
Ethanol concentration after 24 h		
1	Magnesium	0.065
2	Nitrogen	0.121
3	Fiber	0.023
4	Fructose	0.148
5	Potassium	0.109
6	pH	0.077
Ethanol concentration after 36 h		
1	Magnesium	0.240
2	Potassium	0.229
3	Fructose	0.176
4	Zinc	0.175
5	pH	0.097
6	Nitrogen	0.262
Ethanol concentration after 48 h		
1	Phosphorus	0.155
2	Sucrose	0.100
3	Fiber	0.169

4. Discussion

4.1. Estimated versus measured ethanol yields

This study compared measured ethanol yield of four sweet sorghum varieties with estimated yields using five published methods that use sugar yields and composition. There was minimal variability among the four varieties for agronomic traits though the sorghum gene pool has tremendous amount of variability (Ali et al., 2008; Ratnavathi et al., 2011). However, these varieties represent reasonable variation in sugar and mineral components in the juice for purposes of this study. Ethanol yields are often estimated from sugar yields based on assumptions of conversion efficiency. In this study, ethanol yield estimates for sweet sorghum ranged from 1425 to 2622 L ha^{-1} depending on the cultivar and the estimation equation used.

Estimations using Smith 2 (Smith et al., 1987) and Somani and Taylor (2003) very closely matched the measured laboratory ethanol yields in this study (Fig. 1). The other three estimation methods were significantly different from the laboratory produced yields. The theoretical Smith 1 yield (1987, 1993) is calculated based on stoichiometry, and assumes that every sugar molecule is utilized by glycolysis and alcoholic fermentation to produce only ethanol and CO_2 (Gay Lussac law). Under this assumption 5.83 kg hexose or 5.54 kg sucrose will convert to 1 U.S. gal ethanol (3.78 L). Smith and Buxton (1993) use the average of 5.68 kg sugars gal^{-1} ethanol, assuming sugars are a mixture of 50% hexose (glucose and fructose), and 50% sucrose. Sweet sorghum juice generally has a much higher concentration of sucrose to hexoses. In this study sucrose made up between 75.9 and 81.7% of the total sugars (Table 2). Smith 1 estimate also assumed 100% conversion at 1.5 kg L^{-1} ethanol. However, their second estimate (Smith 2) assumes a more conservative efficiency, noting that at least 5% of the sugars are utilized by yeast for other metabolic purposes and that 80% conversion efficiency would be a more realistic estimation of actual ethanol yield. In our study, multiplying theoretical yields by 80% (Smith 2), as suggested by Smith et al. (1987) and others (Dalvi et al., 2011; Rani and Umakanth, 2012), gives estimates that are acceptably close to those obtained in the laboratory for sorghum, as demonstrated by t-test ($t = 0.923$; $p = 0.371$) and Pearson correlation ($r = 0.941$). The theoretical equation (Smith 1) overestimates ethanol yields by 389 L ha^{-1} for sorghum. Thus, our laboratory derived ethanol yields are 82% of theoretical yields that would be estimated by the Smith 1 equation.

The estimation equation used by Hills et al. (1990) calculates the total hexose sugars present in the juice. Hydrolysis of a sucrose molecule into glucose and fructose releases a water molecule, thus a mole of hexose has less mass than a mole of sucrose. An adjustment is made by multiplying %sucrose by a factor of 1.05, then adding %fructose and %glucose. Hills et al. (1990) cite an ethanol conversion rate of 15.02 lbs hexose gal^{-1} ethanol, which corresponds to 1.8 kg hexose L^{-1} ethanol and is more conservative than the 1.5 kg sugar L^{-1} ethanol of Smith and Buxton (1993). In our study this equation over-estimated the sweet sorghum laboratory values slightly, and the difference was significant by t-test ($t = -2.50$, $p = 0.024$).

Tew et al. (2008) proposed an equation based on Brix and %sucrose to estimate hexose sugars. Again, the factor of 1.05 is multiplied by %sucrose to adjust for the mass loss by hydrolysis. Glucose and fructose are then estimated by subtracting %sucrose from total Brix. To convert to ethanol, Tew et al. (2008) propose a conversion rate of 1.7 kg hexose L^{-1} ethanol. Since Brix includes other soluble solids besides convertible sugars, the estimate of ethanol from sugars is highly overestimated. They also use the 100% theoretical conversion rate of 1.7 kg hexose L^{-1} ethanol which compounds their overestimate. Compared to the values we obtained in the laboratory, their equation highly overestimated ethanol yields for sorghum.

The equation of Somani and Taylor (2003) estimates total sugar using Brix and specific gravity measurements. Specific gravity (SG; mass of 1 L) is easily measured using a balance and graduated cylinder or with a hydrometer. Brix is a measurement of soluble solids percentage (mass/mass) of liquid, based on the refractive indices of solutions with known concentrations of sucrose. Brix is easy to measure using a refractometer, but as mentioned previously, Brix can highly over-estimate sugars due to the presence of other solutes. Somani and Taylor (2003) seem to suggest a correction for this by subtracting 3 from the base Brix measurement. Multiplying (Brix − 3) by SG of the liquid gives approximate percent sugars by volume. To calculate ethanol yield, this is then multiplied by a factor of 0.59 L ethanol kg^{-1} sucrose, or 142 U.S. gal ethanol ton^{-1} sucrose. In our study, this equation appears to be acceptable for estimating ethanol yields from sweet sorghum juice ($t = -1.21$; $p = 0.244$; $r = 0.94$) (Fig. 1) and is useful when exact quantification of sugars is impractical or not possible, but simpler Brix and SG measurements can be taken. However, this equation does not take into account possible compositional differences of the total soluble solids. Subtracting with the constant 3 from the Brix measurements changes the percentage of non-sugars from different samples. For example, for a Brix reading of 12, subtracting 3 would constitute 25% adjustment for non-sugars while a Brix of 20 would constitute a correction of 15%.

4.2. Effects of juice quality on fermentation rate

Juice quality may also affect ethanol yield by affecting conversion efficiency by the yeast. In our study, the amounts of hexoses affected the conversion rate after 12 and 24 h but not at 36 or 48 h (Table 6). Stepwise regression models indicated that sucrose content was important in the final ethanol concentration (48 h). Glucose is most often fermented first by the yeast followed by fructose. Sucrose requires hydrolysis to the monosaccharides prior to fermentation and with high levels of fructose fermentation can

be sluggish (Bisson, 1999). Andrzejewski et al. (2013a,b) reported how differences in quality of sweet sorghum juice among cultivars and hybrids affects clarification which in turn can affect conversion rates. Shinnde et al. (2013) found the total soluble solids ($r = 0.56^{**}$), total sugar ($r = 0.56^{**}$) and non-reducing sugar ($r = 0.57^{**}$) were positively correlated with ethanol yield. Ritter et al. (2008) found that glucose was associated to fructose ($r = 0.96^{***}$) as was found in this study ($r = 0.95^{***}$). Similarly, Wang et al. (2012) reported that glucose was positively correlated with fructose ($r = 0.87^{***}$) and sucrose was negatively correlated with glucose ($r = -0.65^{***}$). In our study sucrose and total sugars were highly correlated ($r = 0.94^{***}$), which is similar to Shiringani et al. (2010) ($r = 0.99^{***}$).

In a previous study, pH of sweet sorghum ranged from 4.43 to 4.85 (Davila-Gomez et al., 2011) and 4.95 to 5.47 (Chohnan et al., 2011). Range of pH in this study was intermediate between the two studies (pH 4.8). Fermentation progresses well within this range for most yeast (Bisson, 1999). Nitrogen content in the juice had an important positive effect on early fermentation (after 12 h) as observed through correlations ($r = 0.55$, $p < 0.02$) and from the stepwise regression (Table 6). This may be primarily due to the need of the fermenting yeast for nitrogen in the form of proteins or amino acids (Andrzejewski et al., 2013b). Both nitrogen and zinc are essential elements for growth of fermenting yeast (Bisson, 1999; Stehlik-Tomas et al., 2004; De Nicola and Walker, 2009). Other micro-nutrients are essential but may also be toxic in higher concentrations. Though no individual correlation coefficients were significant between any juice traits and ethanol concentration after 24 h of fermentation, a number or traits fit the regression model (Table 6). Potassium, magnesium, and fiber content can have a negative effect on ethanol content. Han et al. (2012) found that cellulose fiber in juice was negatively correlated with ethanol yield and though fiber had no direct negative correlation with ethanol levels, fiber showed up at each level of fermentation in the stepwise regression analysis (Table 6). For final ethanol levels (48 h), phosphorus was the only other juice component having an effect. Though correlation coefficients for phosphorus and magnesium were not significant, they were negative in value (−0.18 to −0.36 and −0.10 to −0.49, respectively) with ethanol levels at each sampling time.

4.3. Conclusions

In this study, estimates of ethanol yield from field harvest by the Smith 2 equation which multiplies theoretical yields by 80% (Smith et al., 1987) was the most accurate and should be used for future estimations when only juice yields and sugar parameters are available, though the equation of Somani and Taylor (2003) was also quite accurate. Though nitrogen content in the juice is important for fast conversion, in the end the quantity of juice and amounts of sucrose in the juice have the greatest effect on ultimate ethanol production.

Acknowledgement

The researchers would like to thank the Royal Golden Jubilee Ph.D. Program (RGJ) under the Thailand Research Fund, Research and Researcher for Industry (RRi), Plant Breeding Research Center for Sustainable Agriculture, Department of Plant Science and Agricultural Resources, Faculty of Agriculture and Khon Kaen University Research Fund.

References

Ali, M.L., Rajewski, J.F., Baenziger, P.S., Gill, K.S., Eskridge, K.M., Dweikat, I., 2008. Assessment of genetic diversity and relationship among a collection of US sweet sorghum germplasm by SSR markers. Mol. Breed. 21, 497–509.

Andrzejewski, B., Eggleston, G., Lingle, S., Powell, R., 2013a. Development of a sweet sorghum juice clarification method in the manufacture of industrial feedstocks for value-added fermentation products. Ind. Crops Prod. 44, 77–87.

Andrzejewski, B., Eggleston, G., Powell, R., 2013b. Pilot plant clarification of sweet sorghum juice and evaporation of raw and clarified juices. Ind. Crops Prod. 44, 648–658.

Bisson, L.F., 1999. Stuck and sluggish fermentation. Am. J. Enol. Vitic. 50, 17–119.

Broadhead, D.M., Freeman, K.C., Coleman, O.H., Zummo, N., 1978. Registration of Theis sweet sorghum. Crop Sci. 18 (1), 165.

Chohnan, S., Megumi, N., Habibur, R., Youji, N., Takanori, Y., Hiroyuki, O., Yasurou, K., 2011. Fuel ethanol production from sweet sorghum using repeated-batch fermentation. J. Biosci. Bioeng. 111 (4), 433–436.

Dalvi, U.S., Chavan, U.D., Shinde, M.S., Gadakh, S.R., 2011. Assessment of sweet sorghum cultivars for efficient ethanol production. Sugar Tech 13 (3), 186–190.

Davila-Gomez, F.J., Chuck-Hernandez, C., Perez-Carrillo, E., Rooney, W.L., Serna-Saldivara, S.O., 2011. Evaluation of bioethanol production from five different varieties of sweet and forage sorghums (*Sorghum bicolor* (L.) Moench). Ind. Crops Prod. 33, 611–616.

De Nicola, R., Walker, G.M., 2009. Accumulation and cellular distribution of zinc by brewing yeast. Enzyme Microb. Technol. 44, 210–216.

Doggett, H., 1988. Sorghum, second ed. Longman Group, London.

Gomez, K.A., Gomez, A.A., 1984. Statistical Procedures for Agricultural Research, second ed. John Wiley & Sons, New York.

Han, K.J., Pitman, W.D., Kim, M., Day, D.F., Alison, M.W., McCormick, M.E., Aita, G., 2012. Ethanol production potential of sweet sorghum assessed using forage fiber analysis procedures. GCB Bioenergy, 1–9.

Hills, F.J., Lewellen, R.T., Skoyen, I.O., 1990. Sweet sorghum cultivars for alcohol production. Calif. Agric. 44, 14–16.

Hoffmann-Thoma, G., Hinkel, K., Nicolay, P., Willenbrink, J., 1996. Sucrose accumulation in sweet sorghum stem internodes in relation to growth. Physiol. Plant. 97, 277–284.

IBPGR and ICRISAT, 1993. Descriptors for Sorghum [*Sorghum bicolor* (L.) Moench]. International Board for Plant Genetic Resources/International Crops Research Institute for the Semi-Arid Tropics, Rome, Italy/Patancheru, India.

Jia, F., Chawhuaymak, J., Riley, M.R., Zimmt, W., Ogden, K.L., 2013. Efficient extraction method to collect sugar from sweet sorghum. J. Biol. Eng. 7, 1–8.

Laopaiboon, L., Thanonkeo, P., Jaisil, P., Laopaiboon, P., 2007. Ethanol production from sweet sorghum juice in batch and fed-batch fermentations by *Saccharomyces cerevisiae*. World J. Microbiol. Biotechnol. 12, 357–360.

Liu, R., Li, J., Shen, F., 2008. Refining bioethanol from stalk juice of sweet sorghum by immobilized yeast fermentation. Renew. Energy 33, 1130–1135.

Makanda, I., Tongoona, P., Derera, J., 2009. Combining ability and heterosis of sorghum germplasm for stem sugar traits under off-season conditions in tropical lowland environments. Field Crops Res. 114, 272–279.

Mountney, G.J., Gould, W.A., 1988. Practical Food Microbiology and Technology. Van Nostrand Reinhold Company, New York, USA.

Murray, S.C., Rooney, W.L., Hamblin, M.T., Mitchell, S.E., Kresovich, S., 2009. Sweet sorghum genetic diversity and association mapping for brix and height. Plant Genome 2, 48–62.

Pfeiffer, T.W., Bitzer, M.J., Toy, J., Pedersen, J.F., 2010. Heterosis in sweet sorghum and selection of new sweet sorghum hybrid for use in syrup production in Appalachia. Crop Sci. 50, 1788–1794.

Raikar, R.V., 2012. Enhanced production of ethanol from grape waste. Int. J. Environ. Sci. 3, 776–783.

Rani, C.H., Umakanth, A.V., 2012. Genetic variation and trait inter-relationship in F_1 hybrids of sweet sorghum (*Sorghum bicolor* (L.) Moench). J. Trop. Agric. 50 (1–2), 80–83.

Ratnavathi, C.V., Chakravarthy, S.K., Komala, C.V., Chavan, U.D., Patil, J.V., 2011. Sweet sorghum as feedstock for biofuel production: a review. Sugar Tech 13 (4), 399–407.

Ratnavathi, C.V., Suresh, K., Kumar Vijay, B.S., Pallavi, M., Komala, V.V., Seetharama, N., 2010. Study on genotypic variation for ethanol production from sweet sorghum juice. Biomass Bioenergy 34, 947–952.

Ritter, K.B., Jordan, D.R., Chapman, S.C., Godwin, I.D., Mace, E.S., McIntyre, C.L., 2008. Identification of QTL for sugar related traits in a sweet × grain sorghum (*Sorghum bicolor* L. Moench) recombinant inbred population. Mol. Breed. 22, 367–384.

SAS Institute, 1999. SAS User's Guide. Statistics. Version 7. SAS Institute, Cary, NC.

Shen, F., Zeng, Y., Deng, S., Liu, R., 2011. Bioethanol production from sweet sorghum stalk juice with immobilized yeast. Proc. Environ. Sci. 11, 782–789.

Shinnde, M.S., Repe, S., Gaikwad, A.R., Dalvi, U.S., Gadakh, S.R., 2013. Physio-biochemical assessment of sweet sorghum genotypes during post rainy season. J. Acad. Ind. Res. 1 (8), 501–507.

Shiringani, A.L., Frisch, M., Friedt, W., 2010. Genetic mapping of QTLs for sugar-related traits in a RIL population of *sorghum bicolor* L. Moench. Theor. Appl. Genet. 121, 323–336.

Sipos, B., Réczey, J., Somorai, Z., Kádár, Z., Dienes, D., Réczey, K., 2009. Sweet Sorghum as feedstock for ethanol production: enzymatic hydrolysis of steam-pretreated bagasse. Appl. Biochem. Biotechnol. 153, 151–162.

Smith, G.A., Buxton, D.R., 1993. Temperate zone sweet sorghum ethanol production potential. Bioresour. Technol. 43 (1), 71–75.

Smith, G., Bagby, M., Lewellan, R., Doney, D., Moore, P., Hills, F., Campbell, L., Hogaboam, G., Coe, G., Freeman, K., 1987. Evaluation of sweet sorghum for fermentable sugar production potential. Crop Sci. 27, 788–793.

Somani, R.B., Taylor, J.R.N., 2003. Sorghum: a potential source of raw material for agro-industries. In: Alternative Uses of Sorghum and Pearl Millet in Asia. Proceedings of the Expert Meeting, Common Fund for Commodities, CFC Technical Paper No. 34, pp. 146–168, ICRISAT, Patancheru, Andhra Pradesh, India, 1–4 July 2003.

Stehlik-Tomas, V., Zetic, V.G., Stanzer, D., Grba, S., Vahcic, N., 2004. Zinc, copper and manganese enrichment in yeast *Saccharomyces cerevisiae*. Food Technol. Biotechnol. 42 (2), 115–120.

Tew, T.L., Cobil, R.M., Richard Jr., 2008. Evaluation of sweet sorghum and sorghum × sudangrass hybrids as feedstocks for ethanol production. Bioenergy Res. 1 (2), 147–152.

Wang, M., Xin, Z., Tonnis, B., Farrell, G., Pinnow, D., Chen, Z., Davis, J., Yu, J., Hung, Y.C., Pederson, G.A., 2012. Evaluation of sweet sorghum as a feedstock by multiple harvests for sustainable bioenergy production. J. Sustain. Bioenergy Syst. 2, 122–137.

Geoderma 237–238 (2015) 105–116

Contents lists available at ScienceDirect

Geoderma

journal homepage: www.elsevier.com/locate/geoderma

Biochar characteristics and application rates affecting corn growth and properties of soils contrasting in texture and mineralogy

Somchai Butnan [a], Jonathan L. Deenik [b], Banyong Toomsan [c], Michael J. Antal [d], Patma Vityakon [a,*]

[a] Land Resources and Environment Section, Department of Plant Science and Agricultural Resources, Faculty of Agriculture, Khon Kaen University, Khon Kaen 40002, Thailand
[b] Department of Tropical Plant and Soil Science, University of Hawaii, HI 96822, USA
[c] Agronomy Section, Department of Plant Science and Agricultural Resources, Faculty of Agriculture, Khon Kaen University, Khon Kaen 40002, Thailand
[d] Hawaii Natural Energy Institute, University of Hawaii, HI 96822, USA

ARTICLE INFO

Article history:
Received 25 February 2014
Received in revised form 12 July 2014
Accepted 23 August 2014
Available online 7 September 2014

Keywords:
Al and Mn phytotoxicities
Ash content of biochar
Biochar mediated Mn solubility
K luxury consumption
Nutrient availability
Soil pH

ABSTRACT

Benefits of biochar as a soil amendment may vary with its properties, time after its application, and in relation to soil texture and mineralogy. Effects of pyrolysis conditions on biochar properties which, in turn, influence soil fertility and plant growth in two different soils were investigated. A pot experiment employing two types of eucalyptus wood derived biochar, i.e. low (350 °C) and high (800 °C) pyrolysis temperatures, was applied at four rates, i.e., 0, 1, 2, and 4% w/w, once at the beginning of the experiment to a loamy-sand Ultisol and a silty-clay-loam Oxisol. Two consecutive corn crops were grown to investigate biochar temporal effect. Low temperature biochar had lower ash (2.4%) content than its high temperature counterpart (3.9%). Biomass of the first corn crop was significantly depressed under the highest rate of the high temperature biochar compared to control treatment in the sandy Ultisol, but not in the clayey Oxisol. Biomass depression was accompanied by a significant increase in soil pH (5.88) compared to control (4.74), as well as significant increases in tissue K concentrations (43 vs 10.8 g kg^{-1}), and decreases in tissue Ca (2.8 vs 3.8 g kg^{-1}) and Mg (1.3 vs 2.6 g kg^{-1}). Biomass of the second crop increased in most biochar treatments compared to the controls, due to the reduction in phytotoxicity of Al in the Ultisol and Mn in the Oxisol. Both biochars significantly increased soluble Mn concentrations relative to the control (1.39–4.61 vs 1.12 mg l^{-1}), while they decreased tissue Mn concentrations compared to the control (0.08–0.17 vs 0.41 g kg^{-1}) in the Oxisol. Possible mechanisms underlying biochar mediated increases in soil Mn solubility and decreases in corn Mn uptake were discussed. These results showed clearly that lower temperature biochar gave higher benefits to both contrasting textured soils than the higher temperature counterpart in both first (32 days after biochar application, DAA) and second (82 DAA) cropping cycles. The 1–2% w/w rate of the low temperature biochar was appropriate for these soils, the higher rate being more suited to the finer textured soil.
© 2014 Elsevier B.V. All rights reserved.

1. Introduction

Biochar used as a soil amendment to improve soil fertility and plant growth has been the focus of much research in the recent past (Ibrahim et al., 2013). It has shown promise as a sustainable amendment to enhance soil chemical properties (Glaser et al., 2002; Lehmann et al., 2011). Unlike most conventional soil organic materials, which are readily decomposed, the recalcitrant nature of biochar increases its potential value as a soil amending material for the longer term (Chan et al., 2007). Some biochars contain high quantities of ash, which are enriched with a number of plant nutrients, especially cationic elements, such as K, Ca, and Mg (Deenik et al., 2011; Rajkovich et al., 2012; Yuan et al., 2011). Additionally, ash content plays a major role in controlling soil pH which determines cation exchange capacity (CEC) of variable charged soils (Sollins et al., 1988) and nutrient availability (Mengel and Kirkby, 2001).

The chemical characteristics of biochar produced from a feedstock depend considerably on pyrolysis conditions, especially temperature (Antal and Gronli, 2003). At low temperature, biochar chemical composition is closer to the original feedstock while high temperature biochar is closer to graphite (Masiello, 2004). Low temperature biochar has high volatile matter (VM — e.g., bound carboxylic acid, phenol, ketone, and aldehyde functional groups), but lower fixed C and ash contents than the high temperature counterpart (Bourke et al., 2007). Previous studies showed that biochar with high VM content contributed to N immobilization and microbial activity reduction which negatively affected plant growth (Deenik et al., 2010; Spokas et al., 2011).

It is likely that biochar amendment effects depend upon soil properties, especially soil texture and mineralogy. In the tropics, a large proportion of agricultural soils are highly weathered belonging to the order Oxisols and Ultisols, which occupy about 23% and 20% of the tropics worldwide, respectively (Sanchez and Logan, 1992). The mineralogy of

* Corresponding author.
E-mail address: patma@kku.ac.th (P. Vityakon).

http://dx.doi.org/10.1016/j.geoderma.2014.08.010
0016-7061/© 2014 Elsevier B.V. All rights reserved.

these soils consists predominantly of low activity clays with variable charged surface; i.e., kaolinite and oxides and hydroxides of Fe and Al (Naidu et al., 1997). Commonly, a crucial problem of Ultisols and Oxisols is Al toxicity (Lathwell and Grove, 1986). Previous studies showed that biochar application reduced Al toxicity in acid soils (Hossain et al., 2010; Major et al., 2010). Chan et al. (2007) reported that application of greenwaste biochar to an acidic Alfisol soil reduced extractable Al concentration from 0.27 $cmol_c\ kg^{-1}$ in control to 0.12 $cmol_c\ kg^{-1}$ in 50 t biochar ha^{-1}. Nevertheless, excessive application of liming materials including biochar to coarsely textured low buffering capacity soils may lead to abrupt increases in soil pH resulting in deficiencies of some plant nutrients (Kamprath, 1971). For example, K deficiency in radish resulted from application of poultry litter biochars to an acid soil (Chan et al., 2008), and N and P deficiencies in larch (*Larix gmelinii*) resulted from application of Japanese larch wood biochar (Makoto et al., 2011).

Although there have been some studies on the influence of biochars on soil properties and plant growth in soils differing in texture and mineralogy, these studies did not show the interaction effects of biochar types (particularly based on different pyrolysis conditions) and the different soils. For example, Kolb et al. (2009) reported that application of 10% w/w biochar produced from mixed feedstock (bull manure:dairy manure:pine wood = 2:1:1) increased total N in a sandy loam Spodosol, but not in a clay loam Alfisol. Meanwhile, Yeboah et al. (2009) reported that application of savannah wood biochar increased N and P uptake in corn plants grown in a sandy loam, but uptake decreased in a silt loam soil. We propose that biochar materials are characterized by physical and chemical properties that would benefit coarsely textured soils more than soils with fine texture. Biochars possess high porosity and surface area with a potential to beneficially impact soil physical properties by reducing bulk density and increasing water holding capacity in sandy soils with high bulk density and low water retention. Chemically, biochars have the potential to provide nutrient supply and liming potential through ash components and increase nutrient retention by increasing CEC.

The present research addressed two general hypotheses: (i) biochars have higher influence on soil properties and plant growth in a coarse textured Ultisol soil than in a fine textured Oxisol and (ii) biochar produced under higher temperature, and hence lower VM, is more effective at improving soil properties and plant growth than a lower temperature (higher VM) biochar, but the effectiveness is short-lived. Therefore, the objectives of this study were (i) to determine effects of pyrolysis condition on biochar properties; (ii) to evaluate the effects of those biochars and their application rates on soil properties and plant growth in soils contrasting in texture and mineralogy; and (iii) to determine the time effect on biochar benefits.

2. Materials and methods

2.1. Soils

Two soils with contrasting texture and mineralogy were used for this study. The Khorat soil (isohyperthermic Typic Oxyaquic Kandiustults) collected from 0–15 cm depth from a fruit tree research plot at Khon Kaen University, Thailand (16°27′50″ N; 102°48′14″ E) and the Wahiawa soil (kaolinitic isohyperthermic Rhodic Haplustox) from the 0–15 cm depth at the Poamoho Research Station, University of Hawaii, USA (21°32′30″ N; 158°05′15″ W). Soils were air-dried and sieved to pass through a 2-mm sieve and stored in polyethylene containers at room temperature. The Khorat soil was shipped to the University of Hawaii where the greenhouse experiments were performed. Initial physical and chemical properties of Khorat and Wahiawa soils are shown in Table 1.

2.2. Biochars

The biochar feedstock comprised the upper branches of eucalyptus trees (*Eucalyptus camaldulensis*) remaining from tree cuttings used for pulp production from the Mancha Khiri Plantation Forest Station, Khon Kaen province, Thailand. The biochars were produced using two different pyrolysis techniques: Thai traditional kiln (TK) and Flash Carbonization™ (FC) (Table 2). The TK biochar was produced utilizing the traditional practice of local Thai people where the feedstock was subjected to heating (approximately 350 °C) under low O_2 for three days, cooled down with water and air dried for another four days. The FC biochar was produced at the Hawaii Natural Energy Institute at the University of Hawaii using the Flash Carbonization process, which involved exposing the feedstock to a controlled flash fire at 1 MPa pressure for 40 min with peak temperature reaching up to 800 °C in the reaction canister. Both biochars were crushed and subsequently sieved to pass through a 2-mm sieve. The TK biochar was transported to Hawaii and both biochars were stored at room temperature prior to laboratory analysis and further use in a greenhouse experiment.

2.3. Greenhouse experiment

A pot experiment was conducted under greenhouse conditions from August to October 2011. A factorial treatment structure was used with two soil types (Khorat and Wahiawa soils), two biochar types (TK and FC biochars), and four rates of biochar application (0, 1, 2, and 4% w/w). The 14 treatment combinations were arranged in a randomized complete block design (RCBD) with three replications for a total of 42 experimental units. Pots ($d = 0.16$ m, $v = 3016\ cm^3$) were filled with 2 kg air dried soil and four rates of each biochar were applied to the pots and mixed thoroughly with the soils. Corn was grown in these pots for two crops, each crop had a duration of 39 days, and biochars were applied only once before the first crop planting. This allowed the study of time effects of biochar on soil properties and plant growth, i.e. two periods corresponding to the first and the following second crops. The period of the first crop was that from biochar application to the harvest of that crop and accompanying soil sampling at 39 days after biochar application (DAA), while the period designated as the second crop was that from the biochar application to the harvest and soil sampling (82 DAA).

Corn seeds (var. Hawaiian supersweet no. 9) obtained from the University of Hawaii Seed Laboratory (Agricultural Diagnostic Services Center, University of Hawaii) were used as the test plant. Six corn seeds were planted directly into each pot. The seedlings were thinned to two plants per pot at ten days after planting (DAP). The pots were watered with deionized (DI) water once a day to 70% of water holding capacity (WHC) (20.5 and 63.4% w/w for Khorat and Wahiawa soils, respectively).

Table 1
Initial physical and chemical properties of the Khorat and Wahiawa soils used for the plant bioassay experiment.

Soil	Soil particle distribution (%)			Soil texture	Total C	Total N	pH (1: 5 H_2O)	CEC[a] ($cmol_c\ kg^{-1}$)	Mineral N ($mg\ kg^{-1}$)		P ($mg\ kg^{-1}$)	Extractable cations ($mg\ kg^{-1}$)				
	Sand	Silt	Clay		($g\ kg^{-1}$)				NO_3^-	NH_4^+		K	Ca	Mg	Al	Mn
Khorat soil	79.9	17.6	2.5	Loamy sand	6.9	1.28	5.52	0.95	ND[b]	23.59	5.73	14	111	21	11.46	13.46
Wahiawa soil	7.9	35.6	56.5	Silty clay loam	15.3	2.72	6.04	7.86	1.40	28.78	6.26	311	509	161	0.023	516.89

[a] CEC, cation exchange capacity.
[b] ND, not detectable.

Table 2
Chemical properties of Thai traditional kiln (TK) and Flash Carbonization™ (FC) biochars used for the plant bioassay experiment: (a) proximate analysis values (VM, ash, and fC contents) and elemental contents in biochar ash; (b) pH, charge property (pH_0), extractable mineral N (NO_3^- and NH_4^+).

(a) Proximate analysis and ash components

Biochar	Proximate analysis (%)			Elemental content in ash[a] (g kg^{-1})						
	VM[b]	Ash	fC[c]	Si	Al	Fe	Ca	Mg	K	P
TK biochar	35.79	2.35	61.86	0.72	0.14	0.50	5.41	0.43	5.10	0.50
FC biochar	14.65	3.85	81.50	1.04	0.33	2.29	10.42	0.59	7.81	0.86

(b) pH, charge property, and mineral N contents

Biochar	pH	Charge property	Extractable mineral N (mg kg^{-1})	
	(BC[d]:H_2O = 1:5)	pH_0	NO_3^-	NH_4^+
TK biochar	6.52	6.38	0.3	23.96
FC biochar	8.92	8.13	ND[e]	11.87

[a] Dry weight basis of biochar.
[b] VM, volatile matter.
[c] fC, fixed C.
[d] BC, biochar.
[e] ND, not detectable.

This was performed by weighing pots (pot + soil mixture + water) and adding DI water when necessary to maintain the target water content. Miracle-Gro® fertilizer (24% N: 3.5% NH_4^+–N and 20.5% $CO(NH_2)_2$–N; 8% P_2O_5; 16% K_2O; 0.02% B; 0.07% Cu; 0.15% Fe; 0.05% Mn; 0.0005% Mo; and 0.06% Zn) was applied twice in solution at 1 and 25 DAP to achieve N fertilizer rates of 100 kg N ha^{-1} and 50 kg N ha^{-1}, respectively. At 39 DAP, the aboveground biomass was harvested, oven-dried at 70 °C to constant weight, and weighed. Soil samples were also collected, air-dried and sieved to pass through 2-mm screen for later use in chemical analyses. Roots were carefully removed from the rest of the soils. Pieces of biochars attached on the roots were returned to the same pots and were used to grow the second crop of corn. The second crop was planted 4 days after the first crop harvest. The procedures of crop management were the same as the first crop.

2.4. Biochar, soil, and plant analyses

Proximate analysis (VM, ash, and fixed C contents) of biochars was measured following ASTM 1762-84 (American Standard of Testing Material, 2001). The contents of VM, ash, and fixed C of TK biochar were 35.79%, 2.35%, and 61.86%, respectively; while those of FC biochar were 14.65%, 3.85%, and 81.50%, respectively (Table 2). The ash components were measured by Hazen Research, Inc., Golden, Colorado, USA. The pH_0 of biochars was estimated following Gillman (2007). In brief, nine samples at 2 g each of each biochar type were used. The adsorption sites were saturated with Ca^{2+} by equilibrating with 20 ml of 0.1 M $CaCl_2$ for 2 h. The excess Ca^{2+} was removed by centrifugation and discarding of the supernatant. This step was performed 3 times employing lower ionic strength (0.002 M) of $CaCl_2$. Thereafter, pH of the biochar samples was adjusted to cover a gradient that includes the expected pH_0 employing either an acid 0.1 M HCl, or an alkali saturated $Ca(OH)_2$. They were left overnight to reach an equilibrium after which the pH was determined and recorded as $pH_{0.002}$. To obtain pH at 0.05 M ($pH_{0.05}$), the suspension was equilibrated with 0.5 ml of 2 M $CaCl_2$. ΔpH was calculated as the difference between $pH_{0.05}$ and $pH_{0.002}$. The pH_0 is that where ΔpH equals zero.

Soil pH was determined in a 1:5 soil to DI water ratio. Soil total C and N contents were determined using a Shimadzu TOC-VCSH high-sensitivity combustion TOC analyzer (Shimadzu Corp., Kyoto, Japan). Mineral N (NH_4^+ and NO_3^-) was extracted by 2 M KCl extraction. Ammonium was subsequently determined by salicylate–hypochlorite method (Gentry and Willis, 1988) and NO_3^- by Cd reduction method (Mulvaney, 1996) using an EasyChem Discrete Autoanalyzer (EasyChem, Systea Scientific, Oak Brook, IL). Phosphorus was extracted with Bray-2 solution (Jones, 2001) and determined on a Shimadzu UV–VIS spectrophotometer (UVmini 1240, Systea Scientific, Oak Brook, IL) at an absorbance of 820 nm. Basic cations (K^+, Ca^{2+}, and Mg^{2+}) were extracted by 1 M NH_4OAc at pH 7 (Pansu and Gautheyrou, 2006), and Al^{3+} by 1 M KCl (Bertsch and Bloom, 1996), while soluble Mn was measured in a saturated paste extract (Porter et al., 2004). Cations were determined by inductively coupled plasma spectrophotometry on a Thermo Jarrell Ash Atom Scan 16 instrument (Franklin, MA). Soil cation exchange capacity (CEC) was measured by 1 M NH_4OAc extraction method at pH 7 (Pansu and Gautheyrou, 2006), and NH_4^+ concentration for calculation of CEC was determined colorimetrically using a flow-injection analyzer (FIAstar® 5012, FOSS Tecator, Sweden).

Shoot and root biomass of corn were measured by weighing from each pot after they were oven-dried at 70 °C for 72 h or till achieving the constant weight. The shoot tissue samples were ground and sieved to pass through a 2-mm screen. Plant nutrient concentrations (K, Ca, Mg, and Mn) were determined by combusting 0.5 g oven-dried tissue, digesting in 1 M HCl, and measuring on an inductively couple plasma spectrophotometer.

2.5. Statistical analysis

Three-way analysis of variance (ANOVA) was used to determine the effect of soil type, biochar type and application rate, time after biochar application, and their interactions on corn biomass, corn shoot tissue nutrient concentrations, and soil properties. The treatment means were compared using Tukey's Studentized Range Test. The differences between initial pH and Al in the Khorat soil versus those in control treatment in the first crop were compared using paired t-test. All statistical analyses were performed using SAS software version 9.1 (SAS Institute, Cary, NC). Plotting, fitting, and equations of regression analysis, as well as calculations of coefficient of the determination (r^2) were performed using SigmaPlot software version 12.3 (SYSTAT software, Inc., Chicago, IL). In all analyses, differences were considered to be significant at $p \leq 0.05$.

3. Results

3.1. Biochar properties

FC biochar had higher fixed carbon (fC) content, ash content, and ash constituents of mineral oxides, but lower VM content than TK biochar (Table 2). Among the elements in ash some of which are sources of plant macro-nutrients, Ca and K constituted the two highest contents,

while Mg and P were the two lowest in both biochars. In addition, Fe and Ca contents were significantly lower in TK than FC biochars while extractable NH_4^+ was greater in TK than FC and extractable NO_3^- was found only in TK biochar. As a consequence of higher ash content in FC than TK biochar, higher pH was found in the former (pH 8.92) than the latter biochar (pH 6.52).

Pyrolysis temperature influenced pH_0 of biochars used in this study as seen in a higher pH_0 value in FC biochar than in TK biochar (Table 2). pH_0 is the pH at which the net charge (of variable charged materials) equals to zero (Uehara and Gillman, 1981).

3.2. Plant responses

3.2.1. Corn above-ground biomass

Corn biomass responded differently ($p \leq 0.01$) to soils of different textures and mineralogy (Table 3). In the Khorat soil, application of FC biochar immediately negatively affected corn biomass especially at the highest (4%) rate relative to the control (Fig. 1a). However, in the Wahiawa soil, there were no significant effects of both biochars in the first crop relative to the control (Fig. 1b), but significant positive effects appeared only later in the second crop under the higher rates (2 and 4%) (Fig. 1d). It is notable that in the second crop, both biochars produced positive effects in both soils at all rates with the exception of the FC biochar at the low (1%) rate (Fig. 1c and d). Contrary to our hypothesis, the effects of the biochars on corn biomass were not only short-lived, but also carried over from the first to the second crop as shown initially by the significant ($p \leq 0.001$) time effect on the biomass (Table 3). This showed that the time after biochar application exerted significant influence on the biomass. The above results as well as the findings that corn biomass of the second crop in the controls in both soils were significantly depressed compared to those of the first crop (Fig. 1a vs c and b vs d) also testified to this time effect.

Corn biomass also responded differently ($p \leq 0.001$) to the two biochar types produced under different temperature regimes as well as to the three-way interactions of soils × biochar type × time ($p \leq 0.05$) (Table 3). Overall, the TK biochar produced higher corn biomass than the FC biochar in both soils and cropping cycles (Fig. 1). In the first crop cycle, TK biochar produced average corn biomass of 13.2 g pot^{-1}, while FC biochar produced 11.8 g pot^{-1}. Similarly, in the second crop, average corn biomass under TK biochar was 10.1 g pot^{-1}, while that of FC biochar was 8.2 g pot^{-1}. In addition, in the Khorat soil, FC biochar at the highest rate (4%) significantly depressed the biomass in the first crop, while the TK did not cause any significant effect compared to the control (Fig. 1a). Furthermore, in the second crop, the highest rate of FC biochar also significantly depressed corn biomass below the same (4%) and lower (2%) rates of the TK biochar (Fig. 1c). In addition, this highest rate of FC biochar also brought about a growth depression below those of its lower rates.

3.2.2. Tissue nutrient concentrations and ratios

In general, all selected tissue macro-nutrient (K, Ca, Mg) concentrations were significantly affected by type and rate of biochar in the Khorat soil in both the first crop and second crop periods, except K which significantly changed in both soils in the longer term (Table 4).

In the Khorat soil in the first crop, tissue K concentrations increased, while Ca and Mg concentrations decreased with increasing rates of both biochars (except for 1% FC biochar), however significant differences compared to the control were only found at the highest rate (4%) of FC biochar (Table 4). In the second crop, significant increases in K concentrations over the controls were observed under 4% FC biochar in both soils. In the Khorat soil, Mg concentrations were much lower than the TK counterpart at the highest rate of FC biochar. This decrease was substantiated by significantly lower Mg uptake by plants under FC (12.1 mg pot^{-1}) compared with TK (32.6 mg pot^{-1}) biochar. In addition, the 4% rate of FC also depressed the Mg concentration below that of the lower rate (2%).

To further investigate interactions among the cations, ratios of concentrations of Ca:K and Mg:K were considered (Table 5). Significant treatment effects on such ratios were found only in the Khorat soil in both cropping cycles. Tissue Ca:K and Mg:K ratios significantly decreased with increasing rates of both biochars in the first crop while in the second crop, significant decreases of Ca:K and Mg:K ratios were found only at the highest rate of FC biochar compared to 2% FC biochar. There were significant polynomial relationships between extractable soil K concentration and tissue Ca concentration in both the first and second crops. In the first crop, tissue Ca concentrations were significantly reduced by increasing extractable soil K concentration ($r^2 = 0.67$; $p \leq 0.01$) (Fig. 2a). Meanwhile, in the second crop, tissue Ca concentrations increased with soil K concentrations up to a threshold level of 32.5 mg K kg^{-1} beyond which they decreased ($r^2 = 0.43$; $p \leq 0.01$) (Fig. 2b).

Tissue Mn concentrations showed decreasing trends relative to the controls under increasing rates of both biochars in both soils at both times (Table 4). These decreases were significant under the highest rates (4%) of FC biochar. It was notable that in the Wahiawa soil in the second crop, application of both types of biochars significantly decreased tissue Mn concentration below that of the controls, and Mn concentration of the control in the second crop was 2.6 times higher than that of the first crop (Table 4). Manganese to Ca ratios were all below the critical point of 80 (dos Anjos Reis, 2002) in the first cropping cycle suggesting the absence of Mn toxicity (Table 6). In the second planting, however, Mn:Ca reached 121 in the control treatment indicating toxic conditions with both biochars significantly lowering Mn:Ca ratio compared with the control.

3.3. Soil properties

In the first crop cycle, soil pH was not affected by biochar amendment except in the Khorat soil amended with the highest rate of FC biochar (Table 7a). On the other hand, in the sandy soil, pH of the unamended (control) treatment was significantly lower than the initial pH. Meanwhile, in the second crop, significant pH increases over the control were found in higher rates of both biochars in both soils, i.e. at the highest rate of FC and TK biochars in both soils, and at 2% rate of the FC biochar in the Wahiawa soil (Table 7b). Soil pH showed a trend of higher values under FC compared with TK biochar with a significant increase at the highest rate for the FC biochar in the Khorat soil only.

Extractable K and Ca concentrations mostly increased in the first crop with increasing biochar rates in both soils with the exception of that under 1% TK biochar in the Wahiawa soil. However, the increase was significant only at the 4% rate for the FC biochar compared to their respective controls (Table 7a and b). Similarly, Mg concentrations

Table 3
Analysis of variance (ANOVA) showing the effects of soil types, biochar types, biochar application rates, time after biochar application, and their interactions on corn biomass, soil pH, and soil Mn concentration.

Source of variance	df	Corn biomass	Soil properties	
			pH	Mn
Soil (S)	1	**	***	–
Biochar type (Bt)	1	***	***	**
Biochar rate (Br)	3	***	***	***
Time (T)	1	***	***	ns
S × Bt	1	ns	**	–
S × Br	3	ns	*	–
S × T	1	***	ns	–
Bt × Br	3	*	***	**
Bt × T	1	ns	*	***
Br × T	3	***	ns	***
S × Bt × T	3	*	ns	–

*$p \leq 0.05$; **$p \leq 0.01$; ***$p \leq 0.001$; and ns = not significantly different (F-test).

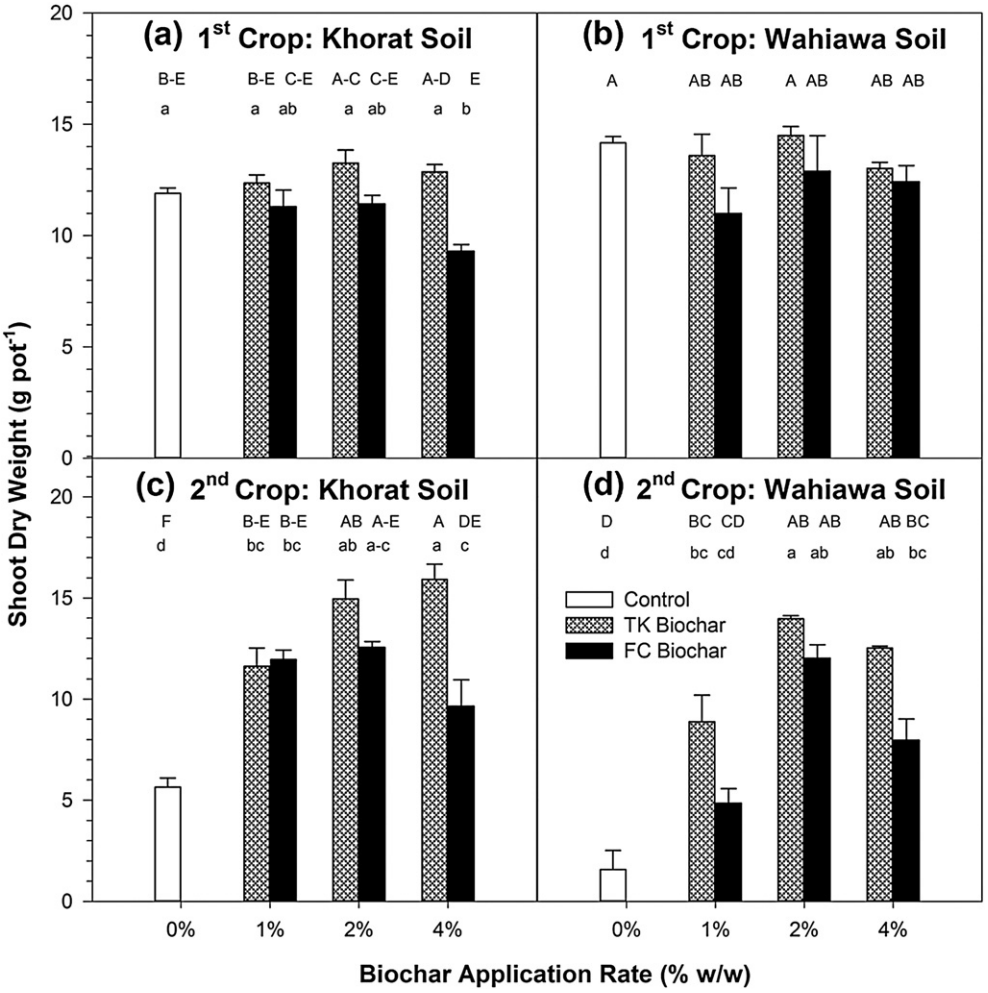


Fig. 1. Different application rates of Thai traditional kiln (TK) and Flash Carbonization™ (FC) biochars affecting corn shoot dry weight: (a) the Khorat soil in the first crop; (b) the Wahiawa soil in first crop; (c) the Khorat soil in the second crop; (d) the Wahiawa soil in the second crop. Bars with the same lower case letter within the same soil type and crop and those with the same upper case letter within a soil type but different crops are not statistically different ($p \leq 0.05$; Tukey's Studentized Range Test). Error bars represent SEM.

also showed a significant increase at the highest application rate of FC biochar in the Khorat soil (Table 7a). In the second crop, K, Ca, and Mg concentrations in the Khorat soil were greatest at the highest rate of FC biochar, and the Ca and Mg concentrations under FC biochar were significantly higher than those of TK biochar at the same rate. Meanwhile, in the Wahiawa soil in the second crop period, K concentration reached a maximum at the highest rate of FC biochar and it was greater than the lower rates (1% TK and 2% TK and FC biochars) (Table 7b). Calcium concentration in the Wahiawa soil was greatest at the highest rate of FC biochar, however, Mg concentrations showed significant decreases in all biochar amended treatments, compared to the controls.

Two elements known to have potential phytotoxic effects in acid soils are Al (in Ultisols, i.e. Khorat soil) and Mn (in Oxisol, i.e. Wahiawa soil) (Porter et al., 2004). Aluminum concentrations in the Khorat soil in the first crop decreased significantly below the control with increasing rates of both biochars (Table 7a). However, in the second crop, significant decreases in Al concentration below the control were only found under 2% and 4% rates of FC biochar. At the end of the first crop, soil pH showed a significant negative effect ($r^2 = 0.89$; $p \leq 0.001$) on extractable Al in the Khorat soil (Fig. 3a). This effect persisted through to the second crop where high soil Al concentration showed a negative effect on shoot ($r^2 = 0.42$; $p \leq 0.01$) (Fig. 3b) and root ($r^2 = 0.49$; $p \leq 0.01$) (Fig. 3c) biomass. For the Oxisol, Mn concentrations in the saturated paste extract were above 0.5 mg L^{-1}, the concentration considered toxic (Porter et al., 2004), and showed a general increase with the addition of biochar (Table 7b).

4. Discussion

4.1. Biochar characteristics as affected by pyrolysis conditions

Pyrolysis temperatures significantly influenced chemical properties of biochars. Similar to previous reports, fC, ash, and VM contents of biochars were primarily affected by pyrolysis temperature (Abdullah et al., 2010; Deenik et al., 2010). High fC and ash, but low VM contents of FC biochar were results of its high production temperature relative to those of the TK biochar. Ash is a principal factor determining elemental contents and pH value of biochars (Yuan et al., 2011). Higher elemental contents of FC compared with TK biochars were the results of higher ash content from elevated temperatures. Yuan et al. (2011) reported that alkalinity and pH of biochars increased with increasing pyrolysis temperatures. In addition, the higher pH of FC than TK biochars was the result not only of higher ash contents in the former biochar, but also progressive loss of acidic surface functional groups (mainly carboxylic acids) and VM under high production temperature (Mukherjee et al., 2011; Singh et al., 2010).

The variability of types and contents of elemental constituents of ash in biochars was influenced mainly by feedstock type and pyrolysis temperature (Antal and Gronli, 2003). Eucalyptus wood has been reported to have Ca and K as its major elemental components (Abdullah et al., 2010). This supports the high contents of Ca and K relative to other elements in both biochars. In addition, the higher melting points of these two elements than other elements contributed to their persistence,

Table 4
Nutrient concentrations in corn shoot tissue in the Khorat and Wahiawa soils as affected by application of different rates of Thai traditional kiln (TK) and Flash Carbonization™ (FC) biochars in the first crop (T1) and second crop (T2) periods.

Treatment	Selected tissue nutrient concentration (g kg^{-1})							
	K		Ca		Mg		Mn	
	T1	T2	T1	T2	T1	T2	T1	T2
Khorat soil								
Control	10.8c†	19.3b	3.84ab	3.48	2.58a	1.19b–d	0.134a	0.281ab
1% TK biochar	15.4c	14.5b	3.23ab	3.76	2.12b	1.16d	0.083b	0.297a
2% TK biochar	20.6bc	14.3b	3.03b	4.63	1.87bc	1.77ab	0.061b–d	0.142bc
4% TK biochar	30.8b	15.1b	3.08ab	4.70	1.65cd	1.75a–c	0.056b–d	0.126bc
1% FC biochar	20.4bc	17.2b	3.99a	4.10	1.97bc	1.46a–d	0.067b–c	0.166a–c
2% FC biochar	28.7b	15.5b	3.17ab	5.88	1.45d	1.89a	0.037c–d	0.179a–c
4% FC biochar	43.0a	31.5a	2.76c	3.58	1.32d	1.17cd	0.034d	0.041c
p-Value	<.0001	0.0003	0.0052	0.055	<.0001	0.0015	<.0001	0.0022
F-test	***	***	**	ns	***	**	***	**
C.V. (%)	17.37	12.62	10.32	17.60	7.39	10.61	17.02	27.51
Wahiawa soil								
Control	44.3	31.2b	2.97	3.38	2.22	2.96	0.159a	0.408a
1% TK biochar	44.0	32.5b	2.90	3.75	2.25	2.86	0.140ab	0.169b
+2% TK biochar	43.6	27.9b	3.18	3.52	2.20	2.79	0.136ab	0.163b
4% TK biochar	44.3	43.7ab	3.37	3.72	2.28	2.21	0.103ab	0.156b
1% FC biochar	56.1	46.2ab	3.14	3.58	2.39	2.69	0.125ab	0.121b
2% FC biochar	47.0	35.9ab	3.58	3.60	2.45	2.26	0.096b	0.093b
4% FC biochar	50.0	53.9a	3.41	3.93	1.94	2.50	0.084b	0.078b
p-Value	0.090	0.016	0.4094	0.962	0.280	0.584	0.006	0.0004
F-test	ns	*	ns	ns	ns	ns	**	***
C.V. (%)	11.06	13.92	12.47	16.66	9.91	17.98	12.77	25.04

*$p \le 0.05$; **$p \le 0.01$; ***$p \le 0.001$; and ns = not significantly different (F-test).
T1 = the first crop period (39 days after biochar application or at the harvest of the first crop), T2 = the second crop period (82 days after biochar application or at the harvest of the second crop).
† Means within a column followed by the same letter are not significantly different at $p \le 0.05$ (Tukey's Studentized Range Test).

and hence to their higher contents compared with other elements lost during pyrolysis (Abdullah et al., 2010; Wu et al., 2011). Elemental content of the TK biochar was also affected by the cooling down process employing water. The use of water in the cooling down process has been reported to leach out some mineral elements from biochars, for example, substantial removal of Ca from biochars via water leaching has been reported by Wu et al. (2011). This earlier finding supports our results which showed significantly lower contents of Fe and Ca in TK compared to FC biochars. The TK biochar not only had lower ash content, but also lost some of these ash constituent elements through water leaching during the cooling down process. The cooling down step involved placing the TK biochar in the open air and applying water to hasten cooling. Lower extractable NH_4^+ concentration in FC than TK biochars was likely the result of N loss due to higher temperature during pyrolysis of FC biochar. At the relatively low temperature reached in the traditional kiln process, a large proportion of N is still retained in biochar structure and NH_3 loss is reduced (Hansson et al., 2004). Presence of NO_3^- in TK biochar was likely due to oxidation of NH_4^+.

Table 5
Corn tissue Ca:K and Mg:K ratios in the Khorat and Wahiawa soils as affected by different application rates of Thai traditional kiln (TK) and Flash Carbonization™ (FC) biochars in the first crop (T1) and second crop (T2) periods.

Treatment	Tissue Ca:K ratio		Tissue Mg:K ratio	
	T1	T2	T1	T2
Khorat soil				
Control	0.356a†	0.164bc	0.239a	0.053b
1% TK biochar	0.211b	0.261a–c	0.139b	0.081ab
2% TK biochar	0.147cd	0.327ab	0.091c	0.111a
4% TK biochar	0.100de	0.328ab	0.053d	0.118a
1% FC biochar	0.195bc	0.256a–c	0.096c	0.085ab
2% FC biochar	0.111ed	0.380a	0.051de	0.114a
4% FC biochar	0.067e	0.114c	0.032e	0.041b
p-Value	<.0001	0.006	<.0001	0.0005
F-test	***	**	***	***
C.V. (%)	10.44	19.97	7.31	13.88
Wahiawa soil				
Control	0.067	0.108	0.050	0.064
1% TK biochar	0.066	0.115	0.051	0.088
2% TK biochar	0.073	0.116	0.051	0.088
4% TK biochar	0.076	0.071	0.051	0.051
1% FC biochar	0.073	0.075	0.056	0.056
2% FC biochar	0.077	0.145	0.053	0.068
4% FC biochar	0.068	0.073	0.039	0.046
p-Value	0.66	0.47	0.17	0.05
F-test	ns	ns	ns	ns
C.V. (%)	14.67	41.34	13.76	19.18

**$p \le 0.01$; ***$p \le 0.001$; and ns = not significantly different (F-test).
† Mean within column followed by the same letter are not significantly different at $p \le 0.05$ (Tukey's Studentized Range Test).

Biochar charge properties were also affected by pyrolysis temperature. The pH_0 of a variable charged material (e.g., soil or biochar) is the pH at which its net surface charge equals zero. When pH is higher than pH_0, net negative surface charge results and consequently the biochar acquires cation exchange capacity (CEC) (Uehara and Gillman, 1981). The TK biochar had lower pH_0 than the FC biochar, hence at the same pH of the environment where the biochars exist, the TK biochar would be expected to have higher CEC than the FC biochar. Lower pH_0 in the TK compared to the FC biochar was a result of lower production temperature preserving acidic functional groups that potentially contribute to CEC (Lau et al., 1986; Solar et al., 1990). Results of this study were consistent with Gaskin et al. (2008), Kloss et al. (2012), and Singh et al. (2010), who reported that CEC of biochars decreased with increasing production temperature. In addition, it is likely that the production process of the TK biochar leads to substantial surface oxidation during the cooling down phase of the pyrolysis process which involves applying water to hasten cooling. This process can enhance surface oxidation or aging of the biochar (Spokas, 2010) leading to increasing CEC. The cooling down process can be likened to the production of activated carbon from charcoal via the use of water vapor to increase its adsorption capacity (Budinova et al., 2006). On the other hand, FC biochar was cooled down in a sealed chamber (Antal, 2004) and hence unlikely to have undergone oxidation.

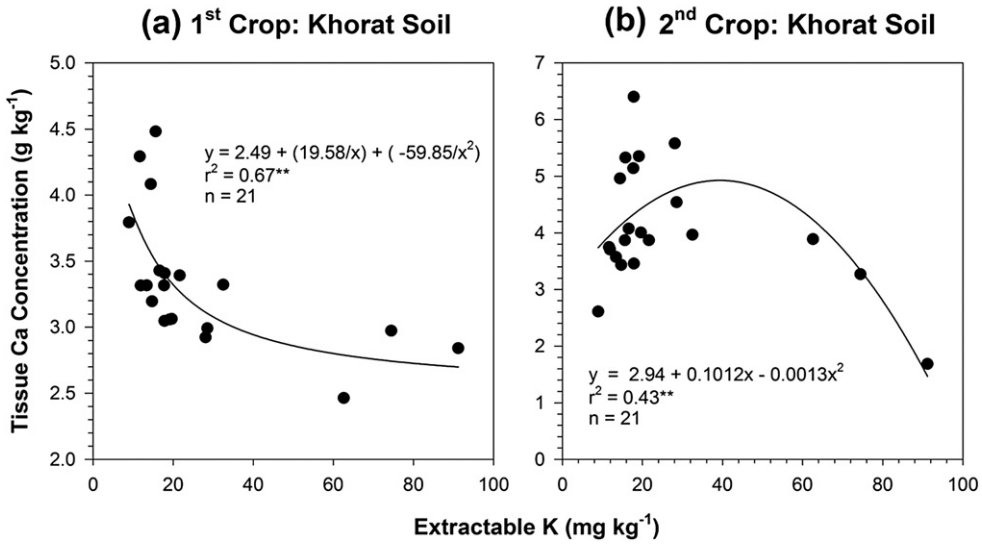


Fig. 2. Relationship between extractable soil K concentration and corn tissue Ca concentration in the Khorat soil: (a) the first crop and; (b) the second crop.

The cooling down process employing water in TK biochar could potentially affect other physical and chemical characteristics. Water vapor may increase specific surface area of the biochar through swelling or expansion of biochar structure (Bangham et al., 1932) as well as increasing its micropores (Budinova et al., 2006). In addition to removal of elemental constituents of biochar, cooling down process employing water could have removed dissolved organic carbon (DOC) compounds including polycyclic aromatic hydrocarbons (PAHs) (Wu et al., 2011). Removal of some biotoxic PAHs by water in TK biochar would be beneficial for its use as a soil amendment.

4.2. Ash content of biochars contributing to soil pH increase

Immediate increases in soil pH at the highest (4%) rate of FC biochar in the Khorat soil were due to high content of "quick lime" or readily soluble compounds in the ash constituents of this biochar in conjunction with low buffering capacity of the sandy soil. However, continued pH increases in both soils in the second crop period under biochar amended treatments were due in part to slow dissolution of $CaCO_3$ derived from CaO (Mengel and Kirkby, 2001), which was a major ash constituent of both biochars (expressed in elemental Ca form in Table 2a). These results are in agreement with Ulery et al. (1993), who reported that the liming effect of biochar application could be divided into two phases: an initial phase where soil pH was increased by readily soluble oxides, hydroxides, and carbonates of K and Na and a later phase associated with less soluble $CaCO_3$.

It is notable that relatively low ash contents of both TK (2.35% ash) and FC (3.85% ash) biochars were used in this study compared to other previous reports (in the range of 14–56%) (Laird et al., 2010; Smider and Singh, 2014). Both biochars increased soil pH, particularly in low buffering capacity (Khorat), soil early in the first cropping cycle (Table 7a) with some delay observed in the high buffering capacity Wahiawa soil (Table 7b). Similar low ash biochars (approximately 4%) have been reported to increase pH of low buffering capacity soils (Alburquerque et al., 2014).

Reduction processes of Fe oxides in the Khorat soil and Mn/Fe oxides in the Wahiawa soil may be an additional factor explaining pH increases during the second crop period. Higher soil pH can be obtained by reduction of Fe and Mn oxides. Localized reduction conditions can occur in microsites containing rapidly decomposing organic compounds (Haynes and Mokolobate, 2001). In this study, these organic compounds likely came from soil organic matter, sorbed biochar compounds, and new corn root exudates.

Table 6
Corn tissue Mn:Ca ratios in the Wahiawa soils as affected by different application rates of Thai traditional kiln (TK) and Flash Carbonization™ (FC) biochars in the first crop (T1) and second crop (T2) periods.

Treatment	Tissue Mn:Ca ratio‡	
	T1	T2
Wahiawa soil		
Control	38.5ab †	121a
1% TK biochar	45.7a	45b
2% TK biochar	41.4ab	46b
4% TK biochar	34.0b–d	42b
1% FC biochar	35.9a–c	34b
2% FC biochar	24.2d	25b
4% FC biochar	26.5cd	20b
p-Value	0.003	<.0001
F-test	***	***
C.V. (%)	7.05	21.59

‡ Mn (mg kg^{-1}), Ca (g kg^{-1}).
† Means within column followed by the same letter are not significantly different at $p \leq 0.05$ (Tukey's Studentized Range Test).
*** $p \leq 0.001$ (F-test).

4.3. Biochars' liming effect reducing soil al toxicity with a consequent increase in corn biomass in the coarse-textured, ultisol soil

Ultisols, in general, and the Khorat soil, in particular, are known to have potential to reduce plant growth due to their acidity and high Al concentration (Vityakon and Seripong, 1989). In the second crop, shoot and root biomass in the unamended Khorat soil were 33% and 18%, respectively, of their maximum biomass achieved in the 4% TK biochar-amended treatment. This depression of shoot and root biomass in the control treatment was caused by 24.8 mg kg^{-1} (0.28 $cmol_c$ kg^{-1}) extractable Al (Table 7a, Fig. 3b and c) equivalent to 45% Al saturation. Corn shoot yield reduction to approximately 40% of maximum yield at approximately 30% Al saturation was reported in an Ultisol soil in the Coastal Plain of North Carolina, USA (Evans and Kamprath, 1970), while 20% Al saturation was found to be the threshold for sorghum shoot yield reduction in a related Ultisol soil in Northeast Thailand. The phytotoxic Al content found in the control was likely due to the

Table 7
Soil pH and extractable elements in the Khorat and Wahiawa soils as affected by application of different rates of Thai traditional kiln (TK) and Flash Carbonization™ (FC) biochars in the first crop (T1) and second crop (T2) periods.

(a) Khorat soil

Treatment	pH		Extractable element							
			K		Ca		Mg		Al	
			(mg kg^{-1})							
	T1	T2	T1	T2	T1	T2	T1	T2	T1	T2
Control	4.74bc[1/†]	5.28b	12c	27.5	106e	102d	11b	8.9ab	24.82a[2/]	10.22ab
1% TK biochar	4.68c	5.12b	15bc	16.5	124de	105d	11b	6.3bc	16.77b	11.08a
2% TK biochar	4.72bc	5.09b	16bc	14.5	147cd	124cd	13b	4.9c	4.84cd	10.65ab
4% TK biochar	4.83bc	5.59b	30b	17.3	225b	180b	17a	5.9bc	1.23cd	6.43bc
1% FC biochar	5.25a–c	5.31b	16bc	14.4	168c	134c	11b	4.4c	6.17c	6.61b
2% FC biochar	5.59ab	5.61b	20bc	13.5	240b	194b	14ab	4.9c	0.33d	1.78cd
4% FC biochar	5.88a	6.46a	76a	36.5	349a	354a	17a	12.3a	0.15d	0.07d
p-Value	0.0015	<.0001	<.0001	0.0528	<.0001	<.0001	<.0001	<.0001	<.0001	<.0001
F-test	**	***	***	ns	***	***	***	***	***	***
C.V. (%)	6.25	3.46	22.77	44.84	6.23	5.69	10.34	18.77	29.01	22.46

(b) Wahiawa soil

Treatment	pH		K		Ca		Mg		Saturated paste Mn (mg L^{-1})	
			(mg kg^{-1})							
	T1	T2	T1	T2	T1	T2	T1	T2	T1	T2
Control	5.37	5.42c[†]	111d	146ab	562b	595b	151	155a	0.81e	1.12c
1% TK biochar	5.20	5.70bc	132cd	82b	531b	529b	135	131b	1.32de	2.38b
2% TK biochar	5.19	5.78a–c	140cd	82b	570b	546b	138	126b	1.87c	2.44b
4% TK biochar	5.20	5.87ab	254ab	171ab	649b	675ab	137	136b	3.18b	4.61a
1% FC biochar	5.45	5.72a–c	196b–d	177ab	609b	607b	138	135b	1.77cd	1.39c
2% FC biochar	5.59	5.97ab	219bc	107b	701ab	655ab	146	132b	3.06b	1.56c
4% FC biochar	5.78	6.10a	329a	261a	883a	796a	145	130b	4.65a	2.37b
p-Value	0.0386	0.0014	<.0001	0.0061	0.0005	0.0006	0.2735	0.0027	<.0001	<.0001
F-test	ns	**	***	**	***	***	ns	**	***	***
C.V. (%)	4.10	2.47	17.86	33.75	10.96	8.69	6.05	4.84	5.37	5.74

*$p \le 0.05$; **$p \le 0.01$; ***$p \le 0.001$; and ns = not significantly different (F-test).
1/ Mean comparison of pH between initial (pH 5.52) and control (first crop period) value was significant ($p \le 0.01$) (paired t-test).
2/ Mean comparison of soil Al concentration between initial (11.46 mg kg^{-1}) and control (first crop period) value was significant ($p \le 0.05$) (paired t-test).
† Means within a column followed by the same letter and those without accompanying letter are not significantly different at $p \le 0.05$ (Tukey's Studentized Range Test).

decreased pH as a consequence of the acidifying effect of basal fertilizer N, i.e., urea and ammonium. Similar pH decrease has been reported in some Ultisols receiving urea fertilizer approximately 30 days after application (Tong and Xu, 2012).

The positive liming effect of both types of biochars on corn biomass grown in the Khorat soil was clearly shown in the second crop. Reduction of soil Al concentrations by biochar application at the end of the first crop significantly improved shoot (Fig. 3b) and root (Fig. 3c) biomass of the second crop. Previous research has shown the benefit of biochar as a liming material to increase soil pH while reducing soil Al contents and Al phytotoxicity in radish (Chan et al., 2007) and tomato (Hossain et al., 2010). Besides increases in soil pH, application of organic materials, like biochar in particular, could reduce soil Al concentration (Haynes and Mokolobate, 2001), due to (i) decreasing soil exchangeable Al through adsorption reactions with solid-phase organic material, i.e., biochars — as aged biochar surfaces were negatively charged, and (ii) decreasing Al activity in soil solution through chelation with soluble organic compounds from biochars (Hue et al., 1986). In addition, it has been demonstrated that biochar with its chemically active surface can adsorb allelochemical compounds rendering them non-toxic to plants (Elmer and Pignatello, 2011; Rogovska et al., 2014; Schulz and Glaser, 2012).

4.4. Biochar affecting available Mn in a Mn-rich Oxisol: can biochar reduce Mn toxicity?

Unlike other Oxisols, the major factor that critically constrains plant growth in some Hawaiian Oxisols is Mn toxicity (Hue et al., 2001). Our results showed clearly that there was a close link between increased saturated paste soil Mn content and depression in corn growth in the unamended Wahiawa soil. To our knowledge, there are few published reports in the scientific literature that investigate biochar influence on Mn phytotoxicity through probing both soils and growing plants simultaneously, e.g. Major et al. (2010). In our study, all rates of application of both biochars showed potential alleviation of Mn toxicity and consequent improvement of corn biomass in the Mn-rich Wahiawa soil. Both biochars significantly reduced tissue Mn concentrations below the critical toxic level of 200 mg kg^{-1} in the second crop (Porter et al., 2004; Reuter and Robinson, 1997). Meanwhile, in the control treatment, tissue Mn concentration was at 408 mg kg^{-1}, which is more than double the toxic level. The positive effect of both biochars in ameliorating Mn toxicity in corn was likely due to increases in Ca availability as a consequence of reducing Mn–Ca competition for plant uptake (Hue and Mai, 2002). This can be seen in significant decreases in tissue Mn:Ca ratios (in the range of 20–46) under applications of both types of biochars relative to the control which showed Mn:Ca of 121 (Table 6). The range of Mn:Ca ratio obtained under the biochar-amended treatments is considered in the same magnitude with the norm value of 17 (dos Anjos Reis, 2002). This suggests that increases in Ca availability by biochar application could mitigate Mn phytotoxicity in the Wahiawa soil. This is supported by evidence that increased Ca uptake in watermelon led to increased plant tolerance to Mn toxicity in the same soil (Hue and Mai, 2002).

Corn biomass depression in the Wahiawa control treatment in the second crop was due to excessive Mn uptake as a consequence of elevated soil Mn concentration. This can be seen in increases in Mn concentrations in saturated soil-paste and corn tissue under control treatment. Saturated paste Mn concentration in the second crop (1.12 mg L^{-1})

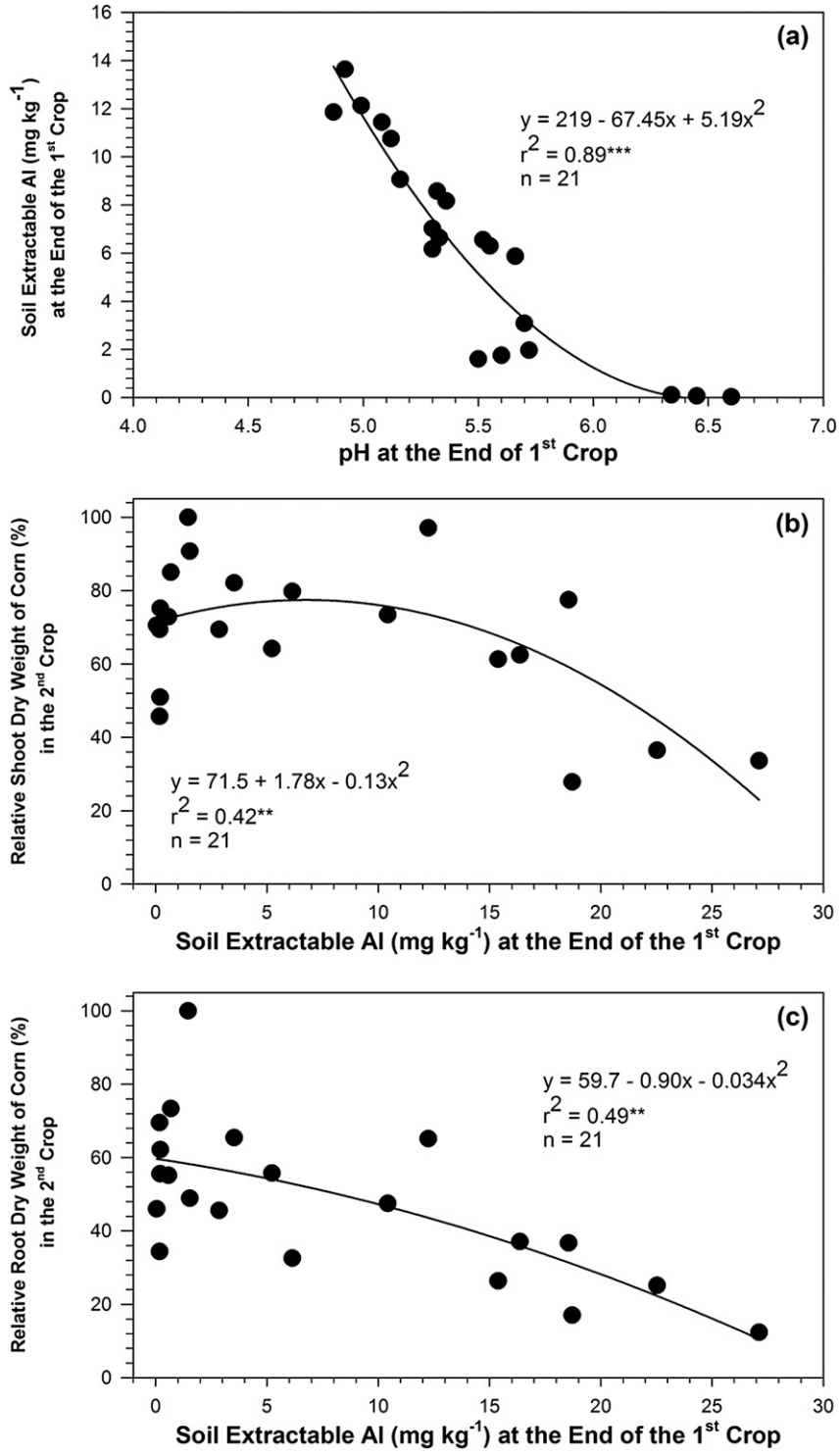


Fig. 3. Relationship between: (a) pH at the end of the first crop and soil extractable Al concentration at the end of the first crop; (b) soil extractable Al concentration at the end of the first crop and relative shoot dry weight of corn in the second crop and; (c) soil extractable Al concentration at the end of the first crop and relative root dry weight of corn in the second crop, in the Khorat soil.

was almost 1.5-fold as much as that of the first crop (0.81 mg L^{-1}) (Table 7b). In parallel, tissue Mn concentration was 2.5-fold greater in the second crop (0.281 g kg^{-1}) than in the first crop (0.134 g kg^{-1}) (Table 4). Reducing conditions in the soil resulting from microbial decomposition of some localized organic matter may have led to Mn oxide reduction with a consequent release of Mn^{2+} (Haynes and Mokolobate, 2001). This microbial decomposition process could also produce various biochemical compounds, e.g., hydroquinone, catechol, ascorbic acid, citric acid, ethylenediamine tetraacetic acid, and salicylic acid (Hue et al., 2001), which together with root exudates could further contribute dissolved Mn in soil solution (Godo and Reisenauer, 1980). Some of these compounds may also be phytotoxic in their own right which could have contributed to depressing growth through allelopathy (Iman et al., 2006).

While tissue Mn concentrations were significantly reduced by biochar treatments, Mn concentrations in the soil saturated paste extracts increased with biochar rates. All treatments had soil Mn concentration higher than 0.5 mg L^{-1}, which is the level considered toxic in the Wahiawa soil (Porter et al., 2004). Although increases in soil Mn could be attributed to both the soil and biochars, those from the biochars were likely non-significant due to its low content, <2 mg kg^{-1} reported in eucalyptus biochar by Carvalho et al. (2013), in reference to that of the Mn-rich Wahiawa soil (517 mg kg^{-1}). Therefore, increases in Mn concentrations with increasing rates of application of both biochars were more likely due to increases in soil Mn solubility from the biochar application.

Manganese solubility in soil systems is complex and determined by several factors including pH, redox potential, and the presence of a range of dissolved organic molecules. Soil Mn solubility may have been increased through dissolution and chelation mechanisms enabled by some biochar-derived dissolved organic molecules. Dissolved organic molecules, such as aliphatic organic acids, e.g., acetic, citric, and oxalic acids, tannic acid, catechol, and gallic acid, have been shown to effectively dissolve and chelate soil Mn in the Wahiawa soil (Hue et al., 2001). Recent research linked dissolution of Mn in soils to reduction reactions rendered by organic substances in aqueous extracts of various biochars including eucalyptus biochars produced at 350 and 450 °C (Graber et al., 2014). These workers have identified a whole host of organic compounds in the biochar extract and demonstrated their strong reducing capacities. Examples of these DOM compounds were sugar acids, aliphatic organic acids, polyphenols, tannins, and humic-like substances. Mn-reducing/solubilizing and chelating organic molecules were likely present in eucalyptus feedstock. Eucalyptus is known to be enriched in hydrolysable tannins (e.g., tannic acid, gallic acid, and catechol) and condensed tannins (e.g., catechin, gallocatechin, and epigallocatechin) (Martius et al., 2012). Catechols, gallic acid derivatives, and acetic acid have been shown to persist after pyrolysis up to the temperature of 600 °C (Kaal et al., 2012). Moreover, pyrolysis of eucalyptus wood could have transformed some condensed tannins to catechol. It has been found that catechin in sorghum grain (Galletti, 1991) and conifer cone scales and seeds (Stankiewicz et al., 1997) were transformed to catechol upon pyrolysis.

Not only biochar-derived dissolved organic molecules that possess reducing power, but also the presence of functional groups on biochar surfaces, e.g. O-containing acidic (carbonyl, lactonic, carboxylic, hydroxyl and phenol) and basic (chromene, ketone, and pyrone) functional groups has reducing properties (Ahmad et al., 2014). Biochar derived from weed plant (*Solanum elaeagnifolium* L.) has been shown to effectively reduce artificially added Cr(VI) to Cr(III) in soils. The reducing capacities were attributed to electron donor functional groups, such as phenolic, hydroxyl, carbonyl and amide, on the biochar surface.

In this study, the higher Mn concentrations in the soil did not translate into higher Mn uptake by the corn plants as indicated by decreased tissue Mn concentrations. Contrary to the present study, Major et al. (2010) reported that high Mn in the biochar amended soils corresponded to increases in total Mn uptake and soybean tissue concentrations. The contrary results suggest that plant response to high soil Mn and Mn uptake mechanisms is species dependent. It has been shown for Fe uptake in non-graminaceous and dicot plants that Fe must be freed from its chelating form prior to the uptake. Meanwhile, graminaceous monocots can readily take up the chelated form. However, the chelating agent must be compatible with the specific uptake mechanism, i.e., the protein transporter in the cell membrane, of the monocots in question, for example mugineic acid has been found to be a compatible chelating agent for corn (White, 2012). It is possible that the biochar induced chelated form of Mn in the Wahiawa soil was not compatible with Mn uptake in the corn. Similar mechanisms may have operated in the case of Mn. Another possible mechanism for low Mn concentration in corn despite increased soil Mn may be related to biochar-derived tannin derivatives, such as gallic and tannic acids, which are known to inhibit the activity of H^+-ATPase, an enzyme required for active uptake of Mn (Erdei et al., 1994; Marschner, 1995). From the biochar standpoint, those used in this study and in Major et al.'s study may have produced different chelating agents due to different feedstock and pyrolysis conditions (Graber et al., 2014; Sánchez et al., 2009).

Our results combined with the work of Graber et al. (2014) show that biochar plays a role in Mn chemistry, and serve as a guide for future research. These results indicate that biochar derived dissolved organic compounds affect Mn solubility, but that plant uptake may be species dependent and dependent on the chelated form of Mn.

4.5. Negative effects on corn of high temperature biochar: K luxury consumption pertaining to high ash and other possible factors

Increases in tissue K concentrations (up to 43 g kg^{-1}) over the control indicated K luxury consumption by corn plants grown in the Khorat soil amended with the highest rate of FC biochar. Excessive concentrations of K can restrict Ca and Mg uptake due to their antagonistic effects (Marschner, 1995). High K content in the FC biochar contributed to luxury K consumption adversely impacting Ca and Mg nutrition of the corn plants. This was shown by deficient levels of Ca and Mg in the corn tissue, which were considerably lower than the critical levels (5 and 1.5 g kg^{-1} for Ca and Mg, respectively) (Reuter and Robinson, 1997). Soil conditions leading to K luxury consumption were shown by increases in soil K contents (Table 7a) under the 4% FC treatment. Increasing soil K significantly decreased tissue Ca concentration (Fig. 2a and b). In addition, ratios of tissue Ca to K (approximately 0.1) and Mg to K (<0.1) significantly decreased under the 4% FC treatment (Table 5). The norm values of Ca:K and Mg:K ratios for optimal corn growth are 0.25 and 0.13, respectively (dos Anjos Reis, 2002). These pieces of evidence jointly indicated the negative effect of K luxury consumption on depressing corn biomass at the highest (4%) rate of FC biochar in the Khorat soil in both planting cycles.

In addition to K luxury consumption, depression of corn biomass under 4% FC biochar in the Khorat soil of both planting cycles may have been partially affected by phytotoxicity of PAHs in biochars produced at high temperature. Henner et al. (1999) reported that naphthalene could potentially delay seed germination and decreased growth of several plants including corn. Previous studies showed that naphthalene was a particulate PAH constituted in eucalyptus biochar (Barbosa et al., 2006). Its contents were increased with increases in pyrolysis temperature (Kloss et al., 2012), but decreased when time of pyrolysis was extended (Barbosa et al., 2006). In this study, FC biochar was produced under higher temperature and shorter pyrolysis period than TK biochar. Moreover, the cooling down process using water could have removed PAHs from TK biochar. Removal of organic carbon from biochar through water leaching was reported by Wu et al. (2011).

4.6. Biochar types and rates appropriate for soils contrasting in texture and mineralogy

Both TK and FC biochars were effective in reducing Al (in the Khorat soil) and Mn (in the Wahiawa soil) toxicities with overall greater benefits to corn growth derived from the TK biochar. This is contrary to our hypothesis that the high temperature biochar would benefit plant growth more than the low temperature biochar, due to its lower VM content and higher ash content. The high ash content, resulting from high production temperature, in the FC biochar produced antagonistic effects on plant nutrition due to excessive K content. In addition, there was a possible phytotoxicity effect rendered by some specific PAHs generated through high production temperature of FC biochar. Results from the greenhouse experiments indicate that the TK biochar made in a traditional manner provides more benefit to soil properties and plant growth than the FC biochar.

For the appropriate application rate, 1% TK biochar is recommended for coarse textured soil, while 2% of the same biochar is recommended

for the fine textured soil. The low (1%) rate of TK biochar is appropriate for the coarse textured soil because higher rate of the same biochar did not produce significantly higher corn biomass in the second crop period due to low buffering capacity of this soil. This rate could improve soil fertility, notably soil pH increases, tissue nutrient balance improvement, reduction of Al phytotoxicity and possible increased adsorption capacity to retain some allelochemicals and toxic elements. For fine textured soil, higher (2%) rate of TK biochar was required to compensate for the higher buffering capacity of this soil compared to coarse textured soil. In addition, 2% TK biochar produced the highest corn biomass and showed the potential to reduce Mn phytotoxicity.

5. Conclusions

Our results showed that biochar production techniques had significant effects on biochar properties and subsequent effects on soil properties and plant growth. Contrary to our expectations, the ash enriched high temperature biochar produced by the Flash Carbonization™ technique was less effective in improving soil properties and plant growth than that produced under the lower temperature traditional kiln technique. In contrast to our hypothesis, high ash content was a major factor responsible for deleterious effects on plant growth. Excessive K in the ash produced K antagonism with other nutrient cations (Ca and Mg). In addition, it is possible that high temperature biochar-derived PAHs caused deleterious effects on plant growth. Our results also showed clearly that the effect of these biochars varied in soils contrasting in texture and mineralogy. As expected, biochar effects, both positive (liming) and negative (cation antagonism), were more readily observed in the less buffered coarse-textured soil. We showed that biochar effects were not short-lived, but persisted for at least 82 days in both soils. We provide further evidence that liming is one of the more important beneficial aspects of biochar. Biochar application effectively reduced the negative effects of Al toxicity in the sandy Ultisol and may have been responsible for Mn detoxification due to retention of Mn on DOM molecules through chelation in the fine-textured Oxisol. Overall, low-temperature biochar was shown to be more effective in improving soil fertility of both soils than its high temperature counterpart. The appropriate rate of the low temperature biochar was found to be 1–2% (w/w), the higher rate being required in the finer textured soil. While further laboratory investigations will be necessary to elucidate the exact mechanisms explaining biochar-mediated Mn chemistry and phytodetoxification in Mn-rich soils observed in some biochars, our data provide evidence that biochar is a promising material to counter the deleterious effects of Mn phytotoxicity in acid soils.

Acknowledgments

This research was funded by the Royal Golden Jubilee Ph.D. Program under the Thailand Research Fund (TRF) (PHD/0222/2549). The research was funded in part by the Government of Thailand's Grants to Khon Kaen University (KKU) (FY 2010 id 532203 and 2011 is 542203-030103), TRF Basic Research Programs (2008 and 2011) (project no. DBG5180007, 2008 and DBG5480001, 2011), the affiliate scholar program under the Memorandum of Understanding between the East–West Center (EWC), the University of Hawaii at Manoa (UHM), and the TRF, and the Water, Energy, and Soil Sustainability (WESS) Program funded by the Sustainability Initiative (Chancellor's Office, University of Hawaii at Manoa). Preparation of the manuscript was under the 2013 KKU Faculty of Agriculture International Publication Promotion Program. The eucalyptus wood and biochar used in this study generously donated by the Mancha Khiri Plantation Forest Station are gratefully acknowledged. The late Goro Uehara (University of Hawaii) and the late Kuan M. Goh (Lincoln University, New Zealand) contributed greatly to this study. This paper is dedicated to the memories of our professors and friends.

References

Abdullah, H., Mediaswanti, K.A., Wu, H., 2010. Biochar as a fuel: 2. Significant differences in fuel quality and ash properties of biochars from various biomass components of mallee trees. Energy Fuels 24, 1972–1979.
Ahmad, M., Rajapaksha, A.U., Lim, J.E., Zhang, M., Bolan, N., Mohan, D., Vithanage, M., Lee, S.S., Ok, Y.S., 2014. Biochar as a sorbent for contaminant management in soil and water: a review. Chemosphere 99, 19–33.
Alburquerque, J.A., Calero, J.M., Barrón, V., Torrent, J., del Campillo, M.C., Gallardo, A., Villar, R., 2014. Effects of biochars produced from different feedstocks on soil properties and sunflower growth. J. Plant Nutr. Soil Sci. 177, 16–25.
American Standard of Testing Material, 2001. Standard Test Method for Chemical Analysis of Wood Charcoal ASTM D 1762-84.
Antal, M.J., 2004. Process for flash carbonization of biomass. United States Patent. Patent Storm, September 14, Number 152276, USA.
Antal, M.J., Gronli, M., 2003. The art, science, and technology of charcoal production. Ind. Eng. Chem. Res. 42, 1619–1640.
Bangham, D.H., Fakhoury, N., Mohamed, A.F., 1932. The swelling of charcoal. Part II. Some factors controlling the expansion caused by water, benzene and pyridine vapours. Proc. R. Soc. Lond. A 138, 162–183.
Barbosa, J.M.d.S., Re´-Poppi, N., Santiago-Silva, M., 2006. Polycyclic aromatic hydrocarbons from wood pyrolysis in charcoal production furnaces. Environ. Res. 101, 304–311.
Bertsch, P.M., Bloom, P.R., 1996. Aluminum. In: Sparks, D.L. (Ed.), Methods of Soil Analysis. Part 3. Chemical MethodsSoil Science Society of America Book Series No. 5. Soil Science Society of America, Wisconsin, pp. 517–550.
Bourke, J., Manley-Harris, M., Fushimi, C., Dowaki, K., Nunoura, T., Antal, M.J., 2007. Do all carbonized charcoals have the same chemical structure? 2. A model of the chemical structure of carbonized charcoal. Ind. Eng. Chem. Res. 46, 5954–5967.
Budinova, T., Ekinci, E., Yardim, F., Grimm, A., Björnbom, E., Minkova, V., Goranova, M., 2006. Characterization and application of activated carbon produced by H3PO4 and water vapor activation. Fuel Process. Technol. 87, 899–905.
Carvalho, M.T.d.M., Madari, B.E., Bastiaans, L., Oort, P.A.J.v., Heinemann, A.B., Silva, M.A.S.d., Maia, A.d.H.N., Meinke, H., 2013. Biochar improves fertility of a clay soil in the Brazilian Savannah: short term effects and impact on rice yield. J. Agric. Rural. Dev. Trop. Subtrop. 114, 101–107.
Chan, K.Y., van Zwieten, L., Meszaros, I., Downie, A., Joseph, S., 2007. Agronomic values of greenwaste biochar as a soil amendment. Aust. J. Soil Res. 45, 629–634.
Chan, K.Y., Zwieten, L.V., Meszaros, I., Downie, A., Joseph, S., 2008. Using poultry litter biochars as soil amendments. Aust. J. Soil Res. 46, 437–444.
Deenik, J.L., McClellan, T., Uehara, G., Antal Jr., M.J., Sonia, C., 2010. Charcoal volatile matter content influences plant growth and soil nitrogen transformations. Soil Sci. Soc. Am. J. 74, 1259–1270.
Deenik, J.L., Diarra, A., Uehara, G., Campbell, S., Sumiyoshi, Y., Antal Jr., M.J., 2011. Charcoal ash and volatile matter effects on soil properties and plant growth in an acid Ultisol. Soil Sci. 176, 336–345.
dos Anjos Reis, R., 2002. DRIS norms universality in the corn crop. Commun. Soil Sci. Plant Anal. 33, 711–735.
Elmer, W.H., Pignatello, J.J., 2011. Effect of biochar amendments on mycorrhizal associations and fusarium crown and root rot of asparagus in replant soils. Plant Dis. 95, 960–966.
Erdei, L., Szabó-Nagy, A., Laszlavik, M., 1994. Effects of tannin and phenolics on the H^+-ATPase activity in plant plasma membrane. J. Plant Physiol. 144, 49–52.
Evans, C.E., Kamprath, E.J., 1970. Lime response as related to percent Al saturation, solution Al, and organic matter content. Soil Sci. Soc. Am. J. 34, 893–896.
Galletti, G.C., 1991. PY–GC–ion trap detection of sorghum grain polyphenols (*syn*. vegetation tannins): preliminary results. Prepr. Pap. Am. Chem. Soc. Div. Fuel Chem. 36, 691–697.
Gaskin, J., Steiner, C., Harris, K., Das, K., Bibens, B., 2008. Effect of low-temperature pyrolysis conditions on biochar for agricultural use. Trans. ASABE 51, 2061–2069.
Gentry, C.E., Willis, R.B., 1988. Improved method for automated determination of ammonium in soil extracts. Commun. Soil Sci. Plant Anal. 19, 721–737.
Gillman, G.P., 2007. An analytical tool for understanding the properties and behaviour of variable charge soils. Aust. J. Soil Res. 45, 83–90.
Glaser, B., Lehmann, J., Zech, W., 2002. Ameliorating physical and chemical properties of highly weathered soils in the tropics with charcoal — a review. Biol. Fertil. Soils 35, 1719–1730.
Godo, G.H., Reisenauer, H.M., 1980. Plant effects on soil manganese availability. Soil Sci. Soc. Am. J. 44, 993–995.
Graber, E.R., Tsechansky, L., Lew, B., Cohen, E., 2014. Reducing capacity of water extracts of biochars and their solubilization of soil Mn and Fe. Eur. J. Soil Sci. 65, 162–172.
Hansson, K.-M., Samuelsson, J., Tullin, C., Åmand, L.-E., 2004. Formation of HNCO, HCN, and NH_3 from the pyrolysis of bark and nitrogen-containing model compounds. Combust. Flame 137, 265–277.
Haynes, R.J., Mokolobate, M.S., 2001. Amelioration of Al toxicity and P deficiency in acid soils by additions of organic residues: a critical review of the phenomenon and the mechanisms involved. Nutr. Cycl. Agroecosyst. 59, 47–63.
Henner, P., Schiavon, M., Druelle, V., Lichtfouse, E., 1999. Phytotoxicity of ancient gaswork soils. Effect of polycyclic aromatic hydrocarbons (PAHs) on plant germination. Org. Geochem. 30, 963–969.
Hossain, M.K., Strezov, V., Chan, K.Y., Nelson, P.F., 2010. Agronomic properties of wastewater sludge biochar and bioavailability of metals in production of cherry tomato (*Lycopersicon esculentum*). Chemosphere 78, 1167–1171.
Hue, N.V., Mai, Y., 2002. Manganese toxicity in watermelon as affected by lime and compost amended to a Hawaiian acid oxisol. HortSci. 37, 656–661.
Hue, N.V., Craddock, G.R., Adams, F., 1986. Effect of organic acids on aluminum toxicity in subsoils. Soil Sci. Soc. Am. J. 50, 28–34.

Hue, N.V., Vega, S., Silva, J.A., 2001. Manganese toxicity in a Hawaiian Oxisol affected by soil pH and organic amendments. Soil Sci. Soc. Am. J. 65, 153–160.
Ibrahim, H.M., Al-Wabel, M.I., Usman, A.R.A., Al-Omran, A., 2013. Effect of *Conocarpus* biochar application on the hydraulic properties of a sandy loam soil. Soil Sci. 178, 165–173.
Iman, A., Wahab, Z., Rastan, S.O.S., Halim, M.R.A., 2006. Allelopathic effect of sweet corn and vegetable soybean extracts at two growth stages on germination and seedling growth of corn and soybean varieties. J. Agron. 5, 62–68.
Jones, J.B., 2001. Laboratory Guide for Conducting Soil Tests and Plant Analysis. CRC Press, Boca Raton.
Kaal, J., Nierop, K.G.J., Kraal, P., Preston, C.M., 2012. A first step towards identification of tannin-derived black carbon: conventional pyrolysis (Py–GC–MS) and thermally assisted hydrolysis and methylation (THM–GC–MS) of charred condensed tannins. Org. Geochem. 47, 99–108.
Kamprath, E.J., 1971. Potential detrimental effects from liming highly weathered soils to neutrality. Soil Crop Sci. Soc. Fla. Proc. 31, 200–203.
Kloss, S., Zehetner, F., Dellantonio, A., Hamid, R., Ottner, F., Liedtke, V., Schwanninger, M., Gerzabek, M.H., Soja, G., 2012. Characterization of slow pyrolysis biochars: effects of feedstocks and pyrolysis temperature on biochar properties. J. Environ. Qual. 41, 990–1000.
Kolb, S.E., Fermanich, K.J., Dornbush, M.E., 2009. Effect of charcoal quantity on microbial biomass and activity in temperate soils. Soil Sci. Soc. Am. J. 73, 1173–1181.
Laird, D.A., Fleming, P., Davis, D.D., Horton, R., Wang, B., Karlen, D.L., 2010. Impact of biochar amendments on the quality of a typical Midwestern agricultural soil. Geoderma 158, 443–449.
Lathwell, D.J., Grove, T.L., 1986. Soil–plant relationships in the tropics. Annu. Rev. Ecol. Syst. 17, 1–16.
Lau, A.C., Furlong, D.N., Healy, T.W., Grieser, F., 1986. The electrokinetic properties of carbon black and graphitized carbon black aqueous colloids. Colloids Surf. 18, 93–104.
Lehmann, J., Rillig, M.C., Thies, J., Masiello, C.A., Hockaday, W.C., Crowley, D., 2011. Biochar effects on soil biota — a review. Soil Biol. Biochem. 43, 1812–1836.
Major, J., Rondon, M., Molina, D., Riha, S.J., Lehmann, J., 2010. Maize yield and nutrition during 4 years after biochar application to a Colombian savanna Oxisol. Plant Soil 333, 117–128.
Makoto, K., Choi, D., Hashidoko, Y., Koike, T., 2011. The growth of *Larix gmelinii* seedlings as affected by charcoal produced at two different temperatures. Biol. Fertil. Soils 47, 467–472.
Marschner, H., 1995. Mineral Nutrition of Higher Plants. Academic Press, London.
Martius, S.v., Hammer, K.A., Locher, C., 2012. Chemical characteristics and antimicrobial effects of some *Eucalyptus* kinos. J. Ethnopharmacol. 144, 293–299.
Masiello, C.A., 2004. New directions in black carbon organic geochemistry. Mar. Chem. 92, 201–213.
Mengel, K., Kirkby, E.A., 2001. Principles of Plant Nutrition, 5th edition. Kluwer Academic Publishers, Dordrecht.
Mukherjee, A., Zimmerman, A.R., Harris, W., 2011. Surface chemistry variations among a series of laboratory-produced biochars. Geoderma 163, 247–255.
Mulvaney, R.L., 1996. Nitrogen — inorganic forms. In: Spark, D.L. (Ed.), Methods of Soil Analysis. Part 3. Chemical MethodsSSSA Book Ser. 5. SSSA, Madison, WI, pp. 1123–1184.
Naidu, R., Kookana, R.S., Sumner, M.E., Harter, R.D., Tiller, K.G., 1997. Cadmium sorption and transport in variable charge soils: a review. J. Environ. Qual. 26, 602–617.
Pansu, M., Gautheyrou, J., 2006. Handbook of Soil Analysis: Mineralogical, Organic and Inorganic Methods. Springer-Verlag, Heidelberg.
Porter, G., Locke, J.B., Hue, N.V., Strand, D., 2004. Manganese solubility and phytotoxicity affected by soil moisture/O_2 levels and green manure additions. Commun. Soil Sci. Plant Anal. 35, 99–116.
Rajkovich, S., Enders, A., Hanley, K., Hyland, C., Zimmerman, A.R., Lehmann, J., 2012. Corn growth and nitrogen nutrition after additions of biochars with varying properties to a temperate soil. Biol. Fertil. Soils 48, 271–284.
Reuter, D.J., Robinson, J.B., 1997. Plant Analysis: An Interpretation Manual. Inkata Press, Melbourne.
Rogovska, N., Laird, D.A., Rathke, S.J., Karlen, D.L., 2014. Biochar impact on Midwestern Mollisols and maize nutrient availability. Geoderma 230–231, 340–347.
Sanchez, P.A., Logan, T.J., 1992. Myths and science about the chemistry and fertility of soils in tropics. In: Lal, R., Sanchez, P.A. (Eds.), Myths and Science of Soils of the TropicsSSSA Special Publication No. 29. SSSA Inc. and ASA Inc., Madison, Wisconsin, pp. 35–46.
Sánchez, M.E., Lindao, E., Margaleff, D., Martínez, O., Morán, A., 2009. Pyrolysis of agricultural residues from rape and sunflowers: production and characterization of bio-fuels and biochar soil management. J. Anal. Appl. Pyrol. 85, 142–144.
Schulz, H., Glaser, B., 2012. Effects of biochar compared to organic and inorganic fertilizers on soil quality and plant growth in a greenhouse experiment. J. Plant Nutr. Soil Sci. 175, 410–422.
Singh, B., Singh, B., Cowie, A., 2010. Characterisation and evaluation of biochars for their application as soil amendment. Aust. J. Soil Res. 48, 516–525.
Smider, B., Singh, B., 2014. Agronomic performance of a high ash biochar in two contrasting soils. Agric. Ecosyst. Environ. 191, 99–107.
Solar, J.M., Leon y Leon, C.A., Osseo-Asare, K., Radovic, L.R., 1990. On the importance of the electrokinetic properties of carbons for their use as catalyst supports. Carbon 28, 369–375.
Sollins, P., Robertson, G.P., Uehara, G., 1988. Nutrient mobility in variable- and permanent-charge soils. Biogeochemistry 6, 181–199.
Spokas, K.A., 2010. Review of the stability of biochar in soils: predictability of O:C molar ratios. Carbon Manage. 1, 289–303.
Spokas, K.A., Novak, J.M., Stewart, C.E., Cantrell, K.B., Uchimiya, M., DuSaire, M.G., Ro, K.S., 2011. Qualitative analysis of volatile organic compounds on biochar. Chemosphere 85, 869–882.
Stankiewicz, B.A., Mastalerz, M., Kruge, M.A., Van Bergen, P.F., Sadowska, A., 1997. A comparative study of modern and fossil cone scales and seeds of conifers: a geochemical approach. New Phytol. 135, 375–393.
Tong, D., Xu, R., 2012. Effects of urea and $(NH_4)_2SO_4$ on nitrification and acidification of Ultisols from Southern China. J. Environ. Sci. 24, 682–689.
Uehara, G., Gillman, G., 1981. The mineralogy, chemistry, and physics of tropical soils with variable charge clays. Westview Press, Boulder.
Ulery, A.L., Graham, R.C., Amrhein, C., 1993. Wood-ash composition and soil pH following intense burning. Soil Sci. 156, 358–364.
Vityakon, P., Seripong, S., 1989. Effects of soil acidity and its amendments (lime and magnesium applications) on sorghum in an Ultisol of Northeast Thailand. The 27th Academic Conference of Kasetsart University: Research Reports in Plant Science, Kasetsart University, Bangkok, Thailand, pp. 81–91 (in Thai with English abstract).
White, P.J., 2012. Ion uptake mechanisms of individual cells and roots: short-distance transport, In: Marschner, P. (Ed.), Marschner's Mineral Nutrition of Higher Plants, Third Edition Academic Press, San Diego, pp. 7–47.
Wu, H., Yip, K., Kong, Z., Li, C.-Z., Liu, D., Yu, Y., Gao, X., 2011. Removal and recycling of inherent inorganic nutrient species in Mallee biomass and derived biochars by water leaching. Ind. Eng. Chem. Res. 50, 12143–12151.
Yeboah, E., Ofori, P., Quansah, G.W., Dugan, E., Sohi, S.P., 2009. Improving soil productivity through biochar amendments to soils. Afr. J. Environ. Sci. Technol. 3, 034–041.
Yuan, J.-H., Xu, R.-K., Zhang, H., 2011. The forms of alkalis in the biochar produced from crop residues at different temperatures. Bioresour. Technol. 102, 3488–3497.

PLOS ONE

RESEARCH ARTICLE

Construction of an SSR and RAD-Marker Based Molecular Linkage Map of *Vigna vexillata* (L.) A. Rich

Rusama Marubodee[1☯], Eri Ogiso-Tanaka[3☯], Takehisa Isemura[3☯], Sompong Chankaew[2], Akito Kaga[3], Ken Naito[3], Hiroshi Ehara[1], Norihiko Tomooka[3]*

1 Graduate School of Bioresources, Mie University, 1577 Kurimamachiya-cho, Tsu, Mie, 514–0102, Japan, **2** Department of Plant Science and Agricultural Resources, Faculty of Agriculture, Khon Kaen University, Khon Kaen, 40002, Thailand, **3** Genetic Resources Center, National Institute of Agrobiological Sciences, Kannondai 2-1-2, Tsukuba, Ibaraki, 305–8602, Japan

☯ These authors contributed equally to this work.
* tomooka@affrc.go.jp

CrossMark
click for updates

OPEN ACCESS

Citation: Marubodee R, Ogiso-Tanaka E, Isemura T, Chankaew S, Kaga A, Naito K, et al. (2015) Construction of an SSR and RAD-Marker Based Molecular Linkage Map of *Vigna vexillata* (L.) A. Rich. PLoS ONE 10(9): e0138942. doi:10.1371/journal.pone.0138942

Editor: Xianlong Zhang, National Key Laboratory of Crop Genetic Improvement, CHINA

Received: May 19, 2015

Accepted: September 4, 2015

Published: September 23, 2015

Copyright: © 2015 Marubodee et al. This is an open access article distributed under the terms of the Creative Commons Attribution License, which permits unrestricted use, distribution, and reproduction in any medium, provided the original author and source are credited.

Data Availability Statement: All relevant data are within the paper and its Supporting Information files.

Funding: Ph.D. scholarship program of Monbukagakusho (MEXT), Japan to RM, Genebank Project of the National Institute of Agrobiological Sciences (NIAS), Japna to NT, study design, data collection and analysis, publication, preparation of the manuscript.

Competing Interests: The authors have declared that no competing interests exist.

Abstract

Vigna vexillata (L.) A. Rich. (tuber cowpea) is an underutilized crop for consuming its tuber and mature seeds. Wild form of *V*. *vexillata* is a pan-tropical perennial herbaceous plant which has been used by local people as a food. Wild *V*. *vexillata* has also been considered as useful gene(s) source for *V*. *unguiculata* (cowpea), since it was reported to have various resistance gene(s) for insects and diseases of cowpea. To exploit the potential of *V*. *vexillata*, an SSR-based linkage map of *V*. *vexillata* was developed. A total of 874 SSR markers successfully amplified single DNA fragment in *V*. *vexillata* among 1,336 SSR markers developed from *Vigna angularis* (azuki bean), *V*. *unguiculata* and *Phaseolus vulgaris* (common bean). An F_2 population of 300 plants derived from a cross between salt resistant (V1) and susceptible (V5) accessions was used for mapping. A genetic linkage map was constructed using 82 polymorphic SSR markers loci, which could be assigned to 11 linkage groups spanning 511.5 cM in length with a mean distance of 7.2 cM between adjacent markers. To develop higher density molecular linkage map and to confirm SSR markers position in a linkage map, RAD markers were developed and a combined SSR and RAD markers linkage map of *V*. *vexillata* was constructed. A total of 559 (84 SSR and 475 RAD) markers loci could be assigned to 11 linkage groups spanning 973.9 cM in length with a mean distance of 1.8 cM between adjacent markers. Linkage and genetic position of all SSR markers in an SSR linkage map were confirmed. When an SSR genetic linkage map of *V*. *vexillata* was compared with those of *V*. *radiata* and *V*. *unguiculata*, it was suggested that the structure of *V*. *vexillata* chromosome was considerably differentiated. This map is the first SSR and RAD marker-based *V*. *vexillata* linkage map which can be used for the mapping of useful traits.

Introduction

Vigna vexillata (L.) A. Rich. is a perennial herb belonging to the genus *Vigna* and considered to be closely related to cowpea (*Vigna unguiculata* (L.) Walp.), the most important food legume in Africa [1]. A domesticated form of *V*. *vexillata*, which has large non-dormant seeds and non-shattering pods named "tuber cowpea", was found cultivated for their flesh tubers and mature seeds in Bali and Timor, Indonesia [2]. Another cultivated form *V*. *vexillata* var. *macrosperma* was described from the specimen from Costa Rica [3]. The protein content of tuberous roots of *V*. *vexillata* is about three times higher (15%) than that of potato and about six times higher than that of cassava [4]. The tuberous roots of wild *V*. *vexillata* have been eaten like sweet potato by local people in Ethiopia and Sudan [5], in Himalayas and in the hills of eastern and northeastern India at altitude between 1,200 and 1,500m [6,7] and in tropical and subtropical Australia [8]. The wild plant has been used also as forage or cover crop in several African countries [9,10] and in Australia [11].

The wild *V*. *vexillata* distributed from Africa, Asia, Australia to Central and South America. Due to its worldwide distribution, *V*. *vexillata* shows a great morphological variation and several botanical varieties are recognized [3,12–14]. Wild *V*. *vexillata* is considered to be an important gene(s) source in cowpea breeding [15], because some of its accessions are highly resistant to the cowpea weevil [16], pod sucking bugs, flower thrips, *Maruca vitrata* (Fabricius) [17] and *Striga gesnerioides* (Scrophulariaceae) [18], powdery mildew [19] and cowpea mottle carmovirus [1,20,21]. In addition, it shows high levels of resistances to various environmental stresses, such as to prolonged water logging [11], to lateritic acid and aluminous soils [6], to infertile sandy loams to fertile heavy-textured clays and to alkaline cracking clay soil [8,22].

Genetic mapping is a powerful approach to understand the function of genes in a variety of biological processes [23]. Discovering genes that control morphological and physiological phenotypes is critical for understanding the mechanism of adaptive evolution and for plant breeding [24]. The SSR (simple sequence repeat) markers have particular advantages for characterization and mapping of gene(s) because of their high reproducibility, co-dominant inheritance, relative abundance, high polymorphism, and ease of genotyping [25]. The SNP (single nucleotide polymorphisms) markers have been developed based on genome sequence information and have been used for mapping gene(s). Among several methods of developing SNP markers, SNP discovery using sequenced RAD (Restriction site Associated DNA) markers have advantages for non-model organisms without prior reference genome sequence information [26,27]. By using the high-throughput sequencing of DNA fragments flanking the restriction sites (RAD tags), a huge number of SNPs could be identified as co-dominant markers efficiently.

To date, several SSR-based linkage maps of *Vigna* crops, including azuki bean (*V*. *angularis* (Willd.) Ohwi & H. Ohashi: [28], [29], [30]), black gram (*V*. *mungo* (L.) Hepper: [31]), mungbean (*V*. *radiata* (L.) R. Wilczek: [32]), rice bean (*V*. *umbellata* (Thunb.) Ohwi & H. Ohashi: [33]) and yardlong bean (*V*. *unguiculata*: [34]) were reported. Based on the comparative genome mapping study using the common SSR markers, it was revealed that all the four *Vigna* crops belonging to the subgenus *Ceratotropis*, i. e., azuki bean, black gram, mungbean and rice bean have highly conserved genome structures, and therefore the QTLs of domestication related traits among these 4 *Ceratotropis* crops could successfully be compared [35].

Recently, two sequencing-based linkage maps of azuki bean and mungbean [36,37]) were reported. However, there are no reports of the linkage map of *V*. *vexillata* consist of the 11 linkage groups which correspond to the number of chromosomes of this promising crops for the future [1,35].

Hence, the objectives of this study were to construct linkage map of *V*. *vexillata* (1) using SSR markers developed from related *Vigna* and *Phaseolus* crops, (2) using RAD markers developed by *de novo* RAD-sequencing and (3) to compare constructed linkage map with those of two most important *Vigna* crops, *V*. *radiata* and *V*. *unguiculata*.

Materials and Methods

Plant materials

An F_2 mapping population was developed from a cross between wild *V*. *vexillata* accession V1 (from USDA, PI 406383, duplicate conserved as JP202334 in the NIAS genebank, National Institute of Agrobiological Sciences, Japan) and V5 (from the Botanic Garden, Meise, NI 936, conserved as JP235869). V1 is a salt tolerant accession collected from Paramaribo, Suriname while V5 is a salt sensitive accession collected at a site 35km E of Santa Marta, Columbia. The V1 was used as a male parent and V5 was a female parent in the cross to produced F_1 seeds. The F_1 plant was self-pollinated to produce 300 F_2 plants which were grown in a greenhouse of NIAS from May 2013.

DNA extraction

Total genomic DNA of the parents and F_2 plants were extracted from fresh leaf tissue using the CTAB method [38] with a slight modification. The DNA was adjusted to 5 ng/μl for SSR marker analysis by comparing with known concentrations of standard λ–DNA on 1.5% agarose gel.

SSR marker analysis

A total of 1336 SSR markers consisting of 329 SSR markers of azuki bean [39], 480 EST-SSR markers of azuki bean [40], 487 SSR markers of cowpea [34,41], and 40 SSR markers of common bean [42–45] were screened (Table 1, S1 Table). For azuki bean SSR, common bean SSR, cowpea SSR (VM primers; Li et al. [41]), each PCR reaction mixture solution was prepared to a volume of 5 μL containing 5 ng DNA, 1x QIAGEN Multiplex PCR Master Mix and 5 pmol of forward and reverse primers. The 5'-end of the reverse primer was fluorescent labeled with one of the four following fluorescent dyes: 6-FAM (blue), VIC (green), NED (yellow) and PET (red) (Applied Biosystems). For azuki bean EST and cowpea SSR (cp primers; Kongjaimun et al. [34]), each PCR reaction mixture solution was prepared to a volume of 5 μL containing 5 ng DNA, 1x QIAGEN Multiplex PCR Master Mix, 1x Q-solution, 2 pmol of forward primer and 20 pmol of reverse primer. The 5'-end of the forward primer was fluorescent labeled with one of the three following fluorescent dyes: FAM (blue), HEX (green) and NED (yellow) (Applied Biosystems). PCR reactions were performed in a GeneAmp PCR System 9700 (Applied Biosystems) The PCR thermal cycling was programmed as follows: 95°C for 15 mins follow by 40 cycles of 94°C for 30 s, 55°C for 90 s, 72°C for 60 s, and a final cycle at 72°C for 10 mins. For azuki bean SSR, common bean SSR, cowpea SSR (VM primers; Li et al. [41]), 1 μL of ten times diluted PCR product was mixed with 8.5 μL of Hi-Di formamide and 0.125 μL of Gene Scan 500 LIZ size standard (Applied Biosystems). For azuki bean EST and cowpea SSR (cp primers; Kongjaimun et al. [34]), 1 μL of five times diluted PCR product was mixed with 8.5 μL of Hi-Di formamide and 0.125 μL of Gene Scan 500 ROX size standard (Applied Biosystems). The mixer was denatured at 95°C for 5 mins and run on an ABI Prism 3100 or 3130xl Genetic Analyzer (Applied Biosystems). Allele size for the highest stutter peak with the height ranging between 500 and 10,000 RFU was recorded and used to create bins for automatic assignment of genotypes. The genotyping was conducted by the GeneMapper 3.0 software (Applied Biosystems) with default settings. After marker screening, 6 or 7 primers with

Table 1. Summary of amplification of SSR and EST-SSR markers from three legumes in *Vigna vexillata* and polymorphic rate between parents V1 and V5.

SSR sources	Marker type	Screened	Amplified (%)[b]	Polymorphic (%)[c]
Azuki bean	SSR[a]	329	257 (78.1)	28 (8.5)
Azuki bean	EST-SSR	480	305 (63.5)	19 (4.0)
Cowpea	SSR	487	273 (56.1)	35 (7.2)
Common bean	SSR	40	39 (97.5)	1 (2.5)
Total		1,336	874 (65.4)	83 (6.2)

[a] One STS marker is included.

[b] (No. of SSR and EST-SSR primer pairs amplified/ No. of SSR and EST-SSR primer pairs screened)*100

[c] (No. of SSR and EST-SSR primer pairs polymorphic/ No. of SSR and EST-SSR primer pairs screened)*100.

doi:10.1371/journal.pone.0138942.t001

different labels and product sizes were put into a single PCR reaction mixture and amplified as a multiplex PCR using the same procedures described above.

SSR linkage map construction and comparison with related species

An SSR genetic linkage map was constructed with JoinMap ver. 4.0 [46]. The calculation was set with a minimum logarithm of the odds (LOD) of 4.0 and a maximum recombination frequency (*r*) of 0.25. Kosambi mapping function [47] was used to calculate the distance between SSR loci. For each marker, chi-square analysis was calculated for goodness of fit to a 1:1 segregation ratio of genotypic classes at P = 0.05, 0.01, and 0.001. Markers were assigned to an LG based on recombination frequencies and LOD values. The recombination frequencies were converted into map distances (cM) using the mapping function of Kosambi [47]. Double crossovers between adjacent loci were confirmed manually. The numbering of linkage groups was named following mungbean linkage map [32]. Based on common SSR markers, the structure of the linkage maps among mungbean (*V*. *radiata*), yardlong bean (*V*. *unguiculata*) and *V*. *vexillata* were compared. In case more than 2 SSR markers of a mungbean linkage group (e.g., LG1) were mapped with several SSR markers of another mungbean linkage group (e.g., LG5), it is estimated that a translocation is occurred.

RAD-seq analysis

RAD-seq analysis was performed based on the protocol of Matsumura et al. with minor modifications [48].

Preparation of adaptors

Adapter-1 for BamHI-digested DNA site was prepared by annealing the two synthesized oligonucleotides 5'-biotin-GTACAGGTTCAGAGTTCTACAGTCCGACGATCXXXXXX-3′ and 5′-GATCXXXXXXGATCGTCGGACTGTAGAACTCTGAACCTGT-3 (XXXXXX correspond to the variable index sequences to identify the individual DNA sample). Adapter 2 for NlaIII-digested DNA site was prepared by annealing of the two complementary oligonucleotides 5′-amino-CAAGCAGAAGACGGCATACGACATG-3′ and 5′-TCGTATGCCGTCTTC TGCTTG-3′.

Library construction and RAD sequencing

DNA library for RAD sequencing was constructed as follows. Each genomic DNA samples (100–300 ng) of parents and 286 F_2 individuals were simultaneously digested with BamHI-HF

and NlaIII and purified. Adaptor-1 and adaptor-2 were ligated to the digested DNA samples and purified. Adaptors ligated biotinylated DNA samples were collected using streptavidin coated magnetic beads (Dynabeads M270, Dynal). Adaptor ligated DNA on the beads was amplified by PCR using Phusion High-Fidelity DNA polymerase (Thermo Fisher Scientific) and the adapter primers. Size of the PCR amplified fragments were checked by electrophoresis in agarose gel. The 96 purified PCR products were pooled and sequenced using the Illumina HiSeq2000 system. The sequencing primer was 5′-CGACAGGTTCAGAGTTCTACAG TCCGACGATC.

Extraction of RAD-tag and bi-allelic RAD-marker detection

Extraction of RAD-tag sequence and bi-allelic RAD-marker detection were conducted using a software, Stacks ver. 1.12 [49]. Sequence reads of low quality and sequence reads with ambiguous six-base variable index sequences were discarded and 85 bp RAD-tag sequence reads were prepared. The RAD-tag sequence reads were classified into those of 2 parental accessions and F_2 individuals based on the six-base variable index sequences. RAD-tags with the sequence reads of less than 2 sequence mismatch were grouped as a stack. Stacks of each parent with less than 3 sequence mismatch were estimated as the stacks derived from a homologous locus. A list of RAD-tag sequences and their count was constructed for each sample. For the genotyping of F_2 individuals, stacks which have more than 20 RAD-tags (minimum stack depth of 20) were used as potential RAD-markers.

Linkage map construction using SSR and RAD-markers

Linkage group construction was conducted by a software R/qtl ver. 1.36.6 [50]. Potential RAD-markers which have genotype data of less than 100 F_2 individuals, which show identical F_2 individuals genotypes, and/or which show significant segregation distortion (chi-squared test, $P < 10^{-5}$) were not used. Suitable values of recombination fractions and LOD scores were estimated using the est.rf command. After these steps, initial linkage group construction was carried out using the formLinkageGroups command with a maximum recombination fraction of 0.25 and LOD threshold of 15. Robustness of linkage groups was checked using plot.rf command. Marker order within a linkage group was estimated using a program TMAP [51]. Some RAD-markers mapped at less than 0.1cM locus were not used for linkage map construction.

Results

Linkage map based on SSR markers

Among 1,336 SSR markers screened, 874 SSR markers (65.4% on average) amplified single DNA fragment (Table 1). The percentage of SSR markers amplified ranged from 56.1% for cowpea SSR markers to 97.5% for common bean SSR markers. Among 874 amplified SSR markers, only 83 SSR markers (6.2%) showed polymorphism between parents. The percentage of polymorphic SSR markers ranged from 2.5% for common bean SSR markers to 8.5% for azuki bean SSR markers.

A total of 82 out of 84 polymorphic SSR loci could be assigned to 11 linkage groups (LGs) covering a total length of 510.5 cM of the *V*. *vexillata* genome at an average marker distance of 7.2 cM (Fig 1, Table 1). Two polymorphic markers (CEDG074a and VES0660) were unlinked and could not be mapped. The number of markers on each LG ranged from 3 (LG1) to 13 (LG9) (Table 2). The length of each LG ranged from 8.6 (LG7) to 93.9 cM (LG9). The average distance between two adjacent markers ranged from 1.4 (LG7) to 15.7 cM (LG1). The LGs 1, 2,

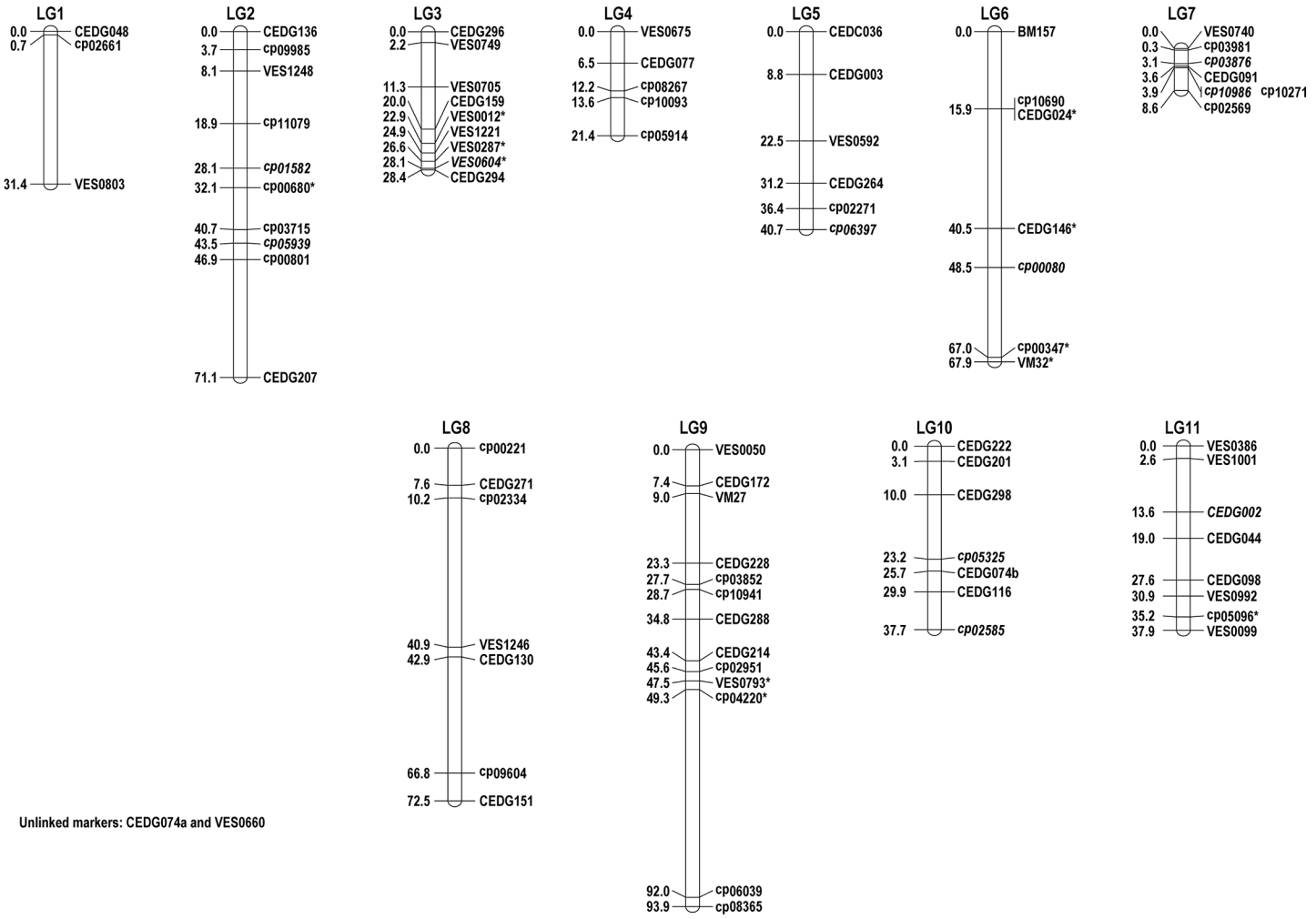


Fig 1. A genetic linkage map of *V. vexillata* constructed from 300 F_2 individuals of intraspecific cross between accessions V1 and V5. Map distances and marker names are shown on the left and right side of the linkage groups, respectively. Marker names in italics indicate dominant loci. Markers showing significant deviation from the expected segregation ratio at 0.05 are indicated with*. SSR markers with prefixes CED are derived from azuki bean. Markers with prefixes cp and VM are derived from cowpea. BM157 (LG6) is derived from common bean. Markers with prefixes VES are EST-SSR markers derived from azuki bean.

doi:10.1371/journal.pone.0138942.g001

6, 8 and 9 had gaps greater than 15 cM between markers. Eight markers (9.8%) showed significant segregation distortion at 5% level (Fig 1).

Linkage map based on SSR and RAD markers

Illumina sequencing with HiSeq2000 yielded a total of 451,012,199 RAD-tag 85-base reads from 494,666,849 raw reads. The number of RAD-tags of parents (V1 and V5) and F_2 individuals was 412,372, 1,138,645 and 450,040,150, respectively (Table 3). The average number of RAD-tags per F_2 individual was 1,597,514.3. RAD-tags were aligned and clustered into 42,517 stacks. Among these stacks, 10,037 candidate RAD loci were inferred and genotyped for 286 individuals of F_2 population. For the analysis of the F_2 mapping population, 5,438 RAD markers which showed homozygote polymorphic genotype between parents were used. Among them, 735 RAD markers together with 84 SSR markers loci were used for the linkage map

Table 2. Comparison of *Vigna vexillata* linkage group with those of *V. radiata* and *V. unguculata*, and some characteristics of the constructed *V. vexillata* SSR linkage map.

Linkage	Corresponding linkage groups of	Length	No. of loci					Average distance between two maker loci
group	*V. radiata* and *V. unguiculata* maps	(cM)	Azuki bean SSR	Cowpea SSR	Common bean SSR	Azuki bean EST-SSR	Total	(cM)
1	1	31.4	1	1	0	1	3	15.7
2	2	71.1	2	7	0	1	10	7.9
3	3	28.4	3	0	0	6	9	3.6
4	4	21.4	1	3	0	1	5	5.4
5	1 and 5	40.7	3	2	0	1	6	8.1
6	6 and 9	67.9	2	4	1	0	7	11.3
7	4	8.6	1	5	0	1	7	1.4
8	8	72.5	3	3	0	1	7	12.1
9	1 and 9	93.9	4	7	0	2	13	7.8
10	10	37.7	5	2	0	0	7	6.3
11	11	37.9	3	1	0	4	8	5.4
Total	**-**	**511.5**	**28**	**35**	**1**	**18**	**82**	**7.2**

Unlinked markers: CEDG074a and VES0660

doi:10.1371/journal.pone.0138942.t002

construction after discarding markers showing identical F_2 genotypes, high level of segregation distortion, and less than 100 F_2 genotypes.

Linkage analysis identified 11 linkage groups (LG1–LG11) containing a total of 475 RAD markers loci and 84 SSR markers loci after the removal of unlinked markers (Table 4, Fig 2). Sequence and SNP position of each RAD-marker was summarized (S2 Table). The map spanned 973.9 cM, with a mean distance between markers of 1.8 cM. The lengths of linkage groups ranged from 71.7 (LG11) to 128.3 cM (LG9). The positions of all SSR markers in an SSR-RAD markers linkage map were consistent with those in SSR markers linkage map.

Comparative linkage maps

Comparative linkage maps based on the common SSR markers were developed (Fig 3). Linkage maps of *V. radiata* (left) and *V. unguiculata* (middle) were highly conserved. Most of the common markers were mapped on the same linkage group with the same order. One reciprocal translocation was found between LG4 and LG7. On the other hand, 3 translocations were detected in *V. vexillata* compared with *V. radiata* (Fig 3, Table 2). Among 11 LGs, the structure of 8 *V. vexillata* LGs (vex LGs 1, 2, 3, 4, 7, 8, 10, 11) was estimated to be conserved with those of *V. radiata* and *V. unguiculata*. Other 3 LGs of *V. vexillata* (vex LGs 5, 6, 9) were composed of the fragments of 2 LGs of *V. radiata* or *V. unguiculata*.

Table 3. RAD-seq results in parents and F_2 populations using HiSeq2000 platform.

Samples	Number of reads	Number of RAD-tag	Mean coverage depth	Mean merged coverage depth
V. vexillata V1	442,165	412,372	12.0	12.7
V5	1,176,089	1,138,645	24.0	25.2
F_2 populations (286 lines)	470,584,049	450,040,150	-	-
Average per F_2 individual	1,670,491	1,597,514.3	30.6	37.0

doi:10.1371/journal.pone.0138942.t003

Table 4. Characteristics of a *V. vexillata* linkage map based on the SSR and RAD markers.

Linkage group	Number of loci			Length (cM)	Average marker interval (cM)
	Total	SSR	RAD		
1	54	3	51	84.5	1.6
2	56	10	46	109.4	2.0
3	58	10	48	91.4	1.6
4	41	5	36	78.0	1.9
5	50	6	44	75.4	1.5
6	54	7	47	89.7	1.7
7	53	8	45	78.8	1.5
8	43	7	36	90.8	2.2
9	55	13	42	128.3	2.4
10	56	7	49	75.9	1.4
11	39	8	31	71.7	1.9
Total	559	84	475	973.9	1.8

doi:10.1371/journal.pone.0138942.t004

Discussion

Transferability of SSR markers

The genetic linkage map developed in this study is the first SSR and RAD markers-based linkage map of *V. vexillata*. In addition, this is the first genetic linkage map consisting of 11 linkage groups that correspond to the haploid chromosome number of *V. vexillata* (n = 11). Former *V. vexillata* linkage map was constructed by 70 RAPD, 47 AFLP and one SSR marker, and was consisted of 14 linkage groups [1].

SSR markers developed in related species of *Vigna* and *Phaseolus* showed good amplification and a total of 874 markers were selected as potentially useful markers for *V. vexillata* (Table 1, S1 Table). However, there were only 83 polymorphic markers between the parents (V1 and V5). This might be explained by the fact that both of the parental accessions were from South America (V1 from Suriname and V5 from Columbia), where the genetic diversity of this species was reported to be low [3]. Baudoin and Maréchal [52] mentioned that there were two main centers of diversity, one in eastern and southern Africa (Zambezian district) and the other in Southeast Asia from Yunnan to Indonesia. Spinosa et al. [53] showed a lower degree of isozyme and RAPD variations in American accessions compared with African accessions. Vanderborght [10] reported that accessions from America showed epigeal germination which might be a recent evolutionary trend since most of the African accessions showed hypogeal germination which is considered ancestral type of germination in *V. vexillata*.

RAD-seq analysis for linkage map construction

SSR markers have been used as useful molecular markers and several SSR based linkage maps were constructed for *Vigna* crops [28–34]. However, we have encountered a problem of low polymorphism in SSR markers (6.2%) between *V. vexillata* parental accessions, hence resulting in a low density SSR linkage map. Recently, RAD-markers have been successfully used to construct a genetic linkage map and to perform QTL mapping in higher plant species [54–56].

By the application of RAD-seq analysis to the genetically close parental accessions of *V. vexillata* (V1 and V5), we could construct a high-density linkage map with 11 linkage groups with 475 RAD-markers (SNPs based of RAD-tag sequence) (S2 Table). Recently, a mungbean (*V. radiata*) and an azuki bean (*V. angularis*) linkage maps were constructed by SNPs using GBS

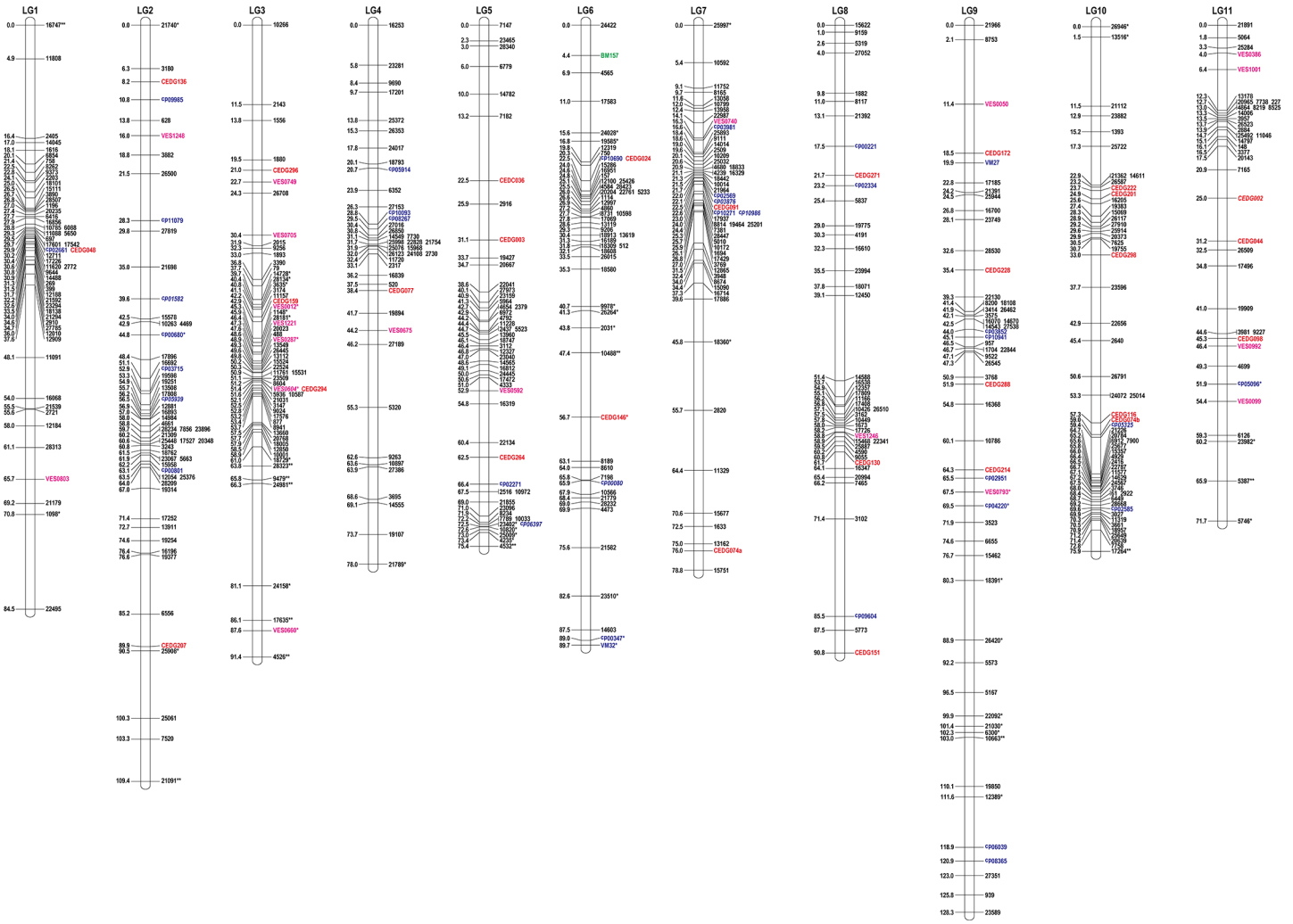


Fig 2. The SSR and RAD markers linkage map of *V. vexillata* constructed from 286 F_2 individuals of intraspecific cross between accessions V1 and V5. Map distances and marker names are shown on the left and right side of the linkage groups, respectively. Marker names in italics indicate dominant loci. Markers showing significant deviation from the expected segregation ratio at 0.05 and at 0.01 are indicated with* and **, respectively. SSR markers with prefixes CED are derived from azuki bean (red text). Markers with prefixes cp and VM are derived from cowpea (blue text). BM157 (LG6) is derived from common bean (green text). Markers with prefixes VES are EST-SSR markers derived from azuki bean (purple text). Markers without prefixes are RAD-markers derived from *V. vexillata* (black text).

doi:10.1371/journal.pone.0138942.g002

method (genotyping-by-sequencing) [35,36]. However, since they used different enzyme (ApeKI) in library preparation, sequence of the DNA fragments flanking the restriction sites could not be compared with RAD-tag sequence of the present study.

Since the genetic linkage map based on the RAD and SSR markers could confirm the linkage group accuracy of SSR-based linkage map, comparative genomic analysis were performed using common SSR markers.

Translocations in *Vigna vexillata*

The present study suggested several translocations occurred in *V. vexillata* chromosomes, while genomic structure of *V. radiata* and *V. unguiculata* was basically conserved with only one translocation. The remarkable chromosomal re-arrangements in *V. vexillata* was surprising because molecular phylogenetic analysis based on RFLP and the sequences of nuclear

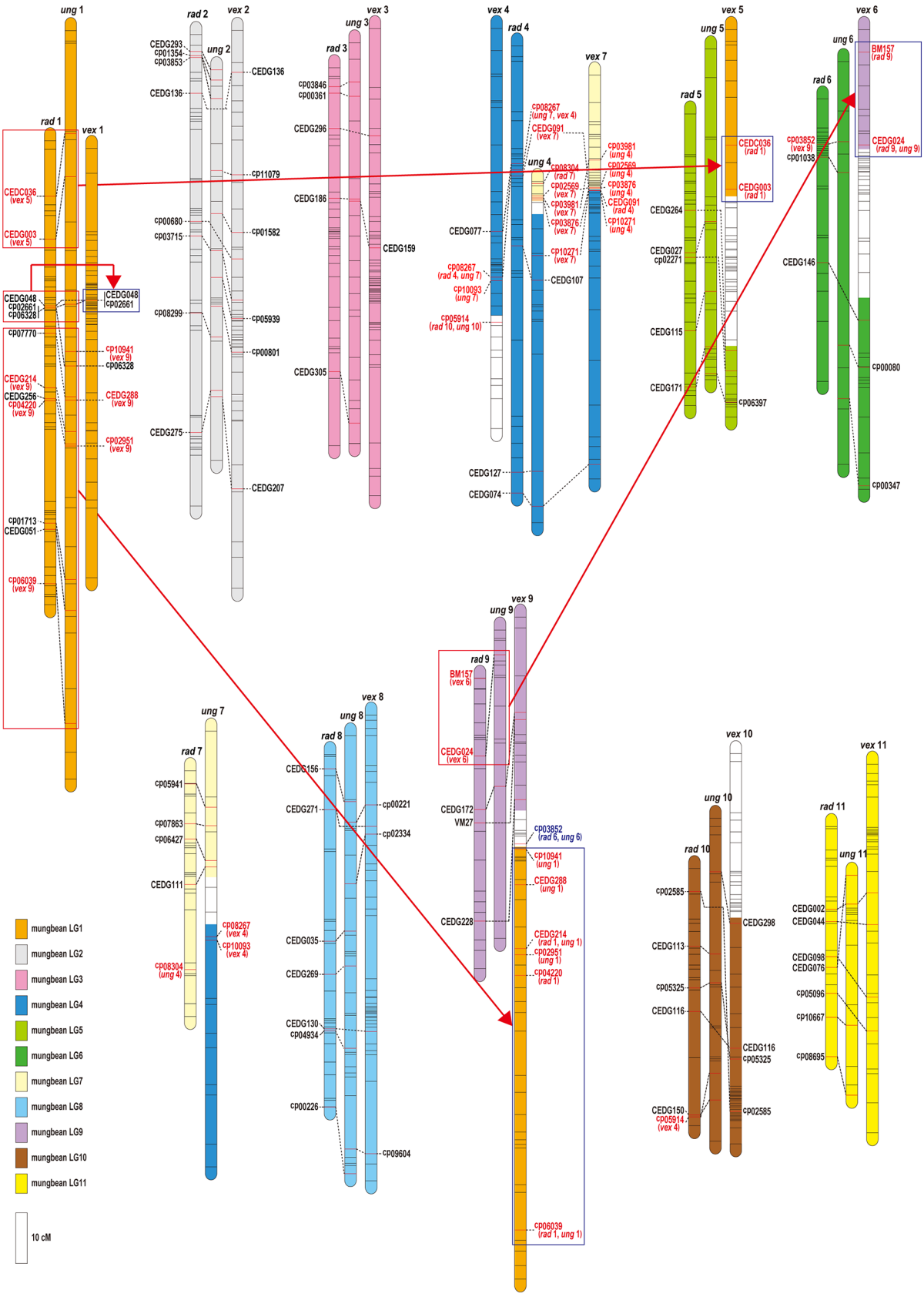

ung 1
rad 1
vex 1
CEDC036 (vex 5)
CEDG003 (vex 5)
CEDG048
cp02661
cp06328
CEDG048
cp02661
cp07770
cp10941 (vex 9)
cp06328
CEDG214 (vex 9)
CEDG256
cp04220 (vex 9)
CEDG288 (vex 9)
cp02951 (vex 9)
cp01713
CEDG051
cp06039 (vex 9)
rad 2
ung 2
vex 2
CEDG293
cp01354
cp03853
CEDG136
CEDG136
cp11079
cp00680
cp03715
cp01582
cp08299
cp05939
cp00801
CEDG275
CEDG207
ung 3
rad 3
vex 3
cp03846
cp00361
CEDG296
CEDG186
CEDG159
CEDG305
vex 4
rad 4
vex 7
cp08267 (ung 7, vex 4)
CEDG091 (vex 7)
ung 4
cp08304 (rad 7)
cp02569 (vex 7)
cp03981 (vex 7)
cp03876 (vex 7)
cp10271 (vex 7)
CEDG107
CEDG077
cp08267 (rad 4, ung 7)
cp10093 (ung 7)
cp05914 (rad 10, ung 10)
CEDG127
CEDG074
cp03981 (ung 4)
cp02569 (ung 4)
cp03876 (ung 4)
CEDG091 (rad 4)
cp10271 (ung 4)
vex 5
ung 5
rad 5
CEDC036 (rad 1)
CEDG003 (rad 1)
CEDG264
CEDG027
cp02271
CEDG115
CEDG171
cp06397
vex 6
ung 6
rad 6
BM157 (rad 9)
CEDG024 (rad 9, ung 9)
cp03852 (vex 9)
cp01038
CEDG146
cp00080
cp00347
vex 9
ung 9
rad 9
BM157 (vex 6)
CEDG024 (vex 6)
CEDG172
VM27
cp03852 (rad 6, ung 6)
cp10941 (ung 1)
CEDG288 (ung 1)
CEDG228
CEDG214 (rad 1, ung 1)
cp02951 (ung 1)
cp04220 (rad 1)
cp06039 (rad 1, ung 1)
ung 7
rad 7
cp05941
cp07863
cp06427
CEDG111
cp08267 (vex 4)
cp10093 (vex 4)
cp08304 (ung 4)
vex 8
ung 8
rad 8
CEDG156
CEDG271
cp00221
cp02334
CEDG035
CEDG269
CEDG130
cp04934
cp00226
cp09604
vex 10
ung 10
rad 10
cp02585
CEDG113
cp05325
CEDG116
CEDG150
cp05914 (vex 4)
CEDG298
CEDG116
cp05325
cp02585
vex 11
rad 11
ung 11
CEDG002
CEDG044
CEDG098
CEDG076
cp05096
cp10667
cp08695
mungbean LG1
mungbean LG2
mungbean LG3
mungbean LG4
mungbean LG5
mungbean LG6
mungbean LG7
mungbean LG8
mungbean LG9
mungbean LG10
mungbean LG11
10 cM

Fig 3. Comparative linkage maps among *Vigna radiata* (left: rad), *V. unguiculata* (middle: ung), and *V. vexillata* (right: vex) based on common SSR markers. Linkage group 4 (LG 4) of *V. vexillata* (vex 4) was placed to the left and LG 7 of *V. vexillata* (vex 7) was placed to the right of LG4 of *V. radiata* (rad 4) to show the relationships of common markers. The positions of common markers were connected by dotted lines. Markers which were mapped on different LGs among 3 *Vigna* species were written in red text. Major translocations were indicated by red arrows. The species abbreviation name and number in parentheses below red text marker names, e.g., (vex 5) indicate that the species and linkage group number on which corresponding marker was mapped.

doi:10.1371/journal.pone.0138942.g003

ribosomal DNA (rDNA) regions suggested that *V. vexillata* was more closely aligned with *V. unguiculata* compared with *V. radiata* [18,57,58]. In addition, morphological studies suggested *V. vexillata* group (subgenus *Plectrotropis*) formed an evolutionary intermediate group between *V. unguiculata* group (subgenus *Vigna*) and *V. radiata* group (subgenus *Ceratotrois)* [52,59].

Similar phenomenon was reported in the comparative analyses among *V. marina*, *V. radiata* and *V. unguiculata* linkage maps [60]. Structure of linkage maps was completely conserved between *V. marina* and *V. radiata*, which belong to the different subgenera, i.e., subgenus *Vigna* and *Ceratotropis*, respectively. On the contrary, one reciprocal translocation between LG4 and 7 was found between *V. marina* and *V. unguiculata*, which belong to the same subgenus *Vigna*. However, since the number of common SSR markers used for developing the comparative linkage map was not sufficient in these studies, it should be confirmed by the comparison of higher density molecular maps or more directly by cytogenetic analysis. Gomathinayagam et al. [61] observed the meiotic chromosomes of a hybrid of *V. vexillata* x *V. unguiculata* and reported high frequency of univalent formation, hence suggested that the genomes of the two species are structurally differentiated.

In addition, it is unknown that the chromosomal re-arrangement of *V. vexillata* suggested in the present study is commonly seen in *V. vexillata* or only occurred in some local accessions (e.g. American accessions). In case of azuki bean (*V. angularis*), we also suggested reciprocal translocation between LG4 and LG6 based on the comparison of SSR-based linkage maps developed for 2 different mapping populations [29,30]. Recently, this translocation event was confirmed to be occurred on a Japanese wild azuki bean parent by BAC-fluorescence in situ hybridization (FISH) analyses [62]. In that study, 21 wild azuki bean accessions collected from various regions of Japan were analyzed and it was found that geographical distribution of accessions with translocated chromosomes were restricted to eastern and northern Japan.

Future perspectives

Vigna vexillata is a promising food crop which could be grown under harsh environmental conditions [63]. There are domesticated accessions collected in Bali, which could be harvested in about 3 months and estimated tuber yield is 18–30 t/ha and seed yields of 0.7–1.2 t/ha [2]. There is another domesticated form (var. *macrosperma*) recognized having large seeds, non-dehiscent pods and bushy plant type [3,64]. *V. vexillata* var. *macroperma* showed earlier maturity with higher seed yield than Bali cultivated accessions [64]. Based on the hybridization study of these 2 domesticated forms (Bali and var. *macrosperma*) with African and Austronesian wild *V. vexillata* accesions, it was revealed that var. *macrosperma* and the wild accessions can be considered to belong to the same gene pool with strong genetic compatibility [65]. In contrast, there were various levels of genetic barriers between the cultivated Bali accessions and the wild accessions. Among several cross combinations tried, there was an Australian wild accession which could produce F_1 plants with a cultivated Bali accession having vigorous growth, but it showed complete F_1 sterility. However, backcrossing both to wild and Bali cultivated parents could produce BC_1 plants, suggesting the possibility of backcross breeding of improving these domesticated forms [66]. As was mentioned in Introduction section, there are wild accessions showing high levels of resistance to various kinds of insects and diseases, and also to various kinds of abiotic stresses. Therefore, diverse wild *V. vexillata* could be used to

incorporate adaptation gene(s) into these domesticated forms to grow under both biotic and abiotic stress environments.

In the breeding procedure, especially using wild germplasm, it is essential to map the position of useful traits and use marker assisted selection in the segregating population [67]. The SSR and RAD-marker based linkage map and SSR markers which produce single amplified DNA fragment in *V*. *vexillata* in the present study could be used as basic genome mapping resources.

Supporting Information

S1 Table. SSR and EST-SSR primers information.
(XLSX)

S2 Table. RAD markers name and sequence.
(XLSX)

Acknowledgments

We appreciate Associate Professor, Dr. Somchai Chakhatrakan, Thammasat University, Thailand who encouraged the first author (RM) to conduct the present study in Japan.

Author Contributions

Conceived and designed the experiments: AK ET KN HE NT. Performed the experiments: RM ET TI SC. Analyzed the data: RM ET TI. Contributed reagents/materials/analysis tools: ET AK NT. Wrote the paper: RM ET TI NT.

References

1. Ogundiwin EA, Thottappilly G, Aken'Ova ME, Pillay M, Fatokun CA. A genetic linkage map of *Vigna vexillata*. Plant Breed. 2005; 124: 392–398.
2. Karuniawan A, Iswandi PRK, Heinzemann J, Grüneberg WJ. *Vigna vexillata* (L.) A. Rich. cultivated as a root crop in Bali and Timor. Genet Resour Crop Evol. 2006; 53: 213–217.
3. Maréchal R, Mascherpa JM, Stainier F. Etude taxonomique d'un groupe complexe d'especes des genres *Phaseolus* et *Vigna* (*Palilionaceae*) sur la base de donnes morphologiques et polliniques, traitees par l'analyse informatique. Boissiera. 1978; 28: 1–273.
4. Chandel KPS, Arora RK, Joshi BS. *Vigna capensis* Walp.–an edible root legume. Curr Sci. 1972; 41: 537.
5. Duke JA. Handbook of Legumes of World Economic Importance. 11th ed. Plenum Press, New York and London; 1981. 345 p.
6. United States of America. National Research Council (NRC). *Vigna vexillata* in Tropical Legumes: Resources for the Future. National Academy of Science. Washington, DC. 1979; 34–36.
7. Sasikumar B, Sardana S. *Vigna vexillata* (Fabaceae), a pulse cum tuber crop of Northeastern Hill Region of India. Econ Bot. 1988; 42(2): 292.
8. Lawn RJ, Cottrell A. Wild mungbean and its relatives in Australia. Biologist. 1988; 35(5): 267–273.
9. Maxted N, Mabuza Dlamini P, Moss H, Padulosi S, Jarvis A, Guarino L. African *Vigna*: an ecogeographic study. International Plant Genetic Resources Institute (IPGRI), Rome, Italy. 2004.
10. Vanderborght T. Some observations on seedlings of *Vigna vexillata* (L.) A. Rich. (Fabaceae). Bull Jard Bot Nat Belg. 1989; 59: 179–187.
11. Miller IL, Williams WT. Tolerance of some tropical legumes to six months of simulated waterlogging. Trop Grasslands. 1981; 15(1): 39–43.
12. Verdcourt B. Studies in the Leguminosae Papilionoidae for the Flora of Tropical East Africa: 4. Kew Bull 1970; 24: 440–442.
13. Verdcourt B. Leguminosae. In Milne-Redhead E and Polhill RM, editors. Flora of Tropical East Africa. Crown Agency for Overseas Governments, London. 1971; 4: 652–655.

14. Garba M, Pasquet RS. The *Vigna vexillata* (L.) A. Richi. gene pool. In Sorensen M, Estrella JE, Hermann EOJ, Luiz SAR, editors. Proceedings of the 2nd International Symposium on Tuber Legumes; 1996 Aug 5–8, Celaya Guanajuato, Mexico. MacKenzie: Copenhagen. 1998; 61–71.
15. Fatokun CA, Perrino P, Ng NQ. Wide crossing in African *Vigna* species. In Singh BB, Mohan Raj DR, Dashiell KE, Jackai LEN, editors. Advances in cowpea research. JIRCAS & IITA, Ibadan, Nigeria; 1997. p. 50–57.
16. Vincenzo L, Terzano R, Cicco N, Cardinali A, Di Venere D, Linsalata V. Seed coat tannins and bruchid resistance in stored cowpea seeds. J Sci Food Agr. 2005; 85: 839–846.
17. Jackai LEN, Padulosi S, Ng Q. Resistance to the legume pod borer, *Maruca vitrata* Fabricius, and the probable modalities involved in wild *Vigna*. Crop Prot. 1996; 753–761.
18. Fatokun CA, Danesh D, Young ND, Stewart EL. Molecular taxonomic relationships in the genus *Vigna* based on RFLP analysis. Theor Appl Genet. 1993; 86: 97–104. doi: 10.1007/BF00223813 PMID: 24193388
19. James AT, Lawn RJ. Inheritance of selected traits in accessions of *Vigna vexillata* (L.) A. Rich of Australian and African origin. Austral J Bot. 1991; 39: 415–429.
20. Thottappilly G, Ng NQ, Rossel HW. Screening germplasm of *Vigna vexillata* for resistance to cowpea mottle virus. Int J Trop Plant Dis. 1994; 12: 75–80.
21. Ogundiwin EA, Thottappilly G, Aken'Ova ME, Ekpo EJA, Fatokun CA. Resistance to cowpea mottle carmovirus in *Vigna vexillata*. Plant Breed. 2002; 121: 517–520.
22. Lawn RJ, Watkinson AR. Habitat, morphological diversity and distribution of the genus *Vigna Savi* in Australia. Aust J Agric Res. 2002; 53: 1305–1316.
23. Baired NA, Etter PD, Atwood TS, Currey MC, Shiver AL, Lewis ZA, et al. Rapid SNP Discovery and Genetic Mapping Using Sequenced RAD Markers. PLoS ONE. 2008; 3 (10): e3376. doi: 10.1371/journal.pone.0003376 PMID: 18852878
24. Baxter SW, Davey JW, Johnson JS, Shelton AM, Heckal DG, Jiggins CD, et al. Linkage Mapping and Comparative Genomics Using Next-Generation RAD Sequencing of a Non-Model Organism. PLoS ONE. 2011; 6 (4): e19315. doi: 10.1371/journal.pone.0019315 PMID: 21541297
25. Varshney RK, Graner A, Sorrells ME. Genic microsatellite markers in plants: features and applications. Trends Biotechnol. 2005; 23: 48–55. PMID: 15629858
26. Miller M, Dunham J, Amores A, Cresko W, Johnson E. Rapid and cost effective polymorphism identification and genotyping using restriction site associated DNA (RAD) markers. Genome Res. 2007; 17: 240–248. PMID: 17189378
27. Baird NA, Etter PD, Atwood TS, Currey MC, Shiver AL, et al. Rapid SNP discovery and genetic mapping using sequenced RAD markers. PLoS ONE. 2008; 3:e3376. doi: 10.1371/journal.pone.0003376 PMID: 18852878
28. Han OK, Kaga A, Isemura T, Wang XW, Tomooka N, Vaughan DA. A genetic linkage map of azuki bean [*Vigna angularis* (Willd.) Ohwi & Ohashi]. Theor Appl Genet. 2005; 111(7):1278–1287. doi: 10.1007/s00122-005-0046-8 PMID: 16193342.
29. Isemura T, Kaga A, Konishi S, Ando T, Tomooka N, Han O, et al. Genome dissection of traits related to domestication in azuki bean (*Vigna angularis*) and comparison with other warm season legumes. Ann Bot. 2007; 100 (5): 1053–1071. PMID: 17728336
30. Kaga A, Isemura T, Tomooka N, Vaughan DA. The genetics of domestication of the azuki bean (*Vigna angularis*). Genetics. 2008; 178(2):1013–1036. doi: 10.1534/genetics.107.078451 PMID: 18245368
31. Chaitieng B, Kaga A, Tomooka N, Isemura T, Kuroda Y, Vaughan DA. Development of a black gram [*Vigna mungo* (L.) Hepper] linkage map and its comparison with an azuki bean [*Vigna angularis* (Willd.) Ohwi and Ohashi] linkage map. Theor Appl Genet. 2006; 113: 1261–1269. PMID: 16932883
32. Isemura T, Kaga A, Tabata S, Somta P, Srinives P, Shimizu T, et al. Construction of genetic linkage map and genetic analysis of domestication related traits in mungbean (*Vigna radiata*). PLos ONE. 2012; 7(8): e41304. doi: 10.1371/journal.pone.0041304 PMID: 22876284
33. Isemura T, Kaga A, Tomooka N, Shimizu T, Vaughan DA. The genetics of domestication of rice bean, *Vigna umbellata*. Annals of Botany. 2010; 106: 927–944. doi: 10.1093/aob/mcq188 PMID: 20880934
34. Kongjaimun A, Kaga A, Tomooka N, Somta P, Shimizu T, Shu Y, et al. An SSR-based linkage map of yardlong bean (*Vigna unguiculata* (L.) Walp. subsp. *unguiculata* Sesquipedalis Group) and QTL analysis of pod length. Genome. 2012; 55: 81–92. doi: 10.1139/G11-078 PMID: 22242703
35. Tomooka N, Isemura T, Naito K, Kaga A, Vaughan D. *Vigna* species. In Singh M, Bisht IS, Dutta M, editors. Broadening the Genetic Base of Grain Legumes. Springer New Delhi Heidelberg New York Dordrecht London; 2014b. Chapter 9, 175–208.

36. Kang YJ, Satyawan D, Shim S, Lee T, Lee J, et al. Draft genome sequence of adzuki bean, *Vigna angularis*. Sci Rep. 2015; 5: 8069 doi: 10.1038/srep08069 PMID: 25626881

37. Kang YJ, Kim SK, Kim MY, Lestari P, Kim KH et al. Genome sequence of mungbean and insights into evolution within *Vigna* species. Nat Commun. 2014; 5: 5443 doi: 10.1038/ncomms6443 PMID: 25384727

38. Lodhi MA, Ye GN, Weeden NF, Reisch BI. A simple and efficient method for DNA extraction from grapevine cultivars and *Vitis* species. Plant Mol Bio Rep. 1994; 12: 6–13.

39. Wang XW, Kaga A, Tomooka N, Vaughan DA. The development of SSR markers by a new method in plants and their applicationto gene flow studies in azuki bean [*Vigna anguicularis* (Willd.) Ohwi & Ohashi]. Theor Appl Genet. 2004; 109: 352–360. PMID: 15014881

40. Chankaew S, Isemura T, Isobe S, Kaga A, Tomooka N, Somta P, et al. Detection of genome domor species of neglected tetraploid crop *Vigna reflexo-pilosa* (créole bean), and genetic structure of diploid species based on newly developed EST-SSR markers from azuki bean (*Vigna angularis*). PLos ONE. 2014a; 9 (8): e104990. doi: 10.1371/journal.pone.0104990 PMID: 25153330

41. Li CD, Fatokun CA, Ubi B, Singh BB, Scoles GJ. Determining genetic similarities and relationships aming cowpea breeding lines and cultivars by microsatellite markers. Crop Sci. 2001; 41: 189–197.

42. Yu K, Park J, Poysa V, Gepts P. Integation of simple sequence repeat (SSR) markers into a molecular linkage map of common bean (*Phaseolus vulgaris* L.). J Hered. 2000; 91: 429–434. PMID: 11218079

43. Gaitán-Solís E, Duque MC, Edwards KJ, Thome J. Microsatellite repeats in common bean (*Phaseolus vulgaris* L.): isolation, characterization, and cross-species amplification in *Phaseolus* ssp. Crop Sci. 2002; 42: 2128–2136.

44. Blair MW, Pedraza F, Buendia HF, Gaitán-Solís E, Beebe SE, Gepts P, et al. Development of a genome-wide anchored microsatellite map of common bean (*Phaseolus vulgaris* L.). Theor Appl Genet. 2003; 107: 1362–1374. PMID: 14504741

45. Guerra-Sanz JM. New SSR markers of *Phaseolus vulgaris* from sequence databases. Plant Breed. 2004; 123, 87–89.

46. Van Ooijen JW. JoinMap Version 4.0. Software for the calculation of genetic linkage maps. Kyazma BV, Wageningen. 2006.

47. Kosambi DD. The estimation of map distances from recombination values. Ann Eugen. 1944; 12: 172–175.

48. Matsumura H, Miyagi N, Taniai N, Fukushima M, Tarora K, et al. Mapping of the gynoecy in bitter gourd (*Momordica charantia*) using RAD-Seq analysis. PLoS ONE. 2014; 9(1): e87138. doi: 10.1371/journal.pone.0087138 PMID: 24498029

49. Catchen JM, Amores A, Hohenlohe P, Cresko W, Postlethwait JH. Stacks: building and genotyping Loci de novo from short-read sequences. G3 (Bethesda). 2011; 1(3): 171–82.

50. Arends D, Prins P, Jansen RC, Broman KW. R/qtl: High-throughput multiple QTL mapping. Bioinformatics. 2010; 26: 2990–2992 doi: 10.1093/bioinformatics/btq565 PMID: 20966004

51. Cartwright DA, Troggio M, Velasco R, Gutin A. Genetic mapping in the presence of genotyping errors. Genetics. 2007; 176(4): 2521–2527. PMID: 17277374

52. Baudoin JP, Maréchal R. Taxonomy and evolution of the genus *Vigna*. In "Mungbean" Proceedings of the Second International Symposium; 1987 Nov 16–20; Bangkok, Thailand. Shanhua, Taiwan: AVRDC; 1988.

53. Spinosa A, Pignone D, Sonnante G. Assessment of genetic variation in a working collection of *Vigna vexillata* A. Rich. By isozyme and RAPD analyses. Genet Resour Crop Evol. 1998; 45: 347–354.

54. Hegarty M, Yadav R, Lee M, Armstead I, Sanderson R, et al. Genotyping by RAD sequencing enables mapping of fatty acid composition traits in perennial ryegrass (*Lolium perenne* (L.)). Plant Biotechnol. 2013; 11: 572–581. doi: 10.1111/pbi.12045

55. Barchi L, Lanteri S, Portis E, Valè G, Volante A, et al. A RAD tag derived marker based eggplant linkage map and the location of QTLs determining anthocyanin pigmentation. PLoS One. 2012; 7: e43740. doi: 10.1371/journal.pone.0043740 PMID: 22912903

56. Pfender WF, Saha MC, Johnson EA, Slabaugh MB. Mapping with RAD (restriction-site associated DNA) markers to rapidly identify QTL for stem rust resistance in *Lolium perenne*. Theor Appl Genet. 2011; 122: 1467–1480. doi: 10.1007/s00122-011-1546-3 PMID: 21344184

57. Goel S, Raina SN, Ogihara Y. Molecular evolution and phylogenetic implications of internal transcribed spacer sequences of nuclear ribosomal DNA in the *Phaseolus-Vigna* complex. Mol Phylogenet Evol. 2002; 22(1): 1–19. PMID: 11796025

58. Choi HW, Kim MY, Lee SH, Sultana S, Bang JW. Molecular cytogenetic analysis of the *Vigna* species distributed in Korea. Genes Genom. 2013; 35: 257–264.

59. Tateishi Y, Ohashi H. Systematics of the azuki bean group in the genus *Vigna*. In Fujii K, Gatehouse AMR, Jhonson CD, Mitchel R, Yoshida T, editors. Bruchids and Legumes: Economics, Ecology and Coevolution. Kluwer Academic Publishers; Netherlands. 1990; 189–199.

60. Chankaew S, Isemura T, Naito K, Ogiso-Tanaka E, Tomooka N, Somta P, et al. QTL mapping for salt tolerance and domestication–related traits in *Vigna marina* subsp. *oblonga*, a halophytic species. Theor Appl Genet. 2014b. doi: 10.1007/s00122-013-2251-1

61. Gomathinayagam P, Ganesh ram S, Rathnaswamy R, Ramaswamy NM. Interspecific hybridization between *Vigna unguiculata* (L.) Walp. and *V. vexillata* (L.) A. Rich. through *in vitro* embryo culture. Euphytica. 1998; 102: 203–209.

62. Wang L, Kikuchi S, Muto C, Naito K, Isemura T, Ishimoto M, et al. Reciprocal translocation identified in *Vigna angularis* dominates the wild population in East Japan. J Plant Res. 2015. doi: 10.1007/s10265-015-0720-0

63. Tomooka N, Naito K, Kaga A, Sakai H, Isemura T, Ogiso-Tanaka E, et al. Evolution, domestication and neo-domestication of the genus *Vigna*. Plant Genet Resour. 2012a; 12(S1): S168–S171.

64. Damayanti F, Lawn RJ, Bielig M. Genotypic variation in domesticated and wild accessions of the tropical tuberous legume *Vigna vexillata* (L.) A. Rich. Crop Pasture Sci. 2010a; 61 (10): 771–784.

65. Damayanti F, Lawn RJ, Bielig M. Genetic compatibility among domesticated and wild accessions of the tropical tuberous legume *Vigna vexillata* (L.) A. Rich. Crop Pasture Sci. 2010b; 61 (10): 786–797.

66. Damayanti F, Lawn R, Bielig M. Expression of qualitative and quantitative traits in hybrids between domesticated and wild accessions of the tropical tuberous legume *Vigna vexillata* (L.) A. Rich. Crop Pasture Sci. 2010c; 61 (10): 798–811.

67. Ashraf M, Foolad MR. Crop breeding for salt tolerance in the era of molecular markers and marker-assisted selection. Plant Breed. 2013; 132: 10–20.

020/2558

Breeding Science 65: 127–137 (2015)
doi:10.1270/jsbbs.65.127

Research Paper

Genetic diversity of the black gram [*Vigna mungo* (L.) Hepper] gene pool as revealed by SSR markers

Anochar Kaewwongwal, Alisa Kongjaimun, Prakit Somta*, Sompong Chankaew, Tarikar Yimram and Peerasak Srinives

Department of Agronomy, Faculty of Agriculture at Kamphaeng Saen, Kasetsart University, Kamphaeng Saen, Nakhon Pathom 73140, Thailand

In this study, 520 cultivated and 14 wild accessions of black gram (*Vigna mungo* (L.) Hepper) were assessed for diversity using 22 SSR markers. Totally, 199 alleles were detected with a mean of 9.05 alleles per locus. Wild black gram showed higher gene diversity than cultivated black gram. Gene diversity of cultivated accessions among regions was comparable, while allelic richness of South Asia was higher than that of other regions. 78.67% of the wild gene diversity presented in cultivated accessions, indicating that the domestication bottleneck effect in black gram is relatively low. Genetic distance analysis revealed that cultivated black gram was more closely related to wild black gram from South Asia than that from Southeast Asia. STRUCTURE, principal coordinate and neighbor-joining analyses consistently revealed that 534 black gram accessions were grouped into three major subpopulations. The analyses also revealed that cultivated black gram from South Asia was genetically distinct from that from West Asia. Comparison by SSR analysis with other closely related *Vigna* species, including mungbean, azuki bean, and rice bean, revealed that level of gene diversity of black gram is comparable to that of mungbean and rice bean but lower than that of azuki bean.

Key Words: *Vigna*, urd bean, domestication, microsatellite marker, plant genetic resources.

Introduction

The genus *Vigna* is a large leguminous taxon comprising 104 described species distributed in tropical and subtropical regions of Africa, Asia, America, and Australia (Lewis *et al.* 2005). It is an important and interesting taxon because up to nine species in this taxon are domesticated as food crops in Asia, Africa, and America. These species include *V. subterranea* (L.) Verdc. (Bambara groundnut), *V. unguiculata* (L.) Walp. (cowpea), *V. vexillata* (L.) (zombi pea), *V. radiata* (L.) Wilczek (mungbean), *V. angularis* (Ohwi) Ohwi & Ohashi (azuki bean), *V. mungo* (L.) Hepper (black gram), *V. aconitifolia* Jacq. (moth bean), *V. umbellata* (Thunb.) Ohwi & Ohashi (rice bean), and *V. reflexo-pilosa* Hayata (créole bean) (Tomooka *et al.* 2006). Seeds, pods, and tubers of these species are sources of dietary proteins, amino acids, carbohydrates, vitamins, and minerals for humans. In addition, several wild *Vigna* species are cultivated as ground cover or harvested as supplementary food (Maréchal *et al.* 1978, Tomooka *et al.* 2006). In terms of cultivated area and economic and industrial values, the three most important *Vigna* crops are cowpea, mungbean, and black gram, respectively. Cowpea is mainly cultivated in Africa, while mungbean and black gram are principally grown in Asia.

Cultivated black gram (also known as urd, urad, or mash; *Vigna mungo* var. *mungo* (L.) Hepper) is believed to have been domesticated in India from its wild progenitor, *Vigna mungo* var. *silvestris* Lukoki, Maréchal, and Otoul (Chandel *et al.* 1984). Based on archeological evidence found in India (Fuller and Harvey 2006), domestication of black gram may have occurred about 4,500 years ago. Early finds of black gram were from Gujarat and the Northern Peninsula in India, where wild black gram populations persist (Fuller and Harvey 2006).

Black gram seeds contain about 25% protein and 65% carbohydrates. The seeds are mainly consumed as soup. Black gram flour and powder are used as major ingredients for several kinds of foods, such as cakes, biscuits, snacks, cookies, and doughnuts. Sprouts produced from black gram are also consumed as a vegetable source of vitamins and minerals. In Thailand and Japan, sprouts from black gram are more preferable than those from mungbean because of their longer shelf life. Black gram is mainly grown in South and Southeast Asian countries, including Afghanistan, Bangladesh, India, Pakistan, Nepal, Myanmar, the

Communicated by J. Abe
Received June 19, 2014. Accepted October 31, 2014.
*Corresponding author (e-mail: pksomta@gmail.com)

Philippines, Sri Lanka, and Thailand. Due to its relative drought tolerance, short life cycle (75–90 days), and ability to fix atmospheric nitrogen in association with soil *Rhizobium* and *Bradyrhizobium* bacteria, the crop is grown as a component in various cropping systems, but chiefly following rice and wheat. Although there is no official record of growing area of black gram, the area is expected to be higher than 5 Mha. India is the largest producer (about 3 Mha), followed by Myanmar (about 1 Mha) and Pakistan (0.5 Mha). Black gram production in Myanmar and Thailand are mainly for exporting seeds to India and Japan.

Seed yield of black gram is low, being about 450–800 kg/ha. There are not many breeding programs for black gram, and most of them are in India, Pakistan, and Thailand. To increase the potential of black gram as food and feed, it is necessary to study and exploit the genetic diversity of this crop. Compared to cowpea and mungbean, there has been less research on black gram, especially in terms of molecular genetic diversity. Genetic variability of black gram has been studied based on morphological and agronomic traits (Ghafoor *et al.* 2001, Gupta *et al.* 2001), seed storage protein (Ghafoor and Ahmad 2005), isozyme markers (Singh *et al.* 2009), DNA markers including random amplified polymorphic DNA (RAPD), inter simple sequence repeat (ISSR), amplified fragment length polymorphism (AFLP), and simple sequence repeat (SSR) (Gupta and Gopalakrishna 2009, Sivaprakash *et al.* 2004, Souframanien and Gopalakrishna 2004). However, these studies have provided little information on the extent of genetic diversity in black gram because each study, except Gupta *et al.* (2001) and Ghafoor *et al.* (2001), employed less than 150 accessions, and the germplasm used in each study originated from only a single geographical region (country). Moreover, the dominant nature of RAPD, ISSR, and AFLP markers make them unsuitable for diversity analysis, because they complicate the calculation of population genetics parameters based on allele frequency (Lynch and Milligan 1994).

SSR (also known as microsatellite) is the marker of choice for molecular genetics study in crops because of its advantages of being co-dominant, multi-allelic, reliable, PCR-based, and easy to score, and requiring a small amount of DNA for analysis. SSR markers from one species can also be used in other related species. Although no SSR marker has been developed from black gram, thousands of them have been developed in other *Vigna* crops, including azuki bean (Wang *et al.* 2004), cowpea (Gupta and Gopalakrishna 2010, Kongjaimun *et al.* 2012), and mungbean (Seehalak *et al.* 2009, Somta *et al.* 2008, 2009, Tangphatsornruang *et al.* 2009). SSR markers from azuki bean, cowpea, and mungbean have shown a high rate of amplification in black gram and thus are useful for genomics study in this crop (Chaitieng *et al.* 2006, Gupta and Gopalakrishna 2010, Somta *et al.* 2009, Tangphatsornruang *et al.* 2009).

In this study, a set of 534 black gram accessions from various origins were assessed by SSR markers from azuki bean and cowpea, with the aims of determining the level of genetic diversity and population structure. The results will be useful for black gram breeders/geneticists to better understand diversity and domestication of the crop.

Materials and Methods

Plant materials and DNA extraction

Five hundred and thirty-four accessions of black gram, including 520 cultivated and 14 wild accessions from various geographical origins covering major growing areas, were used in this study (**Table 1** and **Supplemental Table 1**).

Seeds of each accession were sown in an experimental field of Kasetsart University, Kamphaeng Saen Campus, Nakhon Pathom, Thailand. Young leaves from two or three plants of each accession were collected and extracted for DNA following the method described by Lodhi *et al.* (1994), with the exception that absolute ethanol was used instead of 95% ethanol for DNA precipitation. The DNA concentration was determined by comparison with a known concentration of λ DNA and adjusted to 1 ng/μl for SSR marker analysis.

SSR marker analysis

Ninety-four SSR markers from azuki bean [18 genomic SSRs reported by Wang *et al.* (2004) and 37 EST-SSRs reported by Chankaew *et al.* (2014)] and from cowpea [1 genomic SSR reported by Li *et al.* (2001) and 38 EST-SSRs reported by Kongjaimun *et al.* (2012)] were used to screen for PCR amplification and for potential detection of polymorphism in five black gram accessions (**Supplemental Table 2**). PCR amplification was performed as follows: the PCR mixture was prepared in a total volume of 10 μl containing 4 ng of genomic DNA, 5 pmol of each forward and reverse primer, 1× *Taq* buffer, 200 mM dNTPs, 2 mM $MgCl_2$, and 1 U *Taq* DNA polymerase (Thermo Scientific, Wilmington, USA). The PCR cycling profile for the genomic SSR markers was the same as that described by Somta *et al.* (2008), while that for the EST-SSR markers was the same as that noted by Kongjaimun *et al.* (2012). The SSR markers were amplified using GeneAmp® PCR System 9700 thermocycler (Applied Biosystems, Foster City, USA) or PTC-200 thermocycler (MJ Research, Waltham, USA). The PCR products were separated on 5% denatured polyacrylamide gel (w/v; 19 : 1 acrylamide-bisacrylamide) with 7M urea and 1×TBE buffer. Electrophoresis was run at 80 W constant power for 2 to 3 h (depending on allele size) using Model S2 Sequencing Gel Electrophoresis Apparatus (Biometra, Goettingen, Germany). ϕX174 DNA/*Hinf*I marker (Thermo Scientific, Wilmington, USA) was used as a size standard. The PCR products were visualized by silver staining. Twenty-two polymorphic SSR markers with clear bands were then used to analyze all the DNA samples.

Data analysis

Number of alleles, observed heterozygosity (H_O), gene diversity (expected heterozygosity; H_E), Wright's fixation

Table 1. Sources and number of cultivated black gram accessions used in this study with number of alleles (N_A), gene diversity (H_E), observed heterozygosity (H_O), allelic richness (A_R), and estimated outcrossing rate (t)

Form (status)	Origin	No. of accessions	N_A	H_E	H_O	A_R	t (%)
Cultivated	All	520	178	0.59	0.06	105.77	4.38
	South Asia (C_SA)	245	156	0.57	0.06	62.08	4.60
	Bangladesh (BGD)	2	35	0.55	0.07	32.00	2.30
	India (IND)	240	154	0.57	0.06	44.10	4.66
	Sri Lanka (SLK)	3	43	0.60	0.06	36.46	2.62
	West Asia (C_WA)	143	136	0.52	0.07	57.00	6.21
	Afghanistan (AFG)	8	39	0.26	0.03	27.84	2.35
	Pakistan (PAK)	134	127	0.51	0.07	40.72	6.61
	Iran (IRN)	1	23	ND	0.05	ND	ND
	Himalayan region (Nepal; C_NEP)	92	125	0.51	0.04	56.94	4.17
	Southeast Asia (C_SEA)	25	98	0.54	0.07	58.60	3.73
	Myanmar (MMR)	1	22	ND	0.00	ND	ND
	Philippines (PHL)	3	42	0.49	0.09	34.26	4.17
	Singapore (SGP)	1	22	ND	0.00	ND	ND
	Thailand (THA)	20	90	0.54	0.07	42.26	3.79
	Africa (C_AF)	7	67	0.58	0.06	55.58	2.30
	Cote D'Ivoier (CIV)	2	28	0.40	0.00	26.00	0.00
	Mauritius (MUS)	1	22	ND	0.00	ND	ND
	Senegal (SEN)	2	32	0.43	0.09	28.00	6.27
	Zaire (ZAR)	2	34	0.18	0.09	24.00	16.69
	America (C_AM)	6	63	0.60	0.03	57.24	1.27
	Argentina (GRG)	1	24	ND	0.09	ND	ND
	Colombia (COL)	1	22	ND	0.00	ND	ND
	Trinidad (TTO)	2	29	0.33	0.00	26.00	0.00
	United states of America (USA)	1	22	ND	0.00	ND	ND
	Venezuela (VEN)	1	22	ND	0.00	ND	ND
	Unknown (C_NA)	2	34	0.52	0.05	31.00	2.20
Wild	All	14	115	0.75	0.08	112.81	4.44
	South Asia (India; W_SA)	9	96	0.77	0.10	72.98	5.71
	Southeast Asia (Thailand; W_SEA)	5	46	0.41	0.05	42.19	4.00
Overall		534	199	0.60	0.06	198.10	4.33

Note; ND = not determined.

index (F_{IS}), and allelic richness (A_R) were calculated with software FSTAT 2.9.3.2 (Goudet 2002). F_{IS} was then employed to calculate outcrossing rate (t) using an equation proposed by Weir (1996): $t = (1 - F_{IS})/(1 + F_{IS})$. Polymorphism information content (*PIC*) of each marker was calculated following Anderson *et al.* (1993).

Genetic admixture among black gram accessions was determined with software STRUCTURE 2.3.4 (Pritchard *et al.* 2000). Initially, 20 simulation runs of STRUCTURE were performed based on an independent allele frequency model using K (number of clusters) varying from 1 to 10 with a burn-in period of 10,000 and 50,000 replicates of Markov Chain Monte Carlo (MCMC); the optimum K was then determined based on the *ad-hoc* ΔK method of Evanno *et al.* (2005). Finally, a run with the optimum K, 100,000 burn-in period, and 500,000 MCMC replications were performed to assign individual black gram accessions to clusters.

Nei's genetic distance (D_A) (Nei *et al.* 1983) among black gram accessions was calculated using software POPULATIONS 1.2.31 (Langella 2002) and was then used in a principal coordinate analysis (PCoA) and neighbor-joining analysis using *R*-program 2.10.0 (R Development Core Team 2012) and MEGA6 (Tamura *et al.* 2013), respectively, to depict relationships among the accessions. The neighbor-joining tree was obtained with 1,000 bootstraps.

Results

SSR polymorphism

Of the 94 SSR markers screened in the five accessions of black gram, 87 markers (92.55%) were able to successfully amplify their DNAs, and 37 of the amplifiable markers (42.53%) showed polymorphism (**Supplemental Table 2**). Twenty-two polymorphic markers (12 azuki bean genomic SSRs, 4 azuki bean EST-SSRs, and 6 cowpea EST-SSRs) showing unambiguous DNA bands were selected and used for further analysis of the 534 black gram accessions (**Supplemental Table 3**). The 22 SSR markers detected 199 alleles in total, with the number of alleles per locus ranging from 3 (cp01038 and VES0019) to 23 (CEDG305 and cp05325) and an average of 9.05 alleles per marker (**Tables 1**, **2**).

The PIC values varied from 0.02 (CEDG015) to 0.92 (CEDG305 and cp05325), with an average of 0.60 (**Table 2**). In general, markers showed higher PIC in wild accessions than in cultivated accessions. SSR markers

Table 2. Number of detected alleles, polymorphism information content (*PIC*), and allelic richness of 22 SSR markers in cultivated and wild black gram

Primer (allele size range)	No. of alleles			*PIC*			Allelic richness		
	O[a]	C[b]	W[c]	O[a]	C[b]	W[c]	O[a]	C[b]	W[c]
CEDG013 (82–100)	8	7	5	0.66	0.66	0.66	8.00	4.56	4.95
CEDG015 (151–200)	4	2	3	0.02	0.02	0.25	4.00	1.16	2.78
CEDG056 (200–250)	9	9	6	0.75	0.75	0.81	9.00	5.70	6.00
CEDG088 (110–140)	7	4	6	0.13	0.10	0.71	6.74	1.74	5.53
CEDG092 (140–150)	8	5	4	0.72	0.70	0.56	7.97	4.04	3.96
CEDG097 (82–118)	16	13	8	0.73	0.73	0.78	15.83	6.97	7.45
CEDG103 (80–110)	8	6	5	0.66	0.64	0.72	7.89	3.42	4.96
CEDG111 (150–200)	4	3	4	0.19	0.17	0.72	4.00	1.95	4.00
CEDG173 (110–142)	16	14	6	0.79	0.78	0.76	15.98	6.71	5.95
CEDG279 (153–205)	7	7	5	0.77	0.77	0.69	7.00	5.30	5.00
CEDG305 (106–118)	23	22	7	0.92	0.92	0.81	22.95	11.46	6.91
CEDG006 (100–132)	4	3	3	0.08	0.07	0.59	4.00	1.55	3.00
cp01038 (267–350)	3	3	3	0.49	0.48	0.57	3.00	2.77	2.98
cp01354 (213–267)	8	8	7	0.80	0.80	0.80	8.00	5.46	6.88
cp05325 (200–500)	23	23	10	0.92	0.92	0.87	23.00	11.45	9.97
cp07770 (350–434)	8	8	4	0.79	0.79	0.72	8.00	5.74	4.00
cp10549 (234–300)	12	12	7	0.85	0.85	0.84	11.87	7.40	6.92
cp11079 (210–250)	7	6	5	0.59	0.58	0.77	6.98	3.35	4.98
VES0019 (213–234)	3	3	3	0.45	0.43	0.66	3.00	2.48	3.00
VES0287 (192–234)	10	10	4	0.69	0.67	0.64	10.00	5.55	3.79
VES0670 (102–126)	5	4	5	0.54	0.52	0.73	4.97	2.47	4.92
VES1246 (124–184)	6	6	5	0.69	0.69	0.67	6.00	4.55	4.88
Average	9.05	8.10	5.23	0.60	0.59	0.70	9.01	4.81	5.13
Total	199	178	155						

[a] O = Overall.
[b] C = Cultivated.
[c] W = Wild.

showed comparable A_R between wild and cultivated accessions (**Table 2**).

H_O in cultivated black gram germplasm from different regions or between cultivated and wild germplasm were comparable (**Table 1**). Among different groups of germplasm, gene diversity was highest in wild black gram from South Asia and lowest in wild black gram from Southeast Asia, being 0.77 and 0.41, respectively (**Table 1**). Among the cultivated black gram, gene diversity of America was the greatest but comparable with that of other regions (**Table 1**). Among germplasm from major growing areas (South Asia, West Asia, the Himalayan region, and Southeast Asia), that from South Asia possessed the highest gene diversity, followed by Southeast Asia, West Asia, and the Himalayan region. A_R values in these four regions were almost the same (**Table 1**). However, wild black gram possessed greater A_R than cultivated black gram. Wild black grams from South Asia had higher A_R than those from Southeast Asia (**Table 1**).

Genetic admixture

Population admixture among black gram accessions was determined by STRUCTURE analysis which uses Bayesian algorithm. Based on the *ad-hoc* ΔK measurement method (Evanno *et al.* 2005), the 534 black gram accessions were an admixture of three subpopulations (**Supplemental Figs. 1** and **2**). Subpopulation I, II, and III comprised 159, 188, and 187 accessions, respectively. The majority in subpopulation I were cultivated accessions from South Asia (52%) and all cultivated accessions except one from Southeast Asia (15%), some accessions from West Asia (9%) and Himalayan region (8%). All the wild accessions were included in this subpopulation. Most of the accessions in subpopulation II were from South Asia (82%), with some accessions from the Himalayan region (13%) and West Asia (4%). The majority of accessions in subpopulation III were from West Asia (65%) and the Himalayan region (28%), together with some accessions from South Asia (4%).

Principal coordinate analysis

PCoA revealed that the first three PCs together accounted for 37.37% of the total variation. The first, second, and third PCs accounted for 14.89%, 13.03%, and 9.45%, respectively. Although the scatter plot of black gram germplasm based on PC1 and PC2 showed that there were no clear distinct groups of germplasm, it demonstrated that accessions in the same subpopulation as identified by STRUCTURE analysis were mainly scattered together on the PCoA plot (**Fig. 1**A).

Black grams from South Asia showed the broadest distribution (**Fig. 1**B). They were mainly scattered at the central right and the upper left of the plot. Accessions in the latter group showed much wider distribution than those in the former. Black grams from West Asia showed wide distribution

(**Fig. 1**C). Most of them could be differentiated from black grams from South Asia, while some showed overlapping distribution (**Fig. 1**A). The majority of accessions from West Asia were at the lower middle-left of the PC plot. Black grams from the Himalayan region also showed wide distribution (**Fig. 1**D). Most of them scattered around the center of the plot. About a half of the accessions were associated with accessions from South Asia, while the other half were associated with accessions from West Asia. Black grams from Southeast Asia, America, and Africa, as well as those of unknown origin, showed relatively narrow distribution (**Fig. 1**E), scattering mainly around the left half of the plot. However, most accessions were differentiated from one region to another. Black grams from the American collection showed wide variation, scattering on the upper and lower left of the plot (**Fig. 1**E). Black grams from Africa

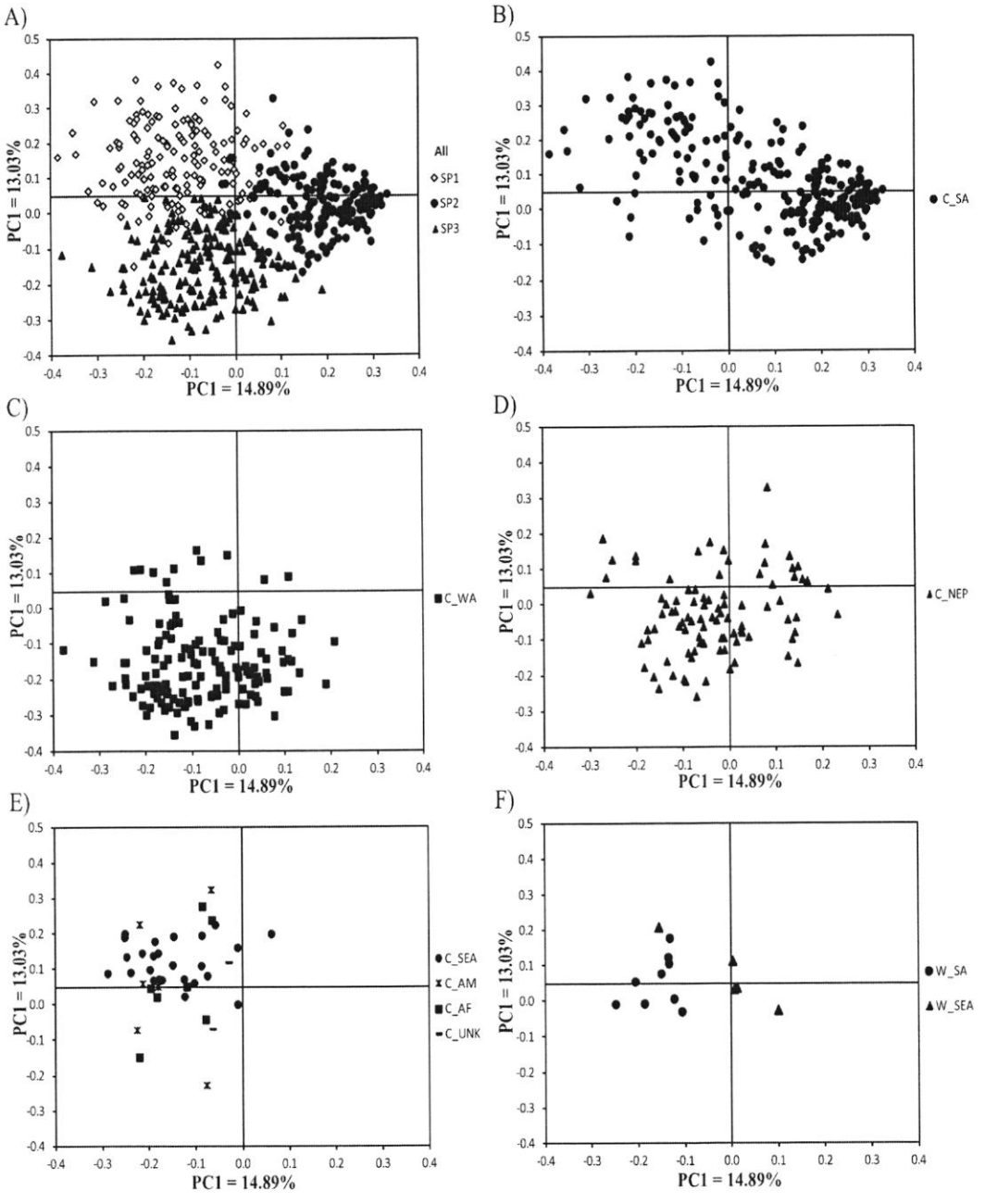


Fig. 1. Distribution of 534 black gram accessions on a scatter plot based on PC1 and PC2 from principal coordinate analysis (PCoA) using Nei's genetic distance (D_A). (A) All accessions, (B) South Asia, (C) West Asia, (D) Himalayan region, (E) Southeast Asia, America, Africa, and unknown origin, and (F) wild germplasm. SP1, SP2, and SP3 in *a* represent accessions of subpopulations I, II, and III, respectively, clustered by STRUCTURE analysis.

showed a similar distribution pattern as those from America (**Fig. 1**E).

Wild black grams from South Asia showed narrow distribution around the middle left half of the plot (**Fig. 1**F). All except one of the wild black grams from Southeast Asia were at the center of the plot and well differentiated from wild black grams from South Asia. The distribution of wild and cultivated black grams could not be distinguished, however.

Neighbor-joining analysis

A phylogenic tree was constructed by neighbor-joining analysis based on D_A among individual black gram accessions. The tree demonstrated that three major clusters exist, in general; accessions in each of the three subpopulations as identified by STRUCUTURE analysis were clustered together (**Fig. 2**). Cluster I is the most diverse cluster and represents subpopulation I. It comprises all wild accessions and many cultivated accessions from South Asia, all cultivated accessions from Southeast Asia and Africa, all except one accession from America, and some accessions from West Asia and the Himalayan region. In this cluster, thirteen accessions (four each from South Asia and West Asia, two from the Himalayan region, and one from Southeast Asia) formed a mini subcluster with all the wild accessions, except two from South Asia. Cluster II principally consisted of accessions from South Asia together with several accessions from the Himalayan region and a few accessions from West Asia. This cluster represents subpopulation III. Accessions from the Himalayan region formed a subcluster in cluster II. Cluster III was mainly composed of accessions from West Asia and the Himalayan region, and represents subpopulation II.

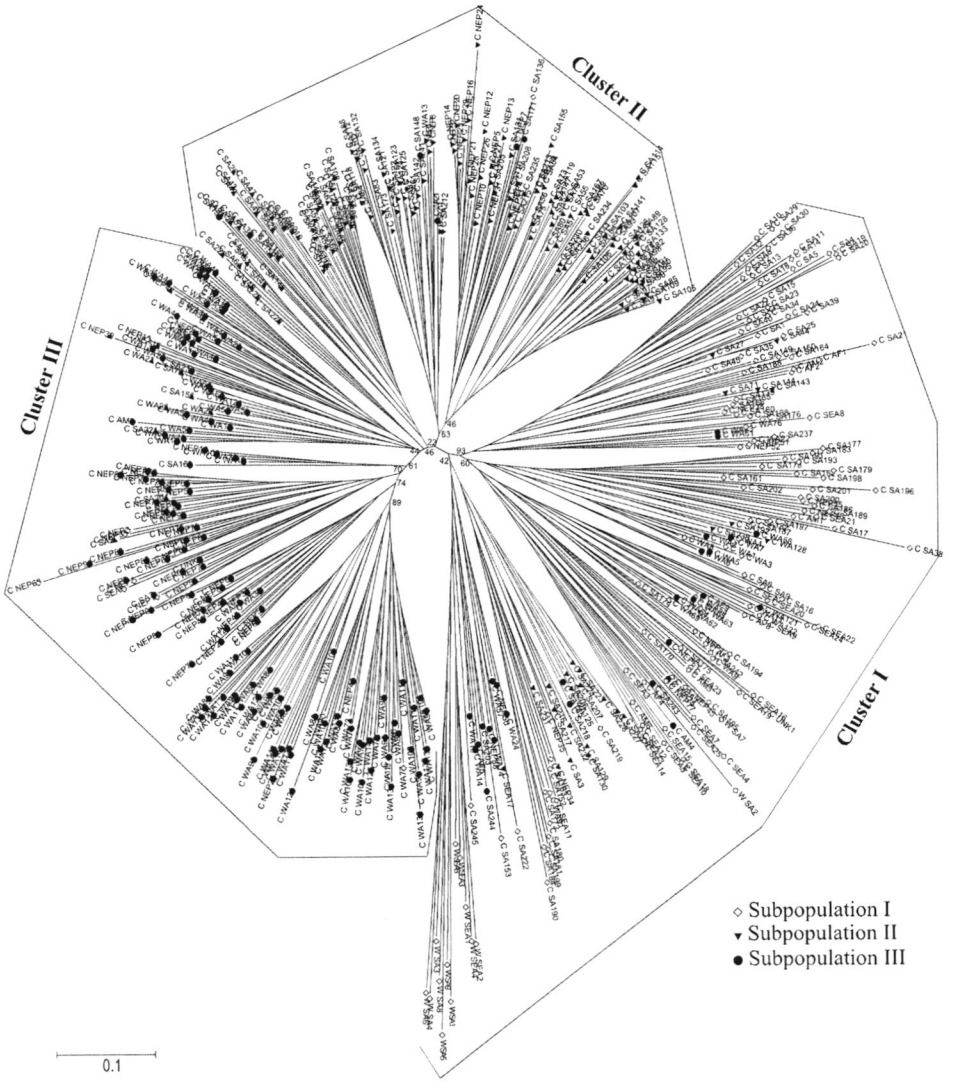


Fig. 2. A neighbor-joining tree of 534 black gram accessions based on Nei's genetic distance (D_A) calculated from SSR allelic data at 22 loci. Diamond, triangle, and circle represent accessions in subpopulations I, II and III, respectively, clustered by STRUCTURE analysis. Bootstrap values at only major nodes are shown.

Table 3. Nei's genetic distance (Nei *et al.* 1983) among different groups of black gram germplasm

Code[a]	C_SA	C_WA	C_NEP	C_SEA	C_AM	C_AF	C_UNK	W_SA
C_WA	0.1331							
C_NEP	0.1181	0.1121						
C_SEA	0.1850	0.1904	0.1902					
C_AM	0.2482	0.2200	0.2537	0.1988				
C_AF	0.2455	0.2363	0.2134	0.2104	0.2571			
C_UNK	0.3565	0.3528	0.2968	0.3271	0.3902	0.3684		
W_SA	0.4186	0.4135	0.4108	0.4144	0.4482	0.4637	0.5957	
W_SEA	0.4548	0.4877	0.4776	0.5024	0.5096	0.5569	0.5718	0.5505

[a] See description for the code in **Table 1**.

Eight accessions from India and one each from Southeast Asia and America were also included in this cluster. Most accessions from the Himalayan region formed a subcluster.

Genetic distance and outcrossing rate

Nei's D_A among black grams of different types and/or from different regions is shown in **Table 3**. The D_A values among cultivated black grams from South Asia, West Asia, and the Himalayan region were low (<0.14). Yet, they showed low distance from cultivated black grams from Southeast Asia. This suggests geographical proximity and a close genetic relationship among them. The D_A values between black grams from Southeast Asia and America or Africa were lower than those between black grams from South Asia or West Asia or the Himalayan region and America or Africa (**Table 3**).

In all cases, D_A between wild and cultivated black grams was moderate (0.41 to 0.56). In general, D_A between cultivated black grams and South Asian wild black grams was lower than D_A between cultivated black grams and Southeast Asian wild black grams. D_A between South Asian and Southeast Asian wild black grams was 0.55, indicating moderate genetic differentiation between wild germplasm from the two regions.

Outcrossing rate in black grams varied among different regions and/or types, with an overall rate of 4.33% (**Tables 1, 4**). Wild black grams showed similar outcrossing rates with cultivated black grams. The minimum outcrossing rate was 1.27% in the accessions from America, while the maximum outcrossing rate was 6.21% in the West Asian cultivated black grams. Based on the country of origin, outcrossing rates were between 0% in Côte d'Ivoire and Trinidad and 16.69% in Zaire.

Discussion

The present study is the first large-scale molecular diversity analysis of black gram, covering accessions from all major growing regions in the world, and including both wild and cultivated types. The use of SSR markers enables comparison of allelic diversity in black gram gene pools with the other crop gene pools in the same genus. In this study the average number of alleles per SSR locus was 9.0. This figure is much lower than that reported for azuki bean (23.9 alleles; 13 SSRs in 548 cultivated and 67 wild accessions) (Xu *et al.* 2008) and mungbean (16.3 alleles; 19 SSRs in 415 cultivated and 189 wild accessions) (Sangiri *et al.* 2007). When only cultivated germplasm was considered, the average number of alleles per SSR locus in black gram (8.1 alleles; **Table 2**) was similar to that in mungbean (7.3 alleles; **Table 4**), Bambara groundnut (*Vigna subterranea*) (7.6 alleles; 22 SSRs in 240 accessions; Somta *et al.* 2011), and rice bean (10.2 alleles; **Table 4**), but still much lower than that in azuki bean (18.5 alleles; **Table 4**). The lower number of alleles found in black gram appears to be due partly to the much smaller number of wild accessions used in this study.

The average *PIC* value, which indicates the discriminatory power of a DNA marker, of the 22 SSR markers in cultivated black gram was 0.59. This value was similar to that in cultivated azuki bean (0.70; Xu *et al.* 2008), rice bean (0.52; Tian *et al.* 2013), and cultivated Bambara groundnut (0.58; Somta *et al.* 2011), but higher than that in mungbean (0.38; Sangiri *et al.* 2007). Markers CEDG305, cp05325, and cp10549 showed higher *PIC* values (>0.80; **Table 2**) than other markers, and thus they are highly informative for cultivar identification of black gram germplasm.

Outcrossing rate of the black gram found in this study (4.33%) is higher than that reported in mungbean (1.06%; Sangiri *et al.* 2007) and is comparable to azuki bean (3.48%; Xu *et al.* 2008), but very much lower than that of rice bean (17.00%; Tian *et al.* 2013) (**Table 4**). Although black gram and mungbean share similar morphological traits and have similar life cycles and ecological habitats (Tomooka *et al.* 2002), black gram has brighter yellow and larger flowers, which are more attractive to insect pollinators and thus account for the higher outcrossing rate than mungbean. The estimated outcrossing rate in mungbean by Sangiri *et al.* (2007) included many wild accessions from Australia, which generally have smaller flowers than those of mungbean from other regions (Lawn and Rebetzke 2006). The difference in outcrossing rate between black gram and rice bean is possibly due to the difference in their flower morphology and life cycle. Black gram has smaller flowers and paler yellow corolla than rice bean (Tomooka *et al.* 2002). Black gram is considered an annual species (Tomooka *et al.* 2002), while rice bean is a perennial species (Tomooka *et al.* 1997). However, it should be noted that the outcrossing rate estimated of black gram in this study was possibly overestimated since bulked DNA samples of each accession were used for the SSR marker analysis (see Materials and Methods). The use of bulked DNA samples may also have caused overestimation for H_O in this study, although the H_O for black gram in this study (0.06) is similar to that reported in mungbean (0.01; Sangiri *et al.* 2007) and azuki bean (0.05; Xu *et al.* 2008) and is lower than that reported in rice bean (0.15; Tian *et al.* 2013).

In Asian *Vigna,* which black gram belongs to, the genetic relationship between cultivated and wild forms of mungbean, azuki bean, and rice bean have been studied. Clear

Table 4. Comparison of gene diversity between black grams and other Asian *Vigna* species

Vigna species	Status and origin	No. of accessions	SSR loci used	N_A[a] (mean per locus)	H_E[b]	T[c]
Black gram	All	534	22	199 (9.04)	0.60	4.33
(*V. mungo*)	Cultivated	420		178 (8.09)	0.59 (87.67%)[d]	
	South Asia (excluding Pakistan)	245		156 (7.09)	0.57	
	West Asia (excluding Pakistan)	143		136 (6.18)	0.52	
	Himalayan region (Nepal)	92		125 (5.68)	0.51	
	Wild	14		115 (5.23)	0.75	
Azuki bean[e]	All	616	13	311 (23.92)	0.76	3.48
(*V. angularis*)	Cultivated	548		240 (18.46)	0.74 (86.05%)[d]	
	East Asia	489		227 (17.46)	0.72	
	Southeast Asia	25		61 (4.69)	0.54	
	Himalayan region (Nepal + Bhutan)	34		72 (5.54)	0.51	
	Wild	68		245 (21.15)	0.86	
Mungbean[f]	All	615	19	309 (16.26)	0.62	1.06
(*V. radiata*)	Cultivated	415		138 (7.26)	0.41 (65.08%)[d]	
	South Asia (including Nepal but excluding Pakistan)	101		105 (5.53)	0.44	
	West Asia (including Pakistan)	112		92 (4.84)	0.45	
	Southeast Asia	131		97 (5.11)	0.32	
	Wild	189		257 (13.53)	0.63	
Rice bean[g]	All	472	13	168 (12.92)	0.61	17.0
(*V. umbellata*)	Cultivated	388		132 (10.15)	0.57 (66.28%)[d]	
	South Asia (excluding Pakistan)	151		106 (8.15)	0.55	
	Southeast Asia (including Nepal)	175		90 (6.92)	0.53	
	Wild	84		245 (18.85)	0.86	

[a] Number of alleles.
[b] Gene diversity.
[c] Percentage of out-crossing rate.
[d] Percentage of gene diversity as compared with its wild species.
[e] Xu *et al.* (2008).
[f] Sangiri *et al.* (2007).
[g] Tian *et al.* (2013).

genetic differentiation between the wild and cultivated gene pools was shown in mungbean (Sangiri *et al.* 2007), but not in azuki bean (Xu *et al.* 2008) and rice bean (Tian *et al.* 2013). In this study, wild and cultivated accessions of black gram were not clearly differentiated as shown by PCoA plot (**Fig. 1**) and phylogenetic tree (**Fig. 2**). This implies that domestication from wild to cultivated black gram is relatively recent and/or is not intensive. However, archaeological evidence suggests that domestication of black gram may be as long as 3,500–4,500 years ago (Fuller and Harvey 2006). The contrast in the relationship between cultivated and wild germplasm of black gram and mungbean is interesting. Both species originated in India, sharing several common morphological characteristics, and are cultivated and utilized in similar ways (Tomooka *et al.* 2002). Compared to wild mungbean, wild black gram has much narrower distribution. The former is present in Africa, Asia, and Australia, while the latter is only found in limited areas of Asia, mainly in India, Myanmar, and Thailand (Tomooka *et al.* 2002). Cultivation of black gram also principally occurs in these countries, while mungbean is more widely cultivated. Narrow geographical distribution and recent or non-intensive domestication of black gram appear to account for the unclear distinction between wild and cultivated forms of this crop.

Gene diversity and A_R from SSR allelic data (**Table 1**) shows that wild black gram possesses higher genetic diversity than cultivated black gram. Although the data revealed that cultivated black grams from all different regions possess a comparable level of gene diversity with low genetic differentiation among each other (**Tables 1**, **3**), the data showed the greatest gene diversity in wild black gram from South Asia. This high diversity is supported by the highest A_R found in the wild black gram from South Asia (**Table 1**). The data also revealed that, among the cultivated black grams, A_R was the highest in accessions from South Asia. This supports the original view of Vavilov (1926) that India is the center of diversity of black gram.

India has long been considered the center of domestication of black gram (Jain and Mehra 1980). Allelic data obtained from SSR markers revealed that cultivated black gram from every region is genetically more similar to Indian wild black gram (W_SA) than to Thai wild black gram (W_SEA) (**Table 3**), although the number and origin of accessions of the wild black gram used in this study were limited. This suggests that cultivated black gram is more likely to be genetically derived from Indian rather than Thai wild black gram and that domestication of black gram was possibly started in India. Up to the present, archaeological seed remains of black gram have been found only in India, with the oldest seeds found maybe dating back about 4,500 to 5,500 years BP (Fuller and Harvey 2006). In addition, the

presence of weedy black gram populations in India (Bisht *et al.* 2005) also supports the long history of domestication of black gram in the country. In this study, black grams from India were separated into two major groups. One group comprises wild and cultivated accessions from various parts of India, the other group comprises only cultivated accessions which mostly come from northern India, especially from the Himalayan foothills, including Uttarakhand, Uttar Pradesh, and Bihar (**Fig. 2** and see also **Supplemental Table 1**). All of the wild accessions with known locality were from Maharashtra (Central Plateau region). Gene diversity of the black grams in the first group was higher than that in the second groups (0.63 vs. 0.46; data not shown). Since wild black gram in India is widespread in the northern parts of Western Ghats, and sporadically occurs in some parts of Rajasthan, Madhya Pradesh, and Maharashtra (Bisht *et al.* 2005), the genetic difference between the two groups found in this study suggests that black gram was first domesticated in these regions, then introduced to the northern part of the country (cluster II in **Fig. 2**) and selected to adapt to the environment.

Black gram and mungbean are closely related species and complement each other as a secondary gene pool. In India, wild black gram and wild mungbean populations generally have the same geographical distribution, although some show distinct distribution (Bisht *et al.* 2005). Based on archaeological findings, wild mungbean was probably domesticated in the Himalayan foothills in the Punjab region, and in the far south of India, while wild black gram was perhaps domesticated in Gujarat and the Northern Peninsula (Fuller and Harvey 2006). Based on protein banding variation in a large set of mungbean germplasm, Tomooka *et al.* (1992) hypothesized that mungbean was domesticated in South Asia, and from there diverse cultivars were introduced to West Asia and Southeast Asia. This hypothesis was supported by SSR allelic data in a large and diverse set of mungbean germplasm that show the same level of diversity between South Asian and West Asian mungbeans, and a high level of diversity in Southeast Asian mungbeans (Sangiri *et al.* 2007). A similar pattern was found in black gram in this study, where cultivated black grams from South Asia, West Asia, and Southeast Asia showed the same level of gene diversity and low genetic distance among each other (**Tables 1**, **3**). Since black gram and mungbean are both domesticated in South Asia, and are grown and used in similar ways, it is possible that they spread to West Asia and Southeast Asia by similar/same process, route, and time period.

Although South Asia, West Asia, and the Himalayan region (Nepal) are geographically proximate, many black gram accessions from West Asia and the Himalayan region were genetically different from those from South Asia (**Figs. 1**, **2**). This suggests that after black gram cultivars from South Asia were introduced into West Asia and the Himalayan region, they were genetically selected and adapted to environments in these two regions, which may be different from their origins. Two major groups exist for black gram from West Asia (**Fig. 2**): one was genetically intermediate between subgroups from South Asia and the Himalayan region, while the other was genetically close to a subgroup from the Himalayan region. This suggests that black gram cultivars in West Asia were introduced from both South Asia and the Himalayan region.

There are two major genetic clusters of black gram from the Himalayan region (Nepal) (**Fig. 2**), one closely associated with a major cluster of black grams from South Asia, especially those from the states near the Himalayan foothills (cluster II; see **Supplemental Table 1** for details on the locality), while the other is associated with black grams from West Asia (cluster III). This suggests that black gram cultivars from the Himalayan region were derived from two different origins. Interestingly, similar results were reported in azuki bean and rice bean. Based on SSR analyses, Xu *et al.* (2008) and Tian *et al.* (2013), respectively, showed that cultivated azuki bean and cultivated rice bean from Nepal were mainly separated into two major groups, western Nepal and eastern Nepal. Although the provenance/locality of many black grams from Nepal is not known, most black grams with known locality (eastern Nepal) were grouped together (cluster III and see also **Supplemental Table 1** for details on the locality). However, gene diversity and A_R between the Himalayan black grams in cluster II and cluster III are comparable (0.42 vs. 0.48 and 2.69 vs. 3.77, respectively; data not shown).

Although cultivated black grams from Southeast Asia possessed high gene diversity (**Table 1**), they mainly showed a close genetic relationship with each other (**Figs. 1**, **2**). The neighbor-joining tree showed that most of the black grams from Southeast Asia were grouped in the same subcluster as some cultivated black grams from South Asia, West Asia, Nepal, Africa, and America, and two wild black grams from South Asia (**Fig. 2**). Thus, this subcluster appears to be different from the others and shows high genetic diversity. In addition, one accession of black gram from Southeast Asia was grouped within a subcluster together with black gram from Nepal (**Fig. 2**). These results suggest that there are multiple times and/or sources of introduction of black gram into Southeast Asia. This is not in line with the history of black gram cultivation in this region; for example, cultivation in Thailand may be only recent (about 60–70 years), using the cultivars introduced from India (Srinives 1990). Additional studies with more accessions from Southeast Asia, especially from Myanmar, which lies between South and Southeast Asia and is possibly a part of the domestication center of black gram, are necessary to clarify the genetic relationship of black grams in this region with those in other regions.

Black gram was introduced to Africa and America in recent times by Indian immigrants (Jain and Mehra 1980) to grow as food and manure crop, which is called "woolly pyrol" in America. Interestingly, gene diversities of cultivated black gram in America and Africa are higher than those in other regions. The neighbor-joining tree revealed that

positions of black grams from these two regions were similar to those from Southeast Asia (**Supplemental Fig. 2**; see also above discussion on black gram from Southeast Asia). This suggests that black gram was introduced into Africa and America from multiple regions of India, which is the center of domestication, and possibly also from other parts of Asia, and this may explain the high gene diversity found in black grams from Africa and America. Based on the plant introduction history of America, a black gram accession was introduced into the country in 1906 from Barbados (Piper and Morse 1914); thus, the introduction of black gram from Asia to America occurred more than 100 years ago. Vertovec (1994) noted that about 95,000 people from India migrated to Trinidad from 1874 to 1917; some of them might have introduced black gram, resulting in the highest gene diversity detected in this study.

Acknowledgements

This study was supported by the Graduate School, Kasetsart University, Thailand, and the Thailand Research Fund (TRF). For providing the black gram germplasm used in this study, we would like to thank the United States Department of Agriculture, USA; Genebank, National Institute of Agrobiological Sciences, Japan; Australian Tropical Crops and Forages Collection, Australia; and Chai Nat Field Crops Research Center, Thailand.

Literature Cited

Anderson, J.A., G.A. Churchill, J.E. Autrique, M.E. Sorells and S.D. Tanksley (1993) Optimizing parental selection for genetic linkage maps. Genome 36: 181–186.

Bisht, I.S., K.V. Bhat, S. Lakhanpaul, M. Latha, P.K. Jayan, B.K. Biswas and A.K. Singh (2005) Diversity and genetic resources of wild *Vigna* in India. Genet. Resour. Crop Evol. 52: 53–68.

Chaitieng, B., A. Kaga, N. Tomooka, T. Isemura, Y. Kuroda and D.A. Vaughan (2006) Development of a black gram [*Vigna mungo* (L.) Hepper] linkage map and its comparison with an azuki bean [*Vigna angularis* (Willd.) Ohwi and Ohashi] linkage map. Theor. Appl. Genet. 113: 1261–1269.

Chandel, K.P.S., R.N. Lester and R.J. Starling (1984) The wild ancestors of urd and mung beans (*Vigna mungo* (L.) Hepper and *V. radiata* (L.) Wilczek). Bot. J. Linn. Soc. 89: 85–96.

Chankaew, S., T. Isemura, S. Isobe, A. Kaga, N. Tomooka, P. Somta, H. Hirakawa, K. Shirasawa, D.A. Vaughan and P. Srinives (2014) Detection of genome donor species of neglected tetraploid crop *Vigna reflexo-pilosa* (créole bean) and genetic structure of diploid species based on newly developed EST-SSR markers from azuki bean (*Vigna angularis*). PLoS One 9: e104990.

Evanno, G., S. Regnaut and J. Goudet (2005) Detecting the number of clusters of individuals using the software STRUCTURE: a simulation study. Mol. Ecol. 14: 2611–2620.

Fuller, D.Q. and E.L. Harvey (2006) The archaeobotany of Indian pulses: identification processing and evidence for cultivation. Environ. Archaeol. 11: 241–268.

Ghafoor, A., A. Sharif, Z. Ahmad, M.A. Zahid and M.A. Rabbani (2001) Genetic diversity in blackgram (*Vigna mungo* L. Hepper). Kaewwongwal, Kongjaimun, Somta, Chankaew, Yimram and Srinives Field Crops Res. 69: 183–190.

Ghafoor, A. and Z. Ahmad (2005) Diversity of agronomic traits and total seed protein in black gram (*Vigna mungo* (L.) Hepper). Acta Biol. Cracov. Bot. 47: 69–75.

Goudet, J. (2002) FSTAT: a program to estimate and test gene diversities and fixation indices. Version 2.9.3.2. Available from http://www.unil.ch/izea/softwares/fstat.html [accessed on 22 May 2011].

Gupta, S., S.R. Gupta, H.K. Dikshit and R.A. Singh (2001) Variability and its characterization in Indian collections of blackgram [*Vigna mungo* (L.) Hepper.]. Plant Genet. Resour. Newsl. 127: 20–24.

Gupta, S.K. and T. Gopalakrishna (2009) Genetic diversity analysis in blackgram (*Vigna mungo* (L.) Hepper) using AFLP and transferable microsatellite markers from azuki bean (*Vigna angularis* (Willd.) Ohwi & Ohashi). Genome 52: 120–129.

Gupta, S.K. and T. Gopalakrishna (2010) Development of unigene-derived SSR markers in cowpea (*Vigna unguiculata*) and their transferability to other *Vigna* species. Genome 53: 508–523.

Jain, H.K. and K.L. Mehra (1980) Evolution adaptation relationships and uses of the species of *Vigna* cultivated in India. *In*: Summerfield, R.J. (ed.) Advances in Legume Science, Royal Botanic Garden Kew, Richmond Surrey, pp. 459–468.

Kongjaimun, A., A. Kaga, N. Tomooka, P. Somta, T. Shimizu, Y. Shu, T. Isemura, D.A. Vaughan and P. Srinives (2012) An SSR-based linkage map of yardlong bean (*Vigna unguiculata* (L.) Walp. subsp. *unguiculata* Sesquipedalis Group) and QTL analysis of pod length. Genome 55: 81–92.

Langella, O. (2002) Populations a free population genetic software. Version 1.2.31. Available from http://bioinformatics.org/~tryphon/populations [Accessed on 12 May 2013].

Lawn, R.J. and G.J. Rebetzke (2006) Variation among Australian accessions of the wild mungbean (*Vigna radiata* ssp. *sublobata*) for traits of agronomics, adaptive, or taxonomic interest. Aust. J. Agric. Res. 57: 119–132.

Lewis, G., B. Schrire, B. Mackinder and M. Lock (2005) Legumes of the world, Kew Royal Botanic Gardens, Richmond Surrey, p. 577.

Li, C.D., C.A. Fatokun, B. Ubi, BB. Singh and G.J. Scoles (2001) Determining genetic similarities and relationships among cowpea breeding lines and cultivars by microsatellite markers. Crop Sci. 41: 189–197.

Lodhi, M.A., G.N. Ye, N.F. Weeden and B.I. Reisch (1994) A simple and efficient method for DNA extraction from grapevine cultivars and *Vitis* species. Plant Mol. Biol. Rep. 12: 6–13.

Lynch, M. and B.G. Milligan (1994) Analysis of population genetic structure using RAPD markers. Mol. Ecol. 3: 91–99.

Maréchal, R., J.M. Mascherpa and F. Stainier (1978) Etude taxonomique d'un groupe complex d'espèces des geners *Phaseolus* et *Vigna* (Papilionaceae) sur la base de données morphologiques et polliniques traitées par l'analyse informatique. Boissiera 28: 1–273.

Nei, M., F. Tajima and Y. Tateno (1983) Accuracy of estimated phylogenetic trees from molecular data. J. Mol. Evol. 19: 153–170.

Piper, C.V. and W.J. Morse (1914) Five oriental species of beans. Bull. USDA 119: 1–32.

Pritchard, J.K., M. Stephens and P. Donnelly (2000) Inference of population structure using multilocus genotype data. Genetics 155: 945–959.

R Development Core Team (2012) R: A language and environment for statistical computing, R Foundation for Statistical Computing, Vienna, Austria.

Sangiri, C., A. Kaga, N. Tomooka, D.A. Vaughan and P. Srinives (2007) Genetic diversity of the mungbean (*Vigna radiata* Leguminosae)

genepool on the basis of microsatellite analysis. Aust. J. Bot. 55: 837–847.

Seehalak, W., P. Somta, W. Sommanas and P. Srinives (2009) Microsatellite markers for mungbean developed from sequence database. Mol. Ecol. Resour. 9: 862–864.

Singh, A.K., A. Mishra and A. Shukla (2009) Genetic assessment of traits and genetic relationship in blackgram (*Vigna mungo*) revealed by isoenzymes. Biochem. Genet. 47: 471–485.

Sivaprakash, K.R., S.R. Prashanth, B.P. Mohanty and A. Parida (2004) Genetic diversity of black gram (*Vigna mungo*) landraces as evaluated by amplified fragment length polymorphism markers. Curr. Sci. 86: 1411–1416.

Somta, P., W. Musch, B. Kongsamai, S. Chanprame, S. Nakasathien, T. Toojinda, W. Sorajjapinun, W. Seehaluk, S. Tragoonrung and P. Srinives (2008) New microsatellite markers isolated from mungbean (*Vigna radiata* (L.) Wilczek). Mol. Ecol. Resour. 8: 1155–1157.

Somta, P., W. Seehalak and P. Srinives (2009) Development characterization and cross-species amplification of mungbean (*Vigna radiata*) genic microsatellite markers. Conserv. Genet. 10: 1939–1943.

Somta, P., S. Chankaew, O. Rungnoi and P. Srinives (2011) Genetic diversity of the Bambara groundnut (*Vigna subterranea* (L.) Verdc.) as assessed by SSR markers. Genome 54: 898–910.

Souframanien, J. and T. Gopalakrishna (2004) A comparative analysis of genetic diversity in blackgram genotypes using RAPD and ISSR markers. Theor. Appl. Genet. 109: 1687–1693.

Srinives, P. (1990) Mungbean breeding and genetic resources in Thailand. *In*: Thavarasook, C., P. Srinives, N. Boonkerd, H. Imai, A. Pookpakdi, P. Laosuwan and U. Pupipat (eds.) Proceedings of the Mungbean Meeting 90. Japan Tropical Agricultural Research Center, Bangkok, pp. 31–41.

Tamura, K., G. Stecher, D. Paterson, A. Filipski and S. Kumar (2013) MEGA6: molecular evolutionary genetics analysis version 6.0. Mol. Biol. Evol. 30: 2725–2729.

Tangphatsornruang, S., P. Somta, P. Uthaipaisanwong, J. Chanprasert, D. Sangsrakru, W. Seehalak, W. Sommanas, S. Tragoonrung and P. Srinives (2009) Characterization of microsatellites and gene contents from genome shotgun sequences of mungbean (*Vigna radiata* (L.) Wilczek). BMC Plant Biol. 9: 137.

Tian, J., T. Isemura, A. Kaga, D.A. Vaughan and N. Tomooka (2013) Genetic diversity of the rice bean (*Vigna umbellata*) genepool as assessed by SSR markers. Genome 56: 717–727.

Tomooka, N., C. Lairungreang, P. Nakeeraks, Y. Egawa and C. Thavarasook (1992) Center of genetic diversity and dissemination pathways in mung bean deduced from seed protein electrophoresis. Theor. Appl. Genet. 83: 289–293.

Tomooka, N., S. Chotechuen, N. Boonkerd, B. Taengsan, S. Nuplean, D.A. Vaughan, Y. Egawa, T. Yogoyama and Y. Tateishi (1997) Collection of seed and nodule samples from wild subgenus *Ceratotropis* species (genus *Vigna*) in central and northern Thailand. Annual report on exploration and introduction of plant genetic resources 13: 189–206.

Tomooka, N., D.A. Vaughan, H. Moss and N. Maxted (2002) The Asian *Vigna*: genus *Vigna* subgenus *Ceratotropis* genetic resources, Kluwer Academic Publishers, The Netherlands, p. 270.

Tomooka, N., A. Kaga and D.A. Vaughan (2006) The Asian *Vigna* (*Vigna* subgenus *Ceratotropis*) biodiversity and evolution. *In*: Sharma, A.K. and S. Sharma (eds.) Plant Genome; Biodiversity and Evolution. Volume 1 part C. Phanerograms (Angiosperms Dicotyledons), Science Publishers, New Jersey, pp. 87–126.

Vavilov, N.I. (1926) Centers of origin of cultivated plants. Bull. Appl. Bot. 26:1–248.

Vertovec, S. (1994) "Official" and "Popular" Hinduism in the Caribbean: historical and contemporary trends in Surinam, Trinidad and Guyana. Contrib. Indian Soc. 28: 123–147.

Wang, X.W., A. Kaga, N. Tomooka and D.A. Vaughan (2004) The development of SSR markers by a new method in plants and their application to gene flow studies in azuki bean [*Vigna angularis* (Willd.) Ohwi & Ohashi]. Theor. Appl. Genet. 109: 352–360.

Weir, B.S. (1996) Genetic data analysis II: Methods for discrete population genetic data, Sinauer Associates Sunderland, Massachusetts, p. 445.

Xu, H.X., J. Tian, N. Tomooka, A. Kaga, T. Isemura, and D.A. Vaughan (2008) Genetic diversity of the azuki bean (*Vigna angularis* (Willd.) Ohwi & Ohashi) gene pool as assessed by SSR markers. Genome 51: 728–738.

022/2558

Theor Appl Genet (2015) 128:1881–1892
DOI 10.1007/s00122-015-2554-5

ORIGINAL PAPER

A single base substitution in *BADH/AMADH* is responsible for fragrance in cucumber (*Cucumis sativus* L.), and development of SNAP markers for the fragrance

Chutintorn Yundaeng[1] · Prakit Somta[2] · Sithichoke Tangphatsornruang[3] · Sompong Chankaew[1] · Peerasak Srinives[2]

Received: 17 May 2014 / Accepted: 5 June 2015 / Published online: 17 June 2015
© Springer-Verlag Berlin Heidelberg 2015

Abstract

Key message **Sequence analysis revealed that an SNP (A1855G) in *CsBADH* of cucumber accession PK2011T202 causes amino acid change in a highly conserved motif, Y163C. Gene mapping showed association between the SNP and the fragrance.**

Abstract Pandan-like fragrance is a value-added trait in several food crops such as rice, vegetable soybean and sorghum. The fragrance is caused by the volatile chemical 2-acetyl-1-pyrroline (2AP). Mutation(s) in *betaine aldehyde dehydrogenase2* (*BADH2*; also known as *aminoaldehyde dehydrogenase2*) gene causes defective BADH2 and results in biosynthesis of 2AP. Recently, cucumber cultivars possessing pandan-like fragrance were discovered in Thailand. In this study, we report an association between *CsBADH* and the fragrance in cucumber accession "PK2011T202". Gene expression analysis of *CsBADH* in leaves of PK2011T202 and "301176" (non-fragrant) at various growth stages revealed that *CsBADH* was expressed in both accessions. Sequence comparison of *CsBADH* showed that PK2011T202 possesses a single base substitution (A1855G) in exon 5 which causes an amino acid change in a highly conserved motif of BADH, Y163C. Single nucleotide-amplified polymorphism markers were developed to detect the SNP polymorphism between the wild-type and fragrance alleles. Since *CsBADH* is located on chromosome 1, quantitative trait locus (QTL) mapping was conducted for this chromosome using an F_2 and a backcross populations developed from the cross between PK2011T202 and 301176. QTL analysis in both populations showed that the major QTL for fragrance, *qFgr*, was co-localized with the *CsBADH*. We concluded that the defect function of CsBADH is responsible for fragrance in cucumber PK2011T202.

Communicated by A. J. Bervillé.

Electronic supplementary material The online version of this article (doi:10.1007/s00122-015-2554-5) contains supplementary material, which is available to authorized users.

✉ Prakit Somta
pksomta@gmail.com

[1] Program in Plant Breeding, Faculty of Agriculture at Kamphaeng Saen, Kasetsart University, Kamphaeng Saen, Nakhon Pathom 73140, Thailand

[2] Department of Agronomy, Faculty of Agriculture at Kamphaeng Saen, Kasetsart University, Kamphaeng Saen, Nakhon Pathom 73140, Thailand

[3] National Center for Genetic Engineering and Biotechnology, 113 Phaholyothin Road, Khlong Nueng, Khlong Luang, Pathumthani 12120, Thailand

Introduction

Cucumber (*Cucumis sativus* L.; *Cucurbitaceae*) ($2n = 2x = 14$) is one of the most economically important vegetable crops in the world with the total production of more than 60 Mt per annum. Cucumber fruits are consumed in fresh or cooked or pickled forms. China is the largest producer followed by Iran and Turkey with the annual production of about 47.31, 1.82, and 1.75 Mt, respectively (FAOSTAT 2013). Traits determining cucumber fruit quality include stripes, spine color, fruit color, weigh, length, diameter and firmness.

India is the center of origin and domestication of cucumber, where cultivated (*C. sativus* var *sativus* L.) and wild (*C. sativus* var. *hardwickii*) forms coexist. Thailand, especially the northern region, is a part of the center of diversity where *C. sativus* var. *hardwickii* and primitive

Author's personal copy

cucumber cultivars are found (de Wilde and Duyfjes 2010). Recently, a few cucumber cultivars with fragrance fruits were found in Thailand. Their fruits and leaves have pandan (*Pandanus amaryllifolius* L.)-like fragrance (Pramnoi et al. 2013) which is the same as those possessed by fragrant rice (*Oryza sativa* L.), soybean [*Glycine max* (L.) Merr.] and sorghum [*Sorghum bicolor* (L.) Moench]. The pandan-like fragrance in the latter three crops is caused by the presence of the volatile chemical compound 2-acetyl-1-pyrroline (2AP) (Buttery et al. 1983; Fushimi and Masuda 2001; Yundaeng et al. 2013). Genetic studies demonstrated that the fragrance in these crops is controlled by a single recessive gene (AVRDC 2003; Ayyangar 1938; Berner and Hoff 1986; Murty et al. 1982; Sood and Siddiq 1978). Gene mapping and molecular genetic studies in these crops demonstrated that mutation(s) in *betainealdehyde dehydrogenase 2* (*BADH2*) (also known as *aminoaldehyde dehydrogenase*; *AMADH2*) gene results in the null and reduced function of BADH2 protein and causes accumulation of 2AP which is responsible for the fragrance (Bradbury et al. 2005; Wanchana 2005; Chen et al. 2008; Kovach et al. 2009; Juwattanasomran et al. 2011, 2012; Yundaeng et al. 2013). In rice, insertion, deletion, or substitution in *OsBADH2* that causes premature stop codon or amino acid change is responsible for fragrance (Bradbury et al. 2005; Shi et al. 2008; Kovach et al. 2009). In case of soybean, deletion or single base substitution in *GmBADH2* results in premature stop codon and amino acid change that associates with the fragrance (Juwattanasomran et al. 2011, 2012). For sorghum, deletion in *SbBADH2* causes premature stop codon and gives rise to the fragrance (Yundaeng et al. 2013). Apart from *OsBADH2*, mutation in *OsBADH1* also associates with fragrance in rice, although the effect is far less than that of *OsBADH2* (Amarawathi et al. 2008).

Genetic control of fragrance in cucumber has been reported recently (Pramnoi et al. 2013). The authors found that the fragrance in fruits and leaves is controlled by a single recessive gene, proposed as *fgr* with no xenia effect for the fragrance. However, molecular basis of the fragrance in cucumber has not yet been determined. Since *BADH* is responsible for the fragrance in rice (Bradbury et al. 2005), soybean (Juwattanasomran et al. 2011), and sorghum (Yundaeng et al. 2013), this gene is hypothesized as the candidate gene responsible for the fragrance in cucumber.

In this paper, we reported a molecular genetic basis of fragrance in cucumber accession PK2011T202. The objectives of this study were (1) to determine the association between the candidate gene *BADH* and the fragrance in cucumber, and (2) to develop a functional marker for the fragrance. Information on the causal gene and the functional marker(s) will be useful for breeding new fragrant cucumber cultivars.

Materials and methods

Plant materials and DNA extraction

Two cucumber accessions, "PK2011T202" and "301176", were used as parents for population development. PK2011T202 is a local cultivar from Thailand which possesses strong pandan-like fragrance; while 301176, an inbred line from Clover Seed Company, Hong Kong possesses no fragrance. These two accessions were the same parents used in inheritance study of fragrance reported earlier by Pramnoi et al. (2013). Quantification of 2AP content in fruit by head-space gas chromatography revealed that PK2011T202 had high 2AP while 301176 had no 2AP (Wongpornchai and Somta, unpublished data). PK2011T202 (as female parent) was hybridized by 301176 to develop F_1 seeds. F_1 plants were grown in a crossing block in which one plant was self-pollinated to produce an F_2 population comprising 123 individuals. Other F_1 plants were backcrossed as female parent to PK2011T202 to develop a BC_1F_1 population comprising 138 individuals. The F_2 plants and 10 plants from each of the parents were grown in an experimental field of Kasetsart University, Kamphaeng Saen Campus, Nakhon Pathom, Thailand during August to October 2013. Similarly, the BC_1F_1 plants and 10 plants from each of the parents were grown in pots (one plant per pot) at Kasetsart University, Kamphaeng Saen Campus, Nakhon Pathom, Thailand during February to April 2014. The materials were used for DNA extraction and fragrance evaluation by olfactory test.

Total genomic DNA of the parental, BC_1F_1 and F_2 plants was extracted from young leaves as per Lodhi et al. (1994) with minor modification. DNA concentration was estimated on 1 % agarose gel electrophoresis by comparing with a known concentration λ DNA, and adjusted to10 ng/μl for DNA marker analysis.

Evaluation for fragrance

The fragrance was evaluated by olfactory test following Sood and Siddiq (1978). At 30 days after planting (DAP), young leaves of parental, F_2, and BC_1F_1 plants were excised and used for the test. The leaves from each plant were weighted for three grams and cut into pieces of about 0.5 × 0.5 cm, put in a 25-ml tube and added with 15 ml of 1.7 % KOH (w/v) at 40 °C for 10 min. Subsequently, the tube was opened and smelled directly by 5 volunteers. The fragrance was scored as 1 (no fragrance), 2 (mildly to moderately fragrance), or 3 (highly fragrance). Average scores of the 5 volunteers were used for segregation and QTL analyses.

Author's personal copy

Chi-square (χ^2) analysis

Chi-square (χ^2) analysis for segregation of fragrance scores in the F_2 and BC_1F_1 populations was performed using the *R*-Program 2.10.0 (R Development Core Team 2010). The plants with score higher than 1.5 were classified as fragrant, while those with score equal to or lower than 1.5 were classified as non-fragrant.

Expression analysis of the *CsBADH*

PK2011T202 and 301176 were grown in pots in a greenhouse under natural condition during May to June 2012. At 15, 30 and 45 DAP, 0.5 g of young fresh leaves from three plants of each accession were harvested for extraction of total RNA using Concert™ Plant RNA Reagent (Invitrogen). Each RNA sample was derived from a single different plant. The RNA was treated with DNA-free™ DNaseI (Ambion) and converted to cDNA using RevertAid H Minus First Strand cDNA Synthesis Kit (Fermentas) according to manufacturer's instruction. cDNA concentration was quantified using ND-1000 Spectrophotometer (NanoDrop Technologies, Inc., DE, USA).

A complete cDNA sequence of *BADH* from melon (*Cucumis melo* L.) (Genbank accession number JN091961), a closely related species to cucumber, was used for BLAST search against reference genome sequences of cucumber lines "Gy14" and "9930" in Phytozome v9.1 database (http://www.phytozome.net/cucumber) and Cucumber Genome Database (http://cucumber.genomics.org.cn), respectively, to identify the candidate gene(s) for BADH in cucumber. Annotated gene sequences identified as *BADH* (*Cucsa.197230* in Gy14 and *Csa005363* in 9930) were used in designing primers for real-time PCR analysis using Primer3 (Rozen and Skaletsky 2000) (Table S1). Primers were also designed for the *ACTIN* based on sequence of Genbank accession number AB698859 (Table S1). Real-time PCR analysis was carried out following Yundaeng et al. (2013). Three analyses (three biological replicates) were conducted at each growing stage. Expression of *CsBADH* was quantified with *ACTIN* normalization using Livak method (Livak and Schmittgen 2001).

Sequencing of the *CsBADH* gene and development of allele-specific markers

Eleven primer pairs (Table S2) were designed to amplify a genomic region of 5.068 kb covering the *CsBADH*. PCR was performed in a total volume of 25 μl containing 20 ng genomic DNA, 1 × *Taq* buffer, 2 mM $MgCl_2$, 0.2 mM dNTPs, 0.1 U *Taq* DNA polymerase (Fermentas), and 0.5 μM each of forward and reverse primers. Amplification was performed in a GeneAmp PCR9700 System (Applied Biosystems) programmed as follows: 94 °C for 3 min, 35 cycles of 94 °C for 30 s, 55 °C for 30 s, 72 °C for 2 min, and 72 °C for 5 min. PCR products were then electrophoresed on agarose gel and purified using E-gel® CloneWell™ Agarose Gels (Invitrogen). The purified PCR products were sequenced by Macrogen Co. Ltd. (South Korea) using BigDye® Terminator v3.1 Cycle Sequencing Kit on an ABI 3730xl DNA Analyzer (Applied Biosystems). The individual sequences were assembled using software Sequencher 5.0 (Gene Code Corporation). The complete sequences of *CsBADH2* of PK2011T202 and 301176 were submitted to GenBank as the accession numbers KJ577629 and KJ577628, respectively.

The *CsBADH* sequences from PK2011T202, 301176, Gy14 and 9930 were aligned using ClustalW (http://www.ebi.ac.uk/clustalw) to identify polymorphic sites among them. Predicted protein sequences encoded from these genes were also aligned using the same software.

Upon identification of a single nucleotide polymorphism (SNP) that may cause the fragrance, single nucleotide-amplified polymorphism (SNAP) markers specific to wild-type and mutant alleles were designed using WebSNAPPER (Drenkard et al. 2000; http://pga.mgh.harvard.edu/cgi-bin/snap3/websnaper3.cgi). The SNAP markers were tested in the parents by PCR amplification. The amplification conditions included 94 °C for 3 min, followed by 28 cycles at 94 °C for 30 s, 60 °C for 30 s, 72 °C for 30 s, and 72 °C for 5 min. The PCR products were run on 1 % agarose gel electrophoresis, stained with ethidium bromide and visualized under ultraviolet light. The markers were then analyzed in the F_2 and BC_1F_1 plants.

Linkage map and QTL analyses

Forty-three simple sequence repeat (SSR) markers evenly covering chromosome 1 of cucumber (Ren et al. 2009) were screened for polymorphism between PK2011T202 and 301176. In addition, 11 SSR markers developed from sequence information of *CsBADH* gene (*Cucsa.197230*) or nearby genomic regions (Table 1) were also used. PCR amplification, electrophoresis and DNA band visualization were performed as described by Somta et al. (2008) with an exception that PCR contained 10 ng of genomic DNA. Polymorphic markers were used to analyze the F_2 and BC_1F_1 populations.

A linkage map was constructed using MapMaker3.0 (Lander et al. 1987) with the LOD score of 3, the maximum recombination frequency (r) of 4.0 and Kosambi's mapping function (Kosambi 1944). QTL analysis was conducted to locate the gene controlling fragrance in the F_2 and BC_1F_1 population by composite interval mapping (CIM) using Windows QTL Cartographer 2.5 (Wang et al. 2012). Significant LOD threshold for the QTL was determined by 10,000 runs of permutation test at $P = 0.01$.

Author's personal copy

Table 1 PCR primers designed for real-time PCR analysis of *CsBADH* and the reference *ACTIN* genes. The annealing temperature for all primers is 58 °C

Primer name	Target gene	Primer sequence	PCR product size (bp)
Cs_BADH	*BADH*	F: GGCTGTTCGTGCCAAGTATT	149
		R: AGTAATCGAAGCACCCAGCA	
Cs_ACTIN	*ACTIN*	F: AGGCCGTTCTGTCCCTCTAC	150
		R: CAGTAAGGTCACGACCAGCA	

Phylogenetic analysis

BADH/AMADH protein sequences of plants [*Arabidopsis thaliana* (AAM13070.1 and AAK44148.1), *Amaranthus hypochondriacus* (AAB58165.1 and AAB70010.1), *Atriplex hortensis* (ABF72123.1 and P42757.1), *Avicennia marina* (AAK55121.1 and BAB18544.1), *Beta vulargis* (BAE07176.1), *Cucumis melo* (AEK81574.1), *C. sativus* (Cucsa.197230), *G. max* (BAG09376.1 and BAG09377.1), *Gossypium hirsutum* (AAR23816.2), *Hordeum vulgare* (BAB62846.1 and BAB62847.1), *Lycium barbarum* (ACQ99195.1), *Leymus chinensis* (BAD86757.1 and BAD86758.1), *O. sativa* (NP_001053016.1_and NP_001061833.1), *Picea sitchensis* (ACN40431.1), *Pisum sativum* (CAC48392.3/CAC48393.2), *Populus trichocarpa* (XP_002322147.2 and DR448910), *Solanum lycopersicum* (AAX73303.1 and ACI43573.1), *Solanum tuberosum* (PGSC0003DMT400083025 and PGSC0003DMT400063205), *Sorghum bicolor* (06g019200.1 + 06g019210.1 and AGZ15751.1), *Spinacia oleracea* (AAA34025.1), *Vitis vinifera* (XP_002283690.1 and XP_002281984.1), *Zea mays* (ACS74867.1 and ACS74868.1), *Zoysia tenuifolia* (BAD34953.1 and BAD34949.1) and *Physcomitrella patens* (EDQ78577.1)] were obtained from GenBank or Phytozome (www.phytozome.net), or Sol Genome (http://solgenomics.net) databases. Phylogenetic analysis was performed using Phylogeny.fr (Dereeper et al. 2008) in which the sequences were subjected to multiple sequence alignments by MUSCLE 3.7, and then to phylogenetic tree construction by maximum likelihood with 1000 bootstraps.

Results

Fragrance variation in the F_2 and BC_1F_1 populations and inheritance of the fragrance

Fragrance scores evaluated by olfactory test of leaves in the F_2 population ranged from 1.0 to 2.8 with the mean of 1.45. Similarly, the fragrance scores in the BC_1F_1 population varied from 1 to 3 with the mean of 1.64. The scores for PK2011T202 and 301176 were 3 (highly fragrant) and 1 (non-fragrant), respectively. Frequency distribution of

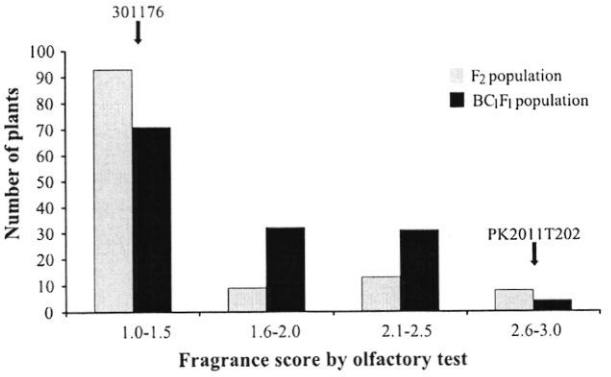


Fig. 1 Frequency distribution of fragrance scores in the F_2 (301176 × PK2011T202) and BC_1F_1 [(301176 × PK2011T202) × PK2011T202] populations evaluated by olfactory test

fragrance scores of both populations in Fig. 1 showed a skewed distribution toward the non-fragrant parent.

Inheritance of the fragrance was determined based on olfactory test in the F_2 and BC_1F_1 populations. In the F_2 population, 30 and 93 F_2 plants were classified as fragrant and non-fragrant, respectively. In the BC_1F_1 population, 71 and 67 plants were classified as fragrant and non-fragrant, respectively. The segregation in the F_2 population fitted well with a 3 (non-fragrant):1 (fragrant) ratio ($\chi^2 = 0.0244$, $P = 0.8759$), while that in the BC_1F_1 population fitted a 1 (non-fragrant):1 (fragrant) ratio ($\chi^2 = 0.1159$, $P = 0.7335$). These indicated that the fragrance in cucumber accession PK2011T202 is conditioned by a single recessive gene.

Identification and expression analysis of *CsBADH*

BLAST search using *CmBADH* against cucumber reference genome sequences at Phytozome and Cucumber Genome databases identified one annotated locus in each database as *CsBADH* gene; *Cucsa.197230* (scaffold01357:699724..704791) in the former and *Csa005363* (chromosome01:1164184..1168771) in the latter databases. CDS comparison revealed that *Cucsa.197230* and *Csa005363* are the same loci. Based on *Cucsa.197230*, *CsBADH* has genomic sequence of 5068 nucleotides, transcript sequence of 2003 nucleotides, coding sequence

Author's personal copy

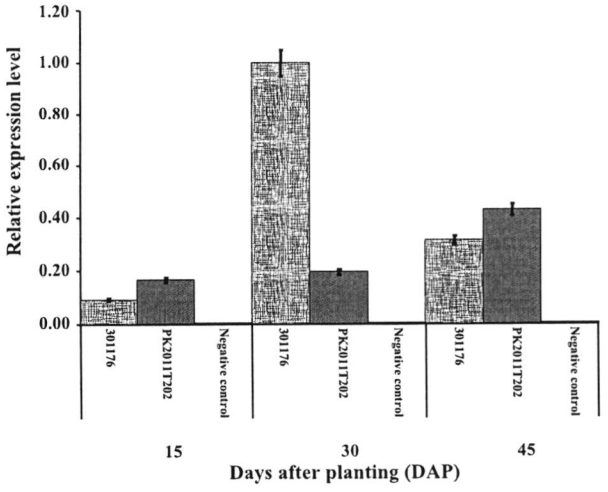


Fig. 2 Expression of *CsBADH2* in fully expanded leaves of PK2011T202 and 301176 at 15, 30 and 45 days after planting (DAP)

(CDS) of 1512 nucleotides from 15 exons, and protein sequence of 503 amino acids.

Expression of *CsBADH* in PK2011T202 and 301176 was determined in leaves at 15, 30 and 45 DAP using real-time PCR analysis. The *CsBADH* showed constitutive expression at all three growth stages of both accessions (Fig. 2). 301176 showed the highest expression level at 30, followed by 45, and 15 DAP, respectively. PK2011T202 had the greatest expression level at 45, followed by 30, and 15 DAP, respectively. The χ^2 test for homogeneity revealed that expression levels of *CsBADH* at all three growth stages in both cucumber varieties were not different ($\chi^2 = 0.43$, P value $= 0.81$). A t test at $P = 0.01$ for *CsBADH* expression level of the two varieties at each growth stages showed that they were not different ($t = 0.5384$ and P value $= 0.6189$; $t = -3.1884$ and P value $= 0.03327$; and $t = 0.4819$ and P value $= 0.6550$, respectively).

Sequence and allele-specific markers of *CsBADH*

Sequences of *CsBADH* in both PK2011T202 and 301176 were determined and compared with the reference sequences to identify mutation(s). The sequence length of *CsBADH* in 301176 was 4594 bp, while that of PK2011T202 was only 4577 bp (Fig. 3). When the sequences of PK2011T202 and 301176 were aligned against the reference sequences, 14 mutations, 6 single base substitutions, and 8 indels were observed. All the substitutions were in exons (exons 1, 2, 4, 5, 8 and 9), while all the indels were in introns (four 1-bp deletion each in intron 1, 4, 8, and 11, a 3-bp deletion in intron 10, a 4-bp deletion in intron 4, a 5-bp deletion in intron 13, and a 6-bp deletion in intron 2). The substitutions in exons 1, 4, 5 and 8 caused amino acid changes. However, only the mutation in exon 5 is unique to the fragrant cucumber PK2011T202. This mutation is the nucleotide change from adenine (A) in 9930, Gy14 and 301176 to guanine (G) in PK2011T202 at the position 1855. The SNP introduced an amino acid change from tyrosine (Y) to cytosine (C) at the position 163 (Y163C) of CsBADH (Fig. 4).

Six SNAP markers were developed to detect the SNP in exon 5; three each for the wild-type (A) and mutant (G) alleles in 301176 and PK2011T202, respectively (Table 2). All three SNAP markers for the wild type amplified DNA band in 301176, while two SNAP markers for the mutant, CsBADH_G1 and CsBADH_G3, amplified DNA band in PK2011T202 (Fig. 5a). DNA band patterns amplified by SNAP markers CsBADH_A1 and CsBADH_G1 in some F_2 plants are shown in Fig. 5b.

Linkage map and QTL analyses

QTL mapping was conducted in the F_2 and BC_1F_1 populations to determine the association between fragrance and *CsBADH*. Marker screening revealed that 11 out of 43 SSR markers gave polymorphism between the parents. The 11 polymorphic SSR markers and the marker CsBADH-AG were used to construct linkage group. The linkage groups in the F_2 and BC_1F_1 populations spanned 61.0 and 152.2 cM in length, respectively (Fig. 5).

Single marker regression analysis in both populations revealed that 10 markers associated with the fragrance. The markers explained 9.74 to 58.83 % of the fragrance variation in the F_2 population and 6.26 to 55.14 % in the BC_1F_1 population (Supplementary Table S3).

LOD thresholds for QTL determined by permutation test of fragrance score in the F_2 and BC_1F_1 populations were 6.1 and 5.7, respectively. CIM identified single major QTL for fragrance score, *qFgr*, in the F_2 and BC_1F_1 populations with LOD scores of 44.45 and 19.96, respectively (Fig. 6). In the F_2 population, the *qFgr* was located 1.1 cM away from the SNAP marker CsBADH-AG and accounted for 80.85 % of the fragrance score variation. The *qFgr* showed additive and dominant effects of non-fragrant (301176) allele at the olfactory scores of −0.34 and −0.58, respectively. In the BC_1F_1 population, the QTL was 1.0 cM from the SNAP marker and explained 43.27 % of the fragrance variation. Additive effect of the non-fragrant allele in this population was −0.72. In both populations, alleles from PK2011T202 increased the fragrance score.

Phylogenetics of CsBADH

Phylogenetic analysis was performed to determine the relationship of CsBADH with other monocot and dicot BADHs/AMADHs. The phylogenetic tree revealed two

Author's personal copy

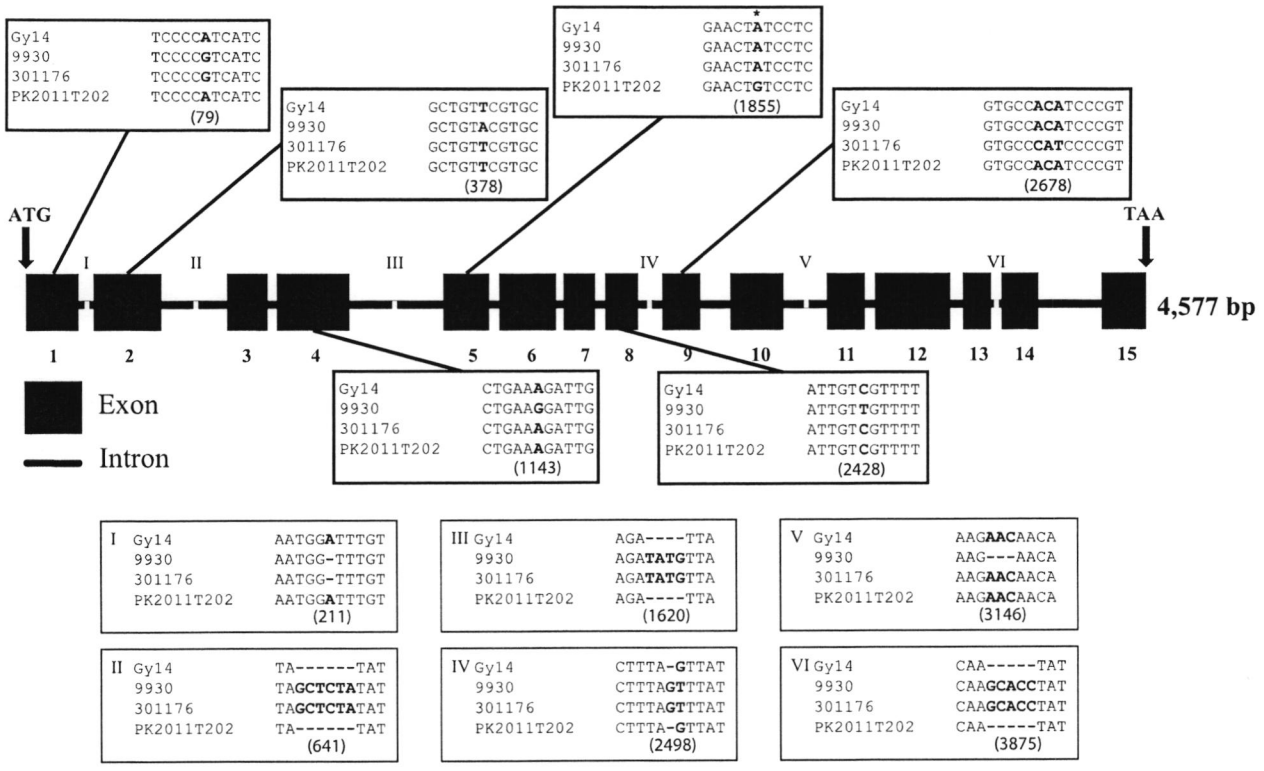


Fig. 3 A scheme depicting the location of SNPs and indels in *CsBADH* among cucumber accession PK2011T202, 301176, and the reference sequences. Start codon (ATG), 15 exons (*solid boxes*), 14 introns (*solid line*) and stop codon (TAA) are illustrated. SNPs and indels are bolded. *Asterisk* indicates the SNP that caused amino acid change specific to PK2011T202. Roman numbers indicate mutations in introns

```
9930          MAISIPTRQLFIDGEWREPVLKKRIPVINPTTEETIGSIPAATAEDVELAVDAARKALARNKGKDWRSASGAVRAKYLRAIAAKITERKSELAKLEAIDCGKPLEEAAWDMDDVAGCFDY 120
Gy14          MAISIPTRQLFIDGEWREPVLKKRIPIINPTTEETIGSIPAATAEDVELAVDAARKALARNKGKDWRSASGAVRAKYLRAIAAKITERKSELAKLEAIDCGKPLEEAAWDMDDVAGCFDY 120
301176        MAISIPTRQLFIDGEWREPVLKKRIPVINPTTEETIGSIPAATAEDVELAVDAARKALARNKGKDWRSASGAVRAKYLRAIAAKITERKSELAKLEAIDCGKPLEEAAWDMDDVAGCFDY 120
PK2011T202    MAISIPTRQLFIDGEWREPVLKKRIPIINPTTEETIGSIPAATAEDVELAVDAARKALARNKGKDWRSASGAVRAKYLRAIAAKITERKSELAKLEAIDCGKPLEEAAWDMDDVAGCFDY 120

                                                                                *
9930          YADLAEGLDAKQKAPVDVPMDTFKSYVLKEPIGVVGLITPWNYPLLMCAWKVAPALAAGCAAILKPSELASVTSLELAEICKDVGLPSGILNVLTGYGPEAGAPLASHPHVDKVAFTGSS 240
Gy14          YADLAERLDAKQKAPVDVPMDTFKSYVLKEPIGVVGLITPWNYPLLMCAWKVAPALAAGCAAILKPSELASVTSLELAEICKDVGLPSGILNVLTGYGPEAGAPLASHPHVDKVAFTGSS 240
301176        YADLAERLDAKQKAPVDVPMDTFKSYVLKEPIGVVGLITPWNYPLLMCAWKVAPALAAGCAAILKPSELASVTSLELAEICKDVGLPSGILNVLTGYGPEAGAPLASHPHVDKVAFTGSS 240
PK2011T202    YADLAERLDAKQKAPVDVPMDTFKSYVLKEPIGVVGLITPWNCPLLMCAWKVAPALAAGCAAILKPSELASVTSLELAEICKDVGLPSGILNVLTGYGPEAGAPLASHPHVDKVAFTGSS 240

9930          ATGSKIMASAAQLVKPVTMELGGKSPIVVFDDVDLDKAAEWAIFGCFWTNGQICSATSRLLVHENIADEFLDKIVQWCKNIKISDPLEEGCRLGPVVSAGQYEKVLKFVSTAEQEGAKIL 360
Gy14          ATGSKIMASAAQLVKPVTMELGGKSPIVVFDDVDLDKAAEWAIFGCFWTNGQICSATSRLLVHENIADEFLDKIVQWCKNIKISDPLEEGCRLGPVVSAGQYEKVLKFVSTAEQEGAKIL 360
301176        ATGSKIMASAAQLVKPVTMELGGKSPIVVFDDVDLDKAAEWAIFGCFWTNGQICSAHPRLLVHENIADEFLDKIVQWCKNIKISDPLEEGCRLGPVVSAGQYEKVLKFVSTAEQEGAKIL 360
PK2011T202    ATGSKIMASAAQLVKPVTMELGGKSPIVVFDDVDLDKAAEWAIFGCFWTNGQICSATSRLLVHENIADEFLDKIVQWCKNIKISDPLEEGCRLGPVVSAGQYEKVLKFVSTAEQEGAKIL 360

9930          YGGVRPKHLKKGYFVEPAIITNVTTSMQIWKEEVFGPVLCVKTFSSEDEAIELANDTIYGLGAAVISNDLERCDRVAKAFQAGIVWINCSQPCFTQAPWGGIKRSGFGRELGEWGLDTYL 480
Gy14          YGGVRPKHLKKGYFVEPAIITNVTTSMQIWKEEVFGPVLCVKTFSSEDEAIELANDTIYGLGAAVISNDLERCDRVAKAFQAGIVWINCSQPCFTQAPWGGIKRSGFGRELGEWGLDTYL 480
301176        YGGVRPKHLKKGYFVEPAIITNVTTSMQIWKEEVFGPVLCVKTFSSEDEAIELANDTIYGLGAAVISNDLERCDRVAKAFQAGIVWINCSQPCFTQAPWGGIKRSGFGRELGEWGLDTYL 480
PK2011T202    YGGVRPKHLKKGYFVEPAIITNVTTSMQIWKEEVFGPVLCVKTFSSEDEAIELANDTIYGLGAAVISNDLERCDRVAKAFQAGIVWINCSQPCFTQAPWGGIKRSGFGRELGEWGLDTYL 480

9930          TVKQVTQYISDEPWGWYKSPSKL 503
Gy14          TVKQVTQYISDEPWGWYKSPSKL 503
301176        TVKQVTQYISDEPWGWYKSPSKL 503
PK2011T202    TVKQVTQYISDEPWGWYKSPSKL 503
```

Fig. 4 Alignment of the amino acid sequences of betaine aldehyde dehydrogenase protein encoded by *CsBADH* from fragrant cucumber PK2011T202, non-fragrant cucumber 301176, and the reference sequence. *Asterisk* indicates amino acid change unique to PK2011T202

Author's personal copy

Table 2 Characteristics of SNAP primer pairs specific to A/G polymorphism in the exon 5 of the *CsBADH* gene. The annealing temperature for all primers is 60 °C

Primer name	Primer sequence	PCR product size (bp)
CsBADH2-A1	F: GCTGATGTCTATCTTTTATTGAAGGAACAA	155
	R: CACAATAAATAAAGTTCATAAAATCCATAATCAC	
CsBADH2-A2	F: TGCTGATGTCTATCTTTTATTGAAGGAAATA	156
	R: CACAATAAATAAAGTTCATAAAATCCATAATCAC	
CsBADH2-A3	F: TGCTGATGTCTATCTTTTATTGAAGGAATTA	156
	R: CACAATAAATAAAGTTCATAAAATCCATAATCAC	
CsBADH2-G1	F: TGATGTCTATCTTTTATTGAAGGAACCG	153
	R: CACAATAAATAAAGTTCATAAAATCCATAATCAC	
CsBADH2-G2	F: GCTGATGTCTATCTTTTATTGAAGGAACAG	155
	R: CACAATAAATAAAGTTCATAAAATCCATAATCAC	
CsBADH2-G3	F: GCTGATGTCTATCTTTTATTGAAGGAATTG	155
	R: CACAATAAATAAAGTTCATAAAATCCATAATCAC	

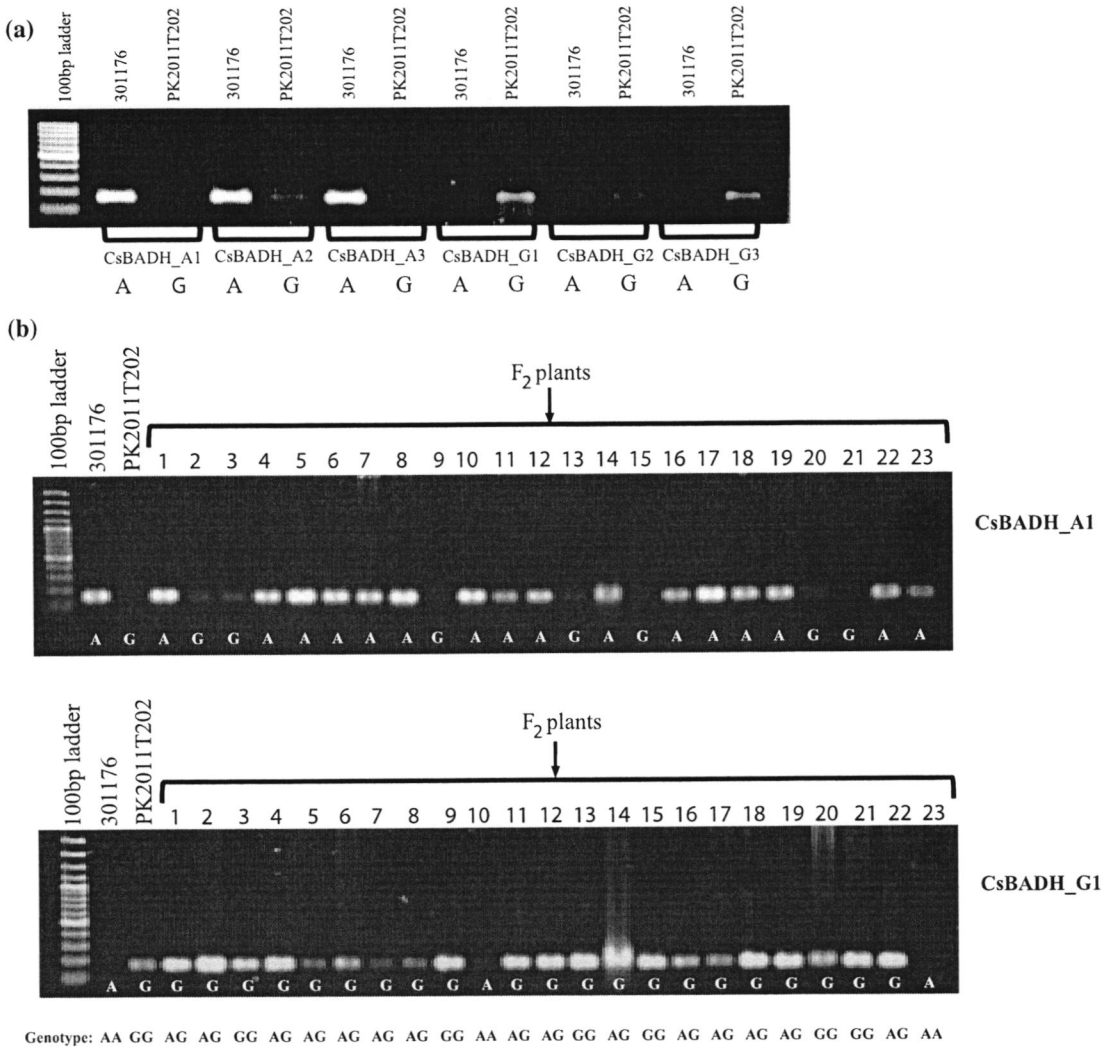


Fig. 5 DNA bands amplified by SNAP markers specific to single nucleotide polymorphism in exon 5 of *CsBADH* in cucumber PK2011T202 and non-fragrant cucumber 301176 (**a**). Segregation of the SNAP marker CsBADH-A1 and CsBADH-G1 in 23 F_2 progenies from the cross between 301176 and PK2011T202 is also shown. Allele detected by each marker in each individual plant is shown at the bottom of the gel (**b**). Genotypes inferred by the two markers are shown at the bottom of the figure

Author's personal copy

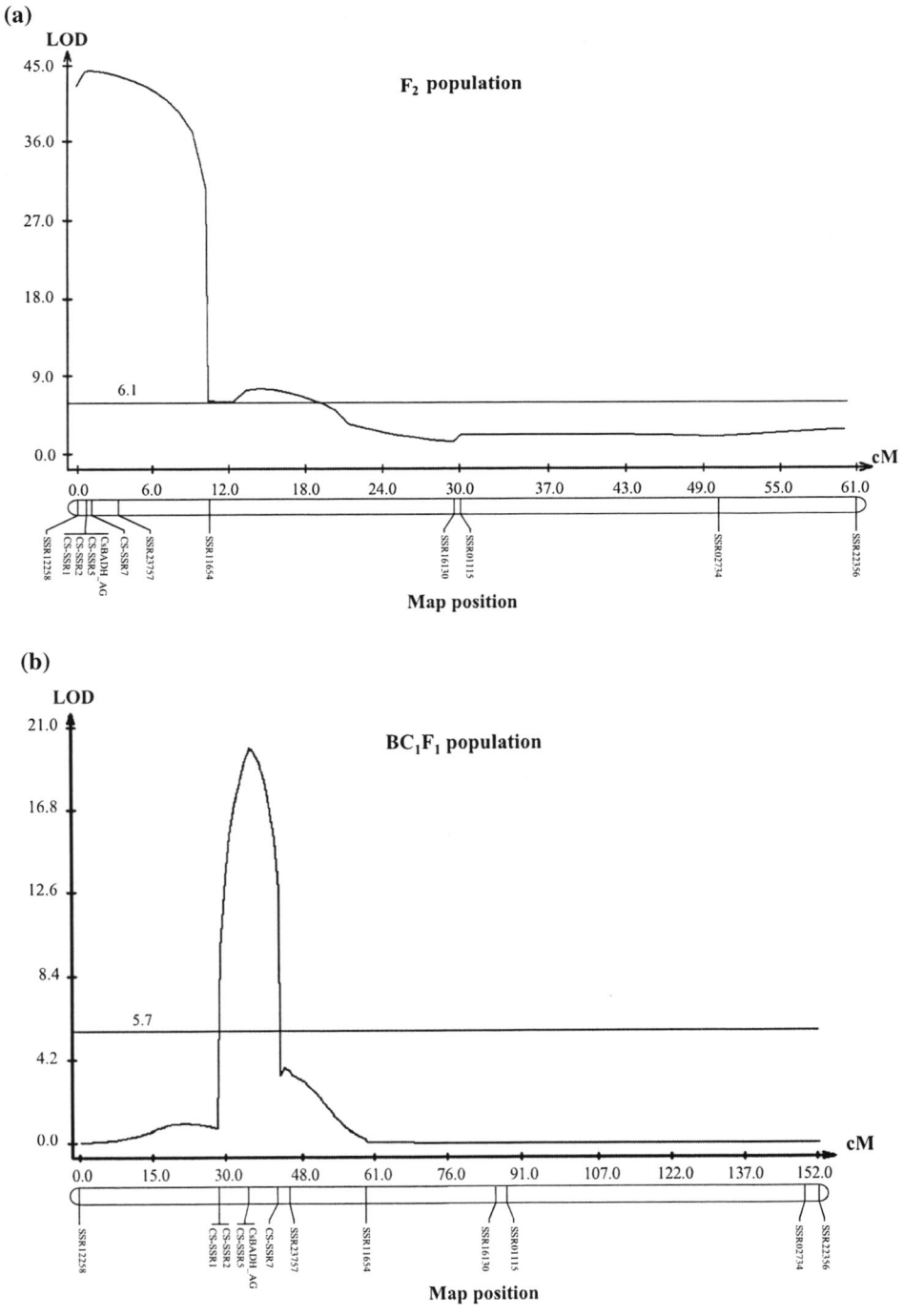


Fig. 6 LOD graph for the major QTL controlling fragrance score (*qFgr*) detected on chromosomes 1 by composite interval mapping in the F_2 (301176 × PK2011T202) and BC_1F_1 [(301176 × PK2011T202) × PK2011T202] populations

major clusters of plant BADHs/AMADHs, each cluster belonged to the respective monocot and dicot groups (Fig. 7). In the dicot group, *P. patens* and *Picea sitchensis* were clustered in this group. Each species of both groups have two homologous sequences of BADHs/AMADHs, with exception in *C. sativus*, *C. melo*, *G. hirsutum*, *L. Barbarum*, *S. oleracea*, *B. vulgaris*, and *P. patens* which have no homologous sequence, and in *Z. mays* which has three homologous sequences. There were two clear orthologous subclusters in the monocots, while there was no clear subcluster in the dicots. The CsBADH identified from this study was closely related to CmBADH, GhBADH and PtBADH2/PtAMADH2 (Fig. 7).

Author's personal copy

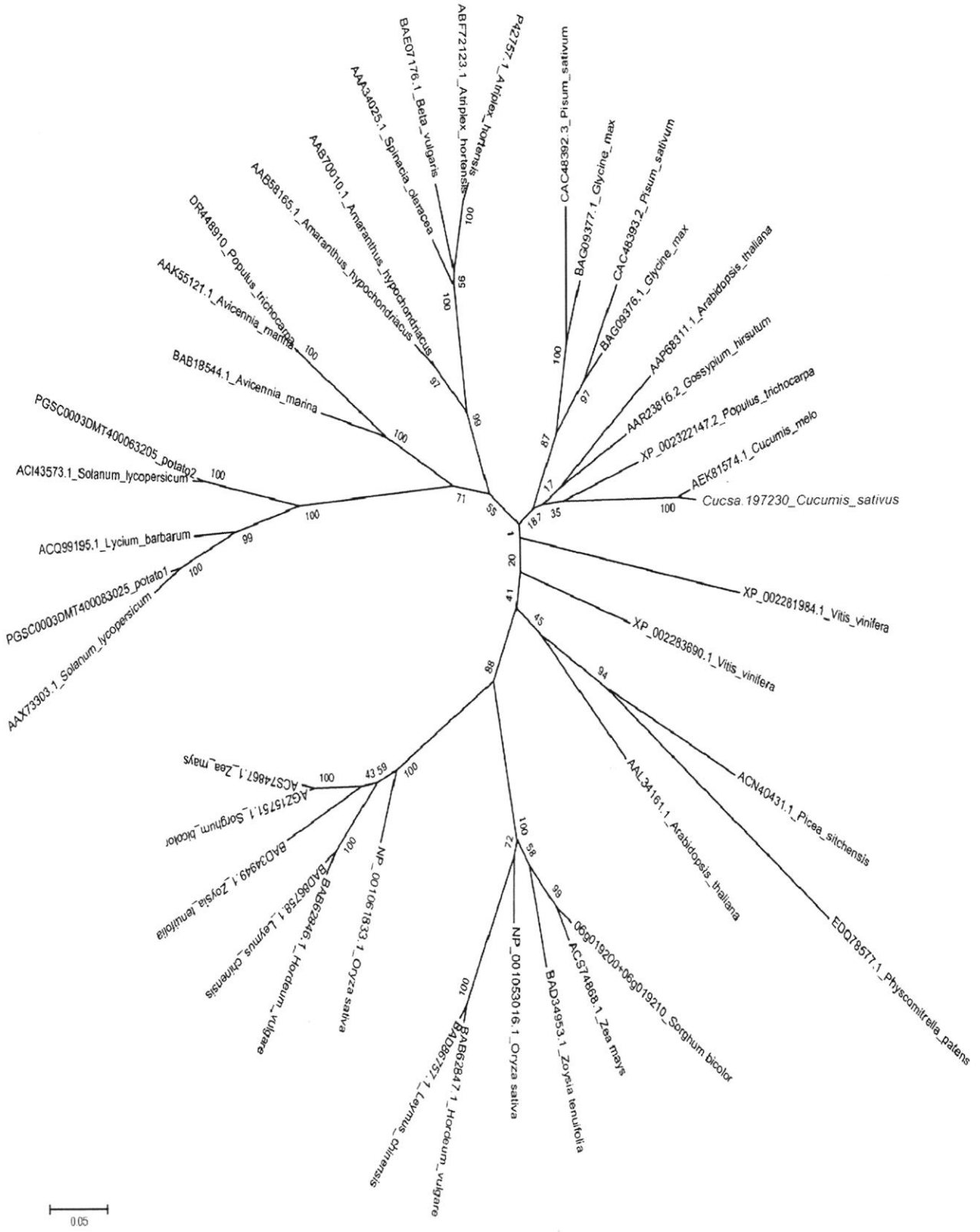


Fig. 7 A phylogenetic tree reconstructed from BADHs/AMADHs sequences of several plant species including cucumber. Bootstrap frequencies are labeled at the dichotomous points

Author's personal copy

Discussion

Fragrance is an important value-added trait of many edible crops. Cultivars with pandan-like fragrance are more preferable to consumers than the non-fragrant ones. Breeding for fragrance is a major objective in rice, vegetable soybean and sorghum breeding programs. The fragrance is mainly the result of the presence in volatile compound 2AP. In this study, segregation analysis confirmed the result of Pramnoi et al. (2013) that the fragrance in cucumber "PK2011T202" is controlled by a single recessive gene. The recessiveness of the fragrance suggests that this trait is created by a loss in gene function.

Studies on fragrance in field crops including rice (Bradbury et al. 2005; Shi et al. 2008; Shao et al. 2011; Amarawathi et al. 2008; Kovach et al. 2009), soybean (Juwattanasomran et al. 2011, 2012) and sorghum (Yundaeng et al. 2013) demonstrated that the fragrance and 2AP synthesis are associated with defected function of BADH2. Silencing *BADH2* in non-fragrant rice and soybean cultivars by RNAi resulted in 2AP production and the fragrance (Niu et al. 2008; Arikit et al. 2010), thus confirming the association between *BADH2* and the fragrance. In this study, we demonstrated that an SNP in gene coding for BADH in cucumber associates with the fragrance. This is the first report on molecular basis of the fragrance in vegetable crops. The SNP A1855G in *CsBADH* is present only in the fragrant cucumber PK2011T202 and results in Y163C change in BADH2. The mutation appears to involve in the fragrance in this cucumber. BADHs (AMADHs) enzymes belong to the aldehyde dehydrogenase families 9 and 10 (Kirch et al. 2005). The substrates of BADHs include betaine aldehyde, 3-aminopropionaldehyde, 3-dimethylsulfoniopropionaldehyde, γ-guanidinobutyraldehyde, and γ-aminobutyraldehyde (GABald) (for details see Fitzgerald et al. 2008). Enzymatic studies in pea (Kopečný et al. 2011), spinach (Díaz-Sánchez et al. 2012), tomato and maize (Kopečný et al. 2013) revealed that Y163 (equivalent to Y160 in spinach; Díaz-Sánchez et al. 2012) is a critically active residue responsible for the specificity of plant BADHs. Y163 maintains overall geometry of the substrate channel that allows appropriate orientation of the substrate, which results in optimal reaction rate (Kopečný et al. 2011). Kopečný et al. (2011) and Kopečný et al. (2013) showed that Y163A mutation of BADH in pea (PsAMADH2 in the original paper) and spinach (SoBADH) results in weak binding to its substrates including GABald, as compared to the wild-type protein. In a proposed pathway for biosynthesis of 2AP (Bradbury et al. 2008), functional BADH2 inhibits the biosynthesis of 2AP by converting GABald to γ-aminobutyric acid, whereas non-functional BADH2 leads to an accumulation of GABald which is then acetylated to form 2AP. Thus, the Y163C mutation in cucumber accession PK2011T202 possibly impairs the binding between BADH/AMADH and GABald, leading to 2AP production and fragrance. A similar finding was reported by Juwattanasomran et al. (2011) that an SNP in *GmBADH2* causes an amino change in a conserved region, G334D, of GmBADH2 that produces the fragrance in vegetable soybean cultivar "Kaori".

In this study, we considered the fragrance as a quantitative trait and evaluated it by sensory test. The QTL detected for the fragrance, *qFgr*, accounted for 80.85 and 43.27 % of the variation of fragrance scores in the F_2 and BC_1F_1 populations, and its position corresponded to a genome region containing *CsBADH2* gene. This supports that the A1855G mutation in *CsBADH2* that causes Y163C change of CsBADH2 is responsible for the fragrance in cucumber accession PKT2011T202. However, the moderate fragrance variation (43.27 %) explained by *qFgr* in the BC_1F_1 population suggests that there may be other genetic factor(s) involving the fragrance in cucumber. We examined association between genotypes detected by the SNAP marker CsBADH-AG and fragrance scores in the F_2 and BC_1F_1 populations and found imperfect association between the marker and the score in both populations. In the F_2 population, one plant showing homozygous alleles from PKT202 had fragrance score of only 1.2 and one plant showing heterozygous alleles had fragrance score higher than 1.5. In the BC_1F_1 population, six plants possessing homozygous alleles from PKT202 had fragrance score lower than 1.5, while eight plants possessing homozygous alleles had fragrance score higher than 1.5. Similar observations have been reported for the fragrance in rice (Amarawathi et al. 2008) and soybean (Juwattanasomran et al. 2011, 2012). The imperfect association between the functional marker and the fragrance score may also arise from the inaccuracy of the sensory test used for evaluation of the fragrance. However, it suggests that apart from *BADH* gene which is the principal cause of the fragrance, there may be also other genetic factor(s) affecting the fragrance in cucumber. Since 2AP is the chemical that is responsible for the fragrance and the biosynthesis pathway of 2AP involves several other chemicals such as proline (Bradbury et al. 2008) which is highly influenced by environmental factors, genetic factor(s) controlling proline can affect fragrance level in cucumber. Moreover, in another pathway proposed for 2AP biosynthesis that is independent of BADH enzyme, Huang et al. (2008) demonstrated that Δ^1-pyrroline-5-carboxylic acid synthetase (P5CS) may react directly with methylglyoxal (MG) leading to 2AP formation in rice, while Wu et al. (2009) showed that P5CS may degrade to 1-pyrroline and interact with MG to produce 2AP. Genetic factor(s) controlling these chemicals may also affect fragrance level in cucumber. In addition, QTL mapping studies for fragrance in rice revealed that the fragrance is controlled

Author's personal copy

by one major QTL (*BADH2* gene) on chromosome 8 and three minor QTLs each on chromosomes 3, 4 and 12 (Amarawathi et al. 2008; Lorieux et al. 1996).

Although fragrance is controlled by a single recessive gene and its evaluation can be achieved by sensory test, improvement of the trait requires repeated evaluations of selfed progenies after each generation of backcross breeding (Juwattanasomran et al. 2011). Using MAS for selection of fragrance cucumber can shorten such steps. Functional marker(s) for a trait is highly demanded for MAS as they perfectly associate with the trait. In this study, an SNP in *CsBADH* gene associated with fragrance in cucumber was identified and enabled us to develop SNAP markers as functional markers for detecting *CsBADH* polymorphism. SNAP is a preferable marker for SNP detection because it is simple, rapid and inexpensive to analyze (Drenkard et al. 2000). The SNAP markers developed in this study can facilitate marker-assisted selection for fragrant cucumber genotypes in a large-scale breeding program using PK2011T202 or other cucumber germplasm that possesses the same fragrance alleles as the gene donor.

Previous phylogenetic analyses showed that flowering plant species possess two homologous BADHs/AMADHs and that there are two orthologous BADHs/AMADHs subgroups in the monocot plants (Arikit et al. 2010; Kopečný et al. 2013). Our phylogenetic analysis gave similar result as the previous reports. Arikit et al. (2010) postulated that the two homologous BADHs/AMADHs in flowering plants had evolved through a duplication of the ancestral gene after the divergence of monocots and dicots, and that the two *BADHs/AMADHs* in each monocot were duplicated in its common ancestor before the divergence, while they were independently duplicated in each species after the divergence of the dicots. Kopečný et al. (2013) found that maize, which is among plants with large genome size (2500 Mbp), has three homologous sequences of BADHs/AMADHs. The authors also noted that number of homologous sequences of BADHs/AMADHs can be higher in species with genome duplications. In our study, however, duplication of *BADH/AMADH* was not detected in cucumber genome, as BLAST search against the two reference genome sequences of cucumber identified only *CsBADH*. Cucumber has a small genome size of only about 367 Mb (Arumanagathan and Earle 1991). Whole genome sequencing revealed that cucumber does not experience recent whole genome duplication and has a few tandem duplications in the genome (Huang et al. 2009). This supports the absence of *BADH/AMADH* duplication in cucumber found in our study.

Author contribution statement C.Y. carried out major part of the experiments and analyzed the data. C.Y., S.C., P. Somta and P. Srinives prepared plant materials. S.T. participated in gene expression analysis and sequencing. P. Somta initiated and coordinated the study, and analyzed the results. C.Y., P. Somta, S.T. and P. Srinives wrote the manuscript. All authors approved the manuscript.

Acknowledgments This research was supported by the Royal Golden Jubilee Ph.D. Scholarship and the TRF Research Career Development Grant (RSA5580057) both of which co-funded by the Thailand Research Fund (TRF) and Kasetsart University to P. Somta and C. Yundaeng.

Ethical standards and conflict of interest All the experiments performed in this study comply with the current laws of Thailand. The authors declare that they have no conflict of interest.

References

Amarawathi Y, Singh R, Singh AK, Singh VP, Mohapatra T, Sharma TR, Singh NK (2008) Mapping of quantitative trait loci for basmati quality traits in rice (*Oryza sativa* L.). Mol Breed 21:49–65

Arikit S, Yoshihashi T, Wanchana S, Uyen TT, Huong NTT, Wongpornchai S, Vanavichit A (2010) Deficiency in the amino aldehyde dehydrogenase encoded by *GmAMADH2*, the homologue of rice *Os2AP*, enhances 2-acetyl-1-pyrroline biosynthesis in soybeans (*Glycine max* L.). Plant Biotechnol J 9:75–87

Arumanagathan K, Earle ED (1991) Nuclear DNA content of some important plant species. Plant Mol Biol Rep 9:229–241

AVRDC (2003) AVRDC progress report 2002. AVRDC-The World Vegetable Center, Shanhua

Ayyangar GNR (1938) Studies in sorghum. J Madras Univ 11:131–143

Berner DK, Hoff BJ (1986) Inheritance of scent in American long grain rice. Crop Sci 26:876–878

Bradbury LMT, Fitzgerald TL, Henry RJ, Jin QS, Waters DLE (2005) The gene for fragrance in rice. Plant Biotechnol J 3:363–370

Bradbury LMT, Gillies SA, Brushett DJ, Waters DLE, Henry RJ (2008) Inactivation of an aminoaldehyde dehydrogenase is responsible for the fragrance in rice. Plant Mol Biol 68:443–449

Buttery RG, Ling LC, Juliano BO, Turnbaugh JG (1983) Cooked rice aroma and 2-acetyl-1-pyrroline. J Agric Food Chem 31:823–826

Chen S, Yang Y, Shi W, Ji Q, He F, Zhang Z, Cheng Z, Liu X, Xu M (2008) *Badh2*, encoding betaine aldehyde dehydrogenase, inhibits the biosynthesis of 2-acetyl-1-pyrroline, a major component in rice fragrance. Plant Cell 20:1850–1861

de Wilde WJJO, Duyfjes BEE (2010) *Cucumis sativus* L. forma *hardwickii* (Royle) W.J. de Wilde & Duyfjes and feral forma *sativus*. Thai For Bull (BOT) 38:98–107

Dereeper A, Guignon V, Blanc G, Audic S, Buffet S, Chevenet F, Dufayard JF, Guindon S, Lefort V, Lescot M, Claverie JM, Gascuel O (2008) Phylogeny.fr: robust phylogenetic analysis for the non-specialist. Nucleic Acids Res 36:465–469

Díaz-Sánchez ÁG, González-Segura L, Mújica-Jiménez C, Rudiño-Piñera E, Montiel C, Martínez-Castilla LP, Muñoz-Clares RA (2012) Amino acid residues critical for the specificity for betaine aldehyde of the plant ALDH10 isoenzyme involved in the synthesis of glycine betaine. Plant Physiol 158:1570–1582

Drenkard E, Richter BG, Rozen S, Stutius LM, Angell NA, Mindrinos M, Cho RJ, Oefner PJ, Davis RW, Ausubel FM (2000) A simple procedure for the analysis of single nucleotide polymorphisms facilitates map-based cloning in Arabidopsis. Plant Physiol 124:1483–1492

Author's personal copy

Fitzgerald TL, Waters DLE, Henry RJ (2008) The effect of salt on betaine aldehyde dehydrogenase transcript levels and 2-acetyl-1-pyrroline concentration in fragrant and non-fragrant rice (*Oryza sativa*). Plant Sci 174:539–546

Food and Agriculture Organization (2013) FAOSTAT. http://faostat.fao.org. Accessed 5 March 2014

Fushimi T, Masuda R (2001) 2-acetyl-1-pyrroline concentration of the vegetable soybean. In: Lumpkin T, Shanmugasundaram S (eds) Proceeding of the 2nd international vegetable soybean conference. Washington State University, Pullman, p 39

Huang TC, Teng CH, Chang JL, Chuang HS, Ho CT, Wu ML (2008) Biosynthetic mechanism of 2-acetyl-1-pyrroline and its relationship with Δ^1-pyrroline-5-carboxylic acid and methylglyoxal in aromatic rice (*Oryza sativa* L.) callus. J Agric Food Chem 56:7399–7404

Huang S, Li R, Zhang Z, Li L, Gu X, Fan Lucas WJ, Wang X, Xie B, Ni P, Ren Y, Zhu H, Li J, Lin K, Jin W, Fei Z, Li G, Staub J, Kilian A, van der Vossen EAG, Wu Y, Guo J, He J, Jia Z, Ren Y, Tian G, Lu Y, Ruan J, Qian W, Wang M, Huang Q, Li B, Xuan Z, Cao J, Asan WZ, Zhang J, Cai Q, Bai Y, Zhao B, Han Y, Li Y, Li X, Wang S, Shi Q, Liu S, Cho WK, Kim J, Xu Y, Heller-Uszynska K, Miao H, Cheng Z, Zhang S, Wu J, Yang Y, Kang H, Li M, Liang H, Ren X, Shi Z, Wen M, Jian M, Yang H, Zhang G, Yang Z, Chen R, Liu S, Li J, Ma L, Liu H, Zhou Y, Zhao J, Fang X, Li G, Fang L, Li Y, Liu D, Zheng H, Zhang QN, Li Z, Yang G, Yang S, Bolund L, Kristiansen K, Zheng H, Li S, Zhang X, Yang H, Wang J, Sun R, Zhang B, Jiang S, Wang J, Du Y, Li S (2009) The genome of the cucumber, *Cucumis sativus* L. Nat Genet 41:1275–1281

Juwattanasomran R, Somta P, Chankaew S, Shimizu T, Wongpornchai S, Kaga A, Srinives P (2011) A SNP in *GmBADH2* gene associates with fragrance in vegetable soybean variety "Kaori" and SNAP marker development for the fragrance. Theor Appl Genet 122:533–541

Juwattanasomran R, Somta P, Kaga A, Chankaew S, Shimizu T, Sorajjapinun W, Srinives P (2012) Identification of a new fragrance allele in soybean and development of its functional marker. Mol Breed 29:13–21

Kirch HH, Schlingensiepen S, Kotchoni S, Sunkar R, Bartels D (2005) Detailed expression analysis of selected genes of the aldehyde dehydrogenase (ALDH) gene superfamily in *Arabidopsis thaliana*. Plant Mol Biol 57:315–332

Kopečný D, Tylichová M, Snegaroff J, Popelková H, Šebela M (2011) Carboxylate and aromatic active-site residues are determinants of high-affinity binding of ω-aminoaldehydes to plant aminoaldehyde dehydrogenases. FEBS J278:3130–3139

Kopečný D, Končitíková R, Tylichová M, Vigouroux A, Moskalíková H, Soural M, Šebela M, Moréra S (2013) Plant ALDH10 family: identifying critical residues for substrate specificity and trapping a thiohemiacetal intermediate. J Biol Chem 288:9491–9507

Kosambi DD (1944) The estimation of map distances from recombination values. Ann Eugen 12:172–175

Kovach MJ, Calingacion MN, Fitzgerald SR McCough (2009) The origin and evolution of fragrance in rice (*Oryza sativa* L.). Proc Natl Acad Sci USA 106:14444–14449

Lander ES, Green P, Abrahamson J, Barlow A, Daly MJ, Lincoln SE, Newberg LA (1987) MAPMAKER: an interactive computer package for constructing primary genetic linkage maps of experimental and natural populations. Genomics 1:174–181

Livak KJ, Schmittgen TD (2001) Analysis of relative gene expression data using real-time quantitative PCR and the $2^{-\Delta\Delta Ct}$ method. Methods 25:402–408

Lodhi MA, Ye GN, Weeden NF, Reisch BI (1994) A simple and efficient method for DNA extraction from grapevine cultivars and *Vitis* species. Plant Mol Biol Rep 12:6–13

Lorieux M, Petrov M, Huang N, Guiderdoni E, Ghesquiere A (1996) Aroma in rice: genetic analysis of a quantitative trait. Theor Appl Genet 93:1145–1151

Murty DS, Nicodemus KD, House LR (1982) Inheritance of basmati and dimpled seed in sorghum. Crop Sci 22:1080–1082

Niu X, Tang W, Huang W, Ren G, Wang Q, Luo D, Xiao Y, Yang S, Wang F, Lu BL, Gao F, Lu T, Liu Y (2008) RNAi-directed downregulation of *OsBADH2* results in aroma (2-acetyl-1-pyrroline) production in rice (*Oryza sativa* L.). BMC Plant Biol 8:100. doi:10.1186/1471-2229-8-100

Pramnoi P, Somta P, Chankaew S, Juwattanasomran R, Srinives P (2013) A single recessive gene controls fragrance in cucumber (*Cucumis sativus* L.). J Genet 92:147–149

R Development Core Team (2010) A Language and Environment for Statistical Computing. R Foundation for Statistical Computing, Vienna. ISBN 3-900051-07-0

Ren Y, Zhang Z, Liu J, Staub JE, Han Y, Cheng Z, Li X, Lu J, Miao H, Kang H, Xie B, Gu X, Wang X, Du Y, Jin W, Huang S (2009) An integrated genetic and cytogenetic map of the cucumber genome. PLoS ONE 4:e5795

Rozen S, Skaletsky HJ (2000) Primer3 on the WWW for general users and for biologist programmers. In: Krawetz S, Misener S (eds) Bioinformatics methods and protocols: methods in molecular biology. Humana Press, Totowa, pp 365–386

Shao GN, TangA Tang SQ, Luo J, Jiao GA, Wu JL, Hu PS (2011) A new deletion mutation of fragrant gene and the development of three molecular markers for fragrance in rice. Plant Breed 130:172–176

Shi WW, Yang Y, Chen SH, Xu ML (2008) Discovery of a new fragrance allele and the development of functional markers for the breeding of fragrant rice varieties. Mol Breed 22:185–192

Somta P, Musch W, Kongsamai B, Chanprame S, Nakasathien S, Toojinda T, Sorajjapinun W, Seehaluk W, Tragoonrung S, Srinives P (2008) New microsatellite markers isolated from mungbean (*Vigna radiata* (L.) Wilczek). Mol Ecol Resour 8:1155–1157

Sood BG, Siddiq EA (1978) A rapid technique for scent determination in rice. Indian J Genet 38:268–275

Wanchana S (2005) Identification of genes controlling grain aroma and amylose content for positional cloning and marker-assisted selection program in rice (*Oryza sativa* L.). Ph.D. Thesis, Kasetsart University, Thailand

Wang S, Basten CJ, Zeng ZB (2012) Windows QTL Cartographer 2.5. Department of Statistics. North Carolina State University, Raleigh

Wu ML, Chou KL, Wu CR, Chen JK, Huang TC (2009) Characterization and the possible formation mechanism of 2-acetyl-1-pyrroline in aromatic vegetable soybean. J Food Sci 74:192–197

Yundaeng C, Somta P, Tangphatsornruang S, Wongpornchai S, Srinives P (2013) Gene discovery and functional marker development for fragrance in sorghum (*Sorghum bicolor* (L.) Moench). Theor Appl Genet 126:2897–2906

A Burning Issue

Rethinking the Transition from Hunter-Gatherer to Industrial Sociometabolic Regimes

A. Terry Rambo

Keywords:

biomass burning
energy and society
fire ecology
industrial ecology
premodern modes of production
socioeconomic metabolism

Summary

Hunter-gatherers are commonly seen as having a fundamentally different sociometabolic regime from agrarian and industrial societies because they are thought to directly appropriate the products of natural ecosystems without modifying those systems in order to enhance their productivity. However, ethnographic and archeological evidence reveals that many hunter-gatherers extensively employed fire to manage their ecosystems so as to increase production of desirable wild resources, thus engaging in "colonization of nature" that is not qualitatively different from that practiced by other types of society. They systematically burned wild vegetation in order to increase populations of edible wild plants consumed by humans and promote growth of forage for game animals. Deliberate ecosystem burning by Australian Aborigines represented an energy expenditure of 1,512 gigajoules per capita per year (GJ/capita/yr), a level of energy use that is more than three times higher than the United States (445 GJ/capita/yr). It is their profligate consumption of biomass energy that explains why the quality of life of many hunter-gatherers was often better than that of traditional settled peasant farmers. Hence, the extent to which hunter-gatherers have a distinct type of sociometabiolic regime is called into question. It can be argued that in the course of social evolution, there have been only two sociometabolic regimes. In one type, which includes hunter-gatherers, swidden agriculturalists, and industrial societies, extrasomatic energy does most of the productive work, whereas in the other type, that of premodern settled agriculturalists, production is largely dependent on human muscle power.

Introduction

The idea that the evolution of more complex human societies is driven by increases in per capita energy consumption is an old one in the social sciences (Ross and Machlis 1983). This belief is founded on the recognition that social systems, just like living organisms and ecosystems, require a continuous supply of energy in order to function (Smil 2004). Energy is required by social systems to coordinate activities of their members, produce food and other necessities, build physical infrastructure, preserve social order within the system, and defend against hostile neighboring social systems. Consequently, it is assumed that as the consumption of energy increases, social systems become larger and more complex (Cook 1971; Cottrell 2009; Debeir et al. 1991; Rambo 1991; Smil 1994, 2004; White 1943, 1959). The anthropologist Leslie White (1943, 1959) even proposed a formula to express the relationship between energy and cultural evolution:

$$E \times T \rightarrow C$$

(in which E is the amount of energy harnessed per capita per year, T is the efficiency with which available technology employs that energy to perform work, and C is the resulting degree of cultural development).

Address correspondence to: Prof. Terry Rambo, Faculty of Agriculture, Khon Kaen University, Khon Kaen 40002, Thailand. *Email*: trryrambo@yahoo.com

© 2014 by Yale University
DOI: 10.1111/jiec.12163

Editor managing review: Heinz Schandl

Volume 19, Number 1

White asserted that culture had evolved through three increasingly complex stages as the amount of energy used per capita had increased. Very small and simple hunter-gatherer societies represented the first stage, larger and more complex agrarian societies based on domesticated plants and animals represented the second stage, and modern industrial societies using fossil fuel (FF) energy represented the third stage. In a widely reproduced graph, Earl Cook (1971) plotted energy consumption of societies at various evolutionary stages. According to his graph, per capita energy consumption increased from 8.4 megajoules per day (MJ/day) for "primitive man" (hunters and gatherers) 1 million years ago, to 50 MJ/day for early agriculturalists (swidden farmers), to 109 MJ/day for advanced agriculturalists (peasant farmers), to 962 MJ/day for "technological man" in the United States of 1970. Cook did not list any sources for the energy consumption figures assigned to premodern societies and it appears that he simply made "common sense" estimates.

Although the belief that increasing per capita use of energy is the main driving force of social evolution has become part of the conventional wisdom of the social sciences, it had never actually been empirically tested until quite recently when scholars associated with the Institute of Social Ecology in Austria, employing what has been labeled as "the Viennese sociometabolic transition approach" (Fischer-Kowalski and Rotmans 2009), published some well-documented analyses of energy use by societies representing different evolutionary stages (Fischer-Kowalski et al. 2011; Haberl 2002; Krausmann et al. 2008). These analyses show the same trends as Cook's earlier rough estimates. Thus, Haberl's (2002) comparative analysis of the energetic metabolism of three societies representing the hunter-gatherer, agricultural, and industrial evolutionary stages shows that daily per capita energy expenditure for hunters and gatherers (Nicobar Islands, India) was 22 MJ, increasing to 208 MJ for an advanced peasant agricultural society still largely reliant on animal draft power (a rice growing village in Northeast Thailand), and climbing to 688 MJ for a modern industrial society (Austria).

In the Viennese approach, the concept of the "sociometabolic regime" (Sieferle 2001) is used to distinguish different socioecological systems and their associated energy systems. It is assumed that the character of the socioecological system is determined by the energy system so that, following the functionalist logic that underlies this conceptual approach, those systems depending on the same source of energy and employing similar kinds of energy conversion technology are expected to display many other similar characteristics as well, including patterns and levels of resource use, demography, settlement pattern, human labor allocation patterns, institutional arrangements, and communications (Krausmann et al. 2008). Three main sociometabolic regimes have been delineated to represent successive stages in the evolutionary history of human society. These are the hunter-gatherer regime, the agrarian regime, and the industrial regime. Each of these "ideal type" regimes is said to be characterized by a distinctive energy system: Hunter-gatherers are said to have an "uncontrolled solar energy system" (Sieferle [1997] as cited in Haberl [2002]), in which humans appropriate the products of photosynthesis of natural ecosystems without attempting to modify those systems in order to enhance their productivity; agrarian regimes rely on a controlled solar energy system, in which they purposively modify ecosystems in order to increase net primary productivity, and industrial regimes have an FF-based energy system which, for at least a short period of time, liberates them from the energetic limits of their ecosystems (Krausmann et al. 2008; Fischer-Kowalski and Haberl 2007; Sieferle 2001). This characterization of the three sociometabolic regimes is essentially a restatement, using the vocabulary of energy systems analysis, of the conventional typology of social evolutionary stages long employed by students of cultural evolution (e.g., White 1943, 1959). The stages in this typology represent a lineal progression from small, simple, and technologically primitive social systems to ever larger, more complex, and technologically advanced systems. Similarly, the identification of the sources of energy and energy conversion technology employed by each regime are basically identical to those earlier suggested by White and other cultural evolutionists. But it is precisely this aspect of their analysis, in particular the assertion that hunters and gatherers employ an uncontrolled solar energy system, in which they simply appropriate the products of natural ecosystems without attempting to increase ecosystem productivity (Fischer-Kowalski and Haberl 1997, 2007; Haberl 2002; Sieferle 2001), that deserves to be challenged in light of the accumulated evidence of ethnographic and archeological research that reveals that many hunting and gathering societies in different parts of the world have systematically modified their ecosystems to serve their needs.

The Sociometabiolic Regime of Hunter-Gatherers

That hunter-gatherers have engaged in a deliberate process of ecosystem management, which Bruce D. Smith (2011) (employing a concept proposed earlier by Laland et al. [2000]) refers to as "niche construction," is widely recognized by anthropologists. Certainly, the once widely held belief that hunting and gathering people always live in harmony with nature and have minimal impacts on nature has now been largely discredited (Rambo 1985). It is now evident that they alter their ecosystems in many ways, both deliberately and as the unintended consequences of their daily activities. In an article reviewing deliberate efforts to manage wild plant and animal resources by small-scale societies, Smith identified six general categories of niche construction:

1. General modification of vegetation communities
2. Broadcast sowing of wild annuals
3. Transplantation of perennial fruit-bearing species
4. In-place encouragement of perennial fruit and nut-bearing species
5. Transplantation and in-place encouragement of perennial root crops, and

6. Landscape modification to increase prey abundance in specific locations (Smith 2011).

All of these actions involve modification of the natural ecosystem in ways intended to increase productivity of resources needed by humans and therefore represent efforts to colonize nature. In particular, many groups of hunters and gatherers have employed fire (and, less frequently, water[1]) to manage their ecosystems in ways intended to increase production of desirable wild plant and animal resources (Goudsblom 1992; Pyne 2005). Fire was used to increase production of forage for game animals, increase populations of wild plants consumed as food by humans, and increase the mobility and exploitative efficiency of human hunters and foragers by clearing low-growing vegetation that slowed their travel and made it difficult to see prey animals (Mellars 1976).

It is not known with any certainty when humans first began using fire to manage natural ecosystems, but there is some evidence that it occurred during the Mesolithic period in Europe (Mellars 1976). Certainly, the practice was very widespread among hunter-gatherers in many parts of the world at the time of first contact with European explorers. Fire was used by aboriginal hunters and gatherers to manage "natural" ecosystems in Australia (Bird et al. 2008; Gould 1971; Hallam 1985; Jones 1969; Lewis 1985; Vigilante et al. 2009), North America (Anderson 1994; Blackburn and Anderson 1993; Hough 1926; Lewis 1982; Lewis and Ferguson 1988; Stewart et al. 2002; Williams 2005), South America (Mistry et al. 2005; Pivello 2011), Africa (Shaffer 2010; Sheuyange et al. 2005), and Asia (Zong et al. 2007). Use of fire to increase ecosystem productivity seems to have been most common among hunters and gatherers residing in deserts, savannas, and seasonally dry forests, but has also been reported for the Canadian boreal forest (Lewis and Ferguson 1988) and even the humid Malaysian rainforest (Rambo 1985). A cross-cultural study of 96 hunting and gathering groups found that 16 burned for hunting, 29 burned to encourage growth of plants, and 51, mostly in areas with high rainfall or at high latitudes, did not burn (Keeley 1995, 256, Table 9.4).[2]

Although burning by hunters and gatherers has often been attributed to their use of fire in hunting, it is their systematic use of deliberately set fires to "clean up" the landscape, as the Australian Aborigines refer to their practice of periodically burning areas covered by mature climax vegetation cover in order to set back the successional clock, and thus increase the productivity of the ecosystem, that would seem to represent deliberate colonization of nature (Bird et al. 2008; Murphy and Bowman 2007; Russell-Smith et al. 1997). By choosing the time of the year and the frequency with which they burn an area, they are able to increase the yield of wild plants that they consume directly, or that are eaten by the wild game animals that they hunt for meat, above the natural level of an unmanaged ecosystem that is burned only when irregularly occurring lightning strikes ignite wild fires. For example, the Cocopa Indians of the American Southwest collected wild grass seed as an important source of food. According to Hough (1926, 66):

> After harvest, the Indians burn off the dry grass to clear the land of rubbish, so that when the new grass springs up the harvest may be facilitated. The Indians believe that the grass is benefitted by burning and their idea appears to be good. This is a case of unintentional fertilization. It also may be seen that a continuation of this process may work a change in the habits of the grass, leading in some respects to its domestication.

Regular burning of savanna vegetation is also widely practiced by hunter-gatherers in order to increase the quantity and nutritive quality of tender shoots and leaves of forage plants that regenerate after the fire. Experiments in North America and Europe have shown that careful use of fire can increase the carrying capacity of the environment for grazing animals by 300% to 700% over that of an unmanaged ecosystem (Mellars 1976). Studies of areas burned by Aboriginal Australians have also found increases in the populations of desired game species and edible wild plants (Bird et al. 2008; Murphy and Bowman 2007; Viglante et al. 2009).

Periodic burning by hunters and gatherers also serves to limit the natural occurrence of huge lightening-ignited wild fires, which are likely to occur after an area has accumulated an excessive fuel load, and may destroy useful species and retard the regeneration of the vegetation communities on which the hunters and gatherers depend for their food (Pyne 2005). By burning different patches within the landscape at different intervals, they also create and maintain a fine-grained mosaic environment with greatly increased edge length that enhances biodiversity (Bird et al. 2008; Lewis and Ferguson 1988).

Although many studies have shown that deliberate burning of natural vegetation by hunters and gatherers increases ecosystem productivity, and it would therefore seem logical to include the biomass energy used in fires in analyses of their sociometabolic regimes, this form of energy use has been largely omitted (with the notable exception of Sieferle et al. [2006]) in analyses employing the Viennese sociometabolic transition approach.[3] Although Sieferle (2011) does acknowledge that hunters and gatherers used fire for hunting[4] and, in the process, changed the character of the natural vegetation so as to create open grasslands that served as pasture for the large herbivores that were their favored prey, he denies that this represented "systematic colonization of nature."[5] Those areas where the ecosystem has been manipulated by hunter-gatherers by burning biomass are referred to as "affected areas," although the land-use structure of these areas is said to be "100% natural vegetation" (Sieferle et al. 2006, Table 2.2), which would seem to imply that the ecosystem has not been significantly modified by human actions. Haberl (2002) also recognizes that hunters and gatherers do use a small amount of final energy (ca. 3.5 gigajoules per capita per year [GJ/capita/yr]) in the camp fires they use for cooking and warmth and that this value would be "several orders of magnitude higher in cases where hunter-gatherers burn down forests during hunting, thus promoting herbaceous vegetation," but he does not include this extrasomatic energy in his analysis of their sociometabolic regime. Others employing the Viennese approach (e.g., Fischer-Kowalski

and Haberl 1997; Fischer-Kowalski et al. 2010; Sieferle 2001) also acknowledge that hunters and gatherers use fire for a variety of purposes, but nevertheless omit it from their sociometabolic analyses on the grounds that "hunter-gatherers do not colonize nature in the sense that they deliberately modify natural systems to make them more productive or convenient for their needs" (Fisher-Kowalski and Haberl 1997. There is a circularity in this logic (hunter-gatherers have a fundamentally different sociometabolic regime because they do not colonize nature → therefore their use of biomass energy to modify their ecosystems is not included into the analysis of their sociometabolic regime → therefore they have a fundamentally different sociometabolic regime) that obscures perception of the actual utilization of energy by hunter-gatherers.

Rethinking the Role of Biomass Energy in Hunter-Gatherer Sociometabolism

The omission of fire energy from analyses of the sociometabolic regime of hunters and gatherers is hardly a minor issue. Although detailed and reliable empirical data are difficult to obtain, the limited available evidence suggests that inclusion of the energy consumed in fires intended to manage their ecosystems would dramatically alter our view of the sociometabolism of hunters and gatherers. The only reasonably comprehensive and reliable data on hunter and gatherer use of fire to manage their ecosystems come from ethnographic studies of the Aborigines who inhabit the savanna ecosystems of Northern Australia.[6] Until recently, these nomadic hunters and gatherers lived in small bands numbering from 20 to 50 people, with a mean population density of 1 person per two square kilometers (1 person/2 km^2) (Jones 1980). Net primary production of the savanna ecosystem is quite low, with estimates of average annual accumulation of biomass in the form of easily burnable leaf litter and understory grasses and shrubs ranging from 140 grams per square meter (g/m^2) (1.4 metric tons per hectare [t/ha]) (Chen et al. 2003, 409, Table 3) to as much as 1,000 g/m^2 (Lacey et al. 1982). Dry plant litter has an average energy content of 4.3 kilocalories per gram (kcal/g) (0.018 MJ/g) (Golley 1961, so if the average fuel load is 140 g/m^2, it would contain 2.52 MJ of energy. According to Lewis (1985), the Aborigines in this area burned between 30% and 50% of their whole territory each year. If they burn just 30% of their territory each year, or 600,000 m^2/person, this would represent a minimum estimate of per capita energy expenditure in the form of biomass burning of 1,512 GJ/capita/yr. This is a level of energy use that is more than three times higher than the United States (445 GJ/per capita/yr) and seven times greater than the European Union (EU) (210 GJ/capita/yr) in 2000 (Haberl et al. 2006, 156). One can, of course, question the accuracy of the ecological values employed in making this estimate, but, even if they were several times lower than the numbers used here (e.g., the area burned per person is smaller or the fuel load lower than the already minimum values employed in this calculation), the total amount of energy used in burning would still be immense.

It is important to include biomass energy used in burning into analysis of the hunter-gatherer sociometabolic regime because it helps to explain the otherwise anomalous finding that the quality of life of hunters and gatherers was generally much better than that of peasant farmers in traditional agrarian states. Although citizens of modern states, who enjoy a high quality of life because they are able to exploit vast quantities of FF energy, commonly perceive hunters and gatherers as having led lives that, in Thomas Hobbes' terms were "poor, nasty, brutish and short," modern ethnographic research does not support this stereotypical view. Indeed, there is considerable evidence that hunters and gatherers were able to adequately feed themselves with a minimum amount of work and also were generally healthier and lived longer than traditional agriculturalists (Cordain et al. 2000; Gurven and Kaplan 2006; Milton 2000).[7] It was their enjoyment of such a high quality of life, despite working only a few hours per day, that led the anthropologist Marshall Sahlins (1974) to refer to hunters and gatherers as "the original affluent society." A recent review of studies of eight contemporary hunting and gathering societies found that individuals spent an average of only 3.7 hours per day in procuring food (Waguespack 2005). This is a reflection of the generally high returns of food calories that they achieve per hour worked. According to a recent review of energy yields for several contemporary hunting and gathering groups (Kuhn and Stiner 2001, 102, Table 5.1), hunting of large game yielded an average of 265.4 MJ per hour (MJ/hr), small game 67.2 MJ/hr, digging of roots and tubers between 25.6 and 43.6 MJ/hr, and collecting seeds and nuts between 14.7 and 27.3 MJ/hr. Another compilation of return rates for hunter-gatherers in Australia, the Great Basin of the United States, the Canadian boreal forest, and the Malaysian rainforest shows a very wide range from 1.1 MJ/hr for grass seed in Australia to 2,991.1 MJ/hr for grasshoppers in the Great Basin (Kelly 1995, 81–82, Table 3-3). Although these figures suggest that procurement of some types of food by hunter-gatherers could be very efficient, it is not possible to extrapolate from these data to an overall estimate of average return rate for any hunter-gatherer society. There have been only a few comprehensive studies of time expended in food procurement by contemporary hunters and gatherers. It is particularly unfortunate that no studies on the productive efficiency of Australian Aborigines were made until after they had been partly resettled on government stations, where they had access to store-bought foods, and also after the government had prohibited regular burning of the environment, so the extent to which the available figures on caloric returns per hour spent in food procurement are representative of the precontact situation is open to serious question.[8] Richard Lee's detailed study of the Kung San of Botswana in southern Africa, who used fire to manage their ecosystem in much the same way as the Australian Aborigines (Sheuyange et al. 2005), is probably the most reliable available study of labor productivity of hunting and gathering in a savanna ecosystem. He found that adults spent, on average, 3.5 hours per day in hunting and foraging and obtained 17.2 MJ for each hour spent in food procurement, so required only 29 minutes of work to procure sufficient food

Table 1 Human labor time needed to produce food in subsistence systems employing different energy sources

	Hunting and gathering (Kung San, Botswana, Africa) Human labor + fire	*Swiddening hill rice (Iban, Sarawak) Human labor + fire*	*Traditional peasant wet rice farming (colonial era Vietnam) Human labor only*	*Traditional peasant wet rice farming (colonial era Java) Human labor only*	*Traditional peasant maize farming (Mexico) Human labor +oxen*	*Semimodernized peasant wet rice farming (Northeast Thailand) Human labor + buffalo + machine power*	*Mechanized wet rice farming (Japan) Human labor + machine power*	*Mechanized wet rice farming (USA) Human labor + machine power*
Time period	28 days	1 annual crop	1 wet season crop	1 wet season crop	1 annual crop	1 wet season crop	1 annual crop	1 annual crop
Yield/t/ha	n.a.	1.1	1.5	1.1	0.94	2.0	6.3	7.37
Yield/MJ	8,373.6	16,837.6	15,383.5	11,383.8	13,986.2	20,205.2	96,203.9	111,043.1
Human labor hours	486	936	2,336	1,680	383	570.2	640	24
MJ/human labor hour	17.2	18	6.6	6.8	36.5	35.4	150.3	4,627.2
Human labor time to feed 1 person/1 day	29 minutes	31 minutes	76 minutes	74 minutes	14 minutes	14 minutes	3 minutes	<1 second
Source of data	Lee (1979) *en passim*	Nielsen and colleagues (2006), Table II	Dumont 1935 *en passim*	Van der Eng 2004,Table 3	Pimentel and Pimentel 2008, Table 10.4	Grünbühel and colleagues (2003), Table II	Pimentel and Pimental 2008, Table 10.12	Pimentel and Pimental 2008, Table 10.14

Note: t/ha = tons per hectare; MJ = megajoules; n.a. = not applicable.

for 1 person for 1 day (Lee 1979).[9] Thus, it does not appear that hunters and gatherers are necessarily less productive than traditional peasant agriculturalists (table 1). Indeed, colonial-era peasants in the densely populated Red River Delta in Vietnam (Dumont 1935) and in Java in Indonesia (Van der Eng 2004), who had to entirely rely on human muscle power to cultivate their paddy fields, had to work more than twice as long as the Kung San to produce sufficient food calories to feed 1 person for 1 day, whereas swidden agriculturalists, such as the Iban of Borneo (Nielsen et al. 2006) or the Tsembaga of Papua New Guinea (Rappaport 1971), who, like all slash-and-burn cultivators, used fire energy to do much of the work of cultivating their fields (McGrath 1987; Rambo 1980), achieved approximately the same output per hour as the Kung San hunters and gatherers.[10] It is only modern industrial farmers who cultivate their fields using FF-powered machinery who achieve a level of labor productivity that greatly exceeds that of hunters and gatherers using fire to manage their ecosystems[11] (Pimentel and Pimentel 2008).

Although their labor productivity was very high, the efficiency with which hunter-gatherers used biomass energy to increase the productivity of their ecosystems by landscape burning was extremely low. The Australian Aborigines had a strongly negative energy output-input ratio for food of 0.0023:1,[12] which is even lower than the output-input ratio of 0.11:1 achieved by the Tsembaga swidden agriculturalists in Papua New Guinea (Rambo 1984). In contrast to the very low efficiencies of these fire-using groups, the traditional wet rice-growing peasants in the Red River Delta of Vietnam, who used only their own muscle power to cultivate their crops, had a strongly positive food energy output/work energy input of approximately 11.9:1 (calculated from data in Dumont [1935]). Even FF-using mechanized American agriculture, which has often been criticized for its inefficient use of energy (e.g., Steinhart and Steinhart 1974), has a positive output-input ratio for maize production of from 4.11:1 (Pimentel 2009) to 10:1 (Gelfand et al. 2010).

The very inefficient use of almost all of the available energy in their environment by hunter-gatherers is reflected in the very low population densities that are characteristic of this sociometabolic regime. For example, the Australian Aborigines, who used 1,535 MJ/capita/yr of energy, had a population density of only 1 person/2 km^2. Swidden agriculturalists, who achieved somewhat greater efficiency in their use of biomass energy for food production, were able to support considerably higher densities. Thus, the Tsembaga tribal swidden farmers in Papua New Guinea, who used 20 times less energy per capita (71 GJ/capita/yr) than the Aboriginal hunter-gatherers, but used it to produce food 48 times more efficiently, had a mean population density of 14 people/km^2. Traditional peasant farmers, who used only their own muscle power to grow their crops, could achieve very high population densities. For example, the wet rice-growing peasants of Vietnam's Red River Delta, who used only 4.24 GJ/capita/yr of energy, had a mean population density exceeding 300 persons/km^2 and reaching as high as 1,500 persons/km^2 (Rambo 1991; Le and Rambo 1993). Thus, the growth of hunter-gatherer societies and, to a somewhat lesser degree, swidden agriculturalists, was very tightly constrained by the total amount of biomass energy available per square kilometer in their territories. If population density should come to exceed the very low carrying capacity of these modes of production, they could no longer maintain the prolific expenditures of energy that gave them high labor productivity. They were forced to shift from a space-based energy system to one based on labor, with a consequent decrease in their quality of life.

Conclusions

Contrary to the conventional belief, hunter-gatherers do not all rely on an "uncontrolled solar energy system," in which they merely appropriate the products of photosynthesis of natural ecosystems without modifying those systems in ways that increase their productivity. Instead, many hunter-gather societies make extensive use of fire to reshape natural ecosystems to serve human needs, thus engaging in "colonization of nature" that is not qualitatively different from that practiced by agricultural societies. Hence, the extent to which hunter-gatherers have a distinct type of sociometabiolic regime is called into question. Indeed, it might even be argued that, in the course of social evolution, there have been only two sociometabolic regimes. In one type, which includes those hunter-gatherer societies that used fire to modify their ecosystems, swidden agriculturalists, and industrial societies, extrasomatic energy does most of the productive work, whereas in the second type, that of hunter-gatherers who do not burn their ecosystems and premodern settled agriculturalists, production is largely dependent on human muscle power, supplemented, in some cases, by draft animals. Members of the first type of regime, because they are able to tap vast resources of biomass energy, either in the form of living vegetation in the case of hunter-gatherers and swidden farmers, or of FFs (i.e., the "subterranean forest" as Sieferle [2001] has memorably called it) in the case of industrial societies, are liberated from total reliance on their own muscle power to produce their food needs.[13]

In any case, I would argue that it is not differences in the amounts of extrasomatic energy that individual hunters and gathers consume that distinguishes the sociometabolic regime of their societies from the regimes of agricultural or industrial societies.[14] Instead, what differentiates hunter-gatherer societies (regardless of whether or not they engage in large-scale modification or their ecosystems by burning) from advanced agrarian and industrial societies is the very small amount of energy that these small and simple social systems expend on integrative activities (Rambo 1991). As Elman Service (1971) has pointed out, the social organization of hunting and gathering bands is characterized by its rudimentariness, with bands lacking any other integrative means than kinship and religious rituals. Because a typical band is composed of fewer than 50 members, who are usually related by descent or marriage, and are in continual face-to-face contact in the course of their

normal daily activities, there is minimal need for special integrative institutions to maintain social cohesion. In such small groups, informal interactions among kinspeople who are coresident within the same band are the primary mechanism for maintaining social cohesion. Interactions among members occur as a matter of course during the ordinary activities of daily life, rather than requiring extra expenditure of time or effort. Consequently, a band does not expend much energy on coordinating the actions of its members or ensuring the maintenance of internal social cohesion. Integration is achieved simply by members spending a few minutes in conversation around the evening campfire to plan the next day's activities, and perhaps devoting a few hours every so often to participating in periodic ritual gatherings. No detailed quantitative studies have been made of the amount of energy expended on social integrative activities by hunting and gathering bands, but, if we assume that each member spends an average of 1 hour a day on such activities, the total amount of energy employed for societal purposes would hardly exceed a few megajoules per day 1991).

In contrast to band societies, where integration is essentially an incidental by-product of the daily routine of life, traditional agrarian states, such as the Chinese or Roman empires, required special purpose-built institutions to create and maintain social cohesion. Such states were composed of millions of members, mostly poor peasants, workers, and slaves. Despite the poverty of most of their subjects, these states themselves had immense administrative and military power. Their ruling elites employed the coercive power of the state to extract heavy taxes (usually paid in grain or forced labor service) from the peasantry. The amount of grain contributed by each peasant household was small, perhaps only a few hundred kilograms (kg) each year, but when combined with the grain contributed by millions of other households, represented a huge stock of energy that could be used to support the functioning of diverse specialized integrative institutions. These institutions included the civil and religious bureaucracies that were responsible for public administration, defense, and the performance of rites and rituals that functioned to maintain societal cohesion. These states also commonly used taxes to support construction of large-scale irrigation and flood control projects designed to improve agricultural yields, which led to what Goudsblom (1992, 54) refers to as the increase in "collective productivity" displayed by advanced agrarian societies. Again, no studies are available of energy expenditure on social integration by agrarian states, but it would certainly have been thousands, even tens of thousands, of GJ/day.[15]

Modern industrial societies are much larger and structurally more complex than traditional agrarian states and require correspondingly greater energy expenditures on their integrative institutions. In addition to a multitude of government agencies that attempt to maintain order and regulate the functioning of these societies, they typically have a vast interlocking array of private corporations, nongovernmental organizations, and voluntary associations that contribute to creation of social solidarity. The operation of these institutions must consume a very large quantity of energy, but, unfortunately, I have been unable to locate any estimates of the total amount of energy used for integrative purposes by any modern industrial society. However, one can gain a sense of the magnitude of these expenditures on social integration by examining the amount of energy expended on communications. Transmission of information among millions of members by means of telephones, the Internet, and the mass media plays a critical role in the integration of modern industrial societies. Complete data are unavailable, but the United States probably expends at least 1,000 terajoules per day (TJ/day) on communications, with much, probably most, of this energy contributing to societal integration.[16]

The admittedly crude estimates of the amount of energy used for integrative purposes by social systems at different evolutionary stages that I have presented can certainly be questioned, but I doubt that any possible revisions will overturn the relative ranking of these different types of societies. That agricultural societies use vastly more energy for societal integration than hunting and gathering bands, and that industrial societies use even greater amounts of energy than agricultural ones, does not seem to be open to question.

It is also evident that the relationship between per capita energy consumption rates and the evolution of more complex social systems is much more problematic than has been commonly assumed. Indeed, if we were to draw a graph showing changes in per capita energy use in the course of social evolution, it would display a U-shaped curve, with the line dipping down from the very high per capita energy consumption level in many hunter-gatherer bands, to a moderately high consumption level by slash-and-burn farmers living in tribal societies, and then falling steeply to a very low per capita consumption level by peasants in traditional agrarian states, before climbing steeply to the very high per capita level of consumption by citizens of modern industrial states (Rambo 1991). It appears therefore that it is time for serious rethinking about the role played by transitions in sociometabolic regimes in the process of cultural evolution.

Acknowledgments

The writing of this article was funded by a grant (BRG5680008) from the Thailand Research Fund (TRF) Basic Research Program to the author, but the views expressed herein are not necessarily shared by the TRF. George W. Lovelace and Gary D. Murfin made helpful comments on an earlier draft of this article, Richard A. Gould guided the author to literature on Australian Aborigine management of wetland resources, and Frank Rasche helpfully translated a key table from German to English. The author is grateful to the three anonymous reviewers whose very helpful comments and criticisms helped to clarify the arguments presented in this article. In doing this research, the author has received invaluable assistance in locating numerous difficult-to-find publications from the librarians of the Research Information Service of the East-West Center, especially Audrey Minei.

Notes

1. Management of water by hunter-gatherers to manipulate ecosystem productivity is much less commonly reported than their use of fire, but some Native American hunters and gatherers are known to have constructed quite extensive systems of canals to irrigate plots of edible wild plants, thereby increasing their productivity. The Owens Valley Paiute, in what is now the American state of California, built earthen dams to divert water from streams into canals that extended for as long as 4 miles to irrigate the wild tubers and grasses that provided carbohydrates consumed by the Indians (Steward 1930). Australian Aborigines, in what is now the state of Victoria, dug extensive canal systems to regulate water levels in wetlands in order to increase the population of wild eels, a major source of protein in their diet (Lourandos 1980). Another group of Aborigines living near the Roper River in the Northern Territories constructed check dams across small streams that helped to maintain the level of water in jungle swamps during the dry season. They did this in order to maintain the habit for wild birds and promote the growth of the wild food that lived in the swamps (Campbell 1965). More than 7000 yr BP, Mesolithic hunters and gatherers in the Lower Yangtze River basin in China intensively managed wild rice growing in coastal swamps and may have constructed bunds to retain nutrient-rich flood waters in their rice fields while blocking inundation by brackish water (Zong et al. 2007).
2. The use of fire by hunter-gathering societies to colonize ecosystems is almost certainly seriously under-reported in the ethnographic literature. It was only in the 1970s that anthropologists began to pay serious attention to this practice, by which time landscape burning had already been suppressed by governments in many parts of the world. In earlier times, most of the vast terrestrial surface area occupied by hunter-gatherers would have been amenable to modification with fire, and I suspect that landscape burning was much more commonly employed by them then.
3. In a book published in German in 2006 (which regrettably I am unable to read), Sieferle and colleagues state that total per capita energy use by hunter-gatherers is much higher (3,810 MJ/capita/yr) than it is for slash-and-burn farmers (950 MJ), settled agriculturalists (73 MJ), and industrial societies (156 MJ) (Sieferle et al. 2006, Table 2.2). Although the amounts of energy used by societies at each social evolutionary stage are different from those in the analysis presented in the present article, the general trend is the same. Curiously, this finding does not seem to have influenced subsequent analyses using the Viennese approach, including Sieferle's (2011) own discussion of the relationship between energy and cultural evolution, in which he states that hunter-gatherers had a total energy use of approximately 10 GJ/capita/yr. I am grateful to an anonymous referee for calling this important work to my attention and sending me a copy of Table 2.2.
4. Sieferle (2011) associates the use of fire by hunter-gatherers to burn the landscape exclusively with its use as a hunting technique. He states that "Fire was also an important instrument for hunting, employed to provoke panic on beasts of prey so that they could more easily be hunted down." Although some hunter-gatherers did occasionally use fire to drive game, it was more commonly employed to deliberately modify the ecosystem (Lewis 1985; Stewart et al. 2002; Williams 2005).
5. Sieferle (2011) argues, following Fischer-Kowalski and Haberl (1997), that "colonization of nature means that humans systematically construct and maintain controlled functional segments within the natural environment" and that "in a strict sense this was only the case with the emergence of agriculture" (Sieferle 2011, 318). But there is no sharp line separating the ways in which hunters and gatherers modify nature and what is done by agriculturalists as Keeley (1995) and Smith (2011) have documented.
6. These estimates employ most of the same data used in Rambo (1991), but have been reworked to use the most conservative available estimates of biomass accumulation.
7. Not only did hunters and gatherers have to spend less time working to meet their subsistence needs than most agriculturalists, but they were also largely free of the degenerative diseases (sometimes called the "diseases of civilization"), such as obesity, diabetes, high blood pressure, and heart disease, that afflict so many people in modern societies (Cordain et al. 2000; Milton 2000). They also enjoyed relatively long lifespans with a modal age of death of 72 years, which, although lower than the 85 years for the United States in 2002 (Gurven and Kaplan 2006, 334–335), is considerably longer than the lifespans of most traditional peasant agriculturalists.
8. The most detailed study, covering a total of 4 months at different times in the annual cycle, of an Aboriginal band in Arnhem Land that had been resettled but returned to the bush for extended periods, found that adults spent an average of 2.6 hours per day in subsistence activities and obtained 4.02 MJ/hr, so needed to work for 2.08 hours to collect sufficient food for 1 person for 1 day (Altman 1987, 92, Table 27; 109, Table 30). An earlier 14-day study of another group of partially sedentarized Aborigines, also in Arnhem Land, found that adults devoted an average of 3 hours and 45 minutes per day to food procurement. It was the height of the dry season, when wild tubers were difficult to find and wild game was relatively scarce, so they obtained 2.9 MJ/hr and spent almost 3 hours to obtain sufficient food to feed 1 person for 1 day (McCarthy and McArthur 1960). A third study by O'Connell and Hawkes (1981, 118, Table 5.A.2) of semisettled Aborigines in the central desert, recorded the time expended and the food energy gained by Aborigines on a number of plant-collecting trips. They report a range of returns from 1.1 to 8.6 MJ/hr (mean = 3.6 MJ/hr or 138 minutes to feed 1 person for 1 day). No data are presented on returns on hunting, which usually provides much greater energy returns per hour than plant foraging under Australian conditions, so actual productivity is probably considerably higher than this. Moreover, their time expenditure data include both procurement and processing time, so are not directly comparable to other studies on agricultural labor productivity.
9. Of course, the Kung San must spend additional time working to process and cook food, collect firewood and water, make and repair tools, and do other household chores (Lee 1984, 51–52), but that is also the case with traditional farmers. My concern in this analysis is solely with efficiency of food production.
10. That Hill and colleagues (1985, 44) found that "no significant difference can be shown to exist between amount of men's subsistence work in foraging societies and subsistence horticultural societies" can be seen as reflecting the fact that both modes of production enjoy very large, and generally unrecognized, subsidies of extrasomatic energy, in the form of fire.
11. Of course, if all of the labor time and energy expended in producing the tools and chemicals on which modern agriculture depends were to be counted, then its labor productivity would be very much lower. As Odum (1967, 60) has pointed out, "the bulk of the persons who work to support the farming process are in cities far

away from the farm, but they are just as necessary to the farm as the man riding the tractor."

12. Assuming that each person expended 4 hours per day on food procurement, this would represent human energy use of approximately 0.2 GJ/capita/yr. Energy utilized in biomass burning would represent 1,572 GJ/capita/yr. No reliable data on the energy value of food obtained are available, but it must have averaged at least 3.5 GJ/capita/yr, assuming that the basic metabolic requirements of the people were being met.
13. Hunter-gatherers and swidden agriculturalists using biomass energy can be grouped together with industrial societies using FF energy into a single sociometabolic regime because none of these systems are constrained by energy. However, they differ in that the societies that depend on biomass energy are space-based systems that cannot support high population densities. In contrast, FF-based industrial societies are not constrained by space. Only the speed with which fossil energy can be extracted from geological deposits and, ultimately, the ability of the global biogeochemical system to absorb the waste products of burning FFs act as constraints on the growth of these societies. I am grateful to an anonymous reviewer for bringing this important distinction to my attention.
14. Per capita energy use is undoubtedly a key metric for explaining differences in the quality of life of people in different societies, but it is largely irrelevant to the explanation of differences in the size and complexity of social systems at different stages of evolution. Trying to differentiate sociometabolic regimes on the basis of per capita energy use is comparable to employing the amount of energy used by individual cells in biological organisms to distinguish simple and complex life forms. Multicellular organisms consume more energy than single-celled ones, but that is a result of their being made up of multiple cells that are united by complex integrative mechanisms and not because each of their individual cells consumes more energy.
15. The Vietnamese kingdom in the mid-1800s, before the French conquest, had a population of some 1.5 million peasant households. Most households were extremely poor, with only approximately 1 ha of rice land, which yielded approximately 1.5 t of paddy rice (Dumont 1935). This represents an energy value of 15.4 GJ, which is barely sufficient to feed a family of five for 1 year. Despite their poverty, each household would have been forced to contribute approximately 300 kg of grain (3 GJ) in taxes to the state (as well as also frequently being forced to send members to work as unpaid laborers on state projects). When multiplied by the 1.5 million peasant households in the kingdom, this represented a huge pool of energy (4.5 million GJ) that was used to support the functioning of the state's integrative institutions, allowing the state to expend more than 12,300 GJ/day of energy to maintain its integrative institutions (Rambo 1991).
16. Operation of the telecommunications system in the United States consumes more than 274 TJ/day of electrical energy (Mathews 2003), whereas operation of television sets uses 454 TJ/day (Ostendorp et al. 2005).

References

Altman, J. C. 1987. *Hunter-gatherers today: An aboriginal economy in North Australia*. Canberra: Australian Institute of Aboriginal Studies.

Anderson, M. K. 1994. Prehistoric anthropogenic wildland burning by hunter-gatherer societies in the temperate regions: A new source, sink, or neutral to the global carbon budget? *Chemosphere* 29(5): 913–934.

Bird, R. B., D. W. Bird, B. F. Codding, C. H. Parker, and J. H. Jones. 2008. The "fire stick farming" hypothesis: Australian aboriginal foraging strategies, biodiversity, and anthropogenic fire mosaics. *Proceedings of the National Academy of Sciences* 105(39): 14796–14801.

Blackburn, T. C., and K. Anderson, eds. 1993. *Before the wilderness: Environmental management by native Californians*. Menlo Park, CA, USA: Ballena.

Campbell, A. H. 1965. Elementary food production by the Australian Aborigines. *Mankind* 6(5): 206–211.

Chen, X., L. B. Hutley, and D. Eamus. 2003. Carbon balance of a tropical savanna of northern Australia. *Oecologia* 137(3):405–416.

Cook, E. 1971. The flow of energy in an industrial society. *Scientific American* 224(3): 134–147.

Cottrell, F. 2009. *Energy & society*. Revised edition. Bloomington, IN, USA: AuthorHouse.

Cordain, L., J. B. Miller, S. B. Eaton, N. Mann, S. H. A. Holt, and J. D. Speth. 2000. Plant-animal subsistence ratios and macronutrient energy estimations in worldwide hunter-gatherer diets. *American Journal of Clinical Nutrition* 71(3): 682–692.

Debeir, J-C., J-P. Deleage, and D. Hemery. 1991. *In the servitude of power: Energy and civilisation through the ages*. London: Zed Books.

Dumont, R. 1935. *La culture du riz dans la delta du Tonkin* [Rice cultivation in the Tonkin Delta]. Paris: Societe d'Editions Geographiques, Maritmes et Coloniales.

Fischer-Kowalski, M. and H. Haberl. 2007. Conceptualizing, observing and comparing socioecological transitions. In *Socioecological transitions and global change: Trajectories of social metabolism and land use*, edited by H. Haberl and M. Fischer-Kowalski, pp.1–30. Cheltenham, UK: Edward Elgar.

Fischer-Kowalski, M. and J. Rotmans. 2009. Conceptualizing, observing, and influencing social-ecological transitions. *Ecology and Society* 14(2): 3–20.

Fischer-Kowalski, M., S. J. Singh, L. Ringhofer, C. M. Grünbühel, C. Lauk, and A. Remesch. 2010. *Sociometabolic regimes in indigenous communities and the crucial role of working time: A comparison of case studies*. Social ecology working paper 121. Vienna: Institute of Social Ecology.

Fischer-Kowalski, M., S. Marina, J. Simron, C. Lauk, A. Remesch, L. Ringhofer, and C. M. Grünbühel. 2011. Sociometabolic transitions in subsistence communities: Boserup revisited in four comparative case studies. *Human Ecology Review* 18(2): 147–158.

Gelfand, I., S. S. Sieglindes, and G. P. Robertson. 2010. Energy efficiency of conventional, organic, and alternative cropping systems for food and fuel at a site in the U.S. Midwest. *Environmental Science & Technology* 44(10): 4006–4011.

Goudsblom, J. 1992. *Fire and civilization*. London: Allen Lane.

Gould, R. A. 1971. Uses and effects of fire among the Western Desert Aborigines of Australia. *Mankind* 8(1): 14–24.

Grünbühel, C. M., H. Haberl, H. Schandl, and V. Winiwarter. 2003. Socioeconomic metabolism and colonization of natural processes in SangSaeng Village: Material and energy flows, land use, and cultural change in Northeast Thailand. *Human Ecology* 31(1): 53–86.

Gurven, M. and H. Kaplan. 2006. Longevity among hunter-gatherers: A cross-cultural examination. *Population and Development Review* 33(2): 321–365.

Haberl, H. 2002. The energetic metabolism of societies. Part II: Empirical examples. *Journal of Industrial Ecology* 5(2): 71–88.

Haberl, H., H. Weisz, C. Amann, A. Bondeau, N. Eisenmenger, K-H. Erb, M. Fischer-Kowalski, and F. Krausmann. 2006. The energetic metabolism of the European Union and the United States: Decadal energy input time-series with an emphasis on biomass. *Journal of Industrial Ecology* 10(4): 151–171.

Hallam, S. J. 1985. The history of aboriginal firing. In *Fire ecology and management in Western Australian ecosystems*, edited by J. R. Ford, pp.7–20. WAIT Environmental Studies Group report no. 14. Perth, WA, Australia: Western Australian Institute of Technology.

Hill, K., H. Kaplan, K. Hawkes, and A. M. Hurtado. 1985. Men's time allocation to subsistence work among the Ache of Eastern Paraguay. *Human Ecology* 13(1): 29–47.

Hough, W. 1926. *Fire as an agent in human culture*. United States National Museum bulletin no. 139. Washington, DC: Smithsonian Institution.

Jones, R. 1969. Firestick farming. *Australian Natural History* 16(7): 224–228.

Jones, R. 1980. Hunters in the Australian coastal savanna. In *Human ecology in savanna environments*, edited by D. Harris, pp.107–146. London: Academic.

Keeley, L. H. 1995. Protoagricultural practices among hunter-gatherers: A cross-cultural survey. In *Last hunters, first farmers: new perspectives on the prehistoric transition to agriculture*, edited by T. D. Price and A. B. Gebauer, pp.243–272. Santa Fe, NM, USA: School of American Research.

Kelly, R. L. 1995. *The foraging spectrum: Diversity in hunter-gatherer lifeways*. Washington, DC: Smithsonian Institution Press.

Krausmann, F., M. Fischer-Kowalski, H. Schandl and N. Eisenmenger. 2008. The global sociometabolic transition: Past and present metabolic profiles and their future trajectories. *Journal of Industrial Ecology* 12(5–6): 637–656.

Kuhn, S. L. and M. C. Stiner. 2001. The antiquity of hunter-gatherers. In *Hunter-gatherers: An interdisciplinary perspective*, edited by C. Panter-Brick, R. H. Layton, and P. Rowley-Conway, pp.99–142. Cambridge, UK: Cambridge University Press.

Lacey, C., J. Walker, and I. Noble. 1982. Fire in Australian tropical savannas. In *Ecology of tropical savannas*, edited by, B. J. Huntley and B. H. Walker, pp.246–272. Berlin: Springer Verlag.

Laland, K. N., J. Odling-Smee, and M. W. Feldman. 2000. Niche construction, biological evolution, and cultural change. *Behavioral and Brain Sciences* 23(1): 131–175.

Le, T. C. and A. T. Rambo, eds. 1993. *Too many people, too little land: The human ecology of a wet rice-growing village in the Red River Delta of Vietnam*. Honolulu, HI, USA: East-West Center.

Lee, R. B. 1979. *The !Kung San: Men, women and work in a foraging society*. Cambridge, UK: Cambridge University Press.

Lee, R. B. 1984. *The Dobe !Kung*. New York: Holt, Rinehart and Winston.

Lewis, H. T. 1982. *A time for burning*. Occasional publication no. 17. Edmonton, Alberta, Canada: University of Alberta, Boreal Institute for Northern Studies.

Lewis, H. T. 1985. Burning the "top end": Kangaroos and cattle. In *Fire ecology and management in Western Australian ecosystems*, edited by J. Ford. WAIT Environmental Studies Group report no. 14. Perth, WA, Australia: Western Australian Institute of Technology.

Lewis, H. T. and T. A. Ferguson. 1988. Yards, corridors, and mosaics: How to burn a boreal forest. *Human Ecology* 16(1): 57–77.

Lourandos, H. 1980. Change or stability?: Hydraulics, hunter-gatherers and population in temperate Australia. *World Archaeology* 11(3): 245–264.

McCarthy, F. D. and M. McArthur. 1960. The food quest and the time factor in Aboriginal economic life. In *Records of the American-Australian scientific expedition to Arnhem Land, vol. 2 anthropology and nutrition*. edited by C. P. Mountford, pp 145–194. Melbourne, Australia: Melbourne University Press.

McGrath, D. G. 1987. The role of biomass in shifting cultivation. *Human Ecology* 15(2): 221–242.

Mathews, H. S. 2003. Electricity use of wired and wireless telecommunications networks in the united states. *ISEE International Symposium on Electronics and the Environment, 2003*, pp. 131–136. Washington, DC: IEEE Computer Society.

Mellars, P. 1976. Fire ecology, animal populations and man: A study of some ecological relationships in prehistory. *Proceedings of the Prehistoric Society* 42: 15–45.

Milton, K. 2000. Hunter-gatherer diets—A different perspective. *American Journal of Clinical Nutrition* 71(3): 665–667.

Mistry, J, A. Berardi, V. Andrade, T. Kraho, P. Kraho, and O. Leonardos. 2005. Indigenous fire management in the *cerrado* of Brazil: The case of the Kraho of Tocantins. *Human Ecology*. 33(3): 365–386.

Murphy, M. R. and D. M. J. S. Bowman. 2007. The interdependence of fire, grass, kangaroos and Australian Aborigines: A case study from central Arnhem Land, northern Australia. *Journal of Biogeography* 34(2): 237–250.

Nielsen, U., O. Mertz, and G. T. Noweg. 2006. The rationality of shifting cultivation systems: Labor productivity revisited. *Human Ecology* 34(2): 201–218.

Odum, H. T. 1967. Energetics of food production. In *The world food problem*, Report of the President's Science Advisory Committee, Panel on World Food Supply, Vol. 3, pp. 55–94. Washington, DC: The White House.

O'Connell, J. F. and K. Hawkes. 1981. Alyawara plant use and optimal foraging theory. In *Hunter-gatherer foraging strategies: Ethnographic and archeological analyses*, edited by B. Winterhalder and E. A. Smith pp. 99–125. Chicago, IL, USA: University of Chicago Press.

Ostendorp, P., S. Foster, and C. Calwell. 2005. *Televisions: Active mode energy use and opportunities for energy savings*. Washington, DC: Natural Resources Defense Council Issue Paper.

Pimentel, D. 2009. Energy inputs in food crop production in developing and developed nations. *Energies* 2(1): 1–24.

Pimentel, D. and M. H. Pimentel. 2008. *Food, energy, and society*. Third edition. Boca Raton, FL, USA: CRC.

Pivello, V. R. 2011. The use of fire in the cerrado and Amazonian rainforests of Brazil: Past and present. *Fire Ecology* 7(1): 24–39.

Pyne, S. J. 2005. *World of fire: The culture of fire on earth*. Seattle, WA, USA: University of Washington Press.

Rambo, A. T. 1980. Fire and the energy efficiency of swidden agriculture. *Asian Perspectives* 23(2): 309–316.

Rambo, A. T. 1985. *Primitive polluters: Semang impact on the Malaysian tropical rain forest ecosystem*. Anthropological papers no. 76. Ann Arbor, MI, USA: University of Michigan, Museum of Anthropology.

Rambo, A. T. 1991. Energy and the evolution of culture: A reassessment of White's law. In *Profiles in cultural evolution: Papers from*

a conference in honor of Elman R. Service, edited by A.T. Rambo and K. Gillogly pp. 291–307. Anthropological papers no. 85. Ann Arbor, MI, USA: University of Michigan Museum of Anthropology.

Rappaport, R. A. 1971. The flow of energy in an agricultural society. *Scientific American* 225(3): 116–132.

Ross, E. A. and G. E. Machlis. 1983. Energetic theories of society: An evaluative review. *Social Inquiry* 53(2–3): 152–178.

Russell-Smith, J., D. Lucas, M. Gapindi, B. Gunbunuka, N. Kapirigi,G.Namingum, K. Lucas, P. Giuliani, and G. Chaloupka. 1997. Aboriginal resource utilization and fire management practice in Western Arnhem Land, monsoonal Northern Australia: Notes for prehistory, lessons for the future. *Human Ecology* 25(2): 159–195.

Sahlins, M. 1974. *Stone age economics*. London: Tavistock Publications.

Service, E. R. 1971. *Profiles in ethnology*. New York: Harper & Row.

Shaffer, L. J. 2010. Indigenous fire use to manage savanna landscapes in southern Mozambique. *Fire Ecology* 6(2): 43–59.

Sheuyange, A., G. Oba, and R. B. Weladji. 2005. Effects of anthropogenic fire history on savanna vegetation in northeastern Namibia. *Journal of Environmental Management* 75(3): 189–198.

Sieferle, R. P. 1997. *Ruckblick auf die natur, eine geschichte des menschen und seiner umwelt* [Looking back on nature. A history of man and his environment]. Munich, Germany: Luchterhand Verlag.

Sieferle, R. P. 2001. *The subterranean forest: Energy systems and the industrial revolution*. Cambridge, UK: The White Horse Press.

Sieferle, R. P. 2011. Cultural evolution and social metabolism. *Geografiska Annaler Series B* 93(4): 315–324.

Sieferle, R. P., F. Krausmann, H. Schandl and V. Winiwarter. 2006. *Das Ende der Fläche* [The end of area]. Zum gesellschaftlichen Stoffwechsel der Industrialisierung (= Umwelthistorische Forschungen; Bd. 2). Köln/Weimar/Wien, Germany: Böhlau.

Smil, V. 1994. *Energy in world history*. Boulder, CO, USA: Westview.

Smil, V. 2004. World history and energy. In *Encyclopedia of energy*, Vol. 6, edited by C. J. Cleveland, pp.549–561. New York: Elsevier Science.

Smith, B. D. 2011. General patterns of niche construction and the management of "wild" plant and animal resources by small-scale pre-industrial societies. *Philosophical Transactions of the Royal Society B* 366(1566): 836–848.

Steinhart, J. S. and C. E. Steinhart. 1974. Energy use if the U.S. food system. *Science* 184(134): 307–316.

Steward, J. H. 1930. Irrigation without agriculture. *Papers of the Michigan Academy of Sciences, Arts, and Letters* 12: 149–156.

Stewart, O. C., H. T. Lewis, and M. K. Anderson, eds. 2002. *Forgotten fires: Native Americans and the transient wilderness*. Norman, OK, USA: University of Oklahoma Press.

Van der Eng, P. 2004. Productivity and comparative advantage in rice agriculture in South-East Asia since 1870. *Asian Economic Journal* 18(4): 345–370.

Vigilante, T., B. P. Murphy, and D. M. J. S. Bowman. 2009. Aboriginal fire use in Australian tropical savannas: Ecological effects and management lessons. In *Tropical fire ecology, climate change, land use and ecosystem dynamics*, edited by M. Cochrane, pp.143–167. Heidelberg, Germany: Springer Praxis.

Waguespack, N. M. 2005. The organization of male and female labor in foraging societies: Implications for early Paleoindian archaeology. *American Anthropologist* 107(4): 666–676.

Williams, G. W. 2005. *References on the American Indian use of fire in ecosystems*. Unpublished manuscript. Washington, DC: USDA Forest Service

White, L. A. 1943. Energy and the evolution of culture. *American Anthropologist* 45(3): 335–356.

White, L. A. 1959. Energy and the evolution of culture. In *The science of culture: A study of man and civilization*, pp. 363–393. New York: Grove.

Zong, Y., Z. Chen, J. B. Innes, C. Chen, Y. Wang, and H. Wang. 2007. Fire and flood management of coastal swamp enabled first rice paddy cultivation in East China. *Nature* 449(7161): 459–462.

About the Author

A. Terry Rambo is a professor in the Program on System Approaches in Agriculture, Faculty of Agriculture, Khon Kaen University, Thailand, and an adjunct senior fellow of the East-West Center, Honolulu, HI, USA.

THE CONTRIBUTION OF SOIL PHYSICOCHEMICAL PROPERTIES TO THE PRESENCE AND GENETIC DIVERSITY OF *BURKHOLDERIA PSEUDOMALLEI*

Rinrapee Ngamsang[1,2], Chotima Potisap[1,3], Atcha Boonmee[1,4], Phrueksa Lawongsa[5], Thotsapol Chaianunporn[6], Surasakdi Wongratanacheewin[1,2], Jorge LM Rodrigues[7] and Rasana W Sermswan[1,3]

[1]Melioidosis Research Center, Khon Kaen University; [2]Department of Microbiology; [3]Department of Biochemistry, Faculty of Medicine, Khon Kaen University; [4]Department of Microbiology, Faculty of Science, Khon Kaen University; [5]Plant Science and Agricultural Resources, Faculty of Agriculture, Khon Kaen University; [6]Department of Environmental Science, Faculty of Science, Khon Kaen University, Khon Kaen; Thailand;[7]Department of Biology, University of Texas at Arlington, TX, USA

Abstract. *Burkholderia pseudomallei* (Bp), the causative agent of melioidosis, is unevenly distributed in the complex soil environment. Physicochemical factors in the soil have been reported to affect microbial communities in the soil. The effect of physicochemical factors on the number and diversity of organisms in the soil has not been reported. Twenty-five each *B. pseudomallei*-positive and -negative soil samples were collected from a melioidosis-endemic area. The amount of Bp in each soil sample was measured by culture and quantitative PCR (qPCR). The following physicochemical properties from each soil sample were measured: pH, total organic carbon (TOC), total nitrogen (TN), carbon to nitrogen ratio (C:N ratio), exchangeable calcium (EC) and extractable iron (EI). All the physicochemical properties measured were significantly different between the Bp-positive and -negative soil samples. The Bp-positive soil samples had lower C:N ratios and lower EC and a higher EI ($p<0.05$) than the Bp-negative samples. The average pH was lower (3.7-5.0) in the Bp-negative samples. Among the Bp-positive soil samples, the EC was negatively correlated with the PCR copy number. The amount of bacteria detected with the qPCR method was higher than with the culture method, suggesting the presence of unculturable forms of bacteria that might re-grow when the environmental conditions was suitable. A total of 117 Bp isolates obtained from the soil samples were classified into 25 groups using BOX-PCR. The genetic diversity of Bp, did not correlate with the physicochemical factors investigated. A suitable pH range and C:N ratio may be important for the presence of Bp. The EI supports the needs and EC probably alters the growth of Bp. The genetic diversity of the bacteria was not influenced by the soil factors

Correspondence: Rasana W Sermswan, Department of Biochemistry, Faculty of Medicine, Melioidosis Research Center, Khon Kaen University, 123 Mitraparb Road, Khon Kaen 40002, Thailand. Tel/Fax: 66 (0) 43 363265, 66 (0) 43 348386; E-mail: rasana@kku.ac.th

investigated in this study. This information shows the environment conducive to the growth of Bp. This gives us information about how to potentially control or decrease Bp in the soil in the future.

Keywords: *Burkholderia pseudomallei*, melioidosis, soil physicochemical factors, qPCR

INTRODUCTION

The gram-negative bacterium *Burkholderia pseudomallei* is the causative agent of melioidosis, an infectious disease in humans and other animals (White, 2003). The disease is endemic in Southeast Asia and northern Australia. Sporadic cases have been reported in travelers to endemic areas (Dance, 1991; Wilks *et al*, 1994). In Thailand, most of the cases occur in the northeastern part of the country. The average annual melioidosis incidence during 1997- 2006 in Ubon Ratchathani Province was 12.7 cases per 100,000 people per year with the highest rate being 21.3 cases per 100,000 people during 2006 (Limmathurotsakul *et al*, 2010). *B. pseudomallei* is a widely distributed environmental saprophyte found in the soil and water of many tropical countries. It is resistant to a variety of adverse environmental conditions (Cheng and Currie, 2005). Humans become infected by inoculation of contaminated soil or water through skin abrasions, by inhalation of contaminated dust and ingestion of contaminated water. Patients with recreational or occupational exposure to mud and surface water, particularly rice farmers, have a greater potential of becoming infected with this bacterium (Heng *et al*, 1998).

The amount of *B. pseudomallei* in the soil has been estimated to be 20-fold higher in northeastern Thailand than in central Thailand (Smith *et al*, 1995). This results in a 10-fold greater incidence of melioidosis in the northeastern Thailand than central Thailand (Suputtamongkol *et al*, 1994). Khon Kaen Province is endemic for melioidosis (Wuthiekanun *et al*, 1995). From our survey as previously reported, Nam Phong District has more *B. pseudomallei* in the soil than any other district in Khon Kaen. *B. pseudomallei* is more culturable in sandy soil at a pH of 5.0 to 6.0, a moisture content >10% and higher chemical oxygen demand (COD) and total nitrogen levels (Palasatien *et al*, 2008).

Soil is a complex environment and a reservoir for microbial communities (Robe *et al*, 2003). Besides the type and amount of microbes affecting the soil microbial community, soil physicochemical properties also have an effect. Besides studying microbial diversity using molecular biology techniques, the study of physicochemical properties of soil is also important (Maron *et al*, 2011). It is important to study the amount and genetic diversity of *B. pseudomallei* in association with the physicochemical properties of the soil where it is endemic. This information could improve measures for controlling and decreasing the amount of *B. pseudomallei* in the soil.

MATERIALS AND METHODS

Soil sampling

Soil samples were collected from the agricultural fields of the Faculty of Agriculture, Khon Kaen University, Khon Kaen, Thailand. To determine the sampling sites, soil samples were collected from 20 randomly selected areas in the fields and the presence or absence of *B. pseudomallei* was determined by the direct culture and

the sites were designated as either positive or negative for *B. pseudomallei*. Then, each site was divided into 25, 1.5 x 1.5 m grids. Soil samples were collected from each grid. The grid locations were marked by a global position system (GPS) device (GPSMAP® 60CSx, Garmin, Lenexa, KS) using the center of each grid. Each soil sample was collected at 15 cm below the soil surface using a spade that was cleaned and disinfected prior to use. One sample was made from a pooled collection 3 sampling locations in a triangle 30 cm from the center of each grid. Soil samples were kept in a closed container at room temperature in the dark until use. Two hundred grams of soil from each sample were used for microbial culture and biological studies, while 300 g of soil were used for physicochemical property analysis.

Soil physicochemical properties

The physicochemical properties of the soil samples were determined at the Department of Land Resources and Environment, Faculty of Agriculture, Khon Kaen University, Khon Kaen, Thailand.

The soil pH was measured by mixing 20 ml sterile distilled water with 20 g soil and stirring to form a paste and then left for 60 minutes; the suspension was then re-stirred and the pH was measured immediately using a pH meter (Jones, 2001).

The total organic carbon (TOC) level of the soil was determined using the dichromate oxidation method according to Walkley and Black (1934).

The total nitrogen (TN) level of the soil, which includes both organic and inorganic forms of nitrogen,was measured using the micro-Kjeldahl digestion method with a 2 g soil sample (Bremner, 1965).

Calcium was extracted from a 5 g soil sample using 1N ammonium acetate (NH_4OAc) and the exchangeable calcium (EC) level was determined using flame photometry (Berry *et al*, 1946).

Iron was extracted from 10 g soil using diethylenetriaminepentaacetic acid solution and the extractable iron (EI) level was measured by flame atomic absorption spectrometry (Lindsay and Norvell, 1978).

Bacterial culture of the soil

B. pseudomallei in the soil was detected by direct and enrichment culture methods as described previously (Wuthiekanun *et al*, 1990). Suspected colonies are wrinkled and violet-purple in color. The bacteria were grown by direct culture; enriched culture was used if the bacteria could not be grown on direct culture. The bacteria were then identified using latex agglutination with a monoclonal antibody specific to *B. pseudomallei* (Samosornsuk *et al*, 1999). At least 5-10 colonies of *B. pseudomallei* from each grid were used for BOX-PCR analysis.

Detection of *B. pseudomallei* by semi-nested PCR

To detect *B. pseudomallei* in soil, the total DNA was extracted from soil samples using a DNA extraction kit (PowerSoil® DNA Isolation Kit; MO BIO Laboratories, Carlsbad, CA). *B. pseudomallei* DNA was detected by semi-nested PCR, using primers for the 16S-23S intergenic spacer (Inglis *et al*, 2005) with slight modification. The first-round primers were Bp1 (5′CGATGATCGTTGGCGCTT) and Bp4 (5′CGTTGTGCCGTATTCCAAT), and the second-round primers were Bp1 and Bp3 (5′ATTAGAGTCGAACAAT). For the first-round PCR, a total volume of 20 µl was used, which consisted of 0.5 units of Taq polymerase (RBC Bioscience, New Taipei City, Taiwan), 1x buffer, 0.2 mM dNTPs, 1.5 mM $MgCl_2$, and 0.2 µM each for Bp1 and Bp4 and 2 µl of DNA template. For the second-round, the Bp1

and Bp3 primers were used and 0.4 µl of the first-round product was used as the DNA template. The amplification conditions for first-round cycling were pre-denaturation at 94°C for 5 minutes, activation of the polymerase, 45 cycles at 94°C for 30 seconds for denaturation, 30 seconds at 55°C for annealing, 45 seconds at 72°C for extension and then 72°C for 7 minutes. Second-round amplification was carried out under the same conditions as the first round, except 50°C was used as the annealing temperature. The PCR products were analyzed with 1% agarose gel-electrophoresis.

DNA extraction of cultured *B. pseudomallei*

B. pseudomallei was cultured in 1.5 ml of Luria-Bertani broth and incubated at 37°C with shaking at 200 rpm for 16 hours. The DNA was extracted from the cell pellets using the SDS and Proteinase K method (Goldenberger *et al*, 1995). The DNA pellet was re-suspended in 30 µl TE buffer (2M Tris-HCl pH 8, 0.5 M EDTA pH 8) and stored at -20°C until used.

BOX-PCR genomic typing

Repetitive sequence-based PCR using the BOXA1R primer (5′CTACG-GCAAGGCGACGCTGACG) (de Versalovic *et al*, 1998) was used for BOX-PCR typing. The 25 µl PCR reaction mixture consisted of 2 units of *Taq* polymerase (Roche, Indianapolis, IN), 1xbuffer, 50 ng DNA templates, 600 µM dNTPs, 1.3 µl of primer (300 ng/µl), 0.2 µl BSA (20 mg/ml) and 10% v/v of dimethyl sulfoxide. Pre-denaturation of template DNA was done at 96°C for 10 minutes and then *Taq* polymerase was subsequently added. The PCR reaction was conducted for 30 rounds using denaturation at 92°C for 30 seconds, primer annealing at 50°C for 1 minute, elongation at 65°C for 8 minutes and then 65°C for 8 minutes. The PCR products were then analyzed with 2% agarose gel-electrophoresis using TAE buffer (Mirza *et al*, 2009).

Quantitative PCR (qPCR)

The quantitative PCR was carried out using the iTaqTMFast SYBR Green Supermix with a ROX kit (Bio-Rad, Hercules, CA). The 20 µl reaction mixture consisted of 10 µl iTaqTM Fast SYBR Green Super mix with ROX, 10 ng of DNA sample and 100 nM of each 16S-23S spacer primer. The expected size of the first round PCR product was 302 bp and the second round was 285 bp. Amplification was performed using the Applied Biosystems 7300 Real-Time PCR System (Applied Biosystems, Carlsbad, CA). The PCR amplification conditions were 95°C for 5 minutes, 40 cycles of denaturation at 95°C for 30 seconds, annealing at 55°C for 30 seconds and then extension at 72°C for 30 seconds. Specificity of the qPCR products was confirmed using melting curve analysis. Standard curves using 10^1-10^7 copies per reaction of 16S-23S intergenic spacer were generated with plasmid DNA containing a fragment of the 16S-23S spacer. The qPCR efficiency (E) was calculated using the equation E=10[-1/slope]. The real-time efficiency of the 16S-23S spacer was 1.79 ± 0.01 and the R^2 of the standard curve was 0.99.

Statistical analysis

The program SPSS, version 16.0 (IBM, Armonk, NY) was used to analyze the physicochemical properties of *B. pseudomallei*-positive and -negative soil. The independent samples *t*-test was used when two separate sets of independent data were normally distributed. The non-parametric test, Mann-Whitney *U* test, was used when two separate sets of independent data were not normally distributed. The generalized linear model (GLM) method was used to study the

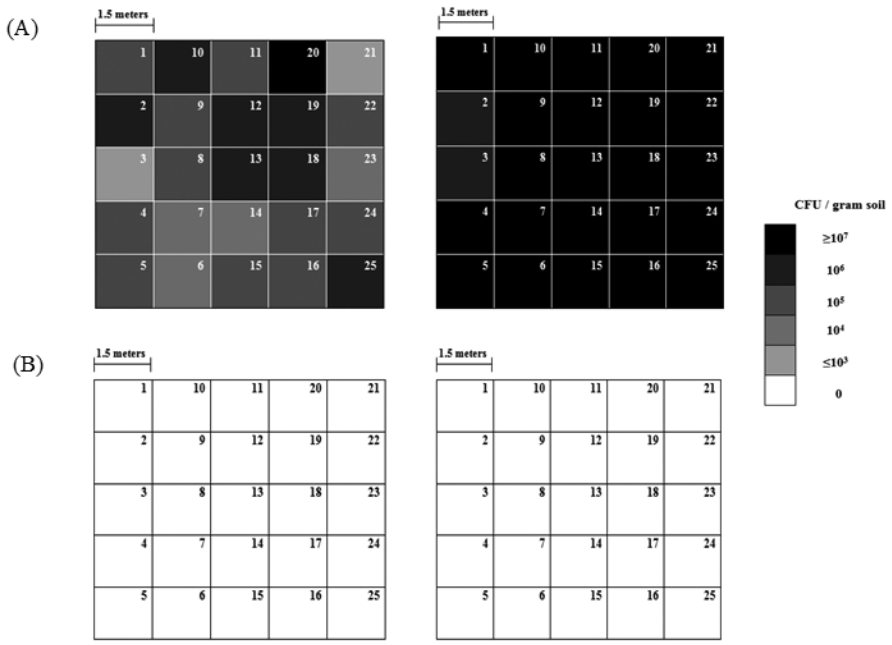


Fig 1–Culture of *B. pseudomallei* from the soil. (A) Colony count obtained from positive soil by direct culture (left) and enriched culture (right). (B) Results of all negative soil direct culture (left) and enriched culture (right).

correlation between soil physicochemical factors and the numbers of *B. pseudomallei* in the positive soil samples.

RESULTS

B. pseudomallei culture and DNA extraction from the soil

The 25 *B. pseudomallei* direct culture positive samples had concentrations of 1×10^3-6.6×10^6 colonies/g of soil. The concentration of *B. pseudomallei* with the enriched culture was $\geq10^7$ colonies/g soils (Fig 1A). The 25 soil sites that positive by culture were all positive by nested-PCR. For the negative site, *B. pseudomallei* was confirmed to be negative by both direct and enriched methods in all 25 sites (Fig 1B). When these 25 negative soil samples were confirmed by nested-PCR, 2 of them were positive for *B. pseudomallei* at the second round of amplification. Therefore, these 2 samples were excluded from physicochemical factors analysis of the negative site.

Physicochemical properties of soil

The pH, TOC, TN, EC, and EI from *B. pseudomallei*-positive and -negative soil sites were compared. The average values for all the physicochemical properties tested were significantly different between the positive and negative sites ($p<0.05$) (Table 1, Fig 2).

The pH for all the soil samples was below 7, indicating generally acidic soil in the study area. The pH values in the *B. pseudomallei*-positive soil site ranged from 4.13 to 5.05 and the average pH value of 4.6 in the *B. pseudomallei*-positive soil was higher than the 4.4 in the *B. pseudomallei*-negative soil (range 3.66 to 4.42).

Table 1
Physicochemical properties of *B. pseudomallei*-positive and -negative soil samples.

Factor	Positive site (n=25)	Negative site (n=23)	p-value
pH	4.578±0.2238	4.149±0.2244	<0.001[b]
Total organic carbon (%)	0.385±0.067	0.559±0.065	<0.001[b]
Total nitrogen (%)	0.027±0.005	0.023±0.004	0.012[a]
Carbon to nitrogen ratios	14.65±1.937	24.69±5.248	<0.001[b]
Exchangeable calcium (mg/kg)	43.60±27.82	67.20±39.85	0.016[a]
Extractable iron (ppm)	45.36±18.44	17.88±7.219	<0.001[b]

Each value represents the mean ± standard deviation.
[a]Significant at p<0.05; [b]Significant at p<0.001.

Table 2
Correlation between real time PCR results and soil physicochemical properties predicted by a generalized linear model.

Variable	Estimate	Std error	t-value	p-value
Intercept	-903375.0	830807.3	-1.087	0.290
pH	333338.4	208090.1	1.602	0.126
Total organic carbon	-482759.4	819030.0	-0.589	0.563
Total nitrogen	-978734.7	8453178.7	-0.116	0.909
Exchangeable calcium	-3432.2	1492.4	-2.300	0.033*
Extractable iron	472.1	2772.4	0.170	0.867

* Statistically significant (p<0.05).

The TOC in the *B. pseudomallei*-positive soil ranged from 0.26% to 0.52%, and the average in the *B. pseudomallei*-positive soil (0.39%) was lower than the 0.56% in the *B. pseudomallei*-negative soil (ranged from 0.30 to 0.63%). The average TN in the *B. pseudomallei*-positive soil was 0.027% (ranged from 0.02% to 0.04%), which was higher than the average of 0.023% (ranged from 0.02% to 0.03%) in the *B. pseudomallei*-negative soil. The C:N ratio in the *B. pseudomallei*-positive soil ranged from 12.23 to 21.00 and the average value is 14.7, which is lower than the average 24.7 in *B. pseudomallei*-negative soil (ranged from 15.20 to 36.69).

The EC in the *B. pseudomallei*-positive soil ranged from 10 to 100 mg/kg and the average value 44 mg/kg was lower than 67 mg/kg in the *B. pseudomallei*-negative soil (ranged from 20 to 190 mg/kg). The EI in the *B. pseudomallei*-positive soil ranged from 17 to 90 ppm and the average of 45.4 ppm was significantly higher than 17.9 in the *B. pseudomallei*-negative soil (ranged from 8 to 35 ppm).

Correlation between the concentration of bacteria in the soil and the soil physicochemical properties

A qPCR with standard curve was used to quantify the amount of *B. pseudomallei*

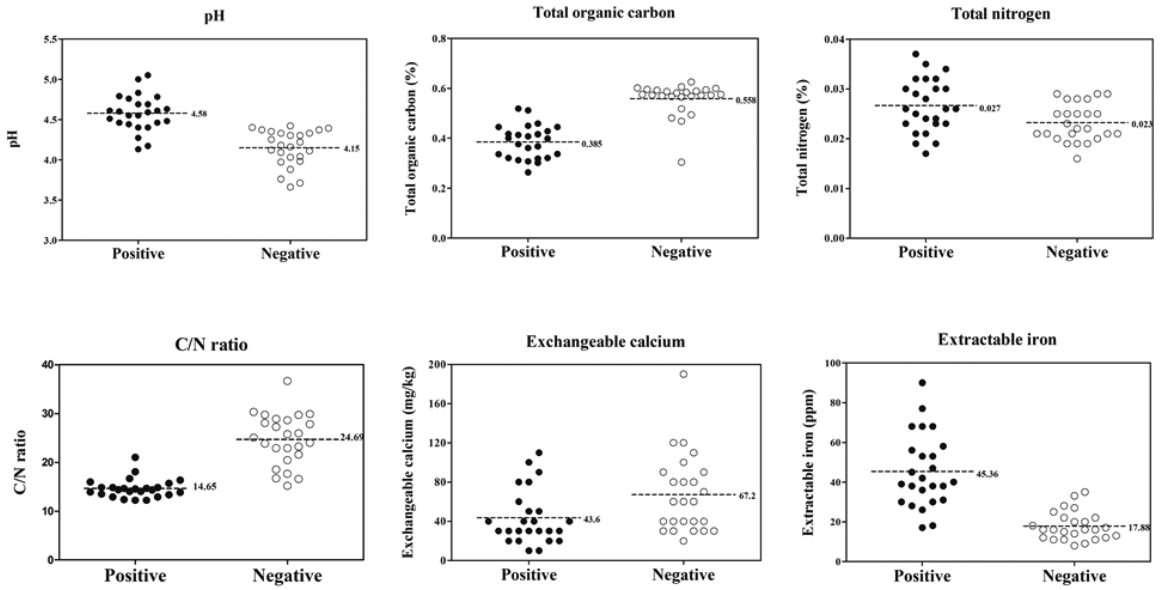


Fig 2–Scatter dot plot of the physicochemical factors investigated in positive and negative soil sites. The pH, total organic carbon, extractable iron and C:N ratio were significantly different between negative and positive soil sites.

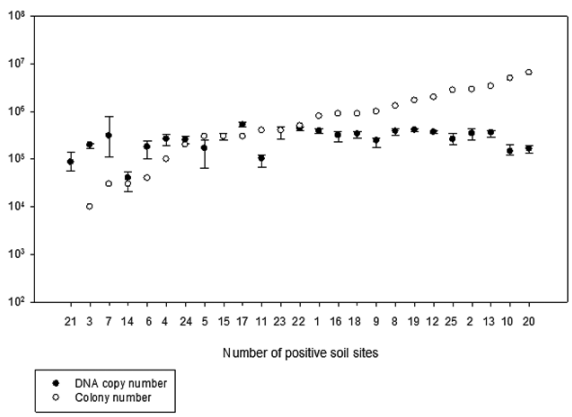


Fig 3–Scatter plots for DNA copy numbers by qPCR and direct soil culture.

in soil. There were 6 sites that DNA copy was higher than colony count, whereas 13 sites showed higher colony count than DNA copy number and 6 sites equivalent (Fig 3). The average of *B. pseudomallei* copy number was 2.82×10^5. The generalized linear model (GLM) method was used to study the correlation between soil physicochemical properties in *B. pseudomallei*-positive soil and DNA copy number of *B. pseudomallei*. The GLM showed only a negative correlation between EC and the number of DNA copies of *B. pseudomallei* ($p<0.05$) (Table 2).

The diversity of *B. pseudomallei*

One hundred seventeen *B. pseudomallei* isolates were collected. Their genotypes were analyzed using a BOX-PCR. Amplification of the *B. pseudomallei* DNA using BOXA1R primers generated variety of numbers and sizes of amplicons. The fingerprint patterns generated by the BOX-PCR consisted of 14-24 DNA fragments with a range of 0.28-10.0 kb. The band patterns from gel-electrophoresis were analyzed and classified into 25 distinct patterns (Fig 4A). Each isolate was classified with the BOX-PCR correlated

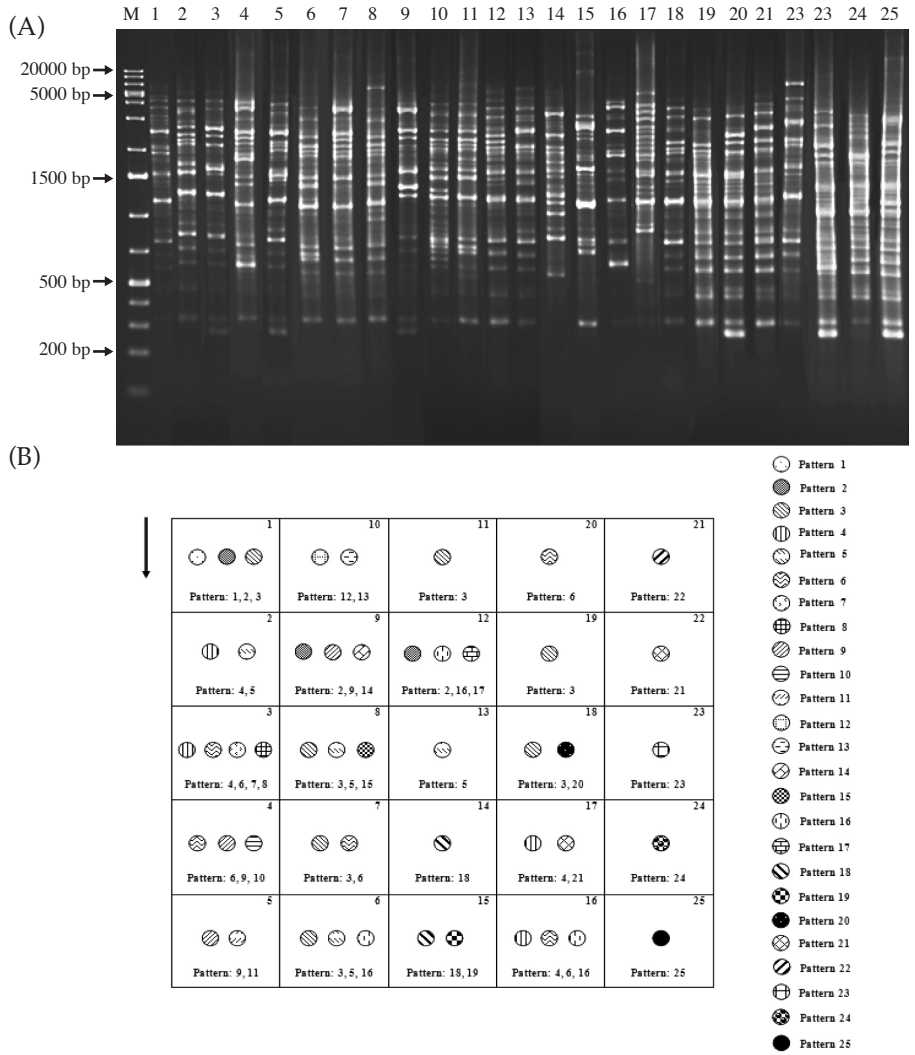


Fig 4–Type and diversity of *B. pseudomallei* in soil. Twenty-five BOX-PCR patterns seen on agarose gel (A) and diversity of *B. pseudomallei* as seen by spots of BOX-PCR obtained from each grid (B).

with its grid (Fig 4B). The more patterns per grid indicated the greater the diversity of *B. pseudomallei.*

The correlation between soil physicochemical properties and the genetic diversity of *B. pseudomallei* at each site was examined by plotting each physicochemical property against the number of genotypes of *B. pseudomallei* in each grid, plotted from the lowest to the highest number. The genetic diversity of *B. pseudomallei* tended to increase with increases in TOC, TN and EI values, but this trend was not significant (Fig 5).

DISCUSSION

B. pseudomallei can be generally found in Thailand, particularly in the northeast where 50.1% of soil samples are positive (Vuddhakul *et al*, 1999). Northeastern Thailand is also known as the endemic area of melioidosis (Suputtamongkol *et al*,

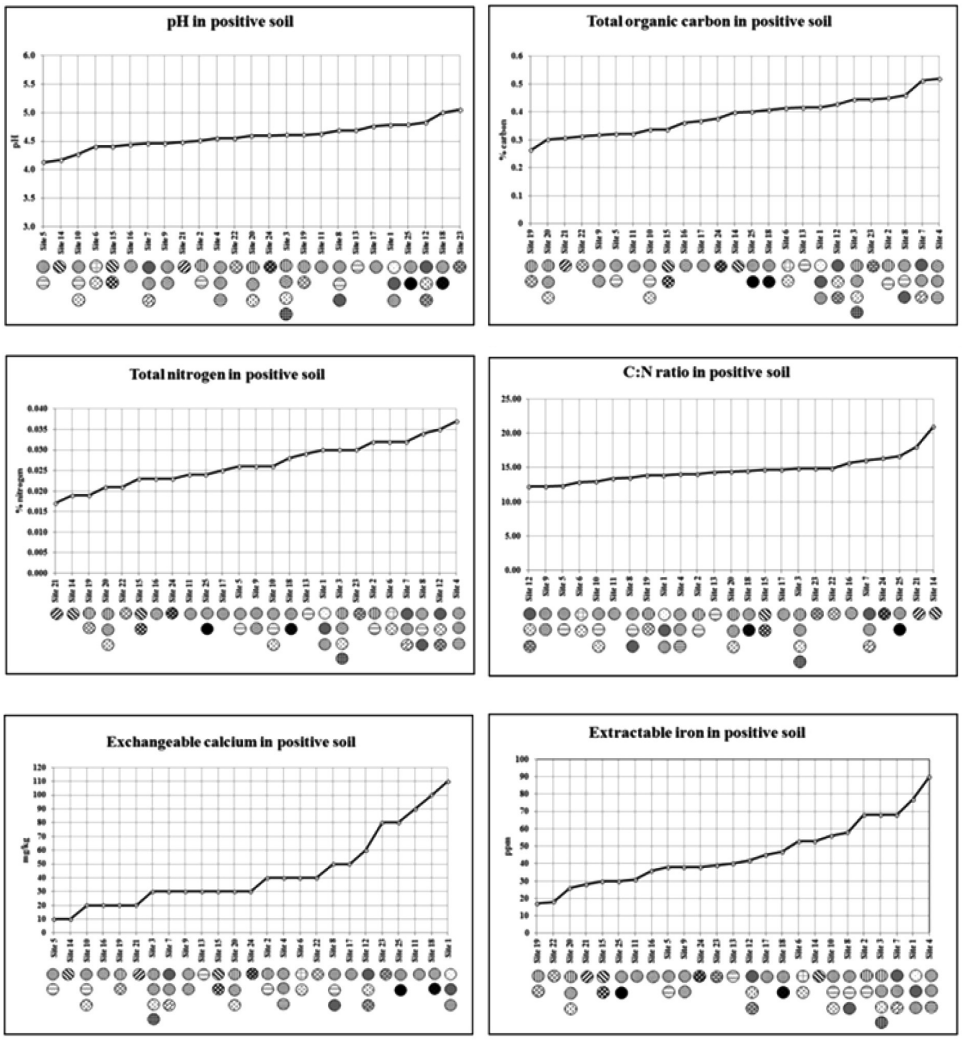


Fig 5–Plot of the diversity of *B. pseudomallei* for each positive site and the values for each physicochemical factor. BOX-PCR banding patterns found at each site (Y axis) and values for the physicochemical factors (X axis).

1999). A soil pH<6, moisture content >10% and higher carbon and nitrogen levels are all important for the growth of *B. pseudomallei* (Palasatien *et al*, 2008).

In our study, *B. pseudomallei*-positive soil sites had significantly different values for pH, TOC, TN, C:N ratio, EC and EI from *B. pseudomallei* -negative soil. The overall pH in the studied area was quite acidic. In this and previous study (Palasatien *et al*, 2008), the *B. pseudomallei*-positive soil samples have a pH less than 6. In the present study, the average pH in the *B. pseudomallei*-negative soil was 4.15 suggesting the pH critical range for *B. pseudomallei* is about 4-6. This finding is in agreement with a previous study that found *B. pseudomallei* cannot survive at pH< 4 (Wang-Ngarm *et al*, 2014). The optimal pH range for most plants and soil bacteria is 5.5-7.1. Soil in the northeastern Thailand is almost acidic (pH < 7)

(Boonsompopphan *et al*, 2008). Nearly half of the soil in northeastern Thailand contains laterite, which is rich in iron and aluminium. Those metal elements have a potential to generate hydrogen ions (H^+) which make the soil acidic (Cawte and Boyd, 2010). Iron is a soil micronutrient in and cofactor for microbial metabolism (Paul, 2006). In this study, distribution of iron rich soil correlated well with *B. pseudomallei*-positive soil. The low pH of the soil helps keep the iron in an available form for microbes.

The presence of and proportions of carbon and nitrogen are important for bacterial growth. TOC is used to describe all organic carbons that enter the soil through decomposition of plant and animal residues, root exudates and metabolites of living and dead microorganisms (Harris, 2007). In this study, the mean TOC level in *B. pseudomallei*-positive soil was lower than in the *B. pseudomallei*-negative soil, suggesting *B. pseudomallei* can survive under tough conditions; it has even been found to survive in water for up to 3 years (Moore *et al*, 2008). In environmental studies, the C:N ratio has been used as an indicator to express the quality of soil suitable for cultivation (Pitty, 1979). The average C:N ratio varies from country to country depending on the soil type, but values between 8 and 17 are generally found (Pitty, 1979). In this study, the mean C:N ratio in *B. pseudomallei*-positive soil (14.65) was lower than in *B. pseudomallei*-negative soil (24.69). Therefore, the pH and C:N ratio could be used for monitoring and controlling *B. pseudomallei* in the environment.

The concentration of *B. pseudomallei* in *B. pseudomallei*-positive soil was 1×10^3-6.6×10^6 CFU/g soil measured by direct culture. Interestingly, *B. pseudomallei*-negative soil was located only 100 m from *B. pseudomallei*-positive soil. The samples were both taken from a grassy field rarely used to feed cattle. In spite of their close location, the physicochemical factors were significantly different from each other.

In this study, nested qPCR was used to confirm the presence of *B. pseudomallei*. Since *B. pseudomallei* bacterium has more than one copy of the 16S-23S spacer, so the qPCR technique should be more sensitive than colony counts to quantify the number of bacteria (Supaprom *et al*, 2007). However, in our study more of the grids had lower PCR copy number than direct culture colony count numbers. Errors may occur with either method, such as errors in soil sampling, efficiency of DNA extraction and bacterial extraction from the soil. The copy numbers detected by nested qPCR was not much different among the positive sites, while colony counts varied by location. Two of the colony-negative grids were positive on the second round of the nested-qPCR, indicating low numbers of bacteria or the presence of unculturable forms of *B. pseudomallei* (Palasatien *et al*, 2008) which can persist throughout the dry environment (Inglis and Sagripanti, 2006).

As we are interested in both culturable and non-culturable forms of *B. pseudomallei* present in soil. The relationship between PCR copy numbers and the physicochemical properties of the bacteria-positive soil was examined. From this study, EC was negatively correlated with PCR copy numbers. An optimum pH of 4-6 was also important for growth of *B. pseudomallei.*

In this study, we used the BOX-PCR to type *B. pseudomallei* as it is simple and could generate high power of discrimination (Martin *et al*, 1992). The BOX-PCR has been recommended to classify *B. pseudomallei* (Currie *et al*, 2007). BOX-PCR using

the BOX-A1R primers, we found 25 patterns when evaluating *B. pseudomallei*. No statistically significant associations were seen between the various *B. pseudomallei* patterns and the various physicochemical factors examined. However, there was a non-significant association with TOC, TN and EI. An EI value of 150 to 200 mg/kg (150-200 ppm) indicates enriched soil. In our study, the average EI result was <150 mg/kg. The average EI was non-significantly higher at *B. pseudomallei*-positive sites than *B. pseudomallei*-negative sites. *B. pseudomallei* has genes coding for a two-component system that can fix iron (Lazar Adler *et al*, 2009). Interestingly, the soil sites with more diversity of *B. pseudomallei* contained higher EI than the sites with less *B. pseudomallei* diversity, suggesting EI as a possible factor affecting *B. pseudomallei* diversity, although these findings were not significant. Further study is needed to confirm this theory.

In conclusion, the studied physicochemical factors were significantly different between *B. pseudomallei*-positive and –negative soil samples. A pH range of 4-6, the C:N ratio and and EI level may be used to follow the presence of *B. pseudomallei*. The EC level may be used to control *B. pseudomallei* growth. It is unclear whether these studied factors could influence the diversity of *B. pseudomallei*.

ACKNOWLEDGEMENTS

This study was supported by the Higher Education Research Promotion and National Research University Project of Thailand, Office of the Higher Education Commission, through the heath cluster, project "Specific Health Problems in the Greater Mekong Sub-region (SHeP-GMS)" of Khon Kaen University. We would like to acknowledge Prof Yukifumi Nawa, Faculty of Medicine Publication Clinic, Khon Kaen University, Thailand for editing the manuscript. We are also grateful to the Faculty of Medicine, Graduate School and Melioidosis Research Center, Khon Kaen University.

REFERENCES

Berry JW, Chappell DG, Barnes RB. Improved method of flame photometry. *Indust Engineer Chem Analyt Ed* 1946; 18: 19-24.

Boonsompopphan B, Vearasilp T, Yost RS, Attanandana T. Field identification of soil series: indexing and retrieving soil information while sharing experience and knowledge. *Soil Sci* 2008; 173: 736-44.

Bremner JM. Total nitrogen. In: Black CA, ed. Methods of soil analysis. Part 2. Madison: American Society of Agronomy, 1965: 1149-78.

Cawte HJ, Boyd WE. Laterite nodules: A credible source of iron ore in iron age northeast Thailand? *Geoarchaeology* 2010; 25: 626-44.

Cheng AC, Currie BJ. Melioidosis: epidemiology, pathophysiology, and management. *Clin Microbiol Rev* 2005; 18: 383-416.

Currie BJ, Gal D, Mayo M, *et al.* Using BOX-PCR to exclude a clonal outbreak of melioidosis. *BMC Infect Dis* 2007; 7: 68.

Dance DA. Melioidosis: the tip of the iceberg? *Clin Microbiol Rev* 1991; 4: 52-60.

de Versalovic J, Bruijn F, Lupski J. Repetitive sequence-based PCR (rep-PCR) DNA fingerprinting of bacterial genomes. In: Bruijn F, Lupski J, Weinstock G, eds. Bacterial genomes: physical structure and analysis. 1st ed. Philadelphia: Springer Science + Business Media, LLC, 1998: 437-54.

Goldenberger D, Perschil I, Ritzler M, Altwegg M. A simple "universal" DNA extraction procedure using SDS and proteinase K is compatible with direct PCR amplification. *PCR Methods Appl* 1995; 4: 368-70.

Harris JA. Microbiological methods for assessing soil quality - Edited by Bloem J,

Hopkins DW & Benedetti A. *Eur J Soil Sci* 2007; 58: 1214-15.

Heng BH, Goh KT, Yap EH, Loh H, Yeo M. Epidemiological surveillance of melioidosis in Singapore. *Ann Acad Med Singapore* 1998; 27: 478-84.

Inglis TJ, Merritt A, Chidlow G, Aravena-Roman M, Harnett G. Comparison of diagnostic laboratory methods for identification of *Burkholderia pseudomallei*. *J Clin Microbiol* 2005; 43: 2201-6.

Inglis TJ, Sagripanti JL. Environmental factors that affect the survival and persistence of *Burkholderia pseudomallei*. *Appl Environ Microbiol* 2006; 72: 6865-75.

Jones JB, Jr. Laboratory guide for conducting soil tests and plant analysis: Boca Raton, New York: CRC Press, 2001.

Lazar Adler NR, Govan B, Cullinane M, Harper M, Adler B, Boyce JD. The molecular and cellular basis of pathogenesis in melioidosis: how does *Burkholderia pseudomallei* cause disease? *FEMS Microbiol Rev* 2009; 33: 1079-99.

Limmathurotsakul D, Wongratanacheewin S, Teerawattanasook N, *et al*. Increasing incidence of human melioidosis in Northeast Thailand. *Am J Trop Med Hyg* 2010; 82: 1113-7.

Lindsay WL, Norvell WA. Development of a DTPA soil test for zinc, iron, manganese, and copper1. *Soil Sci Soc Am J* 1978; 42: 421-28.

Maron PA, Mougel C, Ranjard L. Soil microbial diversity: methodological strategy, spatial overview and functional interest. *C R Biol* 2011; 334: 403-11.

Martin B, Humbert O, Camara M, *et al*, A highly conserved repeated DNA element located in the chromosome of *Streptococcus pneumoniae*. *Nucleic Acids Res* 1992; 20: 3479-83.

Mirza B, Welsh A, Rasul G, Rieder J, Paschke M, Hahn D. Variation in Frankia populations of the Elaeagnus host infection group in nodules of six host plant species after inoculation with soil. *Microb Ecol* 2009; 58: 384-93.

Moore RA, Tuanyok A, Woods DE. Survival of *Burkholderia pseudomallei* in water. *BMC Res Notes* 2008; 1: 11.

Palasatien S, Lertsirivorakul R, Royros P, Wongratanacheewin S, Sermswan RW. Soil physicochemical properties related to the presence of *Burkholderia pseudomallei*. *Trans R Soc Trop Med Hyg* 2008; 102 (suppl 1): S5-9.

Paul EA. Soil microbiology, ecology and biochemistry. 3rd ed. Oxford: Elsevier Science, 2006.

Pitty AF. Geography and soil properties. 1st ed. London: Methuen, 1979.

Robe P, Nalin R, Capellano C, Vogel TM, Simonet P. Extraction of DNA from soil. *Eur J Soil Biol* 2003; 39: 183-90.

Samosornsuk N, Lulitanond A, Saenla N, Anuntagool N, Wongratanacheewin S, Sirisinha S. Short report: evaluation of a monoclonal antibody-based latex agglutination test for rapid diagnosis of septicemic melioidosis. *Am J Trop Med Hyg* 1999; 61: 735-7.

Smith MD, Wuthiekanun V, Walsh AL, White NJ. Quantitative recovery of *Burkholderia pseudomallei* from soil in Thailand. *Trans R Soc Trop Med Hyg* 1995; 89: 488-90.

Supaprom C, Wang D, Leelayuwat C, *et al*. Development of real-time PCR assays and evaluation of their potential use for rapid detection of *Burkholderia pseudomallei* in clinical blood specimens. *J Clin Microbiol* 2007; 45: 2894-901.

Suputtamongkol Y, Chaowagul W, Chetchotisakd P, *et al*. Risk factors for melioidosis and bacteremic melioidosis. *Clin Infect Dis* 1999; 29: 408-13.

Suputtamongkol Y, Hall AJ, Dance DA, *et al*. The epidemiology of melioidosis in Ubon Ratchatani, northeast Thailand. *Int J Epidemiol* 1994; 23: 1082-90.

Vuddhakul V, Tharavichitkul P, Na-Ngam N, *et al*. Epidemiology of *Burkholderia pseudomallei* in Thailand. *Am J Trop Med Hyg* 1999; 60: 458-61.

Walkley A, Black IA. An examination of the

Degtjareff method for determining soil organic matter, and a proposed modification of the chromic acid titration method. *Soil Sci* 1934; 37: 29-38.

Wang-Ngarm S, Chareonsudjai S, Chareonsudjai P. Physicochemical factors affecting the growth of *Burkholderia pseudomallei* in soil microcosm. *Am J Trop Med Hyg* 2014; 90: 480-5.

White NJ. Melioidosis. *Lancet* 2003; 361: 1715-22.

Wilks D, Jacobson SK, Lever AM, Farrington M. Fatal melioidosis in a tourist returning from Thailand. *J Infect* 1994; 29: 87-90.

Wuthiekanun V, Dance DA, Wattanagoon Y, Supputtamongkol Y, Chaowagul W, White NJ. The use of selective media for the isolation of *Pseudomonas pseudomallei* in clinical practice. *J Med Microbiol* 1990; 33: 121-6.

Wuthiekanun V, Smith MD, Dance DA, White NJ. Isolation of *Pseudomonas pseudomallei* from soil in north-eastern Thailand. *Trans R Soc Trop Med Hyg* 1995; 89: 41-3.

Food Sec. (2015) 7:739–746
DOI 10.1007/s12571-015-0463-8

ORIGINAL PAPER

Regulating edible insects: the challenge of addressing food security, nature conservation, and the erosion of traditional food culture

A. Halloran[1] · **P. Vantomme**[2] · **Y. Hanboonsong**[3] · **S. Ekesi**[4]

Received: 17 October 2014 / Accepted: 30 March 2015 / Published online: 28 April 2015
© Springer Science+Business Media Dordrecht and International Society for Plant Pathology 2015

Abstract Entomophagy is a common practice in many regions of the world but there are few examples of national regulations that govern insects for human consumption. Where entomophagy is not common, the current regulatory discourse focuses primarily on food safety and consumer protection. In countries where insects contribute to local diets, nature conservation is often an issue of high importance. This paper investigates the variation in the ways in which entomophagy and its related activities are currently regulated in Thailand, Switzerland, Kenya and Canada. Authoritative bodies who are responsible and the roles they play are discussed. Insects have only recently entered into the sustainable food dialogue, but have not yet been incorporated into policy documents and have been largely omitted from regulatory frameworks. Moreover, even in nations where there is a tradition of consuming a variety of insect species, they do not appear explicitly in dietary guidelines. Although food safety is a major concern, it can undermine the importance of nature conservation, traditional food culture, food security, and potential economic development. Thus, entomophagy should be viewed holistically and development of future legislation must take into consideration its multi-dimensional nature.

✉ A. Halloran
aha@nexs.ku.dk

[1] Department of Nutrition, Exercise and Sports, University of Copenhagen, Rolighedsvej 26, 1958 Frederiksberg C, Denmark

[2] Forestry Department, Food and Agriculture Organization of the United Nations, Viale delle Terme di Caracalla, 00153 Rome, Italy

[3] Entomology Division, Faculty of Agriculture, Khon Kaen University, Khon Kaen 40002, Thailand

[4] International Centre of Insect Physiology and Ecology (icipe), PO Box 30772-00100, GPO, Nairobi, Kenya

Keywords Entomophagy · Regulatory frameworks · Food security · Food safety · Nature conservation · Traditional diets

Introduction

In May 2014, the Food and Agriculture Organization (FAO) of the United Nations and Wageningen University and Research jointly hosted the *Insects to Feed the World Conference* in Ede, The Netherlands. Approximately 450 participants gathered from more than 45 countries to discuss issues related to insects as food and feed. The conference summary concluded that the "major challenges include… : further awareness-raising among the general public to promote insects as healthy food for humans and feed for animals; influencing policy makers to approve insect inclusive food and feed legislations; and further research efforts to provide and expand with validated data the available scientific evidence and benefits of using insects in the food and feed chains" (FAO/WUR 2014). Unsurprisingly, the issue of insect inclusive food and feed legislation featured in the vast majority of the presentations as an unresolved issue.

As noted by Halloran and Münke (2014), the greatest barriers to the growth of an edible insect sector is the lack of all-inclusive legislation that governs the production, use and trade of insects as both food and animal feed. Although the discourse regarding the regulatory frameworks influencing insects as food and feed has gained momentum in the past couple of years, it is not new. For example, at the national level, research regarding the need for the recognition of insects as a food resource in Mexico has been extensively discussed by Ramos-Elorduy and Paoletti (2005). The willingness of some decision making bodies, such as the Directorate-General of Health and Consumers (SANCO) of the European Commission, to discuss the possibilities for incorporating insects into

food and feed legislation has gradually increased. A case in point is that of Laos PDR which proposed a regional food standard for insects in 2010 under the *Proposal for new work on development of regional standards for edible crickets and their products*. This proposal was supported by the neighbouring countries of Cambodia, Thailand and Malaysia (FAO 2010). National governments, such as the Netherlands, are actively funding researchers investigating issues of legislation for governing insect farms, health and safety standards, and marketing through retail outlets (Pascucci and Magistris 2013).

This paper reviews various actions taken or underway in Thailand, Canada, Kenya and Switzerland in order to address and understand the relevant stakeholders and multi-jurisdictional regulations and legislations governing the use of insects as food and feed. It builds on an earlier draft by FAO "*Discussion paper: regulatory frameworks influencing insects as food and feed*" (Halloran and Münke 2014) and assesses regulatory frameworks including legislation, standards and other regulatory instruments which are legally binding or otherwise in the use of insects as food and feed.

Thailand

Thailand boasts a large and successful commercial insect sector that produces primarily for human consumption. Locusts, crickets, giant water bugs, bamboo caterpillars, beetles, palm weevil larvae and ants are the most commonly consumed and marketed in the country and beyond. These species are either wild harvested, semi-cultivated or farmed (Hanboonsong et al. 2013).

Among the various insects, cricket farming is the most advanced. The technology was developed by Kohn Kaen University 15 years ago, and then promoted by the Thai government through a small and micro-community enterprise scheme. Despite the fact that there are over 20,000 operating cricket farms with average production of 7500 tonnes per year, research on commercial production is sparse. Moreover, few production and management standards for cricket farming exist, such as hygiene for minimizing disease outbreaks. In many cases, best practices in breeding, nutrition, or pest control are not well understood by farmers (Hanboonsong et al. 2013).

The Ministry of Public Health is the main authoritative body currently regulating insect production and consumption in Thailand. All products processed from insects that are sold in the local markets and exported have to be passed by law through the Food and Drug Administration (FDA) under the Ministry of Public Health. Insect producers have to apply for a licence, and an inspector from the FDA monitors the production site, and also samples and monitors products for proper hygiene standards on a regular basis.

No specific standards for insects as food exist; thus, they are treated like any other food product under the Food Act of B.E.2522 (1979) (Food and Drug Administration Thailand 2014). This is probably attributed to the fact that Thailand, as well as the greater region of South-eastern Asia has a long history of entomophagy and paradoxically has not developed specific food standards to protect consumer safety. Discussions are now underway on how to make the farm GAP (Good Agriculture Practice) index for cricket farming. This should provide some guideline for farmers to follow at farm sites. However, there is little support from extension services to improve techniques and farming conditions (Hanboonsong et al. 2013).

Many of the insects consumed in Thailand are wild harvested. Environmental and habitat changes have caused their decline. The Royal Forest Department under the Ministry of Natural Resources has played a major role in protecting many insect species. However, Thailand, like many other countries, has struggled to conserve wild insect populations despite the availability of legal regulations for species protection that have been put in place by the government (Boongird 2010). For example, there are four official acts for forest conservation and protection which relate to wild bees (Boongird 2010). Due to declining numbers of palm trees, improved techniques for palm weevil semi-cultivation have been developed. The Department has also developed techniques for semi-cultivating bamboo caterpillars in order to ensure a more sustainable caterpillar harvest (Hanboonsong et al. 2013). Despite ministerial involvement, the insect food industry has been largely overlooked by government in relation to other agri-food industries.

As mentioned by Fellows (2014), the widespread use of E-commerce through internet access has allowed producers in Thailand to easily gain access to high value markets in industrialized countries. Products like dried and flavoured crickets have been exported to Europe (mainly France and Belgium) and even the United States. With the expansion of training and education in computing and information technology in many universities in developing countries, Fellows (2014) predicts that an increased amount of insect products will be available to international markets via internet sales. All insect exports from Thailand must be certified by the Royal Forest Department to ensure that no species listed under the Convention on International Trade in Endangered Species of Wild Fauna and Flora (CITES) are being traded.

Switzerland

Switzerland is an example of a country that has been quick to address requests from its citizens to incorporate insects as food into national legislation. The Federal Department of Home Affairs Ordinance on foodstuffs of animal origin governs

animal-derived food products. However, the Ordinance (Article 2) does not recognize insects as an animal species accepted for food production. In 2013, there was active involvement from civil society, namely the organization Grimiam, in placing insects for both food and feed on the agenda.

On 25 November 2013, Councillor Isabelle Chevalley posed an interpellation (Nr. 13.4013) to the Federal Assembly by asking: *Pourquoi interdire la consommation d'insectes?* (Why forbid the consumption of insects?). The interpellation challenged the Federal Council on the following points (Federal Assembly of the Swiss Parliament 2014a):

1. Is the Federal Assembly prepared to propose to Parliament a legislative amendment to allow the consumption of insects?
2. How can the prohibition of eating insects be justified since hundreds of millions of people have consumed insects for millennia (Aristotle praised the exquisite taste of cicada nymphs)?

These interpellations were welcomed by members of the Federal Assembly, as solutions for sustainable food is an area of interest and priority. The Assembly reported back on 12 February 2014 and addressed the following issues (original text in French) (Federal Assembly of the Swiss Parliament 2014a):

1. Insect consumption in Switzerland is not prohibited and consumers can consume insects they breed or collect in the wild themselves. However, selling and serving insects as food is prohibited as insects have not been described in the food and commodities regulation (LGV, SR 817.02);
2. Reliable scientific data on the risk of allergies and the transmission of disease is needed in order to amend the current legislation;
3. The handling of non-native invertebrates in closed systems and free-range trials is regulated for the sake of environmental protection and biodiversity. However, no standardized methods of breeding and production of insects for food have been created to date.
4. While the rearing of selected insect species could contribute to sustainable food and animal feed production in Switzerland many of the fundamental questions remain unanswered.
5. The consumption of specified insects could contribute to sustainable food production, including as an ingredient for animal feed. However, many fundamental questions currently remain and will need answering in order to come to a final decision.

Following this rebuttal two additional interpellations were made on 21 March 2014: 1) Interpellation Nr. 3273 - *Pourquoi interdire en Suisse la commercialisation d'insectes qui sont consommés couramment dans d'autres pays?* (Why forbid in Switzerland the commercialization of insects that are widely consumed in other countries?) (Federal Assembly of the Swiss Parliament 2014b), and 2) Interpellation Nr. 14.3274 - *Pourquoi interdire l'alimentation des poissons, des volailles et des porcs par des insectes?* (Why forbid the feeding of fish, poultry and pigs with insects?) (Federal Assembly of the Swiss Parliament 2014c). These interpellations were supported by 63 and 68 of 200 councillors, respectively.

The Assembly responded to each of the latter interpellations. In particular, the council noted that insects represent an untapped animal feed source for Switzerland. Switzerland is participating in discussions at the European Union level so as to avoid the negative consequences in case insects are not approved in the European Union. Moreover, the use of insects as feed should be accelerated, pending risk analysis (Federal Assembly of the Swiss Parliament 2014c). In terms of insects that are utilized for human consumption, the Assembly acknowledged that there is a growing evidence base supporting entomophagy. Nonetheless, strict regulations and further evidence would need to be generated in order to protect consumer health and safety. Moreover, selected insect species that are fit for human consumption would need to be pin-pointed (Federal Assembly of the Swiss Parliament 2014b). A round-table discussion of the Swiss Parliament concerning insects as foodstuff will be inaugurated in the first quarter of 2015 (J. Vogel, personal communication, 6 October, 2014).

Kenya

In Kenya, the national food safety and quality system is managed by various statutory government agencies operating from different ministries with the broad objective of promoting public health, and protecting consumers against health hazards while enhancing economic development (FAO/WHO 2005; GAIN 2005). Although the country lacks a defined and published policy on food safety as part of a wider National Food and Nutrition Policy, food laws exist that are designed to protect the consumers. Food safety control agencies operate under the Ministries of (1) Trade, (2) Industrialization, (3) Public Health and Sanitation, and (4) Livestock, Fisheries Development, and Agriculture. A summary of the legal and policy framework of these agencies and the implementing mechanisms for the laws is documented by FAO/WHO (FAO/WHO 2005). The agencies include Kenya Bureau of Standards (KEBS), Kenya Agricultural Research Institute (KARI), Kenya Plant Health Inspectorate Services (KEPHIS), Department of Public Health (DPH), Weights and Measures Department (WMD), Government Chemist's Department, Department of Veterinary Services (DVS), Kenya Dairy Board (KDB), and Horticultural Crops Development Authority (HCDA), among others (GAIN 2005; Mwangi et al. 2009).

The functions of these agencies include sensitization and implementation of codes of hygiene and agricultural practices by stakeholders throughout the food chain. Standards for food and agricultural products are developed by technical committees, with their secretariats at KEBS. Food standards give specifications for the compositional requirements, microbial requirements, the tolerance limits for contaminants, packaging, labeling and the hygiene conditions necessary for manufacture of products. While there are specific standards for various food and feed items, there are no specific standard for use of insects as food and feed. Rather insects are considered as impurities or contaminants in food that have to be eliminated. The majority of the Kenyan standards are adopted from international ones, International Organization for Standardization (ISO) and Codex Alimentarius Commission – Codex (CAC), following the philosophy of the World Trade Organization (WTO) Sanitary and Phytosanitary Standards (SPS) and Technical Barrier to Trade (TBT) agreements (World Bank 2005). There is now support for standards dealing with the use of insects as food and feed and consultations are currently underway with Kenya Bureau of Standards (KEBS) and other relevant agencies to establish a technical committee to draft standards that will govern the application of insects as food and feed.

Kenya Bureau of Standards (KEBS) coordinates all activities concerning the development and implementation of both local and international standards relevant to Kenya (KEBS 2014). Kenya Bureau of Standards is a statutory Public body under the Ministry of Industrialization, operational since July 1974, and mandated by the Standards Act Chapter 496 (NCST 2009). The KEBS board of directors, the National Standards Council, is its policy-making body for supervising and controlling the administration and financial management. To improve on efficiency and provide more effective services to clients, KEBS established a Certification Unit (CU), accredited by the Quality Systems Accreditation Committee (QSAC) that offers certification services. Kenya Bureau of Standards gathers information on quality concerns through industrial visits and receives private complaint samples for analysis in its laboratories as part of quality assurance and testing services components of its operations. KEBS is also the National Codex Contact Point serving as the secretariat of the National Codex Committee (NCC). As the Codex Contact Point, KEBS acts as a link between the Codex Secretariat and Kenya.

In addition to the establishment of standards through KEBS, the main nature conservation authority (i.e., Kenya Wildlife Services), also requires permits for large-scale farming of insects especially crickets. These permits are required in order to: 1) conform to wildlife domestication regulation process; and 2) match regulations on transporting livestock. This is required when moving animals from one zone to another and also includes an approved method of transportation. A zone is a jurisdictional area (part of a district).

The Kenya National Guidelines on Nutrition and HIV/AIDS recognizes entomophagy as a part of traditional food culture, and states that "common sources of animal proteins in Kenya include milk and milk products, beef, poultry, chicken, eggs, fillet, dried small fish (*Rastrineobola argentea*) and edible insects such as termites" (Republic of Kenya 2006; p. 11). Moreover, it recommends that food security in HIV-affected households could be addressed in rural areas by promoting traditional practices of harvesting, preserving and consuming indigenous foods such as edible insects like termites. It is especially recommended when planning for the lean season (Republic of Kenya 2006).

Indigenous foods are allowed for consumption, but not allowed for trade unless registered under the National Bureau of Standards.

Canada

Food and food safety regulation in Canada occurs at federal, provincial and municipal levels. In general, the federal government deals with laws on food pertaining to import and export, novel foods, and interprovincial transport of food. The provincial levels deal with farming and food processing regulation. The municipal level mainly enforces the provincial laws, and also has a few bylaws pertaining to public health. They also work closely with the types of enterprises commonly found in cities and towns (like restaurants, markets, grocery stores etc.) (A. Jean, personal communication, 1 Dec 2014).

Health Canada is the key administrative body in Canada that is responsible for regulations governing the use of insects as food and feed. The Canadian Food Inspection Agency (CFIA) falls under Health Canada and handles issues related to food safety and public health. The CFIA conducts novel food safety assessments under the Food Directorate. The purpose of the directorate is to establish policies, set standards and provide advice and information on the safety and nutritional value of food (A. Jean, personal. communication, 1 Dec 2013).

According to the Government of Canada "since the CFIA's inception in 1997, Canada's demographic make-up has been changing at a fast pace. With immigration continuing to increase and accounting for a large percentage of the country's population, the Agency has found itself facing demands for a larger variety of ethnic and imported foods from an ever increasing number of countries, especially developing countries. This demand, coupled with increasing globalization, has meant that the Agency has had to change and evolve at a fast pace to keep up with consumer's needs" (Government of Canada 2009).

Most of the popular insects used as food around the world do have a history of safe use for human consumption as it is estimated that over 2,000 species of insects are consumed in

80 % of the world's nations (van Huis et al. 2013). Insects that do not have a history of safe use as food may be considered as novel food and, as such, they may need an assessment from the Novel Food Section of the Bureau of Microbial Hazards, Food Directorate, Health Canada. Insects that are not considered as "novel food" may be offered for sale to Canadian consumers as long as they are not in violation of the Food and Drugs Act and Regulations; namely Sections 4, 5 and 7 of the Act and Division 28 of the Regulations. Division 28 of the Food and Drug Regulations applies to Novel Foods, their assessment and their pre-market notification. This process is similar in nature to EU Novel Food legislation (A. Jean, personal communication, 1 Dec 2013).

Canada is one of the most culturally and ethnically diverse countries in the world. It experiences food culture through the exchange of traditions and world cuisines that are adopted as mainstream trends. Ethnic foods are in high demand and readily available at grocery stores and restaurants (Swiss Business Hub Canada 2011). This could partially explain the general legislative stance and attitude that has been seen in Canada by accepting the contribution of entomophagy to human diets worldwide.

Some restaurants across Canada already serve insects on their menus (Gordon 2011). Restaurants may be allowed to sell dishes containing insects so long as the insects used in the dishes meet the Food and Drugs act regulations. However, municipal or provincial health authorities may have provisions in their own regulations that would condition, limit or prohibit the sale of dishes containing insects (A. Jean, personal communication, 1 Dec 2013).

Discussion

Nature conservation

Conservation policy can often fail to integrate biological and cultural conservation (Correal et al. 2009). In many societies, insects are not only considered as food or feed but also medicine and spiritual symbols (van Huis et al. 2013). Giving an example from the African continent, De Prins (2014) notes in her review of *Edible insects: future prospects for food and feed security* that "there is a conflict of interest between those who protect the tropical biodiversity and those who have the ingenuous wish to improve the agricultural economy in Africa" (De Prins 2014; pg. 1). Therefore, the conservation of insects collected from the wild must also be included when developing legal frameworks.

Thailand represents a country where insects as food are being regulated to a certain extent as a response to a growing number of enterprises commercially exploiting the increasing demand for them. However, since the demand for some insect species in Thailand is so huge that it cannot be met by domestic production, an additional supply of insects is received from neighbouring countries such as Lao PDR (Hanboonsong et al. 2013), which may enforce nature conservation laws less rigorously.

While the examples of Thailand and Kenya demonstrate that satisfying the interests of diverse stakeholders may be a difficult undertaking, such an issue can be tackled. In the West, many national and local governments have governed the collection of wild foods such as mushrooms and game and the same could be undertaken for insects. In order to encourage food security and sustainable diets, regulation of wild harvesting, as well as semi-domestication of farmed insects has been promoted, as is typical for Thailand.

The Swiss Federal Assembly has addressed the issue of nature conservation by regulating non-native invertebrates from being handled in closed systems (Einschliessungsverordnung vom 9. Mai 2012; SR 814.912), as well as in free-range trials for research purposes (Freisetzungsverordnung vom 10. September 2008; SR 814.911). However, there has been no standardization in terms of rearing and production of insects for food purposes to date.

Formalization of local economy

As seen in Kenya and Thailand there is a lack of a legal framework governing insects as food. However, this has proved not to be a major barrier to the expansion of the insect food sector. Insects as food have always been a part of the informal economy in those countries where entomophagy is a common practice. However, where entomophagy has not been a component of food culture, as in many western countries, their respective governments did not have the foresight to predict the future need to incorporate insects into legislation. Because of this, there is often little governance of this resource.

In many countries, the collection, farming, processing and marketing of insects is primarily an informal activity. For example, in Kenya, the majority of the insect species that are consumed including termites, crickets, grasshoppers, lake flies and bees are collected from the wild. However, most recently, attempts are being made to rear these insects by developing simple technologies to assure year round availability and transferring these technologies to smallholder producers. In the process of scaling up, issues such as nature conservation, trade, and food safety will have to be addressed and formalization of rules and regulations governing the use of insect as food and feed will become increasingly crucial.

Formalization through regulation can threaten local, informal economy. On the other hand, informal economy provides employment and income, especially in areas of high unemployment. As noted by Nelson and Bruijn "informality offers opportunities of economic necessity to the poor, most of who will never be able to assimilate the costs of formalization, and

partly because it offers others a low cost arena for experimentation that can lead to business growth" (Nelson and De Bruijn 2005; pg. 579). Nonetheless, the informal sector is not homogeneous and formalization can in many cases provide positive outcomes, such as access to international trade as in the cases of Kenya and Thailand. Further, in order for insects as food and feed to develop, governmental involvement is essential in order to develop appropriate legislation to govern the sector.

In Kenya and Thailand care should be taken to ensure that local populations can continue to consume their traditional foods without disrupting the food system due to an increasing demand from export markets and rising prices. An example of this complicated dynamic is given by how the booming export market for quinoa from Southern Bolivia has impacted the environment and home consumption (Jacobsen 2011; Winkel et al. 2012).

Food-base dietary guidelines and food safety

The World Health Organization (WHO) and the FAO have been responsible for the review of new research and information concerning diets worldwide. Due to the dynamic nature of diets, having a single snapshot of nutrient requirements and recommended nutrient intakes in a given region is an ongoing task. Such nutrients include protein, energy, carbohydrates, fats and lipids, a range of vitamins, and minerals and trace elements.

Many countries are dependent on WHO and FAO to provide them with the necessary information, which is often adopted as national dietary guidelines or used as a basis for their own standards. In 1986, Gussow and Clancy, when discussing dietary guidelines for sustainability in the United States, noted that "the human race once enjoyed a diet drawn from a large variety of plant and animal (including insects!) life. Now the world's population depends on a mere handful of species…" A number of studies have shown the importance of insects in the diets of a variety of ethnic groups (van Huis et al. 2013; Christensen et al. 2006); however, the inclusion of insects as food is missing from most national food-based dietary guidelines. For example, termites, crickets and locusts are recognized under the "miscellaneous" food group in the Tanzania Food-based Dietary Guidelines (Lukmanji et al. 2008). However, insects are acknowledged in policy documents, such as the aforementioned Kenya National Guidelines on Nutrition and HIV/AIDS and Uganda Food and Nutrition Policy. Insects are not included in the Canada Food Guide or in the Swiss Food-based Dietary Guidelines. The inclusion of locally consumed insect species may help to valorise the contribution of insects to regional or national diets.

In terms of food safety, Switzerland has taken a precautionary approach to addressing insects as food due to the lack of knowledge of their potentially adverse health effects and standardization of rearing methods. Kenyan legislation is comparable to that of Switzerland when it comes to the precautionary approach. Canada, on the other hand, addresses food safety issues in terms of the sanitary standards of the establishments handling food products. Therefore, insects are treated like most other food products. Thailand has a similar approach. The involvement of FAO in promoting insects as food and feed sources will be crucial in projecting and harmonizing dietary guidelines for insects in consultation with national systems.

Insects as a component of sustainable food policy

There is broad scientific agreement that food systems are both the cause and solution to environmental problems. However, nutrition and sustainability is an emerging discourse in the food policy arena (Lang and Barling 2013). Insects have been highlighted in a number of high-level international conferences, such as "the International Conference on Forests for Food Security and Nutrition at the FAO, Rome May 15–17", 2013 as an important pathway to ensuring food and feed security.

Of the recorded 2000+ edible insect species (Jongema 2014), few scattered studies have analysed the nutritional value of insects (van Huis et al. 2013). However, as demonstrated by Rumpold and Schlüter (2013) insects can provide satisfactory energy, protein, amino acids, monounsaturated and/or polyunsaturated fatty acids, and micronutrients.[1] An effective system of legislation, food safety and agricultural health controls must be judged on its effectiveness and scientific and technical relevance. There is the need for continuous dialogue to inform policy on the use of insects as food and feed. Sufficient political will and socioeconomic priorities will be crucial for the introduction and maintenance of regulations for domestic consumption, trade promotion and the welfare of producers and consumers. Safe and high-quality insect products must result from efficient regulation at all stages of the supply chain in order to minimize the necessity of excessive corrective action having to be taken at a later stage in the process.

However, in order to incorporate insects into sustainable food policy a better understanding of the environmental impact of insect production systems through consequential life cycle assessments is needed while ensuring appropriate legislation is in place to address the concerns highlighted above. Moreover, impact assessment of increased insect consumption and demand, and the effect on ecosystems are needed.

[1] However, it must be noted that there have been no studies published to the knowledge of the authors, which have investigated the bioavailability of micronutrients and proteins from processed and unprocessed insects.

Conclusion

Addressing insects as a novel food focuses primarily on food safety and consumer protection. While these issues are highly relevant, they can also undermine the importance of nature conservation, traditional food systems, and economic development. In those countries where there was never a previous need to address regulations concerning insects as food we find that insects have been partially, or completely left out of legislation and decision making. Thus, the development of future legislation must take into consideration the multi-dimensional nature of insects as food and feed.

Acknowledgments The author would like to acknowledge the following people for their contributions to this study Jürgen Vogel, Association Grimiam and André Jean, Health Canada. This paper is a product of the "GREEiNSECT: Insects for Green Economy" research consortium (www.greeinsect.ku.dk), funded by the Danish International Development Agency's Consultative Research Committee for Development Research Fund.

References

Boongird, S. (2010). Honey and non-honey foods from bees in Thailand. In P. Durst, D. V. Johnson, R. N. Leslie, K. D. Shono, & V. Johnson (Eds.), *Forest insects as food: Humans bite back, 165* (pp. 165–172). Bangkok: Food and Agriculture Organization of United Nations Regional Office for Asia and the Pacific.

Christensen, D. L., Orech, F. O., Mungai, M. N., Larsen, T., Friis, H., & Aagaard-Hansen, J. (2006). Entomophagy among the Luo of Kenya: a potential mineral source? *International Journal of Food Sciences and Nutrition, 57*(3–4), 198–203.

Correal, C., Zuluaga, G., Madrigal, L., Caicedo, S., Plotkin, M., Kuhnlein, H., et al. (2009). *Ingano Traditional Food and Health: phase 1, 2004–2005. Indigenous people's food systems: the many dimensions of culture, diversity and environment for nutrition and health* (pp. 83–108). Rome: CINE/FAO.

De Prins, J. (2014). Book review on edible insects: future prospects for food and feed security. *Advances in Entomology, 2*(1), 47–48.

Food and Drug Administration Thailand (2014). Laws and Regulations. http://www.fda.moph.go.th/eng/food/laws.stm.

FAO. (2010). *Development of regional standard for edible crickets and their products* (Paper presented at the Joint FAO/WHO meeting Food Standards Programme). Bali: FAO/WHO Coordinating Committee for Asia.

FAO/WHO (2005). Practical Actions to Promote Food Safety: Regional conference on food safety for Africa, Final Report. Harare, Zimbabwe. 3 – 6 October 2005.

FAO/WUR (2014). Insects to feed the world: summary report. In P. Vantomme, C. Münke, A. van Huis, J. van Itterbeeck, & A. Hakman (Eds.), Insects to Feed the World. Ede, Netherlands.

Federal Assembly of the Swiss Parliament (2014a). 13.4018 – Interpellation: Pourquoi interdire la consommation d'insectes? http://www.parlament.ch/e/suche/Pages/geschaefte.aspx?gesch_id=20134018. Accessed 25 July 2014.

Federal Assembly of the Swiss Parliament (2014b). 14.3273 – Interpellation: Pourquoi interdire en Suisse la commercialisation d'insectes qui sont consommés couramment dans d'autres pays? http://www.parlament.ch/e/suche/Pages/geschaefte.aspx?gesch_id=20143273. Accessed 2 October 2014.

Federal Assembly of the Swiss Parliament (2014c). 14.3274 – Interpellation: Pourquoi interdire l'alimentation des poissons, des volailles et des porcs par des insectes? http://www.parlament.ch/f/suche/pages/geschaefte.aspx?gesch_id=20143274. Accessed 2 October 2014.

Fellows, P. (2014). Insect products for high-value Western markets. *Food Chain, 4*(2), 119–128.

GAIN (2005). Food and Agricultural Import Regulations and Standards United States Department of Agriculture (USDA) Foreign Agricultural Service. Global Agricultural Information Network Report No. KE 5011. November 2005.

Gordon, D. (2011). Cricket Parantha: creative Vancouverites incorporate insects into contemporary. http://www.foodinsectsnewsletter.org/pdfs/Vij'sArticlebyDGGordon.pdf Accessed December 15 2013.

Government of Canada (2009). ARCHIVED - Annual Report on the Operation of the Canadian Multiculturalism Act 2007–2008. http://www.cic.gc.ca/english/resources/publications/multi-report2008/part1.asp. Accessed 24 June 2014.

Gussow, J. D., & Clancy, K. L. (1986). Dietary guidelines for sustainability. *Journal of Nutrition Education, 18*(1), 1–5.

Halloran, A., & Münke, C. (2014). *Discussion paper: regulatory frameworks influencing insects as food and feed*. Rome: Food and Agriculture Organization of the United Nations.

Hanboonsong, Y., Jamjanya, T., & Durst, P. B. (2013). *Six-legged livestock: edible insect farming, collecting and marketing in Thailand*. Bangkok: Food and Agriculture Organization of the United Nations Regional Office for Asia and the Pacific.

Jacobsen, S. E. (2011). The situation for quinoa and its production in southern Bolivia: from economic success to environmental disaster. *Journal of Agronomy and Crop Science, 197*(5), 390–399.

Jongema, Y. (2014). World list of edible insects. http://www.wageningenur.nl/upload_mm/7/e/6/c79e66db-00d5-44c9-99cb-f38943723db6_LIST%20Edible%20insects%201st%20of%20April.pdf. Accessed 04/06/14.

KEBS (2014). The Outline of Services offered by the Kenya Bureau of Standards, Kenya Bureau of Standards. www.kebs.org. Accessed 27 October 2014.

Lang, T., & Barling, D. (2013). Nutrition and sustainability: an emerging food policy discourse. *Proceedings of the Nutrition Society, 72*(01), 1–12.

Lukmanji, Z., Hertzmark, E., Mlingi, N., Assey, V., Ndossi, G., & Fawzi, W. (2008). *Tanzania food composition Table*. Dar es Salaam: MUHAS- TFNC & HSPH.

Mwangi P., Nambiro, E. and Murithi, F.M. (2009). Safe and High Quality Food Supply Chains and Networks (SAFEACC) project Vegetable and Fruits, Fish and Beef products: The Kenya Component. KARI/Global Food Network.

NCST. (2009). *A Proposed Coordination Structure for Biosafety Regulatory Agencies in Kenya* (NCSTth ed.). Nairobi: The National Council for Science and Technology.

Nelson, E. G., & De Bruijn, E. J. (2005). The voluntary formalization of enterprises in a developing economy—the case of Tanzania. *Journal of International Development, 17*(4), 575–593. doi:10.1002/jid.1176.

Pascucci, S., & Magistris, T. d. (2013). Information bias condemning radical food innovators? The case of insect-based products in the Netherlands. *International Food and Agribusiness Management Review, 16(3)*.

Ramos-Elorduy, J., & Paoletti, M. G. (2005). Insects: a hopeful food source. Ecological implications of minilivestock: potential of insects, rodents, frogs and snails. 263–291.

Republic of Kenya. (2006). *Kenyan national guidelines on Nutrition and HIV/AIDS*. Republic of Kenya: Ministry of Health.

Rumpold, B. A., & Schlüter, O. K. (2013). Nutritional composition and safety aspects of edible insects. *Molecular Nutrition & Food Research, 57*(5), 802–823.

Swiss Business Hub Canada. (2011). *The Canadian food retail sector*. Toronto: Swiss Buisness Hub Canada.

van Huis, A., Van Itterbeeck, J., Klunder, H., Mertens, E., Halloran, A., Muir, G., et al. (2013). *Edible insects: future prospects for food and feed security*. Food and Agriculture Organization of the United Nations

Winkel, T., Bertero, H., Bommel, P., Bourliaud, J., Chevarría Lazo, M., Cortes, G., et al. (2012). The Sustainability of Quinoa Production in Southern Bolivia: from Misrepresentations to Questionable Solutions. Comments on Jacobsen (2011, J. Agron. Crop Sci. 197: 390–399). *Journal of Agronomy and Crop Science, 198(4)*, 314–9.

World Bank (2005). *The Role of Standards under Kenya's Export Strategy Contribution to the Kenya Diagnostic Trade and Integration Study*. World Bank.



Afton Halloran is as PhD fellow within the GREEiNSECT research consortium (greeinsect.ku.dk), a group of public and private institutions investigating how insects can be utilized as novel and supplementary sources of protein in small to large-scale industries in Kenya. Her research focuses on the nutritional, socio-economic and environmental impacts of insect production systems. She formerly worked as a consultant with the Insects for Food and Feed Programme at the Food and Agriculture Organization of the United Nations (FAO). She is a co-author of the FAO's most popular publication "Edible insects: future prospects for food and feed security." At the FAO, she also developed a discussion paper on the regulatory frameworks governing insects as food and feed. Afton holds an MSc in Agricultural Development from the University of Copenhagen where she wrote her thesis on the legitimization and institutionalization of urban agriculture systems in Dar es Salaam, Tanzania and Copenhagen, Denmark. Her research interests include sustainable food systems, food policy, rural–urban interactions, undervalued foods, farmer organizations and sustainable diets.



Paul Vantomme is an agricultural engineer and has worked for FAO since 1978 in agro- forestry projects worldwide. From 1996 onwards he has coordinated the FAO global programme to promote Non-Wood Forest Products (NWFP), particularly wild gathered food products such as mushrooms and medicinal plants (http://www.fao.org/forestry/nwfp/en/). His focus is on enhancing the contribution of wild gathered edible plant and animal products to food security. Mr. Vantomme has wide experience in awareness raising, communication and outreach activities at the global level in the field of NWFP and since 2002 on the promotion of edible insects in particular (http://www.fao.org/forestry/edibleinsects/en/). Mr. Vantomme is another one of the co-authors of the popular FAO publication "Edible insects: future prospects for food and feed security." Mr. Vantomme represents FAO as an international partner of GREEiNSECT.



Dr. Yupa Hanboonsong is an Associate Professor of Entomology at Khon Kaen University, Thailand. Dr. Hanboonsong has also worked as a project leader and technical consultant with the FAO on indigenous foods such as insects in Thailand and Laos. She is a co-author of the FAO publications "Six-legged livestock: Edible insect farming, collecting and marketing in Thailand" and "Edible insects in Lao PDR: Building on tradition to enhance food security." She is a team leader of the research programme on appropriate cricket farming management in Thailand. Dr. Hanboonsong represents the University of Khon Kaen as an international GREEiNSECT partner.



Dr. Sunday Ekesi is a Principal Scientist and Head of the Plant Health Division at the International Centre for Insect Pathology and Ecology (*icipe*). He obtained his PhD from Ahmadu Bello University, Nigeria in 1999 and undertook his post-doctoral research both at *icipe* and Rothamsted Research in the UK. His area of research interest is integrated pest management (IPM) that is based on the use of entomopathogens, baiting techniques, botanicals, orchard sanitation and classical biological control for the management of arthropod pests of horticulture. He has more than 20 years of working experience with arthropod pests of horticultural crops and has coordinated several research projects on the same topic. His current research activities are focusing on filling critical gaps in knowledge that are related to the impact of climate change on ecosystem services with emphasis on pest management and pollination and developing adaptation strategies to cope with changes. Other research activities focus on climate change and adaptation strategies and the use of insects for food and feed. Sunday sits on various international advisory and consultancy panels for the FAO, IAEA, WB and regional projects on fruit flies and several other important arthropod pests. He is currently a member of the International Fruit Fly Steering Committee (IFFSC) and member of the Editorial Board of the Newsletter of Tephritid Co-workers of Europe, Africa and the Middle East. Dr. Ekesi represents *icipe* as an international GREEiNSECT partner.

Ecol Res (2015) 30: 415
DOI 10.1007/s11284-015-1252-8

DATA PAPER

**Itsarapong Voraphab · Yupa Hanboonsong
Youichi Kobori · Hiroaki Ikeda · Takeshi Osawa**

Insect species recorded in sugarcane fields of Khon Kaen Province, Thailand, over three seasons in 2012

Received: 1 August 2014 / Accepted: 15 February 2015 / Published online: 6 March 2015
© The Ecological Society of Japan 2015

Abstract The diversity of insect species in cultivated fields provides a number of ecosystem benefits, including natural pest control and pollination. However, current knowledge of the insect fauna in agricultural landscapes is extremely limited when compared with information available for other ecosystems, such as forests and rivers. Here, we present data on insect diversity, including functional feeding group diversity, in sugarcane fields of Khon Kaen Province, Thailand. Sugarcane is a major Thai crop. We collected insects using light trap systems located in 16 sugarcane field plots. Each light trap was deployed in an individual 0.16 ha plot. Trapping was conducted over three seasons, including both dry and rainy periods, in March, June, and October of 2012. On each trapping day, we collected insects in the evening from 18:00 to 19:30. The traps yielded a total of 98,423 individuals including 143 species belonging to 26 families. We classified collections into five functional feeding groups: herbivores, predators, decomposers, parasitoids, and pollinators. The dominant functional species were herbivores, followed in rank order by predators; most individuals in the traps were predatory species. We assembled an insect fauna data set that will be useful in the study of southeast Asian agricultural ecosystems and provided the data in the Darwin Core Archive format.

Keywords Agricultural ecosystem · Decomposer · Herbivore · Parasitoid · Pollinator · Predator

Ecological Research Data Paper Archives http://db.cger.nies.go.jp/JaLTER/ER_DataPapers/
Accession number: ERDP-2015-01

The complete data set for this abstract published in the Data Paper section of the journal is available in electronic format in *Ecological Research Data Paper Archives* at http://db.cger.nies.go.jp/JaLTER/ER_DataPapers/archives/2015/ERDP-2015-01.

I. Voraphab · Y. Hanboonsong
Division of Entomology, Faculty of Agriculture, Khon Kaen University, Khon Kaen 40002, Thailand

Y. Kobori
Japan International Research Center for Agricultural Sciences, Ishigaki, Japan

H. Ikeda · T. Osawa (✉)
National Institute for Agro-Environmental Sciences, Tsukuba, Japan
E-mail: arosawa@gmail.com
Tel.: +81.78.803.8148
Fax: +81.78.803.8199

T. Osawa
Japan Node of the Global Biodiversity Information Facility, Tsukuba, Japan

frontiers in Plant Science

ORIGINAL RESEARCH
published: 27 November 2015
doi: 10.3389/fpls.2015.01022

Seasonal Patterns of Fine Root Production and Turnover in a Mature Rubber Tree (*Hevea brasiliensis* Müll. Arg.) Stand- Differentiation with Soil Depth and Implications for Soil Carbon Stocks

Jean-Luc Maeght[1,2], Santimaitree Gonkhamdee[3], Corentin Clément[4], Supat Isarangkool Na Ayutthaya[3], Alexia Stokes[2] and Alain Pierret[5]*

[1] Institut de Recherche pour le Développement, UMR 242/iEES – Paris (IRD-UPMC-CNRS-UPEC-UDD-INRA), Bondy, France, [2] INRA, UMR-AMAP, Montpellier, France, [3] Khon Kaen University, Faculty of Agriculture, Khon Kaen, Thailand, [4] International Water Management Institute, Vientiane, Laos, [5] Institut de Recherche Pour le Développement, UMR IEES-Paris – Department of Agricultural Land Management (DALaM), Vientiane, Laos

OPEN ACCESS

Edited by:
Sergio Rossi, Université du Québec à Chicoutimi, Canada

Reviewed by:
Petra Fransson, Swedish University of Agricultural Sciences, Sweden
Aidan M. Keith, Centre for Ecology and Hydrology, UK

***Correspondence:**
Jean-Luc Maeght
jean-luc.maeght@ird.fr

Specialty section:
This article was submitted to Functional Plant Ecology, a section of the journal Frontiers in Plant Science

Received: *11 September 2015*
Accepted: *05 November 2015*
Published: *27 November 2015*

Citation:
Maeght J-L, Gonkhamdee S, Clément C, Isarangkool Na Ayutthaya S, Stokes A and Pierret A (2015) Seasonal Patterns of Fine Root Production and Turnover in a Mature Rubber Tree (Hevea brasiliensis Müll. Arg.) Stand- Differentiation with Soil Depth and Implications for Soil Carbon Stocks. Front. Plant Sci. 6:1022. doi: 10.3389/fpls.2015.01022

Fine root dynamics is a main driver of soil carbon stocks, particularly in tropical forests, yet major uncertainties still surround estimates of fine root production and turnover. This lack of knowledge is largely due to the fact that studying root dynamics *in situ*, particularly deep in the soil, remains highly challenging. We explored the interactions between fine root dynamics, soil depth, and rainfall in mature rubber trees (*Hevea brasiliensis* Müll. Arg.) exposed to sub-optimal edaphic and climatic conditions. A root observation access well was installed in northern Thailand to monitor root dynamics along a 4.5 m deep soil profile. Image-based measurements of root elongation and lifespan of individual roots were carried out at monthly intervals over 3 years. Soil depth was found to have a significant effect on root turnover. Surprisingly, root turnover increased with soil depth and root half-life was 16, 6–8, and only 4 months at 0.5, 1.0, 2.5, and 3.0 m deep, respectively (with the exception of roots at 4.5 m which had a half-life similar to that found between depths of 1.0 and 2.5 m). Within the first two meters of the soil profile, the highest rates of root emergence occurred about 3 months after the onset of the rainy season, while deeper in the soil, root emergence was not linked to the rainfall pattern. Root emergence was limited during leaf flushing (between March and May), particularly within the first two meters of the profile. Between soil depths of 0.5 and 2.0 m, root mortality appeared independent of variations in root emergence, but below 2.0 m, peaks in root emergence and death were synchronized. Shallow parts of the root system were more responsive to rainfall than their deeper counterparts. Increased root emergence in deep soil toward the onset of the dry season could correspond to a drought acclimation mechanism, with the relative importance of deep water capture increasing once rainfall ceased. The considerable soil depth regularly explored by fine roots, even though significantly less than in surface layers in terms of root length density and biomass, will impact strongly the evaluation of soil carbon stocks.

Keywords: deep roots, root phenology, root turnover, soil carbon, root access well, drought

INTRODUCTION

Fine root production and turnover represent 22% of terrestrial net primary production globally (McCormack et al., 2015). Yet there are still major uncertainties about the mechanisms that control fine root production and turnover. With the growing global demand for food and plant-derived commodities, unraveling such mechanisms is becoming increasingly important, particularly with the concomitantly pressing need to develop more sustainable agro-ecosystems. In recent years, rubber tree (*Hevea brasiliensis* Müll. Arg.) plantations have rapidly expanded, especially in marginal regions where the climate is much drier than in the species' natural range and where seasonal drought occurs (Carr, 2011). Soaring prices of natural rubber in the late 2010s influenced governmental policies regarding the expansion of *H. brasiliensis* cultivation. In Thailand, the world's leading latex producer, where the surface area planted with *H. brasiliensis* was multiplied by a factor of 75 between 1980 and 2008, from 24,000 ha^{-1} to 1.8 million ha^{-1} (Carr, 2011). Given the stress that tapping, i.e., the process by which the latex is collected, already imposes on *H. brasiliensis*, the sustainability and profitability of latex production in such areas could greatly benefit from adapting tapping modalities by taking into account the physiological response of trees to water availability (Boithias et al., 2011; Junjittakarn, 2012).

As roots are conduits for nutrients and water from the soil to plants, they have a determining role with regard to tree resilience to a range of environmental constraints, especially water stress (Boyce, 2005; Lobet et al., 2013). Fine roots are also an integrative indicator of plant response to environmental factors (Edwards et al., 2004) and we assume that root production or elongation of *H. brasiliensis* is synchronized with rainfall patterns (Green et al., 2005), although there exists evidence of endogenous controls of root growth (Abramoff and Finzi, 2015). Therefore, we expect that fine root growth is arrested during the dry season, but no data exist to support or refute this hypothesis. Fine roots of trees contribute to soil water extraction (Danjon et al., 2013), while a variable (and most often poorly quantified) share of the water demand is supplied by deep roots (Maeght et al., 2013). The measurement of root growth and survival *in situ* along a deep soil profile is an approach that can bring essential information to understanding how trees cope with water-limiting conditions and tree resilience to such constraints.

Quantifying fine root phenology and mortality down a soil profile, and particularly in deep soils, will also impact the evaluation of belowground carbon stocks, an area where data are scarce (Wauters et al., 2008). This proportion of soil carbon stocks could well contribute to the balance between the release and accumulation of carbon fluxes, currently described as the "missing sink" (Esser et al., 2011). However, to observe and analyze roots non-destructively within the soil matrix is still a major scientific challenge (Virginia and Jarrell, 1987), especially in deep soil layers and most studies have focused on the superficial layers of soil (Stone and Kalisz, 1991; Maeght et al., 2013). Our knowledge of fine root lifespan is also limited, particularly at depth (Eissenstat and Yanai, 1997).

We hypothesize that: (i) rooting in general is deeper than commonly assumed, (ii) fine root phenology and mortality are synchronized with annual patterns of precipitation, (iii) fine roots growing deep in the soil contribute to the resilience of *H. brasiliensis* to frequently occurring drought conditions in N. E. Thailand. Therefore, we measured seasonal patterns of fine root production and turnover in a mature stand of *H. brasiliensis*, down a 4.5 m soil profile during a 3-year observation period. We examined the interactions between fine root dynamics, rainfall, and soil depth and estimated the relative contribution of fine and deep roots to soil carbon.

MATERIALS AND METHODS

Study Site and Climate

The field site was located at Baan Sila Khu-Muang village, Buriram province in North East Thailand (N 15°16′23″, E 103°04′51.3″, 150 m a.s.l.). This region is part of the non-traditional areas for *H. brasiliensis* cultivation established since the 1990s. The experiment was set up in 2006 in a monoclonal plot of 14 years old trees (RRIM 600 clone developed by the Rubber Research Institute of Malaysia), planted at 2.5 m × 7.0 m spacing (∼570 trees ha^{-1}) that had already been tapped for over 4 years to produce latex. Tapping was performed using a semi-spiral cut 2 days out of 3 and is largely adapted to the local climatic conditions. Tapping is usually discontinued for 3–4 months during the dry season. The maximum leaf area index (LAI), measured using 91 m^1 litter traps during the defoliation period (December–February; Isarangkool Na Ayutthaya et al., 2010), was estimated to be 3.9 ± 0.7 (mean ± standard deviation).

This marginal area for rubber tree cultivation is subjected to the Southeast Asian monsoon, with heavy rainfall between April and October. Local microclimate was monitored automatically with a Minimet weather station (Skye Instruments Ltd, UK) attached to a data logger recording air temperature, relative humidity, incident short wave radiation and rainfall at 30-min intervals. Reference evapotranspiration (ET0) was calculated according to Allen et al. (1998) using the data collected from the weather station.

Soil Properties

The soil at the study site was a deep loamy sand with limited water retention capacity, developed on fine sand or coarse silt deposits with a homogeneous sandy loam texture throughout the profile. The Ap horizon was a 0.25 m thick remnant from previous sugar cane (*Sacharum officinarum L.*) cultivation (Hartmann et al., 2006). Clay, silt, and sand contents were 100, 100, and 800 g kg^{-1}, respectively. The clay content increased with depth: from 150 g kg^{-1} in the Bt1 horizon (0.25–0.50 m) to 200 g kg^{-1} in the Bt2 (0.50–1.0 m). Silt content was similar in all soil layers throughout the soil profile (100 g kg^{-1}) while sand decreased to 700 g kg^{-1} at a depth of 1.0 m. From 100 to about 4.0 m, these properties remained fairly stable. The laterite layer was found at a depth of 6.0–7.0 m, as previously observed

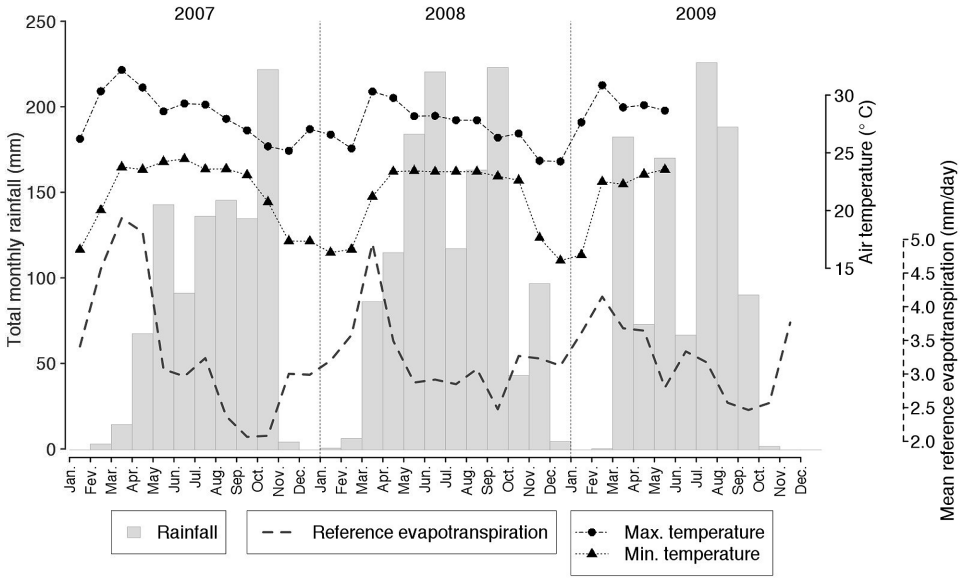


FIGURE 1 | Monthly rainfall, minimum and maximum air temperatures and reference evapotranspiration monitored at the experimental site from January 2007 to December 2009.

in this region (Cawte and Boyd, 2010). The water table was not found within the first 7 m of the profile, even during the rainy season. The soil was acidic with a pH ranging from 5.0 to 5.3. Soil organic carbon content was lower than 10 g kg^{-1} in the topsoil (Isarangkool Na Ayutthaya et al., 2011). Typical bulk soil density was 1.55 g cm^{-3} to a depth of 3.0 m (Gonkhamdee et al., 2009). Additional soil properties can be found in Hartmann et al. (2006) and Isarangkool Na Ayutthaya et al. (2011).

Root Growth Monitoring and Rooting Profiles

Soil Coring

To quantify carbon stocks associated with fine roots, root samples were collected at depths corresponding to the depths covered by root windows. We extracted undisturbed soil cores using standard soil sample steel rings (diameter 53 mm, height 50 mm and 100 cm^3 internal volume, Eijkelkamp Giesbeek, The Netherlands), in the vicinity of the root access well ($n = 12$ at soil depths 0.25, 0.50, 0.75, and 1.0 m; $n = 5$ at soil depths 1.6, 2.8, and 4.0 m). Root samples were analyzed according to Pierret et al. (2007b). Roots were first washed free of soil from the undisturbed soil cores and then imaged using a flatbed scanner (Epson Perfection V700 Photo scanner; Seiko Epson Corp., Japan) in light transmission mode, at a spatial resolution of 600 dpi (pixel size of 0.0423 mm). Special care was taken to separate every root from each other as much as possible, since overlapping roots are known to impair accurate length recovery. Specific root length (SRL) values, i.e., the length of root per unit dry root biomass, obtained from fine root samples collected within the first meter of the soil profile, were used to estimate the root dry biomass (RDB) distribution along the 4.5 m profile observed in the well, based on the following equation:

$$\mathrm{RDB} = \mathrm{RLD} \times [\mathrm{Z}]/\mathrm{SRL} \quad (1)$$

where RDB (in Mg ha^{-1}) is the RDB in a soil depth layer of thickness [Z] (m), RLD is the root length density (m m^{-3}) calculated from soil cores, in this soil layer and SRL the specific root length (m g^{-1}).

Root Access Well

Root growth was studied using the access well technique described in Maeght et al. (2013). An access well (0.9 m in diameter and 4.5 m deep) was installed in July 2006 at a distance of 1.35 m from two trees and 0.5 m aside from a tree row. The access well observation technique is an evolution of basic techniques for root observation at transparent interfaces with soil (Smit et al., 2000). A total of nine observation windows were cut through the concrete walls of the well in staggered rows (with 1.0 and 0.5 m horizontal and vertical spacing, respectively). Each root window included a specifically designed metallic frame supporting, on its upper side, a piece of 8 mm thick glass (0.25 m × 0.30 m) pressed against the soil at a 45° angle by means of two threaded rod actuators. On the frame's lower side, two guide rails allow the insertion of a standard flatbed scanner. Overall, given the geometrical arrangement of windows, the soil depth increments that were accessible were 0.4–0.6, 0.9–1.1, 1.4–1.6, 1.9–2.1, 2.4–2.6, 2.9–3.1, 3.4–3.6, 3.9–4.1, and 4.4–4.6 m. For simplicity, these are referred to as 0.5, 1.0, 1.5, 2.0, 2.5, 3.0, 3.5, 4.0, and 4.5 m hereafter. Due to time and financial constraints, it was not possible to build and monitor replicate root access wells within the framework of this field experiment. More details about the set up of the root access well set be found in Gonkhamdee et al. (2009) and Maeght et al. (2013).

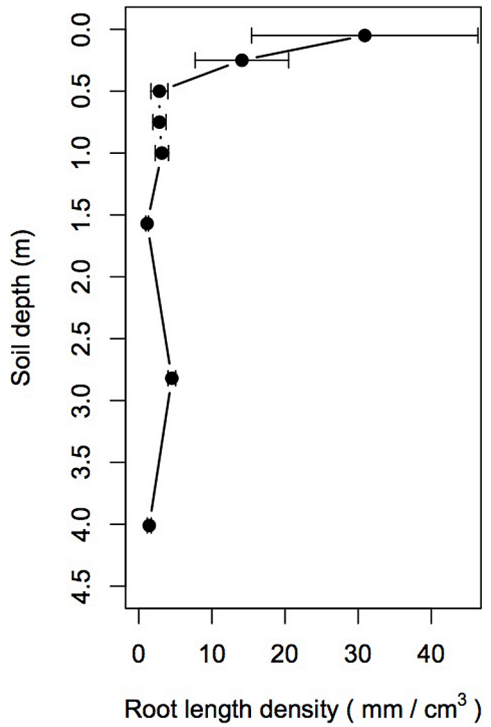


FIGURE 2 | Mean root length density (RLD mm/cm^3) derived from soil coring (n = 12 per depth between 0.05 and 1.0 m; n = 5 below 1.0 m) as a function of soil depth. Note the significant decrease of RLD with increasing soil depth below 0.25 m and the relative increase of RLD between 2.5 and 3.0 m. Dots are mean values and error bars are 95% confidence intervals.

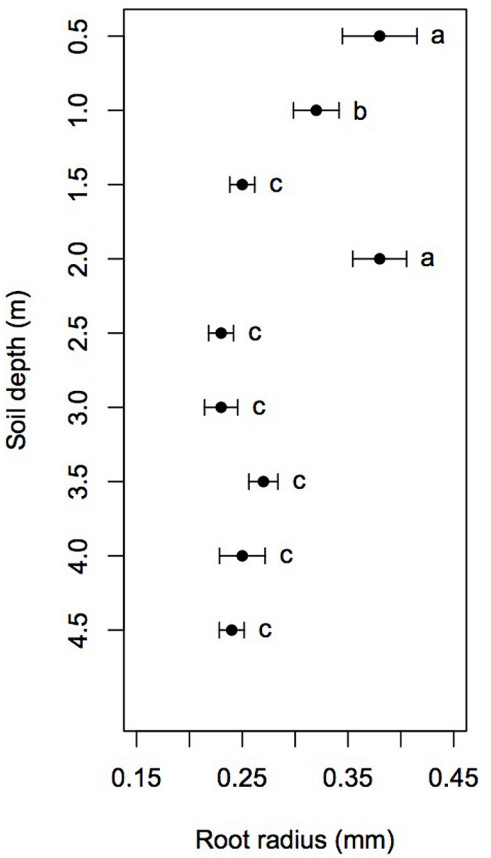


FIGURE 3 | Mean root radius as a function of soil depth (dots) with 95% confidence intervals (error bars). Different letters indicate significant differences (Tukey HSD with $\alpha = 0.05$).

Images of roots were taken using a flatbed scanner (HP Scanjet 4370 Photo scanner at 200 DPI – Hewlett-Packard Development Company, California) and custom software which offers a convenient, faster and more accurate record than manual techniques (Zoon and Tienderen, 1990; Kaspar and Ewing, 1997). Root windows were scanned at monthly intervals during 3 years starting in January 2007. This scanning was started 6 months after setting up the access well to avoid recording overproduction of roots at the onset, as often occurs in mini-rhizotron experiments (Yuan and Chen, 2012). Long-term observations are also highly recommended to avoid the risk of overestimating fine root turnover (Strand et al., 2008). Root growth monitoring was conducted following a procedure described in Maeght et al. (2007). Images of the soil and roots in direct contact with each window were used to estimate root length, radius, and time of root appearance/disappearance (from which root turnover was inferred). We used the Gimp freeware package[1] to digitize roots and classify them as live or senescent. Senescent roots are often difficult to identify with certainty (Majdi et al., 2005). We considered roots as senescent when they exhibited no elongation and/or radius expansion for at least two successive observation dates and when their color turned from white to brown. Senescent roots were considered dead when their color changed to dark brown/black or when they completely disappeared from one observation to the next. A total of more than 1500 roots distributed in 300 images were processed.

Root emergence was quantified as the number of roots appearing between two monthly observations divided by the number of root windows from which this number of roots was derived (number of new roots per cm^2 and per month). Likewise, root mortality was quantified as the number of roots that disappeared between two monthly observations divided by the number of root windows from which this number of roots was derived (number of senescent/dead roots per root window and per month). 95% confidence intervals were computed as an indicator of the variability of root emergence/mortality across windows.

Assuming that all roots had emerged at the same time, the half-life represents the time after which half of all the roots would have died. Half-life values simplify comparisons between the survival

[1]www.gimp.org

of roots that emerged at the onset of the observation period and for which the time of disappearance could actually be recorded and that of roots that emerged much later and which died after the end of the observation period (right-censored data).

Analysis of Root Sample Images

Root length measurements were obtained using IJ_Rhizo's implementation of the method developed by Kimura et al. (1999). IJ_Rhizo (Pierret et al., 2013) is a software designed to measure roots washed from soil samples and developed in the ImageJ[2] macro language. The approach developed by Kimura et al. (1999) is based on discriminating each pixel of the medial axis (or skeleton) of each digitized root according to its number of orthogonal and diagonal (vertical or horizontal) neighbors. We also used IJ_Rhizo to compute frequency distributions of root radius classes (i.e., the cumulated root length par root radius class).

Statistical Analyses

All numerical data processing and statistical analyses were performed within the R environment (version 3.0.2; R Development Core Team, 2013). We first explored our dataset using a principal component analysis (PCA; "ade4" package, version 1.6-2). RLD and root radius values are reported as mean ± 95% confidence interval. We applied analysis of variance with Tukey's HSD *post hoc* tests to determine differences in root radius at different soil depths. We assessed fine root survival at the depth of each root using a Kaplan–Meier survival analysis (Kaplan and Meier, 1958) implemented in the "*survival*" package (version 2.37-4) of the R environment. For each individual root, we recorded the time of emergence and the time to either an event (death) or the end of the study (i.e., roots that were still alive at the time of the last observation were right-censored). Differences in survivorship of roots that emerged at different soil depths (regardless of their actual time of emergence) were assessed by *post hoc* pairwise comparisons using the Mann–Whitney test with a Bonferroni correction. Additionally, a Cox proportional hazards regression model was used to test whether root radius had an influence on root survival. Fine root emergence and mortality determined for each root observation window at monthly intervals are reported as pseudo-medians derived from the Wilcoxon test ± 95% confidence intervals.

A PCA (Supplementary Figure S1) indicated that root emergence was partly explained by rainfall and evapotranspiration, but the two first axes accounted for less than 50% of the variance. Therefore, we resorted here to a more descriptive analysis of fine root dynamics. As (i) roots with lifespans of 30 months and more only occurred between the surface and a depth of 2.0 m, (ii) roots were thicker above 2.0 m (with the exception of the 1.5 m depth increment) and (iii) at depths below 2.0 m, roots emerged at least 12 months later than at depths above 2.0 m, we chose to analyze separately root dynamics above and below the soil depth of 2.0 m.

[2]http://rsbweb.nih.gov/ij/

RESULTS

Climate Measurements

Total annual rainfall during the 3-year period over which the experiment was conducted, was 965, 1265, and 1002 mm, in 2007, 2008, and 2009, respectively (average: 1077 mm; **Figure 1**). Air temperatures increased during the dry season and decreased following the end of the rainy season (with a range from +8.3 to +40.3°C). Reference evapotranspiration (ET0) was found to roughly follow the monsoon regime, with a peak toward the end of the dry season and a subsequent decrease throughout the rainy season (**Figure 1**).

Rooting Profiles

Mean fine RLD derived from soil coring decreased by about one order of magnitude from a depth of 0.05 to 0.5 m, then declined slightly from 0.5 to 1.5 m before further increasing at 2.82 m ($F_{7,55} = 7.49$, $p < 0.001$; **Figure 2**). A *post hoc* Tukey test showed that mean fine RLD was significantly higher at 0.05 m than at all other depths ($p < 0.05$) and that fine root RLD between 0.25 and 4.0 m were not significantly different from each other.

Mean root radius measured in root windows significantly varied with soil depth ($F_{8,89} = 34.15$, $p < 0.001$), reaching 0.38 ± 0.03 mm at 0.5, 0.38 ± 0.02 mm at 2.0 m and 0.32 ± 0.02 mm at 1.0 m. At all other soil depths, mean root radius was fairly constant at 0.23–0.27 mm (**Figure 3**). A *post hoc* Tukey HSD test showed that mean root radii at 0.5 and 2.0 m were significantly higher than those at 1.0 m at $p < 0.05$ and that mean root radius at 1.0 m was itself significantly higher than those at all other soil depths ($p < 0.05$).

Root Emergence and Age Distributions

Roots near the soil surface (0.0–0.5 m) had a significantly longer life span compared to that in deeper soil layers (**Figure 4A**). There was a significant effect of soil depth on root age ($c^2 = 94.93$, $p < 0.001$). Roots with life spans of 30 months and more were only observed between the surface and a depth of 2.0 m.

Roots first emerged in layers close to the soil surface (0.5 and 1.0 m) and at 3.5 m, i.e., within the first 6 months of the observation period. However, at depths of 2.5, 3.0, and 4.0 m, roots did not emerge until 11–17 months after the beginning of the observation period (**Figure 4B**). Root emergence differed significantly depending on soil depth ($F_{8,89} = 34.15$, $p < 0.001$). Root emergence occurred significantly earlier ($p < 0.05$) in the three top windows (means were: 11, 14, and 17 months at 0.5, 1.0, and 1.5 m, respectively) than in the deeper windows (means were: 21–25 months).

Root Survival

Kaplan and Meier (1958) curves showed that, overall, root half-life decreased with soil depth, with the half-life of roots at 0.5 m being in the order of 500 days (>16 months; turnover of 0.73 yr^{-1}). The half-life of roots between 1.0 and 2.5 m was about 180–250 days (6–8 months; turnover 1.46–2.03 yr^{-1}) and that of roots at 3.0 m and below dropped to less than 120 days

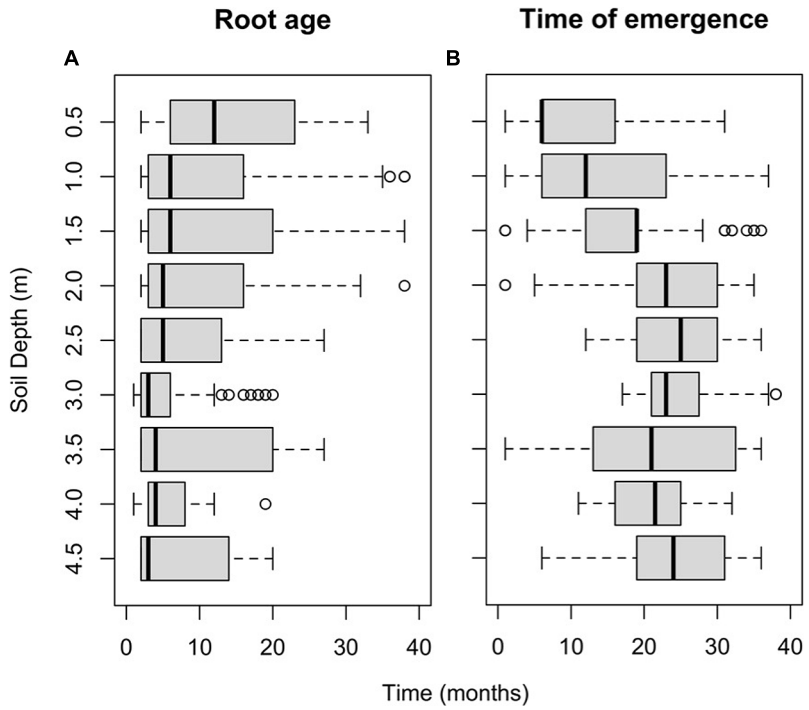


FIGURE 4 | (A) Box-whisker plot of root age distributions in each root window (for live and dead roots combined). **(B)** Distribution of the times of emergence of roots for each root window. The central vertical line indicates the median value, and the left and right edges of boxes (hinges) correspond to the 25th and 75th percentile values, while the whiskers extend 1.5× beyond the spread of the hinges. Data points outside this range (outliers) are indicated with circles.

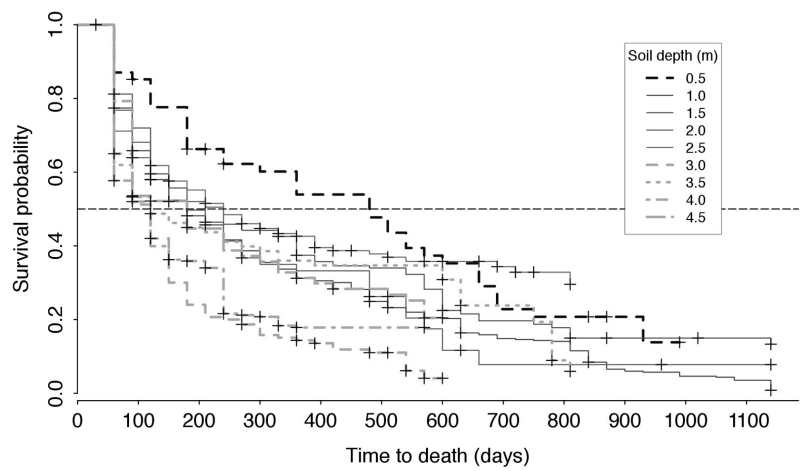


FIGURE 5 | Kaplan–Meier survival probability of roots depending on soil depth (see legend). The dotted horizontal line indicates a survival probability of 50%: the abscissa at which a given Kaplan–Meier curves intersects this line represents the half-life of roots corresponding to this survival curve, i.e., the estimated time required for half of the roots observed at any given point in time to have died.

(∼4 months; turnover 3.04 yr^{-1}), with the exception of roots at 4.5 m; the latter had a half-life similar to that found between 1.0 and 2.5 m (**Figure 5**). Soil depth significantly affected root half-life values ($\chi^2 = 89.9, p < 0.001$) and survival at 0.5 m was longer than that at all other depths ($p < 0.05$) except for 2.5 and 1.5 m, while there was no difference in root survival between depths of 3.5–4.5 m.

Differences in root survival might be related in part, to root branching order, with higher branching order roots (Pregitzer et al., 2002), living longer, i.e., thicker roots observed at 0.5 m (**Figure 3**). This could be putatively associated with slower turnover compared to lower order roots (Yao et al., 2009; Sun et al., 2012). However, a Cox proportional hazards model including root radius as a

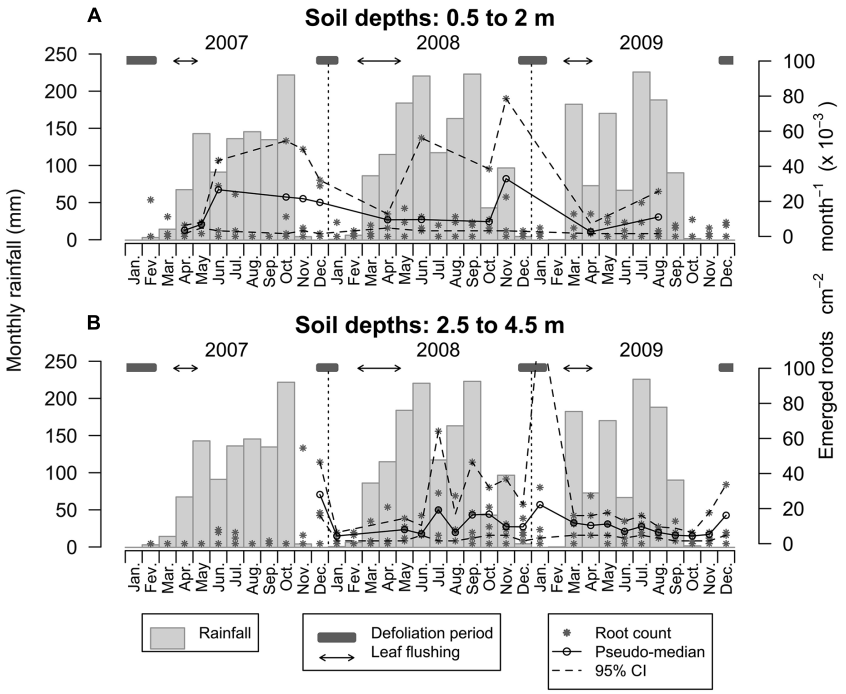


FIGURE 6 | Dynamics of root emergence over 3 years within the top 0.5–2.0 m of the soil profile (A) and between 2.5 and 4.5 m (B). Asterisks are emerging root counts determined in every root window at monthly intervals. Open circles represent the pseudo-median of emerging root counts in root windows ($n = 4$ and $n = 5$ for the upper and lower plots, respectively) and dashed lines are 95% confidence intervals estimated using the Wilcoxon signed rank test.

covariate of soil depth showed that root survival was clearly influenced by soil depth ($p < 0.001$) and not by root radius ($p = 0.25$).

Root Dynamics as a Function of Soil Depth and Rainfall

Root emergence between soil depths of 0.5 and 2.0 m ranged from 1.60 to 107.42 $\times$ 10^{-3} emerging roots cm^{-2} month^{-1}, with an average of 7.33 $\times$ 10^{-3} emerging roots cm^{-2} month^{-1} (**Figure 6A**). Despite much variability, root emergence tended to be lowest in the first 3–4 months of each observed year, followed by an increase that lasted at least until the month of November (although there was much variability between depth increments and observation years, **Figure 6A**). During the first 2 years, root emergence increased approximately 3 months after the first rainfall, usually in the month of June. Root emergence could occur at relatively high rates during defoliation but was generally low during leaf flushing (**Figure 6A**). The dynamics of root emergence observed below 2.0 m was radically different with root emergence ranging from 1.60 to 128.27 $\times$ 10^{-3} emerging roots cm^{-2} month^{-1}, with a mean of 7.11 $\times$ 10^{-3} emerging roots cm^{-2} month^{-1} (**Figure 6B**). There was very limited root growth until the 11th month of the observation period – or 14 months after root windows were installed – (i.e., until the onset of the first dry season and during leaf fall). Beyond that point in time, root emergence subsided until February 2008 and increased again and remained relatively high for 1 year (with a mean of 11.81 $\times$ 10^{-3} emerging roots cm^{-2} month^{-1}). Subsequently, root emergence slowed down and became more stable over time with a mean of 6.57 $\times$ 10^{-3} emerging roots cm^{-2} month^{-1} (**Figure 6B**).

The range of root mortality between soil depths of 0.5 and 2.0 m was 1.60 to 40.08 $\times$ 10^{-3} dead roots cm^2 month, with an average of 6.33 $\times$ 10^{-3} emerging roots cm^{-2} month^{-1} (**Figure 7A**). Root mortality at these soil depths was relatively stable over time with the highest mortality rates observed from August to January. Below a depth of 2.0 m, the range of root mortality was 1.60–78.56 $\times$ 10^{-3} dead roots cm^{-2} month^{-1}, with an average of 5.28 $\times$ 10^{-3} emerging roots cm^{-2} month^{-1} (**Figure 7B**). Following the initial period of root emergence at these soil depths, root mortality tended to remain at relatively high levels from June 2008 until June 2009 (a mean of 10.04 $\times$ 10^{-3} emerging roots cm^{-2} month^{-1}), beyond which it stabilized at a lower level of 6.65 $\times$ 10^{-3} emerging roots cm^{-2} month^{-1}.

Bivariate plots of monthly root length variations as a function of (1) average monthly rainfall, (2) monthly average of minimum daily soil temperature, and (3) average reference evapotranspiration are given in Supplementary Figure S2. There was a weak yet significant (as indicated by the low R-squared and p-values of the regressions) positive relationship between, on the one hand, average monthly rainfall and monthly root length variations (Supplementary Figure S2A) and on the other hand, monthly average of minimum daily soil temperature and monthly root length variations (Supplementary Figure S2C).

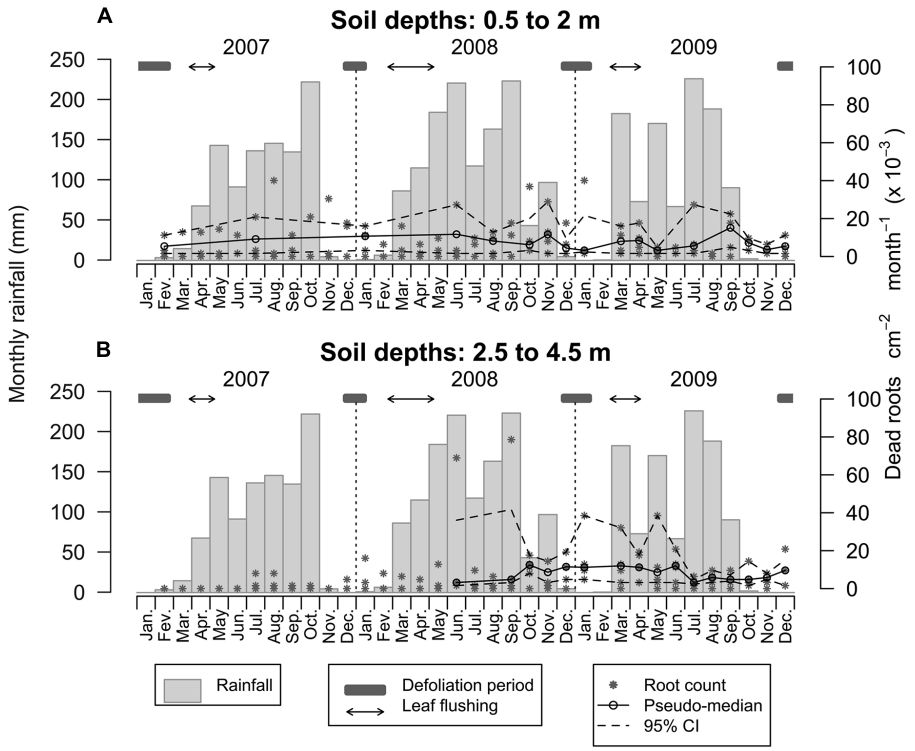


FIGURE 7 | Dynamics of root mortality over 3 years within the top 0.5–2.0m of the soil profile (A) and between 2.5 and 4.5 m (B). Asterisks are emerging root counts determined in every root window at monthly intervals. Open circles represent the pseudo-median of dead root counts in the deeper root windows ($n = 4$ and $n = 5$ for the upper and lower plots, respectively) and dashed lines are 95% confidence intervals estimated using the Wilcoxon signed rank test.

DISCUSSION

Fine Root Emergence

We showed that root phenology differed along the soil profile and was not synchronized with rainfall patterns as we had hypothesized, particularly below a depth of 2.0 m. Within the first 2 m of the soil profile, the highest rates of root emergence occurred about 3 months after the onset of the rainy season, while deeper in the soil, root emergence remained low until the 11th month of the observation period and was not correlated with the rainfall pattern. Therefore, the shallow parts of the root system were more responsive to rainfall, as roots near the soil surface capture water from rainfall more readily than deeper roots. Deep roots only emerged once rainfall became scarcer and may reflect the need for trees to use increasingly deeper water resources during the dry season.

Below 2.0 m, the first peak of root emergence rates occurred in November and December 2007, followed by a period of high root emergence that spanned from July 2008 to January 2009 (with the maximum peak in January 2009). Surprisingly, the highest emergence rates below 2.0 m occurred during the period of aerial dormancy, i.e., with no leaves supplying resources for root growth through photosynthesis. Similar results, whereby broadleaf tree root growth occurs significantly during a period of aerial dormancy, were also found in a Mediterranean climate in *Juglans regia* L. (Germon et al., under revision). Abramoff and Finzi (2015) suggest that endogenous cuing (i.e., any factor that affects growth other than climate), and subsequent allocation of stored non-structural carbohydrates (NSC) are dominant drivers of root growth in subtropical and Mediterranean trees. Although the climate in our study was tropical, distinct rainy seasons are present, but soil and air temperatures remain warm, therefore water supply is likely the main limiting climatic factor, particularly in the upper soil horizons where less buffering exists against soil drying. In deeper soils, thermic and hydric buffering should thus allow for more constant rates of root growth throughout the year if endogenous cuing is not the main driver of growth. However, we found that the peak of deep root growth was delayed until late into the dry season. As tree root and stem NSC usually decline during the growing season and re-accumulate during aerial dormancy (Richardson et al., 2013), NSC re-accumulation rates may differ between shallow and deep roots, with a time lag resulting in delayed deep root growth. Nevertheless, as root emergence rates were so different between shallow and deep roots, it may be that the drivers between the two compartments are separate and distinct, with rainfall driving shallow root growth and endogenous cuing driving deep root growth. However, further studies using isotopes would be needed to support this hypothesis (Trumbore et al., 2006).

Between soil depths of 0.5 and 2.0 m, root mortality was relatively disconnected from variations in root emergence, although higher mortality values occurred toward the end of the rainy season, as did the highest emergence values. Below 2.0 m, from 2008 onward, peaks in root emergence and death were largely synchronized, e.g., in June and September 2008 as well as April–May 2009, suggesting the existence of a mechanism for the replacement of recently senesced roots. It is also possible that deep roots that first grew after the installation of the well, began to die, either because they could not be maintained by the tree (too costly in terms of resources) or because the relatively high rates of emergence during the second year were a response to the disturbance caused by the well installation, as often occurs in rhizotron experiments (Strand et al., 2008). Roots growing in the direction of the well may have had reduced access to resources (since the volume occupied by the well was inaccessible) thus suppressing root emergence (feedback response). Observed differences in root emergence could also be related to the presence/absence of roots in the immediate vicinity of observation windows, prior to their installation which increased the probability for early root emergence in windows near pre-existing roots. The total higher and lower rates of root emergence observed in 2008 and 2009, respectively, may also have been influenced by the total annual precipitation, which in 2009 (1002 mm) was only 79% of that in 2008 (1265 mm). The year 2007 was the driest during the observation period with only 965 mm total annual precipitation. However, the second semester of year 2009, was the driest second semester of the monitoring period with only 78% of the rainfall that had been monitored for the same period in the two preceding years. In the first 3 months of the rainy season 2009 (April–June) it rained less than 60% of that for the same period in 2008. However, the reduced emergence within the first 2 m, putatively related to drier conditions during the rainy season, was not counter-balanced by increased emergence at depth. Therefore, while our data support the hypothesis that deep root emergence might correspond to a safety net against water stress during the dry season, they do not point at the existence of a similar mechanism against dry periods occurring during the wet season.

The peak of evapotranspiration that occurs every year around March–April, was highest in 2007, intermediate in 2008 and lowest in 2009 (it did not occur in 2009 as high rainfall occurred as soon as March 2009). We hypothesize that high evaporative demand may be a signal that triggers root growth at the onset of the rainy season, particularly near the soil surface and the low evapotranspiration observed in 2009 may have resulted in a weaker pattern of root emergence in that year.

At all depths, in 2008, root emergence reached its lowest level throughout the period during which trees had already shed old leaves but not yet started to grow new leaves (i.e., February). Although this pattern could not be observed in the previous and following years, it might correspond to a dormancy state prior to the resumption of physiological activity with the first rains of the season.

Fine Root Turnover

As generally reported in the literature (Chen and Brassard, 2013), we found that soil depth had a significant effect on root turnover, but rather unexpectedly, root turnover increased with soil depth from 0.73 yr^{-1} at 0.5 m to 2–3 yr^{-1} at greater depths, in sharp contrast with what is generally reported (Wu et al., 2013). However, most studies have been concerned with soil depth ranges that were much shallower than those in our study (Baddeley and Watson, 2005; Chen and Brassard, 2013). Similarly, we did not find any evidence that root radius had an influence on longevity, although this has also been reported in the literature (Baddeley and Watson, 2005; Chen and Brassard, 2013). Furthermore, we did not find a linear increase in root turnover with soil depth over the whole 4.5 m range investigated, which is consistent with the theory that several factors, both intrinsic and extrinsic, control fine root life span (Chen and Brassard, 2013). It is known that environmental parameters (e.g., temperature, water content, N availability, CO_2 partial pressure) influence fine root turnover to variable degrees (Vogt et al., 1996). Therefore, we hypothesize that during dry periods, deeper distal roots underwent a physiological pruning process, whereby peripheral organs died, as also observed in shoots of *H. brasiliensis* (Chen and Cao, 2015).

Fine Root Biomass and Carbon

Assuming that the RLD values that we obtained from soil coring are homogeneous over large volumes of soil, it can be inferred that fine root biomass below a depth of 1.0 m could account for more than half of the overall fine root biomass of the rubber trees measured [4.8 t ha^{-1} between 0.0 and 1.0 m compared to 5.8 t ha^{-1} between 1.0 and 4.0 m, with a mean SRL of ∼14 m/g^{-1} for roots ≤1 mm in diameter (Pierret et al., 2007a)]. As roots may also be present below a depth of 4 m (the bedrock was found at 7–8 m), total root biomass may be underestimated. Assuming that rubber tree root tissues have a mean organic carbon content of approximately 47% (Wauters et al., 2008), our results show that rubber tree roots ≤0.5 mm in diameter, on average account for about 5 t C ha^{-1}. This value is similar, although slightly higher, than the 1.91–3.72 5 t C ha^{-1} range reported by Wauters et al. (2008) for coarser roots (2.5–25 mm in diameter) for a range of rubber tree clones from Western Ghana and Brazil. Similarly Cheng et al. (2007) estimated carbon stocks of 16.50 t C ha^{-1} for roots of all sizes, in rubber tree plantations at Hainan Island, China and Yuen et al. (2013) calculated total carbon stocks of the order of 4–32 t C ha^{-1} for rubber trees at six locations in Southeast Asia. Hence, the presence of fine roots at fairly low length densities over considerable soil depths can have important implications with regard to soil carbon accounting. As recently pointed out by Yuen et al. (2013), more attention should be given to sampling roots at appropriate depths if we are to improve baseline data on belowground carbon stocks. In addition, it should be acknowledged that there are still major uncertainties regarding (1) the reliability of coring versus imaging techniques for quantifying fine root biomass and turnover (Yuan and Chen, 2012) and (2) the way different fine root definitions might influence such quantifications (McCormack et al., 2015).

CONCLUSION

We explored the interactions between fine root dynamics, the rainfall regime and soil along a 4.5 m profile using a root access-well. Our results reveal that root growth dynamics in the upper 2 m of soil surface were related mainly to precipitation patterns (Chairungsee et al., 2013). Deeper in the soil, root growth was more independent of rainfall and was likely driven by internal tree carbon allocation. We show that fine root production will impact soil carbon stocks and was higher than commonly reported (e.g., Brunner and Godbold, 2007), particularly at depth. Such an input of fine root related carbon in soils could be all the more significant considering the slow breakdown of fine roots in some sub-tropical tree species (Xiong et al., 2012). One major limitation of this work is that observations are taken from a single location, which means that inference and conclusions cannot be generalized. The results of this study thus advocate in favor of more field studies aimed at assessing precisely the production and fate of fine roots, not only near the soil surface but also very deep in the soil.

AUTHOR CONTRIBUTIONS

JLM and AP designed the experimental setup, implemented it in the field, analysed the data and wrote the paper. SG and SINA performed data collection in the field. CC, AS and SG have contributed significantly to the data analysis, discussing the results and writing of the paper.

ACKNOWLEDGMENTS

This research was funded by the French Institute of Research for Development (IRD), France, the French Institute for Natural Rubber (IFC), France, and Michelin/Socfinco/SIPH Rubber Tree Plantations Companies. We would also like to thank all our Thai counterparts from Khon Kaen University (KKU), Land Development Department (LDD), and the owner of the plantation (Mr. Chaipat Sirichaiboonwat) who kindly welcomed us. The authors also wish to thanks Drs. D. Nandris and F. Do (IRD) for their interest in and support of this research.

SUPPLEMENTARY MATERIAL

The Supplementary Material for this article can be found online at: http://journal.frontiersin.org/article/10.3389/fpls.2015.01022

REFERENCES

Abramoff, R. Z., and Finzi, A. C. (2015). Are above- and below-ground phenology in sync? *New Phytol.* 205, 1054–1061. doi: 10.1111/nph.13111

Allen, R. G., Pereira, L. S., Raes, D., Smith, M., and Ab, W. (1998). *Crop Evapotranspiration - Guidelines for Computing Crop Water Requirements - FAO Irrigation and Drainage Paper 56*. Rome: FAO, 1–15.

Baddeley, J. A., and Watson, C. A. (2005). Influences of root diameter, tree age, soil depth and season on fine root survivorship in *Prunus avium*. *Plant Soil* 276, 15–22. doi: 10.1007/s11104-005-0263-6

Boithias, L., Do, F. C., Isarangkool Na Ayutthaya, S., Junjittakarn, J., Siltecho, S., and Hammecker, C. (2011). Transpiration, growth and latex production of a *Hevea brasiliensis* stand facing drought in northeast Thailand: the use of the WaNuLCAS model as an exploratory tool. *Exp. Agric.* 48, 49–63. doi: 10.1017/S001447971100086X

Boyce, K. C. (2005). "The evolutionary history of roots and leaves," in *Vascular Transport in Plants*, eds N. M. Holbrook and M. A. Zwieniecki (San Diego, CA: Elsevier), 479–500.

Brunner, I., and Godbold, D. L. (2007). Tree roots in a changing world. *J. For. Res.* 12, 78–82. doi: 10.1007/s10310-006-0261-4

Carr, M. K. V. (2011). The water relations of rubber (*Hevea brasiliensis*): a review. *Exp. Agric.* 48, 176–193. doi: 10.1017/S0014479711000901

Cawte, H. J., and Boyd, W. E. (2010). Laterite nodules: a credible source of iron ore in iron age northeast Thailand? *Geoarchaeology* 25, 626–644. doi: 10.1002/gea.20326

Chairungsee, N., Gay, F., Thaler, P., Kasemsap, P., Thanisawanyangkura, S., Chantuma, A., et al. (2013). Impact of tapping and soil water status on fine root dynamics in a rubber tree plantation in Thailand. *Front. Plant Sci.* 4:538. doi: 10.3389/fpls.2013.00538

Chen, H. Y. H., and Brassard, B. W. (2013). Intrinsic and extrinsic controls of fine root life span. *Crit. Rev. Plant Sci.* 32, 151–161. doi: 10.1080/07352689.2012.734742

Chen, J.-W., and Cao, K.-F. (2015). A possible link between hydraulic properties and leaf habits in *Hevea brasiliensis*. *Funct. Plant Biol.* 42, 718–726. doi: 10.1071/FP14294

Cheng, C.-M., Wang, R.-S., and Jiang, J.-S. (2007). Variation of soil fertility and carbon sequestration by planting *Hevea brasiliensis* in Hainan Island, China. *J. Environ. Sci.* 19, 348–352. doi: 10.1016/S1001-0742(07)60057-6

Danjon, F., Stokes, A., and Bakker, M. R. (2013). "Root systems of woody plants," in *Plant Roots Hidden Half*, 4th Edn, eds A. Eshel and T. Beeckman (Boca Raton, FL: CRC Press), 29.1–29.21.

Edwards, E. J., Benham, D. G., Marland, L. A., and Fitter, A. H. (2004). Root production is determined by radiation flux in a temperate grassland community. *Glob. Chang. Biol.* 10, 209–227. doi: 10.1111/j.1365-2486.2004.00729.x

Eissenstat, D. M., and Yanai, R. D. (1997). The ecology of root lifespan advances in ecological research. *Adv. Ecol. Res.* 27, 1–60. doi: 10.1016/S0065-2504(08)60005-7

Esser, G., Kattge, J., and Sakalli, A. (2011). Feedback of carbon and nitrogen cycles enhances carbon sequestration in the terrestrial biosphere. *Glob. Chang. Biol.* 17, 819–842. doi: 10.1111/j.1365-2486.2010.02261.x

Gonkhamdee, S., Maeght, J. L., Do, F., and Pierret, A. (2009). Growth dynamics of fine *Hevea brasiliensis* roots along a 4.5-m soil profile. *Khon Kaen Agric. J.* 37, 265–276.

Green, J. J., Dawson, L. A., Proctor, J., Duff, E. I., and Elston, D. A. (2005). Fine root dynamics in a tropical rain forest is influenced by rainfall. *Plant Soil* 276, 23–32. doi: 10.1007/s11104-004-0331-3

Hartmann, C., Lesturgez, G., Do, F. C., Maeght, J. L., Isarangkool, S., Ayutthaya, N., et al. (2006). "Rubber tree trunk phloem necrosis (TPN) in northeast thailand: 1. Investigations on soil heterogeneities linked to disease outbreak," in *Proceedings of the International Natural Rubber Conference - IRRDB Annual Meetinge*, Ho Chi Minh City, 139–156.

Isarangkool Na Ayutthaya, S., Do, F. C., Pannengpetch, K., Junjittakarn, J., Maeght, J.-L., Rocheteau, A., et al. (2010). Transient thermal dissipation method of xylem sap flow measurement: multi-species calibration and field evaluation. *Tree Physiol.* 30, 139–148. doi: 10.1093/treephys/tpp092

Isarangkool Na Ayutthaya, S., Do, F. C., Pannangpetch, K., Junjittakarn, J, Maeght, J.-L., Rocheteau, A., et al. (2011). Water loss regulation in mature *Hevea brasiliensis*: effects of intermittent drought in the rainy season and hydraulic regulation. *Tree Physiol.* 31, 751–762. doi: 10.1093/treephys/tpr058

Junjittakarn, J. (2012). Short term effects of latex tapping on micro-changes of trunk girth in *Hevea brasiliensis*. *Aust. J. Crop Sci.* 6, 65–72.

Kaplan, E. L., and Meier, P. (1958). Nonparametric estimation from incomplete observations. *J. Am. Stat. Assoc.* 53, 457–481. doi: 10.1080/01621459.1958.10501452

Kaspar, T. C., and Ewing, R. P. (1997). ROOTEDGE: software for measuring root length from desktop scanner images. *Agron. J.* 89, 932. doi: 10.2134/agronj1997.00021962008900060014x

Kimura, K., Kikuchi, S., and Yamasaki, S. (1999). Accurate root length measurement by image analysis. *Plant Soil* 216, 117–127. doi: 10.1023/A:1004778925316

Lobet, G., Hachez, C., and Draye, X. (2013). "Root water uptake and water flow in the soil–root domain," in *Plant Roots: The Hidden Half*, eds Y. Waisel, A. Eshel, and U. Kafkafi (Boca Raton, FL: CRC Press), 24–21.

Maeght, J.-L., Pierret, A., Sanwangsri, M., and Hammecker, C. (2007). "Field monitoring of rice rhizosphere dynamics in saline soils of NE Thailand," in *Proceedings of the International Conference Rhizosphere 2, 26-31 August 2007*, Montpellier, 26–31.

Maeght, J.-L., Rewald, B., and Pierret, A. (2013). How to study deep roots—and why it matters. *Front. Plant Sci.* 4:299. doi: 10.3389/fpls.2013.00299

Majdi, H., Pregitzer, K., Morén, A.-S., Nylund, J.-E., and Ågren, G. I. (2005). Measuring fine root turnover in forest ecosystems. *Plant Soil* 276, 1–8. doi: 10.1007/s11104-005-3104-8

McCormack, M. L., Dickie, I. A., Eissenstat, D. M., Fahey, T. J., Fernandez, C. W., Guo, D., et al. (2015). Tansley review: redefining fine roots improves understanding of below- ground contributions to terrestrial biosphere processes. *New Phytol.* 207, 505–518. doi: 10.1111/nph.13363

Pierret, A., Doussan, C., Pages, L., Do, F. C., Gonkhamdee, S., Maeght, J. L., et al. (2007a). Is impeded root growth related to the occurrence of rubber tree trunk phloem necrosis (TPN)? Preliminary results from NE Thailand. *Paper Presented at IRRDB Annual Meeting*, Siem Reap, 489–498.

Pierret, A., Latchackak, K., Sengtaheuanghoung, O., and Valentin, C. (2007b). Interactions between root growth, slope and soil detachment depending on land use: a case study in a small mountain catchment of Northern Laos. *Plant Soil* 301, 51–64. doi: 10.1007/s11104-007-9413-3

Pierret, A., Gonkhamdee, S., Jourdan, C., and Maeght, J.-L. (2013). IJ_Rhizo: an open-source software to measure scanned images of root samples. *Plant Soil* 373, 531–539. doi: 10.1007/s11104-013-1795-9

Pregitzer, K. S., DeForest, J. L., Burton, A. J., Allen, M. F., Ruess, R. W., and Hendrick, R. L. (2002). Fine root architecture of nine North American trees. *Ecol. Monogr.* 72, 293–309.

R Development Core Team (2013). *R: A Language and Environment for Statistical Computing v.3.0.0*. Vienna: R Foundation for Statistical Computing. Available at: http://www.R-project.org/ [accessed April 2013].

Richardson, S. J., Allen, R. B., Buxton, R. P., Easdale, T. A., Hurst, J. M., Morse, C. W., et al. (2013). Intraspecific relationships among wood density, leaf structural traits and environment in four co-occurring species of Nothofagus in New Zealand. *PLoS ONE* 8:e58878. doi: 10.1371/journal.pone.0058878

Smit, A. L., Bengough, A. G., Engels, C., van Noordwijk, M., Pellerin, S., and van de Geijn, S. C. (2000). *Root Methods: A Handbook*. Berlin: Springer-Verlag, 587.

Stone, E. L., and Kalisz, P. J. (1991). On the maximum extent of tree roots. *For. Ecol. Manage.* 46, 59–102. doi: 10.1016/0378-1127(91)90245-Q

Strand, A. E., Pritchard, S. G., McCormack, M. L., Davis, M. A., and Oren, R. (2008). Irreconcilable differences: fine-root life spans and soil carbon persistence. *Science* 319, 456–458. doi: 10.1126/science.1151382

Sun, J., Gu, J., and Wang, Z. (2012). Discrepancy in fine root turnover estimates between diameter-based and branch-order-based approaches: a case study in two temperate tree species. *J. For. Res.* 23, 575–581. doi: 10.1007/s11676-012-0297-6

Trumbore, S., Da Costa, E. S., Nepstad, D. C., Barbosa De Camargo, P., Martinelli, L. A., Ray, D., et al. (2006). Dynamics of fine root carbon in Amazonian tropical ecosystems and the contribution of roots to soil respiration. *Glob. Change Biol.* 12, 217–229. doi: 10.1111/j.1365-2486.2005.001063.x

Virginia, R. A., and Jarrell, W. M. (1987). "Approaches for studying the function of deep root systems," in *Plant Response to Stress: Functional Analysis in Mediterranean Ecosystems*, Vol. 15, eds J. D. Tenhunen, F. M. Catarino, O. L. Lange, and W. C. Oechel (Berlin: Springer), 107–127.

Vogt, K. A., Vogt, D. J., Palmiotto, P. A., Boon, P., O'Hara, J., and Asbjornsen, H. (1996). Review of root dynamics in forest ecosystems grouped by climate, climatic forest type and species. *Plant Soil* 187, 159–219. doi: 10.1007/BF00017088

Wauters, J. B., Coudert, S., Grallien, E., Jonard, M., and Ponette, Q. (2008). Carbon stock in rubber tree plantations in Western Ghana and Mato Grosso (Brazil). *For. Ecol. Manage.* 255, 2347–2361. doi: 10.1016/j.foreco.2007.12.038

Wu, Y., Deng, Y., Zhang, J., Wu, J., Tang, Y., Cao, G., et al. (2013). Root size and soil environments determine root lifespan: evidence from an alpine meadow on the Tibetan Plateau. *Ecol. Res.* 28, 493–501. doi: 10.1007/s11284-013-1038-9

Xiong, Y., Fan, P., Fu, S., Zeng, H., and Guo, D. (2012). Slow decomposition and limited nitrogen release by lower order roots in eight Chinese temperate and subtropical trees. *Plant Soil* 363, 19–31. doi: 10.1007/s11104-012-1290-8

Yao, S., Merwin, I. A., and Brown, M. G. (2009). Apple root growth, turnover, and distribution under different orchard groundcover management systems. *HortScience* 44, 168–175.

Yuan, Z. Y., and Chen, H. Y. H. (2012). Indirect methods produce higher estimates of fine root production and turnover rates than direct methods. *PLoS ONE* 7:e48989. doi: 10.1371/journal.pone.0048989

Yuen, J. Q., Ziegler, A. D., Webb, E. L., and Ryan, C. M. (2013). Uncertainty in below-ground carbon biomass for major land covers in Southeast Asia. *For. Ecol. Manage.* 310, 915–926. doi: 10.1016/j.foreco.2013.09.042

Zoon, F. C., and Tienderen, P. H. (1990). A rapid quantitative measurement of root length and root branching by microcomputer image analysis. *Plant Soil* 126, 301–308. doi: 10.1007/BF00012833

Conflict of Interest Statement: The authors declare that the research was conducted in the absence of any commercial or financial relationships that could be construed as a potential conflict of interest.

Copyright © 2015 Maeght, Gonkhamdee, Clément, Isarangkool Na Ayutthaya, Stokes and Pierret. This is an open-access article distributed under the terms of the Creative Commons Attribution License (CC BY). The use, distribution or reproduction in other forums is permitted, provided the original author(s) or licensor are credited and that the original publication in this journal is cited, in accordance with accepted academic practice. No use, distribution or reproduction is permitted which does not comply with these terms.

Acta Physiol Plant (2015) 37:88
DOI 10.1007/s11738-015-1826-7

ORIGINAL PAPER

Comparative proteomic analysis of leaves, leaf sheaths, and roots of drought-contrasting sugarcane cultivars in response to drought stress

Siriporn Khueychai[1,2] · Nisachon Jangpromma[2,3] · Sakda Daduang[1,2] · Prasit Jaisil[4] · Khomsorn Lomthaisong[1,2] · Apisak Dhiravisit[5] · Sompong Klaynongsruang[1,2]

Received: 23 September 2014 / Revised: 7 March 2015 / Accepted: 13 March 2015 / Published online: 3 April 2015
© Franciszek Górski Institute of Plant Physiology, Polish Academy of Sciences, Kraków 2015

Abstract A better understanding of drought response proteins may improve our understanding of the mechanisms underlying drought tolerance in sugarcane. In this research, drought-tolerant (K86-161) and drought-sensitive (B34-164) sugarcane cultivars were grown and exposed to drought stress. The changes in protein expression in leafs, leaf sheaths and roots were analyzed using proteomics techniques. Proteins that responded to drought in both cultivars could be classified into four major categories, including energy and metabolism, photosynthesis, antioxidant, and defense protein. Interestingly, an increased abundance of fructose-bisphosphate aldolase under drought was observed in all three organs of K86-161. Elevated expression of oxygen-evolving enhancer protein was also found in leaves and leaf sheaths of K86-161, when compared with their controls. Additionally, SOD was abundant in the leaves and roots of K86-161. Importantly, the expression level of these proteins decreased in B34-164 under drought stress. These contrasting results suggest that these proteins were inhibited by drought stress in the drought-sensitive cultivar. This proteomic research is the first to combine analyses of leaves, leaf sheaths and roots in sugarcane, which may enhance our understanding of drought responses at the molecular level and lead to selective breeding for enhanced drought tolerance.

Keywords Drought-responsive protein · *Saccharum officinarum* L. · Water stress · Water shortage · Two-dimensional polyacrylamide gel electrophoresis (2D-PAGE) · Liquid chromatography coupled to mass spectrometry (LC/MS–MS)

Abbreviations

2D-PAGE	Two-dimensional polyacrylamide gel electrophoresis
LC/MS-MS	Liquid chromatography coupled to mass spectrometry
FC	Field capacity
PWC	Permanent wilting point
IEF	Isoelectric focusing
PRK	Phosphoribulokinase
FNR	Ferredoxin-NADP reductase
RuBP	D-Ribulose 1,5-bisphosphate
ROS	Reactive oxygen species
SOD	Superoxide dismutase

Communicated by M. Hajduch.

Electronic supplementary material The online version of this article (doi:10.1007/s11738-015-1826-7) contains supplementary material, which is available to authorized users.

✉ Sompong Klaynongsruang
Thammasirirak.s@gmail.com; somkly@kku.ac.th

[1] Department of Biochemistry, Faculty of Science, Khon Kaen University, Khon Kaen 40002, Thailand

[2] Protein and Proteomics Research Center for Commercial and Industrial Purposes (ProCCI), Khon Kaen University, Khon Kaen 40002, Thailand

[3] Office of the Dean, Faculty of Science, Khon Kaen University, Khon Kaen 40002, Thailand

[4] Northeast Thailand Cane and Sugar Research Center, Khon Kaen University, Khon Kaen 40002, Thailand

[5] Faculty of Humanities and Social Sciences, Khon Kaen University, Khon Kaen 40002, Thailand

Introduction

Sugarcane (*Saccharum officinarum* L.) is a significant sugar-producing crop and plays a major economic role in countries worldwide (Inman-Bamber 2004; Murata et al. 2007). The production of dryland and upland sugarcane is usually inhibited by drought (Smit and Singels 2006). Drought negatively affects plants by slowing canopy development, the production of new shoots and leaves and by accelerating shoot and leaf senescence (Inman-Bamber 2004). Therefore, improving the productivity of sugarcane under drought stress by increasing drought tolerance is very important.

Several studies have attempted to understand the mechanism underlying drought tolerance in plants (Ripley et al. 2007; Jangpromma et al. 2010a, b, 2012). Plants respond to drought with various strategies; thus, only one mechanism is not enough to improve drought tolerance in plants (Mitra 2001). Recently, much of the information on drought-affected sugarcane has focused on the morphological and physiological characteristics (Inman-Bamber 2004; Smit and Singels 2006; Jangpromma et al. 2010b, 2012). Physiological parameters include leaf chlorophyll content, leaf temperature, leaf relative water content, water use efficiency, aboveground growth, and root characters. Only a few studies have focused on the biochemical and genetic mechanisms of the sugarcane drought response (Sugiharto et al. 2002). Altered gene expression is well characterized but does not necessarily lead to a functional response because post-transcriptional/post-translational changes can prevent a gene response from being translated into a functional protein response (Chaves et al. 2003). Therefore, evaluating the effects of drought stress on the proteome will be a powerful tool for understanding the biochemical mechanisms of drought tolerance in plants.

The proteomic approach has proven to be an effective tool for separating complex protein mixtures. Proteomic strategies have been used to measure changes in protein profiles in response to environmental effects, including water stress (Castillejo et al. 2008; Xiao et al. 2009; Aranjuelo et al. 2011), salt stress (Salekdeh et al. 2002; Caruso et al. 2008), cold stress (Yan et al. 2006), oxidative stress (Ahsan et al. 2008) and radioactivity stress (Klubicova et al. 2010). The use of proteomics to evaluate the effect of progressive water stress has been demonstrated in maize (Riccardi et al. 1998), cotton (Deeba et al. 2012), rice (Salekdeh et al. 2002), and sugarcane (Sugiharto et al. 2002; Jangpromma et al. 2010a). Previous research examining drought in rice leaves identified proteins that were involved in various metabolic pathways. The three most prominently increased proteins were actin-depolymerizing factor, a homolog of the S-like ribonuclease and the chloroplastic glutathione-dependent dehydroascorbate reductase (Salekdeh et al. 2002). Drought stress in the leaf sheaths of a drought-tolerant rice cultivar mostly affects the biochemical pathways involved in defense, energy, metabolism, cell structure, and signal transduction. Prominent changes include the light harvesting complex chain II, SOD, and actin-depolymerizing factor (Ali and Komatsu 2006). Similar metabolic pathways, especially pathways that protect against oxidative damage, are also altered in rice roots subjected to drought (Rabello et al. 2008).

In sugarcane, proteomic research on drought-responsive proteins has focused on the leaves (Sugiharto et al. 2002; Jangpromma et al. 2010a). All the published results have identified proteins associated with drought that can be used as markers in screening for drought-tolerant sugarcane. A search for sugarcane proteins whose expression is controlled by drought stress identified a protein with an apparent molecular mass of 22 kDa. The 22 kDa protein was further identified as a hydrophilic protein that can bind water molecules to the surface of the protein, even when the plant is exposed to a water deficit (Sugiharto et al. 2002; Sugiharto 2004). A similar protein, p18, may be classified in the group of Late Embryogenesis Abundant (LEA) proteins, and may be functional under drought by preventing water loss from sugarcane leaves (Jangpromma et al. 2010a). The literature on the proteomics of sugarcane suggests that research on sugarcane exposed to drought is limited to the leaf.

Leaves are the powerhouses of plants via the photosynthetic pathway (Ripley et al. 2007). The major component of leaves that uses sunlight to convert H_2O and CO_2 into energy is chlorophyll (Tezara et al. 1999). Apart from the leaves, the leaf sheath is similar in function and helps to transport water and nutrients to other organs (Shen et al. 2003). Additionally, the root is another important organ that enables the intake of water and nutrients from the soil and serves to anchor the plant (Miller 1985). The modification of water uptake in the root during water deficit conditions is an important mechanism to avoid drought stress (Jangpromma et al. 2010a, 2012).

To better understand the adaptations of sugarcane to conditions of water shortage, proteomic research on the responses of different organs to drought is needed. Therefore, this study examined the changes of proteins that respond to drought stress in leaves, leaf sheaths, and roots of drought-tolerant and drought-sensitive cultivars of sugarcane using a proteomics approach. The information obtained may lead to a better understanding of the sugarcane mechanisms response to water stress, which could be used to improve the drought tolerance of the plant.

Materials and methods

Plants material and experimental design

Two sugarcane cultivars with contrasting responses to drought, K86-161 and B34-164, were used as representative drought-tolerant and drought-sensitive sugarcane cultivars, respectively. Both sugarcane cultivars were grown in a greenhouse according to a previously described method (Jangpromma et al. 2010b, 2012). Briefly, the cane stalks were cut into short pieces, each piece having one active bud and pre-germinated in germinating trays. Stalks were then planted in plastic pots containing 2 kg of sandy loam soil. The soil moisture content was 11.5 % at field capacity (FC) and 2.67 % at the permanent wilting point (PWC). A factorial experiment in a randomized complete block design with four replications was carried out in a greenhouse. Two water regimes (drought stress and non-stress) were assigned as factor A and two sugarcane cultivars were assigned as factor B (Supplementary Figure 1). Sugarcane plants were grown with daily watering to maintain the soil moisture at FC until 3 weeks old. The K86-161 and B34-164 sugarcane plants were then exposed to drought stress treatment by withholding water for 5 days. The leaves, leaf sheaths, and roots samples were then harvested from stressed and non-stressed plants, rapidly frozen and kept at −70 °C until use.

Preparation of protein extracts

The experimental details have been described previously (Prajanban et al. 2012). Each sample of leaf, leaf sheath or root was ground in a mortar with liquid nitrogen. The powder was then suspended in lysis buffer, which contained 7 M urea, 2 M thiourea, 4 % (w/v) CHAPS, 2 % (w/v) DTT and 0.8 % (w/v) IPG buffer. The supernatant was collected by centrifugation for 30 min at 12,000×*g*, 4 °C. The supernatant was cleaned to remove any contaminating substances with the 2D-clean up kit (Amersham Bioscience, Sweden). The protein pellets were resuspended in rehydration buffer, which contained 7 M urea, 2 M thiourea, 2 % (w/v) CHAPS, 2 mM DTT, 0.8 % (w/v) IPG buffer and 0.2 % bromophenol blue. The protein concentration was determined by the Bradford assay (Bradford 1976) using bovine serum albumin (Amersham Biosciences, USA) as the standard, expressed in µg/µl protein.

Two-dimensional polyacrylamide gel electrophoresis (2D-PAGE)

Two-dimensional (2D) electrophoresis was performed following a modified method that has previously been documented (O'Farrell 1975; Jangpromma et al. 2010a; Prajanban et al. 2012). For the first dimension, 24 cm isoelectric focusing (IEF) gel IPG strips (pH 4–7) were rehydrated for 15 h with rehydration buffer (7 M urea, 2 M thiourea, 2 % (w/v) CHAPS, 2 mM DTT, 0.8 % (w/v) IPG buffer and 0.2 % bromophenol blue) in a reswelling tray (Amersham Biosciences, Sweden) at 20 °C. For analytical and preparative gels, 600 µg of protein was loaded onto the IPG strip. The IEF running condition was a gradient mode using 41.5 kVh. The focused strips were equilibrated twice in equilibration solutions. The first equilibration was performed in a solution containing 6 M urea, 30 % (w/v) glycerol, 2 % (w/v) SDS, 0.002 % (w/v) bromophenol blue, 1.5 % (w/v) DTT and 50 mM Tris–HCl buffer, pH 8.8. The second equilibration was performed in a solution modified by the replacement of DTT by 4 % (w/v) iodoacetamide. After IEF, SDS-PAGE in the second dimension was performed using a 13.5 % polyacrylamide gel. The gel was then stained with colloidal Coomassie brilliant blue G250 solution overnight at room temperature and then destained with distilled water (dH_2O).

Gel imaging and data analysis

The stained gels were photographed with an EPSON scanner (EPSON, USA) at a resolution of 300 dpi and 24 bits. The 2D gel images were imported into ImageMaster 2D Platinum 7.0 software (GE Healthcare). Protein spots were detected automatically by applying the same detection parameters (smooth 2, min area 5 and saliency 40) to the all 2D gel images. After that the automatic spot detections were proved by deleting manually because noise and artifacts are generated through all steps of 2D gel production. The approximate MW of each spot was calculated according to the standard protein band on the 2D gel (phosphorylase b, 97 kDa; albumin, 66 kDa; ovalbumin, 45 kDa; carbonic anhydrase, 30 kDa; trypsin inhibitor, 20.1 kDa; and α-lactalbumin, 14.4 kDa). The acidic and basic components in the range p*I* 4.0–7.0 were calculated according to the position of known proteins spot with near acidic or basic p*I*s. Normalized spot intensity (total spot normalization) for gels was then matched between the groups. Differentially expressed protein spots were evaluated by fold change (the ratio of intensity between drought-treated spots and -untreated spots). Moreover, to exhibit the different protein expression in histogram format, the spot volumes were considered. The normalized spot value was performed by dividing all values with the central tendency and thus giving a ratio for all data. Using this data, all histograms have the same scale and thus it becomes easier to detect matches that do not have homogenous values. After data analysis, the proteins which had changes in their expressions as indicated by

their fold change values were selected for further identification.

Tryptic digestion

Experimental details were previously described by Prajanban et al. (2012). Protein spots were excised from the 2D gels into 96-well plates and washed twice with MilliQ water. Coomassie brilliant blue G250 was removed by destaining with 50 mM ammonium bicarbonate and 50 % methanol. The gel pieces were dehydrated in 100 % acetone nitrile (ACN) and further digested overnight at 37 °C with trypsin solution of 20 ng trypsin in 50 % ACN and 10 mM ammonium bicarbonate. The peptides were extracted by washing three times with 30 µl of 50 % ACN/0.1 % formic acid. The peptide solutions were dried overnight in an incubator at 40 °C. The dried peptides were stored at −20 °C until LC/MS–MS analysis was performed.

Protein identification by liquid chromatography coupled to mass spectrometry (LC/MS–MS)

The digested peptides were subjected to LC/MS–MS according to the method of Prajanban et al. (2012). The dried digested peptides were resuspended with 10 µl of 0.1 % (v/v) trifluoroacetic acid (TFA) and centrifuged for 5 min at 10,000×*g*. The supernatants were collected and injected into a nanoACQUITY system (Waters Corp., Milford, MA, USA) that was composed of a Symmetry C_{18} Trap column and a BEH130 C_{18} analytical reverse phase column (Waters Corp., Milford, MA, USA) at a flow rate of 350 nl/min to attain the highest chromatographic resolution before MS detection. Water and acetonitrile with 0.1 % formic acid added to each were used as solvents A and B, respectively. Each tryptic peptide was detected using a SYNAPT^{TM} HDMS mass spectrometer (Waters Corp., Manchester, UK) in positive nanoelectrospray ion mode. The Quadrupole mass analyzer was adjusted such that ions from *m*/*z* 200 to 1990 were efficiently transmitted. Bioworks 3.2 software (Thermo Electron) was used to process the data and convert to a Mascot generic file for using Mascot search.

Database searching

The raw mass data were converted into .mgf files by data analysis 3.4 Build 169 software and searched using a local Mascot server (http://www.matrixscience.com). Mascot search parameters including a specified trypsin enzymatic cleavage with one possible missed cleavage, taxonomic category of Viridiplantae, MS/MS tolerance of 0.6 Da, a peptide charge of 1+, 2+, 3+ ions, methionine oxidation variable modification and carbamidomethylation (C) fixed modification were used. The p*I*, molecular mass, MASCOT score, number of peptide matches, peptide sequence and sequence coverage were used to evaluate the database search results.

Fig. 1 Leaf protein, leaf sheath, and roots expression of well-watered control and drought-stressed K86-161 sugarcane cultivars visualized by 2D-PAGE. In the first dimension (IEF), 600 µg of protein extracted from the leaf was loaded onto 24 cm IPG strip, pH 4–7. For the second dimension, 13.5 % SDS-PAGE was used. Proteins were detected by colloidal Coomassie brilliant blue G250 staining. The *arrows* indicate proteins responding to drought, which were further identified by LC/MS–MS. **a**, **b** Representative proteins in leaves harvested from well-watered control and drought-stressed K86-161 plants, respectively. **c**, **d** Representative proteins in leaf sheaths harvested from well-watered control and drought-stressed K86-161 plants, respectively. **e**, **f** Representative proteins in roots harvested from well-watered control and drought-stressed K86-161 plants, respectively ▶

Results

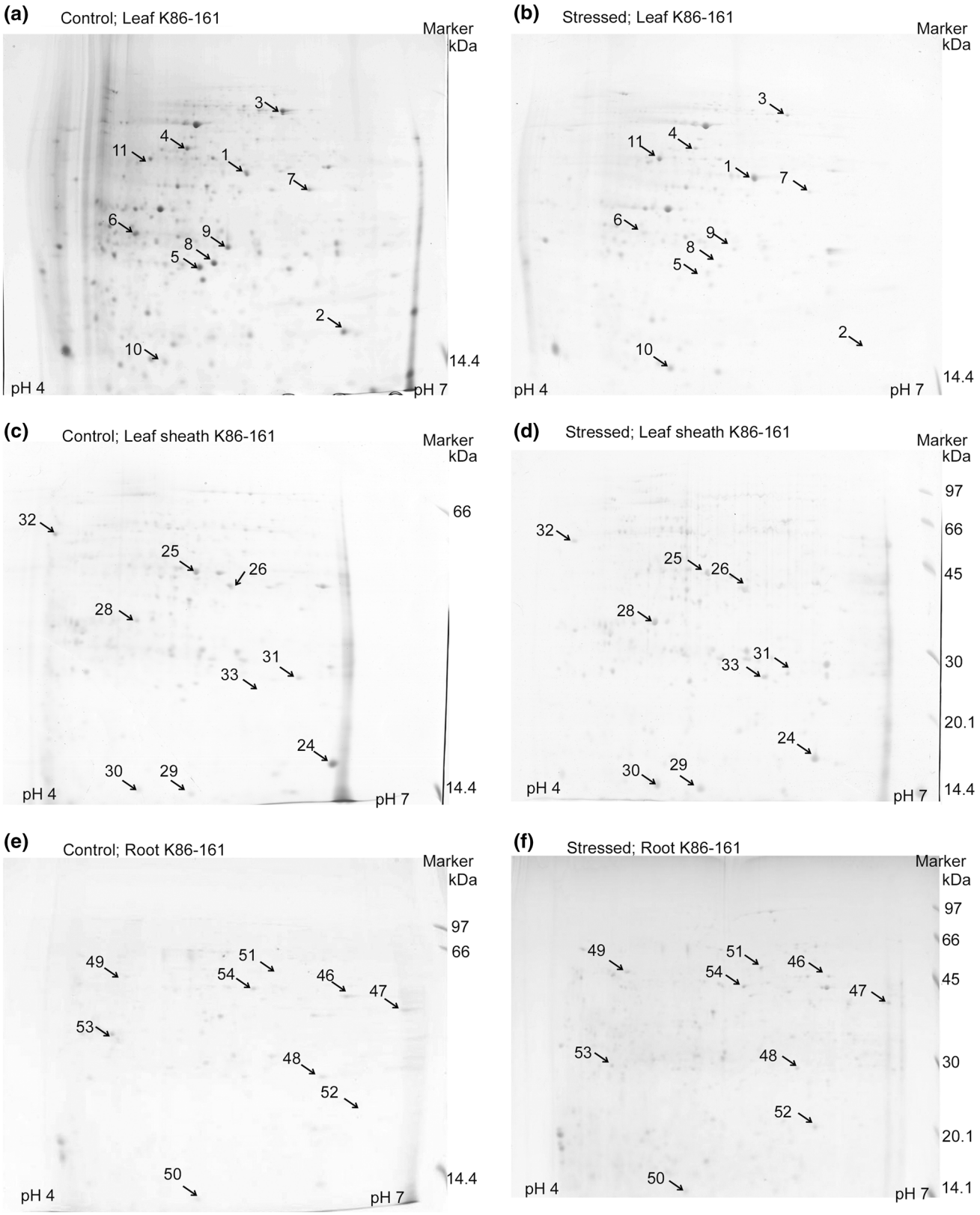
Drought-inducible proteins of sugarcane

K86-161 and B34-164 were subjected to drought and their protein was separated by 2D-PAGE. More than 300 protein spots were found in both drought-tolerant and drought-sensitive sugarcane leaves and leaf sheaths and more than 200 protein spots were found in roots (Figs. 1, 2).

The proteomic changes in the leaves of drought-tolerant sugarcane cultivars are shown in Fig. 1a, b. Three protein spots were up-regulated by drought stress (spots 1, 10, and 11) and 8 protein spots were down-regulated by drought stress (spots 2–9). In drought-sensitive sugarcane leaves, 7 protein spots were down-regulated by drought stress (spots 14, 16–18, and 20–22) (Fig. 2a, b). The LC/MS–MS identification of differentially expressed protein spots in leaves under water stress in both sugarcane cultivars is shown in Table 1

The 2D-PAGE pattern of sugarcane leaf sheaths revealed 18 protein spots that were identified by LC/MS–MS (Table 1). Of these 18 protein spots, 6 were up-regulated in the drought-tolerant sugarcane cultivar (spots 26, 28–32) and 3 were down-regulated (spots 24, 25, and 33) when compared with well-watered control plants (Fig. 1c, d). In the drought-sensitive sugarcane cultivar, four protein spots were up-regulated (spots 40–43) and five protein spots were down-regulated (spots 35–39 and 70) when compared with well-watered control plants (Fig. 2c, d).

In roots, we identified 15 differentially expressed protein spots after water stress in both sugarcane cultivars (Table 1). Four protein spots that were present in drought-stressed K86-161 but absent in well-watered K86-161 are


(a)
Control; Leaf K86-161
Marker kDa
3
4
11
1
7
6
9
8
5
2
10
14.4
pH 4
pH 7
(b)
Stressed; Leaf K86-161
Marker kDa
3
4
11
1
7
6
9
8
5
2
10
14.4
pH 4
pH 7
(c)
Control; Leaf sheath K86-161
Marker kDa
66
32
25
26
28
31
33
24
30
29
14.4
pH 4
pH 7
(d)
Stressed; Leaf sheath K86-161
Marker kDa
97
66
45
32
25
26
28
31
33
30
20.1
24
30
29
14.4
pH 4
pH 7
(e)
Control; Root K86-161
Marker kDa
97
66
49
51
54
46
47
53
48
52
50
14.4
pH 4
pH 7
(f)
Stressed; Root K86-161
Marker kDa
97
66
49
51
46
54
45
47
53
48
30
52
20.1
50
14.1
pH 4
pH 7

indicated in Fig. 1e, f (spots 49–52). In drought-tolerant roots, spots 47, 48, and 54 were up-regulated and spots 46 and 53 were down-regulated (Fig. 1e, f). In contrast, the roots of drought-sensitive sugarcane cultivars showed only 1 protein spot that was present in drought-stressed and absent in well-watered plants (spot 57). One protein spot was up-regulated (spot 73) and 4 protein spots were down-regulated in B34-164 (spots 58, 59, 72, and 74). The identification numbers of these proteins in B34-164 are shown in Fig. 2e, f.

Comparison of the effects of drought on the leaves of drought-tolerant and drought-sensitive cultivars

The drought-responsive proteins found in the leaves of both K86-161 and B34-164 were identified as ATP synthase CF1 alpha subunit (spots 3 and 14), ferredoxin-NADP reductase (spots 7 and 16), phosphoribulokinase (PRK) (spots 11 and 22), and oxygen-evolving enhancer protein (spots 10 and 18) (Table 2). ATP synthase CF1 alpha subunit and ferredoxin-NADP reductase were down-regulated in response to stress. Of four protein types that were found in both drought-exposed K86-161 and B34-164 cultivars, PRK and oxygen-evolving enhancer protein were increased in K86-161 but decreased in leaves of B34-164.

Comparison of the effects of drought on the leaf sheaths of drought-tolerant and drought-sensitive cultivars

In the leaf sheaths of drought-stressed K86-161 and B34-164, RuBisCO large subunit (spots 25 and 39), 2-Cys peroxiredoxin BAS1 (spots 29 and 38), and fructose-bisphosphate aldolase (spots 26 and 35) were expressed in both cultivars (Table 2). In addition, when we compared the expression levels of proteins in drought-stressed plants with well-watered plants, the RuBisCO large subunit protein was down-regulated in both cultivars. In contrast, 2-Cys peroxiredoxin BAS1 and fructose-bisphosphate aldolase were up-regulated in K86-161 but down-regulated in B34-164 under drought-stressed conditions.

Comparison of the effects of drought on the roots of drought-tolerant and drought-sensitive cultivars

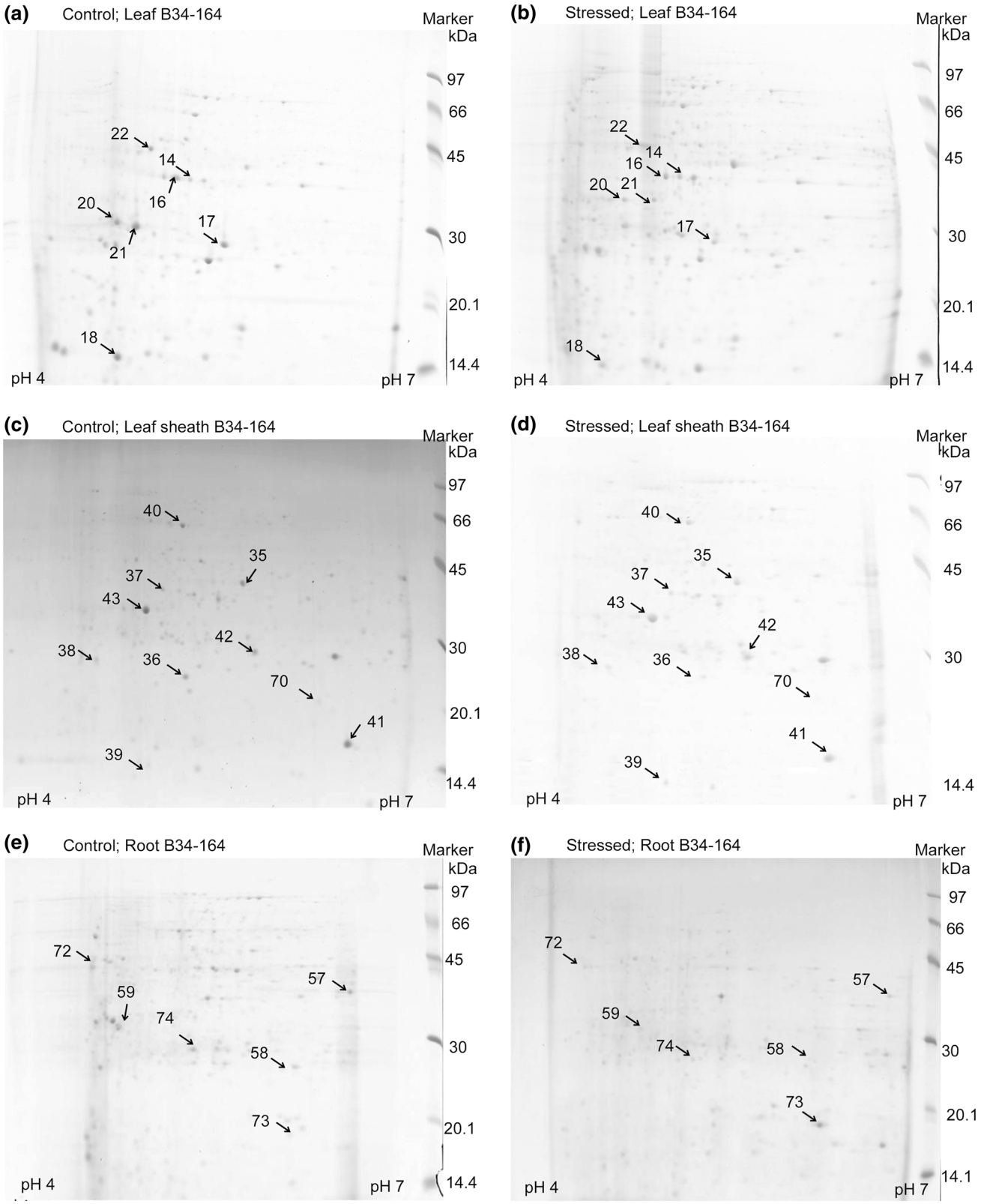
After drought, the proteins up-regulated in both K86-161 and B34-164 roots were identified as fructose-bisphosphate aldolase (spots 47 and 57), SOD (spots 48 and 58) and 14-3-3-like protein (spots 53 and 59) (Table 2). Fructose-bisphosphate aldolase was expressed only in drought-stressed plants. SOD was up-regulated in both cultivars when compared with control plants. Another protein observed in the roots of both sugarcane cultivars was 14-3-3-like protein. When we compared the expression level of 14-3-3-like protein in drought-treated sugarcane with untreated sugarcane, we found that this protein was up-regulated in the drought-tolerant cultivar but was down-regulated in the drought-sensitive cultivar.

Fig. 2 Leaf protein, leaf sheath and roots expression of well-watered control and drought-stressed B34-164 sugarcane cultivars visualized by 2D-PAGE. In the first dimension (IEF), 600 μg of protein extracted from the leaf was loaded onto 24 cm IPG strip, pH 4–7. For the second dimension, 13.5 % SDS-PAGE was used. Proteins were detected by colloidal Coomassie brilliant blue G250 staining. The *arrows* indicate proteins responding to drought, which were further identified by LC/MS–MS. **a**, **b** Representative proteins in leaves harvested from well-watered control and drought-stressed B34-164 plants, respectively. **c**, **d** Representative proteins in leaf sheaths harvested from well-watered control and drought-stressed B34-164 plants, respectively. **e**, **f** Representative proteins in roots harvested from well-watered control and drought-stressed B34-164 plants, respectively

Comparison of protein changes in the leaves, leaf sheaths, and roots following drought

When we compared the protein in the leaves, leaf sheaths, and roots of K86-161, we found that of 31 total protein spots, 9 were expressed only in leaves (spots 2–4, 6–9, 11, and 12), 5 were expressed only in leaf sheaths (spots 24, 29, 30, 32, and 33) and 8 were expressed only in roots (spots 46, 49–55) (Fig. 3a). In leaves and leaf sheaths of K86-161, oxygen-evolving enhancer protein (spots 10 and 28) was up-regulated and RuBisCO large subunit (spots 5 and 25) was down-regulated when compared with well-watered control plants (Fig. 3a). Additionally, the expression of SOD (spots 31 and 48) was up-regulated in leaf sheaths and roots of drought-tolerant sugarcane under water stress (Fig. 3a). Interestingly, fructose-bisphosphate aldolase was highly expressed in all three parts of K86-161 (spots 1, 26, and 47) (Fig. 3a). However, this enzyme was not observed in the leaves of B34-164 (spots 35 and 57) (Fig. 3b). In response to drought in B34-164, this protein was up-regulated only in the root, while it was down-regulated in leaf sheaths.

In the drought-sensitive sugarcane cultivar B34-164, 29 protein spots were up- or down-regulated under drought stress. Among these proteins, 12 proteins were expressed exclusively in leaves (spots 14, 15, 17–23, and 67–69), 7 proteins were expressed exclusively in leaf sheaths (spots 36, 38–43) and 5 proteins were expressed exclusively in roots (spots 58, 59, and 72–74) (Fig. 3b). Ferredoxin-NADP reductase (spots 16 and 37) was down-regulated in both leaves and leaf sheaths. Additionally, fructose-bisphosphate aldolase (spots 35 and 57) was down-regulated in leaf sheaths and up-regulated in the roots of this cultivar (Fig. 3b).


(a)
Control; Leaf B34-164
Marker
kDa
97
66
45
30
20.1
14.4
22
14
16
20
21
17
18
pH 4
pH 7
(b)
Stressed; Leaf B34-164
Marker
kDa
97
66
45
30
20.1
14.4
22
14
16
20
21
17
18
pH 4
pH 7
(c)
Control; Leaf sheath B34-164
Marker
kDa
97
66
45
30
20.1
14.4
40
35
37
43
42
38
36
70
41
39
pH 4
pH 7
(d)
Stressed; Leaf sheath B34-164
Marker
kDa
97
66
45
30
20.1
14.4
40
35
37
43
42
38
36
70
41
39
pH 4
pH 7
(e)
Control; Root B34-164
Marker
kDa
97
66
45
30
20.1
14.4
72
57
59
74
58
73
pH 4
pH 7
(f)
Stressed; Root B34-164
Marker
kDa
97
66
45
30
20.1
14.1
72
57
59
74
58
73
pH 4
pH 7

The identification and characterization of stress-responsive proteins in different organs of sugarcane are summarized in Fig. 4. These proteins can be classified into four major categories based on their function, including energy and metabolism, photosynthesis, antioxidant, and defense protein. The protein categories that respond to drought by up- or down-regulation in both drought-tolerant and drought-sensitive sugarcane cultivars were energy and metabolism and photosynthesis (Fig. 4a–d).

The most notable proteins were fructose-bisphosphate aldolase (energy and metabolism category), oxygen-evolving enhancer protein (photosynthesis category), and SOD (antioxidant protein category). These proteins were increased in the leaf, leaf sheath and root of K86-161 under drought-stressed conditions when compared with the control. Nevertheless, contrasting responses were observed in the B34-164 cultivar.

Discussion

In this study, we used two sugarcane cultivars with contrasting responses to drought, K86-161 and B34-164. The K86-161 cultivar represents a drought-tolerant cultivar based on its physiological traits such as chlorophyll content and root characteristics. The B34-164 cultivar represents a drought-sensitive cultivar because it shows a poor physiological response to drought (Jangpromma et al. 2010b, 2012). After drought treatment, the physiological changes of plants are reported in a parallel paper (Jangpromma et al. 2014). Drought conditions were observed to reduce the relative water content (RWC) for B34-164 higher than K86-161 compared to non-stress plants. The reduction of chlorophyll content was also highest in B34-164. Our results confirmed that K86-161 was more tolerant to drought than the B34-164 cultivar. After drought stress treatment, proteomics, which is a powerful technique for separating complex protein mixtures, was used to identify the proteins which changed under drought stress conditions in leaves, leaf sheaths and roots. The leaf protein spots were similar to a previous report by Jangpromma et al. (2010a) even though the age and growing conditions of the sugarcane were different between the two studies (Jangpromma et al. 2010a). The difference in the number of protein spots among leaves, leaf sheaths, and roots was found and the lowest protein spot was observed for roots. This difference may be because leaves and leaf sheaths have many more metabolic proteins than roots.

In the identification of differentially expressed proteins spot of sugarcane (Table 1), several proteins were found in multiple spots on 2D-PAGE, such as chlorophyll a–b binding protein. The different p*I* or molecular mass of those proteins might be due to the existence of isoforms and post-translational modifications (Lee and Seo 2004).

The proteins responsive during drought in different sugarcane organs are involved in numerous biological pathways and the putative implications of these identified proteins in response to drought are now discussed.

Drought-responsive proteins of drought-tolerant and drought-sensitive cultivar leaves

Four of the identified proteins including ATP synthase CF1 alpha subunit, ferredoxin-NADP reductase, phosphoribulokinase (PRK), and oxygen-evolving enhancer protein were found in both drought-stressed K86-161 and B34-164 leaves (Table 2).

Two down-regulated proteins were involved in energy metabolism and photosynthesis which were ATP synthase CF1 alpha subunit and ferredoxin-NADP reductase. The literature suggests that C4 photosynthesis is highly sensitive to drought stress (Ghannoum 2009). ATP synthase is one of the most commonly used enzymes to measure a plant's capacity for photosynthesis (Tezara et al. 1999). This enzyme plays a central role in energy transduction in chloroplasts (Pradet and Raymond 1983) and mitochondria and in maintaining the function of the chloroplast when the plant is subjected to drought stress. Moreover, the ATP synthase catalyzes an essential reaction for many processes in the cell and water stress substantially decreases CO_2 assimilation by affecting the amount of available ATP.

Differing ATP synthase responses to drought have been reported in plants. Although photosynthesis is sensitive to drought, the expression level of ATP synthase is up-regulated by drought stress in cotton (Deeba et al. 2012), *Phalaenopsis* (Ail et al. 2005), and sugarcane (Jangpromma et al. 2010b). In contrast, drought can reduce the expression of ATP synthase in *Alloteropsis semialata* grass (Ripley et al. 2007), Bermuda grass (Zhaoa et al. 2011), and sunflower (*Helianthus annuus* L.) (Tezara et al. 1999). Our findings support previous findings in other plants that drought reduces the expression level of ATP synthase, but contradict the results in sugarcane reported by Jangpromma et al. (2010a). This contradictory result may be due to the different age and stage of development of the sugarcane plants at the point of drought exposure. In this research, the sugarcane plants were only 1 month old at the point of drought stress and none had fully expanded leaves. Therefore, drought may decrease ATP synthase and inhibit C4 photosynthesis by non-stomatal factors, including the direct effects of reduced leaf and cellular water levels on the activity of enzymes involved in the CO_2 fixation and electron transport reactions and induction of early senescence (Ghannoum 2009). This protein was down-regulated under drought conditions, indicating that it is highly correlated with a water deficit.

Table 1 Drought-responsive protein in leaves, leaf sheaths and roots of the K86-161 and B34-164 cultivars that were identified by LC/MS–MS

Spot ID[a]	Fold change[b]	GI number[c]	p*I*/MW		Sequence coverage (%)	Score	Protein name
			Expt.	Theor.			
Leaves K86-161 cultivar							
Energy- and metabolism-related proteins							
1 ↑	>1.85	195634659	5.76/43000	7.63/41924	20	331	Fructose-bisphosphate aldolase
2 ↓	<2.37	48478778	6.50/16000	5.31/53987	5	44	ATP synthase CF1 beta subunit
3 ↓	<1.07	11467189	6.02/56000	5.80/55729	18	329	ATP synthase CF1 alpha subunit
4 ↓	<1.39	53791714	5.31/53000	5.59/51284	6	212	Putative ATPase beta subunit
Photosynthesis-related proteins							
5 ↓	<2.03	131935	5.50/23000	6.04/53310	42	234	RuBisCO large subunit
6 ↓	>0.22	115780	4.92/30000	5.31/28577	10	146	Chlorophyll a–b binding protein
7 ↓	<1.12	13096165	6.9/38000	7.01/35576	15	193	Ferredoxin-NADP reductase
8 ↓	<2.75	115764	5.50/24000	5.82/26786	8	61	Chlorophyll a–b binding protein 6A
9 ↓	<2.18	195613254	5.61/27000	8.94/28966	21	217	Chlorophyll a–b binding protein 8
10 ↑	>1.02	195619530	5.12/14000	5.59/34783	18	264	Oxygen-evolving enhancer protein 1
11 ↑	>3.66	195645472	4.76/97000	5.75/46078	25	428	Phosphoribulokinase
Leaves B34-164 cultivar							
Energy- and metabolism-related proteins							
14 ↓	<0.36	11466784	5.25/39000	5.95/55687	11	301	ATP synthase CF1 alpha subunit
Photosynthesis-related proteins							
16 ↓	<2.44	357149112	5.14/40000	5.59/39924	13	205	Ferredoxin-NADP reductase
17 ↓	<3.14	195613254	5.500/29000	8.94/28966	23	303	Chlorophyll a–b binding protein
18 ↓	<0.31	195619530	4.71/15000	5.59/34783	19	302	Oxygen-evolving enhancer protein 1
20 ↓	<0.17	115771	4.99/3500	5.14/27912	8	130	Chlorophyll a–b binding protein 1
21 ↓	<4.58	115786	5.08/40000	5.29/28148	15	239	Chlorophyll a–b binding protein
Energy- and metabolism-related proteins							
22 ↓	<0.33	19564542	4.96/46000	5.75/46078	11	277	Phosphoribulokinase
Leaf sheaths K86-161 cultivar							
Energy- and metabolism-related proteins							
24 ↓	<1.17	400404	6.20/16000	5.79/13061	28	205	Nucleoside diphosphate kinase 1
25 ↓	<0.69	379035767	5.28/25000	6.12/19276	19	181	RuBisCO large subunit
26 ↑	>0.21	62732954	5.69/41000	6.85/39556	10	185	Fructose-bisphosphate aldolase
30 ↑	>0.76	226505926	4.44/33000	4.39/24881	10	126	Elongation factor 1-delta 1
Photosynthesis-related proteins							
28 ↑	>1.27	195619530	5.12/35000	5.59/34783	24	349	Oxygen-evolving enhancer protein 1
29 ↑	>0.81	195626524	4.63/27000	5.81/28302	16	210	2-Cys peroxiredoxin BAS1
Leaf sheaths K86-161 cultivar							
Antioxidant-related proteins							
31 ↑	>0.83	1174391	6.00/27000	6.71/25223	29	258	Superoxide dismutase [Mn] 3.4
Defense proteins							
32 ↑	>0.24	439586	4.43/57000	4.45/47180	3	147	Calreticulin, partial
Other proteins							
33 ↓	<1.63	242047384	5.83/26000	8.63/27718	8	8	Hypothetical protein SORBIDRAFT_02g002690
Leaf sheaths B34-164 cultivar							
Energy- and metabolism-related proteins							
35 ↓	<4.48	195634659	5.70/41000	7.63/41924	17	409	Fructose-bisphosphate aldolase

Table 1 continued

Spot ID[a]	Fold change[b]	GI number[c]	p*I*/MW		Sequence coverage (%)	Score	Protein name
			Expt.	Theor.			
Photosynthesis-related proteins							
36 ↓	<1.93	313663913	5.41/24000	5.78/22568	6	57	Ribulose-1,5-bisphosphate carboxylase/oxygenase large subunit
37 ↓	<0.74	356538289	5.26/39000	8.70/40804	12	187	Ferredoxin-NADP reductase
38 ↓	<0.25	357149358	4.83/27000	6.43/28513	20	188	2-Cys peroxiredoxin BAS1
39 ↓	<0.32	164698711	5.11/16000	8.78/19368	28	215	RuBisCO large subunit
Defense proteins							
40 ↑	>1.16	357475607	5.62/38000	8.24/43113	4	23	Cysteine synthase
Other proteins							
41 ↑	>0.22	115436702	6.43/16000	5.71/21631	8	21	Os01g0390300
Leaf sheaths B34-164 cultivar							
Other proteins							
42 ↑	>1.85	242047384	5.77/29000	8.63/27718	24	306	Hypothetical protein SORBIDRAFT_02g002690
43 ↑	>0.28	224062828	5.80/31000	5.45/23292	3	37	Predicted protein
Roots K86-161 cultivar							
Energy- and metabolism-related proteins							
46 ↓	<0.29	1931631	6.28/46000	5.96/44285	8	180	Glutamate dehydrogenase
47 ↑	>0.17	226492743	6.68/41000	6.96/38891	14	162	Fructose-bisphosphate aldolase
Antioxidant-related proteins							
48 ↑	>1.69	1174391	6.04/30000	6.71/25223	13	49	Superoxide dismutase
Defense proteins							
49*	5.12	59799993	4.69/47000	4.78/41240	6	112	Heat shock protein 70
50*	1.03	809576	5.10/14000	5.28/14416	18	81	Cysteine proteinase inhibitor
51*	0.31	226496089	5.70/45000	5.04/51927	5	108	Cysteine protease 1 precursor
52*	2.45	226504442	6.17/20000	6.77/17048	14	124	16.9 kDa class I heat shock protein 1
Other proteins							
53 ↓	<0.71	1345588	4.70/34000	4.75/29732	22	165	14-3-3-like protein GF14-12
54 ↑	>0.31	307103200	5.61/34000	5.44/39524	9	87	Reversibly glycosylated protein
Roots B34-164 cultivar							
Energy- and metabolism-related proteins							
57*	2.97	226492743	6.71/38000	6.96/38891	10	144	Fructose-bisphosphate aldolase
Antioxidant-related proteins							
58 ↓	<1.03	254030293	5.98/26000	7.11/25327	34	360	Superoxide dismutase
Other proteins							
59 ↓	<2.17	37903393	4.62/32000	4.79/28978	26	286	14-3-3-like protein
72 ↓	<0.92	56606827	4.45/58000	4.49/47404	12	136	Calreticulin-like protein
73 ↑	>4.69	242052185	5.12/30000	5.56/17059	12	110	Hypothetical protein SORBIDRAFT_03g006880
74 ↓	<1.57	195605636	5.90/20000	5.53/27278	18	255	Triose phosphate isomerase

[a] The arrow indicates up-(↑) or down-(↓) regulated proteins under water stress; the asterisk (*) indicates that the gene was only expressed under water stress, when compared with the control (well-watered plants)

[b] Fold change was increased or decreased (>/<) compared with the control

[c] NCBI accession number

During photosynthesis, ferredoxin-NADP reductase (FNR) is one of the important final acceptors in transferring electrons from photoreduced photosystem I (PSI) (Balmer et al. 2004). Our results indicate that FNR expression was down-regulated under drought stress conditions. A similar decrease in FNR has also been found in *Populus cathayana*

(Salekdeh et al. 2002) and sunflower (*Helianthus annuus*) (Castillejo et al. 2008). The specific function of FNR under drought stress is still unclear. Nevertheless, some literature have suggested that FNR may play a crucial role in free radical scavenging in plants; these radicals are generated by the reduction of univalent oxygen at the level of PSI in the Mehler reaction (Xiao et al. 2009). The other presumed role of FNR involves maintaining the NADPH/NADP(+) homeostasis of the plastid under various environmental stresses (Xiao et al. 2009).

Two other proteins were increased in drought-tolerant sugarcane cultivar leaves. PRK is an enzyme involved in the Calvin cycle, carbon dioxide fixation and photorespiratory oxidation in which it catalyzes the ATP-dependent phosphorylation of D-ribulose 5-phosphate (Ru5P) to form D-ribulose 1,5-bisphosphate (RuBP) (Katam et al. 2007). A similar increase in PRK expression under drought stress has been reported in cotton (*Gossypium herbaceum* L.) (Deeba et al. 2012) and groundnut (Katam et al. 2007). Hence, the up-regulation of PRK may be important for stabilizing light-independent reactions during photosynthesis.

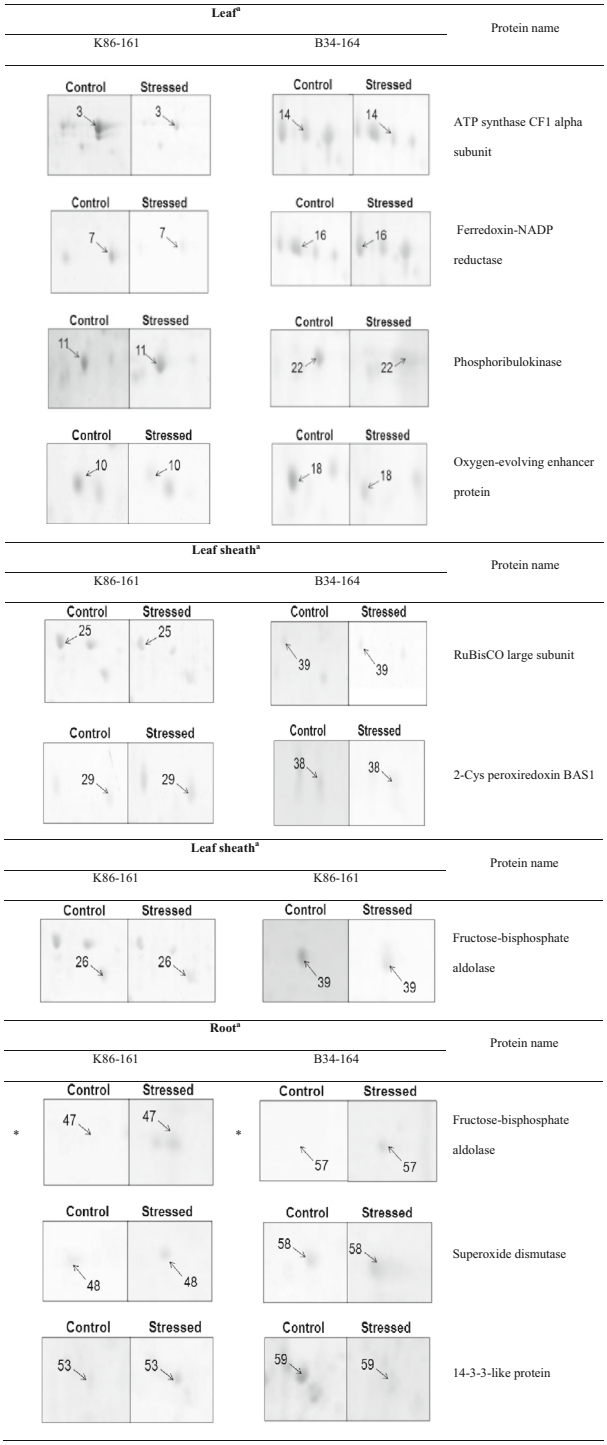
The oxygen-evolving enhancer protein has been associated with the photosystem II (PSII) complex of the photosynthetic pathway, the site of oxygen evolution in all higher plants and algae (Ali and Komatsu 2006). The increased expression of oxygen-evolving enhancer proteins under drought stress was also observed in wheatgrass (*Elymus elongatum* Host) (Gazanchian et al. 2007), *Populus cathayana* (Xiao et al. 2009), and rice (Ail et al. 2005). In the presence of salt, oxygen-evolving enhancer protein can be easily removed from the PSII complex. Therefore, the increased abundance of this protein may be necessary to repair protein damage caused by dissociation and to continue producing oxygen (Gazanchian et al. 2007).

Our results demonstrate that the up-regulation of leaf proteins under drought conditions may play a crucial role in photosynthesis to enhance energy production. Moreover, the drought-tolerant sugarcane cultivar was more capable of withstanding the stress from drought, compared to the drought-sensitive cultivar which had lost the expression of this protein.

Drought-responsive proteins of drought-tolerant and drought-sensitive cultivar leaf sheaths

A few of the leaf sheaths proteins have been documented. Our research was the first report of leaf sheaths proteins changed by drought stress in sugarcane. The possible roles of three proteins that are expressed in both cultivars, i.e., RuBisCO large subunit, 2-Cys peroxiredoxin BAS1, and fructose-bisphosphate aldolase (Table 2) are discussed below.

Table 2 Proteins of K86-161 and B34-164 cultivars those are identical in each organ (i.e., leaf, leaf sheath, and root)



[a] The arrow indicates up-(↑) or down-(↓) regulated proteins under water stress; the asterisk (*) indicates genes that were only expressed under water stress when compared with their control (well-watered plants)

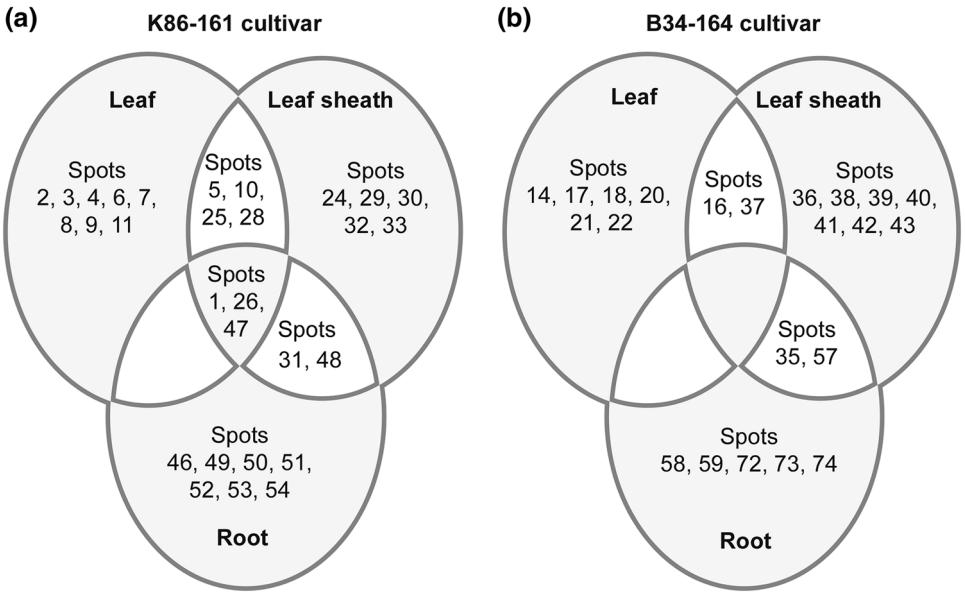


Fig. 3 Changes in protein expression levels in different organs (i.e., leaf, leaf sheath, and root). Sugarcane seedlings were exposed to drought by withholding water for 5 days. Proteins were extracted from leaves, leaf sheaths and roots, separated by 2-DE and detected by colloidal Coomassie brilliant blue G250 staining. **a**, **b** The number of protein spots that respond to drought by up- or down-regulation in different organs of K86-161 and B34-164 cultivars, respectively

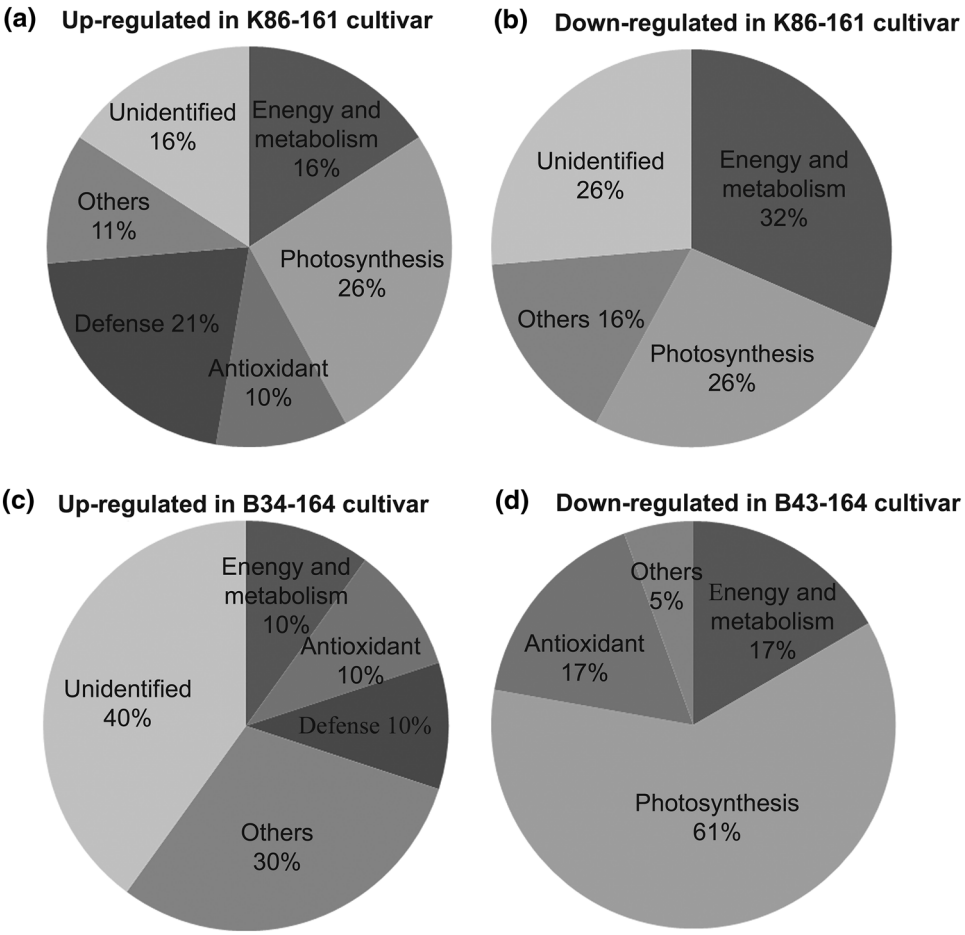


Fig. 4 Functional classification of drought-responsive proteins in the leaf, leaf sheath, and root. **a**, **b** Proteins that respond to drought by up- or down-regulation in K86-161 cultivars, respectively. **c**, **d** Proteins that respond to drought by up- or down-regulation in B34-161 cultivars, respectively

RuBisCO large subunit is a major enzyme in the photosynthetic pathway that plays important roles in maintaining growth and development in leaves and is easily affected by environmental stress (Crafts-Brandner and Salvucci 2000). Our results show that this protein was down-regulated in sugarcane when exposed to drought. Generally, RuBisCO

catalyzes ribulose-1,5-bisphosphate and CO_2 to produce glycerate-3-phosphate (3-PGA), which is then converted to triose phosphate via the photosynthetic transport of electrons (Murata et al. 2007). The down-regulation of this protein was reported under oxidative stress (Ahsan et al. 2008), chilling stress (Yan et al. 2006), salt stress (Caruso et al. 2008), and water stress (Ali and Komatsu 2006). The reduction of RuBisCO was also reported in rice leaf sheaths following water stress (Ali and Komatsu 2006). The rice report suggested that chloroplasts in bundle sheaths are sensitive to drought stress and that the RuBisCO content is reduced due to chloroplast stress. Therefore, we presume that a similar mechanism may occur in sugarcane.

2-Cys peroxiredoxin BAS1 was up-regulated in drought-tolerant sugarcane following water stress conditions. Our results agree with the results of Ali and Komatsu (Ali and Komatsu 2006), who reported the up-regulation of this protein in rice leaf sheaths. 2-Cys peroxiredoxin BAS1 is a nuclear-encoded chloroplast protein that reduces oxidative damage to chloroplast proteins from ROS such as H_2O_2 and alkyl hydroperoxide (Ali and Komatsu 2006). The chloroplast is constantly exposed to free radicals, which leads to oxidative damage by photosynthetic oxygen production and activation (Ali and Komatsu 2006). Aranjuelo et al. (2011) also found the up-regulation of 2-Cys peroxiredoxin in alfalfa (*Medicago sativa* L.) during drought stress. Similar results have also been reported in sugar beets (Hajheidari et al. 2005). However, we observed the opposite response in the drought-sensitive sugarcane cultivar. We presume that 2-Cys peroxiredoxin BAS1 may allow the drought-tolerant sugarcane cultivar to detoxify ROS better than the drought-sensitive cultivar under drought stress conditions.

Another protein that increased under drought stress was fructose-bisphosphate aldolase, which is a key enzyme in the cellular metabolism of plants (Hajheidari et al. 2005; Konishi et al. 2005; Qaisar et al. 2009). This enzyme catalyzes a reversible reaction that splits the aldol fructose 1,6-bisphosphate into triose phosphates dihydroxyacetone phosphate (DHAP) and glyceraldehyde 3-phosphate (GAP) (Qaisar et al. 2009). It is involved in gluconeogenesis, the glycolysis pathway in the cytoplasm, and the Calvin cycle in plastids (Lu et al. 2012). Up-regulation of fructose-bisphosphate aldolase has been observed in cotton under drought stress (Qaisar et al. 2009), in Flax plants under radioactivity (Klubicova et al. 2010) and in rice leaf sheath under salt stress (Abbasi and Komatsu 2004).

Drought-responsive proteins of drought-tolerant and drought-sensitive cultivar roots

At present, little information on the proteomics of roots under drought stress conditions is available in the literature; however, some information is available for rice (Yan et al. 2005), soybean (Panter et al. 1999), and wild watermelon (a C_3 xerophyte) (Yoshimura et al. 2008). Proteomic analysis of roots has also been reported under salt stress conditions in rice and chilling stress conditions in rice (Lee et al. 2009) and maize (*Zea mays* L.) (Li et al. 2007). For sugarcane root, this is the first report of proteins changed by drought stress. This knowledge may lead to a better understanding of the metabolism of drought tolerance in sugarcane.

In this study, the proteins that were noticeably induced during drought in the root of both sugarcane cultivars were fructose-bisphosphate aldolase, SOD and 14-3-3-like protein. For fructose-bisphosphate aldolase, Konishi et al. (2005) suggested that the rate of cellular growth of seedling roots may be enhanced by increasing aldolase. Thus, increased levels of fructose-bisphosphate aldolase in sugarcane root after exposure to drought may stimulate the growth of the root cells, resulting in a more effective uptake of water, which is an important mechanism to avoid drought stress (Songsri et al. 2009; Jangpromma et al. 2010b).

SOD is an efficient antioxidant enzyme that protects cells from a wide range of environmental and biological stresses, including ROS (Azcarate-Peril et al. 2006). Many previous studies have associated high SOD activity with drought stress tolerance in plants (Zang and Komatsu 2007; Jangpromma et al. 2010b). The increased abundance of SOD in sugarcane root under drought stress conditions is similar to other plants such as creeping bentgrass (*Agrostis stolonifera*) (Merewitz et al. 2011), saffron (*Crocus sativus* L.) (Merewitz et al. 2011) and *Lactuca sativa* L. (Ruiz-Lozano et al. 1996). Moreover, the expression level of SOD was higher in the drought-tolerant cultivar than the drought-sensitive cultivar, suggesting that SOD contributes to the better defense mechanism of drought-tolerant sugarcane. The increased expression level or activity of SOD in the root may be associated with increased root viability under stress.

Another root protein belonging to the 14-3-3-like protein was up-regulated in the drought-treated K86-161 but was down-regulated in the drought-treated B34-164. A previous study in cotton reported the up-regulation of 14-3-3-like protein following drought; this protein interacts with metabolic enzymes, signaling proteins, and transcription factors (Deeba et al. 2012). 14-3-3-like protein plays a crucial role in regulating primary metabolism and cellular signal transduction in plants (Chen et al. 2006). The binding of plant 14-3-3 proteins to transcription factors and other signaling proteins results in the regulation of plant development, plant defense, and stress responses (Chen et al. 2006; Xu and Shi 2006). Moreover, research on young tomato roots suggests that 14-3-3 proteins may be

involved in the response to salt stress and potassium and iron deficiency (Xu and Shi 2006).

Comparison of protein responses in the leaves, leaf sheaths, and roots of drought-tolerant and drought-sensitive cultivars

In the total of K86-161 proteins, four proteins that we found interesting were oxygen-evolving enhancer protein, RuBisCO large subunit, fructose-bisphosphate aldolase and SOD. These proteins were particularly interesting since their responses were found in more than one organ, relating to photosynthesis, energy metabolism, and defense mechanisms, which might enhance the adaptation and growth in drought-tolerant sugarcane under water stress. Of these four proteins, the most interesting was fructose-bisphosphate aldolase which was highly expressed in all three organs. Fructose-bisphosphate aldolase appears to be involved in plant growth, mainly through the promotion of ATP synthesis through the glycolytic pathway, which may accelerate cell growth and maintain a higher energy status during water deficiency (Songsri et al. 2009). Therefore, fructose-bisphosphate aldolase is important in all sugarcane organs to withstand the stress of drought.

In the drought-sensitive sugarcane cultivar B34-164, two proteins that we find interesting were ferredoxin-NADP reductase and fructose-bisphosphate aldolase. The expressions of both proteins were down-regulated under drought, except that fructose-bisphosphate aldolase was up-regulated in the roots. The down-regulation of these proteins suggests that drought could inhibit the major components of the photosynthetic pathway in this drought-sensitive sugarcane cultivar. These results indicate that the B34-164 cultivar has a reduced ability to develop, grow and survive under water stress.

Taken together, when plants were exposed to drought stress, we observed the up-regulation of important proteins in the K86-161 cultivar, such as fructose-bisphosphate aldolase, oxygen-evolving enhancer protein, and SOD. These proteins are involved in metabolism, photosynthesis and antioxidant defense under environmental stress which supports the development and growth of the plant. Therefore, these results demonstrate that under drought stress, the K86-161 cultivar adapts and survives better than the B34-164 cultivar.

Conclusions

A large body of work has documented the responses of crops to drought in an attempt to understand the mechanism of drought tolerance. However, an integrated understanding of the functioning of the whole plant in response to drought is needed. Therefore, we analyzed the drought response of sugarcane proteins in three different organs, the leaf, leaf sheath, and root using proteomic methods.

The identification and characterization of stress-responsive proteins in different organs of sugarcane can be classified into four major categories based on their function, including energy and metabolism, photosynthesis, antioxidant and defense proteins. The fructose-bisphosphate aldolase, oxygen-evolving enhancer protein, and SOD are increased in the leaf, leaf sheath, and root of K86-161 under drought-stressed conditions when compared with the control. However, contrasting responses were observed in the B34-164 cultivar.

The increase of these proteins in the K86-161 cultivar suggests that most drought responses are associated with energy and metabolism, photosynthesis and antioxidant defense. Moreover, we propose that drought-tolerant sugarcane can tolerate drought better than drought-sensitive cultivars using these mechanisms. We have reported the first proteomic profiling of the sugarcane response under drought in multiple organs. This knowledge should be useful for improving the stress tolerance of sugarcane via genetic engineering and breeding or developing new tools for screening drought-tolerant sugarcane genotypes.

Author contribution statement S. Khueychai, N. Jangpromma, P. Jaisil and S. Thammasirirak made substantial contributions to conception and design, acquisition of data: laboratory or clinical, analysis of data, drafting of article and final approval of the version to be submitted and any revised version. S. Daduang made substantial contributions to acquisition of data: laboratory or clinical, analysis of data, drafting of article, revised version and final approval of manuscript. K. Lomthaisong and A. Dhiravisit made substantial contributions to drafting of article, revised version and final approval of manuscript.

Acknowledgments This study was financially supported by the National Research University Project through the Bio-Fuel Research Cluster and Protein and Proteomics Research Center for Commercial and Industrial Purposes (ProCCI), Department of Biochemistry, Faculty of Science, Khon Kaen University. This study was supported (in part) by Northeast Thailand Cane and Sugar Research Center Khon Kaen University. We are most grateful to Mr. Werapon Ponragdee, Khon Kaen Field Crop Research Center, for providing sugarcane cultivars.

References

Abbasi FM, Komatsu S (2004) A proteomic approach to analyze salt-responsive proteins in rice leaf sheath. Proteomics 4:2072–2081

Ahsan N, Lee DG, Lee KW, Alam I, Lee SH, Bahk JD, Lee BH (2008) Glyphosate-induced oxidative stress in rice leaves revealed by proteomic approach. Plant Physiol Biochem 46:1062–1070

Ail S, Munir A, Hayat R, Ijaz SS (2005) Enhancing water use efficiency, fixation capacity of mash bean and soil profile nitrate content with phosphorus and potassium application. Agron J 4:340–344

Ali GM, Komatsu S (2006) Proteomic analysis of rice leaf sheath during drought stress. J Proteome 5:396–403

Aranjuelo I, Molero G, Erice G, Avice JC, Nogues S (2011) Plant physiology and proteomics reveals the leaf response to drought in alfalfa (*Medicagosativa* L.). J Exp Biol 62:111–123

Azcarate-Peril MA, Bruno-Bárcena JM, Hassan HM, Klaenhammer TR (2006) Transcriptional and functional analysis of oxalyl-coenzyme A (CoA) decarboxylase and formyl-CoA transferase genes from *Lactobacillus acidophilus*. Appl Environ Microbiol 72:1891–1899

Balmer Y, Koller A, Val G, Schürmann Buchanan BB (2004) Proteomics uncovers proteins interacting electrostatically with thioredoxin in chloroplasts. Photosynth Res 79:275–280

Bradford MM (1976) A rapid and sensitive method for the quantitation of microgram quantities of protein utilizing the principle of protein-dye binding. Anal Biochem 72:248–302

Caruso G, Cavaliere C, Guarino C, Gubbiotti R, Foglia P, Lagana A (2008) Identification of changes in *Triticum durum* L. leaf proteome in response to salt stress by two-dimensional electrophoresis and MALDI-TOF mass spectrometry. Anal Bioanal Chem 391:381–390

Castillejo MA, Maldonado AM, Ogueta S, Jorrín JV (2008) Proteomic analysis of responses to drought stress in sunflower (*Helianthus annuus*) leaves by 2DE gel electrophoresis and mass spectrometry. The Open Proteomics J 1:59–71

Chaves MM, Maroco JP, Pereira J (2003) Understanding plant responses to drought-from genes to the whole plant. Functional Plant Biol 30:239–264

Chen F, Li Q, Sun L, He Z (2006) The rice14-3-3 gene family and its involvement in responses to biotic and abiotic stress. DNA Res 13:53–64

Crafts-Brandner SJ, Salvucci ME (2000) Rubisco activase constrains the photosynthetic potential of leaves at high temperature and CO_2. Plant Biol 97:13430–13435

Deeba F, Pandey AK, Ranjan S, Mishra M, Sharma YK, Shirke PA, Pandey V (2012) Physiological and proteomic respones of cotton (*Gossypium herbaceum* L.) to drought stress. Plant Physiol Biochem 53:6–18

Gazanchian A, Hajheidari M, Sima NK, Salekdeh GH (2007) Proteome response of *Elymus elongatum* to severe water stress and recovery. J Exp Bot 58:291–300

Ghannoum O (2009) C_4 photosynthesis and water stress. Ann Bot 103:635–644

Hajheidari M, Abdollahian-Noghabi M, Askari H, Heidari M, Sadeghian SY, Ober ES, Salekdeh GH (2005) Proteome analysis of sugar beet leaves under drought stress. J Proteomics 5:950–960

Inman-Bamber NG (2004) Sugarcane water stress criteria for irrigation and drying off. Field Crop Res 89:107–122

Jangpromma N, Kitthaisong S, Komatsu S, Daduang S, Jaisil P, Thammasirirak S (2010a) A proteomics analysis of drought stress-responsive proteins as biomarker for drought-tolerant sugarcane cultivars. Am J Biochem Biotechnol 6:89–102

Jangpromma N, Songsri P, Thammasirirak S, Jaisil P (2010b) Rapid assessment of chlorophyll content in sugarcane using a SPAD chlorophyll meter across different water stress conditions. Asian J Plant Sci 9:368–374

Jangpromma N, Thammasirirak S, Jaisil P, Songsri P (2012) Effects of drought and recovery from drought stress on above ground and root growth, and water use efficiency in sugarcane (*Saccharum officinarum* L.). Aust J Crop Sci 6:1298–1304

Jangpromma N, Saito A, Araki T, Jaisil P, Songsri P, Songsri P, Daduang S, Kawaguchi Y, Dhiravisit A, Thammasirirak S (2014) Molecular cloning and characterization in eukaryotic expression systems of a sugarcane cysteine protease inhibitor gene involved in drought tolerance. Tur J Bot 38:724–736

Katam R, Basha SM, Vasanthaiah HN, Naik N (2007) Identification of drought tolerant groundnut genotypes employing proteomics approach. Agric Res 5:1–4

Klubicova K, Danchenko M, Miernyk JA, Rashydov NM, Berezhna VV, Ova AP, Hajduch M (2010) Proteomics analysis of flax grown in chernobyl area suggests limited effect of contaminated environment on seed proteome. Environ Sci Technol 44:6940–6946

Konishi H, Yamane H, Maeshima M, Komatsu S (2005) Characterization of fructose-bisphosphate aldolase regulated by gibberellin in roots of rice seedling. Plant Mol Biol 56:839–848

Lee J, Seo KJ (2004) Post-translational modifications and their biological functions: proteomic analysis and systematic approaches. J Biochem Mol Biol 37:35–44

Lee DG, Ahsan N, Lee SH, Lee JJ, Bahk JD, Kang KY, Lee BH (2009) Chilling stress-induced proteomic changes in rice roots. J Plant Physiol 166:1–11

Li K, Xu C, Zhang K, Yang A, Zhang J (2007) Proteomic analysis of roots growth and metabolic changes under phosphorus deficit in maize (*Zea mays* L.) plants. J Proteomics 7:1501–1512

Lu W, Tang X, Huo X, Xu R, Qi S, Huang J, Zheng C, Wu C (2012) Identification and characterization of fructose 1,6-bisphosphate aldolase genes in *Arabidopsis* reveal gene family with diverse responses to abiotic stresses. Gene 503:65–74

Merewitz EB, Gianfagna T, Huang B (2011) Protein accumulation in leaves and roots associated with improved drought tolerance in creeping bentgrass expressing an *ipt* gene for cytokinin synthesis. J Exp Bot 62:5311–5333

Miller DM (1985) Studies of root function in *zea mays*: iii. Xylem sap composition at maximum root pressure provides evidence of active transport into the xylem and a measurement of the reflection coefficient of the root. Plant Physiol Biochem 77:162–167

Mitra J (2001) Genetics and genetic improvement of drought resistance in crop plants. Curr Sci 80:758–763

Murata N, Takahashi S, Nishiyama Y, Allakhverdiev SI (2007) Photoinhibition of photosystem II under environmental stress. Biochim Biophys Acta 1767:414–421

O' Farrell PH (1975) High resolution two-dimensional electrophoresis of protein. Biol Chem 250:4007–4021

Panter S, Thomson R, Bruxelles Gd, Laver D, Trevaskis B, Udvardi M (1999) Identification with proteomics of novel proteins associated with the peribacteroid membrane of soybean root nodules. Am Phytopath Soc 13:325–333

Pradet A, Raymond P (1983) Adenine nucleotide ratios and adenylate energy charge in energy metabolism. J Plant Physiol 34:199–200

Prajanban BO, Shawsuan L, Daduang S, Kommanee J, Roytrakul S, Dhiravisit A, Thammasirirak S (2012) Identification of five reptile egg whites protein using MALDI-TOF mass spectrometry and LC/MS-MS analysis. J Proteomics 75:1940–1959

Qaisar U, Irfan M, Meqbool A, Zahoor M, Khan MY, Rashid B, Riazuddin S, Husnain T (2009) Identification, sequencing and characterization of a stress induced homologue of fructose bisphosphate aldolase from cotton. Can J Plant Sci 90:41–48

Rabello AR, Guimarães CM, Rangel PHN, da Silva FR, Seixas D, de Souza E, Brasileiro ACM, Spehar CR, Ferreira ME, Mehta A (2008) Identification of drought-responsive genes in roots of upland rice (*Oryza sativa* L). BMC Genom 9:485

Riccardi F, Gazeau P, Vienne D, Zivy M (1998) Protein changes in response to progressive water deficit in maize. Plant Physiol 117:1253–1263

Ripley BS, Gilbert ME, Ibrahim DG, Osborne CP (2007) Drought constraints on C_4 photosynthesis: stomatal and metabolic limitations in C_3 and C_4 subspecies of *Alloteropsis semialata*. J Exp Mar Biol Ecol 58:1351–1363

Ruiz-Lozano JM, Azcon R, Gòmez M (1996) Alleviation of salt stress by arbuscular-mycorrhizal *Glomus* species in *Lactuca sativa* plants. Physiol Plant 98:767–772

Salekdeh GH, Siopongco J, Wade LJ, Ghareyazie B, Bennett J (2002) Proteomic analysis of rice leaves during drought stress and recovery. J Proteomics 2:1131–1145

Shen S, Jing Y, Kuang T (2003) Proteomics approach to identify wound-response related proteins from rice leaf sheath. J Proteomics 3:527–535

Smit MA, Singels A (2006) The response of sugarcane canopy development to water stress. Field Crop Res 98:91–97

Songsri P, Vorasoot N, Jogloy S, Kesmala T, Akkasaeng C, Patanothai A, Holbrook CC (2009) Evaluation of yield and reproductive efficiency in peanut (*Arachis hypogaea* L.) under different available soil water. Asian J Plant Sci 8:465–473

Sugiharto B (2004) Biochemical and molecular studies on sucrose-phosphate synthase and drought inducible protein in sugarcane (*Saccharum offcinarum*). J Ilmu Dasar 5:62–67

Sugiharto B, Ernawati N, Mori H, Aoki K, Yonekura-Sakakibara K, Yamaya T, Sugiyama T, Sakahibara H (2002) Identification and characterization of a gene encoding drought-inducible protein localization in the binder sheath cell of sugarcane. Plant Cell Physiol 43:350–354

Tezara W, Mitchell VJ, Driscoll SD, Lawlor DW (1999) Water stress inhibits plant photosynthesis by decreasing coupling factor and ATP. Letters to Nature 401:114–117

Xiao X, Yanga F, Zhanga S, Korpelainenc H, Li C (2009) Physiological and proteomic responses of two contrasting *Populus cathayana* populations to drought stress. Physiol Plant 136:150–168

Xu WF, Shi WM (2006) Expression profiling of the 14-3-3 gene family in response to salt stress and potassium and iron deficiencies in young tomato (*Solanum lycopersicum*) roots: analysis by real-time RT-PCR. Ann Bot 98:965–974

Yan S, Tang Z, Su W, Sun W (2005) Proteomic analysis of salt stress-responsive proteins in rice root J Proteomics 5:235–244

Yan SP, Zhang QY, Tang ZC, Su WA, Sun WN (2006) Comparative proteomic analysis provides new insights into chilling stress responses in rice. Mol Cell Proteomics 5:484–496

Yoshimura K, Masuda A, Kuwano M, Yokota A, Akashi K (2008) Programmed proteome response for drought avoidance/tolerance in the root of a C3 xerophyte (wild Watermelon) under water deficits. Plant Cell Physiol 49:226–242

Zang X, Komatsu S (2007) A proteomics approach for identifying osmotic-stress-related proteins in rice. Phytochemistry 68:426–437

Zhaoa Y, Dua H, Wanga Z, Huanga B (2011) Identification of proteins associated with water-deficit tolerance in C_4 perennial grass species, *Cynodondactylon* × *Cynodon transvaalensis* and *Cynodon dactylon*. Physiol Plant 141:40–55

Hydrol. Earth Syst. Sci., 19, 1193–1207, 2015
www.hydrol-earth-syst-sci.net/19/1193/2015/
doi:10.5194/hess-19-1193-2015
© Author(s) 2015. CC Attribution 3.0 License.

Hydrology and Earth System Sciences
Open Access

Use of field and laboratory methods for estimating unsaturated hydraulic properties under different land uses

S. Siltecho[1,4,5], C. Hammecker[2], V. Sriboonlue[3,4], C. Clermont-Dauphin[2], V. Trelo-ges[1,4], A. C. D. Antonino[6], and R. Angulo-Jaramillo[7]

[1]Department of Plant Science and Land Resource, Faculty of Agriculture, Khon Kaen University, Khon Kaen, Thailand
[2]Institut de Recherche pour le Développement (IRD), UMR 210, place Viala, Montpellier, France
[3]Department of Agricultural Engineering, Faculty of Engineering, Khon Kaen University, Khon Kaen, Thailand
[4]Ground Water Research Center, Khon Kaen University, Khon Kaen, Thailand
[5]Land Development Regional Office No. 5, Land Development Department, Ministry of Agriculture, Khon Kaen, Thailand
[6]Universidade Federal de Pernambuco, Centro de Tecnologia e Geociências, Departamento de Energia Nuclear, Recife, Brazil
[7]Université de Lyon – UMR5023 Ecologie des Hydrosystèmes Naturels et Anthropisés, Université Lyon 1, ENTPE, CNRS, 3, rue Maurice Audin, 69518 Vaulx-en-Velin, France

Correspondence to: C. Hammecker (claude.hammecker@ird.fr)

Received: 23 April 2014 – Published in Hydrol. Earth Syst. Sci. Discuss.: 10 June 2014
Revised: 26 December 2014 – Accepted: 7 February 2015 – Published: 3 March 2015

Abstract. Adequate water management is required to improve the efficiency and sustainability of agricultural systems when water is scarce or over-abundant, especially in the case of land use changes. In order to quantify, to predict and eventually to control water and solute transport into soil, soil hydraulic properties need to be determined precisely. As their determination is often tedious, expensive and time-consuming, many alternative field and laboratory techniques are now available. The aim of this study was to determine unsaturated soil hydraulic properties under different land uses and to compare the results obtained with different measurement methods (Beerkan, disc infiltrometer, evaporation, pedotransfer function). The study has been realized on a tropical sandy soil in a mini-watershed in northeastern Thailand. The experimental plots were positioned in a rubber tree plantation in different positions along a slope, in ruzi grass pasture and in an original forest site. Non-parametric statistics demonstrated that van Genuchten unsaturated soil parameters (K_s, α and n) were significantly different according to the measurement methods employed, whereas the land use was not a significant discriminating factor when all methods were considered together. However, within each method, parameters n and α were statistically different according to the sites. These parameters were used with Hydrus1D for a 1-year simulation and computed pressure head did not show noticeable differences for the various sets of parameters, highlighting the fact that for modeling, any of these measurement methods could be employed. The choice of the measurement method would therefore be motivated by the simplicity, robustness and its low cost.

1 Introduction

The rubber tree (*Hevea brasiliensis*) has become a crop of high economic interest in the northeast of Thailand since the rise in price of natural rubber on the international market and the policy of the Thai government to extend rubber tree plantation. Despite climatic and edaphic conditions being very different to those of the original growing region (south of Thailand), rubber tree plantation extended by about 170 000 ha between 2004 and 2006 (Rantala, 2006). The introduction of the rubber tree in the northeast of Thailand may also contribute to important land use changes affecting soil and water resources. In this area, the average annual rainfall (1.1–1.2 m) does not completely meet the minimal requirements for rubber trees (1.3 m), and therefore it is necessary to design a wise water management to be able to ensure sustainable rubber tree farming. In order to achieve this practical goal, numerical modeling of water flow in soils is a valu-

able tool for quantifying precisely the water balance and the different mechanisms involved (Soares and Almeida, 2001; Antonino et al., 2004; Anuraga et al., 2006) and therefore for trying to forecast the evolution of the system, as the new land use may be leading to changes in the general water balance. In order to achieve accurate quantification of these changes with modeling, it is therefore necessary to estimate precisely the hydrodynamical properties of the vadose zone.

Several laboratory methods are commonly used to determine the hydraulic properties of soil, like the pressure plate method (Klute and Dirksen, 1986; Bittelli and Flury, 2009) to determine the retention curve, and hydraulic conductivity measurements like hot air, crust, one-step outflow, and sorptivity-based methods (Stolte et al., 1994). Some in situ methods have mainly been developed to measure hydraulic conductivity in the field, like the tension disc infiltrometer (Perroux and White, 1988; Akeny et al., 1991; Angulo-Jaramillo et al., 2000). In any of these cases, the determination of the hydraulic parameters of unsaturated soil is always tedious and time-consuming. Therefore, the quest for alternative methods of determination is a research issue. For example, the development of pedotransfer functions (PTFs), which provide relationships between soil hydraulic parameters and more easily measurable properties such as particle size distribution (PSD), has become successful amongst soil scientists and hydrologists (Bouma, 1989; Pachepsky et al., 2006). They are mainly based on the textural properties of soil, but show some inadequacy in describing structural aspects of soil. Consequently, specific methods taking into account structural properties have been developed to tackle this problem. For example, the Beerkan method (Haverkamp et al., 1996; Braud et al., 2005) is a field and laboratory measurement method that aims to determine retention curves and hydraulic conductivity curves by particle size distribution and single ring infiltration data, in order to describe the contribution of the texture and the structure to hydraulic properties. But, the main interest of this method is to provide an efficient and low cost estimation of soil hydraulic properties. These basic data are processed with the Beerkan Estimation of Soil Transfer parameters (BEST) algorithm according to this theory (Lassabatere et al., 2006) to provide acceptable estimations of hydraulic parameters to a complete characterization of hydraulic characteristic curves. We also compared it to a laboratory evaporation method inspired by the method proposed by Wind (1968), which is based on an evaporation measurement to estimate soil water retention and hydraulic conductivity. Wind's method has become very popular and is constantly improved by the introduction of inverse modeling (Tamari et al., 1993; Simunek et al., 1998a; Richard et al., 2001), and has been adapted for infiltration procedures (Bruckler et al., 2002). Though hydraulic conductivity is well predicted for the dry part of the curve, Wind's method is generally inadequate near saturation for hydraulic gradients that are too low (Tamari et al., 1993; Wendroth et al., 1993; Richard et al., 2001). In this study, we considered only part of the evaporation technique, in order to determine experimentally the retention curve.

Land use changes are known to modify soil properties and especially the unsaturated soil hydraulic characteristics (Zimmermann et al., 2006; Price et al., 2010), as the soil structure might be affected by different tillage methods, different root densities and sizes, and different biological activities of macro-fauna. Therefore, the hydraulic conductivity of the top soil will be affected and the infiltration capacity will be modified. In the context of tropical rain patterns with heavy rainfall followed by long dry periods, with these shallow soils, the infiltration capacity is an important factor in the soil water balance. The efficiency of the rainfall highly depends on the infiltration capacity.

Different land uses such as rubber tree plantation, pasture or natural forest in the same soil series are expected to show very different soil properties. The purpose of this study is to verify this hypothesis and to compare the performance of different measurement techniques for estimating the soil-hydraulic properties of top soil in a typical mini-watershed of northeastern Thailand, in order to model soil water flow accurately.

2 Materials and methods

2.1 Site and soil description

The study area is set up in a small watershed located near Ban Noon Tun, Phra Yuen District, Khon Kaen Province, Thailand (16°19′43.90″ N, 102°45′07.91″ E) at about 19 km southwest of the city of Khon Kaen. This area is subject to a tropical savanna climate, with annual rainfall of 1.3 and 1.96 m in 2007 and 2008, respectively, and an average annual temperature of 29 °C. The site is located in the typically undulating landscape of northeastern Thailand, with an elevation ranging from 165 to 181 m above medium sea level and an average slope of 3.5 % (Fig. 1). The surface area of the mini-watershed is estimated to be 200 m × 104 m, where most of the surface is covered with rubber trees (*Hevea brasiliensis*) and ruzi grass (*Brachiaria ruziziensis*) cultivated for seeds. The area dedicated to rubber tree plantation is approximately 120 m × 104 m, and previously the land was planted with jute (*Corchorus capsularis*), cassava (*Manihot esculenta*) and ruzi grass. Following the governmental policy and the bright economical perspectives for the farmers, the soil use changed to a rubber tree plantation in 2004.

The soil is generally shallow; in the upper part of the toposequence, the soil thickness is about 0.70 m, 0.90 m midslope, and 2.5 m downslope. The soil texture is classified as sand to sandy clay loam, with a bulk density ranging from 1.38 to 1.54×10^3 kg m^{-3}. According to the USDA classification system, the soil fit into three subgroups, i.e., Typic Haplustult, Arenic Paleustalf, and Typic Paleustult. The soil profile is comprised of an unstructured superficial sandy

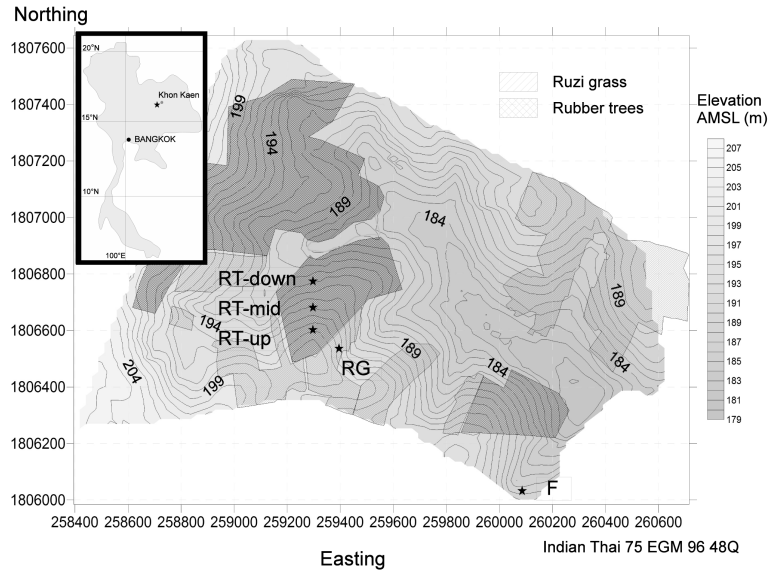


Figure 1. Location of the experimental watershed with the different different land uses and measurement sites; F: forest, RG: ruzi grass, RT-up: rubber tree upslope, RT-mid: rubber tree midslope, RT-down: rubber tree downslope, and location of meteorological station MS.

Table 1. Physical and chemical properties of the topsoil at the different sites.

	Sand	Silt %	Clay	Bulk density kg m^{-3}	Organic matter %	pH
Rubber tree						
Upslope	89.3	7.1	3.5	1.39×10^3	0.49	6.0
Midslope	88.5	7.5	4.1	1.38×10^3	0.71	6.4
Downslope	85.5	12.2	2.3	1.46×10^3	0.70	6.4
Ruzi grass	89.0	7.5	3.5	1.47×10^3	0.63	6.6
Forest	84.6	11.1	4.3	1.54×10^3	0.76	6.4

layer with low clay and organic matter contents, overlying a 0.20 to 0.50 m thick grey clayey layer colored locally with red weathered material from the bedrock (Wiriyakitnateekul et al., 2009). The bedrock, which is also probably the parental material, is a fine red sandstone or siltstone, containing clay minerals and feldspars (orthoclase), thoroughly weathered in its upper part, and densely fractured. The physical and chemical properties of the soil measured in the laboratory (Table 1) show that the texture of the top soil is sandy for rubber trees (upslope and midslope) and ruzi grass and loamy sand for rubber tree (downslope) and forest. Moreover, they show slightly acidic soils with very low organic matter content, though slightly higher in the forest (Table 1).

The first situation considered for measuring soil hydraulic properties was a toposequence of 300 m along a gentle slope (3 %) in the rubber tree plantation (i.e., RT site, Fig. 1) where three positions were selected: upslope, midslope, and downslope. Next to the rubber tree plantations, important extensions of ruzi grass pasture are still present in this small watershed, which are ploughed once a year, during the rainy season, just before sowing. The second measurement site was located in a ruzi grass pasture plot close to the rubber tree plantation (i.e., RG site, Fig. 1). The third measurement site was located in the upper part of the watershed, where an original Dipterocarpus forest has been conserved (i.e., F site, Fig. 1). Experimental soil water flow measurement devices, namely, tensiometers with pressure sensors (SKT 850T, SDEC, Reignac-sur-Indre, France) and soil moisture sensors (Enviroscan probe, Sentek, Stepney SE, Australia), were installed at the different sites (RT upslope, midslope, downslope, RG and F) and monitored every 2 h continuously from 2007 to 2009. Tensiometric data were recorded at 0.10, 0.25, 0.40, 0.60 and 1.10 m and soil moisture was measured at 0.10, 0.30, 0.50, 0.70, 0.90, 1.10 and 1.40 m. Meteorological data (rainfall, temperature, air humidity, wind speed, solar radiation) were recorded continuously at a single site in the small watershed (Fig. 1). At each experimental site (RT upslope, midslope, downslope, RG and F), Beerkan infiltration experiments were performed in the field during the dry season, from November 2007 to February 2008, and soil cylinders were collected for laboratory evaporation method measurements. The soil volumetric water content at 0–0.10 m depth, measured when the Beerkan infiltration experiments were performed, was 0.01 (m^3 m^{-3}) for RT upslope and F and 0.02 for the other sites.

2.2 Estimation of soil unsaturated hydraulic properties

Modeling and quantifying water flow in the vadose zone is mostly described by Richards' equation (Richards, 1931), and in order to solve this equation, one is required to deter-

mine (i) the soil water retention function, relating the pressure head to the soil water content $h(\theta)$,

$$S_e = \left(\frac{\theta - \theta_r}{\theta_s - \theta_r}\right) = \left(1 + (\alpha h)^n\right)^{-m}, \quad (1)$$

$$m = 1 - \frac{k}{n}, \quad (2)$$

and (ii) the hydraulic conductivity based on the Brooks and Corey (1964) model (Eq. 3),

$$\frac{K(\theta)}{K_s} = (S_e(\theta))^{\eta}, \quad (3)$$

or the van Genuchten relationship:

$$K(\theta) = K_s S_e^l \left[1 - \left(1 - S_e^{1/m}\right)^m\right]^2. \quad (4)$$

These equations are defined by several parameters where h is the pressure head (L), S_e is the effective saturation (–), θ ($L^3\,L^{-3}$) is the volumetric water content, θ_r and θ_s are the residual and saturated water content, m (–) and n (–) are shape parameters, and k is an integer usually chosen to be 1 (Mualem, 1976) or 2 (Burdine, 1953). α (L^{-1}) is the scale-fitting parameter, K_s ($L\,T^{-1}$) is the saturated hydraulic conductivity, and l (–) and η (–) are other shape parameters, with l usually considered to be 1/2.

2.2.1 The Beerkan method

The experimental procedure of this method consisted of two distinct processes, i.e., the soil particle size distribution analysis and a single ring infiltration test. According to the theory developed in Braud et al. (2005) and Lassabatere et al. (2006), 3-D axisymmetric infiltration was realized with a zero pressure head at the soil surface. It was achieved with a pulse flux of small volumes of water, and the infiltration tests were performed in situ with a 0.102 m diameter cylinder. The choice of the cylinder diameter for the Beerkan method was motivated by the experience from the literature (Braud et al., 2005) and the availability of the material. As the soil in this area is sandy and has little or no structure, it was assumed that the diameter of the infiltration cylinder would not impact the representativity of measurement.

The infiltration cylinder was driven firmly into the soil for about 0.01 to 0.02 m in order to prevent lateral loss of water from the infiltration cylinder (Fig. 2b). A series of constant volume of water ($120 \times 10^{-6}\,m^3$) was poured into the cylinder and the time was recorded after each volume of water had been completely infiltrated. Each volume represented a maximum of 0.015 m of pounding pressure at the soil surface when the cylinder was freshly refilled. Haverkamp et al. (1998) showed that small variations in pounding pressure did not influence significantly the infiltration rate, and the surface pressure head in the present case could be considered to be nil. The soil surface micro-topographic irregularities

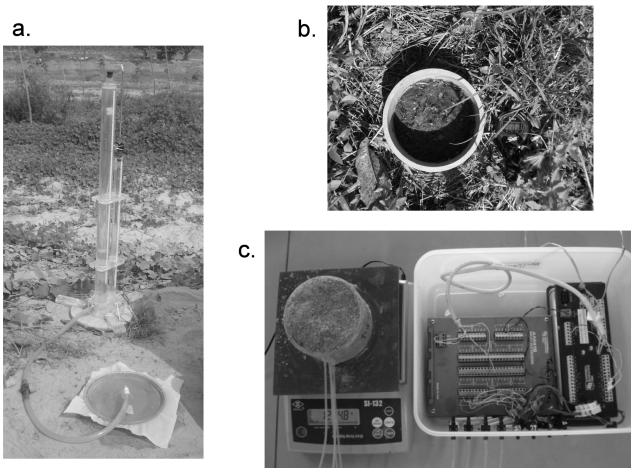


Figure 2. Photographs of some of the experimental measurement methods: **(a)** disc infiltrometer; **(b)** Beerkan method; and **(c)** evaporation method.

in a cylinder of 0.102 m in diameter are therefore negligible as regards the surface pressure. The time reading for each added volume was recorded precisely when the last free water puddle vanished completely from the soil surface. A new volume was added immediately to ensure continuous water supply. This procedure was continued until the steady-state infiltration rate was reached. Undisturbed and disturbed soil samples were collected at the test spot to determine dry bulk density, PSD by the sedimentation method, and initial (θ_0) and final (θ_s) volumetric water content. At each site, when the results were homogeneous, a minimum of three infiltration tests have been conducted. When the variability of infiltration was higher, the number of infiltration tests was increased to seven in some cases. The results were analyzed with the BEST algorithm (Lassabatere et al., 2006) in order to obtain both, the water retention curve (Eq. 1) with the Burdine condition, $k = 2$ (Eq. 2), and the hydraulic conductivity (Eq. 3). The details of this calculation procedure can be found in Lassabatere et al. (2006). However, in order to compare the results with other methods and to be able to use these parameters in numerical models like Hydrus1D (Simunek et al., 2005), the curves obtained with BEST were then adjusted to the van Genuchten with Mualem conditions ($k = 1$ in Eq. 2). The retention curve was plotted according to the Burdine parameters and the equation with the Mualem condition ($m = 1 - 1/n$) was adjusted with a Marquardt procedure to fit the new parameters.

2.2.2 Disc infiltrometer

This common field technique to measure saturated hydraulic conductivity was used at the different sites with the SW080 B device (SDEC, Reignac-sur-Indre, France). The principle of the tension disc infiltrometer is based on maintaining the water in the apparatus under a controlled tension, so that only

pores with lower matric potential can be filled. With this technique, the bio-macropores, cracks and other structures promoting preferential flow can be ignored, to measure hydraulic conductivity strictly in the soil matrix. A tension disc infiltrometer consists of a water reservoir, a Mariotte bubbling tower, and a contact disc of diameter 0.20 m covered with a microporous nylon membrane (with a pore diameter of 20×10^{-6} m). The water reservoir outlet was connected to the center of the disc with a flexible plastic tube (Fig. 2a). The tension applied to water in the device is controlled in the Mariotte tube; the depth of the air inlet under the water surface controls the minimal tension necessary to draw water out of the infiltrometer throughout the disc. Infiltration is realized until it reaches the constant infiltration rate successively with decreasing tension. The soil surface has to be cleared of vegetation and leveled to ensure perfect contact with the infiltration disc. Usually, the soil surface was slightly covered with clean fine sand to get a smooth horizontal surface and to provide a good contact between the base of the disc and the soil below. The relative position of the infiltration disc with the water reservoir is not necessarily constant. Therefore, it is important to measure it in order to calculate the actual water potential head controlled with the immersed tube of the Mariotte device. In order to calculate saturated hydraulic conductivity with the multi-potential method (Perroux and White, 1988; Smettem and Clothier, 1989), the infiltration measurements have been realized for two different tension values and interpreted with Wooding's method (Wooding, 1968; Akeny et al., 1991; Angulo-Jaramillo et al., 2000). The tension values used for the experiments were not always exactly the same, as they were partly controlled by the soil microtopography. But, they were generally between -15 and -10 hPa for the higher tension and between -7 and -3 hPa for the lower tension.

2.2.3 Evaporation method

Two undisturbed soil samples were collected in the field at each location (RT upslope, midslope, downslope, RG, F) by driving a PVC cylinder (height 9 cm and diameter 15 cm) into the previously wetted soil surface. The soil cylinders were air-dried, ensuring that the soil structure was preserved, and slowly saturated with tap water to control the initial water content. Four micro-tensiometers (3×10^{-2} m length $\times$ 1.5×10^{-2} m diameter) filled with de-aired water were connected to pressure transducers (Honeywell 15 PSI model, Honeywell Aerospace Plymouth, Plymouth MN) and inserted into the soil sample at four depths: at 0.011, 0.034, 0.056 and 0.079 m from the top of the soil sample (Fig. 2c). The cylindrical soil sample was dried from the upper surface in a ventilated thermostatic oven at an air temperature of 40 °C, imposing very slow evaporation conditions with a constant evaporation rate of 2.3×10^{-8} m s^{-1}. Pressure and the weight were recorded during evaporation at a regular time interval (30 min) on a data logger (CR10 model, Campbell Scientific, Logan UT). The measurements continued until the air entry limit of the ceramic cup of the tensiometer was reached. The soil was removed from the PVC cylinder and oven-dried at 105 °C during 24 h, and the final water content and dry bulk density were calculated. As the evaporation rate was set to be slow with a quasi steady-state flux, the pressure head gradient in the soil sample was close to zero, with a uniform pressure head profile. Therefore, it was legitimate to derive the retention curve from the average tension measured in the four tensiometers and from the water content variation during the drying of the soil cylinder. The relationship of van Genuchten (1980), Eq. (1) with the Mualem condition ($k = 1$), has been used to fit to the experimental water retention curves.

2.2.4 The inverse method

The original method of Wind is known for introducing some biases into the calculation of the hydraulic conductivity near saturation, especially as the hydraulic gradient is low (Tamari et al., 1993; Wendroth et al., 1993; Richard et al., 2001). Therefore, the same experimental data set as for the evaporation method was used to derive the soil hydraulic parameters by numerical inverse modeling with Hydrus1D (Simunek et al., 2005). The height of the simulated domain was set to 0.09 m, with four observation points corresponding to the positions of the tensiometers in the soil cylinder. The boundary conditions were set to Neumann conditions; namely, the lower boundary condition was set to zero flux and the upper boundary condition was set to the experimental evaporation flux. The inversion procedure is based on the minimization of an objective function describing the difference between observed and computed values. The estimated unsaturated soil characteristics were chosen to be described by the van Genuchten (1980) relationship (Eqs. 1 and 4) with the Mualem condition ($k = 1$, Eq. 2). In order to improve the fitting procedure, the values of θ_r, θ_s, n, and α obtained with the evaporation method and the values of K_s obtained with the disc infiltrometer were used as initial guesses for the inversion procedure. The water content parameters θ_r and θ_s were kept fixed, whereas the parameters n, α, K_s were fitted, and l was set to 0.5.

2.2.5 Pedotransfer function

Many pedotransfer functions relating simple PSD to the soil water characteristics (SWC) and especially the water retention curve have been developed in the last decades (Pachepsky and Rawls, 2003; Mohammadi and Vanclooster, 2011). Therefore, a well-established model was chosen for this study.

The model proposed by Arya et al. (1999) based on the original work of Arya and Paris (1981) is a partly physically based model, deriving from the pore size distribution of a soil from the PSD data, according to the following equation:

$$r_i = R_i \sqrt{\frac{2en_j^{1-\alpha_i}}{3}}, \quad (5)$$

where r_i is the mean pore radius and R_i the mean particle radius for the ith particle size fraction, e is the void ratio of the natural structured soil sample, n_i is the equivalent number of spherical particles in the ith particle size fraction, and α_i is a scale factor. The calculation details for these parameters can be found in Arya et al. (1999). Finally, the pore radii, r_i, are converted into equivalent pressure heads h_i, using the capillary rise equation

$$h_i = \frac{2\eta \cos\Theta}{\rho_w g r_i}, \quad (6)$$

where η is the water surface tension at the air–water interface, Θ is the contact angle, ρ_w is the density of water, and g is the acceleration due to gravity. The volumetric water content, θ_i ($m^3\,m^{-3}$), is obtained from successive summation of water-filled pore volumes according to

$$\theta_i = (\varepsilon S_w) \sum_{j=1}^{j=i} w_j, \quad (7)$$

where ε is the total porosity ($m^3\,m^{-3}$), and S_w is the saturation rate.

2.3 Evaluation of the methods

Experimental soil water flow measurement devices, namely, tensiometers and soil moisture sensors (Enviroscan probe, Sentek, Stepney SE, Australia) were installed in the different soil locations, and were continuously recorded every 2 h for several years. In order to evaluate the goodness of the soil parameter estimation methods, a reference was needed. The final use for these parameters was modeling of soil water flow, and no intrinsic correct values were known, so these parameters were evaluated by modeling with Hydrus1D, a robust and well-documented software (Simunek et al., 2005), and by comparing modeled results with experimental data. The calculation has been performed on a uniform 0.35 m deep domain with two tensiometric boundary conditions measured in the field at 0.10 m as the upper boundary condition and at 0.45 m for the bottom boundary condition. This choice has been motivated by the necessity to perform the simulation with well-constrained boundaries. The development of matric potential during an almost 1-year period was calculated for the intermediate tensiometer located at 0.25 m. These calculations were performed with the combination of the unsaturated soil parameters measured with the different methods (i.e., the Beerkan, disc infiltrometer, PTF, evaporation and inverse methods) and were compared to the experimental tension values measured in the five different locations (i.e., in the forest, ruzi grass, and the three positions in the rubber plantation). The four criteria generally proposed were used to evaluate the performance of modeling (Table 2), namely the root mean squared error (RMSE), the coefficient of determination (CD), the modeling efficiency index (EF) and the coefficient of residual mass (CRM) (Loague and Green, 1991; Kim et al., 1999).

2.4 Statistics

Firstly, the estimated variables, namely saturated hydraulic conductivity (K_s), parameter α and parameter n, were analyzed using standard statistics to calculate their mean and coefficient of variation values. The statistical R package (R Development core team, 2008) was used to test the normality of data frequency distribution with the Anova test.

However, as the number of repetitions were uneven and sometimes very low (from 3 to 10 samples per method tested in each site), Kruskal–Wallis non-parametric tests were also used to check the hypothesis of the same continuous distribution for the different cases. This test determines equality between means or medians of different groups of data, without presuming any specific hypothesis on the distribution.

3 Results

3.1 Beerkan method

With a simple 3-D infiltration experiment combined with PSD analysis, the BEST software (Lassabatere et al., 2006) derived the main shape parameter n and scale parameter K_s and α describing the unsaturated hydraulic properties. The results displayed in Table 3 show relatively low variation between the different sites. Saturated hydraulic conductivity (K_s) ranged from 5.59 to $10.23 \times 10^{-6}\,m\,s^{-1}$ within the different sites and showed a clear gradient along the slope in the rubber tree plantation. The highest values of K_s were found upslope and on the lowest downslope, probably due to the accumulation of finer particles in the lower part, as mentioned by other authors (Heddadj and Gascuel-Odoux, 1999; Jing et al., 2008) describing topographic variation of hydraulic conductivity. Average K_s values were found to be very similar for the soil under ruzi grass and under forest (5.84 and $5.93 \times 10^{-6}\,m\,s^{-1}$, respectively), though the standard deviation was much higher for ruzi grass than for forest (3×10^{-6} and $9 \times 10^{-7}\,m\,s^{-1}$, respectively). Along the slope, the relative standard error on K_s was also quite high, with values ranging from 49 to 62 %. The retention curve parameters, α and n, also showed little variation between the different sites: for most of the cases, the average value of α was 1.4 or $1.5 \times 10^{-4}\,m^{-1}$, except for the forest (F), where α displayed higher values ($2.8 \times 10^{-4}\,m^{-1}$). The shape parameter n followed a similar trend as K_s, namely, decreasing values along the slope (2.33, 2.26 and 2.06, respectively, in the upslope, midslope and downslope positions). Outside the plantation, the average value for n in ruzi grass (R) was within the range previously observed, namely 2.23, but it was significantly

Table 2. Evaluation criteria for performance of modeling.

$\mathrm{RMSE} = \sqrt{\frac{\sum_{i=1}^{N}(T_i - M_i)^2}{N}}$	Indicates that the degree of deviation between the experimental determinations and calculated values tends to zero when the calculated and experimental values tend to be equal.
$\mathrm{CD} = \frac{\sum_{i=1}^{N}(M_i - \overline{M})^2}{\sum_{i=1}^{N}(T_i - \overline{M})^2}$	Describes the ratio between the dispersion of experimental determinations and the dispersion of the calculated values, tending towards unity when the experimental and calculated values are consistent.
$\mathrm{EF} = \frac{\sum_{i=1}^{N}(M_i - \overline{M})^2 - \sum_{i=1}^{N}(T_i - \overline{M})^2}{\sum_{i=1}^{N}(M_i - \overline{M})^2}$	Indicates whether the model provides a better estimate of experimental determinations than the mean value of these determinations. The expected value for EF tends towards 1.
$\mathrm{CRM} = \frac{\sum_{i=1}^{N} M_i - \sum_{i=1}^{N} T_i}{\sum_{i=1}^{N} M_i}$	Indicates whether the model tends to overestimate (CRM < 0) or underestimate (CRM > 0) compared to experimental values. The optimal value for CMR tends towards zero.

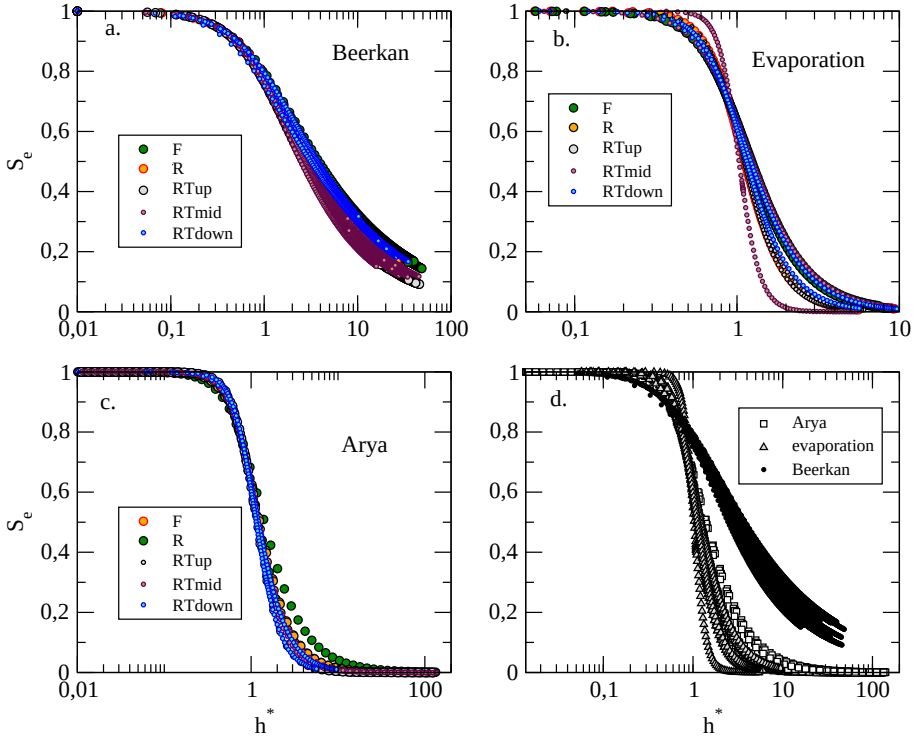


Figure 3. Scaled retention curves for **(a)** the Beerkan method, **(b)** the evaporation method, **(c)** the method based on Arya's PTF, and **(d)** the different methods.

Table 3. Means and standard errors for the main van Genuchten parameters with Mualem conditions ($n = 1/\{1 - m\}$) determined for the different methods at the different sites. The number of samples is indicated in parentheses.

$K_s \times 10^{-6}$ (m s^{-1})				
	Beerkan	Disc infiltrometer	Inverse	
Forest	5.94 ± 0.94 (3)	6.65 ± 4.41 (6)	10.00 ± 2.04 (3)	
Ruzi	5.82 ± 3.55 (4)	6.93 ± 5.45 (7)	18.48 ± 7.12 (3)	
RT downslope	5.59 ± 2.56 (7)	3.48 ± 2.38 (6)	10.18 ± 0.82 (3)	
RT midslope	8.53 ± 4.22 (11)	5.11 ± 4.60 (7)	14.66 ± 8.90 (3)	
RT upslope	10.23 ± 6.38 (10)	6.89 ± 5.31 (6)	22.06 ± 5.27 (2)	
α (m^{-1})				
	Arya	Beerkan	Inverse	Evaporation
Forest	1.5 ± 0.9 (6)	2.8 ± 0.47 (3)	1.8 ± 0.058 (3)	1.8 ± 0.058 (3)
Ruzi	0.6 (1)	1.5 ± 0.56 (10)	1.87 ± 0.21 (3)	1.87 ± 0.21 (3)
RT downslope	0.6 (6)	1.4 ± 0.55 (11)	1.97 ± 0.21 (3)	1.97 ± 0.21 (3)
RT midslope	0.54 ± 0.05 (5)	1.5 ± 0.85 (7)	1.87 ± 0.21 (2)	1.87 ± 0.3 (3)
RT upslope	0.5 (5)	1.5 ± 0.9 (4)	2.55 ± 0.35 (3)	1.97 ± 0.21 (3)
n				
	Arya	Beerkan	Inverse	Evaporation
Forest	2.83 ± 0.17 (6)	2.00 ± 0.03 (3)	2.29 ± 0.09 (3)	3.29 ± 0.50 (3)
Ruzi	1.82 ± 1.22 (3)	2.23 ± 0.11 (4)	2.90 ± 0.44 (3)	3.82 ± 0.69 (3)
RT downslope	2.72 ± 0.07 (6)	2.06 ± 0.02 (7)	2.48 ± 0.29 (3)	3.20 ± 0.54 (3)
RT midslope	3.35 ± 0.14 (5)	2.26 ± 0.06 (11)	2.31 ± 0.08 (3)	2.96 ± 0.14 (3)
RT upslope	3.17 ± 1.01 (6)	2.33 ± 0.03 (10)	2.18 ± 0.02 (2)	3.32 ± 0.67 (3)

lower in the forest situation, with a value of 2. Normalized or scaled retention curves (Fig. 3d) were established with dimensionless values of water content (S_e) and of the matric potential ($h^* = h\,\alpha$), in order to simplify the retention curve $h(\theta)$, and to compare the shape parameters. They showed very similar shapes for all the locations, with a small shift for the F soil samples, indicating differences in shape parameters for the soil in forest resulting from a slightly higher clay content. As hydraulic conductivity is mainly ruled by shape parameters like texture that vary less in local than in scale parameters, scaled hydraulic conductivity curves (not shown here) were all grouped together and were therefore less informative.

3.2 Disc infiltrometer

Results obtained for K_s with the disc infiltrometer showed a behavior similar to that with the Beerkan method, namely, a progressive decrease down the slope in the rubber tree plantation, though the actual values for K_s were systematically lower, namely, 6.9, 5.1 and 3.5×10^{-6} m s^{-1} from upslope to downslope positions, respectively (Table 3). The average values of K_s in the forest and ruzi grass were larger than those for the Beerkan method (6.65 and 6.93×10^{-6} m s^{-1}, respectively). The relative standard errors for this method were significantly larger than for the Beerkan method, with values ranging from 66 to 90 %. The higher dispersion for hydraulic conductivity values derived from the disc infiltrometer could be explained by the fact that measurements are very dependent on the quality of the contact between the disc and the soil surface. Despite all the efforts to meet this requirement, it can be quite difficult to fulfill, and therefore affects the kinetics of infiltration. The precise infiltration surface area was also subjected to uncertainty when sand was applied to improve the contact, as the sand could overlap the actual disc surface. Moreover, in sandy soils, local hydrophobicity can occur (especially in rubber tree plantations, where natural rubber can modify water repellent properties of soil), and therefore affects infiltration dynamics and more specifically the measurements with the disc infiltrometer, as soil suction was the driving force. The presence of macro-pores related to biological activity (earthworms, ants, termites) could also partly explain the differences between the Beerkan method and the disc infiltrometer, as with this latter method, water can only infiltrate into the soil matrix.

3.3 Evaporation method and the associated inverse method

Theoretically, the water retention curve obtained from the evaporation method could be considered a reference, for it corresponds to direct experimental data with no model as-

sumed a priori. In order to compare the results more easily with the other methods, the van Genuchten model with Mualem conditions was used to fit to the experimental retention curves. Parameter α varied only in a very narrow interval between 1.8×10^{-4} and $2.5 \times 10^{-4}\,\mathrm{m}^{-1}$, and was found to be equal for both methods. Nevertheless, the values were found to be slightly larger than for the Beerkan method. Values for shape parameter n are significantly different between the two methods, with higher values for the evaporation method. By comparison, the n values obtained with the Beerkan method are much lower than those derived from the evaporation and inverse methods. The scaled retention curves depicted in Fig. 3c for the evaporation method clearly show slight variations between the different situations. A single soil sample from the RT in the midslope position stood out, with a noticeably larger value for n. Saturated hydraulic conductivity obtained with the inverse method was much more important than when determined with other methods, as it ranged from 10 to $22 \times 10^{-6}\,\mathrm{m\,s}^{-1}$. Regarding K_s along the slope, the same pattern was found, namely, showing an increase along the slope from the bottom to the upper position. Unlike the disc infiltrometer and Beerkan methods, K_s for ruzi grass and for forest soils was found to be very different, with a very high K_s value for ruzi grass: $22 \times 10^{-6}\,\mathrm{m\,s}^{-1}$ instead of $6 \times 10^{-6}\,\mathrm{m\,s}^{-1}$ with the other methods.

3.4 Arya method

Van Genuchten water retention parameters were fitted on the experimental curves and showed little variation for parameter α between the different sites, reflecting a low variability of PSD. On the other hand, the values for α were found to be significantly lower than for the other estimation methods. The shape parameter n showed very high variability, with average values ranging from 1.82 for RG to 3.35 for RT-mid and an important standard deviation running from 3 to 67 %. The scaled retention curves (Fig. 3b) for this method were very similar, though the forest soil samples showed a slightly particular behavior. Nevertheless, when all are represented on the same graph, the slight variations of scaled retention curves corresponding to the location of the soil samples seemed negligible compared to the differences due to the measurement methods (Fig. 3a). The value of the shape parameter n represented by the slope of the retention curve was lowest for the Beerkan method, intermediate for Arya method and highest for the evaporation method. Retention curves obtained with the Arya and Beerkan methods were, respectively, strictly based on PSD, and on PSD partly influenced by infiltration data. As for these methods, the values for n were lower, and the pore size distribution was not as sharp as for the evaporation method. One can therefore suppose that part of the porous volume was not drained with the evaporation method. In fact, by imposing a low evaporation rate to avoid overly important hydraulic gradients inside the soil sample, the energy necessary to draw out water from the smallest or less accessible pores is probably not sufficient.

3.5 Statistical analysis

The number of replicates for each method was not equal, because it depended on (i) the time necessary to perform the measurement, and on (ii) the quality of the measurement. For example, only a few evaporation measurements have been performed, as each measurement took up to 2 weeks to be completed. On the other hand, more Beerkan and disc infiltrometer measurements have been performed, as the infiltration experiments lasted only between 30 and 60 min, and between 2 and 6 h, respectively. The number of results was also controlled by the data processing of the infiltration experiment, as some experiments had finally to be discarded.

The statistical analysis of the van Genuchten unsaturated soil water parameters for the different locations with the different experimental techniques was performed with the Kruskal–Wallis non-parametric method. Both κ^2 and p values (Table 4) showed clearly that measured unsaturated soil water parameters were highly dependent on the measurement techniques. As already pointed out on the scaled retention curves, parameter n seemed to be the most dependent on the type of method, considering the high value of κ^2 and the extremely low p value. The shape parameter α showed the highest κ^2 value, but saturated hydraulic conductivity K_s is also highly dependent on the measurement method. The influence of location was found to be secondary or even negligible, with a p value of 0.11, 0.94 and almost 1 for α, n and K_s, respectively, except for α showing a relatively high value for κ^2 (7.15), but still under the acceptable limit (9.49) for the corresponding degrees of freedom (4). Saturated hydraulic conductivity K_s was therefore not a discriminating parameter for the different situations, whereas parameter n tended to show an evolution with the different sites. When data were considered globally, regrouping all the measurement methods, the variability of the results was higher considering the measurement method rather than the measurement location. When studied separately for each measurement method (Table 4), some parameters seemed to differentiate clearly the different sites. For example, with the Beerkan method, the shape parameter n appeared to be significantly different for the different sites. With the pedotransfer function of Arya, scale parameter α was the most discriminating parameter, with an extremely low p value, though parameter n also showed a low p value (< 0.05). In both cases, it was shown that the particle size distribution and the derived parameters were significantly different at the various sites for these two measurement methods. With the others, no clear distinction between the different sites was observed, as the p values were very high, between 0.15 and 0.86.

Table 4. Medians and parameters of Kruskal–Wallis, chi-squared (κ^2), degree of freedom df, and p value for the van Genuchten parameters for different methods and different sites, in general and in detail for each method, $K_S \times 10^{-6}$ ($m\,s^{-1}$) and α (m^{-1}). B: beerkan, I: inverse, A: Arya, E: evaporation, D: disc. * indicates a statistically significant difference between values.

	General	Arya	Beerkan	Disc inf.	Inverse	Evapor.	κ^2	df	p value
	α	0.6	1.6	–	1.9	1.8	28.171	3	3.34×10^{-6}
	K_S	–	7.15	4.76	12.16	–	19.364	2	6.24×10^{-5}
	n	2.979	2.251	–	2.331	3.117	47.981	3	2.15×10^{-10}
		Forest	RT down	RT mid	RT up	Ruzi			
	α	1.9	1.4	1.6	1.5	1.7	7.15	4	1.28×10^{-1}
	K_S	6.42	4.497	8.39	9.53	6.97	4.40	4	3.54×10^{-1}
	n	2.703	2.597	2.318	2.361	2.387	1.72	4	7.87×10^{-1}
Method	Detail	Forest	RT down	RT mid	RT up	Ruzi	κ^2	df	p value
B	K_S	5.99	4.93	8.81	9.53	4.93	4.251	4	0.3731
	α	2.72	1.39	1.59	1.505	1.44	6.16	4	0.1878
	n	2.01	2.06	2.26	2.33	2.20	24.54	4	6.23×10^{-5}*
I	K_S	92.68	90.00	169.86	190.60	140.28	6.35	4	0.1750
	α	1.80	1.90	1.80	2.55	1.80	6.05	4	0.1955
	n	2.28	2.60	2.28	2.18	3.09	6.77	4	0.1490
A	α	1.5	0.6	0.5	0.5	10.9	21.22	4	0.0003*
	n	2.84	2.72	3.4	3.553	2.84	12.97	4	0.0114
E	α	1.8	1.9	1.8	1.9	1.8	1.29	4	0.8627
	n	3.07	3.42	2.89	3.60	4.01	3.47	4	0.483
D	K_S	44.51	25.85	24.24	58.03	59.71	2.71	4	0.6077

3.6 Modeling validation

Unsaturated soil water parameters are generally determined for use in mathematical models simulating soil water flow. Their evaluation was therefore performed with Hydrus1D, and the computed matric potentials at 0.25 m were compared to the experimental data. The different locations could be divided into two distinctive groups where (i) infiltration was strictly 1-D with vertical water flow, corresponding to the forest and ruzi grass, and (ii) with a possible lateral flow component due to the slope in the rubber tree plantation. The results obtained in the forest and at the ruzi grass sites showed good conformity with the experimental data (Fig. 4) and with RMSE values less than 40 hPa and EF values close to unity, especially for the forest site (0.83–0.95). The numerical simulations obtained with unsaturated soil water parameters issued from the different methods show very few differences. In both cases (F and RG), the best fit was obtained with parameters derived from the combination of the Arya method for retention curves and the disc infiltrometer for hydraulic conductivity. Simulations performed with parameters from the Beerkan method showed a slightly higher RMSE value, whereas the results obtained with the evaporation-method-based parameters seemed to fit worse to experimental data. These trends were confirmed by the other modeling evaluation indexes (DR, EF). CRM showed a systematic small negative value for the forest site, regardless of the measurement method, indicating an underestimation in the computed matric potential values. The scatterplots of computed vs. experimental matric pressure heads (Fig. 5) showed good agreement for all models in the forest and a slight underestimation for the high values in the ruzi grass. For the rubber tree plantation, concordance between computed results and experimental data was much worse (Figs. 4 and 5). The general trend was preserved but often overestimated compared to experimental data, as depicted in Table 4 and quantified by CRM in Table 5. During the rainy season, the fit between computed and experimental matric potential was generally better than during the drier period (Fig. 5). This discrepancy can be explained mainly by the slope in the rubber tree plantation and the inevitable subsurface lateral flow. Indeed, in the soil profile, an impervious clayey layer lying over the bedrock promoted the generation of a perched water table during the rainy season. Though the slope of the terrain was only 3 %, the actual slope of the interface on which the water table built up was more important, as the soil profiles increased from upslope to downslope. It has been shown that 40 % of the annual rainfall actually contributed to lateral flow along the slope (Seltacho et al., 2013). Therefore, the water flow in the field was not 1-D, and could not be com-

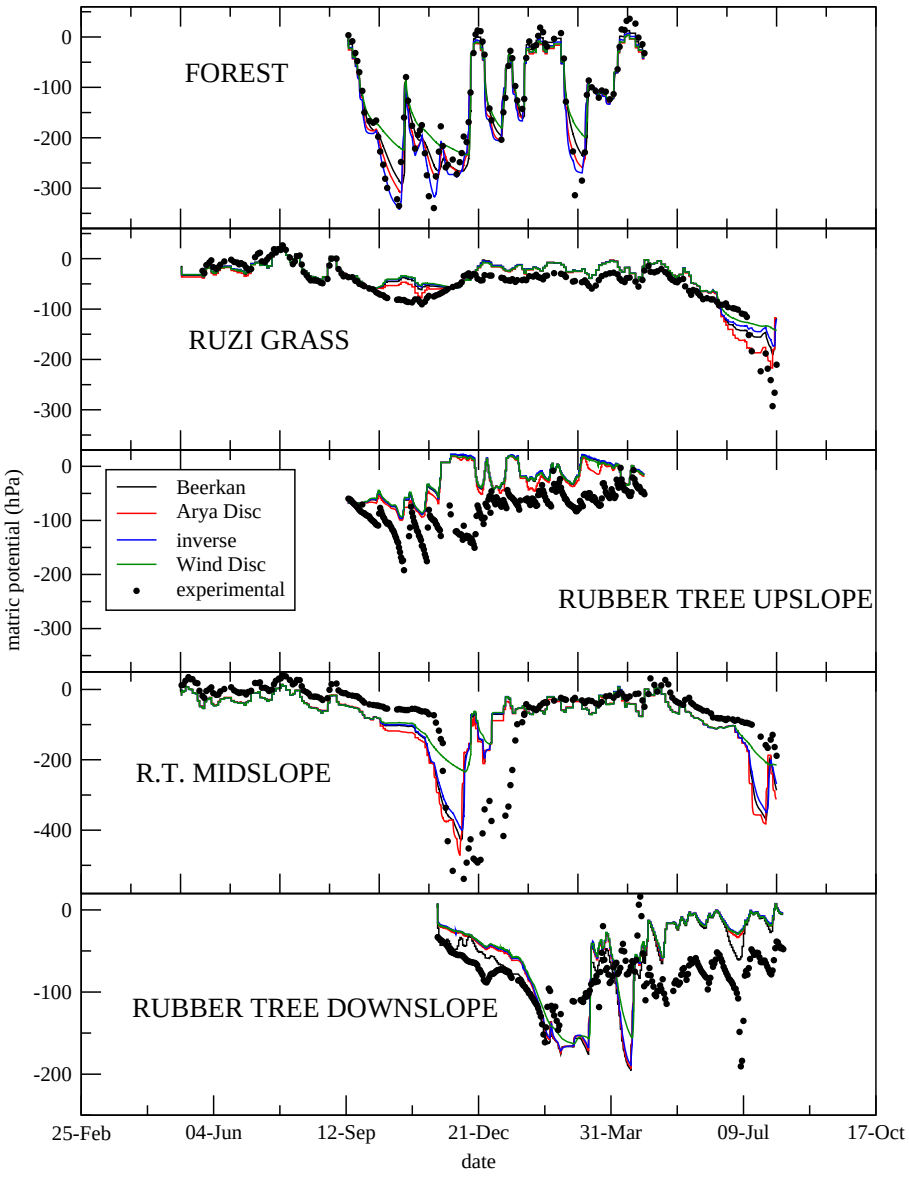


Figure 4. Development of the matric potential at 0.25 m depth in the different locations (black dots) and results of modeling with Hydrus1D (continuous lines).

puted adequately; in upslope and midslope positions, water was lost laterally and accumulated in the downslope position. Nevertheless, when lateral flow was taken into account in a 2-D simulation with Hydrus2D (Seltacho et al., 2013), computed and experimental values fitted well. In any case, when contemplated from a yearly timescale, the differences between the different methods for simulating the water flow in soil seemed negligible in terms of water stock. Regardless of whether the computed results fitted the experimental data, as for forest and ruzi grass, or did not, as with the rubber tree plantation, no method could clearly stand out as being more efficient than any other one in modeling water flow for these different situations. These results are informative about the non-uniqueness of the parameters for modeling water flow in soil. Despite not describing exactly the development of soil water potential, different combinations of soil parameters lead to very similar results when used in Hydrus1D on a yearly timescale. The efforts to determine the soil hydraulic parameters precisely can therefore be seriously questioned. In any case, to improve the modeling performance for a longer time series or to forecast different scenarios, the parameters need to be adjusted by inverse modeling (Seltacho et al., 2013).

Table 5. Four modeling evaluation criteria for matric potential for the different situations with the different parameters used in Hydrus1D.

RMSE (hPa)	Beerkan	Arya disc	Inverse	Evaporation disc
Forest	33.15	27.47	24.09	42.50
Ruzi grass	23.02	22.56	24.45	26.71
RT upslope	64.94	60.06	65.78	64.61
RT midslope	100.59	102.25	99.62	98.25
RT downslope	52.63	49.06	53.21	51.22
DR	Beerkan	Arya disc	Inverse	Evaporation disc
Forest	1.2	1.25	1.05	1.83
Ruzi grass	0.56	1.05	1.42	1.65
RT upslope	0.30	0.35	0.29	0.31
RT midslope	2.43	2.25	2.61	4.87
RT downslope	1.33	0.27	0.24	0.27
ME	Beerkan	Arya disc	Inverse	Evaporation disc
Forest	0.9	0.93	0.95	0.83
Ruzi grass	0.62	0.76	0.72	0.66
RT upslope	−2.47	−1.97	−2.56	−2.44
RT midslope	0.32	0.30	0.33	0.35
RT downslope	0.85	−2.06	−2.60	−2.43
CRM	Beerkan	Arya disc	Inverse	Evaporation disc
Forest	−0.03	−0.06	−0.09	0.08
Ruzi grass	−0.51	0.15	0.24	0.27
RT upslope	0.69	0.62	0.70	0.69
RT midslope	−0.11	−0.15	−0.09	0.02
RT downslope	0.33	0.23	0.35	0.41

4 Discussion

A major result of this study is the apparent high dependence of unsaturated hydraulic properties on the measurement method. Several factors can explain this discrepancy, especially the size of the soil sample on which the measurement has been performed.

The measurements have been performed on soil samples of different sizes for the different methods, depending on the availability of equipment and materials. For example, the diameter of the disc infiltrometer was almost twice the diameter of the infiltration cylinder. However, according to Anderson and Bouma (1997) and Bouma (1980), the representative elementary volume of sandy soil for measuring hydraulic conductivity is usually considered to be around $1 \times 10^{-4}\,m^3$. Consequently, considering the texture (mainly sandy) and especially the lack of structure of the soil in the different locations (except in the forest), the volumes of the soil samples exceed the representative elementary volume. Therefore, despite not having been measured on strictly the same volumes or areas, but still on the order of magnitude (Beerkan $8 \times 10^{-4}\,m^3$, disc infiltrometer $2 \times 10^{-3}\,m^3$, evaporation $1.5 \times 10^{-3}\,m^3$), the results for the different methods should not be affected by the scale.

On the other hand, the differences can be explained by the specific properties of each method with their limitations and inherent assumptions for deriving the parameters.

The Beerkan method is popular for the straightforwardness of the experimental setup and rapid infiltration process; a constant infiltration rate is generally reached in less than an hour. However, the derivation of the unsaturated parameters is based on a rigorous hypothesis about the unsaturated hydraulic properties; namely, they are supposed to follow strictly the retention model of van Genuchten with Burdine's condition and the expression of Brooks and Corey for hydraulic conductivity. Even though this assumption agrees well in most of the cases, situations like bimodal porous networks, for example, are not taken into account.

With the disc infiltrometer, the experiment is more difficult to set up, as it needs a perfectly flat contact between the soil surface and the disc and is prone to many technical failures (leaks, etc.). Moreover, each experiment usually takes a very long time to reach a constant infiltration rate (sometimes several hours for finely textured soils). Wooding's model used to derive saturated hydraulic conductivity from disc infiltration measurements assumes an exponential relationship between hydraulic conductivity and matric potential that is quite different from the van Genuchten function.

The evaporation method is the only one for which the retention curves were actually measured without any a priori model. The slow evaporation rate imposed at the surface generated a very slight tension gradient inside the soil, with a uniform water content distribution. Average water content and pressure head values could therefore be calculated. The drawbacks of this method are the length of time needed for a soil sample to dry completely (up to 2 weeks) and the costly equipment (oven, computer, balance, microtensiometers, pressure gauge, data logger).

The pedotransfer function is an extremely easy method to derive the retention curve based only on particle size distribution. The Arya relationship is physically based, deriving the size of the voids between the grains by assuming a packing model. Nevertheless, as this model, unlike the Beerkan method, is exclusively governed by the PSD and the bulk density of the soil, little information about the the soil structure is available in the computed retention curve.

These technical and theoretical differences between the two infiltration methods can explain the contrast between their results. The shape of the hydraulic conductivity equations, Brooks and Corey for the Beerkan method and an exponential relationship for the disc infiltrometer, are different, especially near saturation. Saturated hydraulic conductivity determined through an exponential function with the Wooding method takes into account pressure head values near saturation, whereas in the BEST procedure, the Brooks and Corey equation is derived over a wider range of pressure head values. Therefore, saturated hydraulic conductivity determined with the disc infiltrometer is higher than when derived with the Beerkan method (Simunek et al., 1998b).

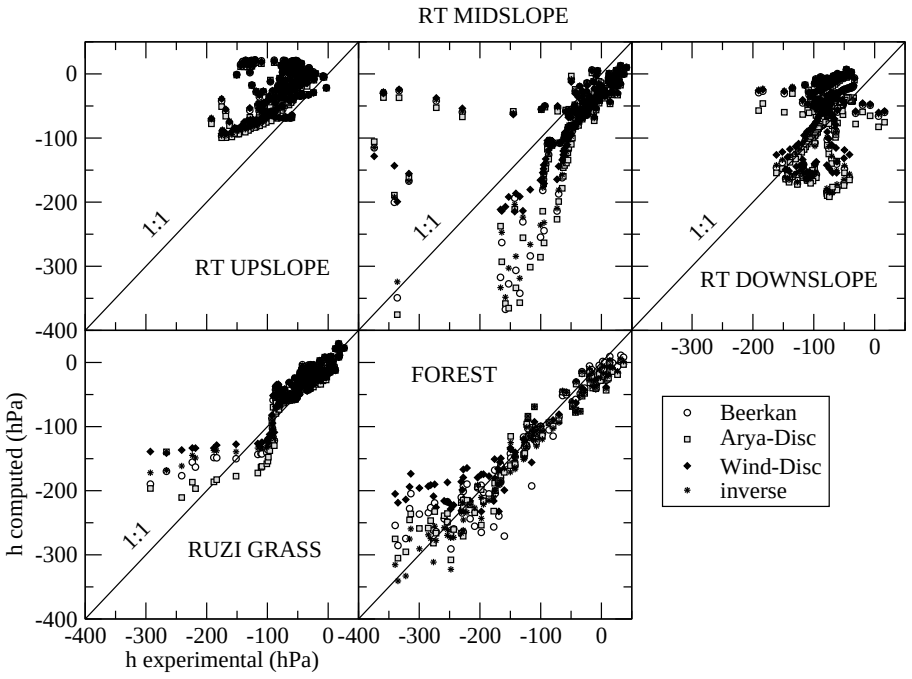


Figure 5. Scatterplots of computed vs. experimental matric potential values in the different locations for different combinations of parameters.

When K_s is derived by inverse modeling from the evaporation experiment, it is systematically higher than with the infiltration methods. The use of the van Genuchten equation (Eq. 4) with Mualem conditions in the fitting procedure seems to be responsible for the overestimation of K_s. More generally, the use of different type of equations, valid in different domains of pressure head or soil water content to derive K_s, invariably leads to a wide range of values. The same conclusions could be drawn for the scale and shape parameters (α and n), as equivalent procedures were used to derive them.

Nevertheless, for each measurement method, a decrease in hydraulic conductivity down the slope in the rubber tree plantation was systematically observed, and could probably be related to the translocation of finer particles downslope (Wiriyakitnateekul et al., 2009). Despite showing slightly higher levels of organic matter, and unlike what would commonly be expected, forest soil had the lowest hydraulic conductivity. The higher content in finer particles (clay and silt) was most probably responsible for lower K_s values at the forest site and to some extent at the ruzi grass site. During the early stages of the rubber tree plantation, the soil surface was not covered and was therefore more vulnerable to erosion. The fine soil particles were translocated downslope and down the soil profile, whereas under forest and ruzzi grass clay translocation was not as active.

The final use of these van Genuchten (VG) parameters was to use them in Hydrus1D to compute the water balance at these different sites. This study showed clearly that the uniqueness of VG parameters did not apply in this case, as many different combinations provided similar or equivalent results when a yearly timescale was considered. The simulation results obtained with the parameters derived from different methods were generally equivalent when the different validation parameters were considered. In any case, to perform efficient and reliable modeling of water flow in soil, these parameters should be carefully adjusted by inverse modeling procedures on experimental data over a time series describing contrasted situations and then validated. The measured VG parameters should be used as appropriate first guess values for the inverse modeling procedure. No single method could be considered without doubt as producing better results than the others. It should therefore be recommended to use the easiest and cheapest methods for the experimental evaluation of the first set of VG parameters and, in this case, the Beerkan method would surely be the best option.

5 Conclusions

In order to determine the unsaturated hydraulic properties of soil for different land use, several experimental methods have been used in a small watershed in northeastern Thailand. They included laboratory methods like the evaporation method, inverse methods and PTF (Arya et al., 1999), and also field evaluations like the Beerkan method and a disc infiltrometer.

Statistical analysis of the results obtained during this study showed clearly that significative differences in VG parame-

ter measurements appeared, depending on the measurement method. Though the impact of land use and position was not completely negligible, the primary factor for measurement variability was found to be in the experimental methods. It was stated that the actual values of VG parameters depend on the method employed to determine them. However, when each measurement method was considered separately, the discrimination by site was significant for the Beerkan method and Arya's PTF method. As both methods are based on particle size distribution, parameters n and α, respectively, could distinguish the different sites. Unsaturated soil properties of this sandy soil seemed to be governed mainly by textural parameters related to the pedogenesis rather than by structural properties associated with land use and management.

Amongst the different methods tested in this study, none could clearly be considered superior to the others in terms of providing better parameters for modeling soil water flow. Therefore, the cheapest and easiest method to derive the VG parameters, like the Beerkan method, should be used to fulfill this task. The important land use changes taking place in northeastern Thailand can therefore be evaluated easily with numerical modeling and the consequences of rubber tree plantation for the water balance on different scales can therefore be predicted (Seltacho et al., 2013).

The Supplement related to this article is available online at doi:10.5194/hess-19-1193-2015-supplement.

Acknowledgements. The work was funded by IRD (Institut de Recherche pour le Développement), UMR210, the Land Development Department (LDD), the Groundwater Research Center of Khon Kaen University and the PHC-Siam Franco-Thai cooperation program. We would also like to express our thanks to the research assistants of IRD for their valuable contribution to the field measurements (Nitjaporn Koonklang, Worraphan Chintachao and Weerawut Yotjamrut), and the staff of the Land Development Department laboratory. Finally, we were very grateful to Apichai Keansuwan and Vachira Jariyapaiboon, respectively, the owner and manager of the rubber tree plantation, for giving us the opportunity to perform this experiment in this field.

In memory of our colleague and friend Roland Poss.

Edited by: B. Kronvang

References

Ankeny, M. D., Ahmed, M., Kaspar, T. C., and Horton, R.: Simple field method for determining unsaturated hydraulic conductivity, Soil Sci. Soc. Am. J., 55, 467–470, 1991.

Anderson, J. L., and Bouma, J.: Relationships between hydraulic conductivity and morphometric data of an argillic horizon, Soil Sci. Soc. Am. Proc., 37, 413–421, 1997.

Angulo Jaramillo, R., Vandervaere, J.-P., Roulier, S., Thony, J.-L., Gaudet, J.-P., and Vauclin, M.: Field measurement of soil surface hydraulic properties by disc and ring infiltrometers: a review and recent developments, Soil Till. Res., 55, 1–29, 2000.

Antonino, A. C. D., Angulo-Jaramillo, R., Hammecker, C., Netto, A. M., Montenegro, S. M. L. G., Lira, C. A. B. O., and Cabral, J. J. S. P. A.: A simplified water transfer model of the reservoir-ebb tide system, including preferential flow, in the semi-arid region in Northeastern Brazil, J. Hydrol., 287, 147–160, 2004.

Anuraga, T., Ruiz, L., Kumar, M. M., Sekhar, M., and Leijnse, A.: Estimating groundwater recharge using land use and soil data: a case study in South India, Agr. Water Manage., 84, 65–76, 2006.

Arya, L. M. and Paris, J. F.: A physicoempirical model to predict the soil moisture characteristics from particle-size distribution and bulk density data, Soil Sci. Soc. Am. J., 45, 1023–1030, 1981.

Arya, L. M., Leij, F. J., Shouse, P. J., and van Genuchten, M. T.: Relationship between the hydraulic conductivity function and the particle-size distribution, Soil Sci. Soc. Am. J., 63, 1063–1070, 1999.

Bittelli, M. and Flury, M.: Errors in water retention curves determined with pressure plates, Soil Sci. Soc. Am. J., 73, 1453–1460, 2009.

Bouma, J.: Field measurement of soil hydraulic properties characterizing water movement through swelling clay soils, J. Hydrol., 4, 149–158, 1980.

Bouma, J.: Using soil survey data for quantitative land evaluation, Adv. Soil S., 9, 177–213, 1989.

Braud, I., De Condappa, D., Soria, J. M., Haverkamp, R., Angulo-Jaramillo, R., Galle, S., and Vauclin, M.: Use of scaled forms of the infiltration equation for the estimation of unsaturated soil hydraulic properties (the Beerkan method), Eur. J. Soil Sci., 56, 361–374, 2005.

Brooks, R. H. and Corey, C. T.: Hydraulic properties of porous media, Hydrol. Paper 3, Colorado State University, Fort Collins, 1964.

Bruckler, L., Bertuzzi, P., Angulo-Jaramillo, R., and Ruy, S.: Testing an infiltration method for estimating soil hydraulic properties in the laboratory, Soil Sci. Soc. Am. J., 66, 384–395, 2002.

Burdine, N. T.: Relative permeability calculation from pore size distribution data, Petr. Trans. Am Inst. Min. Metall. Eng., 198, 71–77, 1953.

Haverkamp, R., Arrue, J. L., Vandervaere, J.-P., Braud, I., Boulet, G., Laurent, J. P., Taha, A., Ross, P. J., and Angulo-Jaramillo, R.: Hydrological and thermal behaviour of the vadose zone in the area of Barrax and Tomelloso (Spain): experimental study, analysis and modeling Project UE no EV5C-CT 92 00 90, Laboratoire d'étude des Transferts en Hydrologie et Environnement, Grenoble, 1996.

Haverkamp, R., Bouraoui, C., Zammit, R., Angulo-Jaramillo, R., and Delleur, J. W.: Soil properties and moisture movement in the unsaturated zone, in: The Handbook of Groundwater Engineering, edited by: Delleur, J. W., CRC, Boca Raton, FL, 2931–2935, 1998.

Heddadj, H. and Gascuel-Odoux, C.: Topographic and seasonal variations of unsaturated hydraulic conductivity as measured by tension disc infiltrometers at the field scale, Eur. J. Soil Sci., 50, 275–283, 1999.

Jing, Y.-S., Zhang, B., Thimm, A., and Zepp, H.: Anisotropy of soil hydraulic properties along arable slopes, Pedosphere, 18, 353–362, 2008.

Kim, D. J., Angulo-Jaramillo, R., Vauclin, M., Feyen, J., and Choi, S. I.: Modeling of soil deformation and water flow in a swelling soil, Geoderma, 92, 217–238, 1999.

Klute, A. and Dirksen, C.: Hydraulic conductivity and diffusivity: laboratory methods, in: Methods of Soil Analysis, Part 1. Physical and Mineralogical Methods, edited by: Klute, A., 2nd Edn., ASA and SSSA, Madison, WI, 687–734, 1986.

Lassabatere, L., Angulo-Jaramillo, R., Soria Ugalde, J. M., Cuenca, R., Braud, I., and Haverkamp, R.: Beerkan, Estimation of soil transfer parameters through infiltration experiments – BEST, Soil Sci. Soc. Am. J., 70, 521–532, 2006.

Loague, K. M. and Green, R. E.: Statistical and graphical methods for solute transport models, J. Contam. Hydrol., 7, 51–73, 1991.

Mohammadi, M. H. and Vanclooster, M.: Predicting the soil moisture characteristic curve from particle size distribution with a simple conceptual model, Vadose Zone J., 10, 594–602, 2011.

Mualem, Y.: A new model for predicting the hydraulic conductivity of unsaturated porous media, Water Resour. Res., 12, 513–522, 1976.

Pachepsky, Y. A., Rawls, W., and Lin, H.: Hydropedology and pedotransfer functions, Geoderma, 131, 308–316, 2006.

Pachepsky, Y. A. and Rawls, W. J.: Soil structure and pedotransfer functions, Eur. J. Soil Sci., 54, 443–452, 2003.

Perroux, K. M. and White, I.: Design for disc permeameters and soil dispersion, Soil Sci. Soc. Am. J., 48, 50–55, 1988.

Price, K., Jackson, C. R., and Parker, A. J.: Variation of surficial soil hydraulic properties across land uses in the southern Blue Ridge Mountains, North Carolina, USA, J. Hydrol., 383, 256–268, 2010.

Rantala, L.: Rubber plantation performance in the Northeast and East of Thailand in relation to environmental conditions, Ms thesis, Dep. of Forest Ecology, University of Helsinky, Finland, 70 pp., 2006.

R Development Core Team: R: A Language and Environment for Statistical Computing, R Foundation for Statistical Computing, Vienna, Austria, available at: http://www.R-project.org (last access: 22 November 2013), 2008.

Richard, G., Sillon, J., and Marloie, O.: Comparison of inverse and direct evaporation methods for estimating soil hydraulic properties under different tillage practices, Soil Sci. Soc. Am. J., 65, 215–224, 2001.

Richards, L. A.: Capillary conduction of liquids through porous media, J. Appl. Phys., 1, 318–333, doi:10.1063/1.1745010, 1931.

Seltacho, S., Sriboonlue, V., Suwanang, N., Wiriyakitnateekul, W., and Hammecker, C.: Quantification and modeling of water flow in sandy soils in Northeast Thailand, in: Advances in Unsaturated Soils, edited by: Caicedo, B., Murillo, C., Colmenares, L. H. J. E., and Berdugo, I. R., CRC Press, London, 573–577, 2013.

Simunek, J., Wendroth, O., and van Genuchten, M. T.: Parameter estimation analysis of the evaporation method for determining soil hydraulic properties, Soil Sci. Soc. Am. J., 62, 894–905, 1998a.

Simunek, J., Wang, D., Shouse, P. J., and Van Genuchten, M. T.: Analysis of field tension disc infiltrometer data by parameter estimation, Int. Agrophys., 12, 167–180, 1998b.

Simunek, J., van Genuchten, M. T., and Sejna, M.: The HYDRUS-1D software package for simulating the movement of water, heat and multiple solutes in a variably saturated media, Version 3.0 HYDRUS, University of California Riverside, Riverside, California, USA, 2005.

Smettem, K. R. J. and Clothier, B. E.: Measuring unsaturated sorptivity and hydraulic conductivity using multiple disc permeameters, J. Soil Sci., 40, 563–568, 1989.

Soares, J. V. and Almeida, A. C.: Modeling the water balance and soil water fluxes in a fast growing Eucalyptus plantation in Brazil, J. Hydrol., 253, 130–147, 2001.

Stolte, J., Freijer, J. I., Bouten, W., Dirksen, C., Halbertsma, J. M., van Dam, J. C., van den Berg, J. A., Veerman, G. J., and Wösten, J. H. M.: Comparison of six methods to determine unsaturated soil hydraulic conductivity, Soil Sci. Soc. Am. J., 58, 1596–1603, 1994.

Tamari, S., Bruckler, L., Halbertsma, J., and Chadoeuf, J. A.: Simple method for determining soil hydraulic properties in the laboratory, Soil Sci. Soc. Am. J., 57, 642–651, 1993.

van Genuchten, M. T.: A closed form equation for predicting the hydraulic conductivity of unsaturated soils, Soil Sci. Soc. Am. J., 44, 892–898, 1980.

Wendroth, O., Ehlers, W., Hopmans, J. W., Kage, H., Halbertsma, J., and Wosten, J. H. M.: Reevaluation of the evaporation method for determining hydraulic functions of unsaturated soils, Soil Sci. Soc. Am. J., 57, 1436–1443, 1993.

Wind, G. P.: Capillary conductivity data estimated by a simple method, in: Water in the Unsaturated Zone, Vol. 1, edited by: Rijtema, P. E. and Wassink, H., Proc. Wageningen Symp., June 1966, Int. Assoc. Scientific Hydrol., Gentbrugge, Belgium, 181–191, 1968.

Wiriyakitnateekul, W. C., Hammecker, C., Anusontpornperm, S., and Boonrod, S.: Clay mineralogy of soils developed on sandstone along a toposequence in Northeast Thailand, XIV International Clay Conference, 14–20 June 2009, Castellaneta Marina, Italy, 520–520, 2009.

Wooding, R. A.: Steady infiltration from a shallow circular pond, Water Resour. Res., 4, 1259–1273, 1968.

Zimmermann, B., Elsenbeer, H., and De Moraes, J. M.: The influence of land-use changes on soil hydraulic properties: implications for runoff generation, Forest Ecol. Manage., 222, 29–38, 2006.

RESEARCH ARTICLE

SABRAO Journal
of Breeding and Genetics
47 (3) 278-290, 2015

GENETICS DIVERSITY BASED ON AGRICULTURAL TRAITS AND PHYTOCHEMICAL CONTENTS IN SPINY BITTER GOURD (*Momordica cochinchinensis* (Lour.) Spreng)

N. BOOTPROM[1], P. SONGSRI[1,*], B. SURIHARN[1], K. LOMTHAISONG[2] and K. LERTRAT[1]

[1]Plant Breeding Research Center for Sustainable Agriculture, Department of Plant Science and Agricultural Resources, Faculty of Agriculture, Khon Kaen University, Khon Kaen 40002, Thailand
[2]Department of Biochemistry, Faculty of Science, Khon Kaen University, Khon Kaen 40002, Thailand
*Corresponding author's email: patcharinso@kku.ac.th
Email addresses of co-authors: namaoy_bio@hotmail.com, bsuriharn@gmail.com, kholom@kku.ac.th, kamol9@gmail.com

SUMMARY

Spiny bitter gourd is a highly nutritious plant as its aril contains high contents of phytochemicals, especially - lycopene and beta carotene. The information on genetic variation in germplasm is important for development of new varieties. The objective of this study was to evaluate the genetic diversity of spiny bitter gourd based on agricultural traits and phytochemical contents. Twenty-six accessions of spiny bitter gourd collected from different parts of Thailand and Vietnam were evaluated in a randomized complete block design with 3 replications at the Fruit Orchard Research Farm, Department of Plant Science and Agricultural Resources, Faculty of Agriculture, Khon Kaen University, Thailand during July to October 2010. Genetic diversity of 26 accessions of spiny bitter gourd was identified based on horticultural traits (fruit fresh weight, aril weight, days to fruit maturity and number of seeds) and phytochemical contents (total carotenoids, lycopene, beta-carotene and lycopene per fruit). High variations were observed in these accessions for all agricultural traits and phytochemical contents. Cluster analysis showed that the 26 accessions of spiny bitter gourd could be grouped into 6 distinct clusters. The results are useful for germplasm conservation, utilization and management for breeding of spiny bitter gourd in the future.

Key words: Breeding, cluster analysis, gac fruit, germplasm, lycopene, beta carotene.

Key findings: Grouping of germplasm into different clusters using agricultural traits and level of phytochemical contents was a mean to identify genetic differences. This knowledge will enable useful information for germplasm conservation, utilization and management for spiny bitter gourd breeders.

Manuscript received: October 13, 2014; Decision on manuscript: February 18, 2015; Manuscript accepted: March 1, 2015.
© Society for the Advancement of Breeding Research in Asia and Oceania (SABRAO) 2015

Communicating Editor: Bertrand Collard

INTRODUCTION

Spiny bitter gourd (*Momordica cochinchinensis* (Lour.) Spreng) is an underutilized tropical vegetable crop in Asia. It's also called baby jackfruit, Gac fruit, sweet gourd, cochinchin gourd. The crop is known under different names in different countries such as Gac in Vietnam, Fak kao in Thailand, Bhat Kerala in India, Moc Niet Tu in China and Mak kao in Laos. It is a member of perennial dioecious cucurbit family (Sanwal *et al.,* 2011). Spiny bitter gourd has

long been used as a food and traditional medicine in East and Southeast Asia (Kubola and Siriamornpun, 2011). Placenta or aril (seed membrane) is an excellent source of bio-accessible carotenoids (lycopene and beta-carotene) (Vuong *et al.,* 2006; Burke *et al.,* 2005). These phytochemicals are beneficial to health as they can reduce the risk of several diseases such as prostate cancer, colon cancer, stomach cancer and cerebral thrombosis (Voung *et al.,* 2006; Ishida *et al.,* 2009). In addition, spiny bitter gourd oil has been readily accepted by women and children of Vietnam, and consumption of the oil can reduce lard intake (Vuong *et al.,* 2002; Vuong and King, 2003; Ishida *et al.,* 2004).

The potential uses of this underutilized crop are as raw material for natural colorant industry, food additive and functional food products because of its high carotenoid content in placenta or seed membrane. Breeding for high and stable carotenoid content and yield is important for industrial utilization of spiny bitter gourd, and the information on genetic diversity among germplasm is also important for effective breeding programs. Unfortunately, this useful information is not available in the literature. The objective of this study was to determine genetic diversity and genetic relatedness among 26 landraces of spiny bitter gourd accessions collected in Thailand and Vietnam using agricultural traits and phytochemical contents. The information is very useful for genetic improvement of this crop.

MATERIALS AND METHODS

Plant material

The 26 spiny bitter gourd accessions were evaluated in study. Twenty-five accessions were collected in Thailand and 1 accession was collected from Vietnam (Table 1).

Table 1. List of spiny bitter gourd accessions used in this study and sites of collection.

Accessions	Collection sites
KKU ac.09-002	Khon Kaen Province, Thailand
KKU ac.09-003	Khon Kaen Province, Thailand
KKU ac.09-004	Khon Kaen Province, Thailand
KKU ac.09-008	Chiang Mai Province, Thailand
KKU ac.09-010	Nakhon Pathom Province, Thailand
KKU ac.09-011	Nong Khai Province, Thailand
KKU ac.09-012	Kalasin Province, Thailand
KKU ac.09-013	Kalasin Province, Thailand
KKU ac.09-016	Khon Kaen Province, Thailand
KKU ac.09-018	Yasothon Province, Thailand
KKU ac.09-019	Hybrid#3
KKU ac.09-020	Hybrid#4
KKU ac.09-027	Kalasin Province, Thailand
KKU ac.09-030	Kalasin Province, Thailand
KKU ac.09-033	Kanchanaburi Province, Thailand
KKU ac.09-034	Chaiyaphum Province, Thailand
KKU ac.10-043	Hybrid#10
KKU ac.10-049	Khon Kaen Province, Thailand
KKU ac.10-077	Hybrid#40
KKU ac.10-080	Hybrid#43
KKU ac.10-086	Hybrid#48
KKU ac.10-087	Nakhon Pathom Province, Thailand
KKU ac.10-090	Samut Songkhram Province, Thailand
KKU ac.10-094	Vietnam
KKU ac.11-138	Ratchaburi Province, Thailand
Kaenpayorm1	Khon Kaen Province, Thailand

These accessions were grown in October 2010 at the Fruit Orchard Research Farm, Department of Plant Science and Agricultural Resources, Faculty of Agriculture, Khon Kaen University, Thailand. The accessions were arranged in a randomized complete block design with 3 replications. The spacing was 6 m between plants within row and 2 m between rows. N-P-K fertilizers formula 15–15–15 were applied at 15, 45 and 90 days after transplanting. Pests and diseases were controlled by weekly applications of insecticides and fungicides. Mini-sprinkler irrigation was available as necessary to avoid drought stress. Metal supports were also constructed for each plot.

The plants that produced male flowers were used as pollinators to pollinate all accessions in the experiment. The receptive flowers were artificially pollinated and the pollinated flowers were tagged and labeled.

Data collection

Data were recorded for fruit fresh weight, aril weight, days to fruit maturity, number of seeds, total carotenoids, lycopene, beta-carotene and lycopene per fruit. The fruits were harvested at ripening maturity which was determined by red skin of the fruits. Days to ripening was determined by numbers of days from artificial pollination to ripening maturity. Aril was separated from the fruits, put in sealable plastic bags and weight. Seed number per fruit was determined by counting filled seeds.

Sample preparation for phytochemical extraction

One fruit was randomly chosen from 3 ripening fruits for each of 3 sampling dates which were considered as 3 replications in unreplicated plot. The ripening fruits were determined by red fruits and red aril. The fruits were cleaned and separated into pulp, peeled seeds and aril. The aril samples were stored in a freezer (-20 ^{o}C) until further analysis.

Carotenoid extraction

Aril samples of 1 g each were oven-dried at 50 ^{o}C for 72 hours, and the dry samples were ground into powder using a mortar and a pestle. The powdered sample (0.1 g) was mixed with 50 ml of hexane : acetone : ethanol (2 : 1 : 1). Water of 5 ml was added into the mixed sample 2 times and the amount of water was 10 ml in total. The supernatant was placed in a round-bottomed flask and evaporated to dryness. The solid residue was re-dissolved in 8 ml of petroleum ether. The final solution of 2 ml was filtered through 0.45 μm membrane filter before injection of 20 μl into the high performance liquid chromatography (HPLC) aperture. Lycopene and beta-carotene were analyzed in triplicate using the HPLC by a method modified from Kubola and Siriamornpun (2011). Analysis was performed using Shimadzu LC-20AD pumps, a SPD-20M diode array detector, and inertsil ODS-3 C-18 column reverse phase (4.6 x 250 mm i.d., 5 μM). The mobile phase consisted of Acetonitrile methanol (solvent A)/ Dichloromethane (solvent B) and Methanol (solvent C) at a flow rate of 1 ml/min. The absorbance was read at 450 nm.

Statistical analysis

The data for the agronomic traits and phytochemical contents were analyzed statistically according to a randomized complete block design. Mean, minimum (min), maximum (max), standard error (SE), coefficient of variation (CV) and F-ratio were determined using Statistix-8 software. Least significant difference (LSD) at the 5% level was used to compare mean differences. The relationships among traits were calculated by the Pearson's correlation analysis using accession means (Ireland, 2010).

Cluster analysis

A data matrix of the 26 accessions was constructed using means for agricultural traits and phytochemical contents. Hierarchical agglomerative clustering was then performed for agricultural traits and phytochemical contents, using the Ward criterion. All calculations were performed using JMP Pro software (version 10.0, SAS institute Inc., Chicago, IL, USA).

RESULTS

Variations in spiny bitter gourd accessions

Variations in 26 accessions of spiny bitter gourd were evaluated for total carotenoids, lycopene, beta-carotene and lycopene per fruit, fruit fresh weight, aril weight, days to fruit maturity and number of seeds (Table 2). High variations were observed for all characters under investigation as indicated by high CV values (5 for days to maturity to 37 for lycopene per fruit) and high F-ratio (9.8 for total carotenoids to 152.7 for fruit fresh weight). The ranges of minimum and maximum values for these characters also indicated variations for these characters. Mean values for these characters are also provided for comparison with other investigations.

It is interesting to note here that some characters such as total carotenoids, lycopene content and lycopene yield per fruit had high CV values (22 - 37), but they had low F-ratios (9.8 - 20.4). In contrast to the above traits, fruit fresh weight, days to fruit maturity and number of seeds had low CV values (5 - 8), but they had high F-ratios (22.0 - 152.7).

Variation in fruit shape was also observed in these spiny bitter gourd accessions (Figure 1). There were 3 different fruit shapes including round (KKU ac. 09-008), elliptical with pointed end (KKU ac.09-002, KKU ac.09-016, KKU ac.09-010, KKU ac.09-003, KKU ac.10-049, Kaenpayorm1, KKU ac.09-018, KKU ac.09-027, KKU ac.09-030, KKU ac.10-090, KKU ac.09-019, KKU ac.10-077, KKU ac.09-004, KKU ac.09-034, KKU ac.09-012, KKU ac.09-033, KKU ac.10-087, KKU ac.10-080, KKU ac.09-011, KKU ac.09-013, KKU ac.09-020, KKU ac.10-043, KKU ac.10-086 and KKU ac.11-138) and flattened (oblate) (KKU ac. 10-094).

KKU ac. 10-094 had the highest fruit fresh weight (1787 g fruit^{-1}), aril weight (393 g fruit^{-1}) and days to fruit maturity (108 days after flowering), whereas KKU ac. 09-010 had the highest number of seeds (53 seed fruit^{-1}). Other accessions had smaller fruits and lower aril weight and matured earlier than KKU ac. 10-094 (Table 3). Also KKU ac. 10-094 had the highest total carotenoids (4041 µg g^{-1} dry weight), beta-carotene (1513 µg g^{-1} dry weight) and lycopene per fruit (52608 µg fruit^{-1}) and its lycopene content was also high although it was lower than 2487 µg g^{-1} dry weight of KKU ac. 09-008. Other interesting accessions included KKU ac. 09-002 because of high total carotenoids, KKU ac. 09-008 because of high total carotenoids and lycopene and KKU ac. 09-016 because of high total carotenoids (Table 4).

Correlations among quantitative characters

Positive and high correlation coefficients between total carotenoids with lycopene ($P \leq 0.01$, $r = 0.83$), beta-carotene ($P \leq 0.01$, $r = 0.74$) and lycopene per fruit ($P \leq 0.01$, $r = 0.73$) were observed. Total carotenoids also had positive correlations with days to fruit maturity ($P \leq 0.05$, $r = 0.46$), aril weight ($P \leq 0.05$, $r = 0.43$) and fruit fresh weight ($P \geq 0.05$, $r = 0.37$) although it was not significant, but it is not associated with number of seeds ($P \geq 0.05$, $r = 0.08$).

Lycopene was positively and significantly associated with beta-carotene ($P \leq 0.05$, $r = 0.48$) and lycopene per fruit ($P \leq 0.01$, $r = 0.62$), but it is not significantly associated with fruit fresh weight, aril weight, days to fruit maturity and number of seeds. Beta-carotene was associated with lycopene per fruit ($P \leq 0.01$, $r = 0.75$), fruit fresh weight ($P \leq 0.01$, $r = 0.59$), aril weight ($P \leq 0.01$, $r = 0.62$) and days to fruit maturity ($P \leq 0.01$, $r = 0.62$), but it is not associated with number of seeds. Similarly, lycopene per fruit was also associated with fruit fresh weight ($P \leq 0.01$, $r = 0.84$), aril weight ($P \leq 0.01$, $r = 0.90$) and days to fruit maturity ($P \leq 0.01$, $r = 0.86$), but it is not associated with number of seeds.

Fruit characters (fruit fresh weight and aril weight) and days to fruit maturity were inter-related with correlation coefficients ranging from $P \leq 0.01$, $r = 0.80$ to $P \leq 0.01$, $r = 0.94$, and fruit fresh weight was also associated with number of seeds ($P \leq 0.05$, $r = 0.44$). However, aril weight and days to fruit maturity were not associated with number of seeds ($P \geq 0.05$, $r = 0.27$) (Table 5).

Table 2. Means, standard errors (SE), minimum (min), maximum (max), coefficient of variation (CV) and F-ratio of quantitative characters of 26 accessions of spiny bitter gourd.

Characters	Mean ± SE	Min - Max	C.V. (%)	F-ratio
Total carotenoid (µg g^{-1} dry weight)	2013 ± 261	840-4041	23	9.8**
Lycopene (µg g^{-1} dry weight)	1051 ± 131	364-2487	22	16.0**
Beta-carotene (µg g^{-1} dry weight)	417 ± 51	100-1513	21	39.6**
Lycopene per fruit (µg $fruit^{-1}$)	9746 ± 2099	2500-52608	37	20.4**
Fruit fresh weight (g $fruit^{-1}$)	578 ± 23	280-1787	7	152.7**
Aril weight (g $fruit^{-1}$)	87 ± 11	48-393	21	36.0**
Days to fruit maturity (days)	60 ± 2	52-108	5	37.8**
Number of seed (seed $fruit^{-1}$)	36 ± 2	21-53	8	22.0**

** significant at $P < 0.01$

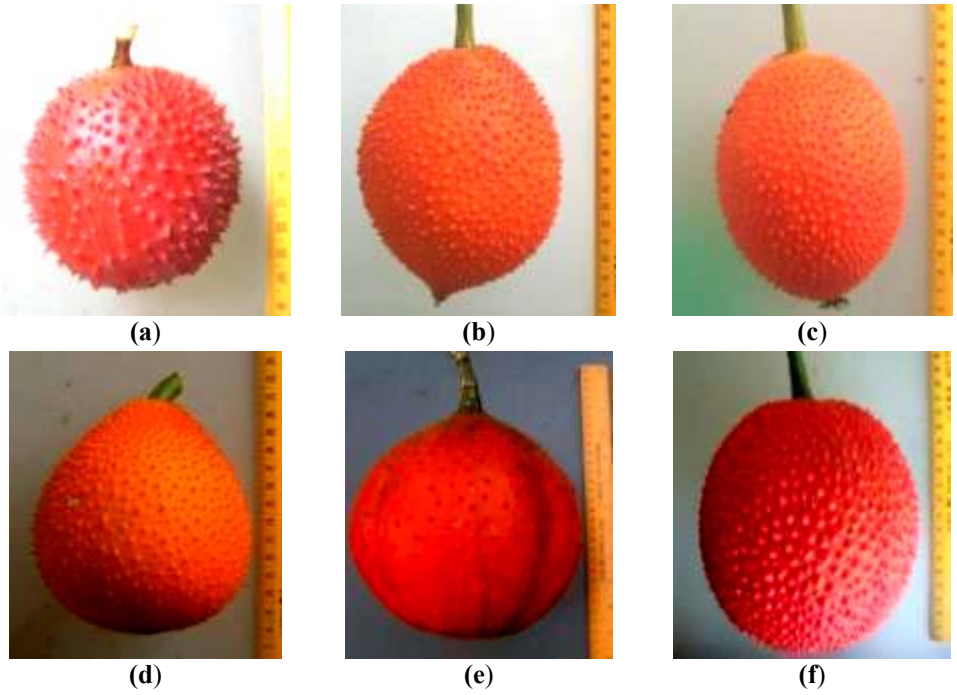


Figure 1. Genetic diversity of fruit types: (a) round; (b) elliptical with pointed end; (c) oval; (d) flattened bottom; (e) flattened (oblate); and (f) semi-cylindrical of *Momordica cochinchinensis* (Lour.) Spreng.

Table 3. Fruit fresh weight (g fruit^{-1}), aril weight (g fruit^{-1}), days to fruit maturity (days) and number of seeds (seeds fruit^{-1}) of 26 spiny bitter gourd accessions.

Accessions	Fruit fresh weight	Aril weight	Days to fruit maturity	Number of seeds
KKU ac.09-002	355 i	65 def	56 f-i	35 g-k
KKU ac.09-003	450 gh	65 def	63 c	23 n
KKU ac.09-004	725 c	110 bc	59 c-h	39 d-g
KKU ac.09-008	280 j	48 f	60 c-f	34 i-l
KKU ac.09-010	715 c	90 bcd	59 c-h	53 a
KKU ac.09-011	410 hi	60 def	58 d-h	34 h-l
KKU ac.09-012	460 gh	73 def	56 f-i	35 g-k
KKU ac.09-013	548 ef	80 cde	55 hi	30 lm
KKU ac.09-016	643 d	80 cde	55 ghi	42 def
KKU ac.09-018	455 gh	85 cde	58 d-h	36 g-k
KKU ac.10-019	478 g	85 cde	57 d-i	22 n
KKU ac.10-020	350 i	58 ef	52 i	21 n
KKU ac.09-027	495 fg	55 ef	59 c-h	28 m
KKU ac.09-030	553 ef	80 cde	58 d-h	37 f-j
KKU ac.09-033	715 c	82 cde	60 c-f	50 ab
KKU ac.09-034	673 cd	72 def	61 cde	33 j-m
KKU ac.10-043	568 e	67 def	60 c-g	44 cd
KKU ac.10-049	365 i	55 ef	62 cd	38 f-i
KKU ac.10-077	503 fg	65 def	55 ghi	37 f-j
KKU ac.10-080	555 ef	62 def	57 e-i	39 e-h
KKU ac.10-086	507 efg	85 cde	57 e-i	35 j-k
KKU ac.10-087	854 b	117 b	55 f-i	48 bc
KKU ac.10-090	645 d	88 bcd	54 hi	48 bc
KKU ac.10-094	1787 a	393 a	108 a	43 de
KKU ac.11-138	445 gh	63 def	59 c-h	31 klm
Kaenpayorm1	503 fg	83 cde	73 b	41 def
Mean	578	87	60	36

Mean in the same column followed with the same letter are not significant at $P < 0.05$ by LSD.

Table 4. Total carotenoids (μg g^{-1} dry weight), lycopene (μg g^{-1} dry weight), beta-carotene (μg g^{-1} dry weight), and lycopene per fruit (μg $fruit^{-1}$) of 26 spiny bitter gourd accessions.

Accessions	Total carotenoid	Lycopene	Beta-carotene	Lycopene per fruit
KKU ac.09-002	3551 a	1274 de	1159 b	13374 b-e
KKU ac.09-003	2599 b	1207 d-g	441 def	7169 f-j
KKU ac.09-004	1443 e-j	835 g-j	219 i-l	9764 c-g
KKU ac.09-008	3412 a	2487 a	141 kl	16024 b
KKU ac.09-010	2226 bcd	1513 cd	384 d-h	14545 bc
KKU ac.09-011	1934 b-g	827 hij	234 i-l	5033 g-j
KKU ac.09-012	1669 d-h	1294 de	358 d-i	9673 c-h
KKU ac.09-013	1550 d-j	555 i-m	242 h-l	4853 g-j
KKU ac.09-016	3447 a	1734 bc	763 c	14316 bcd
KKU ac.09-018	1830 c-h	789 h-k	248 g-k	7475 e-j
KKU ac.10-019	1910 b-g	808 hij	272 g-k	6864 f-j
KKU ac.10-020	925 ij	426 klm	100 l	2846 ij
KKU ac.09-027	2037 b-f	1272 def	715 b	7445 e-j
KKU ac.09-030	1572 d-j	805 hij	302 f-j	6776 f-j
KKU ac.09-033	1321 f-j	979 e-h	326 e-i	8560 c-i
KKU ac.09-034	2241 bcd	1515 cd	642 c	9474 d-h
KKU ac.10-043	1152 hij	364 m	235 i-l	2500 j
KKU ac.10-049	1572 d-j	946 e-h	484 d	6137 f-j
KKU ac.10-077	2150 b-e	900 f-i	382 d-h	6225 f-j
KKU ac.10-080	2465 bc	1791 bc	454 de	11449 b-f
KKU ac.10-086	840 j	400 lm	145 kl	3797 hij
KKU ac.10-087	1750 c-h	750 h-l	173 jkl	10246 b-g
KKU ac.10-090	1768 c-h	653 h-m	360 d-i	6158 f-j
KKU ac.10-094	4041 a	1893 b	1513 a	52608 a
KKU ac.11-138	1285 g-j	490 j-m	392 d-g	3269 ij
Kaenpayorm1	1654 d-i	826 hij	163 jkl	6823 f-j
Mean	2013	1051	417	9746

Means in the same column followed with the same letter are not significant at $p < 0.05$ by LSD.

Table 5. Correlation coefficients among quantitative characters of 26 accessions of spiny bitter gourd.

Characters	Total carotenoid	Lycopene	Beta-carotene	Lycopene per fruit	Fruit fresh weight	Aril weight	Days to fruit maturity
Lycopene	0.83**						
Beta-carotene	0.74**	0.48*					
Lycopene per fruit	0.73**	0.62**	0.75**				
Fruit fresh weight	0.37^{ns}	0.24^{ns}	0.59**	0.84**			
Aril weight	0.43*	0.24^{ns}	0.62**	0.90**	0.94**		
Days to fruit maturity	0.46*	0.34^{ns}	0.62**	0.86**	0.80**	0.89**	
Number of seeds	0.08^{ns}	0.13^{ns}	0.09^{ns}	0.27^{ns}	0.44*	0.27^{ns}	0.18^{ns}

$^{ns, *, **}$ non-significant and significant at 0.05 and 0.01 probability levels, respectively (n = 26)

Cluster analysis

A dendrogram constructed based on agronomic traits and phytochemical contents grouped 26 accessions of spiny bitter gourd into 6 distinct clusters (Figure 2), and the characters of each group were summarized in Table 6.

Cluster A consisted of KKU ac.09-002, KKU ac.09-010, KKU ac.09-016 and KKU ac.10-080. This cluster had total carotenoids between 2226 to 3551 µg g^{-1} dry weight, lycopene between 1274 to 1791 µg g^{-1} dry weight, beta-carotene between 384 to 1159 µg g^{-1} dry weight, lycopene per fruit between 11449 to 14545 µg $fruit^{-1}$, fruit fresh weight between 355 to 715 g $fruit^{-1}$, aril weight between 65 to 90 g $fruit^{-1}$, days to fruit maturity between 55 to 59 days after flowering, number of seeds between 35 to 53 seeds $fruit^{-1}$ and elliptical with pointed end fruit type.

Cluster B had 1 accession (KKU ac. 09-008). This accession had 3412 µg g^{-1} dry weight of total carotenoids, 2487 µg g^{-1} dry weight of lycopene, 141 µg g^{-1} dry weight of beta-carotene, 16024 µg $fruit^{-1}$ of lycopene per fruit, 280 g $fruit^{-1}$ of fresh fruit weight, 48 g $fruit^{-1}$ of aril weight, 60 days after flowering of fruit maturity, 34 seeds $fruit^{-1}$ and round fruit type.

Cluster C comprised KKU ac.09-003, KKU ac.09-019, KKU ac.09-027, KKU ac.09-034, KKU ac.09-011, KKU ac.09-018, KKU ac.09-030, KKU ac.10-077, KKU ac.09-012 and KKU ac.10-049. This cluster had total carotenoids between 1572 to 2599 µg g^{-1} dry weight, lycopene between 789 to 1515 µg g^{-1} dry weight, beta-carotene between 234 to 715 µg g^{-1} dry weight, lycopene per fruit between 5033 to 9673 µg $fruit^{-1}$, fruit fresh weight between 365 to 673 g $fruit^{-1}$, aril weight between 55 to 85 g $fruit^{-1}$, days to fruit maturity between 55 to 63 days after flowering, number of seeds between 22 to 38 seeds $fruit^{-1}$ and elliptical with pointed end fruit type.

Cluster D consisted of KKU ac.09-013, KKU ac.11-138, KKU ac.10-086 and KKU ac.10-020. This cluster had total carotenoids between 840 to 1550 µg g^{-1} dry weight, lycopene between 400 to 555 µg g^{-1} dry weight, beta-carotene between 100 to 392 µg g^{-1} dry weight, lycopene per fruit between 2846 to 4853 µg $fruit^{-1}$, fruit fresh weight between 350 to 555 g $fruit^{-1}$, aril weight between 58 to 80 g $fruit^{-1}$, days to fruit maturity between 52 to 59 days after flowering, number of seeds between 21 to 39 seeds $fruit^{-1}$ and elliptical with pointed end fruit type.

Cluster E consisted of KKU ac.09-004, KKU ac.09-033, KKU ac.10-090, KKU ac.10-087, KKU ac.10-043 and Kaenpayorm 1. This cluster had total carotenoids between 1552 to 1768 µg g^{-1} dry weight, lycopene between 364 to 979 µg g^{-1} dry weight, beta-carotene between 163 to 360 µg g^{-1} dry weight, lycopene per fruit between 2500 to 10246 µg $fruit^{-1}$, fruit fresh weight between 503 to 854 g $fruit^{-1}$, aril weight between 67 to 117 g $fruit^{-1}$, days to fruit maturity between 54 to 73 days after flowering, number of seeds between 39 to 50 seeds/fruit and elliptical with pointed end fruit type.

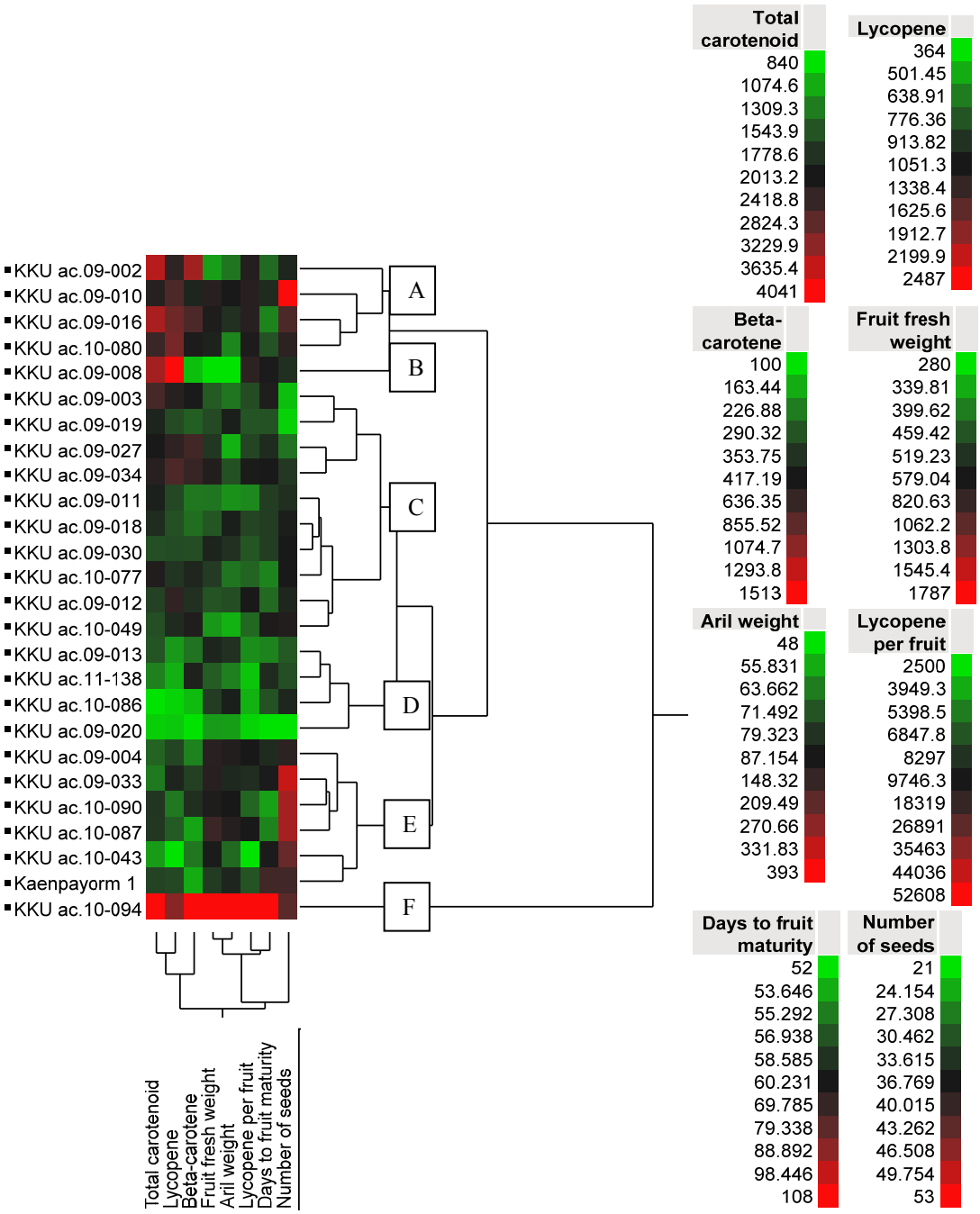


Figure 2. Dendrogram showing genetic relatedness of 26 spiny bitter gourd accessions collected in Thailand and Vietnam. Six main clusters (A to F) were formed. Two-way clustering method was Ward's cluster analysis based on agronomic traits and phytochemicals content (scale: Distance scale)[a].

[a] Cluster together columns as well as rows; the columns must be measured on the same scale.

Table 6. List of sites of collection, total carotenoids (µg g^{-1} dry weight), lycopene (µg g^{-1} dry weight), beta-carotene (µg g^{-1} dry weight), lycopene per fruit (µg $fruit^{-1}$), fruit fresh weight (g $fruit^{-1}$), aril weight (g $fruit^{-1}$), days to fruit maturity (days) and number of seeds (seeds $fruit^{-1}$) in 7 clusters grouped by cluster analysis of 26 spiny bitter gourd accessions.

Groups	Collection in site	Total carotenoids	Lycopene	Beta-carotene	Lycopene per fruit	Fruit fresh weight	Aril weight	Days to fruit maturity	Number of seeds per fruit
1	Khon Kaen (2), Nakhon Pathom (1), Hybrid (1)	2226-3551	1274-1791	384-1159	11449-14545	355-715	65-90	55-59	35-53
2	Chiang Mai (1)	3412	2487	141	16024	280	48	60	34
3	Khon Kaen (2), Yasothon (1), Kalasin (3), Nong Khai (1), Chaiyaphum (1), Hybrid (2)	1572-2599	789-1515	234-715	5033-9673	365-673	55-85	55-63	22-38
4	Kalasin (1), Ratchaburi (1), Hybird (2)	840-1550	400-555	100-392	2846-4853	350-555	55-80	52-59	21-39
5	Samut Songkhram (1), Hybrid (1), Khon Kaen (2), Nakhon Pathom (1), Kanchanaburi (1)	1152-1768	364-979	163-360	2500-10246	503-854	67-117	54-73	39-50
6	Vietnam (1)	4041	1893	1513	52608	1787	393	108	43

The number in parenthesis is the number of accessions.

Cluster F had 1 accession (KKU ac. 10-094) collected from Vietnam. This accession had 4041 µg/g dry weight of total carotenoid, 1893 µg g^{-1} dry weight of lycopene, 1513 µg g^{-1} dry weight of beta-carotene, 52608 µg $fruit^{-1}$ of lycopene per fruit, 1787 g $fruit^{-1}$ of fresh fruit weight, 393 g $fruit^{-1}$ of aril weight, 108 days after flowering to fruit maturity, 43 seeds $fruit^{-1}$ and flattened (oblate) fruit type.

DISCUSSION

Variations in spiny bitter gourd accessions

Spiny bitter gourd is an underutilized vegetable crop in Southeast Asia. People in this region use spiny bitter gourd as coloration in many food recipes such as sticky rice, several sweet recipes and soft drinks. As spiny bitter gourd has very high lycopene and beta-carotene, it has high potential for development as a functional food. This study used fruit characters (fruit fresh weight, aril weight, number of seeds and fruit maturity) and phytochemical characters (lycopene content, beta-carotene content and total carotenoids) to evaluate genetic variability in spiny bitter gourd. This information is limited because the crop is rather new for breeders and horticulturists. In Thailand, the fruit of spiny gourd is usually collected from fence climbers or from wild plants. It is found seasonally in local markets (June to November). Statistical data are lacking. There is very little information on genetic variations, and no cultivar selection has been reported. Germplasm collections are made by villagers with home gardens.

Based on CV values and F-ratios, high variations were observed in 26 accessions of spiny bitter gourd collected in Thailand and Vietnam for fruit fresh weight, aril weight, number of seeds, days to fruit maturity, lycopene content, beta-carotene content and total carotenoids. The results are convincing to use this germplasm collection for breeding purpose.

Scant information on variations in these characters is available in the literature. During literature review, we could not find report on variations in fruit characters and fruit maturity. However, total carotenoids concentration on average was 497 µg g^{-1} fresh material with lycopene dominating and exceeding beta-carotene concentrations by a factor of approximately 5 (408 µg g^{-1} versus 83 µg g^{-1}) (Vuong *et al.,* 2006). Lycopene was found to be predominantly present in the gac seed membrane at a concentration of up to 380 µg g^{-1} of seed membrane (Aoki *et al*., 2002). In another study, mean values obtained in aril tissues were 1342 µg trans, 204 µg cis, and 2227 µg total lycopene; 597 µg trans, 39 µg cis and 718 µg total beta-carotene (Ishida *et al.,* 2004). In comparison of 3 studies, carotenoid concentration, lycopene concentration and beta-carotene concentration in this study (2013 µg g^{-1} total carotenoids, 1051 µg g^{-1} lycopene and 417 µg g^{-1} total beta-carotene) were much higher than those reported by Vuong *et al.* (2006) and Aoki *et al.* (2002) because the results in this study were based on dry weight, but the results in this study seemed to be lower than those reported by Ishida *et al*. (2004). Carotenoid levels in spiny bitter gourd seem to vary widely.

High F-ratio indicated that genotype contributed to large portion of total variation for fruit fresh weight, beta-carotene, days to fruit maturity, aril weight, number of seeds, lycopene per fruit, lycopene and total carotenoid, and improvement of these traits will be easy. In this study, spiny bitter gourd accessions with good fruit characters and high phytochemical characters were identified, and these accessions will be further used in breeding programs.

Correlations among quantitative characters

Correlations among characters are important when breeding for multiple characters is carried out, and selection for one trait may affect other traits. In this study, total carotenoids, lycopene, beta-carotene and lycopene per fruit were inter-related with correlation coefficients ranging from 0.48 between lycopene and beta-carotene to 0.83 between total carotenoids and lycopene. The results also indicated that fruit characters were also interrelated with correlation coefficients ranging from 0.80 between fruit fresh weight and days to maturity and 0.94 between aril weight and fruit fresh weight. It is also interesting to note here that all phytochemicals were also associated with fruit characters as beta-carotene and lycopene per

fruit had strong associations with fruit fresh weight, aril weight and days to fruit maturity, whereas the relationships between total carotenoids and lycopene with fruit fresh weight, aril weight and days to fruit maturity were rather weak. Most characters under investigation were not associated with number of seeds except for fruit fresh weight.

In previous study, inverse correlation between beta-carotene and lycopene concentrations was observed in spiny bitter gourd due to the ripening stage, since lycopene appears earlier than beta-carotene in the carotenogenesis pathway, and less mature fruits contain higher lycopene and lower beta-carotene concentrations than more mature fruits (Vuong *et al.,* 2006).

The results indicated that improvement of fruit characters and phytochemicals at the same time would be possible especially for beta carotene and lycopene per fruit, but it might be difficult to improve total carotenoids and lycopene at the same time with improvement of fruit fresh weight, aril weight and days to fruit maturity because of weak correlations. Improvement of fruit fresh weight would result in increase in seed number. However, high seed number is not necessary for this crop because the crop can be propagated vegetatively, but seeds are still important for breeding purpose.

Cluster analysis

A dendrogram from cluster analysis based on fruit characters and phytochemical characters divided 26 spiny bitter gourd accessions into 6 distinct clusters. The accession from Vietnam (KKU ac. 10-094) formed cluster F which was isolated from other 5 clusters which were the accessions collected in Thailand. KKU ac. 10-094 also had flattened (oblate) fruit shape, whereas other accessions in Thailand had round fruits (cluster B) (KKU ac. 09-008) and elliptical with pointed end fruits (clusters A, C, D and E). Actually, 6 fruit shapes were found in our germplasm collections including round, flattened, elliptical with pointed end, oval, flattened bottom and semi-cylindrical (Figure 1).

It is very interesting to note here that an accession from Vietnam was the out-group of these accessions and it also had many good characters. As spiny bitter gourd is grown and utilized mostly in Vietnam, germplasm in Vietnam is valuable for immediate use and further development. A germplasm collection mission was first carried out in central Vietnam during March 2012, and many accessions were collected for further evaluation and utilization. The results in this study revealed genetic difference of the spiny bitter gourd germplasm in these countries.

In our previous findings in 25 accessions of spiny bitter gourd common to this study, 11 RAPD primers could divide these accessions into 8 clusters (Bootprom *et al.,* 2012). In comparison of the 2 studies, both dendrograms separated the accession KKU ac. 10-094 from Vietnam from other accessions. The clustering pattern based on RAPD markers was not in accordance with the grouping based on fruit and phytochemical characters. The lack of relationships between molecular study and conventional study for grouping of germplasm has also been reported in bitter gourd (*Momordica charantia*) (Paul and Raychaudhuri, 2010). Similarly, in *Cuminum cyminum*, a valuable medicinal plant belonging to family Apiaceae, grouping based on molecular markers and morpho-agronomic traits are different so these 2 systems could not discriminate accessions as in the same way (Rostami-Ahmadvandi *et al.,* 2013).

The results also indicated that agronomic traits and phytochemical contents are useful parameters for evaluation of genetic diversity in spiny bitter gourd. Although newer methods of genetic diversity evaluation in crop plants have been invented and used widely, the conventional methods are still useful and more cost effective.

For development of spiny bitter gourd as functional food and natural food colorant in food industry, more breeding attempts are still required. The breeding activities include germplasm collection, preliminary evaluation of new germplasm and dialell analysis of crosses among accessions for agricultural traits and phytochemical contents to understand heterotic patterns of spiny bitter gourd germplasm and to find appropriate ways for germplasm utilization. The results will enable breeders to make informed decisions about possible heterotic

groups for their breeding programs and germplasm conservation.

CONCLUSION

In this study, grouping of germplasm into different clusters using agricultural traits and level of phytochemical contents was a means to identify genetic differences of 26 spiny bitter gourd accessions. This knowledge will enable useful information for germplasm conservation, utilization and management for the development of spiny bitter gourd in breeding programs.

ACKNOWLEDGEMENTS

The authors acknowledge financial support from the Higher Education Research Promotion and National Research University Project of Thailand, Office of the Higher Education Commission, through the Food and Functional Food Research Cluster of Khon Kaen University and support in part by the Plant Breeding Research Center for Sustainable Agriculture, Faculty of Agriculture, Khon Kaen University and the Thailand Research Fund (TRF), the Commission for Higher Education (CHE) and Khon Kaen University (KKU) supported this work by providing financial supports through the Distinguished Research Professor Grant of Professor Dr. Aran Patanothai. An acknowledgement is extended to Khon Kaen University and the faculty of Agriculture for providing financial support for manuscript preparation activities. We also thank Miss Hannah Wright for assistance with editing our draft paper.

REFERENCES

Aoki H, Kieu NT, Kuze N, Tomisaka K, Van Chuyen N (2002). Carotenoid pigments in gac fruit (*Momordica cochinchinensis* Spreng). *Biosci. Biotechnol. Biochem.* 66: 2479–2482.

Bootprom N, Songsri P, Suriharn B, Chareonsap P, Sanitchon J, Lertrat K (2012). Molecular diversity among selected *Momordica cochinchinensis* (Lour.) Spreng accessions using RAPD markers. *SABRAO J. Breed. Genet.* 44: 406–417.

Burke DS, Smidt CR, Vuong LT (2005). *Momordica cochinchinensis*, *Rosa Roxburghii*, wolfberry, and sea buckthorn-Highly nutritional fruit supported by tradition and science. *Curr. Top Nutraceut. R.* 3: 259–266.

Ireland CR (2010). Experimental statistics for agriculture and horticulture. CABI, UK.

Ishida BK, Turner C, Chapman MH, McKeon TA (2004). Fatty acid and carotenoid composition of gac (*Momordica cochinchinensis* Spreng) fruit. *J. Agric. Food Chem*. 52: 274–279.

Ishida BK, Chapman MH (2009). Carotenoid Extraction from plants using a novel, environmentally friendly solvent. *J. Agric. Food Chem.* 57: 1051–1059.

Kubola J, Siriamornpun S (2011). Phytochemicals and antioxidant activity of different fruit fractions (peel, pulp, aril and seed) of Thai gac (*Momordica cochinchinensis* Spreng). *Food Chem*. 127: 1138–1145.

Paul A, Raychaudhuri SS (2010). Medicinal uses and molecular identification of two *Momordica charantia* varieties – a review. *eJBio*. 6: 43–51.

Rostami-Ahmadvandi H, Cheghamirza K, Kahrizi D, Bahraminejad S (2013). Comparison of morpho-agronomic traits versus RAPD and ISSR markers in order to evaluate genetic diversity among *Cuminum cyminum* L. accessions. *AJCS*. 7: 361–367.

Sanwal SK, Kozak S, Kumar M, Singh B, Deka BC (2011). Yield improvement through female homosexual hybrids and sex genetics of sweet gourd (*Momordica cochinchinensis* Spreng). *Acta Physiol. Plant*. 33: 1991–1996.

Vuong LT, Dueker SR, Murphy SP (2002). Plasma β-carotene and retinol concentrations of children increase after a 30-d supplementation with the fruit *Momordica cochinchinensis* (gac). *Am. J. Clin. Nutr.* 75: 872–879.

Vuong TL, King JC (2003). A method of preserving and testing the acceptability of gac fruit oil, a good source of β-carotene and essential fatty acids. *Food Nutr. Bull.* 24: 224–230.

Vuong LT, Franke AA, Custer LJ, Murphy SP (2006). *Momordica cochinchinensis* Spreng. (gac) fruit carotenoids reevaluated. *J. Food Comp. Anal.* 19: 664–668.

RESEARCH ARTICLE

SABRAO Journal
of Breeding and Genetics
47 (4) 493-501, 2015

GENOTYPIC DIVERSITY OF TRAITS RELATED TO NITROGEN FIXATION IN VALENCIA PEANUT GERMPLASM

S. MAHAKOSEE[1], S. JOGLOY[1,2*], N. VORASOOT[1], B. SURIHARN[1], N. PUPPALA[3] and A. PATANOTHAI[1]

[1]Department of Plant Science and Agricultural Resources, Faculty of Agriculture, Khon Kaen University, Khon Kaen 40002, Thailand
[2]Peanut and Jerusalem Artichoke Improvement for Functional Food Research Group, Khon Kaen University, Muang, Khon Kaen, Thailand
[3]Agricultural Science Center at Clovis, New Mexico State University, Clovis, New Mexico 88101, USA

[*]Corresponding author's email: sjogloy@gmail.com
Co-authors' email addresses: nvorasoot1@gmail.com, bsuriharn@gmail.com, npuppala@ad.nmsu.edu, aran@kku.ac.th

SUMMARY

Peanut can fix atmospheric nitrogen by symbiotic relationship with cowpea-type of rhizobium. Traits related to nitrogen fixation may be useful as select criteria for high nitrogen fixation. Thus the objective of this study was to evaluate 130 accessions of Valencia peanut for traits related to nitrogen fixation including nodule dry weight, biomass and harvest index. The new germplasm of 125 Valencia peanut accessions from New Mexico State University and International Crops Research Institute for Semi-Arid-Tropics (ICRISAT) and the 4 varieties commercially available peanut of Thailand consisting of 3 Valencia peanuts, 1 Spanish and 1 Virginia were planted in randomize complete block design (RCBD) with 4 replications during February to June 2012 and 2013. Nodule dry weight ranged from 0.16 to 0.56 g plant^{-1} with mean of 0.31 g plant^{-1}, and biomass productions ranged from 58.38 to 97.45 g plant^{-1} with mean value of 74.56 g plant^{-1}. Pod yields showed a wide range from 15.00 to 35.84 g plant^{-1} with mean value of 24.39 g plant^{-1}, whereas harvest index values ranged from 0.23 to 0.45 with mean value of 0.33. Base on traits related to nitrogen fixation (nodule dry weight, biomass and harvest index), peanut accessions were separated into 4 groups.

Key words: Nodule dry weight, groundnut (*Arachis hypogaea* L.), biomass production

Key findings: Diversity of nitrogen fixation in Valencia peanut germplasm.

Manuscript received: November 8, 2014; Decision on manuscript: April 12, 2015; Manuscript accepted: May 18, 2015.
© Society for the Advancement of Breeding Research in Asia and Oceania (SABRAO) 2015

Communicating Editor: Bertrand Collard

INTRODUCTION

Seventy eight percent of the total nitrogen pool is available as nitrogen gas in the atmosphere. However, gaseous nitrogen is not directly useful to plants and plants require sufficient mineral nitrogen for growth and development. Gaseous nitrogen can be transformed into mineral nitrogen by lighting, nitrogen fixation by free living organisms, industrial fertilizer production and many systems of symbiotic association between nitrogen fixing organisms and many plant species especially leguminous species such as beans, soybean and peanut (Giller, 2001).

Peanut (*Arachis hypogaea* L.) is traditionally grown under rainfed conditions with erratic rainfall and low soil fertility that affect to growth and peanut yield. Peanut can fix nitrogen of about 80 - 150 kg N ha^{-1} (Giller *et al.*, 1987; Toomsan, 1990). Nitrogen from peanut residues can be beneficial to subsequent crops in a cropping system (McDonagh *et al.*, 1993, 1995; Toomsan *et al*., 1995). Association of rhizobium and root nodules of peanut can fix atmospheric nitrogen into nitrogen compounds that are available for peanut. However, the efficiency of nitrogen fixation in peanut depends on peanut varieties, rhizobium strains and the interaction between peanut variety and rhizobium strain (McDonagh *et al*., 1993).

Measurement of fixed nitrogen is a direct means for determining nitrogen fixing ability and accomplished only in a laboratory where complicated equipment is installed. Several traits have been identified and used as selection criteria and surrogate traits for high nitrogen fixation such as nodule dry weight, biomass production, leaf color score and nitrogenase activity. Strong and positive correlations were found between nitrogen fixation, total nitrogen and total dry matter (Pimratch *et al*., 2004).

The new peanut germplasm of Valencia type from New Mexico State University and the International Crops Research Institute for the Semi-Arid-Tropics (ICRISAT) have not been evaluated for their nodulation efficiency and nitrogen fixation. Valencia peanut type (sub species *fastigiata*) has erect canopy with sequential branching pattern. Leaves of Valencia peanut are pale green and the leaves are larger than those of Virginia type. Valencia peanut has variations in pod size, seeds per pod and seed testa color. Valencia peanut type are early maturing, sweet taste and generally with 3 or 4 kernels per pod (Purseglove, 1977). Thus the objective of this study was to evaluate 130 accessions of Valencia peanut for traits related to nitrogen fixation including nodule dry weight, biomass and harvest index. The characterization of new germplasm sources for economically important traits is very important for breeding and effective utilization of the germplasm.

MATERIALS AND METHODS

Crop management and experimental design

The experiment was conducted at the Field Crop Research Station of Khon Kaen University, Khon Kaen, Thailand (lat 16º, 28' N, long 102º 48' E, 200 m above mean sea level). One hundred and thirty peanut accessions consisting of 125 accessions of Valencia peanut from New Mexico State University and the International Crops Research Institute for the Semi-Arid-Tropics (ICRISAT), 3 peanut varieties (KS1, KS2 and KK4), one Spanish peanut type (KKU40) and one Virginia peanut type (KKU 60) commercially available in Thailand were used in this study (Table 1). The experiment was laid out in a randomized complete block design with 4 replications during February to June 2012 and 2013. Plot size was 2 x 5 m^2 and the spacing was 50 cm between rows and 20 cm between plants within rows.

Seeds were treated with captan (3a,4,7,7a-tetrahydro-2-[(trichloromethyl) thio]-1H-isoindole-1,3 (2H)-dione) at the rate of 5 g kg^{-1} seeds before planting to control fungal diseases. Seeds were planted 3-4 seed $hill^{-1}$ and pre-emergence weeds were controlled by alachlor (2-cholro-2',6'-diethyl-*N*-(methoxymethyl) acetanilide 48%, w/v, emulsifiable concentrate) at the rate of 3 L ha^{-1} at planting after application of water. *Bradyrhizobium* inoculation (mixture of strains THA 201 and THA 205; Department of Agriculture, Ministry of Agriculture and Cooperatives, Bangkok, Thailand) was accomplished by applying a water-diluted commercial peat-based inoculum of *Bradyrhizobium* on the rows of peanut at 2 day after planting. At 10-15 DAP, peanut seedlings were thinned to obtain 2 plants per hill and weeds were controlled by hand weeding. Chemical fertilizer N:P_2O_5:K_2O was applied the rate of 0, 56.25, 37.5 kg ha^{-1}, respectively. Gypsum ($CaSO_4$) at the rate of 312 kg ha^{-1} was applied at 40-45 DAP after weeding control. Carbofuran (2,3-dihydro-2,2-dimethylbenzo-furan-7-ylmethylcarbamate 3% granular) was used at pod setting stage to protect the crop from the subterranean ants (*Dorylus orientalis*).

Table 1. Valencia peanut accessions and seed source.

Entry No.	Accession	Source	Entry No.	Accession	Source	Entry No.	Accession	Source
1	PI468225	New Mexico	45	PI493325	New Mexico	89	Valencia - C	New Mexico
2	PI475913	New Mexico	46	PI493339	New Mexico	90	M C Ran	New Mexico
3	PI475921	New Mexico	47	PI493340	New Mexico	91	ICG 115	India
4	PI475925	New Mexico	48	PI493344	New Mexico	92	ICG 297	Mauritius
5	PI476074	New Mexico	49	PI493360	New Mexico	93	ICG 332	Brazil
6	PI476078	New Mexico	50	PI493373	New Mexico	94	ICG 397	USA
7	PI476079	New Mexico	51	PI493382	New Mexico	95	ICG 1142	Benin
8	PI476089	New Mexico	52	PI493405	New Mexico	96	ICG 1274	Indonesia
9	PI493381	New Mexico	53	PI493415	New Mexico	97	ICG 1399	Malawi
10	PI493521	New Mexico	54	PI493442	New Mexico	98	ICG 2738	India
11	PI493536	New Mexico	55	PI493446	New Mexico	99	ICG 3673	Korea
12	PI493562	New Mexico	56	PI493451	New Mexico	100	ICG 3681	USA
13	PI497447	New Mexico	57	PI493458	New Mexico	101	ICG 4670	Sudan
14	PI497459	New Mexico	58	PI493461	New Mexico	102	ICG 5221	Argentina
15	PI501293	New Mexico	59	PI493470	New Mexico	103	ICG 5475	Kenya
16	PI501985	New Mexico	60	PI493484	New Mexico	104	ICG 5609	Sri Lanka
17	PI536300	New Mexico	61	PI493501	New Mexico	105	ICG 6022	Sudan
18	PI536307	New Mexico	62	PI493523	New Mexico	106	ICG 6201	Cuba
19	PI599612	New Mexico	63	PI493565	New Mexico	107	ICG 6646	Unknown
20	PI602494	New Mexico	64	PI493566	New Mexico	108	ICG 6888	Brazil
21	PI259580	New Mexico	65	PI493584	New Mexico	109	ICG 7181	India
22	PI259601	New Mexico	66	PI493612	New Mexico	110	ICG 8106	Peru
23	PI306361	New Mexico	67	PI493624	New Mexico	111	ICG 8517	Bolivia
24	PI314980	New Mexico	68	PI493629	New Mexico	112	ICG 9315	USA
25	PI315612	New Mexico	69	PI493630	New Mexico	113	ICG 10092	Zimbabwe
26	PI338337	New Mexico	70	PI493660	New Mexico	114	ICG 10474	Cuba
27	PI365564	New Mexico	71	PI493666	New Mexico	115	ICG 10554	Argentina
28	PI390432	New Mexico	72	PI493688	New Mexico	116	ICG 10566	Congo
29	PI406718	New Mexico	73	PI493810	New Mexico	117	ICG 10890	Peru
30	PI407451	New Mexico	74	PI493816	New Mexico	118	ICG 111444	Argentina
31	PI429427	New Mexico	75	PI493865	New Mexico	119	ICG 13856	Uganda
32	PI429430	New Mexico	76	PI494019	New Mexico	120	ICG 13858	Uganda
33	PI493507	New Mexico	77	PI497642	New Mexico	121	ICG 14106	Zaire
34	PI493514	New Mexico	78	DC 2120 (S3873)	New Mexico	122	ICG 14127	Zaire
35	PI493518	New Mexico	79	DC 2440 (S3897)	New Mexico	123	ICG 14710	Cameroon
36	PI502023	New Mexico	80	S-3653	New Mexico	124	ICG 15042	Unknown
37	PI508278	New Mexico	81	S-3881	New Mexico	125	ICG 15309	Brazil
38	PI536121	New Mexico	82	New BG	New Mexico	126	KS 1	Thailand
39	Grif13802	New Mexico	83	23322	New Mexico	127	KS 2	Thailand
40	PI501269	New Mexico	84	S-3840	New Mexico	128	KK4	Thailand
41	PI576604	New Mexico	85	Kremena	New Mexico	129	KKU 60	Thailand
42	Breeding line	New Mexico	86	NM 052565	New Mexico	130	KKU 40	Thailand
43	PI409037	New Mexico	87	Rossita	New Mexico			
44	PI468208	New Mexico	88	Valencia - A	New Mexico			

Pests and diseases were controlled twice a month by applying carbosulfan [2-3-dihydro-2,2-dimethylbenzofuran-7-yl (dibutylaminothio) methylcar-bamate 20% w/v, water soluble concentrate] at the rate of 2.5 L ha^{-1}, methomyl [*S*-methyl-*N*-((methylcarbamoyl)oxy) thioaceti-midate 40% soluble powder] at the rate of 1.0 kg/ha and carboxin [5,6-dihydro-2-methyl-1,4-oxathine-3-carboxanilide 75% wettable powder] at the rate of 1.68 kg ha^{-1}. Sprinkler irrigation system was installed to supply water to the peanut plants from planting to harvest.

Data collection

Soil and weather parameters

Weather data were obtained from nearby meteorological station, Khon Kaen University, Khon Kaen, Thailand for both years.

The soil samples at the depth 0-30 cm were analyzed to determine the physical and chemical properties (Table 2).

Traits measurement

At the final harvest, 5 plants in each plot were randomly selected. Nodules were removed from the roots and oven dried at 80 ºC for 48 h or until the weight was constant and dry weight was measured. Shoot fresh weight was determined in the field. The shoot sample of 1 kg fresh weight was oven-dried at 80 ºC for 48 h or until the weight was constant and dry weight was measured. The pods form harvest area (4.8 m^2) in each plot were removed from the plants and air-dried to obtain approximately 8% moisture content, and pod dry weight was determined. Biomass production was calculated based on shoot dry weight and pods dry weight (without roots). Harvest index was computed as the ratio of total pod weight to total biomass at the final harvest.

Statistical analysis and cluster analyses

Analysis of variance was performed for all characters in each year, error variances were tested for homogeneity, and the data of 2 years with variance homogeneity were combined. The analyses of variance were done using MSTAT-C package (Bricker, 1989).

A data matrix of the 130 accessions was constructed using means of nodule dry weight, biomass and HI. The cluster analysis based on Ward's method and Squared Euclidian distance was performed and the dendrogram was constructed. All calculations were performed in SAS 6.12 (SAS, 2001).

RESULTS

Meteorological conditions and soil properties

Weather conditions

The experiment was conducted under field conditions for 2 years in dry seasons 2012 and 2013. The average air temperatures were 22.4 to 34.7 ºC in 2012 and 23.5 to 35.5 ºC in 2013 (Figure 1). There was rainfall in both years (Figure 1a, 1b). Rainfall in the dry season 2012 was higher than in 2013 especially during late growing season (75-105 DAP). Patterns of weather conditions were similar for 2 years.

Soil properties

The soil is Yasothorn series with sand soil texture in both years, and % sand, % silt and % clay in 2012 and 2013 were 90.23, 7.79 and 1.96, and 92.58, 6.00 and 1.42, respectively (Table 2). pH values were 6.39 in 2012 and 6.63 in 2013, and electrical conductivity (EC) value was 0.04 dS m^1 in both years. Cation exchange capacity (CEC) values were 3.43 c mol/kg in 2012 and 1.88 c mol kg^{-1} in 2013. Organic matter values and total nitrogen values were low in both years, showing nitrogen deficiency in the soil. Available P and exchangeable K were also deficient in both years, whereas exchangeable Ca values were rather high in both years (409 mg kg^{-1} in 2012 and 391 mg kg^{-1} in 2013), indicating that calcium was sufficient.

Table 2. Chemical and physical properties of the soil in the experimental fields of Khon Kaen University at the depth 0-30 cm in 2 years.

Soil properties	pH (1:1 H_20)	EC (1:5 H20) (dS/m)	CEC (c mol/kg)	OM (%)	Total N (%)	Available P (mg/kg)	Exchangeable		Particle size, mum (USDA system)			Soil texture
							K (mg/kg)	Ca (mg/kg)	Sand: 2.0-0.05 (%)	Silt: 0.05-0.002 (%)	Clay: <0.002 (%)	
2012	6.39	0.04	3.43	0.51	0.02	30.8	39.9	409	90.23	7.79	1.96	Sand
2013	6.63	0.04	1.88	0.49	0.01	35.6	42.5	391	92.58	6.00	1.42	Sand

EC = Electrical conductivity, CEC= Cation exchange capacity and OM = Organic matter

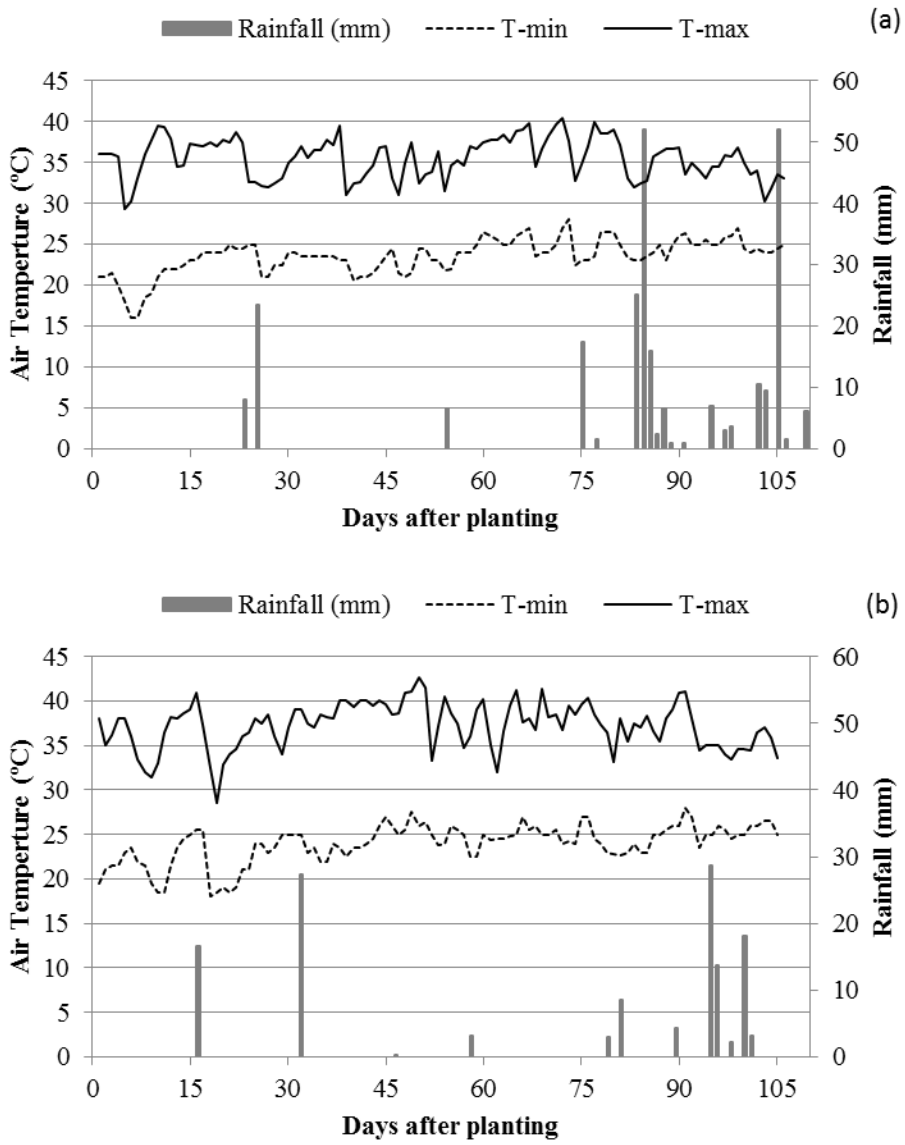


Figure 1 Maximum air temperatures (T-max), minimum air temperatures (T-min) (^{O}C), rainfall (mm), during the crop growth period of Valencia Peanut in the dry season 2012 (a) and 2013 (b)

Nodule dry weight (NDW), pod yield, biomass and harvest index

Years were significantly different for pod yield ($P \leq 0.01$) and nodule dry weight ($P \leq 0.05$), but they were not statistically different for biomass and harvest index (Table 3). Significant differences ($P \leq 0.01$) among peanut genotypes were observed for nodule dry weight, pod yield, biomass and harvest index. However, genotype × year interactions were also significant ($P \leq 0.01$) for all characters and also contributed to lower portions than did genotype.

Peanut genotypes were also different for nodule dry weights, ranging from 0.16 to 0.56 g plant^{-1} with mean of 0.31 g plant^{-1} and biomass production ranging from 58.38 to 97.45 g plant^{-1} with mean value of 74.56 g plant^{-1} (Table 4). Peanut genotypes had a rather wide range for pod yield from 15.00 to 35.84 g plant^{-1} with mean value of 24.39 g plant^{-1}, whereas they had rather narrow range for harvest index from 0.23 to 0.45 with mean value of 0.33.

Table 3. Mean squares for nodule dry weight, biomass, pod yield and harvest index (HI) of 130 peanut accession across 2 years.

Source	DF	Nodule dry weight	Biomass	Pod yield	HI
Years	1	0.72*	20585.7^{ns}	3784.8**	0.014^{ns}
Reps. Within Years	6	0.08	4046.7	59.2	0.060
Accessions	129	0.03**	391.2**	91.2**	0.011**
Accessions x Years	129	0.02**	320**	57.2**	0.005**
Pool error	774	0.01	164.3	9.8	0.003
CV (%)		30.8	17.18	12.76	15.47

^{ns}, *, ** = non-significant and significant at $P \leq 0.05$ and $P \leq 0.01$ probability levels, respectively.

Table 4. Mean, minimum (min), maximum (max) of nodule dry weight (NDW; g plant^{-1}), biomass (g plant^{-1}), pod yield (g plant^{-1}) and harvest index (HI) of 130 peanut accession across 2 years were grouped into 4 clusters.

Cluster	No. accession		NDW	Biomass	PY	HI
1	63	Min	0.19	71.62	17.82	0.24
		Max	0.43	79.77	32.44	0.42
		Average	0.31	75.66	24.79	0.33
2	25	Min	0.22	80.69	20.48	0.23
		Max	0.56	97.45	35.84	0.43
		Average	0.32	84.64	25.46	0.31
3	33	Min	0.18	64.06	19.05	0.27
		Max	0.40	71.21	33.68	0.45
		Average	0.30	68.46	23.68	0.35
4	9	Min	0.16	58.38	15.00	0.26
		Max	0.38	62.83	24.86	0.40
		Average	0.30	61.19	21.20	0.35
Total	130	Min	0.16	58.38	15.00	0.23
		Max	0.56	97.45	35.84	0.45
		Average	0.31	74.56	24.39	0.33
		S.E	0.005	0.30	23.56	0.001

Cluster analysis

Base on traits related to nitrogen fixation including nodule dry weight, biomass and HI, Valencia peanut accessions could be classified into 4 groups ($R^2 = 0.85$) (Figure 2). Sixty three peanut accessions (PI468225, PI476078, PI476079, PI493381, PI493521, PI493536, PI497447, PI501985, PI536300, PI536307, PI599612, PI602494, PI315612, PI406718, PI429427, PI429430, PI493507, PI493514, PI493518, PI502023, PI508278, Grif13802, PI501269, PI576604, Breeding-line, PI409037, PI493339, PI493340, PI493344, PI493405, PI493442, PI493446, PI493484, PI493523, PI493612, PI493624, PI493629, PI493660, PI493666, PI493810, PI493816, PI493865, PI497642, DC 2440 (S3897), M C Ran, ICG 332, ICG 1142, ICG 1399, ICG 2738, ICG 3673, ICG 4670, ICG 5475, ICG 5609, ICG 6201, ICG 6646, ICG 9315 ICG 10890, ICG 13856, ICG 15309, KS 1, K4, KKU 60 and KKU 40) formed group 1, which was the largest group. This group had nodule dry weight ranging from 0.19 to 0.43 g plant^{-1} with mean of 0.31 g plant^{-1}, biomass ranging from 71.62 to 79.77 g plant^{-1} with mean of 75.66 g plant^{-1}, harvest index ranging from 0.24 to 0.42 with mean of 0.33 and pod yield ranging from 17.82 to 32.44 g plant^{-1} with mean of 24.79 g plant^{-1} (Table 4).

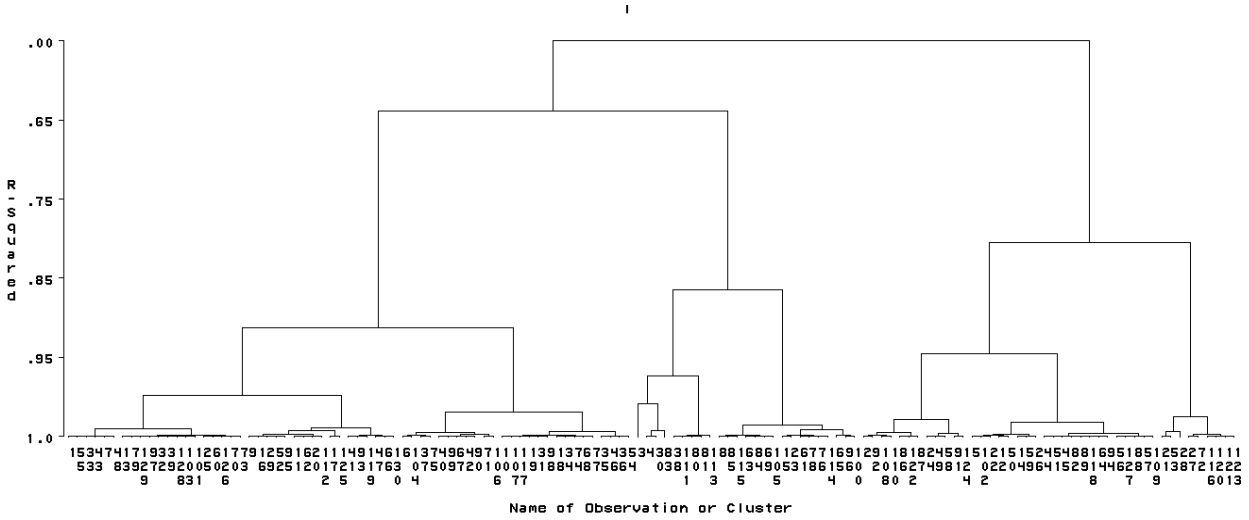


Figure 2. Dendrogram produced by Ward's minimum variance cluster analysis base on mean traits related to nitrogen fixation of 130 Valencia peanut accessions across 2 years.

Group 2 consisted of 25 peanut accessions (PI475921, PI475925, PI476089, PI501293, PI306361, PI407451, PI536121, PI493501, PI493565, PI493584, PI493630, PI494019, DC 2120 (S3873), S-3653, S-3881, 23322, S 3840 Kremena, ICG 1274, ICG 3681, ICG 6022, ICG 8517, ICG 10092, ICG 10474 and ICG 10554). This group had nodule dry weight ranging from 0.22 to 0.56 g plant^{-1} with mean of 0.32 g plant^{-1}, biomass ranging from 80.69 to 97.45 g plant^{-1} with mean of 84.64 g plant^{-1}, HI ranging from 0.23 to 0.43 with mean of 0.31 and pod yield ranging from 20.48 to 35.84 g plant^{-1} with mean of 25.46 g plant^{-1}

Group 3 consisted of 33 accessions (PI475913, PI476074, PI493562, PI497459, PI259601, PI314980, PI338337, PI468208, PI493325, PI493360, PI493373, PI493382, PI493451, PI493458, PI493461, PI493470, PI493566, New BG, NM 052565, Rossita, Valencia – A, Valencia – C, ICG 115, ICG 297, ICG 397, ICG 5221, ICG 6888, ICG 7181, ICG 8106, ICG 111444, ICG 14127, ICG 15042 and KS 2). This group had nodule dry weight ranging from 0.18 to 0.40 g plant^{-1}and mean of 0.30 g plant^{-1}, biomass production ranging from 64.06 to 71.21 g plant^{-1} and mean of 68.46 g plant^{-1}, HI ranging from 0.27 to 0.45 and mean of 0.35 and pod yield ranging from 19.05 to 33.68 g plant^{-1} and mean of 23.68 g plant^{-1}.

Group 4 consisted of 9 accessions (PI259580, PI365564, PI390432, PI493415, PI493688, ICG 10566, ICG 13858, ICG 14106 and ICG 14710). This group had nodule dry weight ranging from 0.16 to 0.38 g plant^{-1} with mean of 0.30 g plant^{-1}, biomass ranging from 58.38 to 62.83 with mean of 61.19 g plant^{-1}, HI ranging from 0.26 to 0.40 with mean of 0.35 and pod yield ranging from 15.00 to 24.86 g plant^{-1} with mean of 21.20 g plant^{-1}

Group 2 consisting of 25 accessions (such as ICG 3681, ICG 6022, ICG 10554, PI493630 and PI407451 etc.) had the highest nodule dry weight, biomass, pod yield and HI, whereas groups 4 consisting of 9 accessions (such as PI390432, PI259580, PI365564, PI493415 and ICG 10566 etc.) had the lowest nodule dry weight, biomass, harvest index and pod yield.

DISCUSSION

The traits related to nitrogen fixation consisting of nodule number, nodule dry weight, leaf color score, biomass production, shoot dry weight harvest index and nitrogenase activity had strong and positive correlations with nitrogen fixation (Philips *et al*., 1989; Pimratch *et al*., 2004, 2008). As most peanut growing soils are not fertile and peanut being a legume is dependent

on atmospheric nitrogen for fixation nitrogen fixation traits are, therefore, closely related to growth parameters and pod yield. Harvest index is correlated with nitrogen fixation, if fixed nitrogen gives more contribution to pod yield than vegetative growth, and nitrogenase activity is related to nitrogen fixation as this parameter is an indirect assessment for nitrogen fixation. Most of the peanut growers are from Semi-Arid Tropics and cannot afford to apply synthetic fertilizers. Selection of varieties with high nodules number and high yield helps growers to reduce the input cost on commercial fertilizers. Selection for surrogate traits as an indirect method for nitrogen fixation is much easier than direct selection for nitrogen fixation which is difficult and can be performed in laboratory.

Genotypic diversity is important source of germplasm for breeding program. Breeders can select peanut accessions for improving the characters. Peanut Genotypes with high nitrogen fixation and high yield should be used as parents in peanut breeding programs for high nitrogen fixation (Pimratch *et al*., 2008). Krishna *et al*. (2004) identified 48 Valencia peanut from 20 different country by using microsatellite makers.

Genotype variations were observed for all characters under study. The Valencia peanut germplasm had high variations in nodule dry weight, biomass production, pod yield and harvest index. The range of variation for nodule dry weight in this study was from 0.16 to 0.56 g plant^{-1}. In previous study using other germplasm under well-irrigated condition, the range of nodule dry weight was from 0.38 to 0.57 g plant^{-1} (Dinh *et al*., 2013). The results in this study were similar to those in previous study.

The peanut accessions were classified into 4 groups based on Squared Euclidian distance matrix which indicated degree of similarity. High values showed high similarity and vice versa. Group 2 consisting of 25 accessions had the highest biomass and pod yield. The accessions in this group should be selected as parents in breeding programs. Group 4 consisting of 9 accessions had low biomass, pod yield and nodule dry weight. In previous investigation, the variation in biomass production ranged from 6,766 -8,875 kg ha^{-1} (Pimratch *et al*., 2008). In this study, the variation in biomass productions ranged from 5,838 to 9,845 kg ha^{-1} was observed.

The peanut genotypes with high nodule dry weight can be used as parents by peanut breeders to incorporate high nitrogen fixation traits into cultivated varieties with high yield and good agronomic traits. The variations in traits related to nitrogen fixation are also important for prediction of the possible success in breeding programs for improving nitrogen fixation in Valencia peanut.

CONCLUSION

This study investigated the variation in nodule dry weight, biomass, pod yield and harvest index in 130 accessions of Valencia peanut germplasm. The results indicated that high variation was observed for all characters under study. The accessions with high biomass production, pod yield and nodule dry weight are promising for use as parents in breeding programs.

ACKNOWLEDGEMENTS

This work was supported by the Higher Education Research Promotion and National Research University Project of Thailand, Office of the Higher Education Commission, through the Food and Functional Food Research Cluster of Khon Kaen University (KKU), Thailand. This work were also partially supported by Peanut CRSP NMS 72 project by USAID through University of Georgia ECG-A-00-0700001-00 and peanut genotypes for this study were kindly provided by ICRISAT, New Mexico State University, USA. Grateful acknowledgement is made to the Thailand Research Fund, for providing financial supports to this research through the Senior Research Scholar Project of Professor Dr. Sanun Jogloy (Project No RTA 5880003). Acknowledgment is extended to the Thailand research fund (IRG5780003), KKU and faculty of agriculture, KKU for providing financial supported for manuscript preparation activities.

REFERENCES

Bricker AA (1989). MSTAT-C User's guide. Michigan State University, East Lansing, MI.

Dinh HT, Kaewpradit W, Jogloy S, Vorasoot N, Patanothai A (2013). Biological nitrogen fixation of peanut genotypes with different

levels of drought tolerance under mid-season drought. *SABRAO J. Breed. Genet*. 45: 491-503.

Giller KE, Nambiar PTC, Srinivasa Rao B, Dart PJ, Day JM (1987). A comparison of nitrogen fixation in genotypes of groundnut (*Arachis hypogaea* L.) using 15N-isotope dilution. *Biol. Fertil. Soil*. 5(1): 23-25.

Giller KE (2001). Nitrogen fixation in tropical cropping systems. 2nd ed. CAB International, Wallingford, UK.

Herridge D, Rose I (2000). Breeding for enhanced nitrogen fixation in crop legumes. *Field Crops Res*. 65: 229-248.

Hoshmand AR (2006). Design of experiments for agriculture and the natural sciences 2nd Ed. Chapman & Hall/CRC, Boca Raton, FL.

Krishna GK, Zhang J, Burow M, Pittman RN, Delikostadinov SG, Lu Y, Puppala N (2004). Genetic diversity analysis in Valencia peanut (*Arachis hypogaea* L.) using microsatellite markers. *Cell. Mol. Biol. Lett*. 9: 685-697.

McDonagh JF, Toomsan B, Limpinuntana V, Giller KE (1993). Estimate of the residual nitrogen benefit of groundnut to maize in Northeast Thailand. *Plant and Soil*. 154: 267-277.

McDonagh JF, Toomsan B, Limpinuntana V, Giller KE (1995). Grain legumes and green manures as pre-rice crops in Northeast Thailand: Legume N_2–fixation, production and residual nitrogen benefits to rice. *Plant and Soil*. 177: 111-126.

Phillips TD, Wynne JC, Elkan GH, Schneeweis TJ (1989). Field evaluations of peanut cultivar-*Bradyrhizobium* specificities. *Peanut Sci*. 16: 54-57.

Pimratch S, Jogloy S, Toomsan B, Jaisil P, Sikhinarum J, Kesmala T, Patanothai A (2004). Evaluation of seven peanut genotypes for nitrogen fixation and agronomic traits. *Songklanakarin J. Sci. Technol*. 26: 295-304.

Pimratch S, Jogloy S, Vorasoot N, Toomsan B, Patanothai A, Holbrook CC (2008). Relationship between biomass production and nitrogen fixation under drought-stress conditions in peanut genotypes with different levels of drought resistance. *J. Agron. Crop Sci*. 194: 15-25.

Purseglove TW. 1977. Tropical crops dicotyledons, Longman Group Ltd., London. pp. 224-235.

SAS Institute (2001). SAS/STAT User's guide, 2nd ed. SAS Institute Inc. Cary.

Toomsan B (1990). Groundnut microbiology research at Khon Kaen University. In: A. Patanothai, ed., Groundnut improvement project, Khon Kaen University. Report of work for 1986-1988. Faculty of Agriculture, Khon Kaen University. Khon Kaen, Thailand. pp. 89-111.

Toomsan B, McDonagh JF, Limpinuntana V, Giller KE (1995). Nitrogen fixation by groundnut and soybean and residual nitrogen benefits to rice in farmers' field in Northeast Thailand. *Plant and Soil*. 175: 45-56.

Copyright of SABRAO Journal of Breeding & Genetics is the property of Society for the Advancement of Breeding Researches in Asia & Oceania and its content may not be copied or emailed to multiple sites or posted to a listserv without the copyright holder's express written permission. However, users may print, download, or email articles for individual use.

Journal of Applied Biological Sciences 9 (2): 23-30, 2015
ISSN: 1307-1130, E-ISSN: 2146-0108, www.nobel.gen.tr

Exogenous Supplementation of Growth Regulators and Temperature Improves Germination of Dormant Jerusalem Artichoke (*Helianthus tuberosus* L.) Seeds under *in vitro* and *in vivo* Conditions

Preeya PUANGSOMLEE WANGSOMNUK[1]* Sudarat KHAMPA[1] Sanun JOGLOY[2]
[1]Department of Biology, Faculty of Science, Khon Kaen University, Khon Kaen, Thailand
[2]Department of Plant Science and Agricultural Resources, Faculty of Agriculture, Khon Kaen University, Khon Kaen, Thailand

*Corresponding author:
Email: prepua@kku.ac.th

Received: April 30, 2015
Accepted: June 09, 2015

Abstract

Jerusalem artichoke (*Helianthus tuberosus* L.) is an important tuber crop but the seed germination is one of the major limiting factors in propagation due to the dormancy of the seeds. To find a solution, we investigated whether exogenous application of the hormones 6-benzylaminopurine (BAP) and gibberellic acid (GA_3) as well as chilling (4 ºC) alone or in combination can be used to alleviate the problem of dormancy under *in vitro* and *in vivo* conditions. In the present study, JA102xJA89 control seeds showed only 11.7 and 13.3% of germination rate under aseptic and greenhouse conditions, respectively. Exogenous supplementation of 8 ppm BAP for seven and two days scored the highest germination rate of 91.7 and 85.0% under aseptic and greenhouse conditions, respectively. In the presence of BAP it was not necessary to chill the seeds or add GA_3 to increase germination, and, in the presence of chilling, it was not necessary to add GA_3. In addition, no variation was observed in germination percentages of different Jerusalem artichoke genotypes when supplemented with 8 ppm of BAP. Two weeks after germination under aseptic conditions the seedlings had the highest survival rate when transplanted under greenhouse conditions which could be applicable for further genetic characterization.

Keywords: Benzylaminopurine; cytokinin; gibberellic acid; chilling; dormancy; germination; Jerusalem artichoke

INTRODUCTION

Jerusalem artichoke (*Helianthus tuberosus* L.) is a perennial herbaceous plant that is grown as an annual crop. It originates from the temperate regions of the northern central part of the USA. *Helianthus* belongs to the Asteraceae family and comprises 50 species [1-2]. The upper plant parts are used for biomass and animal feed, whereas the lower parts such as the tubers are used as feedstock for food and for non-food chemical production. The tubers store nearly 20% of inulin, an indigestible carbohydrate that is beneficial to human health and unique on equation vitamin-mineral complex, valuable foodstuff with high fructose syrup, bio-ethanol and prophylactic potential [1, 3-4]. Chicory (*Cichorium intybus* L.) and Jerusalem artichoke are the inulin storage species [1]. Tubers are consumed by people as vegetable because of its food value, flavour, and inulin content [5-6]. Dried Jerusalem artichoke powder is an important source of soluble dietary fibre, which significantly differs from defatted flax seeds, rye and wheat bran [3]. The Jerusalem artichoke was recently introduced into Thailand for commercial production as a food crop.

Seed dormancy is a nuisance in propagation programs; removing or breaking dormancy has always been a challenge for plant physiologists and dormancy is a serious threat to the improvement of the Jerusalem artichoke crop population [1, 4, 7]. Seed dormancy is defined as the lack of germination in a specified period of time under favorable environmental conditions [8-9]. Two major forms of physiological seed dormancy have been described, namely embryo and seed coat dormancy [10-11]. Physiological dormancy can be divided into three levels: deep, intermediate and slight dormancy [8]. Genotypic constraints, physiological inhibitors and morphologically immature embryos appear to cause a combined dormancy in Jerusalem artichoke seeds. In the physiologically dormant seeds, temperature can break dormancy and promote germination, and there is a list of chemicals such as oxidants, nitrites, nitrates, respiratory inhibitors and growth regulators that have been proven to eliminate seed dormancy [12-13]. Levels of endogenous plant growth regulators are believed to play a major role in overcoming seed dormancy of different species with variable success. The gibberellins promote the endosperm weakening and subsequent endosperm rupture (micropylar endosperm in particular) by induction of cell wall hydrolases, whereas abscisic acid inhibits the induction of cell wall hydrolases and thereby inhibits endosperm weakening and endosperm rupture [14-15].

To increase the rate of germination and to break dormancy, moist chilling and cold stratification have been widely used as pre-sowing treatments. They are cost-effective and simple approaches for overcoming seed dormancy [16]. The mechanism is still not clearly understood, but according to the researchers Nikolaeva, Mozafar and Masoomeh [17-18], moist chilling plays an important role in establishing hormone levels by initiation of appropriate enzyme activity. Gibberellic acid has been shown to promote seed germination, and both GA_3 and pre-chilling also improved the germination rate in the seeds of

Nothofagus obliqua [19-20]. Cold stratification has been found to be an effective method and is also recognized in overcoming physiological dormancy of germinating seeds of many species [21-22]. A previous study reported that 4 ºC treatment was superior to addition of kinetin, BAP and GA_3 in improving seed germination of *Ferula assa-foetida* L. [23]. Removing the hull and seed coat of difficult-to-germinate *Helianthus* species including the Jerusalem artichoke was previously found to be the most effective method and gave rise to 90% germination [24]. BAP is an important growth regulator and plays a key role in breaking of seed dormancy [25]. There are some reports on improvement of sunflower seed germination after application of BAP [26-27]. The aim of this study was to examine the effect of plant growth regulators and the chilling factor both alone and in combination in overcoming seed dormancy of the Jerusalem artichoke under *in vitro* and *in vivo* conditions. For the first time we have established *in vitro* culture protocols for dormancy-breaking of Jerusalem artichoke seeds.

MATERIALS AND METHODS

Effects of the cytokinin 6-benzylaminopurine (BAP), gibberellic acid (GA_3) and chilling at 4 ºC on seed germination under aseptic and greenhouse conditions

Mature achenes of the Jerusalem artichoke (Figure 1a) were harvested from field-grown F_1 hybrids derived from the cross between JA 102 and JA 89 plants. The parental genotypes were kindly donated from the plant genetic resources of Saskatoon Research Centre, Canada (KSRC). All achenes were dry in shade and preserved until used.

In the first experiment, aseptic culture was performed. One thousand two hundred and sixty seeds of JA 102xJA 89 were sterilized with 1.2 and 0.6% sodium hypochlorite for 5 min, and subsequently sodium hypochlorite was removed by washing with sterile distilled water twice for 5 min each. Twenty surface-sterilized seeds were (1) cultured on MS basal medium (pH adjusted to 5.6-5.8) supplemented with various concentrations of BA (Sigma) and GA_3 (Wago, Japan) for seven days (Fig. 1b) and then transferred to plain MS basal medium (MS salt, JRH bio science); (2) subjected to a chilling treatment at 4 ºC for one, two, three or four weeks and then transferred to plain MS basal medium; (3) subjected to combination treatments of BAP (8 ppm) or GA_3 (4 ppm) with/without chilling for four weeks at 4 ºC in a refrigerator and then transferred to plain MS basal medium under the growing conditions 12 hrs photoperiod with approximately 28 $\mu mol.m^{-2}.s^{-1}$ and 25±2 ºC. Non-treated seed culture was used as a control. The detailed treatments are described in Table 1.

In addition, experiments were conducted to determine whether the seeds can germinate sufficiently under greenhouse conditions. Greenhouse experiments were conducted with minor modifications based on the results obtained from the aseptic culture experiments. One thousand one hundred and forty seeds of JA 102xJA 89 were sterilized with 1.2 and 0.6% sodium hypochlorite for 5 min and followed by washing with sterile water twice for 5 min each. Twenty seeds of the Jerusalem artichoke were placed on Whatman No.1 filter paper in Petri dishes, and were imbibed with sterile distilled water supplemented with various concentrations of BAP and GA_3 for 48 hours as well as combinations of BAP (8 ppm) or GA_3 (6 ppm) with/without chilling (4 ºC) for four weeks (Table 1). Pure water-supple- mented cultures which were unchilled were used as a control treatment. The seeds were also incubated at 4 ºC for one, two, three or four weeks in a refrigerator. Seeds were transferred to a peat moss medium (Pindstrup) under greenhouse conditions and water was added once a day.

Table 1. Treatments to study the effect of plant growth regulators and chilling on seed germination of the Jerusalem artichoke JA 102xJA 89 under aseptic culture conditions and greenhouse conditions

Treatment	BA (ppm)	GA_3 (ppm)	Chilling (week)
1	0	0	0
2*	1	0	0
3	2	0	0
4	4	0	0
5	6	0	0
6	8	0	0
7	10	0	0
8*	0	1	0
9	0	2	0
10	0	4	0
11	0	6	0
12	0	8	0
13	0	10	0
14	0	0	1
15	0	0	2
16	0	0	3
17	0	0	4
18	8	4* (6)	0
19	8	0* (0)	4
20	0	4* (6)	4
21	8	4* (6)	4

* Treatment used for aseptic culture conditions only
() Treatment used for greenhouse culture conditions only

Effect of BAP on seed germination of 12 Jerusalem artichoke genotypes

The treatment that gave the best germination results (Table 2) was further tested with seeds of 12 Jerusalem artichoke varieties (Table 3), to determine if there are different responses among varieties. In this case, BAP at the concentration of 8 ppm without chilling was selected to treat the 12 Jerusalem artichoke varieties both under aseptic and greenhouse conditions. Seed preparation and growing conditions were similar to those described previously. The treatments were replicated three times. Germination, dormancy and dead seed percentages were recorded.

Transplanting study of *in vitro* grown seedlings

Pericarps of the Jerusalem artichoke hybrid (JA 102xJA 89) were removed and seeds were cultured under the growing conditions described above. For hardening, seedlings of the *in vitro* germinated seeds that were one, two, three and four weeks old were transferred to plastic containers filled with peat moss. The pots were covered with transparent plastic bags provided with ventilation holes for three days. After hardening, the plastic bags were removed and water was supplied daily. The surviving

plants were counted weekly until four weeks and then transferred to pots with high-quality soil.

Data analysis

We define 'germination' as the stage when the root tips emerge from the seeds [27]. The germination was recorded eight times at 3-day intervals. Ungerminated seeds were then tested for their viability using 0.5% tetrazolium (Sigma) for 12 hours. Final germination rate, dormancy and dead seed percentage were recorded.

Germination, dormancy and dead seed data were analysed using the Statistic 8 software program [28] and mean separation was performed by the Least Significant Difference (LSD) if the F-test was significant at the 0.05 probability level. Graphical presentation was done in Microsoft Excel.

RESULTS

Effects of BAP and GA_3

Supplementation of 1-10 ppm of BAP to the seeds of the Jerusalem artichoke hybrid JA102xJA89 significantly increased seed germination under aseptic (45.0 to 91.7%) and greenhouse conditions (38.3 to 85.0%) when compared to untreated controls (11.7% and 13.3%) after twenty-four days (Table 2). The highest seed germination of 91.7% and 85.0% was recorded at 8 ppm of BAP under both aseptic and greenhouse conditions (Table 2; Figures 2a & 2b).

Supplementation of GA_3 also significantly increased the germination rate except at the lowest concentration of 1 ppm under aseptic conditions (Table 2). However, the germination percentages were generally much lower than those of BAP, ranging from 13.3 to 38.3% for aseptic conditions and 25.0 to 58.3% for greenhouse conditions. There was no significant difference among concentrations from 2 to 10 ppm under aseptic conditions; therefore, the best concentrations could not be clearly determined. The best concentration for greenhouse conditions was recorded at 6 ppm (58.3% germination) (Figure 2d).

For all concentrations tested under aseptic conditions, BAP and GA_3 can significantly reduce dormancy of Jerusalem artichoke seeds (Table 2). The percentages of seed dormancy ranged from 0 to 40% for BAP and 38.3 to 50% for GA_3 compared to 71.7% of the untreated control. BAP at the concentration of 8 ppm gave the lowest percentage of dormancy (0%), whereas GA_3 at all concentrations gave similar results. The total percentage of dead seeds in BAP-treated experiments were much lower than that of GA_3 treatments under aseptic conditions.

Effects of Chilling

Chilling at 4 ºC for one to four weeks can also significantly increase germination (Table 2, Figures 2e & 2f). The germination percentages ranged from 31.7 to 76.7% for aseptic conditions and 33.3 to 75.0% for greenhouse conditions, when compared to 11.7 and 13.3% of the untreated controls. The best treatment for both culture conditions was chilling for four weeks that can give germination rates of 76.7 and 75%.

In contrast to germination, chilling at 4 ºC can reduce seed dormancy and the lowest percentages of dormancy (6.7% for aseptic conditions and 5.0% for greenhouse conditions) were found when the seeds were chilled for four weeks, whereas untreated controls had seed dormancy of 71.7 and 36.7%.

Combined effects of BAP, GA_3 and chilling

Supplementation of BAP, GA_3 and chilling alone significantly improved seed germination under both aseptic and greenhouse conditions. The combined treatment of BAP, GA_3 and chilling also significantly increased seed germination rate under aseptic conditions (33.3 to 86.7%) and greenhouse conditions (30.0 to 55.3) when compared to 11.7 and 13.3% in untreated controls (Table 2). The maximum synergistic treatment effect (86.7%) was observed at 8 ppm BA with combination of chilling at 4 ºC for four weeks. However, BAP at a concentration of 8 ppm alone showed a higher seed germination than combination with chilling. The combination of GA_3 and chilling resulted in less improved germination when compared to other combinations (Table 2 and Figure 2). Treatment with co-applied GA_3 showed significantly lower seed germination compared to treatment without GA_3 under greenhouse conditions (Figure 2h).

Variation in seed germination of Jerusalem artichoke varieties

According to our experiments, 8 ppm BAP concentration was the most effective in breaking seed dormancy and improving germination rate. In this experiment, twelve accessions of Jerusalem artichoke seeds were treated with 8 ppm BAP for scoring of germination and dormancy rate under both aseptic and greenhouse conditions. Seed germination (85.0 to 93.3% and 83.3 to 93.3%) (Figures 3a & 3b), dormancy (0.0% to 5.0% and 0%) and dead seeds (1.7% to 15% and 6.7% to 16.0%) were recorded under aseptic and greenhouse conditions (Table 3). The difference of seed germination percentages among the genotypes was not significant. However, a significant difference was found in the percentage of dead seeds under *in vitro* conditions. The application of 8 ppm BAP alone gave the highest germination percentages from 9 to 18 days under aseptic conditions (Figure 3a) and 6 to 12 days under greenhouse conditions (Figure 3b).

Transplanting of seedlings

Transplanting of seedlings germinated under aseptic conditions to ambient environments usually has a low survival rate and depends on the age of the seedling. The highest survival rate of JA102xJA89 Jerusalem artichoke seedlings was recorded for the seedlings transferred two weeks after germination, followed by seedlings transferred one week, three weeks and four weeks after germination (Figure 3c). The final survival rates were 100%, 95%, 80% and 72% for seedlings of two weeks, one week, three weeks and four weeks, respectively. After transplanting the survival was constant from two to four weeks.

Table 2. Effect of treatments of Jerusalem artichoke JA 102xJA 89 seed germination

Treatment	%Germination		%Dormancy		%Dead seed	
	In vitro	*In vivo*	*In vitro*	*In vivo*	*In vitro*	*In vivo*
Control	11.67 ^{k}	13.33 ^{k}	71.67 ^{a}	36.67 ^{c}	16.67 ^{efg}	50.00 ^{bc}
BA 7 days (2 days)						
1 ppm*	45.00 ^{fg}	ND	40.00 ^{c}	ND	15.00 ^{fg}	ND
2 ppm	48.33 ^{f}	38.33 ^{k}	36.67 ^{cd}	30.00 ^{d}	15.00 ^{fg}	31.67 ^{def}
4 ppm	65.00 ^{e}	46.67 ^{de}	23.33 ^{ef}	23.33 ^{ef}	11.67 ^{ghi}	30.00 ^{efg}
6 ppm	71.67 ^{de}	58.33 ^{c}	15.00 ^{g}	16.67 ^{g}	13.33 ^{gh}	25.00 ^{fght}
8 ppm	91.67 ^{a}	85.00 ^{a}	0.00 ^{j}	3.33 ^{hi}	8.33 ^{hi}	11.67 ^{j}
10 ppm	78.33 ^{cd}	55.00 ^{c}	11.67 ^{ghi}	18.33 ^{fg}	13.33 ^{gh}	26.67 ^{fgh}
GA_3 7 days (2 days)						
1 ppm*	13.33 ^{k}	ND	50.00 ^{b}	ND	36.67 ^{a}	ND
2 ppm	30.00 ^{ij}	26.67 ^{ij}	38.33 ^{c}	51.67 ^{a}	31.67 ^{abc}	21.67 ^{hi}
4 ppm	38.33 ^{gh}	33.33 ^{ghi}	40.00 ^{c}	36.67 ^{c}	21.67 ^{de}	30.00 ^{efg}
6 ppm	35.00 ^{hi}	58.33 ^{c}	38.33 ^{c}	23.33 ^{ef}	26.67 ^{cd}	18.33 ^{ij}
8 ppm	25.00 ^{j}	45.00 ^{ef}	41.67 ^{c}	23.33 ^{ef}	33.33 ^{ab}	31.67 ^{def}
10 ppm	30.00 ^{ij}	25.00 ^{j}	41.67 ^{c}	26.67 ^{de}	28.33 ^{bc}	48.33 ^{c}
Chilling 4ºC						
1 wk	31.67 ^{hij}	33.33 ^{ghi}	40.00 ^{c}	31.67 ^{cd}	28.33 ^{bc}	35.00 ^{de}
2 wks	50.00 ^{f}	53.33 ^{cd}	30.00 ^{de}	28.33 ^{de}	20.00 ^{ef}	18.33 ^{ij}
3 wks	65.00 ^{e}	60.00 ^{c}	18.33 ^{fg}	20.00 ^{fg}	16.67 ^{efg}	20.00 ^{hi}
4 wks	76.66 ^{cd}	75.00 ^{b}	6.67 ^{hij}	5.00 ^{hi}	16.67 ^{efg}	20.00 ^{hi}
Combination						
8 ppm BA + 4 (6) ppm GA_3 for 7 (2) days	80.00 ^{bc}	36.67 ^{gh}	13.33 ^{gh}	6.67 ^{hi}	6.67 ^{i}	56.67 ^{b}
8 ppm BA + 4 ºC for 4 wks	86.67 ^{ab}	53.33 ^{cd}	5.00 ^{ij}	8.33 ^{h}	8.33 ^{hi}	38.33 ^{d}
4 (6) ppm GA_3 + 4 ºC for 4 wks	33.33 ^{hi}	33.33 ^{ghi}	51.67 ^{b}	43.33 ^{b}	15.00 ^{fg}	23.33 ^{ghi}
8 ppm BA +4 (6) ppm GA_3 +4 ºC for 4 wks	81.67 ^{bc}	30.00 ^{hij}	6.67 ^{hij}	1.67 ^{i}	11.67 ^{ghi}	68.33 ^{a}

*Treatments used for aseptic culture condition only
() Treatments used for greenhouse condition only
ND: Not determined
Numbers in the same column with the same letter(s) are not significantly different at 0.05 probability level by the Least Significant Difference (LSD).

Table 3. Percentages of germination and dormancy of seeds of Jerusalem artichoke varieties treated with BAP at concentration of 8 ppm cultured under aseptic and greenhouse conditions

Genotype	% Germination		% Dormancy		% Dead Seed	
	Aseptic	Greenhouse	Aseptic	Greenhouse	Aseptic	Greenhouse
CN 52867	93.3	93.3	0.0	0.0	6.7^{bcd}	6.7
HEL 53	93.3	91.7	5.0	0.0	1.7^{d}	8.3
HEL 54	91.7	93.3	5.0	0.0	3.3^{cd}	6.7
HEL 65	91.7	90.0	1.7	0.0	6.7^{bcd}	10.0
HEL 66	91.7	93.3	3.3	0.0	5.0^{bcd}	6.7
HEL 321	90.0	91.7	1.7	0.0	8.3^{bc}	8.3
HEL 322	93.3	90.0	3.3	0.0	3.3^{cd}	10.0
HEL 335	90.0	83.3	3.3	0.0	6.7^{bcd}	16.0
JA 37	93.0	85.0	0.0	0.0	6.7^{bcd}	15.0
JA 38	91.7	91.7	0.0	0.0	8.3^{bc}	8.3
JA 41	85.0	91.7	0.0	0.0	15.0^{a}	8.3
JA 81	90.0	88.3	0.0	0.0	10.0^{ab}	11.7

Numbers in the same column with the same letter(s) are not significantly different at 0.05 probability level by the Least Significant Difference (LSD).

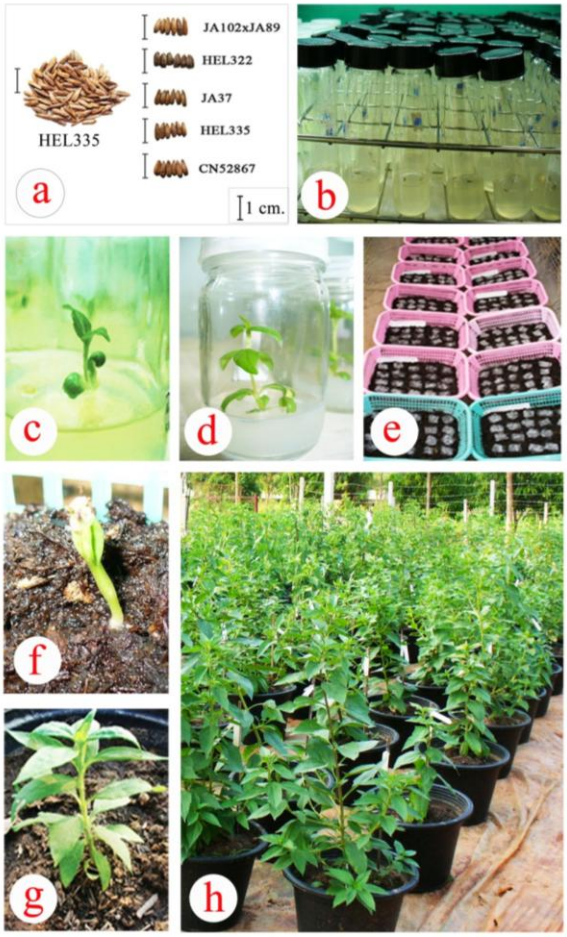


Figure 1. Seed germination in the Jerusalem artichoke: achenes (a); seeds treated under aseptic conditions (b); *in vitro* seedlings on MS basal medium free hormone (c, d); treated seeds transferred to peat moss medium in the greenhouse (e); seedling growth in peat moss medium (f); plants of Jerusalem artichoke in pots (g, h).

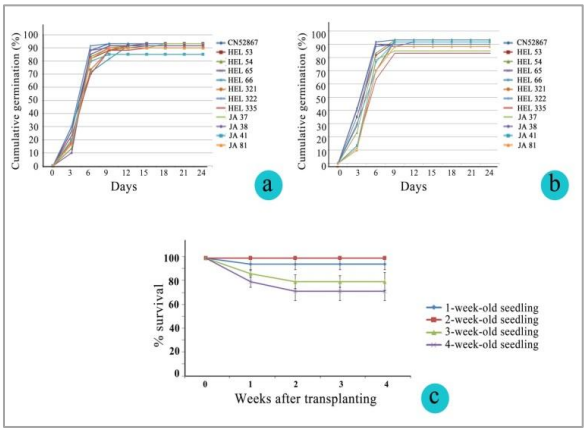


Figure 3. Percentages of cumulative germination of Jerusalem artichoke varieties treated with BAP at a concentration of 8 ppm under aseptic conditions (a) and under greenhouse conditions (b); percentage of survival of JA102xJA89 Jerusalem artichoke seedlings grown *in vitro* and transplanted at different ages under greenhouse conditions (c).

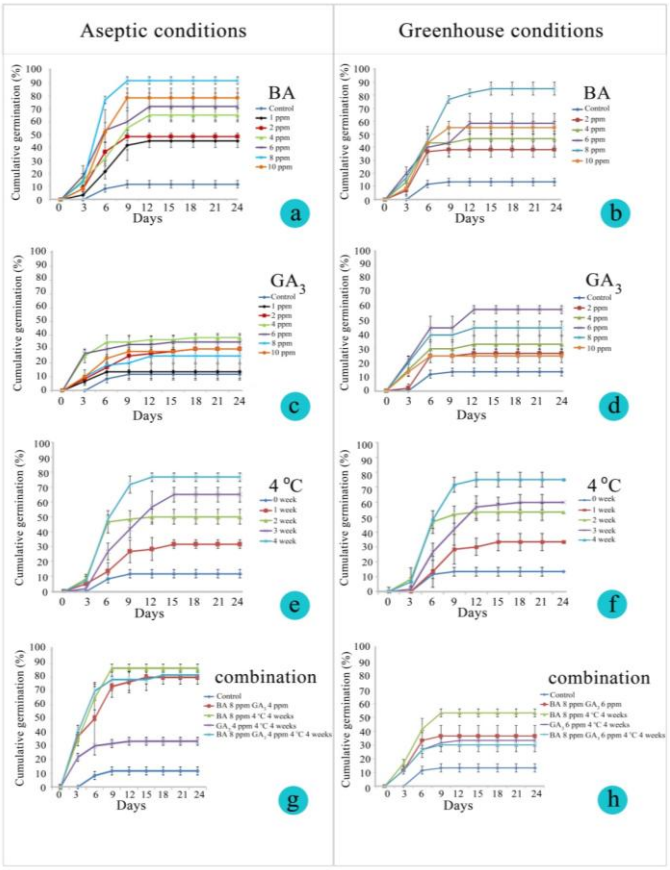


Figure 2. Percentages of cumulative germination of the Jerusalem artichoke hybrid 102xJA89 treated with BAP (a and b), GA_3 (c and d), chilling (e and f), and a combination of growth regulators and chilling at 4 ºC (g and h) under aseptic conditions (a, c, e and g) and greenhouse conditions (b, d, f and h).

DISCUSSION

Plant growth regulators play an important role in the regulation of seed germination and plant growth by breaking seed dormancy. The method to supplement plant growth regulators is one of the key successes in seed germination under laboratory conditions or when cultivation is attempted [29]. Present results demonstrate that supplementation of BAP, GA_3 and chilling is involved in breaking the dormancy of Jerusalem artichoke seeds under both *in vitro* and *in vivo* conditions. Our findings were confirmed by a number of earlier reports in other plants [30-31]. In one report, a treatment of lotus nuts (*Nelumbo nucifera*) supplemented with 0.8-3.5 µM BAP followed by chilling at 4 ºC for four weeks and addition of GA_3 induced the highest germination [31].

Cytokinins regulate diverse processes from embryonic development to adult plant growth [32-33]. Increase in cytokinins may result in the breaking of dormancy, perhaps by overcoming the effect of endogenous inhibitors [34]. Our results show that 8 ppm concentration of BAP (cytokinin) significantly reduces dormancy in the Jerusalem artichoke both *in vivo* and *in vitro* (Table 2 and Figures 2a

& 2b). These results are consistent with those of Nikolic et al [31], who reported that most of the cytokinins including BAP and TDZ influenced seed germination in *Lotus corniculatus* and *Carica papaya*. The cytokinins probably penetrate through the testa and neutralise the inhibitors present in the embryo, thus enabling it to rupture the seed coat [35]. Cytokinins are not necessary for germination, but they can affect the germination inhibitor ABA [36].

Several growth regulators including gibberellins promote germination in dormant or partially dormant seeds. GA is effective in stimulating germination in seeds with a shallow dormancy. Our study showed that under greenhouse conditions GA_3 at 2 and 4 ppm did not markedly affect Jerusalem artichoke seed dormancy, but a 6 ppm concentration of GA_3 significantly reduced dormancy. Application of GA_3 to seeds in a greenhouse at 6 and 8 ppm for two days showed much higher germination and a decrease of dormant and dead seeds compared to the same concentration treated for seven days under aseptic conditions. In contrast to our own findings, Yang et al [37] reported a slightly higher germination percentage of 95% in seeds of the trianda palm (*Areca trianda*) treated with GA_3 (250 mg/l) compared to a germination percentage of 85% when treated with BAP (5-25 mg/l). The supplementation of gibberellins improves seed germination rate by increasing the amino acid availability in embryo and they cause the releasing of hydrolytic enzyme required for digestion of endospermic starch when seeds renew growth at germination [38].

Stratification is the most efficient factor and that in some plants imbibed seeds germination with the highest rate only occurs in chilling temperature. It indicates that glycolysis, respiratory system, pentose phosphate pathway, citric acid cycle and protein synthesis do not start in dry seeds at room temperature [39]. Generally for seed germination, seed imbibition, respiration and protein synthesis will provide necessary energy (ATP) [40]. Evidence shows that under moist-chilling conditions many genes in dormant seeds are active and some of these genes are under control of plant hormones [41]. El-Dengawy also found that chilling at 4 ºC for 60 days lead to high germination of 93% although the differences were not significant when compared with those treated with GA_3 and BAP [41]. In the present work, following stratification for four weeks, 76.7% and 75% seed germination was achieved in aseptic and greenhouse conditions. The results shown in Table 2 and Figures 2e and 2f indicate that four weeks of exposure to chilling significantly improved germination compared to shorter exposure. Figures 2e and 2f showed that cold-exposure for four weeks was the best chilling treatment for Jerusalem artichoke seed germination, even if it is still less effective than BAP treatment. The highest germination percentages were observed in both aseptic and greenhouse conditions as early as 12 days after initiation of germination. Durations of chilling for two and three weeks could be confounded at different evaluation times, but in general seeds chilled for two weeks showed a clearly higher germination percentage than the seeds chilled only for one week.

The participation of more than one plant growth regulator in biological systems is not un-common. An interplay of hormones may result in synergistic, antagonistic, additive, and permissive effects. BAP acts synergistically with gibberellins, chilling and probably also with other plant growth regulators; which might be called a system approach or synergism. Cytokinins (CKs) and gibberellins (GAs) are actively involved in dividing of seed tissues and breaking of dormancy after seed imbibitions which results in germination and growth of the dormant embryos [42-43]. In our study, concomitant application of growth regulators (BAP and GA_3) and chilling all successfully increased the seed germination of the Jerusalem artichoke. The ineffectiveness of exogenous GA_3 along with cold-stratification has previously been reported in *Ferula assa-foetida*, *Heracleum sphondylium* and *Chaerophyllum temulum* [23, 44-45]. We found that seeds treated with 6 ppm GA_3 for two days under greenhouse conditions showed lower percentage of dormancy than under aseptic conditions when seeds were treated with 4 ppm GA_3 for seven days (Table 2). This observation is confirmed by the results of the combined effects of concomitant application of BAP, GA_3 and chilling. The positive effect of BAP (8 ppm) on seed germination was decreased when it was co-applied with GA_3 or chilling at 4 ºC. This is in contrast to Sharifi and Pouresmael [18] who found that the positive effect of BAP was increased when it was co-applied with GA_3 in breaking the seed dormancy of *Bunium persicum*. The exact role of cytokinins in seed germination has yet to be solved. However, cytokinins certainly can break dormancy in seeds with a chilling requirement or with light requirement [46]. Our results indicated that when BAP was present, it was not necessary to include GA_3 and chilling. With chilling it was not necessary to include GA_3. Inclusion of these treatments results in lower germination.

Twelve Jerusalem artichoke varieties were treated with 8 ppm BAP and tested for germination percentages under aseptic and greenhouse conditions. They showed very similar germination percentages, indicating that there was no significant variation in response to 8 ppm BAP (Table 3 and Figures 3a & 3b). The plants later developed well in pots (Figures 1g and 1h).

In conclusion, the results of our investigation clearly demonstrated that plant growth regulators such as BAP and GA_3 as well as chilling can successfully enhance the seed germination of the Jerusalem artichoke. Among the tested growth regulators, 8 ppm BAP was the most effective in increasing seed germination and reducing dormancy. Our findings may also apply to other plant species with low germination rates.

Acknowledgement

The authors are thankful to Dr. Ediga Anjaneyulu, Dr. Hubert Kurzweil and Assoc. Prof. Wichuda Chaisiwamongkol for their valuable suggestions and comments throughout this research work. This work was financially supported by the Higher Education Research Promotion and the National Research University Project of Thailand, the Office of the Higher Education Commission through the Food and Functional Food Research Cluster of Khon Kaen University; the research funding from Khon Kaen University was awarded to the corresponding author.

REFERENCES

[1] Kays SJ, Nottingham SF. 2008. Biology and Chemistry of Jerusalem artichoke: *Helianthus tuberosus* L. CRC Press, Boca Raton, FL.

[2] Yang L, He QS, Corscadden K, Udenigwe CC. 2014. The prospects of Jerusalem artichoke in functional food ingredients and bioenergy production. Biotechnology Reports. 5:77–88.

[3] Liene J, Beitane I. 2014. Comparison of dietary fibre content in different fibre sources. Proceedings of the 9th Baltic Conference on Food Science and Technology "Food for Consumer Well-Being" FOODBALT 2014 Conference Proceedings. Jelgava, LLU.90.

[4] Puttha R, Goggi S, Gleason ML, Jogloy S, Kesmala T, Vorasoot N, Banterng P, Patanothai A. 2014. Pre-chill with gibberellic acid overcomes seed dormancy of Jerusalem artichoke. Agronomy for Sustainable Development. 34:869-878.

[5] Cem B, Esin A. 2012. Chips production from Jerusalem artichoke (*Helianthus tuberosus* L.). Food and Nutrition Sciences. 3(9):1321-1328.

[6] Cem B, Esin A. 2013. Crisp production from Jerusalem artichoke (*Helianthus tuberosus* L.) and investigation of quality parameters. Akademik Gida. 11(2):14-20.

[7] Gedrovica I, Karklina D. 2011. Influence of Jerusalem artichoke powder on dough rheological properties. Proceedings of the 6th Baltic Conference on Food Science and Technology. Jelgava, Latvia, p. 7-12.

[8] Baskin JM, Baskin CC. 2004. A classification system for seed dormancy. Seed Science Research. 14:1-16.

[9] Majidi MM, Barati M. 2011. Methods for breaking seed dormancy in one cultivated and two wild *Onobrychis* species. Seed Science Technology. 39:44-53.

[10] Kucerna B, Cohn MA, Leubner-Metzger G. 2005. Plant hormone interactions during seed dormancy release and germination. Seed Science Research. 15:281-307.

[11] Nasri F, Koshesh SM, Ghaderi N, Akbar Mozafari A, Javadi T. 2014. Improving germination and dormancy breaking in *Alstroemeria ligtu* hybrid seeds. Trakia Journal of
Sciences. 1:38-46.

[12] Gendreau E, Corbineau F. 2009. Physiological aspects of seed dormancy in woody ornamental plants. Propagation of Ornamental Plants. 9(3):151-158.

[13] Arc E, Galland M, Godin B, Cueff G, Rajjou L. 2013. Nitric oxide implication in the control of seed dormancy and germination. Front Plant Science. 4:346.

[14] Muller K, Tintelnot S, Leubner-Metzger G. 2006. Endosperm-limited Brassicaceae seed germination: Abscisic acid inhibits embryo-induced endosperm weakening of *Lepidium sativum* (cress) and endosperm rupture of cress and *Arabidopsis thaliana*. Plant and Cell Physiology. 47:864-877.

[15] Xi W, Liu C, Hou X, Yu H. 2010. Mother of FT and TFL1 regulates seed germination through a Negative feedback loop modulating ABA signaling in *Arabidopsis*. The Plant Cell. 22(6):1733-1748.

[16] Wang BSP, Berjak P. 2000. Beneficial effects of moist chilling on the seeds of black spruce (*Picea mariana* (Mill.) Britton, Sterns & Poggenb.). Annals of Botany. 86:29-36.

[17] Nikolaeva, MG. 1977. Factors controlling the seed dormancy pattern. In: Khan AA, ed. The physiology and biochemistry of seed dormancy and germination. Amsterdam, New York, Oxford: North-Holland Publishing Company. 51-74.

[18] Sharifi M, Pouresmael M. 2006. Breaking seed dormancy in *Bunium persicum* by stratification and chemical substances. Asian Journal of Plant Sciences. 5:695-699.

[19] Ghidiyal, SK. 2003. Provenance testing in *Pinus roxburghii* from Western-central Himalaya. Ph.D thesis, H.N.B. Garhwal University, Srinagar, Garhwal, Uttaranchal, India.

[20] Shafiq, Y. 1980. Effect of gibberellic acid (GA_3) and pre-chilling on germination percent of *Nothofagus obliqua* (Mirb.) Oerst. and *N. procera* Oerst. seeds. Indian Forester. 106:27-33.

[21] Miller, WF. 1971. Duration of stratification period for *Pinus elliotti*. Floresta. 3:83-85.

[22] Stilinovic S, Tucovic A. 1971. Preliminary study on seed of *Abies concolor* Lind. From the seed stand at Avala (Yugoslavia). 95-102. Quoted from Forestry Abstracts. 1971:35.

[23] Hassani SB, Saboora A, Radjabian T, Fallah Husseini H. 2009. Effect of temperature, GA_3 and cytokinins on breaking seed dormancy of *Ferula assa-foetida* L. Iranian Journal of Science and Technology. 33:75-85.

[24] Chandler JM, Jan CC, Beard BH. 1986. Chromosomal differentiation among the annual *Helianthus* species. Systematic Botany. 11:354-371.

[25] Emamipoor Y, Maziah M. 2014. An efficient method in breaking of dormancy from *Bunium persicum* (Boiss.) Fedtsch seeds: a valuable herb of Middle East and Central Asia. Asian Pacific Journal of Tropical Biomedicine. 4:642-649.

[26] Zimmerman Craig, A. 1977. A comparison of breeding system and seed physiologies in three species of *Portulaca* L. Ecology. 58:860-868.

[27] Sharifi M, Pouresmael M. 2006. Breaking seed dormancy in *Bunium persicum* by stratification and chemical substances. Asian Journal of Plant Sciences. 5:695-699.

[28] Statistix8. 2003. Statistix8: Analytical software user's manual. Tallahassee, Florida.

[29] Nadjafi F, Bannayan M, Tabrizi L, Rastgoo M. 2006. Seed germination and dormancy breaking techniques for *Ferula gummosa* and *Teucrium polium*. Journal of Arid Environment. 64:542-547.

[30] Bhattacharya J, Khuspe SS, 2001. *In vitro* and *in vivo* germination of papaya (*Carica papaya* L.) seeds. Scientia Horticultureae 91:39-49.

[31] Nikolic R, Mitic N, Miletic R, Neskovic M, 2006. Effects of cytokinins on *in-vitro* seed germination and early seedling morphogenesis in *Lotus corniculatus* L. Plant Growth Regulators. 25:187-194.

[32] Sakakibara, H. 2006. Cytokinins: activity, biosynthesis, and translocation. Annual Review of Plant Biology. 57:431–449.

[33] Werner T, Schmulling T, 2009. Cytokinin action in plant development. Current Opinion in Plant Biology. 12: 527–538.

[34] Van Staden J, Olatoye, ST, Hall MA, 1973. Effect of light and ethylene on cytokinin levels in seeds of *Spergula arvensis*. Journal of Experimental Botany. 24:662.

[35] Khan AA. 1971. Cytokinins: Permissive role in seed germination. Science. 171:853-859.

[36] Litwack G. 2005. Plant Hormones (ED). Academic Press, Californa, USA.

[37] Yang QH, Ye WH, Yin XJ. 2007. Dormancy and germination of *Areca triandra* seeds. Scientia Horticulture Amsterdam. 113:107-111.

[38] Roychowdhury R, Mamgain A, Ray S, Tah J. 2012. Effect of gibberellic acid, Kinetin and Indole 3-Acetic acid on seed germination performance of *Dianthus caryophyllus* (Carnation) Agriculturae Conspectus. Scientificus. 77:157-160.

[39] Nonogaki H, Bassel GW, Bewley JD. 2010. Germination-still a mystery. Plant Science. 179:574-581.

[40] Bewley JD, Black M, Halmer P. 2006. The encyclopedia of seeds: science, technology and uses. Wallingford, UK: CABI.

[41] El-Dengawy, ER. 2005. Promotion of seed germination and subsequent seedling growth of loquat (*Eriobotrya japonica* (Thunb.) Lindl.) by moist-chilling and GA_3 applications. Scientia Horticulture. 105:331-342.

[42] Sondheimer E, Galson EC. 1966. Effects of abscisin II and other plant growth substances on germination of seeds with stratification requirements. Plant Physiology. 41:1397-1398.

[43] Siobhan MB, McCourt. 2003. Hormone cross-talk in seed dormancy. Journal of Plant Growth Regulators. 22:25-31.

[44] Joshi M, Dhar U. 2003. *In vitro* propagation of *Saussurea obvallata* (DC.) Edgew. An endangered ethnoreligious medicinal herb of Himalaya. Plant Cell Reports. 21:933-939.

[45] Vandelook F, Bolle N, Van Assche JA. 2007. Multiple environmental signals required for embryo growth and germination of seeds of *Selinum carvifolia* (L.) L. and *Angelica sylvestris* L. (Apiaceae). Seed Science Research. 17:283-291.

[46] Copeland LO, McDonald MB. 2001. Principles of seed science and technology. Kluwer Academic Publisher.

http://www.pjbs.org

PJBS

ISSN 1028-8880

Pakistan Journal of Biological Sciences

ANSInet
Asian Network for Scientific Information
308 Lasani Town, Sargodha Road, Faisalabad - Pakistan

Pakistan Journal of Biological Sciences 18 (1): 19-26, 2015
ISSN 1028-8880
© 2015 Asian Network for Scientific Information

ansinet
Asian Network for Scientific Information

RESEARCH ARTICLE OPEN ACCESS

DOI: 10.3923/pjbs.2015.19.26

Changes in Protein Expression in Peanut Leaves in the Response to Progressive Water Stress

[1]Chutipong Akkasaeng, [2]Natpapath Tantisuwichwong, [1]Ni-on Ngamhui, [3]Sittiruk Roytrakul, [1]Sanun Jogloy and [1]Aran Pathanothai
[1]Department of Plant Science and Agricultural Resources, Faculty of Agriculture,
[2]Department of Biology, Faculty of Science, Khon Kaen University, Khon Kaen, 40002, Thailand
[3]Genome Institute, National Center for Genetic Engineering and Biotechnology, 113 Thailand Science Park, Phahonyothin Road, Pathumthani, 12120, Thailand

ARTICLE INFO

Article History:
Received: December 04, 2014
Accepted: January 06, 2015

Corresponding Author:
Chutipong Akkasaeng,
Department of Plant Science and Agricultural Resources,
Faculty of Agriculture,
Khon Kaen University, Khon Kaen, 40002, Thailand

ABSTRACT

This investigation was carried out at the Department of Plant Science and Agricultural Resources, Khon Kaen University in the rainy season of 2011. The objective of this study was to identify proteins in leaves of drought-susceptible peanut plants when regulated by progressive water stresses. The drought-susceptible peanut plants of Khon Kaen 4 cultivar were grown in pots under controlled environment. At day 30 after seed emergence, the plants were subjected to stress conditions for 5 and 6 days. The results showed that withheld water supply for 5 and 6 days gave moderately and severely water stresses, respectively. Under moderate water stress conditions, two up-regulated and eight down-regulated proteins were attained. The up-regulated proteins were striated fibre assembling and flap endonuclease 1. The down-regulated proteins were peptidyl-prolyl cis-trans isomerase FKBP4, tRNA(Ile)-lysidine synthase, chloroplastic, chloroplastic thioredoxin F-type, cytidinedeaminase 7, ALF domain class transcription factor, nudix hydrolase 8, pentatricopeptide repeat super-family protein, putative and ribulose-1,5-bisphosphate carboxylase/oxygenase, a large sub-unit. Under severe water stress conditions, two proteins, i.e., tRNA(Ile) lysidine synthase, chloroplastic and ALF domain class transcription factor did not change their relative abundance significantly where it indicated drought acclimation. The remaining proteins displayed significant changes and the changes were the same as those found in the peanut leaves when deprived water for 5 days. Up-regulated proteins are responsible for alleviating oxidative damages to plant genome and mediating plants responsive to the environmental factors in providing mechanical support, barriers and a rapid transport route. Down-regulated proteins were associated with drought susceptibility of the Khon Kaen 4 peanut plants.

Key words: Peanut, water stress, 2-DE, plant proteome, mass spectrometry

INTRODUCTION

Peanut or groundnut (*Arachis hypogaea*) is one of the most important leguminous crops where matured seeds in pods provide edible oil and protein for human consumption. It is widely grown in the tropics and sub-tropics mainly under rain-fed conditions where drought conditions frequently occur. It has been advocated that when stress conditions occur at a critical growth stage it may result in a drastic reduction or even a failure in crop production (Wright and Nageswara Rao, 1994). Most crop plants possess some mechanisms to avoid drought stress conditions by maximizing water uptake as well

as minimizing water loss. Maximization of water uptake occurs when more assimilates are invested in root proliferation at its depths where water is available. Water loss could be minimized by several mechanisms e.g., a partial closure of stomata in reducingthe absorption of light energy through the rolling leaves and the increasing reflectance ofa dense layer of trichomes, and the reduction in leaf areas, and a rapid senescence of the older leaves (Lopes *et al*., 2011; Marshall *et al*., 2012). Stomata limitation took place during water deficit stress condition could be effectively resulted in a reduction of photosynthetic CO_2 assimilation. As a consequence, the requirement for ATP and NADPH in photosynthetic carbon reduction cycle or Calvin Cycle declines considerably. Light absorption exceeds the capacity for its utilization in the carbon assimilatory reactions and excessive light energy will eventually lead to the production of Reactive Oxygen Species (ROS). The ROS includes superoxide ($O_2^{\bullet -}$), hydrogen peroxide (H_2O_2), hydroxyl radicals ($HO^{\bullet}$), and singlet oxygen ($^1O_2$) as reported by Asada (2006). The ROS accumulation during stress condition greatly depends on the balance between the ROS production and the ROS scavenging. Production and the removal of the ROS must be tightly regulated. However, the equilibrium between production and scavenging of the ROS may be perturbed by a number of the adverse environment stresses including drought conditions. When the level of the ROS exceeded the defense mechanisms, a cell is said to be in a state of oxidative stress. The ROS induces a broad range of DNA damage, including base and nucleotide modifications, especially in the sequences under the high guanosine content, and may even cause strand breaks. It is well documented that oxygenated nucleotides like 8-oxo-guanine can cause the accumulation of hydroxyl radicals ($HO^{\bullet}$). The 7,8-dihydro-8-oxoguanine (GO) is a common oxidative DNA lesion generated by a direct modification via the reactive oxygen species. The GO lesions are and can mispair with adenine during the DNA replication (Tuteja *et al*., 2001). The ROS may cause modification of proteins and some are direct and others are indirect. The direct modification involves alteration of a protein's activity through nitrosylation, carbonylationdisulphide bond formation and glutathionylation. Proteins can be modified indirectly by the conjugation with its breakdown products of fatty acid peroxidation. As a consequence of an excessive amount of the ROS production, it establishes hessite-specific amino acid modification, fragmentation of the peptide chain, aggregation of cross-linked reaction products and alteration of electric charge and an increase in susceptibility of proteins to proteolysis (Sharma *et al*., 2012). It revealed that maintaining proteins in their native conformation, it could prevent the aggregation of non-native proteins, refolding of denatured proteins to their functional conformation and the removal of damaged proteins and polypeptides are all critical for cell survival under water deficit stress conditions (Vierstra, 1993).

As sessile organisms, the plants must cope up with their ever changing environmental conditions in order to survive, the plants must have evolved upon its elaborate mechanisms to perceive with a rapidly respond to a diverse range of biotic stresses. Sensing of the environmental stresses may occur after its stress perception. The plants commonly perceive the stresses by plasma membrane located within the receptors, intracellular or cytoskeleton-associated proteins. The stress perception is transmitted using the signaling cascades taken into the altered gene expression programmes and ultimately resulting in both metabolic adjustment and the altered physiological responses (Osakabe *et al*., 2013). Under oxidative stress, the plants may have its strategies to minimize the ROS generation or maximize detoxification of the overwhelm production of the ROS. A strict control of the ROS levels is very important in preventing their toxicity and to ensure an accurate operation of their signaling functions. In chloroplasts, copper/zinc superoxide (Cu/ZnSOD) causes the dis-mutation of the superoxide radicals into hydrogen peroxide and the ascorbate peroxidase (APX) catalizes the conversion of the H_2O_2 to water. In this process, ascorbate (AsA) is oxidized to mono dehydroascorbate radical (MDA), which is regenerated to the AsA by either reducing the ferredoxin or by NAD (pH), which catalysed by an MDA reductase (MDAR). Dehydroascorbate (DHA) is produced when the MDAR was not able to reduce the MDA to AsA. The DHA is then reduced to the AsA by the DHA reductase (DHAR) using a reduced GSH as an electron donor. Peroxiredoxins(PrxRs) together with the Thioredoxin (Trx) can also provide antioxidative protection enabling the detoxification of the photochemically produced H_2O_2 in the chloroplasts (Miller *et al*., 2008). The PrxRs and trxplayits possessed important roles during the drought and oxidative stress conditions. The SODs are the only plant enzymes capable of scavenging $O_2^{\bullet -}$, whereas the H_2O_2 can be catabolized directly by catalases (CATs) or by Ascorbate Peroxidases (APX), peroxiredoxins, Glutathione Peroxidases (GPX) and the heterogenous group of the guaiacol peroxidases (Gechev and Hille, 2005).

Proteins often mis-fold under the stressful environments and the mis-folded proteins are highly deleterious to the cell because they can form non-physiological interactions with other proteins (Chen *et al*., 2010). Repair proteins called chaperones can, in many instances, restore the native conformation of the wrongly folded proteins. Molecular chaperones are responsible for protein folding, assembly translocation and degradation in a broad array of normal cellular processes.They also function in the stabilization of proteins and membranes, and can assist in protein refolding under stress conditions (Wang *et al*., 2004). The changes in a relative expression of proteins occurred under water stress (Riccardi *et al*., 1998) and the changes are highly variable depending on genotypes of the crop plants. The up or down regulated proteins are associated with drought sensitive or drought tolerant varieties of the crop plants (Benesova *et al*., 2012). However, the changes in abundance of the proteins under different magnitudes of water deficit are not well

documented. The objective of this study was to identify proteins being regulated by the different levels of water stress and relate them to the susceptibility of peanut variety of Khon Kaen 4 to drought stress conditions.

MATERIALS AND METHODS

A drought susceptible variety of peanut crop viz., Khon Kaen 4 cultivar was grown in the composted pots and kept in a Climate Simulator (Model 630, Contherm Scientific Ltd., New Zealand) under controlled environments. On day 30 after seed emergence, water stress was imposed to the plants by withholding water for 5 and 6 days, whilst the plants of the control treatment were adequately supplied with the water. For this experiment, water status of soils and plants was determined. Fully expanded leaflets of the plants in the experiment under both water stress and adequate water supply conditions were harvested. They were frozen in liquid nitrogen and kept at -80°C for a few days and then extraction and separation of proteins were taken place. The leaflets of the plants supplied with adequate water and under water stress for 5 and 6 days were used for protein extraction and separation using two-dimensional gel electrophoresis with the method described by Akkasaeng *et al.* (2007). The proteins were separated in three replicated gels and the proteins in twelve gels were resolved. The proteins were visualized by the silver nitrate staining with the use of the methods described by Heukeshoven and Dernick (1985).

Image analysis: Analyses of gels were performed using ImageMaster 2D Platinum 7.0 (GE Healthcare). Two reference spots with iso-electric point (pI), molecular weight (M_r) of 5.21, 40 and 5.78, 43 were assigned for pI and M_r of all the remaining proteins in each gel were estimated by ImageMaster 2D Platinum 7. Volume parameter was used to indicate the relative abundance of the proteins. Protein spots in six gels were matched and the volume means of the protein spots under water-stress and non-stress conditions were compared. The up-regulated proteins were indicated when the volume means were greater when under stress condition whereas the down-regulated was assigned when their volume means were reduced under stress conditions. Three-dimensional views of the proteins were visualized to provide the supporting evidence for the up or down-regulated proteins. For mass spectrometry analysis, an additional of 2-D gels was provided and the proteins contents were stained with the use of the Coomassie Brilliant Blue G-250 (GelCode™ blue stain reagent, Pierce Biotechnology, USA).

Protein digestion and MALDI-TOF analysis

Chemicals: Acetonitrile (ACN) of LC/MS grade was taken from the J.T. Baker chemicals. A chemical of α-cyano-4-hydroxy-cinnamic acid (HCCA) was taken from the Bruker Daltonik GmbH. Whilst the Trifluor acetic acid peptide (TFA), a sequencing grade was obtained from the Applied Biosystems.

Protein digestion: Proteins spots regulated by water stress were excised from the gels. Proteins were digested in the gel plugs following the methods described by Shevchenko *et al.* (2007). Briefly, proteins in the gel plugs were reduced with a 10 mM DTT in a 100 mM ammonium bicarbonate for 1 h at 56°C and alkylated with a 100 mM iodoacetamine in a 100 mM ammonium bicarbonate for 1 h in the dark at room temperature. The protein in each excised gel was rehydrated in a 20 μL of a 12.5 μg mL^{-1} trypsin in a 100 mM ammonium bicarbonate for 20 min in an ice bath. The in-gel tryptic digestion was carried out at 37°C overnight. The resulting peptides were extracted three times with a 50 μL 0.1% trifluoroacetic acid and a 50% acetonitrile for 20 min each. The pooled extracted samples were then evaporated to its dryness. The dried peptides were dissolved in a 3 μL of 0.1% trifluoroacetic acid.

MALDI TOF analysis: For the preparation of matrix solution, HCCA was saturated in the TA (ACN:0.1% TFA, 1:2). Tryptic peptide sample was mixed with an equal volume of a matrix solution and deposited onto an AnchorChip target plate (Bruker-Daltonics). Cocrystallization of the matrix and sample occurred at ambient temperature. The mass spectra were recorded using a reflector viz., Bruker reflex V (Bruker Daltonik GmbH), a delayed extraction the MALDI-TOF mass spectrometer was equipped with a 2 GHz LeCroy digitizer and a 337 nm N_2laser. The acceleration voltage was 25 kV for the IS1 and 20.2 kV for the IS2. A total of 100 laser shots from three to five different positions were summed up for each peptide sample. The peptide data were acquired using the Flex Analysis software (Bruker Daltonics).

Data bases searching: The peptide data was searched and formulated using the MASCOT software (www.matrixscience.com). Two data bases, i.e., Swiss Prot and NCBInr were used. For the MASCOT search value, a peptide tolerance was ±1.2 to 1.8 Da allowing a maximum of 1 missed cleavage by trypsin. Fixed modification and variable modification were carbamidomethylation of cysteine and an oxidation of methionine, respectively. Identified proteins had its MASCOT scores with probability $p<0.05$.

RESULTS

Withholding water supply for 5 and 6 days severely affected Leaf Water Potential (LWP) as compared with the controlled treatment. The LWPs for the non-stressed and stressed plants under the withholding water supply for 5 days were -0.20 and -0.42 MPa, respectively. On day 6 of the withholding water supply, the LWPs in the non-stressed and stressed plants were -0.23 and -1.11 MPa, respectively (Table 1). On day 5 of the withholding water supply, there were some significant differences in Relative Water Contents (RWC) between the non-stressed and the stressed plants. After the withholding water supply for 5 days, the percentages of the RWCs were 93.7 and 69.4%, respectively. With the

withholding water supply for 6 days, the result showed that the RWC values for the non-stressed and stressed plants were 94.1 and 61.1%, respectively (Table 1).

Reproducibility of the gels and regulated proteins by water stress: Protein spots were clearly resolved and proteomic maps were very similar across the 6 gels using the proteins from leaves of the plants with adequate water supply and water stress for 5 and 6 days (Fig. 1). The total of 1,092 and 1,600 protein spots were reproducibly detected in leaf proteomes of the peanut plants with adequate water supply and those subjected to water stress for 5 days. Withholding water supply for 5 days resulting in some significant changes in a relative abundance of 98 proteins, 43 protein spots of the up-regulated and 55 for the down-regulated. In the controlled and the water-stressed plants for 6 days, 545 and 740 protein spots were attained from the peanut leaves. Water deficit stress conditions caused significant changes in a relative abundance of 71 proteins; 16 showing an increase in a relative abundance and 55 shown a decrease in a relative abundance. However, only 8 down-regulated and 2 up-regulated were identified (Table 2 and Fig 1). For proteomes of the peanut leaves under water stress for 5 days, the relative abundances of the down-regulated proteins were between 0.47 and 5.24 and the magnitudes of the changes were between 1.4 and 2.6. The relative abundances of the up-regulated proteins were 1.1 and 0.63 and the magnitudes of the changes were 1.5 and 1.3, respectively (Fig. 2 and Table 2). The down-regulated proteins include peptidyl-prolyl cis-trans isomerase FKBP4(D1), tRNA(Ile)-lysidine synthase, chloroplastic (D2), thioredoxin F-type, chloroplastic (D3), cytidine deaminase 7(D4), ABI3-like factor (ALF) domain class transcription factor (D5), nudix hydrolase 8 (D6), pentatricopeptide, a repeat super-family protein, putative (D7), ribulose-1,5-bisphosphate carboxylase/oxygenase, a large sub-unit (D8). Two up-regulated proteins are striated fibre assembling (SF-assembling, U1) and the Flap endonuclease 1(U2) where they are clearly shown in Table 2. On day 6 after

Table 1: Leaf water potential and relative water contents of the peanut plants under water stress conditions for 5 and 6 days compared with the plants of adequate water supply. Stress conditions took place at day 30 after seed emergence

Duration of water stress	Leaf water potential (MPa)	Relative water content (%)
5 days		
Adequate water supply	-0.20 (+0.02)	93.7 (+0.1)
Water stress	-0.42 (+0.03)	69.4 (+0.3)
6 days		
Adequate water supply	-0.23 (+0.02)	94.1 (+0.2)
Water stress	-1.11 (+0.04)	61.1 (+0.3)

Figures in the blankets represent Standard errors of means

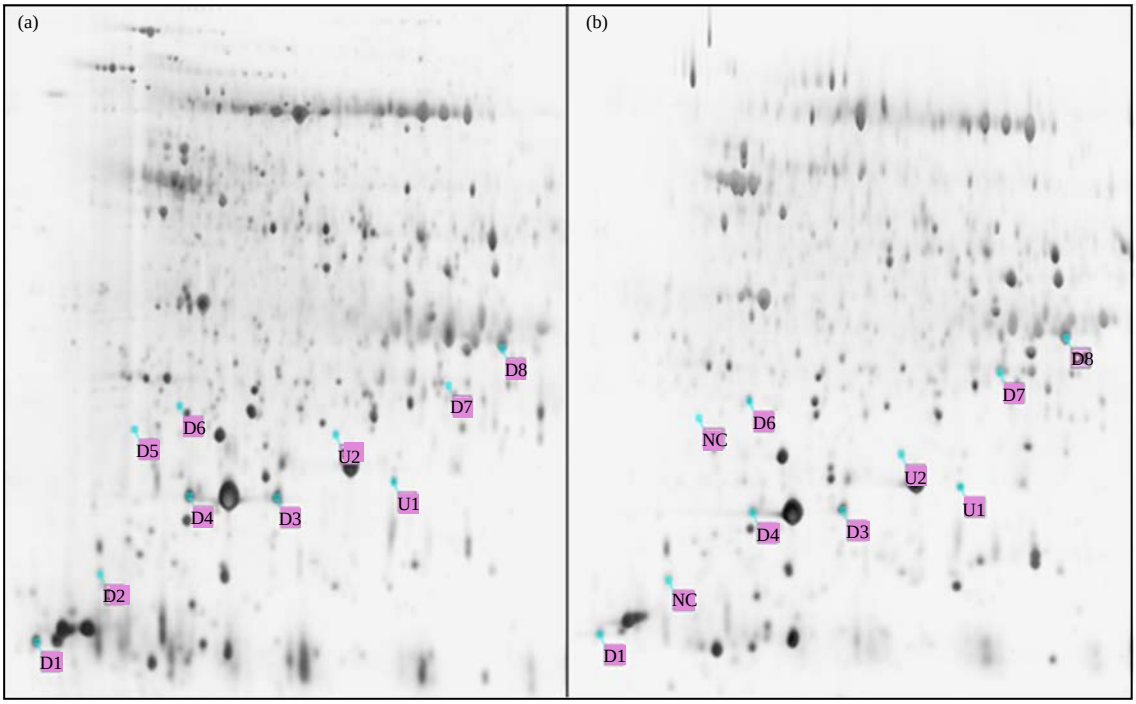


Fig. 1(a-b): Distributions of proteins in leaves of the Khon Kaen 4 peanut plants being regulated by water stress conditions. Proteins were separated using leaves of the peanut plants when under stress for (a) 5 days and (b) 6 days. D: Down-regulated, U: Up-regulated, NC: Non-change. The stress condition was taken place at day 30 after seed emergence

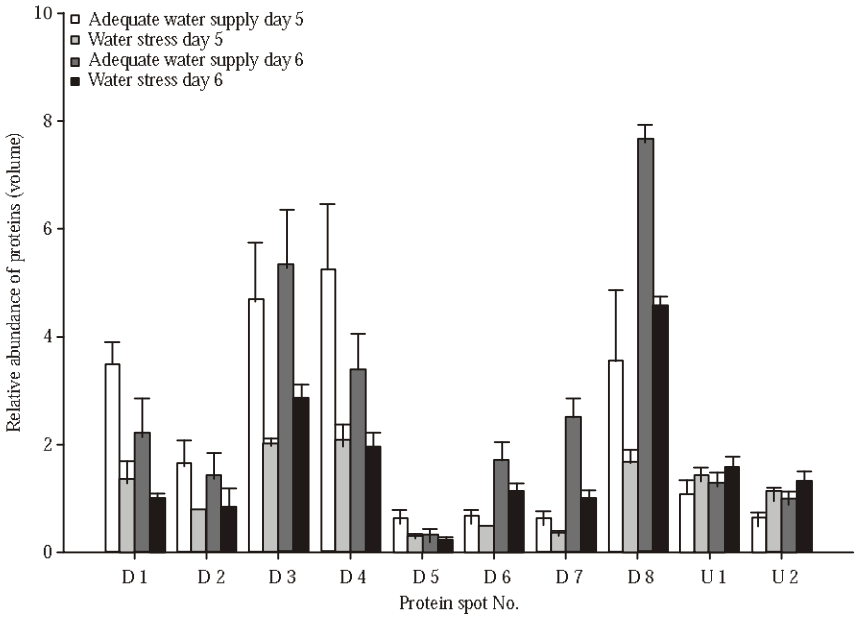


Fig. 2: Relative abundance of proteins of the peanut leaves being influenced by water stress for 5 and 6 days. Water stress commenced at day 30 after seed emergence. D: Down-regulated, U: Up-regulated. Vertical lines represent standard errors of means

Table 2: Spot numbers of the proteins in the peanut leaves as influenced by water deficit when stress conditions took place at day 30 after seed emergence

			Magnitude of change (days)						M_r (kDa)/pI	
Spot No.	Homologous proteins	Organism	5	6	Accession No[a]	Score[b]	Cov[c] (%)	Probability[d]	Theo[e]	Exp[f]
D1	Peptidyl-prolyl cis-trans isomerase FKBP4	*Triticum urartu*	2.6	2.2	EMS65417	85	31	0.005	23.03/8.23	28/4.32
D2	tRNA(Ile)-lysidine synthase, chloroplastic	*Chaetosphaeridium globosum*	2.1	NC	Q8M9Y1	69	29	0.004	40.65/9.9	33/4.62
D3	Thioredoxin F-type, chloroplastic	*Spinacia oleracea*	2.3	1.9	P09856	58	42	0.059	21.24/9.17	40/5.44
D4	Cytidine deaminase 7	*Arabidopsis thaliana*	2.5	1.7	Q9SU87	58	37	0.051	34.22/8.48	40/5.03
D5	ALF domain class transcription factor	*Malus domestica*	2.0	NC	ADL36572	74	26	0.065	47/4.77	74/27.34
D6	Nudix hydrolase 8	*Arabidopsis thaliana*	1.4	1.5	Q8L7W2	60	30	0.039	41.63/6.37	50/4.99
D7	Pentatricopeptide repeat superfamily protein, putative	*Theobroma cacao*	1.8	2.5	XP-007021301	76	15	0.047	84.56/7.14	51/6.24
D8	Ribulose-1,5-bisphosphate carboxylase/oxygenase large subunit	*Lantana camara*	2.1	1.7	AAF22242	79	43	0.022	53.49/6.2	57/6.49
U1	SF-assemblin	*Dunaliella bioculata*	1.3	1.2	P54214	60	23	0.037	31.51/5.41	41/5.98
U2	Flap endonuclease 1	*Ostreococcus tauri*	1.8	1.3	Q013G9	66	40	0.008	43.08/8.94	46/5.71

D: Down-regulated, U: Up-regulated , [a]Accession No: Accession number according to NCBI database, [b]Score, Individual ions, scores indicate identity or extensive homology ($p<0.05$), [c]Cov: Sequence coverage, [d]Probability: Significant homology, [e]Theo: Theoretical, [f]Exp: Experimental, Mr: Molecular weight, pI: Isoelectric point

the withholding water supply, only 7 proteins displayed significant changes. The relative abundance of the proteins was between 1.2 and 5.3 and the magnitudes of the changes were between 1.2 and 2.7 (Fig. 2 and Table 2). Two proteins, i.e., tRNA(Ile)lysidine synthase, chloroplastic (D2) and ALF domain class transcription factor (D5) did not change their relative abundance significantly when under water stress, whilst the remaining proteins displayed significant changes and the changes were the same as those found in the peanut leaves with the deprivation of the water for 5 days (Fig. 2 and Table 2).

DISCUSSION

Withholding water supply created severely water stresses in the Khon Kaen 4 peanut plants. Water stress appeared to be

moderate under 5-day duration but severely found at 6 days of water deprivation which were indicated by the LWPs and RWCs. Under different intensities of the water stresses, there were evidences shown on the differences in the patterns of protein expressions. Under a moderate water stress, there were 43 up and 55 down-regulated proteins. The up-regulated proteins may help to alleviate damages caused by the water deficit and the 55 down-regulated may be associated with the susceptibility of the Khon Kaen 4 peanut plants to water stress conditions. A severe water stress had caused a large decline in numbers of the up-regulated proteins down to 16 proteins, whilst maintaining 55 down-regulated proteins. A severe water stress may have caused a reduction in the up-regulated proteins that may act as the protection mechanisms against damages caused by the water deficit stress conditions.

Roles of the up-regulated proteins by water stress: The ROS causes the DNA base damage and the destruction of the deoxyrobose residues producing chain breaks (Bray and West, 2005). Flap endonuclease 1 (FEN1) occurred as a high-abundant protein with a relative abundance of 1.3 under water stress (Fig. 2). The flap endonuclease has its significant role in DNA repairing by the removal of the DNA damage and the alternate base-excision repair pathways. The DNA repair is essential for maintaining genome stability (Hosfield *et al*., 1998). The up-regulation of the FEN1 could possibly provide protective mechanisms against oxidative damages to the plant genomes under water stress conditions.

Striated Fibre assembling (SF assembling) is the major component of the Striated Microtubule-Associated Fibres (SMAFs) in the flagellar basal apparatus of the green flagellates (Lechtreck *et al*., 2002). Although structures and functions of the SMAFs have been well characterized in the Chlamydomonas reinhardtii (Silflow and Lefebvre, 2001), the roles of these proteins in the higher eukaryotic organisms are somewhat poorly understood. Since the SMAFs are associated with the structural constituents of the cytoskeletons, the proteins may function in mediating the plants in responding to the environmental factors where it provides mechanical support, barriers and the rapid transport routes (Wasteneys, 2004). An increase in the relative abundance of the SF assembling may help to trigger the rapid responses against water stress and to maintain a cellular integrity under water stress and also to alleviate damages from the cellular dehydration.

Down regulated proteins and protein synthesis: ALF domain class transcription factor (D5) is a B3 domain-containing the transcription factor that activates specific ABA-dependent gene expressions. The ALF potentiates chromatin for transcription by mediating histone modifications (Chinnusamy *et al*., 2008). The ABA triggers the assembly of the ABA signaling cascade components leading to the recruitment of the RNA Pol II and GTFs. Both the ALF and ABA are required for specific gene expressions (Ng *et al*., 2006). Water stress may have some adverse effects on specific gene expression due to down-regulation of the ALF domain class transcription factor (D5). However, under a severe water stress condition, this protein did not display a significant change suggesting an acclimated response of the protein to its progressive water stress.

Putative Pentatricopeptide Repeat (PPR) proteins (D7) are in one of the largest families in the plants. The PPR proteins are involved in the RNA processing including editing, maturation, stability, and translation in the plant organelles. The PPR proteins may act as the transacting factors and facilitate the recruitment of other factors for the RNA processing and translation (Saha *et al*., 2007). The down regulation of the PPR protein may perturb RNA processing and translation where it could be critical for the cellular processes.

Chloroplastic tRNA(Ile)-lysidine synthase (D2) converts both the codon specificity of the tRNA(Ile) from the AUG to AUA and its amino acid specificity from methionine to isoleucine (Suzuki and Miyauchi, 2010). The enzyme will definitely modify the amino acid composition of the targeted proteins. However, the involvement of this enzyme under drought stress responses is poorly documented. This protein did not change a relative abundance under a severe water stress.

Cytidine deaminase catalyzes the hydrolyric deamination of cytidine into uridine. The higher plants use cytidine deaminase as editing systems in the conversion of the Cs to the Us in the edited RNAs. In the RNA editing, it occurs mainly in the mitochondria and plastids (Shikanai, 2006). The RNA editing is essential as to express functional proteins but it can also create an initiation or stop codon or remove a stop codon. The editing occurs in the introns and the untranslated regions which may play a significant role in increasing transcript stability (Chateigner-Boutin and Small, 2010; Grennan, 2011). A decline in the abundance of cytidine deaminase 7(D4) may decrease the activity of the RNA editing leading to the production of the non-functional proteins that could be detrimental to cellular processes.

The FK506-binding proteins (FKBPs) belong to the large family of the peptidyl-prolyl cis-transisomerases (PPIases), which catalyses protein folding by accelerating the slow step of the cis-trans isomerisation of the peptidyl-prolyl bonds. The plants of the FKBP also function as molecular chaperone, independently of its peptidylprolyl cis-trans isomerase (Kurek *et al*., 2002). The expression of the genes encoding the FKBPs is regulated by the water stress phenomena (Yu *et al*., 2012). The down-regulation of the peptidyl-prolyl cis-trans isomerase FKBP4 (D1) may adversely affect protein folding during water stress condition and that the damaged proteins could not be recovered under the water stress condition where it rendering this peanut variety to be susceptible to water stresses.

Photosynthesis and oxidative stressunder water stress conditions: Photosynthetic capacity of plants invariably decreases during the drought stress conditions (Chaves *et al*., 2009). Ribulose-1,5-bisphosphate carboxylase/oxygenase

(Rubisco) of a large sub-unit (LS-D8) is a key enzyme responsible for the CO_2 fixation during the photosynthetic process. This protein presents in a large amount with a relatively abundance of 3.5 and 7.6 under an adequate water supply on days 5 and 6 after imposing water stress, respectively. The relative amount of the protein decreased by 2.1 and 1.7 folds under the withholding of water supply for 5 and 6 days, respectively (Fig. 2 and Table 1). The effect of drought conditions on the amount of the Rubisco is somewhat contradictory. Withholding water supply for 3, 6 and 9 days resulted in the progressive declines in photosynthetic rates but have caused to increase amount of the Rubisco LS (Kamal *et al*., 2013). However, the content of the Rubisco LS decreased to 50-75% in the drought stressed leaves of both drought-tolerant and drought sensitive varieties (Demirevska *et al*., 2009). A reduction in the amount of the Rubisco LS in this current experiment may suggest that a decline in photosynthetic capacity of the peanut plants under water stress may be associated with the drought susceptibility of the peanut plants.

Chloroplastic thioredoxins (TRX) F-type must have involved in the regulation of the key carbon-fixation enzymes that are mostly inactive in the dark and activated by the TRXs underillumination (Schurmann and Jacquot, 2000). The lower abundance of the chloroplastic thioredoxin F-type (D3) in the peanut leaves may be attributable to the decreased amount of the activated key enzymes in the carbon fixation process and the photosynthetic capacity of leaves (Yoshida *et al*., 2014).

Nudix (nucleoside diphosphates linked to moiety X) hydrolases play a vital role in the cellular homeostasis by catalyzing the hydrolysis of a variety of nucleoside diphosphate derivatives. ZmNUDX8 (*Zea mays* NUDX8) and AtNUDX2 (*Arabidopsis thaliana* NUDX2) belong to the ADP-ribose pyrophosphatase (ADPR) sub-family (Huang *et al*., 2012). The AtNUDX2 expression could have been induced by salt and drought stress conditions. An over expression of the AtNUDX2 resulted in enhancing tolerance to the oxidative stress by maintaining the NAD^+ and ATP levels (Ogawa *et al*., 2009). The down-regulation of the Nudix hydrolase 8 (D6) in the peanut leaves under water stress conditions may have lowered the capacity of the antioxidant systems to cope up with any oxidative stress conditions.

ACKNOWLEDGMENT

The authors are gratefully appreciated the financial supports provided by the Senior Research Scholar Project of Professor Dr. Aran Pathanothai under the Thai Research Funds and the National Research Council of Thailand.

REFERENCES

Akkasaeng, C., N. Tantisuwichwong, I. Chairam, N. Prakrongrak, S. Jogloy and A. Pathanothai, 2007. Isolation and identification of peanut leaf proteins regulated by water stress. Pak. J. Biol. Sci., 10: 1611-1617.

Asada, K., 2006. Production and scavenging of reactive oxygen species in chloroplasts and their functions. Plant Physiol., 141: 391-396.

Benesova, M., D. Hola, L. Fischer, P.L. Jedelsky and F. Hnilicka *et al*., 2012. The physiology and proteomics of drought tolerance in maize: Early stomatal closure as a cause of lower tolerance to short-term dehydration? PLoS One, Vol. 7. 10.1371/journal.pone.0038017

Bray, C.M. and C.E. West, 2005. DNA repair mechanisms in plants: Crucial sensors and effectors for the maintenance of genome integrity. New Phytologist, 168: 511-528.

Chateigner-Boutin, A.L. and I. Small, 2010. Plant RNA editing. RNA Biol., 7: 213-219.

Chaves, M.M., J. Flexas and C. Pinheiro, 2009. Photosynthesis under drought and salt stress: Regulation mechanisms from whole plant to cell. Ann. Bot., 103: 551-560.

Chen, B., M. Retzlaff, T. Roos and J. Frydman, 2010. Cellular strategies of protein quality control. Cold Spring Harbor Perspect. Biol. 10.1101/cshperspect.a004374

Chinnusamy, V., Z. Gong and J.K. Zhu, 2008. Abscisic acid-mediated epigenetic processes in plant development and stress responses. J. Integr. Plant Biol., 50: 1187-1195.

Demirevska, K., D. Zasheva, R. Dimitrov, L. Simova-Stoilova, M. Stamenova and U. Feller, 2009. Drought stress effects on Rubisco in wheat: Changes in the Rubisco large subunit. Acta Physiol. Plant, 31: 1129-1138.

Gechev, T.S. and J. Hille, 2005. Hydrogen peroxide as a signal controlling plant programmed cell death. J. Cell. Biol., 168: 17-20.

Grennan, A.K., 2011. To thy proteins be true: RNA editing in plants. Plant Physiol., 156: 453-454.

Heukeshoven, J. and R. Dernick, 1985. Simplified method for silver staining of proteins in polyacrylamide gels and the mechanism of silver staining. Electrophoresis, 6: 103-112.

Hosfield, D.J., C.D. Mol, B. Shen and J.A. Tainer, 1998. Structure of the DNA repair and replication endonuclease and exonuclease FEN-1: Coupling DNA and PCNA binding to FEN-1 activity. Cell, 95: 135-146.

Huang, H., H. Cao, Y. Niu and S. Dai, 2012. Expression analysis of nudix hydrolase genes in *Chrysanthemum lavandulifolium*. Plant Mol. Biol. Rep., 30: 973-982.

Kamal, A.H.M., K. Cho, J.S. Choi, Y. Jin, J.S. Park, J.S. Lee and S.H. Woo, 2013. Patterns of protein expression in water-stressed wheat chloroplasts. Bioligia Plantalum, 7: 305-312.

Kurek, I., F. Pirkl, E. Fischer, J. Buchner and A. Breiman, 2002. Wheat $FKBP_{73}$ functions *in vitro* as a molecular chaperone independently of its peptidyl prolyl cis-trans isomerase activity. Planta, 215: 119-126.

Lechtreck, K.F., J. Rostmann and A. Grunow, 2002. Analysis of *Chlamydomonas* SF-assemblin by GFP tagging and expression of antisense constructs. J. Cell Sci., 115: 1511-1522.

Lopes, M.S., J.L. Araus, P.D.R. van Heerden and C.H. Foyer, 2011. Enhancing drought tolerance in C_4 crops. J. Exp. Bot., 62: 3135-3153.

Marshall, A., R.B. Aalen, D. Audenaert, T. Beeckman and M.R. Broadley *et al*., 2012. Tackling drought stress: Receptor-like kinases present new approaches. Plant Cell, 24: 2262-2278.

Miller, G., V. Shulaev and R. Mittler, 2008. Reactive oxygen signaling and abiotic stress. Physiol. Plantarum, 133: 481-489.

Ng, D.W.K., M.B. Chandrasekharan and T.C. Hall, 2006. Ordered histone modifications are associated with transcriptional poising and activation of the phaseolin promoter. Plant Cell, 18: 119-132.

Ogawa, T., K. Ishikawa, K. Harada, E. Fukusaki, K. Yoshimura and S. Shigeoka, 2009. Overexpression of an ADP-ribose pyrophosphatase, *AtNUDX2*, confers enhanced tolerance to oxidative stress in Arabidopsis plants. Plant J., 57: 289-301.

Osakabe, Y., K. Yamaguchi-Shinozaki, K. Shinozaki and L.S.P. Tran, 2013. Sensing the environment: Key roles of membrane-localized kinases in plant perception and response to abiotic stress. J. Exp. Bot., 64: 445-458.

Riccardi, F., P. Gazeau, D. De Vienne and M.M. Zivy, 1998. Protein changes in response to progressive water deficit in maize. Plant Physiol., 117: 1253-1263.

Saha, D., A.M. Prasad and R. Srinivasan, 2007. Pentatricopeptide repeat proteins and their emerging roles in plants. Plant Physiol. Biochem., 45: 521-534.

Schurmann, P. and J.P. Jacquot, 2000. Plant thioredoxin systems revisited. Ann. Rev. Plant Physiol. Plant Mol. Biol., 51: 371-400.

Sharma, P., A.B. Jha, R.S. Dubey and M. Pessarakli, 2012. Reactive oxygen species, oxidative damage and antioxidative defense mechanism in plants under stressful conditions. J. Bot. 10.1155/2012/217037

Shevchenko, A., H. Tomas, J. Havli, J.V. Olsen and M. Mann, 2007. In-gel digestion for mass spectrometric characterization of proteins and proteomes. Nat. Protoc., 1: 2856-2860.

Shikanai, T., 2006. RNA editing in plant organelles: Machinery, physiological function and evolution. Cell. Mol. Life Sci., 63: 698-708.

Silflow, C.D. and P.A. Lefebvre, 2001. Assembly and motility of eukaryotic cilia and flagella. Lessons from *Chlamydomonas reinhardtii*. Plant Physiol., 127: 1500-1507.

Suzuki, T. and K. Miyauchi, 2010. Discovery and characterization of $tRNA^{Ile}$ lysidine synthetase (TilS). FEBS Lett., 584: 272-277.

Tuteja, N., M.B. Singh, M.K. Misra, P.L. Bhalla and R. Tuteja, 2001. Molecular mechanisms of DNA damage and repair: Progress in plants. Crit. Rev. Biochem. Mol. Biol., 36: 337-397.

Vierstra, R.D., 1993. Protein degradation in plants. Ann. Rev. Plant Physiol. Plant Mol. Biol., 44: 385-410.

Wang, W.X., B. Vinocur, O. Shoseyov and A. Altman, 2004. Role of plant heat-shock proteins and molecular chaperones in the abiotic stress response. Trends Plant Sci., 9: 244-252.

Wasteneys, G.O., 2004. Progress in understanding the role of microtubules in plant cells. Curr. Opin. Plant Biol., 7: 651-660.

Wright, G.C. and R.C. Nageswara Rao, 1994. Groundnut Water Relations. In: The Groundnut Crop: A Scientific Basis for Improvement, Smartt, J. (Ed.). Chapman and Hall, London, ISBN: 978-0412408205, pp: 281-325.

Yoshida, K., K. Matsuoka, S. Hara, H. Konno and T. Hisabori, 2014. Distinct redox behaviors of chloroplast thiol enzymes and their relationships with photosynthetic electron transport in *Arabidopsis thaliana*. Plant Cell Physiol., 55: 1415-1425.

Yu, Y., H. Zhang, W. Li, C. Mu, F. Zhang, L. Wang and Z. Meng, 2012. Genome-wide analysis and environmental response profiling of the FK506-binding protein gene family in maize (*Zea mays* L.). Gene, 498: 212-222.

Available online at www.derpharmachemica.com

Scholars Research Library

Der Pharma Chemica, 2015, 7(11):57-63
(http://derpharmachemica.com/archive.html)

ISSN 0975-413X
CODEN (USA): PCHHAX

The synergic retardation effects of both total capsaicinoids and phenolic extracts from some hot chilli peppers on the autooxidation kinetics of oxymyoglobin

Chatrachatchaya Choichayapong[1], Warunee Thongdee[1], Weeranuch Khottawong[1], Suchila Techawongstien[2] and Saksit Chanthai[1,*]

[1]*Department of Chemistry and Center of Excellence for Innovation in Chemistry, Faculty of Science, Khon Kaen University, Khon Kaen, Thailand*
[2]*Department of Plant Science and Agricultural Resources, Faculty of Agriculture, Khon Kaen University, Khon Kaen, Thailand*

ABSTRACT

Both of total capsaicinoids and phenolic compounds were extracted from hot chilli pepper by magnetic stirring method using 90% methanol (at 60℃ for 2 h) and 90% acidified (0.05% HCl) methanol (at ambient temperature) as the extraction solvents, respectively. The capsaicinoids contents in the extract of eight chilli samples were found in the range of 63.76-106.6 mg/g DW with some residual phenolics containing of 16.56-21.91 mg/g DW. For total phenolics extraction, the phenolic contents were almost found in the range of 27.99-39.03 mg/g DW, but the ranges of capsaisinoids still resembled (59.02-113.8 mg/gDW). Thus, these extracts gave rather fixed ratios of both total phenolic antioxidants. For application, the autooxidation kinetics of oxymyoglobin (oxyMb) in the presence of both capsaicinoids and phenolic compounds in the extracts was monitored at 581 nm for 2 h using freshly prepared oxyMb solution. The results showed that the crude extracts could retard effectively the autooxidation reaction of oxyMb. Their observed first-order rate constant (k_{obs}) ratios in the presence of the extracts for both capsaicinoids and phenolic compounds were found in the same range between 0.38-0.50 h^{-1} and 0.29-0.48 h^{-1}, respectively, with respect to those of control. It is, therefore, implied that the phenolic antioxidants in hot chilli can keep serving this stabilized function on the oxygen storage of the protein in muscle.*

Key words: myoglobin, autooxidation, capsaicinoids, phenolic compounds, chilli pepper

---

INTRODUCTION

Hot chilli peppers are known to be good sources of phytochemical compounds including vitamin C, E and A, alkaloids, flavonoids, and carotenoids [1]. Capsaicinoids, the pungent alkaloids, are the main active component of chilli peppers. The naturally occurring capsaicinoids present in hot chilli pepper are capsaicin and other structurally related compounds, namely dihydrocapsaicin, nordihydrocapsaicin, homocapsaicin and homodihydrocapsaicin [2]. Capsaicin and dihydrocapsaicin are responsible for approximately 80-90% of the total capsaicinoids present and contribute greatly to overall pungency [3]. The capsaicinoids accumulate in pericarp and placenta of chilli pepper and their concentrations vary, depending on hotness of species varieties, growing conditions and the harvested time. Capsaicinoids have many useful properties, especially antioxidant properties. Many reports reveal substantial antioxidant activity of chilli pepper extracts of capsaicinoids [4-7]. Phenolic compounds found in hot chilli pepper include both simple phenols and flavonoids [8]. Phenolic compounds arethe common antioxidants which can retard or inhibit lipid oxidationby acting scavengers and can protect against propagation of the oxidative chain like capsaicinoids [9,10]. Based on the antioxidant properties of capsaicinoids and phenolics, these compounds were extracted from various kinds of hot chilli pepper samples and their concentrations were evaluated. In addition, this

study was aimed to investigate the influence of both extracts from the hot chilli pepper samples on the autooxidation rate of oxymyoglobin.

MATERIALS AND METHODS

2.1 Chemicals

All the reagents usedwere analytical reagent (AR) grade including dihydrocapsaicin, gallic acid monohydrate, sodium dithionite, Tris-HCl, sodium carbonate and horse heart myoglobin (Sigma-Aldrich, Germany), Folin-Ciocarteu phenol reagent, methanol, hydrochloric acid (Carlo Erba, Italy).

2.2 Apparatus

Capsaicinoids and phenolics contents in hot chilli pepper extracts and their antioxidant activities were determined using Diode Array UV-Visible spectrophotometer (Agilent 8453,USA). Centrifuge (Hitachi EBA 20, Germany), rotary evaporator (Model B-490 Buchi, Switzerland) and magnetic stirrer (Iowa 52001, Germany) were used for sample preparation.

2.3 Chilli pepper fruits

Eight samples (green, orange and red pepper fruits as labeled sample A-H as shown in Figure 1) used in this study were randomly purchased from a fresh market in Khon Kaen, Thailand.



Figure (1): Pictures of different kinds of hot chilli pepper samples used in this study

2.4 Analysis of total capsaicinoids in the chilli extract

Extraction of capsaicinoids in hot chilli pepper samples were carried out following by Juagsamut et al. (2012) [3]. Briefly, all chilli pepper fruits were dried at 60°C for 4 days and ground to a fine powder using a blender (Philips, Netherlands). The powder was shifted through a 500 µm mesh laboratory sieve (Endecotts Limited, England). Two grams of the ground samples were weighed into a 15 mL centrifuge tube, and 20 mL of 90% methanol was added. The extraction was done by magnetic stirring method at 60°C for 2 h. The extract was centrifuged at 5000 rpm for 10 min and then filtered through a Whatman No.42 filter paper. The solvent in the extract was evaporated to dryness using a rotary evaporator and the residue was dissolved with methanol to make a final volume of 5 mL. Stock standard solution of dihydrocapsaicin (1000 mg/L) was prepared by dissolving dihydrocapsaicin in methanol. Working solutions were prepared by dilution of the stock solution with Tris-HCl buffer solution pH 7.2. The calibration curve of capsaicinoids was obtained in the range of 10-60 mg/L. The absorbance of the solutions was measured at 279 nm [3,4] and total capsaicinoids was determined directly from the calibration curve.

2.5 Analysis of total phenolic compounds in the chilli extract

The total phenolics extract was obtained using the same extraction method as mentioned above [10] but the extraction was carried out at room temperature by using methanol: 0.05% HCl (90:10) as an extraction solvent. The extract was centrifuged, filtered, evaporated and the residue was dissolved with the extraction solvent to make a final volume of 20 mL. The Folin-ciocalteau method as previously described using gallic acid as a standard compound was used to estimate total phenolics content [12]. Stock standard solution (1000 mg/L) of gallic acid was prepared by accurately dissolving with methanol and kept in a dark vial and stored at 4°C prior to use. Working standard solution was prepared by diluting the stock solution. The calibration curve in the range of 1.0-4.5 mg/L was generated by using gallic acid solution with deionized water, Na_2CO_3 and Folin-Ciocalteau reagent. After incubated at room temperature for 90 min, the absorbance of the blue color solution was measured at 745 nm. The total phenolics content in the extract was, therefore, determined from the calibration curve.

2.6 Autooxidation kinetics of oxymyoglobin

Myoglobin, an oxygen-binding protein, was used as an autooxidation reaction model for studying the antioxidant properties of hot chilli extract. The aim of this study was to investigate the effect of dihydrocapsaicin, gallic acid and hot chilli extracts (total capsaicinoids and phenolic compounds) on retardation of the autooxidation reaction of horse heart oxymyoglobin. Myoglobin in ferrous form can bind oxygen molecule reversibly as shown in Figure 2 [13].

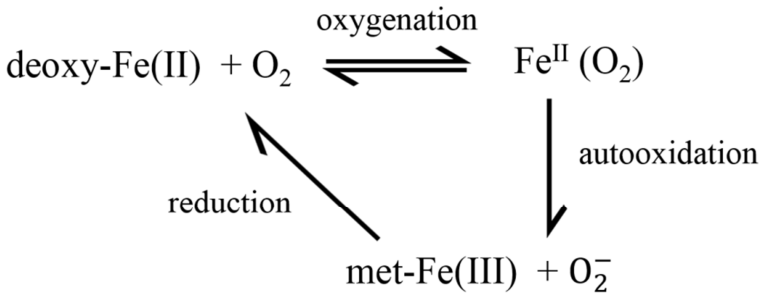


Figure (2): some functional complexes of myoglobin with oxygen molecule [13]

The mechanism for the autooxidation reaction of oxymyoglobin (oxy-Fe^{2+}) to metmyoglobin (met-Fe^{3+}) can be explained by the Fenton reaction as follows [14,15]:

$$Fe^{2+} + O_2 \rightarrow Fe^{3+} + O_2^{-\cdot}$$
$$2O_2^{-\cdot} + 2H^+ \rightarrow H_2O_2 + O_2$$
$$Fe^{2+} + H_2O_2 \rightarrow Fe^{3+} + OH^- + OH^{\cdot}$$

Since temperature is one of important factors affecting the autooxidation kinetics of oxymyoglobin (oxyMb), this reaction rate becomesfaster as the temperature increases. To obtain the optimum temperature for studying the effect of an antioxidant on retardation of the autooxidation of oxyMb, various incubation temperatures were also determined bymonitoring the changes inan oxidation state of iron from (oxy-Fe^{2+}) to (met-Fe^{3+}). The stock solution of horse heart Mb (about 6.2 g/L) was prepared by dissolving the protein with Tris-HCl buffer pH 7.2. An aliquot of the protein solution was converted to oxyform by addition of 10 µL of fresh sodium dithionite solution (100 mg/L) and makes a volume to 4 mL to obtain the final concentration of oxyMb of 300 mg/L. The solution was gently agitated with urging of oxygen gas for a few min until the bright red colored appeared. The oxyMb solution was

quickly transferred to a quartz cell and placed in thermostat connecting with UV-Visible spectrophotometer. The changes in the absorbance in the region of 450-650 nm were recorded at an interval of 5 min for 2 h by varying the incubation temperatures (25, 30, 33, 35, 37, 40 and 50°C). The solution was subject to the absorbance measurement at 581 nm. The absorbance data were analyzed by plotting in terms of $[MbO_2]_t/[MbO_2]_0$ versus time, where the ratio of MbO_2 concentration after time t to that at an initial time $t = 0$). From the slope of each straight line, the observed first-order rate constant, k_{obs} in h^{-1}, was determined. According to the autooxidation reaction of oxyMb, the superoxide radical ($O_2^{\cdot-}$) and hydroxyl radical ($OH^{\cdot}$) which produced by the reaction of ferrous iron in the heme and hydrogen peroxide (H_2O_2) are concerned. The present work was aimed to study the effect of antioxidants including capsaicinoids and phenolic compounds on the autooxidation rate of oxyMb because these compounds could retard the oxidation by scavenging free radical intermediate ($O_2^{\cdot-}$, $OH^{\cdot}$) by donating a hydrogen atom as follows:

$$ROO^{\cdot} + AH \rightarrow ROOH + A^{\cdot}$$
$$RO^{\cdot} + AH \rightarrow ROH + A^{\cdot}$$

Where $ROO^{\cdot}$, $RO^{\cdot}$and AH represents $O_2^{\cdot-}$, $OH^{\cdot}$and antioxidant, respectively. The oxyMb was prepared as described above and followed by the addition of each of various amounts of dihydrocapsaicin or gallic acid. The final concentrations of both dihydrocapsaicin and gallic acid were 5, 10, 20, 30, 40 and 50 mg/L. The oxyMb and the antioxidant solutions were then mixed and measured for k_{obs} values at 37°C at the time interval of 5 min to 2 h. The hot chilli extract was added to the oxyMb solution to get the final concentration of the extract of 10 mg/L. The observed autooxidation rate constant, k_{obs} was determined under the same optimum conditions as described above.

RESULTS AND DISCUSSION

3.1 Total capsaicinoids in hot chilli samples

Total capsaicinoids in eight varieties of hot chilli samples were determined based on dry weight basis as shown in Table 1. The capsaicinoids contents found in these samples were ranged of 63.76-106.62 mg/g DW. Sample A gave the highest content of capsaicinoids, while sample F had the lowest one. According to the extraction solvent for both groups of the compounds, they could be extracted using methanol or the acidified methanol. It is noted that some phenolic compounds can certainly be released into the methanol extract due to very similar organic structure. Therefore, the total phenolics contents in the methanol extract were also found using Folin-Ciocalteau method. It was found that the total phenolics always appeared in the extract of capsaicinoids in the range of 16.56-21.91 mg/g DW.

Table (1): Total capsaicinoids and phenolics contents in hot chilli samples based on dry basis (mg/g DW; *n* = 3)

	Capsaicinoids extract		Phenolics extract	
Sample	Capsaicinoids content	Phenolics content	Phenolics content	Capsaicinoids content
A	106.6	20.22	32.06	113.8
B	83.45	17.98	34.27	90.16
C	64.35	20.13	32.62	60.77
D	74.99	21.40	35.33	80.97
E	75.89	20.28	30.88	92.23
F	63.76	21.91	39.03	83.99
G	64.68	17.98	27.99	59.02
H	72.76	16.56	28.47	64.33

3.2 Total phenolics in hot chilli samples

Total phenolics contents in these eight varieties of chilli samples were also found in the same range (27.99-39.03 mg/g DW) as mentioned above (Table 1) when using methanol: 0.05%HCl (90:10) as the extraction solvent. Sample F gave the highest total phenolics content and sample G showed the lowest one. Based on the phenolic structure, the capsaicinoids contents in the acidified methanol extract were also determined. The results showed that the capsaicinoids also presented in the same range of 59.02-113.81 mg/g DW, slightly higher than those of the methanol extract. It is suggested that an acidified methanol can be effectively used to extract capsaicinoids from the chilli samples. Therefore, it is evident that the each of the hot chilli extracts obtained from both extraction methods contains both of total capsaicinoids and phenolic compounds.

3.3 Effect of temperature on the autooxidation of oxymyoglobin

The horse heart Mb solution was oxygenated to be oxyMb and recorded the Soret peak at 410 nm and visible band at 543 nm and 581 nm (Figure 3). When autooxidation reaction of the protein occurred, the Soret peak tend to slightly blue shifted and the charge transfer bands (543 nm and 581 nm) disappeared. Because of the oxidation of oxyMb is

favored by higher temperature, the observed first-order rate constant (k_{obs}) for the autooxidation reaction at various temperatures was determined.

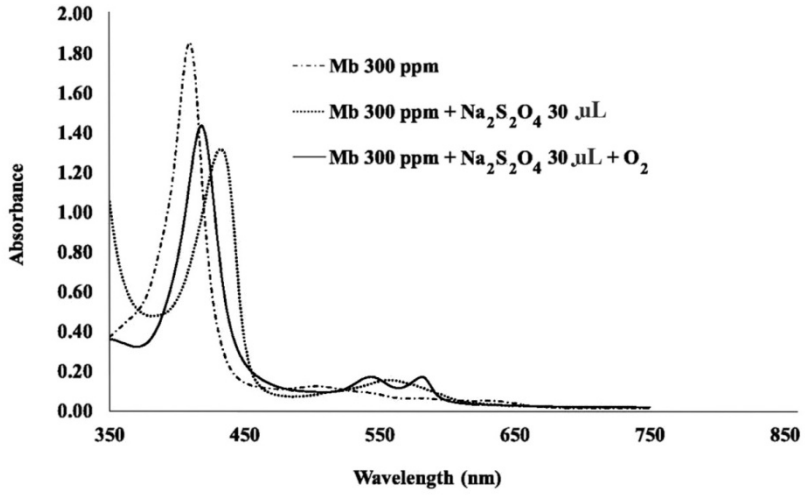


Figure (3): Absorption spectra of metMb, reduced Mb and oxyMb (each 300 mg/L)

The first-order plots for the autooxidation of oxyMb at various temperatures are shown in Figure 4. The results showed that when increase in an incubation temperature, the slope of straight line (k_{obs}) also increased. The k_{obs} values of the plots are 0.179, 0.329, 0.443, 0.626, 0.779, 1.21 and 1.64 attributing from the incubation temperature of 25, 30, 33, 35, 37, 40 and 50°C, respectively. However, 37°C was chosen for studying the effects of antioxidants and hot chilli extracts on retardation of autooxidation reaction of oxyMb because the k_{obs} could be obviously observed. By contrast, the autooxidation rate at higher incubation times was rather difficult to observe because the oxyMb solution was rapidly oxidized.

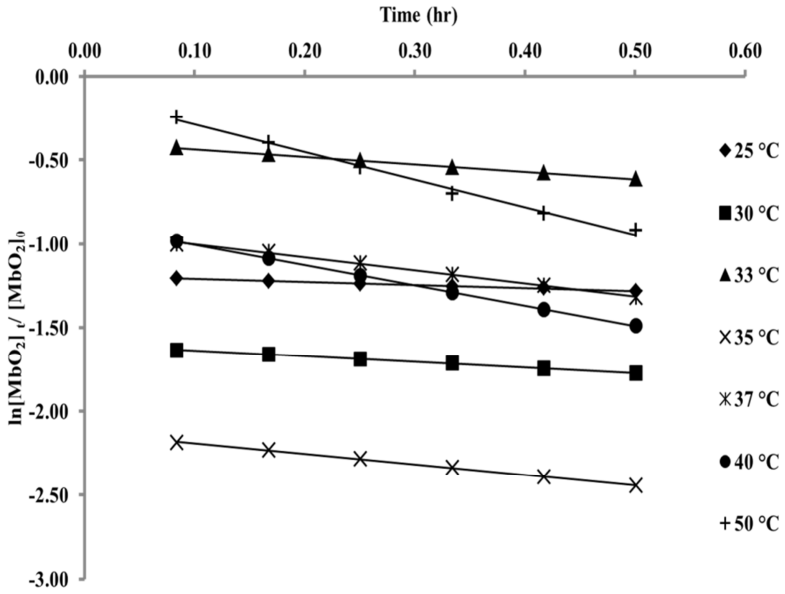


Figure (4): First-order plots for the autooxidation rate of oxyMb at various incubation temperatures

3.4 Effects of dihydrocapsaicin and gallic acid on the autooxidation of oxymyoglobin Dihydrocapsaicin and gallic acid solutions were chosen for capsaicinoids and phonolic compounds as standard antioxidants, respectively. The effect of dihydrocapsaicin and gallic acid concentrations on the autooxidation of oxyMb was preliminary studied. It was found that an increasing of concentrations of both compounds decreased the k_{obs} values compared with oxyMb solution without antioxidants. It is suggested that both dihydrocapsaicin (about 10x less) and gallic acid could stabilize the autooxidation reaction of oxyMb (Table 2).

Table (2): The $*k_{obs}$ ratios of the autooxidation rate of oxyMb in the presence of dihydrocapsaicin and gallic acid at various concentrations

Dihydrocapsaicin (ppm)	$*k_{obs}$ (h^{-1})	Gallic acid (ppm)	$*k_{obs}$(h^{-1})
Control	-	Control	-
5	0.067	5	0.667
10	0.067	10	0.552
20	0.057	20	0.468
30	0.049	30	0.370
40	0.043	40	0.257
50	0.038	50	0.222

$*k_{obs} = k_{obs\ (sample)} / k_{obs\ (control)}$; *where* $k_{obs\ (control)}$ *for dihydrocapsaicin* $= 83.2 \times 10^{-2}$ *and* $k_{obs\ (control)}$ *for gallic acid* $= 78.4 \times 10^{-2}$

According to both capsaicinoids and phenolic extract, no difference in the k_{obs} values of all samples was found (Figure 5 and Table 3). From the results, it is shown that although various chilli samples have different amounts of both capsaicinoids and phenolic compounds, they still exhibit the same retardation of the autooxidation rate of oxyMb, since their antioxidants used are fixed at the same level. In addition, both of the extracts composed of mixed ratios of both total capsaicinoids and total phenolic compounds. Therefore, the effects of the antioxidant capacities of the chilli extracts on retardation of the autoxidation rate of oxyMb were demonstrated under the optimum conditions of their kinetic study.

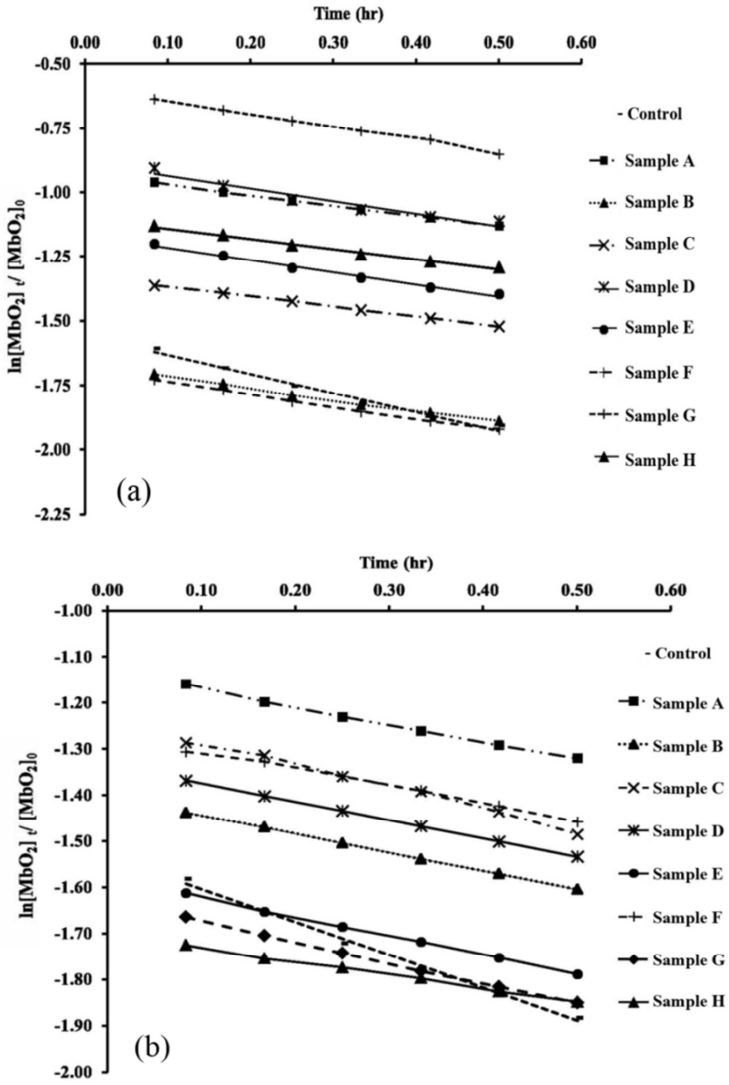


Figure (5): The effect of crude extracts of hot chilli on retardation of the autooxidation rate of oxyMb: (a) capsaicinoids extract and (b) phenolics extract

Table (3): The $*k_{obs}$ ratio of autooxidation rate of oxyMb in the presence of total capsaicinoids and phenolics extracts

Sample	Capsaicinoids extract $*k_{obs}(h^{-1})$	Phenolics extract $*k_{obs}$ (h^{-1})
Control	-	-
A	0.545	0.546
B	0.579	0.565
C	0.522	0.673
D	0.668	0.554
E	0.646	0.583
F	0.644	0.521
G	0.679	0.628
H	0.539	0.411

$*k_{obs} = k_{obs\ (sample)} / k_{obs\ (control)}$; where $k_{obs\ (control)}$ for capsaicinoids = 74.1×10^{-2} and $k_{obs\ (control)}$ for phenolics = 71.1×10^{-2}

Total capsaicinoids and total phenolics were extracted using 90% (v/v) methanol and methanol: 0.05% HCl (90:10, v/v), respectively. The contents of both phenolic compounds in various chilli samples were comparable. Interestingly, these extracts showed their effective antioxidant activities on the retardation of the autooxidation reaction of the oxyMb solution. Therefore, daily consumption of hot chilli by either direct or indirect way of food cooking would be fruitfully benefited for health, in particular to serve stabilization for oxygen storage in such the protein structure.

Acknowledgements
The authors thank the Higher Education Research Promotion and National Research University Project of Thailand, Office of the Higher Education Commission, through the Food and Functional Food Research Cluster of Khon Kaen University, and Department of Chemistry and Center of Excellence for Innovation in Chemistry (PERCH-CIC), Commission on Higher Education and Ministry of Education for financial support.

REFERENCES

[1] Howard L.R., Talcott S.T., Brenes C.H., Villalon B., *Journal of Agricultural and Food Chemistry*, **2000**, 48, 1713-1720.
[2] Hoffman P.G., Lego M.C., Galleto W.G., *Journal of Agricultural and Food Chemistry*, **1983**, 31, 1326-1330.
[3] Juangsamut J., Ruangviriyachai C., Techawongstien S., Chanthai S., *International Food Research Journal*, **2012**, 19, 1217-1226.
[4] Davis C.B., Markey C.E., Busch M.A., Busch K.W., *Journal of Agricultural and Food Chemistry*,**2007**, 25, 5925-5933.
[5] Henderson D.E., Slickman A.M., *Journal of Agricultural and Food Chemistry***, 1999**, 48, 2563-2573.
[6] Rosa A., Deiana M., Casu V., Paccagnini S., Appendino G., Ballero M., Dessi M.A., *Journal of Agricultural and Food Chemistry*, **2002**, 50, 2563-2573.
[7] Tsai T.H., Tsai P.J., Ho S.C., *Journal of Food Sciences*, **2005**, 70, 93-97.
[8] Si W., Liang Y., Ma K.Y., Chen Z.-Y., *Journal of Agricultural and Food Chemistry*, **2012**, 60, 6230-6234.
[9] Navarro J.M., Flores P., Garrido C., Martinez V., *Food Chemistry*, **2006**, 96, 66-73.
[10] Antonious G.F., Kochhar T.S., Jarret R.L., Synder J.C., *Journal of Environmental Science and Health B*, **2006**, 41, 1237-1243.
[11] Chatteree S., Niaz Z., Guatan S., Adhikari S., Pasad S.V., Sharma A., *Food Chemistry*, **2007**, 102, 515-523
[12] Arnnok P., Ruangviriyachai C., Mahachai R., Techawongstien S., Chanthai S., *International Food Research Journal*, **2012**, 16, 235-243.
[13] Shikama K., *Progress in Biophysical and Molecular Bi*ology, **2006**, 91, 83-162.
[14] Hultin H.O., *In: Advance in Seafood Biochemistry*. Frick G.J. and Martin R.E., eds. (**1992**) pp. 99-122.
[15] Chaijan M., *Songklanakarin Journal of Science and Technology*, **2008**, 30, 47-53.
[16] Singleton V.L., Rossi J.A., *American Journal of Enology and Vitticulture*, **1965**, 16, 144-158.

Songklanakarin J. Sci. Technol.
37 (4), 401-408, Jul. - Aug. 2015

http://www.sjst.psu.ac.th

Original Article

Improvement of eri silkworm (*Samia ricini* D.) tolerance to high temperature and low humidity conditions by discontinuous regime

Duanpen Wongsorn[1,2], Sivilai Sirimungkararat[1,2,3]*, and Weerasak Saksirirat[2,3]

[1] *Entomology Section, Department of Plant Science and Agricultural Resources,*

[2] *Cultivation and Product Development Research Group of Wild Silkmoths and Economic Insects for Value Added Creation,*

[3] *Agricultural Biotechnology Research Center for Sustainable Economy and Center of Agricultural Biotechnology (AG- BIO/PERDO-CHE), Faculty of Agriculture, Khon Kaen University, Mueang Khon Kaen, 40002 Thailand.*

Received: 18 March 2015; Accepted: 3 May 2015

Abstract

Improvement of eri silkworm tolerance to high temperature was carried out under high temperature (42±1°C) and low relative humidity (50±5% R.H., relative humidity). Eri silkworm rearing at normal temperature (25±2°C; 80±5% R.H.) served as control treatment and was compared to rearing at high temperatures. Directional selection was undertaken with the batches reared at 42±1°C and 50±5% R.H. until the 5th generation. From 6th, 8th, 10th and 12th generations, rearing was conducted as normal rearing (25±2°C; 80±5% R.H.), while for 7th, 9th, and 11th generations directional selection was done as 1st – 5th generations. Various parameters were used as indexes for high temperature tolerance. When the silkworms were reared until to F12 (12th generation), the survival rate of larva (1st–5th instar) (95.33%) and larva (1st–5th instar) – adult (69.33%) including cocooning rate (80.67%) of F12 were the highest compared to F1 and F11. For cocoon yields among F1, F11, and F12, the highest values of fresh cocoon weight (2.7144 g), pupa weight (2.3490 g), shell weight (0.3671 g), shell ratio(13.53%), total cocoon shell weight(17.01 g), and fresh cocoon/10,000 larvae (25. 16 kg) were achieved from F12, which were significantly different ($P< 0.05$) to F1 and F11. In the same manner for egg yields, F12 provided the maximum numbers in case of eggs/moth (311.33 eggs), total eggs (6,693.33 eggs) and total hatching eggs (4,842.67 eggs) except hatching eggs (73.15%). Of these evaluations between F11 and F1, it was found that F11 was higher than F1 and statistically different ($P<0.05$) in all parameters excluding the percentage of hatching eggs, which was not significant difference. These results indicate that the property of high temperature tolerance was improved and heat tolerant property of eri silkworm (SaKKU1) is heritable. This is a first to report on heat tolerance improvement of eri silkworm. Although it is a first trial that was carried out in a laboratory, it can be applied on eri silkworm rearing in the future to cope with recent global warming trends.

Keywords: eri silkworm, tolerance, high temperature, low humidity, selection

1. Introduction

Eri silkworm (*Samia ricini* D.) is a multivoltine, polyphagous wild silkworm, and feeds on a wide range of host plants (Sirimungkararat, 2014). In addition to industrial insects such as domesticated silkworm (*Bombyx mori*), eri silkworm plays a significant role in various industries, especially the worldwide textile industry. It has also been studied and utilized in various fields such as cosmetic products, processed food supplements, health care products, etc. (Akai, 2002; Sirimungkararat *et al.*, 2010; Sirimungkararat, 2012). Currently, in Thailand, eri silkworm rearing is being widely promoted in

* Corresponding author.
Email address: sivilai@kku.ac.th

government, private and public sectors. The success of sericulture industry normally depends upon several factors such as biotic and abiotic factors, which are of vital importance. Among abiotic factors, the temperature plays a major role on growth and productivity in domesticated mulberry silkworm, *B. mori* (Kumari *et al.*, 2011). Similarly, in eri silkworm the optimum temperature for growth of young stage is about 26-28°C with a relative humidity of 85-90% and at later stage 24-26°C, with 70-80% (Singh and Saratchandra, 2012). Recently, eri silkworm rearing at high temperature as in summer temperatures might be seen as a scenario due to global warming. Temperatures above 35°C often negatively affect growth of eri silkworm. As a result, eri silkworm cannot grow well and eventually be infected easily by the pathogens causing dead, which makes it impossible to maintain eri silkworm varieties. This may also lead to reduce yields in both quantity and quality (Sahu *et al.*, 2006). Eri silkworm was introduced to Thailand several decades ago. It is promoted and researched in various aspects towards industrial level (Sirimungkararat, 2013). In Thailand, the rearing of eri silkworm in hot season, especially from March to April, is hampered by high temperatures. Low yields and high mortality were observed. There has been no research about the impact of high temperature on eri silkworm breeding except Sirimungkararat *et al.* (2013a) on high temperature and high humidity (80±5% R.H.), where the eri silkworm was not able to survive and complete its life cycle, and the study of Wongsorn *et al.* (2014) on the screening of ecoraces tolerant to different high temperatures and low humidity (50±5% R.H.). Ecoraces are populations that have been isolated geographically over centuries and by this have been adapted to particular ecological niches. The ecorace SaKKU1 shows a high temperature tolerance of up to 42±1°C with low relative humidity (50±5%). Hence, improvement of a heat tolerance ecorace or a variety of eri silkworm is one promising solution and a way to adapt to global warming trends and climate changes in the future. Therefore, this present work aims to improve eri silkworm ecorace (SaKKU1) that can tolerate high temperatures and to evaluate the effect of high temperature and low relative humidity on growth and yield of eri silkworm.

2. Materials and Methods

2.1 Eri silkworm stock culture

The eri silkworm ecorace SaKKU1 was selected as the stock to be improved for heat tolerance, based on its morphological character, growth, yields (Wongsorn *et al.*, 2013), genetic characterization (Sirimungkararat *et al.*, 2013a), and preliminary thermotolerant property tested with 42±1°C and 50±5% R.H. The hatched larvae of selected ecorace (SaKKU1) defined as the first filial generation (F1), were reared at room temperature (25±2°C, 80±5% R.H.) until 5th instar day 2. After that the 5th instar day 3 larvae were separated into 2 groups for high temperature treatment (42±1°C, 50±5 %R.H.) and control treatment (25±2°C, 80±5% R.H.).

2.2 High temperature treatment

The method of high temperature treatments or thermal exposure was modified from methods of Suresh Kumar *et al.* (2002), Rao *et al.* (2007), and Singh and Kumar (2010a,b). Briefly, the larvae of 5th instar day 3 (F1) were randomly selected and reared at high temperature of 42±1°C, 50±5% R.H. in an incubator (Umax Scientific: Model Um-TTM004 Leec, England) for 6 hours/day (10:00-16:00). After the high temperature treatment of each day, they were moved to normal temperature condition (25±2°C, 80±5% R.H.). This procedure was performed until the larvae reached to the ripe stage; then they were allowed to spin cocoons at this normal temperature. Cocoon harvesting was carried out on the 7th day. Cocoon yield parameters were assessed on the subsequent days. Adult moths were allowed to mate and couple until laying eggs. When larvae hatched from the mixed eggs from various moths of each treatment, the 1st instar larvae (3-5 hours after hatching) were selected randomly. The completely randomized design (CRD) was used with three replications. Twelve generations (F1-F12) served as treatments. There were three replications per treatment. Each replication contained 50 larvae, which were reared at normal temperature and fed with castor (cultivar TCO 101) leaves as food plant. Rearing was done according to the method of Sirimungkararat *et al.* (2002). When the larvae developed to 5th instar day 3, they were randomly selected and exposed to high temperature as described above. The survival larvae were reared until developing to adults. The male and female moths of each replication were randomized to mate and allowed to lay eggs. After female adults laid eggs and newly hatched larvae developed until to new adult stage, it was defined as filial generation (F). The high temperature exposure experiment was conducted continuously from 1st generation (F1) until F5. For F6, F8, F10, and F12, the eri silkworms were reared at 25±2°C and 80±5% R.H., whereas F7, F9, and F11 were reared under above mentioned high temperature and low humidity (42±1°C, 50±5% R.H.). Details of the improvement plan were based on temperature regime and control treatment conducted at 25±2°C, 80±5% R.H. from F1 to F12 was followed as shown in Figure 1.

2.3 Data collection and statistical analysis

The data pertaining traits *viz*. survival {larva stage (1st - 5th instar), larva stage (1st-5th instar) - adult stage}, cocooning rate, cocoon yields (fresh cocoon weight, pupa weight, shell weight, shell ratio, total cocoon shell weight and fresh cocoon weight/10,000 larvae), and egg yields (eggs/moth, hatching egg percentage, total eggs and total hatching eggs) were recorded. The data were statistically analyzed according to analysis of variance (ANOVA) and the means were compared by using Duncan's multiple range test (DMRT).

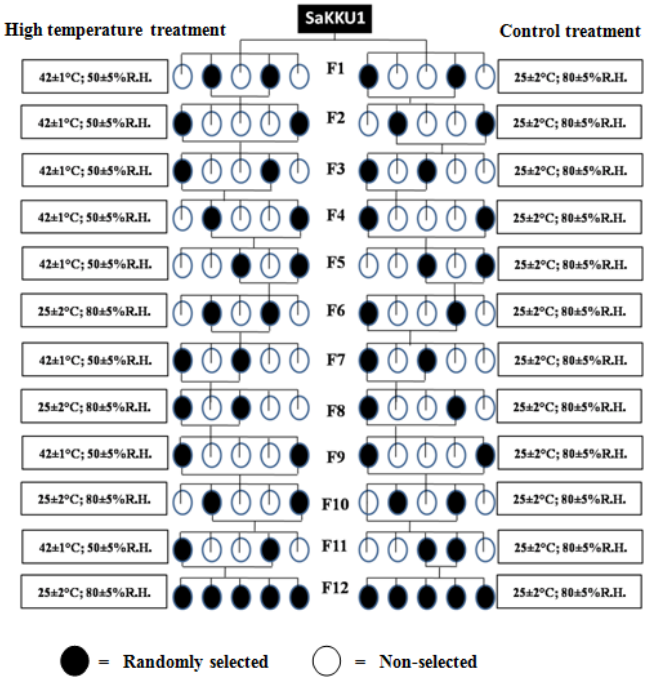


Figure 1. Improvement plan of eri silkworm (*Samia ricini* D.) ecorace SaKKU1 tolerant to 42±1°C and 50±5% R.H. F1-F5, F7, F9, and F11 = 5th instar larvae, day 3 were randomly selected and exposed to high temperature (42±1°C and 50±5% R.H.) for 6 hours/day otherwise were reared at normal temperature until reached to the ripe stage. F6, F8, F10, and F12 = silkworms were reared at normal temperature (25±1°C and 80±5% R.H.).

3. Results

3.1 Survival and cocooning rate of eri silkworm

Rearing eri silkworm at high temperature condition of 42±1°C, 50±5% R.H. in F1-F5 and F7, F9, and F11, while F6, F8, F10, and F12 at 25±2°C, 80±5% R.H. (Table 1) revealed the average values of survival and cocooning rates: survival rate from larva stage (1st-5th instar), the F1 survival rate was 78.33% whereas F5 was 56.00%, which was significantly different ($P<0.05$). When the silkworms were reared until to F11, the survival rate increased practically and F11 had a higher value (85.33%) than F1 (78.33%), which was not significantly different. The result of survival from larva (1st-5th instar) – adult stage showed that F1 (54.17%) was not significantly different from F11 (45.33%). For cocooning rate of F1-F5 treated with high temperature, the rate decreased temporarily. Thereafter, the cocooning rate of high temperature exposed treatments increased continuously until F11 with a maximum of 52.67% and it was significantly different ($P<0.05$) from F1 (34.00%). Moreover, in comparison of all generations treated and non-treated with high temperature, F12 of all checked parameters had higher values and was significant difference ($P<0.05$) from both F11 and F1. In control treatments, means of survival rates and cocooning rate among F1-F12 were similar and comparable. Survival rate at larva stage (1st-5th instar) from F1 to F12 was 97.50 to 100.00%, respectively. While for larva (1st-5th instar) – adult stage from F1 onwards to F12 was from 97.50 to 84.67%, respectively. There were significantly statistical differences ($P<0.05$) between F1 and F12 on both survival rates, but no difference on cocooning rate.

3.2 Cocoon yields of eri silkworm

For cocoon yields, mean values of fresh cocoon weight, pupa weight, shell weight, shell ratio, total cocoon shell weight, and fresh cocoon/10,000 larvae were evaluated under alternatively treated with high temperature condition (F6-F12) (Table 2). The fresh cocoon weight of F1-F5, continuously exposed to 42±1°C, 50±5% R.H., trended to decrease temporarily. Fresh cocoon weight of F5 was 2.1370 g, after that the weight decreased slightly. The value of F11 was 2.0861 g, but not significantly different to F1 (2.2853 g). Pupa weight of F1 was 1.9333 g, however, not significant different to F11 (1.8836 g). For shell weight, the value of F1 (0.2628 g) was higher than of F11 (0.1944 g). Interestingly, when the experiment was continued to F12 all of these checked values of F12 were the highest except when compared to F10 and F8. Shell weight of F11 (0.1944 g) was less than that obtained from F1 (0.2628 g) and significantly different ($P<0.05$). In control treatments, from F1 to F12 a slight decrease was observed. The values of all parameters varied depending on different generations. Fresh cocoon weight of F1 and F12 was from 3.0411 to 2.7270 g, pupa weight of F1 and F12 was from 2.6236 to 2.3322 g and shell weight of F1 and F12 from 0.4037 to 0.3829 g. F1 and F12 were statistically different ($P<0.05$) on fresh cocoon weight and pupa weight, however not significant different on shell weight. In consideration on means of fresh cocoon weight, pupa weight and shell weight of F12 in high temperature treatment, the values were similar and comparable to those obtained from F1-F12 in control treatments. The shell ratio from F1 (11.61%) decreased until F11 (9.65%), and it is significantly different with F11. Statistically, there is no change between F2 (9.73%) and F11 (9.65%). In the case of total cocoon shell weight and fresh cocoon/10,000 larvae, F1 was 6.10 g and 10.55 kg, respectively. Between F2 and F11 of both parameters increased from 1.76 to 3.55 g (total cocoon shell weight) and from 3.68 to 7.42 kg (fresh cocoon/10,000 larvae). Besides, these values are above mean values, with F12 gave a value close to F10, which is close to the highest (F10) and significantly different ($P<0.05$). For the control treatments from F1 to F12 there was a slight increase observed in the shell ratio, but there was a larger decrease in fresh cocoon/10,000 larvae (shell ratio F1 to F12 from 13.36 to 14.11% and fresh cocoon/10,000 larvae F1 to F12, from 29.81 to 26.36 kg). Only the values on fresh cocoon weight/10,000 larvae between F1 and F12 were statistically different ($P<0.05$). Shell ratio, total cocoon shell weight and fresh cocoon/10,000 larvae derived from F12 (after high

Table 1. Survival and cocooning rate of eri silkworm (*Samia ricini* D.) reared at two conditions of 42±1°C, 50±5% R.H. and 25±2 °C, 80±5% R.H.

Generation	42±1 °C and 50±5% R.H. [1/,2/]			25±2 °C and 80±5% R.H. [1/,2/]		
	Survival rate (%)			Survival rate (%)		
	Larva stage (1st - 5th)	Larva (1st - 5th) – adult stage	Cocooning rate (%)	Larva stage (1st - 5th)	Larva (1st - 5th) – adult stage	Cocooning rate (%)
F1	78.33±12.58 c	**54.17±12.58 d**	34.00±7.21 e	97.50±2.50 bc	**97.50±2.50 a**	97.33±3.21 ab
F2	**98.00±2.00 a**	16.67±2.31 g	21.33±4.62 f	96.67±1.15 c	90.00±4.00 a-d	94.00±2.00 b
F3	94.00±5.29 ab	34.67±5.77 f	21.33±2.31 f	99.33±1.15 ab	87.33±5.03 b-d	94.00±2.00 b
F4	97.33±2.31 a	31.33±4.16 f	15.33±3.06 f	**100.00±0.00 a**	85.33±1.15 cd	97.33±2.31 ab
F5	56.00±4.00 d	40.00±2.00 ef	32.67±1.15 e	99.33±1.15 ab	92.00±2.00 a-c	99.33±1.15 a
F6	(98.67±1.15 a)	(90.00±2.00 a)	(98.67±1.15 a)	**100.00±0.00 a**	90.67±3.06 a-c	**100.00±0.00 a**
F7	53.33±5.77 d	36.00±2.00 f	41.33±5.03 de	98.67±1.15 a-c	85.33±5.77 cd	98.00±2.00 a
F8	(99.33±1.15 a)	(79.33±3.06 b)	(98.67±2.31 a)	**100.00±0.00 a**	80.67±8.33 d	98.00±2.00 a
F9	58.67±13.32 d	48.67±6.11 de	46.67±8.33 cd	**100.00±0.00 a**	95.33±3.06 ab	**100.00±0.00 a**
F10	(98.00±2.00 a)	(86.00±5.29 ab)	(94.67±2.31 a)	97.33±2.31 bc	90.00±4.00 a-d	96.00±3.46 ab
F11	85.33±2.31 bc	45.33±3.06 de	**52.67±3.06 c**	99.33±1.15 ab	92.00±9.17 a-c	99.33±1.15 a
F12	(95.33±6.43 ab)	(69.33±1.15 c)	(80.67±11.72 b)	**100.00±0.00 a**	84.67±5.03 cd	96.67±3.06 ab
Mean[3/]	77.63±19.08	38.35±11.63	33.17±13.25	99.01±0.09	89.24±4.79	97.50±2.07
F-test	**	**	**	*	*	*
C.V.(%)	7.56	9.68	10.05	1.25	5.60	2.11

[1/] means followed by the same letter within a column are not significantly different (DMRT, P >0.05). [2/] numbers in parentheses are the values of a generation reared in room temperature 25±2°C humidity 80±5% (F6, F8, F10, and F12). [3/] the values of an average of a generation tested at high temperature (F1-F5, F7, F9 and F11) except in control treatment (25±2°C; 80±5%R.H.).
*, ** = Significantly different at 95 and 99% level, respectively.

temperature exposed treatment, F11) were comparable to the values from F1-F12 in control treatments. These results indicate an improvement in the high temperature tolerance of eri silkworm SaKKU1 in this study.

3.3 Egg yields of eri silkworm

The mean values of egg yields were presented in Table 3. Under the treatment with high temperature eggs/moth, hatching egg percentage, total eggs and total hatching eggs increased from F1 to F12 (149.00 to 311.33, 77.00 to 73.15, 746.11 to 6,693.33 and 444.67 to 4,842.67, respectively) and were significantly different (P<0.05), except hatching eggs. In control treatments, all parameters of F1 and F11 were 346.67 and 357.69, 6,360.03, and 7,524.69, 5,577.93, and 6,631.30 eggs, and 87.78 and 88.37%, for eggs/moth, total eggs, total hatching eggs and hatching eggs, respectively. Of these were not significant differences, although F11 had higher values than F1. In F12 after F11 (high temperature exposure), the average of eggs/moth, total eggs and total hatching eggs increased significantly (P<0.05) from F11. Interestingly, eggs/moth, total eggs and total hatching eggs of F12 in control treatments increased in the same trend as the high temperature treatment regime.

4. Conclusions and Discussion

It is well established in plants and animals that the widespread utilization of hybrids can achieve sustainability, quality and quantity oriented production increasing. Silkworm is the best animal where hybrids are used compulsorily for commercial silk product since the study of Toyama (1906). The goal of breeding is to bring together the desirable genes in appropriate combinations and allow them to recombine so as to improve the genetic performance of maximizing the yield and productivity per unit population (Kumar and Reddy, 1994). The presented study in eri silkworm was carried out to develop suitable high temperature tolerant ecorace for a target environment with high temperature (42±1°C) and low humidity (50±5%) exposed to the larvae from 3rd days of 5th instar until ripe stage. After exposure to high temperature, eri silkworm could grow continuously until a final generation (F12). Survival of larva stage, survival rate larva – adult stage and cocooning rate increased and were significantly different (P<0.05) between F1 and F12, with 78.33 to 95.33%, 54.17 to 69.33% and 34.00 to 80.67%, respectively. These results suggest that the nature of the heat tolerance is heritable and accumulated to the 12th generation. These three parameters of F12 were the highest and most significantly different

Table 2. Cocoon yields of eri silkworm (*Samia ricini* D.) reared at two conditions of 42±1°C, 50±5% R.H. and 25±2°C, 80±5% R.H.

Generation	42±1 °C and 50±5% R.H. [1/, 2/]			25±2 °C and 80±5% R.H. [1/, 2/]		
	Fresh cocoon weight (g)	Pupa weight (g)	Shell weight (g)	Fresh cocoon weight (g)	Pupa weight (g)	Shell weight (g)
F1	2.2853±0.31cde	1.9333±0.16 de	**0.2628±0.03 d**	3.0411±0.03 ab	2.6236±0.02 ab	0.4037±0.01 b-d
F2	**2.5008±0.11 bc**	**2.3139±0.10 ab**	0.2404±0.01 de	2.8929±0.06 bc	2.4617±0.06 c	0.4158±0.03 bc
F3	1.9712±0.14 f	1.7999±0.14 def	0.1634±0.01 gh	**3.0901±0.20 a**	**2.6381±0.19 a**	**0.4533±0.04 a**
F4	1.9812±0.02 f	1.8213±0.04 def	0.1477±0.02 h	2.8927±0.08 bc	2.4753±0.06 bc	0.4202±0.03 b
F5	2.1370±0.12 def	1.8860±0.08 def	0.2465±0.04 de	2.7639±0.10 c	2.3939±0.08 c	0.3740±0.03 d-f
F6	(2.3397±0.07 cd)	(2.0062±0.08 cd)	(0.3337±0.04 c)	2.4731±0.11 d	2.1383±0.06 d	0.3360±0.01 g
F7	1.9367±0.13 f	1.7102±0.14 f	0.2207±0.04 ef	2.4751±0.03 d	2.1375±0.25 d	0.3526±0.02 fg
F8	(2.6030±0.02 b)	(2.1964±0.02 bc)	(0.3937±0.01 ab)	2.5482±0.05 d	2.1343±0.04 d	0.3999±0.01 b-d
F9	1.9046±0.11 f	1.7428±0.11 ef	0.1523±0.01 h	2.8526±0.18 c	2.4105±0.13 c	0.3953±0.01 b-e
F10	(2.8753±0.15 a)	(2.4364±0.15 a)	(0.4067±0.02 a)	2.7935±0.09 c	2.3768±0.07 c	0.3950±0.10 b-e
F11	2.0861±0.16 ef	1.8836±0.18 def	0.1944±0.02 fg	2.4634±0.07 d	2.0900±0.06 d	0.3614±0.03 e-g
F12	(2.7144±0.05 ab)	(2.3490±0.05 ab)	(0.3671±0.01 bc)	2.7270±0.09 c	2.3322±0.07 c	0.3829±0.02 c-f
Mean [3/]	2.1004±0.20	1.8864±0.19	0.2035±0.05	2.7511±0.22	2.3510±0.19	0.3908±0.03
F-test	**	**	**	**	**	**
C.V.(%)	6.10	5.71	8.10	3.74	3.81	4.96

Generation	42±1 °C and 50±5% R.H. [1/, 2/]			25±2 °C and 80±5% R.H. [1/, 2/]		
	Shell ratio (%)	Total cocoon shell weight (g)	Fresh cocoon / 10,000 larvae (kg)	Shell ratio (%)	Total cocoon shell weight (g)	Fresh cocoon / 10,000 larvae (kg)
F1	**11.61±1.01 b**	**6.10±0.68 c**	**10.55±0.21 d**	13.36±0.24 d	19.79±0.87 a-c	**29.81±0.84 a**
F2	9.73±0.86 cd	1.76±0.09 f	3.68±0.46 g	14.46±1.02 b-d	19.40±1.18 a-c	27.00±0.36 cd
F3	8.25±1.12 de	1.75±0.26 f	4.18±0.14 g	14.90±0.76 ab	**21.30±0.63 a**	29.25±1.99 ab
F4	7.37±1.22 e	1.13±0.28 f	3.04±0.39 g	14.66±0.59 bc	20.50±1.66 ab	28.14±1.34 a-d
F5	11.44±1.44 bc	3.27±1.64 e	6.65±0.87 f	13.65±0.58 cd	18.58±1.57 b-e	27.46±1.14 b-d
F6	(14.39±0.60 a)	(16.46±0.04 b)	(23.09±1.00 c)	13.68±0.17 cd	16.80±0.71 e	24.73±1.09 f
F7	11.43±1.32 bc	4.51±0.67 d	7.99±0.91 ef	14.29±0.80 b-d	17.28±1.03 de	24.42±0.33 f
F8	(15.14±0.79 a)	(19.42±0.77 a)	(25.68±0.43 b)	**15.83±0.28 a**	19.59±0.64 a-c	24.97±0.35 ef
F9	8.03±0.26 de	3.59±0.14 de	8.87±0.36 e	13.94±0.86 b-d	19.76±0.33 a-c	28.53±1.81 a-c
F10	(14.15±0.45 a)	(19.25±1.04 a)	(27.23±1.88 a)	14.28±0.28 b-d	18.96±0.59 b-d	26.80±0.23 c-e
F11	9.65±1.54 cd	3.55±0.69 de	7.42±0.29 f	14.81±0.77 a-c	17.95±1.39 c-e	24.47±0.72 f
F12	(13.53±0.40 a)	(17.01±1.05 b)	(25.16±1.30 b)	14.11±0.39 b-d	18.01±1.47 c-e	26.36±1.27 d-f
Mean [3/]	9.69±1.69	3.21±1.64	6.55±2.68	14.33±0.67	18.99±1.33	26.83±1.89
F-test	**	**	**	**	**	**
C.V.(%)	8.94	7.15	6.35	4.35	5.74	4.13

[1/] means followed by the same letter within a column are not significantly different (DMRT, P >0.05). [2/] numbers in parentheses are the values of a generation reared in room temperature 25±2°C humidity 80±5% (F6, F8, F10, and F12). [3/] the values of an average of a generation tested at high temperature (F1-F5, F7, F9 and F11) except in control treatment (25±2°C; 80±5%R.H.). ** = Significantly different at 99% level.

among F1, F11, and F12. In domesticated mulberry silkworm (*B. mori*), the breeder of all the sericultural countries have experienced the influence of environment during the process of breeding. The effect of higher temperature of more than 30°C on mulberry silkworm larvae was reported earlier (He and Oshiki, 1984). Attempts to create higher temperature resistant silkworm races were carried out and showed that the genetically heritable nature of thermotolerance is possible to be

Table 3. Egg yields of eri silkworm (*Samia ricini* D.) reared at two conditions of 42±1 °C, 50±5% R.H. and 25±2 °C, 80±5% R.H

Generation	42±1°C and 50±5% R.H. [1/, 2/]				25±2°C and 80±5% R.H. [1/, 2/]			
	Eggs/moth (eggs)	Hatching eggs (%)	Total eggs (eggs)	Total hatching eggs (eggs)	Eggs/moth (eggs)	Hatching eggs (%)	Total eggs (eggs)	Total hatching egg (egg)
F1	149.00±33.83 d	77.00±12.82 a-d	746.11±474.96 h	444.67±209.71 h	346.67±19.72 c-e	87.78±0.41	6,360.03±687.85 c-e	5,577.93±594.53 de
F2	160.00±79.02 d	**86.38±5.22 a**	982.00±244.52 gh	845.52±259.34 gh	322.16±56.96 de	**92.64±1.66**	5,903.45±922.19 de	5,480.38±927.36 de
F3	199.11±41.13 cd	69.50±6.40 d	1,774.89±274.76 f	1,227.11±237.52 fg	386.17±10.45 a-c	81.96±9.45	8,756.06±234.87 ab	7,263.22±565.16 a-c
F4	234.08±27.53 bc	69.04±5.63 d	1,656.56±429.47 fg	1,106.78±227.60 f-h	401.53±24.13 ab	83.35±2.44	9,017.33±874.28 ab	6,722.67±597.18 b-d
F5	239.11±39.70 bc	75.59±2.38 a-d	3,272.89±576.70 de	2,581.44±629.90 cd	405.13±40.66 ab	88.70±7.17	9,086.73±928.11 ab	8,049.73±694.85 ab
F6	(285.00±14.27 ab)	(82.91±2.12 a-c)	(5,896.40±557.06 b)	(4,844.80±565.85 a)	392.20±23.31 a-c	86.60±1.15	7,816.67±730.95 bc	7,493.20±203.08 a-c
F7	239.80±19.71 bc	81.08±3.35 a-c	2,075.60±101.29 f	1,692.27±198.80 ef	302.20±15.38 e	87.67±4.01	6,947.07±809.88 c-e	6,096.40±749.43 c-e
F8	(308.59±24.82 a)	(84.82±3.21 ab)	(5,127.50±399.62 c)	(4,364.78±517.59 a)	329.48±17.73 de	87.89±1.41	5,485.71±357.82 e	4,795.14±212.30 e
F9	**279.87±16.96 ab**	77.07±6.22 a-d	2,802.27±339.67 e	2,164.10±361.90 de	335.40±18.34 de	90.75±3.45	8,834.60±761.70 ab	8,036.87±430.12 ab
F10	(288.00±29.21 ab)	(74.17±1.78 b-d)	(4,984.27±406.67 c)	(3,702.00±223.77 b)	420.73±51.30 a	87.93±2.15	8,896.80±199.04 ab	7,824.80±155.27 ab
F11	251.75±25.01 abc	83.45±5.49 a-c	**3,601.25±427.82 d**	**3,011.92±397.53 c**	357.69±12.38 b-d	88.37±1.90	7,524.69±925.94 b-d	6,631.30±741.53 b-d
F12	(311.33±23.80 a)	(73.15±3.22 cd)	(6,693.33±562.30 a)	(4, 842.67±474.51 a)	**428.47±41.59 a**	86.95±1.06	**10,207.13±963.63 a**	**8,874.73±845.48 a**
Mean [3/]	219.08±45.70	77.39±6.17	2,113.92±1,035.54	1,635.35±890.13	368.99±41.98	87.55±2.84	7,903.04±800.29	6,903.83±735.38
F-test	**	**	**	**	**	ns	**	**
C.V.(%)	13.38	7.21	12.79	15.11	7.31	4.30	11.56	12.37

[1/] means followed by the same letter within a column are not significantly different (DMRT, P >0.05). [2/] numbers in parentheses are the values of a generation reared in room temperature 25±2°C humidity 80±5% (F6, F8, F10, and F12). [3/] the values of an average of a generation tested at high temperature (F1-F5, F7, F9 and F11) except in control treatment (25±2°C; 80±5%R.H.). ns = non significantly different at 95% level. ** = Significantly different at 99% level.

accumulated by selection using the pupation rate of the silkworm as an index of the thermotolerance on the larvae reared under higher temperature conditions during the 5th instar (Shirota, 1992; Tazima and Ohnuma, 1995). In addition, an increase in the temperature beyond 35°C causes less spinning, mortality of larvae and pupae, poor moth emergence and sterility at adult stage of eri silkworm (Sahu *et al.*, 2006). In this present study, cocoon yields of eri silkworm were obtained regularly from early generation until 12th generation. This indicates that the performance of eri silkworm ecorace with high temperature tolerance improved by directional selection at 42±1°C and low humidity (50±5% R.H.). However, at the same temperature but high humidity (80±5% R.H.) the eri silkworm could not survive and could not complete its life cycle (Sirimungkararat *et al.*, 2013b). This emphasizes that the temperature and relative humidity are the major effective factors on growth and yield of eri silkworm. In the case of domesticated mulberry silkworm, high temperature caused adverse effects on biochemical processes, including the physiology of the worm (Willmer *et al.*, 2004). Rahmathulla (2012) indicated in *B. mori* that relative humidity affects both directly and indirectly the physiological functions of the silkworm and rapidly dry mulberry leaves. Besides, the study of Hussian *et al.* (2011) demonstrated in *B. mori* that rearing silkworm at temperatures, 25±1, 30±1, and 35±1°C and low humidity of 55% R.H. resulted in lowest cocoon yield in almost all tested varieties. Suresh Kumar *et al.* (2001) showed that fresh cocoon and cocoon shell weight of *B. mori* decreased due to high temperature effect and suggested that thermotolerant property was heritable. Similar tendency for the decrease of fresh cocoon weight and cocoon shell weight of high temperature improvement was observed in our study between F1 and F11 of eri silkworm compared to control group. Survival rates of eri silkworm obtained from high temperature treatment increased by directional selection towards F12 in our study. Besides, when all parameters were considered, it was clear that survivals, cocoon yields, and total hatching eggs of F12 were higher than F1 and significantly different ($P<0.05$). This suggests the adaptation of eri silkworm SaKKU1 against higher temperature suppression. There is also evidence that F11, the last generation of high temperature exposure, showed survival rates, which were comparable and not statistically different to the beginning generation (F1). In Thailand, our studies exhibited the thermotolerant property of eri silkworm. Ecorace SaKKU1 can tolerate up to 42±1°C with low humidity (50±5% R.H.) compared to other ecoraces (Sirimungkararat *et al.*, 2013a; Wongsorn *et al.*, 2014). The present study indicates that thermotolerant property of eri silkworm ecorace SaKKU1 is heritable to the progeny. This study is a pioneer work of the improvement of eri silkworm tolerance to high temperature. The derived thermotolerant eri silkworm is used for rearing tests by farmers, which then will be assessed so that new culture methods can be established to cope with recent global warming trend.

Acknowledgements

This research is supported by Plant Genetic Conversation Project Royal under Initiation of Princes Maha Charkri Sirindhorn, KKU-Integrate Multidisciplinary Research Cluster, General Research Fund Fiscal Year 2011-2013 from Khon Kaen University (KKU), Cultivation and Product Development Research Group of Wild Silkmoths and Economic Insects for Value Added Creation, Agricultural Biotechnology Research Center for Sustainable Economy and Center of Agricultural Biotechnology KKU and AG-BIO/PERDO-CHE. Finally, we wish to express our appreciation to Mrs. Somying Chuprayoon, The Queen Sirikit Department of Sericulture for their efforts, comments and improvements of this article.

References

Akai, H. 2002. Development and contribution of international society for wild silkmoths. International Journal of Wild Silkmoth and Silk. 7, 1-10.

He, Y. and Oshiki, T. 1984. Study on cross breeding of a robust silkworm race in low latitude are in China. Journal of Sericultural Science of Japan. 54, 320-324.

Hussian, M., Khan, S.A., Naeem, M., Aqil ,T., Khursheed, R. and Mohsin, A.U. 2011. Evaluation of silkworm lines against variations in temperature and R.H. for various parameters of commercial cocoon production. Psyche. (145640), 1–11.

Kumar, N.S. and Reddy, S.G. 1994. Evaluation and selection of potential parents for silkworm breeding. Proceedings of the National Workshop held, March 18-19, 1994, 63-78.

Kumari, S.S., Subbrarao, S.V., Misra, S. and Murty, U.S. 2011. Screening strains of the mulberry silkworm, *Bombyx mori*, for thermotolerance. Journal of Insect Science. 11(116), 1-14.

Rahmathulla, V.K. 2012. Management of climatic factors for successful silkworm (*Bombyx mori* L.) crop and higher silk production: a review. Psyche. 121234, 1-12.

Rao, P.S., Nayaka, A.R.N., Mamatha, M.T., Sowmyashree, S., Bashai, I. and Ilahi, I. 2007. Development of new robust bivoltine silkworm hybrid SR2xSR5 for rearing throughout the year. International Journal of Industrial Entomology. 14(2), 93-97.

Sahu, M., Bhuyan, N. and Das, P.K. 2006. Eri silkworm, *Samia ricini* (Lepidoptera: Saturniidae) Donovan, seed production during summer in Assam. Proceeding of Regional Seminar on "Prospects and problems of sericulture as an economic enterprise in North West India 2006, Dehradune, India, November 11-12, 2006, 2-3.

Shirota, T. 1992. Selection of healthy silkworm strain through high temperature rearing of fifth instar larvae. Reports of the Silk Science Research Institute. 40, 33-40.

Singh, H. and Kumar, N.S. 2010a. On the breeding of bivoltine breeds of the silkworm, *bombyx mori* L. (Lepidoptera : Bombycidae), tolerant to high temperature and high humidity conditions of the tropics. Psyche. 2010 (892452), 1-15.

Singh, H. and Kumar, N.S. 2010b. On the breeding of bivoltine double hybrid of the silkworm, *Bombyx mori* L. (Lepidoptera : Bombycidae), tolerant to high temperature and low humidity conditions of the tropics. African Journal of Basic and Applied Sciences. 2(3-4), 71–80.

Singh, N.S. and Saratchandra, B. 2012. Eri culture. A P H Publishing Corporation: New Delhi, India.

Sirimungkararat, S. 2012. Eri silkworm products and current status of wild silkmoths in Thailand. The 7th International Conference on Wild Silkmoth and Silk "Southeast Asian Silk", Mahasarakham, Thailand, November 22-24, 2012.

Sirimungkararat, S. 2013. Innovation on eri silk products for the community and economics in Thailand. International Seminar Cum Business Matching on Mekong Silk Road, Khon Kaen, Thailand, November 27-28, 2013.

Sirimungkararat, S. 2014. Eri silkworm rearing in Thailand. International Journal of Wild Silkmoth and Silk. 18, 1-16.

Sirimungkararat, S., Atthathom, T. and Saksirirat, W. 2002. Development of eri-silkworm rearing technique using cassava leaf as food plant and its textile production. Proceeding of XIXth Congress of the International Sericultural Commission, Bangkok, Thailand, September 21-25,2002.

Sirimungkararat, S., Maskhao, S., Wongsorn, D. and Saksirirat, W. 2013a. Effects of high temperature and relative humidity on growths and yields of eri silkworm (*Samia ricini* D.). National Conference on Sericulture 2013, Bangkok, Thailand, June 25-27, 2013. (Abstract in English)

Sirimungkararat, S., Nuchadomrong, S., Saksirirat, W. and Nopparat, T. 2010. By-product of eri silkworm rearing as preliminary cosmetic product development. 6th International Conference on Wild Silkmoths, Tokyo, Japan, September 21-23, 2010.

Sirmungkararat, S., Urairong, H., Wongsorn, D. and Saksirirat, W. 2013b. Searching of microsatellite primers for diversity study of eri silkworm. The Conference of the Queen Sirikit Department of Sericulture, Ministry of Agriculture and Cooperatives, Bangkok, Thailand, June 26-27, 2013. (Abstract in English)

Suresh Kumar, N., Yamamota, T., Basavaraja, H.K. and Datta, R.K. 2001. Studies on the effect of high temperature on F1 hybrids between polyvoltine and bivoltine silkworm races of *Bombyx mori* L. International Journal of Entomology. 2, 123-127.

Suresh Kumar, N., Basavaraja, H.K., Kumar, C.M.K., Reddy, N.M. and Datta, R.K. 2002. On the breeding of "CSR18xCSR19" – a robust bivoltine hybrid of silkworm, *Bombyx mori* L. for the tropics. International Journal of Industrial Entomology. 5(2), 153-162.

Tazima, Y. and Ohnuma, A. 1995. Preliminary experiments on the breeding procedure for synthesizing a high temperature resistant commercial strain of the silkworm, *Bombyx mori* L. Silk Science Research Institute Japan. 43, 1-16.

Toyama, K. 1906. Studies on hybridology of insects. I. On some silkworm crosses, with special reference to Mendel's law of heredity. Bulletin Tokyo Imperial University College of Agriculture 7, 259-293.

Willmer, C.W., Stone, G. and Johnston, I. 2004. Environmental physiology of animal. Blackwell Science, Oxford: UK.

Wongsorn, D., Sirimungkararat, S., Urairong, H., Saksirirat, W. and Chooprayoon, S. 2014. Selection of eri silkworm (*Samia ricini* D.) tolerant ecorace to high temperature. The Conference of the Queen Sirikit Department of Sericulture, Ministry of Agriculture and Cooperatives 2014, Pathum Thani, Thailand, April 2-4, 2014. (Abstract in English)

Songklanakarin J. Sci. Technol.
37 (5), 499-505, Sep. - Oct. 2015

http://www.sjst.psu.ac.th

Original Article

Screening for eri silkworm (*Samia ricini* Donovan) ecoraces using morphological characters, growth, yields, and ISSR marker

Duanpen Wongsorn[1], Weerasak Saksirirat[2,3]*, Sivilai Sirimungkararat[1,2,3], and Hathairat Urairong[4]

[1] *Entomology Section, Department of Plant Science and Agricultural Resources,*

[2] *Cultivation and Product Development Research Group of Wild Silkmoths and Economic Insects for Value Added Creation,*

[3] *Agricultural Biotechnology Research Center for Sustainable Economy and Center of Agricultural Biotechnology (AG- BIO/PERDO-CHE), Faculty of Agriculture, Khon Kaen University, Mueang, Khon Kaen, 40002 Thailand.*

[4] *Biotechnology Research and Development Office, Sirinthorn Genetic Resources Building, Department of Agriculture, Ministry of Agriculture and Cooperatives, Pathum Thani, 12110 Thailand.*

Received: 14 February 2015; Accepted: 18 May 2015

Abstract

The selection of eri silkworm ecoraces with high yield and distinct morphological characters is necessary for variety improvement. The five ecoraces SaKKU1, SaKKU2, SaKKU3, SaKKU4 and SaKKU5 were derived mostly by international academic cooperation. They were cultured using castor leaves of TCO 101 cultivar as food plant at 25±2°C, 80±5% R.H. Based on morphological characters, they are similar, except the body of the 5th instar larva of SaKKU1 is clearly covered with more creamy white powder and the mature larva has a shiny dominant yellow color. The duration of the life cycle among ecoraces was also similar; 46-53 days (SaKKU1), 42-53 days (SaKKU2), 42-52 days (SaKKU3), 40-56 days (SaKKU4) and 41-52 days (SaKKU5). SaKKU1 had the highest survival rate at larval stage (1st – 5th instar) (100.00%) and larva (1st – 5th instar) - adult (88.89%), including the predominant heaviest average larva weight of all instars, 0.0317 g (2nd instar), 0.2206 g (3rd instar), 1.0788 g (4th instar), 4.0102 g (5th instar), and 8.9940 g (5 days of 5th instar), which was significantly different ($P<0.05$) to other ecoraces. Moreover, this ecorace gave the highest average yields: fresh cocoon weight (3.8016 g), pupa weight (3.2532 g), shell weight (0.5287 g), shell ratio (14.01%), fresh cocoon weight/10,000 larvae (38.01 kg), eggs/moth (531.13 eggs), total eggs (6,375.27 eggs) and total hatching eggs (6,006.13 eggs), which was also significantly different ($P<0.05$) than other ecoraces. Of those properties, especially survival rates and yields, this ecorace (SaKKU1) is favored for further varietal improvement program. In parallel, genetic relationship analysis of eri silkworm ecoraces using inter-simple sequence repeat (ISSR) technique was also carried out. The result revealed from dendrogram analysis that SaKKU1 was the farthest distance than other ecoraces, especially against SaKKU3. Based on all above results, the SaKKU1 ecorace was considered to be the most suitable for heat tolerant variety improvement.

Keywords: screening, ecorace, eri silkworm, yield, ISSR marker

* Corresponding author.
Email address: weerasak@kku.ac.th

1. Introduction

Eri silkworm (*Samia ricini* Donovan), Lepidoptera: Saturniidae), a commercial silk producing insect, is believed to have originated in the Brahmaputra Valley of India (Jolly *et al*., 1979) and had restricted distribution in India, China, and Japan for two centuries (Peigler, 1993; Singh and Benchamin, 2002). The primary food plant of this polyphagous insect is castor (*Ricinus communis* L.), but it also feeds on a wide range of food plants such as Kesseru (*Heteropanax fragrans*), Tapioca (*Manihot esculenta*), Ceara rubber tree (*Manihot glaziovii*), Variegated tapioca (*Manihot esculenta variegata*), and Gulancha Phool/Champa (*Plumeria acutifolia*) (Sirimungkararat *et al*., 2005). Besides, the new food plants and the alternative food plant are also very suitable to feed eri silkworm in some cases (Sirimungkararat *et al*., 2005; Buamuangpia *et al*., 2014). The wild *S. canningi* silkworm (the progenitor of the domesticated *S. ricini*) completes one to three generations per year depending on geographical position and climatic condition of region; however, up to six generations occur in the domesticated cultures (Neupane *et al*., 1990). Populations of eri silkworm that have been commercially exploited are present in different regions of north-east India showing wide variations in morphological and quantitative characters such as absolute silk content, larval weight, cocoon weight, cocoon shell weight, and silk ratio (Siddiqui *et al*., 2000). Eri silkworm was introduced to Thailand around 1974 by technical cooperation of the Department of Agricultural Ministry of Agriculture and Cooperatives, for cultivation test of highland project in northern Thailand (Wongtong *et al*., 1980). However, due to the density of host plants in mountainous area, the eri silkworm rearing was proposed for other parts of the country where the host plants were sufficient and the farmers have skills also with indigenous knowledge on sericulture. The Northeast of Thailand is a largest planting area of cassava (*Manihot esculenta*), a host plant of eri silkworm, and the farmer has knowledge on sericulture as the way of life. Therefore, several research projects have focused on rearing technique, machine and appliance development, textile, eri food and cosmetic products including exploitation of eri rearing waste. Of those, our studies were published in series (Sirimungkararat *et al*., 2002; 2005; 2007a. 2007b; 2010; 2012; 2013a; 2013b; 2014). In order to preserve the natural biodiversity present among these populations, attempts are being made to know the basic morphological characters, growth, yield and the genetic variation of each population. As molecular markers are stable and environmentally independent, they are increasingly being preferred to phenotypic traits to detect genetic variation not only among populations but also between individuals within a population. There are a number of DNA marker systems to be applied for this purpose such as RFLP (restriction fragment length polymorphism) (Mahendran *et al*., 2006), RAPD (random amplified polymorphic DNA) (Lui *et al*., 2010), SCAR marker (sequence characterized amplified region) (Saha and Kundu, 2006), and ISSR (Chatterjee *et al*., 2004; Kar *et al*., 2005; Vijayan *et al*., 2006; Pradeep *et al*., 2011). The objective of this study aimed to evaluate the eri ecoraces from basic morphological characters, growth, some quantitative traits and genetic basis variability, leading to the most suitable ecorace for heat tolerance improvement program.

2. Materials and Methods

2.1 Eri silkworm ecoraces

Five ecoraces of eri silkworm were derived by local collecting and international academic cooperation between Thailand, India, and Japan, which were coded as SaKKU1, SaKKU2, SaKKU3, SaKKU4 and SaKKU5. The larvae of all ecoraces were fed with castor leaves cultivar TCO 101, at room temperature 25±2°C and 80±5% relative humidity (R.H.). The rearing method was modified from Sirimungkararat *et al.* (2002).

2.2 Morphological characters, life cycle, survival and yields of eri silkworm

Eri silkworm ecoraces were investigated for morphological characters of larva, life cycles, survival rates, and also the yield components of cocoons and eggs, based on rearing conditions described previously. The following data were recorded: weight and size of each instar (24 hrs after molting), survival rates from $1^{st} - 5^{th}$ larva instar and larva ($1^{st} - 5^{th}$ instar)– adult, cocoon yields (fresh cocoon weight, pupa weight, shell weight, shell ratio, total cocoon shell weight and fresh cocoon weight/10,000 larvae), and egg yields (eggs/moth, hatching eggs, total eggs, and total hatching eggs). Weighing of cocoon or pupa with four decimal, a balance Sartorius BP 210S, Germany was used. The experimental design known as completely randomized design (CRD) was used. The ecoraces served as treatments with three replications. Each replication contained 50 larvae of eri silkworm. Analysis of variance (ANOVA) was done and means of the treatments were compared statistically using Duncan's multiple range test (DMRT).

2.3 Genetic relationship study of eri silkworm using inter-simple sequence repeat technique

Ten mature 5^{th} instar larvae of each ecorace were taken for DNA extraction using silk glands. The glands were washed with 70% ethanol to remove traces of sericin and then crushed in pre-chilled mortar and pestle with liquid nitrogen. Genomic DNA from 10 individual larvae of each ecorace was extracted separately by using phenol:chloroform extraction method (Chatterjee *et al*., 2004). Five inter-simple sequence repeat (ISSR) primers were used for the study UBC811 ($(GA)_8C$), UBC818($(CA)_8G$), UBC848($(CA)_8AGG$), UBC857 ($(CA)_8CTG$) and UBC888(CGTAGTCGT $(CA)_7$). The polymerase chain reaction (PCR) was performed in an MJ Research

thermal cycler, PTC200, using 20 µl reaction mixture containing 30 ng DNA, 2.0 µl of 10xPCR buffer (MBI Fermentas), 0.2 mM dNTP, 2.5 mM $MgCl_2$, 0.15 µl M primer and 0.10 µl *Tag*DNA polymerase (recombinant) (5 U/µl). The PCR products were resolved on 1.5% agarose gel, in Tris-Boric Acid-EDTA buffer, stained with ethidium bromide (0.5 µg/ml). The genetic variability in the population was analyzed using phylogenetic tree based on Neighbor-Joining method.

3. Results

3.1 Morphological characters, life cycle, survival and yields of eri silkworm

The eri silkworm is a multivotine (polyvoltine) wild silkmoth, and has complete metamorphosis. The five ecoraces had similar morphological characters in all development stages: egg, larva, pupa and adult, both in shape and color having similar characteristics. There was only one that was somewhat different. The ripe larva of SaKKU1 showed shiny distinct yellow color than other ecorace (Table 1).

In the cultivation of eri silkworm using castor leaves cultivar TCO 101, it was shown that all ecoraces had similar life cycle durations of 46-53, 42-53, 42-52, 40-56 and 41-52 days for ecorace SaKKU1, SaKKU2, SaKKU3, SaKKU4, and SaKKU5, respectively. The shortest life cycle was 40 days (ecorace SaKKU4). The age of both female and male moths of SaKKU1 (10-14 days) was longer than other ecoraces, with values between 4-12 days for males (4-12 days) and females (5-12 days).

The survival of the larval stage (1^{st}–5^{th}) (Table 2), the rate of SaKKU1 was the highest (100.00%), which differed statistically from other ecoraces ($P<0.05$). Whereas, the survival of larval stage (1^{st}–5^{th}) – adult, the ecorace SaKKU1 still had a maximum rate (88.89%) with no statistical difference compared to ecorace SaKKU4 (85.56%)

Table 1. Phenotypic characters of five different ecoraces of eri silkworm (*Samia ricini*) fed with leaf of castor cultivar TCO 101.

Characters	Ecorace				
	SaKKU1	SaKKU2	SaKKU3	SaKKU4	SaKKU5
Voltinism	Multivotine	Multivotine	Multivotine	Multivotine	Multivotine
Egg color	Creamy white	Creamy white	Creamy white	Creamy white	Creamy white
Larval color (5-days-old 5^{th} instar)	Greenish light blue with more white powder cover body	Greenish light blue with slight white powder cover body	Greenish light blue with slight white powder cover body	Greenish light blue with slight white powder cover body	Greenish light blue with slight white powder cover body
Larval color (ripe larva)	Distinct yellow	Yellow	Yellow	Yellow	Yellow
Larval marking	Plain	Plain	Plain	Plain	Plain
Cocoon color	Creamy white	Creamy white	Creamy white	Creamy white	Creamy white
Cocoon shape	Oval	Oval	Oval	Oval	Oval
Moth color (both sexes)	Blackish gray	Blackish gray	Blackish gray	Blackish gray	Blackish gray

Table 2. Survival (mean±SD) of eri silkworm (*Samia ricini*) fed with leaf of castor cultivar TCO 101.

Ecorace	Survival (%)	
	Larva (1^{st} – 5^{th} instar)	Larva(1^{st} – 5^{th} instar) – Adult
SaKKU1	100.00±0.00 a	88.89±5.09 a
SaKKU2	64.44±1.92 d	64.44±1.92 d
SaKKU3	74.44±5.09 c	71.11±1.92bc
SaKKU4	85.56±5.09 b	85.56±5.09 a
SaKKU5	76.67±8.82 bc	73.33±5.77 b
F-test	**	**
C.V. (%)	**6.44**	**5.61**

Means followed by the same letter within a column are not significantly different (DMRT, $P>0.05$). ** = Significantly different at 99% level.

The average weights of silkworms of various ages were shown in Table 3. The 1st instar in all ecorace was similar and did not differ statistically. But the 2nd, 3rd, 4th, 5th, and 5day of 5th instar of ecorace SaKKU1 had the highest values (0.0317, 0.2206, 1.0788, 4.0102, and 8.9940 g, respectively), which differed statistically significant ($P<0.05$) from other ecoraces. The weight of mature silkworms (5 days of 5th instar) of ecorace SaKKU2 - SaKKU5 ranged from 5.4544 to 6.0649 g, which was not significantly different.

As well as the average body size of the silkworm in each instar and growth, it was found that the ecorace SaKKU1 had still larger body size than other ecoraces, with means of 0.10 × 0.48, 0.23 × 1.14, 0.42 × 2.31, 0.86 × 3.97, 1.25 × 6.61 and 1.63 × 9.02 cm for 1st, 2nd, 3rd, 4th, 5th, and 5 day of 5th instar, respectively. The body size of eri larvae of ecorace SaKKU2, SaKKU3, SaKKU4 and SaKKU5 in each instar were similar: 1st instar (0.10 × 0.45 - 0.47 cm), 2nd instar (0.15 × 0.89 - 0.98 cm), 3rd instar (0.38 - 0.40 × 1.96 - 2.02 cm), 4th instar (0.63 - 0.71 × 3.11 - 3.28 cm), 5th instar (1.00 - 1.09 × 5.20 - 5.33 cm), and 5 day of 5th instar (1.39 - 1.44 × 7.17 - 7.49 cm).

The average output of cocoon yields (Table 4) showed that ecorace SaKKU1 had the highest in various yields of fresh cocoon weight (3.8016 g), pupa weight (3.2532 g), shell weight (0.5287 g), shell ratio (14.01%), total cocoon shell weight (15.86 g) and fresh cocoon weight/10,000 larvae (38.01 kg), which is still higher and the difference is highly significant compared to the other ecoraces.

For egg yields (Table 5), the number of eggs/moth, total eggs, and total hatching eggs, SaKKU1 remained the most effective ecorace (531.13, 6,375.27 and 6,006.13 eggs, respectively) and were significantly different ($P<0.05$) compared to the others. The hatching egg percentage of all ecoraces were similar and did not differ statistically, whereas ecorace SaKKU1 had the highest value (94.33%), followed by ecorace SaKKU2 (93.74%) and SaKKU5 (92.57%), respectively.

Table 3. Mean (mean±SD) weights of eri larva (*Samia ricini*) of different instars fed with leaf of castor cultivar TCO 101.

Ecorace	Mean weights of larva (g)					
	1st instar	2nd instar	3rd instar	4th instar	5th instar	5 days of 5th instar
SaKKU1	0.0020	**0.0317±0.001 a**	**0.2206±0.002 a**	**1.0788±0.09 a**	**4.0102±0.13 a**	**8.9940±0.42 a**
SaKKU2	0.0020	0.0120±0.001 c	0.1371±0.008 c	0.5487±0.04 b	2.5116±0.23 b	6.0649±0.24 b
SaKKU3	0.0020	0.0166±0.001 b	0.1338±0.004 c	0.6055±0.06 b	2.4689±0.05 b	5.5984±0.61 b
SaKKU4	**0.0021**	0.0123±0.001 c	0.1573±0.008 b	0.5303±0.05 b	2.4963±0.38 b	5.4544±0.11 b
SaKKU5	0.0020	0.0136±0.002 c	0.1323±0.016 c	0.6422±0.07 b	2.3978±0.20 b	5.6790±0.37 b
F-test	**ns**	**	**	**	**	**
C.V.(%)	**4.30**	**6.93**	**5.76**	**9.74**	**8.09**	**6.13**

Means followed by the same letter within a column are not significantly different (DMRT, $P>0.05$).
ns = Non significantly different at 95% level
** = Significantly different at 99% level

Table 4. Yields (mean±SD) of eri silkworm (*Samia ricini*) fed with leaf of castor cultivar TCO 101.

Ecorace	Average yield					
	Fresh cocoon weight (g)	Pupa weight (g)	Shell weight (g)	Shell ratio (%)	Total cocoon shell weight (g)	Fresh cocoon weight/ 10,000 larvae (kg)
SaKKU1	**3.8016±0.41 a**	**3.2532±0.37 a**	**0.5287±0.04 a**	**14.01±0.59 a**	**15.86±1.07 a**	**38.01±1.42 a**
SaKKU2	2.4591±0.21 b	2.1584±0.18 b	0.2879±0.03 b	11.64±0.23 b	5.57±0.65 c	24.59±2.37 b
SaKKU3	2.0100±0.14 b	1.8695±0.12 b	0.2570±0.03 b	11.93±0.59 b	5.71±0.23 c	20.10±1.67 b
SaKKU4	2.4169±0.16 b	2.1094±0.14 b	0.2943±0.02 b	12.16±0.12 b	7.34±0.23 b	24.17±3.11 b
SaKKU5	2.3943±0.14 b	2.0971±0.13 b	0.2856±0.01 b	11.94±0.32 b	6.57±083 bc	23.95±2.04 b
F-test	**	**	**	**	**	**
C.V. (%)	**8.93**	**9.07**	**7.67**	**3.39**	**8.42**	**8.93**

Means followed by the same letter within a column are not significantly different (DMRT, $P>0.05$).
** = Significantly different at 99% level.

Table 5. Egg yields (mean±SD) of eri silkworm (*Samia ricini*) fed with leaf of castor cultivar TCO 101.

Ecorace	Average yield				
	Eggs/moth (eggs)	Hatching eggs (%)	Total eggs (eggs)	Total hatching eggs (eggs)	Male : Female
SaKKU1	**531.13**±30.28 **a**	94.33±2.60	**6,375.27±320.11 a**	**6,006.13±277.33 a**	1: 2.32
SaKKU2	353.87±45.67 b	93.74±3.27	4,027.87±297.22 b	3,762.07±321.00 b	1:1.31
SaKKU3	272.40±37.32 b	88.87±5.73	2,413.07±263.37 b	2,174.13±321.00 b	1:1.72
SaKKU4	322.87±35.62 b	91.75±5.26	3,990.20±311.01 b	3,663.20±272.33 b	1:1
SaKKU5	310.20±27.65 b	92.57±2.96	3,194.60±255.41 b	2,602.27±266.13 b	1:1.30
F-test	**	**ns**	**	**	-
C.V.(%)	**12.62**	**4.52**	**25.79**	**24.57**	-

Means followed by the same letter within a column are not significantly different (DMRT, P >0.05).
ns = Non significantly different at 95% level. ** = Significantly different at 99% level.

3.2 Genetic relationship study of eri silkworm using inter-simple sequence repeat technique

The five primers of inter-simple sequence repeat (ISSR) produced 34 different DNA fragments of all ecoraces varying from 200 to 2,700 bp (data not shown). The data of DNA fragments were analyzed to obtain a dendrogram using Neighbor-Joining method as illustrated in Figure 1. Based on the dendrogram, the ecorace SaKKU3 was the most closely related to ecorace SaKKU5. Obviously, the ecorace SaKKU1 resulted in an outgroup against SaKKU3 and other ecoraces.

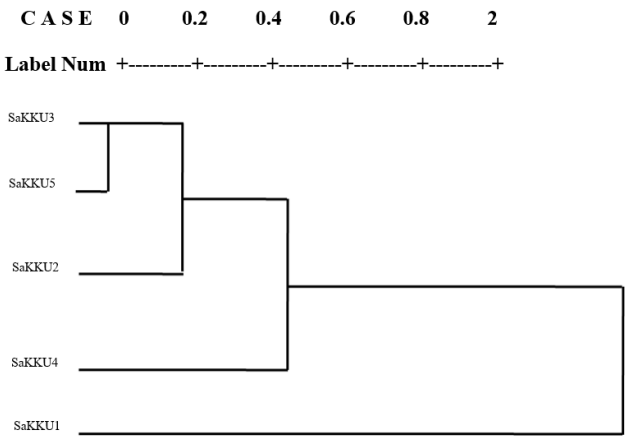


Figure 1. Dendrogram showing grouping of the five ecoraces of eri silkworm (*Samia ricini*)

4. Conclusions and Discussion

Our results on morphological study clearly indicated that the 5th instar larva of ecorace SaKKU1 showed more white powder covering larva body, with distinct yellow color than other ecoraces. These characters were supported by the ISSR data, which exhibited the outgroup of SaKKU1 with the farthest distance from SaKKU3 and other ecoraces. Five ecoraces have been also studied for their genetic relationships using simple sequence repeat (SSR) by our previous study (Sirimungkararat *et al*., 2013a) using primer SCO 1293 and could be characterized by the genetic difference of SaKKU1 among other ecoraces. For non-mulberry silkworms, molecular techniques have been used to identify differences in populations, such as RAPD for eri silkworm (Zuo *et al*., 2001; Shivashankar *et al*., 2013) and RFLP (restriction fragment length polymorphism) for the wild tasar silkmoth (Mahendran *et al*., 2006). Moreover, in the present study the ISSR technique was reliable due to specific primer of repeat bases.

In general, the objective of variety improvement in sericulture is to develop the pure variety or hybrid variety to withstand environmental conditions and to provide highest yields in both quality and quantity. The present study focuses on the screening of the best ecorace of eri silkworm for improvement against high temperature and other unfavorable environment. Therefore, the selection of ecorace is necessary to conduct to achieve the most suitable ecorace. Our result indicated that the ecorace SaKKU1 is the best ecorace, showing the highest survival rates (larval stage 100%, larva – adult 88.89%), the heaviest larva weight of 2nd – 5th instar and of 5th instar day 5. Both cocoon yields and eggs yield were statistically significant among other ecoraces (P<0.05). It is possible that the ecorace SaKKU1 responded to the food plant (castor cultivar TCO 101) better than other ecoraces. Among ecoraces the response may depend on different food plants. However, feeding one ecorace eri silkworm with the same plant but not the same variety resulted in different growth and yield expression (Sirimungkararat *et al*., 2013b; Sirimungkararat *et al.,* 2012). Whereas, Chandrashekhar *et al*. (2013) revealed that different varieties of castor had varying nutritional properties. Besides, environmental factors such as temperature, light, humidity and larval density in the rearing containers can affect the life cycle of eri

silkworm (Hans and Sundaramoorthy, 2003). In addition, Kalpana and Reddy (1988) reported that the yield of mulberry silkworm was less dependent on genetic potential of each line than on rearing environments.

Analysis of genetic difference of eri ecoraces by using ISSR exhibited that the SaKKU3 and SaKKU5 were closely related. Obviously, the SaKKU1 was the most different from other ecoraces, especially from the SaKKU3. Although the yields obtained from all ecoraces are similar, the SaKKU1 showed the best performance and potential to be subjected in the variety improvement program. The ISSR technique can be characterized on different genetic information, which correlated to the morphological characterization e.g. the SaKKU1 5th instar larva had color and cuticle powder different to other ecoraces, and also the genetic divergence was the most distinct. Besides the ISSR, the SSR (Simple sequence repeat or microsatellite) could be also applied in eri silkworm ecorace for population characterization by using SCO 1293 primer, the SaKKU1 and SaKKU4 had no inter-population polymorphism, whereas SaKKU5 had the most polymorphism (Sirimungkararat *et al*., 2013a). However, other technique, e.g. RAPD (Random amplified polymorphic DNA) for genetic characterization of silkworm (Zuo *et al*., 2001; Shivashankar *et al*., 2013) including eri silkworm, mulberry silkworm and oak silkworm (*Antheraea pernyi*) (Liu *et al*., 2010) and the RFLP (restriction fragment length polymorphism) were also applied in the genetic characterization study. Based on our result, the SaKKU1 ecorace is the most appropriate to be used in the variety improvement program.

Acknowledgements

This research was financially supported by Plant Genetic Conservation Project under The Royal Initiative of Her Royal Highness Princess Maha Chakri Sirindhorn, the general supporting research fund of fiscal year 2011-2013, Khon Kaen University (KKU), KKU-Integrate Multidisciplinary Research Cluster, and the Cultivation and Product Development Research Group of Wild Silkmoths and Economic Insects for Value Added Creation, KKU, Thailand. Thanks are also extended to Center of Agricultural Biotechnology (AG-BIO/PERDO-CHE) and Agricultural Biotechnology Research Center for Sustainable Economy, KKU for access to supporting equipment and facilities.

References

Buamuangpia, C., Sirimungkararat, S., Pitirit, T. and Saksirirat, W. 2014. Efficiency of alternation of food plants on rearing and yields of eri silkworm (*Samia ricini* D.). National Conference on Sericulture, Pathum Thani, Thailand. April 2-4, 2014, 332-343.

Chandrashekhar, S., Sannappa, B., Manjunath, K.G. and Govindan, R. 2013. Nutritive value of leaves in different genotypes of castor (*Ricinus communis* L). Indian Journal of Plant Sciences. 2(2), 22-27.

Chatterjee, S.N., Vojayan, K., Roy, G.C. and Nair, C.V. 2004. ISSR profiling of genetic variability in ecotypes of *Antheraea mylitta* Drury, the tropical tasar silkworm. Russian Journal of Genetics. 40(2), 152-159.

Jolly, M.S., Sen, S.K., Sonwalkar, T.N. and Prasad, G.K. 1979. Non-mulberry silks. FAO: Rome. Italy.

Hans, D. and Sundaramoorthy, S. 2003. Life cycle duration of *Philosamia ricinii* (L.) on thirteen released castor varieties as different host plants for appraisal of best variety/ varieties. Asian Journal Experimental Science. 17(1), 11-15.

Kalpana, G.V. and Reddy, S.G. 1988. Synthesis of bivoltine race of silkworm *Bombyx mori* for tropical climate. International Congress on Tropical Sericulture Practice, Bangalore, India, February 18-23, 1988, 451-458.

Kar, P.K., Vijayan, K., Mohandas, T.P., Nair, C.V., Saratchandra, B. and Thangavelu, K. 2005. Genetic variability and genetic structure of wild and semi-domestic populations of tasar silkworm (*Antheraea mylitta*) ecorace Daba as revealed through ISSR markers. Genetica. 125, 173-183.

Liu, Y.Q., Qin, L., Li, Y.P., Wang, H., Xia, R.X., Qi, Y.H., Li, X.S., Lu, C. and Xiang, Z.H. 2010. Comparative genetic diversity and genetic structure of three Chinese silkworm species *Bombyx mori* L. (Lepidoptera : Bombycidae), *Antheraea pernyi* Guerin-Meneville and *Samia cynthia ricini* Donovan (Lepidoptera : Saturniidae). Neotropical Entomology. 39(6), 967-976.

Mahendran, B., Padhi, B.K., Ghosh, S.K. and Kundu, S.C. 2006. Genetic variation in ecoraces of tropical tasar silkworm, *Antheraea mylitta* D. using RFLP technique. Current Science. 90(1), 100-103.

Neupane F.P., Thapa, R.B. and Parajulee, M.N. 1990. Life and seasonal histories of the eri silkworm, *Samia cynthia ricini* Hutt. (Lepidoptera: Saturniidae), in Chitwan, Nepal. Journal of Institute of Agriculture: Animal Science. 11, 113-120.

Pradeep, A.R., Awasthi, A.K., Singh, C.K., Anuradha, H.J., Guruprasad, C., Rao, P. and Vijayaprakash, N.B. 2011. Genetic evaluation of eri silkworm *Samia cynthia ricini*: ISSR loci specific to high and low altitude regimes and quantitative attributes. Journal of Applied Genetics. 15, 1-12.

Peigler, R.S. 1993. Wild silks of the world. American Entomologist. 39, 151-161.

Saha, M. and Kundu, S.C. 2006. Molecular identification of tropical tasar silkworm (*Antheraea mylitta*) ecoraces with RAPD and SCAR Marker. Biochemical Genetics. 44(1/2), 75-88.

Shivashankar, M., Chandan, N. and Nagananda, G.S. 2013. Genetic diversity analysis of eri silkworm by RAPD. Journal of Chemical, Biological and Physical Sciences. 3(1), 326-335.

Siddiqui A.A., Saha, L.M. and Das, P.K. 2000. Genetic variability and correlation studies of some quantitative

traits in eri silkworm. International Journal of Wild Silkmoth and Silk. 5, 234-237.

Singh, K.C. and Benchamin, K.V. 2002. Biology and ecology of the eri silkmoth *Samia ricini* (Donovan) (Saturniidae): a review. Bulletin of Indian Academy of Sericulture. 6, 20-33.

Sirimungkararat, S., Atthathom, T. and Saksirirat, W. 2002. Development of eri-silkworm rearing technique using cassava leaf as food plant and its textile production. Proceedings of the XIXth Congress of the International Sericultural Commission, Bangkok, Thailand, September 21-15, 2002.

Sirimungkararat, S., Saksirirat, W. and Wongsorn, D. 2014. Ideal edible insect: High value, safety food and innovative products with complete value chain of eri silkworm (*Samia ricini* D.) in Thailand. Proceeding of International Conference Insects to Feed the World, Ede, The Netherlands. May 14-17, 2014.

Sirimungkararat, S., Urairong, H., Wongsorn, D. and Saksirirat, W. 2013a. Searching of microsatellite primers for diversity study of eri silkworm. Proceeding of National Conference on Sericulture 2013, Bangkok, Thailand, June 25-27, 2013.

Sirimungkararat, S., Sangtamat, T., Saksirirat, W. and Wongsorn, D. 2007a. Effect of some major and alternate food plants on growth of eri silkworm (*Samia ricini* D.). International Journal Wild Silkmoth and Silk. 12, 29-34.

Sirimungkararat, S., Sangtamat, T., Saksirirat, W. and Waikakul, Y. 2005. New food plants for eri silkworm rearing. International Journal of Wild Silkmoth and Silk. 10, 27-34.

Sirimungkararat, S., Saksirirat, W., Wongsorn, D. and Apinakpong, K. 2012. Yield response of eri silkworm (*Samia ricini*) on major food plant in Thailand. Proceeding of The 7th International Conference on Wild Silkmoth and Silk "Southeast Asian Silk". Mahasarakham, Thailand, November 22-24, 2012.

Sirimungkararat, S., Saksirirat, W. Wongsorn, D. and Maskao, S. 2013b. Use of castor commercial line for increasing yield of eri silkworm. Khon Kaen Agriculture Journal. 41 (supplement), 185-191.

Sirimungkararat, S., Saksirirat, W., Nopparat, T. and Nathongkham, A. 2010. Edible products from eri silkworm (*Samia ricini* D.) and mulberry silkworm (*Bombyx mori* L.) in Thailand. In Edible forest insects as food: humans bite back. Durst, P.B., Johnson, D.V., Leslie, R.N. and Shono, K. editors, FAO: Bangkok, Thailand, pp. 189-200.

Sirimungkararat, S., Kamoltip, S., Suksirirat, W., Sangtamat, T. and Wongsorn, D. 2007b. Eri silk yarn producing and innovative textile products. International Journal Wild Silkmoth and Silk. 12, 21-28.

Vijayan, K., Anuradha, H.J., Nair, C.V., Pradeep, A.R., Awasthi, A.K., Saratchandra, B. S., Rahman, A.S., Singh, K.C., Chakraborti, R. and URs, S.R. 2006. Genetic diversity and differentiation among populations of the Indian eri silkworm, *Samia cynthia ricini*, revealed by ISSR markers. Journal of Insect Science. 30, 1-11.

Wongtong, S., Areekul, P., Onlamoon, A. and Tragoolgarn, S. 1980. Research on wild silkworm cultivation in the highlands of northern Thailand. Final Report of Highland Agriculture Project 1976-1980. Bangkok, Thailand.

Zuo, Z.-H., Mu-Yan, G., Xue-Min, W. and Yuan-Lin, C. 2001. Application of RAPD technique in genetic relationship study of silk insect I. Genetic variance in eri silkworm. Hereditas. 23(2), 128-130.

The Potential of Phosphate-Solubilizing Bacteria from the Eggplant Fields

K. Sungthongwises[1], M. Matsuoka[2], K. Ohnishi[2], S. Tanaka[2] and C.B. Iwai[1]
[1] Department of Plant Science and Agricultural Resources, Faculty of Agriculture, Khon Kaen University, Khon Kaen, Thailand
[2] Faculty of Agriculture, Kochi University (Nankoku campus), Kochi, Japan

Keywords: bio-inoculums, eggplant, phosphate-solubilizing bacteria (PSB)

Abstract

The present study aims to identify the diversity and the efficiency of phosphate-solubilizing bacteria (PSB) with a strong potential as bio-inoculums from eggplant fields. Phosphorus is considered as the principal yield-limiting nutrient along with nitrogen. Accordingly it is a primary constraint to plant growth in many terrestrial ecosystems especially, in acid sandy soils with high levels of P fixation by Fe and Al oxides. The potential of phosphate solubilizing bacteria (PSB) to increase soluble P by enhancing solubilization of insoluble P compounds was isolated and evaluated in this experiment. Six different PSB strains isolated from eggplant fields were screened for their efficiency in P solubilization. The PSB isolated from eggplant field soils solubilized 770-1,548 mg/L of P. Stepwise multiple regression analysis and P solubility kinetics indicated that the major mechanism of P solubilization by PSB is the pH reduction through the release of organic acids. Especially, *Klebsiella pneumoniae* strain M-AI-2 isolate code Ek04 and *Gluconacetobacter* sp. isolate code Ek01 in the eggplant field seem to have the capacity to solubilize insoluble forms of $AlPO_4$ and $FePO_4$ which are the main forms of insoluble phosphates in acid sandy soils.

INTRODUCTION

N, P and K are major essential macronutrients for plant growth and development especially, phosphorus is considered for ATP synthesis. ATP is an essential energy-provider molecule for the metabolism of organic compounds containing P such as sugar phosphates, phospholipids, nucleic acids, nucleotides and coenzymes which are key molecules for biological metabolisms (Schachtman et al., 1998). PSB have been used to increase soluble forms of available P for plant growth by plant root exudation and microorganisms produce phosphatases. The phosphatases efficiency is related to various factors such as the microbial fauna, the soil temperature and humidity and more particularly the associated bacteria communities (Zahran, 1999). Phosphatases activity can be induced by low inorganic phosphorus concentrations in the soil solution, but other factors can play a significant role as the environmental conditions, the physiological state of the plant, the type of rooting system, the age of the plant and the location of ectomycorrhiza on the root (Antibus et al., 1997).

The analysis of the ability of bacterial isolates to solubilize insoluble P form to available P form will enable to create a highly valuable basis for the use of these isolates as bio-inoculums or bio-fertilizer to increase crops yield. Godinho et al. (2010) found that *Bacillus subtilis*, *Kocuria rosea* and *Microbacterium arborescens* from sand dunes of goa are good plant growth promoters as biofertilizers for promoting growth in eggplant field according to it having ACC deaminase activity and other attributes like IAA, HCN production, siderophore production and phosphate solubilization. ACC deaminase activity might have produced better root growth in the initial stages of crop growth by reducing the level of ethylene in the roots of the developing plants thereby increasing the root length and growth. This resulted in healthy plants due to balanced nutrient availability and uptake, which in turn increased plant biomass. The potential of PSB *Bacillus megaterium* and potassium solubilizing bacteria (KSB) *Bacillus mucilaginosus* in combination did not significantly enhance soil availability of P and K. PSB increased

higher soil P availability than KSB and promote growth of eggplant in Korea (Han and Lee, 2005). The location of ectomycorrhiza on the eggplant root particularly in the isolation of phosphate-solubilizing bacteria and their P solubilization capacity in the phosphorus cycle remains poorly studied. The objectives of this research were to isolate phosphate-solubilizing bacteria (PSB) from eggplant fields, evaluate their P solubilization capacity and identify the PSB in Kochi, Japan.

MATERIALS AND METHODS

Soil Sampling

The experiment was conducted within Kochi prefecture, Japan. Kochi prefecture is characterized by a semi-arid tropical climate with a distinct rainy season from May to September. Soil samples were collected from eggplant fields from the soil surface until a depth of 10 cm in order to isolate phosphate solubilizing bacteria. The soil samples were analyzed for pH, total N, total P, available P and exchangeable K (Table 1).

Isolation of Phosphate Solubilizing Bacteria by Enrichment Culture

To extract bacteria from soil, 5 g of soil samples were transferred to the National Botanical Research Institute phosphate growth medium (NBRIP). Per liter, this growth liquid medium contains 10 g glucose with 5 g of different insoluble forms of phosphate ($AlPO_4$, $Ca_3(PO_4)_2$ and $FePO_4$), 5 g $MgCl_2 \cdot 6H_2O$, 0.25 g $MgSO_4 \cdot 7H_2O$, 0.2 g KCl and 0.1 g $(NH_4)_2SO_4$. Additionally, modified NBRIP media, containing either $FePO_4$ or $AlPO_4$ as the sole source of P, were also used for the initial screening step. The pH of the agar medium was adjusted to 7.0. Tricalcium phosphate was autoclaved separately and the other sterile ingredients were aseptically mixed after autoclaving. Erlenmeyer flasks containing 50 ml of the medium with inoculants were incubated for 7 days at 30°C on a IWAKI Incubator shaker at medium speed (150 cycles min^{-1}). For the following week, 5 ml of this incubated medium with inoculants were transferred into 50 ml Erlenmeyer flasks again with new liquid medium for 7 more days at 30°C on a IWAKI Incubator shaker at medium speed (150 cycles min^{-1}). At the end of each week in NBRIP growth liquid media, aliquots of each dilution were spread on NBRIP medium and incubated at 30°C for 14 days. Colonies were selected from the plates on the basis of the appearance of a clear halo; the clones were further purified on minimal medium based on each insoluble phosphate forms. Once purified, each isolate was stored as a glycerol stock at -80°C.

Mineral Phosphate Solubilization Assays

The phosphate solubilizing (PS) activity of each of the isolates was determined by molybdenum-blue method (Murphy and Riley, 1962). The isolates were grown in NBRIP liquid medium containing different insoluble forms of phosphate ($AlPO_4$, $Ca_3(PO_4)_2$ and $FePO_4$) for 3 days at 30°C on a IWAKI Incubator shaker at medium speed (150 cycles min^{-1}). The solubilization efficiencies were determined by reaction with ammonium molybdate for phosphorus compounds as ammonium phosphomolybdate and reduced with a compound ascorbic acid to molybdenum blue. Then, the isolates were incubated for 30 min at room temperature for color development. And finally, the absorption of light in the wavelength range 595 nm was measured by 680 XR Microplate Reader.

PCR Amplification of 16S rRNA and Sequencing

The gene-encoding 16S rRNA was amplified from selected strains by the polymerase chain reaction (PCR) using bacterial universal primers proR2 (5'-AGAGTTTGATCMTGGCTCAG-3') and 907R (5'-CCGTCAATTCCTTTRAGTTT-3') (Weisburg et al., 1992). The PCR mix consisted of 0.25 μM of each primer, 1X PCR buffer and 0.2 U of Taq DNA polymerase. A suspension of cells on MilliQ water, coming from a fresh colony grown on nutrient agar, was used as target DNA. The following cycle conditions were used: 85°C for 5 min, followed by 35 cycles of 95°C for 1 min, 55°C for 1 min and 72°C for 2 min, and a final extension step at 72°C for 3 min (Lane, 1991). The

PCR products were purified from agarose gels with the PCR Clean-up Gel Extraction Kit (Macherey-Nagel, Germany) and sequenced. The nucleotide sequences were compared using the BlastN program (Altschul et al., 1997), and the closest match of known phylogenetic affiliation was used to assign the isolated strains to specific taxonomic groups.

RESULTS AND DISCUSSION

Isolation of PSB from Eggplant Fields

The screening strategy employed during this research enabled the identification of PSB colonies on NBRIP medium containing different insoluble forms of phosphate ($AlPO_4$, $Ca_3(PO_4)_2$ and $FePO_4$) as sole P source. No colonies exhibiting a clear halo were observed on agar plates supplemented with either $FePO_4$ or $AlPO_4$. Approximately 6 bacterial isolates showed clear halos of $Ca_3(PO_4)_2$ solubilization. Some obvious differences in the size of the halos of different isolates were observed (not shown). This preliminary observation suggested the existence of bacterial isolates exhibiting different degrees of PS efficiencies in the soil samples collected. To confirm this observation, the 6 purified isolates were tested following the protocol of Murphy and Riley (1962), a method previously shown to be a reliable and qualitative indicator of the PS activity of different bacterial isolates. Table 2 shows the OD595 nm shift of the culture supernatants of each of the 6 PSB isolates after a 3-day cultivation period in NBRIP medium. Indeed, some isolates did not show any significant change in the absorbance of the supernatant while others exhibited OD595 nm changes in the absorbance. Furthermore, we noticed that the most dramatic changes in the color of the supernatant correlated with a total solubilization of $Ca_3(PO_4)_2$ in the medium. Based on these results we selected 6 isolates exhibiting the highest PS activities for further studies. The solubilization efficiencies of these isolates were calculated and are shown in Table 2. After evaluating their P solubilization capacity, we concluded that all of the 6 isolates can solubilize $Ca_3(PO_4)_2$ better than $FePO_4$ and $AlPO_4$ especially the isolates with the code Ek04. Moreover, isolate codes Ek01 and Ek04 look interesting for solubilizing $FePO_4$ and $AlPO_4$, which are the main forms of insoluble phosphates in acid sandy soils.

Effect of Soil Properties in Eggplant Fields Crop Productions on PSB

After identification by enrichment culture, we found bacteria from the eggplant field that could solubilize insoluble phosphate in solid media. Six isolates were evaluated for their P solubilization capacity, all 6 isolates can solubilize $Ca_3(PO_4)_2$ better than $FePO_4$ and $AlPO_4$ especially the isolates with the code Ek04 that came from the eggplant field in Kochi University. These findings might be linked to the soil pH that was between 5.4-5.5 (Table 1) which is not too low and not higher than 6.5. Poehlman (1991) found that the suitable soil pH for rhizobia activity was around 5.5 and that rhizobia exhibit varied responses to acidity. Moreover, Taylor et al. (1991) reported that acidity had more severe effects on rhizobial multiplication than did Al stress and low P conditions. However, phosphorus is also particularly important for the activity of the rhizobia species. In addition, the growth rate of most rhizobia strains is reduced by low levels of P (Al-Niemi et al., 1997). The strains of rhizobia differ markedly in their tolerance to phosphorus deficiency (Beck and Munns, 1985). This P stress response occurred when the medium P concentration decreased below 1 mM.

Identification of PSB Isolates

Nucleotide sequencing of PCR-amplified 16S rRNA genes and sequence comparison with available data in the GenBank using the BLAST algorithm (Altschul et al., 1997) allowed us to identify the majority of the PSB isolates (Table 3). Based on a sequence identification of 94% or greater (Van Waasbergen, 2004), they were all affiliated to the β- or γ- sub-divisions of the *Proteobacteria*: one isolate was similar to species of the *Klebsiella* genus, another three were similar to *Gluconacetobacter* sp. and

one was closely related to *Sphingobacterium* sp. *Klebsiella pneumonia* in the eggplant fields which solubilize $Ca_3(PO_4)_2$ better than $FePO_4$ and $AlPO_4$. *Klebsiella pneumonia* strain M-AI-2 seems to be more interesting to solubilize $AlPO_4$ and $FePO_4$. Moreover, *Gluconacetobacter* sp. isolate code Ek01 in the eggplant field in Kochi University can solubilize $FePO_4$ as well.

CONCLUSION

Klebsiella pneumoniae showed the highest P solubilization capacity in the eggplant fields. *Klebsiella pneumoniae* strain M-AI-2 and *Gluconacetobacter* sp. isolate code Ek04 and Ek01 in the eggplant field in Kochi University seem to have the capacity to solubilize insoluble forms of $AlPO_4$ and $FePO_4$. Moreover, the soil pH from different areas has an effect on rhizobial multiplication and their activities in the soil**.**

ACKNOWLEDGEMENTS

This research was supported thanks to a cooperation between the Japan Society for the Promotion of Science and Kochi University under the Invitation Program for East Asian Young Researchers on Field science towards the resolution of environmental and food problems in Southeast Asia and the kind support of the research institute of molecular genetics at Kochi University (Japan) and Khon Kaen University (Thailand).

Literature Cited

Al-Niemi, T.S., Kahn, M.L. and McDermott, T.R. 1997. P metabolism in the bean-*Rhizobium tropici* symbiosis. Plant Physiol. 113:1233-1242.

Altschul, S.F., Madden, T.L., Schaffer, A.A., Zhang, J., Zhang, Z., Miller, W. and Lipman, D.J. 1997. Gapped BLAST and PSI-BLAST: a new generation of protein database search programs. Nucleic Acids Res. 25:3389-3402.

Antibus, R.K., Bower, D. and Dighton, J. 1997. Root surface phosphatase activities and uptake of ^{32}P-labelled inositol phosphate in field-collected gray birch and red maple roots. Mycorrhiza 7:39-46.

Beck, D.P. and Munns, D.N. 1985. Effect of calcium on the phosphorus nutrition of *Rhizobium meliloti*. Soil Sci. Soc. Am. J. 49:334-337.

Godinho, A., Ramesh, R. and Bhosle, S. 2010. Bacteria from sand dunes of goa promoting growth in eggplant. World J. of Agri. Sci. 6:555-564.

Han, H.S. and Lee, K.D. 2005. Phosphate and potassium solubilizing bacteria effect on mineral uptakes, soil availability and growth of eggplant. Res. J. of Agri. and Biol. Sci. 1:176-180.

Lane, D.J. 1991. 16S/23S rRNA sequencing. p.130-141. In: E. Stackebrandt and M. Goodfellow (eds.), Nucleic Acid Techniques in Bacterial Systematics, Wiley, Chichester.

Murphy, J. and Riley, J.P. 1962. A modified single solution method for the determination of phosphate in natural waters. Anal. Chem. Acta. 27:31-36.

Poehlman, J.M. 1991. The Mungbeans. Mohan Primlani for Oxford and IBH Publishing Co. Pvt. Ltd. New Delhi, India. 343p.

Schachtman, D.P., Reid, R.J. and Ayling, S.M. 1998. Phosphorus uptake by plants: from soil to cell. Plant Physiol. 116:447-453.

Taylor, R.W., Williams, M.L. and Sistani, K.R. 1991. Nitrogen fixation by soybean-*Bradyrhizobium* combinations under acidity, low P and high Al stresses. Plant Soil. 131:293-300.

Van Waasbergen, L.G. 2004. What makes a bacterial species? When molecular sequence data are used, is rRNA enough? p.339-356. In: R.V. Miller and M.J. Day (eds.), Microbial Evolution: Gene Establishment, Survival and Exchange, ASM Press, Washington, DC.

Weisburg, W.G., Barns, S.M., Pelletier, D.A. and Lane, D.J. 1992. 16S ribosomal DNA amplification for phylogenetic studies. J. of Bacteriology 173:697-703.

Zahran, H.H. 1999. *Rhizobium*-legume symbiosis and nitrogen fixation under severe

conditions and in an arid climate. Microbiol. Molecu. Bio. Rev. 63:968-989.

Tables

Table 1. Soil properties in eggplant fields in Kochi, Japan.

Soil properties	Eggplant field in Kochi University	Eggplant field around Kochi University
pH (1:1 H_2O)	5.53	6.80
Total nitrogen (%)	0.156	0.179
Total phosphorous (mg/kg)	1,107.87	10,544.22
Available phosphorous (mg/kg)	300.29	4,285.71
Exchangeable potassium (mg/kg)	244.01	1,527.25

Table 2. Phosphate solubilizing effectiveness of tested bacteria, 3 days after inoculation.

Isolate code	Solubilized phosphate (mg P/L) from		
	$Ca_3(PO_4)_2$	$FePO_4$	$AlPO_4$
Ek01	805	93	0
Ek02	941	0	0
Ek03	943	0	15
Ek04	1,548	47	161
Ek05	770	0	0
Ek06	912	0	0

Table 3. Identification of PSB isolates from soil samples of an eggplant fields in Kochi by 16S rRNA sequencing after inoculation.

Isolate code	Length of 16S rRNA gene sequenced	GenBank accession no.	Most closely related organism/species (strain)	Accession no.	% gene identity
Ek01	546	lcl/19025	*Gluconacetobacter* sp.	EF493039.1	99
Ek02	710	lcl/39135	*Gluconacetobacter* sp.	EF493039.1	99
Ek03	990	lcl/26231	*Gluconacetobacter* sp.	EF493039.1	99
Ek04	938	lcl/51159	*Klebsiella pneumoniae*/ M-AI-2	FJ828890.2	99
Ek05	966	lcl/30399	Uncultured bacterium clone MS-115	GQ477848.1	99
Ek06	983	lcl/27533	*Sphingobacterium* sp. 21	CP002584.1	94

ResearchGate

See discussions, stats, and author profiles for this publication at: https://www.researchgate.net/publication/285359447

Comparisons of nutrient status between regular season and off-season cropping of Curcuma alismatifolia Gagnep

Article *in* Acta horticulturae · October 2015

DOI: 10.17660/ActaHortic.2015.1104.68

CITATIONS
0

READS
52

2 authors:



Soraya Ruamrungsri
Chiang Mai University
101 PUBLICATIONS **186** CITATIONS
SEE PROFILE



Panupon Hongpakdee
Khon Kaen University
12 PUBLICATIONS **6** CITATIONS
SEE PROFILE

Some of the authors of this publication are also working on these related projects:



Accumulation mechanism related with Plant nutrition View project



Control flowering in Nelumbo nucifera as a cut flower View project

All content following this page was uploaded by Panupon Hongpakdee on 07 December 2015.

The user has requested enhancement of the downloaded file.

Comparisons of nutrient status between regular season and off-season cropping of *Curcuma alismatifolia* Gagnep.

S. Ruamrungsri[1] and P. Hongpakdee[2]

[1]Department of Plant Science and Natural Resources, Faculty of Agriculture, Chiang Mai University, Chiang Mai 50200, Thailand; [2]Department of Plant Science and Agricultural Resources, Faculty of Agriculture, Khon Kaen University, Khon Kaen 40002, Thailand.

Abstract

The present work investigated the nutrient status in plant tissue and plant growth between regular season (RS) and off-season (OS) cropping of *Curcuma alismatifolia* Gagnep. at flowering stage. To use this species for year-round cut flower or rhizomes production it was necessary to establish adequate cultivation techniques. The determination of nitrogen (N), phosphorous (P) and potassium (K) status in plants is basic information that can be used to evaluate the optimum crop fertilizer requirement. At flowering stage (12 weeks after planting: WAP), the nutrient contents in plant component and plant growth of *Curcuma* plants under the different cropping systems were analysed. N content in old rhizomes, old storage roots and new rhizomes was significantly increased under the OS cropping, but the opposite result was found in leaves. The highest N content was observed in leaves under RS condition (353.23 mg plant^{-1}). Higher P content was found in leaves and inflorescence under the RS cropping (87.95 and 60.84 mg plant^{-1}), while RS cropping tissue contained less P content in new rhizomes (9.68 mg plant^{-1}). K content significantly decreased in leaves, old rhizomes and new rhizome under the OS cropping (228.26, 14.19 and 2.11 mg plant^{-1}). The OS cropping system resulted in reduced N, P and K content in most aboveground organs, increased dry matter accumulation in below ground organs (old storage roots, new rhizomes and new storage roots) and decreased dry matter accumulation in leaves and inflorescences. Poor quality of plant (decrease in height, canopy and total leaves areas) was also found in OS cropping.

Keywords: *Curcuma*, dry matter, nutrition out of season

INTRODUCTION

Generally in geophytes, cyclic patterns of growth, flowering and rest periods involve a sequence of specific endogenous processes, which are expressed in the growth and differentiation of the shoot and storage organ (Le Nard and De Hertogh, 1993). The developmental transitions are partially associated with changes in the levels of nutrient status, which are probably involved in the control of growth and dry matter accumulation. These developmental changes follow the seasonal fluctuation in the environmental conditions (temperature, day length, light intensity, relative humidity and water status) (Flaishman and Kamenetsky, 2006). Moreover, the changes in some levels of nutrient status i.e., nitrogen (N), phosphorus (P) and potassium (K) were reflected plant responses to those environmental changes (Mengel and Kirkby, 1987; Noquet et al., 2003).

Curcuma alismatifolia Gagnep. belongs to the member of *Zingiberaceae* geophytes, which normally grow in the rainy season (or regular season) and become dormant in winter. Off-season cropping of this species in Thailand is practised for avoiding surplus production of cut flower or rhizome during the regular season and hence increases profitably for growers. A problem with off-season cropping of this species is reduced quality of flowers and rhizomes (Hongpakdee et al., 2010). The wholesale value of potted *Curcuma* production in The Netherlands by commercial auction was estimated to be 1.3 million euros (Flower Council of Holland, 2009) which makes the crop a valuable product for Thailand.

Nutritional programs used in *C. alismatifolia* production are important since growth, flower quality, and rhizome yields respond to the amount of N applied, and a deficiency of N can substantially decrease yields (Ohtake et al., 2006). A previous study found the optimum nutrient levels (Lee et al., 2008) and the critical N levels for only regular season cropping of *Curcuma* production (Inkham et al., 2011). However, no detailed information on nutrition and dry matter partitioning of this species is available concerning year round production. Therefore, the objective of this study was to evaluate the N, P and K status along with dry matter partitioning in *C. alismatifolia* at flowering stage.

MATERIALS AND METHODS

C. alismatifolia Gagnep. 'Chiang Mai Pink' rhizomes were planted in 6×12 inch plastic bags as used in commercial practices, containing 2.35 L of potting medium of soil, rice husks and rice husk charcoal at 1:1:1 ratio by volume. Plants were irrigated daily with 450 mL water throughout the growth periods without the run-off solution, and each bag was supplied with 7.5 g of 16-16-16 (N-P-K) granular fertilizer commencing at the stage of first leaves fully expanded and subsequently supplied through the flowering stage, twice a month till the termination of the trial. Plants were assessed under translucent plastic covered greenhouse at Chiang Mai University. Long term climatic averages for the experimental site are presented in Figure 1. The plants were grown under two seasonal cropping treatments being from July to October 2008 as regular season (RS) and from November 2008 to February 2009 as off-season (OS).

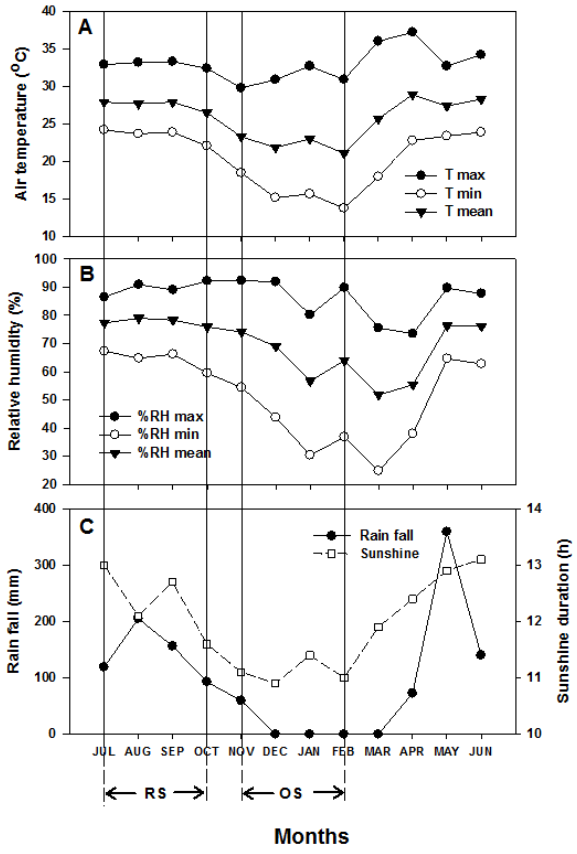


Figure 1. Air temperature (A), relative humidity (B) and rain fall and sunshine duration (C) automatically recorded at Multiple Cropping Centre: MCC, Faculty of Agriculture, Chiang Mai University weather station between regular season (RS) cover from July to October 2008 as rainy season and off-season (OS) cover from November 2008 to February 2009 as winter in Chiang Mai, Thailand.

At flowering stage (12 weeks after planting: WAP), 30 plant samples (10 plants replication^{-1}) were collected to determine the dry matter contents and nutrient status for leaves, inflorescence, old rhizomes, old storage roots, new rhizomes and new storage roots. Each plant component was washed with tap water initially and subsequently with de-ionized water two times, then dried and ground into powder. Dried samples were digested using a Kjeldahl digest solution (Ohyama et al., 1991) to determine total N concentration by a modified indophenols method, P concentration was quantified by the ammonium molybdate method (Davidescu and Davidescu, 1972) and K concentration was determined by atomic absorption spectrophotometry using a $HClO_4$-HNO_3 digestion modified method (Mizukoshi et al., 1994).

The data were analysed for statistical significance using Statistic 8 analytical software (SXW Tallahassee, FL, USA). Student's t-test was used in experiments to determine significant differences in plant growth, dry matter accumulation and nutrient contents.

RESULTS AND DISCUSSION

At flowering, the OS condition seemed to reduce N, P and K contents in almost all aboveground parts (leaves and inflorescence) (Figure 2) and reduced plant height, canopy and total leaf area (Table 1). This occurrence might be explained by the lower temperature (22.3°C) and shorter day condition (11.1 h) of the OS treatment compared with the RS treatment (27.5°C and 12.4 h, respectively). The reduced temperature and day length probably affected the rate of nutritional up take by roots, since low temperatures in root zone had been reported to reduce the up take rate of both NH_4^+ and NH_3^+ (Mengel and Kirkby, 1987) and affected the K^+ influx outside of roots (Ching and Barbers, 1979). Reductions of photoperiods from 16 to 8 h have also been reported to decrease N up take in *Medicago sativa* (Noquet et al., 2003). In *Curcuma*, some evidence might confirm that low temperature (15°C) stimulates the translocation of N as represented by higher ^{15}N distribution to old rhizome and old storage roots or delay in export of N to other plant organs (Khuankaew et al., 2014). Likewise our work showed higher N accumulation in OS plant below ground parts (old rhizomes, old storage roots, new rhizomes and new storage roots) than that of RS plant below ground parts (Figure 2).

Some research has shown that cool conditions severely inhibited the uptake of P in corn (Engels et al., 1992). In contrast our study showed an increase in P content for new rhizomes and storage roots under the low temperature in OS conditions (Figure 2). This finding might be due to be the function of P in energy conservation and transfer in cell (Marschner, 1995), brought about by the greater dry matter accumulation in OS belowground parts (Figure 2), due to more carbon partitioning, and sink-source competition between root and shoot under OS than RS conditions. Khuankaew (2010) reported that P in storage organs of *C. alismatifolia* was used during initial plant growth and flowering. In potatoes, the tuber (storage organs) became the principal site of phosphate accumulation (Poder et al., 1988). However, P deficiency also promoted root growth and reduced shoot growth by increasing root-shoot mass ratio and root surface in several plants (Wittenmayer and Merbach, 2005).

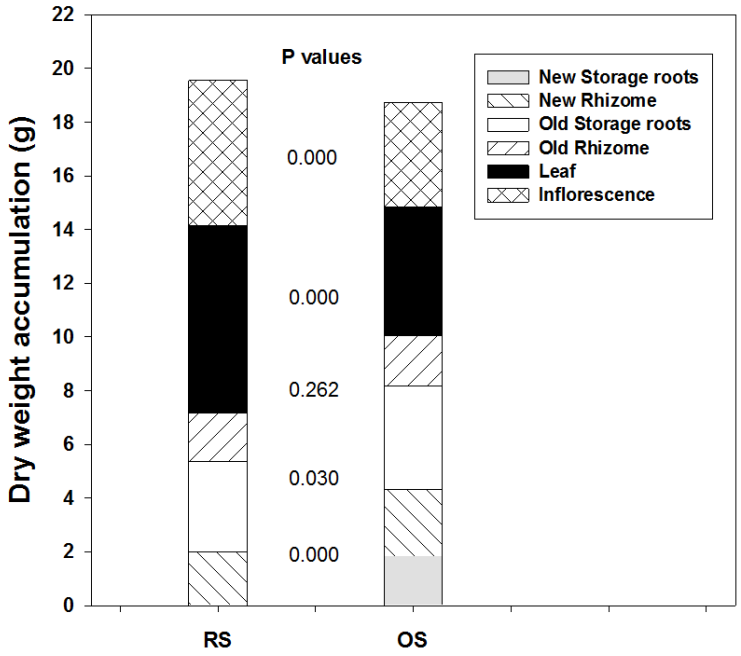


Figure 2. Dry weight accumulation (g) of component plant parts of *Curcuma* plants when grown under regular season (RS) or off-season (OS) cropping at flowering stage (12 WAP). Significant levels for aboveground (inflorescence + leaves) and belowground (old rhizomes + old storage roots + new rhizomes + new storage roots) dry weight accumulation were both P=0.00. Formation of new storage roots is delayed under RS conditions and is represented as non-dry weight accumulation in this organ.

The decreased K content in leaves, old rhizomes and new rhizomes under OS condition (Table 2) supports the finding of Ching and Barbers (1979) who reported that low temperature reduced K^+ influx outside the root and less growth in *Zea mays*. Also reducing K content could be partially related to the decrease in aboveground dry matter accumulation of OS plant (Figure 2) resulting in poor growth and compacted shorter plant (Table 1 and Figure 3E), due to the important role of K in meristematic growth and by the contribution of K^+ to the osmotic potential of the cell (Marschner, 1995). Nevertheless, the various concentrations of K supplied to *C. alismatifolia* did not affect any plant growth parameters, except on the number of green bracts (Ruamrungsri et al., 2005).

Table 1. Plant height, plant canopy, total leaf area and compactness index of *Curcuma* plants grown under regular season (RS) or off-season (OS) cropping at flowering stage (12 WAP). Values are means ± SE (n=30).

Treatment	Plant height (cm)	Plant canopy (cm)	Total leaf area (cm^2)	Compactness index ($cm^2\ cm^{-1}$)
RS	59.7±0.88	24.6±0.34	370±1.38	6.23±0.11
OS	26.2±1.03	16.1±0.26	290±2.87	11.0±0.40
t-test	*	*	*	*

*Significant by Student's *t*-test at p<0.05.

Table 2. Nitrogen (N), phosphorus (P) and potassium (K) contents (mg per plant) of various organs of *Curcuma* plants between regular season (RS) and off-season (OS), at the flowering stage (12 WAP). Values are means ± SE (n=3). New storage root forming delays under RS conditions represent as non-nutrient content (NC) in this organ.

Organs	Nutrient content (mg plant^{-1})					
	Nitrogen (N)		Phosphorus (P)		Potassium (K)	
	RS	OS	RS	OS	RS	OS
			Aboveground			
Leaves	350±8.06	300±1.45*	88.0±3.64	64.7±0.47*	340±1.84	230±7.87*
Inflorescence	160±8.03	170±5.54^{ns}	60.8±2.02	50.9±2.48*	200±3.68	190±2.43
			Underground			
Old rhizome	89.9±1.16	110±4.56*	28.0±2.23	22.7±1.76^{ns}	18.9±1.03	14.2±1.11*
Old storage root	41.8±1.57	60.8±2.19*	46.4±3.39	45.0±2.25^{ns}	94.0±2.18	110±1.40^{ns}
New rhizome	110±4.10	120±1.93*	9.68±1.57	25.5±1.79*	67.6±3.28	2.11±2.43*
New storage root	NC	66.4±1.22	NC	10.4±0.59	NC	110±8.29*
Total	**760±15.7**	**830±20.8***	**230±6.75**	**220±3.49^{ns}**	**720±13.0**	**690±21.5^{ns}**

*Significant by Student's t-test at p<0.05.

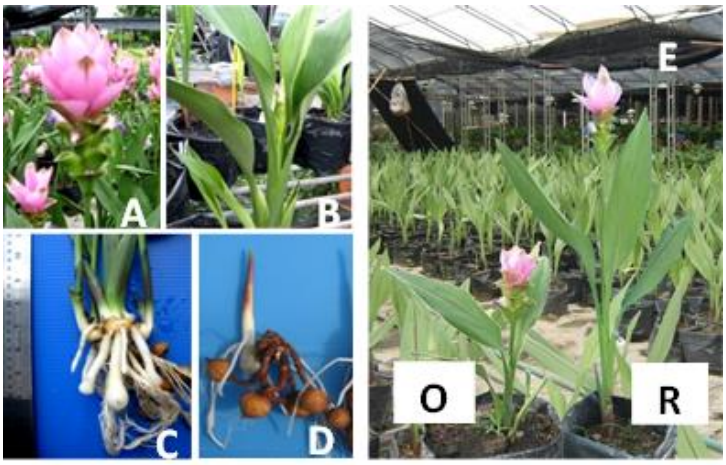


Figure 3. *C. alismatifolia* plant components: inflorescence (A), leaf (B), new rhizomes and new storage roots (C) and old rhizomes and old storage roots (D). Decrease in aboveground dry matter accumulation of *Curcuma* under off-season (OS) condition represent as smaller plant size than plant grown under regular season (RS) (E).

CONCLUSIONS

The unfavourable conditions in OS, such as low temperature or short day length, resulted in a decrease of N, P, and K contents in *Curcuma* aboveground parts, but induced an increase of all nutrients in below ground parts and more dry matter accumulation. This finding partially concerns the poor aboveground plant growth under OS condition. To improve the better nutrition of targeted element in this species, day length extension or warming temperature setting in greenhouse might be a possible technique for OS production. The present study exhibits the basic information to evaluate optimal crop fertilizer requirement in year round production of *Curcuma* plant.

ACKNOWLEDGEMENTS

This project was financially supported by Khon Kaen University and Chiang Mai University, Thailand. We thank the H.M. the King's Initiative Centre for Flower and Fruit Propagation for valuable support. Thanks to Prof. Dr. Takuji Ohyama from Niigata University,

Japan for technical advice.

Literature cited

Ching, P.C., and Barbers, S.A. (1979). Evaluation of temperature effects on K uptake by corn. Agron. J. *71*, 1040–1044 http://dx.doi.org/10.2134/agronj1979.00021962007100060035x.

Davidescu, D., and Davidescu, V. (1972). Evaluation of Fertility by Plant and Soil Analysis (London, UK: Abacus Press).

Engels, C., Munkle, L., and Marschner, H. (1992). Effect of root zone temperature and shoot demand on uptake and xylem transport of micronutrients in maize (*Zea mays* L.). J. Exp. Bot. *43*, 537–547 http://dx.doi.org/10.1093/jxb/43.4.537.

Flaishman, M., and Kamenetsky, R. (2006). Florogenesis in flower bulbs: classical and molecular approaches. In Floriculture, Ornamental and Plant Biotechnology, Vol. II, J. Texeira da Silva, ed. (Kagawa, Japan: Global Science Books), p.33–43.

Flower Council of Holland. (2009). Background information on Curcuma Siam Scarlet. www.flowercouncil.org/int/product/novelties/plants/2007/p06NL_Siam_ad.asp.

Hongpakdee, P., Siritrakulsak, P., Ohtake, N., Sueyoshi, K., Ohyama, T., and Ruamrungsri, S. (2010). Changes in endogenous abscisic acid, trans -zeatin riboside, indole-3-acetic acid levels and the photosynthetic rate during the growth cycle of *Curcuma alismatifolia* Gagnep. in different production seasons. Europ. J. Hort. Sci. *75*, 204–213.

Inkham, C., Sueyoshi, K., Ohtake, N., Ohyama, T., and Ruamrungsri, S. (2011). Critical nitrogen level determination in *Curcuma alismatifolia* Gagnep. Europ. J. Hort. Sci. *76*, 188–193.

Khuankaew, T. (2010). Assimilation and translocation of nitrogen and carbon in *Curcuma alismatifolia* Gagnep. Ph.D. Thesis (Niigata, Japan: Niigata University).

Khuankaew, T., Tanabata, S., Yamamoto, M., Ishikawa, S., Tsutsumi, K., Ohtake, N., Sueyoshi, K., Ohyama, T., Sato, T., Anuwong, C., and Ruamrungsri, S. (2014). Temperature affects N and C assimilation and translocation in *Curcuma alismatifolia* Gagnep. J. Hortic. Sci. Biotechnol. *8*, 287–292.

Le Nard, M., and De Hertogh, A.A. (1993). Bulb growth and development and flowering. In The Physiology of Flower Bulbs, A.A. De Hertogh, and M. Le Nard, eds. (Amsterdam, The Netherlands: Elsevier), p.29–43.

Lee, J.S., Lee, A.K., and Suh, J.K. (2008). Optimum nutrient level on growth, flowering and rhizome production in *Curcuma.* J. Plant Nutr. *31*, 2183–2195 http://dx.doi.org/10.1080/01904160802463270.

Marschner, H. (1995). Mineral Nutrition of Higher Plants (London, UK: Academic Press).

Mengel, K., and Kirkby, E.A. (1987). Nitrogen. In Principles of Plant Nutrition, K. Mengel, and E.A. Kirkby, eds. (Worblaufen-Bern, Switzerland: Intl. Potash Inst.), p.347–384.

Mizukoshi, K., Nishiwaki, T., Ohtake, N., Minagawa, R., Kobayashi, K., Ikarashi, T., and Ohyama, T. (1994). Determination of tungstate concentration in plant materials by HNO_3- $HClO_4$ digestion and colorimetric method using thiocyanate. Bull. Fac. Agri. Niigata Univ. *46*, 51–56.

Noquet, C., Meuriot, F., Caillot, S., Avice, J.C., Ourry, A., Cunningham, S.M., and Volenec, J.J. (2003). Short-day photoperiod induces changes in N uptake, N partitioning and accumulation of vegetative storage proteins in two *Medicago sativa* cultivars. Funct. Plant Biol. *30*, 853–863 http://dx.doi.org/10.1071/FP03099.

Ohtake, N., Ruamrungsri, S., Ito, S., Sueyoshi, K., Ohyama, T., and Apavatjrut, P. (2006). Effect of nitrogen supply on nitrogen and carbohydrate constituent accumulation in rhizomes and storage roots of *Curcuma alismatifolia* Gagnep. Soil Sci. Plant Nutr. *52*, 711–716 http://dx.doi.org/10.1111/j.1747-0765.2006.00094.x.

Ohyama, T., Ito, M., Kobayashi, K., Araki, S., Yasuyoshi, S., Sasaki, O., Yamazaki, T., Sayoma, K., Tamemura, R., Izuno, Y., and Ikarashi, T. (1991). Analytical procedures of N, P, K content in plant and manure materials using H_2SO_4-H_2O_2 Kjeldahl digestion Method. Bull. Fac. Agri. Niigata Univ. *43*, 111–120.

Poder, D., Suleiman, S., and Penot, M. (1988). Phosphate transport in potato cuttings: effect of gibberellic acid and abscisic acid. Physiol. Plant. *72*, 385–388 http://dx.doi.org/10.1111/j.1399-3054.1988.tb05849.x.

Ruamrungsri, S., Suwanthada, C., Ohtake, N., Sueyoshi, K., Ohyama, T., and Apavatjrut, P. (2005). Effect of nitrogen and potassium on growth and development of *Curcuma alismatifolia* Gagnep. Acta Hortic. *673*, 443–448 http://dx.doi.org/10.17660/ActaHortic.2005.673.56.

Wittenmayer, L., and Merbach, W. (2005). Plant responses to drought and phosphorus deficiency: contribution of phytohormones in root-related processes. J. Plant Nutr. Soil Sci. *168*, 531–540 http://dx.doi.org/10.1002/jpln.200520507.

View publication stats

Latex Yield of *Hevea brasiliensis* Poorly Indicates Soil Drought

S. Isarangkool Na Ayutthaya[1,a] and F.C. Do[2]
[1] Horticultural Section, Department of Plant Science and Agricultural Resources, Faculty of Agriculture, Khon Kaen University, Thailand
[2] IRD, UMR Eco&Sols, SupAgro-INRA, Montpellier F-34060, France

Keywords: rubber tree, *Hevea brasiliensis*, yield, soil drought, indicator

Abstract

Predawn leaf water potential, sap flux density or tree transpiration and whole-tree hydraulic conductance are known indicators of soil drought on rubber tree (*Hevea brasiliensis*). However, these parameters are difficult to access for farmers, in contrast to latex yield which is recorded every day. Hence, the aim of this study was to evaluate the potential use of latex yield as indicator of soil drought in the marginal rainfall areas. The experiment was done during intermittent drought in the rainy season in a representative rubber plantation located in Buriram province, northeast Thailand. The results showed that while the relative transpiration declined by 66% for severe soil drought, the number of rubber sheets per hectare and per tapping decreased slightly by 18% and did not differ for mild drought. Other yield parameters per tapping such as fresh latex per tree or dry rubber content did not differ significantly despite tendencies between severe drought and well-watered period. Finally, the latex yield per tapping does not appear to be a sensitive indicator of soil drought.

INTRODUCTION

To benefit from the increasing demand for natural rubber, the cultivation of *Hevea brasiliensis* has been extended into drought-prone areas like those in the southern part of northeast Thailand. However, severe droughts have induced important branch diebacks and tree mortality (Isarangkool Na Ayutthaya et al., 2011) and in combination with latex tapping it can induce tapping panel dryness or trunk phloem necrosis syndromes (Pellegrin et al., 2007; Do et al., 2011). Hence, an indicator of water stress can be useful to suspend latex tapping when trees suffer a substantial drought.

Leaf water potential, transpiration or sap flux density, tree hydraulic conductance, stomata or leaf conductance, photosynthesis, or trunk fluctuation are known indicators of soil drought (Orwig and Abrams, 1997; Chandrashekar et al., 1998; Goldhamer et al., 1999; Moriana et al., 2003; Intrigliolo and Castel, 2005; Isarangkool Na Ayutthaya et al., 2011). However, these parameters are difficult to access for farmers. In contrast to this, latex yield is recorded almost every day and previous results support its response to soil moisture status (Gururaja Rao et al., 1990; Raj et al., 2005). Hence, the idea of this study was to evaluate the potential use of latex yield as indicator of soil drought. The benefit of this work could help the farmers for decision of stop tapping when the soil drought occurs for tree protection.

In northeast Thailand the tapping period lasts between 8 and 9 months including the rainy season and the first part of the dry season before defoliation. The system of tapping includes two days of tapping and one day of rest (2d/3). Hence there are 150-160 days of tapping during the stage of fully mature leaves. Isarangkool Na Ayutthaya et al. (2011) have assessed for the main clone used in the area (RRIM600) thresholds of relative extractable water (REW; dimensionless) corresponding to drought intensity: mild-drought between 0.5 and 0.2 REW and severe drought below 0.2 REW. Thus, the aim of this work was to quantify the effect of soil drought intensity in a constraining rainy season on latex yield as measured by the number of rubber sheets per hectare and tapping, and on latex yield parameters as fresh latex volume and dry rubber content.

[a] isupat@kku.ac.th

MATERIALS AND METHODS

Field Site

The experiment was conducted in a 5.3-ha plot, planted at 2.5×7.0 m spacing and tapped for 4 years. The plantation is located at Baan Sila (15°16'23"N; 103°04'51.3"E), Khu-Muang district, Bureerum province, northeast Thailand. The rainy season lasts approximately from April to October and the annual amount of rainfall averages 1176 mm. This experiment was done during the rainy season 2007, from May to October, the cumulated rainfall being 20% lower than the long-term average.

Soil Water Content Measurements

Volumetric soil water content (θ) was measured with a neutron probe (3322, Troxler, Research Triangle Park, North Carolina, USA) calibrated for the experimental soil. Twelve tubes 2 m long were set up in pars; of each pair, one tube located in the planting line between two trees, and the other in the middle of the inter-row. The top soil between 0-0.4 m comprised the major fluctuation of soil water content. Average field capacity and permanent wilting point were equal to 19.8 and 7 $cm^3/100\ cm^3$ of soil in this layer. Additionally, θ was measured continuously with a capacitive probe (EnvironSCAN System, Sentek Sensor Technologies, South Australia, Australia) within a single tube close to a tube dedicated to neutron probe measurement. Capacitive sensors were located at the same levels as neutron probe measurements. For each capacitive sensor, θ was estimated from a cross-calibration with the neutron probe measurements over the whole season range. To estimate continuous change of the average soil water profile, linear regressions were performed between θ of the average soil water profile and θ of the profile continuously measured with the capacitive probe (Isarangkool Na Ayutthaya et al., 2011). Relative extractable water (REW) was calculated according to Breda et al. (2006).

Reference Evapotranspiration (ET_0)

The local microclimate was monitored automatically in an open field, at a distance of 50 m from any trees. A datalogger (Minimet automatic weather station, Skye Instruments Ltd., Llandrindod Wells, UK) recorded half-hourly values of air temperature, relative humidity, incoming short wave radiation, wind speed and rainfall. The reference evapotranspiration (ET_0) was calculated according to Allen et al. (1998).

Tree Transpiration (ET)

Tree transpiration was measured from 6 sampled trees using the transient thermal dissipation method (TTD, Do and Rocheteau, 2002; Isarangkool Na Ayutthaya et al., 2010) which is a modification of the continuous thermal dissipation method of Granier (1985). The comparison of ET was done according three 10-days periods of contrasted relative extractable water: well-watered (REW>0.5), mild drought (REW around 0.3) and severe drought (REW around 0.1).

Number of Rubber Sheets

The number of rubber sheets was recorded as usual after every tapping day for the share of the sale between the tapper and the owner. The comparison of rubber sheets between periods of contrasted water availability was done as for tree transpiration.

Latex Volume and Dry Rubber Content

Fresh volume of latex was measured from 18 sampled trees in a severe drought period on 25 July 2007 and in a well-watered period on 23 August 2007, 11 September 2007 and 27 September 2007. The dry rubber content (DRC) was measured by sampling for each volume 10 g and drying it in a hot air oven at 65°C until constant weight. The calculation of DRC followed Equation 1.

$$DRC = \frac{D.W.}{F.W.} \quad x \quad 100 \qquad (1)$$

where D.W. is dry weight and F.W. is fresh weight.

Dry Rubber per Tree and Dry Rubber per Hectare

Dry rubber per tree was calculated from the latex volume in each tree and multiplied by the DRC in each period. The dry rubber production per hectare was also calculated using the dry rubber production per tree multiplied by the number of trees per hectare.

Data Analysis

Soil droughts effects on yields were analyzed using a one-way analysis of variance (SPSS 11.5, SPSS Inc., New York, NY, USA). Post hoc comparisons of means were performed using the Duncan's test.

RESULTS AND DISCUSSION

Soil Drought and Tree Transpiration

Recurrent periods of 10 to 20 days without rainfall occurred between May and September (Fig. 1A). They induced variable decreases of REW (Fig. 1B). REW decreased below 0.5 for a long period in June-July. Despite high evaporative demand (ET_0), ET showed successive decreases following change in REW. In the contrasted periods of REW, ET decreased significantly by 26% in mild drought and 66% in severe drought (Table 1). These results confirmed the soil drought effect on whole tree transpiration (Gururaja Rao et al., 1990; Granier et al., 1999; Breda et al., 2006; Isarangkool Na Ayutthaya et al., 2011).

Soil Drought and Number of Rubber Sheets

The variation of the number of rubber sheets is plotted versus REW and ET changes in Figure 1B. The increase at the onset of the tapping season, mid-May, corresponded to the natural phenomena of the starting metabolism of latex synthesis. After this, the production seems sensitive to the peaks of soil drought. However, later in August and September, the tendency was not clear. The ANOVA supported a significant tendency over the contrasted periods of REW in June, July and August (Table 1). However, the production decrease was modest (18%) for the severe drought and it was not significant for the mild-drought.

This result indicates that very high water stress is required to influence latex yield. Our results differed from previous results of Gururaja Rao et al. (1990) and Raj et al. (2005) which showed a substantial decrease of latex yield (40-50%) under soil drought. The explanation may come from the very different eco-climatic conditions. Previous studies originated from traditional rainfall area of India (annual rainfall around 2000 mm), while the present research was done in marginal rainfall area (annual rainfall around 1200 mm). It is possible that in our conditions, rubber trees were more acclimated to adverse conditions and less sensitive to drought.

Soil Drought and Latex Yield Parameters per Tree

Under soil drought, the fresh latex volume per tree tended to decrease (Table 2) while the dry rubber content tended to increase (Fig. 2). However, the trends were not statistically significant. Gururaja Rao et al. (1990) showed similar tendencies but statistically significant. They clearly report lower dry rubber content of latex during the wet period. It appears logical to find a decrease of the latex water content under water-limited conditions. The question could even be "why it is not more important under severe soil drought?" The relationship between DRC and latex per tapping per tree

expresses a significant negative tendency (Fig. 3): highest latex flow corresponds to higher water content. This result extends in water limited conditions a result already known in non-limiting conditions (Pakianathan et al., 1989). Latex production induced by tapping appears as a dominant process that overcomes other sinks of water and carbon. The relationships between latex yield, drought and growth deserve further research (Carr, 2011).

CONCLUSIONS

The results showed that while the relative transpiration declined by 66% for severe soil drought, the number of rubber sheets per hectare and per tapping decreased slightly by 18% and did not differ for mild-drought. Other yield parameters per tapping such as fresh latex per tree or dry rubber content did not differ significantly despite tendencies between severe-drought and well-watered period. Finally, the latex yield per tapping does not appear as a sensitive indicator of soil drought.

ACKNOWLEDGEMENTS

Many thanks to French and Thai counterparts from the Research Institute for Development (IRD), Khon Kaen University and the Land Development Department. We particularly thank the Land Development Department of Bangkok and Dr. Darunee Chairod for assistance with neutron probe measurements. We are grateful to Dr. Daniel Nandris for his support as coordinator of the agreement program between IRD and the French Institute for Rubber. Finally, we deeply thank the plantation holder (Mr. Chaipat Sirichaiboonwat) who welcomed us so kindly into his rubber tree plantation. This Thai-French research was funded by the French Research Institute for Development (IRD), the French Institute for Rubber (IFC), by Michelin/Scofinco/SIPH Plantations Companies and by the fund of Khon Kaen University.

Literature Cited

Allen, R.G., Pereira, L.S., Raes, D. and Smith, M. 1998. Crop evapotranspiration: guidelines for computing crop water requirements. Irrigation and Drainage Paper No. 56, FAO, Rome.

Breda, N., Huc, R., Granier, A. and Dreyer, E. 2006. Temperate forest trees and stands under severe drought: a review of ecophysiological responses, adaptation processes and long-term consequences. Ann. For. Sci. 63:1-20.

Carr, M.K.V. 2012. The water relations of rubber (*Hevea brasiliensis*): a review. Expl. Agric. 48(2):176-193.

Chandrashekar, T.R., Nazeer, M.A., Marattukalam, J.G., Prakash, G.P., Annamalainathan, K. and Thomas, J. 1998. An analysis of growth and drought tolerance in rubber during the immature phase in a dry subhumid climate. Expl. Agric. 34:287-300.

Do, F. and Rocheteau, A. 2002. Influence of natural temperature gradients on measurements of xylem sap flow with thermal dissipation probes. 2. Advantages and calibration of a non-continuous heating system. Tree Physiol. 22:649-654.

Do, F.C., Pierret, A., Couteron, P., Lesturgez, G., Boithias, L., Isarangkool Na Ayutthaya, S., Junjittakarn, J., Gonkhamdee, S., Maeght, J.L., Hartmann C. and Nandris, D. 2011. Spatial distribution of *Hevea brasiliensis* trunk phloem necrosis within a plot: aggregation but no evidence of constraint on cumulated growth. For. Path. 41:90-100.

Goldhamer, D.A., Fereres, E., Mata, M., Girona, J. and Cohen, M. 1999. Sensitivity of continuous and discrete plant and soil water status monitoring in peach trees subjected to deficit irrigation. J. Amer. Soc. Hort. Sci. 124(4):437-444.

Granier, A. 1985. Une nouvelle méthode pour la mesure des flux de sève dans le tronc des arbres. Ann. For. Sci. 42:193-200.

Granier, A., Breda, N., Biron, P. and Villette, S. 1999. A lumped water balance model to evaluate duration and intensity of drought constraints in forest stands. Ecol. Model. 116:269-283.

Gururaja Rao, G., Sanjeeva Rao, P., Rajagopal, R., Devakumar, A.S., Vijayakumar K.R. and Sethuraj, M.R. 1990. Influence of soil, plant and meteorological factors on water relations and yield in *Hevea brasiliensis*. Int. J. Biometeorol. 34:175-180.

Intrigliolo, D.S. and Castel, J.R. 2005. Usefulness of diurnal trunk shrinkage as a water stress indicator in plum trees. Tree Physiol. 26:303-311.

Isarangkool Na Ayutthaya, S., Do, F.C., Pannengpetch, K., Junjittakarn, J., Maeght, J.-L., Rocheteau, A. and Cochard, H. 2010. Transient thermal dissipation method of xylem sap flow measurement: multi-species calibration and field evaluation. Tree Physiol. 30:139-148.

Isarangkool Na Ayutthaya, S., Do, F.C., Pannangpetch, K., Junjittakarn, J., Maeght, J.-L., Rocheteau, A. and Cochard, H. 2011. Water loss regulation in mature *Hevea brasiliensis*: effects of intermittent drought in the rainy season and hydraulic regulation. Tree Physiol. 31:751-762.

Moriana, A., Orgaz, F., Pastor, M. and Fereres, E. 2003. Yield responses of a mature olive orchard to water deficits. J. Amer. Soc. Hort. Sci. 128(3):425-431.

Orwig, D.A. and Abrams, M.D. 1997. Variation in radial growth responses to drought among species, site, and canopy strata. Trees. 11:474-484.

Pakianathan, S.W., Haridas, G. and d'Auzac, J. 1989. Water relations and latex flow. p.233-256. In: J. d'Auzac, J.-L. Jacob and H. Chrestin (eds.), Physiology of Rubber Tree Latex. CRC Press, Inc, Florida.

Pellegrin, F., Duran-Vila, N., Van Munster, M. and Nandris, D. 2007. Rubber tree (*Hevea brasiliensis*) trunk phoem necrosis: aetiological investigations failed to confirm any biotic causal agent. For. Path. 37:9-21.

Raj, S., Das, G., Poten, J. and Dey, S.K. 2005. Relationship between latex yield of *Hevea brasiliensis* and antecedent environmental parameters. Int. J. Biometeorol. 49:189-196.

Ryan, M.G. 2011. Tree responses to drought. Tree Physiol. 31:237-239.

Tables

Table 1. Effect of drought on tree transpiration (ET) and number of rubber sheets per hectare per tapping (*n*=10 days).

Period	REW	ET (mm day^{-1})	No. sheet	% reduction of ET	% reduction of no. sheet
Well-watered	0.83a[1]	1.97a	10.57a	-	-
Mild drought	0.27b	1.45b	9.85ab	26.4	6.8
Severe drought	0.10c	0.67c	8.70b	66.0	17.7
P-value	<0.01	<0.01	<0.05		

[1] Letters following means express the results of multiple mean comparisons over the same column.

Table 2. Effect of severe drought on latex per tapping per tree, dry rubber (D.W.) per tapping per tree, D.W. per tapping per hectare and dry rubber content (DRC) (*n*=18 sampling trees).

Date	REW	Period	Latex/tree (ml)	D.W. (g tree^{-1})	D.W (kg ha^{-1})	DRC (%)
25-Jul-07	0.08	Severe drought	49.20	19.61	11.20	39.86
23-Aug-07	0.79	Well-watered	61.42	22.70	12.96	36.96
11-Sep-07	0.72	Well-watered	58.76	22.45	12.82	38.20
27-Sep-07	0.96	Well-watered	65.02	25.00	14.28	38.45
P-value			ns[1]	ns	Ns	ns

[1] ns = non-significant difference.

Figures

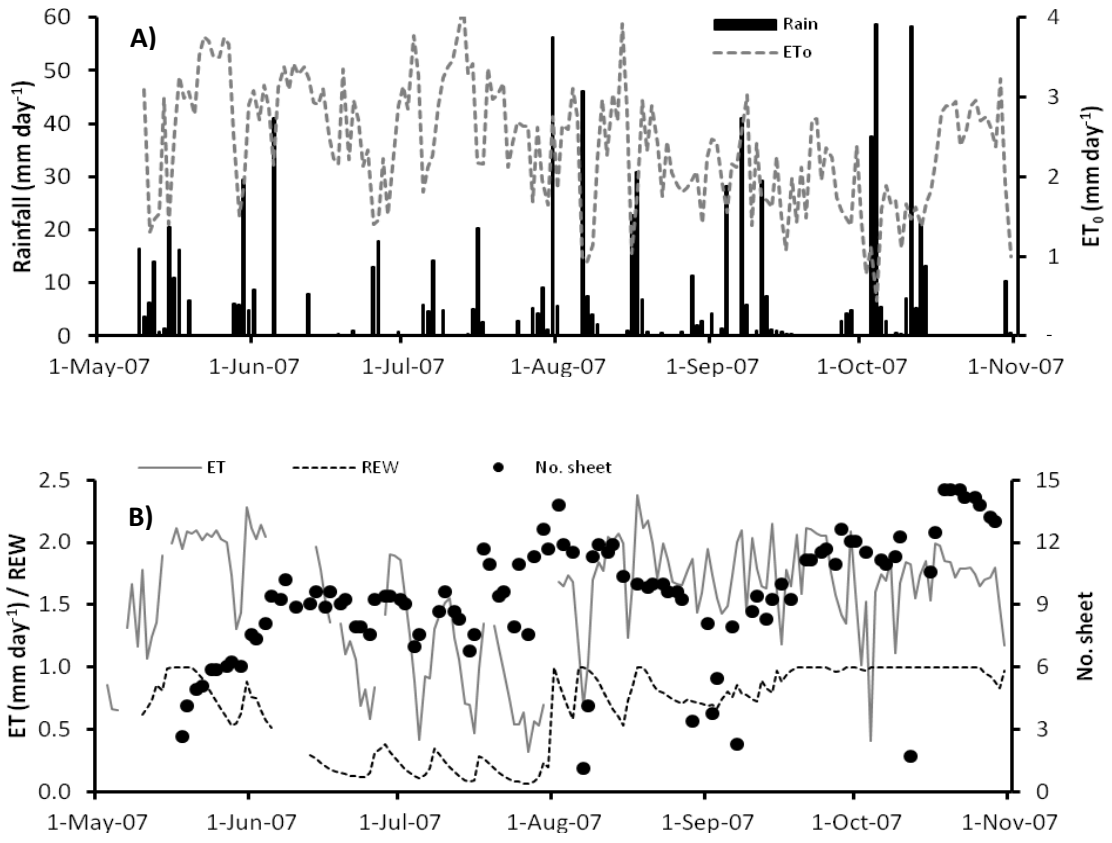


Fig. 1. Change of A) rainfall and reference evapotranspiration (ET_0), B) tree transpiration (ET), number of rubber sheets per hectare and relative extractable water content (REW) during rainy season (May-October 2007) with intermittent drought.

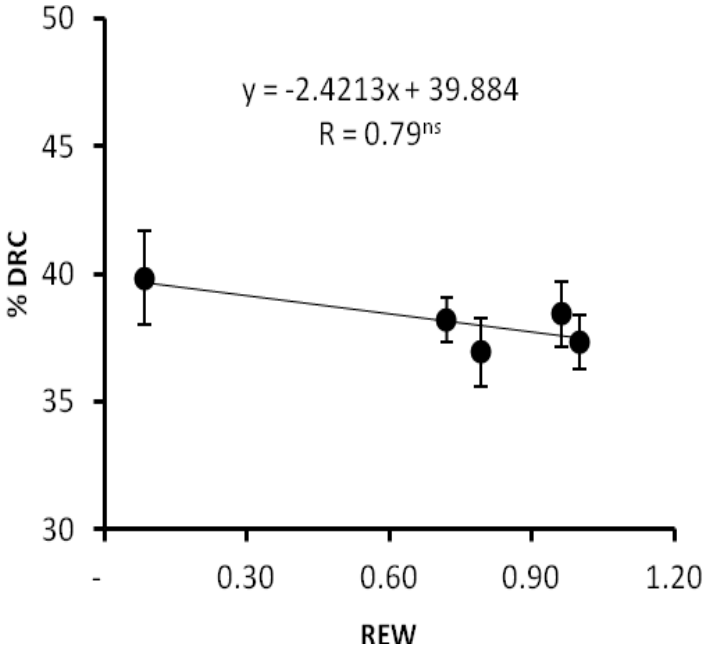


Fig. 2. Relationship between dry rubber content (DRC) and relative extractable soil water (REW). The vertical bars represent the standard error. ns indicates non-significant correlation.

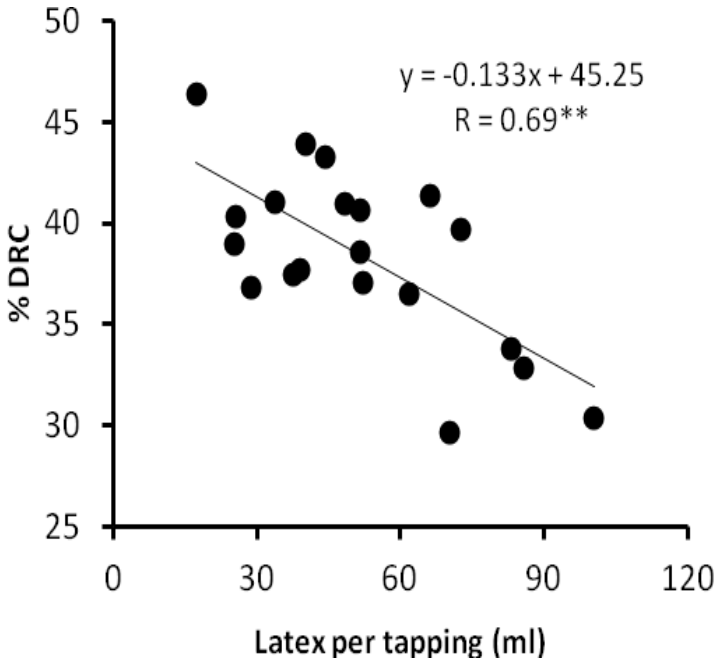


Fig. 3. Relationship between percentage of dry rubber content (DRC) and latex per tapping per tree. ** indicates a highly significant correlation with 99% probability.

AGRIVITA VOLUME 37 No. 2 *JUNE - 2015* *ISSN : 0126-0537*

QTLs CONTROLLING SEED WEIGHT AND DAYS TO FLOWERING IN MUNGBEAN [*Vigna radiata* (L.) Wilczek], THEIR CONSERVATION IN AZUKI BEAN [*V. angularis* (Ohwi) Ohwi & Ohashi] AND RICE BEAN [*V. umbellata* (Thunb.) Ohwi & Ohashi]

Prakit Somta[1*)], Sompong Chankaew[2)], Alisa Kongjaimun[1)] and Peerasak Srinives[1)]

[1)] Department of Agronomy, Faculty of Agriculture at Kamphaeng Saen, Kasetsart University, Nakhon Pathom 73140, Thailand
[2)] Department of Plant Science and Agricultural Resources, Khon Kaen University, Khon Kaen 40002, Thailand
[*)] Corresponding author E-mail: pksomta@gmail.com

Received: May 12, 2015/ Accepted: May 12, 2015

ABSTRACT

Mungbean (*Vigna radiata* (L.) Wilczek) is a socio-economically important legume crop of Asia. Varieties with large seed size and early maturity are preferred in commercial production. This study was to identify quantitative trait loci (QTL) controlling seed weight and days to flowering in mungbean. The mapping population comprises 155 F_2-derived lines from a cross between Kamphaeng Saen 1 (large-seeded and early flowering) and V4718 (small-seeded and late flowering). The F_2 population was analyzed with 67 simple sequence repeat markers. The F2:3 families were evaluated for 100-seed weigh and days to flowering in two years, 2008 (one season) and 2011 (two seasons). Composite interval mapping identified six QTLs for 100-seed weight and 5 QTLs for days to flowering. Three genomic regions harbored QTLs for both seed weight and days to flowering, revealing association between the two traits. Comparison of QTLs for both traits found in this study with those reported in azuki bean [*Vigna angularis* (Willd.) Ohwi & Ohashi] and rice bean [*Vigna umbellata* (Thunb.) Ohwi & Ohashi] revealed that several QTLs are conserved among the three *Vigna* species.

Keywords: comparative mapping, flowering, mungbean, quantitative trait loci, seed size

INTRODUCTION

Mungbean (*Vigna radiata* (L.) Wilczek) is an important legume crop of Asia. The crop is grown principally for its dry seeds, although young pods are sometimes consumed and other plants parts can be used as fodders. Mungbean seeds contain 20-25% of proteins and 65-70% of carbohydrates (Poehlman, 1990). It is a major inexpensive source of dietary proteins and amino acids for people in South, East and Southeast Asia. Seed and flour of mungbean are used to prepare several kinds of food. Mungbean sprout is consumed as a popular vegetable containing high vitamin C and iron. Mungbean is grown in the total production area of about 5.5 million ha of which 90% is in Asia (Somta and Srinives, 2007), although the real production area is believed to be much higher. Major producing countries include India, China, Myanmar, Thailand and Viet Nam where India is the largest producer in an area of about 3 million ha annually. China, Myanmar, Thailand and Viet Nam are also the chief exporters of mungbean grain and products.

Mungbean is usually grown after rice or other cereal crops, or sometimes intercropped with other field and tree crops. It is relatively tolerant to drought and can be harvested within 60-90 days depending on varieties (Fernandez and Shanmugasundaram, 1988). This makes mungbean suitable for several cropping systems. Most commercial mungbean cultivars are large-seeded with 100-seed weight being 0.60 to 0.75 gram and early maturity (55 to 75 days after sowing). Seed size is positively correlated with yield. Large seed has advantage in field germination and establishment. It is also desirable for sprout industry in that large seeds always yield larger sprouts than small seeds. Very early maturing cultivars are desirable because they can escape drought condition. Therefore, large seed size and early maturity are major goals in mungbean breeding programs (Fernandez and Shanmugasundaram, 1988).

Accredited SK No.: 81/DIKTI/Kep/2011
http://dx.doi.org/10.17503/Agrivita-2015-37-2-p159-168

Better understanding of the genetic control of these two traits will be useful for improving new mungbean cultivar(s).

Like most seed crops, genetics of seed size and flowering time have been well studied in mungbean. Seed size is a polygenic trait with high heritability (>80%) (Imrie *et al*., 1985; Humphry *et al*., 2005; Yimram *et al*., 2009). Similarly, days to flowering is controlled by polygenes which has moderate to high heritability (43% to 93%) (Yimram *et al*., 2009). Quantitative trait loci (QTL) controlling seed weight of mungbean has been identified (Fatokun *et al*., 1992; Humphry *et al*., 2005; Sompong *et al*., 2012). Fatokun *et al.* (1992) reported that seed weight is controlled by one major and three minor QTLs. Humphry *et al*. (2005) found that the trait is controlled by as many as 11 QTLs with moderate to minor effect. Sompong *et al*. (2012) reported that five QTLs with moderate to minor effect govern seed size. In contrast to seed weight, there is only a single report on QTL for days to flowering in mungbean. Sompong *et al.* (2012) identified three QTLs, two major and one minor, for days to flowering.

In this paper, we report QTLs for seed weight and days to flowering in mungean and conservation of these QTLs with other related species.

MATERIALS AND METHODS

Plant Materials

An F_2 population comprising 155 lines derived from a cross between Kamphaeng Saen 1 (here after called as KPS1) and V4718. KPS1 is a popular commercial mungean cultivar from Thailand. It has large seed size (about 6.4 g per 100 seeds) and is early flowering (30-35 days after planting). V4718 is a mungbean germplasm originated from India with small seed size (about 3.3 g per 100 seeds) and moderate flowering (40-50 days after planting).

Measurement of Seed Weight and Days to Flowering

The parents and F_2 progenies were individually grown in pots during February to April 2007. DNA of each entry was extracted from leaves using a CTAB method (Lodhi *et al*., 1994). The parents and $F_{2:3}$ progenies were sown in a randomized complete block design (RCBD) with three replicates in two seasons, viz. rainy (August to December, 2008) and dry (January to March 2011). Each replicate contained 20 to 25 plants. In each entry, days to first flowering was recorded, seeds were harvested and weighed for 100 seed weight (g). The parents and $F_{2:4}$ progenies were sown in a RCBD with three replicates in dry season during September 2011 to January 2012. Seed weigh and days to flowering were recorded as described in the $F_{2:3}$ generation.

SSR Marker Analysis

KPS1 and V4718 were screened for DNA polymorphism using 753 primer pairs of simple sequence repeat (SSR) markers [433 from mungbean (Gwag *et al*., 2006; Tangphatsornruang *et al*., 2009; Somta *et al*., 2008; Seehalak *et al*., 2009; Somta *et al*., 2009), 188 from azuki bean [*V. angularis* (Ohwi) Ohwi & Ohashi] (Wang *et al*., 2004), 46 from cowpea [*V. unguiculata* (L.) Walp.] (Li *et al*., 2001), and 86 from common bean (*Phaseolus vulgaris* L.) (Gaitán-Solís *et al*., 2002; Blair *et al*., 2003; Guerra-Sanz, 2004; Buso *et al*., 2006)]. Polymorphic markers were then used to analyze the F_2 population. DNA marker analysis was carried out as per Somta *et al.* (2008).

Linkage Map Construction and QTL Analysis

Genetic linkage maps were constructed using Join Map 3.0 with the minimum logarithm of the odds (LOD) at 3.0 and the maximum recombination frequency (*r*) at 0.5. The recombination frequency was converted into genetic distance (centimorgan; cM) using Kosambi mapping function (Kosambi, 1943). Linkage groups were named after azuki bean linkage map (Han *et al*., 2005) based on the common markers. QTL for seed weight and days to flowering was detected by composite interval mapping (CIM) using WinQTL Cartographer version 2.5 (Wang *et al*., 2011). Genome-wise significant LOD threshold of 3 was used to declare QTL.

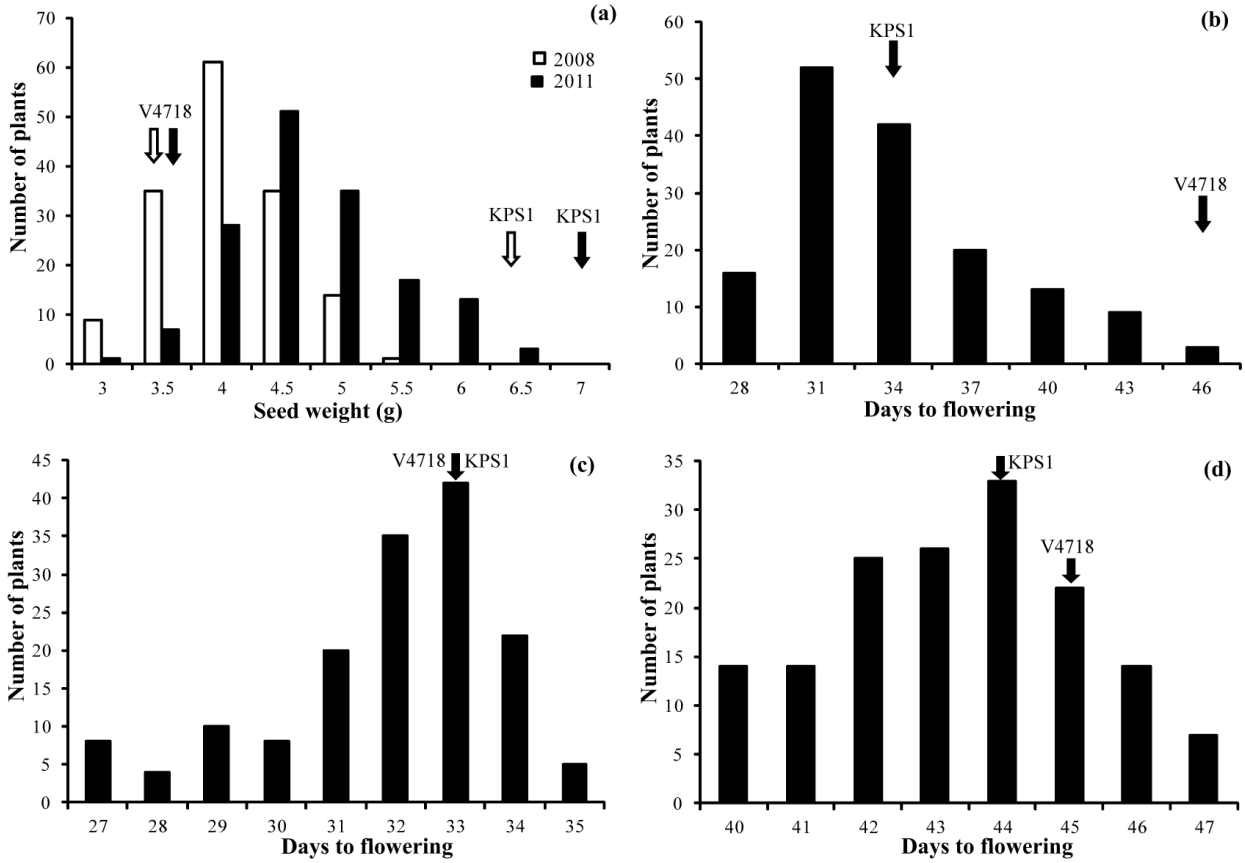


Figure 1. Frequency distribution of seed weight of $F_{2:3}$ population grown in rainy season 2008 and early dry season of 2011 (a), and of days to flowering grown in rainy season 2008 (b), and early (c) and late (d) dry seasons of 2011

RESULTS AND DISCUSSION

Seed Weight

Seed of KPS1 was about one fold larger than V4718. One hundred-seed weight of KPS1 and V4718 grown in the rainy season of 2008 were 6.62 g and 3.27 g in that order, and those grown in the dry season of 2011 were 6.75 g and 3.30 g, respectively. In the $F_{2:3}$ population grown in the rainy season of 2008, their 100-seed weights varied between 2.77 g and 5.36 g with an average of 3.79 g. For the population grown in dry season of 2011, 100-seed weight ranged from 2.78 g to 6.30 g with an average of 4.50 g. As expected, frequency distributions of seed weight in both seasons were continuous (Figure 1). A few progenies had smaller seed weight than V4718, but none of them were larger than KPS1.

Days to Flowering

KPS1 flowered earlier than V4718 when grown in rainy season (long photoperiod condition) of 2008, but they showed almost the same flowering time when grown in the dry season of 2011 (short photoperiod condition). In the rainy season of 2008, days to flowering of KPS1 and V4718 were 33 and 44, respectively. Days to flowering of both KPS1 and V4718 in the early dry season of 2011 were 33, while those in the late dry season of 2011 were 44 and 45 days, respectively. Days to flowering of the $F_{2:3}$ population grown in the rainy season of 2008 was between 26.7 and 45.3 with an average of 32.7 days. For the F_3 population grown in early dry season of 2011, days to flowering varied from 26.5 to 35.5 with an average of 31.6 days. In case of the $F_{2:4}$ population which was grown in the late dry season of 2011, days to flowering ranged from 40 to 47 with an average of 43.2 days. The

transgressive segregation suggests that both KPS1 and V4718 possess both positive and negative alleles for seed weight. There was a positive correlation between days to flowering measured in different populations and seasons. Frequency distribution of days to flowering in all generations and seasons demonstrated continuous segregation (Figure 1). Transgressive segregation was found in all seasons, suggesting that the parents possess both positive and negative alleles for days to flowering.

Correlation between Traits and between Seasons

There were positive correlations of seed weight or days to flowering measured in different seasons (data not shown). The correlation was moderate for seed weight and relatively low for days to flowering, suggesting different degrees of environmental effect on the two traits. Correlation between seed weight and days to flowering was significant and negative being -0.48 ($P < 0.0001$) and -0.24 ($P = 0.0023$) for the $F_{2:3}$ population grown in 2008 and 2011, respectively. Negative correlation between seed weight and earliness (days to flowering and maturity) in mungbean have been reported previously (Siddique *et al.,* 2006).

Mungbean Linkage Map

There was low polymorphism between genomes of V4718 and KPS1. Out of 753 SSR markers screened, 496 (65.87%) amplified DNA of the two genotypes (data not shown), but only 69 (13.91%) of the amplifiable markers were polymorphic. Only 56 polymorphic markers could be assigned to the linkage map (Figure 2), while 13 markers were unlinked. The linkage map consisted of 11 linkage groups (LGs). The total map distance was 995.6 cm with and an average density of 17.78 cm per marker. Comparison of our linkage map with azuki bean map reported by Han *et al.* (2005) based on 30 common markers revealed that all of the markers were conserved on both maps with a few inversions of marker order (data not shown). This indicates high genome homology between mungbean and azuki bean.

QTLs for Seed Weight and Days to Flowering

Six QTLs locating on different LGs were identified for seed weight (Figure 2; Table 1). Five and two QTLs for this trait were found in $F_{2:3}$ population planted in the rainy season of 2008 and dry season of 2011, respectively, in which only one QTL, *qSW5.1*, was common between the seasons. The phenotypic variance explained (PVE) by these QTLs varied between 5.9 (*qSW2.2*) to 22.1% (*qSW2.1*). PVE of the *qSW5.1* in both seasons were very similar. The number of QTLs for seed weight found in this study was only about a half of those reported by Humphry *et al.* (2005) who reported 11 QTLs for seed weight in a RIL from a cross between wild and cultivated mungbeans. The lower number of QTLs found in our study was possibly stem from narrow difference in seed size of the parents used. However, the number of QTLs for seed size found in our study was very similar to those reported by Sompong *et al.* (2012). Although there is small number of common markers between the two studies, the QTLs on LG2 and LG10 appear to be common, especially *qSW2.2* in this study and *SD100WT2.1* reported by them were both linked to the same marker VR413.

Five QTLs were detected for days to flowering (Figure 2; Table 1). All the QTLs were detected in the $F_{2:3}$ population grown in rainy season of 2008. The PVE of these QTLs ranged from 18.2 for *qDFL4.1* to 32.0% for *qDFL5.1*. Only one QTL, *qDFL2.2*, was detected in the $F_{2:3}$ population grown in dry season of 2011, and only QTL *qDFL2.1* was identified in the $F_{2:4}$ population grown in the same season. The PVE of *qDFL2.1* and *qDFL2.2* found in these two seasons was only about a half of that in the same QTL in the rainy season of 2008. The marked difference in number of QTLs for days to flowering found in rainy and dry seasons is very likely due to effect of photoperiod. Mungbean is a short-day plant (Poehlman, 1990). This caused high and low variation in days to flowering in the rainy season (long photoperiod; 19 days) and dry season (short photoperiod; 7 or 9 days), respectively (data not shown). This resulted in difference number of QTLs detected in such different environments.

Table 1. QTL controlling seed weight and days to flowering in the F_2 (KPS1 x V4718) population as detected by composite interval mapping

Trait	Plant generation-Season	QTL name[1]	LG[2]	Marker interval	LOD score	PVE[3] (%)	Additive effect	Dominant effect
Seed weight	$F_{2:3}$-rainy, 2008	*qSW2.1*	2A	DMBSSR160 - GBssrMB087	10.4	22.1	-0.33	-0. 08
		qSW2.2	2B	VR413 - CEDG284	3.6	5.9	-0.17	-0.08
		qSW4.1	4	CEDG088 - CEDG232	3.2	7.8	-0.19	0.08
		qSW5.1	5	CEDG014 - MBSSR39	6.7	11.6	-0.19	-0.19
		qSW10.1	10 B	CEDG198 - VR293	3.4	8.1	-0.18	-0.17
	$F_{2:3}$-dry, 2011	*qSW5.1*	5	CEDG014 - MBSSR39	3.2	9.1	-0.24	-0.15
		qSW11.1	11	MBSSR164 - VR304	3.8	13.0	-0.30	-0.27
Days to flowering	$F_{2:3}$-rainy, 2008	*qDFL2.1*	2A	CEDAAG002 - DMBSSR160	7.4	29.6	3.50	-2.05
		qDFL2.2	2A	DMBSSR160 - GBssrMB087	10.9	29.1	2.75	-2.20
		qDFL4.1	4	DMBSSR167 - VRSSR035	6.7	18.2	2.00	-2.26
		qDFL5.1	5	CEDG014 - MBSSR39	4.5	32.0	0.42	7.27
		qDFL6.1	6	VR095 - CEDG037	5.0	31.0	-0.08	7.02
	$F_{2:3}$-dry, 2011	*qDFL2.2*	2A	CEDAAG002 - DMBSSR160	5.1	12.6	1.10	0.21
	$F_{2:4}$-dry, 2011	*qDFL2.1*	2A	DMBSSR160 - GBssrMB087	4.3	23.2	5.14	-0.65

Remarks: [1] QTLs of the same trait that showed similar position and effect in the different seasons were assigned the same name; [2] Linkage group; [3] Percentage of phenotypic variance explained by the QTL

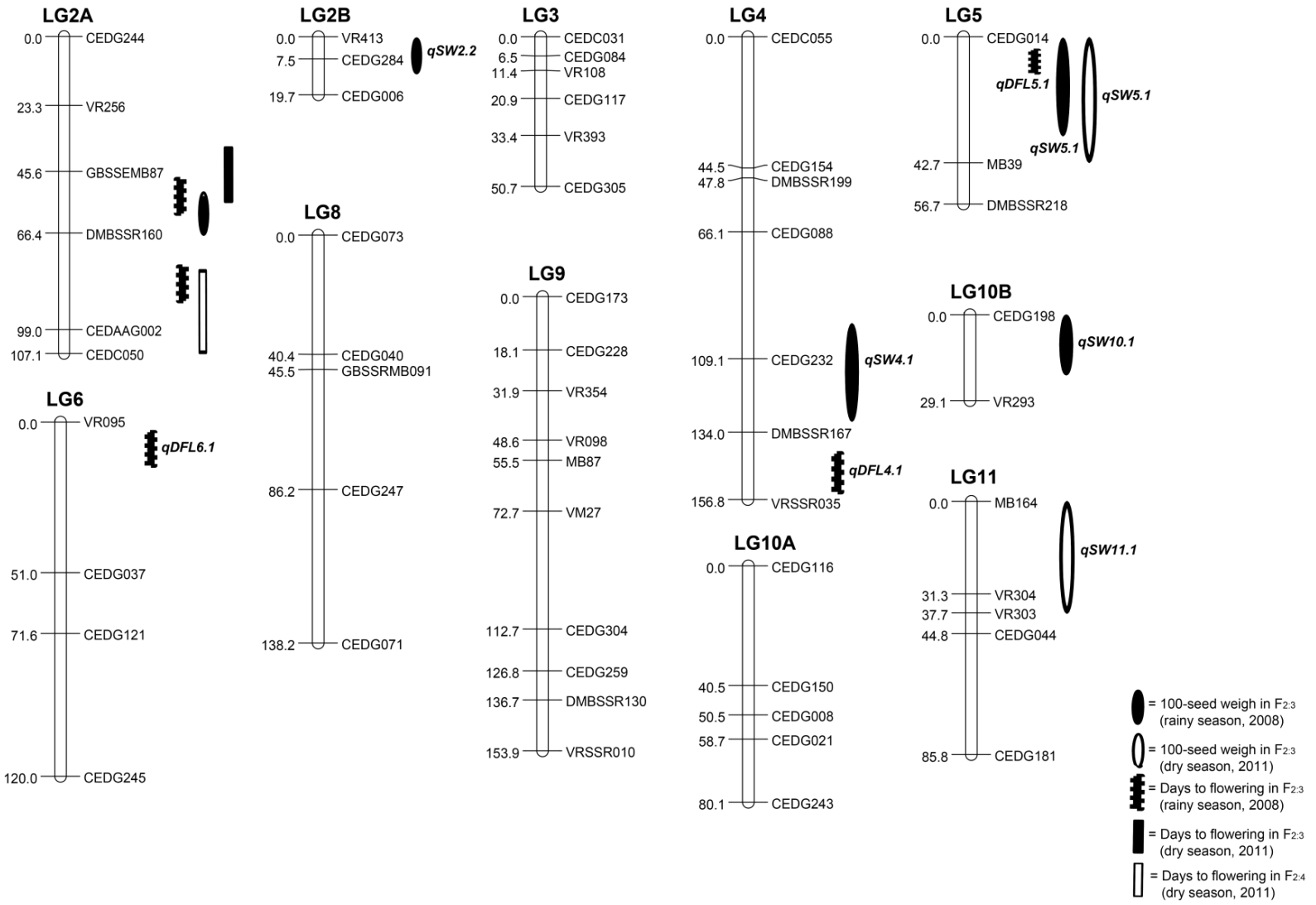


Figure 2. Linkage map and locations of QTLs controlling seed weight and days to flowering of F_2 population developed from a cross between KPS1 and V4718 mungbeans

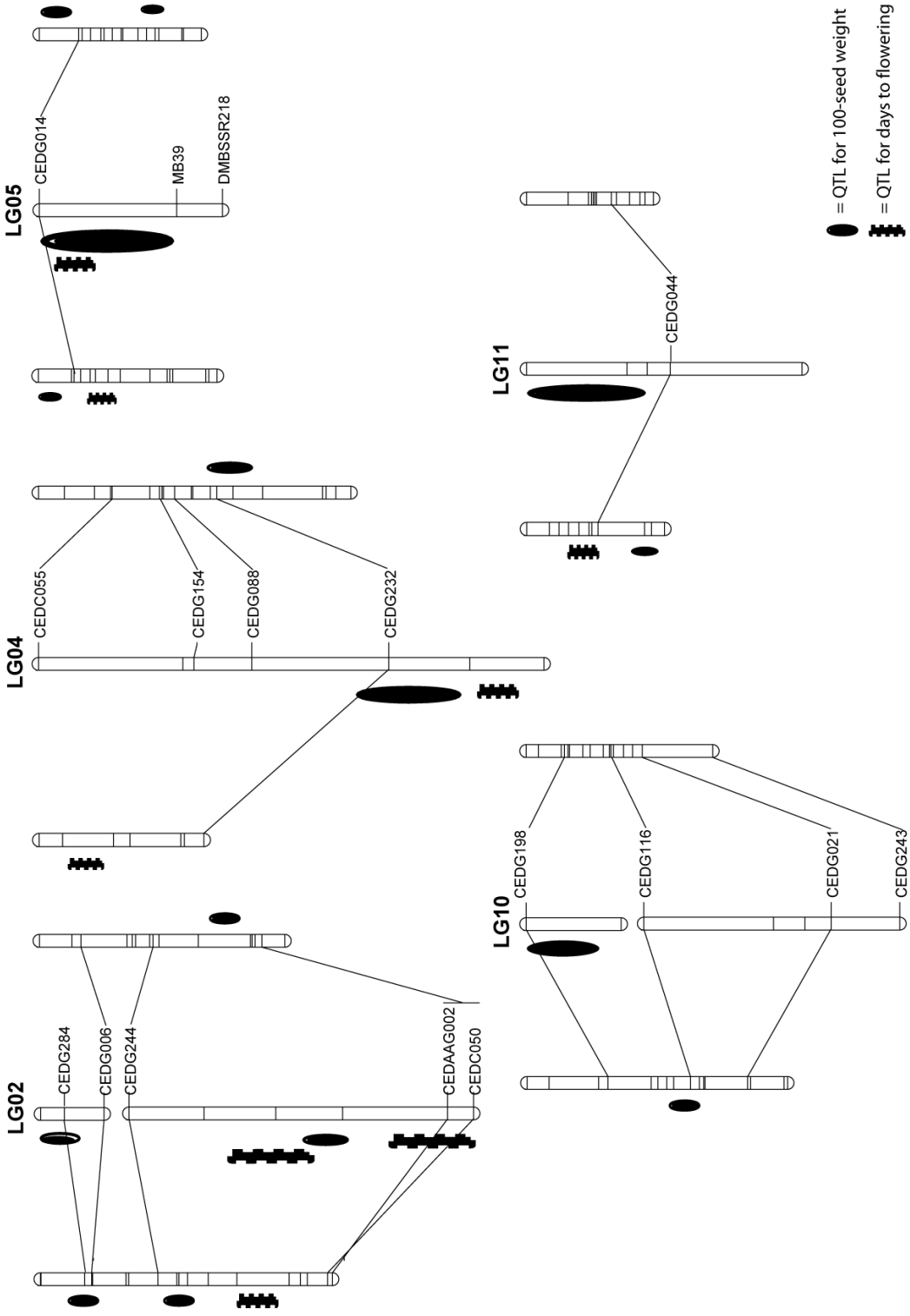


Figure 3. A comparative QTL map for seed weight and days to flowering of azuki bean, mungbean and rice bean. In each linkage group, common markers between maps are connected by lines. Linkage maps of azuki bean, mungbean and rice bean are on the right, middle and left, respectively. Size of QTL symbol does not relate to genetic effect

Since the *qDFL2.1* and *qDFL2.2* were found in both photoperiod conditions, they can be considered important loci controlling flowering time in mungbean. *qDFL4.1, qDFL5.1 and qDFL* which were identified in rainy season may be specific to long photoperiod regime in mungbean. Nonetheless, the number of QTLs for days to flowering found in this study is higher than those reported by Sompong *et al.* (2012) who found only three QTLs for days to flowering. Based on common markers, only QTL on LG4 are likely the same QTL in the two studies (data not shown).

Co-localization or linkage of QTLs for seed weight and days to flowering was found on LGs 2A, 4 and 5. On LG2A and 5, QTLs for seed weight and days to flowering were overlapped (*qSW2.1* vs. *qDFL2.2* and *qSW5.1* vs. *qDFL5.1*). *qSW4.1* and *qDFL4.1* were linked at the lower part of LG4. These support the significant correlation between the two traits.

Comparison of Seed Weight and Days to Flowering QTLs between Mungbean and Azuki Bean, and Rice Bean

High genome conservation among species in the genus *Vigna* has been demonstrated (Fatokun *et al*., 1992; Somta *et al*., 2006; Isemura *et al*., 2007, 2010; Kongjaimun *et al*., 2012). Mungbean, azuki bean and rice bean belong to the subgenus *Ceratotropis* which are known as Asian *Vigna* because they are all originated in Asia. QTLs for seed weight and flowering time have been reported in azuki bean (Isemura *et al*., 2007; Kaga *et al*., 2008) and rice bean (Isemura *et al*., 2010). Comparison of QTL locations for seed weight and flowering time of mungbean in the present study with those of azuki bean and/or rice bean (Figure 3) further supports previous findings. Several QTLs for seed weight and days to flowering of the three *Vigna* species were found on the same LG. Some of them are linked to the same markers or located in the similar genomic regions. For example, a seed size QTL for azuki bean, rice bean and mungbean on LG5 are all linked by marker CEDG014 (Figure 3). These QTLs are possibly the same locus. On the same LG, a QTL for flowering time of mungbean and azuki bean were located in the similar genomic region (Figure 3). It is worth noting that although the QTLs for flowering time on LG4 of azuki bean and mungbean appear to far apart, they are both major QTLs for this trait (Table 1; Kaga *et al*., 2008). The high genome conservation among *Vigna* species is useful for comparative and candidate gene mappings of important traits among species in this taxon.

CONCLUSION

Nine genomic regions harboring six QTLs for 100-seed weight and 5 QTLs for days to flowering was identified in $F_{2:3}$ families of KPS1 x V4718 grown in one rainy season (long day condition) and two dry seasons (short day condition) of two years. Only two of the nine genome regions harbored both QTLs for seed weight and days to flowering detected in rainy season, while the other regions each harbored only a single QTL for a trait. This results suggested substantial effect of day length on the two traits. Therefore, breeding for seed weight and days to flowering simultaneously for different day length conditions in mungbean would be difficult. When the QTLs detected in this study were compared with those QTLs detected previously in azuki bean and rice bean, two genome regions each on linkage groups 2 and 5 containing QTLs for seed weight were found to be common among the three legumes. This suggested that those QTLs can be used as candidates for map-based cloning of seed weight QTLs.

ACKNOWLEDGEMENTS

This study was financially supported by the Center of Advanced Studies for Agriculture and Food, Kasetsart University, under the National Research University program of the Office of the Higher Education Commission, Ministry of Education, Thailand.

REFERENCES

Blair, M.W., F. Pedraza, H.F. Buendia, E.Gaitán-Solís, S.E. Beebe, P. Gepts and J. Tohme. 2003. Development of a genome-wide anchored microsatellite map for common bean (*Phaseolus vulgaris* L.). Theor. Appl. Genet. 107: 1362–1374.

Buso, G.S.C., Z.P.S. Amaral, R.P.V. Brondani and M.E. Ferreira. 2006. Microsatellite markers for the common bean *Phaseolus vulgaris*. Mol. Ecol. Notes. 6: 252–254.

Fatokun, C.A., D.I. Menancio-Hautea, D. Danesh and N.D. Young. 1992. Evidence for orthologous seed weight genes in cowpea and mung bean based on RFLP mapping. Genetics. 132 (3): 841–846.

Fernandez, G.C.J. and S. Shanmugasundaram. 1988. The AVRDC mungbean improvement program: The past, present and future. In: Shanmugasundaram, S. and B.T. McLean. (Eds.) Mungbean. Proceeding of the Second International Symposium. Asian Vegetable Research and Development Center. Taiwan. p. 55-70.

Gaitán-Solís, E., M.C. Duque, K.J. Edwards and J. Tohme. 2002. Microsatellite repeats in common bean (*Phaseolus vulgaris*): Isolation, characterization, and cross-species amplification in *Phaseolus* ssp. Crop Sci. 42 (6): 2128–2136.

Guerra-Sanz, J.M. 2004. New SSR markers of *Phaseolus vulgaris* from sequence databases. Plant Breeding. 123(1): 87–89.

Gwag, J.G., J.W. Chung, H.K. Chung, J.H. Lee, K.H. Ma, A. Dixit, Y.J. Park, E.G. Cho, T.S. Kim and S.H. Lee. 2006. Characterization of new microsatellite markers in mung bean, *Vigna radiata* (L.). Mol. Ecol. Notes. 6 (4): 1132–1134.

Han, O.K., A. Kaga, T. Isemura, X.W. Wang, N. Tomooka and D.A. Vaughan. 2005. A genetic linkage map for azuki bean [*Vigna angularis* (Willd.) Ohwi & Ohashi]. Theor. Appl. Genet. 111: 1278–1287.

Humphry, M.E., C.J. Lambrides, S.C. Chapman, E.A.B. Aitken, B.C. Imrie, R.J. Lawn, C.L. MacIntyre and C.J. Liu. 2005. Relationships between hard-seededness and seed weight in mungbean (*Vigna radiata)* assessed by QTL analysis. Plant Breeding. 124: 292–298.

Imrie, B.C., Z.U. Ahmed and J.P.J. Eerens. 1985. Heritability of seed weight in mungbean. SABRAO J. Breed. Genet. 17: 173–175.

Isemura, T., A. Kaga, S. Konishi, T. Ando, N. Tomooka, O.K. Han and D.A. Vaughan. 2007. Genome dissection of traits related to domestication in azuki bean (*Vigna angularis*) and comparison with other warm-season legumes. Ann. Bot. 100(5): 1053–1071.

Isemura, T., A. Kaga, N. Tomooka, T. Shimizu and D.A. Vaughan. 2010. The genetics of domestication of rice bean, *Vigna umbellata*. Ann. Bot. 106 (6): 927–944.

Kaga, A., T. Isemura, N. Tomooka and D.A. Vaughan. 2008. The genetics of domestication of the azuki bean (*Vigna angularis*). Genetics. 178(2):1013–1036.

Kongjaimun, A., A. Kaga, N. Tomooka, P. Somta, D.A. Vaughan and P. Srinives. 2012. The genetics of domestication of yardlong bean, *Vigna unguiculata* (L.) Walp. ssp. *unguiculata* cv.-gr. *Sesqui-pedalis*. Ann. Bot. 109(6): 1185-1200.

Kosambi, D.D. 1943. The estimation of map distances from recombination values. Ann. Eugen. 12 (1): 172–175.

Li, C.D., C.A. Fatokun, B. Ubi, B.B. Singh and G.J. Scoles. 2001. Determining genetic similarities and relationships among cowpea breeding lines and cultivars by microsatellite markers. Crop Sci. 41 (1): 189–197.

Lodhi, M.A., G.N. Ye, N.F. Weeden and B.I. Reisch. 1994. A simple and efficient method for DNA extraction from grapevine cultivars and *Vitis* species. Plant Mol. Biol. Rep. 12 (1): 6–13.

Poehlman, J.M. 1990. The mungbean. Oxford and IBH Publishing Co. Pvt. Ltd. New Delhi.

Seehalak, W., P. Somta, W. Sommanas and P. Srinives. 2009. Microsatellite markers for mungbean developed from sequence database. Mol. Ecol. Resour. 9 (3): 862–864.

Siddique, M., M.F.A. Malik and S.I. Awan. 2006. Genetic divergence, association and performance evaluation of different genotypes of mungbean (*Vigna radiata*). Int. J. Agric. Biol. 8 (6): 793–795.

Sompong, U., P. Somta, V. Raboy and P. Srinives. 2012. Mapping of quantitative trait loci for phytic acid and phosphorus contents in seed and seedling of mungbean (*Vigna radiata* (L.) Wilczek). Breed. Sci. 62 (1): 87–92.

Somta, P., A. Kaga, N. Tomooka, K. Kashiwaba, T. Isemura, B. Chaitieng, P. Srinives and D.A. Vaughan. 2006. Development of an interspecific *Vigna* linkage map between *Vigna umbellata* (Thunb.) Ohwi & Ohashi and *V. nakashimae* (Ohwi) Ohwi &

Ohashi and its use in analysis of bruchid resistance and comparative genomics. Plant Breeding. 125 (1): 77–84.

Somta, P. and P. Srinives. 2007. Genome research in mungbean (*Vigna radiata* (L.) Wilczek) and blackgram (*V. mungo* (L.) Hepper). Sci. Asia. 33 (Supplement 1): 69–74.

Somta, P., W. Musch, B. Kongsamai, S. Chanprame, S. Nakasathien, T. Toojinda, W. Sorajjapinun, W. Seehalak, S. Tragoonrung and P. Srinives. 2008. New microsatellite markers isolated from mungbean (*Vigna radiata* (L.) Wilczek). Mol. Ecol. Resour. 8 (5): 1155–1157.

Somta, P., W. Seehalak and P. Srinives. 2009. Development, characterization and cross-species amplification of mungbean (*Vigna radiata*) genic microsatellite markers. Conserv. Genet. 10: 1939–1943.

Tangphatsornruang, S., P. Somta, P. Uthaipaisanwong, J. Chanprasert, D. Sangsrakru, W. Seehalak, W. Sommanas, S. Tragoonrung and P. Srinives. 2009. Characterization of microsatellites and gene contents from genome shotgun sequences of mungbean (*Vigna radiata* (L.) Wilczek). BMC Plant Biol. 9: 137.

Wang, X.W., A. Kaga, N. Tomooka and D.A. Vaughan. 2004. The development of SSR markers by a new method in plants and their application to gene flow studies in azuki bean (*Vigna angularis* (Willd.) Ohwi & Ohashi). Theor. Appl. Genet. 109: 352–360.

Wang, S., C.J. Basten, and Z.B. Zeng. 2011. Windows QTL cartographer 2.5. Department of Statistics. North Carolina State University. Raleigh. North Caroline.

Yimram, T., P. Somta and P. Srinives. 2009. Genetic variation in cultivated mungbean germplasm and its implication in breeding for high yield. Field Crops Res. 112 (2-3): 260–266.

Kyoto University

Homegardens of the Cao Lan, a Tai-Speaking Ethnic Minority in Vietnam's Northern Mountains

Pijika Timsuksai,* Nguyen Dinh Tien,** and A. Terry Rambo***

The Cao Lan are a Tai-speaking ethnic group living in the Midlands of Northern Vietnam. Homegardens are an important component of their agroecosystem. The ecological structures of each homegarden of 17 households of the Cao Ngoi village in Tuyen Quang province were described and modal patterns identified. Most homegardens have organically shaped planting areas with indeterminate boundaries, polycentric planting patterns, and contain multiple species within the same bed or planting area. All of the gardens have multiple vegetation levels, with the largest share having 5 levels and a majority having more than 50% of their planting area covered by overlapping vegetation layers. Biodiversity is high with a total of 113 species recorded. Most plant species are used for food, but smaller numbers have ornamental, medicinal, and construction uses or are used for animal fodder, as stimulants, or for other purposes.

Comparison of the modal structure of the Cao Lan homegardens with several Tai minority groups in Northeast Thailand, shows that, although the Cao Lan have been geographically isolated from other Tai groups for many centuries, their homegardens share a similar structural pattern, one commonly referred to as the tropical forest type. This structure is very different from the temperate type gardens of the Kinh in Vietnam with whom the Cao Lan share a common environment and are in frequent contact. The persistence of a common structural pattern among these related Tai ethnic groups, despite their inhabiting different environments, and having had no direct contact with each other for a very long time, suggests that culture exerts a strong influence over agroecosystem structure.

Keywords: Cao Lan ethnic minority, ethnobotany, agroecosystem structure, indigenous knowledge, biodiversity

* พิจิกา ทิมสุกใส, Program on System Approaches in Agriculture, Faculty of Agriculture, Khon Kaen University, Khon Kaen 40002, Thailand

** Nguyễn Đình Tiến, Center for Agricultural Research and Ecological Studies (CARES), Vietnam National University of Agriculture, Gia Lam, Hanoi, Vietnam

*** Program on System Approaches in Agriculture, Faculty of Agriculture, Khon Kaen University, Khon Kaen 40002, Thailand; The East-West Center, Honolulu, Hawaii 96848-1601, USA
Corresponding author's e-mail: trryrambo@yahoo.com

© Center for Southeast Asian Studies, Kyoto University

NII-Electronic Library Service

Kyoto University

Introduction

After Terra's pioneering descriptions of the different types of homegardens associated with different ethnic groups in the Indo-Malayan region (Terra 1952–53; 1954; 1958), few additional studies were published about Southeast Asian homegardens until the 1980s when homegardens emerged as a major focus of agroforestry research. Much of this research was concerned with describing the architecture, species composition, and functions of homegardens of different ethnic groups in the tropics. Since that time, a considerable number of studies have been published describing the structure, species diversity, and functions of homegardens of ethnic groups in different Southeast Asian countries, including Burma (Terra 1954), Indonesia (Soemarwoto and Soemarwoto 1984; Wiersum 2006), Laos (Kou *et al.* 1990; The SUAN Secretariat 1990; Dyg and Saleumsy 2004; Nawata *et al.* 2009), Thailand (Moreno-Black *et al.* 1996; Jiragorn and Nantana 1999; Nawata *et al.* 2009; Thanakorn *et al.* 2010; Kamonnate *et al.* 2012), and the Philippines (Snelder 2008). There has also been considerable research on homegardens in Vietnam (Le Trong Cuc *et al.* 1990; Karyono *et al.* 1993; Hodel *et al.* 1999; Dao Trong Hung *et al.* 2001; Luu Ngoc Trinh *et al.* 2003; Vlkova *et al.* 2011) but it has mostly been focused on the Kinh (ethnic Vietnamese), the majority ethnic group. Only a very few studies have been done on the homegardens of ethnic minorities. In the case of the Cao Lan, a Tai speaking minority group living in the Northern Mountain region, there are only 2 brief reports (Gillogly and Nghiem Phuong Tuyen 1992; Le Trong Cuc and Rambo 2001) which describe the species composition of their homegardens but not their ecological structure or the functions of the different species.

It was in order to obtain information about the structure and species composition and functions of Cao Lan homegardens, that we carried out a short field study in a Cao Lan community in Tuyen Quang province in Northern Vietnam. This case study was done as part of a larger comparative study of the ecological structures of homegardens of different ethnic groups in Northeast Thailand and Vietnam which was designed to assess the relative importance of culture and environment as determinants of agroecosystem structure (Pijika 2014). The aims of this paper are to describe the modal ecological structure of the Cao Lan homegardens, identify all of the plant species grown in these gardens and categorize their functions, and compare the modal structure of the Cao Lan gardens with those of their Kinh neighbors and ethnically related Tai minority groups in Northeast Thailand.

NII-Electronic Library Service

Kyoto University

Background

The Cao Lan Ethnic Group

The Cao Lan speak a language belonging to the Tai family of languages. They are one of 54 officially recognized ethnic groups in Vietnam. They are known officially as San Chay (also often called Cao Lan-San Chi). They first immigrated to Vietnam from China beginning in the 1600s. The Cao Lan numbered about 169,000 people in 2009. They are mainly settled in Tuyen Quang, Bac Can, and Thai Nguyen provinces. Settlements of this ethnic group are also scattered in Yen Bai, Vinh Phuc, Phu Tho, Bac Giang, and Quang Ninh provinces (Dang Nghiem Van *et al.* 2000; Sumitre *et al.* 2003; Ethnologue: Languages of the World 2013). According to the 1999 census, a few thousand San Chay live in the Central Highlands, mostly in Dac Lac with smaller numbers in Binh Phuoc, Dong Nai, Gia Lai, and Kon Tum provinces (General Statistical Office 2001). It is likely that these people migrated south to the New Economic Zones in the 1980s.

According to Gregerson and Edmondson (1998), the Cao Lan-San Chay ethnic group is actually a composite of two groups with two different languages and two non-overlapping cultures. The Cao Lan language has been classified as a Central Tai language of the Kam-Tai sub-branch of the Tai-Kadai language family, while the San Chay language is Han Chinese. In their view ". . . the Cao Lan and San Chay do not live in a classical diglossic situation of high language vs low language, but as two groups with mostly different identities despite a small overlap today and a common link in the past," when these groups lived in close proximity along the border areas of Hunan, Guangdong, and Guangxi provinces of China (*ibid.*, 152).

According to Gregerson and Edmondson's field study, some Tai speaking Cao Lan groups refer to themselves as San Chay, although this is the official name of the Han-speaking group. Both Cao Lan and San Chay write using Chinese characters. Some older San Chay people can also speak a Tai language just as some elderly Cao Lan can speak and write in the Han language. It can be concluded that, "All these facts tell us that the two were in some sense one nationality with two partially overlapping speech communities whose original bilingualism has developed into separated mostly monolingualism through separation, as the majority of the San Chay live in Quang Ninh and the Cao Lan live mostly in Tuyen Quang, Thai Nguyen, and Bac Giang" (*ibid.*).

The Study Village

Cao Ngoi village is in Dong Loi commune, Son Duong district of Tuyen Quang province. This village is quite isolated and far away from the main road. The distance from the Son Duong district capital to the village is about 50 km, or 2 hours travel by bus (Fig. 1). The

NII-Electronic Library Service

Kyoto University

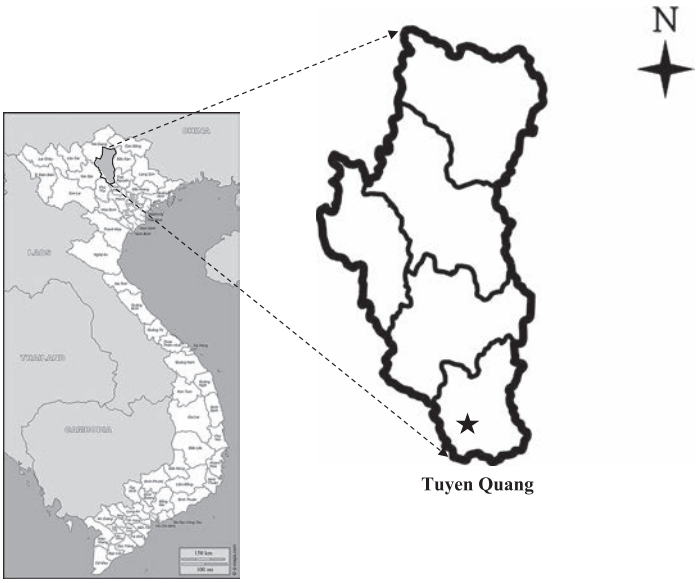


Fig. 1 Map Showing Location of Cao Ngoi Village, Son Duong District, Tuyen Quang Province

narrow and very rough dirt road that connects the village to the main highway crosses paddy fields in lowlands, then climbs up on to the upper terrace with sugarcane fields and acacia tree plantations, before it descends into the narrow valley hidden between steep sloped mountains where Cao Ngoi village is located.

According to the oral traditions of the villagers, Cao Ngoi village was established about 200 years ago by a group of 7 Cao Lan households who migrated there from Hoa Binh province. There are now 21 households with 76 people living there. They all speak the Cao Lan language in their daily activities in the village and also can converse in Vietnamese when dealing with outsiders. Traditionally, Cao Lan was written using Chinese characters but now only one older man in the village can read it. Nowadays the villagers wear Vietnamese style clothes for daily life but they still wear the traditional Cao Lan dress on special occasions.

The villagers live in the traditional Cao Lan style houses which are built on stilts made from large tree trunks. The bottom of each stilt rests on a large flat stone. Most houses have palm leaf roofs. Some houses have walls and floors made of wooden planks and others have woven bamboo walls and floors. They are entered by a wooden ladder on the side of the house. The space underneath the floor of the house is used to store firewood, agricultural equipment, motorcycles and bicycles, and wooden planks for house repairs. A fire-place made of clay is set on the floor of the house and is used for cooking

NII-Electronic Library Service

Kyoto University



Fig. 2 Traditional Cao Lan Style House and Components; (a) Cao Lan House, Well, and Courtyard, (b) Fireplace inside the House, (c) Balcony, (d) Animal Pens under the House

and heating. The ancestral shrine is mounted on a side wall of the house. Agricultural products such as rice grain and dried maize are stored inside the house. Some houses have large attached balconies built from bamboo where they do laundry and sun-dry food (Fig. 2).

The nearest neighboring Cao Lan village is about 4 km away, or 30 minutes by motorcycle, and the nearest market is about 10 km away. The nearest Kinh (ethnic Vietnamese) village is more than 5 km away. A rudimentary 1 room kindergarten in the village has 1 volunteer teacher and 2 very young students. The nearest primary and secondary schools are about 17 km away in Kinh villages. The older children have to ride bicycles to school there early in the morning and return in the afternoon. The trip takes them almost 3 hours each way.

Natural Conditions of the Study Village

Cao Ngoi village is situated at 169 m above sea level at 21°35'40.18''N, 105°20'52.38''E. The climate is classified as humid subtropical. The soil is infertile sandy loam, with poor drainage in the mountain valley. Although this area has scattered rain all year round with a mean annual rainfall of 1,500 mm (Nguyen Thi Mui 2006), there is a relatively dry

NII-Electronic Library Service

Kyoto University

season from August through January and a relatively wet season from February through July. The rains start from late February, with the heaviest rain in July, and then decrease after that with only a slight amount of rain in December. According to the village headman mean temperatures range from 15°C in winter to 35°C in summer. In the village there is a waterfall which the villagers use for electricity generation, for daily household use, to irrigate paddy fields, and which now serves as a tourist attraction in the summer.

The Agricultural System and Its Components

The agricultural system in the village includes paddy fields, upland fields, homegardens, and livestock. The total area of paddy fields is about 5 ha, with an average area per household of about 1,000 m^2. Two rice crops are grown per year with an average yield of about 4 tons of unhusked rice per crop. The fields are irrigated with water from the stream flowing down from the mountainside into the village. Upland field crops are planted under 3 systems: 1) sugarcane on land belonging to the villagers (under contract to the sugar mill), 2) Acacia trees (*Acacia mangium* Willd) on their own land (under contract to the State Forest Enterprise [SFE]), and 3) Acacia on SFE land (the villagers work as wage laborers for the SFE). The 16 household-owned sugarcane fields cover 8.8 ha. The sugar mill provides the farmers with seedlings and fertilizer. After the harvest, they have to repay the cost of these inputs to the mill. Fourteen hectares, owned by 16 households, are planted with Acacia under contract to the SFE, with the owners receiving 63% of the income at harvest. On the Acacia land owned by the SFE, the villagers who are employed by the SFE receive a regular wage for caring for the trees.

Seventeen households have homegardens (*an toon* in the Cao Lan language). Homegardens include vegetable plots and fruit trees. The gardens surround the houses but are mostly sited in front of the houses. The front side of the house is determined by the location of the ancestor's shrine. Within the homegarden are the house, animal pens, fish pond, bee hives, fenced vegetable plots, fruit trees, a concrete paved area for sun-drying crops, and an old-style pit toilet located deep in the garden. The average area of homegardens in this village is almost 3 *sao* or about 1,004 m^2 (1 *sao* = 360 m^2, the traditional measurement unit used in the Northern Vietnam region). The 2 smallest homegardens are only 1 *sao*, 6 gardens are 2 *sao*, 4 each are 3 and 4 *sao*, with the largest garden having an area of almost 6 *sao* (2,000 m^2).

Livestock include about 60 cattle and buffalo, 100 goats (belonging to 5 households), 300 chickens, Muscovy ducks and geese, and 1 or 2 pigs per household. There are 11 fish ponds belonging to 11 households. Six households have honey bee hives.

NII-Electronic Library Service

Kyoto University

Methodology

Selection of Study Site and Study Households

Cao Ngoi village was selected based on discussions with knowledgeable district officers about Cao Lan settlements that maintained their ethnic traditions and met the following criteria: 1) located in rural area, 2) ethnically homogeneous, and 3) the main purpose of their homegardens was production for household consumption. The village was also selected because it was located some distance away from Kinh villages in a remote area in the mountains, and had no recent connections with other Tai groups in Thailand.

Because of the small size of the community, it was not necessary to employ sampling. Instead, all 17 households having homegardens were included in the survey.

Data Collection and Data Analysis

Data collection was carried out for 12 days during September 2012. Data were collected at two levels: 1) community level information on village history and ethnic identity was collected in semi-structured interviews with the village headman and village elders, 2) household level information was collected in semi-structured interviews with garden owners and by making direct observations of their gardens, including measurement of horizontal and vertical dimensions, and enumeration of plant species. Data were collected on homegarden components, functions of individual species, and structural characteristics (horizontal and vertical). These data were recorded on sketch maps, photographs, architectural drawings, and species checklists.

Data on all of the homegardens were entered into an Excel database, which was used to compile tables of characteristics for all gardens of households.

Data analysis employed the classification system for describing the characteristics of homegardens developed by Pijika (2014). This system includes horizontal structural dimensions, vertical dimensions, and measurement of species composition and diversity.

Horizontal dimensions include:

- Shape of planting area or plot: *Geometric* forms include plots or beds with square, rectangular, or circular shapes. *Organic* forms include planting areas with irregular or curvilinear shapes.
- Definition of boundaries of planting areas or plots: Boundaries can be *sharp* and clearly marked or *indeterminate* and ill-defined.
- Arrangement of individual plants within planting areas or beds: Individual plants can be planted in parallel lines (*lineal*) or in multiple clusters of plants, usually including representatives of two or more species (*polycentric*).

NII-Electronic Library Service

Kyoto University

- Species composition within each plot: Planting areas or beds can be planted with only a single kind of plant species (*mono-species*) or with a mixture of two or more different species (*multi-species*).

Vertical dimensions include:

- Number of levels of vegetation: Plants of different species have different heights, which were recorded for 5 levels: Level 1 = 1 meter or less, Level 2 = 1.01–5 m, Level 3 = 5.01–10 m, Level 4 = 10.01–15 m, Level 5 = >15 m. All plants in the garden may be of the same height (*single level*) or they may have different heights (*two or more levels*).
- Canopy overlap: The share of the garden area in which the canopies of plants of different heights overlap each other (*non-overlapping*, *<50% overlapping*, *>50% overlapping*).

Species composition and diversity are measured in terms of the:

- Total number of species growing in the garden.
- Species richness, that is the number of species present by using Shannon-Wiener diversity index (H) (Magurran 1988)

$$H = -\sum_{i=1}^{s} pi \ln pi$$

where *pi* is proportion of the species relative to the total number of plants, and *S* is the number of species recorded.

- Species abundance, that is how equally abundant the species are by using Simpson's index (D) (*ibid.*)

$$D = \sum_{i=1}^{s} (pi)^2$$

where *pi* is proportion of the species relative to the total number of plants, and *S* is the number of species recorded.

NII-Electronic Library Service

Kyoto University

Results and Discussion

The Structure of Cao Lan Homegardens

The frequencies with which different structural characteristics of Cao Lan homegardens occur are shown in Table 1. The modal pattern of Cao Lan homegardens is organic shaped planting areas (Fig. 3a) with indeterminate boundaries (Fig. 3c), polycentric plantings (Fig. 3b) of multiple species in the same bed (Figs. 3b and 3d), and having multiple levels (Figs. 3a and 3d) of overlapping canopy layers (Fig. 3a). A large majority of homegardens (72%) have an organic shape of their planting area, 72% have an indeterminate boundary, 78% have a polycentric planting pattern, and 61% have multiple species within the same bed or planting area. All gardens have multiple vegetation levels, with the largest share

Table 1 Modal Pattern of the Cao Lan Homegardens of Cao Ngoi Village, Tuyen Quang Province, Northern Vietnam (n = 17) (Gray shading indicates most common form)

Structural Dimension	Alternatives Forms (%)		Modal Pattern
Horizontal characteristics			
Shape of planting areas	All Geometric	0	Organic
	>50% Geometric	0	
	>50% Organic	28	
	All Organic	72	
Boundary definition of planting area	All Sharp	6	Indeterminate
	>50% Sharp	0	
	>50% Indeterminate	22	
	All Indeterminate	72	
Arrangement of individual plants within planting areas	All Lineal	11	Polycentric
	>50% Lineal	4	
	>50% Polycentric	7	
	All Polycentric	78	
Species composition within planting area	All Mono-species	22	Multi-species
	>50% Mono-species	17	
	>50% Multi-species	0	
	All Multi-species	61	
Vertical characteristics			
No. of vegetation levels	1	0	5 levels
	2	0	
	3	25	
	4	30	
	5	45	
Share of planting area covered by overlapping layers	Non-overlapping	0	Extensive
	<50% Overlap	44	
	>50% Overlap	56	

NII-Electronic Library Service

Kyoto University



Fig. 3 Homegardens of the Cao Lan of Cao Ngoi Village; (a) Organic, Multi-level and Overlapping Canopy, (b) Polycentric and Multi-species, (c) Indeterminate Boundary, (d) Multi-level and Multi-species

(88%) having 5 levels. More than half (56%) of the gardens have more than 50% of their planting area covered by overlapping vegetation layers.

A comparative study by Pijika (2014) of homegarden structures of 8 different ethnic groups in Northeastern Thailand and Central and Northern Vietnam, including 6 Tai groups (Phu Tai, Nyaw, Yoy, Lao, Kalaeng, and Cao Lan) and 2 Mon-Khmer groups (Viet and Kinh), identified 3 distinctive types of garden structures. The homegardens of most of the Tai groups (Kalaeng, Lao, Nyaw, Yoy, and Cao Lan) have structures that resemble the tropical forest type (Nair 2001), which is characterized by having an organic shape, indeterminate boundaries of planting areas, polycentric planting patterns, multi-species composition, multiple vegetation levels, and extensive canopy overlap. The homegardens of both of the Vietnamese groups (Viet and Kinh) have a temperate type structure (Niñez 1984), with geometric shapes, sharp boundaries, lineal planting patterns, mono-species composition, only a few levels of vegetation, and relatively limited canopy overlap. Fig. 4 compares, the modal structural pattern of the homegardens of the Cao Lan of Cao Ngoi village to that of the Yoy, a typical Tai minority group in Northeast Thailand, and the Kinh of Central Vietnam. It shows that the structure of the Cao Lan homegardens is very similar to the tropical forest type structure found among ethnically-related Tai groups in Northeast Thailand, but is very different from the temperate type garden structure of their Kinh neighbors in Vietnam.

NII-Electronic Library Service

Kyoto University

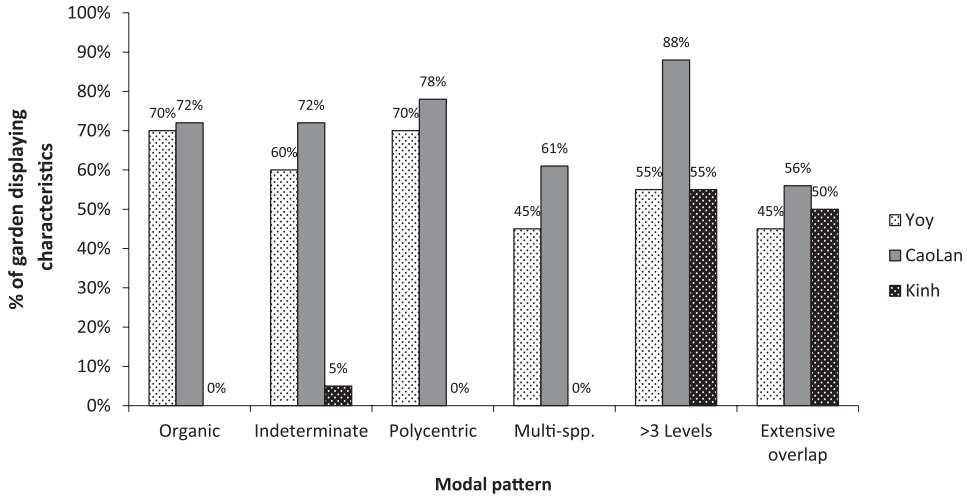


Fig. 4 Comparison of Modal Structural Patterns of Homegardens of Cao Lan with the Yoy, a Related Tai Ethnic Group in Northeast Thailand, and Their Kinh Neighbors in Vietnam (% of gardens of each group displaying characteristics)

Species Composition, Diversity, and Functions

Different plant species are scattered around in different parts of the gardens so as to optimize to their habitats in the different micro-zones of gardens. The total number of plant species found in all 17 gardens was 113. Table 2 presents a detailed list of all species grouped according to their functions. The mean number of species per garden was 25, with a range from 11 to 46 species. Six gardens had 11–20 species, 6 gardens had 21–30 species, 4 gardens had 31–40 species, and only 1 garden had more than 40 plant species.

The most common species are banana (*Musa* spp.) which was found in 15 gardens, ginger (*Zingiber officinale*) and taro (*Colocasia esculenta* Schott.) (14 gardens), guava (*Psidium* sp.) (13 gardens), Ceylon spinach (*Basella albe* L.), sweet potato (*Ipomoea batatas* [L.] Lam) and papaya (*Carica papaya*) (12 gardens), and Indian red wood (*Chukrasia tabularis* A. Juss.) (11 gardens).

Plant species richness was measured using the Shannon-Wiener's index (H), in which the higher the index number, the greater the diversity (Table 3). Species richness in the homegardens ranges from H = 1.25–3.04. One homegarden had the highest richness with 35 plant species (H = 3.04). The least rich were 2 gardens with 11 species each (H = 1.25 and 1.36).

The relative abundance of species was measured using Simpson's index (D) (Table 3). Forty-seven percent of homegardens have the lowest number of plants for each spe-

NII-Electronic Library Service

Kyoto University

Table 2 List of Plant Species in Cao Lan Homegardens

Scientific Name	Common English Name	Cao Lan Name	Vietnamese Name	No. and Percentage of Homegardens Having Species (%)
Vegetable:				
Corchorus olitorius	Tossa jute	Phặc rau đay	Rau đay	2 (11.8)
Solanum spp.	Egg plant	Mặc cơ	Cây cà	8 (47.1)
Solanum spp.	Egg plant (purple)	Mặc cơ	Cây cà tím	5 (29.4)
Luffa aegyptiaca Mill.	Gourd loofa	Cơ mặc kèo	Cây mướp	7 (41.2)
Basella albe L.	Ceylon spinach	Cơ mùng tơi	Cây mồng tơi	12 (70.6)
Brassica juncea	Mustard greens	Phặc cạt	Rau cải	10 (58.2)
Perilla frutescens var. *Crispa*	Shiso	Phặc hòm làng	Cây tía tô	9 (52.9)
Amaranthus gracilis Desf.	Chinese spinach, Amaranth	Phặc lồm	Rau dền	5 (29.4)
Sauropus androgynus (L.) Merr.	Pak wan tree, Star gooseberry	Phặc rau ngót	Cây rau ngót	6 (35.3)
Piper sarmentosum Roxb.	Wild betal leaf bush	Cơ phặc pạt	Lá lốt	4 (23.5)
Vigna unguiculata subsp. *sesquipedalis* (L.) Verdc.	Yard long bean	Cơ mặc tổ	đậu đũa	4 (23.5)
Lactuca indica	Indian lettuce	Phặc bàu	Bồ công anh	3 (17.6)
Artemisia vulgaris L.	Mugwort	Cơ ngải	Cây ngải cứu	6 (35.3)
Persicaria odorata	Vietnamese mint	Cơ phặc lặt léo	Rau răm	3 (17.6)
Artemisia lactiflora Wall ex. Bess.	Sagebrush	Cơ phặc ngoi	Cây ngải tía	1 (5.9)
Ficus spp.	Ficus	Cơ lá sung	Cây sung	3 (17.6)
Colocasia gigantea	Colocasia	Cơ moong linh	Cây dọc mùng	10 (58.8)
Vigna unguiculata subsp. *unguiculata*	Cowpea	Mạc tô phừng	Cây đỗ đũa	3 (17.6)
Benincasa hispida	Winter melon	Cơ mặc qua	Cây bí đao	8 (47.1)
Carica papaya	Papaya	Cơ mặc mời	Cây đu đủ	12 (70.6)
Oroxylum indicum (L.) Kurz	Broken Bones Tree	Cơ núc nác	Cây núc nác	5 (29.4)
Ipomoea batatas (L.) Lam.	Sweet potato	Cơ bảy mền	Cây khoai lang	12 (70.6)
Spice:				
Citrus aurantifolia (Christm.) Swingle.	Lime	Cơ mặc chanh	Cây chanh	9 (52.9)
Zingiber officinale[b)]	Ginger	Cơ hằng gừng	Cây gừng	14 (82.4)
Capsicum frutescens L.	Bird pepper	Cơ hằng chìu	Cây ớt	5 (29.4)
Cymbopogon citratus (DC.) Stapf	Lemon grass	Cơ ha hom	Cây sả	7 (41.2)
Curcumic longa[b)]	Turmeric	Cơ kình	Cây nghệ	9 (52.9)
Eryngium foetidum L.	Long coriander	Phặc hòm nàm	Rau mùi tàu	5 (29.4)
Ocimum basilicum L.	Sweet basil	Phặc húng chói	Húng lìu	4 (23.5)
Mentha cordifolia Opiz.	Spearmint	Phặc hòm nhàu	Cây bạc hà	4 (23.5)
Allium tubreosum Rottler.ex Spreng	Chinese chive	Cà cấu sái	Cây hẹ	5 (29.4)
Alpinia galanga (L.) Willd.	Galangal	Cơ nàng lèo	Cây giềng	4 (23.5)
Atalantia citroides Pierre ex Guill.	–	Cơ mạc chanh đông	Cây chanh rừng	2 (11.8)
Garcinia Cowa Roxb.	Garcinia	Cơ mặc láu xơng	Cây tai chua	2 (11.8)
Fortunella japonica	–	Cơ mạc quất	Cây quất	3 (17.6)
Allium fistulosum	Spring onion	Cơ xông	Cây rau hành	3 (17.6)
Melissa officinalis L.	Kitchen mint	Cơ phặc hom	Húng lìu	2 (11.8)
Carbohydrate source:				
Colocasia esculenta Schott.	Taro	Cơ phực	Cây môn sọ	14 (82.4)
Pachyrhizus erosus (L.) Urb.	Yam Bean	Cơ mền cạt	Cây củ đậu	5 (29.4)
Maranta arundinacea L.	Arrow root	Cơ miền tinh	Dong riềng	5 (29.4)
Manihot esculenta L.	Cassava	Cơ miền mười	Cây sắn	7 (41.2)
Dioscorea bulbifera L.	Aerial yam	Cơ miền bàn	Cây củ mài	2 (11.8)
Vigna radiata	Mungbean	Đậu nho nhe	Cây đậu xanh	3 (17.6)

NII-Electronic Library Service

Kyoto University

Table 2 Continued

Scientific Name	Common English Name	Cao Lan Name	Vietnamese Name	No. and Percentage of Homegardens Having Species (%)
Fruit:				
Averrhoa carambola	Star fruit	Cơ mặc phừng	Cây khế	8 (47.1)
Psidium sp.	Guava	Cơ mặc ổi	Cây ổi	13 (76.5)
Musa spp.[c)]	Banana	Cơ mặc cói tơi	Cây chuối tây	10 (58.8)
Musa spp.[c)]	Banana	Cơ mặc cói lừng	Chuối tiêu	8 (47.1)
Musa balbisiana Colla[c)]	Banana	Cơ mặc cói mòng	Cây chuối hột	15 (88.2)
Prunus armeniaca L.	Apricot	Cơ mây mai	Cây mai	2 (11.8)
Mangifera indica L.	Mango	Cơ mặc xoài	Cây xoài	9 (52.9)
Artocarpus heterophylus Lamk.	Jack fruit	Cơ mặc mẹt	Cây mít	6 (35.3)
Citrus maxima (Burm.f.) Merr.	Pomelo	Cơ mặc pọc	Cây bưởi	10 (58.8)
Prunus persica[d)]	Peach	Cơ mặc đào	Cây đào	4 (23.5)
Zizyphus mauritiana Lamk.	Jujube	Cơ mặc táo	Cây táo	3 (17.6)
Annona squamosa L.	Sugar apple, Castard apple	Cơ mạc na	Cây na	6 (35.3)
Litchi chinensis L.	Lychee	Cơ mặc pai	Cây vải	4 (23.5)
Ananas comosus (L.) Merr.	Pineapple	Cây mặc ló	Cây dứa	3 (17.6)
Syzygium jambos (L.) Alston	Rose apple	Cơ soi	Cây roi	4 (23.5)
Prunus salicina	Plum	Cơ mạc mắn	Cây mận	4 (23.5)
Dimocarpus longen Lour.	Longan	Cơ mạc nhãn	Cây nhãn	3 (17.6)
Diospyros spp.	Persimmon	Cơ mặc hồng	Cây hồng ngâm	5 (29.4)
Manilkara zapota	Sapodilla	Cơ hồng xiêm	Cây hồng xiêm	2 (11.8)
Lucua mamona Gaerten	Lekima, Egg tree	Mạc lai cay	Cây trứng gà	3 (17.6)
Food dyes:				
Peristrophe bivalvis L.	–	Cơ bay sơn	Cây nhuộm cơm	2 (11.8)
Momordica cochinchinnensis (Lour.) Spreng	Spring bitter cucumber	Cơ mò pít	Cây gấc	5 (29.4)
Boehmeria nivea	Ramie	Cơ bảy đáy	Lá gai	6 (35.3)
Medicine:				
Iris domestica (L.) Goldblatt & Mabb.	Blackberry lily	Cơ rẻ quạt	Cây rẻ quạt	1 (5.9)
Crinum asiaticum L.	Crinum lily	Cơ cun	Hoa lá náng/Tỏi lợi tía	3 (17.6)
Plantago major L.	Plantain	Cơ mã đề	Cây mã đề	6 (35.3)
Drynaria quercifolia (L) J. Sm	Basket fern	Et tai thên	Ráng bay	1 (5.9)
Ocimum gratissimum L.	Tree basil	Cơ hương nhu	Cây hương nhu	7 (41.2)
Zingiber cassumunar Roxb.	Cassumunar ginger	Cơ kinh màng	Cây gừng dùng làm thuốc	1 (5.9)
Xanthium spp.	Cocklebur	Cơ phăn pọt	Cây ké	2 (11.8)
Litsea cubeba (Lour.) Pers	May Chang, Aromatic litsea	Mây thu hênh	Cây màng tang	2 (11.8)
Crinum asiaticum	Crinum Lily, Cape Lily, Poison Bulb, Spider Lily	Cơ cồn	Cây lá náng	3 (17.6)
Abutilon indicum (L.) Sweet.	Indian mallow	Cơ cối xay	Cây cối xay	4 (23.5)
Stimulants:				
Camellia sinensis (L.) Kuntze	Tea	Cơ xa	Cây chè	2 (11.8)
Areca catechu Le.	Betel nut, Areca palm	Cơ mặc làng	Cây cau	9 (52.9)
Piper betle L.[d)]	Betel	Cơ đau	Trầu không	5 (29.4)
Nicotiana tabacum L.	Tobacco	Cơ xin bay	Cây thuốc lá	2 (11.8)
Aesthetic:				
Celosia argentea L.	Cockcomb, Chinese wool	Hoa lợn cảy	Hoa mào gà	4 (23.5)
Gerbera jamesonii Bolus	Gerbera	Va đồng tiền	Hoa đồng tiền	2 (11.8)
Cymbidium aloifolium (L.) Sw.	Aloe-leafed Cymbidium	Phong lan	Hoa phong lan	3 (17.6)
Ficus annlata	Banyan tree	Cơ xì	Cây si	3 (17.6)
Rosa spp.	Rose	Cơ hoa hồng	Hoa hồng	4 (23.5)
Celosia cristata L.	–	Cơ lân cạy	Hoa mào gà	3 (17.6)
Eckipja prortraja	–	Cơ mây moong	Cây thực mực	3 (17.6)

NII-Electronic Library Service

Kyoto University

Table 2 Continued

Scientific Name	Common English Name	Cao Lan Name	Vietnamese Name	No. and Percentage of Homegardens Having Species (%)
Ficus bengalensis	Banyan tree	Cơ mây lồng	Cây đa	4 (23.5)
Streblus asper Lour.	Siamese rough bush	Cơ xích xàn	Cây duối	2 (11.8)
Portulaca grandiflora Hook.	Moss-rose	Cơ mười giờ	Hoa mười giờ	1 (5.9)
Chrysanthemum spp.	Chrysanthemum	Cơ hoa cúc	Cây hoa cúc	2 (11.8)
Rhododendorn arboretum Smith	Delavay's Rhododendron	Cơ va hải đường	Cây Hoa hải đường	2 (11.8)
Hura crepitans L.	Monkey's pistol	Cơ vông	Cây vông	3 (17.6)
Cyperus papyrus L.	Papyrus	Nhứ	Cây lác dù	1 (5.9)
Alstonia scholaris (L.) R. Br.	Blackboard tree, Indian devil tree, Ditabark, Milkwood pine, White cheesewood and Pulai	Cơ enh chau	Cây Hoa sữa	3 (17.6)
Arfeuillea arborescens Pierre ex Radlk.	–	Cơ độc cày	Cây xương cá	4 (23.5)
Mila sp.	Cactus	Cơ xương rồng	Cây xương rồng	1 (5.9)
Fodder:				
Colocasia esculenta (L.) Schott.	Taro	Cơ moon	Khoai nước	8 (47.1)
Sterculia lanceolate Cav.	Po pha sam	Cơ mời liền	Cây sảng	4 (23.5)
Panicum maximum	Elephant grass	Cơ cỏ voi	Cơ voi	3 (17.6)
Diplazium esculentum (Retz.) Sw.	Vegetable fern	Cơ mây lưng	Rau dướng	3 (17.6)
Morus alba L.	Mulberry	Cơ mày môn	Cây dâu	3 (17.6)
Construction materials:				
Duabanga sonneratioides Ham.	–	Cơ mây tùng	Cây phay	6 (35.3)
Bambusa spp.[a)]	Bamboo	Cơ mây tê lung	Cây luồng	5 (29.4)
Bambusa spp.[a)]	Bamboo	Cơ mười họp	Cây tre	4 (23.5)
Azadirachta indica A. Juss.	Quinine	Mời liềm hăm	Cây xoan dâu	9 (52.9)
Caesalpinia pulcherrima	Peacock's Crest	Cơ phượng	Cây hoa phượng	1 (5.9)
Wrightia pubescens	–	Cơ mời mòng	Cây mức lông mềm	4 (23.5)
Chukrasia tabularis A. Juss.	Indian red wood, Bastard cedar, Chittagong wood, Indian Mahogany, Burmese almond wood, Jamaica cedar	Cơ mai lát	Cây gỗ lát hoa	11 (64.7)
Corypha lecomtei L.	Lan palm	Cơ gui	Cây cọ	4 (23.5)
Food wrapping:				
Stachyphrynium placentarium (Lour.) Clausager & Borchs.	–	Cơ thong chanh	Lá dong	7 (41.2)
Weaving:				
Gossypium hirsutum L.	Cotton	Mây thoong tooc	Cây bông bạc	1 (5.9)
Firewood:				
Trema orientalis (L.) Bl.	Poison Peach, Charcoal tree	Cơ tặp dêt	Cây hu	3 (17.6)

Notes: [a)] secondary function as food, [b)] as medicine, [c)] as pig fodder, [d)] aesthetic

cies ranging from 0.01–0.25, followed by 4 homegardens (23.5%) ranging from 0.51–0.75, and 2 homegardens (11.8%) in the range of 0.26–0.50. Only 3 homegardens (17.7%) have the highest frequency of occurrence of each species.

All species were categorized according to their primary use: food and food-related, medicine, aesthetic, stimulants, fodder, construction materials, and other uses (Table 4).

NII-Electronic Library Service

Kyoto University

Table 3 Species Composition and Diversity in the Cao Lan Homegardens of Cao Ngoi Village, Tuyen Quang, Northern Vietnam (n = 17)

	Diversity	No. of Homegardens (%)
Richness (Shannon-Wiener index, H)	1.01–1.50	2 (11.8%)
	1.51–2.00	5 (29.4%)
	2.01–2.50	4 (23.5%)
	2.51–3.00	5 (29.4%)
	>3.00	1 (5.9%)
Abundance (Simpson's index, D)	0.01–0.25	8 (47.0%)
	0.26–0.50	2 (11.8%)
	0.51–0.75	4 (23.5%)
	0.76–1.00	3 (17.7%)

Table 4 Primary Functions of Plant Species in the Cao Lan Homegardens (number and percentage)

Functions (no. and % of species)	Type	No. and % of Plant Species (n=113 species)
Food 66 (58.4%)	Vegetable	22 (19.5%)
	Fruit	20 (17.7%)
	Spice	15 (13.3%)
	Carbohydrate source	6 (5.3%)
	Food dye	3 (2.6%)
Aesthetic 17 (15.0%)	Ornamental	17 (15.0%)
Medicine 10 (8.9%)	–	10 (8.9%)
Construction materials 8 (7.1%)	House repair	7 (6.2%)
	Roofing	1 (0.9%)
Fodder 5 (4.4%)	Pig	3 (2.6%)
	Cattle	1 (0.9%)
	Silkworm	1 (0.9%)
Stimulants 4 (3.5%)	–	4 (3.5%)
Other use 3 (2.7%)	Food wrapping	1 (0.9%)
	Weaving	1 (0.9%)
	Firewood	1 (0.9%)

The majority of plant species (58.4%) are used for food, followed by 17 ornamental species (15.0%), 10 medicinal species (8.9%), 8 species for construction (7.1%), 5 species for animal fodder (4.4%), 4 species used as stimulants (3.5%), and 1 species each for other

NII-Electronic Library Service

Kyoto University

uses including food wrapping, firewood, and weaving. No species are used for ritual or to sell for cash. Only 7 species serve multiple functions: Ginger is used for spice and medicine, the fruit of three species of banana (*Musa* spp.) are used for human food and the stalks as food for pigs, and bamboo shoots are eaten as human food and the stalks used as construction materials, peach is used for food and serves an aesthetic function, and betel is used as a stimulant and for aesthetic purposes.

A small number of species are used as stimulants (areca nut [*Areca catechu* Le.] and betel leaf [*Piper betle* L.]), as food dye for cooking sticky-rice cake (spring bitter cucumber [*Momordica cochinchinnensis* (Lour.) Spreng], ramie [*Boehmeria nivea*, and *Peristrophe bivalvis* L.]), and as food-wrapping leaves [*Stachyphrynium placentarium* (Lour.) Clausager & Borchs.]. Three households have mulberry trees in their gardens, the leaves of which used to be used to feed silkworms that yielded thread that was formerly used to weave cloth and one household grows cotton, which also used to be used for weaving.

Conclusions

The homegardens of the Cao Lan of Cao Ngoi village are an important component of their agroecosystem. The many different species of plants grown in these gardens provide food and other necessities for the people as well as fodder for their livestock. With a total of 113 species the gardens also contribute to conservation of biodiversity.

Although the Cao Lan of Cao Ngoi village have been geographically isolated from other Tai groups for many centuries, their homegardens display a tropical forest type garden structure that closely resembles that of several Tai groups in Northeast Thailand. This type of homegarden structure is very different from the temperate type structure of the gardens of their Kinh neighbors in Vietnam with whom they share a common environment and are in frequent contact. The persistence of a common structural pattern among these related Tai ethnic groups, despite their inhabiting different environments, and having had no direct contact with each other for a very long time, suggests that culture exerts a very strong influence over agroecosystem structure. This finding provides empirical support for Richard O'Conner's (1995) earlier suggestion that culture and agriculture are tightly linked together to form durable "agro-cultural complexes" that offer a useful key to reconstruction of the cultural history of Southeast Asia.

Accepted: October 28, 2014

NII-Electronic Library Service

Kyoto University

Acknowledgments

This paper is part of the first author's thesis research for a doctoral degree in Systems Agriculture, Graduate School, Khon Kaen University. The research was supported by a fellowship from the Higher Education Research Promotion and National Research University Project of Thailand, Office of the Higher Education Commission (HERP-NRU) which was administered by Sakon Nakhon Rajabhat University. Additional funding was provided by a grant (BRG5680008) from the Thailand Research Fund (TRF) Basic Research Program to the corresponding author. The views expressed in this paper are those of the authors and are not necessarily shared by the Higher Education Commission or TRF. We would like to thank Prof. Fukui Hayao and Assoc. Prof. Suchint Simaraks of the Khon Kaen University Program on System Approaches in Agriculture, and Dr. Jefferson Fox of the East-West Center, for their helpful suggestions about this research. Prof. Tran Duc Vien, President of Vietnam National University of Agriculture (VNUA) helped to arrange our fieldwork in Vietnam and Dr. Nguyen Thi Bich Yen, Deputy Director of the VNUA Center of Agricultural Research and Ecological Studies (CARES) provided logistic support for our field study. We owe a special debt to the Cao Ngoi villagers for the very great cooperation they extended to our research.

References

Dang Nghiem Van; Chu Thai Son; and Luu Hung. 2000. *Ethnic Minorities in Vietnam*. Ha Noi: The Gioi Publishers.

Dao Trong Hung; Tran Chi Trung; and Le Trong Cuc. 2001. Agroecology. In *Bright Peaks, Dark Valleys: A Comparative Analysis of Environmental and Social Conditions and Development Trends in Five Communities in Vietnam's Northern Mountain Region*, edited by Le Trong Cuc and A. Terry Rambo, pp. 51–83. Ha Noi: The National Political Publishing House.

Dyg, Pernille M.; and Saleumsy Phithayaphone. 2004. Home Gardens in the Lao PDR—Linkages between Agricultural Biodiversity and Food Security. In *Proceedings of Symposium on Biodiversity for Food Security: 14 October 2004, Vientiane, Lao PDR*, pp. 52–59. Vientiane: Ministry of Agriculture and Forestry of Lao PDR.

Ethnologue: Language of the World. 2013. Cao Lan, accessed August 10, 2013, http://www.ethnologue.com/language/mlc.

General Statistical Office. 2001. *Population and Housing Census Vietnam 1999: Completed Census Results*. Hanoi: Nha Xuat ban Thong ke.

Gillogly, Kathleen A.; and Nghiem Phuong Tuyen. 1992. Cao Lan Culture and Biodiversity in Historical Context: Environmental Change among an Ethnic Minority of the Midlands of Northern Vietnam. Working paper No. 3. Honolulu: East-West Center, Environment and Policy Institute.

Gregerson, Kenneth J.; and Edmondson, Jerold A. 1998. Some Puzzles in Cao Lan. In *Proceedings of the International Conference on Tai Studies*, pp. 151–163. Accessed March 2, 2013, http://sealang.net/sala/archives/pdf8/gregerson1998puzzles.pdf.

Hodel, Urs; Gessler, Monika; Hoang Huu Cai; Vo Van Thoan; Nguyen Thi Van Ha; Nguyen Thi Xuan Thu; and Tran Thi Ba. 1999. *In Situ Conservation of Plant Genetic Resources in Home Gardens of Southern Vietnam*. Rome: IPRGI.

Jiragorn Gajaseni; and Nantana Gajaseni. 1999. Ecological Rationalities of the Traditional Homegarden System in the Chao Phraya Basin, Thailand. *Agroforestry Systems* 46: 3–23.

Kamonnate Srithi; Chusie Trisonthi; Prasit Wangpakapattanawong; Prachaya Srisanga; and Balslev, Henrik. 2012. Plant Diversity in Hmong and Mien Homegardens in Northern Thailand. *Economic*

NII-Electronic Library Service

Kyoto University

Botany 66(2): 192–206.

Karyono; Dinh Xuan Hung; Dao Anh Thu; and Nguyen Duc Minh. 1993. Biological Diversity. In *Too Many People, Too Little Land: The Human Ecology of a Wet Rice-Growing Village in the Red River Delta of Vietnam*, edited by Le Trong Cuc and A. Terry Rambo, pp. 94–103. Report of the SUAN-EWC-CREC workshop on sustainable rural resources management and biological diversity conservation held in Hanoi and Thai Binh province from 15–26 July 1991, Occasional paper no. 15. Honolulu: East-West Center, Program on Environment.

Kou Chansina; Terd Charoenwatana; McArthur, Harold; Bounmy Phonegnotha; and Uehara, Goro. 1990. The Agroecosystem of Ban Semoun. In *SUAN Regional Secretariat, Swidden Agroecosystems in Sepone District, Savannakhet Province, Lao PDR, Report of the 1991 SUAN-EAPI-MAF Agroecosystem Research Workshop Savannakhet Province, Lao PDR: 20 June–2 July 1991*, pp. 25–43. Khon Kaen: Khon Kaen Press.

Le Trong Cuc; and Rambo, A. Terry, eds. 2001. *Cao Lan Farmers of the Midlands: A Case Study of the Environmental and Social Conditions in the Ngoc Tan Hamlet, Phu Tho Province, Vietnam*. Research report No. 4. Project on monitoring development trends in Vietnam's Northern mountain region. Ha Noi: Center for Natural Resources Environmental Studies (CRES), Upland working group, Vietnam National University.

Le Trong Cuc; Gillogly, Kathleen A.; and Rambo, A.Terry. 1990. Homegardens and Livestock. In *Agroecosystems of the Midlands of Northern Vietnam: A Report on a Preliminary Human Ecology Field Study of Three Districts in Vinh Phu Province*, edited by Le Trong Cuc, Kathleen A. Gillogly, and A. Terry Rambo, pp. 118–151. Occasional paper No. 12. Honolulu: East-West Center, East-West Environment and Policy Institute.

Luu Ngoc Trinh; Watson, Jessica W.; Nguyen Thi Ngoc Hue; Nguyen Ngoc De; Nguyen Van Minh; Phan Thi Chu; Sthapit, Bhuwon Ratna; and Eyzaguirre, Pablo B. 2003. Agrobiodiversity Conservation and Development in Vietnamese Home Gardens. *Agriculture, Ecosystems and Environment* 97: 317–344. doi: 10.1016/s0167-8809(02)00228-1.

Magurran, Anne E. 1988. *Ecological Diversity and Its Measurement*. London: Croom Helm.

Moreno-Black, Geraldine; Prapimporn Somnasang; and Sompong Thamathawan. 1996. Cultivating Continuity and Creating Change: Women's Home Garden Practices in Northeastern Thailand. *Agriculture and Human Values* 13(3): 3–11.

Nair, P. K. Ramachandran. 2001. Do Tropical Homegardens Elude Science, or Is It the Other Way Around? *Agroforestry Systems* 53: 239–245.

Nawata, Eiji; Uchida, Yukari; and Wada, Yasushi. 2009. Home Gardens. In *An Illustrated Eco-history of the Mekong River Basin,* edited by Tomoya Akimichi, pp. 29–32. Bangkok: White Lotus.

Nguyen Thi Mui. 2006. Country Pasture/ Forest Resource Profiles, Vietnam, accessed October 21, 2013, http://www.fao.org/ag/Agp/AGPC/doc/Counprof/vietnam/vietnam.htm.

Niñez, Vera K. 1984. *Household Gardens: Theoretical Considerations on an Old Survival Strategy*. Research Series Report No. 1. Lima: International Potato Center (CIP), Potatoes in Food Systems.

O'Conner, Richard. A. 1995. Agriculture Change and Ethnic Succession in Southeast Asian States: A Case for Regional Anthropology. *The Journal of Asian Studies* 54(4): 968–996.

Pijika Timsuksai. 2014. A Comparative Ecological Study of Homegardens of Different Ethnic Groups in the Sakon Nakhon Basin, Northeast Thailand, and Some Related Groups in Vietnam. Doctoral thesis in Systems Agriculture, Graduate School, Khon Kaen University.

Snelder, Denyse J. 2008. Smallholder Tree Growing in Philippine Back Yards: Homegarden Characteristics in Different Environmental Settings. In *Smallholder Tree Growing for Rural Development and Environmental Services: Lessons from Asia,* edited by Denyse J. Snelder and Rodel D. Lasco, pp. 37–74. Netherlands: Springer.

NII-Electronic Library Service

Kyoto University

Soemarwoto, Otto; and Soemarwoto, Idjah. 1984. The Javanese Rural Ecosystem. In *An Introduction to Human Ecology Research on Agricultural Systems in Southeast Asia*, edited by A. Terry Rambo and Percy E. Sajise, pp. 254–287. University of Philippines at Los Baños.

Sumitre Pitiphat สุมิตร ปิติพัฒน์; Pichet Saiphan พิเชฐ สายพันธ์; Narisa Dejsupa นาริสา เดชสุภา; and Tiemchit Puangsonchit เทียมจิตร์ พ่วงสมจิตร์. 2003. Yai tai lae cao lan: Gloom charttipa tai nai vietnam neui ไย้ ไต และเกาลาน: กลุ่มชาติพันธุ์ไทในเวียดนามเหนือ [Giay, Tay, and Cao Lan: Tai ethnic groups in Northern Vietnam]. Bangkok: Thammasart University Press.

Terra, G. J. A. 1958. Farm systems in South-East Asia. *Netherlands Journal of Agriculture Science* 6(3): 157–182.

————. 1954. Mixed-Garden Horticulture in Java. *The Malayan Journal of Tropical Geography* 1: 33–43.

————. 1952–53. Some Sociological Aspects of Agriculture in Southeast Asia. *Indonesie* 6: 297–316, 439–463.

Thanakorn Lattirasuvan; Tanaka, Sota; Nakamoto, Kenji; Hattori, Daisuke; and Sakurai, Katsutoshi. 2010. Ecological Characteristics of Home Gardens in Northern Thailand. *Tropics* 18(4): 171–184.

The SUAN Secretariat, Farming System Research Project, Khon Kaen University. 1990. *Two Upland Agroecosystems in Luang Prabang Province, LAO PDR: A Preliminary Analysis*. Report on The SUAN-LAO seminar on rural resources analysis, Vientiane and Luang Prabang, Lao PDR: 4–14 December 1989. Khon Kaen: Khon Kaen Press.

Vlkova, Martina; Polesny, Zbynek; Verner, Vladimir; Banout, Jan; Dvorak, Marek; Havlik, Jaroslav; Lojka, Bahdan; Ehl, Petr; and Krausova, Jitka. 2011. Ethnobotanical Knowledge and Agrobiodiversity in Subsistence Farming: Case Study of Home Gardens in Phong My Commune, Central Vietnam. *Genetic Resources and Crop Evolution* 58: 629–644. doi: 101.1007/s10722-010-9603-3.

Wiersum, K. Freerk. 2006. Diversity and Change in Homegarden Cultivation in Indonesia. In *Tropical Homegardens: A Time-Tested Example of Sustainable Agroforestry*, edited by B. Mohan Kumar and P. K. Ramachandran Nair, pp. 13–24. Netherlands: Springer.

NII-Electronic Library Service

http://www.pjbs.org

PJBS

ISSN 1028-8880

Pakistan Journal of Biological Sciences

ANSInet
Asian Network for Scientific Information
308 Lasani Town, Sargodha Road, Faisalabad - Pakistan

Pakistan Journal of Biological Sciences 18 (4): 185-190, 2015
ISSN 1028-8880
© 2015 Asian Network for Scientific Information

RESEARCH ARTICLE OPEN ACCESS

DOI: 10.3923/pjbs.2015.185.190

Sugarcane White Leaf Disease Incidences and Population Dynamic of Leafhopper Insect Vectors in Sugarcane Plantations in Northeast Thailand

Chiranan Rattanabunta and Yupa Hanboonsong
Department of Plant Science and Agricultural Resources, Faculty of Agriculture, Khon Kaen University, Maung District, Khon Kaen, 40002, Thailand

ARTICLE INFO
Article History:
Received: May 30, 2015
Accepted: July 09, 2015

Corresponding Author:
Yupa Hanboonsong
Department of Plant Science and Agriculture Resources,
Faculty of Agriculture,
Khon Kaen University,
Khon Kaen, 40002, Thailand

ABSTRACT
The work consisted of two experiments, i.e. Experiment 1 was conducted under controlled environments where sugarcane plants were used as hosts. This investigation aimed to monitor the occurrence of the Sugarcane White Leaf disease and the abundance of Leafhopper insect vectors and also the work aimed to provide useful information in understanding some aspects on epidemiology of the Sugarcane White Leaf disease. A Completely Randomized Design with three replications was used to justify growth and development of Leafhopper insects as affected by different temperatures: 20 (T1), 25 (T2), 30 (T3) and 35°C (T4). Experiment 2 was carried out to determine the numbers of Leafhopper insects with the use of light traps in the sugarcane Field 1 (ratoon plants), Field 2 (newly planted), Field 3 (newly planted) and Field 4 (ratoon plants). The results of Experiment 1 showed that growth and development of Leafhopper insects were highly affected by temperatures i.e. the higher the environmental temperature the faster the growth and development of the insects to reach its full adulthood. At 20°C, Leafhopper insects took 12 days to lay eggs whereas at 25°C the insects took only 6 days. Male reached its adulthood approximately 9 days earlier than female when cultured at 25°C and became approximately one week at 30°C or higher. The results of Experiment 2 showed that the majority of Leafhopper insects were found within the months of June and July for both newly planted and ratoon crops. A small amount was found in May and August with an exceptional case of Field 4 where the highest number of Leafhopper insects was found in April followed by June and July. For Sugarcane White Leaf disease, the disease was found in all months of the year except February for Fields 2 and 3. Newly planted sugarcane plants attained much smaller percentages of disease than those of the ratoon plants.

Key words: Leafhopper insect vector, newly planted plants, ratoon plants, Sugarcane White Leaf disease

INTRODUCTION

Sugarcane plant (*Saccharum officinarum* L.) is one of many important economic crops being cultivated annually in Thailand, particularly in many provinces in both the Central Plain and Northeastern regions of the country. Sugarcane plant has long been cultivated by a large number of growers of more than 90 countries in the tropical and subtropical regions. The crop plants provide a considerable amount of sugar in stems when it reaches a full stage of growth. In Northeast Thailand, sugarcane plantations have been established in many provinces such as Udon Thani, Burirum, Khon Kaen, Korat, Mukdahan,

Chaiyaphume, Mahasarakham and other provinces where numbers of sugar mills are located. It has been advocated that the largest sugarcane exporter in the 2011 was Brazil followed by Thailand, Australia and India (FAO., 2011). The low cane contents and the poor sugar yields have been considered to be a significant problem caused by several contributing factors such as poor soil fertility, salinity, drought, pests and diseases. Of many important sugarcane diseases, Sugarcane White Leaf disease (SWL) collaborated with Phytoplasma has long been considered as one of the most significant threats to sugarcane production in the Asian countries (Kumarasinghe and Jones, 2001; Marcone, 2002; Burgess, 2010). The SWL disease can spread out largely among sugarcane plantations by a mean of Phytoplasma-infected cane stalks where two species of phloem feeding Leafhoppers have been naturally and commonly inhabited. They include *Matsumuratettixhiroglyphicus* (Matsumura) and *Yamatotettixflavovittatus* (Matsumura). These two species of Leafhoppers are important vectors and once the plantation is infested these vector species could easily multiply themselves and become vectors to carry out the disease of Sugarcane White Leaf more rapidly with time (Matsumoto *et al*., 1969; Chen, 1974; Maramorosch *et al*., 1975; Hanboonsong *et al*., 2002, 2006). As a part of sugarcane integrated management program to be applied for the development of a large scale plantation, an investigation on vector population levels may possibly provide some essential information for growers of the sugarcane plants in making their decision on any control measurements against the infestation of the disease. This investigation aimed to monitor the occurrence of the Sugarcane White Leaf disease and the abundance of Leafhopper insect vectors and also the work aimed to provide useful information in understanding some aspects on epidemiology of the Sugarcane White Leaf disease. Furthermore, there is a limited published work on Sugarcane White Leaf disease in Thailand, particularly in the northeastern region.

MATERIALS AND METHODS

For this study, two experiments were carried out, i.e. Experiment 1 was carried out from May-September 2012 at Khon Kaen University, Khon Kaen, Thailand under controlled environments where sugarcane plants were used as Leafhoppers hosts. A Completely Randomized Design (CRD) with three replications was used. Four treatments were carried out with the use of a day old Leafhopper insects (*M. hiroglyphicus*). The insects were cultured at 20°C (T1), 25°C (T2), 30°C (T3, control) and 35°C (T4). Six Leafhopper insects were used for each replication. This experiment was carried out to provide some initial information on growth behavior of the insects as affected by different environmental temperatures. With the first experiment the following parameters were used, i.e., numbers of days to lay egg, numbers of days to reach molting stages of its growth (larvae stages of growth from stages 1-5) and number of days to reach a full adulthood stage as influenced by the temperatures. For Experiment 2, the experiment was carried out under field conditions during February-November 2012. Four field areas of the sugarcane plantation were used. This experiment was carried out to determine numbers of Leafhopper insects available in different areas of the four sites of the sugar plantations (Fields 1 up to 4), particularly in different months of the year. The four sites are located within the area of the Non sa-art District, Udon Thani Province, Northeast Thailand. This area was considered as the most infested area of Sugarcane White Leaf disease of the northeastern region of the country (Wongkaew *et al*., 1997; Marcone, 2002). The four sites of the sugarcane plantations include: Field 1 for ratoon plants, Field 2 for newly planted plants, Field 3 for newly planted plants and Field 4 for ratoon plants. The four sites are located nearby each other of the same district of the province. The KK88-92 sugarcane variety was used in all experimental fields. An area of 1600 m^2 of each site occupied with sugarcane plants was chosen for experimental observations. The sugarcane plants were sown at distances of a 50×80 cm within rows and between rows, respectively. The experimental observations commenced when the sugarcane plants reached an age of four months old for both newly planted and the first year ratoon plants. Thirty rows of seventy planted holes of sugarcane plants of each field were randomly marked for both Leafhopper insects and Sugarcane White Leaf disease determinations. The percentages of the Sugarcane White Leaf disease were monthly determined and calculated throughout the study period. The meteorological data on radiant energy, minimum and maximum temperatures, relative humidity, wind speed and rainfall were recorded throughout the experimental period (Table 1). The soil samples were taken at random from each field to the depth of approximately 30 cm at the beginning of the experimental period and they were used for the determinations of soil nitrogen (N), soil phosphorous (P), soil potassium (K), soil Organic Matter (OM) and soil pH. Soil analysis was carried out in the laboratory of the Department of Plant Science and Agricultural Resources, Khon Kaen University (Table 2).

Of the four chosen sugarcane fields of the experimental sites, the populations of the Leafhopper insects (*M. hiroglyphicus*) were observed and collected twice a month with the use of four light traps where each light trap was combined with the use of a sticky plastic sheet. Each sticky plastic sheet was fixed with a PVC plastic pipe frame (50×50 cm in width and length), white cloth, transparent plastic sheet and a light source (black light-blue 20 W). The insect sticky glue obtained from the Beetle Glue, Green Plana Co., Ltd., Thailand was applied as a thin layer on both sides of

Table 1: Mean values of meteorological data measured at the sugarcane experimental fields (Fields 1-4) from February to November 2012 at Udon Thani Province, Northeast Thailand

Experimental sites	Radiant energy (MJ/m^2 day^{-1})	Mini. temp. (°C)	Max. temp. (°C)	Relative humidity (%)	Wind speed (m sec^{-1})	Rainfall (mm day^{-1})
Field 1	15.30	21.74	31.32	71.32	1.29	3.65
Field 2	13.59	21.67	31.47	71.84	0.80	3.74
Field 3	15.02	21.90	31.60	71.72	1.18	4.04
Field 4	15.10	21.69	31.79	72.28	1.03	5.44

Table 2: Mean values of soil analysis data on nitrogen, phosphorus, potassium, organic matter and pH of the Oxic Paleustults great soil group at sugarcane experimental field (Fields 1-4) at Udon Thani Province, Northeast Thailand

Field number	Nitrogen (%)	Phosphorus (ppm)	Potassium (ppm)	Organic matter (%)	pH
Field 1	0.08^a	63.60^c	47.00^a	1.56^a	4.60^c
Field 2	0.06^b	104.60^a	25.00^d	1.23^d	5.50^a
Field 3	0.06^b	101.80^b	44.00^b	1.27^c	4.90^b
Field 4	0.07^a	47.70^d	36.00^c	1.29^b	4.40^d
F-test	*	**	**	**	**
C.V. (%)	22.08	0.19	3.29	1.12	3.07

Letters in each column indicated least significant differences of probability (p) of **: 0.01 and *: 0.05 of Duncan's Multiple Range Test. C.V. %: Covariant percentages

the plastic sheet of each frame. The light traps were placed (one trap for each field) at 1 m away from the border rows of the sugarcane plants at a height of 1 m from 18:00-21:00 PM for insect pest attraction. All of the trapped insects in each field were identified for Leafhopper (*M. hiroglyphicus*) populations and individual Leafhoppers were used for each counting period under an illuminated microscope unit in the laboratory. The number of Leafhopper insect vectors was calculated monthly. The obtained data were calculated where appropriate with the use of a computer program (SAS., 1998).

RESULTS

Experiment 1: The results showed that number of days to reach the first day in laying eggs of T1 up to T4 ranged from 5.76-12.14 days for T4 and T1, respectively. The differences were large and highly significant (Table 3). A decrease in temperature highly increased number of days to reach a stage of laying eggs. At larvae stage 1, the results showed that number of days to reach stage 1 of molting ranged from 2.48-5.36 days for T4 and T1, respectively. The differences were large and highly significant. A similar trend was found with stage 2 up to stage 5 where number of days in molting highly increased with a decrease in environmental temperature. This trend was found from stage 1 up to the last stage (stage 5). The differences were large and highly significant. The number of days to reach a full growth for both male and female highly increased with a decrease in environmental temperature where male Leafhoppers attained number of days ranged from 18.32-21.78 days for T4 and T1, respectively and female ranged from 25.11-30.70 days for T4 and T1, respectively. A decrease in temperature highly increased number of days to reach a full growth of adulthood stage. High environmental temperature tremendously hastened life of the Leafhoppers where the female Leafhoppers possessed much higher number of days to reach a full adulthood stage of growth than the male Leafhoppers. Male required a shorter period of time to reach its full adulthood stage than female insects.

Experiment 2: With meteorological data, the results showed that mean values of radiant energy from the sun of Field 1 up to Filed 4 ranged from 15.02-15.59 MJ/m^2/day for Field 3 and Field 2, respectively (Table 1). Mean values of minimum temperature ranged from 21.67-21.90°C for Field 2 and Field 3, respectively whilst mean values of maximum temperature ranged from 31.32-31.79°C for Field 1 and Field 4, respectively. Mean values of relative humidity ranged from 71.32-72.28% for Field 1 and Field 4, respectively. Mean values of wind speed ranged from 0.80-1.29 m sec^{-1} for Field 2 and Field 1, respectively. Mean values of rainfall ranged from 3.65-5.44 mm day^{-1} for Field 1 and Field 4, respectively.

For soil analysis data, the results showed that mean values of soil nitrogen (N) ranged from 0.06-0.08 for Field 3 and Field 1, respectively (Table 2). Mean values of soil phosphorus (P) ranged from 47.7-104.6 ppm for Filed 4 and Field 2, respectively. Mean values of soil potassium (K) ranged from 25.0-47.0 ppm for Field 2 and Field 1, respectively. Mean values of soil sodium (Na) ranged from 1.3-1.4 ppm for Field 1 and Field 4, respectively. Mean values of soil Organic Matter (OM) ranged from 1.23-1.56% for Field 2 and Field 1, respectively. Mean values of soil pH ranged from 4.4-5.5 for Field 4 and Field 2, respectively. Mean values of electrical conductivity ranged from 0.02-0.03 dS m^{-1} for Field 1 and Field 4, respectively.

With the results on Leafhopper insect vectors and Sugarcane White Leaf disease of Field 1 up to Field 4, the results showed that there were no Leafhoppers found from

Table 3: Growth stages and development of the *Matsumuratettix hiroglyphicus* insects cultured under controlled environments at different treatments and temperature at the Faculty of Agriculture, Khon Kaen University, Khon Kaen, Thailand

		Days							
Treatments	Temperature	Egg laid	Stage 1	Stage 2	Stage 3	Stage 4	Stage 5	Male	Female
T1	20°C	12.14[a]	5.36[a]	5.14[a]	5.42[a]	5.66[a]	5.32[a]	21.78[a]	30.70[a]
T2	25°C	6.72[b]	3.10[b]	3.46[b]	3.64[b]	4.46[b]	4.24[b]	20.96[a]	28.40[ab]
T3	30°C	6.26[c]	2.36[c]	2.74[c]	3.46[b]	3.92[c]	4.06[b]	20.02[a]	26.04[b]
T4	35°C	5.76[c]	2.48[c]	2.50[c]	2.58[c]	3.22[d]	3.70[c]	18.32[b]	25.11[b]
F-test		**	**	**	**	**	**	**	**
C.V. (%)		18.65	20.61	23.95	19.14	16.55	18.76	9.46	6.37

Letters in each column indicated least significant differences at probability (p) of 0.05 of Duncan's Multiple Range Test. C.V. %: Covariant percentages

Table 4: Monthly numbers of Leafhopper insects (*Matsumuratettix hiroglyphicus*) and infected percentages of Sugarcane White Leaf disease (SWLD) of sugarcane experimental fields (Fields 1-4) recorded from February to November 2012 at Udon Thaini Province, Northeast Thailand

	Field 1		Field 2		Field 3		Field 4	
Months	Insect number	SWLD (%)	Insect number	SWLD (%)	Insect number	SWLD (%)	Insect number	SWLD (%)
February	0	0.19	0	0	0	0	0	1.12
March	0	0.31	0	0.03	0	0.05	0	2.10
April	0	5.19	0	0.14	0	0.29	208.50	11.24
May	12.00	23.16	24.50	0.34	11.50	0.41	12.00	54.36
June	174.00	29.04	251.50	1.08	308.50	0.46	190.00	72.55
July	218.00	29.90	530.40	1.74	446.00	0.48	151.50	86.00
August	3.00	30.24	8.50	1.84	9.00	0.75	2.00	86.94
September	0	36.38	0	1.95	0	0.94	0	89.38
October	0	34.91	0	1.33	0	0.79	0	85.20
November	0	32.83	0	1.12	0	0.54	0	80.19

February to April for Fields 1, 2 and 3 but with a large number of Leafhopper insects (208.5 individuals) was found in April for Field 4 (ratoon plants). Mean values of Leafhopper insects found in May ranged from 11.50-24.50 individuals for Field 3 and Field 2, respectively (Table 4). Mean values of Leafhopper insects found in June ranged from 174.00-308.50 individuals for Field 1 and Field 3, respectively. Mean values of Leafhopper insects found in July ranged from 151.50-530.00 individuals for Field 4 and Field 2, respectively. Mean values of Leafhopper insects found in August ranged from 2.00-9.00 individuals for Field 4 and Field 3, respectively. There were no Leafhopper insects found in September up to November, 2011 in Field 1 up to Field 4 of the province of Udon Thani.

For the distribution of the Sugarcane White Leaf disease, the results showed that White Leaf disease infested from February until November where Field 1attained percentages ranged from 0.19-36.38 for February and November, respectively (Table 4). Field 2 attained infested percentages ranged from 8.5-530 for August and July, respectively. Field 3 possessed infestation % ranged from 9.00-446 for August and July, respectively. Field 4 attained infestation % ranged from 2.00-208 for August and April, respectively.

DISCUSSION

With the results carried out under controlled environments on the effect due to different levels of temperature of the Experiment 1, the results showed that Leafhopper insects (*M. hiroglyphicus*) tremendously responded to low and high environmental temperatures, i.e. the results on growth revealed that the higher the temperature the shorter the number of days to reach its adulthood stage. The differences were large and highly significant. The results agree with the work reported by Hanboonsong *et al.* (2006). The results evidently showed that under controlled conditions at 20°C, Leafhopper insects reached its maturity stage at day 12 and started to lay eggs whereas at 25°C the Leafhopper insects could be able to use number of days to lay eggs twice earlier than those of the growth at 20°C (day 6 only) hence a warm environmental temperature hastened maturity age of the insects tremendously. The results indicated that at a high environmental temperature of 25°C or higher, the Leafhopper insects could be able to reach its maturity stage much earlier and able to multiply its populations more rapidly with time. Thus with the environmental temperature in the tropical areas like in Thailand, Leafhopper insects could be able to multiply its populations more rapidly with time throughout the year provided that its hosts are available. It was found that male Leafhopper insects reached its adulthood stage earlier than female insects about one week earlier when the environmental temperature was higher than 25°C. The results suggested that Leafhopper insects could easily remain in any worm climate like in any other Asian countries and they could be ready to act as vectors for the spread out of diseases at any time of the year. The spread out of the disease must be attributable to the

suitable climatic conditions where radiant energy from the sun attained a mean value greater than 13.5 MJ m^{-1} day^{-1} and mean values of rainfall ranged from 3.6-5.4 mm day^{-1} with a mean value of minimum temperature higher than 21°C. Thus this tropical climate favors the rapid multiplication of Leafhopper insects. That is why Sugarcane White Leaf disease could remain in the sugarcane plantations when growers always preserve their sugarcane plants for any new coming planting season or even in the ratoon plants for the second crop.

It has been widely advocated that the majority of soils in Northeast Thailand are those of the Oxic Paleustults great soil group with a relatively poor fertility (Trelo-ges *et al*., 2002). With the soil analysis data, in most cases, the soil indicated unfavorable conditions for growth of the sugarcane plants, e.g., mean values of soil phosphorus (P) ranged from 47.7-104.6 ppm for Fields 4 and 2, respectively. These extremely high mean values of P could have been attributed to the previous history of chemical fertilizers added to the soil. Amount and type of fertilizer application could have been carried out without any soil analysis information hence it is a waste of capital investment. Soil available P should not be exceeded a mean value of 50 ppm since higher P could provide toxic effect on growth of the crop plants and soil pH should be at a range of 6-6.5 (1:2.5 soil: water by volume). This range of soil pH could facilitate a better release of soil nutrients around the roots zone of the crop plants. Furthermore, the attained mean values of potassium (36-47 ppm for Fields 4 and 1, respectively) were inadequately available for growth of the crop plants. Mean value of the potassium in inorganic soils should be at least 80 ppm (Mengel and Kirkby, 1987; Miller and Donahue, 1990; Suksri, 1998a, b; Kasikranan, 2011). The high mean values of organic matter (1.23-1.56% for Fields 2 and 1, respectively) must be attributable to the previous history of the added amount of crop residues to the soil hence soil nitrogen levels were moderately supplied.

With number of Leafhopper insects (*M. hiroglyphicus*) in Field 1 up to Field 3, the results showed that the collected numbers of Leafhopper insects, in most cases, were highest in the month of July followed by June and May whereas in Field 4 the numbers of insects were highest in April followed by June and least with August. The results indicated that Leafhopper insects were able to multiply its populations more rapidly with time in the rainy season, particularly in the months of May up to August. This must be attributable to the rapid growth of the sugarcane plants since the plant stand was nearly 2 m in height. However, with Field 4 (ratoon crop), it was found that the highest numbers of Leafhopper insects were found in the month of April followed by the months of June and July. The highest amount of the insects found in April must be attributable to the high amount of available sugarcane plants of the ratoon crop where the Leafhopper insects used them for sources of food and hosts. The rapid increases in the amount of insects may be due to the low value of soil Ca^{2+} due to the low value of soil pH resulted in a low amount of Ca^{2+} in leaves and stems of the sugarcane plants where the juices available in sugarcane leaves and stems could be of a high palatability for the insects (Suksri, 1999). Therefore, growers should add more of dolomite and organic residues to their lands to attain a suitable mean value of soil pH within a range from 6-6.5 as described earlier.

The severely high percentages of Sugarcane White Leaf disease were found with Field 2 and Field 4. This must be attributable to the rapid growth of the existing ratoon plants continued to supply food for the insects without any vacancy period whilst the percentages of those newly sown plants of Fields 2 and 3 (lesser than 2%) were tremendously lower than those of the ratoon plants. The results suggested that the plants of the ratoon crop may not be of advantages when it comes to the high percentages of the diseases those remain in the plots for the coming rainy season. The disease could spread out easily when Leafhopper insects multiply its populations, particularly in the rainy season (April-August). However, the first ratoon crop should remain in the plots or not it depended on economic returns where growers must evaluate the margin of the profit. The use of some chemical supplies such as insecticides, herbicides and others chemical substances may not be of significant advantages since some hazardous effects may be degrading the quality of the products derived from the sugarcane plants.

To sum up, the results of Experiment 1 carried out under controlled environmental temperatures revealed that growth and development of Leafhopper insects were highly affected by temperature levels, i.e. the higher the environmental temperature the faster the growth and development of the Leafhopper insects to reach its full adulthood stage hence tropical environmental temperature from 25-35°C suited most for a rapid multiplication of this insect vector. The results on the distribution of Leafhopper insects found among different months of the year in the sugarcane plantation of Field 1 up to Field 4 of the Experiment 2 indicated that the majority of Leafhopper insects were found within the months of June up to July for both newly planted and ratoon plants. A small number was found in May and August with exceptional case of Field 4, ratoon plants, i.e. high numbers of Leafhopper insects were found in April. With the Sugarcane White Leaf disease, in most cases, were severely found with the ratoon plants of Fields 1 and 4. The left out of ratoon plants for second crop may not be of a high advantage due to a certain amount of Leafhopper insects and disease remained in the sugarcane fields of the sugarcane plantation.

ACKNOWLEDGMENTS

The researchers wish to express their sincere thanks to: The National Research University Project through Research Cluster of Khon Kaen University Thailand for their full-time financial assistance, the Department of Plant Science and Agricultural Resources, Khon Kaen University for facilities provided and lastly Assist. Prof. Dr. Krirk Pannangpetch for his kind assistance on the collection of the meteorological data.

REFERENCES

Burgess, L., 2010. Sugarcane diseases in Laos. The Crawford Fund. http://archive-org.com/page/3482689/2014-01-06/http://www.crawfordfund.org/states/nsw/news/sugarcane.html.

Chen, C.T., 1974. Sugarcane white leaf disease in Thailand and Taiwan. Sugarcane Pathologists' Newsletter, 11/12: 23.

FAO., 2011. FAOSTAT, Food and agricultural commodities production. Food and Agriculture Organization of the United Nations.

Hanboonsong, Y., C. Choosai, S. Panyim and S. Damak, 2002. Transovarial transmission of sugarcane white leaf phytoplasma in the insect vector *Matsumuratettix hiroglyphicus* (Matsumura). Insect Mol. Biol., 11: 97-103.

Hanboonsong, Y., W. Ritthison, C. Choosai and P. Sirithorn, 2006. Transmission of sugarcane white leaf phytoplasma by *Yamatotettix flavovittatus*, a new leafhopper vector. J. Econ. Entomol., 99: 1531-1537.

Kasikranan, S., 2011. An investigation on different harvesting methods on young pods of KKU # 922 maize (*Zea mays* L.) cultivar for baby corn production. Pak. J. Biol. Sci., 14: 461-465.

Kumarasinghe, N.C. and P. Jones, 2001. Identification of white leaf disease of sugarcane in Sri Lanka. Sugar Tech, 3: 55-58.

Maramorosch, K., M. Kimura and S. Chareonridhi, 1975. Mycoplasma-like organisms associated with white leaf disease of sugarcane in Thailand. FAO Plant Prot. Bull., 23: 137-139.

Marcone, C., 2002. Phytoplasma diseases of sugarcane. Sugar Tech, 4: 79-85.

Matsumoto, T., C.S. Lee and W.S. Teng, 1969. Studies on sugarcane white leaf disease of Taiwan, with special reference to the transmission by a leafhopper, *Epitettix hiroglyphicus* mats. Jpn. J. Phytopathol., 35: 251-259.

Mengel, K. and E.A. Kirkby, 1987. Principles of Plant Nutrient. 4th Edn., International Potash Institute, Bern, Switzerland.

Miller, W.M. and R.L. Donahue, 1990. Soils: An Introduction to Soils and Plant Growth. 6th Edn., Prentice Hall, Englewood Cliffs, New Jersey, ISBN-10: 0138202265.

SAS., 1998. SAS/STAT User's Guide. Version 6, SAS Institute Inc., Cary, North Carolina, USA.

Suksri, A., 1998a. Effects of dolomite on growth and seed yields of soybeans (*Glycine max* L.) grown on oxic paleustult soil in Northeast Thailand. Pak. J. Biol. Sci., 1: 215-218.

Suksri, A., 1998b. Rainy season soybean (*Glycine max* L.) as influenced by nitrogen and potassium fertilisers grown on oxic paleustults soil in Northeast Thailand. Pak. J. Biol. Sci., 1: 399-401.

Suksri, A., 1999. Some Agronomic and Physiological Aspects in Growing Crops in Northeast Thailand. 1st Edn., Khon Kaen University Press, Khon Kaen, Thailand, pp: 212.

Trelo-Ges, V., S. Ruaysoongnern and T. Chuasavathi, 2002. Effect of earthworm activities (*Pheretema* sp.) on the changes in soil chemical properties at different soil depths of nampong soil series (ustoxic quartzipsamment) in Northeast Thailand. Pak. J. Biol. Sci., 5: 32-35.

Wongkaew, P., Y. Hanboonsong, P. Sirithorn, C. Choosai and S. Boonkrong *et al*., 1997. Differentiation of phytoplasmas associated with sugarcane and gramineous weed white leaf disease and sugarcane grassy shoot disease by RFLP and sequencing. Theor. Applied Genet., 95: 660-663.

Songklanakarin J. Sci. Technol.
37 (2), 171-181, Mar.-Apr. 2015

http://www.sjst.psu.ac.th

Original Article

Mapping temporal extent of Chiang Mai floods using coupled 1-D and quasi 2-D floodplain inundation models

Kowit Boonrawd and Chatchai Jothityangkoon*

School of Civil Engineering, Institute of Engineering,
Suranaree University of Technology, Mueang, Nakhon Ratchasima, 30000 Thailand.

Received: 12 August 2013; Accepted: 29 December 2014

Abstract

A coupling of a 1-D flood routing model and quasi 2-D floodplain inundation model is applied for mapping space-time flood extent. The routing model is formulated based on a non-linear storage-discharge relationship which is converted from an observed and synthetic rating curve. To draw the rating curve, required parameters for each reaches are estimated from hydraulic properties, floodplain geometry and vegetation and building cover of compound channels. The shape of the floodplain is defined by using fitting exercise based on the reverse approach between past and simulated inundation flood extent, to solve the current problem of inadequate topographic input data for floodplain. Mapping of daily flood can be generated relying on flat water levels. The quasi 2-D raster model is tested and applied to generate more realistic water surface and is used to estimate flood extent. The model is applied to the floodplains of Chiang Mai, north of Thailand and used to estimate a time series of hourly flood maps. Extending from daily to hourly flood extent, mapping development provides more details of flood inundation extent and depth.

Keywords: Upper Ping River, flood map, raster model, rating curve

1. Introduction

To assess an impact of severe flood and at the same time mitigate economic and social losses, mapping of flood-plain inundation extent including flood depth and flood duration is an important tool for the improvement of flood management systems. Extrapolation work from historical to future potential flood mapping under different possibilities and scenarios are necessary information for stake holders in choosing appropriate measures to reduce flood risks. The magnitude and frequency of floods possibly tend to increase in near future which is the consequence of climate and human induced changes (IPCC, 2007).

* Corresponding author.
Email address: cjothit@sut.ac.th

The devastating results of past floods in Chiang Mai City, particularly in the core economic and residential zones, has brought great public concern about the performance of flood protection and warning systems managed by local authorities. Questions are also being raised by the local people on what are the potential impacts of future land use changes, the forest loss to agricultural plantation, and the uncontrolled urban expansion (Chatchawan, 2005; CENDRU, 2013).

Flood inundation mapping can be formulated in a number of ways including historical flood investigation through field survey and/or remote sensing survey, using hydrological or hydraulic modeling or their combination. Compared to different approaches, hydraulic modeling gives advantages over other methods. It incorporates spatial terrain data and generates the space-time variation of flood depth and magnitudes. One dimensional (1-D) hydraulic modeling of full St. Venant equation is still a standard practice. By

receiving design flood inputs, it can simulate flood magnitude and depth downstream and convert to flood inundation extent such as MIKE, HEC (Fread, 1993; Ervine and MacLeod 1999; De Kok and Grossmann, 2010). The limitation of this method is that the map of flood inundation extent is drawn by linear interpolation of flood characteristics between each cross section. Recently, many cases of uncertainties are studied in form of probabilistic flood inundation map (Merwade *et al.*, 2008; Sarhadi *et al.*, 2012)). To overcome this limitation, two dimensional (2-D) hydraulic models have been proposed to have advantages over 1-D modeling (Horritt and Bates, 2002; Tayefi *et al.*, 2007; Cook and Merwade, 2009). Recent advances in availability of remotely sensed topographic data and high computational capability, allows 2-D flood inundation modeling based on finite difference and finite element numerical method to become practical tools to estimate floodplain inundation extent, flood depth and depth-averaged velocity vector for each node and time step (Bates and De Roo, 2000).

However, the application of the complex 2-D models require massive input data together with consuming high computational cost and time which makes this model less attractive for large-scale floodplain analysis. Application of simplified raster-based hydraulic model is widely used due to some advantages over full 2-D model to simulate dynamic flood inundation (Bradbrook *et al.*, 2004; Yu and Lane, 2006). The raster based model can simply integrate spatial topographic data and process them with high computational efficiency. These models consist of coupling the 1-D and 2-D model representing channel flow and flow over the floodplain (Bates and De Roo, 2000; Yin *et al.*, 2013). The raster-based storage model is developed further to adaptive time step diffusion model (Hunter *et al.*, 2005), including inertial term (Bates *et al.*, 2010) for high efficiency of computation with stable solutions. To improve the quality of river flood inundation prediction with given high resolution of topographic data, comparison study of different hydraulic models were examined for different topographic complexity (Tayefi *et al.*, 2007). However, scarcity of high resolution and detailed topographic data for floodplain, i.e. Lidar and synthetic aperture radar (SAR), still exists in developing countries.

2. Approaches for Floodplain Inundation Model

2.1 Storage-discharge approach

The 1-D channel routing model proposed here is based on a conceptualization of each channel link in the network as non-linear storages. The water balance of each channel reach is modeled by solving equation $dS_c/dt=I(t)-Q(t)$, combined with a non-linear storage (S_c) to discharge (Q). The storage-discharge relationship expresses as a power function $S_c = kQ^m$ where k and m are model parameters, $I(t)$ represents the summation of upstream channel reaches and lateral inflow. The parameter k and m are estimated a priori for each of the stream reaches. These parameters reflect different physical properties of river flow transition from normal to extreme floods or from in-bank to over-bank flow (Jothityangkoon and Sivapalan, 2003; Jothityangkoon *et al.*, 2013).

For estimation of k and m in study river, recorded stage-discharge curve (rating curve) are used, together with surveyed data on the geometry of main channel, cross section of floodplain and length of the river reach. The estimation of the rating curves beyond recorded data can be achieved by a simple hydraulic approach. The compound channel is subdivided to main channels and floodplain sections, and discharges in each section are estimated separately. For the main channel, the measured rating curve can be used and estimated Manning coefficient given cross section area and slope of the channel at this stream gauge. At the other cross sections without measured rating curve, synthetic rating curves can be estimated given cross section area, slope of the channel and simulated Manning coefficient from neighbor cross section. Details of this procedure are described by Jothityangkoon and Sivapalan (2003) and Jothityangkoon *et al.* (2013). To capture the effect of houses and other buildings on the floodplain, the flow resistance in floodplain due to its size and spacing is considered in the same manner as the case of vegetation on the floodplain.

2.2 Raster based storage cell approach

(1) Diffusive model

The advantages of the storage cell formulation are that (i) it is a simple concept to calculate flow rate. Computational times and costs are much lower than solving numerical solution of full shallow water equations, (ii) this method interface well with a regular grid-based cell representing topographic characteristics generating from current remote sensing technology. For these reasons, this method is popular for floodplain inundation modeling (Hunt *et al.*, 2007). The volumetric flow rate between floodplain cells is calculated by using Manning equation,

$$Q_x^{i,j} = \frac{h_f^{5/3}}{n}\left(\frac{h^{i-1,j} - h^{i,j}}{\Delta x}\right)^{1/2} \Delta y \qquad (1)$$

where $Q_x^{i,j}$ is the flow rate in x direction at node (i, j), $h^{i,j}$ is the elevation of free water surface at node (i, j), Δx and Δy are the cell dimensions on rectangular coordinate [L], n is the Manning 's friction coefficient [$L^{-1/3}T$], h_f is the difference between the highest free water surface from two cells and the highest elevation of floodplain bed between nodes.

Interaction between inflow outflow and water surface height within a cell can be explained by water balance or continuity equation of the storage cell $\Delta h / \Delta t = \Delta Q /(\Delta x \Delta y)$. Using finite difference method, this equation is solved to,

$$\frac{{}^{t+\Delta t}h^{i,j} - {}^{t}h^{i,j}}{\Delta t} = \frac{{}^{t}Q_x^{i-1,j} - {}^{t}Q_x^{i,j} + {}^{t}Q_y^{i,j-1} - {}^{t}Q_y^{i,j}}{\Delta x \Delta y} \qquad (2)$$

where ${}^{t}h$ and ${}^{t+\Delta t}h$ are flow depth at time t and $t+\Delta t$, ${}^{t}Q_x^{i,j}$ is flow rate at time t and Δt is the time step.

Assuming that the depth-averaged velocity u is constant with steady and uniform flow in x direction, 1D Saint-Venant equation or momentum equation is simplified to an ordinary non-linear differential equation (neglecting acceleration and advection term),

$$S_0 + \frac{\partial h_f}{\partial x} + \frac{n^2 u^2}{h_f^{4/3}} = 0 \tag{3}$$

where S_0 is the bed slope, if flood wave propagates over flat plane, S_0 = 0, analytical solution can be derived (Hunter *et al.*, 2005),

$$h(x,t) = \left[\frac{7}{3}\left(C - n^2 u^2 (x - ut)\right)\right]^{\frac{3}{7}} \tag{4}$$

where h is the water depth which is a function of location on space x and at any time t, C is a constant depending on the initial condition form integration results.

(2) Inertial Model

For inertial model formulation, only advection term is neglected from 1-D Saint-Venant equation. By assuming flow in a rectangular channel a momentum equation in term of flow per unit width (q) [L^2T^{-1}] is:

$$\frac{\partial q}{\partial t} + \frac{gh\partial(h+z)}{\partial x} + \frac{gn^2 q^2}{R^{4/3} h} = 0 \tag{5}$$

where z is the bed elevation [L], R is the hydraulic radius [L], g is the gravity acceleration [LT^{-2}]. For wide shallow flow, R is assumed equal h. Equation 5 can be discretize with respect to the time step Δt and q_t in the friction term is replaced by a $q_{t+\Delta t}$ (the third term in Equation 5). Equation 5 is rearranged to give flows at the next time step, derived by Bates *et al.* (2010):

$$q_{t+\Delta t} = \frac{q_t - gh_t \Delta t \frac{\partial (h_t + z)}{\partial x}}{1 + gh_t \Delta t n^2 q_t / h_t^{10/3}} \tag{6}$$

2.3 Reverse engineering approach

For some developing countries with inadequate available hydrological input data, Hagen *et al.* (2010) proposed a parsimonious model based on the reverse engineering approach to generate nationwide flood hazard maps from past inundation extents. Motivated by this study, floodplain characteristics can be defined from the map of observed flood extent and depth for lacking good quality of DEM. To evaluate the quality of flood inundation estimation, observed and simulated inundation maps are compared by considering fit index (F).

$$F = 100 * \left(\frac{A_{op}}{A_o + A_p - A_{op}} \right) \tag{7}$$

where A_{op} is the inundated area where both observed and simulated flood extent are completely are overlaid, A_o is the total observed area of inundation, and A_p is the total simulated area of inundation. F varies between zero to 100; zero means no overlap between simulated and observed inundated area and 100 means a perfect match.

3. Application to Chiang Mai Municipality

3.1 Study area

The Upper Ping River catchment is located in the north of Thailand (see Figure 1). The river flows southward through the valley of Chiang Mai. The catchment area upstream of stream gauge station P1 (Navarat Bridge) and P68 (Ban Nam Tong) are 6,350 and 6,430 km^2, respectively. The flood study area covers about half of Chiang Mai municipality (40.2km^2) and two districts (Pa Daet, 25 km^2 and Nong Hoi, 3.67 km^2) which lie on the floodplain of the Upper Ping River.

3.2 Historical flood map and flood warning system

The severe floods usually arrive during August and September. The recent ones (in the past 20 years) occurred

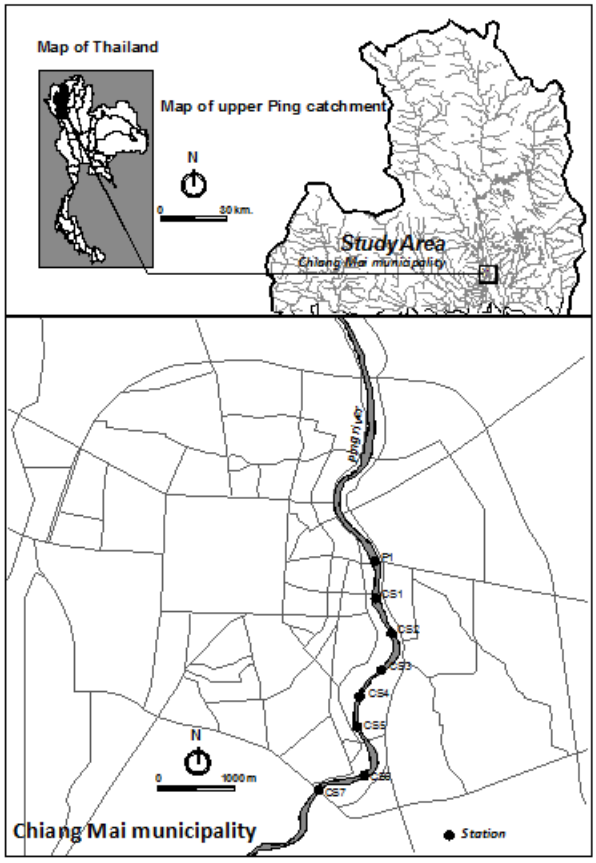


Figure 1. Location map of the Upper Ping River Basin, study reach and floodplain of Chiang Mai Municipality.

in 1994, 1995, 2001, 2005, and 2011 with maximum water levels at the P1 station of 4.43, 4.27, 4.18, 4.93 and 4.94 m, respectively. From an experience in observed flood routing from past flooding events between input flood hydrograph at stream gauge P.67 (Ban Mae Tae, 32 km upstream of P1) and output hydrograph at P1, it was found that if the maximum depth of flood at P.67 equals 4.70 m, the maximum depth of flood at P.1 equals 3.7 m, within about 7-8 hrs later (Chatchawan, 2005). Based on this correlation and observed relationship between flood level at P1 and flood depth measured in the city during flood events, flood warning system for Chiang Mai city was set up in the form of flood hazard maps. Chiang Mai flood maps given by Civil Engineering Natural Disaster Research Unit (CENDRU) Chiang Mai University divides inundation areas into seven zones depending on upstream referenced water level at P1 (Chatchawan, 2005; CENDRU, 2013).

3.3 Parameter estimation for 1-D routing model

Figure 2 presents required hydraulic information at a cross section. Details of using these parameters for floodplain resistance model are presented in Appendix B: Flow resistance for one-dimensional over-bank flow in Jothityangkoon and Sivapalan (2003). Provided channel cross-section, measured rating curve at station P1 and channel bed slope, a Manning coefficient is estimated first by fitting the simulated with the observed rating curve, prior converting to the effective Chezy coefficient of the main channel (C_m). The Chezy coefficient in the flood plain is assumed to be the same as C_m.

3.4 Application of the model for flood extent estimation

Estimation procedures consist of four main steps (Figure 4).

(1) Formulate 1-D floodplain inundation model by fitting the simulated to observed flood extent maps based on assumed floodplain cross section (step 1-6 in Figure 4), upstream boundary condition and inputs are observed flood peaks at station P1.

(2) Convert input flood hydrograph to daily flood extent maps using 1-D flood routing model and flat water level assumption (step 7 in Figure 4).

(3) Simulate a time series of hourly flood extent maps by using 1D raster model (step 8-9 in Figure 4). After channel cross sections are converted to grid based-storage cells in series and given water surface elevation in main channel of the river, flow rates from Equation 1 and water surface elevations from Equation 2 are simultaneously calculated for each time step to generate water surface elevation on floodplain for each cross section. Upstream boundary condition and inputs are water surface elevations in the main channel at each cross section.

(4) Generate a pilot map of 3-D floodplain inundation extent 2-D raster model (step 10 in Figure 4). Similar to the

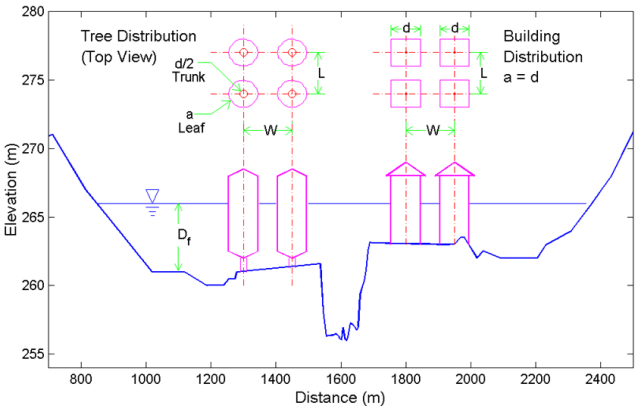


Figure 2. Required hydraulic information at a cross section, parameters for tree and building distribution on floodplain, L= W = 6-8 m (trees), = 10-15 m (building), a = 7-7.5 m (trees), = 9.5-12 m (building), d = 0.3-0.4 m (trees), = 9.5-12 m (building),and β = 0.2-0.5 (trees), = 0.4-0.8 (building).

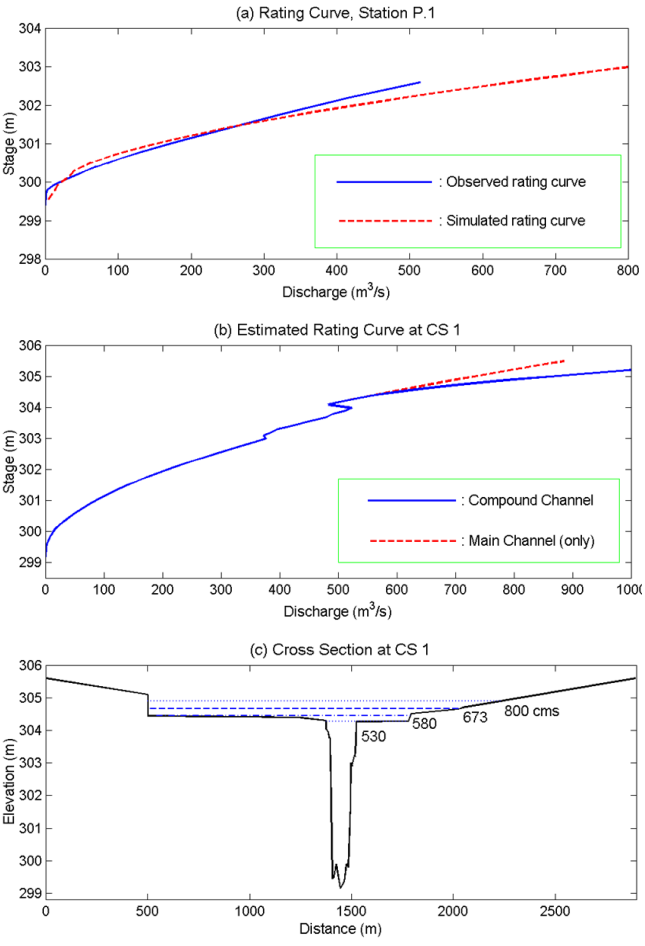


Figure 3. Steps to estimate flood extent at CS 1 (a) comparison of the measured and simulated rating curves for main channel at Station P1, (b) synthetic rating curve at CS 1, (c) estimated flood extents on both size of cross section at CS 1.

previous step, except the flow rates are determined on both directions (x: on floodplain, y: along main channel). Water surface elevation are generate for floodplain at each cross section and between cross sections.

3.5 Approach to estimate 3-D flood map

Hourly flood extent mapping from previous section is generated from the interpolation of water surface level from seven cross sections of floodplain. To test whether the raster models are able to simulate 2-D flood propagation over more realistic floodplain topography, grid-based storage cell from step 10 in Figure 4 is generated again from 1-D to 2-D in a short interval of a floodplain cross section.

4. Results and Discussion

4.1 Synthetic rating curves and flood extent for different water levels and flood peaks

Given surveyed cross section and channel slope of Ping River at stream gauge P1 (slope = 0.0087), simulated rating curve fit to observed rating curve can be drawn with assumed Manning $n = 0.065$ for in-bank flow in main channel (Figure 3a). Figure 3b presents an example of estimated rating curves at cross section CS1 for two cases: (i) main channel only, (ii) compound channel including the effect of trees and/or building distribution. The parameter m and k from calculated storage-discharge curve for seven cross sections are in the range of $m = 0.66$-0.72 (for main channel) 1.55-2.15 (for floodplain) and k = 18417-4536 (main channel) and 0.19-20.35 (floodplain).

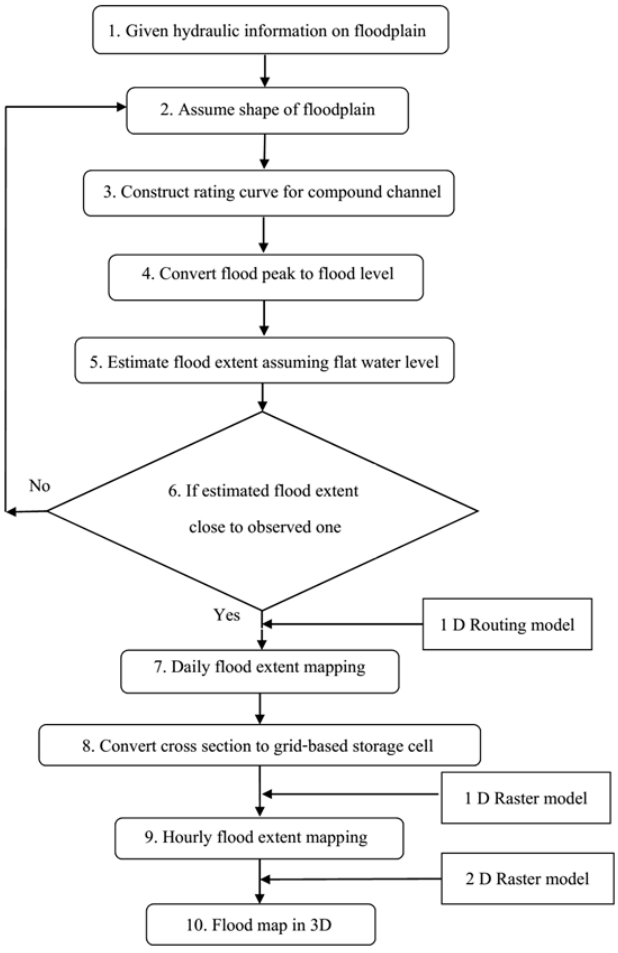


Figure 4. Flowcharts for constructing a map of floodplain inundation extent.

The next cross section (CS1) is about 450 m downstream of P1 where there is no stream gauge; a synthetic rating curve is drawn by using n the same as P1 and surveyed cross sections from the profile and cross section surveying project along Ping River for Chiang Mai 's flood warning, completed in 2007 by the Royal Irrigation Department. The rating curve is extended to over-bank flows on floodplain based on trial and error processes until assumed shape of floodplain provides a good fit between estimated and observed flood extent and inundation depth in the form of flood inundation mapping (see Figure 4). Final shape of compound channel at CS1 is shown in Figure 3c. Over-bank flow occurs when Q>510 m^3/s. For Q = 530 m^3/s, water level, inundation extent from left and right river bank are 304.28, 1, and 255 m (line of sight toward downstream). The estimated distance of inundation extent for Q = 530 m^3/s can be plotted on the map in Figure 5b. Plan view of the flood map shows that there is no over-bank flow on the right bank of Ping River but over-bank is found on the left bank. Estimated and observed flood extents on the left bank are identical. Inundation extents for the other Qs are estimated and plotted in the flood map; see Figure 5c, d, e, and f. By using the method similar to CS1 step 1 to 6 in Figure 4, water level and inundation extent from the river bank are calculated for the other six cross sections (CS2-CS7) downstream of CS1. The estimated distant of inundation extent for all cross sections with the same Q is plotted in the same map to present the boundary and area of inundation cover. These maps present a good agreement between observed and simulated flood extent where the fit index is higher than 75%. Some discrepancies between estimated and observed inundation extent are found, for example, at CS2, Q = 580 m^3/s and at CS5, Q = 600 m^3/s, mostly are underestimations.

4.2 Daily flood extent mapping

Flood plain inundation modeling from a snap shot of inundation extent on floodplain can be used to simulate a time series of flood extent. Moderate daily flood events during 19-22 September 2005 with Q = 164, 543, 679 and 472 m^3/s are selected as an input to the proposed floodplain inundation model and used to generate daily floodplain inundation extents. Figure 6 presents a time series of daily flood map showing an expansion and contraction of flood extent along both sides of the Ping River. However, verification of these results with satellite images during this flood event is

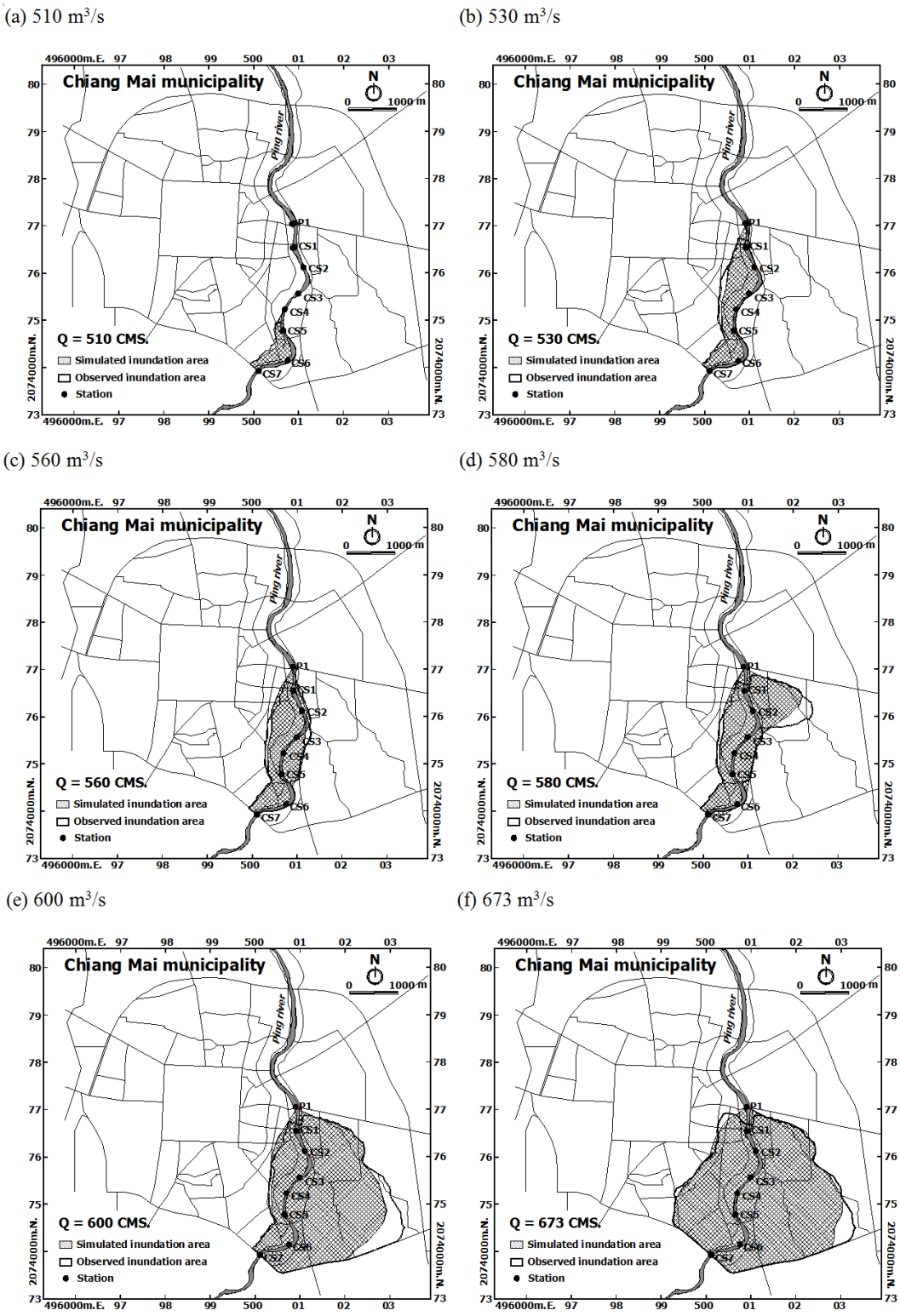


Figure 5. Comparison of observed and simulated flood inundation extent when flood peaks are (a) 510 m³/s, (b) 530 m³/s, (c) 560 m³/s, (d) 580 m³/s, (e) 600 m³/s, and (f) 673 m³/s

required. The results of flood routing model show that the simulated flood hydrograph from each river reaches are almost identical. This indicates that the attenuation of hydrograph due to the effect of routing in short channel storages (3,850 m from P1 to CS7) with some lateral inflows is not significant.

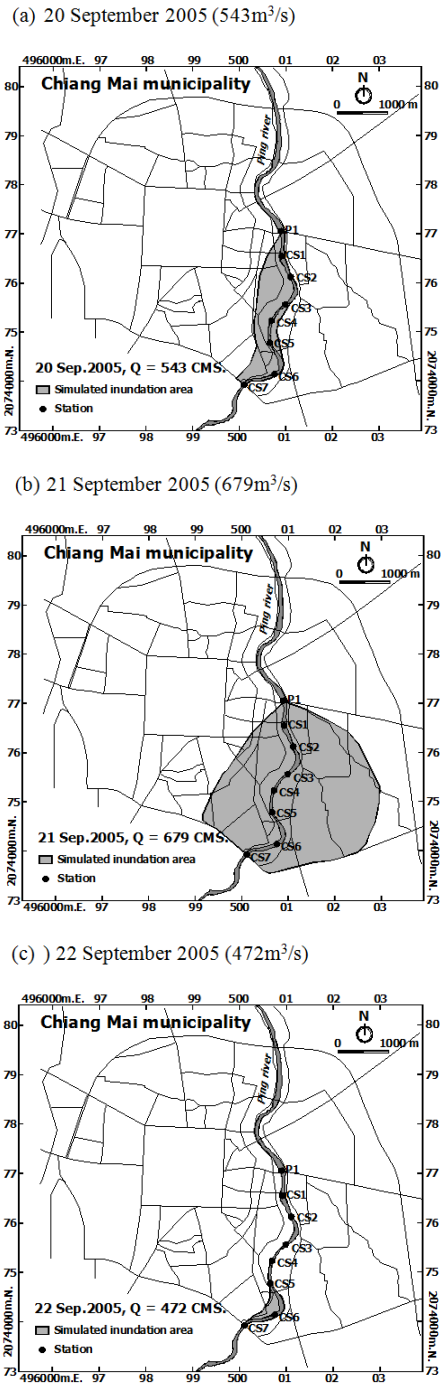


Figure 6. Simulation of daily flood inundation extent with (a) 20 September 2005 (543 m^3/s), (b) 21 September 2005 (679 m^3/s), (c) 22 September 2005 (472 m^3/s).

4.3 Hourly flood extent mapping

4.3.1 Testing of raster model

Equations 1-6 were used to determine the water surface profile of encroached flood level by converting to MATLAB codes based on numerical approaches. The formulation of 2 types of raster models was assessed through the tests of numerical exercises similar to Bates *et al.* (2010) as follow: Test 1: Flood wave propagation over a horizontal floodplain and comparison to an analytical solution; Test 2: Flood wave run-up on slope floodplain and comparison to a numerical solution; and Test 3: Tidal cycle of wetting and drying or rising and falling hydrograph on slope floodplain.

For the first test, using $u = 1$ ms^{-1}, $\Delta x = 50$ m, $\Delta t = 0.2$ s, $n = 0.01$ $m^{-1/3}s$ to represent possible roughness on floodplain, total time = 3,600 s and maximum water level = 0.93 m, analytical solution from Equation 4 is presented in Figure 7a. Given initial condition, $h(t)$ at x=0 from Equation 4, the diffusive and inertial models can generate the water surface curve almost fit to the curve from analytical solution. The inertial model performs better than the diffusive model.

For the second test, there is no direct analytical solution. The solution of Equation 3 can be obtained by numerical method using 4th order Runge-Kutta method. The common parameter values for this test similar to Test 1, but including $S_0 = 10^{-3}$, $n = 0.09$ $m^{-1/3}s$, maximum water level = 8.5 m, Δt = 0.05 and 0.02 s for inertial and diffusive model, respectively. Maximum Δt is chosen to give no instability. Figure 7b shows estimated water surface elevation from the diffusive and inertial model compare to the numerical model.

For the third test, to investigate the simulation results from the whole cycle of flow reversals including rising front

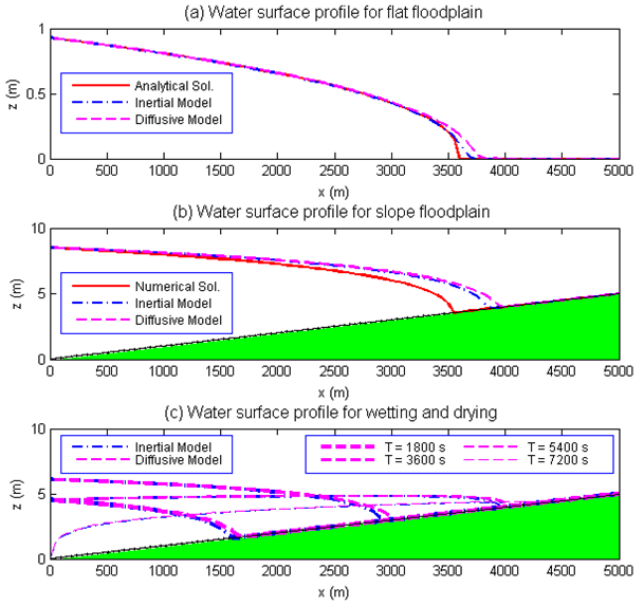


Figure 7. Testing results of raster model (a) simulated water surface elevation (z) at t = 3600 s and Δx = 50 m for wave propagation over a horizontal floodplain section using diffusive model, inertial model compare to analytical model, (b) z at t = 3,600 s and Δx = 50 m for wave propagation up an incline floodplain section using diffusive model, inertial model compare to numerical solution, (c) a time series of z at different time during wetting and drying for wave propagation up an incline floodplain section using diffusive model and inertial model.

of flood waves during floodplain wetting and recession front during floodplain drying, a sinusoidal wave boundary condition is used at $x = 0$, with wave amplitude 6.1 m period 4 hrs and $S_0 = 10^{-3}$ for simulation period 7,200 s. There is no analytical solution for this test. Only the difference between the inertial and diffusive model is investigated (Figure 7c).

4.3.2 Simulation of one dimensional hourly flood extent

Test 1 to 3 are series of idealized case with increasing complexity. To demonstrate the numerical performance of the raster model working over complex topography, surveyed data at each cross-section is interpolate to grid-based storage cell with fine spatial resolution $\Delta x = 50$ m. A time series of observed flood hydrograph (during 20-21 September 2005) is interpolated for selected time step with smooth shape transition from daily to hourly or smaller time step. Receiving these input hydrograph, the inertial and diffusive model can be used to simulate a time series of water surface profile (Figure 8). For a longer duration (48 hrs), the diffusive model generates distance of flood extent longer than the inertial model. At a corner of steep river banks, simulated water levels likely encroached into the river banks. This unrealistic water profile can be minimized if the resolution of Δx is decreased less than 50 m. The final step is the same as in Section 4.1, as the distance of inundation extent from all cross sections are combined to draw the map of time series of f loodplain inundation extents, as shown in Figure 9.

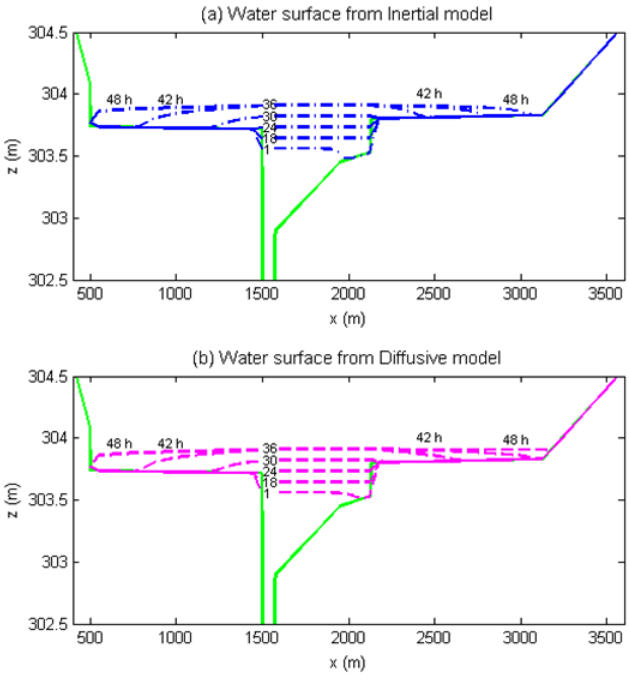


Figure 8. Simulated hourly flood levels at cross section No. 5 between 20 September 2005 to 21 September 2005.

4.4 Flood extent in 3-D

A pilot test of 2-D grid-based storage cells are generated with a distance of 2,500 m along the Ping River downstream of CS6 and assuming an input flood level with constant depths of 0.95 m for the left bank and 1.20 m for the right bank, shown in Figure 10. This 3-D map shows a more realistic shape of flood wave propagation on the floodplain. The upper and lower surface represents propagated water surface and floodplain surface, respectively.

5. Conclusions

By using a synthetic rating curve for compound channel which includes the effect of trees and buildings distribution on floodplain, floodplain inundation model based on flat water surface assumption can be formulated with a number of selected channel cross sections. Although the vertical resolution of existing DEM (based on scale 1:50,000)

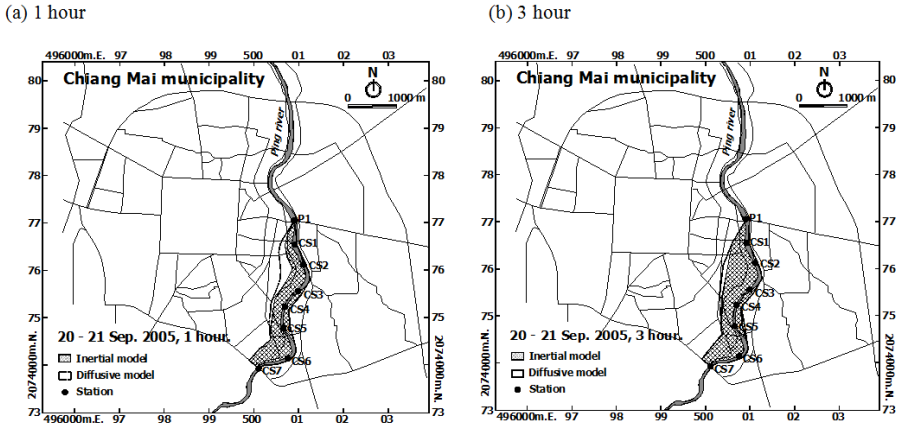
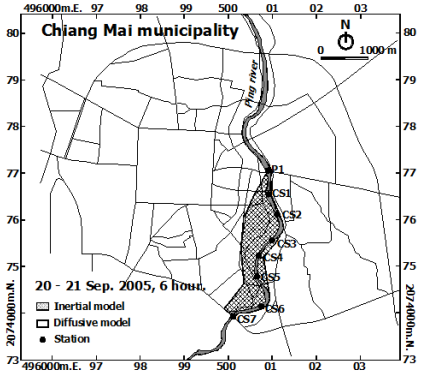
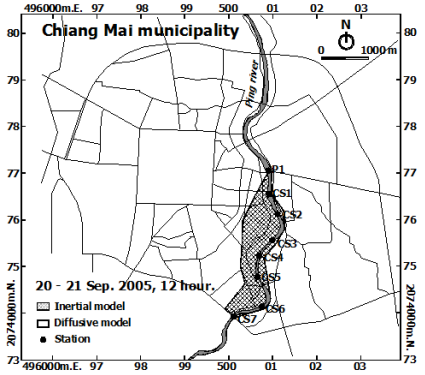


Figure 9. Comparison of simulated hourly flood map and inundation extent from inertial and diffusive model between 20-21 September 2005 with different simulation times (a) 1 hr, (b) 3 hrs, (c) 6 hrs, (d) 12 hrs, (e) 18 hrs, (f) 24 hrs, (g) 30 hrs, (h) 36 hrs, (i) 42 hrs, and (j) 48 hrs.

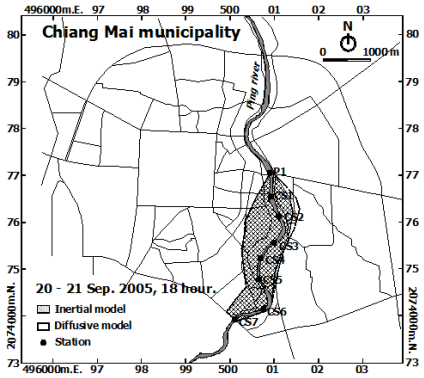
(c) 6 hour



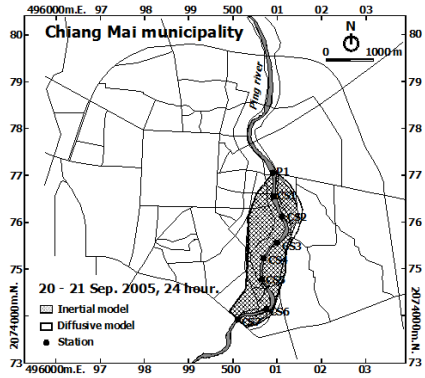
(d) 12 hour



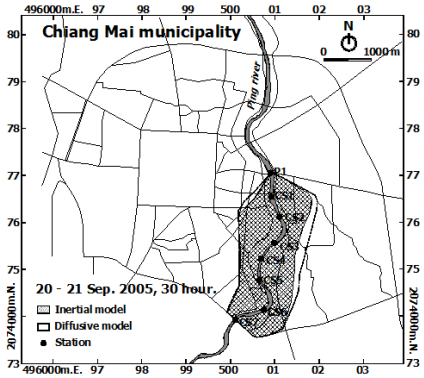
(e) 18 hour



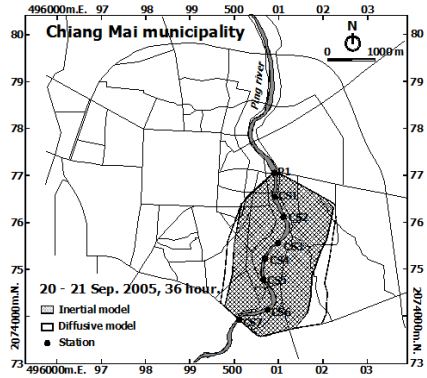
(f) 24 hour



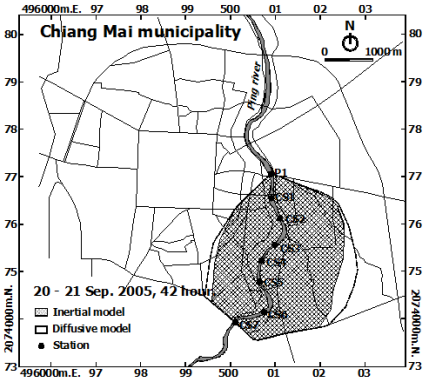
(g) 30 hour



(h) 36 hour



(i) 42 hours



(j) 48 hours

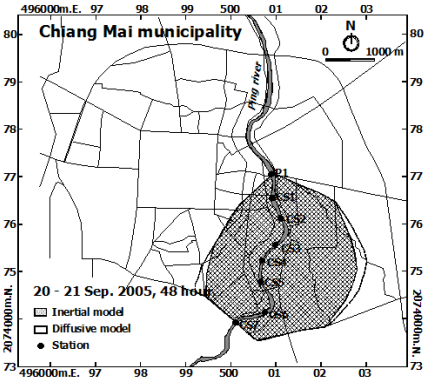


Figure 9. Continued

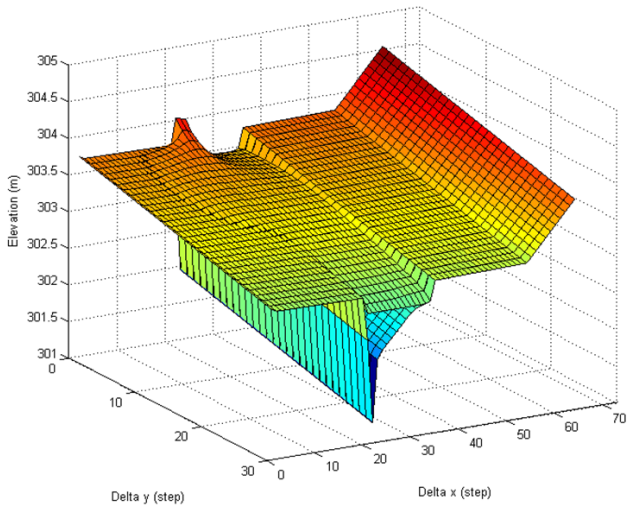


Figure 10. Simulated hourly flood inundation extent in 3-D map downstream of section CS6 generated from 2-D raster model (diffusion model) with 1,500 m length along the channel, slope = 0.0005, n = 0.09 $m^{-1/3}s$, $\Delta x = \Delta y$ = 50 m, Δt = 0.1 s., Running time = 3 hrs.

for the floodplain of Chiang Mai Municipality is too low to represent any change of flood level, the assumed shape of floodplain can be defined and tested from a good fit between observed and simulated flood extent using the reverse engineering approach. This model can be used with confidence to construct a daily flood extent map.

To generate a time series of flood inundation maps from daily to hourly extents, a raster model consisting of diffusive and inertial formation are applied. The inertial model performs slightly better than the diffusive model for a horizontal floodplain and a slope floodplain, when compare to the analytical solution. The difference of simulated water level between the inertial and diffusive model become less pronounced for more complexity of floodplain topography and when receiving dynamic wetting and drying hydrograph. Inertial model can generate stable results with a time step larger than diffusive model due to increased stability with the addition of the inertial term. This study did not consider the computational performance and efficiency between different models.

If digital elevation data at a fine spatial resolution are available from an airborne laser altimetry survey or LiDAR data, then this data can be used to simulate more reliable inundation map and apply to the whole flooding area of Chiang Mai municipality, including the assessment of flood inundation extent from flood peaks with different exceedance probability or return period (Yin *et al.*, 2013). The accuracy of flow patterns on floodplain depends on land surface characteristics and properties which can be interpreted from high resolution topographic information such as LiDAR data. This simplified floodplain inundation modeling are potential and alternative tools for developing countries where no spatial input data with high resolution are available.

Acknowledgements

The authors are grateful to Rajamangala University of Technology Isan (RMUTI) for financial support in form of a PhD Scholarship to the first author. We wish to acknowledge the Thai Meteorological Department, Royal Irrigation Department for providing field data. Special thanks go to Dr. Panya Polsan for his assistance to access hydrologic data.

References

Bates, P. D. and De Roo, A. P. J. 2000. A simple raster-based model for flood inundation simulation. Journal of Hydrology. 236, 54-77.

Bates, P. D., Horritt, M. S. and Fewtrell, T. J. 2010. A simple inertial formulation of the shallow water equations for efficient two-dimensional flood inundation modelling. Journal of Hydrology. 387, 33-45.

Bradbrook, K. F., Lane, S.N., Waller, S. G. and Bates, P.D. 2004. Two dimensional diffusion wave modelling of flood inundation using a simplified channel representation. International Journal River Basin Management. 2(3), 211–223.

CENDRU. 2013. General Information of the Upper Ping Basin (in Thai). Available from: http://cendru.eng.cmu.ac.th/flooding/?name=/chapter1/cp1_1/artical1 [April 5, 2013].

Chatchawan, S. 2005. Flood situation and flood protection report in Chiang Mai municipal area 2005 (in Thai). Proceedings of the Academic Conferences: Towards Society Harmony, Thai Development Research Institute Foundation, Chon Buri, Thailand, November 26-27, 2005.

Cook, A. and Merwade, V. 2009. Effect of topographic data, geometric configuration and modeling approach on flood inundation mapping. Journal of Hydrology. 377, 131-142.

De Kok, J. L. and Grossmann, M. 2010. Large-scale assessment of flood risk and the effects of mitigation measures along the Elbe River. Nature Hazards. 52, 143-166.

Ervine, D. A. and MacLeod, A. B. 1999. Modelling a river channel with distant floodbanks. Proceedings of the Institute of Civil Engineers, Water Maritime and Energy, 136(1), 21-33.

Fread, D. L. 1993. Flow routing (Chap. 10). In Handbook of Applied Hydrology, D.R. Maidment, editor. McGraw-Hill, New York, U.S.A.

Hagen, E., Shroder Jr., J. F., Lu, X. X. and Teufert, J. F. 2010. Reverse engineered flood hazard mapping in Afghanistan: A parsimonious flood map model for developing countries. Quaternary International. 226, 82-91.

Horritt, M. S. and Bates, P.D. 2002. Evaluation of 1D and 2D numerical models for predicting river flood inundation. Journal of Hydrology. 268(1), 87-99.

Hunter, N. H., Bates, P. D., Horritt, M. S. and Wilson, M. D. 2007. Simple spatially-distributed models for predicting flood inundation: a review. Geomorphology. 90, 208-225.

Hunter, N. H., Horritt, M. S., Bates, P. D., Wilson M. D. and Werner, M. G. F. 2005. An adaptive time step solution for raster-based storage cell modelling of floodplain inundation. Advances in Water Resources. 28, 975-991.

Jothityangkoon, C., Hirunteeyakul, C., Boonrawd, K. and Sivapalan, M. 2013. Assessing the impact of climate and land use changes on extreme floods in a large tropical catchment. Journal of Hydrology. 490, 88-105.

Jothityangkoon, C. and Sivapalan M. 2003. Towards estimation of extreme floods: examination of the roles of runoff process changes and floodplain flows. Journal of Hydrology. 281, 206-229.

IPCC, 2007. Climate Change 2007: The Scientific Basis, Cambridge University Press, Cambridge, U.K.

Merwade, V.M., Olivera, F., Arabi, M. and Edleman, S. 2008. Uncertainty in flood inundation mapping – current issues and future direction. ASCE Journal of Hydrologic Engineering. 13(7), 608-620.

Sarhadi, A., Soltani, S. and Modarres, R. 2012. Probabilistic flood inundation mapping of ungauged rivers: Linking GIS techniques and frequency analysis, Journal of Hydrology. 458-459, 68-86.

Tayefi, V., Lane, S. N., Hardy, R. J. and Yu, D. 2007. A comparison of one- and two-dimensional approaches to modelling flood inundation over complex upland floodplains. Hydrological Processes. 21(23), 3190-3202.

Yin, J., Yu, D., Yin, Z., Wang, J. and Xu, S. 2013. Multiple scenario analyses of Huangpu River flooding using a 1D/2D coupled flood inundation model. Natural Hazards. 66, 577-589.

Yu, D. and Lane S.N. 2006. Urban fluvial flood modelling using a two-dimensional diffusion wave treatment, part 1: Mesh resolution effects. Hydrological Processes. 20, 1541-1565.